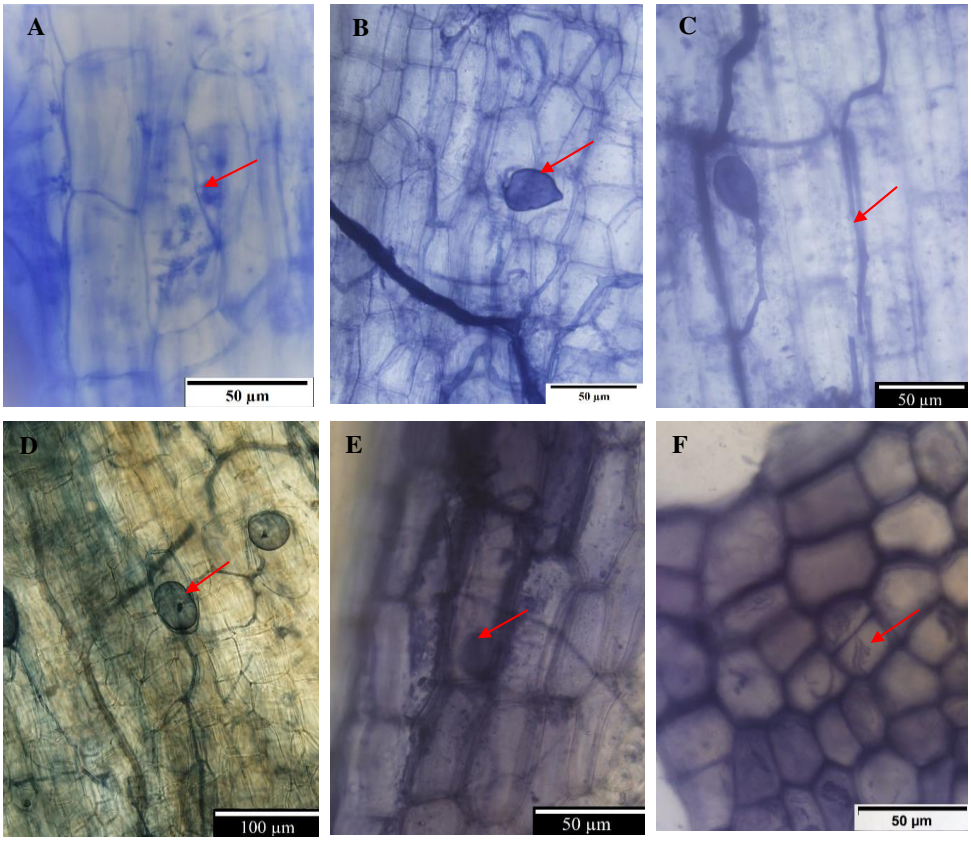
Applied Ecology and Environmental Research

International Scientific Journal



VOLUME 19 * NUMBER 2 * 2021

Published: March 31, 2021
http://www.aloki.hu
ISSN 1589 1623 / ISSN 1785 0037
DOI: http://dx.doi.org/10.15666/aeer

COMPLEXITY, CONNECTANCE AND LINK DENSITY IN CONTINENTAL FOOD WEBS: DISSIMILARITIES IN AQUATIC AND TERRESTRIAL FOOD WEBS AND THEIR HABITATS

VITEKERE, K.[1, 2] – HUA, Y.[3*] – JIANG, G.[1*]

[1]*Feline Research Center of National Forestry and Grassland Administration, College of Wildlife and Natural Protected Areas, Northeast Forestry University, Harbin 150040, China*

[2]*Tayna Center for Conservation Biology, University of Nature Conservation and Development at Kasugho, Goma 167, North-Kivu, Democratic Republic of Congo*

[3]*Guangdong Provincial Key Laboratory of Silviculture, Protection and Utilization, Guangdong Academy of Forestry, Guangzhou 510520, China*

[*]*Corresponding authors*
e-mails: wildlife530@hotmail.com and jgshun@126.com

(Received 10th Aug 2020; accepted 22nd Oct 2020)

Abstract. Both terrestrial and aquatic food webs are characterized by similar key parameters: connectance, robustness, and linkage. Ecosystems vary in basic structures and by processes that govern their dynamics and complexity. A study of complexity, connectance and link density in terrestrial and aquatic food webs, was conducted. We used 49 food webs apportioned in 23 terrestrials, 15 lacustrine and 11 rivers. The results revealed that aquatic food webs presented a difference in superiority of average connectance and link density, ($p \sim 0.05$), depicting an absence of differences in means. A regression test revealed that connectance and link density are inversely correlated in terrestrial food webs and contrary in other habitats, which was the same case for connectance and the average length of chain. We assume that connectance should be positively correlated with other parameters (fluxes and interaction strengths) in terrestrial habitat as its variations were not explained by link density or the average length of chain. This study revealed a higher estimate of connectance in aquatic habitats compared to their terrestrial counterparts. Aquatic habitats are potentially characterized by high values of parameters related to the connection (interactions quality, organisms' growth, and food web size) while terrestrial ones are more branded by features depicting constancy (productivity, complexity, and diversity).
Keywords: *average length chain, ecosystems, interactions, stability, terrestrial, lacustrine, rivers*

Introduction

It is largely known that complex structures such as ecosystems or societies are empirically simplified into three principal aspects: quality, quantity, and stability (Worm and Duffy, 2003). In ecosystems, quality refers to species richness, quantity to biomass or production of living matter and stability to resilience capacity (McCann, 2012). There is interdependence among a wide range of ecological network properties (Vermaat et al., 2009; Gravel et al., 2011). Organisms always interact within habitats when they are linked by feeding behaviour or habit. Interconnected species by such links constitute a food web which are networks of who eats whom within an ecosystem (Cohen et al., 1990; Canning and Death, 2017).

Most ecologists are concerned about biodiversity loss due to human threats on natural habitats (Gilbert, 2009; Bolchoun et al., 2017), but less attention has been given on the imbalance from the destabilization of food web complexity and interactions in an ecosystem (McCann, 2000; Worm and Duffy, 2003; Hagen et al., 2012), and these facts

http://www.aloki.hu ● ISSN 1589 1623 (Print) ● ISSN1785 0037 (Online)
DOI: http://dx.doi.org/10.15666/aeer/1902_817831
© 2021, ALÖKI Kft., Budapest, Hungary

have often been neglected based on the debated opinion that such imbalances take place on much longer time scales (Koch et al., 2014). Naturally, species conservation should imply protection of complex interactions in ecosystem since these interactions networks express essential patterns in species coexistence within habitats (Montoya et al., 2006; Bascompte and Jordano, 2007). This assumption stipulates that the complexity characteristics of species interactions, mostly measured by network connection, are an interesting feature of fit communities that generally protects them from diverse destabilizations (Polis, 1991). Unfortunately, the previous overview indicates that conservation efforts were not implemented to the protection of strongly connected communities but were focused on one species' conservation patterns (Boogert et al., 2006; Tylianakis et al., 2010; Heleno et al., 2012; Jordano, 2016). Thus connectance, a useful parameter in understanding dynamics of a food web is one of the most basic and standard metrics to characterize species interaction (Gilbert, 2009; Heleno et al., 2012). It highlights the robustness of an ecological network (Romanuk et al., 2017).

In a food web, the influence of structure on stability has been widely proved, yet the key factors for determining stability remain nonobvious (Rooney and McCann, 2012). The species richness is the basis of the complex structure in food webs (Hall and Raffaelli, 1991), including the topology and interactions patterns. This complicity shows that the link density grows with the increasing of taxon (Martinez et al., 1999; Gravel et al., 2011). Each species may link to other species including itself, but in food web chain if a species A feeds on species B, this link is not equal if B could feed on A.

Terrestrial and aquatic food webs are characterized by the same parameters as connectance, robustness and linkage. Nonetheless, primary structures of ecological unit and their regular features constitute basic differences in ecosystems (Lindeman, 1942; Strong, 1992; Chase, 2000; Mougi and Kondoh, 2016). The literature shows dissimilarities amongst food webs from terrestrial and aquatic habitats, specifically in the species' growth both in rate and size, and autotrophs' dietary features (Shurin et al., 2006). Except cited parameters, further differences between aquatic and terrestrial food webs according to complexity, connectance and linkage (even robustness, Dunne et al., 2002a) still need to be clarified, and in addition, the common and dissimilarities in food webs topology between terrestrial and aquatic ecosystems have not yet been wholly clarified (Rossi et al., 2015). Only a few studies have explored the role of habitat on a small subset of trophic interacting species (Melian et al., 2005). Indeed, many researchers approve dissimilarities in terrestrial and aquatic ecological networks, yet at the trophic pathways level little studies have quantified these disparities (Shurin et al., 2006; van Altena et al., 2016). Hence two issues emerge: (1) Do food webs from aquatic and terrestrial habitats have the same proportions of link density? (2) Amongst these environmentally different food webs, does one might be more connected than another? This study attempts to compare three attribute patterns (connectance, link density and average length of chain) between aquatic and terrestrial food webs and bring out major features presence magnitude influencing food webs in these two habitats type.

Methods

Study presentation

We conducted literature review found from diverse research browsers to collect as many documents as possible related to all attributes used in this study and those related

http://www.aloki.hu ● ISSN 1589 1623 (Print) ● ISSN1785 0037 (Online)
DOI: http://dx.doi.org/10.15666/aeer/1902_817831
© 2021, ALÖKI Kft., Budapest, Hungary

to any characteristic depicting difference in habitats influencing a food web. We realized that the functioning of food webs and their structure are mostly characterized and influenced by their own different structural attributes. These attributes are constitutive elements of the complexity (diversity, connectance, robustness, nestedness, pathway proliferation and link distribution) and portray the state of the community networks (Canning and Death, 2017). Though, all of them don't necessarily influence stability of the food web (May, 1973; Riede et al., 2010). In our study methodology, we preferred first to understand these attributes; (a) connectance which is the fraction of undertaken interactions from the pool of all probable interactions between members of a network (May, 1973; Calizza et al., 2015). (b) Trophic link which is a reported feeding relationship between two species in a food web (Martinez, 1992). Ecologists use different criteria to decide how much foods validate the presence or the absence of a link (Cohen and Briand, 1984). (c) Average length chain which represents the average link number of chain within a food web from the basis till the top predators, without considering loops (Calizza et al., 2015). (d) Robustness which is the opposite of fragility, and it relates to the preservation of network integrity and so has effects on stability (Gilbert, 2009). (e) Nestedness: a network always has two kinds of species: generalists and specialists (Henle et al., 2004). Thus the interactions in a network are nested when the species interacting with specialists constitute a subgroup of the species interacting with generalists (Tylianakis et al., 2010).

Analysis

Many food webs of different habitats were considered in this study. Selection of the food webs was based on criteria such as common elements and belonging to the same collection (*Table 1*). We calculated the connectance (Gardner and Ashby, 1970; Williams and Martinez, 2000; van Altena et al., 2016; Romanuk et al., 2017) by

$$C=L/S^2 \qquad \text{(Eq.1)}$$

where C represents the connectance; L is the number of trophic links and S is the species richness.

The link density was computed (Hall and Raffaelli, 1993; Bersier et al., 1999; Tylianakis et al., 2010; Gravel et al., 2011; Calizza et al., 2015) by

$$LD= L/S \qquad \text{(Eq.2)}$$

where DL indicates link density L and S are same as *equation (1)*.

Analysis of variance (ANOVA) was used to test if there was a significant difference within connectance of different habitats' food webs and link density values. Normality of the data was checked using the Shapiro test and the homoscedasticity using the Bartlett test (Koller et al., 2007; James et al., 2013). We demonstrated the involvement of connectance with two other attributes (link density and the average length of chain) by the correlation test (Pearson test), and we computed the regression boxplots to demonstrate this correlation power (Koller et al., 2007). Due to the outputs of the correlation test, multiple regressions were computed (in R software) by postulating the connectance as the dependent variable with link density and average length of chain as predictors, to predict how predictors influence the dependent variable, and how they are really associated (Faraway, 2016). We made a set of principal functioning patterns in

http://www.aloki.hu ● ISSN 1589 1623 (Print) ● ISSN1785 0037 (Online)
DOI: http://dx.doi.org/10.15666/aeer/1902_817831
© 2021, ALÖKI Kft., Budapest, Hungary

aquatic and terrestrial ecosystems which govern the feeding interactions from previous studies and discussed about their properties and influences on food web within studied habitats. The interpretation of estimates from computed attributes and dissimilarities pulled from literature constituted the basis of inferences herein this study.

Table 1. *Analyzed food weds (Source: Cohen et al., 1990)*
a. *Terrestrial food webs*

Food webs name in the collection	*S*	*L*	*C*	*LD*	*ALC*	No
Prairie, Manitoba	15	27	0.12	1.8	2.4	23
Willow forest, Manitoba	12	18	0.13	1.5	2.7	24
Aspen communities, Manitoba	24	37	0.06	1.54	2.93	25
Aspen forest, Manitoba	32	56	0.05	1.75	2.93	26
Wytham Wood, England	22	39	0.08	1.77	2.89	27
Salt meadow, New Zealand	32	35	0.03	1.09	1.96	28
Rain forest, Malaysia	11	15	0.12	1.36	1.88	40
Sand beach, California	14	23	0.12	1.64	2.44	50
Trelease Woods, lllinois	29	61	0.07	2.1	2.37	59
Montane forest, Arizona	33	69	0.06	2.09	2.36	60
Barren regions, Spitsbergen	8	10	0.16	1.25	2	61
Reindeer pasture, Spitsbergen	11	12	0.10	1.09	3	62
Sand beach, South Africa	21	36	0.08	1.71	2.38	74
Old field New Jersey	22	39	0.08	1.77	1.84	90
Shigayama coniferous forest, Japan	10	13	0.13	1.3	3	91
High Himalayas community, Tibet	18	18	0.06	1	2	92
Alpine tundra, Montana	26	70	0.10	2.69	2.12	93
Tundra, Prudhoe, Alaska	10	12	0.12	1.2	2.5	95
Tundra, Yamal Peninsula, Siberia	9	16	0.20	1.78	1.92	96
Tundra, South Yamal, Siberia	11	17	0.14	1.55	2	97
Sand dunes, Namib Desert, Namibia	17	39	0.13	2.29	3.54	98
Sonora Desert, Arizona	48	138	0.06	2.88	2.51	99
Rajasthan Desert, India	22	59	0.12	2.68	3.34	100

b. *Lacustrine food webs*

Food webs names in the collection	*S*	*L*	*C*	*LD*	*ALC*	No
Lough Ine Rapids, Ireland	9	13	0.16	1.44	2.86	9
Moosehead Lake, Maine	17	32	0.11	1.88	3	19
Lake Nyasa, rocky shore, Malawi	31	95	0.10	3.06	2.13	38
Lake Nyasa, sandy shore, Malawi	33	70	0.06	2.12	1.8	39
Lake Texoma, Texas	19	68	0.19	3.58	4.43	46
Lake Rybinsk, Russia, USSR	16	32	0.13	2	5.15	71
Heney Lake, pelagic zone, Quebec	17	32	0.11	1.88	3.95	72
Hafner Lake, Austria	10	15	0.15	1.5	2.38	73
Vorderer Finstertaler Lake, Austria	9	14	0.17	1.56	2.75	75
Neusiedler Lake, Austria	14	17	0.09	1.21	2.67	76
Lake Abaya, Ethiopia	13	24	0.14	1.85	3.63	77
Lake George, Uganda	16	27	0.11	1.69	3.15	78
Lake Piijirvi, offshore, Finland	21	29	0.07	1.38	3.41	79
Lake Piijirvi, littoral zone, Finland	27	70	0.10	2.59	3.35	80
Lake PyhajiU-vi,littoral zone, Finland	25	67	0.11	2.68	2.45	83

http://www.aloki.hu ● ISSN 1589 1623 (Print) ● ISSN1785 0037 (Online)
DOI: http://dx.doi.org/10.15666/aeer/1902_817831
© 2021, ALÖKI Kft., Budapest, Hungary

c. *Rivers (and creeks) food webs*

Food Webs name in the collection	*S*	*L*	*C*	*LD*	*ALC*	No
Crocodile Creek, Malawi	29	48	0.06	1.66	1.93	33
River Clydach, Wales	12	27	0.19	2.25	2.56	34
Morgan's Creek, Kentucky	13	36	0.21	2.77	2.72	35
River Rheidol, Wales	18	75	0.23	4.17	3.16	63
Linesville Creek, Pennsylvania	19	28	0.08	1.47	1.67	64
Yoshino River rapids, Japan	13	25	0.15	1.92	1.85	65
River Thames, England	10	18	0.18	1.8	2.93	66
Mudflats, Mississippi River, Iowa	21	62	0.14	2.95	3.94	67
Crystal River Estuary, Florida	14	28	0.14	2	2.49	70
Lestijoki River Rapids, Finland	16	42	0.16	2.63	1.95	88
River Cam, England	18	32	0.10	1.78	2.89	89

S: number of species; *L*: number of links; *C*: connectance; *LD*: link density; *ALC*: average length of chain; No: number of food web in Cohen's collection

Results

Data set and fitness of statistical tests

The analysed food webs were from Cohen et al. (1990) collection. Among the 55 continental food webs of the collection, 49 were studied (*Table 1*). They are apportioned in 23 terrestrials, 15 lacustrine and 11 rivers and creeks which are referred to as simply rivers' food web in this study. Within the sample, 18 food webs (36.73%) of the considered collection were from America, 16 (32.65% of the collection) from Europe, Africa and Asia had 7 food webs each (constituted 14.28% of our data set for each continent) and only one food web from Oceania which represented 2.04%. We computed their studied attributes: connectance, link density and the average length chain. All tests (except one) to verify the requirements of the analysis proved that our data were fitted for ANOVA. Shapiro test $p = 0.957$ and Bartlett test $p = 0.400$ for connectance, Shapiro test $p = 0.001$ and Bartlett test $p = 0.296$ for link density. The Shapiro test for link density had $p < 0.050$, but it didn't influence the analysis as other requirements were successfully fulfilled (e.g. James et al., 2013).

Findings for studied attributes of food webs in three habitats

Findings revealed differences between connectance within three habitats ($p = 0.012$), with averages of 0.101; 0.118 and 0.149 for terrestrial, lacustrine and rivers, respectively. Comparing link density values, the $p = 0.048$ (~0.05), revealed an absence of significant difference and averages were 1.732; 2.028 and 2.308 for terrestrial, lacustrine and rivers respectively. Their boxplots (*Figure 1*) represent these averages and they revealed an increasing pace from terrestrial to rivers' habitat.

The correlation tests of connectance with link density and connectance with average length of chain revealed an inversely correlated relation in terrestrial habitats (*Table 2*); on the other hand, in two other habitats (lacustrine and rivers) they were positively correlated but not significantly.

http://www.aloki.hu ● ISSN 1589 1623 (Print) ● ISSN1785 0037 (Online)
DOI: http://dx.doi.org/10.15666/aeer/1902_817831
© 2021, ALÖKI Kft., Budapest, Hungary

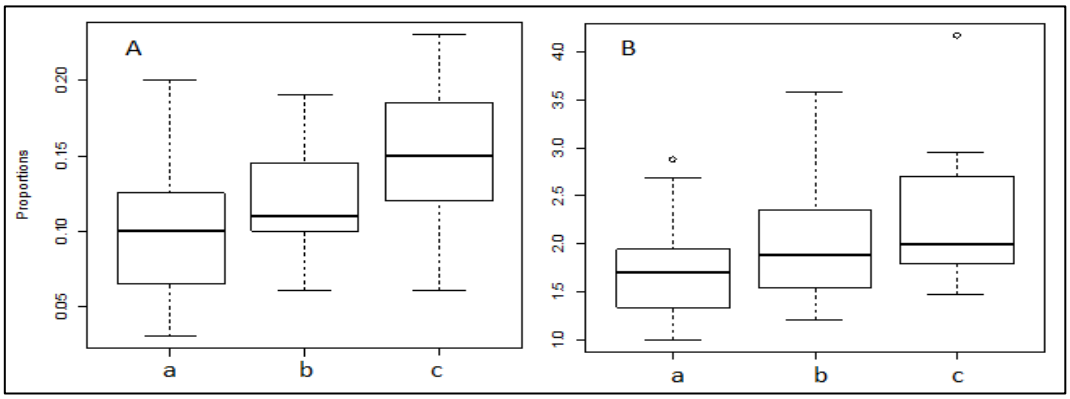


Figure 1. *Different averages rate of connectance (A) and link density (B) in food webs, a: terrestrial; b: lacustrine and c: rivers*

Table 2. *Correlation estimates of attributes in three habitats*

Estimated Parameters	Terrestrial		Lacustrine		Rivers	
	C-LD	***C-ALC***	***C-LD***	***C-ALC***	***C-LD***	***C-ALC***
r	-0.054	-0.041	0.178	0.362	0.727	0.420
r-squared	0.003	0.002	0.031	0.131	0.529	0.177
p-value	0.803	0.849	0.520	0.184	0.011	0.1973

C: connectance, *LD*: link density and *ALC*: average length of chain

A more thorough visual examination was needed, so we used scatter diagrams and variations as demonstrated through the boxplots histogram (*Figure 2*).

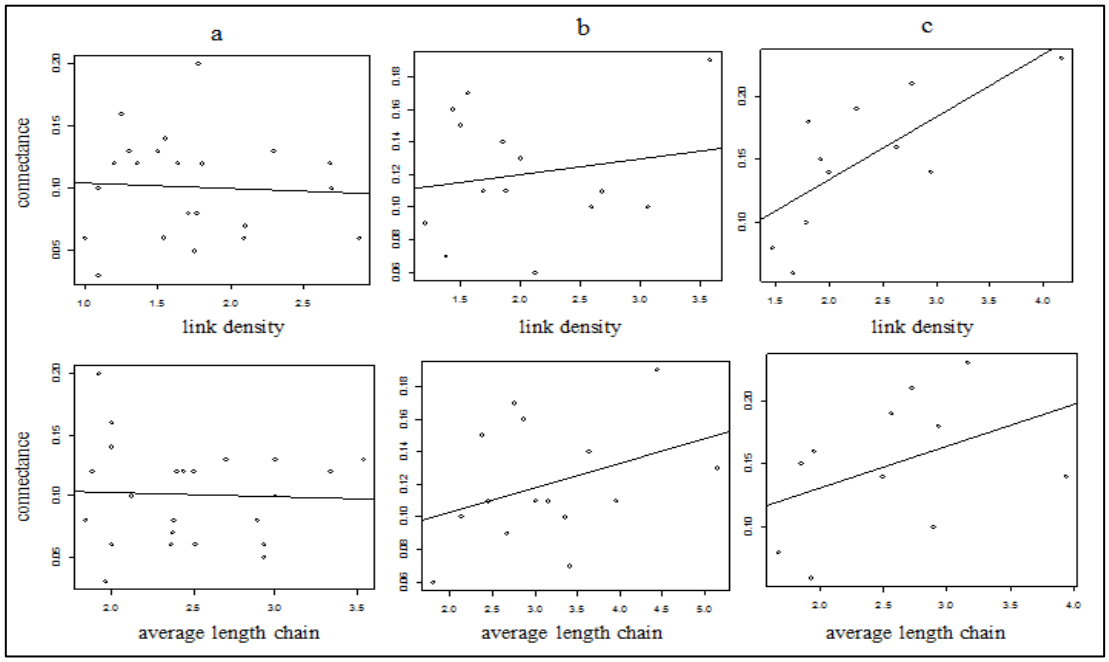


Figure 2. *Correlation diagrams (column a: terrestrial, column b: lacustrine and column c: rivers)*

http://www.aloki.hu ● ISSN 1589 1623 (Print) ● ISSN1785 0037 (Online)
DOI: http://dx.doi.org/10.15666/aeer/1902_817831
© 2021, ALÖKI Kft., Budapest, Hungary

We computed a multiple regression test for these three attributes (*Table 3*). The model depicted lesser influences of both link density and average length of chain on the connectance (dependent variable) in all habitats, except link density in rivers which had $p < 0.05$. Within lacustrine food webs, correlations of connectance with link density; and connectance with average length of chain were positive but weak, with 3.19% and 13.13% of explained variations. In rivers, an average and positive correlation (*Table 2*) for connectance with link density was brought out (with 52.95% as explained variation). According to connectance with average length of chain, a positive but non-significant correlation was found (17.72% explained variation).

Table 3. *Multi-regression models output for three different habitats' attributes; with connectance as the dependent variable and link density and average length of chain as predictors*

Estimated parameters	Terrestrial			Lacustrine			River		
	Inter	***C-DL***	***ALC***	***Inter***	***LD***	***ALC***	***Inter***	***LD***	***ALC***
Estim	0.113	-0.003	-0.002	0.061	0.006	0.014	0.032	0.048	0.001
SE	0.049	0.017	0.019	0.043	0.014	0.011	0.051	0.019	0.022
t	2.265	-0.203	-0.012	1.427	0.479	1.271	0.628	2.449	0.067
p-value	0.034	0.841	0.900	0.179	0.641	0.228	0.547	0.040	0.949

Inter: intercept, Estim: estimates, *SE*: standard error, *t*: test-values, *C*: connectance, *LD*: link density and *ALC*: average length of chain

Differential view of habitats

After computing attributes of studied food webs; we retrieved important dissimilarities which refer directly or indirectly to at least one of the major attributes within a feeding network, in either terrestrial or aquatic habitat (*Table 4*). There are many internal characteristics in both of these two habitats, but we chose the most important cited in previous food webs studies, and these characteristics seemed to be largely documented. Although the habitat type cannot portray the entire food web characteristics, the dynamics of ecosystem features contribute to the functioning of food web patterns within a habitat and can exert a certain influence.

Table 4. *Other peculiarities in two different habitats' food webs*

Attributes	A-food webs	T-food webs	Sources
Productivity	low	high	(Chase, 2000)
Complexity	low	high	(Chase, 2000)
Omnivory	low	high	(Thompson et al., 2012a)
Diversity	low	high	(Strong, 1992; Caizza et al., 2015)
Trophic levels	more than(4)	less than(3)	(Hairston and Hairston, 1993)
Trophic cascades	common	rare	(Chase, 2000)
Interactions	strong	weak	(Polis, 1999)
Size-structured	strong	less	(Shurin et al., 2006)
Growth rates	fast	slow	(Shurin et al., 2006)
Elton's rule (biomass pyramid)	not applied	applied	(Elton, 1927)
Primary producers	unicellular	multicellular	(Linderman, 1942)
Nutrients	more	less	(Linderman, 1942)
Living plants consumption	great	little	(Shurin et al., 2006)

A: Aquatic and T: terrestrial

http://www.aloki.hu ● ISSN 1589 1623 (Print) ● ISSN1785 0037 (Online)
DOI: http://dx.doi.org/10.15666/aeer/1902_817831
© 2021, ALÖKI Kft., Budapest, Hungary

Discussion

Data set and methodological assessment

The choice of our food web samples from the Cohen et al. (1990) collection was justified as this collection remains one of the most detailed and well explained. Only continental food webs constituted our sample. Wetlands and estuarine food webs were excluded due to interpretation issues of the location definition, as stated by Cohen (1994), and the dichotomy between oceans and continents excludes coastal zones, which some argue give them an intermediate status. Our methodology was adapted to use tests in the study, and allowed us to calculate estimates of studied attributes (connectance, link density and length of the chain) chosen because of their importance in measuring connectivity of a food web as stressed by Tylianakis et al. (2010), and making comparisons between food webs belonging to two habitats type: terrestrial and aquatic. Despite that the methodological approaches were mostly based on empirical facts in the food webs estate, we assumed this analysis was not ultimately perfect due to the complexity of food web domain, referring to Power (1992) who admitted the difficulties in applying food web theories to real ecosystems. Nevertheless, despite in real networks, food webs are greatly complex than the literature could let us think (Polis, 1988; Bolchoun et al., 2017), this study brought out details about differences in food webs in different habitats type. We used the geometric average length of chain.

Features of studied attributes in three habitats' food webs

The connectance values were different among three habitats ($p = 0.012$) with aquatic food webs being more connected. The features diversity within ecosystems should probably justify this dissimilarity. Ecological systems vary in their basic configurations that govern their features and complexity (Lindeman, 1942; Strong, 1992; Chase, 2000; Riede et al., 2010), and they differ within terrestrial and aquatic habitat. Food webs' parameters such as quality and quantity of interactions, the size of the structure (Dunne et al., 2002b), and growth rate of organisms have a central role in depicting this difference as they are stronger in aquatic than terrestrial habitats (Polis, 1999; Shurin et al., 2006) that would explain the dissimilarity in food web connections as found in our results, despite analyses of Riede et al. (2010) and Rossi et al. (2015) demonstrated that ecosystem-specific differences were of minor importance in food webs features. However, comparing the observed *p-value* to the 0.01 threshold there were no significant differences. Accordingly, these estimates did not have a high variation between habitats as intragroup variances were the same ($p = 0.4005$, Bartlett test) and averages were 0.101; 0.118 and 0.149 for terrestrial, lacustrine and river food webs, respectively. Our findings corroborated those of Riede et al. (2010) when they studied the scaling of food web properties from five different food web habitats (estuary, lake, marine, river and terrestrial). These slight differences found in averages show the difference of connectivity features between terrestrial and aquatic food webs, yet the average values demonstrate clearly the non-significant aspect of that difference, as it was demonstrated by results found.

The average values for connectance and link density in aquatic habitats were higher than terrestrial. Calizza et al. (2015) observed that link density and connectance always describe the complex structure of the food webs regarding their size dissimilarities, while the average length chain portrays the average number of trophic transfers from detritus resources to top predators. Thus these two metrics are linked by such feature.

http://www.aloki.hu ● ISSN 1589 1623 (Print) ● ISSN1785 0037 (Online)
DOI: http://dx.doi.org/10.15666/aeer/1902_817831
© 2021, ALÖKI Kft., Budapest, Hungary

Indeed, trophic links are one of attributes which have never lacked in a food web (Neutel et al., 2002; Pinnegar et al., 2005) since food web studies shown that a great number of species (more than 95%) are within three links of one another (Gravel et al., 2011). The upper limit of links is the square of the species number; each species cannot be linked to more species than exist in a web. The lowest link number is species' number minus one, as each species must be connected to a food web with at least one link (Martinez, 1992; Gravel et al., 2011). Nonetheless, some habitats have a high number of links, connectance and average length of chain as stated by Dunne et al. (2004) which agree with this study as aquatic food webs were revealed to be more connected.

Terrestrial habitat had an inverse correlation between connectance and two other attributes (link density and average length of chain), with *R-squared* values of 0.003 and 0.002 estimates, respectively, and explained variations of only 0.30% and 0.20%, respectively for link density and average length of chain. When the species richness approaches infinity, it generates the smallest connectance (Gilbert, 2009); and endorses the inverse proportionality with link density. As connectance and link density are inversely connected in terrestrial food webs, Dunne (2012) stated that the highest number of links in a food web is consequently, the square of the species number present in that food web. A positive correlation is always found between species and the number of links within a trophic chain, contrary with connectance. As links and species are positively correlated in term of number, interactions will depend on the correlation because they are underlying and defined by link number. These results corroborate the theory stipulated that food webs should not accumulate the largest numbers of species (McCann et al., 1998) therefore connectance and robustness wouldn't be affected. However, connectance, in its simple interpretation cannot be considered as an indicator of stability, as its value is typically attributed (Helano et al., 2012). In this optic, it should be careful to interpret connectance values in order to avoid a generalization of a trend in specific case as new approaches introduced the notion of weighted and unweighted connectance (Van Altena et al., 2016). Yet, in general the studied connectance remains unweighted as the weighted connectance has never been used in the complexity-stability context and it is focused on flux transmission in a food web.

While interpreting correlation, researchers always conclude that "there is no strong relationship between the two variables". This explanation is simply a reflection of reality. It is then necessary to leave the simple correlations and make multiple-regressions, so we computed a multiple regression test (*Table 3*). This test even elucidates the lack of dependence amongst connectance with link density and average length of chain in all habitats (except link density in rivers), but the prediction of influence in this association remains blurry, particularly in terrestrial food webs. Specific internal features of an ecosystem explain that connectance in terrestrial food webs withstands whatever the effects of the length of chain. For example, productivity, complexity (Chase, 2000), diversity (Strong, 1992), and omnivory (McCann and Hastings, 1997) are all strong in terrestrial habitats, and they are key attributes in depicting stability. Yet recently, it has been stated that a very strong omnivory effect can destabilize a food web (Gellner and McCann, 2012).

Compared to terrestrial habitats, link density and average length of chain in lacustrine food webs are less responsible for connectance variations (3.19% and 13.13%, respectively). The explained variation values were low, thus other probable factors such as fluxes and interaction strengths should empirically explain this disparity as the more

http://www.aloki.hu ● ISSN 1589 1623 (Print) ● ISSN1785 0037 (Online)
DOI: http://dx.doi.org/10.15666/aeer/1902_817831
© 2021, ALÖKI Kft., Budapest, Hungary

consistently flux rates are distributed over links in a food web, the more stable the webs are (van Altena et al., 2016).

Rivers depicted positive correlations with average values for explained variations (52.95% for link density and 17.72% for average length of chain). That demonstrated the difference between terrestrial and aquatic habitats. Evidence shows that although food webs share a fundamental organization that depends on the number of species and network linkages (Dunne et al., 2004), it is useful to recognize whether there are fine structural differences between different habitats type. Cohen (1994) found contrasts between marine food webs as they had greater link density and length of chain than their equivalents in terrestrial and freshwater ecosystems. Obviously, the properties of food webs are actually dissimilar in each specific habitat. In this perspective, the scale-dependence of most food web properties has been well recognized because they change as species richness and complexity change (Martinez, 1993; Riede et al., 2010). Nonetheless, it was proved that some food web properties remain scale-invariant (Sugihara et al., 1989; Cohen et al., 1990; Hall and Raffaelli, 1993) with one exception the links/species ratio (Strong, 1988; Martinez, 1994). This could be a plausible explanation for these findings according to the correlation between connectance and link density, especially in aquatic food webs, as terrestrial food webs tended to conform to the scale invariant properties patterns.

Differential view of food webs in habitats

Trophic cascades are more observed in aquatic food webs, even though facts have never been proved (Chase, 2000). Yet, Hairston et al. (1960) assumed that reduction of the abundance of herbivores in terrestrial food webs when apex carnivores are numerous, allows plants to flourish, and leads to a trophic cascade. Therefore, the most obvious understanding of this fact is that species on which the robustness of a food web is most dependent should be the greatest priority for conservation (McDonald-Madden et al., 2016). In aquatic habitat a trophic cascade may be natural, but in a terrestrial habitat it should depend on apex carnivores. We stress that the Elton's rule (biomass pyramid) is not often applied in aquatic food webs contrary to terrestrial (Elton, 1927). It was well documented that in ascending movement within a food web chain, the biomass decreases at each level. A perfect illustration of the energy transfer through a chain in a food web is a pyramid of biomass. Nonetheless, seasonal disparities in the turnover degree of species at a specific level might result in superior or inferior values for the quantity of biomass sampled at a precise period than the normal quantity across the year. Thus, the turnover is easily triggered in aquatic habitats because of the high abundance of nutrients (Lindeman, 1942) and leads to failure to apply Elton's rule. However, eutrophication is mainly responsible for high nutrient abundance in aquatic habitats (Khan et al., 2014), therefore the pyramid of energy is the best representation of the transfer of energy in a chain of a food web which is applicable in both aquatic and terrestrial habitats.

Terrestrial ecosystems present a high diversity and complexity level (Strong, 1992; Hairston and Hairston, 1993) that induces high productivity (Chase, 2000). Indeed, in terrestrial systems, plant defence is widespread (Polis, 1999) but aquatic systems promote small and floating species, rather than those that are generally well self-defended (Polis and Strong, 1996; Persson, 1999). Accordingly, plant defence also increases complexity in terrestrial habitats. However, this complexity (and diversity) might be influenced by seasonality (Pimm, 1982; Thompson et al., 2012b) and even

http://www.aloki.hu ● ISSN 1589 1623 (Print) ● ISSN1785 0037 (Online)
DOI: http://dx.doi.org/10.15666/aeer/1902_817831
© 2021, ALÖKI Kft., Budapest, Hungary

with high complexity, terrestrial food webs have fewer interactions than aquatic ones (Polis, 1999). We assumed that connectance should be positively correlated with interactions because this study found a high connectance in aquatic than in terrestrial habitat. Thus food webs of freshwater are more connected than terrestrial, which is in agreement with Dunne et al. (2004) for marine areas. Robustness increases with connectance (Dunne et al., 2002a, 2004; Canning and Death, 2017) and regarding species loss (Gilbert, 2009) food webs of freshwater habitats are more robust than their terrestrial counterparts. Marine food webs depicted the same feature (Dunne et al., 2004), as this system allows its food webs to remain robust to a selected loss of well-connected species, due to their high connectance (Albert and Barabasi, 2000; Zhao et al., 2016; Canning and Death, 2017). This fact pertains to the theory of "a loss of less connected species in a chain creates a positive change in the connectance" (Gilbert, 2009), and we infer that habitats in continental waters have more robust food webs than terrestrial as it is the case for marine habitats.

The Trophic levels are more abundant in aquatic food webs than in terrestrial (Hairston and Hairston, 1993). Some ecologists stipulate that there is no evidence for such trend, principally because of issues to estimate the species diversity or richness and links of small sized organisms in aquatic (Schmid-Araya et al., 2002), terrestrial, and soil ecosystems (Mikola and Setälä, 1998). Many trophic levels can present omnivory, which has a positive role in food web stability, contrary to what early studies stipulated (McCann and Hastings, 1997). This attribute is low in aquatic than in terrestrial food webs (Thompson et al., 2012a), and should explain why omnivory cannot influence robustness (Dunnne et al., 2002) as both of them are not highly present in a food web. However, Gellner and McCann (2012) stipulated that strong omnivory can destabilize a food web. Definitively, although food web dissimilarities exist between ecosystems, landscapes or habitats, the "who feed on whom patterns" are more similar within food web pertaining to those habitat types (e.g. Riede et al., 2010; Rossi et al., 2015).

Conclusion

Despite numerous studies by ecologists using multi methodological ways, food web research domain remains complex. Researchers always approve issues in applying food web theories to the real world in ecosystems. Different inferences have been established, but most of them are specific or isolate case, therefore they do not reveal the actual situation in many landscapes. After a documentary analysis, we realised that aquatic food webs are more studied than terrestrial; they are more connected and robust as robustness increases with connectance. Nevertheless, aquatic food webs are more sensitive than terrestrial ones to the loss of connected species in a chain. Many links reduce robustness so it is not necessarily true that more links bring stability, which needs to be empirically proved. Complexity is higher in terrestrial food webs than in aquatic, because many links determine the complexity, and they are opposite to robustness which is high in aquatic systems. Unlike in aquatic systems, connectance and link density are inversely correlated in terrestrial ecosystems. Although food webs share a fundamental organization, there are fine structural differences between habitats. Yet this study should not be the ultimate confirmation of facts underlying its findings since more studies are required to demonstrate new patterns which could support such inferences. Consequently, we suggest researchers to continue going beyond this study in the same thematic.

http://www.aloki.hu ● ISSN 1589 1623 (Print) ● ISSN1785 0037 (Online)
DOI: http://dx.doi.org/10.15666/aeer/1902_817831
© 2021, ALÖKI Kft., Budapest, Hungary

Acknowledgements. This research was funded by North China Leopard Monitoring Demonstration of NFGA, National Natural Science Foundation of China (NSFC 31872241). We thank our colleagues in the Feline Research Center of National Forestry and Grassland Administration of the Northeast Forestry University for their valuable advices and suggestions during the preparation of this study; we particularly thank Meadhbh Molloy and Chula Mwagona Pateson for language corrections and valuable orientations.

REFERENCES

[1] Albert, R., Barabasi, A. L. (2000): Topology of evolving networks: local events and universality. – Physical Review Letters 85: 5234-5237.
[2] Bascompte, J., Jordano, P. (2007): Plant–animal mutualistic networks: the architecture of biodiversity. – Annual Review of Ecology, Evolution, and Systematics 38: 567-593.
[3] Bersier, L. F., Dixon, P., Sugihara, G. (1999): Scale-invariant or scale-dependent Behavior of the link density property in food webs: a matter of sampling effort? – American Naturalist 153: 676-682.
[4] Bolchoun, L., Drossel, B., Allhoff, K. T. (2017): Spatial topologies affect local food web structure and diversity in evolutionary metacommunities. – Scientific Reports 7: 1-11.
[5] Boogert, J. N., Paterson, M. D., Laland, K. N. (2006): The Implications of Niche Construction and Ecosystem Engineering for Conservation Biology. – BioScience 56: 570-578.
[6] Calizza, E., Costantini, M. L., Rossi, L. (2015): Effect of multiple disturbances on food web vulnerability to biodiversity loss in detritus-based systems. – Ecosphere 6: 1-20.
[7] Canning, A. D., Death, R. G. (2017): Trophic cascade direction and flow determine network flow stability. – Ecological Modelling 355: 18-23.
[8] Chase, J. M. (2000): Are there real differences among aquatic and terrestrial food webs? – Trends in Ecology & Evolution 15: 408-412.
[9] Cohen, J. E., Briand, F. (1984): Trophic links of community food webs. – Proceedings of the National Academy of Sciences 81: 4105-4109.
[10] Cohen, J. E., Briand, F., Newman, C. M. (1990): Community food webs: data and theory. – Springer-Verlag, New York.
[11] Cohen, J. E. (1994): Marine and continental food webs: three paradoxes? – Philosophical Transactions of the Royal Society B Biological 343: 57-69.
[12] Dunne, J. A., Williams, R. J., Martinez, N. D. (2002a): Network structure and biodiversity loss in food webs: robustness increases with connectance. – Ecological Letters 5: 558-567.
[13] Dunne, J. A., Williams, R. J., Martinez, N. D. (2002b): Food-web structure and network theory: the role of connectance and size. – Proceedings of the National Academy of Sciences 99: 12917-12922.
[14] Dunne, J. A., Williams, R. J., Martinez, N. D. (2004): Network Structure and Robustness of Marine Food Webs. – Marine Ecology Progress Series 273: 291-302.
[15] Dunne, J. A. (2012): Food webs: Computational complexity theory, techniques and applications. – Springer-Verlag, New York.
[16] Elton, C. (1927): Animal Ecology. – MacMillan, New York.
[17] Faraway, J. J. (2016): Linear models with R. – Chapman and Hall/CRC, New York.
[18] Gardner, M. R., Ashby, W. R. (1970): Connectance of large dynamical (cybernetic) systems: critical values for stability. – Nature 228: 784-784.
[19] Gellner, G., McCann, K. (2012): Reconciling the Omnivory-Stability Debate. – American Naturalist 179: 22-37.
[20] Gilbert, A. J. (2009): Connectance indicates the robustness of food webs when subjected to species loss. – Ecological Indicators 9: 72-80.

http://www.aloki.hu ● ISSN 1589 1623 (Print) ● ISSN1785 0037 (Online)
DOI: http://dx.doi.org/10.15666/aeer/1902_817831
© 2021, ALÖKI Kft., Budapest, Hungary

[21] Gravel, D., Canard, E., Guichard, F., Mouquet, N. (2011): Persistence Increases with Diversity and Connectance in Trophic Metacommunities. – PLoS ONE 6: e19374. doi:10.1371/journal.pone.0019374.
[22] Hagen, M., Kissling, W. D., Rasmussen, C., Carstensen, D. W., Dupont, Y. L., Kaiser-Bunbury, C. N., O'Gorman, E. J., Olesen, J. M., De Aguiar, M. A. M., Brown, L. E., Alves-Dos-Santos, I., Guimarães, P. R., Maia, K. P., Marquitti, F. M. D., Vidal, M. M., Edwards, F. K., Genini, J., Jenkins, G. B., Trøjelsgaard, K., Woodward, G., Jordano, P., Ledger, M. E., Mclaughlin, T., Morellato, L. P. C., Tylianakis, J. M. (2012): Biodiversity, Species Interactions and Ecological Networks in a Fragmented World. – Advances in Ecological Research 46: 89-120.
[23] Hairston, N. G., Smith, F. E., Slobodkin, L. B. (1960): Community structure, population control, and competition. – American Naturalist 94: 421-425.
[24] Hairston Jr, N. G., Hairston Sr, N. G. (1993): Cause-effect relationships in energy flow, trophic structure, and interspecific interactions. – American Naturalist 142: 379-411.
[25] Hall, S. J., Raffaelli, D. G. (1991): Food-web patterns: lessons from a species-rich web. – Journal of Animal Ecology 60: 823-842.
[26] Hall, S. J., Raffaelli, D. G. (1993): Food webs: theory and reality. – Advances in Ecological Research 24: 187-239.
[27] Heleno, R., Devoto, M., Pocock, M. (2012): Connectance of species interaction networks and conservation value: Is it any good to be well connected? – Ecological Indicators 14: 7-10.
[28] Henle, K., Davies, K. F., Kleyer, M., Margules, C., Settele, J. (2004): Predictors of species sensitivity to fragmentation. – Biodiversity & Conservation 13: 207-251.
[29] James, G., Witten, D., Hastie, T., Tibshirani, R. (2013): An introduction to statistical learning. – Springer, New York.
[30] Jordano, P. (2016): Chasing ecological interactions. – PLOS Biology 14: e1002559.
[31] Khan, F. A., Naushin, F., Rehman, F., Masoodi, A., Irfan, M., Hashmi, F. (2014): Eutrophication: global scenario and local threat to dynamics of aquatic ecosystems. – In: Eutrophication: causes, consequences and control. Springer, Dordrecht.
[32] Koch, H., Frickel, J., Valiadi, M., Becks, L. (2014): Why rapid, adaptive evolution matters for community dynamics. – Frontiers in Ecology and Evolution 2: 1-17.
[33] Koller, D., Friedman, N., Džeroski, S., Sutton, C., McCallum, A., Pfeffer, A., Abbeel, P., Wong, M. F., Heckerman, D., Meek, C., Neville, J. (2007): Introduction to statistical relational learning. – MIT Press, Massachusetts.
[34] Lindeman, R. (1942): The trophic-dynamic aspect of ecology. – Ecology 23: 399-418.
[35] Martinez, N. D. (1992): Constant connectance in community food webs. – American Naturalist 139: 1208-1218.
[36] Martinez, N. D. (1993): Effects of Resolution on Food Web Structure. – Oikos 66: 403-412.
[37] Martinez, N. D. (1994): Scale-Dependent Constraints on Food-Web Structure. – American Naturalist 144: 935-953.
[38] Martinez, N. D., Hawkins, B. A., Dawah, H. A., Feifarek, B. P. (1999): Effects of sampling effort on characterization of food-web structure. – Ecology 80: 1044-1055.
[39] May, R. M. (1973): Stability and Complexity in Model Ecosystems. – University Press, Princeton.
[40] McCann, K. S., Hastings, A. (1997): Re-evaluating the omnivory-stability relationship in food webs. – Proceedings of the Royal Society of London 264: 1249-1254.
[41] McCann, K. S., Hastings, A., Huxel, G. R. (1998): Weak trophic interactions and the balance of nature. – Nature 395: 794-798.
[42] McCann, K. S. (2000): The diversity–stability debate. – Nature 405: 228-233.
[43] McCann, K. S. (2012): Mathematical Ecology. – University Press, Oxford.

http://www.aloki.hu ● ISSN 1589 1623 (Print) ● ISSN1785 0037 (Online)
DOI: http://dx.doi.org/10.15666/aeer/1902_817831
© 2021, ALÖKI Kft., Budapest, Hungary

[44] McDonald-Madden, E., Sabbadin, R., Game, E. T., Baxter, P. W. J., Chadès, I., Possingham, H. P. (2016): Using food-web theory to conserve ecosystems. – Nature Communications 7: 10245. doi: 10.1038/ncomms10245.
[45] Melian, C. J., Bascompte, J., Jordano, P. (2005): Spatial structure and dynamics in a marine food web. – Aquatic Food Webs 1: 19-24.
[46] Mikola, J., Setälä, H. (1998): No evidence of trophic cascades in an experimental microbial-based soil food web. – Ecology 79: 153-164.
[47] Montoya, J. M., Pimm, S. L., Sole, R. V. (2006): Ecological networks and their fragility. – Nature 442: 259-264.
[48] Mougi, A., Kondoh, M. (2016): Food-web complexity, meta-community complexity and community stability. – Scientific Reports 6: 24478. doi: 10.1038/srep24478.
[49] Neutel, A. M., Heesterbeek, J. A., De Ruiter, P. C. (2002): Stability in real food webs: weak links in long loops. – Science 296: 1120-1123.
[50] Persson, L. (1999): Trophic cascades: abiding heterogeneity and the trophic level concept at the end of the road. – Oikos 85: 385-397.
[51] Pimm, S. L. (1982): Food webs. – Chapman and hall, New York.
[52] Pinnegar, J. K., Blanchard, J. L., Mackinson, S., Scott, R. D., Duplisea, D. E. (2005): Aggregation and removal of weak-links in food-web models: system stability and recovery from disturbance. – Ecological Modelling 184: 229-248.
[53] Polis, G. A. (1988): Exploitation competition and the evolution of interference, cannibalism, and intraguild predation in age/size-structured populations. – In: Size-structured populations. Springer Berlin, Heidelberg.
[54] Polis, G. A. (1991): Complex trophic interactions in deserts: an empirical critique of food-web theory. – American Naturalist 138: 123-155.
[55] Polis, G. A., Strong, D. R. (1996): Food web complexity and community dynamics. – American Naturalist 147: 813-846.
[56] Polis, G. A. (1999): Why are parts of the world green? Multiple factors control productivity and the distribution of biomass. – Oïkos 86: 3-15.
[57] Power, E. M. (1992): Top-down and bottom-up forces in food webs: do plants have primacy. – Ecology 73: 733-746.
[58] Riede, J. O., Rall, B. C., Banasek-Richter, C., Navarrete, S. A., Wieters, E. A., Emmerson, M. C., Jacob, U., Brose, U. (2010): Scaling of food-web properties with diversity and complexity across ecosystems. – Advances in Ecological Research 42: 139-170.
[59] Romanuk, T. N., Zhou, Y., Valdovinos, F. S., Martinez, N. D. (2017): Robustness trade-offs in model food webs: invasion probability decreases while invasion consequences increase with connectance. – Advances in Ecological Research 56: 263-291.
[60] Rooney, N., McCann, K. S. (2012): Integrating food web diversity, structure and stability. – Trends in Ecology & Evolution 27: 40-46.
[61] Rossi, L., di Lascio, A., Carlino, P., Calizza, E., Costantini, M. L. (2015): Predator and detritivore niche width helps to explain biocomplexity of experimental detritus-based food webs in four aquatic and terrestrial ecosystems. – Ecological Complexity 23: 14-24.
[62] Schmid-Araya, J. M., Hildrew, A. G., Robertson, A., Schmid, P. E., Winterbottom, J. (2002): The importance of meiofauna in food webs: evidence from an acid stream. – Ecology 83: 1271-1285.
[63] Shurin, J. B., Daniel, S., Gruner, D. S., Hillebrand, H. (2006): All wet or dried up? Real differences between aquatic and terrestrial food webs. – Proceedings of the Royal Society of London 273: 1-9.
[64] Strong, D. R. (1988): Food web theory: a ladder for picking strawberries? – Ecology 69: 1647-1676.
[65] Strong, D. R. (1992): Are trophic cascades all wet? Differentiation and donor control in speciose ecosystems. – Ecology 73: 747-754.
[66] Sugihara, G. K., Schoenly, K., Trombla, A. (1989): Scale invariance in food web properties. – Science 245: 48-52.

http://www.aloki.hu ● ISSN 1589 1623 (Print) ● ISSN1785 0037 (Online)
DOI: http://dx.doi.org/10.15666/aeer/1902_817831
© 2021, ALÖKI Kft., Budapest, Hungary

[67] Thompson, R. M., Dunne, J. A., Woodward, G. (2012a): Freshwater food webs: towards a more fundamental understanding of biodiversity and community dynamics. – Freshwater Biology 57: 1329-1341.
[68] Thompson, S. A., Sydeman, W. J., Santora, J. A., Black, B. A., Suryan, R. M., Calambokidis, J., Peterson, W. T., Bograd, S. J. (2012b): Linking predators to seasonality of upwelling: Using food web indicators and analysis to infer trophic connections. – Progress in Oceanography 101: 106-120.
[69] Tylianakis, J. M., Laliberté, E., Nielsen, A., Bascompte, J. (2010): Conservation of species interaction networks. – Biological Conservation 143: 2270-2279.
[70] Van Altena, C., Hemerik, L., De Ruiter, P. C. (2016): Food web stability and weighted connectance: the complexity-stability debate revisited. – Theoretical Ecology 9: 49-58.
[71] Vermaat, J. E., Dunne, J. A., Gilbert, A. J. (2009): Major dimensions in food-web structure properties. – Ecology 90: 278-82.
[72] Williams, R. J., Martinez, N. D. (2000): Simple rules yield complex food webs. – Nature 404: 180-183.
[73] Worm, B., Duffy, J. E. (2003): Biodiversity, productivity and stability in real food webs. – Trends in Ecology & Evolution 18: 628-632.
[74] Zhao, L., Zhang, H., O'Gorman, E. J., Tian, W., Ma, A., Moore, J. C., Stuart, R., Borrett, S. R., Woodward, G. (2016): Weighting and indirect effects identify keystone species in food webs. – Ecological Letters 19: 1032-1040.

http://www.aloki.hu ● ISSN 1589 1623 (Print) ● ISSN1785 0037 (Online)
DOI: http://dx.doi.org/10.15666/aeer/1902_817831
© 2021, ALÖKI Kft., Budapest, Hungary

ARBUSCULAR MYCORRHIZAS IN THE ROOTS OF *AFZELIA AFRICANA*, *ENTADA AFRICANA*, AND *PTEROCARPUS ERINACEUS*

DJOTAN, A. K. G.[1,2,4*] – MATSUSHITA, N.[1] – VAARIO, L. M.[1,3] – YOROU, N. S.[4] – FUKUDA, K.[1]

[1]*University of Tokyo, Graduate School of Agricultural and Life Sciences (Laboratory of Forest Botany), 1-1-1, Yayoi, Bunkyo-ku, Tokyo 113-8657, Japan*
(phone: +81-807-805-0737)

[2]*University of Abomey-Calavi, Graduate School of Environment Planning (Laboratory of Forest Sciences), BP 1493 Abomey -Calavi, Benin*
(phone: +81-907-284-0398)

[3]*University of Helsinki, Department of Forest Sciences, PO Box 27, FI-00014 Helsinki, Finland*
(phone: +358-505-706-228)

[4]*University of Parakou, Research Unit "Tropical Mycology and Plants-Soil Fungi Interactions", BP 123 Parakou, Benin*
(phone: +229-9424-3866)

[*]*Corresponding author*
e-mail: geoffroydjotan@yahoo.fr; phone: +81-807-805-0737

(Received 25th May 2020; accepted 20th Aug 2020)

Abstract. *Afzelia africana*, *Entada africana*, and *Pterocarpus erinaceus* are economically important tropical tree species in Africa. In this study, we performed morphological and molecular analyses to examine the mycorrhizal status of these species in their natural habitat in Benin, West Africa. Fine roots were examined using trypan blue staining. Putative arbuscular mycorrhizal fungi (AMF) were identified by extracting root DNA and sequencing the large subunit region of ribosomal DNA. Operational taxonomic units (OTUs) were positioned on a consensus phylogenetic tree produced using maximum likelihood and neighbor-joining models. Morphological analyses revealed vesicles, arbuscules, and inter- and intracellular hyphae in roots of all three tree species. Molecular analyses revealed 39 AMF OTUs, among which 18 were from roots of *E. africana*, 15 from *P. erinaceus*, and 9 from *A. africana*. These OTUs belonged to *Glomus*, *Nanoglomus*, *Rhizoglomus*, *Sclerocystis*, *Septoglomus*, and *Scutellospora*; two unidentified species belonged to the family Glomeraceae. This is the first study to report AMF in roots of *A. africana*, *E. africana*, and *P. erinaceus* in Benin, and opens new avenues for future studies.
Keywords: *AMF, Benin, LSU, mycorrhiza, plant improvement, tropical tree species, Wari-Maro forest, West Africa*

Introduction

Mycorrhizas are essential symbiotic associations that allow nutrient transfer between fungi and the roots of living plants (Brundrett, 2004). Mycorrhizal symbioses provide multiple benefits for the functioning of natural ecosystems (Smith and Read, 2008), including nutrition enhancement (Clark and Zeto, 2000; Bücking and Kafle, 2015; Bunn et al., 2019), drought stress alleviation (Sharma et al., 2015; Dar et al., 2018), soil pathogen resistance (Talavera et al., 2001; Makoi and Ndakidemi, 2009), and growth of the host plant, as well as soil structure stabilization (Aggarwal et al., 2011). In tropical forests, most Dipterocarpaceous and Myrtaceaous trees form ectomycorrhizal symbioses, and many other angiosperm species form arbuscular mycorrhizas (Wang and Qiu, 2006;

http://www.aloki.hu ● ISSN 1589 1623 (Print) ● ISSN 1785 0037 (Online)
DOI: http://dx.doi.org/10.15666/aeer/1902_833848
© 2021, ALÖKI Kft., Budapest, Hungary

Smith and Read, 2008; Brundrett, 2009). However, information on the mycorrhizal status of valuable tree species is limited for West African tropical forests. Ectomycorrhiza in *Afzelia africana* Sm. have previously been reported (Redhead, 1968; Ba and Thoen, 1990; Yorou et al., 2008); however, the presence of arbuscular mycorrhizal fungi (AMF) in the roots of this species has not been confirmed, and there have been no reports of the mycorrhizal status of *Entada africana* Guill. & Perr. or *Pterocarpus erinaceus* Poir.

Afzelia africana is a vulnerable species (African Regional Workshop, 1998), also known as African mahogany. It is a deciduous tree belonging to the Detarioideae subfamily (Fabaceae), that is valued for the quality of its hard, reddish wood (Bayer and Waters-Bayer, 1999; Sinsin et al., 2004) and for the high nutritional value of its leaves as cattle feed (Sinsin, 1993). Seeds of this species germinate easily; however, the low recruitment rate of seedlings hinders natural regeneration (Padonou et al., 2013), particularly in its fire-prone natural habitats (Bationo et al., 2001). As a consequence of human pressures (Houehanou et al., 2019) and seedling recruitment issues, the population of *A. africana* is decreasing; only adult trees of this species are commonly observed in its natural habitats (Padonou et al., 2013). However, despite the frequent pruning of these adult trees, they continue to persist.

Entada africana, a species of least concern (Botanic Gardens Conservation International, International Union for Conservation of Nature SSC Global Tree Specialist Group, 2019) known as fake locust bean, is a deciduous tree species belonging to the subfamily Caesalpinioideae (Fabaceae); all of its organs are used as traditional medicines (Tibiri et al., 2007, 2010). The roots, stem bark, and leaves of this species contain many phytochemical classes of compounds including polyphenols, terpenes, and alkaloids (Sanogo et al., 1998; Ahua et al., 2007; Tibiri et al., 2007, 2010; Mbatchou et al., 2011), which can be further improved by mycorrhizal associations (Sbrana et al., 2014).

Pterocarpus erinaceus, known as African rosewood, is a deciduous tree species belonging to the subfamily Faboideae (Fabaceae), that has high wood quality (Traoré et al., 2010; Segla et al., 2017). This species is selectively logged in natural forests (Adjonou et al., 2010; Rabiou et al., 2015); the processed wood is exported to China, India, and other countries (Segla et al., 2017). The species is also valued as animal feed (Olafadehan, 2013). It is now an endangered species (Barstow, 2018) due to its low growth rate (Dumenu and Bandoh, 2016) and overexploitation (Dumenu, 2019).

Our long-term research goals are to test the potential of mycorrhizas for improving seedling recruitment in *A. africana*, the growth rate of *P. erinaceus*, and the quality and quantity of phytochemical production in *E. africana*. As a first step, in this study, we investigated the mycorrhizal status of these three tree species through anatomical observation of their roots and molecular detection of putative mycorrhizal fungi.

Materials and Methods

Study site and sampling

Sampling was conducted in the Wari-Maro Forest Reserve in Benin, West Africa, in July 2019. The reserve includes dense forests, woodlands, and savannahs in the Sudano-Guinean phytodistrict defined by Aubréville (1970) and White (1983) in the tropical climate zone (8.80–9.20°N, 1.95–2.45°E) overlapping the Tchaourou and Bassila districts (*Fig. 1*) (Salako et al., 2014; DIVA-GIS, 2018; Djotan et al., 2018). Samples were collected and transported to Japan under official regulations.

http://www.aloki.hu ● ISSN 1589 1623 (Print) ● ISSN 1785 0037 (Online)
DOI: http://dx.doi.org/10.15666/aeer/1902_833848
© 2021, ALÖKI Kft., Budapest, Hungary

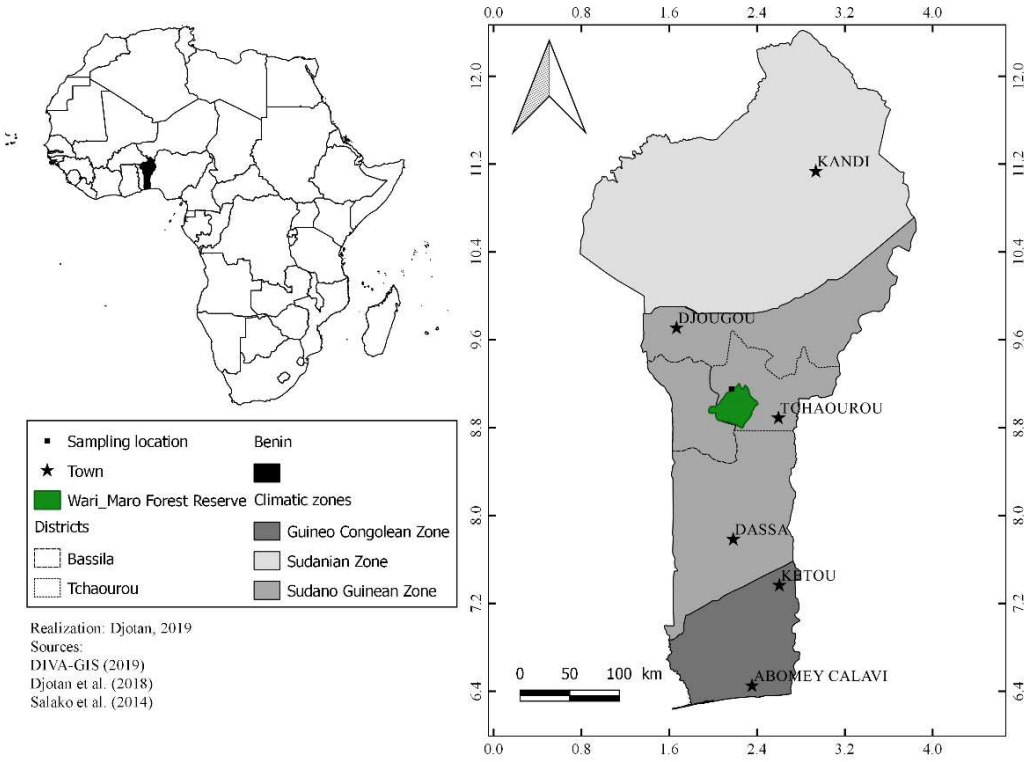


Figure 1. *Sampling locations. Green polygon indicates the Wari-Maro Forest Reserve, which overlaps two districts of central Benin, West Africa. Samples were collected around the black point within the polygon*

Five individual trees of each species were randomly sampled in the forest reserve. We collected 50 g of fine roots, including first- and second-order lateral roots, from each tree. We ensured that the collected roots belonged to the targeted tree by tracing the excavated roots to the base of the tree. Each root system sample was kept fresh within its rhizosphere and transported to the laboratory in a plastic test tube. Roots were washed three times with running tap water to remove soil particles attached to the root surface, and then preserved in 60% ethanol until further use.

Staining and anatomical observation

The root segments were cleaned and stained (Phillips and Hayman, 1970), and stained roots were preserved in lacto-glycerol until observation (Brundrett et al., 1984). For each tree, 10 root segments (length, 1 cm) were randomly cut, mounted with lacto-glycerol, and observed under a microscope (BX50, Olympus, Tokyo, Japan) fitted with a camera (DP71, Olympus) featuring standard bright-field optics. Based on the resulting microscopy images, we calculated the colonization frequencies of arbuscular mycorrhiza for each species as the number of tree samples of the species in which mycorrhizal features were observed (n = 5). Colonization intensity was calculated as the relative length of slide-mounted roots containing mycorrhizal features to the total length of observed roots (Giovannetti and Mosse, 1980; Fujimaki et al., 2001). We confirmed AMF colonization by observation of arbuscules, vesicles, intracellular hyphae, or intercellular hyphae with branches inside cells.

http://www.aloki.hu ● ISSN 1589 1623 (Print) ● ISSN 1785 0037 (Online)
DOI: http://dx.doi.org/10.15666/aeer/1902_833848
© 2021, ALÖKI Kft., Budapest, Hungary

DNA extraction, polymerase chain reaction (PCR) amplification, and sequencing

To identify the root fungal community composition, DNA was extracted from root segments (three randomly selected 1 cm root segments) of each sampled tree using the DNeasy Plant Mini Kit (Qiagen, Hilden, Germany) according to the manufacturer's instructions.

We performed 10-fold dilution of the extracted root DNA samples for use as a DNA template for PCR. We used the nested PCR method to amplify the large subunit (LSU) region of the fungal ribosomal DNA (rDNA) (Gollotte et al., 2004). We used the eukaryote-specific primer LR1 (5'-GCATATCAATAAGCGGAGGA-3') (Van Tuinen et al., 1998), and the fungus-specific primer FLR2 (5'-GTCGTTTAAAGCCATTACGTC-3') (Trouvelot et al., 1999) in the first round of PCR. The resulting PCR products were diluted 100-fold and used as a template for second-round PCR with the general AMF nested primers FLR3 (5'-TTGAAAGGGAAACGATTGAAGT-3') and FLR4 (5'-TACGTCAACATCCTTAACGAA-3') (Gollotte et al., 2004). Both rounds of PCR were performed in a 6 µL reaction mixture containing 1× KAPA2G Robust HotStart ReadyMix with dye (KAPA Biosystems, Wilmington, MA, USA), 0.5 µM of each primer, and 1 µL DNA template. The PCR protocol for each round consisted of an initial denaturation at 95°C for 2 min, 30 cycles of denaturation at 95°C for 90 s, annealing at 54°C for 10 s, extension at 72°C for 30 s, and a final extension at 72°C for 2 min. The second-round PCR products were cloned into the T-vector pMD20 (Takara Bio, Shiga, Japan) using the TaKaRa DNA Ligation Kit Mighty Mix and *Escherichia coli* HST08 Premium Competent Cells (TaKaRa Bio) according to the manufacturer's instructions. Each recombinant *E. coli* colony was randomly selected and boiled in 30 µL sterile water for 10 min at 98°C. DNA fragments were amplified from the supernatant by PCR using a primer specific to the vector. The PCR products were purified using the Illustra ExoProStar system (GE Healthcare, Chicago, IL, USA) according to the manufacturer's instructions, and sequenced by Macrogen Japan Co. (Tokyo, Japan). Eight colonies were sequenced from each root sample that showed positive results following amplification.

Data analysis and phylogeny

Nucleotide sequences received from Macrogen Japan were cleaned and submitted to the CD-HIT Suite online tool (Huang et al., 2010) for operational taxonomic Unit (OTU) clustering. OTU clusters were formed at 99% similarity. Non-AMF OTUs were removed from the data, and the most representative OTU cluster sequences were blasted using the MEGA-X web service menu (Kumar et al., 2018). Additional sequences of the LSU region of other glomeromycotan species were added to the data, and sequences were aligned using the Muscle alignment tool of MEGA-X. The sequences of OTUs generated in this study are available in the National Center for Biotechnology Information (NCBI) GenBank database (links are provided in the Data Availability section).

Evolutionary history was inferred using a maximum likelihood (ML)-based general time reversible model (Nei and Kumar, 2000), and the neighbor-joining (NJ) method (Saitou and Nei, 1987) with the MEGA-X software (Kumar et al., 2018). For the first method, initial trees for the heuristic search were obtained automatically by applying NJ and BioNJ algorithms to a matrix of pairwise distances estimated using the maximum composite likelihood approach, and then selecting the topology with the highest log likelihood value. A discrete gamma distribution was used to model evolutionary rate

http://www.aloki.hu ● ISSN 1589 1623 (Print) ● ISSN 1785 0037 (Online)
DOI: http://dx.doi.org/10.15666/aeer/1902_833848
© 2021, ALÖKI Kft., Budapest, Hungary

differences among sites (5 categories + G, parameter = 1.0112). In the second method, evolutionary distances were computed using the p distance method (Nei and Kumar, 2000) and expressed as numbers of base differences per site. These analyses involved 83 nucleotide sequences including 39 OTUs obtained in this study; all sequences are available in the GenBank database. We eliminated all positions with less than 95% site coverage using the partial deletion option. In total, 301 positions were included in the final dataset. The ML model tree with the highest log likelihood value (–5161.09) is shown. The tree was outgrouped with *Paraglomus occultum* FJ461883, drawn to scale, with branch lengths measured in terms of the number of substitutions per site. For each model, the percentage of trees in which the associated taxa clustered together in a bootstrap test (Felsenstein, 1985) with 1000 replicates is shown next to each branch (NJ/ML).

Statistical analysis

Differences in colonization intensity between species were tested using one-way analysis of variance (ANOVA), and means were compared using Tukey's honestly significant difference (HSD) test with the R v. 3.5.2 software (R Core Team, 2016).

Results

Mycorrhizas were present in the roots of all of the sampled trees, but at different intensities (*Fig. 2, Table 1*); intensity was higher in *E. africana* (84 ± 19%) than in *P. erinaceus* (48 ± 24%) and *A. africana* (48 ± 30%). There were no significant differences in the intensity of mycorrhizal colonization between *P. erinaceus* and *A. africana*.

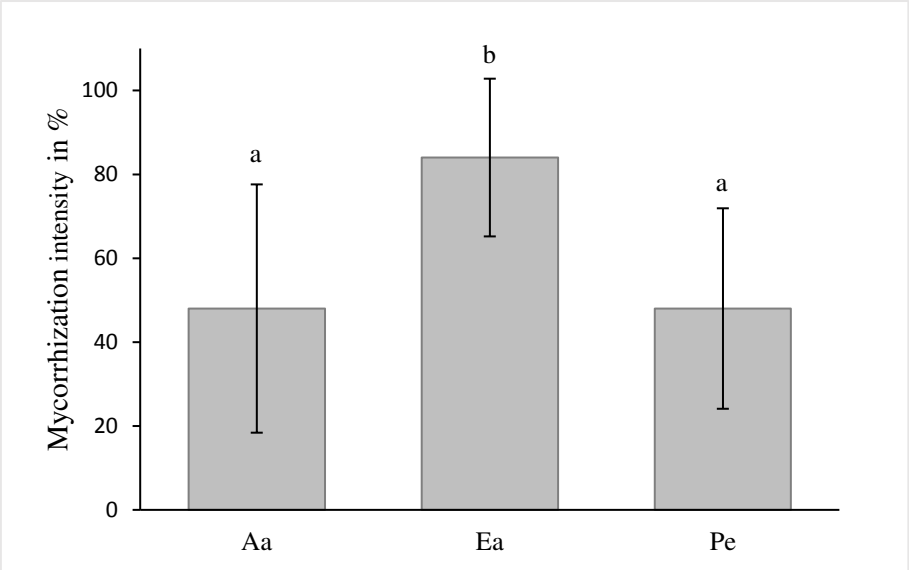


Figure 2. *Mycorrhizal colonization intensity (mean ± standard error) in roots of three tree species. Identical letters indicate no significant difference among the tested species (Tukey's honest significant difference [HSD] test, $p < 0.05$; $n = 5$). Aa,* Afzelia africana*; Ea,* Entada africana*; Pe,* Pterocarpus erinaceus

http://www.aloki.hu ● ISSN 1589 1623 (Print) ● ISSN 1785 0037 (Online)
DOI: http://dx.doi.org/10.15666/aeer/1902_833848
© 2021, ALÖKI Kft., Budapest, Hungary

Table 1. *One-way analysis of variance table for the intensity of mycorrhizal colonization (AMF%). The factor "Species" has 3 levels (*Afzelia africana, Entada africana, *and* Pterocarpus erinaceus*). AMF% is significantly different among species*

Factor	Df	Sum Sq	Mean Sq	F value	Pr(>F)
Species	2	4320	2160	5.5385	0.01977*
Residuals	12	4680	390		

Signif. codes: 0 '***' 0.001 '**' 0.01 '*' 0.05 '.' 0.1 ' ' 1

We found vesicles, arbuscules, and intra- and intercellular hyphae in stained roots of *A. africana*, *E. africana*, and *P. erinaceus* (*Fig. 3*). We detected 39 AMF OTUs, including 9 from *A. africana*, 18 from *E. africana*, and 15 from *P. erinaceus*. Three OTUs (1, 8, and 15) were present in two tree species, whereas the others were species-specific (*Table 2*).

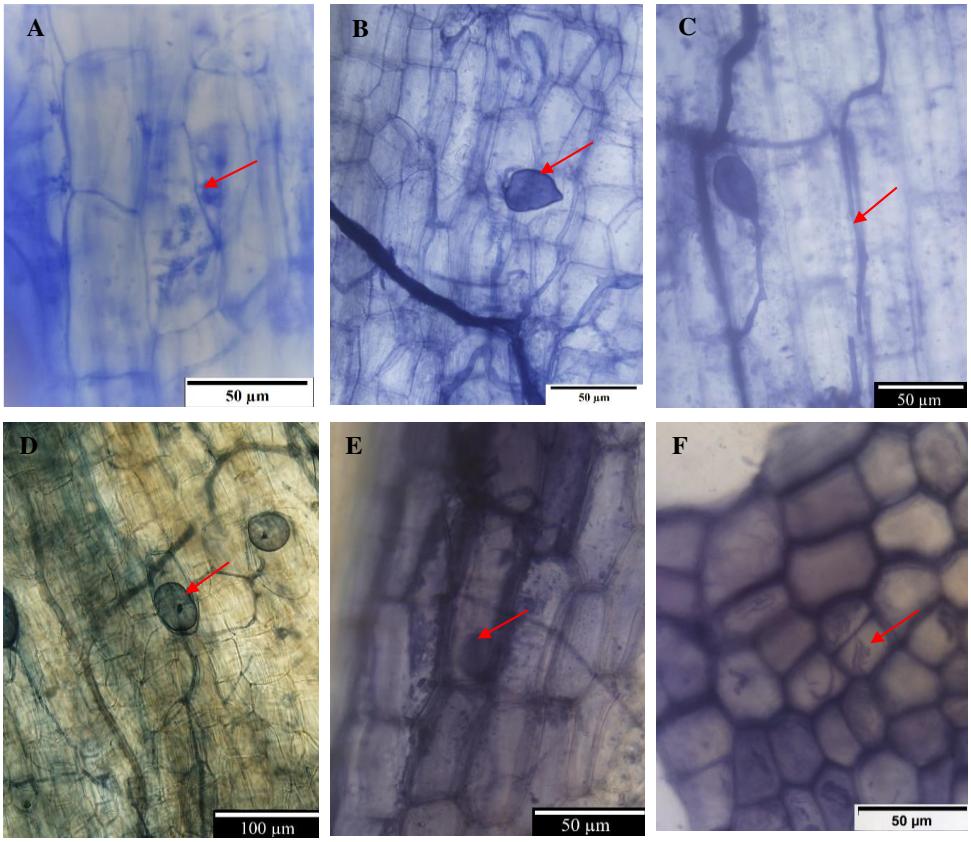


Figure 3. *Micrographs of trypan blue-stained roots taken with an Olympus DP71 camera fitted to an Olympus BX50 microscope. Arrows indicate finely branched arbuscules (A) and terminal vesicles (B) in roots of* A. africana*, intercellular hyphae (C) and terminal vesicles (D) in roots of* E. africana*, and non-terminal vesicles (E) and intercellular hyphae (F) in roots of* P. erinaceus

Using a threshold of percentage of identity equal to or greater than 95%, we identified OTUs 2, 14, 15, and 31 as *Scutellospora erythropa* (in *E. africana*), *Rhizoglomus dalpeae* (in *E. africana*), *Septoglomus deserticola* (in *A. africana*), and *Glomus trimurales* (in *E. africana*), respectively (*Table 2*).

http://www.aloki.hu ● ISSN 1589 1623 (Print) ● ISSN 1785 0037 (Online)
DOI: http://dx.doi.org/10.15666/aeer/1902_833848
© 2021, ALÖKI Kft., Budapest, Hungary

Table 2. *Glomeromycotan operational taxonomic units (OTUs) detected in this study, ordered by their presence and abundance in all three tree host species*

OTUs	OTUs Freq (%)				Access no.	Closest BLAST match				
	Aa	Ea	Pe	All species		Score	e value	Access no.	Identity (%)	Species
1	42	0	8	14	MN920713	652	0	GQ149222	98.13	uncultured Glomeromycotina
2	0	13	0	5	MN920719	551	1.00E-152	AM086173	98.71	*Scutellospora erythropa*
3	21	0	0	5	MT408134	654	0.00E+00	HG515449	98.91	uncultured Glomeromycotina
4	0	0	17	5	MT408150	616	3.38E-172	HE858414	96.28	uncultured *Glomus*
5	0	10	0	4	MN920715	580	1.00E-161	MH504073	94.71	uncultured *Sclerocystis*
6	0	10	0	4	MN920717	610	2.00E-170	MH504060	96.04	uncultured *Sclerocystis*
7	0	10	0	4	MT408139	628	4.32E-176	MH504023	97.07	uncultured *Sclerocystis*
8	0	3	8	4	MT408144	462	4.67E-126	JF798534	90.42	uncultured Glomeromycotina
9	0	0	13	4	MT408154	660	0.00E+00	HG515449	99.18	uncultured Glomeromycotina
10	0	0	8	3	MN920710	632	4.00E-177	HE858414	97.07	uncultured Glomerales
11	0	6	0	3	MN920712	612	5.00E-171	MH504023	96.28	uncultured *Sclerocystis*
12	0	6	0	3	MN920714	606	2.00E-169	KM879707	95.99	uncultured Glomeromycotina
13	0	6	0	3	MN920716	588	9.00E-164	HQ857172	95.17	uncultured fungus
14	0	6	0	3	MN920718	682	0	MN130954	99.73	*Rhizoglomus dalpeae*
15	5	0	4	3	MT408133	592	5.65E-165	JQ048925	95.21	*Septoglomus deserticola*
16	0	0	8	3	MT408149	588	7.27E-164	GQ149222	95.19	uncultured Glomeromycotina
17	0	0	4	1	MN920708	645	0	HG515449	98.90	uncultured Glomeromycota
18	0	0	4	1	MN920709	466	4.00E-127	JF798534	90.50	*Glomus* sp.
19	0	3	0	1	MN920711	588	9.00E-164	JQ048925	94.96	*Septoglomus deserticola*
20	5	0	0	1	MN920720	523	3.00E-144	GQ149222	92.25	uncultured Glomeromycotina
21	5	0	0	1	MT408132	641	5.57E-180	GQ149222	97.59	uncultured Glomeromycotina
22	5	0	0	1	MT408135	652	0.00E+00	HG515449	98.91	uncultured Glomeromycotina
23	5	0	0	1	MT408136	518	9.56E-143	GQ149222	91.98	uncultured Glomeromycotina
24	5	0	0	1	MT408137	551	9.42E-153	GQ149222	93.58	uncultured Glomeromycotina
25	5	0	0	1	MT408138	641	5.57E-180	GQ149222	97.59	uncultured Glomeromycotina

http://www.aloki.hu ● ISSN 1589 1623 (Print) ● ISSN 1785 0037 (Online)
DOI: http://dx.doi.org/10.15666/aeer/1902_833848
© 2021, ALÖKI Kft., Budapest, Hungary

OTUs	OTUs Freq (%)				Access no.	Closest BLAST match				
	Aa	Ea	Pe	All species		Score	e value	Access no.	Identity (%)	Species
26	0	3	0	1	MT408140	617	9.35E-173	MH504023	96.53	uncultured *Sclerocystis*
27	0	3	0	1	MT408141	580	1.23E-161	MH504073	94.71	uncultured *Sclerocystis*
28	0	3	0	1	MT408142	586	2.64E-163	MH504073	94.97	uncultured *Sclerocystis*
29	0	3	0	1	MT408143	575	5.71E-160	MH504073	94.44	uncultured *Sclerocystis*
30	0	3	0	1	MT408145	595	4.38E-166	MH504023	95.47	uncultured *Sclerocystis*
31	0	3	0	1	MT408146	636	2.56E-178	JN937265	97.58	*Glomus trimurales*
32	0	3	0	1	MT408147	566	3.45E-157	JQ048925	93.90	*Septoglomus deserticola*
33	0	3	0	1	MT408148	531	1.00E-146	HG515434	92.88	uncultured Glomeromycotina
34	0	0	4	1	MT408151	652	0.00E+00	HG515449	98.91	uncultured Glomeromycotina
35	0	0	4	1	MT408152	649	0.00E+00	HG515449	98.63	uncultured Glomeromycotina
36	0	0	4	1	MT408153	652	0.00E+00	HG515449	98.91	uncultured Glomeromycotina
37	0	0	4	1	MT408155	652	0.00E+00	HG515449	98.91	uncultured Glomeromycotina
38	0	0	4	1	MT408156	660	0.00E+00	HG515449	99.18	uncultured Glomeromycotina
39	0	0	4	1	MT408157	649	0	HG515449	98.63	uncultured Glomeromycotina
Total	100	100	100	100						

Aa, Afzelia africana; Ea, Entada africana; Pe, Pterocarpus erinaceus

http://www.aloki.hu ● ISSN 1589 1623 (Print) ● ISSN 1785 0037 (Online)
DOI: http://dx.doi.org/10.15666/aeer/1902_833848
© 2021, ALÖKI Kft., Budapest, Hungary

Phylogenetic groups based on consensus trees and 80% bootstrap replicates revealed 3 genera (*Nanoglomus, Rhizoglomus,* and *Septoglomus*) in roots of *A. africana*; 4 genera (*Rhizoglomus*, *Scutellospora*, *Nanoglomus*, and *Septoglomus*) in the roots of *E. africana*; and 4 genera (*Glomus*, *Rhizoglomus*, *Sclerocystis*, and *Nanoglomus*) in roots of *P. erinaceus* (*Fig. 4*). Overall, phylogenetic inference classified 39 OTUs among which 2 (OTUs 8, and 18) were unidentified at the genus level, in the Glomeraceae, and only one OTU, which was identified as *Scutellospora erythropa*, in the Gigasporaceae.

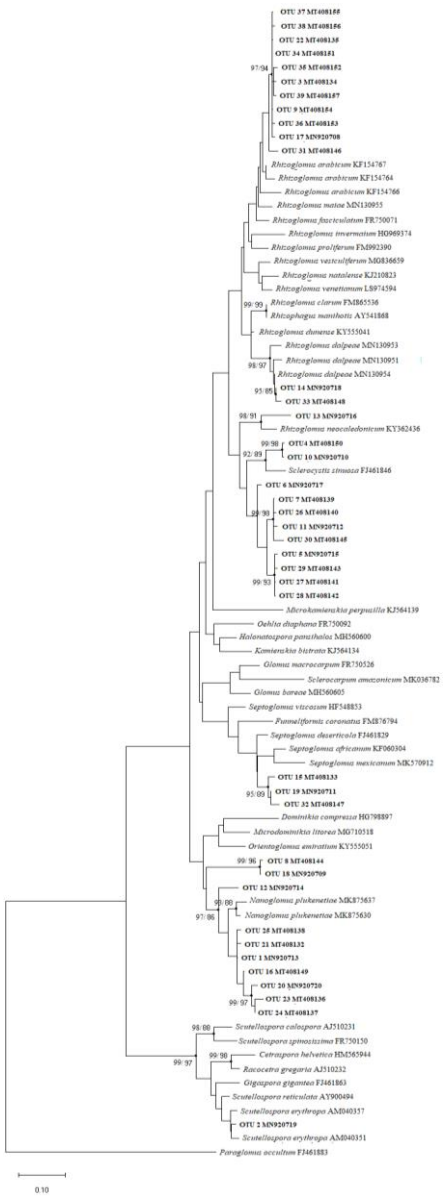


Figure 4. *Maximum likelihood (ML) phylogenetic tree obtained following analyses of large subunit (LSU) sequence data from arbuscular mycorrhizal fungi (AMF) in roots of A. africana, E. africana, and P. erinaceus sampled in Benin. The ML tree was constructed using a general time-reversible model assuming a discrete gamma distribution.* Paraglomus occultum *FJ461883 was used as an outgroup. Neighbor-joining (NJ) and ML bootstrap values ≥ 80% (NJ/ML) are provided at nodes marked with black dots. Operational taxonomic units (OTUs) generated in this study are indicated as OTU#; the scientific names of downloaded OTUs are indicated, followed by their accession numbers*

http://www.aloki.hu ● ISSN 1589 1623 (Print) ● ISSN 1785 0037 (Online)
DOI: http://dx.doi.org/10.15666/aeer/1902_833848
© 2021, ALÖKI Kft., Budapest, Hungary

Discussion

To the best of our knowledge, this study is the first to report microscopic and molecular evidence of arbuscular mycorrhiza in roots of *A. africana*, *E. africana*, and *P. erinaceus* in their natural habitats. Structurally, *E. africana* showed the highest intensity of mycorrhizal colonization. Our basic local alignment search and phylogeny analyses revealed *Nanoglomus* spp., *Rhizoglomus* spp., and *Septoglomus* sp. as putative AMF in the roots of *A. africana*. *Rhizoglomus* spp., *Scutellospora sp*., *Nanoglomus* spp., *Septoglomus* spp., and one genus-unidentified Glomeraceaous species (OTU 8) were putative AMF in the roots of *E. africana*, whereas those found in the roots of *P. erinaceus* were *Glomus* sp., *Rhizoglomus* spp., *Sclerocystis* spp., *Nanoglomus* sp., and one genus-unidentified Glomeraceaous species (OTU 18).

A critical review (Brundrett, 2009) emphasized past misdiagnosis related to the types of mycorrhizal features used during identification of mycorrhiza. McGonigle et al. (1990) recommended caution in the use of hyphae and vesicles, because unlike arbuscules, these features can appear sporadically in some non-mycorrhizal species. In the present study, we relied not only on the observation of morphological characteristics such as arbuscules, vesicles, and intra- and intercellular hyphae in stained roots, but also on DNA analyses. We also referred to illustrations of morphological features (Yuan et al., 2011; Priyadharsini et al., 2012; Claassens et al., 2018) to confirm features observed in our micrographs.

Some LSU sequences generated in the current study matched uncultured arbuscular mycorrhizal (AM) species according to the Basic Local Alignment Search Tool (BLAST), indicating a lack of molecular and mycological data on the tropical AMF community. This lack of data may also explain the positions of two OTUs on the phylogenetic tree, which corresponded to Glomeraceaous species but were not identified to the genus level.

Most OTUs (38 of 39) belonged to Glomeraceae, whereas only one belonged to Gigasporaceae. This result is consistent with a previous review of AMF species in tropical forests, which described Glomeraceae (78 of 228 species) as the most dominant family and Gigasporaceae (6 of 228 species) as one of the least represented families (Marinho et al., 2018). *Rhizoglomus dalpeae*, recently described by Błaszkowski et al. (2019) in Benin as a new species, was identified from roots of *E. africana*. The host tree in our study was collected from an inselberg within the Wari Maro forest reserve. The habitat within this reserve is a harsh environment, similar to the location where the fungus described by Błaszkowski et al. (2019) was collected.

Thoen and Ba (1989) reported that *A. africana* is ectomycorrhizal but is not associated with any endomycorrhiza. The same authors evaluated *A. africana* seed germination and seedling infection, and found that its seedlings exhibit early ectomycorrhizal infection. Yorou et al. (2008) also described the formation of ectomycorrhiza between *A. africana* and *Tomentella* species; however, they did not discuss its arbuscular mycorrhizal status. In the present study, we applied morphological and molecular methods to confirm that *A. africana* roots contained AMF, and therefore hypothesize that this species may be dual-mycorrhizal. In our study, all sampled *A. africana* individuals were adult trees, implying that arbuscular mycorrhiza are formed in adult trees of this species. In addition, Thoen and Ba (1989) conducted their research in Senegal, whereas our study was conducted in Benin. Dual mycorrhizae have been reported in West Africa for *Afzelia pachyloba* Harms, *Gilbertiodendron dewevrei* (De Wild.) J. Leonard, *Uapaca guineensis* Müll. Arg., and *Uapaca staudtii* Pax (Newbery et al., 1988; Thoen and Ba, 1989).

http://www.aloki.hu ● ISSN 1589 1623 (Print) ● ISSN 1785 0037 (Online)
DOI: http://dx.doi.org/10.15666/aeer/1902_833848
© 2021, ALÖKI Kft., Budapest, Hungary

Therefore, we agree with the claim of Thoen and Ba (1989) that roots of adult individual trees should also be examined to avoid erroneous conclusions, because dual mycorrhizal colonization may be more common than previously thought. The high resistance to harsh environmental conditions shown by *A. africana* may be explained by such dual mycorrhizal colonization. We could not identify the *Nanoglomus* fungus found in roots of *A. africana* to the species level; however, its arbuscules and terminal vesicles were comparable to those reported by Corazon-Guivin et al. (2019) describing *Nanoglomus plukenetiae* as new fungal species.

AMF colonization intensity and the number of OTUs were higher in *E. africana* roots than in those of *A. africana* and *P. erinaceus*. The high mycorrhizal dependency of this species may be explained by its ecology. All sampled *E. africana* individuals were growing on shallow and rocky soils of an inselberg, where the absorption of soil resources may be difficult without fungal associations. *R. dalpeae* was previously found to originate from an inselberg with severe environmental conditions in Benin (Błaszkowski et al., 2019), an environment like the one of our research site. The association between *E. africana* and *R. dalpeae* as a mycorrhizal fungal partner could explain the adaptation strategies of the plant to such a harsh environment. A previous study (Tamilarasi et al., 2008) suggested that rhizosphere microorganisms influence the antibacterial properties of medicinal plants; the effects of AMF colonization on medicinal properties should be examined in *E. africana*, which is a medicinal tree species that contains many types of phytochemical compounds (Sanogo et al., 1998; Ahua et al., 2007; Tibiri et al., 2007, 2010; Mbatchou et al., 2011).

Because *P. erinaceus* is a slow-growing species (Dumenu and Bandoh, 2016), it is not used in plantations, and its overexploitation in natural forests is causing a gradual decline in its population (Barstow, 2018). In 2016, to prevent its extinction from natural habitats, as has occurred in other African countries, the Government of Benin banned the logging and export of *P. erinaceus* to China, India, and other countries. Previous studies have reported mycorrhizae in *P. angolensis* DC. (Hengari et al., 2004), *P. soyauxii* Taub. (Onguene et al., 2011), *P. marsupium* Roxb. (Verma et al., 2016), and *P. officinalis* (Saint-Etienne et al., 2006; Fougnies et al., 2007) but not in *P. erinaceus*. The current study reports the first evidence that *P. erinaceus* can form arbuscular mycorrhizae, which may be exploited to improve *P. erinaceus* growth in West Africa.

Conclusion

This study was the first to examine AMF in the roots of three valuable tropical forest tree species in their natural habitats. We confirmed that *A. africana*, *E. africana*, and *P. erinaceus* are all AMF host trees species. *E. africana* showed a relatively high dependence on AMF. At a genus level, 3 genera were identified in *A. africana*, and 4 in *E. africana* and *P. erinaceus*. At a species level, *Glomus trimurales*, *Scutellospora erythropa*, and *Rhizoglomus dalpeae* were identified from the roots of *E. africana*, and *Septoglomus deserticola* from the roots of *A. africana*. Our findings represent a theoretical basis for future applications of mycorrhizal technologies to improve the recruitment and growth of these three tree species following germination of seeds in a controlled environment. Future researches should examine the contribution of AMF to the resistance of *A. africana* in harsh environmental conditions, the effects of AMF colonization on medicinal properties in *E. africana*, and the potential growth-promoting activities of AMF in *P. erinaceus*.

http://www.aloki.hu ● ISSN 1589 1623 (Print) ● ISSN 1785 0037 (Online)
DOI: http://dx.doi.org/10.15666/aeer/1902_833848
© 2021, ALÖKI Kft., Budapest, Hungary

Acknowledgements. We thank M. AGOKOLI and forest officers AKINDELE and YEVIDE for their support during our data collection efforts in Benin.

Author contributions. The first author conducted this work under the supervision of the co-authors.

Competing interests. The authors declare that they have no competing interests.

Data availability. The complete sequences generated in this study are available in the GenBank database at the following websites: https://submit.ncbi.nlm.nih.gov/subs/?search=SUB6744268 and https://submit.ncbi.nlm.nih.gov/subs/?search=SUB7335363.

REFERENCES

[1] Adjonou, K., Ali, N., Kokutse, A. D., Novigno, S. K. (2010): Etude de la dynamique des peuplements naturels de Pterocarpus erinaceus Poir. (Fabaceae) surexploités au Togo. – Bois et Forêts Des Tropiques, CIRAD (Centre de Cooperation Internationale en Recherche Agronomique Pour le Developpement) 306(4): 45-55.

[2] African Regional Workshop (1998): *Afzelia africana*. – Conservation & sustainable management of trees Zinbabwe July 1996, The IUCN Red List of Threatened Species 1998: e.T33032A9751552, available at: https://doi.org/https://dx.doi.org/10.2305/IUCN.UK.1998.RLTS.T33032A9751552.en.

[3] Aggarwal, A., Kadian, N., Tanwar, A., Yadav, A., Gupta, K. K. (2011): Role of arbuscular mycorrhizal fungi (AMF) in global sustainable development. – Journal of Applied and Natural Science 3(2): 340-351.

[4] Ahua, K. M., Ioset, J. R., Ioset, K. N., Diallo, D., Mauël, J., Hostettmann, K. (2007): Antileishmanial activities associated with plants used in the Malian traditional medicine. – Journal of Ethnopharmacology 110(1): 99-104.

[5] Aubréville, A. (1970): Flore du Cameroon: Légumineuses Ceasalpinoidées. – Muséum national d'histoire naturelle Laboratoire de phanérogamie, Paris.

[6] Ba, A. M., Thoen, D. (1990): First syntheses of ectomycorrhizas between *Afzelia africana* Sm. (Caesalpinioideae) and native fungi from West Africa. – New Phytologist 114(1): 99-103.

[7] Barstow, M. (2018): *Pterocarpus erinaceus*. – The IUCN Red List of Threatened Species 2018: e.T62027797A62027800.

[8] Bationo, B. A., Ouedraogo, S. J., Guinko, S. (2001): Longévité des graines et contraintes à la survie des plantules d' *Afzelia africana* Sm. dans une savane boisée du Burkina Faso. – Annals of Forest Science 58(1): 69-75.

[9] Bayer, W., Waters-Bayer, A. (1999): La Gestion Des Fourrages. – CTA, Wageningen, The Netherlands.

[10] Błaszkowski, J., Niezgoda, P., Piątek, M., Magurno, F., Malicka, M., Zubek, S., Mleczko, P., Yorou, N. S., Jobim, K., Vista, X. M., Lima, J. L. R., Goto, B. T. (2019): *Rhizoglomus dalpeae*, *R. maize*, and *R. silesianum*, new species. – Mycologia 111(6): 965-980.

[11] Botanic Gardens Conservation International and International Union for Conservation of Nature SSC Global Tree Specialist Group. (2019): *Entada africana*. – The IUCN Red List of Threatened Species 2019: e.T144292247A14902860.

[12] Brundrett, M. (2004): Diversity and classification of mycorrhizal associations. – Biological Reviews 79 (3): 473-495.

[13] Brundrett, M. C. (2009): Mycorrhizal associations and other means of nutrition of vascular plants: understanding the global diversity of host plants by resolving conflicting information and developing reliable means of diagnosis. – Plant and Soil 320: 37-77.

[14] Brundrett, M. C., Piché, Y., Peterson, R. L. (1984): A new method for observing the morphology of vesicular–arbuscular mycorrhizae. – Canadian Journal of Botany 62(10): 2128-2134.

http://www.aloki.hu ● ISSN 1589 1623 (Print) ● ISSN 1785 0037 (Online)
DOI: http://dx.doi.org/10.15666/aeer/1902_833848
© 2021, ALÖKI Kft., Budapest, Hungary

[15] Bücking, H., Kafle, A. (2015): Role of arbuscular mycorrhizal fungi in the nitrogen uptake of plants: current knowledge and research gaps. – Agronomy 5(4): 587-612.
[16] Bunn, R. A., Simpson, D. T., Bullington, L. S., Lekberg, Y., Janos, D. P. (2019): Revisiting the 'direct mineral cycling' hypothesis: arbuscular mycorrhizal fungi colonize leaf litter, but why? – ISME Journal 13(8): 1891-1898.
[17] Claassens, A., Nock, C. J., Rose, M. T., van Zwieten, L., Rose, T. J. (2018): Colonisation dynamics of arbuscular mycorrhizal fungi and dark septate endophytes in the sugarcane crop cycle. – Rhizosphere 7: 18-26.
[18] Clark, R. B., Zeto, S. K. (2000): Mineral acquisition by arbuscular mycorrhizal plants. – Journal of Plant Nutrition 23(7): 867-902.
[19] Corazon-Guivin, M. A., Cerna-Mendoza, A., Guerrero-Abad, J. C., Vallejos-Tapullima, A., Carballar-Hernández, S., da Silva, G. A., Oehl, F. (2019): *Nanoglomus plukenetiae*, a new fungus from Peru, and a key to small-spored Glomeraceae species, including three new genera in the '*Dominikia* complex/clades'. – Mycological Progress 18(12): 1395-1409.
[20] Dar, Z. M., Masood, A., Asif, M., Malik, M. A. (2018): Review on arbuscular mycorrhizal fungi: an approach to overcome drought adversities in plants. – International Journal of Current Microbiology and Applied Sciences 7(3): 1040-1049.
[21] DIVA-GIS. (2018): Free geographic (GIS) data for any country in the world. Administrative areas data for Benin. – Available at: www.diva-gis.org/datadown (accessed 13 March 2018).
[22] Djotan, A. K. G., Aoudji, K. N. A., Codjia, A. F. S., Gbètoho, A. J., Koura, K., Ganglo, J. C. (2018): How far can climate changes help to conserve and restore *Garcinia kola* Heckel, an extinct species in the wild in Benin (West Africa). – International Journal of Biodiversity and Conservation 10(5): 203-213.
[23] Dumenu, W. K. (2019): Assessing the impact of felling/export ban and CITES designation on exploitation of African rosewood (*Pterocarpus erinaceus*). – Biological Conservation 236: 124-133.
[24] Dumenu, W. K., Bandoh, W. N. (2016): Exploitation of African rosewood (*Pterocarpus erinaceus*) in Ghana: a situation analysis. – Ghana Journal of Forestry 32: 1-15.
[25] Felsenstein, J. (1985): Confidence limits on phylogenies: an approach using the bootstrap. – Evolution 39(4): 783-791.
[26] Fougnies, L., Renciot, S., Muller, F., Plenchette, C., Prin, Y., de Faria, S. M., Bouvet, J. M., Sylla, S. Nd., Dreyfus, B., Ba, A. M. (2007): Arbuscular mycorrhizal colonization and nodulation improve flooding tolerance in *Pterocarpus officinalis* Jacq. seedlings. – Mycorrhiza 17(3): 159-166.
[27] Fujimaki, R., Tateishi, T., Kohzu, A., Saito, M., Tokuchi, N. (2001): Characterization of arbuscular mycorrhizal colonization of 4 plant species in a Japanese red cedar plantation. – Soil Microorganisms 55(2): 121-128.
[28] Giovannetti, M., Mosse, B. (1980): An evaluation of techniques for measuring vesicular arbuscular mycorrhizal infection in roots. – New Phytologist 84(3): 489-500.
[29] Gollotte, A., van Tuinen, D., Atkinson, D. (2004): Diversity of arbuscular mycorrhizal fungi colonising roots of the grass species *Agrostis capillaris* and *Lolium perenne* in a field experiment. – Mycorrhiza 14(2): 111-117.
[30] Hengar, S. N., Valentine, A. J., Theron, J. M. (2004): The effect of the colonisation extent of arbuscular mycorrhizal fungi on the growth of pot grown *Pterocarpus angolensis* seedlings. – Southern African Forestry Journal 202(1): 13-20.
[31] Houehanou, T. D., Prinz, K., Hellwig, F., Assogbadjo, A. E., Gebauer, J., Glele Kakaï, R. L., Sinsin, B. (2019): Morphological trait variation and relationships of *Afzelia africana* Sm. caused by climatic conditions and anthropogenic disturbance in Benin (West Africa). – Genetic Resources and Crop Evolution 66(5): 1091-1105.
[32] Huang, Y., Niu, B., Gao, Y., Fu, L., Li, W. (2010): CD-HIT Suite: a web server for clustering and comparing biological sequences. – Bioinformatics 26(5): 680-682.

http://www.aloki.hu ● ISSN 1589 1623 (Print) ● ISSN 1785 0037 (Online)
DOI: http://dx.doi.org/10.15666/aeer/1902_833848
© 2021, ALÖKI Kft., Budapest, Hungary

[33] Kumar, S., Stecher, G., Li, M., Knyaz, C., Tamura, K. (2018): MEGA X: Molecular Evolutionary Genetics Analysis across computing platforms. – Molecular Biology and Evolution 35(6): 1547-1549.
[34] Makoi, J., Ndakidemi, P. (2009): The agronomic potential of vesicular-arbuscular mycorrhiza (VAM) in cereals-legume mixtures in Africa. – African Journal of Microbiology Research 3(11): 664-675.
[35] Marinho, F., da Silva, I. R., Oehl, F., Maia, L. C. (2018): Checklist of arbuscular mycorrhizal fungi in tropical forests. – Sydowia 70: 107-127.
[36] Mbatchou, V. C., Ayebila, A. J., Apea, O. B. (2011): Antibacterial activity of phytochemicals from *Acacia nilotica*, *Entada africana*, and *Mimosa pigra* L. on Salmonella typhi. – Journal of Animal & Plant Sciences 10(1): 1248-1258.
[37] McGonigle, T. P., Miller, M. H., Evans, D. G., Fairchild, G. L., Swan, J. A. (1990): A new method which gives an objective measure of colonization of roots by vesicular-arbuscular mycorrhizal fungi. – New Phytologist 115(3): 495-501.
[38] Nei, M., Kumar, S. (2000): Molecular evolution and phylogenetics. – Oxford University Press, New York.
[39] Newbery, D. M., Alexander, I. J., Thomas, D. W., Gartlan, J. S. (1988): Ectomycorrhizal rain-forest legumes and soil phosphorus in Korup National Park, Cameroon. – New Phytologist 109(4): 433-450.
[40] Olafadehan, O. A. (2013): Feeding value of *Pterocarpus erinaceus* for growing goats. – Animal Feed Science and Technology 185(1-2): 1-8.
[41] Onguene, N. A., Ngonkeu, L. E. M., Kuyper, T. W. (2011): Growth response of *Pterocarpus soyauxii* and *Lophira alata* seedlings to host soil mycorrhizal inocula in relation to land use types. – African Journal of Microbiology Research 5(17): 2391-2398.
[42] Padonou, E. A., Kassa, B., Assogbadjo, A. E., Chakeredza, S., Babatoundé, B., Glèlè Kakaï, R. (2013): Differences in germination capacity and seedling growth between different seed morphotypes of *Afzelia africana* Sm. in Benin (West Africa). – Journal of Horticultural Science and Biotechnology 88(6): 679-684.
[43] Phillips, J. M., Hayman, D. S. (1970): Improved procedures for clearing roots and staining parasitic and vesicular-arbuscular mycorrhizal fungi for rapid assessment of infection. – Transactions of the British Mycological Society 55(1): 158-161.
[44] Priyadharsini, P., Muthukumar, T., Pandey, R. R. (2012): Arbuscular mycorrhizal and dark septate fungal associations in shallot (*Allium cepa* L. var. *aggregatum*) under conventional agriculture. – Acta Botanica Croatica 71(1): 159-175.
[45] R Core Team. (2016): R: a language and environment for statistical computing. – R Foundation for Statistical Computing, Vienna, available at: www. R-proje ct. org.
[46] Rabiou, H., Bationo, B., Segla, K., Diouf, A., Adjonou, K., Kokutse, A., Radji, R., Mahamane, A., Kokou, K., Saadou, M. (2015): Estimation de volume commercial du bois de *Pterocarpus erinaceus* Poir. (Fabaceae) dans les zones sahélo-soudaniennes et Soudaniennes du Niger et du Burkina Faso (Afrique de l'ouest). – Journal of Applied Biosciences 87: 8131-8143.
[47] Redhead, J. F. (1968): Mycorrhizal associations in some Nigerian forest trees. – Transactions of the British Mycological Society 51(3-4): 377-387.
[48] Saint-Etienne, L., Paul, S., Imbert, D., Dulormne, M., Muller, F., Toribio, A., Plenchette, C., Ba, A. M. (2006): Arbuscular mycorrhizal soil infectivity in a stand of the wetland tree *Pterocarpus officinalis* along a salinity gradient. – Forest Ecology and Management 232(1-3): 86-89.
[49] Saitou, N., Nei, M. (1987): The neighbor-joining method: a new method for reconstructing phylogenetic trees. – Molecular Biology and Evolution 4(4): 406-425.
[50] Salako, V. K., Fandohan, B., Kassa, B., Assogbadjo, A. E., Idohou, A. F. R., Gbedomon, R. C., Chakeredza, S., Dulloo, M. E., Kakai, R. G. (2014): Home gardens: an assessment of their biodiversity and potential contribution to conservation of threatened species and crop wild relatives in Benin. – Genetic Resources and Crop Evolution 61(2): 313-330.

http://www.aloki.hu ● ISSN 1589 1623 (Print) ● ISSN 1785 0037 (Online)
DOI: http://dx.doi.org/10.15666/aeer/1902_833848
© 2021, ALÖKI Kft., Budapest, Hungary

[51] Sanogo, R., Germanò, M. P., D'Angelo, V., Guglielmo, M., de Pasquale, R. (1998): Antihepatotoxic properties of *Entada africana* (Mimosaceae). – Phytotherapy Research 12(S1): 157-159.
[52] Sbrana, C., Avio, L., Giovannetti, M. (2014): Beneficial mycorrhizal symbionts affecting the production of health-promoting phytochemicals. – Electrophoresis 35(11): 1535-1546.
[53] Segla, K. N., Rabiou, H., Adjonou, K., Guibal, D., Bationo, A. B., Mahamane, A., Kokou, K., Langbour, P., Kokutse, A. D., Chaix, G. (2017): Useful near infrared spectroscopy model calibrations on solid wood samples of *Pterocarpus erinaceus* (Poir.) for physical, mechanical and colour properties. – Journal of Near Infrared Spectroscopy 25(4): 256-266.
[54] Sharma, N., Yadav, K., Cheema, J., Badda, N., Aggarwal, A. (2015): Arbuscular mycorrhizal symbiosis and water stress: a critical review. – Pertanika Journal of Tropical Agricultural Science 38(4): 427-453.
[55] Sinsin, A. B. (1993): Phytosociologie, Écologie, Valeur Pastorale, Production et Capacité de Charge des Pâturages Naturels Du Périmètre Nikki-Kalalé Au Nord-Bénin. – Université libre de Bruxelles.
[56] Sinsin, B., Matig, O. E., Assogbadjo, A. E., Gaoué, O. G., & Sinadouwirou, T. (2004). Dendrometric characteristics as indicators of pressure of *Afzelia africana* Sm. dynamic changes in trees found in different climatic zones of Benin. Biodiversity & Conservation, 13(8), 1555-1570.
[57] Smith, S., Read, D. (2008): Mycorrhizal symbiosis. – 3rd. ed. Academic Press. New York
[58] Talavera, M., Itou, K., Mizukubo, T. (2001): Reduction of nematode damage by root colonization with arbuscular mycorrhiza (*Glomus* spp.) in tomato-*Meloidogyne incognita* (Tylenchida: Meloidogynidae) and carrot-*Pratylenchus penetrans* (Tylenchida: Pratylenchidae) pathosystems. – Applied Entomology and Zoology 36(3): 387-392.
[59] Tamilarasi, S., Nanthakumar, K., Karthikeyan, K., Lakshmanaperumalsamy, P. (2008): Diversity of root associated microorganisms of selected medicinal plants and influence of rhizomicroorganisms on the antimicrobial property of *Coriandrum sativum*. – Journal of Environmental Biology 29(1): 127-134.
[60] Thoen, D., Ba, A. M. (1989): Ectomycorrhizas and putative ecto-mycorrhizal fungi of *Afzelia africana* Sm. and *Uapaca guineensis* Müll. Arg. in southern Senegal. – New Phytologist 113(4): 549-559.
[61] Tibiri, A., Banzouzi, J. T., Traore, A., Nacoulma, G. O., Guissou, I. P., Mbatchi, B. (2007): Toxicological assessment of methanolic stem bark and leaf extracts of *Entada africana* Guill. and Perr., Mimosaceae. – International Journal of Pharmacology 3(5): 393-399.
[62] Tibiri, A., Sawadogo, R. W., Ouedraogo, N., Banzouzi, J. T., Guissou, I. P., Nacoulma, G. O. (2010): Evaluation of antioxidant activity, total phenolic and flavonoid contents of *Entada africana* Guill. et Perr. (Mimosaceae) organ extracts. – Research Journal of Medical Sciences 4(2): 81-87.
[63] Traoré, B., Brancheriau, L., Perré, P., Stevanovic, T., Diouf, P. (2010): Acoustic quality of vène wood (*Pterocarpus erinaceus* Poir.) for xylophone instrument manufacture in Mali. – Annals of Forest Science 67: 815.
[64] Trouvelot, S., Van Tuinen, D., Hijri, M., Gianinazzi-Pearson, V. (1999): Visualization of ribosomal DNA loci in spore interphasic nuclei of glomalean fungi by fluorescence in situ hybridization. – Mycorrhiza 8(4): 203-206.
[65] Van Tuinen, D., Jacquot, E., Zhao, B., Gollotte, A., Gianinazzi-Pearson, V. (1998): Characterization of root colonization profiles by a microcosm community of arbuscular mycorrhizal fungi using 25S rDNA-targeted nested PCR. – Molecular Ecology 7(7): 879-887.
[66] Verma, R. K., Thakur, A. K., Verma, P., Mishra, Y. (2016): Arbuscular mycorrhization and growth performance of *Pterocarpus marsupium* seedling raised from different seed sources of Chhattisgarh, India. – Indian Journal of Tropical Biodiversity 24(2): 151-157.
[67] Wang, B., Qiu, Y. L. (2006): Phylogenetic distribution and evolution of mycorrhizas in land plants. – Mycorrhiza 16(5): 299-363.

http://www.aloki.hu ● ISSN 1589 1623 (Print) ● ISSN 1785 0037 (Online)
DOI: http://dx.doi.org/10.15666/aeer/1902_833848
© 2021, ALÖKI Kft., Budapest, Hungary

[68] White, F. (1983): The vegetation map of Africa south of the Sahara. – 2nd ed. UNESCO, Paris.
[69] Yorou, S. N., Agerer, R., Raidi, S. (2008): '*Afzeliaerhiza beninensis*' + *Afzelia africana* Smith. – Description of Ectomycorrhizae 11(12): 1-8.
[70] Yuan, Z. L., Chen, Y. C., Ma, X. J. (2011): Symbiotic fungi in roots of *Artemisia annua* with special reference to endophytic colonizers. – Plant Biosystems 145(2): 495-502.

http://www.aloki.hu ● ISSN 1589 1623 (Print) ● ISSN 1785 0037 (Online)
DOI: http://dx.doi.org/10.15666/aeer/1902_833848
© 2021, ALÖKI Kft., Budapest, Hungary

PHYTOPLANKTON COMPOSITION AND ECOLOGICAL TOLERANCE OF THE AUTOTROPHIC PICOPLANKTON IN ATANASOVSKO LAKE (BLACK SEA COASTAL LAGOON, BULGARIA)

BELKINOVA, D.[1,2] – TENEVA, I.[1*] – BASHEVA, D.[1] – NEYKOV, N.[3] – MOTEN, D.[1] – GECHEVA, G.[1] – APOSTOLOVA, E.[1] – NAIMOV, S.[1]

[1]*Plovdiv University "Paisii Hilendarski", 24 Tsar Assen Str., Plovdiv 4000, Bulgaria*

[2]*Institute of Biodiversity and Ecosystem Research, Bulgarian Academy of Sciences, 23 Acad. G. Bonchev Str., Sofia 1113, Bulgaria*

[3]*National Institute of Meteorology and Hydrology, Sofia, Bulgaria*

[*]*Corresponding author*
e-mail: teneva@uni-plovdiv.bg; phone: +359-32-261-514; fax: +359-32-261-566

(Received 31st Oct 2020; accepted 21st Dec 2020)

Abstract. Atanasovsko Lake is a coastal lagoon used for salt extraction for many years. Its salinity varies within a wide range (from 6.3 to > 72‰). Despite these extreme conditions, phytoplankton blooms are often observed. Therefore, our aim was to study the key abiotic drivers and ecological optimum of the picoplankton in a 5-year period (2013-2017). The taxonomic composition, long-term dynamics and abiotic drivers of the autotrophic picoplankton (APP) has been investigated in North Saltern of the coastal lagoon in Atanasovsko Lake. The APP species were identified by using a polyphasic approach based on molecular and phylogenetic analyses of 16S/18S rDNA in combination with cytomorphological and ecological characterization. *Picochlorum oklahomense* (Trebouxiophyceae, Chlorophyta) and marine *Synechococcus sp*. (Synechococcales, Cyanobacteria) were the dominant genotypes within the APP. The relative biovolume of the APP to the total phytoplankton biovolume was strongly variable (from 36 to 99%) as the salinity and temperature were found to be the main abiotic drivers of its dynamics. Salinity between 30-59‰ and mid-summer temperature above 24°C provide an ecological optimum for the APP development at a relative biovolume of 93%. This is the first record of *Picochlorum oklahomense*/*Synechococcus* sp. assemblage within the APP composition of a European coastal lagoon.
Keywords: *ecology, hypersaline lakes, Synechococcus, Picochlorum oklahomense, 16S/18S DNA*

Introduction

Over the last decade, a number of studies have focused on the autotrophic picoplankton (APP) in saline inland waters of Europe (Felföldi et al., 2009; Somogyi et al., 2011, 2014; Keresztes et al., 2012; Paranhos et al., 2017). Unusually high abundance of APP with extraordinarily high picoplankton productivity was registered in soda lakes in the Carpathian Basin (Felföldi et al., 2009). The APP abundance in hypersaline lakes is higher than those in freshwater and marine environments with similar trophic conditions, and the contribution of the APP to the total phytoplankton community can reach up to 90-100% (Somogyi et al., 2014). The selective advantage of pico-sized primary producers in turbid waters is related to the more effective utilization of the light and nutrients (Agustí, 1991; Reynolds, 2006; Felföldi et al., 2009) and reducing grazing pressure (Paranhos et al., 2017). These results confirmed the assumption of Krienitz et al. (2012) that APP has a key position as a highly productive

http://www.aloki.hu ● ISSN 1589 1623 (Print) ● ISSN 1785 0037 (Online)
DOI: http://dx.doi.org/10.15666/aeer/1902_849866
© 2021, ALÖKI Kft., Budapest, Hungary

primary producer in saline environments and therefore, more attention should be paid to its distribution.

Saline waters also include coastal lagoons and salterns. Coastal lagoons are shallow brackish or marine water bodies separated from the ocean by a barrier island, spit, reef, or sand bank (Barnes, 1980; Kennish and Paerl, 2010; Kennish, 2015). They are formed on shallow banks and are only 12% of the coastal shorelines worldwide (Kennish, 2015). Most of them are situated along African coast (17.9% from shoreline) and North America (17.6%), and only 5.3% are on European territory (Kennish, 2015). Lagoons are characterized with spatial and temporal natural variability, which is not typical for the other aquatic ecosystems (Barnes, 1980). This variability is represented as a strong ecological stress, which forms the community structure. Due to the rarity of these habitats and species that they sustain, coastal lagoons are of primary conservational importance.

Studies on the picophototrophic communities in coastal lagoons and salterns are scarce (Ayadi et al., 2004; Estrada et al., 2004; Elloumi et al., 2009; Schapira et al., 2010). The available results analyzed mainly the dynamics of APP abundance under the influence of abiotic and biotic drivers (Elloumi et al., 2009; Schapira et al., 2010). The reports about the taxonomic composition of APP are even rarer. By applying molecular-genetic methods, a new species *Picocystis salinarum* (Prasinophyceae) has been described from the San Francisco salterns, California, USA (Lewin et al., 2001). Annual domination of the green algae *Picochlorum sp*. and *Picocystis sp*. was recorded in a coastal lagoon in San Diego, California, USA (Wang et al., 2014).

The object of our study was Atanasovsko Lake, a coastal lagoon located on the Black Sea coast in Southeast Bulgaria. The major part of the lake was modified as salterns. Atanasovsko Lake includes a variety of habitats and it is located along the second largest migration route of birds from Europe to Africa, Via Pontica. Our aim was to study the key abiotic drivers and ecological optimum of the picoplankton towards abiotic drivers in a 5-year period.

This is the first study on the taxonomic composition and long-term dynamics of the abundance of APP in a European coastal lagoon.

Materials and methods

Site description

Atanasovsko Lake is a coastal lagoon separated from Black Sea via sand spit, about 1 km long (*Fig. 1A,B*). It is below the sea level (-1.5 m a.s.l.). The volume of the lake is 3.2 mil. m^3, the average depth is 0.3 m, and the surface is 10.9 km^2 (Gecheva et al., 2017).

The lake has been used for salt production since 1906 and was separated by dykes on small basins for salt extraction. The key factor for the lake is the mechanism of salt production and sea-freshwater exchange (Hubenov et al., 2015). Freshwater supply is via atmospheric deposition (rainfall) and river waters (Azmaka and Vetrenska rivers). The inflow of seawater is achieved via sluice from April and continues with varying intensity throughout the summer until the autumn. Due to the decrease in rainfall and the continuous evaporation of water from the crystallization basins, salinity increases almost twice from spring to autumn every year (Ivanov et al., 1964), reaching extreme values in some years – up to 169‰ (Botev, 1997).

http://www.aloki.hu ● ISSN 1589 1623 (Print) ● ISSN 1785 0037 (Online)
DOI: http://dx.doi.org/10.15666/aeer/1902_849866
© 2021, ALÖKI Kft., Budapest, Hungary

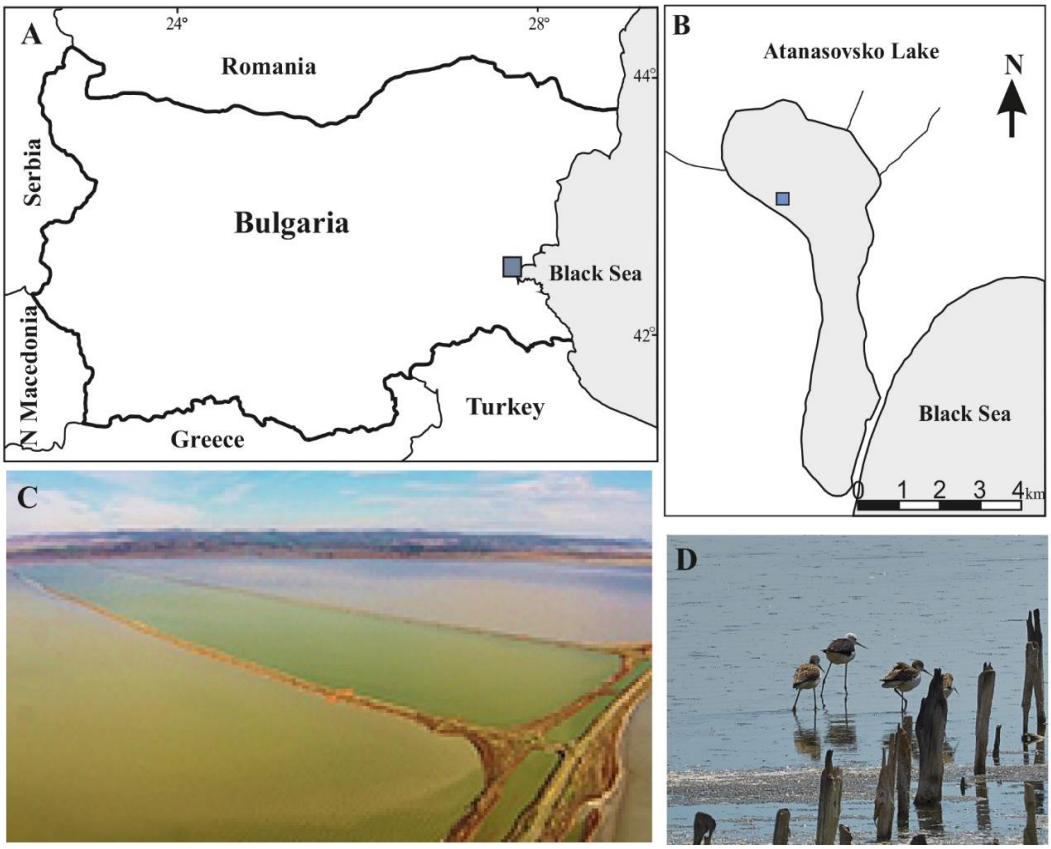


Figure 1. *Atanasovsko Lake.* ***A:*** *Map of Bulgaria (the square shows the location of Atanasovsko Lake);* ***B:*** *Map of Atanasovsko Lake (the square shows the location of the study pond North Saltern);* ***C:*** *Study pond North Saltern with an intensive bloom of APP;* ***D:*** *Habitat of APP, with a high abundance of waterfowl*

Our study was focused on a small basin in the North Saltern (N 42°34'16.4"; E 27°28'04.4") for the period 2013-2017 (*Fig. 1C*). The pond is characterized by variable salinity and intensive blooms of picoplankton. Atanasovsko Lake is one of the most significant wetlands for conregations of waterfowl along the Bulgarian Black Sea coast (*Fig. 1D*).

Sample techniques

Water samples for physico-chemical analyzes were taken five times per each year (2013, 2014, 2015, 2016 and 2017) during the months March, June, July, September and October in the pond North Saltern. The parameters pH, conductivity, temperature and dissolved oxygen/oxygen saturation were measured *in situ* with Multi 3410 SET B TetraCON 952-3 (WTW). Nutrients were analyzed by pHotoFlex STD (WTW) following adopted standards (N-NO_2: EN 26777; N-NO_3: ISO 7890-1; N-NH4: ISO 7150/1; P-PO_4: EN ISO 6878). During the study period (2013-2017) twenty-five water samples were collected for physico-chemical analyzes. Chlorophyll-*a* concentration was determined spectrophotometrically (M107 Visible Spectrophotometer, Spectronic Camspec Ltd., Leeds, UK) according to ISO 10260: 2002. North Saltern waters were classified as mixo- to hypersaline according to the Venice System (Anonymous, 1958).

http://www.aloki.hu ● ISSN 1589 1623 (Print) ● ISSN 1785 0037 (Online)
DOI: http://dx.doi.org/10.15666/aeer/1902_849866
© 2021, ALÖKI Kft., Budapest, Hungary

The phytoplankton sampling was performed three times per year (2013-2017) during the summer season from June to September. In 2015, phytoplankton samples were collected two times instead three times. Due to the shallow depth and lack of vertical salt gradient in the lake, samples were collected with a Meyer bottle from the sub-surface layer and fixed *in situ* with formaldehyde (4% final concentration). During the study period (2013-2017), 14 phytoplankton samples were analyzed.

Isolation and cultivation of the APP species

The APP species were isolated by streaking cells across agar plates (Andersen and Kawachi, 2005) from living natural samples in 2016 when were registered unusual highly-dense phytoplankton blooms. The strain PACC 8945 was isolated from a bloom sample in June 2016 (T=27°C; S=30.3‰) and cultured on liquid medium with seawater (Schlösser, 1982), modified by addition of Na_2CO_3 (pH=8.5). The strain PACC 8946 was isolated from a bloom sample in July 2016 (T=27.6°C; S=59‰) and cultured on liquid medium with artificial seawater (Eddy, 1956). Algal cultures were maintained in a laboratotory at room temperature (22°C±2°C) and a 15:9 hour light:dark cycle. Two unialgal strains (PACC 8945, PACC 8946) were deposited in Plovdiv Algal Culture Collection (PACC) of Plovdiv University in Bulgaria.

Extraction of DNA, PCR amplification and sequencing of the prokaryotic species (16S DNA)

Genomic DNA was extracted from the cultured cyanobacterial mass by the Proteinase-K extraction method. The concentration of the DNA and its purity was measured on a NanoDrop 2000 UV-Vis spectrophotometer (Thermo Fisher Scientific, Wilmington, DE, USA). The integrity of the extracted DNA was visualized on an agarose gel by ethidium bromide staining and UV transillumination (MiniBIS Pro gel documentation system, DNR Bio-Imaging Systems Ltd., Jerusalem, Israel). Isolated DNA was used to perform PCR amplification of 16S DNA. 16S DNA was amplified by using the primers 27F (5'-AGAGTTTGATCCTGGCTCAG-3') and 1492R (5'-CGGTTACCTTGTTACGACTT-3'). PCR reactions were conducted using PuReTaq™ Ready-To-Go™ PCR beads (GE Healthcare, Buckinghamshire, UK) where the final mixture contained 1.5 U of Taq DNA polymerase, 10 mM of Tris–HCl pH 9, 50 mM of KCl, 1.5 mM of $MgCl_2$, 200 µM of each dNTP, 5 pmol of each of the two primers, 100 ng of genomic DNA, and water to a final volume of 25 µl. Amplification was done in a TC-412 thermal cycler (Techne, Cambridge Ltd., UK) using the following program: initial denaturation for 5 minutes at 94°C, followed by 30 cycles of 60 seconds at 95°C, 60 seconds at 53°C, 2 minutes at 72°C, and final elongation step of 10 minutes at 72°C. All PCR products were analyzed by electrophoresis in a 1.5% agarose gel in Tris-acetate-EDTA (TAE) buffer with GeneRuler™ 100 bp DNA Ladder Plus as a size marker (Fermentas Life Sciences), stained with ethidium bromide, and visualized under UV trans-illumination. After visualizing the bands under UV light, amplified product was cut out of the gel and purified using a DNA extraction kit (Fermentas Life Sciences).

The purified product of 16S DNA was sent for direct sequencing (Eurofins MWG Operon, Ebersberg, Germany). Sequencing was done employing the same primers used for PCR amplification. The nucleotide sequence of 16S rRNA gene obtained from DNA sequencing was compared with other cyanobacterial sequences from the NCBI database using BLAST (http://www.ncbi.nlm.nih.gov/BLAST). The sequence was deposited in

http://www.aloki.hu ● ISSN 1589 1623 (Print) ● ISSN 1785 0037 (Online)
DOI: http://dx.doi.org/10.15666/aeer/1902_849866
© 2021, ALÖKI Kft., Budapest, Hungary

the GenBank (Nacional Center for Biotechnology Information, NCBI) under accession number MN061337.

Extraction of DNA, PCR amplification and sequencing of the eukaryotic species (18S DNA)

The dominant eukaryotic species were cultured under aseptic conditions and genomic DNA was isolated. Five milliliters of microalgae culture were harvested by centrifugation at 14 000 RPM on Eppendorf 5424R centrifuge and used for DNA preparation. Genomic DNA from the strain PACC 8946 was isolated using QIAamp DNA Mini Kit (QIAGEN) according to the manufacturer requirements. The DNA concentration and quality was determined spectrophotometrically at a wavelength of 260 nm using Epoch microtiter plate reader and T3 plate protocol. Ribosomal DNA encoding genes were amplified according Yamamoto et al. (2003). Briefly, the reaction was carried out in a 50 µl reaction mixture that contained 1x reaction buffer, 200 µM dNTPs, 0.2 µM 5'-PCR 1-primer (ACCTGGTTGATCCTGCCAGT), 0.2 µM 3'-PCR 3-primer (CCTTCYGCAGGTTCACCTAC), 100 ng microalgal genomic DNA, and 1 unit of Q5 High Fidelity DNA polymerase (New England Biolabs). The samples were placed in a thermocycler and subjected to 30 PCR cycles of denaturation at 95°C for 60 s, annealing at 66°C for 60 s, and extension at 72°C for 60 s. There was a final extension step at 72°C for 10 min. PCR amplicon was separated on a 0.8% agarose gel and purified with the QIAquick Gel Extraction Kit (QIAGEN). The Microsynth Company (Switzerland) performed the sequencing using ABI automated sequencers. Chromatograms were corrected manually with DNA Star software (Lasergene, USA). The resulted nucleotide sequence was deposited in the GenBank under accession number MN088860, subjected to Blastn analysis and compared with other related sequences from the NCBI database. Thirty-three sequences with highest similarity to the query were chosen for further phylogenetic analysis.

Phylogenetic analysis

Multiple sequence alignment of the prokaryotic and eukaryotic species/strains was performed separately by using the ClustalW program built in the phylogenetic software MEGA 7 (Kumar et al., 2016). Phylogenetic trees were computed by MEGA 7 using the maximum-likelihood (ML), and neighbor-joining (NJ) algorithms (Nei and Kumar, 2000). All algorithms were performed with 1000 bootstrap replicates. Nucleotide positions containing gaps and missing data were eliminated from the data set (complete deletion option). *Escherichia coli* str. K-12 (NR102804) was used as an outgroup for the prokaryotic species/strains. The analysis of the eukaryotic species/strains involved 34 nucleotide sequences.

Phytoplankton counting and biovolumes

The taxonomic composition of the nano- and microplankton was determined with a light microscope Amplival (magnification up to 1000 x). Phytoplankton counting was performed on an inverted microscope by the method of Utermöhl (1958). The algal biovolume was determined on the basis of formulas for geometric shapes (Hillebrand et al., 1999). Nano- and microplankton cell size measurements were performed on each species at least on ten individuals. The cell biovolume of picoplankton species were calculated by measuring of 50 cells. The total phytoplankton biovolume was calculated

http://www.aloki.hu ● ISSN 1589 1623 (Print) ● ISSN 1785 0037 (Online)
DOI: http://dx.doi.org/10.15666/aeer/1902_849866
© 2021, ALÖKI Kft., Budapest, Hungary

as the sum of the biovolumes of all species in each sample. The relative biovolume of the APP community was determined as a percentage of the total biovolume. We accept that the APP community (pro- and eukaryotic members) was dominant when there is a relative biovolume of more than 50% of the total biovolume, according to Somogyi et al. (2014).

Statistical analysis

The methodology of generalized additive models (GAMs) (Hastie and Tibshirani, 1990; Stasinopolus et al., 2016) was used to determine the empirical relationships between abundance of APP, total phytoplankton biovolume and abiotic factors. The required computations were performed with the gam and gamlss R packages developed by these authors (R core team 2019). GAMs allow non-linear relationships between the covariates (predictors) via smoothing spline functions and response as opposed to the traditional generalized linear models in which the predictors are included linearly.

Results

Environmental conditions and trophic status

The lagoon is characterized by high summer temperatures, with average values ranging from 19.2 to 24.2°C (*Table 1*). Lowest temperature (7.8°C) was measured in October 2014, while highest summer temperature (29.8°C) was measured in July 2015. North Saltern waters are alkaline, with pH ranging from 8.6 to 9.1. During the summer season, super oxygen saturation was observed, reaching >200% in June 2016 as a result of the intensive blooming of APP. Nutrients had constant high levels. The ammonium nitrogen ($N\text{-}NH_4$) had highest values in the mid-summer (>1.5 mg L^{-1}). Nitrite nitrogen ($N\text{-}NO_2$) increased from spring to summer, while the nitrate nitrogen ($N\text{-}NO_3$) was usually under the detection limit. The levels of $P\text{-}PO_4$ were high, which indicates that there is no P-limitation of the phytoplankton.

Table 1. *Environmental conditions and chlorophyll-a in 2013-2017*

		Parameter										
Year		**T, °C**	**pH**	**DO, mg L^{-1}**	**OS, %**	**C, mS cm^{-1}**	**S, ‰**	**$N\text{-}NO_2$, mg L^{-1}**	**$N\text{-}NO_3$, mg L^{-1}**	**$N\text{-}NH_4$, mg L^{-1}**	**$P\text{-}PO_4$, mg L^{-1}**	**Chl-*a*, µg L^{-1}**
2013	**min**	17.2	8.36	7.5	89.6	45.9	30.1	0.11	<0.2	0.13	0.60	8.7
	max	25.1	8.7	15.4	158.9	78.3	54.3	0.21		>1.5	4.5	26.7
	mean	**21.1**	**8.6**	**11.1**	**124.8**	**65.3**	**43.6**	**0.15**		**n.a.**	**1.97**	**17.7**
2014	**min**	7.8	8.4	10.0	116.1	60.9	39.9	0.11	<0.1	0.14	0.74	9.4
	max	29.3	9.4	14.9	147.2	71.7	49.3	0.61	0.78	>1.5	1.8	37.8
	mean	**19.2**	**8.8**	**11.9**	**127.6**	**66.1**	**44.5**	**0.26**	**n.a.**	**n.a.**	**1.3**	**25.2**
2015	**min**	10.0	8.4	8.1	97.3	11.4	6.3	0.08	<0.1	0.05	0.15	1.5
	max	29.8	8.9	14.8	129.0	60.3	40.2	0.17		0.74	0.85	2.1
	mean	**19.6**	**8.6**	**10.5**	**109.8**	**31.6**	**19.8**	**0.12**	**n.a.**	**0.33**	**0.43**	**1.8**
2016	**min**	18.6	8.6	6.4	79.9	41.3	26.1	0.12	<0.2	0.14	0.27	256.3
	max	27.6	9.5	19.7	>200	83.1	59	0.18	19.3	>1.5	0.69	305.6
	mean	**24.1**	**9.1**	**12.1**	**97.9**	**59**	**40**	**0.14**	**n.a.**	**n.a.**	**0.48**	**280.9**
2017	**min**	17.5	8.7	7.9	72.6	62.8	41.8	0.078	<0.2	0.12	0.08	331.7
	max	29.6	9.1	16.6	172.5	128.6	>72	0.153		>1.5	0.21	400.6
	mean	**24.2**	**8.9**	**11.3**	**136.4**	**97.6**	**n.a.**	**0.12**	**n.a.**	**n.a.**	**0.16**	**366.2**

Legend: Temperature (T), Dissolved oxygen (DO), Oxygen saturation (OS), Conductivity (C), Salinity (S), Chlorophyll-a (Chl-a), n.a. - *not applicable*

http://www.aloki.hu ● ISSN 1589 1623 (Print) ● ISSN 1785 0037 (Online)
DOI: http://dx.doi.org/10.15666/aeer/1902_849866
© 2021, ALÖKI Kft., Budapest, Hungary

Chlorophyll-*a* varied in an extremely wide range from 1.8 to 366.2 μg L^{-1}, but in the prevailing part of the study period indicated hypertrophic conditions according to the fixed boundary system on an OECD report (OECD, 1982). Salinity was controlled by the technological requirements for salt production and naturally increases from spring to autumn. Due to the shallow nature of the lagoon, salinity was strongly influenced by the meteorological conditions, e.g. after a rainy spring in 2015, the salinity reached 40.2‰ only in September. The same year, the mid-seasonal salinity had a minimum value of 19.8‰, which corresponds to the mixosaline zone. With exception of 2015, the average salinity of North Saltern was above 40‰, which is typical for the hypersaline waters. The extreme variations of the salinity in North Saltern over the five-year study period ranged from 6.3 to > 72‰.

Identification of the prokaryotic APP

The 16S DNA sequence analysis of the strain PACC 8945 showed a high percentage of identitties with NCBI 16S rDNA sequences belonging to genus *Synechococcus*. Since the taxonomy of the order Synechococcales and in particular of the genus *Synechococcus* is still problematic, the obtained in this study nucleotide sequence (MN061337) was also used for phylogenetic analyses. For the purpose of the phylogenetic analyses, sequences of representatives of the genera *Synechococcus* (freshwater, marine and species inhabiting waters with very high salinity), *Prochlorococcus*, *Cyanobium* and the newly proposed *Parasynechococcus* were selected.

Determination of the phylogenetic position of different taxa is the first and most important criterion in the classification process. The most commonly used molecular-genetic marker that provides an excellent framework for testing phylogenetic hypotheses is the 16S rRNA gene. The phylogenetic tree obtained from the ML analysis in this study is shown in *Figure 2*. Four distinct clades could be distinguished in the phylogenetic reconstruction, here named Clade 1, Clade 2, Clade 3, and Clade 4 (*Fig. 2*). The first clade (Clade 1) comprises *Synechococcus* marine strains and strains suggested as members of a new genus *Parasynechococcus* (Coutinho et al., 2016). The representatives of genus *Parasynecococcus* are not monophyletic, but rather showed polyphyly, being scattered in the phylogenetic tree. These phylogenetic positions do not confirm the separation of *Parasynecococcus* as a new genus. The topology demonstrates the need of new markers that, in combination with 16S DNA, could contribute to solving such problems.

The second clade (Clade 2) includes the studied PACC 8945 strain, which is positioned close to a strain isolated from a hypersaline water reservoir in Romania and strains isolated from the Red Sea and the Pacific Ocean, each with salinity between 36 and 55 g L^{-1} (Keresztes et al., 2012; Coutinho et al., 2016).

Clade 3 combines representatives of the genus *Prochlorococcus* (*Prochlorococcus marinus*). The phylogenetic tree shows pronounced monophily and potential for distinguishing between low light intensity (LLI) and high light intensity (HLI) strains of genus *Prochlorococcus*. Clade 4 consists of freshwater cyanobacterial strains of the genera *Synechococcus* and *Cyanobium*. The phylogenetic reconstruction based on the neighbor-joining (NJ) algorithm showed a similar topology.

http://www.aloki.hu ● ISSN 1589 1623 (Print) ● ISSN 1785 0037 (Online)
DOI: http://dx.doi.org/10.15666/aeer/1902_849866
© 2021, ALÖKI Kft., Budapest, Hungary

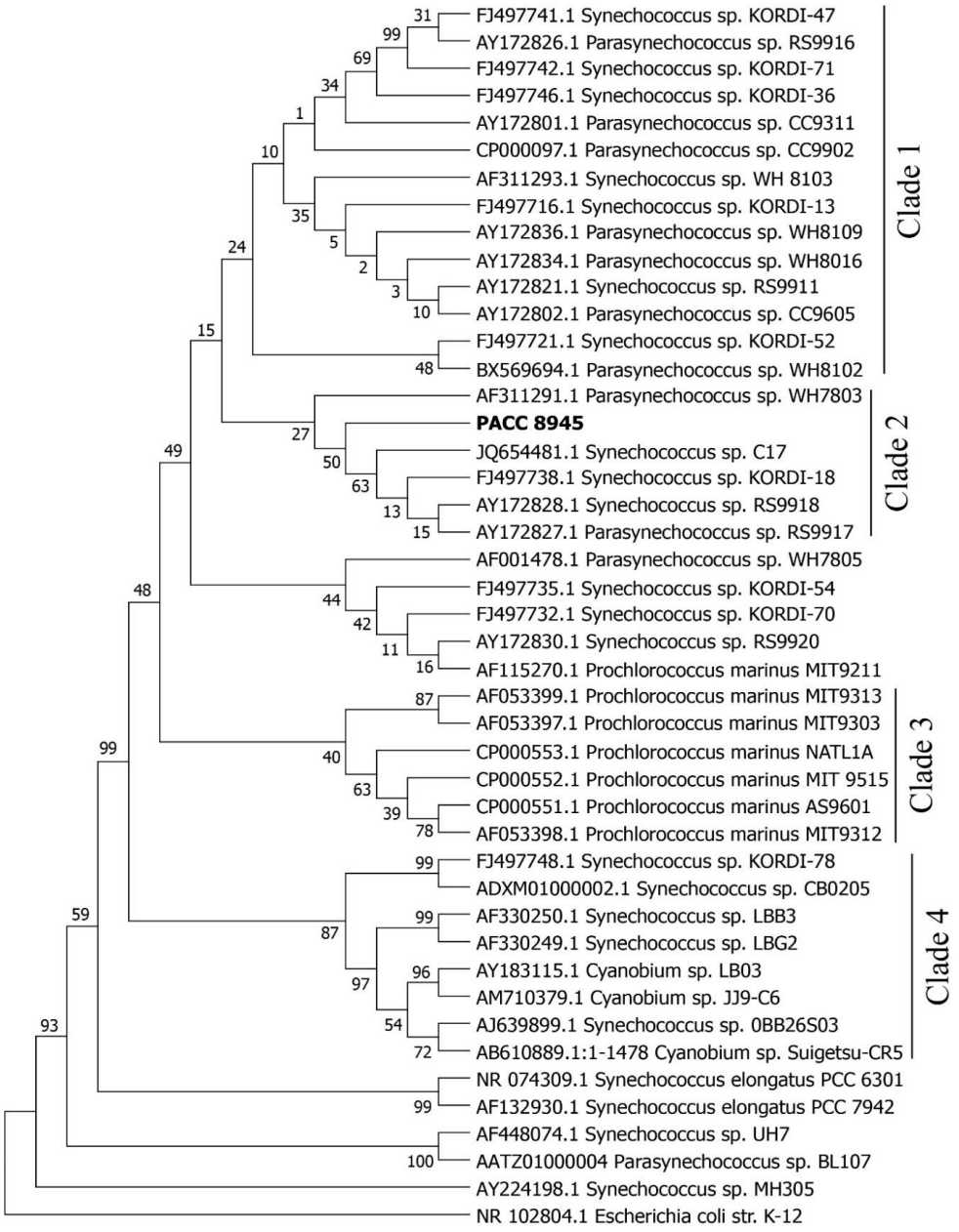


Figure 2. *A Maximum-Likelihood (ML) phylogenetic tree based on 16S DNA sequences. The analysis includes 16S DNA sequences of cyanobacterial strains from the genera Synechococcus, Prochlorococcus, Cyanobium, Parasynechococcus. Numbers show the bootstrap support. The 16S DNA sequence of E coli str. K-12 was used as an outgroup. Access numbers in GenBank are given before the name of the species*

Identification of the eukaryotic APP

For analysis of the phylogenetic relationships and for construction of the phylogenetic tree, 18S DNA sequences from different genera that have been shown homology with the target nucleotide sequence were selected.

The applied selection included the following genera *Picochlorum, Nanochlorum, Nannochloris, Pseudochloris, Marvania, Chlorella, Auxenochlorella* and *Coccomyxa*.

http://www.aloki.hu ● ISSN 1589 1623 (Print) ● ISSN 1785 0037 (Online)
DOI: http://dx.doi.org/10.15666/aeer/1902_849866
© 2021, ALÖKI Kft., Budapest, Hungary

The phylogenetic tree (*Fig. 3*) consisted of 2 clades: the main clade, including species from genera *Picochlorum, Nanochlorum* and *Nannochloris*, and clade 2, which contains species of the taxonomically distant genera *Pseudochloris, Marvania, Chlorella* and *Auxenochlorella*.

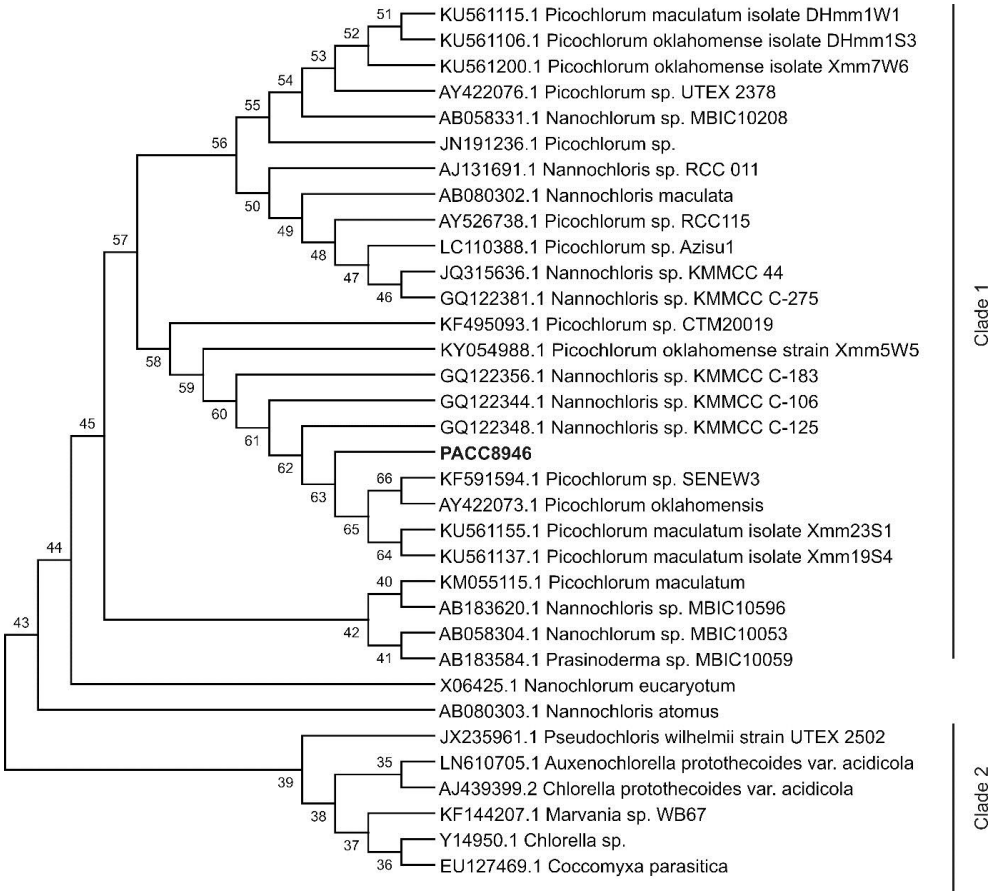


Figure 3. *Molecular phylogenetic analysis based on 18S DNA sequences of species from the genera Picochlorum, Nanochlorum, Nannochloris, Prasinoderma, Pseudochloris, Auxenochlorella, Chlorella, Marvania and Coccomyxa. The tree with the highest log likelihood is shown*

Studied isolate PACC 8946 indicated practical identity of the 18S DNA sequence with the holotype of *Picochlorum oklahomense* (GenBank accession AY422073) and *Picochlorum* sp. SENEW3 (GenBank accession KF591594) from a poikilohaline pond of San Elijo Lagoon, USA (Henley et al., 2004; Wang et al., 2014).

The cytomorphological features of the eukaryotic species (strain PACC 8946) revealed also similarity with *Picochlorum oklahomense.* We observed small rounded cells (d = 2-3 μm) with one laterale chloroplast, without pyrenoide (*Fig. 4A,B*). Reproduction was carried out by autosporulation into two or four daughter cells (*Fig. 4C,D*). The mother cells reached approximately 5 μm in size.

Following the polyphasic approach of the current classification and taking in account the genetic similarity of strain PACC 8946 with *Picochlorum oklahomense*, and similarity in the cytomorphological and ecological markers, we identified the eukaryotic assemblage of APP from the North Saltern as *Picochlorum oklahomense* Hironaka.

http://www.aloki.hu ● ISSN 1589 1623 (Print) ● ISSN 1785 0037 (Online)
DOI: http://dx.doi.org/10.15666/aeer/1902_849866
© 2021, ALÖKI Kft., Budapest, Hungary

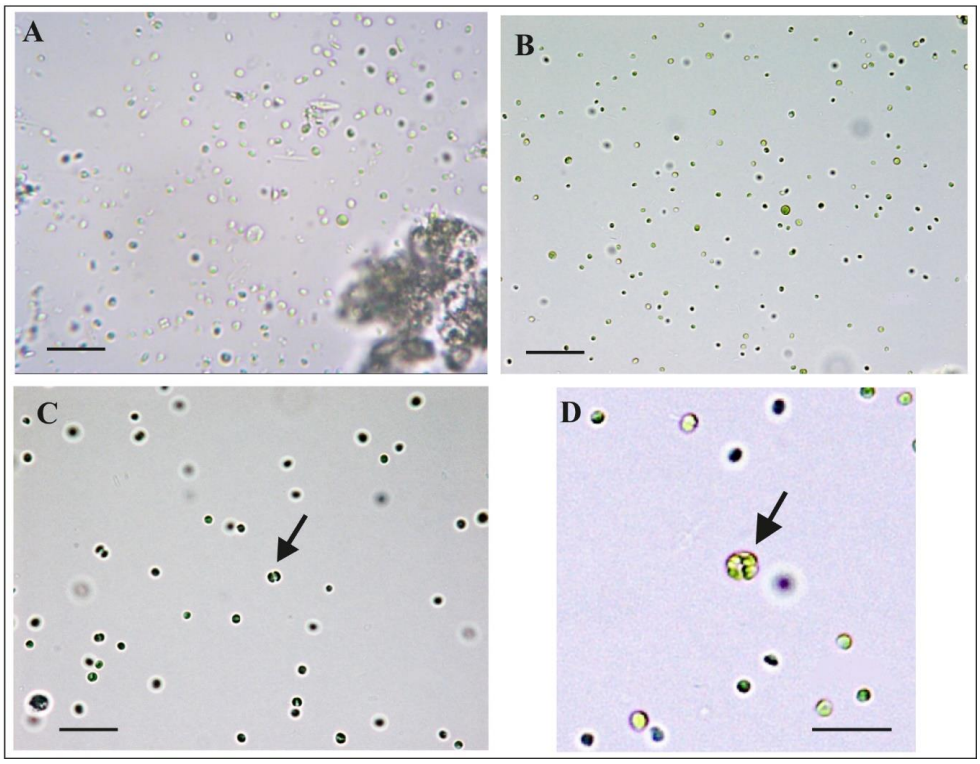


Figure 4. *Photomicrographs of Picochlorum oklahomense.* ***A:*** *Field sample, containing spherical cells of Picochlorum, Synechococcus and pennate diatom;* ***B, C, D:*** *Picochlorum oklahomense, strain PACC 8946, isolated from field sample, collected in Atanasovsko Lake;* ***C:*** *Autosporulation into two daughter cells;* ***D:*** *Autosporulation into four daughter cells. The arrow indicates autosporulation. Scale bars = 10 μm*

Taxonomic composition, abundance and biovolume of the phytoplankton community

During the study period, we found a small number of species (from 10 to 19), which belonged to seven taxonomic groups: Cyanobacteria, Prasinophyceae, Trebouxiophyceae, Chlorophyceae, Bacillariophyceae, Dinophyceae and Cryptophyceae (*Table 2*). Common species that accompanied the APP throughout the study period were diatoms (*Cocconeis placentula*, *Cylindrotheca closterium*, *Triblionella punctata* and *Planothidium delicatulum*), green algae (*Oocystis sp.*) and the dinoflagellate *Katodinium fungiforme*.

The total biovolume of the phytoplankton varied within a very wide range - from 0.6 to 121.7 mm^3 L^{-1} (2015 and 2016, respectively) (*Table 3*). With exception of 2015, APP community was dominant, forming above 50% of the total biovolume. Highest mid-seasonal levels of the total biovolume (65.4 mm^3 L^{-1}) were recorded in 2016, when the APP formed over 93% from the biovolume. The contribution of the APP to the total phytoplankton biovolume reached a maximum value of 99.3% in July 2016 (T=27.6°C; S=59‰). During the same month, the APP was in a state of intensive blooming, with an extremely high abundance of 240.1×10^6 cells mL^{-1}. We found that a key factor for the intensive blooms of APP in 2016 was the salinity range 30-59‰, combined with the higher average annual temperature of 24.1°C (*Table 1*). Conversely, in 2015, the relative biovolume of APP accounted for only 1/3 of the total biovolume and the abundance of APP was significantly lower: mean 0.16×10^6 cells mL^{-1}.

http://www.aloki.hu ● ISSN 1589 1623 (Print) ● ISSN 1785 0037 (Online)
DOI: http://dx.doi.org/10.15666/aeer/1902_849866
© 2021, ALÖKI Kft., Budapest, Hungary

Table 2. *Main cyanobacterial and algal morphotypes in Atanasovsko Lake during the period 2013-2017*

Year	2013	2014	2015	2016	2017
Cyanobacteria					
Prokaryotic APP	●	●	●	●	●
Komvophoron breve	●	●			●
Merismopedia punctata			●		
Phormidium bulgaricum	●				●
Phormidium chlorinum			●		
Pseudanabaena minima		●	●	●	●
Prasinophyceae					
Polyblepharides amylifera			●		
Pyramimonas micron		●		●	●
Trebouxiophyceae					
Eukaryotic APP	●	●	●	●	●
Closteriopsis acicularis			●		
Oocystis sp.	●	●	●	●	●
Provasoliella ovata					●
Chlorophyceae					
Monoraphidium griffithii			●		
Monoraphidium arcuatum			●		
Bacillariophyceae					
Amphora sp.		●		●	●
Cocconeis placentula		●	●	●	●
Cyclotella caspia		●	●	●	●
Cylindrotheca closterium	●	●	●	●	●
Navicula capitatoradiata		●			●
Nitzschia longissima	●	●	●	●	●
Planothidium delicatulum	●	●	●	●	●
Triblionella punctata	●	●	●	●	●
Dinophyceae					
Katodinium fungiforme	●	●	●	●	●
Cryptophyceae					
Hillea fusiformis		●	●	●	●
Teleaulax acuta				●	●

Table 3. *Parameters of the phytoplankton community in Atanasovsko Lake during the period 2013-2017*

Date	TB, $mm^3\ L^{-1}$	CAPPTB, %	AbAPP, $\times 10^6$ cells mL^{-1}
12 June 2013	8.7	58.0	1.62
29 July 2013	16.8	72.2	4.62
01 Sept.2013	26.7	83.8	5.43
10 June 2014	4.1	75.4	0.74
19 July 2014	15.8	88.0	2.63
13 Sept. 2014	12.3	59.2	2.12
17 June 2015	0.6	36.6	0.13
27 July 2015	0.8	35.1	0.18
09 June 2016	62.2	97.0	32.30
27 July 2016	121.7	99.3	240.11
16 Sept. 2016	12.4	84.1	5.48
10 June 2017	36.1	98.5	7.10
21 July 2017	5.3	13.8	1.15
11 Sept. 2017	55.5	51.1	6.00

Abbreviations: TB (Total biovolume); CAPPTB (Contribution of APP to the total phytoplankton biovolume); AbAPP (Abundance of APP)

http://www.aloki.hu ● ISSN 1589 1623 (Print) ● ISSN 1785 0037 (Online)
DOI: http://dx.doi.org/10.15666/aeer/1902_849866
© 2021, ALÖKI Kft., Budapest, Hungary

Statistical analysis

Marked correlations in bold (*Table 4*) are significant at p-value < 0.05. There is a strong linear relationship between the response of variables C (Conductivity) and S (Salinity), total phytoplankton biovolume (TB) and abundance of APP (AbAPP). The correlations between the explanatory variables (covariates) T (temperature), C, S, N-NO_2, N-NO_3, N-NH_4, P-PO_4 and the response variables TB, AbAPP, CAPPTB (Contribution of APP to the total phytoplankton biovolume) is not significant. This means that the relationship between the response and covariates is not linear.

Table 4. *Pearson correlation matrix*

	T	C	S	N-NO_2	N-NO_3	N-NH_4	P-PO_4	AbAPP	TB	CAPPTB
T	1.00	0.18	0.13	−0.03	−0.25	0.18	**−0.61**	0.18	0.09	−0.36
C	0.18	1.00	**0.96**	0.12	−0.01	0.48	−0.15	0.13	0.33	−0.04
S	0.13	**0.96**	1.00	0.06	0.02	0.50	−0.13	0.22	0.34	0.03
N-NO_2	−0.03	0.12	0.06	1.00	0.38	0.22	0.13	0.34	0.36	−0.03
N-NO_3	−0.25	−0.01	0.02	0.38	1.00	0.22	−0.07	−0.09	−0.11	−0.08
N-NH_4	0.18	0.48	0.50	0.22	0.22	1.00	0.26	0.17	0.06	−0.13
P-PO_4	**−0.61**	−0.15	−0.13	0.13	−0.07	0.26	1.00	−0.10	−0.11	0.18
AbAPP	0.18	0.13	0.22	0.34	−0.09	0.17	−0.10	1.00	**0.87**	0.40
TB	0.09	0.33	0.34	0.36	−0.11	0.06	−0.11	**0.87**	1.00	**0.54**
CAPPTB	−0.36	−0.04	0.03	0.03	−0.08	−0.13	0.18	0.40	**0.54**	1.00

Abbreviations: T (Temperature); C (Conductivity); S (Salinity), AbAPP (Abundance of APP), TB (Total biovolume); CAPPTB (Contribution of APP to the total phytoplankton biovolume)

The generalized additive models (GAMs) allow non-linear relationships between the responses AbAPP, TB and smoothing spline functions of the covariates T, S, N-NO_2, N-NO_3, N-NH_4 and P-PO_4. Only the cubic spline functions of the covariates T and S are highly significant and the response TB within GAMs model with gamma distribution and log-link function. Deviance explained by this model is 87% whereas the correlation between measured and model predicted values is 0.71. Similarly, the GAMs model with log-link function, response AbAPP and cubic spline functions of the covariates T and S explain 88% of the deviance whereas the correlation between measured and model predicted values is 0.76. The parameter estimates, standard errors, parameter estimates divided by their estimated standard errors, p-value and significant codes are given in *Table 5*. The AbAPP and TB measured and predicted values are presented in *Table 6*.

Table 5. *GAMs model: response variables TB and AbAPP, cubic spline models of the covariates temperature (T) and salinity (S)*

Gamma distribution terms	**Estimate**	**Std. error**	**t value**	**Pr (>|t|)**	**Sc.**	**Estimate**	**Std. error**	**t value**	**Pr(>|t|)**	**Sc.**
	TB					**AbAPP**				
μ link function: log										
Intercept	2.115	0.854	2.476	0.076		2.022	1.245	1.624	0.178	
cs (T)	−0.099	0.032	−3.134	0.042	*	−0.135	0.048	−2.843	0.047	*
cs (S)	0.064	0.008	7.780	0.002	**	0.059	0.012	4.875	0.008	**
Scale link function - log										
Intercept	−0.821	0.183	−4.483	0.014	*	−0.440	0.178	−2.482	0.068	

Significance codes (Sc): '**' 0.01 '*' 0.05

http://www.aloki.hu ● ISSN 1589 1623 (Print) ● ISSN 1785 0037 (Online)
DOI: http://dx.doi.org/10.15666/aeer/1902_849866
© 2021, ALÖKI Kft., Budapest, Hungary

Table 6. *The measured and GAMs model predicted values with response variables TB and AbAPP, and cubic spline functions of the covariates temperature (T) and salinity (S)*

Case	Observed TB	Predicted TB	Observed AbAPP	Predicted AbAPP
1	8.73	11.69	1.62	1.57
2	16.81	16.97	4.62	4.99
3	26.68	27.99	5.43	5.91
4	4.14	4.213	0.74	0.77
5	15.76	14.89	2.63	4.53
6	12.31	10.93	2.12	1.44
7	0.58	0.73	0.13	0.14
8	0.81	0.94	0.18	0.24
9	62.21	37.71	32.30	23.37
10	121.73	78.50	240.11	107.35
11	12.38	81.18	5.48	102.89
12	36.08	30.09	7.10	6.92
13	5.34	5.496	1.15	0.87
14	55.52	57.47	6.00	14.69

These GAMs results are preliminary of an ongoing and extended study and should be considered with caution because of the small time-series sample size.

Discussion

North Saltern waters are alkaline, rich in ammonium nitrogen (often above the detection range) and phosphate (*Table 1*). Similar high nutrient levels have been reported by Wang et al. (2014) for the San Elijo lagoon, California. The high biogenic load of the lagoons is due to the long water stay and thus the repeated nutrient recycling (Kennish and Paerl, 2010). An additional source of nitrogen and phosphorus loading may be wintering and migrating aquatic birds (Boros et al., 2008), which have high abundance in Atanasovsko Lake as part of the Via Pontica migration route. Salinity of the North Saltern increased naturally from spring to autumn every year, and this cyclic pattern is also characteristic of other lagoons (Wang et al., 2014). Due to the shallow nature of the lake (0.3 m), salinity was strongly influenced by the meteorological conditions (Hubenov et al., 2015). In the last two years, the average seasonal values of chlorophyll-*a* have been in the range of hypereutrophic conditions (*Table 1*). According to Kennish and Paerl (2010) many coastal lagoons are eu- and even hypertrophic.

The APP community in North Saltern was represented by small (2-3 μm) spherical to oval or cylindrical cells (*Fig. 4A*), which cannot be identified by using the classical optical miscroscopy. The reviewed literature showed that pico-sized taxa (< 3 μm) are evaluated via convergent evolution and are characterized by extremely high phylogenetic and physiological diversity (Krienitz et al., 2012; Somogyi et al., 2013). Following the application of molecular genetic methods for Class Trebouxiophyceae, a number of marine or saline picoplankton species belonging to the genera *Picochlorum, Chloroparva* and *Pseudochloris* have been identified (Henley et al., 2004; Somogyi et al., 2011, 2013). A large variety of marine coccoid picoplankton lines was also found in Prasinophyceae (Krienitz et al., 2012). *Mychonastes* spesies (Chlorophyceae) were described from brackish and fresh waters.

http://www.aloki.hu ● ISSN 1589 1623 (Print) ● ISSN 1785 0037 (Online)
DOI: http://dx.doi.org/10.15666/aeer/1902_849866
© 2021, ALÖKI Kft., Budapest, Hungary

The conducted molecular-genetic and phylogenetic analyses proved that the APP in Atanasovsko Lake is an assemblage of two basic genotypes: *Picochlorum oklahomense* Hironaka (Chlorophyta, Trebouxiophyceae) and marine *Synechococcus* sp. (Synechococcales, Cyanobacteria). This finding was confirmed by cytomorphological charateristics of the cultures and ecological data. At present, the species *Picochlorum oklahomense* have been reported from very distinct and isolated habitats. They are parts of limno- and halosphere, such as the saline pool in Salt Plains National Wildlife Refuge of Oklahoma, USA (Henley et al., 2004), inland hypersaline lakes in Romania (Keresztes et al., 2012) and the coastal lagoon in southern California (Wang et al., 2014). These isolated habitats provide specific conditions for development of ensembles dominated by *Picochlorum oklahomense* and marine *Synechococcus* sp. (in Transylvanian lakes, Romania and Atanasovsko Lake, Bulgaria) or *Picocystis salinarum* (San Elijo lagoon, California). Confirmed habitats have the following common characteristics: shallow, with variable salinity, hypertrophic and with high summer temperatures. Three of them (San Elijo lagoon, salt pans of Oklahoma and Atanasovsko lake) maintain high abundance from waterfowl. This confirmed the suggestion of Keresztes et al. (2012) that the distribution of picoplankton species between isolated habitats is via waterfowl transfer.

The low number of associated phytoplankton species included representatives from 7 taxonomic groups (*Table 2*). Most of these species are cosmopolitan in marine or salty waters, euryhaline – e.g. diatoms *Cylindrotheca closterium, Triblionella punctata*, prasinophycean *Polyblepharides amylifera, Pyramimonas micron* (Ettl, 1983; Popovský and Pfiester, 2008). They were reported from coastal, inland haline lakes or freshwater basins with high mineralization. In 2015, the year with decreased salinity – 19.8‰ (*Table 1*), we identified species that are widespread in freshwater (sometimes also in slight salty) habitats as cyanobacteria *Merismopedia punctata*, *Phormidium chlorinum* and green algae *Monoraphidium griffithii*, *M. arcuatum* and *Closteriopsis acicularis* (Komárek and Fott, 1983; Komárek and Anagnostidis, 1999, 2005). According to Vadrucci et al. (2013), the large gradient of salinity and biogenic load are the most important factors that select taxonomic composition in coastal lagoons. Phytoplankton communities in coastal lagoons exhibit high inter- and intra-ecosystem taxonomic heterogeneity due to their spatial and temporal variability in the hydrogeological and geomorphological characteristics. This makes harder the development of indices for assessment of the ecological status of coastal lagoons.

During the 5-year period, the phytoplankton community in North Saltern was dominated by APP, which often reached extremely high abundance – from 10^6 to 10^8 cells mL^{-1} (*Table 3*), to a state of visible blooming of water (*Fig. 1C*). The high abundance of APP in shallow, turbid lakes is explained by the increased surface-to-volume ratio of the cells, which provides better utilization of light and more efficient absorption of nutrients (Felföldi et al., 2009). Similar abundance of the APP (10^6 to 10^8 cells mL^{-1}) and share in total biomass 90-100% was reported by Felföldi et al. (2009) for eutrophic shallow lakes similar to the Atanasovsko Lake. The results showed that the contribution of APP to the total biovolume is highly variable (from 36 to 99%) - *Table 3*. Concerning the ecological factor abundance of APP a nonparametric regression model is proposed between the response abundance of APP and the salinity and temperature (*Table 5*) as the main abiotic drivers. In a study of picoplankton dynamics in an Australian lagoon, Schapira et al. (2010) also identified salinity as a key factor in the abundance of APP.

http://www.aloki.hu ● ISSN 1589 1623 (Print) ● ISSN 1785 0037 (Online)
DOI: http://dx.doi.org/10.15666/aeer/1902_849866
© 2021, ALÖKI Kft., Budapest, Hungary

We registered highest APP abundance in 2016 at salinity range 30-59‰ and average summer temperatures above 24°C (*Tables 1 and 3*). These conditions stimulated the blooms of the picoplankton with a contribution of APP to the total phytoplankton biovolume > 93%. As an ecological optimum for APP predominance (over 99% of total biovolume) we defined salinity 59‰ and temperature 27.6°C, at which the abundance of APP reached values similar with the reported maximum (1.08×10^8 cells mL^{-1}) in extremely shallow turbid soda lakes (Somogyi et al., 2009). Temperature values in the lake during 2016 were close to the optimum growth temperature of 30°C in cultures of *Picochlorum* sp., strain SENEW3 (Wang et al., 2014).

Concerning salinity, the wide-ranging halotolerance of *Picochlorum oklahomense* is well known and accepted as an important species-specific ecological characteristic (Henley et al., 2004; Wang et al., 2014). Although in culture experiments Wang et al. (2014) found that the growth rate of *Picochlorum* sp. (SENEW3) decreases at salinity values above 50‰, in our samples from Atanasovsko Lake the optimum salinity appears to be higher (59‰). In natural samples from Cabdic Lake (Romania), the coexistence *Picochlorum oklahomense/Synechococcus* sp. was found at similar to the Atanasovsko Lake physico-chemical conditions: temperature = 28.2°C and salt concentration 55 g L^{-1} (Keresztes et al., 2012).

Conclusions

Due to the extremely small size (2-3 μm) and the lack of sufficient morphological features for taxonomic identification, the APP species in North Saltern of Atanasovsko Lake were identified by molecular and phylogenetic analyzes of 16S/18S DNA. The APP species showed genotype identity with marine *Synechococcus* sp. (Synechococcales, Cyanobacteria) and *Picochlorum oklahomense* (Trebouxiophyceae, Chlorophyta). Our analysis demonstrated the possibility to apply these molecular methods for identification of picoplankton species from natural sample isolates.

By using a polyphasic approach, based on molecular, morphological and ecological characteristics of natural samples and isolates, we collected data for the *Picochlorum oklahomese/Synechococcus* sp. assemblage. This is the first report for *Picochlorum oklahomese* and marine *Synechococcus* sp. as part of APP in a European coastal lagoon. North Saltern is characterized by a continuous salinity gradient in the limits of mixo- to hypersalinity zone (6.3 to 72‰). Waters are alkaline, with high levels of nutrients (ammonia, phosphate) and high summer temperatures.

The main abiotic drivers that control the taxonomic composition and abundance of the APP are salinity and temperature. Salinity between 30 and 59‰ and an average summer temperature above 24°C provide an ecological optimum for growth of APP at a relative biovolume > 93%.

We think that APP, in which *Picochlorum oklahomese* is associated with *Synechococcus* sp. or *Picocystis salinarum* is distributed in more coastal lagoons or inland hypersaline lakes with similar to the Atanasovsko Lake characteristics. We suggest that the distribution of the picoplankton species is related to the waterfowl and these picoplankton species may be found in more habitats with a high abundance of waterfowl or along their migration routes.

Future research on the taxonomic composition of autotrophic picoplankton in coastal lagoons and salt marshes needs to be expanded, since it plays a key role as a primary producer.

http://www.aloki.hu ● ISSN 1589 1623 (Print) ● ISSN 1785 0037 (Online)
DOI: http://dx.doi.org/10.15666/aeer/1902_849866
© 2021, ALÖKI Kft., Budapest, Hungary

Acknowledgments. This work was supported by the Bulgarian National Science Fund (research grant DN 01/2) and the project LIFE11 NAT/BG/000262 with the acronym Salt of Life.

REFERENCES

[1] Agustí, S. (1991): Allometric scaling of light absorption and scattering by phytoplankton cells. – Canadian Journal of Fisheries and Aquatic Sciences 48: 763-767. https://doi.org/10.1139/f91-091.

[2] Andersen, R., Kawachi, M. (2005): Traditional Microalgae Isolation Techniques. – In: Andersen, R. (ed.) Algal Culturig Techniques. Elsevier Academic Press, Burlington.

[3] Anonymous (1958): The Venice system for the classification of marine waters according to salinity. – Limnology and Oceanography 3: 346-347. https://doi.org/10.4319/lo.1958.3.3.0346.

[4] Ayadi, H., Abid, O., Elloumi, J., Bouaïn, A., Sime-Ngando, T. (2004): Structure of the phytoplankton in two lagoons of different salinity in the Sfax saltern (Tunisia). – Journal of Plankton Research 26: 669-679. https://doi.org/10.1093/plankt/fbh047.

[5] Barnes, R. S. K. (1980): Coastal Lagoons. – Cambridge University Press, Cambridge.

[6] Boros, E., Nagy, T., Pigniczki, C., Kotymán, L., Balogh, K. V., Vörös, L. (2008): The effect of aquatic birds on the nutrient load and water quality of soda pans in Hungary. – Acta Zoologica Hungarica 54(S1): 207-224.

[7] Botev, I. (1997): Hydrological regime of Atanasovsko Lake. – In: Michev, T. (ed.) Ecology and Conservation of Atanasovsko Lake Nature Reserve. Collection of Final Scientific Reports of Experts. BSBCP, Sofia, pp. 10-17. (in Bulgarian).

[8] Coutinho, F., Tschoeke, D. A., Thompson, F., Thompson, C. (2016): Comparative genomics of *Synechococcus* and proposal of the new genus *Parasynechococcus*. – PeerJ 4(3): e1522. https://doi.org/10.7717/peerj.1522.

[9] Eddy, B. P. (1956): The suitability of some algae for mass cultivation for food, with special reference to *Dunaliella bioculata*. – Journal of Experimental Botany 21: 372-380. https://doi.org/10.1093/jxb/7.3.372.

[10] Elloumi, J., Carrias, J. F., Ayadi, H., Sime-Ngando, T., Bouaïn, A. (2009): Communities structure of the planktonic halophiles in the solar saltern of Sfax, Tunisia. – Estuarine Coastal and Shelf Science 81(1): 19-26. https://doi.org/10.1016/j.ecss.2008.09.019.

[11] Estrada, M., Peter, H., Gasol, M. J., Casamayor, O. E., Pedrós-Alió, C. (2004): Diversity of planktonic photoautotrophic microorganisms along a salinity gradient as depicted by microscopy, flow cytometry, pigment analysis and DNA-based methods. – FEMS Microbiology Ecology 49: 281-293. https://doi:10.1016/j.femsec.2004.04.002.

[12] Ettl, H. (1983): Chlorophyta I, Phytomonadina. – In: Ettl, H., Gerloff, J., Heynig, H., Mollenhauer, D. (eds.) Süßwasserflora von Mittelueropa Bd. 9. VEB Gustav Fischer Verlag, Jena.

[13] Felföldi, T., Somogyi, B., Márialigeti, K. L., Vörös, L. (2009): Characterization of photoautotrophic picoplankton assemblages in turbid, alkaline lakes of the Carpathian Basin (Central Europe). – Journal of Limnology 68: 385-395. https://doi.org/10.4081/jlimnol.2009.385.

[14] Gecheva, G., Varadinova, E., Belkinova, D., Michov, S., Gyuzelev, G., Hristeva, Y. (2017): Ecological status assessment of a hypersaline lake: case study of Atanasovsko Lake, Bulgaria. – Acta Zoologica Bulgarica 8: 145-151.

[15] Hastie, T. J., Tibshirani, R. J. (1990): Generalized Additive Models. – 1st ed. Boca Raton, Florida: Chapman & Hall/CRC.

[16] Henley, W. J., Hironaka, J. L., Guillou, L., Buchhem, M. A., Buchhem, I. A., Fawley, M. W., Fawley, K. P. (2004): Phylogenetic analysis of the *'Nannochioris*-like' algae and diagnoses of *Picochiorum okiahomensis* gen. et sp. nov. (Trebouxiophyceae, Chlorophyta). – Phycologia 43: 641-652. https://doi.org/10.2216/i0031-8884-43-6-641.1.

http://www.aloki.hu ● ISSN 1589 1623 (Print) ● ISSN 1785 0037 (Online)
DOI: http://dx.doi.org/10.15666/aeer/1902_849866
© 2021, ALÖKI Kft., Budapest, Hungary

[17] Hillebrand, H., Dürseken, D., Kirschtel, D., Pollingher, U., Zohary, T. (1999): Biovolume calculation for pelagic and benthic microalgae. – Journal of Phycology 35: 403-424. https://doi.org/10.1046/j.1529-8817.1999.3520403.x.
[18] Hubenov, Z., Kenderov, L., Pandourski, I. (2015): Invertebrate animals (Metazoa: Invertebrata) of the Atanasovsko Lake, Bulgaria. – Historia naturalis bulgarica 22: 45-71.
[19] Ivanov, K., Sotirov, A., Rozhdestvensky, A., Vodenicharov, D. (1964): The lakes of Bulgaria. – Proceedings of the Institute of Hydrology and Meteorology 16: 1-243. (In Bulgarian).
[20] Kennish, M. J., Paerl, H. W. (2010): Coastal lagoons: critical habitats of environmental change. – In: Kennish, M. J., Paerl, H. W. (eds.) Coastal Lagoons: Critical Habitats of Environmental Change. Boca Raton, CRC Press, pp. 1-15.
[21] Kennish, M. J. (2015): Coastal Lagoons. – In: Kennish, M. (ed.) Encyclopedia of Estuaries. Springer.
[22] Keresztes, Z. G., Felföldi, T., Somogyi, T., Székely, G., Dragoş, N., Márialigeti, K., Bartha, C., Vörös, L. (2012): First record of picophytoplankton diversity in Central European hypersaline lakes. – Extremophiles 16(5): 759-769. https://doi.org/10.1007/s00792-012-0472-x.
[23] Komárek, J., Fott, B. (1983): Chlorophyta (Grünalgen) Ordnung: Chlorococcales. – In: Huber-Pestalozzi, G. (ed.) Das Phytoplankton des Süßwassers: Systematik und Biology 7(1). E. Schweizerbart'sche Verlagsbuchhandlung (Nägele u. Obermiller), Stuttgart.
[24] Komárek, J., Anagnostidis, K. (1999): Cyanoprokaryota 1 Teil: Chroococcales. – In: Ettl, H., Gärtner, G., Heynig, H., Möllenhauer, D. (eds.) Süßwasserflora von Mitteleuropa 19(1). Gustav Fischer Verlag, Stuttgart.
[25] Komàrek, J., Anagnostidis, K. (2005): Cyanoprokaryota, 2: Oscillatoriales. – In: Ettl, H., Gärtner, G., Heynig, H., Möllenhauer, D. (eds.) Süßwasserflora von Mitteleuropa 19(2). Gustav Fischer Verlag, Stuttgart.
[26] Krienitz, L., Bock, C., Kotut, K., Luo, W. (2012): *Picocystis salinarum* (Chlorophyta) in saline lakes and hot springs of East Africa. – Phycologia 51: 22-32. https://doi.org/10.2216/11-28.1.
[27] Kumar, S., Stecher, G., Tamura, K. (2016): MEGA7: molecular evolutionary genetics analysis version 7.0 for bigger datasets. – Molecular Biology and Evolution 33: 1870-1874. https://doi.org/10.1093/molbev/msw054.
[28] Lewin, R. A., Krienitz, L., Goericke, R., Takeda, H., Hepperle, D. (2001): *Picocystis salinarum* gen. et sp. nov. (Chlorophyta) - a new picoplanktonic green alga. – Phycologia 39: 560-565. https://doi.org/10.2216/i0031-8884-39-6-560.1.
[29] Nei, M., Kumar, S. (2000): Molecular Evolution and Phylogenetic. – Oxford University Press, New York.
[30] OECD (1982): Eutrophication of Waters. Monitoring, assessment and control. – Final Report, OECD cooperative programme on monitoring of inland waters (Eutrophication control), Environment Directorate, OECD, Paris.
[31] Paranhos, R., Somogyi, B., Pálffy, K., Balogh, K., Botta-Dukát, Z., Vörös, L. (2017): Unusual behaviour of phototrophic picoplankton in turbid waters. – PLoS ONE 12(3): e0174316. https://doi.org/10.1371/journal.pone.0174316.
[32] Popovský, J., Pfiester, L. A. (2008): Dinophyceae. – Spectrum Akademischer Verlag, Heidelberg.
[33] R Core Team (2019): R: A language and environment for statistical computing. – Vienna, Austria. URL: https://www.R-project.org/.
[34] Reynolds, C. S. (2006): The ecology of phytoplankton. – Cambridge University Press, Cambridge.
[35] Schapira, M., Buscot, M., Pollet, T., Leterme, S., Seuront, L. (2010): Distribution of picophytoplankton communities from brackish to hypersaline waters in a South Australian coastal lagoon. – Saline Systems 6(1): 2. https://doi.org/10.1186/1746-1448-6-2.

http://www.aloki.hu ● ISSN 1589 1623 (Print) ● ISSN 1785 0037 (Online)
DOI: http://dx.doi.org/10.15666/aeer/1902_849866
© 2021, ALÖKI Kft., Budapest, Hungary

[36] Schlösser, U. (1982): Sammlung von Algenkulturen. – Berichte der Deutschen Botanischen Gesellschaft 95: 181-276. https://doi.org/10.1111/j.1438-8677.1982.tb02862.x.

[37] Somogyi, B., Felföldi, T., Vanyovszki, J., Ágyi, Á., Márialigeti, K., Vörös, L. (2009): Winter bloom of picoeukaryotes in Hungarian shallow turbid soda pans and the role of light and temperature. – Aquatic Ecology 43(3): 735-744. https://doi.org/10.1007/s10452-009-9269-0.

[38] Somogyi, B., Felföldi, T., Solymosi, K., Makk, J., Nomonnay, Z. G., Horváth, G., Turcsi, E., Böddi, B., Márialigeti, K., Vörös, L. (2011): *Chloroparva pannonica* gen. et sp. nov. (Trebouxiophyceae, Chlorophyta) - a new picoplanktonic green alga from a turbid, shallow soda pan. – Phycologia 50: 1-10. https://doi.org/10.2216/10-08.1.

[39] Somogyi, B., Felföldi, T., Solymosi, K., Flieger, K., Márialigeti, K., Böddi, B., Vörös, L. (2013): One step closer to eliminating the nomenclatural problems of minute coccoid green algae: *Pseudochloris wilhelmii*, *gen. et sp. nov*. (Trebouxiophyceae, Chlorophyta). – European Journal of Phycology 48(4): 427-436. https://doi.org/10.1080/09670262.2013.854411.

[40] Somogyi, B., Vörös, L., Pálffy, K., Székely, G., Bartha, C., Keresztes, Z. (2014): Picophytoplankton predominance in hypersaline lakes (Transylvanian Basin, Romania). – Extremophiles 18: 1075-1084. https://doi.org/10.1007/s00792-014-0685-2.

[41] Stasinopoulos, M. D., Rigby, R. A., Heller, G., Voudouris, V., Bastiani, F. (2017): Flexible Regression and Smoothing Using GAMLSS in R. – 1st ed.: CRC Press.

[42] Utermöhl, H. (1958): Zur Vervollkommnung der quantitativen Phytoplankton-Methodik. – Schweizerbart, Stuttgart.

[43] Vadrucci, M. R., Stanca, E., Mazziotti, C., Umani, S. F., Georgia, A., Moncheva, S., Romano, A., Bucci, R., Ungaro, N., Basset, A. (2013): Ability of phytoplankton trait sensitivity to highlight anthropogenic pressures in Mediterranean lagoons: A size spectra sensitivity index (ISS-phyto). – Ecological Indicators 34: 113-125. http://dx.doi.org/10.1016/j.ecolind.2013.04.013.

[44] Wang, S., Lambert, W., Giang, S., Goericke, R., Palenik, B. (2014): Microalgal assemblages in a poikilohaline pond. – Journal of Phycology 50: 303-309. https://doi.org/10.1111/jpy.12158.

[45] Yamamoto, M., Nozaki, H., Miyazawa, Y., Koide, T., Kawano, S. (2003): Relationship between presence of a mother cell wall and speciation in the unicellular microalga *Nannochloris* (Chlorophyta). – Journal of Phycology 39: 172-184. https://doi.org/10.1046/j.1529-8817.2003.02052.x.

http://www.aloki.hu ● ISSN 1589 1623 (Print) ● ISSN 1785 0037 (Online)
DOI: http://dx.doi.org/10.15666/aeer/1902_849866
© 2021, ALÖKI Kft., Budapest, Hungary

CELLULOLYTIC BACTERIA CAPABLE OF NITROGEN FIXATION IN SALINE-SODIC GRASSLAND SOILS

WANG, H. L.[2] – GONG, Z. K.[2] – WU, J. H.[1] – WANG, D.[1] – LIU, D. B.[1*] – WANG, D. L.[1]

[1]*Key Laboratory of Vegetation Ecology, School of Life Science, Northeast Normal University, Changchun 130024, China*
(e-mail: wujh719@nenu.edu.cn (Wu, J. H.); wangdan920811@163.com (Wang, D.); liudb635@nenu.edu.cn (Liu, D. B.); wangd@nenu.edu.cn (Wang, D. L.))

[2]*School of Chemistry and Life Science, Changchun University of Technology, Changchun 130012, China*
(e-mail: wanghonglei@ccut.edu.cn (Wang, H. L.); gongzhongkuo@163.com (Gong, Z. K.))

[*]*Corresponding author*
e-mail: liudb635@nenu.edu.cn

(Received 22nd Jul 2020; accepted 19th Nov 2020)

Abstract. Cellulolytic plate bacteria are considered to be the major drivers of litter decomposition and play critical roles in soil conditioning and nutrient cycling. With the goal to identify strategies used by soil cellulolytic bacteria to overcome nitrogen limitation characteristic of saline-sodic grasslands, cellulolytic strains were isolated from the soil of such habitats in northeast China and their abilities to fix nitrogen were evaluated. Sequencing of the 16S rRNA gene indicated that *Streptomyces* strains were the most abundant cellulolytic microorganisms in this saline-sodic soil. Most of the isolates exhibited extracellular carboxymethyl cellulase (CMCase) and xylanase activities. Importantly, all the cellulolytic isolates from grassland soils with various vegetation types demonstrated nitrogen-fixing activities ranging from 10.80 to 33.36 nmol $C_2H_4 \cdot h^{-1} \cdot ml^{-1}$. The cellulolytic isolates also exhibited indole-3-acetic (IAA) acid production abilities ranging from 2.40 to 80.69 $\mu g \cdot ml^{-1}$. These findings provided the first evidence that cellulolytic bacteria likely adapted to the low-nitrogen saline-sodic grassland soils with the acquisition of nitrogen-fixing abilities.
Keywords: *cellulolytic microorganisms, saline-sodic soils, phylogenetic analysis, nitrogen-fixing activity, IAA activity*

Introduction

Salinity inhibits plant growth due to the low osmotic potential of the soil solution, ion toxicity and ion imbalance which further reduce nutrient uptake (Rengasamy, 2006; Yan et al., 2013), as well as negatively impacts the turnover of soil organic matter by reducing the activity and quantity of microbial biomass in the soil (Tripathi et al., 2006; Yan et al., 2013). Compared to non-saline soils, microbial activity and biomass in salt-affected soils was lower; yet, they still play effective roles in soil conditioning and nutrient cycling (Yan et al., 2012; Orhan et al., 2015). Evidently, microorganisms have developed some strategies to overcome the stress conditions commonly encountered in saline-sodic soils.

The major impact of salinity on soil microorganisms has resulted in extensive studies on the mechanisms of microbial resistance and adaptation to high salinity. Another important environmental factor for soil microbial community is nitrogen-deficiency in salt-affected soils (Liu et al., 2013). Previous researches revealed that nitrogen fixation was considered as one of the most vital sources of nitrogen in nitrogen-deficient soils (Welsh et al., 1996; Reef et al., 2010). Major types of biological nitrogen fixation include symbiotic and free-living nitrogen fixation in natural ecosystems. The best known

http://www.aloki.hu ● ISSN 1589 1623 (Print) ● ISSN1785 0037 (Online)
DOI: http://dx.doi.org/10.15666/aeer/1902_867879
© 2021, ALÖKI Kft., Budapest, Hungary

nitrogen fixers form symbiotic associations with plants, but are limited to select plant groups such as legumes, alders, and cycads (Poly et al., 2001). The free-living nitrogen fixing bacteria are not limited to growth with specific plant taxa, and may, therefore, play widespread roles in ecosystems (Kennedy et al., 2004; Unkovich and Baldock, 2008). These free-living nitrogen-fixing bacteria may be closely involved in the development of soil ecosystems by providing nitrogen supplies and promoting plant growth (Kennedy et al., 2004). In salt-affected habitats, the high nitrogen demand by plant and soil microorganisms may favor the growth of free-living nitrogen-fixing bacteria to convert dinitrogen gas into biologically available N (i.e. ammonia, NH_3). Specifically, some studies have observed the occurrence of nitrogen fixation in organic-matter rich and N-deficient soils (Sistla et al., 2012; Shiau et al., 2017), suggesting that microbial populations involved in soil organic matter decomposition might also have nitrogen-fixing capabilities as a strategy of adaptation to N deficiency.

Soil salinity and alkalinity are the main concerns in many grasslands, especially for the eastern and central of Eurasian steppes (from China, Mongolia, to Kazakhstan and Russia). In Northeast China, large sections of steppes have suffered from deterioration due to alkalization and salinization (Wang et al., 2003). The steppe soil is characterized by higher alkalinity (pH 8.5-11.0) and salinity (salt content > 0.5%), but low nutrient availability (Xin et al., 2012). In this saline-sodic grassland soils, plant litter cellulose, hemicellulose and lignin, were the main source of organic matter (Liu et al., 2013; Trujillo-Cabrera et al., 2013). Decomposer microorganisms are considered to be the major drivers of litter decomposition and play critical roles in soil conditioning and nutrient cycling (Liu et al., 2006; Xin et al., 2012). To break down plant litter, decomposer microorganisms require N-nutrients from the surrounding soils to maintain their activities (Schimel et al., 2003; Shiau et al., 2017). When the soil is N-deficient, it is expected that activities of soil decomposer microorganisms, plant litter decomposition, and nutrient cycling would stop, which would in turn hinder plant biomass production, unless alternative N sources are available (Schimel et al., 2003; Liu et al., 2006). Interestingly, the grassland investigated in this study, with saline-sodic soils, maintained relatively high plant biomass production (about 150-170 $g \cdot m^{-2} \cdot year^{-1}$) (Zhao et al., 2019). Thus, soil microorganisms in this grassland likely possess unique strategies to overcome N-deficiency and sustain litter decomposition and nutrient cycling. Up to now, the decomposer microorganisms in the saline-sodic soil have received increasing attention. However, very little is known about the specific mechanisms that the decomposer microorganisms employ to adapt to N-deficiency frequently encountered in saline-sodic soils in order to sustain nutrient cycling and support primary production in these environments.

For this work, we targeted cellulolytic bacteria as representatives of the soil microbial communities involved in plant litter decomposition and organic matter turnover. Soil cellulolytic bacteria were isolated from low-nitrogen saline-sodic grassland soil in Jilin, China and characterized for activities of cellulolysis and nitrogen fixation. The objective of this study was to understand the potential adaptation strategy of the cellulolytic bacteria to low-nitrogen in saline-sodic soils. We hypothesized that cellulolytic bacteria from the saline-sodic soil with nitrogen-deficiency would evolve nitrogen fixing activities within such adverse environment.

http://www.aloki.hu ● ISSN 1589 1623 (Print) ● ISSN1785 0037 (Online)
DOI: http://dx.doi.org/10.15666/aeer/1902_867879
© 2021, ALÖKI Kft., Budapest, Hungary

Materials and methods

Soil samples and isolation of cellulolytic bacteria

Soil samples were collected from a saline-sodic grassland, located at the Grassland Ecological Research Station of Northeast Normal University, Jilin Province, China (44˚ 45′N, 123˚ 45′E). The climate is semi-arid continental with mean annual temperature 4-7°C and annual precipitation 280–400 mm. The soils were mixed saline and alkaline (pH 8.0–11.0). The vegetation was meadow steppe predominated by perennial *Leymus chinensis*, and other common species include grasses such as *Phragmites australis*, *Calamagrostis epigejos* and *Chloris virgata*; forbs such as *Kalimeris integrifllia*., *Suaeda glauca* and *Kochia sieversiana* (*Figure 1*).



Figure 1. *The saline-sodic grassland for collecting soil samples*

The soil samples in the saline-sodic grassland were obtained from *L. chinensis* soil, *C. virgata* soil and weeds soil (dominated by *P. australis, C. epigejos* and *S. baicalensis*) respectively. Soil samples (0–15 cm depth) were randomly collected from five sites in every types of soil, mixed together to form a single composite sample, placed in a sterile glass bottles and transferred to the laboratory in cool boxes. Each sample was separated into two parts: one was used for the isolation of cellulolytic bacteria; while the rest was air-dried to constant weight at room temperature for the determination of a suite of soil chemico-physical properties.

The cellulolytic strains were isolated on CMC-Na (carboxymethyl-cellulose, sodium salt) agar plates, which were prepared with Mandels' nutrient salts medium (Mandels, 1975) with 1% CMC-Na and 2% agar (w/v). After cultured at 30°C for 5 d, the colonies on this CMC agar medium were observed. And based on the size, color and morphology, the different colonies were picked and transferred to fresh CMC agar media plates, and then incubated at 30°C for 120 h. Pure cultures were obtained through repeated streaking on CMC-Na agar plate. After cultivation at 30ºC for 120 h, the plates were stained with 0.1% (w/v) Congo red solution for 10 min, and then washed with 0.1 M NaCl solution on each individual colony (Xu et al., 2015). A clear zone on the culture plate, indicating cellulolytic activity, was used to identify the cellulase-producing strains. The differences of isolates were performed with light microscopy and their sequences of 16S rRNA genes.

http://www.aloki.hu ● ISSN 1589 1623 (Print) ● ISSN1785 0037 (Online)
DOI: http://dx.doi.org/10.15666/aeer/1902_867879
© 2021, ALÖKI Kft., Budapest, Hungary

Molecular identification of cellulolytic bacteria

The 16S rRNA genes of the isolates were amplified using a forward primer 27F (5'-AGAGTTTGATCCTGGCTCAG-3') and a reverse primer 1492R (5'-TACCTTGTTACGATT-3') in a PCR thermal cycler (Bio-Rad, USA) under the following conditions: 94ºC for 5 min, 35 cycles of 30 sec each at 94ºC, 45 sec at 56ºC, 120 sec at 72ºC, and a final step of 10 min at 72ºC. The PCR products were purified using a High Pure PCR Product Purification Kit (Roche, Germany). The amplified fragments were sent to Comate Bioscience Co. Ltd. (Changchun, China) for sequencing. The obtained sequences were processed following previous described protocols (Zhang et al., 2011). First, sequences with chimeric artifacts were removed by the program Chimera Check at the Ribosomal Database Project (Cole et al., 2003). The surviving 16S rRNA gene sequences were searched for homology using the BLAST program at the National Center for Biotechnology Information (NCBI), aligned with homologous sequences using Clustal X (Thompson et al., 1997), and used for the construction of phylogenetic trees by the neighbor-joining algorithm (1000 bootstrap re-samplings) with Mega-X (Tamura et al., 2007).

Enzymatic assays and IAA producing traits

Each isolate was inoculated into 100 ml of liquid CMC-Na or corn straw media (Mandels' nutrient salts solution 100 ml, 1.0% (w/v) 1-cm long corn straw 5.0 g, pH 8.5). Cultivation was carried in a rotary incubator (120 rpm) at 30°C for 5 d. Subsequently, the cells were separated from the culture medium by centrifugation at 14000 g for 20 min at 4°C. The supernatants were used as the source of the extracellular crude enzyme extract to measure the activities of CMCase (with the CMC-Na medium) and xylanase (with the corn straw medium). CMCase activity was measured by mixing 1 ml of crude enzyme extract with 1 ml of 1% (w/v) low-viscosity CMC-Na solution in 50 mM phosphate buffer (pH 8.5) and incubated at 50°C for 30 min. The reducing sugar generated by CMCase activity was determined using the dinitrosalicylic acid procedure (Miller, 1969). One unit of CMCase activity (IU) was defined as the amount of enzyme releasing 1 μmol of reducing sugars per minute under the assay conditions. Xylanase activity was assayed by the same method with birch wood xylan as the substrate (Sigma-Aldrich Co. Ltd., St. Louis, USA). One unit of xylanase activity (IU) was defined as the amount of enzyme releasing 1 μmol of reducing sugars per minute under the assay conditions.

Nitrogen fixing efficiency of isolates were estimated by using acetylene reduction assay (ARA) (Hardy et al., 1973). All the isolates were grown at 30°C for 48 h in N-free liquid medium. Following incubation, the cotton plugs were replaced with rubber stoppers (subba-seal). 10% of air inside the tubes was evacuated with syringe and replaced by the same amount of pure acetylene gas. These were further incubated at 30°C for 24 h and then reduction of acetylene to ethylene was measured with a gas chromatograph (Agilent 6890 GC, USA) using a flameionization detector. Nitrogenase activity was defined as the amount of ethylene generated (nmol $C_2H_4 \cdot ml^{-1} \cdot h^{-1}$).

The production of IAA, which was considered as a plant growth promoting compound, was determined for all isolates according to the method of Leveau and Lindow (2005). Briefly, an aliquot (1 ml) of the supernatant, obtained after centrifugation of a bacterial culture grown in LB medium (1% tryptone, 1.0% yeast extract and 1.0% NaCl) supplemented with L-tryptophan (0.5 mg/ml), was mixed with 2 ml Salkowski reagent (1 ml 0.5 M $FeCl_3$ in 50 ml 35% $HClO_4$) and 50 μl of 10-mM orthophosphoric acid. The

http://www.aloki.hu ● ISSN 1589 1623 (Print) ● ISSN1785 0037 (Online)
DOI: http://dx.doi.org/10.15666/aeer/1902_867879
© 2021, ALÖKI Kft., Budapest, Hungary

reaction mixture was incubated at 25°C in the dark for 30 min. The absorbance of the pink color which developed after incubation was determined at 530 nm.

Analysis of soil chemo-physical properties

Various parameters of the soil samples were determined according to previously described methods. The soil pH and EC were determined using a soil-water ratio of 1:5. The soil organic carbon (SOC) content was measured using the Mebius method and by Walkley-Black acid digestion (Holguin and Bashan, 1996). The total nitrogen content (TN) was determined using an autoanalyzer (Foss 2100, FOSS Kjeltec1) with the Kjeldahl method following vitriol digestion. The total phosphorus (TP) content was measured colorimetrically after P extraction by Na_2CO_3 fusion (Yeomans and Bremner, 1988). Soil available nitrogen (AN) was measured using determination methods as previously described (Zhang et al., 2013).

Results

Soil chemo-physical properties

The chemo-physical properties of the sampling soil were summarized in *Table 1*. Based on the composition of 1:5 soil to water extracts, the electrical conductivity (EC) of surface soil ranged from 0.11 $ms \cdot cm^{-1}$ to 0.25 $ms \cdot cm^{-1}$, their pH ranges from 8.68 to 10.03. The *L. chinensis* soil group had the lowest pH and EC value, and the highest soil pH and EC values were observed in the weeds soil group. The analysis results of soil sample showed that the organic carbon content was 6.0–13.1 $g \cdot kg^{-1}$, total N 0.60-1.41 $g \cdot kg^{-1}$, available nitrogen 0.06–0.12 $g \cdot kg^{-1}$ and total P 4.55–6.24 $mg \cdot kg^{-1}$. The SOC and TN contents were highest in the *L. chinensis* soil and lowest in the weeds soil.

Table 1. *The chemo-physical properties of saline-sodic soil samples*

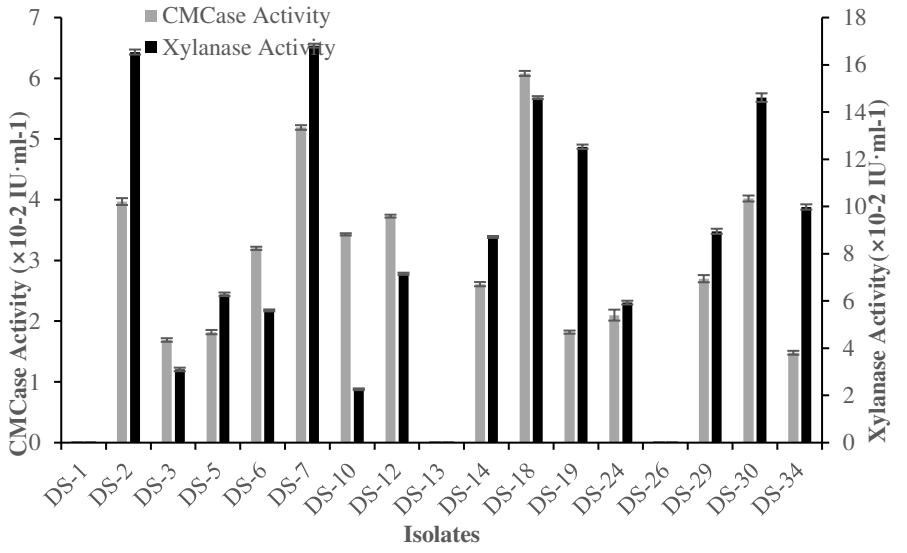
Soils	pH	Organic carbon ($g \cdot kg^{-1}$)	Total nitrogen ($g \cdot kg^{-1}$)	Available nitrogen ($g \cdot kg^{-1}$)	Total phosphorus ($mg \cdot kg^{-1}$)	Electric conductivity ($ms \cdot cm^{-1}$)
L. chinensis soil	8.68	13.1	1.41	0.09	4.55	0.11
C. virgate soil	9.47	10.9	1.18	0.12	6.24	0.19
Weeds soil	10.03	6.0	0.60	0.06	4.88	0.25

Diversity and abundance of cellulolytic bacteria

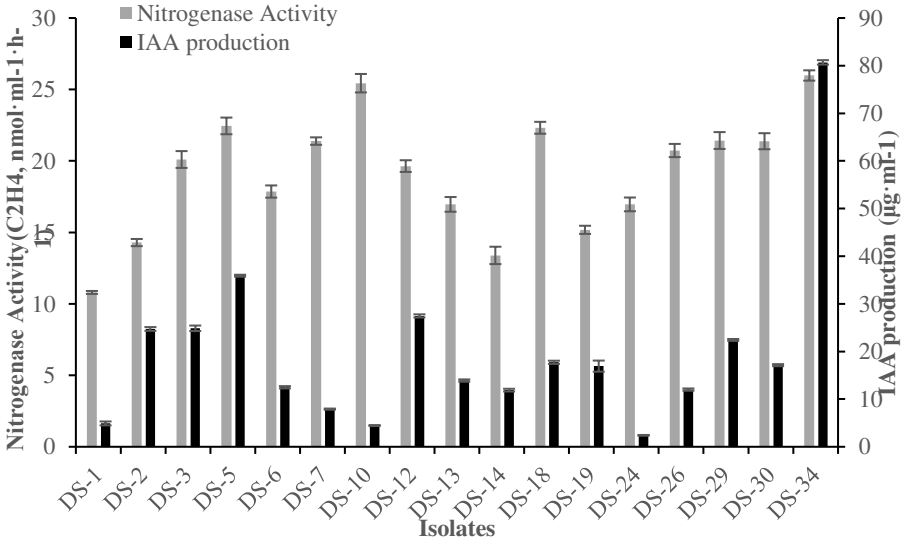
A total of 17 cellulolytic isolates were obtained in the *L. chinensis* soil, *C. virgata* soil and weeds soil. Through 16S rDNA gene phylogenetic analysis of the 17 isolates, it was confirmed that 11 strains were classified as *Streptomyces*, two strains as *Microbacteriums*, and one strain each as *Arthrobacters*, *Flavobacterium, Nocardioide* and *Lechevalieria* (*Figure 2*). No cellulolytic mold or yeast was isolated. In these isolates, 10 strains were obtained from *L. chinensis* soil (DS-1, DS-5, DS-6, DS-10, DS-13, DS-19, DS-24, DS-26, DS-29, DS-30), 9 strains from *C. virgata* soil (DS-2, DS-3, DS-5, DS-7, DS-10, DS-12, DS-13, DS-14, DS-30) and 4 strains from weed soil (DS-13, DS-18, DS-30, DS-34) respectively. The 16S rDNA fragment sequences of the 17 isolates showed 98–100% similarity to known corresponding strains. Strains DS-5 (*Streptomyces pratensis*), DS-10

http://www.aloki.hu ● ISSN 1589 1623 (Print) ● ISSN1785 0037 (Online)
DOI: http://dx.doi.org/10.15666/aeer/1902_867879
© 2021, ALÖKI Kft., Budapest, Hungary

(*Arthrobacter aurescens*), DS-13 (*Streptomyces toxytricini*), DS-30 (*Streptomyces massasporeus*) were obtained from both the *L. chinensis* soil and *C. virgata* soil. Strains DS-13 and DS-30 were also obtained from weed soil.



A



B

Figure 2. *Enzymatic assays and IAA production of the cellulolytic isolates. A: The CMCase and Xylanase activity measured by the isolates. B: The Nitrogenase activity and IAA production measured by the isolates. The reported values correspond to the mean value from three independent experiments in triplicate and the error bars to one standard deviation from the mean value*

The abundance of total cultivable bacteria and cellulolytic bacteria is presented in *Figure 3*. The abundance of total bacteria ($1.44–1.78\times10^7 CFU\cdot g^{-1}$) and cellulolytic bacteria ($1.6–2.3\times10^6 CFU\cdot g^{-1}$) was similar in different vegetation's soils (*Figure 3*). Based on the morphology and 16S rDNA gene phylogenetic analysis, we found that the *Streptomyces* strains were high abundant cellulolytic microorganisms in the grassland soil

http://www.aloki.hu ● ISSN 1589 1623 (Print) ● ISSN1785 0037 (Online)
DOI: http://dx.doi.org/10.15666/aeer/1902_867879
© 2021, ALÖKI Kft., Budapest, Hungary

of this study (accounting for more than 71% abundance in the *L. chinensis* soil, 71% abundance in the *C. virgata* soil and 86% abundance in the weed soil respectively). Especially, 2 *Streptomyces* strains DS-13 (*Streptomyces toxytricini*) and DS-30 (*Streptomyces iakyrus*) were obtained from the *L. chinensis* soil, *C. virgata* soil and weed soil.

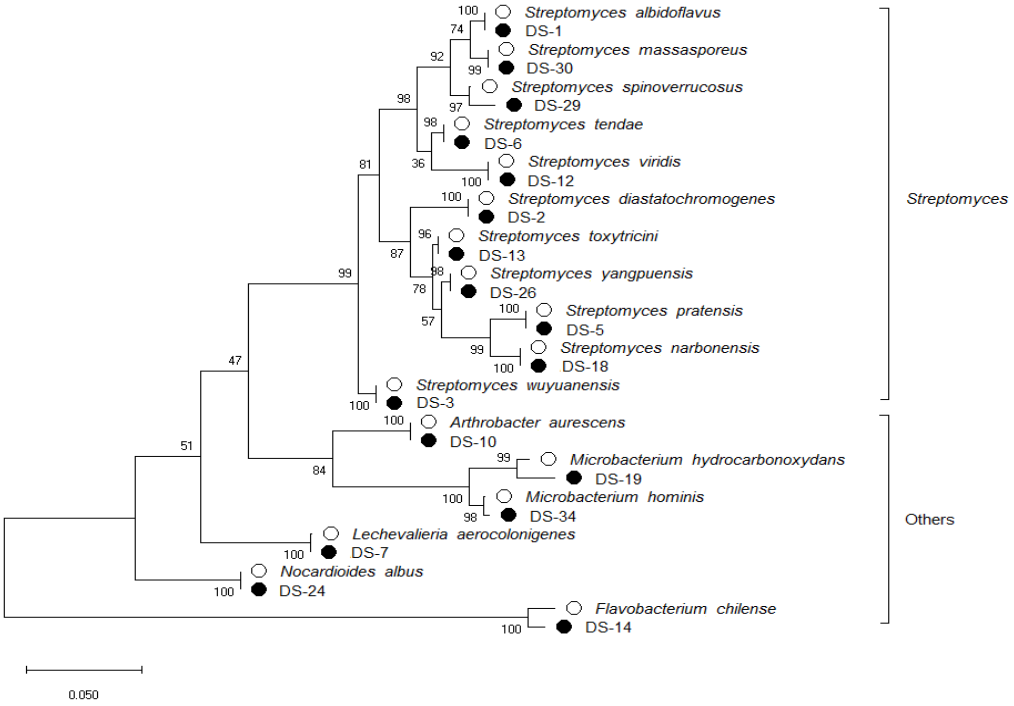


Figure 3. *Maximum Likelihood phylogenetic tree showing the relationships of partial 16S rRNA gene sequences cloned from saline-sodic grassland soil with closely related strains. The numerical values at branch nodes indicate bootstrap values per 1000 re-samplings. The scale bars indicate the number of nucleotide substitutions per sequence position. ●: isolates characterized in the study; ○: known strains closely related to the isolates identified in this study*

Enzymatic activities and IAA producing traits

After being cultured in the Mandel nutrient salts medium supplemented with CMC, all the isolates showed higher extracellular CMCase activity in the CMC media, except for the strains DS-1, DS-13 and DS-26 in which cellulolytic enzymes might distribute on the cell surface by attaching to or being inserted in the cell wall (*Figure 4*). The highest extracellular CMCase activity (6.08×10^{-2} IU·ml^{-1}) was observed for isolate DS-18 (*Streptomyces zaomyceticus*) in CMC media. Compared with CMCase activity, we found that most isolates showed considerably higher extracellular xylanase activity. When the cellulolytic isolates were inoculated on nitrogen-free CMC agar plate, all the isolates were able to develop colonies after three days. Biological nitrogenase activity of these isolates ranged from 10.80 to 25.98 nmol $C_2H_4 \cdot ml^{-1} \cdot h^{-1}$ (*Figure 4*). All the cellulolytic isolates exhibited IAA producing abilities ranging from 2.40 to 80.69 μg·ml^{-1} (*Figure 4B*). The same strains isolated from different vegetation's grassland soils had similar enzymic activities (including CMCase, xylanase and nitrogenase) and IAA producing activities.

http://www.aloki.hu ● ISSN 1589 1623 (Print) ● ISSN1785 0037 (Online)
DOI: http://dx.doi.org/10.15666/aeer/1902_867879
© 2021, ALÖKI Kft., Budapest, Hungary

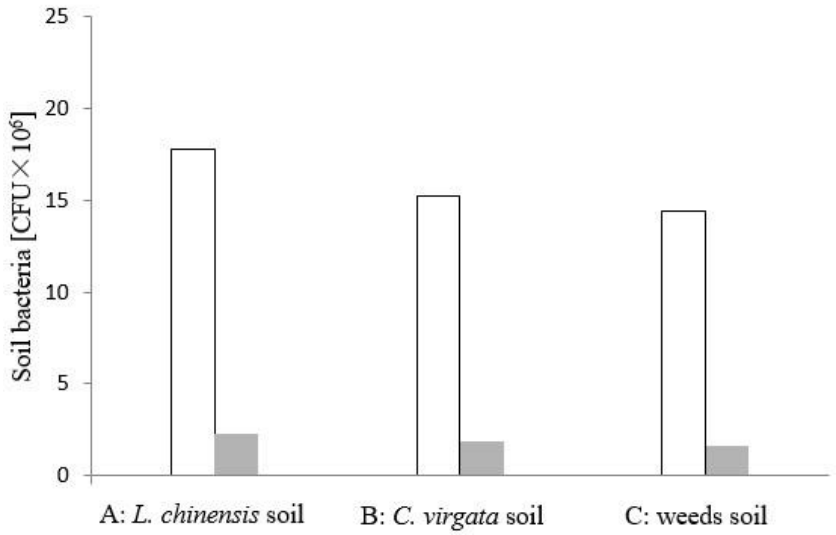


Figure 4. *Colony-forming units of culturable bacteria and cellulolytic soil bacteria in grassland soil. White bars, the abundance of total bacteria; light gray bars, the abundance of cellulolytic bacteria*

Discussion

Abundance and diversity of cellulolytic isolates

For this study, a traditional culture-dependent approach was used because the cellulolytic microbial community is very diverse phylogenetically and the cellulolytic enzymes are also very diverse (Trujillo-Cabrera et al., 2013). Our results showed that the cellulolytic isolates belonged to the Genus *Streptomyces*, *Microbacteriums*, *Arthrobacters*, *Flavobacterium, Nocardioide* and *Lechevalieria*, and cellulolytic *Streptomyces* strains (*Figure 2*) were the high abundant cellulolytic microorganisms in this saline-sodic grassland soil.

In nature, actionobacteria are known to occur not only in normal environments, but also in extreme environments, which are characterized by acidic/alkaline pH, salinity, low levels of available moisture, and nutrients (Zenova et al., 2011). As the represented genera of actinomycetes, the *Streptomyces* bacteria with the largest number of species and varieties are ubiquitous, are well adapted to the life in the soil where they grow by tip extension and branch through the soil searching for nutrients. *Streptomyces* bacteria can secrete large numbers of enzymes that break down insoluble organic polymers, including chitin and cellulose, into substituent sugars for binding and uptake by multiple ABC transporters (Chater et al., 2010; Thompson et al., 2010). These traits of the *Streptomyces* stains confer a competitive advantage over many other bacteria. In this study, the abundance of cellulolytic bacteria ($1.6–2.3\times10^6$ CFU·g^{-1}) was similar in different vegetation's soils (*Figure 3*), and the *Streptomyces* strains were high abundant cellulolytic microorganisms. To date, several studies on the diversity of cellulolytic bacteria isolated from different soils or environments have been performed. Ulrich et al. found that the cellulolytic community composition was dominated by *Streptomyces* (67%) in the silty sand soil and loam soil (Ulrich et al., 2008). Schlatter et al. (2009) revealed similar result that the addition of cellulose or lignin led to the high *Streptomyces* densities in a native soil. In our studied soils, plant litter cellulose, hemicellulose and lignin, were the main

http://www.aloki.hu ● ISSN 1589 1623 (Print) ● ISSN1785 0037 (Online)
DOI: http://dx.doi.org/10.15666/aeer/1902_867879
© 2021, ALÖKI Kft., Budapest, Hungary

source of organic matter, and the cellulolytic bacterial community was clearly highest abundance by *Streptomyce*. Especially, 2 *Streptomyces,* strains DS-13 (*Streptomyces toxytricini*) and DS-30 (*Streptomyces iakyrus*), were obtained from the *L. chinensis* soil, *C. virgata* soil and weed soil. Our results suggested that the cellulolytic *Streptomyces* strains were likely an ecologically significant cellulolytic group, which play a vital litter decomposing role in the soil.

Nitrogen fixing characteristics of cellulolytic isolates

In saline-sodic soils, soil salinity affects the soil chemico-physical properties and soil nutrient availability. Our analysis of soil chemico-physical properties revealed that the saline-sodic soil in this study was saline-alkaline, severely oligotrophic, especially low total nitrogen (0.60–1.41 $g \cdot kg^{-1}$) and available nitrogen (0.06–0.12 $g \cdot kg^{-1}$) (*Figure 4*). Notably, when the cellulolytic isolates from these soils were inoculated on nitrogen-free CMC agar plate, all the isolates were able to develop colonies after three days. Biological nitrogenase activity of these isolates ranged from 10.80 to 25.98 nmol $C_2H_4 \cdot ml^{-1} \cdot h^{-1}$ (*Figure 4*). In soils, soil decomposer microorganisms play a vital role in soil structure maintenance, organic matter decomposition, biogeochemical cycling, and plant nutrient availability. Cellulose is the most abundant polymers in plant litter and cellulolytic microorganisms are considered to be the major drivers of litter decomposition in the saline-sodic soils (Liu et al., 2013; Trujillo-Cabrera et al., 2013). Soil nutrient availability has long been suggested as one of the most important controlling factors affecting the rate of litter decomposition, because decomposers (microorganisms) require nutrients to maintain their activities (Swift et al., 1979; Sinsabaugh et al., 1993). The results in this study showed that the saline-sodic soil was low-nitrogen soil (total N 0.60–1.41 $g \cdot kg^{-1}$) (*Table 1*). In such soil, the decomposers, i.e. cellulolytic microorganisms, are likely to develop strategies to overcome low-nitrogen and sustain cellulolytic activities.

Especially, members of the genus *Streptomyces* were higher abundant nitrogen fixing cellulolytic microorganisms in the grassland soil. Nitrogen fixing genes in actinobacteria have been presumed to have a narrow distribution, mostly restricted to the genus Frankia (Gtari et al., 2012). So far, only one nitrogen fixing heterotrophic *Streptomyces* strain from the arid soils in South Dakota Badlands is documented (Dahal et al., 2017). This is the first known report that cellulolytic *Streptomyces* strains in saline-sodic soils resisted the nitrogen-lacking environment, maintained their cellulolytic process and triggered the recycling of nutrients by the strategy of free nitrogen-fixing.

Nitrogen is the main growth-limiting nutrient for plants and microorganisms. Therefore, bacteria with N-fixation capabilities have a competitive advantage in N-deficient soils (Kennedy et al., 2004). In this study, all the cellulolytic isolates were cellulolytic nitrogen fixing bacteria, which not only decomposed cellulose in saline-sodic condition, but also exhibited nitrogen-fixation activities ranging from 10.80 to 25.98 nmol $C_2H_4 \cdot h^{-1} \cdot ml^{-1}$ (*Figure 4B*). This is most likely a typical adaptive and evolutionary paradigm that soil cellulolytic microorganisms adopted to low-nitrogen in saline-sodic environment. Previous studies also showed that the coastal saline soils can provide conducive conditions for N_2 fixation (Sengupta and Chaudhuri, 1991), and N_2 fixation can be a significant source of nitrogen in the coastal saline habitats (Welsh et al., 1996; Reef et al., 2010). In our studied soils, the cellulolytic bacteria meet their nitrogen requirements for cellulolytic processes by nitrogen fixation when growing in a cellulose-rich and low-nitrogen environment. All the isolates displayed detectable acetylene reduction activity with the highest activity reaching 25.98 nmol $C_2H_4 \cdot h^{-1} \cdot ml^{-1}$ (*Figure 4B*),

http://www.aloki.hu ● ISSN 1589 1623 (Print) ● ISSN1785 0037 (Online)
DOI: http://dx.doi.org/10.15666/aeer/1902_867879
© 2021, ALÖKI Kft., Budapest, Hungary

in agreement with those of several earlier studies on nitrogen fixing bacteria, signifying their ability to grow on low-nitrogen habitats (Sengupta and Chaudhuri, 1991; Unkovich and Baldock, 2008). Meanwhile, cellulolytic bacteria are considered to be the major drivers of litter decomposition and play critical roles in soil conditioning and nutrient cycling. In this sense, the cellulolytic nitrogen fixing bacteria is "the impeller and operator" of the nutrients recycling in low-nitrogen saline-sodic ecosystems. So far, only a few reports were documented on cellulolytic nitrogen-fixing bacteria. Waterbury and coworkers showed that cellulose served as the growth substrate for a nitrogen-fixing aerobic bacterium that existed in symbiotic relation with shipworms (Waterbury et al., 1983). Leschine et al. (1988) also reported four trains of nitrogen-fixing, cellulose-fermenting bacteria from freshwater mud and soil. These studies agree with our result that the nitrogen-fixing cellulolytic bacteria could hold competitive advantages in a situation of cellulose-rich and N-deficiency.

In addition, production of IAA has been implicated in virtually all aspects of plant growth and development (Teale et al., 2006). Many microorganisms including bacteria and fungi are able to synthesize IAA (Teale et al., 2006). In this study, IAA production in cultures amended with tryptophan was detected in all isolated strains, and the amount produced was dependent upon bacterial isolates. Variation among isolates was found not only among species but also within species, such as the case of *Streptomyces* isolates. The 11 *Streptomyces* isolates showed significantly different quantitative IAA production (*Figure 4B*). In conclusion, all the isolated cellulolytic bacteria exhibited the ability to produce IAA (*Figure 4B*), meaning that synthesis of phytohormones by these cellulolytic bacteria likely played an important role for plant growth in saline-sodic soils. This IAA producing characteristic is likely a typical adaptive paradigm that soil cellulolytic microorganisms respond to oligotrophic saline-sodic environment.

Conclusions

In this study, we isolated unique cellulolytic bacteria capable of nitrogen-fixation from low-nitrogen saline-sodic soils, with higher abundant cellulolytic isolates closely related to *Streptomyces*. These cellulolytic isolates appeared to exhibit nitrogen fixing characteristic. This is the first known report that cellulolytic bacteria in low-nitrogen soil environment exhibited nitrogen-fixing activities as a potential strategy for adaptation to nitrogen limitation, providing a new insight into potential mechanisms adopted by the microbial community to sustain ecological functions in adverse soil environments. The IAA producing characteristics of all isolates meant that these cellulolytic bacteria likely played an important role for plant growth in saline-sodic grassland.

In our studied saline-sodic soils, the cellulolytic bacteria meet their nitrogen requirements for cellulolytic process by nitrogen fixation. As the vast amounts of cellulose are available in different environments (such as grassland soils, crop field soils. forest soils, and composts), the cellulolytic bacteria with nitrogen-fixing characteristics have obvious competitive advantage over other soil cellulolytic bacteria. So it is possible that the similar adapting mechanisms and specificities for cellulolytic bacteria are widely existing strategies in other cellulose-rich habitats. Furthermore, these cellulolytic nitrogen-fixing bacteria may have a potential use in improving soil fertility and promoting plant growth.

http://www.aloki.hu ● ISSN 1589 1623 (Print) ● ISSN1785 0037 (Online)
DOI: http://dx.doi.org/10.15666/aeer/1902_867879
© 2021, ALÖKI Kft., Budapest, Hungary

Acknowledgements. This research was supported by the National Key Research and Development Program of China (2016YFC0500602).

Data availability. The chimera-checked 16S rRNA gene sequences reported in this paper were deposited to GenBank under the following accession numbers: KX863512.1 (DS-1), KX863718.1 (DS-2), KY007162.1 (DS-3), KY007161.1 (DS-5), KY007163.1–KY007164.1 (DS-6–DS-7), KY007166.1 (DS-10), KY1009689.1 (DS-12), KY007169.1 (DS-13), KY1009687.1 (DS-14), KY007174.1 (S-19), KY007177.1 (DS-22), KY007179.1 (DS-24), KY007181.1 (DS-26), KY007182.1 (DS-29), KY007185.1 (DS-30), KY007188.1 (DS-34).

REFERENCES

[1] Chater, K. F., Biró, S., Lee, K. J., Palmer, T., Schrempf, H. (2010): The complex extracellular biology of Streptomyces. – FEMS Microbiol Rev. 34: 171-198.

[2] Cole, J. R., Chai, B., Marsh, T. L., Farris, R. J., Wang, Q., Kulam, S. A., Chandra, S., McGarrell, D. M., Schmidt, T. M., Garrity, G. M., Tiedje, J. M. (2003): The Ribosomal Database Project (RDP-II): previewing a new autoaligner that allows regular updates and the new prokaryotic taxonomy. – Nucleic Acids Res. 31: 442-443.

[3] Dahal, B., Nandakafle, G., Perkins, L., Brözel, V. S. (2017): Diversity of free-Living nitrogen fixing Streptomyces in soils of the badlands of South Dakota. – Microbiol Res. 195: 31-39.

[4] Gtari, M., Ghodhbane-Gtari, F., Nouioui, I., Beauchemin, N., Tisa, L. (2012): Phylogenetic perspectives of nitrogen-fixing actinobacteria. – Arch Microbiol. 194: 3-11.

[5] Hardy, R. W. F., Burns, R. C., Holsten, R. D. (1973): Applications of acetylene-ethylene assay for measurement of nitrogen fixation. – Soil. Biol. Biochem. 5: 47-81.

[6] Holguin, G., Bashan, Y. (1996): Nitrogen-fixation by Azospirillum brasilense CD is promoted when co-cultured with a mangrove rhizosphere bacterium (Staphylococcus sp.). – Soil Biol. Biochem. 28: 1651-1660.

[7] Kennedy, I. R., Choudhury, A. T. M. A., Kecskés, M. L. (2004): Non-symbiotic bacterial diazotrophs in crop-farming systems: can their potential for plant growth promotion be better exploited? – Soil Biol Biochem. 36(8): 1229-1244.

[8] Leveau, J. H. J., Lindow, S. E. (2005): Utilization of the plant hormone indole-3-acetic acid for growth by Pseudomonas putida strain 1290. – Appl. Environ Microbiol. 71(5): 2365-2371.

[9] Liu, P., Huang, J., Han, X., Sun, O. J., Zhou, Z. (2006): Differential responses of litter decomposition to increased soil nutrients and water between two contrasting grassland plant species of Inner Mongolia, China. – Appl. Soil Ecol. 34: 266-275.

[10] Liu, S. H., Kang, Y. H., Wan, S. Q., Jiang, S. F., Liu, S. P., Sun, J. X. (2013): Effect of drip irrigation on soil nutrients changes of saline-sodic soils in the Songnen plain. – Paddy Water Environ. 11: 603-610.

[11] Mandels, M. (1975): Microbial sources of cellulase. – Biotechnol. Bioeng. Symp. 5: 81-105.

[12] Miller, G. L. (1969): Use of dinitrosalicylic acid reagent for determination of reducing sugar. – Anal Chem. 31: 426-428.

[13] Orhan, F., Gulluce, M. (2015): Isolation and characterization of salt-tolerant bacterial strains in salt-affected soils of Erzurum, Turkey. – Geomicrobiol. J. 32: 521-529.

[14] Poly, F., Ranjard, L., Nazaret, S., Gourbière, F., Monrozier, L. J. (2001): Comparison of nifH gene pools in soils and soil microenvironments with contrasting properties. – Appl. Environ. Microb. 67: 2255-2262.

[15] Reef, R., Feller, I. C., Lovelock, C. E. (2010): Nutrition of mangroves. – Tree Physiol. 30: 1148-1160.

[16] Rengasamy, P. (2006): World salinization with emphasis on Australia. – J. Exp. Bot. 57: 1017-1023.

http://www.aloki.hu ● ISSN 1589 1623 (Print) ● ISSN1785 0037 (Online)
DOI: http://dx.doi.org/10.15666/aeer/1902_867879
© 2021, ALÖKI Kft., Budapest, Hungary

[17] Schimel, J. P., Weintraub, M. N. (2003): The implications of exoenzyme activity on microbial carbon and nitrogen limitation in soil: a theoretical model. – Soil Biol. Biochem. 35: 549-563.
[18] Schlatter, D., Fubuh, A., Xiao, K., Hernandez, D., Hobbie, S., Kinkel, L. (2009): Resource amendments influence density and competitive phenotypes of Streptomyces in soil. – Microb. Ecol. 57: 413-420.
[19] Sengupta, A., Chaudhuri, S. (1991): Ecology of heterotrophic dinitrogen fixation in the rhizosphere of mangrove plant community at the Ganges river estuary in India. – Oecologia 87: 560-564.
[20] Shiau, Y. J., Lin, M. F., Tan, C. C., Tian, G. L., Chiu, C. Y. (2017): Assessing N2 fixation in estuarine mangrove soils. – Estuar Coast Shelf S. 189: 84-89.
[21] Sinsabaugh, R. L., Antibus, R. K., Linkins, A. E., McClaugherty, C. A., Rayburn, L., Repert, D., Weiland, T. (1993): Wood decomposition: nitrogen and phosphorus dynamics in relation to extra cellular enzyme activity. – Ecology 74: 1586-1593.
[22] Sistla, S. A., Asao, S., Schimel, J. P. (2012): Detecting microbial N-limitation in tussock tundra soil: implications for arctic soil organic carbon cycling. – Soil Boil. Biochem. 55: 78-84.
[23] Swift, M. J., Heal, O. W., Anderson, J. M. (1979): Decomposition in terrestrial ecosystems. – Berkeley: University of California Press.
[24] Tamura, K., Dudley, J., Nei, M., Kumar, S. (2007): MEGA4: molecular evolutionary genetics analysis (MEGA) software version 4.0. – Mol. Biol. Evol. 24: 1596-1599.
[25] Thompson, J. D., Gibson, T. J., Plewniak, F., Jeanmougin, F., Higgins, D. G. (1997): The CLUSTAL_X windows interface: flexible strategies for multiple sequence alignment aided by quality analysis tools. – Nucleic Acids Res. 25: 4876-4882.
[26] Thompson, B. J., Widdick, D. A., Hicks, M. G., Chandra, G., Sutcliffe, I. C., Palmer, T., Hutchings, M. I. (2010): Investigating lipoprotein biogenesis and function in the model Gram-positive bacterium Streptomyces coelicolor. – Mol Microbiol. 77(4): 943-956.
[27] Tripathi, S., Kumari, S., Chakraborty, A., Gupta, A., Chakrabarti, K., Byapadhyay, B. K. (2006): Microbial biomass and its activities in salt-affected coastal soils. – Biol. Fert. Soils 42: 273-277.
[28] Trujillo-Cabrera, Y., Ponce-Mendoza, A., Vásquez-Murrieta, M. S., Rivera-Orduña, F. N., Wang, E. T. (2013): Diverse cellulolytic bacteria isolated from the high humus, alkaline-saline chinampa soils. – Ann Microbiol. 63: 779-792.
[29] Ulrich, A., Klimke, G., Wirth, S. (2008): Diversity and activity of cellulose- decomposing bacteria, isolated from a sandy and a loamy soil after long-term manure application. – Microb. Ecol. 55(3): 512-522.
[30] Unkovich, M., Baldock, J. (2008): Measurement of asymbiotic N2 fixation in Australian agriculture. – Soil Biol. Biochem. 40: 2915-2921.
[31] Wang, Z. C., Li, Q. S., Li, X. J., Song, C. C., Zhang, G. X. (2003): Sustainable agriculture development in saline-alkali soil area of Songnen plain, northeast China. – Chin. Geogr. Sci. 13: 171-174.
[32] Waterbury, J. B., Calloway, C. B., Turner, R. D. (1983): A cellulolytic nitrogen-fixing bacterium cultured from the gland of deshayes in shipworms (bivalvia: teredinidae). – Science 221: 1401-1403.
[33] Welsh, D. T., Bourgues, S., de Wit, R., Herbert, R. A. (1996): Seasonal variations in nitrogen-fixation (acetylene reduction) and sulphate-reduction rates in the rhizosphere of Zostera noltii: nitrogen fixation by sulphate reducing bacteria. – Mar. Biol. 125: 619-628.
[34] Xin, W. D., Yin, X. Q., Song, B. (2012): Contribution of soil fauna to litter decomposition in Songnen sandy lands in northeastern China. – J. Arid Environ. 77: 90-95.
[35] Xu, J. X., Wang, X. F., Hu, L., Zhen, J. X., Xu, W. N., Dai, B. L., Wu, B. (2015): A novel ionic liquid-tolerant Fusarium oxysporum BN secreting ionic liquid-stable cellulase: Consolidated bioprocessing of pretreated lignocellulose containing residual ionic liquid. – Bioresour Technol. 181: 18-25.

http://www.aloki.hu ● ISSN 1589 1623 (Print) ● ISSN1785 0037 (Online)
DOI: http://dx.doi.org/10.15666/aeer/1902_867879
© 2021, ALÖKI Kft., Budapest, Hungary

[36] Yan, N., Marschner, P. (2012): Response of microbial activity and biomass to increasing salinity depends on the final salinity, not the original salinity. – Soil Biol. Biochem. 53: 50-55.
[37] Yan, N., Marschner, P. (2013): Response of soil respiration and microbial biomass to changing EC in saline soils. – Soil Biol. Biochem. 65: 322-328.
[38] Zenova, G. M., Manucharova, N. A., Zvyagintsev, D. G. (2011): Extremophilic and extremotolerant actinomycetes in different soil types. – Eurasian Soil Sci. 44: 417-436.
[39] Zhang, Y., Zamudio Cañas, E. M., Zhu, Z. E., Linville, J. L., Chen, S., He, Q. (2011): Robustness of archaeal populations in anaerobic co-digestion of dairy and poultry wastes. – Bioresour Technol. 102: 779-785.
[40] Zhang, N. Y., Guo, R., Song, P., Guo, J. X., Gao, Y. Z. (2013): Effects of warming and nitrogen deposition on the coupling mechanism between soil nitrogen and phosphorus in Songnen Meadow Steppe, northeastern China. – Soil Biol. Biochem 65: 96-104.
[41] Zhao, Y. N., Yang, B., Li, M. X., Xiao, R. Q., Rao, K. Y., Wang, J. Q., Zhang, T., Guo, J. X. (2019): Community composition, structure and productivity in response to nitrogen and phosphorus additions in a temperate meadow. – Sci. Total. Environ. 654: 863-871.

http://www.aloki.hu ● ISSN 1589 1623 (Print) ● ISSN1785 0037 (Online)
DOI: http://dx.doi.org/10.15666/aeer/1902_867879
© 2021, ALÖKI Kft., Budapest, Hungary

THE INVESTIGATION OF TOXIC ELEMENT POLLUTION AND RADIOACTIVITY ANALYSES OF MARINE SEDIMENTS IN THE GULF OF GEMLIK (BURSA, TURKEY)

YÜMÜN, Z. Ü.[1*] – KAM, E.[2] – DINÇER, A. R.[1] – ÖNCE, M.[1] – YÜMÜN, S.[1]

[1]*Environmental Engineering Department, Çorlu Engineering Faculty, Namık Kemal University, 59860 Çorlu, Tekirdağ, Turkey*
(e-mail: adincer@nku.edu.tr; melike-once@hotmail.com; sevinc.yumun@gmail.com)

[2]*Physics Department, Faculty of Arts and Sciences, Yildiz Technical University, Davutpaşa Campus, 34220 Esenler/İstanbul, Turkey*
(e-mail: erolkam@yildiz.edu.tr)

**Corresponding author*
e-mail: zyumun@nku.edu.tr

(Received 4th Sep 2020; accepted 19th Jan 2021)

Abstract. In this study, the Toxic element pollution and radioactivity of marine sediments in the Gulf of Gemlik was determined. Enrichment factor (EF) and Pollution index (PI) analyses have been applied to determine toxic element pollution. According to the enrichment factor results, the EFNi in BH-1 was between 3 < EFNi < 5, and the other EF values are all below 3. In radionuclide analysis, the Ra-226 and Th-232 values were found to be below the global average value in all locations. It is estimated that the K-40 values, which are above the world average values in the BH-1 drillings, are due to the intensive agricultural activities in that part of the study area. Cs-137 values were found to be 5.3 Bq/kg in the BH-1/1 drilling location. This finding is very important in terms of environmental pollution. In other locations, samples have been found to be below the Cs-137 MDA. The K-40 value has been found to be the highest in Kurşunlu. The Th-232 value has been found to be highest in Fıstıklı, which was below the world average value. There is a parallel between Pollution Index, Enrichment Factor and Radioactivity analysis.
Keywords: *Marmara Sea, Gemlike, elements, radioactive pollution, enrichment factors, Holocene sediment*

Introduction

Industrial development has increased rapidly in the last hundred years and consumption has also risen at the same rate. The increase in consumption has increased the amount of waste and has also caused environmental pollution. With the use of fossil fuels and uncontrolled agriculture (over-application of fertilizer and use of pesticides) the discharge of solid, liquid and gas wastes enter to environment without decontamination, and anthropogenic pollution start to occur in the natural environment.

A specific term for pollution by humans was defined for the first time in 1922 by Alexei Petrovich Pavlov as “anthropogenic pollution” (Bampton, 1999). Toxic matters (heavy metals, natural and artificial radionuclides) derive from anthropogenic pollution sources are significantly dangerous to the environment due to their toxic effects and their accumulation in living things (Omgbu and Kokogbo, 1993).

Gemlik, which is located in the South of the Marmara Region, is one of the developed districts of Bursa with an area of 413 km² (Koday and Baki, 2014). Gemlik Bay was formed during the late Pliocene-Early Pleistocene on the central branch of the

http://www.aloki.hu ● ISSN 1589 1623 (Print) ● ISSN 1785 0037 (Online)
DOI: http://dx.doi.org/10.15666/aeer/1902_881900
© 2021, ALÖKI Kft., Budapest, Hungary

North Anatolian Fault (NAF). The gulf is an 11 × 36 km pull-apart basin developed in the east-west direction with right lateral strike-slip faults. The deepest part of the gulf is -113 m, and the gulf forms a closed basin (Ünlü and Alpar, 2006). The area is polluted by many industrial and domestic wastes and is at risk of anthropogenic pollution, as it is a closed basin. In regard to anthropogenic pollution sources, in the vicinity of Gemlik Bay, there is a high density of industry, including manufacturing plants for textiles, metals, refineries, food (olive and olive oil), soap and cement (Alpar et al., 2006). The most important feature of Gemlik Bay which is located on south Marmara shelf is the separation from Marmara pit with a ridge which is 50 m deep. There are many faults in Gemlik Bay that are compatible with the faults on the land, and some of them control the formation of the bay. Apart from the resources in Gemlik and the Armutlu Peninsula, there are many thermal mineral water sources in the investigated area (Meriç et al., 2005). There are also several ports to the south of the bay. Ports have regional, national and international strategic importance. Various scientific studies have been done in the past years regarding heavy metal and radioactive pollution (Yümün, 2017; Yümün and Önce, 2017; Kam and Önce, 2016; Meriç et al., 2005; Akçay et al., 2003; Okuş et al., 2007; Ünlü and Alpar, 2006). In his study of Yümün (2017), the effect of heavy metal pollution on foraminifera in the Western Marmara Sea (Turkey), is investigated the effects of heavy metals on the foraminiferal assemblages of Holocene deposits in the West Sea of Marmara. The effects of the Quaternary foraminiferal assemblages and heavy metals on foraminifera were investigated by Yümün and Önce (2017). In some stations, shell anomalies were observed in foraminifera, and the chemical, physical, biological and geological environmental conditions as well as heavy metals and biochemical parameters were investigated. Akçay et al. (2003) investigated heavy metal pollution levels in Turkey's economically important Gediz and Büyük Menderes River. Gao and Chen (2012) investigated metal pollution in Bohai Bay in the Bohai Sea. Okuş et al. (2007) stated that Gemlik Bay is polluted by heavy metals and other pollutant groups due to domestic and industrial waste waters. Ünlü and Alpar (2006) investigated the grain-size distribution of Gemlik Bay surface sediments, organic carbon content, heavy metal pollution and PAH distribution. In this study, no significant correlation was observed between total organic carbon content and PAH concentrations. Kam and Önce (2016) determined the heavy metal concentrations in the existing sediments to the southwest of the Marmara Sea.

In this study, heavy metal and radioactive pollution of Gemlik Bay and its surroundings have been investigated. In addition, using the Fe, Zn, As, Co, Cu, Mn, Ni and Pb heavy metal concentrations, an enrichment factor (EF) has been calculated. Further, natural and artificial radionuclides have been measured by radiological analyses. Using the measured radionuclides, the natural radioactivity results of Gemlik Bay and its surroundings have been determined. Gemlik Bay is a very active region in terms of industry and ship traffic. In addition, urbanization and tourism facilities are quite high in this region. This study was conducted to draw attention to the effects of heavy metal and radioactivity contamination due to maritime traffic and industry on human environment.

While some of the previous studies (Yümün, 2017; Yümün and Önce, 2017; Meriç et al., 2005; Akçay et al., 2003; Okuş et al., 2007; Ünlü and Alpar, 2006; Gao and Chen, 2012; Omgbu and Kokogbo, 1993; Koday and Baki, 2014; Bampton, 1999) were taken as a reference in terms of method, some studies (Yümün, 2017; Kam and Önce, 2016; Alpar et al., 2006) were taken as reference because they were conducted in the Marmara

http://www.aloki.hu ● ISSN 1589 1623 (Print) ● ISSN 1785 0037 (Online)
DOI: http://dx.doi.org/10.15666/aeer/1902_881900
© 2021, ALÖKI Kft., Budapest, Hungary

Sea. Previous studies conducted in the Marmara Sea do not include Gemlik-Bandırma Bays. Comparison of the values obtained from previous studies (Heavy metals, radioactivity and foraminifers) with this study aims to compare different regions of the Marmara Sea.

Materials and methods

In the study, 46 samples have been collected from two boreholes (BH-1 and BH-2) in 2016 and four Core-Box samples (Core-1, Core-2, Core-3 and Core-4) have been collected from Gemlik Bay in 2019. Drilling samples were taken from boreholes at sea floor to depth by rotary method using hydraulic machines. With the Core-Box method, Core samples were taken with free fall up to a maximum depth of 1 m. All of the core samples and the upper slime and current sediment sections of the drilling samples are discharged at 10 cm intervals. In order to avoid any difficulties in the sieve analysis of the samples taken, the sample amount is taken between 10-20 grams.

The working area location and sample points are shown in *Figure 1* and the sample coordinates are shown in *Table 1*. For geochemical analysis the samples were first milled. Geochemical analysis of these ground samples for the following elements (Fe, Zn, Al, Mn, As, B, Cd, Co, Cr, Cu, Ni, Na, Mg, K, Ca, P, Bi, Mo, Pb, Pt, Sb, Sn, Se and Hg) was carried out using the SPECTROBLUE model Induced Matched Plasma-Optic Emission Spectrometer (ICP-OES) device at NABİLTEM (Namık Kemal University Central Research Laboratory). In laboratories, the samples are analyzed with ICP-OES devices after being dissolved by the method (king water method, triple acid method, melting method, TS ISO 14869-1, TS ISO 14869-2 etc.) suitable for the analysis to be performed (TSE, 2004a, b).

Table 1. *BH and core sample coordinates*

Sample No	The dates of sample collection	Coordinates		Water depth (m)	Sample size (m)
		Longitude (North)	Latitude (East)		
GMK-1 (BH-1)	10.10.2016	40° 27.498’	28° 58.104’	27.00	12.80
GMK-2 (BH-2)	15.0.2016	40° 27.513’	29° 5.479’	35.60	13.30
CORE-1	01.05.2019	40° 27.888’	29° 1.797’	81.00	0.70
CORE-2	01.05.2019	40° 27.943’	28° 52.497’	75.00	1.00
CORE-3	01.05.2019	40° 22.500’	28° 59.678’	98.00	1.00
CORE-4	01.05.2019	40° 25.769’	29° 8.317’	12.00	1.00

The element concentrations obtained by geochemical analysis were evaluated with the Pollution Index (PI) method, and the pollution conditions of the sample locations were obtained. The pollution situation map of Gemlik Bay was prepared by using the PI values and the Kriging Method. Kriging is an advanced geostatistical procedure that generates an estimated surface from a scattered set of points with z-values. The kriging method is a geostatistical method that provides the creation of density maps by statistically evaluating the positions of the measured points in the field. It is a method that quantifies the distances between points by interpolation method in both horizontal and vertical directions.

http://www.aloki.hu ● ISSN 1589 1623 (Print) ● ISSN 1785 0037 (Online)
DOI: http://dx.doi.org/10.15666/aeer/1902_881900
© 2021, ALÖKI Kft., Budapest, Hungary

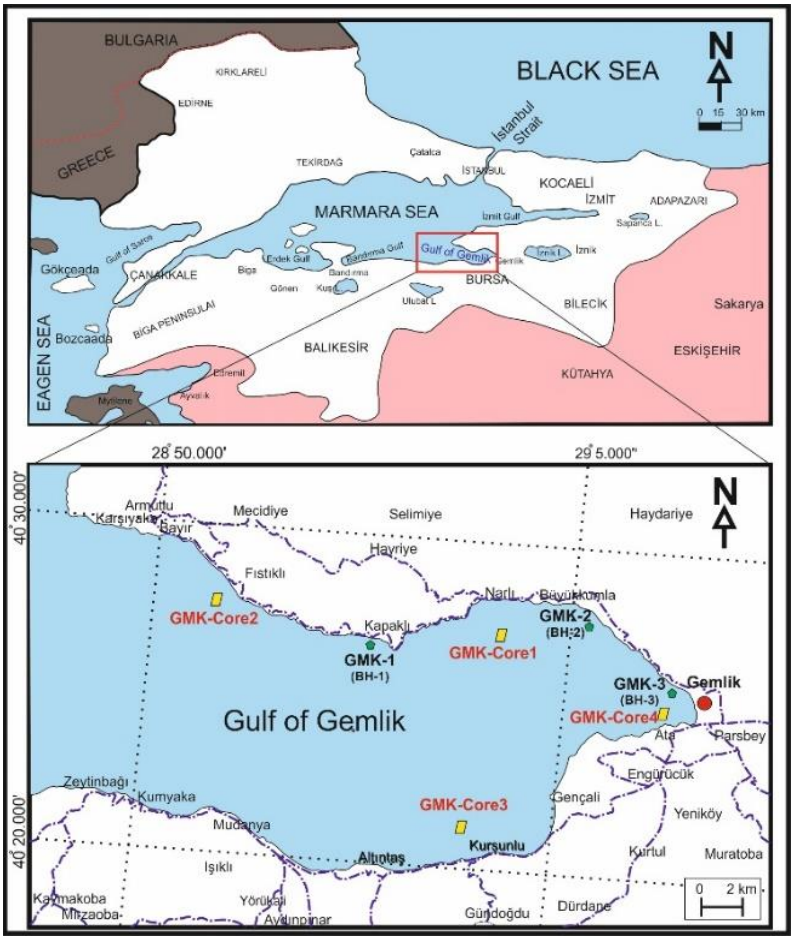


Figure 1. *Location map of investigation area*

The normalized enrichment factor (EF) was widely used in many studies (Buat-Menard, 1979; Hornung et al., 1989; Dickinson et al., 1996; Pekey, 2006) to determine anthropological effects on sediments. In this study, using the results of the heavy metal analysis, the enrichment factor (EF) of the metals (Zn, As, Co, Cu, Ni, Pb and Mn) has been calculated. The enrichment factor is a widely used value in the evaluation of different environments over time and in the calculation of anthropogenic additives in metal pollution (Morillo et al., 2002; Adamo et al., 2005; Valdés et al., 2005). The enrichment factor is calculated by using the following formula:

$$EF = (Cn/Cref)/(Bn/Bref) \quad \text{(Eq.1)}$$

In this formula, EF is the enrichment factor, Cn is the metal value measured in the study, Cref is the value of the working metal in the reference medium (Shell), Bn is the measured value of the reference element in operation and Bref is the value of the reference element in the reference environment (Shell).

In the calculation and evaluation of this factor, unlike other pollution indices, normalization is performed by selecting a reference element. Although there is no definite acceptance in the selection of the element to be used for normalization, it is generally used in geochemically inactive materials such as aluminium, iron, lithium, zirconium and titanium, which can be easily encountered in fine-grained materials

http://www.aloki.hu ● ISSN 1589 1623 (Print) ● ISSN 1785 0037 (Online)
DOI: http://dx.doi.org/10.15666/aeer/1902_881900
© 2021, ALÖKI Kft., Budapest, Hungary

(Reinmann et al., 2000; Schiff and Weisberg, 1999; Sutherland, 2000; Ray et. el., 2006; Huerta-Diaz et al., 2008; Essien et al., 2009; Mohiuddin et al., 2010; Zhang et al., 2011; Galuszka et al., 2014; Park et al., 1997; Feng et al., 1998; Baptista Neto et al., 2000; Esen et al., 2008; Taylor et al., 1995).

Within the scope of this study, the element iron has been considered as a reference element due to its lack of large variations in the cores. In addition, natural environmental and artificial radioactivity results of Gemlik Bay and its surroundings have been determined by radionuclide analyses. In this study, ASTM E181- 98 (2003) Standard Test Methods were used for Detector Calibration and Analysis of Radionuclides. For radionuclide analysis, samples have been first prepared for radioactive analysis at room temperature in a laboratory environment.

The radioactivity analyses of the samples were carried out in the TAEK (Technology Development Department Analytical Measurement Unit). Samples were first passed through a 100-micron sieve to a fine powder. The powdered samples were placed in 1000 ml Marinelli flasks and sealed to prevent contact with air. After weighing, the samples were stored for radioactive equilibrium between radium, thorium and other degradation products for 40 days (Yümün and Kam, 2017). Gamma spectrometry analysis of the sediment was performed with a coaxial high purity germanium compound HPGe detector (Canberra GX5020).

Results

Vertical distribution of sediments in drilling and core samples

The vertical sections of the drillings (BH-1 and BH-2) in the study area are given in *Figure 2,* and the vertical sections of the core samples (Core-1, 2, 3 and 4) are given in *Figures 3* and *4*. The samples in the BH-1 are brown-grey, sandy clay, grey-coloured in the middle, sandy-silty clay with high water content and fine, blackish-grey sandy clay at the highest level. The samples in the BH-2 are greenish grey, mollusc shale and clay-cemented sandy silt and sandy clay, blackish medium sand and silty clay in the middle and blackish-grey, clayey fine sand at the highest level.

The Core-1 section contains dark grey coloured, high water content, fine sandy, silty clay. the Core-2 section contains dark grey coloured, high water content, fine sandy, sandy clay. The Core-3 section contains grey coloured, high water content, fine sandy, silty clay and the Core-4 section contains dark grey coloured, mollusc shale with interbedded fine sand, sandy clay. Drilling samples were taken during drilling and core samples were obtained from the highest levels of the ground section.

Toxic element analysis of drilling and core samples by geochemical analysis

Geochemical analysis results for BH-1, BH-2 and core samples are given in *Tables 2, 3, 4* and *5*. According to the results, Hg measured 0 ppm at all levels in BH-1 drillings. The concentration values of Zn, As, B, Cd, Co, Cr, Cu, Ni Pb, Pt and Sb are between 0 and 300 ppm, and these elements are defined as first group elements.

The concentration values of Na, Mg, K, Ca, P, S, Fe, Al and Mn are determined to be > 300 ppm, and these elements are evaluated as the second group (*Tables 2, 3, 4* and *5*). The 300 ppm limit value was used for the first time in this study, and it facilitates the graphical representation of the analysis results. In future studies, taking into account the measurement ranges, it can be taken as a value greater or less than 300 ppm.

http://www.aloki.hu ● ISSN 1589 1623 (Print) ● ISSN 1785 0037 (Online)
DOI: http://dx.doi.org/10.15666/aeer/1902_881900
© 2021, ALÖKI Kft., Budapest, Hungary

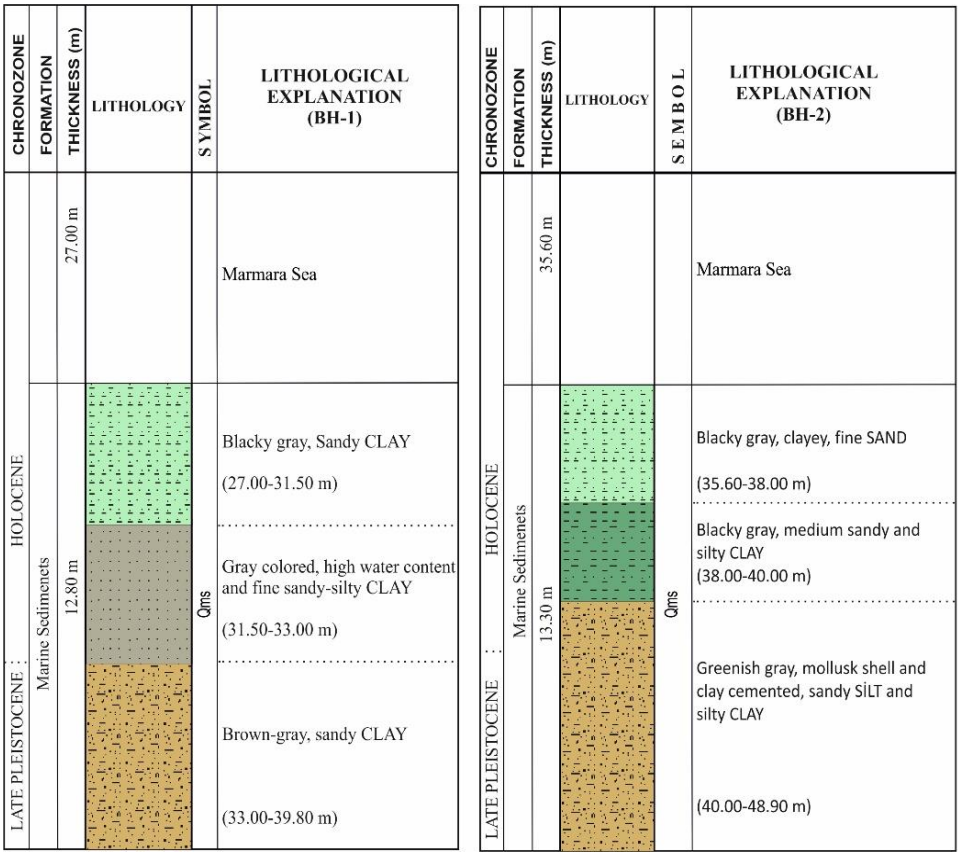


Figure 2. *Vertical distribution of current sediments in BH-1 and BH-2 locations*

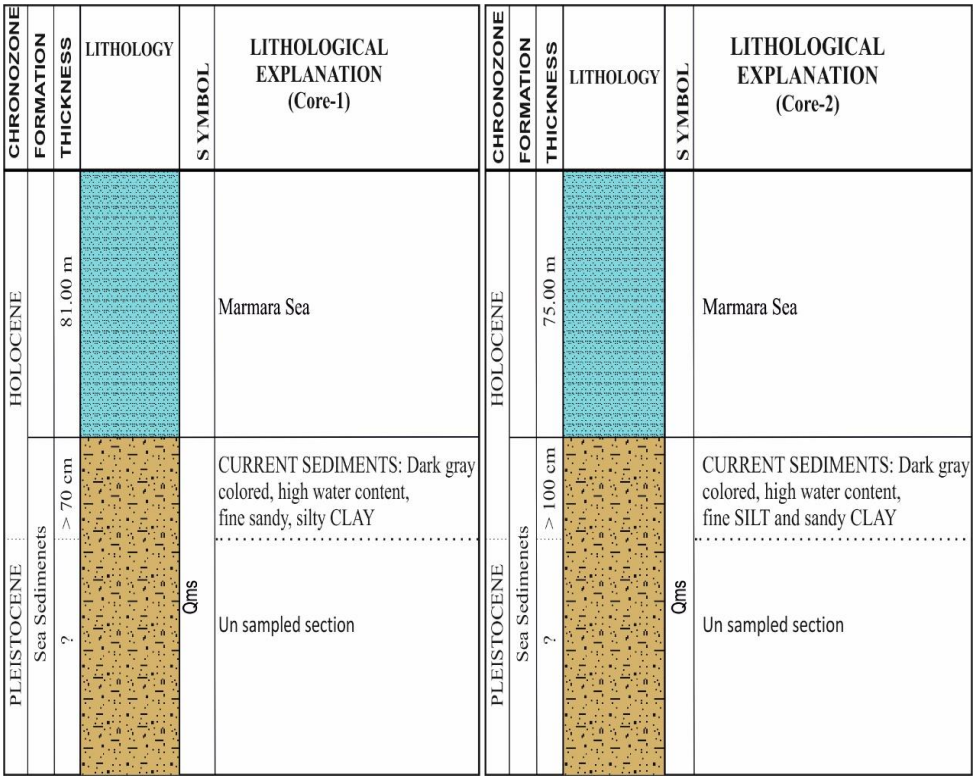


Figure 3. *Vertical distribution of current sediments in CORE-1 and CORE-2 locations*

http://www.aloki.hu ● ISSN 1589 1623 (Print) ● ISSN 1785 0037 (Online)
DOI: http://dx.doi.org/10.15666/aeer/1902_881900
© 2021, ALÖKI Kft., Budapest, Hungary

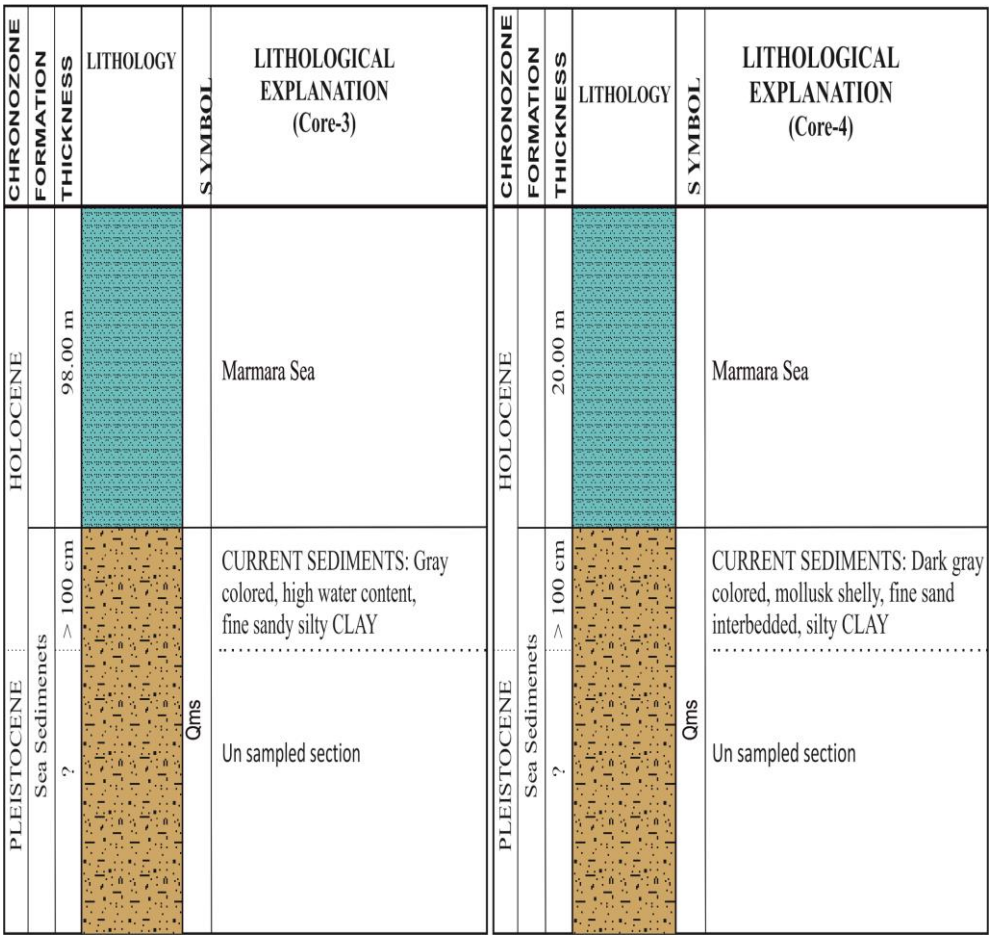


Figure 4. *Vertical distribution of current sediments in CORE-3 and CORE-4 locations*

There are urban settlements on the shores of the sample locations (locations of drilling and core samples) of the Marmara Sea. This shows that the main responsible for heavy metal pollution are agricultural activities and urban settlements. In the drilling and core sample locations, it was found that the concentrations of the first group elements have been lower in the deep and relatively higher in the surface samples. It was also observed by Yümün (2017) and Yümün and Önce (2018) that the concentrations of some of the first group elements are high at the upper levels of the borehole and relatively lower at the depths. The use of these elements in agricultural fertilizers and pesticides in the current period is seen as a reason for this situation. In addition, it is an important reason for the high level of industrial wastes in the current period.

To evaluate the spatial (horizontal) distribution of the first and second groups of elements, each of the drilling samples was calculated by itself. The mean values of the core samples were calculated separately for each sample. At the concentration values of the second group of elements, there is not much differentiation from the upper level to the lower level of the drilling and cores. As a result, Max./Min./ and average value of firs group elements respectively are (Zn:152.60/74.20/120.10; As: 5.57/0.59/3.23; B: 30.99/12.01/19.63; Cd: 1.71/0.94/1.158; Co: 18.03/5.98/12.9; Cr: 13.28/4.70/8.93; Cu:55.56/17.83/38.3; Ni:18.76/7.25/12.6; Pb: 40.33/20.82/32.4; Pt: 1.41/0.51/0.93; Sb: 1.28/0.39/0.91; Hg: 0/0/0) in GMK-1.

http://www.aloki.hu ● ISSN 1589 1623 (Print) ● ISSN 1785 0037 (Online)
DOI: http://dx.doi.org/10.15666/aeer/1902_881900
© 2021, ALÖKI Kft., Budapest, Hungary

Another result achieved, Max./Min./ and average value of first group elements respectively are GMK-2 (Zn: 96.50/66.70/81.88; As:9.58/1.59/5.067; B:39.40/15.36/30.265; Cd: 2.09/0.81/1.319; Co: 23.94/14.00/19.04; Cr: 97.67/49.43/78.72; Cu: 65.80/31.66/49.61; Ni: 146.12/ 62.29/106.11; Pb: 11.79/1.66/6.88; Pt: 1.64/0.71/1.054; Sb: 1.89/0.71/1.265; Hg: 0.74/0.00/0.14) in GMK-2. As the results of GMK-2 samples, Max./Min./ and average value of second group elements respectively are (Al: 18770.80/8292/ 13978.89; Ca: 10833.60/5071.40/6485.45; Fe: 34471.90/14008.90/25790.82; K: 3174.80/1223.30/2303.54: Mg: 5981.90/3300.20/4957.90; Mn: 491.60/283.70/386.75; Na: 3998.70/717/2253.48; P: 225.40/108.10/178.62; S: 8473.60/2384.30/4701.51) in GMK-1. Another result achieved, Max./Min./ and average value of second group elements respectively are (Al: 18884.80/9690.40/15429.49: Ca: 32119.50/5116.40/10300.23; Fe: 38680.50/25373.90/ 33341.11; K: 7493.50/4070.80/5287.81; Mg: 12774.10/8236.10/11278.92; Mn: 567.30/290.30/397.93; Na: 8216.80/3803.40/5557.04; P: 433.40/214.50/331.52; S: 5576.20/1434.90/3002.35) in GMK-2.

In addition, the arithmetic mean of each measurement value for each element was calculated (*Table 4* and *Fig. 5*). As a result of these calculations, Zn, As, B, Cd, Cr, Ni, Pt and Hg values, which are supposed to spread to the environment as a result of agricultural activities, are at the highest levels in Core-1. Zn, As, B, Cr, Ni and Hg values in Core-2 are higher than the average values. The values of Zn, B, Cd, Ni and Pb in the GMK-2 drilling are higher than the average values.

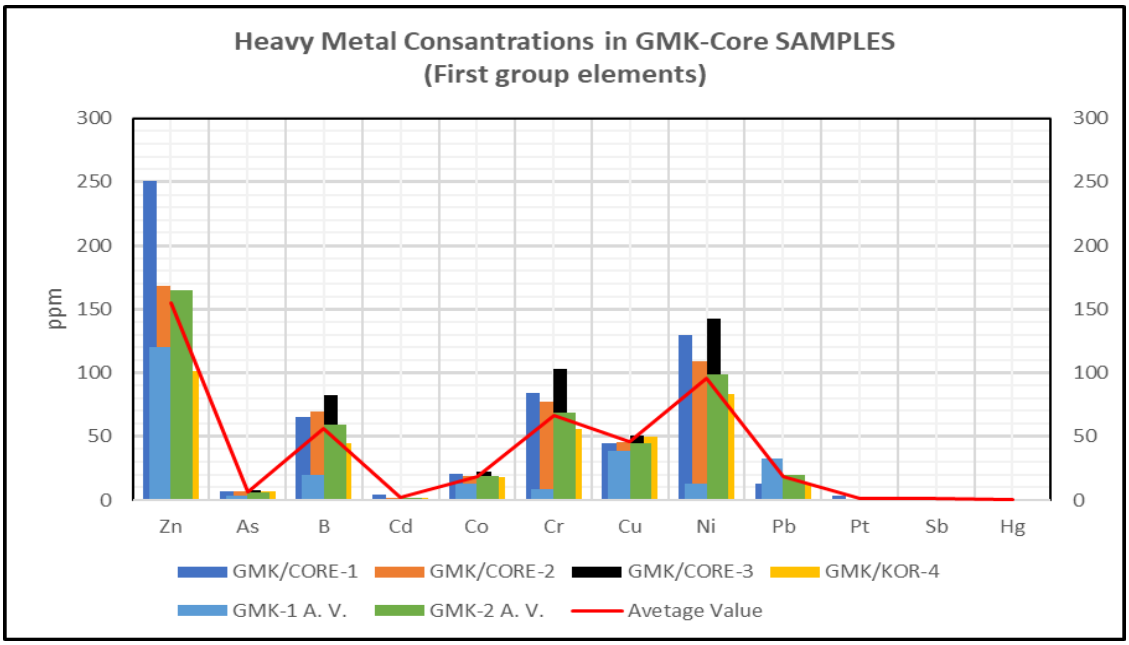


Figure 5. *Heavy metal concentrations in GMK-core samples (first group elements)*

Al, Ca, Fe, K, Mg, Mn and P values of the second group are the highest values in the Core-1, Core-2 and Core-3 locations (*Table 5* and *Fig. 6*). In the Core-4 Location, Na, Mn and P values are highest. High values in the core locations indicate that the heavy metal density in the current period is higher than those of the previous periods. The average values of the drilling samples represent older periods than today because the

http://www.aloki.hu ● ISSN 1589 1623 (Print) ● ISSN 1785 0037 (Online)
DOI: http://dx.doi.org/10.15666/aeer/1902_881900
© 2021, ALÖKI Kft., Budapest, Hungary

samples were taken from deeper locations. The fact that the samples representing the current period are rich in heavy metals is an indicator of the presence of mechanisms that pollute the marine environment. Sea transportation in the region and drugs and fertilizers use occurring due to olive cultivation are seen as the main causes of pollution.

Table 2. *Geochemical analysis of the first group elements in BH-1 (GMK-1) and BH-2 (GMK-2) drilling*

Sample No	Zn	As	B	Cd	Co	Cr	Cu	Ni	Pb	Pt	Sb	Hg
	ppm	ppm	ppm	ppm	ppm	ppm	ppm	ppm	ppm	ppm	ppm	ppm
GMK-1/27-28	119.60	5.57	25.58	1.54	15.25	13.28	37.31	18.76	20.82	1.28	1.28	0.00
GMK-1/28-29	98.60	3.68	18.19	0.94	8.87	7.28	21.22	9.82	27.41	0.85	0.83	0.00
GMK-1/29-30	100.90	5.29	30.99	1.06	9.70	7.05	28.39	10.56	37.06	0.97	0.81	0.00
GMK-1/30-31	108.70	3.14	20.60	0.94	10.73	7.51	28.58	9.90	30.48	0.81	0.67	0.00
GMK-1/31-32	129.00	4.39	23.26	1.35	15.37	10.66	42.00	13.89	33.91	0.99	0.39	0.00
GMK-1/32-33	121.90	4.28	24.17	0.96	14.23	8.09	37.86	11.98	40.33	0.75	0.97	0.00
GMK-1/33-34	105.10	2.93	21.34	0.79	10.93	7.85	31.88	10.93	28.15	0.67	0.88	0.00
GMK-1/34-35	74.20	2.09	20.24	0.53	5.98	4.70	17.83	7.25	24.73	0.50	0.75	0.00
GMK-1/35-36	117.40	2.28	12.01	1.19	12.41	7.21	42.06	10.97	36.66	1.12	1.24	0.00
GMK-1/36-37	152.60	0.59	14.43	1.59	18.03	10.74	62.70	15.09	39.19	1.20	0.82	0.00
GMK-1/37-38	139.90	2.37	14.97	1.15	14.92	9.92	48.67	14.02	36.68	0.94	0.72	0.00
GMK-1/38-39	149.30	1.82	15.31	1.71	17.70	10.98	55.56	15.65	33.53	1.41	1.26	0.00
GMK-1/39-40	144.40	3.55	14.15	1.31	14.22	10.80	43.80	14.40	31.73	0.51	1.20	0.00
Average value of BH-1	**120.1**	**3.23**	**19.63**	**1.158**	**12.9**	**8.93**	**38.3**	**12.6**	**32.4**	**0.93**	**0.91**	**0.00**
GMK-2/35-36	96.50	5.41	36.35	1.94	18.84	80.13	55.06	98.83	11.79	1.58	0.82	0.74
GMK-2/36-37	80.80	4.08	34.07	0.81	18.26	76.92	49.62	95.75	7.36	0.71	1.09	0.00
GMK-2/37-38	73.50	3.28	28.77	1.40	17.40	66.80	44.79	87.42	1.66	0.83	1.27	0.00
GMK-2/38-39	66.70	2.39	21.36	1.10	15.26	57.81	35.50	73.50	3.60	1.00	0.89	0.00
GMK-2/39-40	68.60	1.59	15.36	1.17	14.00	49.43	31.66	62.29	6.61	1.12	1.30	0.00
GMK-2/40-41	74.20	2.69	21.92	1.29	17.95	79.10	46.76	98.81	7.03	0.99	1.89	0.00
GMK-2/41-42	74.10	2.22	20.88	1.43	17.76	70.27	46.73	94.99	5.62	1.30	1.35	0.00
GMK-2/42-43	85.70	7.36	30.01	1.66	20.38	90.95	58.79	120.67	7.15	1.40	1.35	0.70
GMK-2/43-44	80.70	6.15	37.41	0.89	18.98	75.85	50.69	101.65	5.87	0.90	1.65	0.59
GMK-2/44-45	76.50	3.49	35.52	1.34	17.62	74.22	46.96	98.22	2.31	1.09	1.39	0.00
GMK-2/45-46	94.50	8.41	39.40	0.77	22.65	92.16	40.04	124.75	9.78	0.12	0.71	0.00
GMK-2/46-47	89.10	6.42	37.29	1.44	21.39	92.80	60.35	134.43	9.12	1.12	1.22	0.00
GMK-2/47-48	81.10	5.78	27.60	0.83	19.71	83.69	53.13	121.77	9.27	0.82	1.38	0.00
GMK-2/48-49	89.80	7.16	36.24	1.62	21.53	92.96	58.28	132.41	6.65	1.19	1.54	0.00
GMK-2/49-50	96.40	9.58	31.80	2.09	23.94	97.67	65.80	146.12	9.42	1.64	1.12	0.00
Average value of BH-2	**81.88**	**5.067**	**30.265**	**1.319**	**19.04**	**78.72**	**49.61**	**106.11**	**6.88**	**1.054**	**1.265**	**0.14**
Earth crust (Mason and Moore, 1982)	70	1.8	-	-	25	-	55	75	13	-	-	

http://www.aloki.hu ● ISSN 1589 1623 (Print) ● ISSN 1785 0037 (Online)
DOI: http://dx.doi.org/10.15666/aeer/1902_881900
© 2021, ALÖKI Kft., Budapest, Hungary

Table 3. *Geochemical analysis of the second group elements in BH-1 (GMK-1) and BH-2 (GMK-2) drilling*

Sample No	Al	Ca	Fe	K	Mg	Mn	Na	P	S
	ppm	ppm	ppm	ppm	ppm	ppm	ppm	ppm	ppm
GMK-1/27-28	14956.60	9122.70	28954.60	2747.10	5700.60	419.40	3998.70	210.70	3382.80
GMK-1/28-29	10406.10	6094.10	20531.10	1499.10	4048.90	326.60	2605.80	146.80	3786.80
GMK-1/29-30	11701.20	5615.70	22252.60	1918.20	4346.00	348.50	3259.90	132.00	8473.60
GMK-1/30-31	13214.00	5071.40	23189.70	2017.60	4259.30	374.80	2660.90	160.60	5036.90
GMK-1/31-32	18490.00	5329.60	30178.50	3064.60	5981.90	401.80	3368.10	225.40	3605.90
GMK-1/32-33	14658.60	5840.30	25922.40	2326.50	5272.70	377.20	2987.80	185.60	6175.90
GMK-1/33-34	12124.70	10833.60	21336.30	2080.30	4733.70	358.30	2886.10	170.80	4792.70
GMK-1/34-35	8292.00	5761.10	14008.90	1223.30	3300.20	283.70	1814.00	108.10	6098.30
GMK-1/35-36	11580.40	4812.50	24439.50	2116.20	4724.90	370.30	1537.70	175.00	5155.30
GMK-1/36-37	18770.80	5268.20	34471.90	3174.80	5824.20	459.20	962.00	236.00	2384.30
GMK-1/37-38	15727.40	5301.40	28463.60	2581.70	5306.10	397.30	1507.40	201.00	3006.90
GMK-1/38-39	17620.50	6191.10	32291.40	2892.90	5385.50	491.60	717.00	204.30	3912.10
GMK-1/39-40	14183.30	9069.10	29240.20	2302.60	5568.70	419.00	989.90	165.80	5308.10
Average value of BH-1	**13978.89**	**6485.45**	**25790.82**	**2303.45**	**4957.90**	**386.75**	**2253.48**	**178.62**	**4701.51**
GMK-2/35-36	17169.60	10304.30	35698.90	6689.30	11915.10	362.20	8216.80	359.50	2265.80
GMK-2/36-37	15420.50	10497.80	32142.50	5808.40	10678.20	353.70	6168.90	327.30	2099.90
GMK-2/37-38	13726.40	9507.50	31460.80	4437.00	10190.30	342.60	4915.20	307.20	2291.10
GMK-2/38-39	12133.60	6007.20	27949.20	3812.40	9319.00	380.60	4067.50	205.00	4834.10
GMK-2/39-40	9690.40	5204.20	25373.90	2516.70	8236.10	290.30	3803.40	214.50	1640.00
GMK-2/40-41	13146.80	7332.20	31076.80	4070.80	10341.90	375.70	3965.80	271.30	1666.50
GMK-2/41-42	12071.30	7494.80	30204.50	3662.30	10349.80	364.40	4181.10	262.50	1758.70
GMK-2/42-43	15307.30	7442.70	35929.80	4929.40	12081.30	434.50	5297.50	315.80	4463.60
GMK-2/43-44	15440.50	16867.50	33498.40	5820.10	10992.70	415.50	5520.50	574.60	5002.30
GMK-2/44-45	14580.80	14639.20	31457.20	5095.80	10944.60	352.30	5658.50	298.80	4582.80
GMK-2/45-46	21749.60	32119.50	40377.10	6390.50	15475.20	505.40	6893.60	433.40	5576.20
GMK-2/46-47	18108.80	7598.70	36051.30	7493.50	12651.00	408.40	6936.20	336.10	2422.30
GMK-2/47-48	15421.10	6170.80	32852.10	4972.40	10968.30	369.30	5215.10	296.80	2884.80
GMK-2/48-49	18884.80	8200.60	37363.60	7359.90	12774.10	446.70	6810.90	360.40	2112.20
GMK-2/49-50	18590.90	5116.40	38680.50	6258.60	12266.20	567.30	5704.60	409.60	1434.90
Average value of BH-2	**15429.49**	**10300.23**	**33341.11**	**5287.81**	**11278.92**	**397.93**	**5557.04**	**331.52**	**3002.35**

Table 4. *Mean values of Group 1 elements in drilling and core samples*

Sample No	Zn	As	B	Cd	Co	Cr	Cu	Ni	Pb	Pt	Sb	Hg
GMK/CORE-1	250.90	6.66	65.04	3.98	20.74	84.28	45	129.45	13.26	3.49	1.60	0.61
GMK/CORE-2	168.50	7.13	69.54	1.58	18.8	77.27	45.62	109.16	16.34	1.14	1.38	0.65
GMK/CORE-3	121.50	7.76	82.14	0.57	22.32	103.18	50.6	142.67	16.88	0	1.77	0.00
GMK/CORE-4	101.30	6.48	44.60	1.64	18.38	55.82	49.49	83.46	11.73	1.19	1.02	0.00
GMK-1 A. V.	120.10	3.23	19.63	1.158	12.9	8.93	38.3	12.6	32.4	0.93	0.91	0.00
GMK-2 A. V.	165.25	6.19	59.088	1.822	18.69	68.42	44.88	98.47	19.72	1.39	1.42	0.135
Average value of Gulf of Gemlik	**154.59**	**6.24**	**56.67**	**1.79**	**18.64**	**66.317**	**45.648**	**95.97**	**18.39**	**1.36**	**1.35**	**0.233**

http://www.aloki.hu ● ISSN 1589 1623 (Print) ● ISSN 1785 0037 (Online)
DOI: http://dx.doi.org/10.15666/aeer/1902_881900
© 2021, ALÖKI Kft., Budapest, Hungary

Table 5. *Mean values of group-2 elements in drilling and core samples*

Sample No	Al	Ca	Fe	K	Mg	Mn	Na	P	S
Core-1	20103.60	23893.70	37460.90	11050.20	15491.70	954.20	16492.80	365.20	3113.90
Core-2	18861.40	28558.60	34994.70	10293.50	14441.30	561.80	16654.70	322.80	5744.20
Core-3	21236.90	27808.30	39166.50	13499.10	16654.90	817.70	19783.30	418.60	3247.40
GMK/CORE-4	7644.80	11144.10	7754.30	22947.00	538.40	2637.90	35132.30	18475.20	450.50
GMK-1 A. V.	13978.89	6485.446	25790.82	2303.45	4957.90	386.7462	2253.49	178.62	4701.51
GMK-2 A. V.	15429.49	10300.23	33341.11	5287.81	11278.92	397.9267	5557.04	331.52	3002.35
Average value of Gulf of Gemlik	17922.06	19409.26	34150.81	8486.81	12564.94	623.67	12148.27	323.35	3961.87

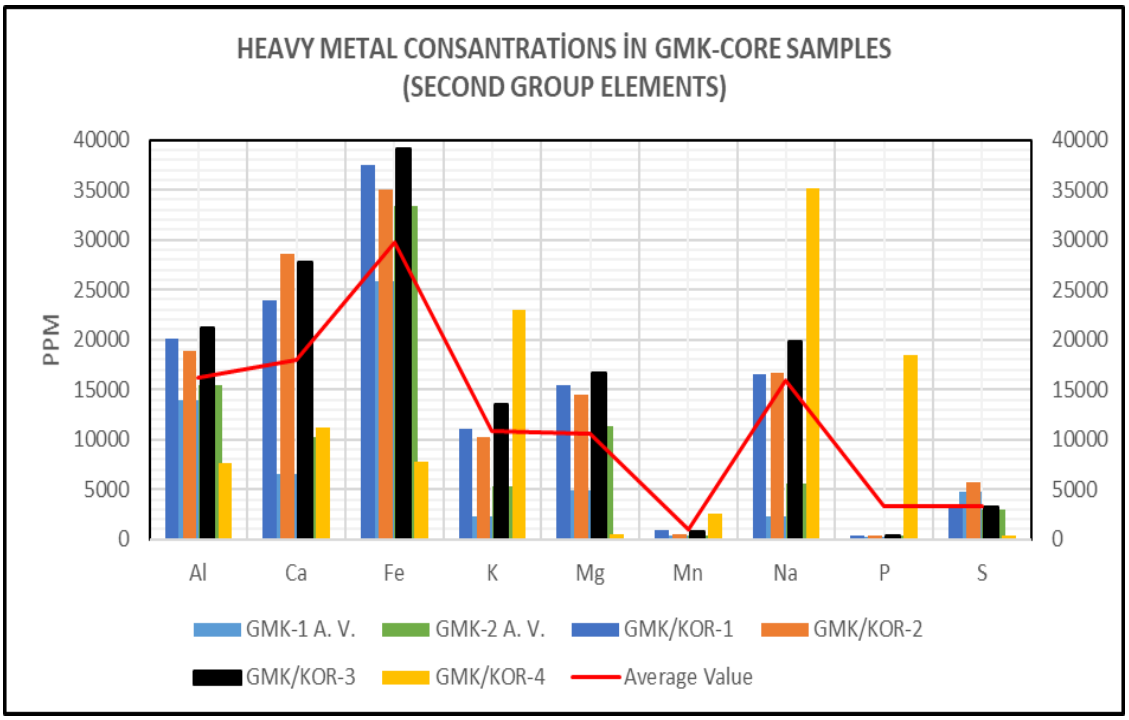


Figure 6. *Mean values of group 2 elements in drilling and core samples*

Evaluation of the pollution of Gemlike Bay with analysis of the pollution index (PI)

An average value, defined as a Pollution Index (PI), was first described by Yümün (2017) in order to simplify the results of geochemical analysis of all core and drilling samples taken from the western part of the Sea of Marmara. This method, which is also considered by many researchers, is used in this study. In the pollution index calculations, the geochemical analysis results of the sediments from the East Marmara Sea have been used. The calculations were performed by dividing the individual totals of the heavy metal measurement values to the total average value by the number of measurements (*Table 6*). In this study, a pollution-zone map was created by the Kriging method to visually evaluate the pollution analysis of Gemlik Bay (*Fig. 7*).

It is seen that PI > 1 in the vicinities of Narlı (Gemlik-Bursa) and Büyükkumla (Gemlik-Bursa) and Kurşunlu, Gemlik Fıstıklı and Kumyaka in the pollution-zone map;

http://www.aloki.hu ● ISSN 1589 1623 (Print) ● ISSN 1785 0037 (Online)
DOI: http://dx.doi.org/10.15666/aeer/1902_881900
© 2021, ALÖKI Kft., Budapest, Hungary

these values are above the threshold of dangerous in terms of pollution. The pollution between Kumkaya, Fıstıklı and Narlı (Gemlik-Bursa) and Büyükkumla (Gemlik-Bursa) is thought to be caused by agricultural activities and ship traffic. The pollution values of Gemlik and Kursunlu are caused by industrial wastes and ship traffic.

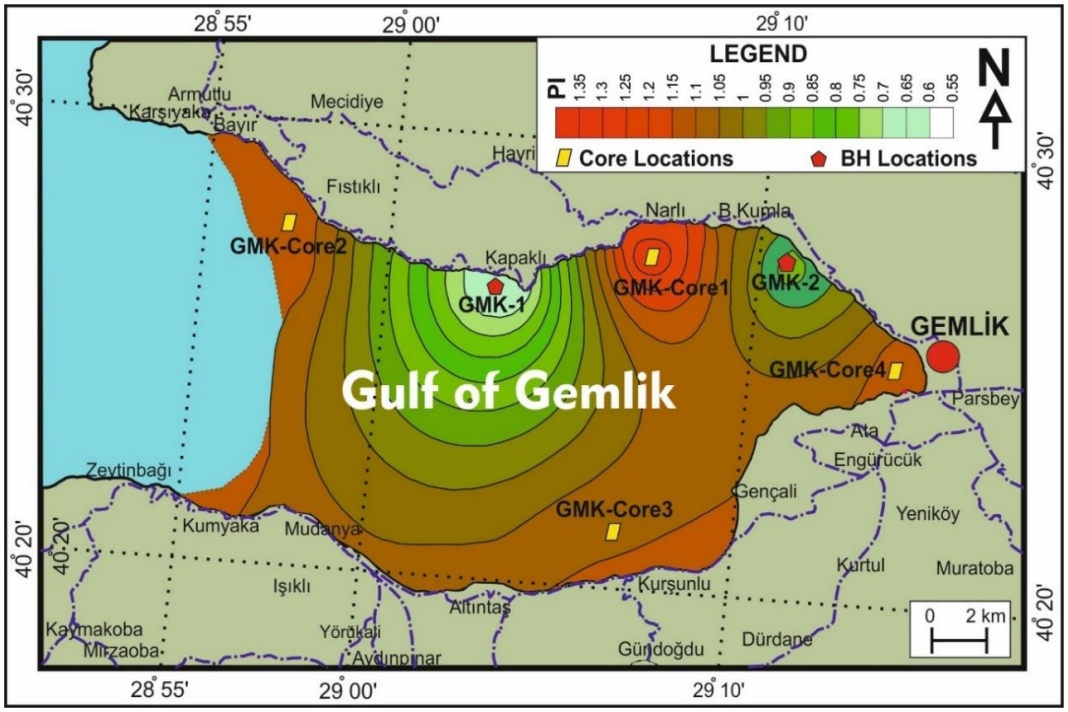


Figure 7. *Pollution-zone map generated by the Kriging method to PI values*

Table 6. *Gemlik Bay pollution index (PI) values*

Sample No	Y	X	PI
CORE-1	672101.00	4481326.00	1.325
CORE-2	658957.00	4481138.00	1.146
CORE-3	669332.26	4471289.20	1.086
CORE-4	681410.00	4477624.00	1.124
GMK-1 A. V.	666899.00	4480487.00	0.5739
GMK-2 A. V.	677320.00	4480755.00	0.8691

Radiological analysis of BH and core samples

The results of radiological measurements of the sediment samples obtained from the sampling locations are given in *Table 7*. At the same time significant natural radionuclides in soil and their world average specific activities are given in *Table 8*. According to the measurement results, Ra-226 has been found below the world average value in all locations. The K-40 values are above the world average values in the BH-1 sounding are from the intensive agricultural activities in that part of the study area. In the BH-2 drilling, K-40 values are below average. Th-232 values have been found to be below the world average value (30 Bq/kg) in BH-1 and BH-2 drillings except for BH-2/3 (the highest value in BH-2/3 (39.85 Bq/kg)). The Cs-137 values have reached the highest

http://www.aloki.hu ● ISSN 1589 1623 (Print) ● ISSN 1785 0037 (Online)
DOI: http://dx.doi.org/10.15666/aeer/1902_881900
© 2021, ALÖKI Kft., Budapest, Hungary

value by exceeding 5.3 Bq/kg in BH-1/1 drilling. The high Cs-137 in this area draws attention to the presence of artificial radioactivity. In all other locations, Cs-137 is below the background level. According to these results, the study area has not contained any unnatural radioactivity except BH-1/1. In addition, the measurement of the high Cs-137 value in the top layer of drilling is an indication of anthropogenic pollution. In the core samples, the K-40 value was determined to be the highest (498 Bq/kg) in Kurşunlu, and this value was above the world average value. Th-232 was found to be the highest in Fıstıklı (42.82 Bq/kg), and this value is above the world average value. Ra-226 has also been found to be the highest in Fıstıklı, but this value has been below the world average value. Cs-137 is below the background level in all core samples. When the results are examined, it is seen that natural and artificial radionuclides increase in sediment as an effect of anthropogenic pollution in the study area.

Table 7. *Radiological measurement results of GMK-1 (BH-1), GMK-2 (BH-2) Core-1, Core-2 and Core-3 (background is natural value of radionuclides of rocks)*

Sample No	K-40 (Bq/kg)	Th-232 (Bq/kg)	Ra-226 (Bq/kg)	Cs-137 (Bq/kg)
GMK-1/1	**853 ± 29.21**	Background	Background	**5.3 ± 29.21**
GMK-1/2	**497 ± 22.29**	Background	23.24 ± 4.80	Background
GMK-1/3	**530 ± 23.02**	25.87 ± 5.7	17.91 ± 4.12	Background
GMK-2/1	82.42 ± 9.06	Background	Background	Background
GMK-2/2	143.45 ± 11.95	7.63 ± 2.65	8.91 ± 2.82	Background
GMK-2/3	**595 ± 24.39**	**39.85 ± 6.24**	25.34 ± 5.03	Background
CORE-1	396 ± 19.89	Background	**39.85 ± 6.24**	Background
CORE-2	359 ± 18.94	**42.82 ± 6.54**	28.51 ± 5.30	Background
CORE-3	**498 ± 22.31**	**36.58 ± 6.05**	**39.85 ± 6.24**	Background

Table 8. *Significant natural radionuclides in soil and their world average specific activities (UNSCEAR, 2000) (MDA is measurement value that is less than detection limits of measurement tools)*

Radionuclide[a]	Concentration in soil (Bq kg^{-1})		Dose coefficient [I20, S49] (nGy h-1 per Bq kg^{-1})	Absorbed dose rate in air (nGy h^{-1})	
	Median value[a]	Population-weighted value [a]		Median value	Population-weighted value
^{40}K	400	420	0.0417	17	18
^{228}U series	35	33	0.462	16	15
^{232}Th series	30	45	0.604	18	27
Cesium-137	< MDA = 2.1				
Total				51	60

[a]Values from *Table 5* (UNSCEAR, 2000)

Radionuclide values were taken from 43 countries from 7 continents (Africa, North America, East Asia, West Asia, West Europe, East Europe, and South Europe) to represent world averages (UNSCEAR, 2000). In the study conducted by UNSCEAR (2000),

http://www.aloki.hu ● ISSN 1589 1623 (Print) ● ISSN 1785 0037 (Online)
DOI: http://dx.doi.org/10.15666/aeer/1902_881900
© 2021, ALÖKI Kft., Budapest, Hungary

arithmetic averages of the radionuclide values obtained from 43 countries were accepted as the average natural radionuclide content of the soils for the whole world (*Table 8*).

Enrichment factor results for Gemlik Bay

Natural soil values and the enrichment factor values calculated for Gemlik Bay are given in *Tables 9, 10* and *11*. According to the results of the enrichment factors, EFNi has found to be between 3-5 and other EF values have been lower than 3. The fact that EFNi is between 3-5 indicates that Ni is becoming enriched in the region. Specifically, the enrichment of Ni shows that the drainage waters of agricultural origin pollute the area. The calculated EF value, being close to 1, indicates the earth's crust, while its value between 3-5 indicates the earth's crust. And EF value greater than 5 indicates that the enrichment is not of crustal origin (Galuszka et al., 2014; Halstead et al., 2000; Mason and Moore, 1982).

Table 9. *Enrichment factor calculations of BH-1 drilling*

Sample No	EF ZN	EF AS	EF CO	EF CU	EF NI	EF PB	EF MN
GMK-1/27-28	0.34	0.02	0.95	0.85	**2.32**	0.36	0.68
GMK-1/28-29	0.29	0.04	**1.16**	**1.06**	**3.14**	0.19	0.61
GMK-1/29-30	0.31	0.06	**1.15**	0.86	**3.16**	0.16	0.64
GMK-1/30-31	0.3	0.06	**1.08**	0.89	**3.51**	0.2	0.67
GMK-1/31-32	0.33	0.03	0.98	0.79	**3.26**	0.23	0.87
GMK-1/32-33	0.3	0.05	0.91	0.75	**3.24**	0.17	0.74
GMK-1/33-34	0.28	0.06	0.98	0.74	**2.93**	0.2	0.64
GMK-1/34-35	0.26	0.11	1.17	0.86	**2.9**	0.15	0.56
GMK-1/35-36	0.29	0.08	0.98	0.64	**3.34**	0.17	0.59
GMK-1/36-37	0.32	0.15	0.96	0.6	**3.43**	0.23	0.78
GMK-1/37-38	0.28	0.05	0.95	0.64	**3.04**	0.2	0.75
GMK-1/38-39	0.3	0.08	0.91	0.64	**3.09**	0.25	0.68
GMK-1/39-40	0.28	0.05	1.03	0.73	**3.05**	0.24	0.64
Average	**0.29**	**0.06**	**1.01**	**0.77**	**3.10**	**0.21**	**0.68**
EF analysis	EF Zn < 1	EFAs < 1	EFCo ≤ 1	EFCu < 1	3 < EFNi < 5	EFPb < 1	EFMn < 1

Discussion

With the geochemical analysis performed by ICP-OES method, toxic element concentration distributions were calculated and pollution analysis of the study area was made. The concentration distributions obtained were analyzed with the Pollution Index (PI) method defined by Yümün (2017). According to the PI results, it has been observed that the pollution is high especially in port areas with heavy ship traffic. The ship traffic in the Narlı, Gemlik and Kurşunlu parts of the Marmara Sea is also seen in the high *Figure 8*. It is seen that PI and Enrichment Factors (EFCo, EFCu, EFPb) are also high in areas with high ship traffic. The Map of Waterways in the Sea of Marmara given in *Figure 8* has been examined to determine whether the areas with high marine pollution have a relationship with sea traffic (http://apelasyon.com/Yazi/536-deniz-yollari). The highly polluted areas determined in the PI map, the areas with high values in the Enrichment Factor calculations exactly overlap with the heavy traffic areas seen in the Sea Waterways map given in *Figure 8*.

http://www.aloki.hu ● ISSN 1589 1623 (Print) ● ISSN 1785 0037 (Online)
DOI: http://dx.doi.org/10.15666/aeer/1902_881900
© 2021, ALÖKI Kft., Budapest, Hungary

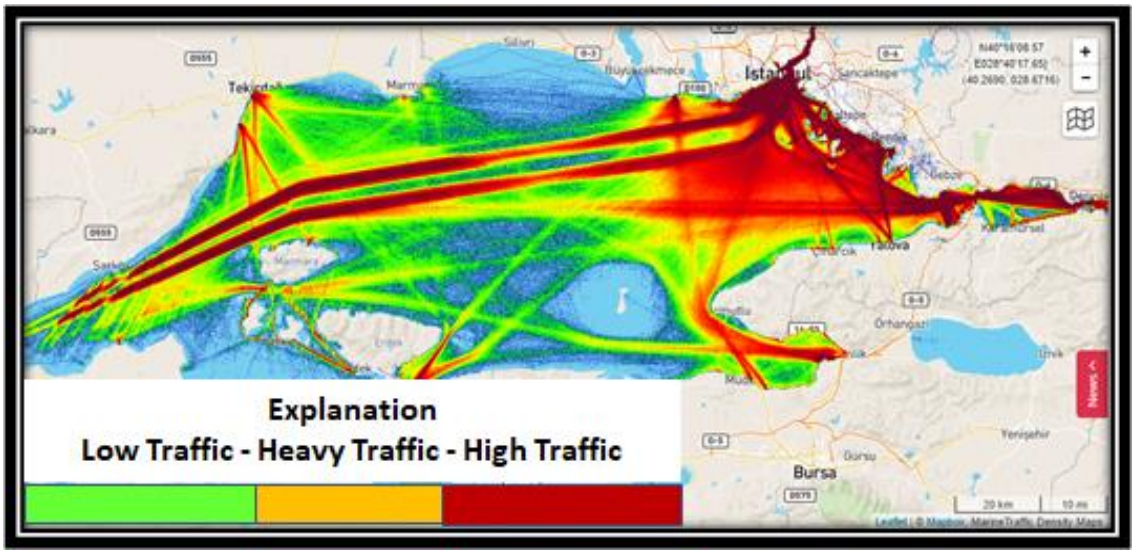


Figure 8. *Waterways of the Marmara Sea (marine traffic) (http://apelasyon.com/Yazi/536-deniz-yollari)*

Table 10. *Enrichment factor calculations of BH-2 drilling*

	EF ZN	**EF AS**	**EF CO**	**EF CU**	**EF NI**	**EF PB**	**EF MN**
GMK-2/35-36	0.52	0.02	0.95	0.71	0.54	0.79	0.9
GMK-2/36-37	0.56	0.02	0.88	0.71	0.5	**1.13**	0.83
GMK-2/37-38	0.6	0.03	0.9	0.77	0.54	**4.92**	0.76
GMK-2/38-39	0.59	0.07	0.92	0.87	0.57	**2.02**	0.61
GMK-2/39-40	0.52	0.04	0.91	0.88	0.61	1	0.63
GMK-2/40-41	0.59	0.02	0.87	0.73	0.47	1.15	0.66
GMK-2/41-42	0.57	0.03	0.85	0.71	0.48	1.4	0.63
GMK-2/42-43	0.59	0.02	0.88	0.67	0.45	1.31	0.67
GMK-2/43-44	0.58	0.03	0.88	0.73	0.49	1.48	0.71
GMK-2/44-45	0.58	0.05	0.89	0.74	0.48	3.54	0.79
GMK-2/45-46	0.6	0.02	0.89	1.11	0.49	1.07	0.82
GMK-2/46-47	0.57	0.01	0.84	0.66	0.4	1.03	0.84
GMK-2/47-48	0.57	0.02	0.83	0.68	0.4	0.92	0.79
GMK-2/48-49	0.58	0.01	0.87	0.71	0.42	1.46	0.8
GMK-2/49-50	0.56	0.01	0.81	0.65	0.4	1.07	0.62
Average	**0.57**	**0.03**	**0.87**	**0.76**	**0.48**	**1.62**	**0.73**
EF analysis	EFZn < 1	EFAs < 1	EFCo < 1	EFCu < 1	EFNi < 1	EFPb > 1	EFMn < 1

Apart from ship traffic, the region is also a very busy area in terms of agricultural activities.

Olive cultivation is particularly intensive in the region (*Fig. 9*). It is seen that olive farming is done entirely in the land areas around the study area. This is shown on the Turkey Olive Production Map (https://s.milimaj.com/others/image/harita/turkiye-2019-zeytin-uretim-haritasi.png) released by the Turkey Statistical Institute.

http://www.aloki.hu ● ISSN 1589 1623 (Print) ● ISSN 1785 0037 (Online)
DOI: http://dx.doi.org/10.15666/aeer/1902_881900
© 2021, ALÖKI Kft., Budapest, Hungary

Table 11. *Enrichment factor calculations of Core samples (Core-1. Core-2. Core-3. Core-4)*

	EF ZN	EF AS	EF CO	EF CU	EF NI	EF PB	EF MN
GMK/CORE-1	0.21	0.02	0.9	0.92	0.43	0.73	0.4
EF analysis	EFZn < 1	EFAs < 1	EFCo < 1	EFCu < 1	EFNi < 1	EFPb < 1	EFMn < 1
GMK/CORE-2	0.29	0.03	0.93	0.84	0.48	0.56	0.64
EF analysis	EFZn < 1	EFAs < 1	EFCo < 1	EFCu < 1	EFNi < 1	EFPb < 1	EFMn < 1
GMK/CORE-3	0.45	0.02	0.88	0.85	0.41	0.6	0.49
EF analysis	EFZn < 1	EFAs < 1	EFCo < 1	EFCu < 1	EFNi < 1	EFPb < 1	EFMn < 1
GMK/CORE-4	0.49	0.01	0.96	0.78	0.63	0.78	0.78
EF analysis	EFZn < 1	EFAs < 1	EFCo < 1	EFCu < 1	EFNi < 1	EFPb < 1	EFMn < 1

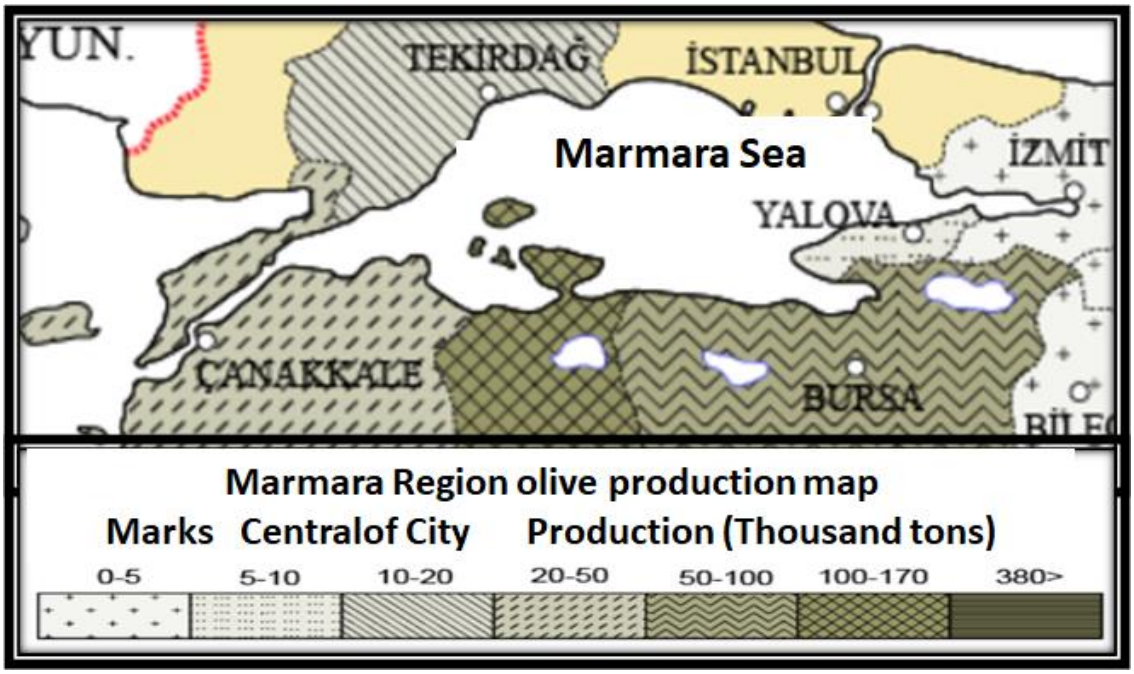


Figure 9. *Olive production density map around Gemlik (Bursa/Turkey) (https://s.milimaj.com/others/image/harita/turkiye-2019-zeytin-uretim-haritasi.png)*

Conclusions

In this study, the heavy metal and radioactive pollution of Gemlik Bay was investigated. Two drillings (BH-1 and BH-2) were conducted and four core samples (CORE-1, CORE-2, CORE-3 and CORE-4) were taken from the gulf. According to the results of geochemical analysis, Ag, Bi, Mo, Sn and Se concentrations were determined as 0 ppm in all samples. In Gemlik BH-1 drilling, in addition to other elements, mercury (Hg) was detected at 0 ppm. The concentration values of Zn, As, B, Cd, Co, Cr, Cu, Ni Pb, Pt and Sb are between 0-300 ppm, and these elements are defined as the first group of elements. The concentration values of Na, Mg, K, Ca, P, S, Fe, Al and Mn have been determined to be > 300 ppm, and these elements have been evaluated as the second group ın this study. The pollution index (PI) values have been calculated by using the results of elemental analysis. Pollution-zone maps were created with the Kriging method by using pollution parameters obtained in this way. The pollution-zone map

http://www.aloki.hu ● ISSN 1589 1623 (Print) ● ISSN 1785 0037 (Online)
DOI: http://dx.doi.org/10.15666/aeer/1902_881900
© 2021, ALÖKI Kft., Budapest, Hungary

shows that Narlı (Gemlik-Bursa) and Büyükkumla (Gemlik-Bursa) and Kursunlu, Gemlik Fıstıklı and Kumyaka have values approximately PI > 1, indicating a dangerous level of pollution. The pollution between Kumkaya, Fıstıklı and Narlı (Gemlik-Bursa) and Büyükkumla (Gemlik-Bursa) is thought to be caused by agricultural activities and ship traffic. The pollution in Gemlik and Kursunlu is thought to be caused by industrial wastes, agriculture and ship traffic. In addition, using the results of the Fe, Zn, As, Co, Cu, Mn, Ni and Pb heavy metals analysis, the enrichment factor of each heavy metal (EF) was calculated. According to the enrichment factor results, EFNi in the BH-1 drilling is in the range of 3 < EFNi < 5, and other EF values are below 1. The results obtained in this study were compared with the study given below. The calculated EF value result is close to 1 (EF < 1) depending on the earth crust origin. The fact that the enrichment values are between 3 and 5 is controversial depending on the shell origin. EF > 5 values are considered to be nonshell origin (Galuszka et al., 2014; Halstead et al., 2000). Since the EF value obtained in this study is less than 3, it is thought to be Earth Crust Origin.

The fact that the EFNi value is between 3 and 5 indicates that Ni is becoming enriched in the region. Specifically, the enrichment of Ni shows that the drainage waters of agricultural origin pollute the area. Natural and artificial radionuclides have been measured by radiological analyses, and the environmental and artificial radioactivity results of Gemlik Bay and its surroundings have been determined. The Ra-226 value has been found to be below the world average value at all locations. It is estimated that the K-40 values above the world average values in the BH-1 drilling are from the intensive agricultural activities in that part of the study area. However, K-40 values are below the average in the BH-2 drillings. There is little or no agricultural activity on the land near the BH-2 drilling zone. Th-232 values have been found to be above the world average value (30 Bq/kg) in BH-2/3 (39.85 Bq/kg) but below that value in other locations. The Cs-137 value has reached the highest value by exceeding 5.3 Bq/kg in the BH-1/1 drilling. The fact that Cs-137 is high in the upper level of the drilling draws attention to the presence of artificial radioactivity. The fact that the Cs-137 radionuclide increased above the measurable limit at this location revealed the level of impact of nuclear activity on the region. In other locations, Cs-137 is at the background level. In the core samples, the K-40 value has been found to be the highest in Kurşunlu (498 Bq/kg), and this value is above the world average value. The value of Th-232 is the highest in Fıstıklı (42,82 Bq/kg), and this value is above the average value. The Ra-226 value has been found to be the highest in Fıstıklı, but this value is below the average value.

The Pollution Index was obtained as > 1 in core samples and < 1 on average values of the drilling samples. This situation shows that pollution has increased in marine environment in the current period. It is seen that Radioactivity is also high in places where the Pollution Index is high. This shows that there is a close relationship between elemental pollution and radioactive pollution. An example of this is the fact that Cs-137 (5.3 ± 29.21) values are higher in samples taken from the upper level of GMK-1 boring, and the background value of CS-137 in samples taken from below level. Again, the radioactivity values obtained in Core-3 samples are above the world average values and the PI value is > 1, which is an important data for showing environmental pollution. It is possible to say the same situation within the enrichment factor. In order to determine the environmental pollution, there was a parallelism between Pollution Index, Enrichment Factor and Radioactivity analysis.

http://www.aloki.hu ● ISSN 1589 1623 (Print) ● ISSN 1785 0037 (Online)
DOI: http://dx.doi.org/10.15666/aeer/1902_881900
© 2021, ALÖKI Kft., Budapest, Hungary

Acknowledgements. The authors thank the RORO Company and the Gemlik Harbour Authority for their support, and the Namık Kemal University Central Research Laboratory (NABİLTEM) for the geochemical analysis, and the Çekmece Nuclear Energy Agency for radiological analysis. The author also thanks Yıldız Technical University Scientific Research Projects Commission for accepting and financing this study (Project no: FBA-2018-3351) and Tekirdağ Namik Kemal University Scientific Research Projects Commission for accepting and financing this study (Project no: NKUBAP.42.GA.19.193)

REFERENCES

[1] Adamo, P., Arienzo, M., Imperato, M., Naimo, D., Nardi, G., Stanzione, D. (2005): Distribution and partition of heavy metals in surface and sub-surface sediments of Naples city port. – Chemosphere 61: 800-809.
[2] Akçay, H., Oğuz, A., Karapire, C. (2003): Study of heavy metal pollution and speciation in Buyak Menderes and Gediz river sediments. – Water Research 37: 813-822.
[3] Alpar, B., Ünlü, S., Kırbaşıoğlu, C. (2006): Records of anthropogenic pollution in sediment of Gemlik Bay (Marmara Sea, Turkey) during the last 15 years. – Geophysical Research Abstracts 8: 00392.
[4] ASTM E181-98 (2003): Standard Test Methods for Detector Calibration and Analysis of Radionuclides. – ASTM, West Conshohocken, PA.
[5] Bampton, M. (1999): Anthropogenic Transformation. – In: Environmental Geology. Encyclopedia of Earth Science. Springer, Dordrecht. https://doi.org/10.1007/1-4020-4494-1_17.
[6] Baptista Neto, J. A., Smith, B. J., Mc Allister, J. J. (2000): Heavy Metal Concentrations in Surface Sediments in a Nearshore Environment, Jurujuba Sound, Southeast Brazil. – Environmental Pollution 109: 1-9.
[7] Buat-Menard, P., Chesselet, R. (1979): Variable in fluence of the atmospheric flux on the trace metal chemistry of oceanic suspended matter. – Earth Planet Science Lett 42: 399-411.
[8] Dickinson, W. W., Dunbar, G. B., Mc Leod, H. (1996): Heavy metal history from cores in Wellington Harbour, New Zealand. – Environmental Geology 27: 59-69.
[9] Esen, E., Kucuksezgin, F., Uluturhan, E. (2008): Assessment of trace metal pollution in surface sediments of Nemrut Bay, Aegean Sea. – Environmental Monitoring and Assessment 160(1-4): 257-266.
[10] Essien, J. P., Antai, S. P., Olajire, A. A. (2009): Distribution, seasonal variations and ecotoxicological significance of heavy metals in sediments of cross river estuary mangrove swamp. – Water, Air, and Soil Pollution 197: 91-105.
[11] Feng, H., Cochran, J. K., Lwiza, H., Brownawell, B. J., Hirschberg, D. J. (1998): Disribution of heavy metal and PCB contaminants in the sediments of an urban estuary: the Hudson River. – Marine Environmental Research 45: 69-88.
[12] Galuszka, A., Migaszewski, Z. M., Zalasiewicz, J. (2014): Assessing the Anthropocene with geochemical methods. – Geological Society, London, Special Publications 395: 221-238.
[13] Gao, X. L., Chen, C. T. A. (2012): Heavy metal pollution status in surface sediments of the coastal Bohai Bay. – Water Res 46: 1901-1911.
[14] Halstead, M. J., Cunninghame, R. G., Hunter, K. A. (2000): Wet deposition of trace metals to a remote site in Fiordland, New Zealand. – Atmospheric Environment 34: 665-676.
[15] Hornung, H., Karm, M. D., Cohen, Y. (1989): Trace metal distribution on sediments and benthic fauna of Haifa Bay, Israel. – Estuarine, Coastal and Shelf Science 29: 43-56.
[16] https://desktop.arcgis.com/en/arcmap/10.3/tools/3d-analyst-toolbox/how-kriging-works.htm#:~:text=Kriging%20is%20a%20multistep%20process,directional%20bias%20in%20the%20data.

http://www.aloki.hu ● ISSN 1589 1623 (Print) ● ISSN 1785 0037 (Online)
DOI: http://dx.doi.org/10.15666/aeer/1902_881900
© 2021, ALÖKI Kft., Budapest, Hungary

[17] Huerta-Diaz, M. A., Delgadillo-Hinojosa, F., Hernández-Ayón, M., Segovia-Zavala, J. A., García-Esquivel, Z., López-Zárate, H., Siqueiros- Valencia, A., Galindo-Bect, S. (2008): Diagnosis of trace metal contamination in sediments: the example of Ensenada and El Sauzal, two harbors in Baja California, Mexico. – Marine Environmental Research 66: 345-358.
[18] Kam, E., Önce, M. (2016): Pollutıon potentıal of heavy metals ın the current sea sedıments between bandırma (Balıkesir) and lapseki (Çanakkale) ın the marmara sea. – Journal of Engineering Technology and Applied Sciences 1: 141-148.
[19] Koday, S., Baki, G. (2014): Port of Gemlik. – Atatürk University Journal of the Institute of Social Sciences 18: 431-454.
[20] Mason, B. J., Moore, C. B. (1982): Principles of Geochemistry. 4th Ed. – Wiley, New York.
[21] Meriç, E., Avşar, N., Nazik, A., Alpar, B., Yokeş, B., Barut, İ. F., Ünlü, S. (2005): Foraminifera, ostrakod and mollusc fauna of gemlik bay surface sediments, sedimentological, hydrochemical and biochemical properties of the region with morphological abnormalities observed in foraminiferal shells. – Journal of Mining Tetics Search 131: 21-48.
[22] Mohiuddin, K. M., Zakir, H. M., Otomo, K., Sharmin, S., Shikazono, N. (2010): Geochemical distribution of trace metal pollutants in water and sediments of downstream of an urban river. – International Journal of Environmental Science and Technology 7: 17-28.
[23] Morillo, J., Usero, J., Gracia, I. (2002): Heavy metal fractionation in sediments from the Tinto River (Spain). – International Journal of Environmental & Analytical Chemistry 82: 245-257.
[24] Okuş, E., Balkıs, N., Müftüoglu, E., Aksu, A. (2007): Metal (Pb, Cd and Hg) inputs via the rivers to the Southern Marmara Sea Shelf, Turkey. – J. Black Sea/Medit. Environ. 13. http:// www.blackmeditjournal.org/index.asp (accessed: April 1, 2014).
[25] Omgbu, J. A., Kokogbo, M. A. (1993): Determination of Zn, Pb, Cn and Hg in soils of Ekpan, Nigeria. – Environ Int 19: 611-612.
[26] Park, J., Presley, B. J. (1997): Trace metal contamination of sediments and organisms from the Swan Lake area of Galveston Bay. – Environmental Pollution 98: 209-221.
[27] Pekey, H. (2006): The distribution and sources of heavy metals in Izmit Bay surface sediments affected by a polluted stream. – Marine Pollution Bulletin 52(10): 1197-1208.
[28] Ray, A. K., Tripathy, S. C., Patra, S., Sarma, V. V. (2006): Assessment of Godavari estuarine mangrove ecosystem through trace metal studies. – Environment International 32: 219-223.
[29] Riemann, L., Steward, G. F., Azam, F. (2000): Dynamics of bacterial community composition and activity during a mesocosm diatom bloom. – Applied and Environmental Microbiology 66: 578-587.
[30] Schiff, K. C., Weisberg, S. B. (1999): Iron as a reference element for determining trace meta enrichment in southern California coastal shelf sediments. – Marine Environmental Research 48: 161-176.
[31] Sutherland, B. R. (2000): Internal wave reflection in uniform shear. – Quarterly Journal of the Royal Meteorological Society 126: 3255-3286.
[32] Taylor, S. R., Mc Lennan, S. M. (1995): The geochemical evolution of the continental crust. – Reviews of Geophysics 33: 241-265.
[33] TSE ISO 14869-1 (2004a): Soil Quality - Dissolution for the Determination of Total Element Content - Part 1: Dissolution with Hydrofluoric and Perchloric Acids. – TSE (Turkish Standardized Institute), Ankara.
[34] TSE ISO 14869-2 (2004b): Soil Quality - Dissolution for the Determination of Total Element Content - Part 2: Dissolution with Alkaline Fusion. – TSE (Turkish Standardized Institute), Ankara.

http://www.aloki.hu ● ISSN 1589 1623 (Print) ● ISSN 1785 0037 (Online)
DOI: http://dx.doi.org/10.15666/aeer/1902_881900
© 2021, ALÖKI Kft., Budapest, Hungary

[35] Ünlü, S., Alpar, B. (2006): Distribution and sources of hydrocarbons in surface sediments of Gemlik Bay (Marmara Sea, Turkey). – Chem. 64: 764-777.
[36] UNSCEAR (2000): United Nations. Sources and Effects of Ionizing Radiation. Volume I: United Nations Scientific Committee on the Effects of Atomic Radiation, 2000 Report to the General Assembly, with scientific annexes. – United Nations Sales Publication E.00.IX.3 and E.00.IX.3. United Nations, New York.
[37] Valdés, J., Vargas, G., Sifeddine, A., Ortlieb, L., Guinez, M. (2005): Distribution and enrichment evaluation of heavy metals in Mejillones Bay (23oS), Northern Chile: geochemical and statistical approach. – Marine Pollution Bulletin 50: 1558-1568.
[38] Yümün, Z. Ü. (2017): The Effect of heavy metal pollution on foraminifera in the western Marmara Sea (Turkey). – Journal of African Earth Sciences 129: 346-365.
[39] Yümün, Z. Ü., Kam, E. (2017): Effects of radionuclides on the recent foraminifera from the clastic sediments of the Çanakkale Strait-Turkey. – Journal of African Earth Science 131: 179-182.
[40] Yümün, Z. Ü., Önce, M. (2017): Monitoring heavy metal pollution in foraminifera from the Gulf of Edremit (northeastern Aegean Sea) between Izmir, Balıkesir and Çanakkale (Turkey). – Journal of African Earth Sciences 130: 110-124.
[41] Zhang, C., Qiao, Q., Piper, J. D., Huang, B. (2011): Assessment of heavy metal pollution from a Fe-smelting plant in urban river sediments using environmental magnetic and geochemical methods. – Environmental Pollution 159: 3057-3070.

http://www.aloki.hu ● ISSN 1589 1623 (Print) ● ISSN 1785 0037 (Online)
DOI: http://dx.doi.org/10.15666/aeer/1902_881900
© 2021, ALÖKI Kft., Budapest, Hungary

A COMPARATIVE STUDY ON THE ADSORPTION PROPERTIES OF HEAVY METAL Cr IN LAKE SEDIMENT AND SOIL

JIANG, Y.[1] – MA, X. L.[1*] – SUN, F. Y.[1] – GUO, Y. X.[1] – REN, L. J.[1,2] – WANG, Y. J.[1] – XIE, Z. L.[3*]

[1]College of Resources and Environment, Jilin Agricultural University, Changchun 130118, China
(phone: +86-138-3340-6073; fax: +86-0431-8453-1264)

[2]Hebei puni testing technology co., LTD. Shijiazhuang 050011, China
(phone: +86-184-4398-4987; fax: +86-0431-8453-3110)

[3]College of Plant Science, Jilin University, Changchun 130062, China
(phone: +86-151-3343-7521; fax: +86-0431-8516-6245)

[*]Corresponding authors
e-mail: 491277643@qq.com; phone: +86-180-0442-2753; fax: +86-0431-8453-1264 (Ma, X. L.)
e-mail: xiezl@jlu.edu.cn; phone: +86-139-4488-3685; fax: +86-0431-8783-6260 (Xie, Z. L.)

(Received 21st Oct 2020; accepted 19th Jan 2021)

Abstract. (1) Background: In order to study chromium (Cr) adsorption characteristics of sediment and shore soil in Xinlicheng Reservoir, Changchun City, Jilin Province, and to discuss the contribution of pH and organic matter adsorption, to explore the accumulation law of Cr in sediment and soil. (2) Methods: OECD Guideline106 equilibrium adsorption method was used in this study. The adsorption kinetics data of Cr in sediment and black soil were fitted by Elovich equation and parabolic diffusion equation. The Freundlich and D-R models were used to fit the adsorption thermodynamic data of Cr. (3) Results: the isothermal adsorption curve of Cr by sediment and soil was "S" type, and K_f sediment $>K_f$ soil. Thermodynamic parameters $\Delta G<0$, $\Delta H>0$, to demonstrate the adsorption of Cr was a spontaneous endothermic process, high temperature was beneficial to the spontaneity of adsorption; Within the pH range of the test, higher and lower pH values were not conducive to the adsorption of Cr by sediment and soil. With the increase of pH, the adsorption capacity of Cr by soil and sediment first increased and then decreased. The adsorption amount of Cr in sediment and soil was the smallest at the pH 3, and the adsorption amount was the largest at the pH 7. However, the difference between adsorption of Cr in the sediment under different pH was not significant ($p>0.05$), and the adsorption of Cr in the soil under different pH was significant ($p<0.05$). Compared with the soil and sediment without organic matter removal, the adsorption capacity of removing organic matter was significantly reduced ($p<0.05$), and the contribution rates of organic matter in sediment and soil to Cr were 50.38% and 48.40%, respectively. Consequently, the content of organic matter played a key role in the adsorption of Cr in soil and sediment.
Keywords: *chromium, sediment and soil, adsorption characteristics, pH, organic matter content*

Introduction

Heavy metals are non-biodegradable accumulative pollutants. The pollution problem is of global concern due to the toxic, persistent and non-degradable nature of excessive heavy metals in the environment. Chromium (Cr), a common heavy metal, is characterized by bioaccumulation, high toxicity, carcinogenicity and mutagenicity, and can cause human cancer, severe diarrhea and kidney damage even at low concentrations (Song et al., 2019). Chromium is among the top hazardous substances priority of the Superfund (Jiang et al., 2018).

Heavy metals in soil mainly come from chemical fertilizers, pesticides, industrial wastewater and irrigation sewage and soil parent material. Chromium (VI) has strong

http://www.aloki.hu ● ISSN 1589 1623 (Print) ● ISSN1785 0037 (Online)
DOI: http://dx.doi.org/10.15666/aeer/1902_901914
© 2021, ALÖKI Kft., Budapest, Hungary

fluidity, solubility and durability, which leads to polluted water, soil and sediment. Especially during heavy rain, pollutants enter the sediment in the riparian zone along with a large amount of soil, mud and sand, and sediment become the carrier, destination and storage place for various substances to migrate and transform in the water environment (Pan and Ding, 2011; Drinčić et al., 2018; Zhang et al., 2019). Through adsorption or chemical and physical combination, soil and sediment tend to accumulate heavy metals. They are both carriers and reservoirs for heavy metals, which play an important role in the migration of heavy metals.

In recent years, soil heavy metal pollution has received considerable attention by many researchers, and related studies have been published. These researches have shown that adsorption is an important process to control the presence of heavy metals in solid phase, including soil and sediment. Adsorption and desorption have been demonstrated closely related to soil properties, including pH, organic matter, cation exchange capacity, and clay minerals, etc. A large number of studies have shown that pH is a main contributing factor. Zhang et al. (2017) studied the migration rule of Cr(VI) in the soil of vegetable base, and found that the initial concentration of heavy metal Cr and environmental pH value exerted an influence on the adsorption process of Cr(VI). Liu et al. (2018) proposed that the adsorption capacity of the adsorbent is closely related to pH, which may change the existing form of Cr, thus changing the leaching rate of heavy metals in the soils. Dong et al. (2009) studied the adsorption of Cr(VI) in moderately polluted farmland soil in northeast China and the effect of pH value on the adsorption, and found that the adsorption capacity of Cr(VI) in soil decreased against the increase of pH, and the migration rate of Cr(VI) in soil and groundwater increased, which caused greater harm to the environment. Fonseca et al. (2009) studied the adsorption of Cr by acidic soils in Portugal and found that the mobility of Cr(VI) was low in acidic soils. In addition to soil pH, soil organic matter is also one of the important properties that affect the availability of heavy metals. Major contributor to the ability of exchangeable forms of organic matter to retain heavy metals. Zeng et al. (2011) found that Cr content in soil and Cr content in rice tissue were negatively correlated with soil pH value, but positively correlated with organic matter content. Vega et al. (2006) found that the main soil components affecting the adsorption of one or more heavy metals were organic matter, Fe oxide, sidrite and chlorite content, and CEC. In order to probe into the heavy metal pollution of the soil of the Luona River deposit in Tibet, and the surrounding sediment, Qiao et al. (2020) conducted a study and found that Cr pollution in the soil mainly comes from river water and sediment polluted by heavy metals.

The present study focuses on the migration of heavy metal Cr in the sediment of Xinlicheng Reservoir, and the soil at the entrance of the reservoir, Changchun city, Jilin Province, China, and identifies the value of soil pH and organic matter content as influencing factors so that scientific basis is provided for the future restoration of heavy metal contaminated soil around lakes and reservoirs.

Materials and methods

Samples for test

The basin of Xinlicheng Reservoir is slightly rectangular in shape with an average width of 20.7 km. Chromium pollution sources in the water of Xinlicheng Reservoir mainly come from sewage discharge from surrounding factories and Cr migration

http://www.aloki.hu ● ISSN 1589 1623 (Print) ● ISSN1785 0037 (Online)
DOI: http://dx.doi.org/10.15666/aeer/1902_901914
© 2021, ALÖKI Kft., Budapest, Hungary

caused by rainfall. The soil samples were collected from the river inlet, and the surface layer of 0-20 cm soil was collected by quartering method. The soil type was black soil, the land is agricultural cultivated land, the crop is maize, and NPK compound fertilizer is applied. The sediment is collected at surface layer (0-10 cm) by grab dredger, that is, sampling points are equidistant from the upstream of the reservoir (5 km, 10 km, 15 km away from the reservoir), and the sampling point is 2 m away from the shore, repeated 3 times for each collection. After the samples collected at the three sampling points were mixed and naturally air-dried indoors, the impurities such as animal and plant residues and rocks were removed, and then the samples were ground through a 10 and 100-mesh sieve for storage. The basic physical and chemical properties of the tested soil samples are shown in *Table 1*.

Table 1. *Physicochemical properties of test soil*

Sample	Unit weight /(g·m^{-3})	OM/ (g /kg)	T_N / %	T_P / %	Cr /mg·kg^{-1}	Mechanical composition%			
						Sand	Coarse silt	Fine silt	Clay
Sediment	1.79	41.23	0.15	0.12	33.73	10.48	33.97	24.12	31.43
Black soil	1.65	34.65	0.12	0.09	26.55	4.84	51.43	22.96	20.77

Test design

Adsorption kinetics

Adsorption kinetics test was used to evaluate the equilibrium time of subsequent adsorption isotherm tests. In the adsorption kinetics test, soil and water ratio 20:1 was used in 50 ml polyethylene centrifuge tube, and 1.00 g soil sample and 20 ml Cr solution with a concentration of 200 mg·L^{-1} were added, respectively. They oscillate for 1, 5, 10, 20, 30, 60, 120, 240, 360, 480, 720, 1440 min at the temperature of 25℃. After centrifugation at 4000 r·min^{-1} for 10 min, the concentration of Cr in the supernatant was determined by filtration with 0.45 um microporous membrane (Dali-Youcef et al., 2006).

Adsorption isotherm

The 1.00 g samples of sediment and soil were added into a 50 mL polyethylene centrifuge tube to study the adsorption isotherm of Cr on sediment and soil. The influence of univariate time on the adsorption of Cr on sediment and black soil was studied when different initial concentrations of Cr were 50, 100, 200, 300, 400 and 500 mg·L^{-1}, respectively. Adsorption kinetics on the basis of constant temperature oscillation at 25℃ to obvious equilibrium, the test tube with Cr solution added as blank, centrifugation, filtration, determination and other steps are the same as Adsorption kinetics (Arias et al., 2006).

Influence of temperature on adsorption isotherm

The adsorption of Cr onto sediment and soil at 15℃, 25℃ and 35℃ was studied by referring to the batch adsorption test. The influence of single variable temperature on the adsorption of Cr onto sediment and black soil at different initial concentrations of 50, 100, 200, 300, 400 and 500 mg·L^{-1} was determined (Abat et al., 2012).

http://www.aloki.hu ● ISSN 1589 1623 (Print) ● ISSN1785 0037 (Online)
DOI: http://dx.doi.org/10.15666/aeer/1902_901914
© 2021, ALÖKI Kft., Budapest, Hungary

Influence of pH on adsorption isotherm

The solutions of 0.1 mol·L^{-1} HCl and 1.0 mol·L^{-1} NaOH were used to adjust the pH values of different Cr solutions to 3, 5, 7, 9 and 11. According to Adsorption isotherm method, adsorption isothermal determination was conducted at 25℃ to study the effect of pH change of a single variable on the adsorption of Cr on sediment and black soil.

Influence of organic matter content on adsorption isotherm

The organic matter in sediment and soil was removed by H_2O_2 digestion. The bottom mud and soil samples were weighed after air drying, and soaked with 6% H_2O_2 for 24 h, and after that 30% H_2O_2 100 ml was added for several times. Repeated treatment was made till no bubbles emerged from the samples. The residual H_2O_2 was removed by heating method and finally washed with deionized water.

Organic matter samples were taken respectively (with non-removed organic matter samples as the control), and the adsorption isotherm was determined at 25℃ according to Adsorption isotherm method, to study the influence of changes in single variable organic matter on sediment and soil Cr adsorption.

Analysis of adsorption data

Adsorption kinetic model

Elovich equation:

$$q_t = a + bln_t \quad \text{(Eq.1)}$$

Parabolic diffusion equation:

$$S/_{S_{max}} = a + bt^{1/2} \quad \text{(Eq.2)}$$

where, a is the adsorption constant related to the maximum adsorption capacity, and b is the adsorption rate coefficient, which can be interpreted as how fast the reaction rate decreases. The Elovich equation is used to explain the adsorption process of heterogeneous diffusion because the activation energy varies greatly during the reaction.

Isothermal fitting equation (Fan et al., 2012):

The Freundlich equation:

$$q_e = K_F C_t^{1/n} \textit{ (Nonlinear form)} \quad \text{(Eq.3)}$$

D-R equation:

$$lnq_e = lnq_m - k\varepsilon^2 \quad \text{(Eq.4)}$$

where, q_e is the adsorbed amount of Cr (mg·g^{-1}); q_m is the maximum adsorption capacity, k is the constant related to the adsorption energy, ε is the adsorption potential of Polanyi, K_F is the constant, n is the affinity value of the constant. All these formula

http://www.aloki.hu ● ISSN 1589 1623 (Print) ● ISSN1785 0037 (Online)
DOI: http://dx.doi.org/10.15666/aeer/1902_901914
© 2021, ALÖKI Kft., Budapest, Hungary

symbols respectively represent the maximum adsorption capacity of Cr and the adsorption capacity.

Thermodynamic parameter equation (Chen et al., 2011):

$$\Delta G = -RT \ln K_F \quad \text{(Eq.5)}$$

$$\Delta G = \Delta H - T\Delta S \quad \text{(Eq.6)}$$

Type: ΔG for the change of Gibbs free energy ($kJ \cdot mol^{-1}$), ΔG<0 indicates that reactions can occur spontaneously, ΔG>0 reaction can't occur spontaneously; ΔH is the standard enthalpy change ($kJ \cdot mol^{-1}$), ΔH<0 indicates the reaction is exothermic, while ΔH>0 indicates the reaction is endothermic; T(K) is the absolute temperature; R is the ideal gas constant = 8.314×10^{-3} $KJ \cdot mol^{-1} \cdot K^{-1}$; ΔS is the standard entropy change ($KJ \cdot mol^{-1} \cdot K^{-1}$), ΔS<0 means chaotic degree is reduced, ΔS>0 indicates confusion degree is increased; K_F stands for thermodynamic equilibrium constant. When the 1/T and lnK are used to draw horizontal and vertical curves, ΔH and ΔS can be obtained according to the slope and intercept, respectively.

All tests were performed in triplicate.

Results and discussion

Adsorption kinetics of Cr

Figure 1 depicts the adsorption of heavy metal Cr in sediment and soil at 25℃ and shows that the whole adsorption process of metal Cr in sediment and soils consist of two stages, the rapid adsorption stage and the slow equilibrium adsorption stage. Within 0-120 min, with the increase of adsorption time, the adsorption amount of Cr by sediment and black soil increases significantly, and the concentration of Cr in solution decreases rapidly. However, within 120-1440 min can be categorized into the slow equilibrium stage. At this stage, the change of Cr concentration in solution gradually tends to be in equilibrium. Kinetic test demonstrates that the adsorption equilibrium time of Cr in sediment and soil is 1440 min, and the maximum adsorption amount of Cr in sediment and black soil is 1665.02 $mg \cdot kg^{-1}$ and 1079.04 $mg \cdot kg^{-1}$, respectively. In the rapid adsorption stage, the adsorption capacity of Cr by sediment and black soil reaches 79.21% and 78.97% of the total adsorption capacity, respectively. With the passage of adsorption time, the heavy metal Cr in the solution is in full contact with the sediment and the black soil, and gradually occupies the adsorption site in the adsorbent, so the adsorption capacity of the sediment and the black soil gradually increases (Tokunaga et al., 2001; Li et al., 2013). The higher adsorption capacity of Cr in sediment may be due to the high content of organic matter in sediment, which can provide more adsorption points for Cr (Liu and Dai, 2015). In the process of Cr adsorption by sediment and soil, some components in the sediment and soil may form complex with Cr, transfer the Cr adsorbed on the surface of sediment and soil to the interior of particles, and lead to more Cr forming precipitation on the surface of sediment and black soil. When the adsorption time reaches 2 h, the adsorption amount of Cr in the bottom mud and black soil reaches about 80% of the total adsorption amount, and the equilibrium adsorption state can be

http://www.aloki.hu ● ISSN 1589 1623 (Print) ● ISSN1785 0037 (Online)
DOI: http://dx.doi.org/10.15666/aeer/1902_901914
© 2021, ALÖKI Kft., Budapest, Hungary

reached at 24 h. Thus, it can be seen that the bottom mud and black soil have a strong accumulation capacity for heavy metal Cr.

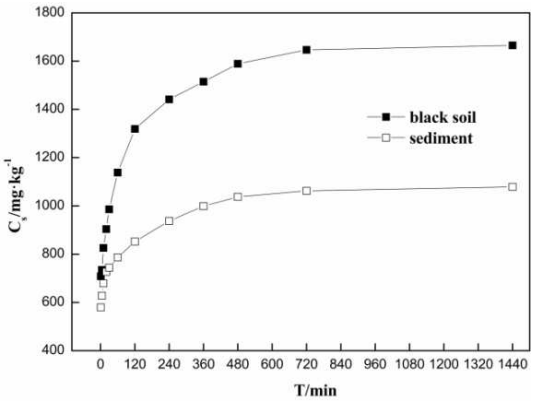


Figure 1. *The adsorption kinetics curves of Cr in black soil and sediment*

Elovich equation and parabolic diffusion equation were used to fit Cr adsorption kinetic data, so as to understand Cr adsorption mechanism in sediment and soil. Generally, the better the model is, the greater the R^2 value will be. *Table 2* shows the fitting parameters of the equation. It can be seen that the adsorption correlation coefficient R^2 of Elovich equation for Cr in sediment and soil was 0.9444 and 0.9569, respectively, which being greater than that of the parabolic diffusion equation (R^2 0.8105 and 0.8485, respectively), indicating that Elovich equation was more suitable for descriptions the Cr adsorption kinetics characteristics in sediment and soil. The higher the constant **a** value in Elovich equation, the higher the adsorption rate, and therefore the metal Cr is more likely to accumulate in the sediment. Elovich equation is an empirical equation, which is used to describe the adsorption behavior of pollutants on the non-uniform solid adsorption surface and is suitable for the process in which the activation energy changes greatly during the reaction process. The adsorption process involves not only particle diffusion but also multiple forces.

Table 2. *Parameters of the kinetics adsorption models for Cr in sediment and black soil*

Soil type	Elovich equation			Parabolic diffusion equation			
	a	b	R^2	a	b	s	R^2
Sediment	526.6285	161.1724	0.9444	30.6494	1.0879	26.9135	0.8105
Black soil	512.2667	78.3782	0.9569	122.2293	2.6892	5.3592	0.8485

Note: R stands for correlation coefficient; $p<0.01$ indicates significant correlation

Adsorption isotherm

The isotherm of heavy metal Cr in sediment and soil at 25℃ are introduced in *Figure 2* and *Figure 3*. From the Figures, with the increase of Cr concentration, the adsorption isotherms of Cr on the sediment and soil are on a gradual upward trend of slope, but the adsorption does not reach the saturation state. Within the test concentration range, when the initial concentration of Cr is 500 mg·kg^{-1}, the equilibrium adsorption capacity of sediment and soil to Cr reaches 8623.43 and 8396.40 mg·kg^{-1}, respectively. The

http://www.aloki.hu ● ISSN 1589 1623 (Print) ● ISSN1785 0037 (Online)
DOI: http://dx.doi.org/10.15666/aeer/1902_901914
© 2021, ALÖKI Kft., Budapest, Hungary

adsorption trend of Cr by different adsorbents (sediment and black soil) is roughly the same, but the adsorption amount is significantly different.

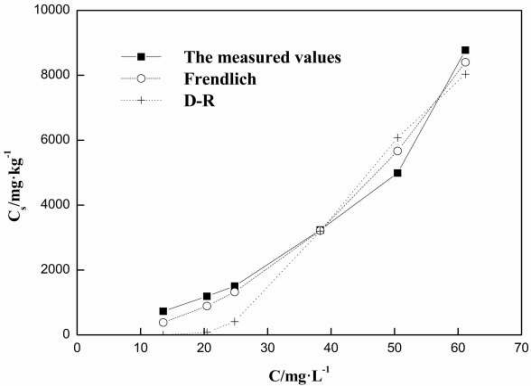


Figure 2. *Adsorption isotherms of Cr in sediment*

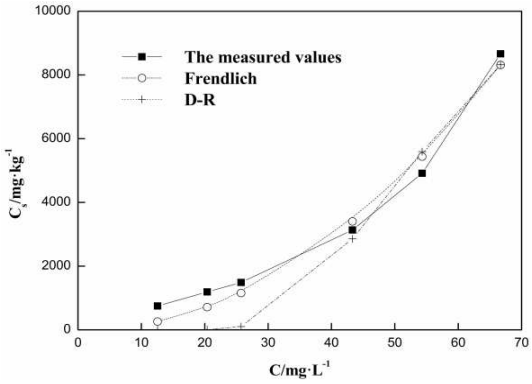


Figure 3. *Adsorption isotherms of Cr in black soil*

The isothermal adsorption curve of Cr by sediment and soil shows an "S" type. Through the adsorption isotherm data fitting, it is found that the Freundlich (Alemayehu et al., 2011) and D-R model has better data fitting effect than Langmuir model, which can explain the adsorption mechanism of Cr on sediment and soil more reasonably. *Table 3* shows the adsorption parameters of Freundlich and D-R. In the Freundlich model fitting, chromium adsorption coefficient R (0.9882 and 0.9834) in sediment and soil is higher than that of D-R model (0.9663 and 0.9675). This is mainly because when the concentration of Cr is less than 500 mg L^{-1}, the adsorption of Cr by sediment and soil does not reach saturation state. The Freundlich equation's adsorption constant K_f represents the adsorption capacity of the adsorbent. K_f sediment is 0.4439 larger than K_f soil, indicating that the sediment is more likely to absorb the metal Cr than the soil.

Table 3. *Parameters of the kinetics adsorption models for Cr in sediment and black soil*

Soil type	Freundlich model			D-R model			
	K_f	n	r	q_m	b	k	r
Sediment	1.8293	0.4882	0.9882**	14677.4102	0.1789	372.7705	0.9663**
Black soil	1.3854	0.4835	0.9834**	18359.7303	0.0346	581.1108	0.9675**

Note: n=12, r0.05=0.0.576, r0.01=0.708, **Represents significance level (p<0.01)

http://www.aloki.hu ● ISSN 1589 1623 (Print) ● ISSN1785 0037 (Online)
DOI: http://dx.doi.org/10.15666/aeer/1902_901914
© 2021, ALÖKI Kft., Budapest, Hungary

Adsorption thermodynamics

Temperature is not only an important environmental factor affecting adsorption but also an important condition affecting adsorption membrane properties. The thermodynamic curves of Cr adsorption in sediment and soil are depicted in *Figure 4* and *Figure 5*. It can be seen from the Figures that the adsorption of Cr in sediment and soil are 8623.40, 8776.82, 8911.64 $mg \cdot kg^{-1}$ and 8396.40, 8666.46, 8846.86 $mg \cdot kg^{-1}$ under the temperatures of 15℃, 25℃ and 35℃, respectively. With temperature increasing, the adsorption capacity of Cr in sediment and soil gradually enhances. It indicates that the higher the temperature is, the more favorable it is for Cr adsorbed on the bottom mud and soil surface to diffuse into the particle interior, and conducive to the transformation from thermodynamic unstable compound state to stable compound state.

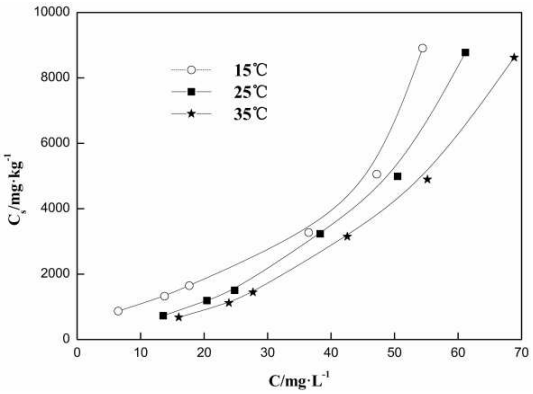


Figure 4. *Thermodynamic curves of Cr in sediment*

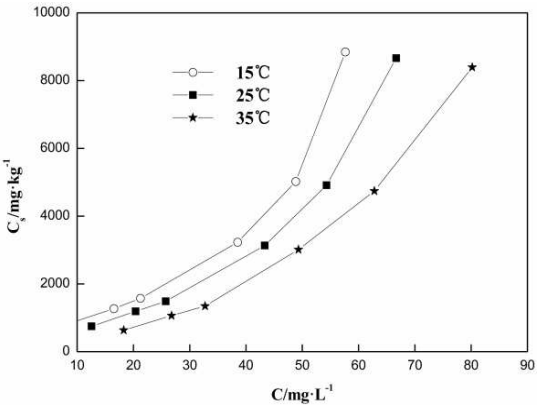


Figure 5. *Thermodynamic curves of Cr black soils*

Table 4 and *Table 5* show the adsorption thermodynamic parameters of Cr in sediment and soil. It can be seen that the Freundlich model has the best fitting effect, and the Q_m value increases with the increase of temperature, which further demonstrates that high temperature is conducive to the adsorption of Cr in sediment and soil. It can be observed from *Table 5* that within the test temperature range (15, 25 and 35℃), ΔG are less than zero; ΔH>0 shows that sediment and soil adsorption of Cr process is a

http://www.aloki.hu ● ISSN 1589 1623 (Print) ● ISSN1785 0037 (Online)
DOI: http://dx.doi.org/10.15666/aeer/1902_901914
© 2021, ALÖKI Kft., Budapest, Hungary

spontaneous endothermic process, and high temperature is beneficial to spontaneous adsorption. The adsorption of heavy metals by adsorbents experiences an endothermic process, and the experimental results are consistent with the trend of (Singh et al., 2017). ΔG and ΔH show that seasonal differences exist in sediment, soil buffer capacity Cr, liquidity and activity of (Lyubchik et al., 2004; Alothman et al., 2013).

Table 4. *Adsorption simulation equation parameters for different temperatures*

Sample type	Temperature (°C)	Freundlich equation			D-R equation		
		K_f	n	R^2	q_m	k	R^2
Sediment	15	1.430	0.488	0.9902	14279.30	452.5590	0.8990
	25	1.829	0.488	0.9776	14677.41	372.7706	0.8753
	35	3.313	0.513	0.9008	21766.84	470.4402	0.8118
Black soil	15	1.015	0.487	0.9948	14445.38	632.5860	0.9161
	25	1.385	0.483	0.9364	18359.73	581.1089	0.8757
	35	1.756	0.479	0.9382	21138.22	506.8181	0.8435

Table 5. *Adsorption thermodynamic parameters of Cr in sediment and soil*

Soil type	ΔG			ΔH	ΔS
	15℃	25℃	35℃		
Sediment	-0.8507	-1.9506	-3.0504	30.8503	0.1105
Black soil	-0.0702	-0.6309	-1.3306	20.2406	0.0708

Effect of pH on Cr adsorption

A variety of factors can affect the adsorption of metal Cr by the adsorbent. *Figure 6* shows the effect of different pH values on the adsorption of metal Cr. It can be seen that with the increase of pH value, the adsorption capacity of sediment and soil to Cr first increases and then decreases. When the pH value of the experimental environment was 3, chromium has the lowest adsorption capacity in sediment and soil, which was 3090.62 $mg \cdot kg^{-1}$ and 2256.62 $mg \cdot kg^{-1}$, respectively. When pH was 7, it reaches the turning point of adsorption, and the maximum adsorption capacity was 3140.02 and 2406.84 $mg \cdot kg^{-1}$, respectively.

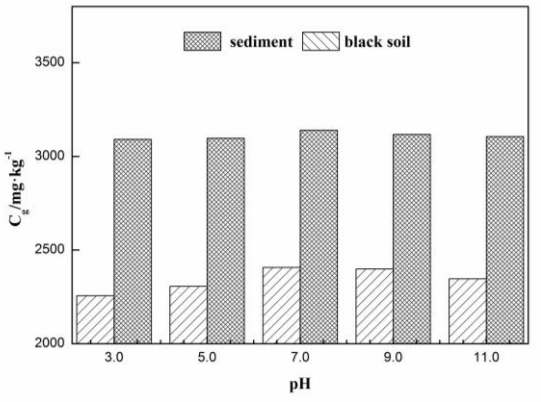


Figure 6. *Effect of pH on Cr adsorption in sediment and black soil*

http://www.aloki.hu ● ISSN 1589 1623 (Print) ● ISSN1785 0037 (Online)
DOI: http://dx.doi.org/10.15666/aeer/1902_901914
© 2021, ALÖKI Kft., Budapest, Hungary

When the pH value was within the range of 7-9, the adsorption effect of heavy metal Cr reaches the maximum level in sediment and soils, and the adsorption capacity of Cr was stronger in sediment. When pH was 11, the content of OH^- in the solution increases, and the competitive adsorption from H^+ decreases. At this time, the activity of Cr decreases, thus reducing the migration ability of Cr in soil and sediment. The adsorption amount of Cr in sediment and soil was the smallest when the pH was 3, and the adsorption amount was the largest when the pH was 7. Within the pH range of the test, higher and lower pH values were not conducive to the adsorption of Cr by sediment and soil. With the increase of pH, the adsorption capacity of Cr by soil and sediment first increased and then decreased. The adsorption amount of Cr in sediment and soil was the smallest at the pH 3, and the adsorption amount was the largest at the pH 7. However, the difference between adsorption of Cr under different pH in the sediment was not significant ($p>0.05$), and the adsorption of Cr under different pH in the soil was significant ($p<0.05$). This may be due to the higher content of organic matter in the sediment, and higher organic matter makes the sediment have a higher adsorption capacity of Cr, so the impact of organic matter content was greater than the pH value.

The reason for this phenomenon was assumed to be that when pH was 3, the solution contains a large number of H^+, and the presence of H^+ produces competitive adsorption with Cr. The pH changes the existing form of Cr in sediment and soil. The lower the pH is, the greater the potential difference of the system will be, thus making it easier for some Cr(VI) to be converted into Cr(III). Cr(III) produces precipitation benefit, reducing the equilibrium concentration of Cr(VI) in solution (Chen et al., 2015). The pH affects H^+ concentration in sediment and soil. The lower the pH, the higher the H^+ concentration, the dissociation of hydroxyl group (-OH) on the surface of soil colloidal particles will be affected, and the potential balance of the colloidal group will be destroyed (Liu et al., 2012). With the increase of pH, the content of H^+ in the solution decreases gradually, competitive adsorption decreases, and OH^- increases. The content of calcium carbonate and hydroxyl (-OH) in the colloidal core in the soil was high, which strengthens the adsorption and fixation of Cr by carbonate and oxide in the soil (Zhang et al., 2017). When pH value continues to rise, the increase of OH^- concentration will reduce the proton adsorption sites on the surface of adsorbent, enhance the electro negativity of sediment and soil surface, and weaken the adsorption capacity of anionic groups such as $HCrO_4^-$, CrO_4^{2-} and $Cr_2O_7^{2-}$, resulting in the decline of Cr adsorption capacity (Wang et al., 2013).

Effects of organic matter on Cr adsorption

As one of the most active solid components in soil chemistry, soil organic matter has a strong adsorption effect on pollutants, thus affecting their migration behavior. When the content of organic matter was high, these organic matter can be complexed with heavy metal ions, thus changing the adsorption property of soil and sediment. The cation exchange capacity in soil and sediment was restricted by oxygen-containing functional groups in humus. Therefore, the humic acid in organic matter can change the cation exchange capacity and thus affect the adsorption capacity of soil and sediment to Cr. *Figure 7* and *Figure 8* show the changes of Cr adsorption before and after removal of organic matter from sediment and soil. It can be seen that before and after the removal of organic matter, when the concentration of Cr added in the solution was at most 500 $mg \cdot L^{-1}$, the Cr adsorption capacity of sediment reached 8776.82 and 5836.58 $mg \cdot kg^{-1}$, and the Cr adsorption capacity of soil was 8646.46 and

http://www.aloki.hu ● ISSN 1589 1623 (Print) ● ISSN1785 0037 (Online)
DOI: http://dx.doi.org/10.15666/aeer/1902_901914
© 2021, ALÖKI Kft., Budapest, Hungary

5826.52 mg·kg^{-1}, respectively, moreover, the difference of adsorption amount for Cr between before and after the removal of organic matter in sediment and soil was significant (P <0.05). According to the formula of contribution rate = (Q-Q removal) /Q removal, the contribution rate of organic matter in sediment and soil to Cr was 50.38% and 48.40%, respectively. This is related to the organic matter content of the sediment and soil. Organic matter provides large amounts of pollutants adsorption points, and has a strong surface adsorption capacity. The organic matter can reduce hexavalent Cr to trivalent Cr in sediment and soil, and make it into a fixed precipitation state and the organic combination state and lose activity (Agrafioti et al., 2014).

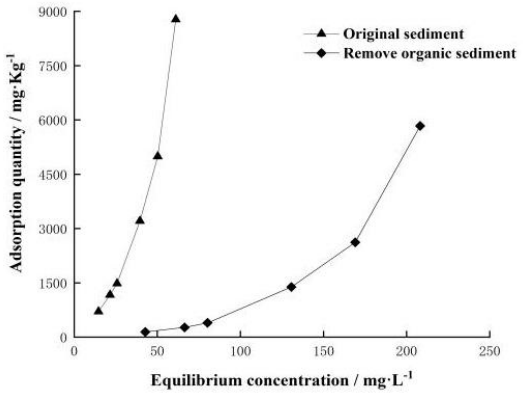


Figure 7. *Adsorption isotherm of Cr onto sediment before and after removal of organics*

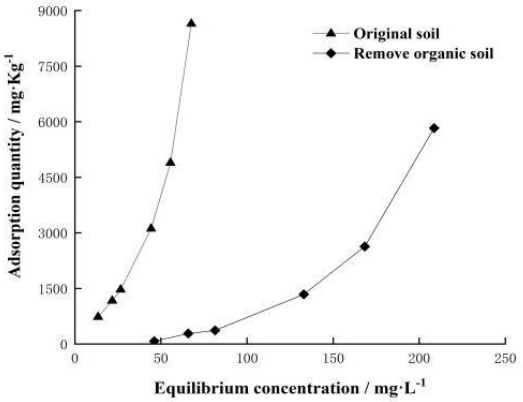


Figure 8. *Adsorption isotherm of Cr onto soil before and after removal of organics*

Conclusion

(1) Compared with the soil, the lake sediment had a strong adsorption capacity for Cr under the same condition, and the maximum adsorption amount of Cr in sediment and soil was 1,665.02 mg·kg^{-1} and 1079.04 mg·kg^{-1}, respectively. The isothermal adsorption curve of Cr in sediment and soil showed an "S" type, and the Freundlich equation was better to describe the thermodynamic characteristics of Cr adsorption.

(2) Within the temperature range designed in the experiment, the thermodynamic parameters G<0, ΔH>0, indicates that sediment and soil adsorption of Cr process is

http://www.aloki.hu ● ISSN 1589 1623 (Print) ● ISSN1785 0037 (Online)
DOI: http://dx.doi.org/10.15666/aeer/1902_901914
© 2021, ALÖKI Kft., Budapest, Hungary

spontaneous and endothermic, and high temperature is beneficial to the spontaneity of the adsorption.

(3) In the test pH range, higher and lower pH values are not conducive to the adsorption of Cr by sediment and soil. With the increase of pH value, the adsorption capacity of soil and sediment to Cr first increased and then decreased. The adsorption capacity of Cr by sediment and soil is minimum at pH 3 and maximum at pH 7. Therefore, in acidic and alkaline environment, it is not conducive to the fixation of Cr in soil and sediment, which increases the environmental risk of Cr.

(4) The contribution rate of organic matter in sediment and soil to Cr was 50.38% and 48.40%, respectively. After the organic matter is removed, the adsorption capacity was significantly reduced, the activity of Cr increases and resulted in the increase of the environmental risk of Cr.

This article studied the adsorption characteristics of Cr in sediment and soil, and effects of the value of pH and content of organic matter on the absorption capacity of Cr, in order to seek effective control measures of the Cr environmental risk in soil and sediment through adjusting the environmental conditions such as temperature, the content of organic matter and pH and so on.

Acknowledgements. The research was funded by the National Natural Science Foundation of China (Grant No.: 31672051), the Development Plan of Jilin Provincial Department of Science and Technology (Grant No.: 20200402013NC), Project of Natural Science Foundation of Jilin Province (20200201217JC) and Jilin Provincial Department of Education (Grant No.: JJKH20200337KJ).

Conflicts of Interests. The authors declare no conflict of interests.

REFERENCES

[1] Abat, M., McLaughlin, M. J., Kirby, J. K., Stacey, S. P. (2012): Adsorption and desorption of copper and zinc in tropical peat soils of Sarawak, Malaysia. – Geoderma 175-176: 58-63.

[2] Agrafioti, E., Kalderis, D., Diamadopoulos, E. (2014): Arsenic and chromium removal from water using biochars derived from rice husk, organic solid wastes and sewage sludge. – Journal of Environmental Management 133: 309-314.

[3] Alemayehu, E., Thiele-Bruhn, S., Lennartz, B. (2011): Adsorption behaviour of Cr(VI) onto macro and micro-vesicular volcanic rocks from water. – Separation & Purification Technology 78(1): 55-61.

[4] Alothman, Z., Naushad, M., Ali, R. (2013): Kinetic, equilibrium isotherm and thermodynamic studies Drinčić Aof Cr (VI) adsorption onto low-cost adsorbent developed from peanut shell activated with phosphoric acid. – Environmental Science & Pollution Research 20(5): 3351-3365.

[5] Arias, M., Pérez-Novo, C., López, E., Soto, B. (2006): Competitive adsorption and desorption of copper and zinc in acid soils. – Geoderma 133(3-4): 151-159.

[6] Chen, X., Chen, G., Chen, L., Chen, Y., Lehmann, J., McBride, M. B., Hay, A. G. (2011): Adsorption of copper and zinc by biochars produced from pyrolysis of hardwood and corn straw in aqueous solution. – Bioresource Technology 102(19): 8877-8884.

[7] Chen, S. Y., Wang, C. D., Li, S. X. (2015): Different pH on the adsorption of Cr (VI) in purple soil. – Environmental engineering 857-860.

[8] Dali-Youcef, N., Ouddane, B., Derriche, Z. (2006): Adsorption of zinc on natural sediment of Tafna River (Algeria). – Journal of Hazardous Materials 137(3): 1263-1270.

http://www.aloki.hu ● ISSN 1589 1623 (Print) ● ISSN1785 0037 (Online)
DOI: http://dx.doi.org/10.15666/aeer/1902_901914
© 2021, ALÖKI Kft., Budapest, Hungary

[9] Dong, D., Zhao, X., Hua, X., Liu, J., Gao, M. (2009): Investigation of the potential mobility of Pb, Cd and Cr(VI) from moderately contaminated farmland soil to groundwater in northeast, China. – Journal of Hazardous Materials 162(2-3): 1261-1268.
[10] Drinčić, A., Zuliani, T., Ščančar, J., Milačič, R. (2018): Determination of hexavalent Cr in river sediments by speciated isotope dilution inductively coupled plasma mass spectrometry. – Science of the Total Environment 637-638: 1286-1294.
[11] Fan, T., Liu, Y., Feng, B., Zeng, G., Yang, C., Zhou, M., Zhou, H., Tan, Z., Wang, X. (2008): Biosorption of Cadmium(II), Zinc(II) and Lead(II) by Penicillium simplicissimum: Isotherms, kinetics and thermodynamics. – Journal of Hazardous Materials 160(2-3): 655-661.
[12] Fonseca, B., Maio, H., Quintelas, C., Teixeira, A., Tavares, T. (2009): Retention of Cr(VI) and Pb(II) on a loamy sand soil: kinetics, equilibria and breakthrough. – Chemical Engineering Journal 152(1): 212-219.
[13] Jiang, B., Gong, Y. F., Gao, J. N., Sun, T., Liu, Y. J., Oturan, N., Oturan, M. A. (2018): The reduction of Cr (VI) to Cr (III) mediated by environmentally relevant carboxylic acids: State-of-the-art and perspectives. – Journal of hazardous materials 365: 205-226.
[14] Li, Y., Liu, W., Chen, F., Zhao, Q. (2013): Adsorption properties of thiol-functionalized bentonite for heavy metals. – Chinese Journal of Environmental Engineering 7(8): 3013-3018.
[15] Liu, Z. J., Chen, L., Dong, Y., Li, Y. Y., Wang, P. (2012): The ionic strength, pH and concentration of humic acid on 63 Ni (Ⅱ) on gamma Al203 adsorption. – The effect of chemical and nuclear radiation chemistry 34(6): 369-373.
[16] Liu, H., Dai, J. L. (2015): The effect of organic matter and organic acid on the chromium release in sediment. – Advanced Materials Research 1081: 88-92.
[17] Liu, W., Jin, L. D., Xu, J., Liu, J., Li, Y. Y., Zhou, P. P., Wang, C. C., Dahlgren, R. A., Wang, X. D. (2018): Insight into pH Dependent Cr (VI) Removal with Magnetic Fe3S4. – Chemical Engineering Journal 359: 564-571.
[18] Lyubchik, S. I., Lyubchik, A. I., Galushko, O. L., Tikhonova, L. P., Vital, J., Fonseca, I. M., Lyubchik, S. B. (2004): Kinetics and thermodynamics of the Cr (Ⅲ) adsorption on the activated carbon from co-mingled wastes. – Colloids & Surfaces A Physicochemical & Engineering Aspects 242(1-3): 151-158.
[19] Pan, D. M., Ding, S. L. (2011): Advances in adsorption, migration and accumulation of chromium in soil and plants. – Western leather 33(2): 22-25.
[20] Qiao, D., Wang, G., Li, X., Wang, S., Zhao, Y. (2020): Pollution, sources and environmental risk assessment of heavy metals in the surface amd water, sediments and surface soils around unexploited Rona Cu deposit, Tibet, China. – Chemosphere 248: 125988. https://doi.org/10.1016/j.chemosphere.2020.125988.
[21] Singh Rathore, A., Kishore Gupta, G., Kapur, M., Kumar Mondal, M. (2017): Study on mass transfer characteristics for Cr (VI) removal by adsorption onto residual black toner ink. – Environmental Progress & Sustainable Energy 36(4): 1022-29.
[22] Song, L., Liu, F. Q., Zhu, C. Q., Li, A. M. (2019): Facile one-step fabrication of carboxymethyl cellulose based hydrogel for highly efficient removal of Cr (VI) under mild acidic condition. – Chemical Engineering Journal 369: 641-651.
[23] Tokunaga, T. K., Wan, J., Firestone, M. K. (2001): Chromium diffusion and reduction in soil aggregates. – Environmental Science & Technology 35(15): 3169-74.
[24] Vega, F. A., Covelo, E. F., Andrade, M. L. (2006): Competitive sorption and desorption of heavy metals in mine soils: influence of mine soil characteristics. – Journal of Colloid & Interface Science 298(2): 582-592.
[25] Wang, T., Liu, W., Xiong, L., Xu, N., Ni, J. (2013): Influence of pH, ionic strength and humic acid on competitive adsorption of Pb (Ⅱ), Cd (Ⅱ) and Cr (Ⅲ) onto titanate nanotubes. – Chemical Engineering Journal 215-216: 366-374.

http://www.aloki.hu ● ISSN 1589 1623 (Print) ● ISSN1785 0037 (Online)
DOI: http://dx.doi.org/10.15666/aeer/1902_901914
© 2021, ALÖKI Kft., Budapest, Hungary

[26] Zeng, F., Ali, S., Zhang, H., Ouyang, Y., Qiu, B., Wu, F., Zhang, G. (2011): The influence of pH and organic matter content in paddy soil on heavy metal availability and their uptake by rice plants. – Environmental pollution 159(1): 84-91.
[27] Zhang, X., Tong, J., Hu, B. X., Wei, W. (2017): Adsorption and desorption for dynamics transport of hexavalent chromium (Cr (VI)) in soil column. – Environmental Science & Pollution Research International 25(5): 1-10.
[28] Zhang, L. X., Tang, S. Y., He, F. X., Liu, Y., Mao, W., Guan, Y. T. (2019): Highly efficient and selective capture of heavy metals by poly(acrylic acid) grafted chitosan and biochar composite for wastewater treatment. – Chemical Engineering Journal 378: 122215.

http://www.aloki.hu ● ISSN 1589 1623 (Print) ● ISSN1785 0037 (Online)
DOI: http://dx.doi.org/10.15666/aeer/1902_901914
© 2021, ALÖKI Kft., Budapest, Hungary

SPATIOTEMPORAL DISTRIBUTION CHARACTERISTICS OF WINTER WHEAT (*TRITICUM AESTIVUM* L.) WATER REQUIREMENTS AND ITS CLIMATIC DRIVING FACTORS DURING A LONG-TERM PERIOD (1969-2019): A STUDY OF SHANDONG PROVINCE, CHINA

CONG, X. – KONG, K. – XU, J. – XU, Z. H.* – WANG, R. Z. – JIAO, Z. – ZHANG, H. W.

School of Water Conservancy and Environment, University of Jinan, Jinan 250022, PR China (e-mail: congxin1994@126.com)

**Corresponding author*
e-mail: xu4045@126.com; phone:+86-186-6898-0091

(Received 24th Oct 2020; accepted 21st Dec 2020)

Abstract. Understanding the change of water requirement (*ET*) for crop production under climate change can provide scientific support for the management of agricultural water resources. The objective behind this study was to analyze spatiotemporal distribution characteristics of *ET*, effective rainfall (P_e), irrigation requirement (*IR*) and aridity index (*AI*) of winter wheat, and evaluate the driving force of *ET* changes as a result of the variation of climatic factors. Daily meteorological data from 18 meteorological stations from 1969 to 2019 distributed throughout Shandong Province, China were collected. Five climatic variables including maximum daily temperature (T_{max}), minimum daily temperature (T_{min}), relative humidity (*RH*), wind speed (*WS*), and sunlight hours (*SH*), were selected to identify their contribution to the variability of *ET*. Results indicated that (1) *ET* distribution differed significantly both in temporal and spatial scale on a general, and decreased -14.11-3.88 mm decade^{-1}. (2) T_{max} was the most influential climatic variable related to *ET* variability with sensitivity coefficient of 0.36, followed by *RH* (-0.34), *SH* (0.13), *WS* (0.11) and T_{min} (-0.07). (3) Declines of *WS* and *SD* were indicated by the decrease of *ET* while the increase of T_{max} and the decrease of *RH* contributed to enhancing *ET*.
Keywords: *water requirement, effective precipitation, irrigation requirement, Mann-Kendall, spatiotemporal characteristics, sensitivity analysis, winter wheat*

Introduction

At present, climate change and freshwater shortage have been regarded as the two most important global issues (Wu et al., 2019). China is a grain-producing country, generating more than half of the world's wheat and corn (Yin et al., 2016). In modern China, the shortage of water resource turns to be the biggest constraint of the agricultural development (Zhang et al., 2018). For example, the major grain producing provinces of China, Henan and Shandong, have both been facing significant trend of decreasing total water resources since the 21st century (Wu et al., 2020). Worse, with global warming due to climate change, irrigation requirements are increasing (Yuan et al., 2015). This creates a huge gap between the supplied and required agricultural water resources.

Crop water requirement (*ET*) is considered as an important basis for planning and design of irrigation water management, which is different due to the influence of soil, climate, crop growth status and management methods. In recent years, extensive research has aimed at exploring the spatial and temporal characteristics of *ET* and the effects of climate on *ET*. Sun et al. (2013) analysed the *ET* data of winter wheat at 356 stations in China from 1961 to 2010, and concluded that the water demand of winter wheat (*Triticum aestivum* L.) in the whole growth period showed a downward trend in recent 50 years. Liu and Lin (2004)

http://www.aloki.hu ● ISSN 1589 1623 (Print) ● ISSN 1785 0037 (Online)
DOI: http://dx.doi.org/10.15666/aeer/1902_915932
© 2021, ALÖKI Kft., Budapest, Hungary

studied the influence of climate warming on water demand of main crops in North China. They thought that climate warming had the greatest impact on water demand of winter wheat, followed by cotton and summer maize. Gao et al. (2019) determined the impacts of climate change on crop water requirements in the double cropping system in Northern China using the annual accumulated temperature above 0℃.

In this study, Shandong Province was selected as the research object. The winter wheat planting area of Shandong is maintained at 2×10^5 hm^2 all the year round, and the total wheat yield accounts for 18% of the national wheat output. Since the amount of precipitation is very low in most of the region during the winter wheat cropping season, irrigation is essential for wheat growth. In Shandong, drought is the impact of wheat production to enhance the first limiting factor. So, it is of great significance to study the crop water requirements in the context of climate change.

There are few synthetic studies on the spatial-temporal variation of *ET* on wheat and the impacts of the driving factors on *ET* both nationally and regionally in the main grain production area - Shandong Province, and the mechanisms responsible for changing *ET* remain uncertain. Given the important role of the Shandong farming region for the Chinese food security and the characteristics of little rainfall in wheat growing season, to fill this gap, this paper investigates three issues: (i) to estimate the temporal-spatial variations of *ET*, effective precipitation (P_e), irrigation requirement (*IR*) and aridity index (*AI*) under a historical data (1969-2019); (ii) to quantify the contributions of climate work on *ET* of winter wheat; (iii) to analyse the mechanisms responsible for changing *ET*. The results will help understand the mechanisms of *ET* change caused by climate change and provide a reference for the scientific irrigation of winter wheat in Shandong Province.

Materials and Methods

Study area

Located in the eastern coast of China, the Shandong Province ranges from the latitudes of 34°22′N to 38°24′N and the longitudes of 114°47′E to 122°42′E, with an area of 15.79×10^4 km^2 that is covered by 15 prefecture-level cities (*Fig. 1*). The region is dominated by a temperate monsoon climate with a mean annual temperature range between 6℃ and 8℃, and a mean annual precipitation of 370.6-505.3 mm, of which approximately 70% occurs from June to September (statistics during 1969-2019). Summer high temperature and rain, sufficient light conditions are suitable for agricultural planting. The major cropping pattern is the winter wheat-summer maize double cropping system. Generally, the winter wheat is sown in early October in the previous year and harvested in early or mid-June in the following year, and the timing of sowing and harvesting for summer maize are at the end of May and September in the same year, respectively.

Data and sources

The data includes daily meteorological data and agricultural statistics data. Daily meteorological data were downloaded from the China meteorological data sharing service system (http://cdc.cma.gov.cn/), which included a total of 18 meteorological stations distributed throughout Shandong Province (*Fig. 1*). It includes daily maximum daily temperature (T_{max}), minimum daily temperature (T_{min}), relative humidity (*RH*), wind speed (*WS*), sunshine hours (*SH*) and precipitation (*P*). Then, the gaps of data were filled using the following strategies: (1) linear interpolation when the number of consecutive missing

http://www.aloki.hu ● ISSN 1589 1623 (Print) ● ISSN 1785 0037 (Online)
DOI: http://dx.doi.org/10.15666/aeer/1902_915932
© 2021, ALÖKI Kft., Budapest, Hungary

data was < 5 and substitution with the mean value of other years when the number of consecutive missing data was ≥5 for all variables except for precipitation, and (2) replacement with the value on the same day based on the nearest meteorological station for only the precipitation data. Agricultural statistics data mainly includes crop growth period, which were downloaded from agrometeorology material in China meteorological data sharing service system. In addition, the winter wheat yield of each city from 2000 to 2018 came from the Shandong Statistic Year Book.

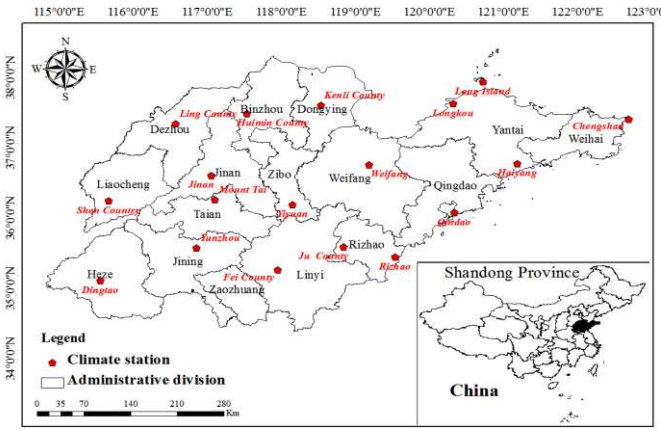


Figure 1. *Location of meteorological stations in Shandong Province, China*

Methods

Crop water requirements (ET)

It is calculated as the crop water requirements (*ET*, mm d^{-1}) using the crop coefficient (K_c) and reference evapotranspiration (ET_0, mm d^{-1}) recommended by the FAO (Allen et al., 1998). The *ET* is calculated as follows (*Eq. 1*):

$$ET = K_c \times ET_0 \quad \text{(Eq.1)}$$

The crop coefficient K_c, is defined for the initial growing stage (K_{cini}), dormancy season (K_{cdor}), mid-season (K_{cmid}) and end-season (K_{cend}). Notably, the crop coefficient of winter wheat over initial growing stage and the dormancy period were set to 0.6 (K_{cini}) (Dong et al., 2013; Sun et al., 2013) and 0.4 (K_{cdor}) (Tao et al., 2003). The values in mid-season and end-season were obtained by single crop coefficient approach (Allen et al., 1998) and were listed in *Table 1*.

Then, based on the K_{cini}, K_{cdor}, K_{cmid}, K_{cend} and crop phenology period, the daily crop coefficient could be computed by linear interpolation. The single crop coefficient approach was used to calculate the crop coefficients, as follows (*Eq. 2*):

$$K_c = K_{ctab} + [0.04(U_2 - 2) - 0.04(RH_{min} - 45)]\left(\frac{h}{3}\right)^{0.3} \quad \text{(Eq.2)}$$

where K_{ctab} is the crop coefficient of corresponding growth stage, U_2 is the wind speed at 2 m height (m s^{-1}), RH_{min} is the average value of daily minimum relative humidity in corresponding growth stages (%), h is the average height of crops in corresponding growth stages (cm).

http://www.aloki.hu ● ISSN 1589 1623 (Print) ● ISSN 1785 0037 (Online)
DOI: http://dx.doi.org/10.15666/aeer/1902_915932
© 2021, ALÖKI Kft., Budapest, Hungary

Table 1. *Growth period and crop coefficient of winter wheat*

Meteorological stations	**Beginning date of initial growth period**	**End date of initial growth period**	**Beginning date of dormancy season**	**End date of dormancy season**	**Beginning date of mid-season**	**End date of mid-season**	**Harvest date**	K_{cini}	K_{cdor}	K_{cmid}	K_{cend}
	Sowing date (date/month)	Tillering stage (date/month)	Overwintering period (date/month)	Green return period (date/month)	Jointing stage (date/month)	Heading date (date/month)	Mature period (date/month)				
Ling County	9 October	30 October	3 December	1 March	4.13 April	5 May	10 June	0.6	0.4	1.15	0.4
Huimin	9 October	30 October	3 December	1 March	4.13 April	5 May	10 June	0.6	0.4	1.15	0.4
Kenli	9 October	30 October	3 December	1 March	4.13 April	5 May	10 June	0.6	0.4	1.16	0.4
Long Island	3 October	23 October	14 December	15 March	4.16 April	7 May	15 June	0.6	0.4	1.19	0.4
Longkou	3 October	23 October	14 December	15 March	4.16 April	7 May	15 June	0.6	0.4	1.19	0.4
Chengshantou	3 October	23 October	14 December	15 March	4.16 April	7 May	15 June	0.6	0.4	1.17	0.4
Shen County	9 October	30 October	3 December	1 March	4.13 April	5 May	10 June	0.6	0.4	1.17	0.4
Jinan	12 October	1 November	17 December	27 February	4.06 April	28 April	7 June	0.6	0.4	1.17	0.4
Mount Tai	12 October	1 November	17 December	27 February	4.06 April	28 April	7 June	0.6	0.4	1.16	0.4
Yiyuan	12 October	1 November	17 December	27 February	4.06 April	28 April	7 June	0.6	0.4	1.15	0.4
Weifang	5 October	27 October	17 December	26 February	4.07 April	30 April	10 June	0.6	0.4	1.16	0.4
Qingdao	3 October	23 October	14 December	15 March	4.16 April	7 May	15 June	0.6	0.4	1.18	0.4
Haiyang	3 October	23 October	14 December	15 March	4.16 April	7 May	15 June	0.6	0.4	1.18	0.4
Dingtao	10 October	5 November	17 December	17 February	4.01April	24 April	5 June	0.6	0.4	1.15	0.4
Yanzhou	12 October	1 November	17 December	27 February	4.06 April	28 April	7 June	0.6	0.4	1.18	0.4
Fei County	5 October	27 October	17 December	26 February	4.07 April	30 April	10 June	0.6	0.4	1.18	0.4
Ju county	5 October	27 October	17 December	26 February	4.07 April	30 April	10 June	0.6	0.4	1.18	0.4
Rizhao	5 October	27 October	17 December	26 February	4.07 April	30 April	10 June	0.6	0.4	1.18	0.4

http://www.aloki.hu ● ISSN 1589 1623 (Print) ● ISSN 1785 0037 (Online)
DOI: http://dx.doi.org/10.15666/aeer/1902_915932
© 2021, ALÖKI Kft., Budapest, Hungary

The daily T_{max}, T_{min}, RH, SH, WS used to calculate ET_0 using the FAO Penman-Monteith equation (Allen et al., 1998), as follows (*Eq. 3*):

$$ET_0 = \frac{0.408\Delta(R_n-G)+\gamma(900/T+273)U_2(e_s-e_a)}{\Delta+\gamma(1+0.34U_2)} \quad \text{(Eq.3)}$$

where Δ is the slope of the saturation vapor pressure-temperature curve (kPa℃$^{-1}$), R_n is the net radiation (MJ m^{-2} d^{-1}), G is the soil heat flux (MJ m^{-2} d^{-1}), γ is the psychrometric constant (kPa ℃$^{-1}$), T is the average air temperature (℃), e_s is the saturation vapor pressure (kPa) and e_a is the actual air vapor pressure (kPa).

Effective precipitation (P_e)

The effective rainfall (P_e, mm) is the fraction of the rainfall excluding surface runoff, deep percolation or evaporation, which is calculated by the *US* Department of Agriculture Soil Conservation, as cited by Döll and Stefan (2002). Calculated as follows (*Eq. 4*):

$$\begin{cases} P_e = P\,(4.17 - 0.2P)/4.17 \cdots P < 8.3 \\ P_e = 4.17 + 0.1P \cdots\cdots\cdots\cdots P \geq 8.3 \end{cases} \quad \text{(Eq.4)}$$

Irrigation requirement (IR)

Following FAO 46, the irrigation requirement (*IR*, mm) during the growing season is defined as the difference between the *ET* and the P_e (Smith, 1992). The calculation formula is as follows (*Eq. 5*):

$$IR = \begin{cases} ET - P_e \cdots ET > P_e \\ 0 \cdots\cdots\cdots ET \leq P_e \end{cases} \quad \text{(Eq.5)}$$

Aridity index (AI) and drought frequency (DF)

AI is meaningful to water resource management. It is defined as the quotient of the difference between *ET* and P_e and *ET* (Shen et al., 2013). The specific calculation equation is as follows (*Eq. 6*):

$$AI = (ET - P_e)/ET \quad \text{(Eq.6)}$$

DF is the number of times in a certain period that drought series accounts for the total series length, which is defined as the quotient of the *N* and *n* (He et al., 2017). It was calculated by using the following equation:

$$DF = \frac{N}{n} \times 100\% \quad \text{(Eq.7)}$$

where, *N* is the number of times of drought at a certain level in growth stage; *n* is the length of the time series.

The division of agricultural drought grades was based on the national standard "Agricultural Drought Grades" and "Standardized Precipitation Evaporation Index (*SPEI*)". The detailed calculation of *SPEI* can be found in the Vicente-Serrano's research (2010). The *SPEI* calculations for this study used the computational procedures of the

http://www.aloki.hu ● ISSN 1589 1623 (Print) ● ISSN 1785 0037 (Online)
DOI: http://dx.doi.org/10.15666/aeer/1902_915932
© 2021, ALÖKI Kft., Budapest, Hungary

University of Nebraska approved by the World Meteorological Organization. According to the drought classification standard formulated by China Meteorological Administration, the drought grades of the region are divided, as shown in *Table 2*.

Table 2. *Classification of agricultural drought grades based on crop deficit index*

Grade type	Index range of *AI*	*SPEI*
No drought (*ND*)	*AI*≤35%	*SPEI*≥-0.5
Light drought (*LD*)	35%<*AI*≤50%	-1≤*SPEI*<-*0.5*
Moderate drought (*MD*)	50%<*AI*≤65%	-1.5≤ *SPEI*<-1
Severe drought (*SD*)	65%<*AI*≤80%	-2≤ *SPEI*<-1.5
Extreme drought (*ED*)	*AI*>80%	*SPEI*<-2

Trend analysis, abrupt change detection and mapping

The linear equation is usually used to describe the change trend of climate elements. The equation is as follows (*Eq. 8*):

$$y(t) = a + bt \quad \text{(Eq.8)}$$

In the formula, *t* is the time series, *a* is the empirical coefficient, which can be obtained by the least square method in the regression analysis method; *b* is the trend change rate, when *b* is positive (negative), it indicates that the air temperature elements have an increasing (decreasing) trend, and *10b* is the climate tendency rate, which represents the change rate of the temperature element in 10 year.

Abrupt change detection is used to check the possible change point of the time series that has an effect on the trend analysis results (Villarini et al., 2012; Gu et al., 2017). In this study, a comprehensive test about the mutation characteristics of *ET*, P_e, *IR* and *AI* were giving by using Mann-Kendall abrupt test and moving t-test technique. The reason for using the two methods is that moving t-test helps to deal with the multiple point mutations after using the Mann-Kendall abrupt test, which ensures the accuracy of the test results (Deng et al., 2018). Similarly, the level of significance was set to 0.05.

The data of *ET*, P_e, *IR* and *AI* in wheat growth period were interpolated by inverse distance weighted interpolation (IDW) in ArcGIS 10.2 to obtain the corresponding spatial distribution.

Sensitivity analysis

In this paper, the one-at-a-time (OAT) was used to analyze the sensitivity of the *ET* of wheat to its impact factors. The sensitivity of the *ET* to one factor can be expressed as (Eq.9) (Wang et al., 2019):

$$Sx_i = \lim_{\Delta x_i \to 0} \left(\frac{\Delta ET / ET}{\Delta x_i / x_i} \right) = \frac{\partial ET}{\partial x_i} \times \frac{x_i}{ET} \quad \text{(Eq.9)}$$

where, Sx_i is sensitivity coefficient of the influencing factors; *ET*, ΔET are irrigation requirement and the change of it; x_i, Δx_i is the influencing factors of irrigation requirement and its change.

http://www.aloki.hu ● ISSN 1589 1623 (Print) ● ISSN 1785 0037 (Online)
DOI: http://dx.doi.org/10.15666/aeer/1902_915932
© 2021, ALÖKI Kft., Budapest, Hungary

Previous research showed that the principal weather parameters affecting evapotranspiration were *T*, *RH*, *WS* and radiation. By significance test, the T_{max}, T_{min}, *RH*, *WS*, *SH* were selected for the sensitivity analysis.

Results and Discussion

Characteristics of ET, P_e, IR and AI

Temporal characteristics and abrupt change

The trends of the annual *ET*, P_e, *IR*, and *AI* of the winter wheat growth period in Shandong Province from 1969 to 2019 were shown in *Fig. 2*. As a whole, Shandong experienced a decrease in *ET*, P_e and *IR*, and *AI* remained relatively unchanged during the study period. Further, the ranges of the variations in the P_e were relatively small compared with the range of the *ET* and *IR* over the whole province. The *ET* and *IR* ranged from 380-475 mm and 242-397 mm, respectively, with the maximum occurring in 1978 and the minimum in 1998. The P_e ranged from 51 to 138 mm, the maximum occurred in 2011 and the minimum occurred in 1998. The *AI* ranged between 0.64 and 0.88, with the maximum occurring in 2011 and the minimum occurring in 2009. The coincidence of the occurrence time of the maximum value of each index indicated that the *IR* and *AI* were greatly influenced by the *ET* and P_e.

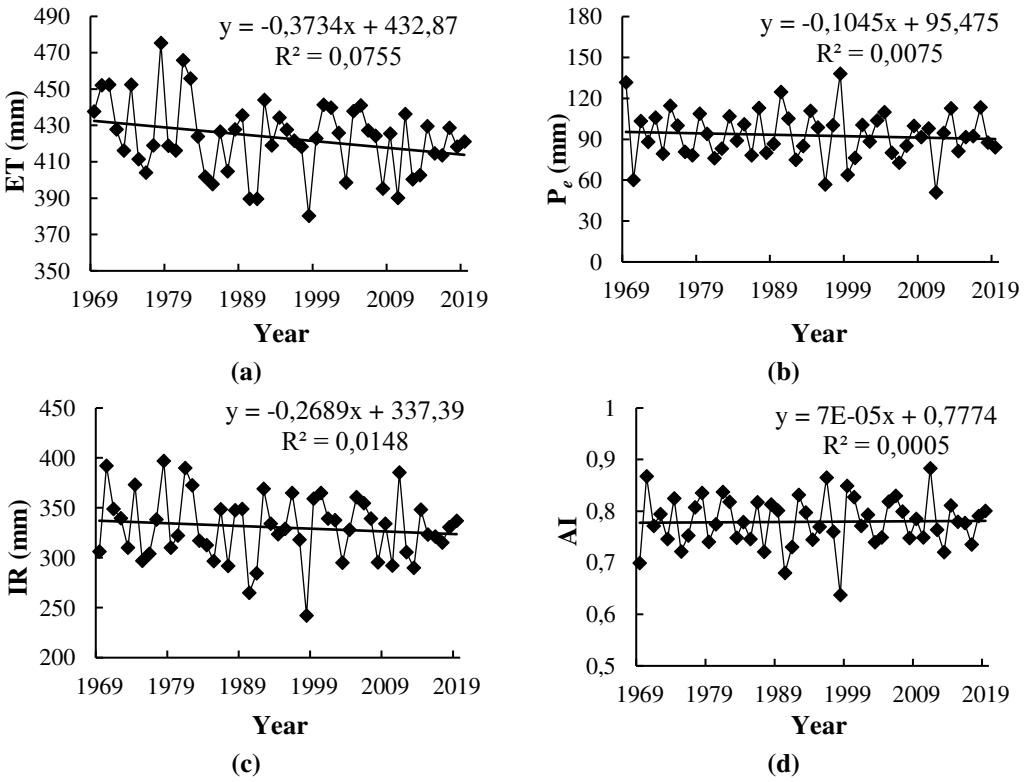


Figure 2. *Interannual variation of (a) ET; (b) P_e; (c) IR; (d) AI in winter wheat growth period*

According to Mann-Kendall abrupt test, there were seven obvious focuses in the reconfidence interval of UF and UB curves (*Fig. 3a*). Then, through the moving t-test, only one point was the mutation point, which was located in 1984 (*Fig. 3b*). This showed

http://www.aloki.hu ● ISSN 1589 1623 (Print) ● ISSN 1785 0037 (Online)
DOI: http://dx.doi.org/10.15666/aeer/1902_915932
© 2021, ALÖKI Kft., Budapest, Hungary

that 1984 was the abrupt change point of *ET* from rising to decreasing. Similarly, P_e, *IR* and *AI*, which have passed the Mann-Kendall abrupt test, had multiple intersections in the confidence interval between UF and UB (*Fig. 3c,e,g*). However, through the moving t-test, all the intersections were not abrupt points (*Fig. 3d,f,h*).

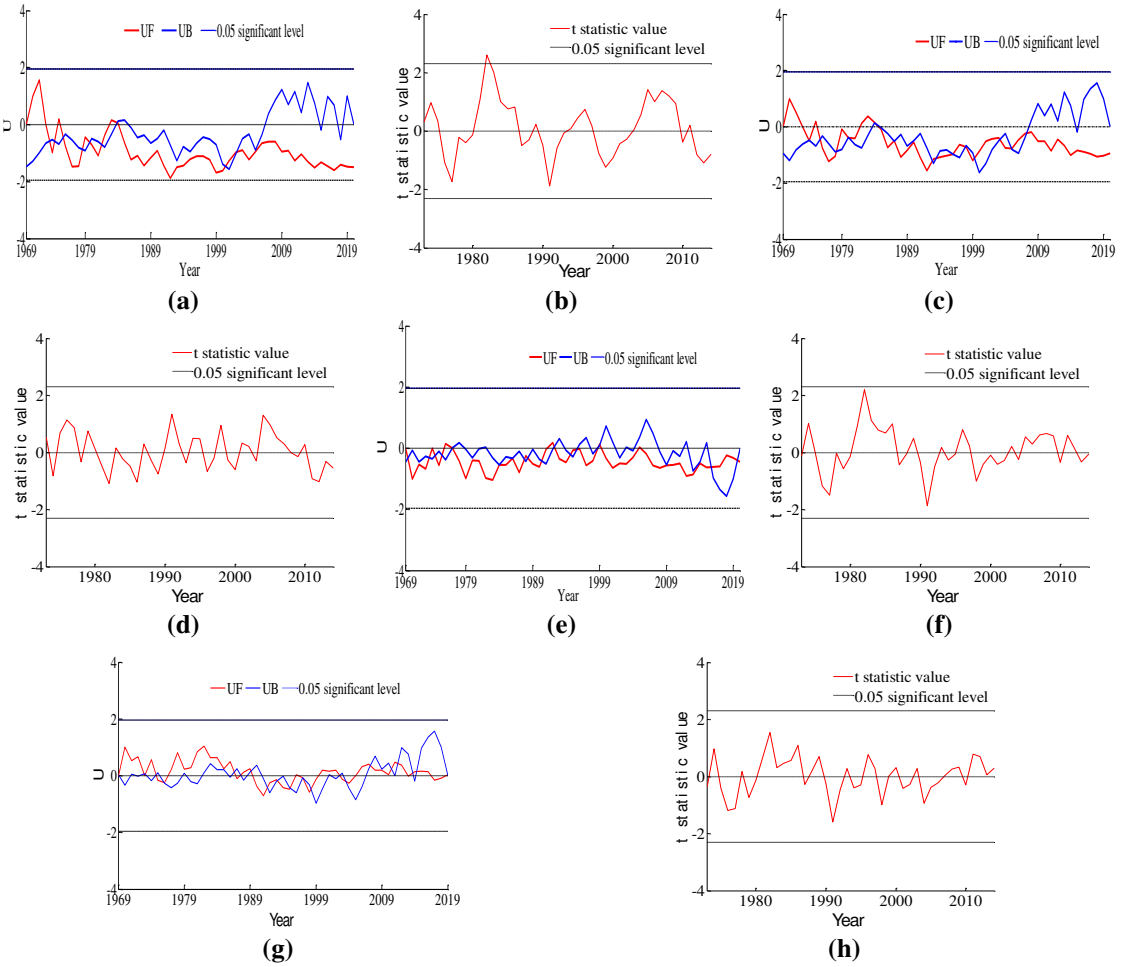


Figure 3. *Time series of (a,b) ET; (c,d) P_e; (e,f) IR; (g,h) AI mutation test curve of winter wheat*

In this paper, the simplified water balance formula was adopted to estimate the *ET*, P_e, *IR* and *AI* during the winter wheat growth stage in the Shandong Province, and this formula considers the ET_0 and K_c. This study showed that the *ET*, P_e, *IR* had been downward tendency and with different degree, and *AI* had no significant trend from 1969 to 2019. The results of this study were basically consistent with the conclusions of Ma et al. (2010). *ET* levels present a steady upward trend from 1969 to 1984 prior to dramatically declining. But now, the abrupt change of ET_0 levels-related research was few, the study of the abrupt change of *ET* levels of winter wheat was much rarer. And ET_0 was calculated by *ET*, the trend of ET_0 was similar in theory. Therefore, this paper discussed the changes of ET_0 analyzed by other scholars. Liang et al. (2010) discovered an abrupt change appeared in 1982 for annual ET_0 of the Taoer River basin of Northeast China; ET_0 levels decreased from 1961 to 1982 and then increased in China as indicated by Wang et al. (2017), and this time point was close to the time in which the valley value of annual *ET* happens in this study (*Fig. 3*).

http://www.aloki.hu ● ISSN 1589 1623 (Print) ● ISSN 1785 0037 (Online)
DOI: http://dx.doi.org/10.15666/aeer/1902_915932
© 2021, ALÖKI Kft., Budapest, Hungary

Spatial-temporal variation

The spatial distribution characteristics of the *ET*, P_e, *IR* and *AI* in Shandong Province were shown in *Fig. 4*. In terms of spatial variation of four indexes, in the winter wheat season, the distribution patterns of *ET* and *IR* were similar, they gradually decreased from the northwest to southeast, and a high-value center was located around the higher terrain area in the southwest region where the *ET* reached 500 mm and *IR* reached 400 mm. The spatial distribution of *IR* of winter wheat in this paper was consistent with the related research (Liu et al., 2013). There was also a remarkable gradient of distribution of P_e. It decreased from southeast to northwest, and the distribution of effective rainfall in coastal area was larger than that in inland area, and that in mountain area was larger than that in plain. The spatial pattern of *AI* was similar to that of *ET* and *IR*, with lower than 0.8 of *AI* within the strip expanding from the mid-northwest of the Shandong to the Jiaodong Peninsula where the *AI* in eastern Shandong was relatively low.

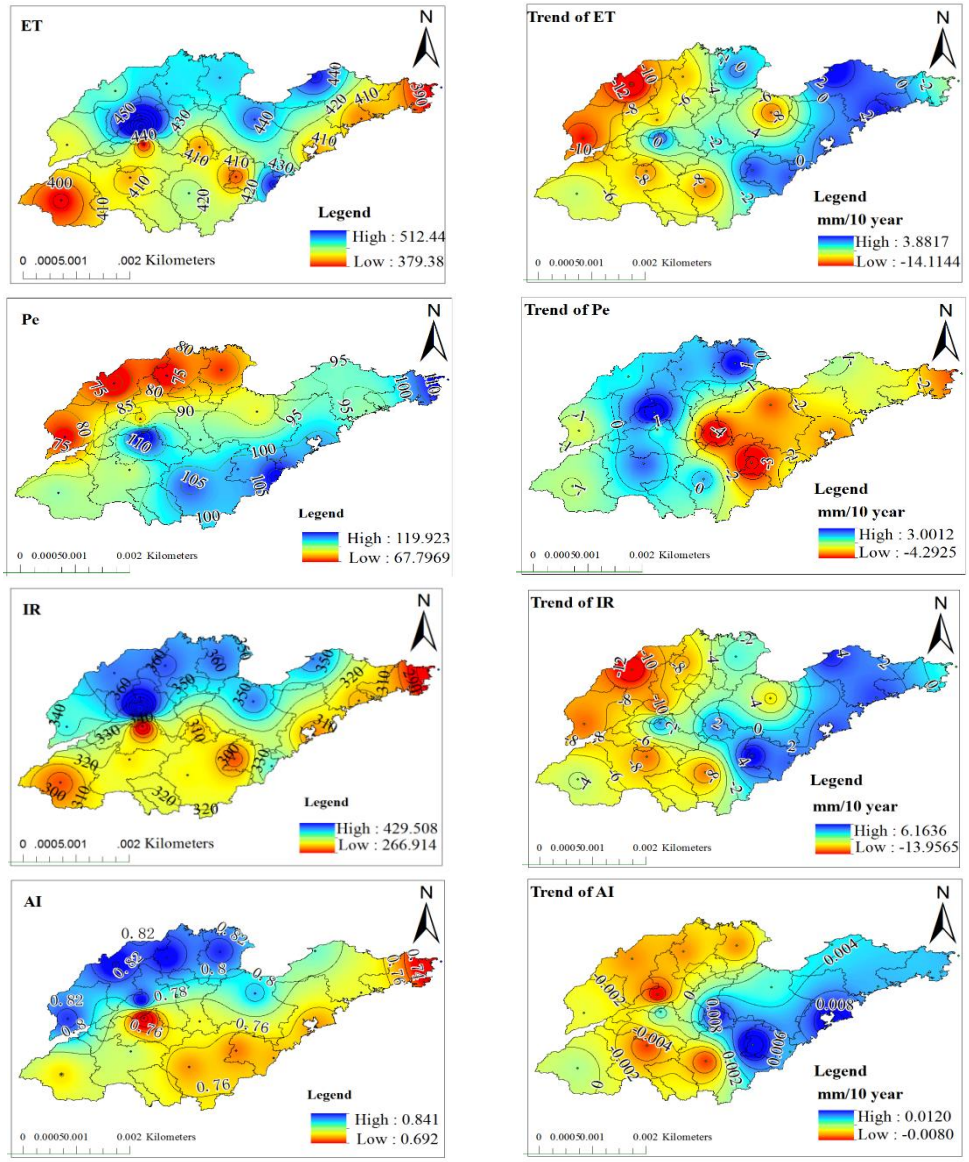


Figure 4. *Spatial and temporal variation in ET, P_e, IR and AI for winter wheat from 1969 to 2019*

http://www.aloki.hu ● ISSN 1589 1623 (Print) ● ISSN 1785 0037 (Online)
DOI: http://dx.doi.org/10.15666/aeer/1902_915932
© 2021, ALÖKI Kft., Budapest, Hungary

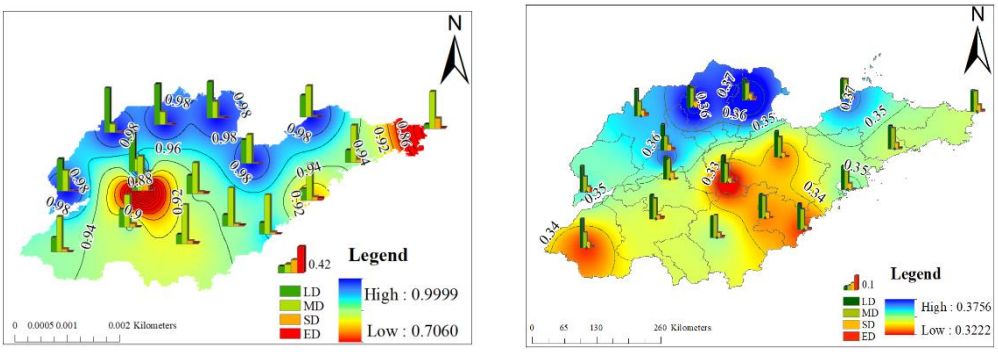
The *IR* was calculated by combining *ET* with P_e together for the winter wheat growth. Nevertheless, the spatial distribution of the corresponding stations of *ET* and P_e trends were distinctly different. For the four indexes, the overall spatial pattern of the trend in *IR* was similar to that of the trend in *ET*. The regions with increasing *ET* and *IR* mainly occurred in Jiaodong Peninsula. The *ET* and *IR* in the rest of the Shandong showed a decreasing trend. However, it can be clearly found that the *ET* and *IR* decreased with a trend of 10-12 mm decade^{-1} in most of northwest parts of the Shandong, within which the *ET* and *IR* in some regions, including the southwestern Shandong and near Bohai Bay in the middle of Shandong, decreased significantly by 2-8 mm decade^{-1}. The trend of P_e showed three zonal distributions from west to east. Among them, the P_e decreased with a trend of 0-1 mm decade^{-1}in the central part of Shandong, while P_e was showing an increasing trend in the rest of two regions. The increasing trend of P_e in the east was more obvious than that in the west, with an average of 3 mm decade^{-1}. For the *AI*, the overall spatial pattern of the trend in *AI* was similar to that of the trend in P_e. Apart from a clear reduction of the value in whole region with a decreasing trend of *AI*, only the area where the 0.01 mm decade^{-1} rising trend in *AI* occurred consisted of three parts, are the Jinan, the Linyi and the Jining.

On the whole, the results showed that the total effective precipitation in Shandong Province could not meet the water demand of winter wheat during the growth period, especially in the northern Shandong. The multi-year average *IR* values in this study were 330.04 mm for the winter wheat. From the spatial point of view, the imbalance of precipitation and water demand in time and space leads to the aggravation of drought in northern region. Although, the result of the variation of *IR* over Shandong in this study shows a decreasing trend (*Fig. 4*). On a time scale, the significantly decreasing *IR* accompanied by significantly decreasing *ET* and P_e revealed that the decreasing trend of *ET* is more significant than P_e. On a regional scale, the decline of *IR* in western region was attributed to both the significantly decrease in *ET* and slight increasing P_e. A decreasing pattern of water shortage for winter wheat in different regions of China can also be found in many existing studies. For example, Cao et al. (2018) have discovered the *IR* for winter wheat in Hebei Province showed the decreasing trend with the rate of -3.74 mm decade^{-1}. Wu et al. (2020) have suggested that the water shortage for winter wheat in the north of Anhui Province decreased in a 2.0 mm decade^{-1}.

Temporal-spatial distribution characteristics of drought in winter wheat growth period

The drought in Shandong analyzed by using *AI* and the 9-month *SPEI* for the period 1969-2019 was shown in *Fig. 5*. In terms of drought grade, it can be seen that the relative drought degree in the north-south direction of the two methods was consistent, although the drought frequency obtained by *AI* method was significantly higher than that by *SPEI* method. The frequency of drought in different grades was higher in the northwest part than in the southeast areas. The high frequency drought areas mainly occur in Dongying, Binzhou, Dezhou, Yantai and Liaocheng. It is worth noting that Xu and Han (2018) have also researched the distribution of drought frequency in Shandong Province by *SPEI*, and concluded that on the monthly scale, severe and above drought was higher in the north and lower in the south. The northwest of Shandong Province has large evaporation and relatively less precipitation, which is the driest climate area and high drought risk area in Shandong Province.

http://www.aloki.hu ● ISSN 1589 1623 (Print) ● ISSN 1785 0037 (Online)
DOI: http://dx.doi.org/10.15666/aeer/1902_915932
© 2021, ALÖKI Kft., Budapest, Hungary



(a) AI **(b) SPEI**

Figure 5. *The spatial distribution of frequency of potential moderate and above drought in winter wheat growth from 1969 to 2019*

Sensitivity analysis of ET of winter wheat to meteorological factors

Sensitivity of crop water productivity at different scale to influencing factors was analyzed by using OAT method. For the five climatic factors, in terms of Shandong Province as a whole, *ET* was positively correlated with T_{max}, *WS* and *SH*, and was negatively correlated with T_{max} and *RH*. That was, wheat *ET* increased as T_{max}, *WS* and *SH* increased, and increased as the T_{max} and *RH* decreased. Results of sensitivity analysis for *ET* showed that there were obvious differences between the influencing factors. *ET* was most sensitive to T_{max} and *RH*, followed by *SH* and *WS*. However, *ET* has lower sensitivity to T_{min} (*Fig. 6*).

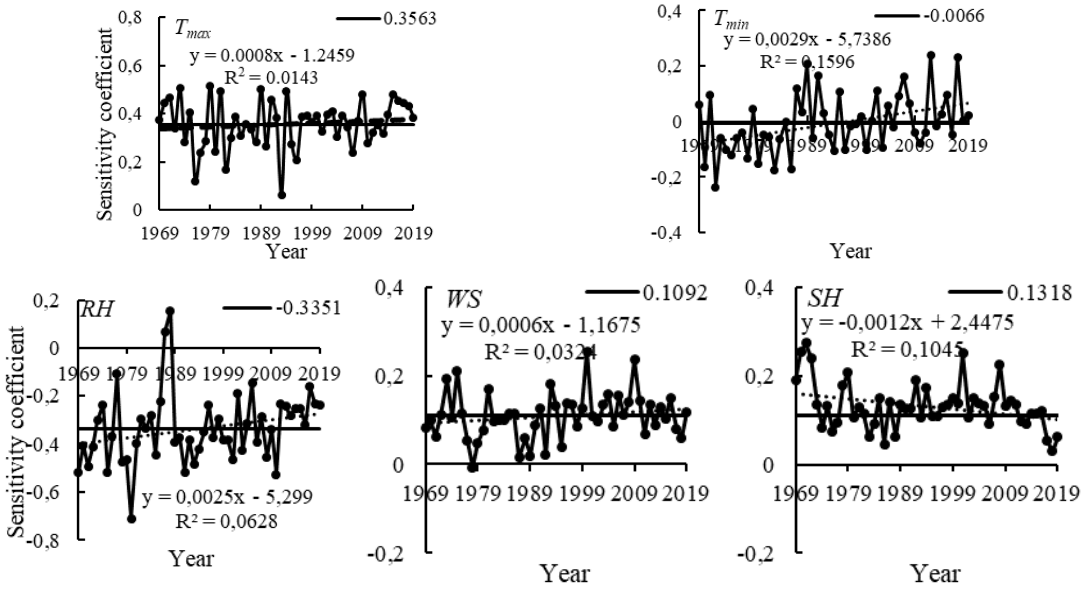


Figure 6. *Annual variation of sensitivity coefficient of meteorological factors from 1969 to 2019*

As observed from *Fig. 7*, the sensitivity coefficient of T_{max} (ST_{max}) decreased progressively from the southwest to northeast over Shandong, reached the minimum at the mountainous and hilly area in the middle and south, and then increases in the part of the area near the Yellow Sea. The spatial distribution of the sensitivity coefficient of T_{min}

http://www.aloki.hu ● ISSN 1589 1623 (Print) ● ISSN 1785 0037 (Online)
DOI: http://dx.doi.org/10.15666/aeer/1902_915932
© 2021, ALÖKI Kft., Budapest, Hungary

(ST_{min}) showed a pattern that is contrary to ST_{max}, and there was a discernable transition zone of ST_{min} from the southwest to northeast, expect mountainous and hilly area in the middle and south. The sensitivity coefficient of *RH* (*SRH*) over Shandong was negative. Different from the distribution of other parameters, *SRH* showed no regularity in variation of Shandong, with the largest value found in Liaocheng and the smallest value found in Weihai. The sensitivity coefficient of *WS* (*SWS*) decreased progressively from the northwest to southeast over Shandong. Similar to *SWS*, the sensitivity coefficient of *SH* (*SSH*) decreased from northwest to southeast, with the largest value found in Taian and Jinan and the smallest value found in Rizhao and Weihai. In general, *SH* and *WS* were the main controlling factors in the central hilly area, and the T_{max} and *RH* were the main control factor of *ET* in other areas, which was consistent with the finding from north region of China (Zheng and Wang, 2015; Fan and Thomas, 2018).

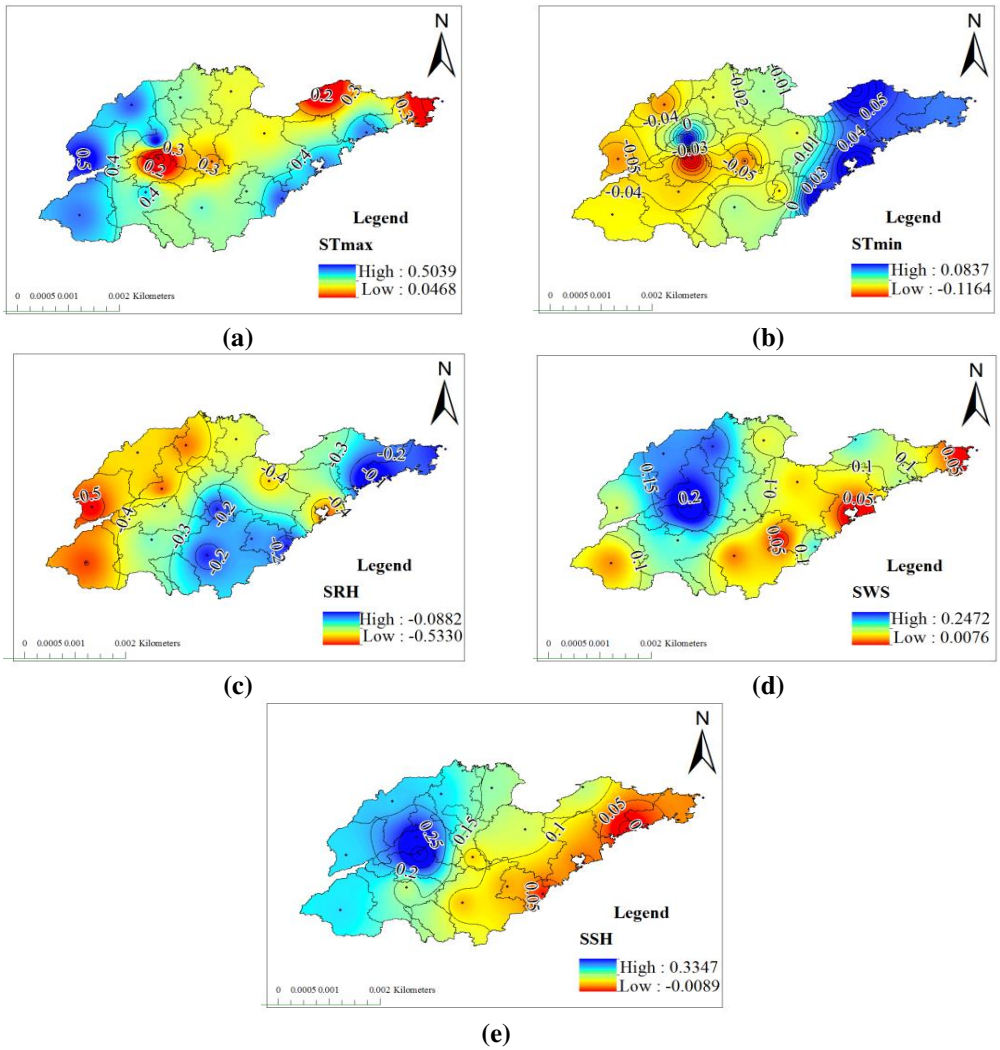


Figure 7. *Sensitivity coefficients of meteorological on ET of winter wheat over Shandong from 1969 to 2019*

The *Fig. 7* revealed that the potential evapotranspiration of crops is positively promoted by T_{max}, *SH* and *WS* and the increase of *RH* will cause the decrease of potential evapotranspiration. The results are in line with previous studies (Liu et al., 2005; Hu et

http://www.aloki.hu ● ISSN 1589 1623 (Print) ● ISSN 1785 0037 (Online)
DOI: http://dx.doi.org/10.15666/aeer/1902_915932
© 2021, ALÖKI Kft., Budapest, Hungary

al., 2017). T_{max} can transfer energy to crops and affect crop transpiration rate. *WS* determines the transfer of water vapor in the air, which has influence on the atmospheric evapotranspiration. *SH* affects the amount of solar radiation during wheat growth period, solar radiation is the energy of soil water vaporization and crop transpiration, which can directly determine the amount of *ET*. *RH* indicates how high the water vapor saturation in the air is. The higher the water saturation is, the less water vapor can be contained in the air for crop transpiration and soil water evaporation, which leads to the interannual variation of wheat water demand opposite to that of relative humidity. Moreover, the attribution analysis suggested that daily average maximum temperature and relative humidity was the most influential factor to the *ET*, followed by the sunshine duration and wind speed (*Fig. 6*). Wang et al. (2017) considered suggested the decreasing trend of ET_0 in Huang-Huai-Hai region was mainly governed by significant decrease in sunshine, which was quite different with this study. The results of this study are basically consistent with the conclusions of Yang et al. (2012) and Liu et al. (2005). Due to the differences in the regional scope, research period and spatial dimensions, there are also some differences. Above all, the variability of *ET* is a synthesis process of climatic variables change. The T_{max} rise may lead to increase of *ET* while the decrease of *WS* and *SD* and the increase of *RH* potentially cause the decrease. This study reveals the descent rate of *WS* and *SD* in study during 1969-2019 was higher than the increase rate of T_{max} and decrease of *RH*, resulting in decreasing trend of *ET*.

Interannual variation of main meteorological factors

In order to study the interannual variation of the above four meteorological factors, the linear tendency rate of meteorological factors with time was calculated (*Table 3*). From 1969 to 2019, the T_{max} showed a very significant upward trend, while the *RH*, *WS* and *SH* showed a very significant downward trend. The change trend of the research results was similar to that of T_{max} (0.045), *RH* ($7e^{-6}$) and *WS* (-0.019) obtained by Wang et al. (2019) using the Sen's slope estimator in Eastern China during 1979-2015.

Table 3. *Propensity rate of meteorological factors during the growing period of winter wheat*

Factor	T_{max}	*RH*	*WS*	*SH*
Coefficients	0.32	-0.04	-0.45	-0.29

It can be seen from *Fig. 8* that the interannual variation characteristics of wheat water requirement and T_{max}, *WS* and *SH* in Shandong Province from 1969 to 2019 were generally consistent, but contrary to the interannual variation characteristics of *RH*. This was consistent with the results of sensitivity analysis. Combined with the results in *Table 3*, it can be analyzed that the change of *ET* is the comprehensive performance of *ET* increase caused by temperature rise and decrease of *ET* caused by wind speed decrease. This is consistent with Wang's (2019) point of view that since the 1990s, a region greatly influenced by *WS* is Shandong, where the impact on ET_0 of T_{max} is counteracted by the largest decrease in *WS* to a great extent. At the same time, a research suggested that the change of *SH* was the major factor influencing the variability of ET_0, followed by *WS*, *RH* and *T* in the Yellow River Basin.

http://www.aloki.hu ● ISSN 1589 1623 (Print) ● ISSN 1785 0037 (Online)
DOI: http://dx.doi.org/10.15666/aeer/1902_915932
© 2021, ALÖKI Kft., Budapest, Hungary

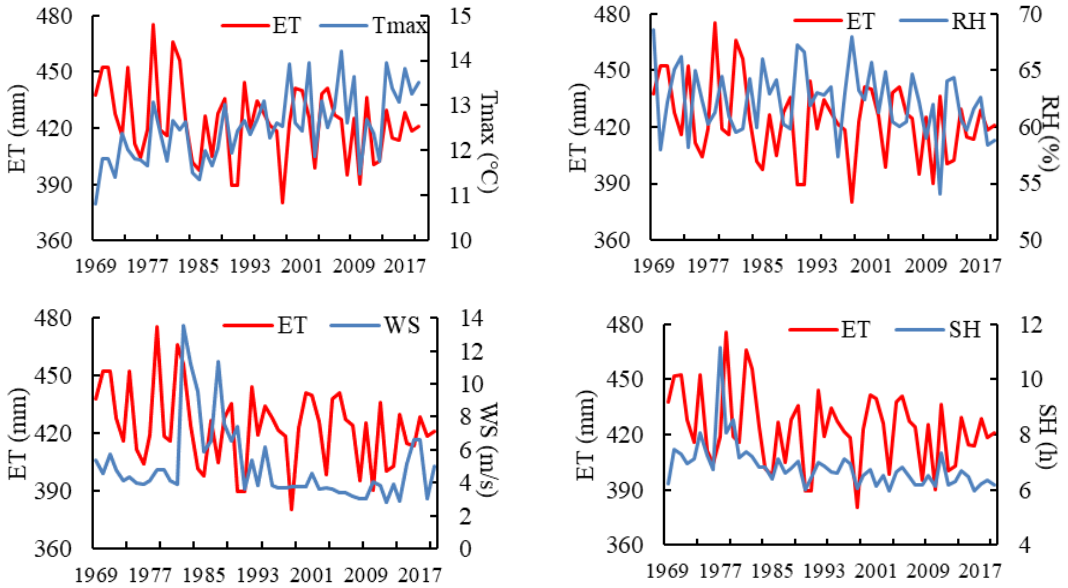


Figure 8. *Variation characteristics of meteorological factors and water requirement of winter wheat during growth period*

Changes of winter wheat yield under the background of climate change

ET variability under different climatic conditions may produce either positive or negative effects on crop yield per unit area. In spite of droughts caused by abnormal climate change, wheat yields in Shandong have been increasing in the past 20 years (*Fig. 9*), implying that the changing *ET* in Shandong Province played a negligible role in agriculture, which corroborates with the extant literature (Piao et al., 2010). He indicated that on a countrywide basis-the consequences of recent climate change on agriculture have been limited both because climate trends remained moderate compared to natural variability, and because technological progress has brought more than all benefits, in particular improved agricultural practice.

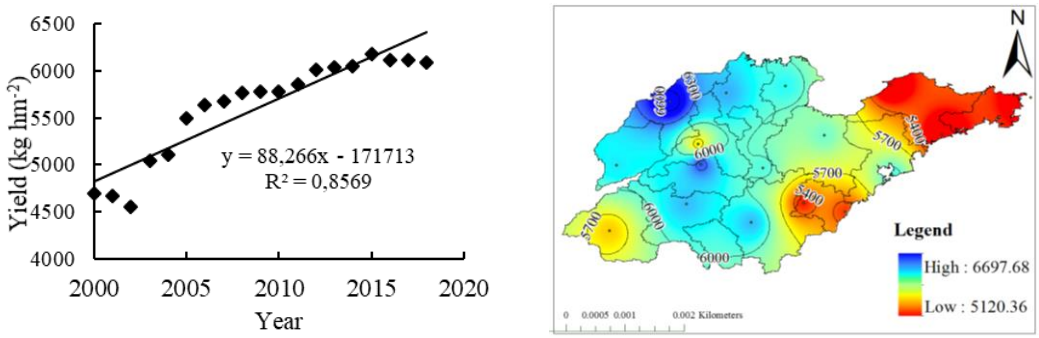


Figure 9. *Distribution of winter wheat yield in Shandong Province from 2000 to 2018*

The results showed that wheat yield increased year by year regardless of the fluctuation of *EI*, P_e and *IR*, which may be due to the effect of supplementary irrigation on yield. For example, although the long-term tendency of *IR* was declining for winter wheat, a large

http://www.aloki.hu ● ISSN 1589 1623 (Print) ● ISSN 1785 0037 (Online)
DOI: http://dx.doi.org/10.15666/aeer/1902_915932
© 2021, ALÖKI Kft., Budapest, Hungary

amount of groundwater was consumed by winter wheat annually in the northern Shandong to maintain high yield, which represented the most important factor for groundwater drawdowns. In addition, the increasing grain yield may mainly benefit from technological progress, such as irrigation system improving and seed amelioration. However, the increasing trend of *ET* may be large enough in some local regions to offset a significant portion of the increases in average yields that arose from technological progress (Lobell et al., 2011). For example, the increasing *ET* in western Jiaodong Peninsula induced by humidity reduction and temperature increment may enhance wheat water stress, resulting in greater water requirements for agriculture production and causing reduction in agriculture yield (*Fig. 9*). Several studies have described that the wheat cultivars renewal and improved crop management practices have offset the negative effects of climatic change on yield (Tao et al., 2012; Wang et al., 2012).

Building the climate-wheat yield relationship without considering the management effects have been large enough to be worthy of attention. Many scholars attempted to differentiate the effects of management and climate change on the crop yield. For example, a research showed that the increase in temperature increased winter wheat yield by 3.0-6.0% in northern part of the NCP during 1980-2009 (Xiao and Tao, 2014). At the same time, Xiong et al. (2012) found that wheat showed reduced yield (-9.7%) owing to climate factors, whilst offset by CO_2 fertilization (overall change 0.9%) in China during 1961-2010. Even, Liu et al. (2016) showed that at global and national scales, global wheat yield was projected to decline between 4.1% and 6.4% with a 1ºCF global temperature increase. It is reported that in the future, the temperature, precipitation and solar radiation in the North China Plain will change significantly (Liu et al., 2018). Therefore, a detailed analysis of climate change and wheat response is essential for wheat growth and management adaptation.

Conclusion

Under the background of climate change, water shortage is becoming more and more serious in North China in recent years. Improve irrigation management system and stabilizing the yield of crops have become the main production objectives in similar areas. Therefore, understanding of *ET* of crop in present situation and development trend, and analysis the influence reason is still the scholars concern.

Based on meteorological data from 15 prefecture-level cities in Shandong Province, this paper used the Penman-Monteith formula and crop coefficient method to determine the water requirements of the winter wheat. To a certain extent, it improved the calculation accuracy of water demand and water shortage, which was of great significance for reasonable guidance of wheat irrigation in Shandong Province.

A temporal analysis of the entire region indicated that a turning point occurred in 1984 for the temporal variability of *ET*. A spatial analysis of the entire region indicated that the *ET*, *IR*, and *AI* were the largest on the northwestern Shandong and displayed a decreasing trend from northwest to southeast. Additionally, the *ET* decreased in the western Shandong, and the *ET* in the rest of the area increased with a trend of 0-2 mm decade^{-1}. And the overall spatial pattern of the trend in *IR* was similar to that of the trend in *ET*. The northwest of Shandong has large evaporation and relatively less precipitation, which is the driest climate area and high drought risk area in Shandong.

In the sensitivity analysis of *ET* of winter wheat to its influencing factors, the T_{max} was the major factor dominating variability of *ET* in Shandong, followed by *RH*, *SH*, *WS* and

http://www.aloki.hu ● ISSN 1589 1623 (Print) ● ISSN 1785 0037 (Online)
DOI: http://dx.doi.org/10.15666/aeer/1902_915932
© 2021, ALÖKI Kft., Budapest, Hungary

T_{min}, respectively. Sensitivity analysis of the *ET* revealed that the T_{max} was the most positively correlated with the *ET* among all the meteorological factors, with sensitivity coefficient of 0.3563, whereas the meteorological factor with the maximum negative correlation was *RH*, with sensitivity coefficient of -0.3351. Significant declines of *WS* and *SH* were responsible for the decrease of *ET* in the entire Shandong from 1969 to 2019 while the increase of T_{max} and the decrease of *RH* contributed to the enhancement of *ET*.

In this study, factors influencing the irrigation requirements of crops were analysed only from a meteorological point of view. With regard to global climate change anomalies, the long-term agricultural water management should be adopted for the continued development. Furthermore, it is necessary to further study the impacts of various agricultural technologies throughout the region to provide a more accurate scientific basis for water management in Shandong farmland.

Acknowledgements. This project was jointly supported by Provincial water conservancy research and technology promotion project of Shandong Province (SDSLKY201803).

REFERENCES

[1] Allen, R. G., Pereira, L. S., Raes, D., Smith, M. (1998): Crop evapotranspiratione guidelines for computing crop water requirements. – FAO Irrigation and Drainage Paper 56: 1-15.

[2] Cao, Y. Q., Li, W. J., Zhu, M. M. (2018): Temporal and spatial characteristics of water deficit of winter wheat and cotton in Hebei Province. – Research of Soil and Water Conservation 25(06): 348-356+364+416-417.

[3] Deng, Y., Jiang, W., He, B., Chen, Z., Jia, K. (2018): Change in intensity and frequency of extreme precipitation and its possible teleconnection with large-scale climate index over the China from 1960 to 2015. – Journal of Geophysical Research: Atmospheres 123: 2068-2081.

[4] Döll, P., Stefan, S. (2002): Global modeling of irrigation water requirements. – Water Resource Research 38(4): 8-1-8-10.

[5] Dong, C., Yang, X., Yang, J., Xie, W., Ye, Q., Zhao, J., Li, K. (2013): The temporal variation characteristics and spatial distribution laws of drought of spring maize in Northern China. – Scientia Agricultura Sinica 46: 4234-4245.

[6] Fan, Z. X., Thomas, A. (2018): Decadal changes of reference crop evapotranspiration attribution: Spatial and temporal variability over China 1960-2011. – Journal of Hydrology 560: 461-470.

[7] Gao, J. Q., Yang, X. G., Zheng, B. Y., Liu, Z. J., Zhao, J., Sun, S., Li, K. N., Dong, C. Y. (2019): Effects of climate change on the extension of the potential double cropping region and crop water requirements in northern China. – Agricultural and Forest Meteorology 268: 146-155.

[8] Gu, X., Zhang, Q., Singh, V. P., Shi, P. (2017): Changes in magnitude and frequency of heavy precipitation across China and its potential links to summer temperature. – Journal of Hydrology 547: 718-731.

[9] He, B., Liu, Z. J., Yang, X. G., Sun, S. (2017): Temporal and spatial variations of agrometeorological disasters of main crops in China in a changing climate (Ⅱ): drought of cereal crops in Northwest China. – Chinese Journal of Agrometeorology 38(1): 31-41.

[10] Hu, Q., Dong, B., Pan, X. B., Wang, X. X., Wei, P., Zhao, H. H., Zhang, X. T. (2017): Spatiotemporal variation and causes analysis of dry-wet climate at different time scales in North China Plain Chinese. – Journal of Agrometeorology 38(05): 267-277.

http://www.aloki.hu ● ISSN 1589 1623 (Print) ● ISSN 1785 0037 (Online)
DOI: http://dx.doi.org/10.15666/aeer/1902_915932
© 2021, ALÖKI Kft., Budapest, Hungary

[11] Liang, L. Q., Li, L. J., Liu, Q. (2010): Temporal variation of reference evapotranspiration during 1961-2005 in the Taoer River basin of Northeast China. – Agricultural and Forest Meteorology 150: 298-306.
[12] Liu, X. Y., Lin, E. D. (2004): Impact of climate change on water requirement of main crops in North China. – Journal of Hydraulic Engineering 2: 77-82.
[13] Liu, X. Y., Li, Y. Z., Hao, W. P. (2005): Trend and causes of water requirement of main crops in North China in recent 50 years. – Transactions of the Chinese Society of Agricultural Engineering 10: 155-159.
[14] Liu, Q., Mei, X. R., Yan, C. G., Ju, H., Yang, J. Y. (2013): Dynamic variation of water deficit of winter wheat and its possible climatic factors in Northern China. – Acta Ecologica Sinica 33(20): 6643-6651.
[15] Liu, B., Asseng, S., Müller, C., Ewert, F., Elliott, J., et al. (2016): Similar estimates of temperature impacts on global wheat yield by three independent methods. – Nature Climate Change 6: 1130-1136.
[16] Liu, Q., Yan, C. G., Ju, H., Garré, S. (2018): Impact of climate change on potential evapotranspiration under a historical and future climate scenario in the Huang-Huai-Hai Plain, China. – Theoretical and Applied Climatology 132(1): 387-401.
[17] Lobell, D. B., Schlenker, W., Costa-Roberts, J. (2011): Climate trends and global crop production since 1980. – Science 333(6042): 616-620.
[18] Ma, J. H., Liu, Y., Yang, X. G., Wang, W. F., Xu, C. Y., Zhang, X. Y. (2010): Characteristics of climate resources under global climate change in the North China Plain. – Acta Ecologica Sinica 30(14): 3818-3827.
[19] Piao, S. L., Ciais, P., Huang, Y., Shen, Z. H., Peng, S. S., Li, J. F., Zhou, L. P., Liu, H. Y., Ma, Y. C., Ding, Y. H., Friedlingstein, P., Liu, C. Z., Tan, K., Yu, Y. Q., Zhang, T. Y., Fang, J. Y. (2010): The impacts of climate change on water resources and agriculture in China. – Nature 467: 43-51.
[20] Shen, Y. J., Li, S., Chen, Y. N., Qi, Y. Q., Zhang, S. W. (2013): Estimation of regional irrigation water requirement and water supply risk in the arid region of northwestern China 1989-2010. – Agricultural Water Management 128(1): 55-64.
[21] Smith, M. (1992): Cropwat: a computer program for irrigation planning and management. – FAO Irrigation and Drainage Paper 46: 1-123.
[22] Sun, S., Yang, X. G., Li, K. N., Zhao, J., Ye, Q., Jie, W. J., Dong, C. Y., Liu, H. (2013): Analysis of spatial and temporal characteristics of water requirement of winter wheat in China. – Transactions of the Chinese Society Agricultural Engineering 29(15): 72-82.
[23] Tao, F., Yokozawa, M., Hayashi, Y., Lin, E. (2003): Changes in agricultural water demands and soil moisture in China over the last half-century and their effects on agricultural production. – Agricultural and Forest Meteorology 118: 251-261.
[24] Tao, F., Zhang, S., Zhang, Z. (2012): Spatiotemporal changes of wheat phenology in China under the effects of temperature, day length and cultivar thermal characteristics. – European Journal of Agronomy 43: 201-212.
[25] Vicente-Serrano, S. M., Beguería, S., López-Moreno, J. I. (2010): A multiscalar drought index sensitive to global warming: the standardized precipitation evapotranspiration index. – Journal of Climate 23: 1696-1718.
[26] Villarini, G., Smith, J. A., Serinaldi, F., Ntelekos, A. A., Schwarz, U. (2012): Analyses of extreme flooding in Austria over the period 1951-2006. – International Journal of Climatology 32(8): 1178-1192.
[27] Wang, J., Wang, E., Yang, X., Zhang, F., Yin, H. (2012): Increased yield potential of wheat–maize cropping system in the North China Plain by climate change adaptation. – Climatic Change 113: 825-840.
[28] Wang, Z., Xie, P., Lai, C., Chen, X., Wu, X., Zeng, Z., Li, J. (2017): Spatiotemporal variability of reference evapotranspiration and contributing climatic factors in China during 1961-2013. – Journal of Hydrology 544: 97-108.

http://www.aloki.hu ● ISSN 1589 1623 (Print) ● ISSN 1785 0037 (Online)
DOI: http://dx.doi.org/10.15666/aeer/1902_915932
© 2021, ALÖKI Kft., Budapest, Hungary

[29] Wang, Z., Ye, A., Wang, L., Liu, K., Cheng, L. (2019): Spatial and temporal characteristics of reference evapotranspiration and its climatic driving factors over china from 1979-2015. – Agricultural Water Management 213: 1096-1108.
[30] Wu, D., Fang, S. B., Li, X., He, D., Zhu, Y. C., Yang, Z. Q., Xu, J. X., Wu, Y. J. (2019): Spatial-temporal variation in irrigation water requirement for the winter wheat-summer maize rotation system since the 1980s on the North China Plain. – Agricultural Water Management 214: 78-86.
[31] Wu, Y. C., Sun, P., Li, N., Sun, M., Yang, M. G., Jiang, M. M. (2020): Characteristics of water need and shortage for winter wheat on Northern Anhui Plain in the past 60 years. – Journal of Xichang University (Natural Science Edition) 34(2): 6-12+128.
[32] Wu, Y., Li, X., Ma, Z. Y., Sun, S. H., Jia, R. B. (2020): Water resources carrying capacity evaluation based on support vector machine in Shandong Province. – Journal of Safety and Environment 10: 1-10.
[33] Xiao, D., Tao, F. (2014): Contributions of cultivars, management and climate change to winter wheat yield in the North China Plain in the past three decades. – European Journal of Agronomy 52: 112-122.
[34] Xiong, W., Holman, I., Lin, E., Conway, D., Li, Y., Wu, W. (2012): Untangling relative contributions of recent climate and CO_2 trends to national cereal production in China. – Environmental Research Letters 7: 044014.
[35] Xu, Z. H., Han, M. (2018): Spatio-temporal distribution characteristics of drought in Shandong Province and it relationship with ENSO. – Chinese Journal of Eco-Agriculture 26(08): 1236-1248.
[36] Yang, X. L., Song, W. Z., Wang, H., Shi, Q. H., Chen, F., Zhu, Q. Q. (2012): Spatio-temporal variations of winter wheat water requirement and climatic causes in Huang-Huai-Hai Farming Region. – Chinese Journal of Eco-Agriculture 20(03): 356-362.
[37] Yin, X. G., Olesen, J. E., Wang, M., Öztürk, I., Chen, F. (2016): Climate effects on crop yields in the Northeast Farming Region of China during 1961-2010. – The Journal of Agricultural Science 154: 1190-1208.
[38] Yuan, Z., Yan, D. H., Yang, Z. Y., Yin, J., Yuan, Y. (2015): Temporal and spatial variability of drought in Huang-Huai-Hai River Basin, China. – Theoretical and applied Climatology 122: 755-769.
[39] Zhang, K. X., Pan, S. M., Zhang, W., Xu, Y. H., Cao, L. G., Hao, Y. P., Wang, Y. (2015): Influence of climate change on reference evapotranspiration and aridity index and their temporal-spatial variations in the yellow river basin, china, from 1961 to 2012. – Quaternary International 380-381: 75-82.
[40] Zhang, C., Chen, X. X., Li, Y., Ding, W., Fu, G. T. (2018): Water-energy-food nexus: concepts, questions and methodologies. – Journal of Cleaner Production 195: 625-639.
[41] Zheng, C., Wang, Q. (2015): Spatiotemporal pattern of the global sensitivity of the reference evapotranspiration to climatic variables in recent five decades over China. – Stochastic environmental research and risk assessment 29: 1937.

http://www.aloki.hu ● ISSN 1589 1623 (Print) ● ISSN 1785 0037 (Online)
DOI: http://dx.doi.org/10.15666/aeer/1902_915932
© 2021, ALÖKI Kft., Budapest, Hungary

GREENHOUSE AND FIELD EVALUATION OF PHYTOREMEDIATION FOR NITROGEN AND PHOSPHORUS IN A RIPARIAN BUFFER STRIP

GOUDARZIAN, P.[1*] – YAZDANI, M. R.[1] – MATINKHAH, S. H.[2]

[1]*Department of Desertification, Faculty of Desert Studies, Semnan University, Semnan, Iran (phone: +98-913-107-8249)*

[2]*Department of Natural Resources, Isfahan University of Technology, Isfahan 84156-83111, Iran (phone: +98-913-328-8275)*

**Corresponding author*
e-mail: P.goudarzian1986@gmail.com; phone: +98-938-912-3965

(Received 11th Mar 2019; accepted 19th Jan 2021)

Abstract. In this research, greenhouse and field studies were conducted to evaluate the efficiency of Riparian Buffer Strips' (RBS) phytoremediation properties for N and P removal. In the field study, RBSs were investigated according to their perimeter, area, path, and length on the banks of Zayandeh-rood River, Iran. In the greenhouse study, the phytoremediation of dominant species (*Fraxinus rotundifolia*) and proposed species (*Aianthus altissima*) was investigated. The results of measurements done on the concentrations of N and P in soil showed that N and P concentrations in soil increased considerably from the beginning of the farm to the end of the farm and then sharply decreased from the beginning of the RBS to the end of it. Results revealed that in general, the efficiency of phytoremediation in removal of pollution was highest under low concentrations of pollution, lowest in average concentrations, and eventually moderate in highest concentrations (P value< 0.05).
Keywords: *arid and semi-arid basin, eutrification, hyper accumulators non-point pollutants, riparian soil*

Introduction

The shortage and pollution of water are regarded as critical problems in many countries. The contamination of surface and ground waters by nitrogen (N) and phosphorus (P) is a major factor affecting water supplies in many parts of the world (Wang et al., 2002; Boz et al., 2013). Similarly, P is recognized as the most critical nutrient-limiting factor that can induce water pollution (Xiang et al., 2009). Regarding the dangers resulting from the increase of P in water, controlling its input into waters, especially rivers, is very important (Sibrell et al., 2009). High concentrations of N in surface waters can also lead to pollution, and in turn, to instability of the ecosystem (Hefting and Klein, 1998).

Most agricultural soil in Iran is contaminated with high doses of Nitrogen and Phosphorus due to the utilization of Urea and Triple Superphosphate over the last decades. P absorption is fast during initial stages but it decreases over time and eventually the P sediments as mineral Phosphates (with low plant absorption) (Malakouti, 2011).

Eutrification caused by N and P (Stefanidis et al., 2020) negatively affects water quality (Lin et al., 2020), the aquatic ecosystems (Lusiana et al., 2020), and the nutrient cycles (Maciej et al., 2020) resulting in a decrease in species diversity and an increase in the biomass of less desirable species (Boyd, 2020). Therefore, besides controlling the P,

http://www.aloki.hu ● ISSN 1589 1623 (Print) ● ISSN 1785 0037 (Online)
DOI: http://dx.doi.org/10.15666/aeer/1902_933952
© 2021, ALÖKI Kft., Budapest, Hungary

removal of N is also important for solving the problem of water pollution. Agricultural runoff can transport sediment, pesticides and nutrients, especially N and P, to surface water and have an impact on the environment (Otto et al., 2008). Due to the ever-growing population of the world on one hand, and the gradual increase of environmental pollutions and the deterioration of agricultural land on the other, a great challenge has arisen in the field of food security, both quantitatively and qualitatively. However recently, research into the application of buffer zones has provided the grounds for the introduction of an environmentally-friendly technology to reduce the non-spot pollution in not only the soil, but also the runoff. Riparian buffer strips (RBS) are an efficient and economical way to reduce agricultural non-point source pollution (De Souza et al., 2013). The effect is usually highly satisfactory, with abatements of 70–98% for P and 70–95% for N (Borin et al., 2005; Anbumozhi et al., 2005). Phytoremediation of contaminated soils within RBS has proven to be cost effective and environmentally friendly (Wang et al., 2002). Euliss et al. (2008) assess phytoremediation for petroleum contaminants in an RBS and indicated that plants enhanced degradation of target contaminants through their phytoremediation capability. Xiang et al. (2009) suggested that phytoremediation is an effective technology for N and P removal from polluted water. In accordance with the results of Aguiar et al. (2015), buffer zones composed of woody soils were more effective in P (99.9%) and N (99.9%) removal when compared to shrub (66.4% and 83.9%, respectively) or grass vegetation area (52.9% and 61.6%, respectively). Fallahi et al. (2012) showed that plant type is very important regarding the effectiveness of plant properties for phytoremediation. Taheri et al. (2014) indicated that *Fraxinus rotundifolia* is one of the effective species for phytoremediation. Several studies have investigated RBS effectiveness in removing suspended solids, nutrients and pesticides from agricultural runoff (Anbumozhi et al., 2005; Schilling and Jacobson, 2014; Aguiar et al., 2015) or phytoremediation for N and P (Wang et al., 2002; Xiang et al., 2009). Few studies have been done to evaluate the phytoremediation of N and P in RBS in both greenhouse and field conditions. Moreover, studies about them are limited in Middle Eastern countries. Therefore, this research was done with the aim of assessing the use of phytoremediation to reduce N & P contaminants in both greenhouse and RBS. In addition to contaminant quantification, the cumulative effect of roots was evaluated over the 6-month study period.

Materials and methods

Study timeline

The overall timeline of the current study includes five stages and covers a period of two years (24 months) from Mar. 2016 to Feb. 2018. These stages include Buffer Zone sampling and analysis of the RBZs data (Field Study – Mar. to Aug. 2016), Greenhouse Preparation and Deployment phase (3 months – Sep. 2016 to Nov. 2017), Greenhouse Study phase (6 months – Des. to May. 2017), Database Lock (3 months – Jun. to Aug. 2017), and finally, Data Analysis and Report (6 months – Sep. 2017 to Feb. 2018).

Field study

The Zayandeh-Rood River in center of Iran, one of the most polluted sites in this region is an example of the anthropogenic impacts on the environment in the last four

http://www.aloki.hu ● ISSN 1589 1623 (Print) ● ISSN 1785 0037 (Online)
DOI: http://dx.doi.org/10.15666/aeer/1902_933952
© 2021, ALÖKI Kft., Budapest, Hungary

decades that have proven to be extremely deleterious due to the rapid development of agriculture (Sanayei et al., 2009). The semi-arid Zayandeh-Rood River Basin is one of the most strategic and important river basins of Iran (Madani and Marino, 2009). This river basin, with an area of 41,347 km^2, is located between the 50° 24′ to 53° 24′ longitudes and 31° 11′ to 33° 42′ latitudes (*Fig. 1*).



Figure 1. *Buffer zone plots along agricultural land around Zayandeh-Rood – The route with the highest Concentration*

The Zayandeh-Rood River Basin covers an area of about 26,917 km^2 in central Iran. The main traditional staple crops of the basin are wheat, rice, barley, and corn, which are highly water consumptive and polluting. Zayandeh-Rood River, with an average flow of 1400 million m^3, including 650 million m^3 of natural flow and 750 million m^3 of transferred flow, is the main surface water resource of the basin (Gohari et al., 2013). *Table 1* summarizes some of the main characteristics of this basin.

Table 1. *General characterizes of the Zayandeh-rood basin (Gohari et al., 2013)*

Attribute	Value
Physiographic and hydrologic	
Elevation range (m)	1470-3974
Annual average precipitation range (mm)	50-1500
Average temperature range (°C)	3-30
Annual potential evapotranspiration (mm)	1500
Average humidity (%)	24-57
River length (Km)	350
Average natural flow (MCM)	650
Average transferred flow (MCM)	750
Agricultural	
Irrigation efficiency (%)	34-42
Agricultural water use (%)	73
Irrigated area (ha)	270,000
Rain fed area (ha)	30,000

http://www.aloki.hu ● ISSN 1589 1623 (Print) ● ISSN 1785 0037 (Online)
DOI: http://dx.doi.org/10.15666/aeer/1902_933952
© 2021, ALÖKI Kft., Budapest, Hungary

The river water is used for drinking, industrial and agricultural purposes. In its west–east journey, Zayandeh-Rood River passes several agricultural areas (Gohari et al., 2013). The determination of pollutants throughout the river is important and has a great role in controlling the ecological condition of this body of water. The first step was finding appropriate fields with agricultural lands that are adjacent to RBS along river through field studies, using remote sensing (RS) and data analysis. The area and perimeter of agricultural land was then determined and analyzed. The Polygon centers were determined with a "place mark" and then coordinates were calculated. One buffer zone site was selected for our study.

As agricultural application is the biggest source of non-point pollution on the national scale, samples were collected along 3 parallel transects from the beginning to the end of the farm and beginning to the end of the buffer zone at the depth of 30 cm and then analyzed in laboratory for N and P concentrations. Species biometrics were investigated in the field. Results are shown in *Table 2*. Two of the fast growing and drought-contamination resistant species, the rich "*Fraxinus rotundifolia Mill"* and also the newly proposed "*Aianthus altissima*", were evaluated in the greenhouse study (Taheri et al., 2014; Li et al., 2015; Yang et al., 2015).

Table 2. *Biometrics of tree species at plot 9*

Dominant species	Family	Average diameter at breast (cm)	Average height (m)	Diameter standard deviation (cm)	Height standard deviation (m)
Fraxinus rotundifolia Mill	Oleaceae	20.15	11.25	2.68	0.79
Salix alba L.	Salicaceae	29.45	10.55	2.4	0.91
Elaeagnus angustifolia L.	Elaeagnaceae	18.80	9.37	1.50	1.51
Populus nigra L	Salicaceae	19.10	17.00	1.01	1.01
Morus alba L.	Moraceae	19.85	12.50	1.10	1.45

Greenhouse evaluation

At first, in order to design the greenhouse study, 30 canals were inserted into soil (50 cm × 50 cm × 2 m). In order to avoid water loss, a plastic layer and then a half tube and finally another plastic layer were placed in the soil (*Diagram 1*). Next, an experiment was conducted with ash (*Fraxinus rotundifolia* Mill) as the dominant species in the region, and Heaven tree (*Aianthus altissima*) as the proposed species. Potassium nitrate and Potassium phosphate solutions were used to create concentrations of 5, 10 and 50 mg L^{-1}. To move the water from the beginning to the end of the canal, a slope of 5% was created. Three replicates were included for statistical validity. During early March, 40 young seedlings of *Fraxinus rotundifolia* and 40 young seedlings of *Aianthus altissima* were planted in the canals, so that four plants were placed in each canal to assess cumulative effect of the roots. A total of 10 canals were left un-vegetated as control to consider the role of soil in remediation. To decrease evaporation, soil surface was coated with sand and aluminum foil. Irrigation was done with pure water at the rate of twice per week; after being planted 3 months, plants were irrigated with polluted water. After being planted 4 months (in late spring), water was collected at the end of the canals and the concentrations of N and P were determined in laboratory. One month later, the collected water was circulated in canals and the concentrations of N and P were again determined in laboratory. Finally, after 6 months, the circulated water was again collected and the pollution was determined in laboratory. Therefore, sampling was

http://www.aloki.hu ● ISSN 1589 1623 (Print) ● ISSN 1785 0037 (Online)
DOI: http://dx.doi.org/10.15666/aeer/1902_933952
© 2021, ALÖKI Kft., Budapest, Hungary

done in three stages. Total P (inorganic and organic) was determined by oxidation of unfiltered samples with potassium persulfate, and analyzing at 885 nm wavelength on the spectrophotometer upon color development with an ammonium molybdate-ascorbic acid-antimony method (Genchi, 1990). Total N (inorganic and organic) was determined in unfiltered samples by oxidation with potassium persulfate (Genchi, 1990) upon color development with the salicylic acid method; samples were analyzed at 410-nm wavelength on the spectrophotometer (spectrophotometer UV-Vis- Camspec M350 Double Beam) (Cataldo et al., 1975).

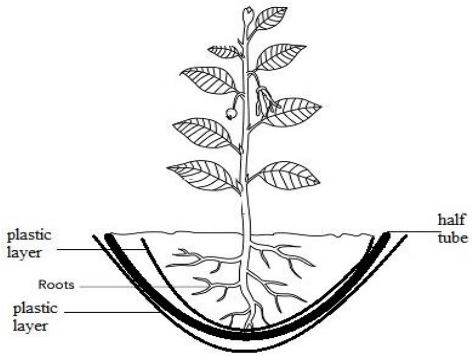


Diagram 1. *Canal design to avoid water loss*

Statistical analysis

Analysis of the results was done using IBM SPSS version 21. A two-way analysis of variance was conducted to explore the effect of the species and the concentration levels on the reduction of the contamination of N and P. The concentration levels were presented as 5 mg/L, 10mg/L, and 50 mg/L. Based on the results from the initial analysis, multiple one-way ANOVA tests (with Tukey HSD as the Post-hoc test) were conducted to compare the N and P reductions for each concentration level and at different times for each of the species. Homogeneity of Variance was tested using Levene's Test of Equality of Error Variances.

Results

Field evaluation

The total length of Zayande-rood River from Zardkuhe Bakhtiari to Gavkhuni marsh is estimated to be 461.65 Km. The distribution of RBSs in Zayandeh-rood basin with measurements of perimeter, area, length, latitude and longitude along agricultural land are given in *Appendix A*. Coordinates of the starting and the end point of the path are (32.5447° and 51.519°) and (32.6237° and 51.722°), respectively. The largest area of buffer zone is at plot 9 (32.6298 and 51.5614) and the smallest area of buffer zone is at plot 26 (32.5895 and 51.5449). Moreover, the greatest length is located at plot 39 (32.438 and 51.5838) and the shortest length is attributed to plot 41 (32.6416 and 51.5775). Furthermore, the largest perimeter of buffer zone is at plot 33 (32.5731 and 51.5231) and the smallest perimeter is at plot 30 (32.5866 and 51.5375).

The results of measuring the concentrations of N and P in the field RBS with a width of 10 m at plot 9 revealed that the highest concentrations of N and P are related to the

http://www.aloki.hu ● ISSN 1589 1623 (Print) ● ISSN 1785 0037 (Online)
DOI: http://dx.doi.org/10.15666/aeer/1902_933952
© 2021, ALÖKI Kft., Budapest, Hungary

end of the farm and the lowest concentrations are related to the end of the buffer zone. N and P concentrations in soil increased considerably from the beginning of the farm to the end of the farm and then sharply decreased from the beginning of the buffer zone to the end of it, as average concentrations of N and P dropped from 0.33 mg L^{-1} to 0.035 mg L^{-1} and from 6.97 mg L^{-1} to 1.74 mg L^{-1}, respectively (*Fig. 2a, b*).

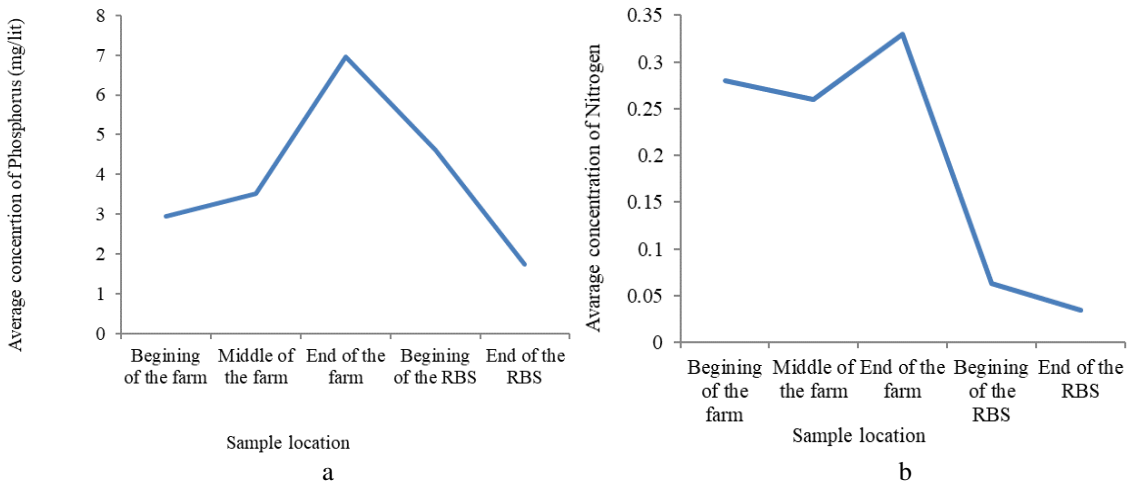


Figure 2. *Alterations in average concentration of P (a) and N (b) in the farm and the RBS*

According to the results of the Tukey Test presented in *Table 3,* the changes in the concentration of N from the beginning to the end of the farm is significant ($p < 0.05$), and the same applies to the concentration of P ($p < 0.05$). Likewise, the concentrations of N and P contaminants decrease significantly from the beginning to the end of the RBS ($p < 0.05$ for both).

Table 3. *Multiple comparison of field RBS nitrogen and phosphorus by Tukey HSD*

Dependent variable: nitrogen						
Tukey HSD						
(I) Point	(J) Point	Mean difference (I-J)	Std. error	Sig.	95% confidence interval	
					Lower bound	Upper bound
Beginning of the farm	Middle of the farm	-.45833	.567240	.925	-2.15573	1.23906
	End of the farm	-2.51000*	.567240	.002	-4.20739	-.81261
	Beginning of the RBS	-.45000	.567240	.930	-2.14739	1.24739
	End of the RBS	1.10500	.567240	.326	-.59239	2.80239
Middle of the farm	Beginning of the farm	.45833	.567240	.925	-1.23906	2.15573
	End of the farm	-2.05167*	.567240	.013	-3.74906	-.35427
	Beginning of the RBS	.00833	.567240	1.000	-1.68906	1.70573
	End of the RBS	1.56333	.567240	.080	-.13406	3.26073
End of the farm	Beginning of the farm	2.51000*	.567240	.002	.81261	4.20739
	Middle of the farm	2.05167*	.567240	.013	.35427	3.74906
	Beginning of the RBS	2.06000*	.567240	.013	.36261	3.75739
	End of the RBS	3.61500*	.567240	.000	1.91761	5.31239
Beginning of the RBS	Beginning of the farm	.45000	.567240	.930	-1.24739	2.14739
	Middle of the farm	-.00833	.567240	1.000	-1.70573	1.68906
	End of the farm	-2.06000*	.567240	.013	-3.75739	-.36261
	End of the RBS	1.55500	.567240	.083	-.14239	3.25239

http://www.aloki.hu ● ISSN 1589 1623 (Print) ● ISSN 1785 0037 (Online)
DOI: http://dx.doi.org/10.15666/aeer/1902_933952
© 2021, ALÖKI Kft., Budapest, Hungary

End of the RBS	Beginning of the farm	-1.10500	.567240	.326	-2.80239	.59239
	Middle of the farm	-1.56333	.567240	.080	-3.26073	.13406
	End of the farm	-3.61500*	.567240	.000	-5.31239	-1.91761
	Beginning of the RBS	-1.55500	.567240	.083	-3.25239	.14239
Dependent variable: phosphorus						
Beginning of the farm	Middle of the farm	.12167	.057171	.247	-.04941	.29274
	End of the farm	-.33333*	.057171	.000	-.50441	-.16226
	Beginning of the RBS	.22833*	.057171	.006	.05726	.39941
	End of the RBS	.28250*	.057171	.001	.11142	.45358
Middle of the farm	Beginning of the farm	-.12167	.057171	.247	-.29274	.04941
	End of the farm	-.45500*	.057171	.000	-.62608	-.28392
	Beginning of the RBS	.10667	.057171	.366	-.06441	.27774
	End of the RBS	.16083	.057171	.072	-.01024	.33191
End of the farm	Beginning of the farm	.33333*	.057171	.000	.16226	.50441
	Middle of the farm	.45500*	.057171	.000	.28392	.62608
	Beginning of the RBS	.56167*	.057171	.000	.39059	.73274
	End of the RBS	.61583*	.057171	.000	.44476	.78691
Beginning of the RBS	Beginning of the farm	-.22833*	.057171	.006	-.39941	-.05726
	Middle of the farm	-.10667	.057171	.366	-.27774	.06441
	End of the farm	-.56167*	.057171	.000	-.73274	-.39059
	End of the RBS	.05417	.057171	.875	-.11691	.22524
End of the RBS	Beginning of the farm	-.28250*	.057171	.001	-.45358	-.11142
	Middle of the farm	-.16083	.057171	.072	-.33191	.01024
	End of the farm	-.61583*	.057171	.000	-.78691	-.44476
	Beginning of the RBS	-.05417	.057171	.875	-.22524	.11691

Greenhouse evaluation (model experiment)

Figure 3 shows the comparison of phytoremediation between *Fraxinus rotundifolia* and *Aianthus altissima* for N and P. According to *Tables 4* and *5,* efficiency of trees in removal of pollution is the highest in lowest concentrations of pollution, the lowest in average concentration, and finally medium in the highest pollution concentration (P value< 0.05 for both). *Figures 4* and *5* show phytoremediation of each species separately and Descriptive Statistics of N and P removal by each species in each time period are given in *Appendices D, E, F, G.*

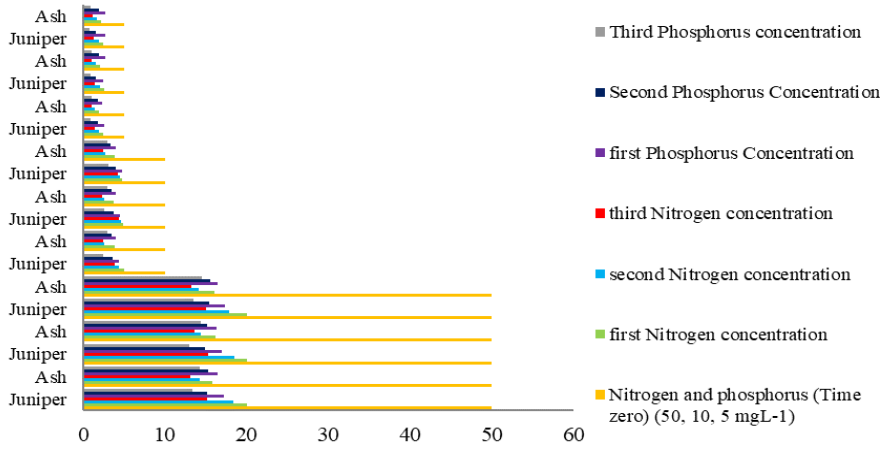


Figure 3. *Comparison of phytoremediation between Fraxinus rotundifolia and Aianthus altissima for N and P in three time periods*

http://www.aloki.hu ● ISSN 1589 1623 (Print) ● ISSN 1785 0037 (Online)
DOI: http://dx.doi.org/10.15666/aeer/1902_933952
© 2021, ALÖKI Kft., Budapest, Hungary

Table 4. *Multiple comparison of Aianthus altissima nitrogen and phosphorus concentration by Tukey HSD*

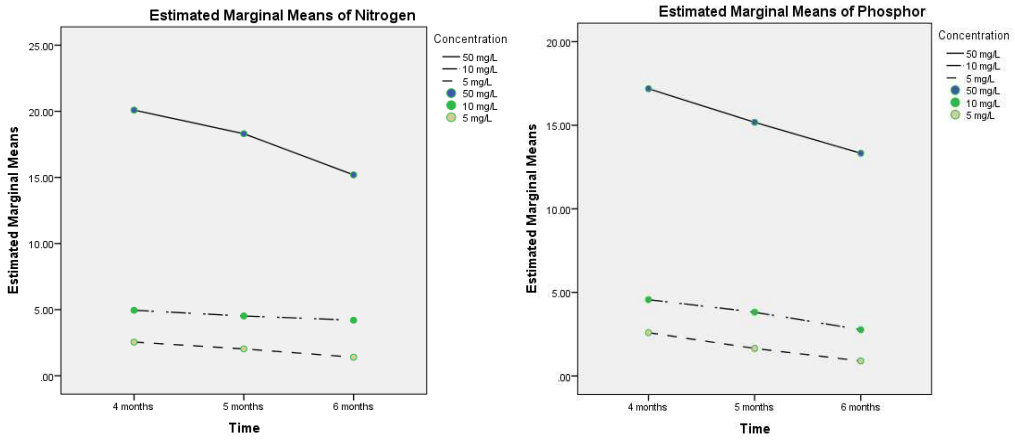
Dependent variable: nitrogen						
(I) Concentration	**(J) Concentration**	**Mean difference (I-J)**	**Std. error**	**Sig.**	**95% confidence interval**	
					Lower bound	**Upper bound**
50 mg/L	10 mg/L	13.3055*	.08107	.000	13.0986	13.5124
	5 mg/L	15.8724*	.08107	.000	15.6655	16.0793
10 mg/L	50 mg/L	-13.3055*	.08107	.000	-13.5124	-13.0986
	5 mg/L	2.5669*	.08107	.000	2.3600	2.7738
5 mg/L	50 mg/L	-15.8724*	.08107	.000	-16.0793	-15.6655
	10 mg/L	-2.5669*	.08107	.000	-2.7738	-2.3600
Dependent variable: phosphorus						
50 mg/L	10 mg/L	11.5133*	.09789	.000	11.2635	11.7632
	5 mg/L	13.5178*	.09789	.000	13.2680	13.7676
10 mg/L	50 mg/L	-11.5133*	.09789	.000	-11.7632	-11.2635
	5 mg/L	2.0044*	.09789	.000	1.7546	2.2543
5 mg/L	50 mg/L	-13.5178*	.09789	.000	-13.7676	-13.2680
	10 mg/L	-2.0044*	.09789	.000	-2.2543	-1.7546

Table 5. *Multiple comparison of Fraxinus rotundifolia nitrogen and phosphorus concentration by Tukey HSD*

Dependent variable: nitrogen						
(I) Concentration	**(J) Concentration**	**Mean difference (I-J)**	**Std. error**	**Sig.**	**95% confidence interval**	
					Lower bound	**Upper bound**
50 mg/L	10 mg/L	11.5535*	.05792	.000	11.4057	11.7013
	5 mg/L	12.9469*	.05792	.000	12.7991	13.0948
10 mg/L	50 mg/L	-11.5535*	.05792	.000	-11.7013	-11.4057
	5 mg/L	1.3935*	.05792	.000	1.2456	1.5413
5 mg/L	50 mg/L	-12.9469*	.05792	.000	-13.0948	-12.7991
	10 mg/L	-1.3935*	.05792	.000	-1.5413	-1.2456
Dependent variable: phosphorus						
50 mg/L	10 mg/L	11.9049*	.04847	.000	11.7812	12.0286
	5 mg/L	13.5380*	.04847	.000	13.4143	13.6617
10 mg/L	50 mg/L	-11.9049*	.04847	.000	-12.0286	-11.7812
	5 mg/L	1.6331*	.04847	.000	1.5094	1.7568
5 mg/L	50 mg/L	-13.5380*	.04847	.000	-13.6617	-13.4143
	10 mg/L	-1.6331*	.04847	.000	-1.7568	-1.5094

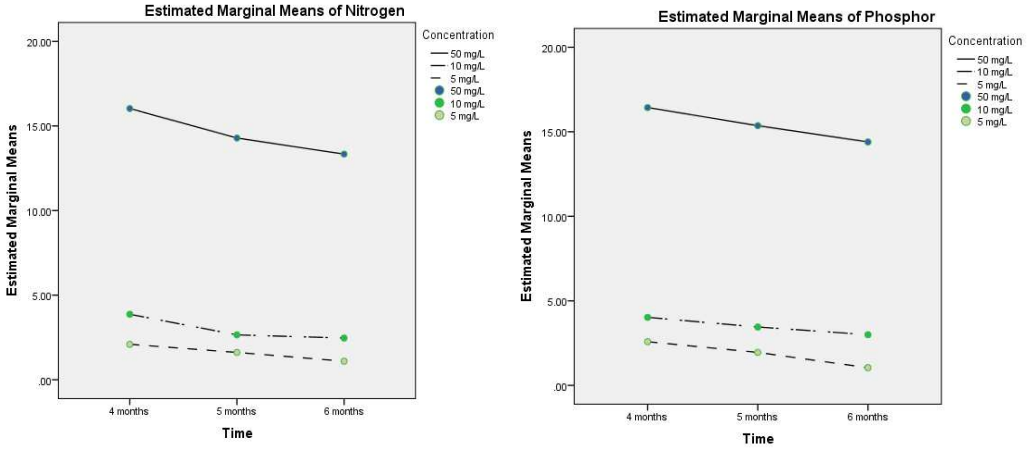
Statistical comparison of the two species (using factorial two-way ANOVA) reveals a significant difference in both N and P concentration reduction between the species (*Table 6*). Considering the homogeneity of Variance (Levene's Test of Equality of Error Variances), it is necessary to perform separate one-way ANOVAs with Tukey HSD as the Post-hoc test to compare the N and P reductions for the different concentration levels and at different times for each of the species.

http://www.aloki.hu ● ISSN 1589 1623 (Print) ● ISSN 1785 0037 (Online)
DOI: http://dx.doi.org/10.15666/aeer/1902_933952
© 2021, ALÖKI Kft., Budapest, Hungary



a **b**

Figure 4. *N (a) and P (b) removal by Aianthus altissima in three time periods*



a **b**

Figure 5. *N (a) and P (b) removal by Fraxinus rotundifolia in three time periods*

Results from the follow-up one-way ANOVAs show that the highest N reduction occurs at the early stage (i.e. 4 months) and much lesser reduction occurs in the second and third stages (i.e. 5 and 6 months, respectively), as N reduction in *Aianthus altissima* and *Fraxinus rotundifolia* is about 60% and 68% at the first, and then reaches to almost 63% and 71% at the second, eventually reaching 69% and 74% at the third stage, respectively (P value< 0.05) (*Tables 7* and *8*). Similarly, P declines sharply at the early stage and reduction in the second and third stages are much lesser, whereas P reduction in *Aianthus altissima* and *Fraxinus rotundifolia* is about 65% and 67% at first and then reaches to almost 70% and 69% at the second and 74% and 71% at the third stages, respectively (P value< 0.05) (*Tables 7* and *8*). It seems that *Fraxinus rotundifolia* is more effective in N reduction than *Aianthus altissima*, and vice versa, P declines more than N in *Aianthus altissima* (P value< 0.05). P reduction in *Fraxinus rotundifolia* is almost equivalent to the reduction of N (a little more) (*Tables 7* and *8*) (P value< 0.05).

http://www.aloki.hu ● ISSN 1589 1623 (Print) ● ISSN 1785 0037 (Online)
DOI: http://dx.doi.org/10.15666/aeer/1902_933952
© 2021, ALÖKI Kft., Budapest, Hungary

Table 6. *Tests of between-subjects effects for the two-way ANOVA– Aianthus altissima and Fraxinus rotundifolia*

Dependent variable: nitrogen						
Source	**Type III sum of squares**	**df**	**Mean square**	**F**	**Sig.**	**Partial eta squared**
Corrected MODEL	777.985[b]	5	155.597	6264.251	.000	1.000
Intercept	942.359	1	942.359	37938.845	.000	1.000
Type	19.845	1	19.845	798.949	.000	.985
Concentration	748.262	2	374.131	15062.301	.000	1.000
Type * concentration	9.879	2	4.939	198.852	.000	.971
Error	.298	12	.025			
Total	1720.642	18				
Corrected total	778.283	17				
Dependent variable: phosphorus						
Corrected model	725.008[b]	5	145.002	5926.186	.000	1.000
Intercept	1122.527	1	1122.527	45877.453	.000	1.000
Type	.842	1	.842	34.429	.000	.742
Concentration	723.722	2	361.861	14789.197	.000	1.000
Type * concentration	.443	2	.222	9.055	.004	.601
Error	.294	12	.024			
Total	1847.829	18				
Corrected total	725.302	17				

[a]Time = 4 months
[b]R squared = 1.000 (Adjusted R squared = .999)

Table 7. *Multiple comparison of. Aianthus altissima nitrogen and phosphorus time by Tukey HSD*

Dependent variable: nitrogen						
(I) Time	**(J) Time**	**Mean difference (I-J)**	**Std. error**	**Sig.**	**95% confidence interval**	
					Lower bound	**Upper bound**
4 months	5 months	.9100*	.08107	.000	.7031	1.1169
	6 months	2.2645*	.08107	.000	2.0576	2.4714
5 months	4 months	-.9100*	.08107	.000	-1.1169	-.7031
	6 months	1.3544*	.08107	.000	1.1475	1.5613
6 months	4 months	-2.2645*	.08107	.000	-2.4714	-2.0576
	5 months	-1.3544*	.08107	.000	-1.5613	-1.1475
Dependent variable: phosphorus						
4 months	5 months	1.2333*	.09789	.000	.9835	1.4832
	6 months	2.4511*	.09789	.000	2.2013	2.7009
5 months	4 months	-1.2333*	.09789	.000	-1.4832	-.9835
	6 months	1.2178*	.09789	.000	.9680	1.4676
6 months	4 months	-2.4511*	.09789	.000	-2.7009	-2.2013
	5 months	-1.2178*	.09789	.000	-1.4676	-.9680

http://www.aloki.hu ● ISSN 1589 1623 (Print) ● ISSN 1785 0037 (Online)
DOI: http://dx.doi.org/10.15666/aeer/1902_933952
© 2021, ALÖKI Kft., Budapest, Hungary

Table 8. *Multiple comparison of Fraxinus rotundifolia nitrogen and phosphorus time by Tukey HSD*

Dependent variable: nitrogen						
(I) Time	**(J) Time**	**Mean difference (I-J)**	**Std. error**	**Sig.**	**95% confidence interval**	
					Lower bound	**Upper bound**
4 months	5 months	1.1461*	.05792	.000	.9983	1.2939
	6 months	1.6993*	.05792	.000	1.5515	1.8472
5 months	4 months	-1.1461*	.05792	.000	-1.2939	-.9983
	6 months	.5532*	.05792	.000	.4054	.7010
6 months	4 months	-1.6993*	.05792	.000	-1.8472	-1.5515
	5 months	-.5532*	.05792	.000	-.7010	-.4054
Dependent variable: phosphorus						
4 months	5 months	.7584*	.04847	.000	.6347	.8822
	6 months	1.5331*	.04847	.000	1.4094	1.6568
5 months	4 months	-.7584*	.04847	.000	-.8822	-.6347
	6 months	.7747*	.04847	.000	.6510	.8984
6 months	4 months	-1.5331*	.04847	.000	-1.6568	-1.4094
	5 months	-.7747*	.04847	.000	-.8984	-.6510

In addition, results revealed that soil has an important role in N and P reduction (*Fig. 6*). Canals without trees indicate significant reduction. Generally, P reduction is about 32% and N reduction is about 30% (*Appendices F* and *G*) (P value< 0.05). It seems that P is more available than N in soil (*Tables 9* and *10*), which could be related to stronger P bonds than those of N with soil clay particles as well as little movement of P through soil clay particles.

Table 9. *Multiple comparison of soil nitrogen and phosphorus time by Tukey HSD*

Dependent variable: nitrogen						
(I) Time	**(J) Time**	**Mean difference (I-J)**	**Std. Error**	**Sig.**	**95% confidence interval**	
					Lower bound	**Upper bound**
4 months	5 months	1.5343*	.14963	.000	1.1524	1.9161
	6 months	2.7576*	.14963	.000	2.3757	3.1395
5 months	4 months	-1.5343*	.14963	.000	-1.9161	-1.1524
	6 months	1.2233*	.14963	.000	.8415	1.6052
6 months	4 months	-2.7576*	.14963	.000	-3.1395	-2.3757
	5 months	-1.2233*	.14963	.000	-1.6052	-.8415
Dependent variable: phosphorus						
4 months	5 months	1.4822*	.17440	.000	1.0371	1.9273
	6 months	2.9422*	.17440	.000	2.4971	3.3873
5 months	4 months	-1.4822*	.17440	.000	-1.9273	-1.0371
	6 months	1.4600*	.17440	.000	1.0149	1.9051
6 months	4 months	-2.9422*	.17440	.000	-3.3873	-2.4971
	5 months	-1.4600*	.17440	.000	-1.9051	-1.0149

http://www.aloki.hu ● ISSN 1589 1623 (Print) ● ISSN 1785 0037 (Online)
DOI: http://dx.doi.org/10.15666/aeer/1902_933952
© 2021, ALÖKI Kft., Budapest, Hungary

Table 10. *Multiple comparisons of soil nitrogen and phosphorus concentration by Tukey HSD*

Dependent variable: nitrogen						
Tukey HSD						
(I) Concentration	(J) Concentration	Mean difference (I-J)	Std. error	Sig.	95% confidence interval	
					Lower bound	Upper bound
50 mg/L	10 mg/L	30.2731*	.14963	.000	29.8912	30.6549
	5 mg/L	33.5341*	.14963	.000	33.1522	33.9160
10 mg/L	50 mg/L	-30.2731*	.14963	.000	-30.6549	-29.8912
	5 mg/L	3.2610*	.14963	.000	2.8792	3.6429
5 mg/L	50 mg/L	-33.5341*	.14963	.000	-33.9160	-33.1522
	10 mg/L	-3.2610*	.14963	.000	-3.6429	-2.8792
Dependent variable: phosphorus						
50 mg/L	10 mg/L	30.7044*	.17440	.000	30.2593	31.1495
	5 mg/L	33.2800*	.17440	.000	32.8349	33.7251
10 mg/L	50 mg/L	-30.7044*	.17440	.000	-31.1495	-30.2593
	5 mg/L	2.5756*	.17440	.000	2.1305	3.0207
5 mg/L	50 mg/L	-33.2800*	.17440	.000	-33.7251	-32.8349
	10 mg/L	-2.5756*	.17440	.000	-3.0207	-2.1305

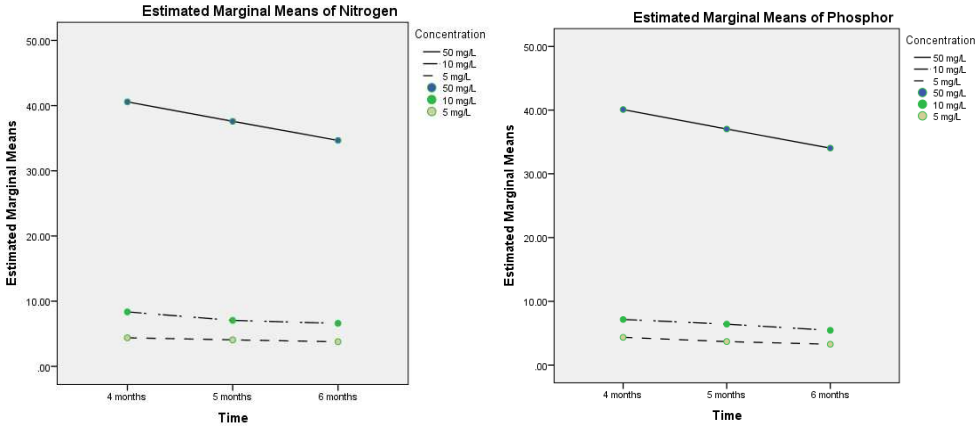


Figure 6. *N (a) and P (b) removal by soil in three time periods*

Discussion

Medium to long term monitoring is necessary to fully understand environmental sustainability and efficiency of RBSs. Therefore, measurements of perimeter, area, length, latitude and longitude of RBS plots along agricultural land on the banks of Zayandeh-rood River are such a helpful tool for future studies and for understanding the RBS efficiency. In this research, our focus was on plot 9 as it encompasses the largest area of buffer zone (total area = 4.3 ha). Results in this plot suggest that N and P removal occurs through an RBS. RBS seems to be more efficient in removal of P compared to N. Generally, results obtained from the RBS showed that N and P were accumulated from the beginning to the end of the farm, as there was a 0.12% increase per meter for N and a 0.50% increase per meter for P. Subsequently, at the beginning of

http://www.aloki.hu ● ISSN 1589 1623 (Print) ● ISSN 1785 0037 (Online)
DOI: http://dx.doi.org/10.15666/aeer/1902_933952
© 2021, ALÖKI Kft., Budapest, Hungary

the root system in the mentioned trees in the RBS, a 1.38% reduction per meter for N concentration and a 0.59% reduction per meter for P concentration were observed at the beginning of the RBS. Eventually, due to the final completion of phytoremediation and the integral effect of root system in the trees in the RBS, a 0.3% reduction in N concentration and a 1.47% reduction in P concentration were measured at the end of the RBS.

It should be noted that significant reductions of these two pollutants can be due to the composition of ash, willow, poplar, buckthorn and mulberry, based on their effective phytoremediation properties (*Table 2*). Woody vegetation has deep rooting systems and is more effective in P and N removal than shrubs and grass areas (Aguiar et al., 2015). They have a significant energy advantage over grassy plants (Glibovytska et al., 2019). They cover broader surface and volume of soil that make them able to accumulate higher amounts of pollutant in their bigger organs. Additionally, tree species are suggested as the most affordable vegetation type for phytoremediation with profounder root system, being appropriate to be planted in less fertile sites with a frail structure and a higher rate of transpiration (Haroni et al., 2019). The costs of phytoremediation would be reduced if other regarded vegetation are replaced with tree species (EPA, 2000). The ability of a RBS to remove N and P from water or soil is influenced by the type and quantity of existing vegetation and by soil condition (Mikkelsen and Vesho, 2000; Wang et al., 2002) Indeed, the effectiveness of phytoremediation is also affected by different contamination levels of wastewater (Assif and Saeed, 2020).

Previous studies of N and P attenuation in RBSs have indicated that they reduce suspended soil particulates considerably (Schilling and Jacobson, 2014; Aguiar et al., 2015) because of their flatter slopes and high surface roughness and in doing so, they often reduce P concentrations in streams (Mikkelsen and Vesho, 2000).

Since the greatest reduction occurs after 4 months, it could be concluded that phytoremediation is very active in early spring, and that after this period, the trees' capacity will decrease. Perhaps, it is because the root system achieves its highest function in this time period. According to Mali et al. (2019) growth stage significantly influenced the nutrient uptake, and during the winter dormant period, plant uptake is generally very low or nonexistent in RBSs (Haycock and Pinay, 1993). Groffman et al. (1992) showed that plant uptake was the dominant sink for N during growing season in RBSs. Ebrahimi et al., 2019 showed that Plant species and the growth season influence the efficiency of plant uptake that is associated with root systems properties.

According to the results obtained from soil, it is suggested that soil has an important role in N and P reduction, as well. Boz et al. (2013) claimed that soil microbial community composition and activity could be affected by suitable manipulation of the environment they live in. If correctly applied, such an approach could become a very effective way to remediate excess of chemicals. Furthermore, we could suggest that in this regard, tree root systems could provide macro-pores and create rapid inflow routes which will be used for transmission of N and P into the soil profile. Therefore, it could decrease the efficiency of Phytoremediation. Another possible explanation for the effectiveness of the root system in these two species, as they are necessarily mycorrhizal, is that the Arbuscular Mycorrhizal fungi have boosted the uptake of the N and P contaminants through the roots. According to (Bücking and Kafle, 2015), mycorrhizal fungi play a crucial role in the uptake of nutrients, such as phosphate and nitrate, in many plant species. This means that this N and P contaminant removal could have been improved by the mycorrhizal fungi and through the roots of the species

http://www.aloki.hu ● ISSN 1589 1623 (Print) ● ISSN 1785 0037 (Online)
DOI: http://dx.doi.org/10.15666/aeer/1902_933952
© 2021, ALÖKI Kft., Budapest, Hungary

studied here. Mycorrhizal fungi could have affected the results of the current study in yet another way. According to (Kebrabadi et al., 2014), the highest colonization percentage of mycorrhizal fungi is in spring, which corresponds with the timing of this current study. The findings of the current study revealed that the highest rate of contaminant reduction was in early spring, which corresponds with the results of (Kebrabadi et al., 2014; Mali et al., 2019). According to the results of the current study, *Aianthus altissima* was more efficient than *Fraxinus rotundifolia* in reduction of P (Li et al., 2015; Yang et al., 2015), and as stated in Taheri et al. (2014), *Fraxinus rotundifolia* is an effective species for phytoremediation of N. Thus, combining these two species can be more helpful to remove excess N and P and avoid water eutrophication.

Systematic evaluation of the greenhouse studies conducted based on the results from the field study suggests that RBZs with emphasis on the phytoremediation applications are beneficial environmentally friendly technique with the potential to rectify the contamination issue due to the eutrification caused by the agricultural runoff. Therefore, investigating the existing plant species in RBZs to determine species with higher phytoremediation capabilities, and the utilization of such results in the design of the RBZs, is of prime importance to future studies. Utilization of phytoremediation properties in buffer zones necessitates the integration of the results from background studies with agricultural skills and technique. Successful contamination remediation programs can be achieved through correct integration of the field conditions and the planting of the proper species to increase the access of the plant to the contamination, which in turn, emphasizes the need for bilateral field and greenhouse studies.

Conclusion

According to the results of the current study, when runoff passes through the buffer zone, P and N contaminations decrease significantly. Generally, the average N and P contamination reaches its highest levels at the end of the farm and the beginning of the RBS; however, the average contamination falls down to its minimum by the end of the RBS, which proved our first hypothesis, stating that RBSs are effective tools to reduce N and P contamination. As a result, we can conclude that the best approach to prevent the non-spot contamination is to create RBSs on the banks of rivers and other water resources which are vulnerable to contamination. The results of the current study revealed that an RBS, based on phytoremediation properties, may be a helpful and friendly technique to deal with the problem of agricultural runoff pollution in the process of purifying eutrophicated water.

Moreover, the findings of the current study revealed that, as Aguiar et al. (2015), Lou et al. (2017) and Seo et al. (2017) claimed, plants with deep root systems, like *Fraxinus rotundifolia* and *Aianthus altissima* are more effective in reducing N and P contaminants and Mixed cultivation can enhance the effects of phytoremediation. Due to the existing inter-species differences in phytoremediation of different contamination, biofilters using a mixture of plants are proposed (Irga et al., 2019).

Therefore, it is concluded that in creating RBSs for the purpose of contaminant removal, combining the two species of *Fraxinus rotundifolia* and *Aianthus altissima* could be an ideal and will result in effective removal of N and P contaminants. It is worth mentioning that *Fraxinus rotundifolia* is one of the most common species in this region and numerous ecological and geographical ranges are allocated to it. Moreover, it is available and inexpensive and, as the results of the current study also showed, has

http://www.aloki.hu ● ISSN 1589 1623 (Print) ● ISSN 1785 0037 (Online)
DOI: http://dx.doi.org/10.15666/aeer/1902_933952
© 2021, ALÖKI Kft., Budapest, Hungary

effective properties in remediation of N and P. Noteworthy, *Aianthus altissima* is a species which is resistant to drought and pollution, so it could be considered as an applicable species to be planted in RBSs.

Recommendations for further research

The selection of appropriate plants for phytoremediation is an open field for study, as different combinations of woody plants with deep root systems could have different effects on N and P contaminant removal. In our current study, we examined the beneficial effect of two species of woody plants which were commonplace to the region. However, examining the N and P contaminant reduction capability of other woody species can be subject to further research.

Another area for research could be the investigation of the role of mycorrhizae fungi on the reduction or removal of N and P contaminants. The findings of this study revealed that there might be a close direct relationship between the mycorrhizae activity and the reduction of the N and P contaminants.

REFERENCES

[1] Aguiar Jr, T. R., Raseraa, K., Parronc, L. M., Britod, A. G., Ferreira, M. T. (2015): Nutrient removal effectiveness by riparian buffer zones in rural temperate watersheds: the impact of no-till crops practices. – Agricultural Water Management 149: 74-80.

[2] Anbumozhi, V., Radhakrishnan, J., Yamaji, E. (2005): Impact of riparian buffer zones on water quality and associated management considerations. – Ecological Engineering 24: 517-523.

[3] Asif, M., Saeed, S. (2020): Study of Effectiveness of phytoremediation at different contamination level of wastewater. – Hydrol Current Research 11(314): 1-5.

[4] Borin, M., Vianello, M., Morari, F., Zanin, G. (2005): Effectiveness of buffer strips in removing pollutants in runoff from a cultivated field in North-East Italy. – Agriculture. Ecosystems and Environment 105: 101-114.

[5] Boyd, C. E. (2020): Eutrophication (chapter 15). – In: Water Quality. Springer, Cham, Switzerland, pp. 311-322.

[6] Boz, B., Rahman, M., Bottegal, M., Basaglia, M., Squartini, A., Gumiero, B., Casella, S. (2013): Vegetation, soil and hydrology management influence denitrification activity and the composition of nirK-type denitrifier communities in a newly afforested riparian buffer. – New Biotechnology 6: 675-684.

[7] Bücking, H., Kafle, A. (2015): Role of arbuscular mycorrhizal fungi in the nitrogen uptake of plants: current knowledge and research gaps. – Agronomy 5(4): 587-612.

[8] Cataldo, D. A., Haroon, M., Schrader, L. E., Youngs, V. L. (1975): Rapid colorimetric determination of nitrate in plant tissue by nitration of salicylic acid. – Communications in Soil Science and Plant Analysis 6: 71-80.

[9] De Souza, A. L. T., Fonseca, D. G., Liborio, R. A., Tanaka, M. O. (2013): Influence of riparian vegetation and forest structure on the water quality of rural low-order streams in SE Brazil. – Forest Ecology and Management 298: 12-18.

[10] Ebrahimi, N., Stoddard, F. L., Hartikainen, H., Seppänen, M. M. (2019): Plant species and growing season weather influence the efficiency of selenium biofortification. – Nutrient Cycling in Agroecosystems 114(2): 111-124.

[11] EPA (2000): Guidelines for Preparing Economic Analyses. EPA 240- R-00-003. – US Environmental Protection Agency, Washington, DC.

http://www.aloki.hu ● ISSN 1589 1623 (Print) ● ISSN 1785 0037 (Online)
DOI: http://dx.doi.org/10.15666/aeer/1902_933952
© 2021, ALÖKI Kft., Budapest, Hungary

[12] Euliss, K., Ho, C., Schwab, A. P., Rock, S., Banks, N. K. (2008): Greenhouse and field assessment of phytoremediation for petroleum contaminants in a riparian zone. – Bioresource Technology 99: 1961-1971.
[13] Fallahi, F., Ayati, B., Ganjidoust, H. (2011): Lab scale study of n removal by phytoremediation. – Journal of Water & Wastewater 1: 57-65. (In Persian).
[14] Genchi, G. (1990): Azoto e fosforo totali. – Nova Thalassia 11: 171-179 (in Italian).
[15] Glibovytska, N. I., Karavanovych, K. B., Kachala, T. B. (2019): Prospects of phytoremediation and phytoindication of oil-contaminated soils with the help of energy plants. – Journal of Ecological Engineering 20(7): 147-154.
[16] Gohari, A., Eslamian, S., Mirchi, A., Abedi-Koupaei, J., Massah Bavani, A., Madani, K. (2013): Water transfer as a solution to water shortage: a fix that can Backfire. – Journal of Hydrology 491: 23-39.
[17] Groffman, P. M., Arthur, J. G., Simmons, R. C. (1992): Nitrate dynamics in riparian forests; microbial studies. – Journal of Environmental Quality 21: 666-671.
[18] Haroni, N. N., Badehian, Z., Zarafshar, M., Bazot, S. (2019): The effect of oil sludge contamination on morphological and physiological characteristics of some tree species. – Ecotoxicology 28(5): 507-519.
[19] Haycock, N. E., Pinay, G. (1993): Groundwater nitrate dynamics in grass and poplar vegetated riparian buffer strips during the winter. – Journal of Environmental Quality 22: 273-278.
[20] Hefting, M. M., Jeroen de Klein, J. M. (1998): N removal in Buffer strips along a lowland stream in the Netherlands: a pilot study. – Environmental Pollution 102: 521-526.
[21] Irga, P. J., Pettit, T., Irga, R. F., Paull, N. J., Douglas, A. N., Torpy, F. R. (2019): Does plant species selection in functional active green walls influence VOC phytoremediation efficiency? – Environmental Science and Pollution Research 26(13): 12851-12858.
[22] Kebrabadi, B. Z., Daryayi, M. G., Matinizadeh, M., Salehi, A. (2014): Investigation and identification of mycorrhizal symbiosis in rhizosphere ash (Fraxinus rotundifolia). – Bulletin of Environment, Pharmacology and Life Sciences 3: 43-48.
[23] Li, Y., Chen, C., Wen, K., Li, G., Cao, P., Zhang, Y., Tackett, T. M. (2015): Abandoned reverse osmosis membrane effects on phytoremediation of saline soils with trees. – Ecological Engineering 84: 660-667.
[24] Lin, S. S., Shen, S. L., Zhou, A., Lyu, H. M. (2020): Assessment and management of lake eutrophication: a case study in Lake Erhai, China. – Science of The Total Environment 751. https://doi.org/10.1016/j.scitotenv.2020.141618.
[25] Lou, J., Qi, S., Peng, L., Xie, X. (2017): Enhanced phytoremediation capacity of a mixed-species plantation of Eucalyptus globulus and Chickpeas. – Geochemical Exploration 182: 201-205.
[26] Lusiana, E. D., Buwono, N. R., Mahmudi, M., Noviasari, P. P. (2020): Nutrient limit estimation for eutrophication modelling at Sengguruh Reservoir, Malang, Indonesia. – Nature Environment and Pollution Technology 19: 361-365.
[27] Maciej, K., Piotr, Z., Magdalena, G., Jolanta, E. K., Joanna, K., Irina, F. (2020): Effect of eutrophication and humification on nutrient cycles and transfer efficiency of matter in freshwater food webs. – Hydrobiologia 847: 2521-2540.
[28] Madani, K., Mariño, M. A. (2009): System dynamics analysis for managing Iran's Zayandeh-Rud river basin. – Water Resour Manage 23: 2163-2187.
[29] Malakouti, M. (2011): Relationship between balanced fertilization and healthy agricultural products (a review). – Journal of Crop and Weed Ecophysiology 4(16): 133-150.
[30] Mali, S. S., Naik, S. K., Jha, B. K., Singh, A. K., Bhatt, B. P. (2019): Planting geometry and growth stage linked fertigation patterns: impact on yield, nutrient uptake and water productivity of Chilli pepper in hot and sub-humid climate. – Scientia Horticulturae 249: 289-298.
[31] Mikkelsen, K., Vesho, L. (2000): Riparian Soils: A Literature Review. – Center for Streamside Studies, University of Washington Water Center, Washington.

http://www.aloki.hu ● ISSN 1589 1623 (Print) ● ISSN 1785 0037 (Online)
DOI: http://dx.doi.org/10.15666/aeer/1902_933952
© 2021, ALÖKI Kft., Budapest, Hungary

[32] Otto, S., Vianello, M., Infantino, A., Zanin, G., Di Guardo, A. (2008): Effect of a full-grown vegetative filter strip on herbicide runoff: maintaining of filter capacity over time. – Chemosphere 71: 74-82.
[33] Sanayei, Y., Ismail, N., Talebi, S. M. (2009): Determination of heavy metals in Zayandeh Rood River, Isfahan-Iran. – World Applied Sciences Journal 6: 1209-1214.
[34] Schilling, K. E., Jacobson, P. (2014): Effectiveness of natural riparian buffers to reduce subsurface nutrient losses to incised streams. – Catena 114: 140-148.
[35] Seo, B. H., Kim, H. S., Kuppusamy, S., Kim, K. H., Kim, K. R. (2017): Enhanced nitrogen and phosphorus removal by woody plants with deep-planting technique for the potential environmental management of carcass burial sites. – Sustainability 9(1): 155.
[36] Sibrell, P. L., Montgomery, G. A., Ritenour, K. L., Tucker, T. W. (2009): Removal of pus from agricultural wastewaters using adsorption media prepared from acid mine drainage sludge. – Water Research 43: 2240-2250.
[37] Stefanidis, K., Christopoulou, A., Poulos, S., Dassenakis, E., Dimitriou, E. (2020): Nitrogen and phosphorus loads in Greek rivers: implications for management in compliance with the water framework directive. – Water 12: 1-18.
[38] Taheri, M., Madadi, R., Jafari, S., Mortazavi, N. (2014): Evaluation some ornamental species cultivated in Tehran, in terms of refining ability heavy metals from soil. – International Journal of Biosciences 9: 26-33.
[39] Wang, Q., Cui, Y., Dong, Y. (2002): Phytoremediation of polluted waters potentials and prospects of wetland plants. – Acta Biotechnologica 22: 199-208.
[40] Xiang, W., Yang, X. E., Zed, R. (2009): Phytoremediation facilitates removal of N and P from eutrophicated water and release from sediment. – Environmental Monitoring and Assessment 157: 277-285.
[41] Yang, Y., Liang, Y., Ghosh, A., Song, Y., Chen, H., Tang, M. (2015): Assessment of arbuscular mycorrhizal fungi status and heavy metal accumulation characteristics of tree species in a lead–zinc mine area: potential applications for phytoremediation. – Environmental Science and Pollution Research 22(17): 13179-13193.

APPENDIX

Appendix A. *Distribution of RBS in Zayandeh-rood basin with measurements of perimeter, area, length, latitude, and longitude along agricultural land*

Plot number	Perimeter (Km)	Area (Ha)	Path length (Km)	Latitude	Longitude
1	0/99	0/5	0/48	32/6414	51/5758
2	0/45	0/18	0/19	32/6421	51/5744
3	0/29	0/07	0/13	32/6413	51/5702
4	0/24	0/11	0/11	32/6424	51/572
5	0/98	0/52	0/48	32/6381	51/5644
6	0/6	0/54	0/27	32/6348	51/5622
7	0/46	0/24	0/22	32/6333	51/5628
8	0/22	0/09	0/1	32/631	51/5617
9	1/47	4/31	0/28	32/6298	51/5614
10	0/47	0/36	0/16/	32/6334	51/5628
11	2/19	2/04	0/94	32/6272	51/5656
12	0/63	0/56	0/3	32/6206	51/5672
13	0/68	0/89	0/2	32/6198	51/5665
14	0/74	1/6	0/29	32/6108	51/5668
15	0/4	0/38	0/16	32/6091	51/5661
16	0/21	0/28	0/16	32/6077	51/5664
17	0/88	0/61	0/19	32/6064	51/5661

http://www.aloki.hu ● ISSN 1589 1623 (Print) ● ISSN 1785 0037 (Online)
DOI: http://dx.doi.org/10.15666/aeer/1902_933952
© 2021, ALÖKI Kft., Budapest, Hungary

18	3/17	3/84	1/38	32/5963	51/5645
19	0/51	0/24	0/24	32/5977	51/5653
20	0/51	0/25	0/24	32/5952	51/5599
21	0/72	0/27	0/36	32/5942	51/5596
22	0/6	0/26	0/27	32/5937	51/5554
23	0/52	0/17	0/25	32/5903	51/5252
24	0/82	0/24	0/4	32/5895	51/5486
25	0/21	0/14	0/15	32/5889	51/5459
26	0/19	0/05	0/09	32/5895	51/5449
27	0/5	0/24	0/19	32/5902	51/5422
28	0/45	0/22	0/19	32/5869	51/5387
29	1	1/05	0/32	32/5854	51/5362
30	0/13	0/09	0/06	32/5866	51/5375
31	0/22	0/07	0/1	32/586	51/5355
32	0/36	0/14	0/17	32/5854	51/534
33	4/65	2/53	2/06	32/5731	51/5267
34	0/86	0/6	0/41	32/5777	51/5267
35	1/01	0/8	0/44	32/5687	51/5206
36	3/06	3/02	1/24	32/5662	51/5223
37	0/97	1	0/36	32/5662	51/5223
38	0/21	0/2	0/09	32/5626	51/5197
39	4/27	2/09	2/1	32/6438	51/5838
40	0/46	0/24	0/2	32/6429	51/5781
41	0/19	0/9	0/04	32/6416	51/5775
42	1/15	0/86	0/53	32/6446	51/5851
43	2/04	1/27	0/91	32/6424	51/5945
44	0/29	0/25	0/13	32/6429	51/5898
45	0/53	0/38	0/25	32/6434	51/5917
46	0/66	0/53	0/3	32/6394	51/6023
47	0/81	0/41	0/4	32/6398	51/6053
48	0/94	0/61	0/42	32/6402	51/6078
49	0/53	0/44	0/23	32/6373	51/6354
50	0/4	0/22	0/16	32/6393	51/6369
51	0/35	0/23	0/14	32/6399	51/638

Appendix B. *Descriptive statistics of N removal by Aianthus altissima in three time periods*

Time	Concentration	Mean	Std. deviation	N
4 months	50 mg L^{-1}	20.0901	.03499	3
	10 mg L^{-1}	4.9536	.15663	3
	5 mg L^{-1}	2.5430	.08154	3
	Total	9.1956	8.23779	9
5 months	50 mg L^{-1}	18.3067	.33262	3
	10 mg L^{-1}	4.5200	.09849	3
	5 mg L^{-1}	2.0300	.07211	3
	Total	8.2856	7.59484	9
6 months	50 mg L^{-1}	15.1933	.16803	3
	10 mg L^{-1}	4.2000	.26458	3
	5 mg L^{-1}	1.4000	.10000	3
	Total	6.9311	6.31631	9
Total	50 mg L^{-1}	17.8634	2.15441	9
	10 mg L^{-1}	4.5579	.36517	9
	5 mg L^{-1}	1.9910	.50129	9
	Total	8.1374	7.19743	27

http://www.aloki.hu ● ISSN 1589 1623 (Print) ● ISSN 1785 0037 (Online)
DOI: http://dx.doi.org/10.15666/aeer/1902_933952
© 2021, ALÖKI Kft., Budapest, Hungary

Appendix C. *Descriptive statistics of P removal by Aianthus altissima in three time periods*

Time	Concentration	Mean	Std. deviation	N
4 months	50 mg L^{-1}	17.1867	.16623	3
	10 mg L^{-1}	4.5633	.22502	3
	5 mg L^{-1}	2.5900	.14000	3
	Total	8.1133	6.86022	9
5 months	50 mg L^{-1}	15.1767	.25325	3
	10 mg L^{-1}	3.8167	.17786	3
	5 mg L^{-1}	1.6467	.12897	3
	Total	6.8800	6.29528	9
6 months	50 mg L^{-1}	13.3233	.30436	3
	10 mg L^{-1}	2.7667	.28746	3
	5 mg L^{-1}	.8967	.05033	3
	Total	5.6622	5.80644	9
Total	50 mg L^{-1}	15.2289	1.68705	9
	10 mg L^{-1}	3.7156	.80761	9
	5 mg L^{-1}	1.7111	.74139	9
	Total	6.8852	6.17158	27

Appendix D. *Descriptive statistics of N removal by Fraxinus rotundifolia in three time periods*

Time	Concentration	Mean	Std. deviation	N
4 months	50 mg L^{-1}	16.0300	.16823	3
	10 mg L^{-1}	3.8695	.05367	3
	5 mg L^{-1}	2.0955	.09425	3
	Total	7.3317	6.56958	9
5 months	50 mg L^{-1}	14.2867	.07767	3
	10 mg L^{-1}	2.6533	.05508	3
	5 mg L^{-1}	1.6167	.12014	3
	Total	6.1856	6.09288	9
6 months	50 mg L^{-1}	13.3333	.25166	3
	10 mg L^{-1}	2.4667	.05774	3
	5 mg L^{-1}	1.0970	.07515	3
	Total	5.6323	5.80768	9
Total	50 mg L^{-1}	14.5500	1.19454	9
	10 mg L^{-1}	2.9965	.66149	9
	5 mg L^{-1}	1.6031	.44078	9
	Total	6.3832	5.96662	27

Appendix E. *Descriptive statistics of P removal by Fraxinus rotundifolia in three time periods*

Time	Concentration	Mean	Std. deviation	N
4 months	50 mg L^{-1}	16.4333	.08622	3
	10 mg L^{-1}	4.0253	.02397	3
	5 mg L^{-1}	2.5833	.20232	3
	Total	7.6807	6.59506	9
5 months	50 mg L^{-1}	15.3633	.16653	3
	10 mg L^{-1}	3.4533	.05508	3
	5 mg L^{-1}	1.9500	.06000	3
	Total	6.9222	6.36489	9
6 months	50 mg L^{-1}	14.3967	.08622	3
	10 mg L^{-1}	3.0000	.04359	3
	5 mg L^{-1}	1.0460	.05011	3
	Total	6.1476	6.24466	9
Total	50 mg L^{-1}	15.3978	.88830	9
	10 mg L^{-1}	3.4929	.44652	9
	5 mg L^{-1}	1.8598	.67785	9
	Total	6.9168	6.18496	27

http://www.aloki.hu ● ISSN 1589 1623 (Print) ● ISSN 1785 0037 (Online)
DOI: http://dx.doi.org/10.15666/aeer/1902_933952
© 2021, ALÖKI Kft., Budapest, Hungary

Appendix F. *Descriptive statistics of N removal by soil in three time periods*

Time	Concentration	Mean	Std. deviation	N
4 months	50 mg L^{-1}	40.5748	.40448	3
	10 mg L^{-1}	8.3589	.32265	3
	5 mg L^{-1}	4.3858	.09633	3
	Total	17.7731	17.18955	9
5 months	50 mg L^{-1}	37.5933	.46972	3
	10 mg L^{-1}	7.0567	.05033	3
	5 mg L^{-1}	4.0667	.05033	3
	Total	16.2389	16.06984	9
6 months	50 mg L^{-1}	34.6667	.57735	3
	10 mg L^{-1}	6.6000	.26458	3
	5 mg L^{-1}	3.7800	.02646	3
	Total	15.0156	14.79225	9
Total	50 mg L^{-1}	37.6116	2.59314	9
	10 mg L^{-1}	7.3385	.81786	9
	5 mg L^{-1}	4.0775	.26834	9
	Total	16.3425	15.46038	27

Appendix G. *Descriptive statistics of P removal by soil in three time periods*

Time	Concentration	Mean	Std. deviation	N
4 months	50 mg L^{-1}	40.0833	.60575	3
	10 mg L^{-1}	7.1567	.14844	3
	5 mg L^{-1}	4.3467	.14572	3
	Total	17.1956	17.21188	9
5 months	50 mg L^{-1}	37.0267	.08622	3
	10 mg L^{-1}	6.4233	.56012	3
	5 mg L^{-1}	3.6900	.41869	3
	Total	15.7133	16.03263	9
6 months	50 mg L^{-1}	34.0367	.46199	3
	10 mg L^{-1}	5.4533	.28572	3
	5 mg L^{-1}	3.2700	.17349	3
	Total	14.2533	14.87032	9
Total	50 mg L^{-1}	37.0489	2.64625	9
	10 mg L^{-1}	6.3444	.80737	9
	5 mg L^{-1}	3.7689	.52679	9
	Total	15.7207	15.48488	27

http://www.aloki.hu ● ISSN 1589 1623 (Print) ● ISSN 1785 0037 (Online)
DOI: http://dx.doi.org/10.15666/aeer/1902_933952
© 2021, ALÖKI Kft., Budapest, Hungary

MORINGA *(MORINGA OLEIFERA)* LEAF NUTRITIONAL COMPOSITION AS INFLUENCED BY SOIL PHYSICAL AND CHEMICAL PROPERTIES AND TREE AGE UNDER DIVERSE AGRO-ECOLOGICAL CONDITIONS

BOPAPE-MABAPA, M. P.[1,2*] – AYISI, K. K.[2] – MARIGA, I. K.[1] – MASHAO, F. M.[2]

[1]*University of Limpopo, Department of Plant Production, Soil Science and Agricultural Engineering, Private Bag X1106, Sovenga 0727, Republic of South Africa*

[2]*University of Limpopo, Risk and Vulnerability Science Centre, Private Bag X1106, Sovenga 0727, Republic of South Africa*

[*]*Corresponding author*
e-mail: paulina.mabapa@ul.ac.za; phone: +27-72-200-9692

(Received 18th Oct 2019; accepted 12th Feb 2020)

Abstract. A study was carried out in the five districts of the Limpopo Province in South Africa to determine the influence of soil physical and chemical properties on the nutritional composition of moringa leaves. Soil samples under moringa canopy and 5 m away from the base of the trees as well as fresh leaf samples were collected from 31 moringa plantations in Limpopo Province during the summer season (November 2015 to January 2016). Soils at a depth of 0 to 30 and 30 to 60 cm were grouped according to textural classes and analyzed for physical and chemical properties. The harvested leaves were dried at room temperature and their nutritional compositions were determined. The study revealed improved soil nutritional composition under moringa trees, mainly in areas where the trees were more than three years old as compared to control. A higher nutritional composition was also recorded in soils with higher clay content relative to low clay soils. The results of leaf nutritional composition revealed no significant differences between the soil textural classes. The study concluded that moringa can be produced in many locations and on diverse soils of the Limpopo Province without negatively affecting leaf nutritional composition.
Keywords: *locations, miracle plant, nutrients, soil textural classes, weather*

Introduction

Moringa is gaining global attention due to its beneficial aspects such as food supplementation, medication, industrial purposes and for water purification properties (Fahey, 2005; Moyo et al., 2011; Oshunsanya et al., 2015; Lamidi et al., 2017). Almost all parts of the moringa tree are utilized for various purposes, for both human food and livestock feed as well as for its medicinal values (Lamidi et al., 2017). Moringa trees have been planted in many developing countries including South Africa, with the aim to combat malnutrition amongst poor families and significantly contribute to reducing food insecurity (Fahey, 2005; Jongrungruangchok et al., 2010; Gandji et al., 2018). The dried nutritional leaf powder can be used to fortify meals during dry seasons when there is a lack of other green leafy vegetables (Kumssa et al., 2017). There is considerable variation in moringa nutritional composition of the dried leaf powder depending on factors such as the genetic background of the plant and prevailing environmental conditions (Moyo et al., 2011).

Besides its nutritional composition, moringa is reported to increase soil fertility litter fall and its leaves can also be used as a nutrient-agent for biofertilizer production (Adiaha, 2017). A study conducted by Undie et al. (2013) showed that moringa leaves can serve

http://www.aloki.hu ● ISSN 1589 1623 (Print) ● ISSN1785 0037 (Online)
DOI: http://dx.doi.org/10.15666/aeer/1902_953970
© 2021, ALÖKI Kft., Budapest, Hungary

as an alternative source of soil organic matter and can be a replacement for inorganic fertilizers for optimum crop production. The moringa tree is also strongly recommended for inclusion in agroforestry systems since its relatively deep root system minimizes moringa's competitiveness with companion crops for nutrient uptake in the system. This ultimately it helps to improve soil organic matter and fertility where moringa is grown (Ashfaq et al., 2012).

Moringa tree thrives under harsh conditions, where the majority of agricultural crops cannot survive, especially in tropical and subtropical areas (Leone et al., 2016). The tree grows best at a temperature ranging between 25 to 35ºC, but can still survive extreme temperatures of up to 48ºC and tolerate a soil pH of 5.0 to 9.0 (Amaglo, 2006; Saini et al., 2016). Besides being tolerant from various environmental conditions, it is a fast growing tree that is known for its drought-tolerance abilities and can reach a height of 6 to 7 m within 12 months of establishment in areas receiving a rainfall of less than 400 and up to 1500 mm/annum (Morton, 1991; Odee, 1998; Amaglo, 2006; Yamato et al., 2009). Its survival to drought conditions is attributed to the presence of water storing organs in the root system and its symbiosis with mycorrhizal fungi (Yamato et al., 2009). Studies by Yamato et al. (2009), Muthukumar et al. (2006) and Cosme et al. (2014) reported on the colonization of arbuscular mycorrhizal (AM) fungi in moringa species and showed that the AM association contributes towards soil nutrients uptake, drought tolerance and disease resistance of the host plant.

Moringa is found in all countries, particularly those which experience malnutrition (Ashfaq et al., 2012). However, in South Africa, moringa is a fairly new crop that is grown by few farmers (Pakade et al., 2013) in provinces such as Kwa-Zulu Natal, Mpumalanga, and Limpopo (Lekgau, 2011). In Limpopo Province, the majority of farmers grow the tree on a small area of fewer than two hectares (Mabapa et al., 2017). Majority of such farmers grow the tree for household purposes. Mabapa et al. (2017), reported that moringa is produced in all districts of the Limpopo province. There is, however, limited information on the influence of soil characteristics on the mineral composition of moringa leaves. This study was established to investigate and compare the nutritional composition of *Moringa oleifera* leaves produced under diverse soil textural classes and types in the Limpopo Province.

Materials and Methods

Study area

The study was conducted during the summer season from November 2015 to January 2016 in all the five districts of the Limpopo Province (23.4013° S, 29.4179° E), namely Capricorn, Sekhukhune, Waterberg, Mopani, and Vhembe. Limpopo province falls within the summer rainfall region of South Africa, with the western part being semi-arid and the eastern part largely sub-tropical. Typical rainfall for the province ranges from 200 mm in the hot dry areas to more than 1500 mm in the high rainfall areas, with most of it falling between October and April (Limpopo, D.F.E.D, 2004). The province experiences the highest temperatures during the months of October to March. Temperatures peak in December and January at about an average of 25ºC. The lowest temperatures occur in July with an average of 15ºC (Tshiala et al., 2011).

http://www.aloki.hu ● ISSN 1589 1623 (Print) ● ISSN1785 0037 (Online)
DOI: http://dx.doi.org/10.15666/aeer/1902_953970
© 2021, ALÖKI Kft., Budapest, Hungary

Data collection

Soil samples and fresh leaf samples were collected from the fields of 31 farmers who produce moringa on an area of 0.5 ha and above. The farmers were identified through a survey conducted by Mabapa et al. (2017). Profile of sampled moringa trees with the sampled areas is presented in *Table 1*. Fully expanded leaf samples were harvested from the lower, mid and upper parts of the five trees canopy from each location. A representative of five soil samples and gravimetric soil moisture were also determined from each location. Preliminary assessment of sampled soils revealed that the five districts had a variable textural class; therefore, the textural classes were grouped and used as treatments for the overall analysis of soil and leaf nutrition across locations.

Table 1. *Locations and profile of moringa trees examined from the 5 districts in the Limpopo Province*

Number	District	Location/Area	Tree Age (Years)	Soil Textural Class	Clay Percentage
1	Capricorn	Polokwane	7	Loamy Sand	18
2	Capricorn	Matlala	2	Sandy Loam	19.5
3	Capricorn	Polokwane	2	Sandy Loam	25
4	Capricorn	Lebowakgomo	3	Sandy Clay Loam	26.5
5	Capricorn	Ga-phasha	3	Sandy Clay Loam	30
6	Capricorn	Makotse	5	Sandy Clay Loam	31.5
7	Capricorn	Tooseng	4	Loamy Sand	26
8	Mopani	Nkowankowa	1	Loamy Sand	18.5
9	Mopani	Milliekloof	1	Loamy Sand	17
10	Mopani	Woster	3	Sandy Loam	21.5
11	Mopani	Ofcolaco	2	Sandy Clay Loam	30
12	Mopani	Sekororo	5	Sandy Loam	28
13	Mopani	Woster	3	Sandy Clay Loam	31
14	Mopani	Lorraine	4	Sandy Clay	42
15	Mopani	Baloon	6	Sandy Clay	44
16	Mopani	Eiland	4	Sandy Loam	17.5
17	Sekhukhune	Driekop	10	Sandy Loam	16
18	Sekhukhune	Denilton	4	Loamy Sand	20
19	Sekhukhune	Dithabaneng	5	Loamy Sand	28
20	Vhembe	Makwarela	3	Sandy Clay Loam	31.5
21	Vhembe	Thohoyandou	3	Sandy Loam	27.5
22	Vhembe	Ha-Budeli	3	Sandy Clay	38.5
23	Vhembe	Tshakhuma	5	Clay Loam	49
24	Vhembe	Tshiande	5	Clay Loam	52
25	Vhembe	Ha-Mutsha	2	Clay Loam	56
26	Vhembe	Thohoyandou	2	Sandy Loam	28
27	Vhembe	Lufule	2	Sandy Loam	20.5
28	Vhembe	Ha-Dumase	2	Sandy Clay Loam	30.5
29	Vhembe	Tshipise	4	Sandy Loam	22
30	Waterberg	Mmapela	3	Clay	60
31	Waterberg	Mokopane	4	Sandy Clay Loam	32.5

Soil sampling and analysis

Soil samples were taken under moringa canopy and 5 m away from the trees (as control) to determine the impact of the change in soil property beneath the moringa canopy area. Soils were sampled at a depth of 0 to 30 and 30 to 60 cm using an auger with the dimension of 8 x 15 cm, to determine physical and chemical characteristics (*Tables 1 and 2*) from each location.

http://www.aloki.hu ● ISSN 1589 1623 (Print) ● ISSN1785 0037 (Online)
DOI: http://dx.doi.org/10.15666/aeer/1902_953970
© 2021, ALÖKI Kft., Budapest, Hungary

Table 2. *Chemical and physical characteristics samples from the different locations in the Limpopo Province*

		Locations														
		1	**2**	**3**	**4**	**5**	**6**	**7**	**8**	**9**	**10**	**11**	**12**	**13**	**14**	**15**
Tree age		**7**	**5**	**2**	**3**	**3**	**5**	**4**	**1**	**1**	**3**	**2**	**5**	**3**	**4**	**6**
Soil Properties	**Depth (cm)**															
Moringa N (%)	0 – 30	0.04	0.04	0.14	0.08	0.08	0.08	0.06	0.04	0.04	0.04	0.40	0.04	0.11	0.04	0.04
Moringa N (%)	30 – 60	-	0.04	0.10	0.07	0.04	0.04	0.04	0.04	0.04	0.04	0.40	0.05	0.04	0.04	0.04
Control N (%)	0 – 30	0.04	0.04	0.09	0.04	0.08	0.04	0.10	0.06	0.06	0.04	0.40	0.09	0.09	0.04	0.04
Control N (%)	30 – 60	-	0.04	0.05	0.04	0.05	0.04	0.04	0.04	0.04	0.04	0.40	0.04	0.04	0.04	0.04
Moringa P (mg/L)	0 – 30	54	4	3	5	8	5	80	8	7	5	7	7	15	10	3
Moringa P (mg/L)	30 – 60	-	2	5	4	2	3	48	3	4	1	3	7	6	10	2
Control P (mg/L)	0 – 30	03	1	2	5	6	3	98	17	7	1	8	4	4	22	4
Control P (mg/L)	30 – 60	-	1	3	3	3	3	11	13	3	1	3	4	4	13	1
Moringa K (mg/L)	0 – 30	248	191	117	581	226	209	398	83	35	139	136	83	238	47	215
Moringa K (mg/L)	30 – 60	-	223	108	439	139	141	133	34	30	102	120	71	259	55	208
Control K (mg/L)	0 – 30	566	211	107	514	277	278	273	77	77	353	212	89	89	101	135
Control K (mg/L)	30 – 60	-	151	52	228	190	296	157	35	35	384	105	41	41	108	120
Moringa Ca (mg/L)	0 – 30	968	593	1050	2964	2482	2353	737	354	472	582	743	1820	2400	414	550
Moringa Ca (mg/L)	30 – 60	-	716	1003	2810	3040	2732	624	384	389	682	717	1970	1718	397	506
Control Ca (mg/L)	0 – 30	660	321	897	2810	1326	1005	712	422	422	472	646	1004	1004	627	823
Control Ca (mg/L)	30 – 60	-	243	715	3166	1903	1089	565	337	337	442	756	1164	1164	782	702
Moringa pH (KCl)	0 – 30	6.37	4.99	5.56	6.52	7.53	6.61	7.84	5.57	5.73	7.44	5.97	6.54	6.73	7.06	4.95
Moringa pH (KCl)	30 – 60	-	5.20	5.58	6.94	7.16	6.91	8.02	5.18	5.30	7.38	5.57	6.26	7.52	7.04	4.95
Control pH (KCl)	0 – 30	5.49	4.78	4.41	6.88	5.86	6.92	7.82	5.51	5.51	5.53	5.13	6.64	6.64	7.46	6.1
Control pH (KCl)	30 – 60	-	3.95	4.28	7.17	5.60	7.22	7.86	5.29	5.20	5.50	5.22	6.63	6.63	6.85	5.58
Moringa Org C (%)	0 – 30	0.6	0.4	1.15	1.60	1.30	1.50	1	0.80	0.50	0.40	1.10	0.7	1.50	0.40	1.40
Moringa Org C (%)	30 – 60	-	0.4	1	1.40	0.80	0.60	0.70	0.40	0.40	0.40	1.10	0.7	1.00	0.50	1.60
Control Org C (%)	0 – 30	0.7	0.4	1.12	0.9	1.20	0.50	1.40	0.90	0.90	0.40	1.40	1.7	1.70	0.50	1.30
Control Org C (%)	30 – 60	-	0.4	1	0.7	0.80	0.40	0.50	0.40	0.40	0.50	1.10	0.4	0.40	0.40	1.40

http://www.aloki.hu ● ISSN 1589 1623 (Print) ● ISSN1785 0037 (Online)
DOI: http://dx.doi.org/10.15666/aeer/1902_953970
© 2021, ALÖKI Kft., Budapest, Hungary

		Locations															
		16	**17**	**18**	**19**	**20**	**21**	**22**	**23**	**24**	**25**	**26**	**27**	**28**	29	30	31
Tree age		**4**	**10**	**4**	**5**	**3**	**3**	**3**	**5**	**5**	**2**	**2**	**2**	**2**	4	3	4
Soil Properties	**Depth (cm)**																
Moringa N (%)	0 – 30	0.04	0.06	0.04	0.04	0.06	0.07	0.11	0.08	0.19	0.12	0.09	0.04	0.12	0.05	0.15	0.08
Moringa N (%)	30 – 60	0.04	0.09	0.04	0.04	0.04	0.09	0.04	0.08	0.07	0.20	0.21	0.07	0.04	0.04	0.05	0.05
Control N (%)	0 – 30	0.12	0.08	0.08	0.04	0.11	0.11	0.06	0.09	0.16	0.33	0.04	0.04	0.04	0.04	0.04	0.11
Control N (%)	30 – 60	0.04	0.06	0.06	0.05	0.07	0.07	0.09	0.10	0.07	0.27	0.18	0.04	0.04	0.04	0.1	0.1
Moringa P (mg/L)	0 – 30	46	100	36	20	51	44	7	83	15	34	22	28	8	11	26	53
Moringa P (mg/L)	30 – 60	39	54	8	3	10	13	22	59	20	26	13	26	2	7	3	2
Control P (mg/L)	0 – 30	32	16	16	9	2	2	12	17	15	11	15	67	14	14	2	4
Control P (mg/L)	30 – 60	20	9	9	3	1	1	46	9	6	6	12	3	8	8	5	2
Moringa K (mg/L)	0 – 30	238	389	331	131	512	603	185	407	282	331	183	202	158	79	566	164
Moringa K (mg/L)	30 – 60	228	372	333	104	253	302	238	336	168	294	267	210	50	69	148	49
Control K (mg/L)	0 – 30	155	292	219	294	187	187	999	200	133	254	270	357	91	91	116	149
Control K (mg/L)	30 – 60	126	265	226	96	213	213	482	195	77	194	134	126	80	80	169	111
Moringa Ca (mg/L)	0 – 30	965	1572	827	1156	1641	2602	2453	1653	1842	1738	1120	1050	1875	970	3442	902
Moringa Ca (mg/L)	30 – 60	992	1530	574	1780	856	1882	1670	1610	2686	1719	1833	1044	869	899	3174	916
Control Ca (mg/L)	0 – 30	1314	1119	119	1467	741	2741	1849	979	1668	1192	1942	1213	629	629	2587	1491
Control Ca (mg/L)	30 – 60	1364	1301	310	1641	926	2917	2326	812	2730	1040	1751	515	625	625	2813	1694
Moringa pH (KCl)	0 – 30	6.86	7.61	6.51	7.72	7.5	7.46	6.63	7.01	5.64	7.6	5.78	6.5	5.85	6.36	7.44	6.5
Moringa pH (KCl)	30 – 60	6.74	7.48	5.67	7.64	7.39	7.15	7.2	6.88	7.42	7.31	5.66	6.39	5.46	6.24	7.21	6.36
Control pH (KCl)	0 – 30	5.60	4.57	4.50	7.70	7.02	7.02	7.37	5.76	5.93	5.12	6.94	6.46	5.86	5.86	7.18	6.72
Control pH (KCl)	30 – 60	5.52	5	5.00	7.60	7	7	7.09	5.56	6.96	4.82	5.9	5.06	5.98	5.98	7.21	6.83
Moringa Org C (%)	0 – 30	0.70	0.7	0.4	0.4	0.6	0.9	1.40	1.7	2.7	1.80	1.4	0.4	1.3	1.1	1.7	1.1
Moringa Org C (%)	30 – 60	0.40	0.7	0.4	0.4	0.4	0.6	0.80	1.7	1.4	2.40	2.8	1.0	0.7	0.7	0.6	0.7
Control Org C (%)	0 – 30	1.50	0.8	0.5	0.4	1.4	1.4	1.30	1.6	2.2	3.60	0.7	0.7	0.4	0.4	0.4	1.1
Control Org C (%)	30 – 60	0.06	0.5	0.3	0.4	10	6	1.20	1.6	1.5	3.10	2.2	0.4	0.4	0.4	0.9	0.4

http://www.aloki.hu ● ISSN 1589 1623 (Print) ● ISSN1785 0037 (Online)
DOI: http://dx.doi.org/10.15666/aeer/1902_953970
© 2021, ALÖKI Kft., Budapest, Hungary

Gravimetric soil moisture percentage was also determined from the same depths. Zip-lock plastic bags were used to keep soil for moisture retention before measurement. Fresh soil moisture weight was determined immediately after sampling using a battery-operated top loading weighing balance (RADWAG, W/C6/12/C1/R model). Soils were placed in aluminum drying pans and dried in an oven (Scientific oven Economy, 240 litres, Model 223) for 24 hours at a temperature of 105ºC. Gravimetric soil moisture percentage was determined when the soil samples had reached a constant weight, using a method described by Black (1965). Soils textural classes were determined based on particle size distribution and soil samples were analysed for P, K, Ca, Mg, Zn, Mn, Cu (mg/L), pH (KCl), organic carbon, total N (%), using analytical methods used by the soil fertility and analytical services section in Kwa-Zulu Natal (Manson and Roberts, 2000).

Nutrients determination in moringa leaves

Samples of moringa leaves collected from different locations were shade-dried at room temperature (24ºC) for 72 hours, to ease the defoliation from the rachis. Dried leaf samples were ground to pass through a 2 mm sieve and samples from the aforementioned locations within each soil textural class were bulked and mixed thoroughly. A 10 g sample of a fine fraction was used to determine their chemical composition. The analyses were carried out in triplicate. Crude protein was determined using the Kjeldahl method (AOAC, 1990). Other minerals such as N, P, Ca, and Fe were determined using atomic absorption procedure (Gaines and Mitchell, 1979).

Statistical analysis

The data collected were subjected to analysis of variance using Statistix 10.0 to determine the effect soil texture on measured variables. Where significant F-values from the treatment effect were found, means were separated by the least significant difference (LSD) at a probability level of 0.05. Linear correlation and regression analyses were performed using Statistix 10.0 and Microsoft Excel to determine the relationship between soil and leaf nutrient properties of moringa trees.

Results

Profile of sampled locations which included districts, location, tree age and soil textural classes are presented in *Table 1*. The results showed that moringa is grown in all the districts of the Limpopo Province. It was observed that 55% of the farmers had three years and lesser experience in moringa farming. Majority of the sampled locations were dominated by sandy loam soil.

The mean annual temperature, annual rainfall, locations where moringa is growing in the Limpopo Province and soil textural classes are shown in *Figs. 1 and 2*. Many areas of the Limpopo Province experience high temperature to an extent such that the average could be more than 23ºC (*Fig. 1*). The province also receives erratic annual rainfall ranging between 300 to 500 mm (*Fig. 2*).

Figs. 1 and 2 showed that moringa can grow on various soils textural classes depending on the location where a farmer is growing the trees in the Limpopo Province. Weather data collected from the nearest weather station of each location during the study period is shown in *Fig. 3*. It was observed that the average maximum temperature ranged

http://www.aloki.hu ● ISSN 1589 1623 (Print) ● ISSN1785 0037 (Online)
DOI: http://dx.doi.org/10.15666/aeer/1902_953970
© 2021, ALÖKI Kft., Budapest, Hungary

between 30 to 35ºC with minimum temperature raging between 15 to 22ºC and a total rainfall of between 75 to 200 mm during the study period (*Fig. 3*).

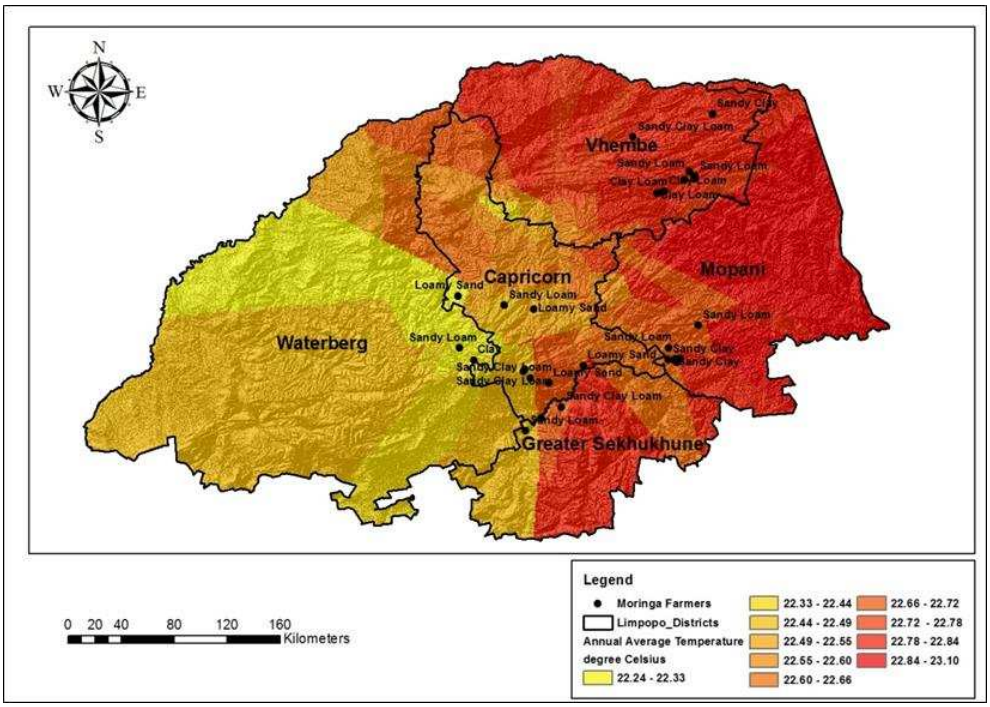


Figure 1. *Average annual temperature and soil textural classes from various locations where moringa is growing in Limpopo Province*

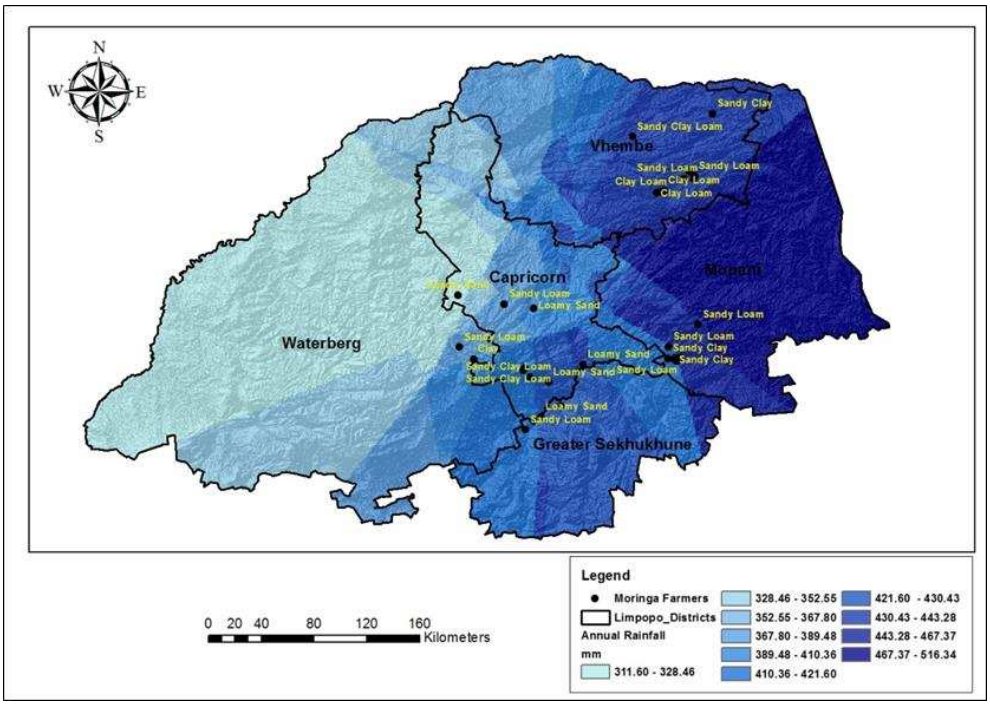


Figure 2. *Total annual rainfall and soil textural classes from various locations where moringa is growing in Limpopo Province*

http://www.aloki.hu ● ISSN 1589 1623 (Print) ● ISSN1785 0037 (Online)
DOI: http://dx.doi.org/10.15666/aeer/1902_953970
© 2021, ALÖKI Kft., Budapest, Hungary

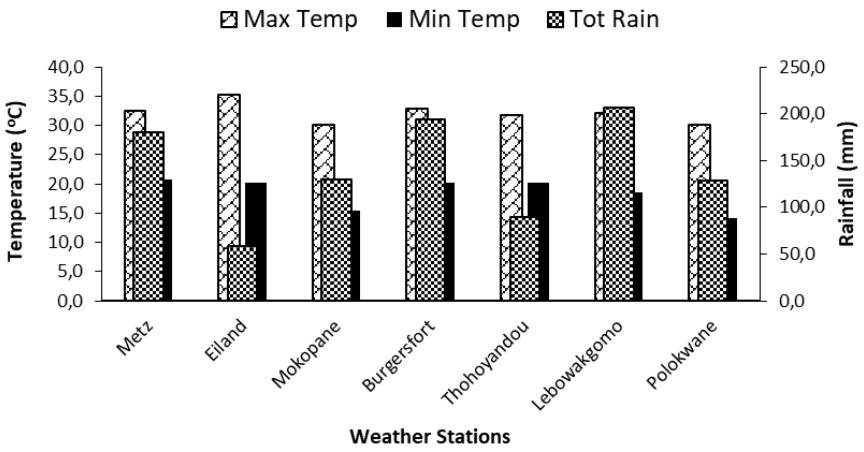


Figure 3. *Weather data collected from 2011 until 2016 during the study from selected locations in Limpopo Province*

Chemical properties of the soil samples collected from the selected 31 locations are shown in *Table 2*. In many cases, the chemical composition in the soil at 0 to 30 cm depth was relatively higher compared to the lower depth of 60 cm in both the control and moringa canopy samples (*Table 2*).

Nitrogen and phosphorus were found to be very low at all locations. The nitrogen content increased slightly by 33 percent mainly in soils with a higher clay content of more than 30 percent, while a reduction of 35 percent was also noticed in sandy soils and the constant results between control and nitrogen content were 32 percent (*Table 2*). The range for phosphorus concentration was between 3 and 100 mg/l under moringa canopy and 2 and 98 mg/l under control. There was also a decrease in P content with an increase in sampling depth.

Out of 31 locations, 17 (55 percent) locations recorded higher potassium content under moringa canopy compared to the control. A total of 22 (71 percent) locations also showed an increase in calcium content where there was moringa trees (*Table 2*). The soil pH ranged from 4.95 to 8.02, under moringa trees, while the control ranged from 3.5 to 7.86. The results thus reveal that moringa may have the potential to ameliorate acidic soils. The soil organic carbon ranged between 0.4 to 2.7% under moringa canopy and 0.06 to 3.6% under the control (*Table 2*). It was observed that where soils had high clay content (>30 percent) the amount of organic carbon under moringa canopy had slightly increased.

A significant positive relationship was observed between soil nitrogen with soil calcium (0.40**) and organic carbon (0.73***). Soil calcium also had a positive relationship with organic carbon (0.30**) and soil potassium (0.45**). As the tree matures the amount of phosphorus increased in many occasions which led to a positive relationship of 0.27* (*Fig. 4*). Soil pH had a positive relationship with soil phosphorus (0.23*), potassium (0.21*) and calcium (0.13*) (*Fig. 5*).

Findings from this study showed that the concentration of soil nitrogen, phosphorus, potassium, calcium and organic carbon was significantly dependent on soil textural class whereas pH was not affected (*Table 3*). It was observed that an increase in clay content (>45 percent) in the soil, improved the soil chemical composition. Soil potassium and calcium content were more than 550 and 3000 mg/L under the clay textured soil (*Table 3*).

http://www.aloki.hu ● ISSN 1589 1623 (Print) ● ISSN1785 0037 (Online)
DOI: http://dx.doi.org/10.15666/aeer/1902_953970
© 2021, ALÖKI Kft., Budapest, Hungary

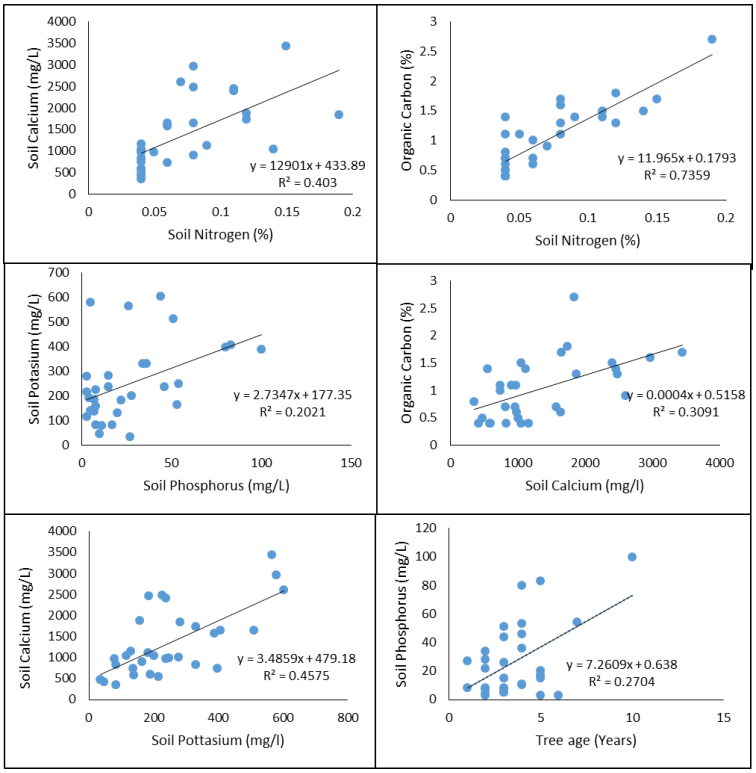


Figure 4. *Correlation and linear relationship effects of tree age and soil properties under the moringa tree canopy*

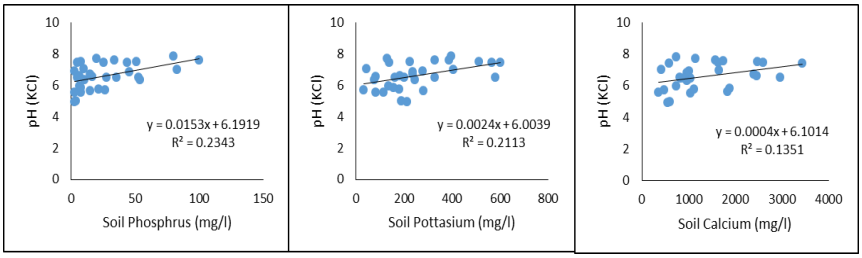


Figure 5. *Correlation and linear relationship analysis of soil pH and other physical properties under moringa tree canopy*

Table 3. *Effect of soil textural class on physical and chemical properties of soil sampled under moringa trees at different locations in Limpopo Province*

Treatment	Soil Chemical properties					
	Soil N (%)	Soil P (mg/L)	Soil K (mg/L)	Soil Ca (mg/L)	pH (KCl)	Soil Org C (%)
Clay	0.15^{a}	26.00 ^{b}	566.00^{a}	3442.0^{a}	7.44^{a}	1.70$^{a\ b}$
Clay Loam	0.13^{a}	44.00^{a}	340.00^{ab}	1751.5 ^{b}	6.75^{a}	2.06^{a}
Sandy Clay Loam	0.08 ^{b}	18.75^{c}	286.63^{ab}	1744.3 ^{b}	6.69^{a}	1.12 ^{bc}
Sandy Clay	0.06 ^{b}	6.66 ^{d}	222.40 ^{b}	1139.3 ^{bc}	6.21^{a}	1.06^{bcd}
Sandy Loam	0.06 ^{b}	28.00^{ab}	149.00 ^{b}	1132.4 ^{bc}	6.51^{a}	0.82 ^{cd}
Loamy Sand	0.04 ^{b}	37.50^{a}	204.33 ^{b}	755.33 ^{c}	6.62^{a}	0.61 ^{d}
$LSD_{0.05}$	0.07	25.34	146	646.27	--	0.39
Significance	***	**	**	***	ns	***

Significance levels: *P < 0.05, **P < 0.01, ***P < 0.001, ns means not significant

http://www.aloki.hu ● ISSN 1589 1623 (Print) ● ISSN1785 0037 (Online)
DOI: http://dx.doi.org/10.15666/aeer/1902_953970
© 2021, ALÖKI Kft., Budapest, Hungary

Findings from the study further revealed that soil textural classes containing higher clay content under the moringa tree had a more positive influence on other soil chemical properties as compared to the control (*Fig. 6*). High clay content had a significant influence on soil phosphorus, potassium, calcium, potassium and organic carbon (*Fig. 6*). Gravimetric soil moisture was relatively low (<10%) across all soil textural classes. However, the soil moisture was significantly higher under the moringa tree as compared to the control. Gravimetric soil moisture ranged between 4 – 8.3% under moringa canopies and from 2.5-7.8 under the control (*Fig. 7*).

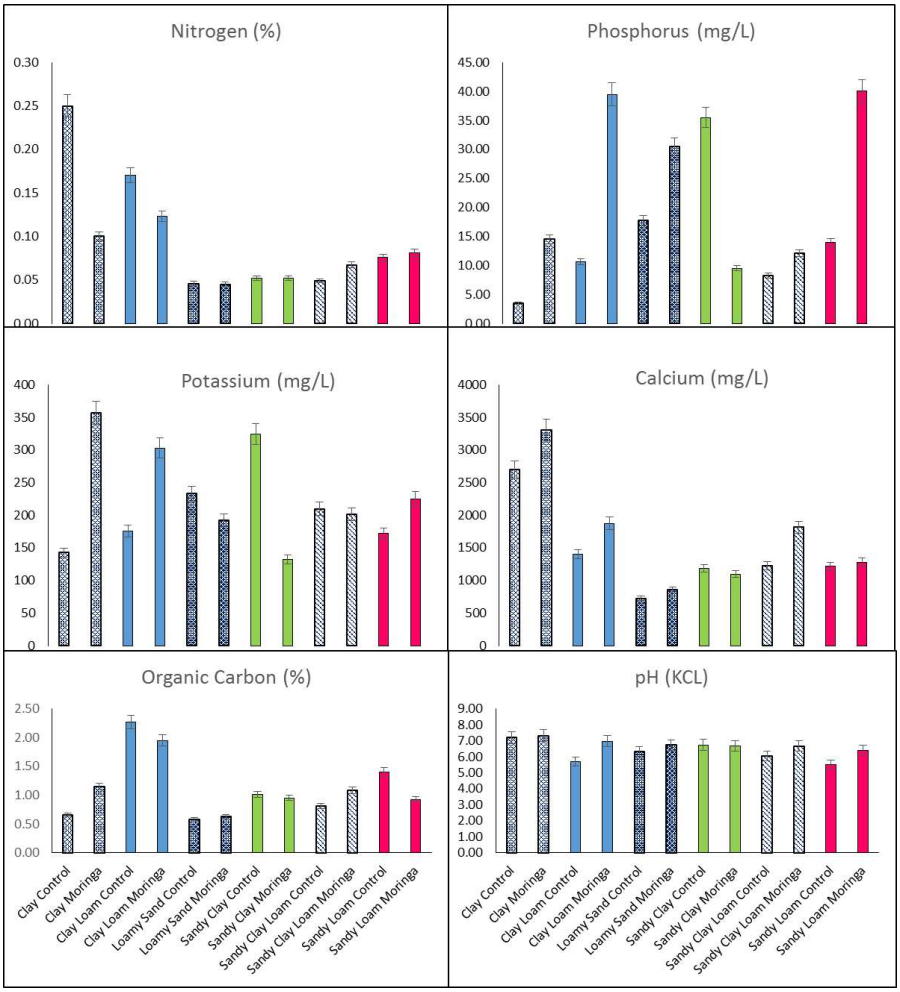


Figure 6. *Textural classes and chemical properties of soils sampled under moringa trees and control (5 m away) at different locations in Limpopo Province*

Findings from this study showed that soil textural classes did not significantly affect the nutritional composition of moringa leaves. Across the various textural classes, leaf nutritional composition was however within levels required to meet dietary requirements for both humans and livestock (*Table 4*). An assessment of association test among the nutritional parameters studied showed a positive linear regression between leaf phosphorus content and leaf nitrogen (0.39**) and that of leaf protein (0.32**) content (*Fig. 8*).

http://www.aloki.hu ● ISSN 1589 1623 (Print) ● ISSN1785 0037 (Online)
DOI: http://dx.doi.org/10.15666/aeer/1902_953970
© 2021, ALÖKI Kft., Budapest, Hungary

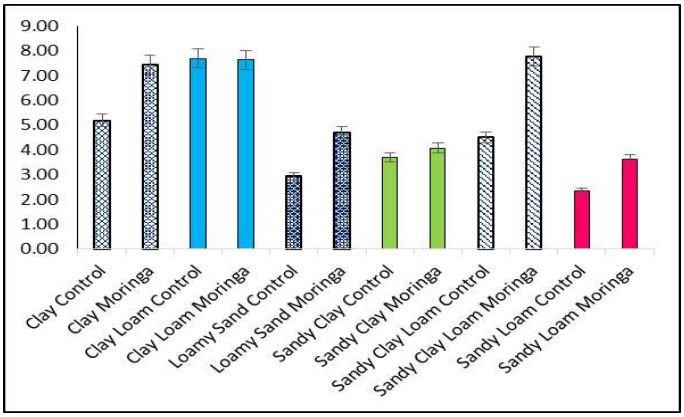


Figure 7. *Textural classes and gravimetric moisture (%) of soils sampled under moringa trees and control (5 m away) at different locations in Limpopo Province*

Table 4. *Effect of soil textural class on the nutritional composition of moringa leaf powder obtained from different locations in Limpopo Province*

Treatment	Leaf N (%)	Crude Protein (%)	Leaf Ca (%)	Leaf P (%)	Leaf Fe (mg/kg)
Clay	5.31[a]	33.20[a]	2.68[a]	0.27[a]	144.00[a]
Clay Loam	3.99[a]	26.38[a]	1.64[a]	0.21[a]	174.00[a]
Sandy Clay Loam	4.70[a]	29.42[a]	2.21[a]	0.23[a]	164.63[a]
Sandy Clay	4.60[a]	28.76[a]	2.60[a]	0.21[a]	163.67[a]
Sandy Loam	4.68a	29.28[a]	2.26[a]	0.23[a]	151.90[a]
Loamy Sand	5.21[a]	31.55[a]	1.99[a]	0.28[a]	167.00[a]
$LSD_{0.05}$	--	--	--	--	--
Significance	ns	ns	ns	ns	ns

Significance levels: ns means none significance

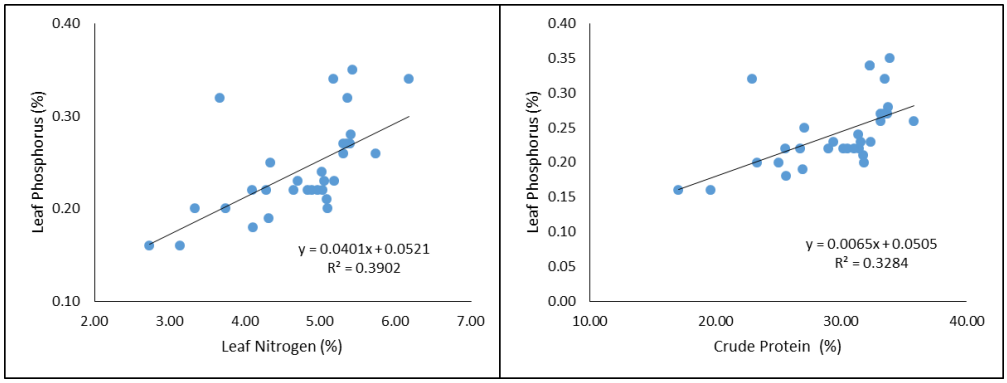


Figure 8. *Regression and linear relationships analysis of moringa leaf phosphorus, nitrogen, and crude protein*

Analysis among soil nutrient ions revealed several significant positive correlations extending to the following: nitrogen and calcium (0.63***); nitrogen and organic carbon (0.86***), potassium and pH (0.46**); potassium and calcium (0.68***); calcium and pH (0.37*) and lastly calcium and organic carbon (0.56***) (*Table 5*). Gravimetric soil moisture did not correlate with any of the parameters measured whereas tree age only revealed a moderate positive correlation with phosphorous (0.52***) (*Table 5*).

http://www.aloki.hu ● ISSN 1589 1623 (Print) ● ISSN1785 0037 (Online)
DOI: http://dx.doi.org/10.15666/aeer/1902_953970
© 2021, ALÖKI Kft., Budapest, Hungary

Table 5. *Pearson's correlation between soil properties and moringa leaf nutritional composition obtained from different locations of the Limpopo Province*

	Gravimetric soil moisture (%)	Tree age (Yrs)	Soil N (%)	Soil P (mg/L)	Soil K (mg/L)	Soil Ca (mg/L)	pH (KCl)	Soil Org C (%)	Leaf N (%)	Crude Protein (%)	Leaf Ca (%)	Leaf P (%)
Gravimetric soil Moisture (%)	1											
Tree Age (Yrs)	-0.14±0.43 ns	1										
Soil N (%)	0.16±0.39ns	-0.14±0.45 ns	1									
Soil P (Mg/L)	-0.20±0.27 ns	0.52±0.00***	-0.09±0.65 ns	1								
Soil K (Mg/L)	-0.04±0.82 ns	0.19±0.31 ns	0.27±0.14 ns	0.45±0.01**	1							
Soil Ca (Mg/L)	0.29±0.11 ns	-0.03±0.89 ns	0.63±0.00***	0.03±0.88 ns	0.68±0.00 ***	1						
pH (KCL)	0.11±0.57 ns	0.27±0.15 ns	-0.04±0.85 ns	0.48±0.01**	0.46±0.01**	0.37±0.04 *	1					
Soil Org C (%)	0.28±0.13 ns	-0.06±0.74 ns	0.86±0.00***	-0.08±0.67 ns	0.27±0.14 ns	0.56±0.00***	-0.150.41 ns	1				
Leaf N (%)	-0.05±0.79 ns	0.09±0.64 ns	-0.12±0.51 ns	0.25±0.17 ns	0.33±0.07 ns	0.01±0.94 ns	0.160.39 ns	-0.22±0.23 ns	1			
Crude Protein (%)	-0.01±0.94 ns	0.11±0.56 ns	-0.03±0.89 ns	0.16±0.37 ns	0.33±0.07 ns	0.07±0.70 ns	0.070.72 ns	-0.14±0.44 ns	0.96±0.00***	1		
Leaf Ca (%)	0.23±0.21 ns	0.03±0.85 ns	-0.16±0.38	-0.05±0.79 ns	0.23±0.22 ns	0.24±0.19 ns	0.290.11 ns	-0.19±0.30 ns	0.11±0.56 ns	0.09±0.63 ns	1	
Leaf P (%)	-0.19±0.28 ns	0.09±0.61 ns	-0.03±0.86 ns	0.37±0.06 ns	0.24±0.19 ns	-0.04±0.84 ns	-0.02±0.93 ns	-0.14±0.47 ns	0.63±0.00***	0.57±0.00 ***	-0.04±0.84 ns	1
Leaf Fe (mg/kg)	-0.03±0.86 ns	0.07±0.69 ns	-0.02±0.92 ns	0.17±0.36 ns	0.16±0.39 ns	0.04±0.81 ns	0.21±0.26 ns	-0.09±0.60 ns	-0.25±0.17 ns	-0.25±0.17 ns	0.13±0.48 ns	-0.18±0.33 ns

Significance levels: *P < 0.05, **P < 0.01, ***P < 0.001, ns- not significant

http://www.aloki.hu ● ISSN 1589 1623 (Print) ● ISSN1785 0037 (Online)
DOI: http://dx.doi.org/10.15666/aeer/1902_953970
© 2021, ALÖKI Kft., Budapest, Hungary

Discussion

During the study period, Limpopo Province experienced high temperatures accompanied by erratic rainfall. The highest total rainfall received was approximately 200 mm throughout the season. This was probably due to El Niño effect which was associated with the dry summer season. El Niño is the below normal rainfall phenomenon with above normal temperatures which lead to devastating effect in the farming sector. A 92% chance of extreme El Niño conditions was predicted to occur in January 2016 (Mpheshea and Landman, 2017). This situation was experienced in many regions of Limpopo Province, including the areas where this study was conducted.

In most of the study areas, soil nitrogen content was generally observed to be low under both moringa trees and the control. The standard or critical soil test values in mg/kg reported in the literature are 20-30 (N), >15 (P), 80-200 (K), >2000 (Ca), >80 (Mg), >5 (Fe), 3-150 (Zn) and 50-1000 (Mn) (Havlin et al., 2013). Although nitrogen was relatively low, the presence of moringa trees and mainly those over 5 years showed a slightly improved in the nitrogen content in the soil. This improvement might be due to litter fall from moringa leaves. Nitrogen is required by plants for assimilation into protein, and these mainly occur in non-leguminous plant species. Many pasture plants and mature trees derive a large portion of nitrogen from litter and leaf fall (Peverill et al., 1999; Lamb et al., 2014). There are also climatic factors which affect the quantity of soil nitrogen and impact soil organic carbon, which influences soil total nitrogen content. Largely, rainfall and temperature control mineralization, immobilization, denitrification, and leaching of soil nitrogen (Peverill et al., 1999).

Large quantities of plant residues are retained in the soil by many crops, and recycling of nitrogen from these residues may add a large portion of nitrogen to the soil for the benefit of the subsequent crop. This was evident in moringa, whereby younger trees utilized more nitrogen but within the older plants, the nitrogen concentration was relatively higher especially in the clay-dominated soils. Soils in this study were generally low in nitrogen content, however, on relative terms; the N content of the soils under moringa canopy was slightly higher. The slight increase could be due to low rainfall that affected the decomposition of organic matter in some moringa production areas. Similarly, soil phosphorus concentration was generally low but an increase of 65% was observed under moringa tree species as compared to the control. From the current study, phosphorus was below the recommended rate of more than 10-20 mg/kg (Peverill et al., 1999; Havlin et al., 2013), in some locations.

Results from the current study showed that potassium and calcium were not limiting nutrients for plant growth in all the study locations. The recommended soil potassium and calcium are reported to be 120-200 mg/kg and 600 – 4000 mg/kg (Peverill et al., 1999). Calcium concentration increases when the soil pH becomes neutral or alkaline. Furthermore, an increase in potassium by 71% was observed under moringa canopy as compared to the control across all locations. These results are in agreement with findings by Singh et al. (2012) who reported highest available phosphorus, potassium and calcium under plantations of Ber (*Ziziphus mauritiana* Lamk), moringa (*Moringa olerifera* Lam), Karonda (*Carissa congesta* Wt.) and Khejri (*Prosopis cineraria* L. Druce) tree species as compared to control soil. The presence of root hairs increases the absorption of P in many plant species and also deeper root system which could absorb the nutrients at some depth and deposited at the surface.

http://www.aloki.hu ● ISSN 1589 1623 (Print) ● ISSN1785 0037 (Online)
DOI: http://dx.doi.org/10.15666/aeer/1902_953970
© 2021, ALÖKI Kft., Budapest, Hungary

Furthermore, it is reported that most terrestrial plants have a symbiosis with arbuscular mycorrhizal (AM) fungi and such colonization has been reported in moringa, where it increases the surface area for P absorption (Peverill et al., 1999; Yamato et al., 2009; Cosme et al., 2014). On the other hand, the fungus has the ability to absorb P from soil solutions with very low P concentration, thus effectively supplementing the amount of accessible phosphorus to the plant root system (Peverill et al., 1999). The presence of AM fungi mainly in areas with low soil moisture assists in alleviating the problems of reduced mineralization, poor uptake of nutrients and failure of the crop (Muthukumar et al., 2006; Yamato et al., 2009).

Soil pH under moringa canopy was variable, ranging from moderate to slightly acidic as well as slightly to moderately alkaline, all of which favour the growth of moringa plant. Generally, the pH was also slightly improved under moringa trees as compared to the control. A soil pH range of 5.0-6.5 is reported to be optimal for growth of most crop species as it increases the availability of calcium element until a pH concentration of 8 (Peverill et al., 1999). From the current study soils under moringa had a good pH level which does not affect nutrient uptake by the tree. Litterfall in moringa assists in pH balancing for ease of nutrient uptake (Singh et al., 2012; Dunsin and Odeghe, 2015).

Over 52 percent of the locations under moringa canopy had a satisfactorily organic carbon content which was above 1 percent at the upper 0-30 cm depth as compared to the control. A commendable increase was observed from the trees that were more than 5 years old and with high soil clay content (*Table 2*). According to Peverill et al. (1999), under relatively low rainfall condition and for soils intended for crop production**,** soil organic carbon is classified to be low, normal and high when the value is <0.9%, 0.9 to 1.45% and >1.45%, respectively. When the field is intended for pasture production, the values are considered to be low, normal and high when they are <1.74%; 1.74 to 2.62% and >2.62%. Typically, the amount of organic carbon is reduced with increasing soil depth. Similar results were reported by Peverill et al. (1999), who indicated that soil organic carbon is higher at the soil surface and decreases exponentially with depth.

At all locations where data was collected, farmers rely on rainfall for crop water needs. During the study period, many locations of the Limpopo Province experienced drought which affected the production of agricultural crops. During the study, it was found that the rainfall was less than 210 mm with a maximum temperature of above 30ºC at all locations (*Fig. 1*). This might have affected nutrient uptake mainly in soils with a high percentage of sand due to high infiltration rate. The soils which are low in potassium are likely to be light textured in the areas receiving high rainfall of more than 600 mm annually (Singh et al., 2012).

The low rainfall received during the study period might have also affected microbial activities and led to slow release of nutrients by the plants. The change in organic carbon% was mainly observed from locations where the soil had some clay in their textural classes, displayed reasonable water holding capacity and the trees were more than 5 years of age. Singh et al. (2012) reported that favourable soil and moisture condition improved the organic carbon of moringa by up to 0.13% compared to control soil with an organic carbon content of 0.04%. Under conditions where warm temperatures prevail, there is a decrease in soil organic carbon due to increased decomposition rate by soil microorganisms (USDA-NRCS, 2009).

Peverill et al. (1999) further reported that factors such as topography, climatic conditions, soil texture and moisture content affect the amount of organic carbon present in the soil. Usually, a steep slope has higher soil organic matter content because of the

http://www.aloki.hu ● ISSN 1589 1623 (Print) ● ISSN1785 0037 (Online)
DOI: http://dx.doi.org/10.15666/aeer/1902_953970
© 2021, ALÖKI Kft., Budapest, Hungary

deposition of organic debris that dominates in clay soils, wetter environments, and finely textured soils. Soil organic carbon serves as the energy source for soil micro-organisms and therefore improves the stability of the soil aggregates. In general soil organic carbon is considered to be low, moderate and high for various soil textural classes. For example, values for different soil types are as follows: sand (<0.5, 0.5-1 and >1%), sandy loam (<0.7, 0.7-1.4 and >1.4%), clay loam or clay (<1.2, 1.2-2 and >2%); these findings were reported by Peverill et al. (1999). The higher gravimetric soil moisture under moringa canopies relative to the control in some of the study locations might be due to litter fall, which covered the soil and possibly reduced the rate of evaporation. However, gravimetric soil moisture was relatively low; this might be due to drought and scanty rainfall received during the season. These findings are in par with Yamato et al. (2009), who reported a soil water content of less than 5%, although the study was conducted during the rainy season. This was attributed to high temperature which accelerated drought.

No significant differences were found when correlating moringa leaf powder nutritional content and soil properties. The non-significant results on leaf nutritional composition found in this study agrees with the general findings that moringa can be produced under adverse environmental conditions without compromising the leaf nutritional quality. Studies by Anwar et al. (2007) and Kumssa et al. (2017) reported similar findings showing that moringa grows well under different conditions such as the humid tropics or hot dry environments as well as low fertility environments. The tree also survives in less fertile soils and is rarely affected by drought (Morton, 1991; Anwar et al., 2007). A study by Lamidi et al. (2017), reported that crude protein was not significantly influenced by harvesting locations ranging from 23.9 to 27.6%. Another study revealed that agro-ecological conditions have no significant effect on the level of moringa leaf nutrients (Asante et al., 2014).

The study that was conducted evaluating eleven leaf samples of moringa from various locations in Thailand reported protein content ranging between 19.15-28.80 (Jongrungruangchok et al., 2010), which was relatively low as compared to protein content found in leaves used in the current study which ranged between 26.38 – 33.20%. Higher concentration of Ca and Mg (3.65 and 0.75 mg/mL) were reported by Anjorin et al. (2010), however, in contrary, their study showed that mineral content in moringa leaves differed significantly with locations.

The concentrated amount of nitrogen, calcium, and phosphorus in the leaves are sufficient, rendering the leaf as a suitable material to be considered in biofertilizer production for soil fertility management and improved crop production (Adiaha, 2017; Mokgophi, 2017). The green leaves are nutritionally rich and can be used as green manure for soil fertility improvement (Mridha, 2015). Moringa leaves can serve as an alternative source of organic matter and calcium or replacement of expensive inorganic fertilizers which majority of smallholder farmers are unable to afford, including facilitating of soil pH and nutrients release for subsequent plant growth (Undie et al., 2013). The leaves improve soil concentration of N, K, Ca and organic carbon (Undie et al., 2013; Adiaha, 2017). A study conducted under two agro ecological conditions of South Africa also revealed that dried moringa leaves assist to concentrate the high nutrient content of moringa leaves (Moyo et al., 2011), as such it can be used during the time of drought when there is scarcity of food (Thurber and Fahey, 2009; Lamidi et al., 2017). Pakade et al. (2013) recommended that the high levels of trace elements found in moringa are safe

http://www.aloki.hu ● ISSN 1589 1623 (Print) ● ISSN1785 0037 (Online)
DOI: http://dx.doi.org/10.15666/aeer/1902_953970
© 2021, ALÖKI Kft., Budapest, Hungary

for human consumption and the leaves contain a substantial amount of flavonols which make the tree to be a natural antioxidant.

Conclusion

This study revealed that moringa can grow under soils with diverse textural classes. The tree showed a capability to recycle soil nutrients and improve soil fertility. Soil phosphorus was found to increase under older trees, indicating the potential of moringa to enhance phosphorus nutrition on marginal soils. In general, under many instances, improvement in soil pH and other soil nutrient elements such as calcium and potassium was observed across the study locations. Also, soil organic carbon showed slight increase mainly under older trees. Under the situation where a large portion of the leaves are not harvested for processing, the leaves are allowed to drop on the soil surface and decompose to improve soil structure and mineral elements. This was predominant in soils with high clay content and with older trees that are more than three years of age. Moringa has the potential to contribute towards human and livestock dietary needs and foster rural development, due to its considerable benefits. It is therefore recommended that, the tree should be introduced to other parts of South Africa, for reduction of malnutrition to the vulnerable communities.

Acknowledgements. This project was funded by NRF-Thuthuka; NRF-RVSC; VLIR-IUC-University of Limpopo. To the farmers who grow moringa in the Limpopo Province for allowing samples collection in their fields.

REFERENCES

[1] Adiaha, M. S. (2017): Potential of *Moringa oleifera* as a nutrient–agent for biofertilizer production. – World News of Natural Sciences 10: 101-104.

[2] Amaglo, N. (2006): How to Produce Moringa Leaves Efficiently? – In: Workshop on Moringa and other highly nutritious plant resources: Strategies, standards, and markets for a better impact on nutrition in Africa (Vol. 2). Accra, Ghana, November 16-18.

[3] Anjorin, T. S., Ikokoh, P., Okolo, S. (2010): Mineral composition of *Moringa oleifera* leaves, pods, and seeds from two regions in Abuja, Nigeria. – International Journal of Agriculture and Biology 12: 431-434.

[4] Anwar, F., Latif, S., Ashraf, M., Gilani, A. H. (2007): *Moringa oleifera*: a food plant with multiple medicinal uses. – Phytotherapy Research 21: 17-25.

[5] AOAC. (1990): Official Methods of Analysis. Association of Official Analytical Chemists. – 15th edition, Helrick, K. (ed.), Arlington.

[6] Asante, W. J., Nasare, I. L., Tom-Dery, D., Ochire-Boadu, K., Kentil, K. B. (2014): Nutrient composition of *Moringa oleifera* leaves from two agro-ecological zones in Ghana. – African Journal of Plant Science 8: 65-71.

[7] Ashfaq, M., Basra, S. M., Ashfaq, U. (2012): Moringa: A miracle plant for agro-forestry. – Journal of Agriculture and Social Sciences 8: 115-122.

[8] Black, C. A. (1965): Methods of Soil Analysis. Part 1 Physical and mineralogical properties. – American Society of Agronomy, Madison, Wisconsin, USA.

[9] Cosme, M., Franken, P., Mewis, I., Baldermann, S., Wurst, S. (2014): Arbuscular mycorrhizal fungi affect glucosinolate and mineral element composition in leaves of *Moringa oleifera*. – Mycorrhiza 24: 565-570.

http://www.aloki.hu ● ISSN 1589 1623 (Print) ● ISSN1785 0037 (Online)
DOI: http://dx.doi.org/10.15666/aeer/1902_953970
© 2021, ALÖKI Kft., Budapest, Hungary

[10] Dunsin, O., Odeghe, T. O. (2015): Response of sweet bell pepper to moringa leaf extract and organo-bio degradable fertilizer. – Asian Journal of Agriculture and Biology 3: 117-123.
[11] Fahey, J. W. (2005): *Moringa oleifera*: A review of the medical evidence for its nutritional, therapeutic, and prophylactic properties. Part 1. – Trees for Life Journal 1: 5.
[12] Gaines, T. P., Mitchell, G. A. (1979): Boron determination in plant tissue by the azomethine H method. – Communications in Soil Science and Plant Analysis 10: 1099-1108.
[13] Gandji, K., Chadare, F. J., Idohou, R., Salako, V. K., Assogbadjo, A. E., Kakaï, R. G. (2018): Status and utilization of *Moringa oleifera* Lam: A review. – African Crop Science Journal 26: 137-156.
[14] Havlin, J. L., Tisdale, S. L., Nelson, W. L., Beaton, J. D. (2013): Soil fertility and fertilisers. – 8th ed. Upper Saddle River, Prentice Hall, 528.
[15] Jongrungruangchok, S., Bunrathep, S., Songsak, T. (2010): Nutrients and minerals content of eleven different samples of *Moringa oleifera* cultivated in Thailand. – Journal of Health Research 24: 123-127.
[16] Kumssa, D. B., Joy, E. J., Young, S. D., Odee, D. W., Ander, E. L., Magare, C., Gitu, J., Broadley, M. R. (2017): Challenges and opportunities for moringa growers in southern Ethiopia and Kenya. – PloS one 12: e0187651.
[17] Lamb, J. A., Fernandez, F. G., Kaiser, D. E. (2014): Understanding nitrogen in soils. – University of Minnesota Extension (Revised), pp. 1-5.
[18] Lamidi, W. A., Murtadha, M. A., Ojo, D. O. (2017): Effects of planting locations on the proximate compositions of *Moringa oleifera* leaves. – Journal of Applied Sciences and Environmental Management 21: 331-338.
[19] Lekgau, J. (2011): *Moringa oleifera:* A Tree Giving Life to Rural Communities. – National Agricultural Marketing Council, USA.
[20] Leone, A., Spada, A., Battezzati, A., Schiraldi, A., Aristil, J., Bertoli, S. (2016): *Moringa oleifera* seeds and oil: characteristics and uses for human health. – International journal of Molecular Sciences 17: 2141.
[21] Mabapa, M. P., Ayisi, K. K., Mariga, I. K., Mohlabi, R. C., Chuene, R. S. (2017): Production and utilization of moringa by farmers in Limpopo Province, South Africa. – International Journal of Agricultural Research 12: 160-171.
[22] Manson, A. D., Roberts, V. G. (2000): Analytical Methods Used by the Soil Fertility and Analytical Services Section. – KZN Agri-Report No. N/A/2001/04. KwaZulu-Natal Department of Agriculture and Environmental Affairs, Pietermaritzburg, South Africa.
[23] Mokgophi, M. M. (2017): Characterisation of vermicomposts and leachate of agroforestry species: C*hamaecytisus tagasaste*, M*oringa oleifera* and *Vachellia karroo* and their potential as soil fertility amendment. – MSc Dissertation, University of Limpopo, 43p.
[24] Morton, J. F. (1991): The horseradish tree, *Moringa pterygosperma* (Moringaceae) - A boon to arid lands? – Economic Botany 45: 318-333.
[25] Moyo, B., Masika, P. J., Hugo, A., Muchenje, V. (2011): Nutritional characterization of *Moringa oleifera* Lam leaves. – African Journal of Biotechnology 10: 12925-12933.
[26] Mpheshea, L. E., Landman, W. A. (2016): Predicting the extreme 2015/16 El Niño event. – available at: www.researchspace.csir.co.za.
[27] Mridha, M. A. U. (2015): Prospects of moringa cultivation in Saudi Arabia. – Journal of Applied Environmental and Biological Sciences 5: 39-46.
[28] Muthukumar, T., Senthilkumar, M., Rajangam, M., Udaiyan, K. (2006): Arbuscular mycorrhizal morphology and dark septate fungal associations in medicinal and aromatic plants of Western Ghats, Southern India. – Mycorrhiza 17: 11-24.
[29] Odee, D. (1998): Forest biotechnology research in drylands of Kenya: The development of Moringa species. – Dryland Biodiversity 2: 7-8.
[30] Oshunsanya, S. O., Fagbenro, J. A., Oyewo, T. O. (2015): Growth and mineral composition of *Moringa oleifera* seedlings as affected by soil texture under water stress conditions. – Journal of Applied Agricultural Research 7: 151-160.

http://www.aloki.hu ● ISSN 1589 1623 (Print) ● ISSN1785 0037 (Online)
DOI: http://dx.doi.org/10.15666/aeer/1902_953970
© 2021, ALÖKI Kft., Budapest, Hungary

[31] Pakade, V., Cukrowska, E., Chimuka, L. (2013): Metal and flavonol contents of *Moringa oleifera* grown in South Africa. – South African Journal of Science 109: 01-07.
[32] Peverill, K. I., Sparrow, L. A., Reuter, D. J. (1999): Soil analysis: an interpretation manual. – CSIRO publishing, Collingwood, Victoria. Australia. ISBN 0643 063 765.
[33] Saini, R. K., Sivanesan, I., Keum, Y. S. (2016): Phytochemicals of *Moringa oleifera*: A review of their nutritional, therapeutic and industrial significance. – Biotechnology 6: 203.
[34] Singh, I. S., Awasthi, O. P., Singh, R. S., More, T. A., Meena, S. R. (2012): Changes in soil properties under tree species. – Indian Journal of Agricultural Sciences 82: 146-151.
[35] Thurber, M. D., Fahey, J. W. (2009): Adoption of *Moringa oleifera* to combat under-nutrition viewed through the lens of the "Diffusion of Innovations" theory. – Ecology of Food and Nutrition 48: 212-225.
[36] Tshiala, F. M., Olwoch, J. M., Engelbrecht, F. A. (2011): Analysis of temperature trends over Limpopo Province, South Africa. – Journal of Geography and Geology 3: 13-19.
[37] Undie, U. L., Kekong, M. A., Ojikpong, T. (2013): Moringa (*Moringa oleifera* Lam.) leaves effect on soil pH and garden egg (*Solanum aethiopicum L.*) yield in two Nigeria agro-ecologies. – European Journal of Agriculture and Forestry Research 1: 17-25.
[38] USDA-Natural Resources Conservation Service. (2009): Soil Quality Indicators: Total organic carbon. – available at: https://www.nrcs.usda.gov.
[39] Yamato, M., Ikeda, S., Iwase, K. (2009): Community of arbuscular mycorrhizal fungi in drought-resistant plants, moringa spp., in semiarid regions in Madagascar and Uganda. – Mycoscience 50: 100-105.

http://www.aloki.hu ● ISSN 1589 1623 (Print) ● ISSN1785 0037 (Online)
DOI: http://dx.doi.org/10.15666/aeer/1902_953970
© 2021, ALÖKI Kft., Budapest, Hungary

EFFECT OF BIO-STIMULANTS (HUMIC ACID, SALICYLIC ACID AND CHITOSAN) ON ROSE PERIWINKLE (*CATHARANTHUS ROSEUS* L.)

NOFAL, E. M. S.[1] – MENESY FARDOUS, A.[1] – ABD EL-HADY, W. M.[2] – SHEHAB EL-DEEN EMAN, G.[2*]

[1]*Hort. Dept., Agric. Fac., Kafr El-Sheikh Univ., Kafr El-Sheikh, Egypt*

[2]*Ornamental Plants and Landscape Gardening Research Department, Horticulture Research Institute, Agriculture Research Center, Giza, Egypt*

**Corresponding author*
e-mail: shehabeldin.iman@yahoo.com

(Received 2nd Apr 2020; accepted 7th Oct 2020)

Abstract. The present research was conducted during two successive seasons of 2017 and 2018 at the green house of the Horticulture Research Station, Mansoura, Egypt (31°2'4" N - 31°23'42" E) to study the influence of some bio-stimulants (humic acid, salicylic acid and chitosan) on vegetative and rooting growth parameters as well as some chemical constituents of a local variety of Catharanthus roseus L. (Vinca rosae, G. Don) (Periwinkle). The treatments involved ten applications i.e. control treatment, humic acid at 2, 4 and 6 ml/l, salicylic acid at 100, 150 and 200 mg/l and chitosan at 100, 200 and 300 mg/l. They were performed six times at fortnightly intervals during the two growing seasons under greenhouse conditions (25 ± 1 °C and 40-50% R.H). The obtained results showed that all vegetative growth and root parameters, (plant height, branch No., leaf area, root length) and their fresh and dry weights were significantly increased due to the applied bio-stimulants when compared to control treatment. Likewise, the chemical constituents of chlorophyll a and b in the leaves as well as their N, P and K% and total alkaloids also experienced a gain. The best results were provided by chitosan treatments at the rates of 300 and 200 mg/l, followed by humic acid at 6 ml/l then salicylic acid at 200 mg/l.
Keywords: *bio-fertilizer, deacetylchitin, fulvic acid and antioxidant 2-hydroxybenzoic acid, periwinkle*

Introduction

Catharanthus roseus L. (*Vinca rosae* G. Don) from the family of Apocynaceae is native and endemic in Madagascar, other English terms occasionally used include, Cape periwinkle, rose periwinkle, rosy periwinkle and "old maid" periwinkle (*Fig. 1*). It has long been cultivated as a herbal medicine and ornamental annual summer plant in flower beds and flower border, as they can grow up to 1 m tall with oval to oblong leaves and while the flowers are creamy or pink with red center, the fruit is a pair of follicles. It is well known in folk medicine for the treatment of diabetes (Harridy, 1986) and for anti-cancer treatments (Nejat et al., 2015).

The bio-stimulants are a category of relatively new products of diverse formulations that positively affect plants vital processes (Calvo et al., 2014).

Humic substances are the most widely distributed organic products of biosynthesis on the face of earth, exceeding the amount of carbon contained in all living organisms by approximately one order of magnitude. The major functional groups of humic acid include carboxyl, phenolic hydroxyl, alcoholic hydroxyl, ketone and quinoid (Russo and Berlyn, 1990). The mechanism of humic acid in promoting plant growth is thought to be related to the increase in cell membrane permeability, oxygen uptake, respiration, photosynthesis, phosphorus uptake, and root cell elongation as plant growth factors proposed by many authors to explain the promotive effect of humic acid on such plant

http://www.aloki.hu ● ISSN 1589 1623 (Print) ● ISSN 1785 0037 (Online)
DOI: http://dx.doi.org/10.15666/aeer/1902_971980
© 2021, ALÖKI Kft., Budapest, Hungary

measurement (Cacco and Dell Agnolla, 1984 and Russo and Berlyn, 1990). In addition, humic acid has beneficial effects on soil structure, its chemical properties and its content of the available microrganisms that increase nutrient uptake and particularly important for transportation and availability of micronutrients (Bohme and Thi lua, 1997).



Figure 1. *Catharanthus roseus L.*

Salicylic acid is a phenolic phytohormone found in plants with the beneficial roles of stimulating photosynthesis, ion uptake and transport and as antioxidant against free radical ions to protect plant cell from damage. In addition, it regulates some aspects of disease resistance in plants (Volt et al., 2009).

Chitosan is a natural biopolymer of seed weed extract that stimulate nutrient's uptake, photosynthesis and increase chlorophyll content, increases the availability and uptake of water and nutrients and enzyme activities that influence plant growth and development (Guan et al., 2009), besides cell enlargement (Malekpoor et al., 2016 and Salahna et al., 2017).

Therefore, due to the economic importance of bio-stimulates, the present study was designed to find out the response of *Chatharanthus roseus* growth to different levels of humic acid, salicylic acid and chitosan.

http://www.aloki.hu ● ISSN 1589 1623 (Print) ● ISSN 1785 0037 (Online)
DOI: http://dx.doi.org/10.15666/aeer/1902_971980
© 2021, ALÖKI Kft., Budapest, Hungary

Materials and methods

The present experiments were conducted in the greenhouse of Horticulture Research Station at Mansoura (120 km at North of Nile Delta) (31°2'4" N - 31°23'42" E) Egypt during two successive seasons of 2017 and 2018 as the first season was replicated in the second one to refine the obtained results, which is a common procedure in Egypt. The aim was to detect the effect of different levels of some biostimulants on the vegetative and rooting growth of periwinkle besides its contents of some chemical constituents.

Seeds of a local variety of periwinkle blackish color with pyriform to obviate shape, were planted in trays (on March) and after one month the obtained transplants were transplanted in plastic pots of 8 cm diameter as one plant/pot filled with sand and silt at 1:1 (v/v). Two months later the plants, were transplanted in 25 cm diameter plastic pots of grey color and filled with the same soil mixture with the addition of monocalcium phosphate ($CaH_4P_2O_8$) at 50 mg/pot and disinfected with a local fungicide (No-Blight) and watered whenever needed.

Humic acid was added with irrigation water as preferable method for such compound at levels of 2, 4 and 6 ml/l. However, salicylic acid was foliar sprayed at 100, 150 and 200 mg/l while chitosan was foliar sprayed at 100, 200 and 300 mg/l. The foliar spraying was conducted to run off plants. This made 9 treatments in addition to the control treatment (check treatment) without any additions in a complete randomized design without interaction in 3 replicates (each replicate contained 10 plants).

At the end of every season (on November 5th) the following parameters were recorded: a) Vegetative growth (plant height (cm), No branches/plant, leaf area (cm^2) (calculated by CI-202 Portable Laser Leaf Area Meter (CID Bio-Science Made In USA) besides the fresh and dry weights of the aerial parts of the plant. b) Root length (cm) and the fresh and dry weights of the roots (g)/plant. c) Some chemical composition parameters of a certain leaf on the plant median part as (1) N% in the dried leaf according Chapman and Pratt (1978), (2) P% in the dried leaf by the method of A.O.A.C. (1980), (3) K% in the dried leaf according to Jackson (1973), (4) Chlorophyll a and b content in the fresh leaf (mg/g f.w.) according to Krishnan et al. (1996), (5) Total alkaloids % was done according to Masoud et al. (1968).

The experimental layout was split plot design. Statistical analysis: Data were statistically analyzed using analysis of variance (ANOVA) and the means of treatments were compared using L.S.D test at 5% (Steel and Torrie, 1980) with the statistical package program, SPSS.

Results

Vegetative growth parameters and fresh and dry weights of the aerial plant parts

Data presented in *Table 1* revealed that all bio-stimulant treatments significantly increased plant height, branch No/plant and leaf area over control. The significantly tallest plants resulted from the treatment of chitosan at either 200 or 300 ppm as there were non-significant differences in between in the two seasons. This was followed with significant differences by the treatment of humic acid at 6 ml/l then the treatment of salicylic acid at 200 mg/l. A somewhat similar trend was obtained for branch No/plant with exception for the treatment of 300 ppm chitosan which gave significantly higher values than the control in both seasons.

http://www.aloki.hu ● ISSN 1589 1623 (Print) ● ISSN 1785 0037 (Online)
DOI: http://dx.doi.org/10.15666/aeer/1902_971980
© 2021, ALÖKI Kft., Budapest, Hungary

For leaf area the significantly highest records were obtained from the treatment of 300 ppm chitosan followed with chitosan treatment at 200 ppm with significant differences in between in the first season while one the differences were insignificant in the second. Other biostimulant treatments gave significantly less values in this concern.

Table 1. *Effect of humic acid, salicylic acid and chitosan on some vegetative growth parameters and fresh and dry weight of plants in two seasons of Periwinkle*

Treatments	Plant height (cm)	No. of branches/plant	Fresh weight of aerial plants parts (g)	Dry weight parts/plant (g)	Leaf area (cm^2)
First season (2017)					
Control	22.52h	4.33g	11.98g	2.09g	11.25j
Humic acid 2 ml/l	26.62f	6.67f	14.55f	2.69ef	13.24h
Humic acid 4 ml/l	31.34d	8.00de	17.45de	3.45cd	14.64f
Humic acid 6 ml/l	37.64b	9.67bc	21.37b	4.54b	17.12c
Salicylic acid 100 mg/l	24.55g	5.00g	13.16fg	2.39fg	12.72i
Salicylic acid 150 mg/l	29.12e	7.00ef	16.28e	3.11de	14.03g
Salicylic acid 200 mg/l	35.29c	8.67cd	20.38bc	4.40b	16.26d
Chitosan 100 mg/l	33.51c	8.33d	18.96cd	3.73c	15.32e
Chitosan 200 mg/l	40.50a	10.33b	23.50a	4.70ab	18.16b
Chitosan 300 mg/l	41.91a	12.00a	24.52a	5.15a	18.95a
LSD 5%	1.85	1.32	1.66	0.51	0.17
Second season (2018)					
Control	24.32f	5.67f	12.70g	2.31g	11.19g
Humic acid 2 ml/l	28.18e	7.67e	16.65f	2.88ef	13.71f
Humic acid 4 ml/l	33.15d	9.00d	18.67de	3.69cd	15.12e
Humic acid 6 ml/l	40.39b	10.33c	22.31b	4.81ab	17.84b
Salicylic acid 100 mg/l	25.94f	6.00f	14.15fg	2.56fg	13.09f
Salicylic acid 150 mg/l	31.19d	8.67de	17.45e	3.33de	14.63e
Salicylic acid 200 mg/l	37.34c	10.33c	21.70bc	4.68b	17.18c
Chitosan 100 mg/l	35.47c	9.33cd	20.30cd	4.06c	16.05d
Chitosan 200 mg/l	43.33a	11.67b	24.94a	4.90ab	19.08a
Chitosan 300 mg/l	44.37a	14.00a	26.65a	5.23a	19.64a
LSD 5%	1.98	1.24	1.73	0.51	0.64

For fresh and dry weights of the aerial plant parts, all biostimulant treatments gave significantly heavier weights than control in both seasons. The significantly heaviest values resulted from the treatments of 200 and 300 ppm chitosan in both seasons without significant differences in between. This was followed by other bio-stimulant treatments which recorded significantly less values. The significantly heaviest fresh and dry weights of the plant aerial parts due to bio-stimulant treatments are a reflection on their stimulatory effects of such compounds on the aforementioned vegetative growth parameters especially the treatments of chitosan at 200 and 300 ppm.

Length of the root, fresh and dry weights of the roots per plant

Data presented in *Table 2* showed that all bio-stimulant treatments gave significantly longer roots than control. The highest values with utmost significance resulted from the treatments of chitosan at 300 ppm followed by chitosan at 200 ppm with significant differences between them in the first season and non-significant differences in the second one.

The other bio-stimulant treatments gave significantly less values in most cases.

http://www.aloki.hu ● ISSN 1589 1623 (Print) ● ISSN 1785 0037 (Online)
DOI: http://dx.doi.org/10.15666/aeer/1902_971980
© 2021, ALÖKI Kft., Budapest, Hungary

For fresh and dry weights of roots per plant, data in the same table cleared that all treatments gave significantly heavier weights than the control in both seasons.

The significantly understanding values resulted from the treatment of chitosan at 300 ppm followed by chitosan at 200 ppm with non-significant differences in most cases between them except for the dry weight in the second season in the treatment of 300 ppm chitosan in the criterion of root dry weight per plant. These results are reflections of such aforementioned treatment effects on recording longer root.

Table 2. *Effect of humic acid, salicylic acid and chitosan on root and fresh and dry weights/plants of periwinkle during two seasons*

Treatments	Root length (cm)	Fresh weight of root (g)	Dry weight of root (g)
First season (2017)			
Control	16.19h	3.58f	0.65f
Humic acid 2 ml/l	18.51fg	4.70def	0.94e
Humic acid 4 ml/l	21.16e	5.53bcd	1.20d
Humic acid 6 ml/l	24.71bc	6.66ab	1.56b
Salicylic acid 100 mg/l	17.47gh	4.18ef	0.77f
Salicylic acid 150 mg/l	19.30f	5.38cde	1.07de
Salicylic acid 200 mg/l	23.52cd	6.50abc	1.46bc
Chitosan 100 mg/l	22.28de	5.69bcd	1.36c
Chitosan 200 mg/l	25.41b	7.41a	1.71a
Chitosan 300 mg/l	27.51a	7.52a	1.84a
LSD 5%	1.81	1.26	0.14
Second season (2018)			
Control	17.13h	3.75f	0.69i
Humic acid 2 ml/l	19.55fg	4.95def	1.00gh
Humic acid 4 ml/l	22.17de	5.83bcd	1.29ef
Humic acid 6 ml/l	26.01b	7.08ab	1.66bc
Salicylic acid 100 mg/l	18.03gh	4.44ef	0.85h
Salicylic acid 150 mg/l	20.30ef	5.66cde	1.13fg
Salicylic acid 200 mg/l	24.59bc	6.48bc	1.54cd
Chitosan 100 mg/l	23.45cd	6.10bcd	1.43de
Chitosan 200 mg/l	26.49b	7.91a	1.78b
Chitosan 300 mg/l	28.73a	7.95a	1.97a
LSD 5%	1.91	1.36	0.15

Some chemical composition parameters

Leaf content of chlorophyll a and b

Data presented in *Table 3* showed that all bio-stimulant treatments significantly increased both chlorophyll a and b over control in the two seasons.

The significantly highest contents resulted from treatment of chitosan at 300 and 200 ppm with non-significant differences between them for chlorophyll (b) while there were significant results for chlorophyll (a). The other biostimulant treatments gave significantly less values in the majority of cases.

N, P and K% in the leaves

Presented data in *Table 4* revealed that all bio-stimulant treatments significantly increased N, P and K% in the leaves over control in the two seasons. The significantly

http://www.aloki.hu ● ISSN 1589 1623 (Print) ● ISSN 1785 0037 (Online)
DOI: http://dx.doi.org/10.15666/aeer/1902_971980
© 2021, ALÖKI Kft., Budapest, Hungary

highest percentages for the three mineral elements were recorded for the treatment of chitosan at 300 ppm followed by the treatment of chitosan at 200 ppm with significant differences in between in all cases. However, the remainder bio-stimulant treatments recorded significantly less values.

Table 3. *Effect of humic acid, salicylic acid and chitosan on the content of pigments (chlorophyll a and b) of periwinkle during two seasons*

Treatments	Chlorophyll a (mg/g f.w)	Chlorophyll b (mg/g f.w)
First season (2017)		
Control	0.397j	0.264i
Humic acid 2 ml/l	0.443h	0.298g
Humic acid 4 ml/l	0.487f	0.330e
Humic acid 6 ml/l	0.577c	0.383b
Salicylic acid 100 mg/l	0.414i	0.285h
Salicylic acid 150 mg/l	0.472g	0.317f
Salicylic acid 200 mg/l	0.537d	0.365c
Chitosan 100 mg/l	0.507e	0.343d
Chitosan 200 mg/l	0.607b	0.415a
Chitosan 300 mg/l	0.621a	0.412a
LSD 5%	0.012	0.006
Second season (2018)		
Control	0.412j	0.275i
Humic acid 2 ml/l	0.463h	0.312g
Humic acid 4 ml/l	0.511f	0.345e
Humic acid 6 ml/l	0.596c	0.404b
Salicylic acid 100 mg/l	0.436j	0.298h
Salicylic acid 150 mg/l	0.494g	0.333f
Salicylic acid 200 mg/l	0.563d	0.384c
Chitosan 100 mg/l	0.533e	0.360d
Chitosan 200 mg/l	0.638b	0.435a
Chitosan 300 mg/l	0.650a	0.429a
LSD 5%	0.007	0.007

Total alkaloid %

The effects of the different bio-stimulants (humic acid, salicylic acid and chitosan) on total alkaloids % of Periwinkle plant leaves are presented in *Table 4*. Data proved that adding the bio-substances to plants significantly increased total alkaloids % to the highest values for the treatments of chitosan at 300 mg and 200 mg/l, humic acid at 6 ml/l and salicylic acid at 200 mg/l for the 1st and 2nd seasons, respectively.

Discussion

The results revealed that all treatments increased and enhanced all vegetative growth parameters. These results are supported by El-Sayed et al. (2016) on *Cycas*, Gad et al. (2016) on *Ixora coccinea* and El-Khateeb et al. (2018) on *Spathiphyllum wallisii*.

The stimulatory effects of chitosan on the foregoing results may be due to stimulation of the availability and uptake of nutrients and water besides, the increase

http://www.aloki.hu ● ISSN 1589 1623 (Print) ● ISSN 1785 0037 (Online)
DOI: http://dx.doi.org/10.15666/aeer/1902_971980
© 2021, ALÖKI Kft., Budapest, Hungary

in enzyme activities required for producing the metabolites necessary for the plant growth and development.

Table 4. *Effect of humic acid, salicylic acid and chitosan on minerals NPK % and total alkaloid in the leaves of periwinkle during two seasons*

Treatments	N%	P%	K%	Total alkaloids (mg/g d.w.)
First season (2017)				
Control	1.37i	0.227j	1.65j	0.097h
Humic acid 2 ml/l	1.64g	0.254h	1.93h	0.112f
Humic acid 4 ml/l	1.80e	0.282f	2.22f	0.126e
Humic acid 6 ml/l	2.11b	0.324c	2.77c	0.148b
Salicylic acid 100 mg/l	1.52h	0.243i	1.76i	0.103g
Salicylic acid 150 mg/l	1.72f	0.272g	2.11g	0.123e
Salicylic acid 200 mg/l	2.00c	0.312d	2.60d	0.142c
Chitosan 100 mg/l	1.92d	0.293e	2.41e	0.135d
Chitosan 200 mg/l	2.16b	0.347b	2.95b	0.153b
Chitosan 300 mg/l	2.23a	0.363a	3.05a	0.164a
LSD 5%	0.04	0.006	0.05	0.005
Second season (2018)				
Control	1.44i	0.236j	1.74j	0.101g
Humic acid 2 ml/l	1.73g	0.266h	2.03h	0.117f
Humic acid 4 ml/l	1.87e	0.295f	2.32f	0.132e
Humic acid 6 ml/l	2.23b	0.337c	2.88c	0.155b
Salicylic acid 100 mg/l	1.59h	0.254i	1.84i	0.107g
Salicylic acid 150 mg/l	1.79f	0.286g	2.19g	0.129e
Salicylic acid 200 mg/l	2.09c	0.326d	2.74d	0.149c
Chitosan 100 mg/l	2.00d	0.306e	2.55e	0.142d
Chitosan 200 mg/l	2.26b	0.361b	3.09a	0.160b
Chitosan 300 mg/l	2.34a	0.379a	3.20a	0.173a
LSD 5%	0.05	0.006	0.06	0.006

Humic acid increases cell membrane permeability, oxygen uptake, respiration and nutrients uptake by plants which reflect on producing healthy plants.

Likewise, are the stimulatory effects of salicylic acid on plant growth and development. This is supported by other researchers as Malekpoor et al. (2016) on *Ixora collinear* and Salachna et al. (2017) on *Verbena bonariensis*.

All treatments increased the averages of root length, fresh and dry weights of roots. These results are in agreement with El-Khateeb et al. (2010) on *Calia secundiflora* plants who found that humic acid at 1% increased root length, fresh and dry weight of root. Also El-Khateeb et al. (2018) on *Spathiphyllum wallisii* plants stated that the foliar application of both humic acid at 1 ml/l and chitosan at 0.1 g/l were the best treatments for increasing the root length. The stimulatory effects of chitosan on root growth may be due to its stimulatory influences on uptake and availability of nutrients to give healthy plants. For humic acid, it promotes root growth via improving better structure of soil texture and increasing soil microorganisms, cell enlargement and water status necessary for vigorous root growth according to Malekpoor et al. (2016). This is supported by the findings of Basil and Salachna et al. (2017) on *Verbena bonariensis* concerning chitosan.

http://www.aloki.hu ● ISSN 1589 1623 (Print) ● ISSN 1785 0037 (Online)
DOI: http://dx.doi.org/10.15666/aeer/1902_971980
© 2021, ALÖKI Kft., Budapest, Hungary

The chlorophyll a and b content increased by all treatments due to bio-stimulant treatment application is attributed to their promotive effect on photosynthesis and cell enlargement and especially foliar spraying chitosan which enhances the uptake of nutrients necessary for such process. In this concern, Hadrami et al. (2010) and Hadwiger (2013) stated that chitosan has been recognized as a product to enhance crop production due to its bioactivities, biodegradability growth stimulation and seed germination, increasing nutrients uptake, reducing oxidative stress, increasing photosynthesis, chlorophyll content and chloroplast enlargement in the leaves. The obtained results are supported with those of Castro et al. (2016) on cariader, Madhavi (2013) on isabgol and Boogar et al. (2014) on *Petunia hybrid.*

All bio-stimulant treatments rose N, P and K% in the leaves over control in the two seasons.

The explanation in these criteria lies in the fact that all bio-stimulants induce plant uptake for nutrients necessary for plant growth and development accompanied with the enhancement of those enzyme activities responsible for vigorous growth of the plants as previously mentioned. The superiority for chitosan may be due to its role in the enhancement of nutrients uptake, reducing oxidative stress and its antifungal, antiviral and antibacterial properties as mentioned by Hadrami et al. (2010) and Hadwiger (2013).

Similar results were obtained by Kim et al. (2005) on basil, Nasiroleslami and Safaridolatabad (2014) on dill plants and Boshra A. El-Sayed et al. (2016) on *Cycas* plant.

The treatments gave significant increment in total alkaloids %. *Catharanthus roseus* plant contains 130 bioactive terpenoid indole alkaloids, among which vinblastine and vincristine are regarded as the most important (Nejat et al., 2015). The above results are in agreement with those obtained by Qifang et al. (2010) who stated that salicylic acid treatment resulted in a significant increase of vinblastine, vindoline and catharanthrine of Periwinkle plants. Also Idrees et al. (2011) found that, total alkaloids content was improved by salicylic acid application in Periwinkle plants.

Conclusion

To obtain high quality plants with balanced chemical constituents and highest content of total alkaloids of periwinkle, the plants of 3 months old should be foliar sprayed with chitosan (a seaweed extract) at either 300 or 200 ppm (from the economic point of view) at fortnightly intervals commencing after two months from transplanting.

REFERENCES

[1] A. O. A. C. (1980): Official Methods of Analysis. 12th Ed. – Association of Official Analysis Chemists, Washington, DC.

[2] Bohme, M., Thi Lua, H. (1997): Influence of mineral and organic treatments in the rizosphere on the growth of tomato plants. – Acta Hortic 450: 161-168.

[3] Boogar, A. R., Shirmohammadi, E., Geikloo, A. (2014): effect of humic acid application qualitative characteristic and micronutrient status in *Petunia hybrid* L. – Bull. Env. Pharmacol. Life Sci. Col 3(9): 15-19.

[4] Cacco, G., Dell Agnolla, G. (1984): Plant regulator activity of soluble humic substances. – Can. J. Soil Sci. 64: 25-28.

[5] Calvo, P., Nelson, L., Kloepper, J. W. (2014): Agricultural uses of plant biostimulants. – Plant Soil. 383: 3-41. DOI: 10.1007/5 11104-014-2131-8.

http://www.aloki.hu ● ISSN 1589 1623 (Print) ● ISSN 1785 0037 (Online)
DOI: http://dx.doi.org/10.15666/aeer/1902_971980
© 2021, ALÖKI Kft., Budapest, Hungary

[6] Castro, Q. T., Avelelas, F. P., Leandro, S. (2016): Chitosan seed soaking: germination and growth of *coriandrum sativum* and *Solanum bycopersicum.* – Front. Mar. Sci. Conference Abstract, International Meeting on Marine Research, Peniche, Portugal. DOI: 10.3389/conf.
[7] Chapman, H. D., Pratt, P. F. (1978): Methods of Analysis for Soils, Plants and Waters. – Univ California Div. Agric. Sci, Oakland, pp. 12-19.
[8] El-Khateeb, M. A., Nasr, A. A., Fahmy, A. N., Dorgham, A. H. (2010): Effect of GA3 and growth bio-stimulants on growth and chemical composition of *Calia secundiflora* plants. – J. Horti. Sci. and Ornamental Plants 2(2): 118-124.
[9] El-Khateeb, M. A., El-Adaawy, A. E., Saber, A. A. (2018): Growth and quality of *Spathiphyllum wallisii* L. plants as affected by foliar sprays of algae, chitosan, atomic and humic acid. – Bio-Sci. Res. 15(2): 618-627.
[10] El-Sayed, B. A., Noor El-Deen, T. M., Abdel-Galeil, L. M., Aly, W. A. (2016): Effect of natural activator (BIOHORM) and humic acid on growth and quality of *Cycas* plant. – Scientific J. Flowers & Ornamental Plants 3(1): 79-86.
[11] Gad, M. M., Abdul-Hafeez, E. Y., Ibrahim, O. H. M. (2016): Foliar application of salicylic acid and gibberellic acid enhances growth and flowering of *Ixora coccinea* L. plants. – J. Plants Production, Mansoura Univ. 7(1): 85-91.
[12] Guan, Y., Jin, H., Xian, W., Chenia, W. (2009): Seed priming with chitosan improves maize germination and seedling growth in relation to physiological changes under low temperature stress. – J. Zhejiang Univ. Sci. 10: 427-433.
[13] Hadrami, A. E., Adam, L. R., Hadrami, I. E., Daayf, F. (2010): Chitosan in plant protection. – Mar. Drugsoy 8: 968-987.
[14] Hadwiger, L. A. (2013): Multiple effects of chitosan on plant system: solid science of hype. – Plant Sci. 20(8): 42-49.
[15] Harridy, M. A. I. (1986): Physiological studies on periwinkle plant *Catharanthus roseus* G. Don. – Ph. D. Thesis. Fac. Agric., Cairo University.
[16] Idrees, M., Naeem, M., Aftab, T., Khan, M., Moinuddin, M. A. (2011): Salicylic acid mitigates salinity stress by improving antioxidant defence system and enhances vincristine and vinblastine alkaloids production in periwinkle (*Catharanthus roseus*). – Acta Physiologiae Plantarum 33(3): 987-999.
[17] Jackson, M. L. (1973): Soil Chemical Analysis. – Prentice Hall of India Private Limited, New Delhi.
[18] Kim, H. J., Chen, F., Wang, X., Rajapakse, N. C. (2005): Effect of chitosan on the biological properties of sweet basil (*Ocimun basilicum* L.). – J. Agric. Food Chem. 53(9): 696-701.
[19] Krishnan, P., Ravi, I., Nayak, S. K. (1996): Methods for determining leaf chlorophyll content of rice: a reappraisal. – Ind. J. Experim. Bio. 34: 1030-1033.
[20] Mahdavi, B. (2013): Seed germination and growth responses of isabgol (*Plantago ovata* Forsok) to chitosan and salinity. – Inter. J. Agric. and Crop Sci. 5(10): 1084-1088.
[21] Malekpoor, F., Pirbalouti, A. G., Salami, A. (2016): Effect of foliar application of chitosan on morphological and physiological characteristics of basil under reduced irrigation. – Res. on Crops 17(2): 354-359.
[22] Masoud, A. N., Sciuchett, I. A., Farnsworth, N. R., Blomste, R. N., Meer, W. A. (1968): Effect of gibberellic acid on growth of *Catharanthus roseus.* – J. Pharm. Sci. 57: 589-593.
[23] Nasiroleslami, E., Safaridolatabad, S. (2014): The comparison of organic and biologic fertitilizers effects on growth and essential oil of dill (*Anthum gravcolens* L.). – Inter. J. Biosciences 5(7): 65-74.
[24] Nejate, N., Valdiani, A., Cahill, D., Tan, Y. H., Maziah, M., Abiri, R. (2015): Ornamental exterior versus therapeutic interior of Madagascar periwinkle (*Catharanthus roseus*): the two faces of a versatile herb. – The Scientific World Journal. DOI: 10.1155/2015/982412.

http://www.aloki.hu ● ISSN 1589 1623 (Print) ● ISSN 1785 0037 (Online)
DOI: http://dx.doi.org/10.15666/aeer/1902_971980
© 2021, ALÖKI Kft., Budapest, Hungary

[25] Qifang, P., Yu, C., Quan, W., Fang, Y., Shihai, X., YueSheng, T., JingYa, Z., Xiaofen, S., Kexuan, T. (2010): Effect of plant growth regulators on the biosynthesis of vinblastine, vindoline and catharanthine in *Catharanthus roseus*. – Plant Growth Regulation 60(2): 133-141.
[26] Russo, R. O., Berlyn, G. P. (1990): The use of organic bio-stimulants to help low input sustainable agriculture. – J. Sustain. Agric 1: 19-42.
[27] Salachna, P., Byczynska, A., Jezziorska, I., Udycz, E. (2017): Plant growth of *Verbena bonariensis* L. after chitosan gellan gum or iota carrageenan foliar application. – World Scientific News 62: 111-123.
[28] Steel, R. G. D., Torrie, J. H. (1980): Principles and Procedures of Statistics. – McGraw-Hill Book Co., Inc., New York, pp. 377-400.
[29] Volt, A. C., Dempsey, D. A., Klessing, D. F. (2009): Salicylic acid, a multifaceted hormone to combat disease. – Annual Review of Phytopathology 47: 177-206.

http://www.aloki.hu ● ISSN 1589 1623 (Print) ● ISSN 1785 0037 (Online)
DOI: http://dx.doi.org/10.15666/aeer/1902_971980
© 2021, ALÖKI Kft., Budapest, Hungary

EFFECT OF DIFFERENT SEED MOISTURE CONTENT AT HARVEST ON SOME MORPHOLOGICAL AND YIELD CHARACTERISTICS OF DIFFERENT RICE CULTIVARS (*ORYZA SATIVA* L.)

ABOUKHADRAH, S. H.[1] – MOHAMED, A. A. A.[1] – ELKHOBY, W.[2] – SHAHEN, F. F.[2*]

[1]*Agronomy Department, Fac. of Agric., Kafr-El-Sheikh Univ., Kafr-El-Sheikh, Egypt*

[2]*Rice Research & Training Center, Field Crop Research Institute, ARC, Giza, Egypt*

**Corresponding author*
e-mail: Shahin.fathy@yahoo.com

(Received 15th Apr 2020; accepted 7th Oct 2020)

Abstract. This experiment study the effects of different seed moisture contents (22, 20, 18, 16 and 14%) on some morphological and yield characters of some rice cultivars, Sakha 105, Sakha 106, Giza 179, Giza 178, Giza 182 and hybrid 2034. The moisture contents were assigned in main plot, while the rice cultivars were assigned in subplot, the main cultural practices were applied according to Rice Research &Training Center. The results showed that, the highest seed volume was recorded under the highest moisture content, but the lowest moisture content resulted in the lowest values for the remaining studied characters, on the other hand Sakha 106 was recorded to have the highest seed volume, plant height and 1000 grain weight, while, the Hybrid 2034 and Giza 178 were recorded the highest germination % and grain yield t/ha, which means the seeds should be died to 14% after harvesting and before storage to maintain the seed viability and increase the productivity. Finally, we concluded that, highest seed volume, plant height and 1000 grain weight was recorded in the case of Sakha 106, while the highest germination % and grain yield (t/ha) was recorded in the Hybrid 2034 and Giza 178, which means that the seeds should be dried to 14% moisture content after the harvested and before storage to maintain the seed viability and increase the productivity. Finally, the optimum date for harvesting rice cultivars under study should be determined.
Keywords: *rice varieties, grain weight and germination*

Introduction

Rice is the most important stable food for more than half of the world's population, mostly in the developing countries. It is ranked after wheat directly and after maize by two places among food crops in the world (Badawai, 2005). Human consumption accounts for 85% of total production for rice, compared with 72% for wheat and 19% for maize (Aidy et al., 2002). The total cultivated area in Egypt was 0.858 million fed. (3.603.600 m^2), and the total production was 1.32 million ton (RRTC, 2015). High quality seed produce high rice production**.** Seed of improved varieties can trigger change and help bring about agricultural production objectives. High quality seed lots may improve crop yield in two ways: first, because seedling emergence from the seedbed is rapid and uniform, leading to the production of vigorous plants, and second because the percentage of seedling emergence is high, so optimum plant population density could be achieved under a wide range of environmental condition. These are the main motivations for farmers, who are interested in buying and cultivating vigorous seeds, thus production of high-quality seeds is an important strategy for seed producers. Seed maturation is one of the main components of seed quality and a prerequisite for successful germination and emergence. The rice cultivars significantly differed in all studied traits; rice cultivar Giza 178 exceeded all cultivars in grain and straw yields as well as yield components as yielder

http://www.aloki.hu ● ISSN 1589 1623 (Print) ● ISSN 1785 0037 (Online)
DOI: http://dx.doi.org/10.15666/aeer/1902_981991
© 2021, ALÖKI Kft., Budapest, Hungary

cultivar under stress conditions (RRTC, 2015). The moisture content in rice seed is considered as the main factor in high quality seed which increase rice production (Chen, 2003). So, the present investigation was aimed to study the effect of moisture content on some morphological and yield characters of some rice cultivars.

Materials and methods

Two experiment was conducted at experimental farm of Sakha agricultural research station, kafr El sheikh, Egypt, during three seasons, 2015, 2016 and 2017, to study the effect of different levels of moisture contents on some morphological and yield characters of some rice cultivars, the six rice cultivars were collected for every season during October 2015 and 2016 with different moisture content (14, 16, 18, 20, 22%) and storage up to sowing in May 1st 2016 the samples were collected during harvest in the field with different moisture content and kept or stored up to start the next season in May. Optimum to sowing date for rice crop this method was repeated during the 2017 season, the design experiment was split plot design with three replications, the main plot was assigned for moisture contents and the cultivars were assigned in subplot with plot size (5 m^2) and the remaining cultural practices were applied according to RRTC (2015). The measurements were recorded on grain volume, germination %, plant height, seed set %, 1000 grain weight and grain yield (t/ha) according to SES to IRRI (2008).

Table 1. *Monthly maximum and minimum temperature (Co), relative humidity % and wind velocity (km/h) at RRTC Sakha, Kafr EL-Skeikh province during 2016 and 2017 seasons*

Month	2016 season					2017 season				
	Temperature (°C)		Relative humidity (%)		Wind velocity (km/h)	Temperature (°C)		Relative humidity (%)		Wind velocity (km/h)
	Max	Min	7.30AM	13.30PM		Max	Min	7.30AM	13.30PM	
April	25.64	13.7	78.30	78.50	95.70	27.8	20.0	80.9	48.9	74.0
May	30.19	18.79	77.30	46.10	114.60	31.2	23.8	75.6	43.9	95.8
June	30.85	21.14	78.80	51.20	105.30	33.6	25.3	75.5	48.0	98.6
July	33.00	22.40	85.20	54.30	97.30	35.2	25.4	82.6	51.0	89.5
August	35.10	25.00	83.8	51.70	91.20	34.9	25.2	82. 4	51.4	76.0
Sept.	34.60	23.80	82.70	46.50	95.30	32.8	23.5	83.1	48.3	68.7
Oct.	29.90	20.60	80.90	54.10	87.00	29.5	20.6	82.5	49.6	57.9

Statistical analysis

All the data collected were subjected to analysis of variance according to Gomez and Gomez (1984). Treatment means were compared using L.S.D. All statistical analysis was performed using analysis of variance technique by means of "COSTAT" computer software.

Results

The main characters for rice cultivars were show in *Table 2*. The rice varieties were related to different types:

1. Japonica type had high moisture content.
2. Indica/Japonica type had moderate moisture content.
3. Indica type had low moisture content.

http://www.aloki.hu ● ISSN 1589 1623 (Print) ● ISSN 1785 0037 (Online)
DOI: http://dx.doi.org/10.15666/aeer/1902_981991
© 2021, ALÖKI Kft., Budapest, Hungary

Table 2. *The main characters for the studied rice cultivars*

Cultivars	Pedigree	Plant height	1000 grain wight	Grain yield t/ha	Disease reaction (blast)
SAKHA 105	Japonica	98	29	10.100	R
SAKHA 106	Japonica	105	28	10.250	R
GIZA 178	Indica/Japonica	100	21	10.500	R
GIZA 179	Indica/Japonica	90	26	10.400	R
GIZA 182	Indica	90	25	9.500	R
SK 2034 (H1)	Indica/Japonica	100	25	11.200	R

The data in *Table 3* showed the effect of different levels for moisture content on grain volume, germination% and plant height, where, in the case of seeds harvested at 14% moisture content the germination% increased and plant height enhanced, while in the case of seeds harvested at 22% moisture content the seed volume increased and the germination% and plant height decreased indicating that increased seed moisture content increased seed size then volume and quality.

Table 3. *Mean performance of some rice varieties with their interaction for grain volume germination % and plant height during 2016 and 2017 seasons*

Treatments %	Grain volume (cm^3)		Germination (%)		Plant height (cm)	
Moisture	**2016**	**2017**	**2016**	**2017**	**2016**	**2017**
14	2.22	2.04	92.05	90.82	101.88	100.77
16	2.37	2.18	88.06	87.05	96.18	93.88
18	2.44	2.33	84.02	82.72	92.5	91.23
20	2.72	2.55	76.44	78.35	89.6	88.63
22	3.00	2.71	59.69	57.29	86.52	85.37
F-test	**	**	**	**	**	**
LSD 0.05	0.145	0.148	0.520	0.312	0.083	0.659
Cultivars						
SAKHA 105	2.77	2.57	84.46	83.25	91.84	93.13
SAKHA 106	2.79	2.57	84.78	83.74	98.48	96.57
GIZA 178	2.11	2.08	82.99	83.04	96.64	95.81
GIZA 179	2.96	2.84	83.32	83.19	85.19	83.83
GIZA 182	2.21	2.17	82.14	81.93	88.94	86.99
SK 2034 (H1)	2.60	2.40	84.60	83.93	98.79	98.54
F-test	**	**	**	**	**	**
LSD 0.05	0.119	0.118	0.462	0.293	0.077	0.680
Interaction moisture × varieties	**	**	**	**	**	**

*Highly significant at 0.05% probability

The data in *Table 4* show the effect of moisture content of some rice cultivars on seed set %, 1000 grain weight and grain yield (t/ha.) during 2016 and 2017 seasons. The highest values for seed set %, 1000 grain weight and grain yield (t/ha.) were recorded at 14% moisture content, while at 22% moisture content undesirable values were recorded for the studied characters, indicating that 14% moisture content enhances crop growth rate then

http://www.aloki.hu ● ISSN 1589 1623 (Print) ● ISSN 1785 0037 (Online)
DOI: http://dx.doi.org/10.15666/aeer/1902_981991
© 2021, ALÖKI Kft., Budapest, Hungary

increases the yield attribute finally grain yield (t/ha.). For the rice cultivars, in the rice cultivar, Giza 179 desirable values were recorded for seed set % and 1000 grain weight, but the indicia/japonica cultivars (Egyptian hybrid 1 and Giza 179) recorded the highest grain yield (t/ha.) compared to the japonica rice cultivars (SAKHA 105 and SAKHA 106).

Table 4. *Mean performance of some rice varieties with their interaction for seed set, grain weight and grain yield characters during 2016 and 2017 seasons*

Treatments	**Seed set (%)**		**1000- grain weight (g)**		**Grain yield (t/ha)**	
Moisture %	**2016**	**2017**	**2016**	**2017**	**2016**	**2017**
14	95.76	94.15	22.58	22.72	11.35	10.92
16	87.56	85.59	23.04	23.66	10.28	9.80
18	82.86	80.87	23.71	24.63	10.11	9.56
20	76.73	75.56	24.77	25.38	9.02	9.04
22	74.94	72.61	26.13	26.49	8.40	3.28
F- test	**	**	**	**	**	**
LSD 0.05	0.425	0.308	0.693	0.229	0.545	0.547
Varieties						
SAKHA 105	83.28	80.98	25.88	25.83	9.40	8.54
SAKHA 106	83.88	82.07	25.93	26.92	9.59	8.99
GIZA 178	84.57	82.57	20.66	2079	10.21	9.49
GIZA 179	84.89	82.91	25.35	25.59	10.30	9.80
GIZA 182	82.05	80.01	23.62	24.79	8.97	8.44
SK 2034 (H1)	84.01	82.00	22.86	23.60	11.47	11.44
F-test	**	**	**	**	**	**
LSD 0.05	0.362	0.240	0.542	0.229	0.477	0.428
Interaction moisture × varieties	**	**	**	**	**	**

**Highly significant at 0.05% probability

The interaction between moisture content and rice varieties are presented in *Table 5* and *Figure 1,* the grain volume affected by the different levels of moisture content, where the high moisture content with most of the rice cultivars recorded the highest value for grain volume compared with the low moisture content.

Table 5. *Grain volume (cm^3) as affected by the interaction between some rice varieties and different moisture content during 2016 and 2017 seasons*

Moisture	**Varieties**											
	SAKHA105		**SAKHA106**		**GIZA178**		**GIZA179**		**GIZA182**		**HYBRID1**	
	2016	**2017**	**2016**	**2017**	**2016**	**2017**	**2016**	**2017**	**2016**	**2017**	**2016**	**2017**
14	2.30	2.10	2.50	2.30	1.80	1.66	2.66	2.66	2.66	1.80	2.10	1.93
16	2.50	2.30	2.56	2.36	1.85	1.68	2.80	2.80	2.80	1.90	2.46	2.26
18	2.73	2.53	2.59	2.49	1.90	1.70	2.70	2.70	2.70	2.03	2.56	2.36
20	3.06	2.86	2.62	2.80	1.95	1.75	3.17	3.17	3.17	2.25	2.86	2.66
22	3.26	3.06	3.68	2.92	2.50	1.83	3.50	3.50	3.50	2.45	3.03	2.83
LSD 0.05 at 2016/2017	0.266/0.261											

http://www.aloki.hu ● ISSN 1589 1623 (Print) ● ISSN 1785 0037 (Online)
DOI: http://dx.doi.org/10.15666/aeer/1902_981991
© 2021, ALÖKI Kft., Budapest, Hungary

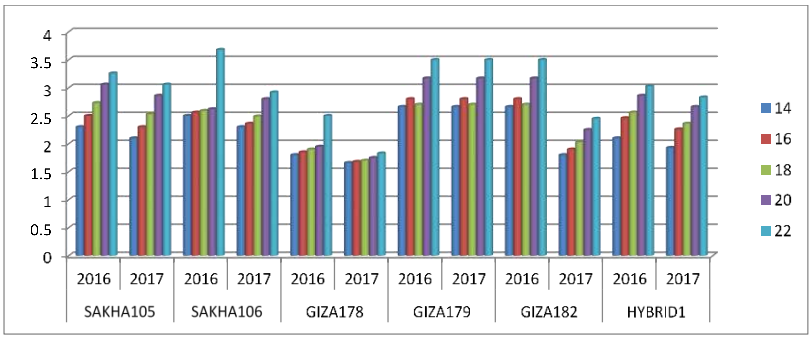


Figure 1. *Grain volume (cm^3) as affected by the interaction between some rice and varieties and different moisture content during 2016 and 2017 seasons*

The results in *Table 6* and *Figure 2* showed. the interaction between rice varieties and different levels of moisture content, the highest value for 1000-grain weight was recorded in the case of the variety Sakha 106 with 14% moisture content compared to the variety Giza 178 with a moisture content of 28%, during the two seasons. Equally for 1000 grain weight the highest values were recorded (27.38 and 28.78 g) when the rice variety Sakha 106 was used with a moisture content of 14%, but the lowest values were recorded (20.69 and 21.72 g) with the rice variety Giza 178 at moisture content 22% during 2016 and 2017 seasons, respectively.

Table 6. *1000 grain weight (g) as affected by the interaction between some rice varieties and different moisture content during 2016 and 2017 seasons*

Moisture	VARIETIES											
	SAKHA105		SAKHA106		GIZA178		GIZA179		GIZA182		HYBRID1	
	2016	2017	2016	2017	2016	2017	2016	2017	2016	2017	2016	2017
14	27.00	27.00	29.16	29.16	21.66	21.66	27.55	27.66	24.83	28.00	22.66	25.46
16	26.66	22.66	26.33	27.33	21.33	21.33	25.66	26.66	24.66	25.33	24.00	25.00
18	26.00	22.50	25.66	26.66	20.66	20.66	24.66	25.66	23.33	24.33	22.00	24.00
20	25.50	25.00	24.33	26.00	20.00	20.33	24.46	24.66	23.00	23.66	21.33	22.33
22	25.00	24.00	23.55	25.00	19.66	20.00	24.33	23.33	22.66	22.66	20.33	21.33
LSD 0.05 at 2016/2017	1.212/1.012											

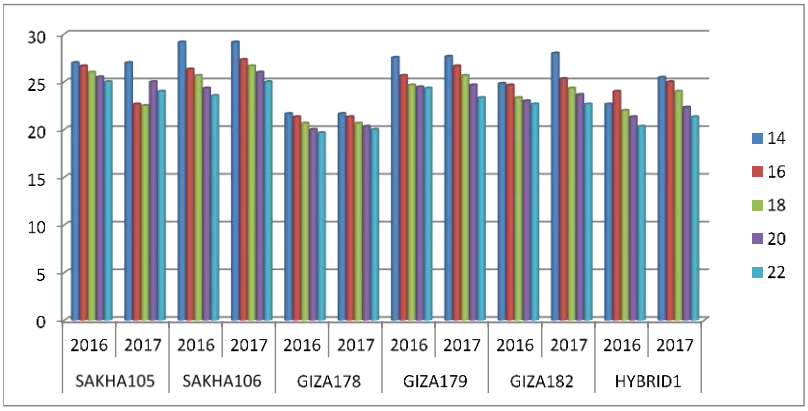


Figure 2. *1000 grain weight (g) as affected by the interaction between some rice and different varieties moisture content during 2016 and 2017 seasons*

http://www.aloki.hu ● ISSN 1589 1623 (Print) ● ISSN 1785 0037 (Online)
DOI: http://dx.doi.org/10.15666/aeer/1902_981991
© 2021, ALÖKI Kft., Budapest, Hungary

That affected on delay the physiological maturity of the seed embryo, then decreased the viability for seed germination and crop growth rate. For rice cultivars, the highest values for grain volumes were recorded in the japonica rice cultivars Sakha 106 and Sakha 105 while in indica/japonica rice cultivars, Giza 178 and Egyptian Hybrid1 the highest values were recorded for germination %, moreover in the Sakha 106 and hybrid 2034 rice cultivars the highest values were recorded for plant height that referred to the genetic background for the studied cultivars. That affected on delay for physiological maturity of the seed embryo, then decreased the viability for seed germination and crop growth rate. For rice cultivars, the highest values for seed volumes were recorded in the japonica rice cultivars Sakha 106 and Sakha 105, while in indica/japonica rice cultivars, Giza 178 and Egyptian hybrid the highest values were recorded for germination %, moreover in the Sakha 106 and hybrid 1 rice cultivars the highest values were recorded for plant height that referred to the genetic background for the studied cultivars.

The results in *Table 7* and *Figure 3* showed the interaction between rice varieties and different levels of moisture content on Germination %, the rice variety Giza 178 recorded the highest value of germination at 14% moisture content, while, in the variety Giza 179 the lowest value was recorded at 22% moisture content, indicating that the Japonica type may be highly affected with high moisture content compared to the indica and indica/Japonica types. Seed vigor is an important aspect of quality, which is controlled by field stand, establishment ability and performance. The problems associated with establishing vigorously growing seedlings are often related to poor seed quality.

Table 7. *Germination % as affected by interaction between some rice and different varieties moisture content during 2016 and 2017 seasons*

Moisture	Varieties											
	SAKHA105		SAKHA106		GIZA178		GIZA179		GIZA182		HYBRID1	
	2016	2017	2016	2017	2016	2017	2016	2017	2016	2017	2016	2017
14	93.50	90.33	91.33	90.60	94.60	93.66	91.13	90.13	91.50	92.43	94.60	92.93
16	88.96	87.26	86.33	85.33	88.16	87.16	87.43	86.40	88.66	87.66	88.73	87.73
18	84.33	83.33	83.36	81.66	82.76	83.20	83.33	81.33	84.90	83.16	85.30	83.23
20	80.25	78.23	79.33	77.66	79.66	78.00	78.33	78.00	80.76	79.50	79.66	78.66
22	76.90	75.93	76.00	75.00	76.56	75.33	75.76	74.70	76.16	75.16	76.73	75.73
LSD 0.05 at 2016/2017	0.975/1.033											

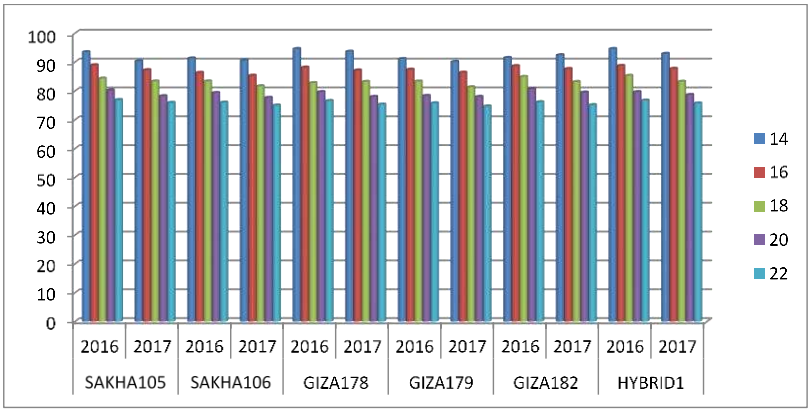


Figure 3. *Germination % as affected by the interaction between some rice varieties and different moisture content during 2016 and 2017 seasons*

http://www.aloki.hu ● ISSN 1589 1623 (Print) ● ISSN 1785 0037 (Online)
DOI: http://dx.doi.org/10.15666/aeer/1902_981991
© 2021, ALÖKI Kft., Budapest, Hungary

The information in *Table 8* and *Figure 4* showed the interaction between rice varieties and different levels of moisture content for plant height, the lower the moisture content was the longer stature for plant height was recorded in all studied cultivars indicating that low moisture content produce good seedling vigor then normal crop growth rate and high productivity.

Table 8. *Plant height (cm) as affected by the interaction between some rice genotypes and different moisture content during 2016 and 2017 seasons*

Moisture	Varieties											
	SAKHA105		SAKHA106		GIZA178		GIZA179		GIZA182		HYBRID1	
	2016	2017	2016	2017	2016	2017	2016	2017	2016	2017	2016	2017
14	104.0	105.0	108.0	106.6	102.0	105.6	93.66	92.00	98.00	96.00	105.6	99.33
16	96.00	94.00	100.7	99.33	99.70	98.33	87.00	85.00	91.00	89.00	101.70	97.66
18	89.80	91.53	97.60	95.40	97.20	95.00	84.40	83.46	88.00	86.00	98.00	96.00
20	86.90	89.70	94.50	92.56	93.60	91.43	81.70	80.83	85.00	83.26	96.23	94.03
22	82.50	85.46	91.60	88.90	90.73	88.63	79.20	77.86	82.70	80.70	92.40	90.70
LSD 0.05 at 2016/2017	2.027/3.264											

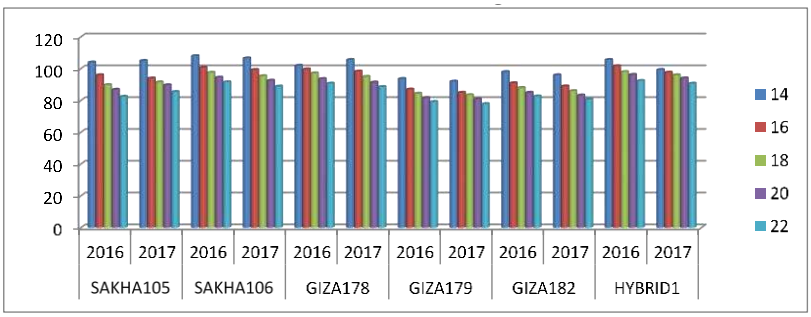


Figure 4. *Plant height (cm) as affected by the interaction between some rice and varieties with different moisture content during 2016 and 2017 season*

The results in *Table 9* and *Figure 5* showed the grain yield as affected by interaction between rice varieties and different levels of moisture content during two seasons, the rice variety Egyptian hybrid 1 recorded the highest value with 14% moisture content compared to SAKHA 105 with 22% moisture content during the two years.

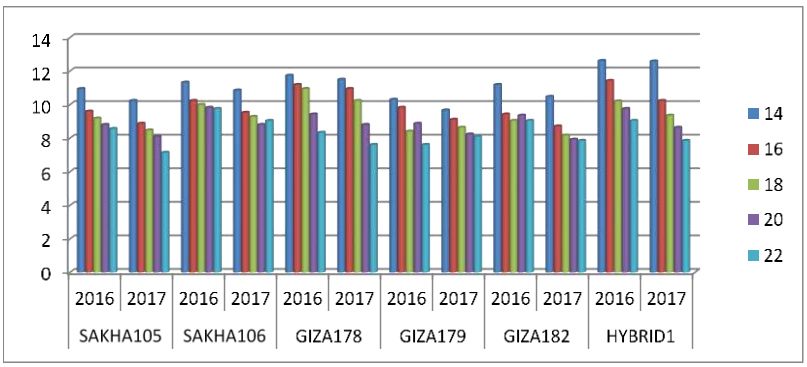


Figure 5. *Grain yield (t/ha.) as affected by the interaction between some rice and varieties with different moisture content during 2016 and2017 seasons*

http://www.aloki.hu ● ISSN 1589 1623 (Print) ● ISSN 1785 0037 (Online)
DOI: http://dx.doi.org/10.15666/aeer/1902_981991
© 2021, ALÖKI Kft., Budapest, Hungary

Table 9. *Grain yield (t/ha.) as affected by the interaction between some rice and different varieties and moisture content during 2016 and 2017 season*

Moisture	Varieties											
	SAKHA105		SAKHA106		GIZA178		GIZA179		GIZA182		HYBRID1	
	2016	2017	2016	2017	2016	2017	2016	2017	2016	2017	2016	2017
14	10.94	10.23	11.32	10.85	11.73	11.49	10.30	9.66	11.18	10.47	12.61	12.58
16	9.59	8.87	10.23	9.52	11.18	10.94	9.82	9.11	9.42	8.71	11.42	10.23
18	9.18	8.47	9.99	9.28	10.94	10.23	8.40	8.63	9.04	8.16	10.2	9.35
20	8.80	8.09	9.82	8.80	9.42	8.80	8.87	8.23	9.35	7.92	9.75	8.63
22	8.56	7.14	9.75	9.04	8.33	7.61	7.61	8.09	9.04	7.85	9.04	7.85
LSD 0.05 at 2016/2017	0.132/0.159											

The results in *Table 10* and *Figure 6* showed the interaction between rice varieties and different levels of moisture content for seed set % in the two years, the Sakha 106 rice varieties with 14% moisture content recorded the highest for seed set% compared to Giza 182 rice variety which recorded undesirable value with high moisture content during the two years, indicating that the Giza 182 as indica type was sensitive to high moisture content and low physiological maturity.

Discussion

High quality seed reflects the need to emphasize seed testing, focusing on physical purity, germination capacity and moisture content, and also seed health tests, varietals purity evaluations and seedling vigor tests. Seed quality control and certification is mainly based on crop inspection and laboratory testing to ensure that, the seed meets minimum standards laid down in the regulations. High quality seed reflects on the increasing national income. Seeds are tested according to the procedures of International Seed Testing Association (ISTA) and Organization for Economic Co-operation and Development (OECD). From the above results it could be concluded that, to increase the seed equality and productivity, the seeds should be harvested at 14% moisture content, these results were in agreement with Kibar et al. (2010), Genkawa et al. (2008) and Pimratcha et al. (2019). Also, the results indicated that the cultivars with low moisture content should be harvest to get high seed quality, these results were confirmed by Sharif and Ghadi (2013) and Li et al. (2019). Also, the results may be referred to the genetic make-up whereas the Giza 178 having lightweight grain, as well as, indicated to the seed with 14% moisture content may be enhancement the crop growth rate then enhancement the yield and yield attributes. Dissimilar results obtained by Khalil (2015), the high differences between the rice variety and moisture content for 1000 grain weight. These results may refer to the hybrid which exhibited the hybrid vigor compared to the other varieties the highest and stabile values for grain yield per unit area may be referred to the stable weather condition through growing seasons as shown in *Table 1* and *Photos 1* and *2* (Abo Yousef et al., 2018; Chu et al., 2018; Fatima et al., 2018; Yong et al., 2019). High quality seeds have the capacity to provide vigorous seedlings over a wide range of environments. Deterioration of high-quality seed can render seed worthless for

http://www.aloki.hu ● ISSN 1589 1623 (Print) ● ISSN 1785 0037 (Online)
DOI: http://dx.doi.org/10.15666/aeer/1902_981991
© 2021, ALÖKI Kft., Budapest, Hungary

planting although its germination percent remains relatively high seed deterioration is a progressive process from the time of physiological maturity until the seed is dead.

Table 10. *Seed set % as affected by the interaction between some rice and different varieties and moisture content during 2016 and 2017 seasons*

Moisture	Varieties											
	SAKHA105		SAKHA106		GIZA178		GIZA179		GIZA182		HYBRID1	
	2016	2017	2016	2017	2016	2017	2016	2017	2016	2017	2016	2017
14	94.00	92.33	98.10	98.10	96.00	94.00	97.00	95.00	94.00	92.00	95.50	93.50
16	86.80	84.80	86.49	84.49	88.20	86.24	89.14	87.14	86.30	84.30	87.72	85.72
18	82.37	80.55	82.00	80.00	83.64	81.64	84.54	82.55	81.83	79.84	83.18	81.18
20	78.00	75.33	77.76	75.76	79.30	77.30	77.16	75.16	74.59	72.56	78.87	76.85
22	74.90	71.90	74.70	71.76	75.19	73.17	76.00	74.00	73.56	71.56	74.78	72.78
LSD 0.05 at 2016/2017	0.564/0.533											

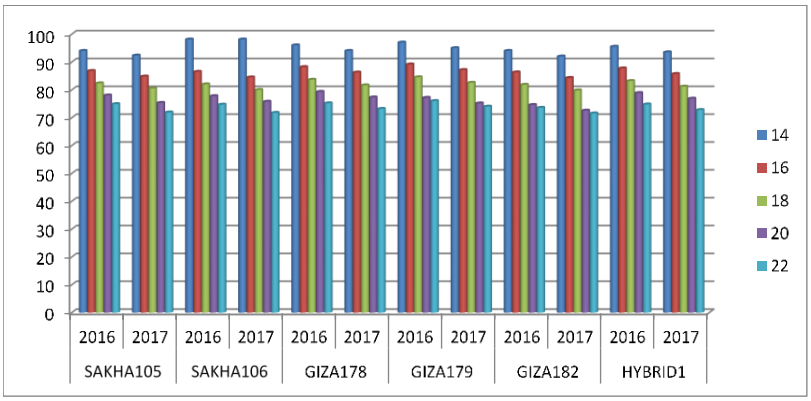


Figure 6. *Seed set % as affected by the interaction between some rice and varieties different moisture content during 2016 and 2017 season*



Photo 1. *Rice varieties at harvest and the different rice varieties under study*

http://www.aloki.hu ● ISSN 1589 1623 (Print) ● ISSN 1785 0037 (Online)
DOI: http://dx.doi.org/10.15666/aeer/1902_981991
© 2021, ALÖKI Kft., Budapest, Hungary



Photo 2. *Rice varieties at harvest*

Conclusion

From these results it could be concluded that, the desirable values were recorded for the lowest moisture content, but the highest moisture content undesirable values were recorded for all studied characters, on the other hand the highest seed volume, plant height and 1000 grain weight were recorded in Sakha 106, while the highest germination % and grain yield (t/ha) were recorded in the Hybrid 2034 and Giza 178, which means seeds dried to 14% moisture content should be harvested and stored to maintain the seed viability and increase the productivity. Finally, the optimum date for harvesting the rice cultivars under study should be determined.

REFERENCES

[1] Abo Yousef, M. I., Abd El Aty, M. S., Talha, I. A., Hammoud, S. A. (2018): Response of some rice varieties to different doses of X rays on the yield and its related characters. – 4th International Conference on Biotechnology Application in Agriculture (ICBAA), 4-7 April, Hurghada, Egypt.

[2] Aidy, I., Draz, R. E., Shatta, A. (2002): Seed production. – Egyptian Journal of Agricultural Research 83(5a): 91-95.

[3] Badawai, I. A. T (2005): Sustainability of rice production in Egypt. – Egyptian Journal of Agricultural Research 83(5a): 23-30.

[4] Chen, C. (2003): Evaluation of air oven moisture content determination methods for rough rice. – Biosystems Engineering 86(4): 447-457.

[5] Chu, G., Chen, T., Chen, S., Xu, C., Wang, D., Zhang, X. (2018): Agronomic performance of drought-resistance rice cultivars grown under alternate wetting and drying irrigation management in southeast China. – The Crop Journal 6(5): 482-494.

[6] Fatima, P., Chand, P., Singh, S. K., Purushottam, Mishra, A., Kumar, P. (2018): Effect of water stress on morphological traits and yield in rice genotypes. – Current Journal of Applied Science and Technology 31(2): 1-8.

[7] Genkawa, A. T. T., Uchino, B. A., Inoue, A. F., Tanaka, B., Hamanaka, D. (2008): Development of a low-moisture content storage system for brown rice: storability at decreased moisture contents. – Biosystems Engineering 4(99): 515-522.

[8] Gomez, K. A., Gomez, A. A. (1984): Statistical Procedures for Agricultural Research. 2nd Ed. – John Wiley and Sons, Inc., New York.

[9] IRRI (2008): Standard Evaluation System for Rice. 3rd Ed. International Rice Testing Programs. – International Rice Research Institute, Manila.

http://www.aloki.hu ● ISSN 1589 1623 (Print) ● ISSN 1785 0037 (Online)
DOI: http://dx.doi.org/10.15666/aeer/1902_981991
© 2021, ALÖKI Kft., Budapest, Hungary

[10] ISTA (2012): International Seed Testing Association. Seed testing No. 143 April 2012.
[11] Khalil, F., Fouda, M. (2015): Effect of moisture content on seed quality and seedling characters in rice. – Master of Science in (Agronomy) Department of Agronomy, Faculty of Agriculture, Kafr EL-Sheikh University.
[12] Kibar, H., Öztürk, T., Esen, B. (2010): The effect of moisture content on physical and mechanical properties of rice (Oryza sativa L.). – Spanish Journal of Agricultural Research 8(3): 741-749.
[13] Li, R., Li, M., Ashraf, U., Liu, S., Zhang, J. (2019): Exploring the relationships between yield and yield-related traits for rice varieties released in China from 1978 to 2017. – Front. Plant Sci. 10: 543.
[14] OECD (2012): Organization for Economic Co-operation and Development. Crop production. OECD-FAO Agricultural Out-look (Edition 2019).
[15] Pimratcha, S., Mungkunkamchaob, T., Kesmalac, T. (2019): Variations in morphological traits, agronomic traits and traits related to drought tolerance in indigenous Thai rice varieties. – Science Asia 45: 99-108.
[16] RRTC (2015): National Rice Research Program: Final Results of 2014 Growing Season. – RRTC, Sakha, Egypt.
[17] Sharif, I., Ghadi, M. (2013): Effect of moisture content on some physical characteristics of three varieties of commercial rice in Iran. – International Journal of Agric. Science 3(1): 62-69.
[18] Yang, X., Wang, B., Chen, L., Li, P., Cao, C. (2019): The different influences of drought stress at the flowering stage on rice physiological traits, grain yield, and quality. – Scientific Reports 9: 3742.

http://www.aloki.hu ● ISSN 1589 1623 (Print) ● ISSN 1785 0037 (Online)
DOI: http://dx.doi.org/10.15666/aeer/1902_981991
© 2021, ALÖKI Kft., Budapest, Hungary

A COMPREHENSIVE OVER 100 YEARS HISTORY OF MOUFLON (*OVIS MUSIMON*) IN POLAND: FROM THE PROMISING BEGINNING IN 1902 TO QUESTIONABLE FUTURE IN 2014 – A CASE STUDY OF WILDLIFE MANAGEMENT HISTORY

NASIADKA, P.[1*] – WAJDZIK, M.[2] – SKUBIS, J.[3]

[1]*Department of Forest Zoology and Wildlife Management, Institute of Forest Sciences, Warsaw University of Life Sciences, ul. Nowoursynowska 159, 02-776 Warsaw, Poland*

[2]*Department of Forest Biodiversity, Faculty of Forestry, University of Agriculture in Cracow, Al. 29-Listopada 46, 31-425 Kraków, Poland*
(e-mail: rlwajdzi@cyf-kr.edu.pl; phone: +48-60-477-5704)

[3]*Department of Wildlife Management and Forest Protection, Faculty of Forestry, Poznań University of Life Sciences, ul. Wojska Polskiego 71 D, 60-625 Poznań, Poland*
(e-mail: skubis@up.poznan.pl; phone: +48-50-719-2365)

**Corresponding author*
e-mail: nasiadek@wl.sggw.pl; phone: +48-60-834-2007

(Received 15th Apr 2020; accepted 27th Jan 2021)

Abstract. Mouflon (*Ovis musimon*) is an alien species in Poland, and a good example of how former customs in hunting become a problematic situation in modern wildlife management. The objective of the study was to document the history of the mouflon, its introductions and the reason for their failures, as well as the changes in population numbers between 1902 and 2014. The history of mouflons was tracked in three periods: 1902-1945, 1946-1981, and 1982-2014. The earliest introductions took place in the Sudeten mountains in 1902. About 50% of next introductions were unsuccessful because of severe winters, lack of supplemental feeding, poaching, and predation by stray dogs, as well as the consequences of inbreeding. Currently less than 3.000 mouflons inhabit the Sudeten mountains in south and the lowlands in western Poland. They occur in 23 local populations. In all locations, mouflon inhabit big forests which represent typical stands composition and potential understory sites. In mountains there are *Picea abies* stands on *Dentario Enneaphyllidis-Fagetum* sites, and in lowlands – *Pinus sylvestris* stands on *Galio Silvatici-Carpinetum* sites respectively. Unfortunately, existing populations need constant protection by hunters that cause legitimate questions about the sense of further breeding of this species for the purpose of hunting.
Keywords: *alien species, introductions, hunting, history of wildlife management, Poland*

Introduction

At least two features of the mouflon (*Ovis musimon,* synonymously known as *O. ammon, O. gmelini, O. aries)* turn it into an exceptional ungulate species occurring in Poland. Firstly, unlike the red deer (*Cervus elaphus* L.), roe deer (*Capreolus capreolus* L.) or wild boar (*Sus scrofa* L.) the mouflon, is a typical forest wild ungulate and all existing populations or introductions undertaken in the past took place in large and dense forest complexes. Forests were to be the area where mouflons should enrich the hunted fauna and, actually, mouflons presently inhabit them causing much less damage to farm crops, so typically ascribed to the deer family (Tomiczek and Türcke, 2003; Cerkal and Muska, 2010).

The second feature (expressed even in its Latin names) is that although the mouflon is inseparably linked to the history of humans in Europe, very little is known about the

http://www.aloki.hu ● ISSN 1589 1623 (Print) ● ISSN 1785 0037 (Online)
DOI: http://dx.doi.org/10.15666/aeer/1902_9931017
© 2021, ALÖKI Kft., Budapest, Hungary

origin and ecology of this large herbivorous species introduced outside the area of its natural habitat (Geist, 1991; Nasiadka et al., 2015).

Discussions used to arise already at the level of origin, and taxonomic classification of the species, which in the last 100 years or so has been thoroughly modified (Chessa et al., 2009). Basically, they concerned the number of wild sheep species and mouflon's ranking among them. At the beginning of the 20th century the mouflon was regarded as one of four or even nine species of wild sheep (Lydekker, 1913; Nasonov, 1923; Heindleder et al., 2002). Later, in the 1950s, Tsalkin (1951) narrowed the number of species to one – *O. ammon* or two – *O. ammon* and *O. nivicola/canadensis*. In the 1970s, when the species began to be distinguished on the basis of the number of chromosomes, Nadler and et al. (1973) suggested the division of wild sheep into four groups with the mouflon (*O. musimon*) being classified into one group with the urial (*O. vignei*) and the argali (*O. ammon*). Unfortunately, both Nadler and et al. (1973), and Valdez and et al. (1978) pointed out to the fact that different species of wild sheep in the areas of their joint occurrence (e.g. northern Iran) can interbreed with each other and produce fertile offspring. This only further complicates the systematics of the species concerned (Nadler et al., 1971).

If the IUCN definitions are to be respected, at present, mouflons should be regarded as one of three wild Eurasian sheep, along with the argali and urial.

Yet another issue which has not been conclusively solved pertains not only to the origin of the species itself but of the mouflons occurring in Europe contemporarily. The question is whether they are indeed the primordial forms of wild sheep which migrated to Europe from Central Asia, or if they are a feral form of sheep previously domesticated, a hybrid between domesticated sheep and mouflons or perhaps yet another combination of domesticated sheep and their wild counterparts (Heindleder et al., 2002).

Domesticated primitive sheep, which arrived in Europe 10 to 4 thousand years B.C. during the so-called Neolithic Revolution, could have been the ancestors of mouflons (Wilson and Reeder, 2005). At that time, the development of agriculture as well as the domestication of animals took place in the region of the Fertile Crescent (areas along the Tigris, Euphrates and Nile rivers). These processes were followed by the increase in human populations and migrations of people (Barker, 2006; Simmon, 2007). It was very likely that during the a.m. agricultural revolution one or several species of the Central-Asian wild sheep were domesticated (*O. orientalis, O. musimon?*). They are thought to have settled, first, in the Mediterranean basin together with migrating people. Then, either with advancing civilization or as animals escaping from farms, they colonized areas further north. However, these populations no longer exist. The mouflon, thus, disappeared completely from the continent of Europe about three thousand years B.C., whereas the animals remaining from Neolithic introductions on Sardinia and Corsica gave rise to the next stage of the European history of this species (Payne, 1968).

The undisputable fact is that all mouflon populations now living in the wild in Europe originated, more often than not, from intentional introductions. At present, the European range of distribution of the mouflon covers 21 countries, although the population numbers in these countries differ considerably. The most numerous populations which consist of more than 50% of the total number of European mouflons live in three countries: the Czech Republic (ca. 20%), Germany (ca. 19%), and Hungary (ca. 13% of the European population). Some 30% of mouflons inhabit three more countries: Austria, continental France, and Slovakia. The remaining group of 15 countries is inhabited by local populations numbering no more than 1-2 thousand individuals in separate, isolated groups (Tomiczek and Türcke, 2003).

http://www.aloki.hu ● ISSN 1589 1623 (Print) ● ISSN 1785 0037 (Online)
DOI: http://dx.doi.org/10.15666/aeer/1902_9931017
© 2021, ALÖKI Kft., Budapest, Hungary

The introductions of mouflons, both those in the early 20th century and those carried out after the Second World War, were aimed, principally, at the introduction of an additional hunted species or – in sporadic cases – of animals for breeding purposes. At that time, the validity of introducing an alien species for hunting purposes was not questioned. The mouflon was a little-known species, had a different appearance than native species and had an interesting trophy (i.e. horns). This was enough for the species to spread all over continental Europe. Now, the mouflon is a game species in 20 European countries. Hunting the species is most popular in Slovakia, the Czech Republic and Hungary, where the horns are highly valued as trophies among hunters. In the remaining European countries, mouflons are hunted in order to control their local population numbers, but also for their horns and, not less importantly, for their meat (Tomiczek and Türcke, 2003).

Poland is a country where the mouflon definitely represents a niche species, numbering approximately 3000 individuals, and their clustered distribution is linked to introduction programmes. Compared with its populations in the neighbouring countries of the Czech Republic or Slovakia, in Poland the mouflon is not regarded as an attractive trophy animal (Wajdzik et al., 2014). Moreover, not being a native species among the native fauna, it sometimes raises discussions on its future fate and triggers critical voices on the justification for maintaining local populations (Szczęśniak, 2011; Dębiec, 2014). On the other hand, however, the mouflon is a hunted species in Poland, consequently the hunters are legally obliged by law – The Act on Hunting, to protect this species and to care for its preservation (Brachmański, 2011).

Unfortunately, the current state of knowledge about the Polish mouflon is so poor that, practically, crucial decisions cannot be taken and the dilemma remains unsolved (Nasiadka et al., 2015). Evident proof of this may be the fact that so far the only bibliography devoted to mouflons, and their history on Polish territory, dates from the early 1950s (Szczepkowki in 1951). Publications from later years have a very diverse form (from press reports to the results of a few studies) and are scattered in many sources. What is more, these materials were mostly published in Polish and are practically unavailable to scientists dealing with wild ungulates and their history in Europe.

This paper was aimed at gathering and summing up as many details as possible on the history over 100-year-long presence of the mouflon in Poland, its introductions, changes in population numbers, and reasons for failures, as of 1902, i.e. from the first introduction of this species to the areas that are presently on Polish territory.

One of the objectives of this paper was also to discuss the further fates of either introduced or spontaneously emerging populations of this species outside its natural range of distribution. The history of the mouflon in Poland can be a very good example of a fragment of the history of European wildlife management (dead end?), when during over 100 years the focus has been shifted from hunting – breeding and shooting for the trophy (for the quantity and quality of as many species as possible) to the sustainable management of native species populations to preserve them and protect their habitats (Riley et al., 2002).

Methods

Research studies on the history of introductions and on current distribution and size of the populations of mouflons in Poland were performed for three time periods: 1902-1945, 1946-1981, and 1982-2014 using two types of sources. The very periods of time

http://www.aloki.hu ● ISSN 1589 1623 (Print) ● ISSN 1785 0037 (Online)
DOI: http://dx.doi.org/10.15666/aeer/1902_9931017
© 2021, ALÖKI Kft., Budapest, Hungary

were primarily dictated by the different quality and availability of source data that varied depending on the specific period to which they pertained.

No statistical data (from foresters or hunters) was available for the years 1902-1945, thus the history of mouflons in that period was reconstructed, primarily, on the basis of the data contained in publications by authors of the time. When describing the first occurrences of mouflons in the present territory of Poland, these authors often provided data on the numbers of released mouflons, their origin, as well as on either the development or the reasons for the failure of breeding efforts. This data is the sole and extremely valuable source of information about mouflons. Furthermore, the specificity of years 1902-1945 consisted in a stormy history resulting, among others, in the changes of borders within Europe, due to which Poland reappeared on the map of the continent in 1918. This period was characterized by high geopolitical dynamics. Over short periods, depending on the specific state an area belonged to, the systems of management, data collection and its archivisation in the same area could change significantly. The same changes regarded game animals and hunting. A short period of stabilisation between 1918 and 1939 was followed by a further extensive 'reshuffling' of states, their borders, and political systems, similar to what had occurred two decades earlier.

After 1945, the territory of Poland shifted west by several hundred kilometers**,** onto lands previously belonging to Germany. This had a significant effect on the presence of mouflons among hunted animal species in Poland. Scarce and inadequate hunting statistics was one of the consequences of the difficult post-war era, and these no longer exist. In the 1950s the principal source of information about mouflons were, as in earlier years, a few press releases, and the first Polish monograph of the mouflon written by Szczepkowski (1951). This data has often been the only preserved evidence of the introductions of mouflons (i.e. the origins of local populations) and their fortunes in subsequent years. In the same period, methods of inventories of game animals as well as hunting data bases were developed and standardized. It finally led to a unified system for monitoring populations of hunted animals which consisted in calculating the estimated number of hunted animals at the end of "game management year", i.e. on 31 March. The responsibility for running these inventories falls on some 2,500 hunting clubs which lease about 4,700 hunting grounds, as well as on 430 forest districts, and, to a lesser extent, on 23 national parks.

Since 1982, data coming from hunting clubs, i.e. from the highest number of wildlife habitats, is transferred to a databank at the Research Station of the Polish Hunting Association in Czempiń near Poznań city. Since then, a standardised system has been in operation not only for data collection on game animals, but also for keeping the data and processing it (e.g. for the purposes of national statistics by the Central Statistical Office of Poland). Therefore, the 1982 to 2014 (to time of changes in rules of data preparing by hunting clubs in 2014) period was treated in our study as the third substantially cohesive period of mouflons inhabiting Poland. Information about this period comes from hunting statistics and from statistics of the State Forests National Forest Holding.

The term "successful introduction" in these studies means that a local mouflon population exists from the time of the first introduction to the present day. The fact whether there were additional re-introductions in the meantime or not, or whether there were periods when mouflons did not occur in a given area (practically there were no such situations), does not affect the meaning of the definition: successful introduction.

http://www.aloki.hu ● ISSN 1589 1623 (Print) ● ISSN 1785 0037 (Online)
DOI: http://dx.doi.org/10.15666/aeer/1902_9931017
© 2021, ALÖKI Kft., Budapest, Hungary

The mouflons were after the first introduction, the mouflons are now, it means that the introduction was successful.

The paper uses official and commonly available geographical names of mountain ranges in which there are or there were mouflons in Poland.

The names of the forest districts and their locations are taken from the official State Forest National Forest Holding catalog: https://www.bdl.lasy.gov.pl/portal/en

Results

The beginning. Years 1902-1945

Although the mouflon appeared on the present-day territory of Poland in 1902, its earlier history and arrival on the European continent is worth mentioning. There is no doubt that the contemporary European mouflon populations came from Sardinia and/or Corsica, and that they were first introduced to the Vienna area in 1730 (Tomiczek and Türcke, 2003). According to mentioned authors, the other milestones important to the development of mouflon population in Europe, include: 1858 – their introduction to the area of Hluboka (presently the Czech Republic); 1868 – introductions to the Jelenec area (Slovakia); 1870 – introduction to the Casentino area (central Italy); 1902 – introductions in the Sudeten mountains (Poland); 1903 – Gohrde region (northern Germany), and in 1906 – in the Harz mountains (Germany) (Tomiczek and Türcke, 2003). Another date that deserves particular attention is 1899 as it marks the beginning of mouflon breeding in Hungary near Betler. The breeding there began with 47 animals brought in from Linz in Austria (Jezierski, 1955).

As mentioned earlier, the first mouflons were brought to lands in present-day Poland in 1902. According to Łabęcki (2008), it was Count von Seidlitz-Sandreczki – one of many representatives of German-Czech-Polish families of the Sudeten region, who came out with the idea of the introduction (Łabęcki, 2008). He brought five mouflons from the hunting ground of Nagyappone in Slovakia, and introduced them to the Sowie mountains, near Bielawa village. The breeding progressed well, and in 1929 this mouflon herd amounted to about twenty individuals. Next came successful introductions to the Karkonosze mountains – in the period 1912-1913, in the Central Sudeten mountains near Wałbrzych in 1913 and 1921, and in the Śnieżnik massif – in 1928-1929 (Piegert and Uloth, 2000). At that time, the German introductions were very successful. Up to the outbreak of the Second World War, this region was inhabited by approximately 200-300 mouflons and their number, despite huntings, continued growing.

In 1934, mouflons were released in another region of Poland, namely in the Carpathians. Four ewes and two rams were brought there from Hamburg and, after a year spent in a pen, they were let loose together with their lambs. This location also proved correct. The originators of the project decided to select a mountainous area in the Starzawa Forest District (henceforth abbreviated as F.D.) – presently the Ukraine, which was free of such large predators as wolf, lynx and brown bear, actually not an easy task in the Western Carpathians at the time (Szczepkowski, 1951). Until 1939, this region was inhabited by ca. 20 individuals. They survived the war there, and traces of their presence can be found in the first Russian post-war publications about fauna of Ukraine (Szczepkowski, 1951 after Bobrinskij et al., 1944). At the beginning of the 1960s this population ceased to exist.

http://www.aloki.hu ● ISSN 1589 1623 (Print) ● ISSN 1785 0037 (Online)
DOI: http://dx.doi.org/10.15666/aeer/1902_9931017
© 2021, ALÖKI Kft., Budapest, Hungary

The lowland forests of Spała in Central Poland, was the next mouflon introduction site in Poland. Mouflons were brought to the Spalskie Forests in 1937. These were two rams and four ewes which gave birth to lambs the following year. Unfortunately, any further breeding efforts were thwarted by war, and the fate of the animals kept in the several-hectare large enclosure remains unknown (Szczepkowski, 1951; Jezierski, 1955).

Very little is known about the introduction of mouflons during the II WWR. However, at least three attempts are known to have been undertaken by Germans. The first was performed in 1939 in the forested hills of the Gdańsk Pomeranian region near Kartuzy (now the Kartuzy F.D.). Nine animals were released there and they survived until 1946 (Szol and Olej, 1946; Nowak, 1968).

The remaining two introduction attempts took place in 1941 and 1942, in the lowland forests of western Poland, in the Notecka Primeval Forest. At first, they consisted in enclosure-based breeding of mouflons which were subsequently released into the wild. In what is now the Wronki F.D., breeding started with four rams and ten ewes and they were at first kept in an enclosure. These mouflons were released in 1942. One year later, another breeding attempt began in the Sieraków F.D., and – in the same year – after a short quarantine period, the mouflons (their initial number remains unknown) formed a wild population there (Nowak, 1968). From post-war publications it is known that the breeding in those locations had been initially successful. Up to the end of war, 30 and 35 mouflons survived in Sieraków and Wronki, respectively (Nowak, 1968). Their numbers later declined. In 1948, 23 mouflons were still alive in Sieraków, whereas only 9 individuals remained in Wronki (Ostrowski, 1949). According to Nowak (1968), the year 1950 should be regarded as the end date of these populations (Nowak, 1968).

The above-mentioned releases were not the only ones that were attempted during the Second World War. Some others, whose history cannot be reconstructed today, include the presence of about ten mouflons in the period 1947-1949 near the city of Bytom in southern Poland (Ostrowski, 1949). This group, observed over three years and considered large for mouflons, must have arrived in the area still before 1945. A similar situation occurred in the area near Toruń, where mouflons were observed shortly after the war. In 1949, two individuals of unknown origin were spotted there (Nowak, 1968). The close distance to the pre-war border with Germany and the large forested lands in this area also allow the presumption that a breeding site of mouflons had existed in this part of the country before the end of WWII. The 1902-1945 locations of successful introductions and releases of mouflons, as well as the sites where the animals have failed to survive in the area of contemporary Poland are presented in *Figure 1*.

Years 1946-1981. Better documentations, worse statistics

The papers and simple statistics published in these years showed that, basically, in the post-war period the presence of mouflons in Poland was documented, and the widespread failure of introductions and the declines in numbers of local populations were widely discussed (Nasiadka et al., 2015).

In addition to the already existing populations, two attempts to introduce mouflons to lowland forests were undertaken between 1946 and 1981. The first was carried out in the north of the Mazovia region and ended in failure. In 1950, two rams and four ewes purchased in the former Czechoslovakia were placed in a quarantine enclosure in the Ciechanów F.D. According to Nowak (1968), one released pair did not survive (poaching, predation by stray dogs) and because of that the remaining four animals were

http://www.aloki.hu ● ISSN 1589 1623 (Print) ● ISSN 1785 0037 (Online)
DOI: http://dx.doi.org/10.15666/aeer/1902_9931017
© 2021, ALÖKI Kft., Budapest, Hungary

transferred to another location, which remains unknown. The second introduction was carried out more than two decades later in the Pomeranian forests of Sławno F.D. In 1973, three rams and two ewes were released there, and one year later, five more ewes were added. All these animals started a local population which still exist today (Solarz, 2011).

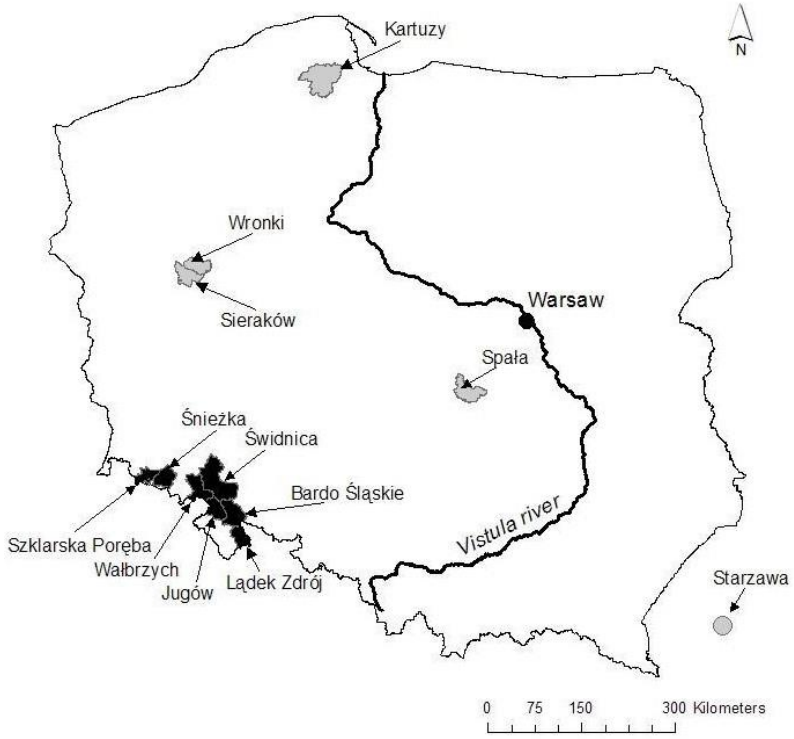


Figure 1. *Introductions of mouflons in Poland during years 1902-1945 (black colour – successful, gray – failed introductions)*

Another attempt to introduce mouflons to the Świętokrzyskie mountains (the Łagów F.D.) – the only mountain range in Poland that is not connected to the country's mountainous region in the south – ended in a rather dramatic fashion. In 1952, two rams, one ewe, and two lambs brought from the Sudeten mountains were placed in a quarantine enclosure. In the same year, at the beginning of winter, the mouflons were released and thus a wild population was formed. Four years later, in 1956, as many as seven mouflons were recorded there (Nowak, 1968), and after two more years, in 1958, this population was reinforced by four more rams and five ewes from Czechoslovakia (Krysztofik, 1962). The same author reported on the successful development of the population in the Świętokrzyskie mountains which in 1962 amounted to as many as 25-30 animals inhabiting both managed forests and the National Park. This situation did not last long, however, because it was already in 1965 when the population ceased to grow, whereas in subsequent years it collapsed completely. Nowak (1968) reported that at the beginning of 1968, there were a mere three mouflons living in the Świętokrzyskie mountains, while the last confirmed sighting was made in 1973 (Nowak, 1968; Solarz, 2011). This year can be deemed to mark the end of the history of mouflons in the area.

http://www.aloki.hu ● ISSN 1589 1623 (Print) ● ISSN 1785 0037 (Online)
DOI: http://dx.doi.org/10.15666/aeer/1902_9931017
© 2021, ALÖKI Kft., Budapest, Hungary

The years between 1946 and 1980 witnessed dynamic changes also at the sites of the first introductions at the beginning of the 20th, namely in the Sudeten mountains. These mountains consist of a number of smaller ranges where introductions took place at various times with strongly variegated sizes of local mouflon populations. Łabęcki (2008) also reported on an interesting natural introduction (migrations) of mouflons. In line with his report, as of 1948 there were sightings of mouflons in the Stołowe mountains, that were not introduced either before or after the war. Taking into consideration the fact that they were large-sized herds numbering: 54 individuals in 1948, 151 in 1949, and as many as 195 in 1950, it is justified to assume that these mouflons originated in the Czech population. In 1957, the last records were made of 22 mouflons in the Stołowe mountains, and thereafter the population vanished until 1989 (Łabęcki, 2008).

Similar events occurred in the Kamienne and Wałbrzyskie mountains. Prior to 1945, in these locations there had been no introductions. However, in the 1948-1958 there were records of several to even several dozen mouflons (Szczepkowski, 1951; Łabęcki, 2008). In subsequent years, the presence of the species was noted sporadically up until 1987. Since that date, the present-day population has inhabited that area.

The introduction of mouflons in the Kaczawskie mountains (the Jawor F.D.), i.e. outside the Sudeten mountains, has been successful**.** The first group of animals: five rams and ten ewes, were brought there in 1969 from Germany, from the Uhlenstein F.D. in the Harz mountains. The animals were released from pen in 1970. Since that year there has been a free-roaming herd of mouflons, which was "beefed up" by more animals in the following years: by four rams and five ewes in 1971, and by three rams and eight ewes in 1976 (Łabęcki, 2008) (*Fig. 2*).

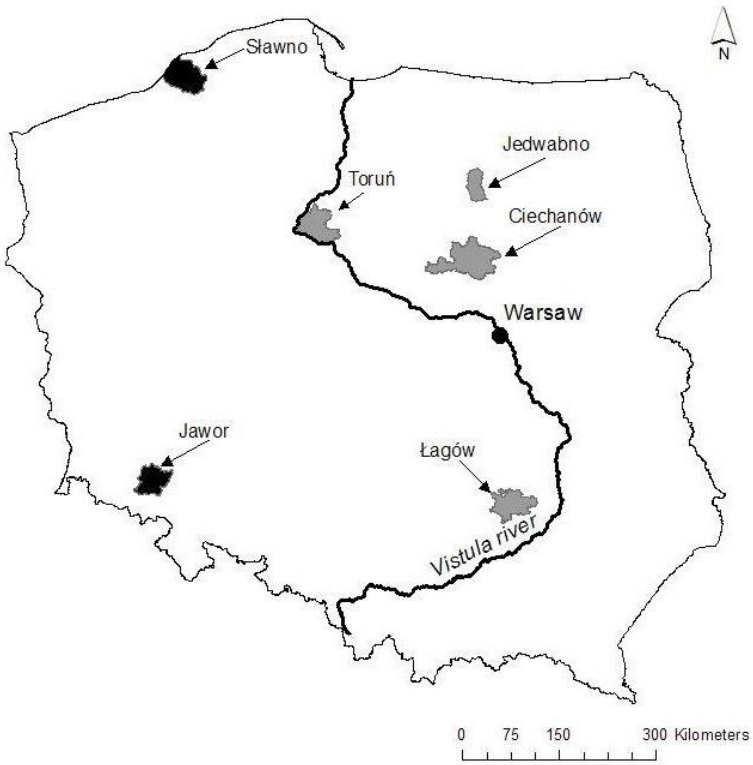


Figure 2. *Introductions of mouflons in Poland during years 1946-1981 (black colour – successful, gray – failed introductions)*

http://www.aloki.hu ● ISSN 1589 1623 (Print) ● ISSN 1785 0037 (Online)
DOI: http://dx.doi.org/10.15666/aeer/1902_9931017
© 2021, ALÖKI Kft., Budapest, Hungary

1982-2014. Better statistics, worse information

This period has two distinctive features in Poland. The first is the increased interest in mouflons, their purchases and introductions among hunting clubs, as well as the emergence of the issue of the adverse effect of mouflons on the environment (Jakubowski and Zalewski, 2000; Bobek et al., 2014). Compared with earlier decades, this period is referred to as a "renaissance" of scientific interest in mouflons in Poland (Nasiadka et al., 2015).

The second feature, unfortunately of an adverse nature when seen from the viewpoint of the consequences of introduction of alien species, involves the increased number of uncontrolled introductions and almost no information about the reasons for failures in this period.

In the aforementioned last three decades, mouflons were reported in a total of more than 50 locations in the lowland part of Poland, and continuously monitored in the Sudeten mountains (*Fig. 3*).

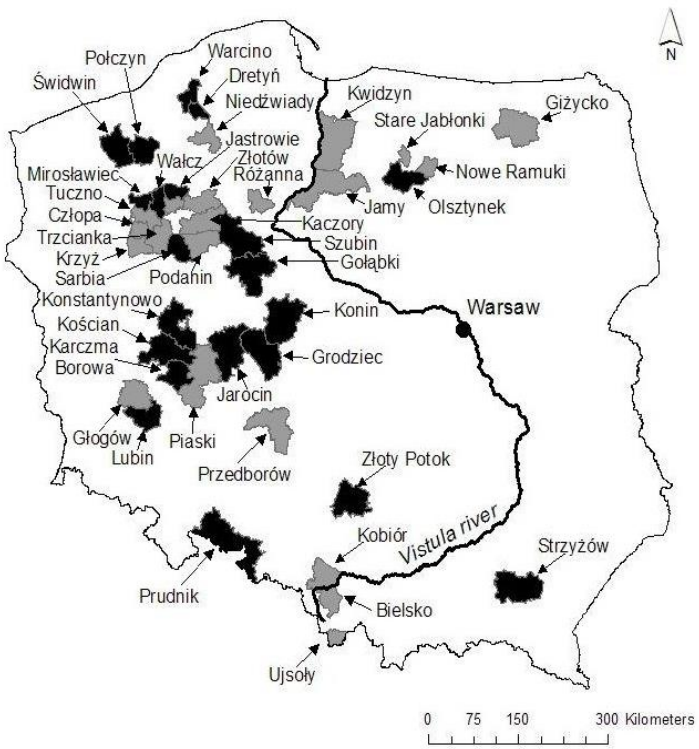


Figure 3. *Introductions of mouflons in Poland during years 1982-2014 (black colour – successful, gray – failed introductions)*

The intensity of introductions has been uneven. Initially, in 1982-1991 mouflons were brought to six F.D., including three forested areas in the northeastern part of the country: Olsztynek, Stare Jabłonki, and Nowe Ramuki; single site in the lower Vistula river basin – Jamy F.D.; Wałcz F.D. in the Pomerania in northern Poland; and Bielsko F.D. in Upper Silesia.

In the following ten years (1992-2001), the number of introductions rose to nine. However, the highest number of introductions and observations of "fugitives" (usually single animals) was noted in the next period, i.e. the years 2002-2011. Hunters released

http://www.aloki.hu ● ISSN 1589 1623 (Print) ● ISSN 1785 0037 (Online)
DOI: http://dx.doi.org/10.15666/aeer/1902_9931017
© 2021, ALÖKI Kft., Budapest, Hungary

and observed groups of 1-20 mouflons – a total of 191 individuals – in 27 places distributed throughout the whole of Poland.

In the above-referred period, the introductions of mouflons did not take place only in central and eastern Poland, i.e. the least forested areas and with severe climate.

In recent years (2012-2014), the intensity of releases has also been quite high. Just in the last three years, hunters have confirmed the presence of 39 mouflons in four new locations: in Jarocin, Świdwin, Krzyż and Połczyn F.D. (*Fig. 4a*).

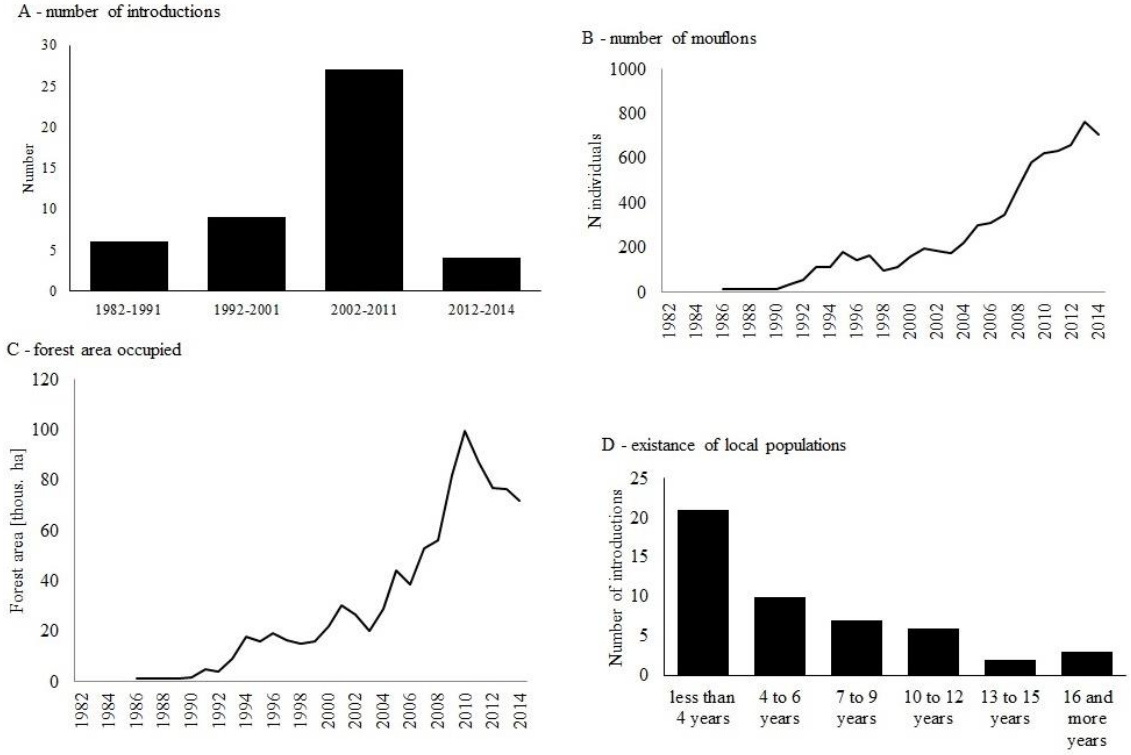


Figure 4. *Characteristics of introductions and history of local populations of mouflons in lowland Poland during the period of 1982-2014*

Despite earlier attempts, lowland mouflon population arose only at the end of the period 1982-2014. At the beginning of this period, only a few to a dozen mouflons lived at large. Over time, there has been an increase in the number of introductions and mouflon population increased to about 700 individuals in 2014. It is worth mentioning that the first successful release of mouflons in that period, carried out in a typical lowland landscape, took place as late as in 1986 in the region of Masuria, in the Olsztynek F.D. The increase in numbers in that period shows two phases. In the first phase (1982-2001) it was slow and strongly correlated with the intensity of releases which was then minor. In subsequent years, beginning in 2002, the mouflon population grew systematically, slowly at the beginning, and rapidly after 2006. It is very likely, that it was the result of intensive introductions made by hunters and not an effect of the development of previously established populations (*Fig. 4b*).

As a consequence of introductions, the area of forests inhabited by mouflons outside mountains has extended. In 1986, mouflons inhabited a single Olsztynek F.D., occupying the area of 1,400 ha. Almost 30 years later the relevant forest area amounted

http://www.aloki.hu ● ISSN 1589 1623 (Print) ● ISSN 1785 0037 (Online)
DOI: http://dx.doi.org/10.15666/aeer/1902_9931017
© 2021, ALÖKI Kft., Budapest, Hungary

to more than 70 thousand hectares. It was, nevertheless, still smaller than the area occupied in 2010, i.e. in the period of the most intensive introduction activities, which amounted to ca. 100 thousand hectares. During the period of the fastest increase in the numbers of mouflons the area occupied by them increased by nearly 50% (*Fig. 4c*).

The history of the local populations that emerged in that time was very diverse. Taking into account the dynamics of releases, populations with history not exceeding three years dominated there. There were 21 of them, accounting for 43%, of all populations which emerged after 1981. Populations that have lasted increasingly longer have become gradually less numerous. Only a few populations survived longer than 13 years. These were represented by mouflons in the following forest districts: Lubin and Dretyń (13-15 years), Wałcz, Olsztynek, Szubin and Lubin – for more than 16 years (7% of all populations) (*Fig. 4d*).

Collected material shows that out of 49 introductions, more than a half (28) ended in failure. The time survived by released groups of mouflons was diverse but the largest group (18 introductions, 64%) comprised animals which did not survive more than three years. About 20% of introductions failed when the animals were still recorded four to six years after introduction. In cases where the animals were still observed after seven to nine years, the percentage of failure was only ca. 10%. Only in one case – in Niedźwiady F.D. (northern Poland) – the local population ceased to exist after 11 years.

Quite the opposite age structure pattern was found in the populations which still exist. The least numerous (15%) are the populations which were set up in 2009-2010, whereas the most numerous were those which have been around for more than 12 years. No failures were registered among introductions in which animals survived for more than 12 years (*Fig. 5*).

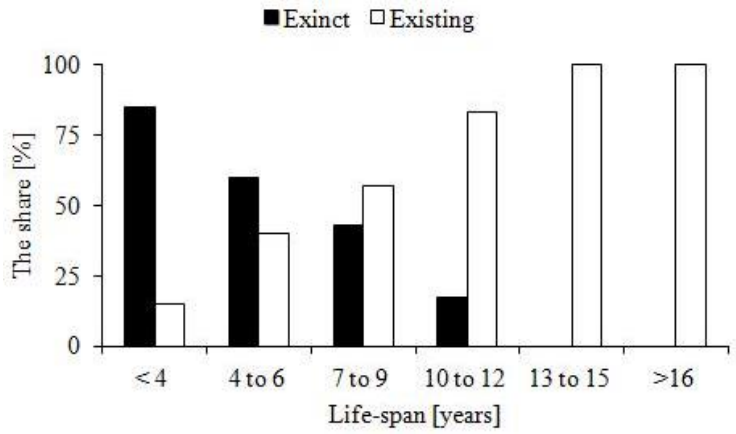


Figure 5. *Proportions of populations introduced after 1982 and extinct before 2014 and population which exist till 2014 in different classes of life-spans*

It seems that the period of 7 to 9 years from the establishment of a population is the threshold value, because at this point similar number of introductions ended in success as in failure. If the mouflons survived this period, the chance for forming a permanent population was, and still is, very high (*Fig. 5*).

For 23 populations of mouflons currently inhabiting lowland Poland it means that a mere ten of them (five which, so far, survived 10 to 12 years, two surviving 13 to 15 years, and three that have lived more than 16 years) stand a major chance of

http://www.aloki.hu ● ISSN 1589 1623 (Print) ● ISSN 1785 0037 (Online)
DOI: http://dx.doi.org/10.15666/aeer/1902_9931017
© 2021, ALÖKI Kft., Budapest, Hungary

continued survival. The duration of populations which were set up after 2007 (i.e. three populations which, so far, have survived 1-3 years, four surviving 4-6 years, and four surviving 7-9 years) does not yet guarantee that stable populations will emerge in these places.

No less dynamic changes occurred in mountain populations, i.e. those in the Polish part of the Sudeten. During the years 1982-2014 there were two evident increases in the numbers of mouflons, separated by periods of stabilization. Between 1982 and 1989 there was the first period of stabilization during which the population of mouflons fluctuated around ca. 500 individuals. Only three years later, the number of mouflons doubled, probably due to the migration of animals from the Czech Republic. This situation lasted, with minor fluctuations (between 1,200 and 1,600 individuals) for nearly 19 years, until 2008. Since 2009 the number of mouflons again grew at a more rapid rate reaching its peak value of 2274 individuals in 2013; so far, this is the greatest value ever recorded in the post-war history of mouflons in Poland (*Fig. 6*).

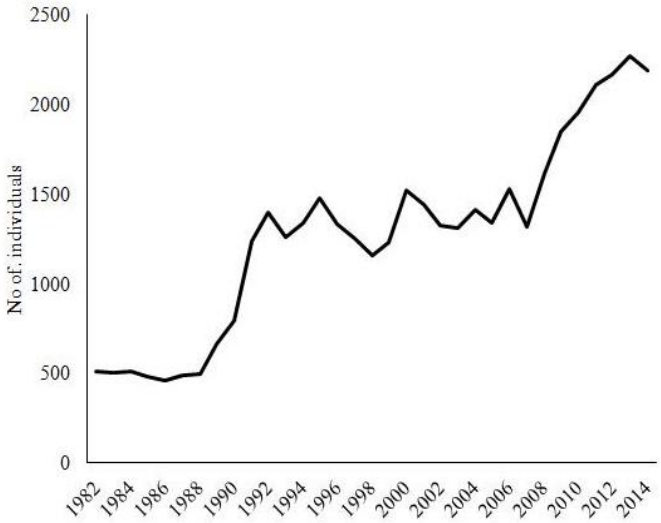


Figure 6. *Changes in the number of mouflons in Polish part of the Sudeten Mt. in the period 1982-2014*

The changes of the numbers of mouflon populations in mountains, were not similar in various ranges within the Sudeten. In some of the ranges, the local populations grew steadily whereas in the others declines were noted. Systematic growth was registered in the Sowie and Bardzkie mountain where the most numerous populations of the Sudeten mouflons lived (ca. 48%). Since 1982, the population there has increased almost fourfold, from ca. 250 to 1,000 animals. A similar phenomenon was observed in the Śnieżnik massif, where only a small fraction (5%) of the whole Sudeten population lives. Also there, over three decades, the number of mouflons tripled, from ca. 30 individuals in 1982 to more than 100 in 2014.

Undoubtedly the highest dynamics characterized the populations from the Wałbrzyskie and Kamienne mountain ranges. Mouflons inhabiting those areas, whose number in 1982 was estimated at ca. 20 individuals, now represent the second largest population in Poland amounting to more than 500 animals.

During the same time, population declines were noted in two ranges of the Sudeten mountains. It was most evident in the Karkonosze inhabited by a small

http://www.aloki.hu ● ISSN 1589 1623 (Print) ● ISSN 1785 0037 (Online)
DOI: http://dx.doi.org/10.15666/aeer/1902_9931017
© 2021, ALÖKI Kft., Budapest, Hungary

group of mouflons (ca. 2.5%). While in 1982 ca. 140 mouflons lived in that area, 32 years later, i.e. in 2014 – only 54 individuals were still present. Thus, there was an almost threefold drop, although it is important to take into account that this location is near the Polish-Czech border so the animals at large are likely to move freely across this border. Therefore, the numbers estimated on only one side of the frontier can be misleading and certainly cannot represent accurately the dynamics of the population.

This situation is similar to that of mouflons living in the Stołowe mountains. These mouflons came as migrants from the Czech Republic and they are probably a fraction of much more numerous population inhabiting the Stołowe mountains on the Czech side. Nevertheless, an almost tenfold increase in their numbers was noted in the 1998-2014 period. Since 1998, when the first 7 individuals were observed, the population has risen to ca. 70 animals and now constitutes ca. 3.2% of all mouflons in the Sudeten mountains according to the 2014 inventory.

The most dynamic changes were recorded in the Kaczawskie mountains. Mouflon population increased there between 1982 and 1994 and then regressed until 2008. This stage was followed, again, by a period of gradual growth which continues until the present day. The amplitude of changes which occurred over the last 30 years in the Kaczawskie mountains shows that this fairly numerous population (16.5%) is still unstable and reacts quickly both to factors limiting its number and to the releases which were carried out in this place in order to improve the quality of individuals (*Fig. 7*).

Constraints and reasons of failures

Even though the intensity of introductions of mouflons in Poland was different in various time intervals within the 1902-2014 period, some of the introductions turned out to be a success whereas others were failed. The failure rate in introductions of mouflons reaches nearly 50% and is yet another feature which distinguishes this species from other wild ungulates in Poland. Not all of the introductions were properly documented, nor their history described in scientific journals or those popularising the knowledge of game management or nature protection. Nevertheless, the available references permit determination of the chief causes of failed introductions or major declines in their numbers (*Table 1*).

Poaching and predation by stray dogs was the most often cited cause of failed mouflon introductions until the 1960s. According to the available information, there was no place in Poland where introduced mouflons would not fall victim to poachers or stray dogs. In some cases, they brought about the disappearance of the whole local populations, e.g. in the Sieraków, Wronki and Ciechanów F.D. (Krysztofik, 1962; Nowak, 1968; Solarz, 2011), or adversely affected the population dynamics, as was the case of some mountainous populations (Nowak, 1968; Łabęcki, 2008). In the post-war period, two or more adverse phenomena frequently overlapped with one another. For example, in the Sudeten, mouflon migrations between Poland and Czech Republic occurred in parallel with poaching and stray dogs, leading to a considerable drop in the number of mouflons in the area of the mountains belonging to Poland. But a reverse phenomenon i.e. rapid increase in "Polish" mouflon populations in the Sudeten area was also observed (Łabęcki, 2008). It is probably due to the proximity of much larger mouflon population at the Czech side of the mountains which has prevented the animals inhabiting the Polish side of the Sudeten mountains from disappearing.

http://www.aloki.hu ● ISSN 1589 1623 (Print) ● ISSN 1785 0037 (Online)
DOI: http://dx.doi.org/10.15666/aeer/1902_9931017
© 2021, ALÖKI Kft., Budapest, Hungary

Table 1. *Known reasons of decline or collapse of local populations of mouflons in Poland since 1902*

Location	Population set up [year]	Decline or extinction [year/s]	Reason of decline or extinction	Does population exist?	Source
Bardzkie Mt.*	1902	1948, 1952, 1987	Poaching and stray dogs, parasitic diseases, inbred	Yes	Łabęcki, 2008 Solarz, 2011
Sowie Mt.*	1902	1952, 1987	Poaching and stray dogs, severe winters, lack of protection and supplemental feeding, migration to C.R., parasitic diseases, inbred	Yes	Nowak, 1968 Nowakowski et al., 2009; Olech and Fruba, 2009
Karkonosze *	1912	1952	Poaching and stray dogs, severe winters, lack of protection and supplemental feeding, migration to C.R.	Yes	Solarz, 2011 Nowakowski et al., 2009
Wałbrzyskie Mt.*	1914	1952, 1958	Severe winters, lack of protection and supplemental feeding, poaching	Yes	Nowak, 1968 Łabęcki, 2008
M. Śnieżnik *	1928	1952	Poaching and stray dogs, severe winters, lack of protection and supplemental feeding, migration to C.R.	Yes	Nowak, 1968 Łabęcki, 2008 Nowakowski et al., 2009
Starzawa	1934	1944	Consequences of World War II	No	Szczepkowski, 1951
Spała	1937	1939	Consequences of World War II	No	Szczepkowski, 1951
Kartuzy	1939	1946	World War II, post war time	No	Szol and Olej, 1946
Sieraków	1942	1950	Poaching, predation of wolfs	No	Nowak, 1968 Solarz, 2011
Wronki	1942	1950	Poaching, predation of wolfs	No	Nowak, 1968 Solarz, 2011
Bytom	1947	1947	Single observation of 9-10 mouflons and unknown reason of disappearance	No	Ostrowski, 1949
Kamienne Mt. *	1948	1952, 1958	Severe winters, lack of protection and supplemental feeding, poaching, migration to C.R.	Yes	Łabęcki, 2008 Nowak, 1968
Stołowe Mt. *	1948	1957	Poaching and stray dogs, lack of supplemental feeding	Yes	Łabęcki, 2008 Nowakowski et al., 2009
Toruń	1949	1949	Single observation of 2 mouflons of unknown origin and unknown reason of disappearance	No	Nowak, 1968
Ciechanów	1950	1950	Poaching, translocation of animals to unknown place	No	Nowak, 1968
Świętokrzyskie Mt.	1951	1960, 1973	Stray dog, poaching, migration to Świętokrzyski National Park	No	Krysztofik, 1962 Solarz, 2011
Kaczawskie Mt.*	1967	1981	Migration to adjacent hunting grounds	Yes	Łabęcki, 2008
Jedwabno	1981	1982	Migrations, predation of stray dogs	No	Jakubowski and Zalewski, 2000
Stare Jabłonki	1987	1988	Migrations	No	Jakubowski and Zalewski, 2000
Nowe Ramuki	1988	1990	Predation of stray dogs	No	Jakubowski and Zalewski, 2000

*Parts of Sudeten Mt.

http://www.aloki.hu ● ISSN 1589 1623 (Print) ● ISSN 1785 0037 (Online)
DOI: http://dx.doi.org/10.15666/aeer/1902_9931017
© 2021, ALÖKI Kft., Budapest, Hungary

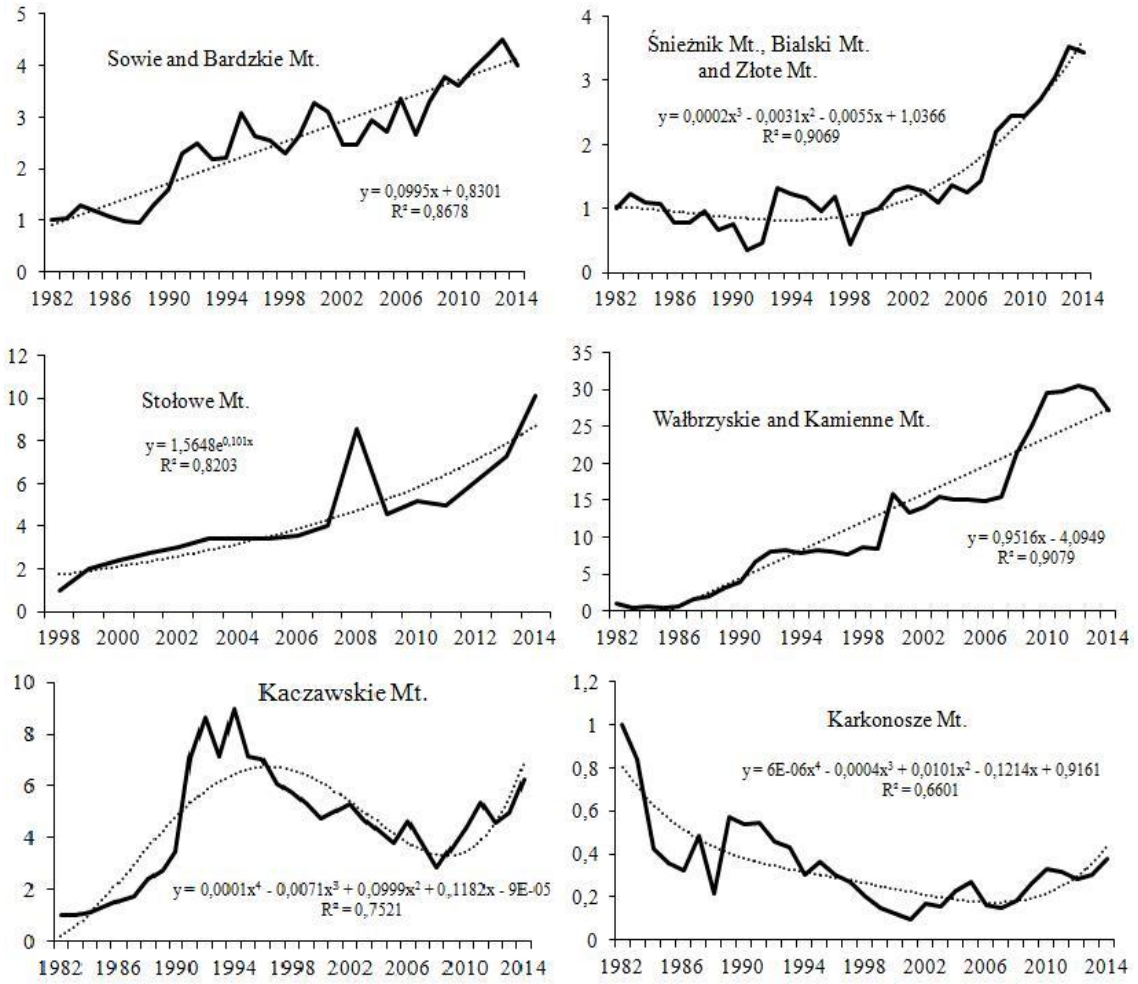


Figure 7. *Trends and relative changes in the number of mouflons in different parts of Sudeten Mt. in the period 1982-2014 (The number of mouflons in 1982, and 1998 for Stołowe Mt. was taken as 1)*

In the case of Świętokrzyskie mountains, the only mountains apart from the Sudeten, disturbances caused by poaching and predation by stray dogs have resulted in the migration of mouflons from the sites of release to the nearby National Park where, deprived of additional feeding during severe winters, their population vanished in early 1970s (Krysztofik, 1962; Solarz, 2011).

Severe winters in Poland and the lack of winter extra feeding, particularly at times of thick snow cover, was the third most often cited reason for the disappearance of mouflon populations. Moreover, it was true not only for the area of mountain ranges but for lowlands as well (*Table 1*).

Poland's climate may also be disadvantageous to mouflons because both its high humidity (good for survival of parasites) and severe winters (debilitating the animals) favour parasitic diseases. Negative effects of both factors on mouflons were reported e.g. by Skálova et al. (2007), and Krozova et al. (2008) from Czech Republic as well as by Meana et al. (1996). As a rule, parasitic infection does not have a lethal effect on the host. However, under unfavourable conditions, parasitic invasions can significantly affect the health and survival rate of the animals. In Poland, according to Kozakiewicz

http://www.aloki.hu ● ISSN 1589 1623 (Print) ● ISSN 1785 0037 (Online)
DOI: http://dx.doi.org/10.15666/aeer/1902_9931017
© 2021, ALÖKI Kft., Budapest, Hungary

and Maszewska (1984), Sołtysiak and Bartczak (1991) and Pacoń (1994) pulmonary and gastrointestinal parasitosis are most frequent and the most harmful.

More or less spontaneous migrations of mouflons also accounted for their failed introductions. A detailed analysis of this phenomenon was presented by Jakubowski and Zalewski (2000) on the basis of unsuccessful introductions in northeastern Poland in the Masuria region in three forest districts: Jedwabno, Stare Jabłonki, and Nowe Ramuki. After their introductions, the animals remained only a short time near the place of their release, and afterwards migrated, for unknown reasons, from a dozen to several dozens of kilometres. They vanished there only one or two years later.

Towards the end of the 1990s, another factor began to negatively affect local populations. It was the inbreeding among animals closely related genetically as they lived in small populations composed of initially small numbers of individuals. Initially the inbreeding was expressed as the deformation of male mouflon horns and mostly concerned isolated populations in the Sudeten mountains (Nowakowski et al., 2009; Olech and Fruba, 2009).

For the time being, the most serious effect of the deformation was the lowering of the value of the horns as hunting trophies, however the problem seems to be serious enough to prompt some forest districts (e.g. Jawor, Bardo Śląskie, Jugów, and Świdnica) to begin, on a major scale, to release mouflons from other localities in order to increase the genetic diversity of the populations living locally (Łabęcki, 2008; Olech and Fruba, 2009).

Current number and distribution

According to data collected for this study, in spring 2014 Polish mouflon population totalled an estimated 2,901 mouflons. This data differs by 57 animals from the official statistics amounting to 2,958 mouflons (GUS Forestry, 2014). This difference probably results from the different status of mouflons kept in enclosures. According to Polish Hunting Law only mouflons living at large in hunting areas should be considered as hunted animals and only these animals are counted in spring and recorded in hunting statistics. Unfortunately, after purchasing mouflons hunters usually keep them in enclosures for a few years and for e.g bookkeeping reasons, they take them into account in hunting statistics.

In Poland, mouflons currently inhabit 24 locations in two types of landscape: mountains (the Sudeten mountains) and lowlands (predominantly in western Poland) (*Fig. 8*). Their population numbers are very diverse, both between the mountainous areas and lowlands, as well as within the Sudeten mountains themselves. Some 75% of the whole Polish population of mouflons live in mountains. The most numerous populations occur in the Sowie and Bardzkie ranges, within the eastern Sudeten mountains. Their total numbers are estimated at ca. 1,000 individuals which corresponds to ca 50% of all mountain mouflons. The next sizeable populations are those of the Wałbrzyskie and Kamienne ranges where inventories show ca. 500 animals (25%), followed by the population in the Kaczawskie range – ca. 350 individuals (16%). The least numerous populations of mouflons live in the Karkonosze and Stołowe mountains where 50 and 70 mouflons were recorded, respectively, in the spring of 2014 (*Fig. 8*). It must be nevertheless underlined that, because of the transboundary nature of the Karkonosze and Stołowe mountains, these mouflons are certainly parts of more numerous Czech populations living on the southern slopes of the Sudeten mountains.

http://www.aloki.hu ● ISSN 1589 1623 (Print) ● ISSN 1785 0037 (Online)
DOI: http://dx.doi.org/10.15666/aeer/1902_9931017
© 2021, ALÖKI Kft., Budapest, Hungary

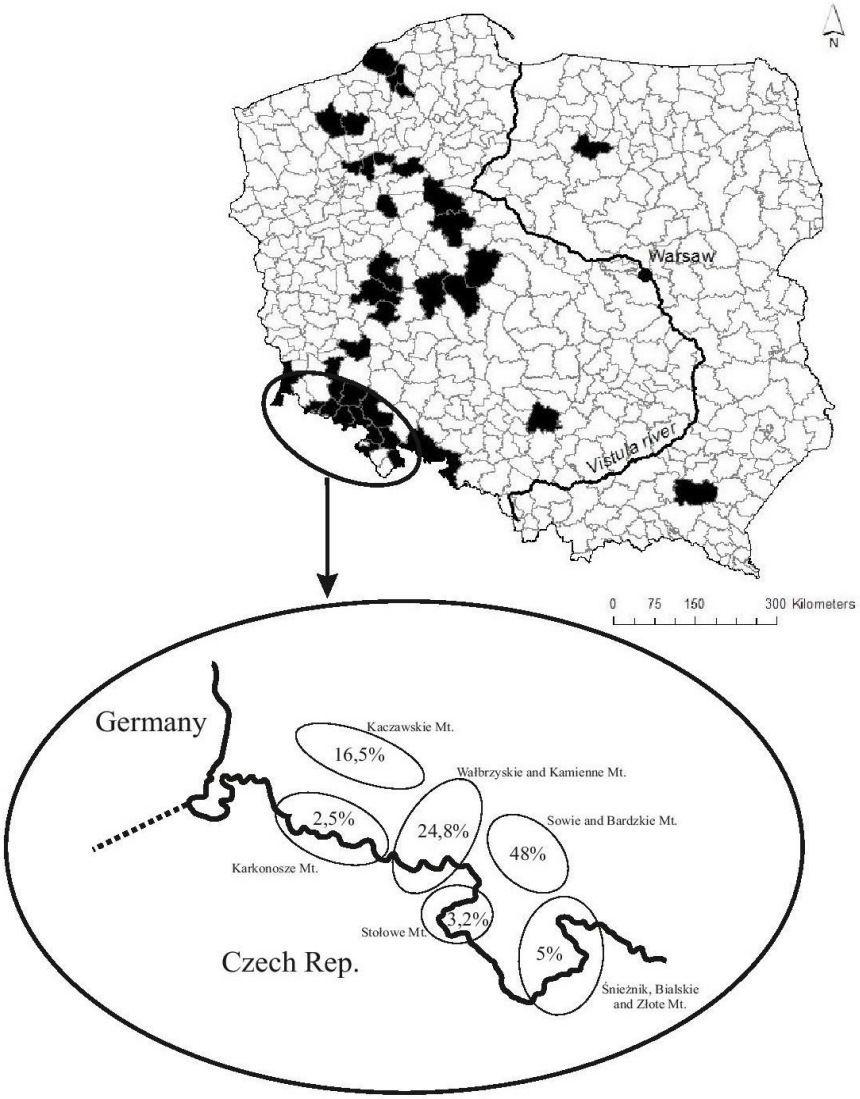


Figure 8. *Location of isolated populations of mouflons in forest districts in lowland Poland and distribution of mouflons in different ranges of Sudeten Mt. in 2014*

The remaining purposeful introductions or migrations of mouflons resulted in the emergence and continued existence of local populations in 23 sites, situated mainly in the lowland forests of western Poland. The only exception is Prudnik F.D. on the eastern border of the Sudeten mountains. Because of the close vicinity of mouflons living in the Sowie mountains, this population, which emerged in 2003, could be considered as mouflons of the Sudeten mountains.

Another exceptional local population includes mouflons living in southeastern Poland, in Strzyżów F.D. This population came to exist in 2005 as an initiative of local hunters (Kiebała, 2013). Despite unfavourable climate in the Carpathian region, the mouflons multiplied from ca. 20 individuals in 2005 to more than 40 individuals in 2014. Today, they represent the southeastern most population of mouflons in Poland.

Similar situation prevails in northeastern Poland, in Olsztynek F.D. The local mouflons living in the area and inhabiting the forests of the Dynowskie foothills, were

http://www.aloki.hu ● ISSN 1589 1623 (Print) ● ISSN 1785 0037 (Online)
DOI: http://dx.doi.org/10.15666/aeer/1902_9931017
© 2021, ALÖKI Kft., Budapest, Hungary

introduced by local hunters 18 years ago and it was the sole successful introduction among several attempts made in the Mazuria region. According to hunting statistics, there were ca. 60 mouflons in the Olsztynek F.D. in the spring of 2014. This population size was reached from the initial herd of some 6-8 animals brought there in 1986. They all have survived, as well as those in Strzyżów, only because they were protected by the hunters.

All the remaining lowland populations of mouflons in Poland occur in the western part of the country, predominantly in the Wielkopolska region, and in the central part of Pomerania. This land is notable for its greater woodiness and it is generally less populated compared with central or southern parts of the country. Moreover, the western part of Poland, which features the Atlantic climate, is warmer, has more precipitation and less severe winters than central and eastern Poland which have a severe continental climate (hot and dry summers, freezing winters).

In Poland, (except for two National Parks in the Stołowe and Karkonosze mountains) mouflons inhabit managed forests typical of local soil and climatic conditions. As a rule, these are forests transformed by humans in previous centuries, and are presently predominated by economically important tree species. In the lowlands, mouflons were released into potentially fertile habitats typical of mixed forests and mixed coniferous forests, such as *Galio-silatici – Carpinetum, Pino – Quercetum*, *Leycobrio – Pinetum*, and *Fago – Carpinetum*. Unfortunately, due to human activities these forests only partly retained their natural floristic composition. By the time mouflons were introduced, these were Scots pine (*Pinus sylvestris*)-dominated forests whereas such species typical of these habitats as oaks (*Quercus sp.*), birches (*Betula sp.*), lime trees *(Tilia sp.)* and hornbeams *(Carpinus betulus)* constituted (and they still constitute today) only small proportions of the tree stands.

Forest districts of Grodziec, Sarbia, and Jastrów represent mouflon breedings in typical commercial pine forests where the proportion of Scots pine exceeds 90% (*Table 2*).

In the Sudeten mountains the situation is very much alike. Taking into account soil and climatic conditions, these mountains should be characterized by strongly diversified plant species – both in the ground cover and in the tree stands. Unfortunately, most forests of the region are dominated by single-species spruce (*Picea abies*) forests set up for the needs of industry in the XIX and XX centuries (Zoll, 1963; Trampler et al., 1990).

Table 2. *Locations and environmental characteristics of forests occupied by local populations of mouflons in Poland in 2014*

F.D. location (expect Sudeten Mt.)	Year of introduction	GPS	Forest area* [ha]	Landscape	Dominant type of vegetation T: Canopy trees (%) P: Potential plant communities
Sudeten Mt.	1902	50.478 N 16.461 E	Ca. 350 000	Lowland (300-500 m a.s.l.) and medium (500-1500 m a.s.l.) mountains (1602 m a.s.l. – highest point)	T: *Picea abies (70%)* P: *Dentario enneaphyllidis – Fagetum, Luzulo nemorosae – Fagetum, Abieti – Picetum (montanum)*
Jawor	1969	50.512 N 15.543 E	15 060	Low and medium hills (690 m a.s.l. – highest point)	T: *Quercus sp. (45%), Picea abies (32%)* P: *Galiosilatici-Carpinetum, Dentario enneaphylli-Fagetum*
Sławno	1973	54.409 N 16.626 E	24210	Lowland	T: *Pinus sylvestris (51%)*, *Fagus silvatica (15%)* P: *Stellario-Carpinetum typicum, Melico-Fagetum*

http://www.aloki.hu ● ISSN 1589 1623 (Print) ● ISSN 1785 0037 (Online)
DOI: http://dx.doi.org/10.15666/aeer/1902_9931017
© 2021, ALÖKI Kft., Budapest, Hungary

Olsztynek	1986	53.579 N 20.206 E	18 230	Lowland/hills (312 m a.s.l. – highest point)	T: *Pinus sylvestris (52%), Betula sp. (14%)* P: *Stellario-Carpinetum typicum,*
Wałcz	1986	53.371 N 16.470 E	16 090	Lowland	T: *Pinus sylvestris (85%)* P: *Leucobryo-Pinetum, Fago-Quercetum petraeae, Pino-Quercetum*
Lubin	1991	51.486 N 16.135 E	21 320	Lowland	T: *Pinus sylvestris (76%)* P: *Galiosilvatici-Carpinetum, Calamagrostio-Quercetum petraeae*
Szubin	1999	53.065 N 17.666 E	26 730	Lowland	T: *Pinus sylvestris (82%)* P: *Leucobryo-Pinetum, Pino-Quercetum, Ficario-Ulmetum chrysosplenietosum*
Dretyń	2000	54.092 N 17.010 E	14 300	Lowland	T: *Pinus sylvestris (82%)* P: *Melico-Fagetum, Pino-Quercetum, Fago-Quercetum petraeae*
Prudnik	2003	50.393 N 17.461 E	16 770	Low and medium hills (785 m a.s.l. – highest point)	T: *Quercus sp. (42%), Pinus sylvestris (21%)* P: *Galiosilvatici-Carpinetum*
Kościan	2003	51.995 N 16.727 E	17 920	Lowland	T: *Pinus sylvestris (70%)* P: *Galiosilvatici-Carpinetum, Ficario-Ulmetum chrysosplenietosum*
Gołąbki	2004	52.774 N 17.841 E	15 710	Lowland	T: *Pinus sylvestris (75%)* P: *Galio silvatici-Carpinetum*
Grodziec	2004	51.991 N 17.980 E	31 700	Lowland	T: *Pinus sylvestris (93%)* P: *Galio silvatici-Carpinetum, Pino-Quercetum*
Strzyżów	2005	49.880 N 21.883 E	29020	Low and medium hills (534 m a.s.l. –highest point)	T: *Abies alba (32%), Fagus silvatica (32%)* P: *Tilio-Carpinetum typicum, Deutario glaudulosae-Fagetum*
Karczma Borowa	2006	51.854 N 16.631 E	13 110	Lowland	T: *Pinus sylvestris (70%)* P: *Galio silvatici-Carpinetum, Ficario-Ulmetum chrysosplenietosum*
Konin	2007	52.357 N 18.385 E	17 990	Lowland	T: *Pinus sylvestris (78%)* P: *Pino-Quercetum, Galio silvatici-Carpinetum, Potentillo albae-Quercetum typicum*
Sarbia	2007	52.997 N 16.798 E	19 920	Lowland	T: *Pinus sylvestris (93%)* P: *Galio silvatici-Carpinetum, Leucobryo-Pinetum*
Mirosławiec	2008	53.330 N 16.180 E	14 500	Lowland	T: *Pinus sylvestris (85%)* P: *Fago-Quercetumpetraeae*
Jastrowie	2009	53.401 N 16.660 E	17 540	Lowland	T: *Pinus sylvestris (91%)* P: *Galio silvatici-Carpinetum, Fago-Quercetum petraeae, Leucobryo-Pinetum*
Warcino	2009	54.228 N 16.934 E	19 320	Lowland	T: *Pinus sylvestris (73%)* P: *Melico-Fagetum, Luzulopilosae-Fagetum*
Złoty Potok	2010	50.747 N 19.252 E	27 280	Lowland	T: *Pinus sylvestris (78%)* P: *Pino-Quercetum, Tilio-Carpinetum, Leucobryo-Pinetum*
Konstantynowo	2010	52.283 N 16.822 E	18 410	Lowland	T: *Pinus sylvestri (68%), Quercus sp. 18%)* P: *Galiosilvatici-Carpinetum*
Świdwin	2012	53.856 N 15.783 E	23 850	Lowland	T: *Pinus sylvestris (55%), Fagus silvatica (12.8%)* P: *Fago-Quercetum petraeae*
Jarocin	2012	51.974 N 17.467 E	24 230	Lowland	T: *Pinus sylvestris (68%), Quercus sp. (20%)* P: *Galio silvatici-Carpinetum, Ficario-Ulmetum chrysosplenietosum*
Połczyn	2014	53.740 N 16.219 E	24 400	Lowland	T: *Pinus sylvestris (58%), Fagus silvatica (14%)* P: *Melico-Fagetum, Pino-Quercetum*

*Total forested area of F.D.

http://www.aloki.hu ● ISSN 1589 1623 (Print) ● ISSN 1785 0037 (Online)
DOI: http://dx.doi.org/10.15666/aeer/1902_9931017
© 2021, ALÖKI Kft., Budapest, Hungary

As regards potential plant communities, the forests of the Sudeten mountains can provide ample fodder and shelter to mouflons, particularly in the lower parts of the mountains. The vegetation of *Dentario enneaphzllidis – Fagetum, Luzulo nemorosae – Fagetum*, and *Abietiti – Picetum montanum* communities, which occupy ca. 70% of the mountain area at an altitude between 500 m a.s.l. and 1000 m a.s.l. (Gorzelak, 1995), can constitute a sufficient fodder base both in summer time (grasses, herbs) and in winter (shrubs) (*Table 2*).

To sum up, in present-day Poland, mouflons live in small, isolated groups inhabiting managed mountain and lowland forests with impoverished natural potential diversity.

Discussion

The history of the mouflon in Poland closely matches the experience obtained in many other efforts to introduce animals for hunting purposes or for their protection (Griffith et al., 1989; Kleiman, 1989; Wolf et al. 1996). This species came into existence, both in Poland and other countries of continental Europe, following some trends reigning in game management at the turn of the XIX and XX centuries. In line with these, the owners of great estates, depending on their tastes and financial resources imported various animal species for hunting. These animals, usually after short time spent in quarantine enclosures, were released into the environment and there often bred under the care of the owners and then hunted down (Long, 2003). In Poland, the principles for importing mouflons have not changed significantly with time. Changes consisted in the replacement of landowners by hunting clubs and the estates – by hunting grounds. The basic mechanism of keeping mouflons in the wild has remained unchanged. Namely, it involves the permanent and far-reaching protection of the species in its natural environment which – as it turns out – is the key factor for the survival of local populations.

Compared with other introductions, the fortunes of mouflons in Poland have demonstrated relatively high effectiveness of their introductions (ca. 50%). Fischer and Lindenmayer (2000) in their analysis of more than 180 cases of reintroductions, supplementations, and translocations made over 20 years, showed that, depending on the criteria they applied, the success rate of introductions only rarely exceeded 30%, irrespective of the animal species involved. Obviously, there is a separate question of the satisfaction felt by the hunting community who would definitely welcome an even higher percentage of successful introductions (Fischer and Lindenmayer, 2000).

The reasons for failed introductions of mouflons in Poland have turned out to be partly convergent with results obtained by other authors. Wolf et al. (1996), in their reanalysis of 421 cases of reintroductions described by Griffith et al. (1989), compiled the ranking of 19 factors with either positive or negative impact on the success of the actions undertaken. Among other factors they included: the quality of the environment, the number of animals introduced, the improvement of living conditions of animals, predation, hunting, competition etc.

The reasons for the disappearance of ca. 50% of local populations of mouflons in Poland, and what is more, soon after their formation, fit at least three factors which are also stressed by Wolf et al. (1996) as being important. These are: poaching – which prevailed particularly in the post-war period, predation by stray dogs, and to a lesser extent by wolves, and finally, severe environmental conditions in winter. The latter factor is compatible with habitat improvement, and primarily with supplemental feeding

http://www.aloki.hu ● ISSN 1589 1623 (Print) ● ISSN 1785 0037 (Online)
DOI: http://dx.doi.org/10.15666/aeer/1902_9931017
© 2021, ALÖKI Kft., Budapest, Hungary

in winter. The number of introduced mouflons and the frequency of introductions are also important. These are also compatible in the case of the species under consideration. For example, in the Sudeten mountains, the introduction of a small number of animals resulted in inbreeding. As a consequence, additional introductions had to be carried out. In this case, the survival of the population would be rather unrealistic in the long run, and human intervention (subsequent introductions) would be necessary.

As opposed to the ranking given by Wolf et al. (1996), the success of the introduction of mouflons in Poland only slightly depended on the quality of the environment. All Polish introductions were performed in forests whose stand compositions were mostly distorted. Moreover, their plant communities were typical of other localities. In lowland Poland, the only exception could be that of the Olsztynek F.D. where there are some kind of hills. A thesis can thus be put forward that it was not so much the quality of habitat but rather the protection and supplemental feeding which had and still has an effect on the survival of mouflons in Poland. However, this aspect has to do with economic burden which is another important factor responsible for the success or failure of reintroduction. This problem was mentioned e.g. by Lindburg (1992), and – with respect to reintroduction projects of other species – also by Kleiman et al. (1991), Bennet (1992), as well as Bangs and Fritts (1996).

Another, separate issue, undoubtedly pertaining not only to the presence of mouflon in Poland and its future, is the necessity to undertake studies that meet the needs of society and decision-makers in order to define the relationship between the objectives of present game management stemming e.g. from the Convention on the Conservation of European Wildlife and Natural Habitats (and the European Charter on Hunting and Biodiversity), and the remnants of old fashions and habits involving alien game animals, disregarding their traditional, economic or recreational importance. What strategy should be adopted for alien species that are already permanently associated with the places of their introduction, are socially accepted, and over time have become not only a hunting attraction?

In the case of the Polish mouflon, the wolf population that has been growing for last decades (Chapron et al., 2014) probably can significantly reduce the number or even eliminate the mouflon from currently inhabited places. However, natural mechanisms will not always „eliminate" questions about other, often numerous alien species. According to official data, there may be more than 300 alien animal species in Poland (Głowaciński et al., 2012). There are also species clearly associated with the history of hunting, such as: fallow deer (*Dama dama*), sika deer (*Cervus nippon*), American mink (*Mustela vison)*, raccoon dog (*Nyctereutes procyonoides*), raccoon (*Procyon lotor*), muskrat (*Ondatra zibethicus*) or even a pheasant (*Phasianus colchicus*), which has been a permanent element of the Polish agricultural landscape for centuries.

The change in the approach to wildlife management, which results from the state of knowledge, understanding of natural processes and social expectations, still leaves open questions as to the future of alien species.

Conclusions

Studies on the history and current distribution of mouflons in Poland lead to several detailed conclusions:

1. In Poland, mouflons inhabit two types of environment, the highlands in the Sudeten mountains, and lowlands – mainly in the western, warmer part of the country.

http://www.aloki.hu ● ISSN 1589 1623 (Print) ● ISSN 1785 0037 (Online)
DOI: http://dx.doi.org/10.15666/aeer/1902_9931017
© 2021, ALÖKI Kft., Budapest, Hungary

2. Local lowland populations are small isolated groups of animals living in the commercial forests typical of the respective regions. Mountain populations in the near-border zone probably remain in contact with mouflons in the Czech Republic. In the other ranges of the Sudeten mountains they also form isolated populations.

3. The main factors affecting the dynamics of mouflon populations in Poland include: severe winters, lack of supplemental feeding, predation by stray dogs, and the consequences of inbreeding. Another significant factor affecting the future of mouflons may also be the development of the wolf population in Poland.

A separate issue, which should certainly be of interest to scientists (not only ecologists, but also sociologists, historians, etc.) is the question of redefining the term "alien species". Over 100 years ago, the introduction of animals beyond their natural range was not questioned. This was often done for hunting purposes. With time, it turned out that some of these introductions were ineffective (e.g. 50% of mouflon introduction in Poland). The consequences of some have a practically small or ambivalent impact on the surrounding environment (pheasant, muskrat), and some have an unfavorable impact (sika deer, American mink, Canadian beaver). However, all of them pose an ethical problem in their further treatment – to accept, maintain or eliminate populations. For example, in modern societies, would there be consent to the elimination of a pheasant that is common in the environment and well known in society? Or, is it only historically justified to maintain a niche mouflon which, though small in number but still locally plays an important historical and social role?

Acknowledgements. The authors would like to thank Lucjan Łabęcki from the Regional Directorate of State Forests in Wrocław for their help in collecting historical data on mouflons in the Sudeten Mountains. We also thank the Research Station of the Polish Hunting Association in Czempiń for providing source data about mouflons in hunting clubs in Poland.

REFERENCES

[1] Bangs, E. E., Fritts, S. H. (1996): Reintroducing the gray wolf to central Idaho and Yellowstone National Park. – Wildlife Society Bulletin 24: 402-413.

[2] Barker, G. (2006): The Agricultural Revolution in Prehistory. Why Did Foragers Become Farmers? – Oxford University Press. London.

[3] Bennet, J. (1992): A glut of gibbons in Sarawak - is rehabilitation the answer? – Oryx 26: 157-164.

[4] Bobek, B., Frąckowiak, W., Furtek, J., Merta, D. (2014): Integration of introduced mouflons with the local population in the Sudeten Mountains. – Balkan Journal of Wildlife Research 1(1): 82-86.

[5] Bobrinskij, J. N., Kuznecow, B. A., Kuzjakin, A. P. (1944): Identifier of Mammals. – CCCP, Moscow (in Russian).

[6] Brachmański, A. (2011): We will not exterminate the mouflon. Interview with Andrzej Tetke, district hunter from Wałbrzych. – Łowiec Polski 2: 16-18 (in Polish).

[7] Cerkal, R., Muska, F. (2010): Damage caused by wild game animals to field crops in the Czech Republic - a historical summary from 1786 to the year 2005. – Journal für Kulturplanzen 62(2): 35-41.

[8] Chapron, G., Kaczensky, P., Linnell, J. D. C., von Arx, M., Huber, D., Andrén, H., López-Bao, J. V., Adamec, M., Álvares, F., Anders, O., Balčiauskas, L., Balys, V., Bedő, P., Bego, F., Blanco, J. C., Breitenmoser, Urs., Brøseth, H., Bufka, L., Bunikyte, R., Ciucci, P., Dutsov, A., Engleder, T., Fuxjäger, Ch., Groff, C., Holmala, K., Hoxha, B.,

http://www.aloki.hu ● ISSN 1589 1623 (Print) ● ISSN 1785 0037 (Online)
DOI: http://dx.doi.org/10.15666/aeer/1902_9931017
© 2021, ALÖKI Kft., Budapest, Hungary

Iliopoulos, Y., Ionescu, O., Jeremić, J., Jerina, K., Kluth, G., Knauer, F., Kojola, I., Kos, I., Krofel, M., Kubala, J., Kunovac, S., Kusak, J., Kutal, M., Liberg, O., Majić, A., Männil, P., Manz, R., Marboutin, E., Marucco, F., Melovski, D., Mersini, K., Mertzanis, Y., Mysłajek, R. W., Nowak, S., Odden, J., Ozolins, J., Palomero, G., Paunović, M., Persson, J., Potočnik, H., Quenette, P. Y., Rauer, G., Reinhardt, I., Rigg, R., Ryser, A., Salvatori, V., Skrbinšek, T., Stojanov, A., Swenson, J. E., Szemethy, L., Trajçe, A., Tsingarska-Sedefcheva, E., Váňa, M., Veeroja, R., Wabakken, P., Wölfl, M., Wölfl, S., Zimmermann, F., Zlatanova, D., Boitani, L. (2014): Recovery of large carnivores in Europe's modern human-dominated landscapes. – Science 346(6216): 1517-19.

[9] Chessa, B., Pereira, F., Arnaud, F., Amorim, A., Goyache, F., Mainland, I., Kao, R. R., Pemberton, J. M., Beraldi, D., Stear, M. J., Alberti, A., Pittau, M., Iannuzzi, L., Banabazi, M. H., Kazwala, R. R., Zhang, Y. P., Arranz, J. J., Ali, B. A., Wang, Z., Uzun, M., Dione, M. M., Olsaker, I., Holm, L. E., Saarma, U., Ahmad, S., Marzanov, N., Eythorsdottir, E., Holland, M. J., Ajmone-Marsan, P., Bruford, M. W., Kantanen, J., Spencer, T. E., Palmarini, M. (2009): Revealing the history of sheep domestication using retrovirus integrations. – Science 324: 532-536.

[10] Dębiec, T. (2014): Difficult decision. – Głos Lasu 4: 20-22 (in Polish).

[11] Fischer, J., Lindenmayer, D. B. (2000): An assessment of the published results of animal relocations. – Biological Conservation 96: 1-11.

[12] Geist, V. (1991): On the taxonomy of giant sheep (*Ovis ammon* Linnaeus, 1766). – Canadian Journal of Zoology 69(3): 706-723.

[13] Głowaciński, Z., Okarma, H., Pawłowski, J., Solarz, W. (eds.). (2012): Alien Species in the Fauna of Poland. – Institute of Nature Protection Polish Academy of Science i Cracow, Cracow.

[14] Gorzelak, A. (1995): Forests and forest management in the Sudeten Mountains. – Prace IBL (B) 25: 7-35 (in Polish).

[15] Griffith, B., Scott, J. M., Carpenter, J. W., Reed, C. (1989): Translocation as a species conservation tool: status and strategy. – Science 245: 477-480.

[16] GUS - Forestry 2014 (2014): Statistical Information and Elaborations. – Central Statistical Office, Warsaw.

[17] Heindleder, S., Kaupe, B., Wassmuth, R., Janke, A. (2002): Molecular analysis of wild and domestic sheep questions current nomenclature and provides evidence for domestication from two different subspecies. – Proceedings of the Royal Society, London (B) 269: 893-904.

[18] Jakubowski, M., Zalewski, K. (2000): Muffelwild in Masuren - Erfolge und Misserfolge bei der Einbürgerung. – Zeitschrift für Jagdwissenschaft 46: 45-50.

[19] Jezierski, W. (1955): Mouflon (monographic sketch). – Pomorsko-poznański Biuletyn Łowiecki 9(32): 20-31 (in Polish).

[20] Kiebała, M. (2013): Introduction and management of the mouflon population (*Ovis aries musimon*, Linnaeus, 1758) in the Strzyżów Forest District. – Dissertation. Postgraduate studies. Wszechnica Polska University, Warsaw (in Polish).

[21] Kleiman, D. G. (1989): Reintroduction of captive mammals for conservation. – BioScience 39: 152-161.

[22] Kleiman, D. G., Beck, B. B., Dietz, J. M., Dietz, L. A. (1991): Costs of a re-introduction and criteria for success: accounting and accountability in Golden Lion Tamarin Conservation Program. – Symposia of the Zoological Society London 62: 125-142.

[23] Kozakiewicz, B., Maszewska, I. (1984): Occurrence and treatment of mouflon parasitosis (*Ovis musimon* L.) in breeding conditions at a hunting center in the Wielkopolska Region. – Medycyna Weterynaryjna 9: 536-538 (in Polish).

[24] Krozova, V., Lamka, J., Szotáková, B., Vokral, I., Srpová, V., Urbánková, M., Kubícek, V., Nobilis, M., Skálová, L. (2008): Dicrocoeliosis of Old Mouflon Ewes - Effect on Biotransformation Enzymes and Metabolism of Anthelmintics In Vitro. – The Open Veterinary Science Journal 2(1): 23-32.

http://www.aloki.hu ● ISSN 1589 1623 (Print) ● ISSN 1785 0037 (Online)
DOI: http://dx.doi.org/10.15666/aeer/1902_9931017
© 2021, ALÖKI Kft., Budapest, Hungary

[25] Krysztofik, E. (1962): Mouflons in the Świętokrzyski National Park. – Łowiec Polski 23/24: 11 (in Polish).
[26] Łabęcki, L. (2008): Mouflon (*Ovis musimon*) in Lower Silesia, Poland. – Dissertation. Postgraduate Studies. Agricultural University in Cracow, Cracow (in Polish).
[27] Lindburg, D. G. (1992): Are wildlife reintroductions worth the cost? – Zoo Biology 11: 1-2.
[28] Long, J. L. (2003): Introduced Mammals of the World: Their History, Distribution and Influence. – CSIRO Publishers, Collingwood.
[29] Lydekker, R. (1913): Catalogue of the Ungulate Mammals in the British Museum (National History). Vol. 1. Artiodactyla. – British Museum, London.
[30] Meana, A., Luzón-Peña, M., Santoago-Moreno, J., DeBulnes, A., Gómez-Bautista, M. (1996): Natural infection by gastrointestinal and bronchopulmonary nematodes in mouflons (*Ovis musimon*) ant their response to netobimin treatment. – Journal of Wildlife Disease 32(1): 39-43.
[31] Nadler, C. F., Lay, D. M., Hassinger, J. D. (1971): Cytogenetic analyses of wild sheep populations in northern Iran. – Cytogenetics 10: 137-152.
[32] Nadler, C. F., Korobitsina, K. V., Hoffmann, R. S., Vorontsov, N. N. (1973): Cytogenetic differentiation, geographic distribution and domestication of palearctic sheep (Ovis). – Zeitschrift für Säugetierkunde 38: 109-125.
[33] Nasiadka, P., Wajdzik, M., Skubis, J. (2015): Current state of research on mouflon (*Ovis musimon*) as a basis for management, protection or elimination of this species from Poland. – Sylwan 159(5): 381-391 (in Polish).
[34] Nasonov, N. (1923): Distribution geographique des mouton sauvages du monde ancient. – Akademija Nauk SSSR, St. Petersburg (in Russian).
[35] Nowak, E. (1968): Mouflon in Poland. – Łowiec Polski 11: 4-5 (in Polish).
[36] Nowakowski, P., Chudoba, K., Piasecki, M. (2009): European muflon (*Ovis orientalis musimon* Schreber, 1782) in the ecosystem of Lower Silesia. – Annales Universitatis Mariae Curie-Skłodowska Lublin - Polonia, Sectio EE XXVII(4): 7-13.
[37] Olech, W., Fruba, A. (2009): Attempt to Link Genetic Profile to Occurrence Horn Deformation in the Polish Population of the Mouflon (*Ovis Musimon*). – Final Report on the Expertise for the Directorate General of State Forests Carried Out at the Department of Genetics and General Animal Breeding, Faculty of Animal Sciences, Warsaw University of Life Sciences, Warsaw (in Polish).
[38] Ostrowski, J. (1949): Mouflons. – Łowiec Polski 1/2: 10-12 (in Polish).
[39] Pacoń, J. (1994): Mouflon, deer and roe deer parasites from Lower Silesia. – Wiadomości Parazytologiczne 40(3): 279-292 (in Polish).
[40] Payne, S. (1968): The origin of domestic sheep and goats: a reconsideration in the light of the fossil evidence. – Proceedings of the Prehistoric Society 34: 368-384.
[41] Piegert, H., Uloth, W. (2000): Das Europäische Mufflon. – DSV-Verlag GmbH, Edition Naturlife, Hamburg.
[42] Riley, S. J., Decker, D. J., Carpenter, L. H., Organ, J. F., Siemer, W. F., Mattfeld, G. F., Parsons, G. (2002): The Essence of Wildlife Management. – Wildlife Society Bulletin 30(2): 585-593.
[43] Simmons, A. H. (2007): The Neolithic Revolution in the Near East; Transforming Human Landscape. – The University of Arizona Press, Tucson.
[44] Skálová, L., Kríová, V., Cvilink, V., Szostakova, B., Storkánova, L., Velik, J. (2007): Mouflon (*Ovis musimon*) dicrocoeliosis: effect of parasitosis on the activities of biotransformation enzymes and albendazole metabolism in liver. – Veterinary Parasitology 146(3-4): 254-262.
[45] Solarz, W. (2011): Muflon *Ovis Ammon* Linnaeus, 1758. – In: Głowaciński, Z.; Okarma, H.; Pawłowski, J.; Solarz, W. (eds.) Alien Species in the Fauna of Poland. Institute of Nature Protection Polish Academy of Science in Cracow, Cracow.

http://www.aloki.hu ● ISSN 1589 1623 (Print) ● ISSN 1785 0037 (Online)
DOI: http://dx.doi.org/10.15666/aeer/1902_9931017
© 2021, ALÖKI Kft., Budapest, Hungary

[46] Sołtysiak, Z., Bartczak, R. (1991): Invasion of pulmonary nematodes from the Protostrongylidae family in the mouflons living in the Sowie Mountains. – Medycyna Weterynaryjna 47(4): 160-161 (in Polish).
[47] Szczepkowski, J. (1951): Muflon. – PWRiL, Warszawa (in Polish).
[48] Szczęśniak, E. (2011): The presence of mouflons (Ovis aries musimon) in Poland - is it really necessary? – Chrońmy Przyrodę Ojczystą 2: 99 (in Polish).
[49] Szol, J. T., Olej, N. (1968): Mouflons in Poland. – Łowiec Polski 3(48): 119 (in Polish).
[50] Tomiczek, H., Türcke, F. (2003): Das Muffelwild. – Franck-Kosmos Verlag GmBH & Co KG, Stuttgart.
[51] Trampler, T., Kliczkowska, A., Dmyterko, E., Sierpińska, A. (1990): Forest and Nature Regionalization on Ecological and Physiographic Basis. – PWRiL, Warszawa (in Polish).
[52] Tsalkin, V. I. (1951): Mountain sheep of Europe and Asia: materials on the fauna and flora of the USSR. – Moscow Society of Naturalists, New Series, Zoology Department 27: 255-265 (in Russian).
[53] Valdes, R., Nadler, C. F., Bunch, T. D. (1978): Evolution of wild sheep in Iran. – Evolution 32: 56-72.
[54] Wajdzik, M., Witek, K., Nasiadka, P., Skubis, J. (2014): Trophy quality of mouflons in the Bardzkie Mountains. – Sylwan 158(12): 911-919 (in Polish).
[55] Wilson, D., Reeder, D. M. (eds.) (2005): Mammal Species of the World. A Taxonomic and Geographic Reference. – Johns Hopkins University Press, Baltimore.
[56] Wolf, C. M., Griffith, B., Reed, C., Temple, S. A. (1996): Avian and mammalian translocations: update and reanalysis of 1987 survey data. – Conservation Biology 10: 1142-1154.
[57] Zoll, T. (1963): Analysis of the condition of forests in the Sudeten Mountains. – Zeszyty Problemowe Podstaw Nauk Rolniczych 37: 123-144 (in Polish).

http://www.aloki.hu ● ISSN 1589 1623 (Print) ● ISSN 1785 0037 (Online)
DOI: http://dx.doi.org/10.15666/aeer/1902_9931017
© 2021, ALÖKI Kft., Budapest, Hungary

EFFECTS OF CADMIUM - SALT INTERACTIONS ON GROWTH AND SOME GENES IN WHEAT

DOĞRU, H. – ERGÜN, N.*

Mustafa Kemal University, Science and Art Faculty, Biology Department, Antakya, Hatay, Turkey

**Corresponding author*
e-mail: ergun.nuray@gmail.com

(Received 11th Jul 2020; accepted 19th Jan 2021)

Abstract. Due to the increase in human population and anthropogenic factors, agricultural lands have been affected by salinization and heavy metal pollution has increased. In this study, the effects of cadmium and salt interactions on Konya - 2002 and Dağdaş - 94 varieties of *Triticum aestivum* L. seedlings were investigated. Catalase and glutathione reductase activities were determined as well as proline content and expression of TaMYB73, TaSRG and TaERF1 genes. Cd and salt applications caused an increase in catalase, glutathione reductase activities and free proline content in both cultivars. With Cd and salt applications, Dağdaş - 94 variety was more resistant than Konya - 2002. TaMYB73 expression did not increase under either treatment. Dağdaş exhibited the highest increase in gene expression. High NaCl and Cd concentrations caused an increase in ERF1 expression in Dağdaş variety. Increased TaSRG expression in Dağdaş under low NaCl concentrations has probably been associated with salt tolerance. Increased TaSRG expression with Cd administration in Konya probably corresponded to genes related to Cd resistance.
Keywords: *catalase, glutathione reductase, TaMYB73, TaSRG, TaERF1*

Introduction

Cereals meet half of the protein and carbohydrate requirements of humans. Therefore, they rank first among the cereals cultivated (Durán et al., 2007).

Currently, abiotic stress (including temperature, water, light, NaCl and pH) leads to the loss of more than half of the product. Salinity affects the yield of soils used to cultivate wheat (*Triticum aestivum* L.), leading to the inefficiency of 10 million hectares of land annually. Salt stress is mainly caused by evaporation and lack of rainfall (Doğan and Çarpıcı, 2015).

Salt stress reduces the growth and yield of plants, especially in climatic zones with low rainfall. Salinity is a major threat to modern agriculture, hindering crop growth and development (Isayenkov and Maathius, 2019). Salts in the soil dissolve with irrigation and rainfall; leaking to lower soil layers; and may even reach the sea, which can mix with groundwater. In arid regions, salt washing and evaporation lead to the accumulation of salt on the soil surface referred to as salt stress.

High concentrations of salt ions in salty soils lead to reduced water absorption in plants, rendering toxic effects and enzymatic activity changes. The deterioration in the ion balance and lack of water reduces the nutrient transport and membrane permeability of plants. Vital functions in plants such as photosynthesis and respiration are inhibited; the growth of roots and aboveground parts is retarded; and the number of buds decreases.

According to Doğan and Çarpıcı (2015), salty lands were reportedly improved by the elimination of infertile effects of saline soils; however, the methods for this

http://www.aloki.hu ● ISSN 1589 1623 (Print) ● ISSN1785 0037 (Online)
DOI: http://dx.doi.org/10.15666/aeer/1902_10191031
© 2021, ALÖKI Kft., Budapest, Hungary

improvement are time - consuming and exhausting. Therefore, the selection of salt-resistant species and varieties in saline soils is very important. Species grown in suitable environments will increase the yield, and hence wheat production.

Currently, heavy metal pollution is gradually increasing worldwide due to industrialization and human activities. Cadmium (Cd, the atomic number of 48) is a heavy metal that exerts a serious threat to human health; it is one of the most dangerous heavy metal pollutants in the ecosystem, and it is toxic to living organisms. Due to the long - term use of phosphorous manure and sewage sludge, low or moderate concentrations of cadmium are observed in agricultural soils in several parts of the world (Tirry et al., 2018). Meanwhile, proline is a key osmoregulatory amino acid that ensures the integrity of proteins as well as activates enzymes in plants under salt (NaCl) stress. Proline content increases when plants are exposed to stress conditions (Öncel et al., 2000).

Heavy - metal contamination in plants causes genotoxic effects; thus, mutation - like changes are observed in the DNA structure. Batır (2014) has examined the effect of lead (Pb) and copper (Cu) on artichoke (*Cynara scolymus* L.) seedlings by physiological, biochemical and molecular methods. Different concentrations of heavy metals lead to a decrease in the root length and ratio of the total soluble protein in seedlings. The randomly amplified polymorphic DNA - polymerase chain reaction Randomly Amplified Polymorphic DNA - Polymerase Chain Reaction (RAPD - PCR) screening method was employed to determine the genotoxic effects of heavy metal stress on seedlings. Compared to control group seedlings, those exposed to heavy metal stress exhibit different changes such as new bands and/or loss of bands in their RAPD profiles. As a result, the genomic template stability of artichoke seedlings exposed to Pb and Cu stress changes according to their RAPD profiles.

He et al. (2012) have reported that the TaMYB73 (myeloblastosis oncogene) gene stimulates NaCl dehydration and several phytohormones under NaCl stress conditions and that the overexpression of the relevant gene increases the tolerance to salt stress by playing a role in the ionic stress response in *Arabidopsis*. MYB is a transcription factor. Previously, the MYB transcription factor has been reported to play a role in plant responses to biotic and abiotic stresses, cell development and signal transfer (Wang et al., 2016).

He et al. (2011) have reported that the wheat TaSRG gene serves as a transcription agent in plant varieties and increases tolerance. Also, in their study, the TaSRG gene function is related to salt tolerance. Ethylene - responsive factor (ERF) transcription factors constitute a family including 147 members according to plant species. The ERF gene expression is crucial for adaptation to several biotic and abiotic stresses (Cheng et al., 2013).

Wheat plays an important role in the nutrition of the population in the world and Turkey. Abiotic factors such as salt and heavy metal pollution are known to decrease wheat yield. Therefore, the selection of both stress-resistant wheat varieties is a decisive factor for agricultural production. It is known that plants develop tolerance to stress factors. It is important to determine the biochemical, physiological and molecular mechanisms that ensure the tolerance of wheat to salt and heavy metal stress.

Owing to the limited number of studies on the salt application in wheat seedlings exposed to heavy metal stress, in this study, effects of the applications of salt (100 mM, 200 mM), cadmium (10 mM) and salt–cadmium (100 mM NaCl + 10 mM Cd, 200 mM NaCl + 10 mM Cd) on the free proline content, as well as CAT and GR activities, on

http://www.aloki.hu ● ISSN 1589 1623 (Print) ● ISSN1785 0037 (Online)
DOI: http://dx.doi.org/10.15666/aeer/1902_10191031
© 2021, ALÖKI Kft., Budapest, Hungary

wheat (*T. aestivum* L. cv. Konya - 2002, Dağdaş - 94) seedlings were investigated, and biochemical parameters, as well as TaMYB73, TaSRG, TaERF transcription factors, were examined by molecular biological methods. Also, the Konya - 2002 and Dağdaş - 94 wheat varieties were compared in terms of the specified parameters, and whether these varieties exhibit tolerance to different salt concentrations and Cd stress was investigated. Biochemical studies were spectrophotometrically conducted for CAT and GR activities and free proline content, and real-time PCR (RT - PCR) was employed for TaMYB73, TaSRG and TaERF.

Materials and Methods

Materials

Wheat is one of the most important cereal in Turkey. Therefore, our study common varieties of wheat produced in Turkey (*T. aestivum* L. cv. Konya - 2002 and *T. aestivum* L. cv Dağdaş -94) were used. Wheat seeds were obtained from the Directorate of Bahri Dağdaş International Agricultural Research Institute (Konya, Turkey). The Konya - 2002 wheat variety is known to be sensitive to drought but exhibits good resistance to incubation, winter and cold (Anonym, 2020). The Dağdaş - 94 wheat variety is known to be resistant to drought, incubation and cold (Öztürk and Aydin, 2017).

Methods

Plant Growth Conditions

Seeds were sterilized by 20 - min incubation in a 2% sodium hypochlorite solution, washed with pure water, and incubated in pure water for 1 h to swell. Then, the seeds were placed in perlite - containing pots and incubated at 24 ± 2 °C for germination. The seeds were watered with 200 mL of pure water on average for 7 days and transferred to 1 - L plastic pots containing the Arnon–Hoagland nutrient solution after germination. Seedlings in the plastic pots were grown at 24/16 °C day/night conditions for 5 days. At the end of the fifth day, the pots were divided into 12 groups (Öncel et al., 2000; Ergün and Öncel, 2012).

Group 1 (Konya control): The growth conditions (24/16 °C day/night) were maintained constant since the day the seedlings were taken into the water culture on the 10th day.

Group 2 (Konya NaCl 100 mM): The seedlings were treated with 100 mM NaCl on the 6th day.

Group 3 (Konya cadmium group): The seedlings were treated with 10 mM Cd at the beginning of the 6th day.

Group 4 (Konya NaCl 100 mM + cadmium): The seedlings were treated with 100 mM NaCl and 10 mM Cd at the beginning of the 6th day.

Group 5 (Konya NaCl 200 mM): The seedlings were treated with 200 mM NaCl on the 6th day.

Group 6 (Konya NaCl 200 mM + cadmium): The seedlings were treated with 200 mM NaCl and 10 mM Cd at the beginning of the 6th day.

Group 7 (Dağdaş control): The growth conditions (24/16 °C day/night) were maintained constant since the day the seedlings were taken into the water culture on the 10th day.

http://www.aloki.hu ● ISSN 1589 1623 (Print) ● ISSN1785 0037 (Online)
DOI: http://dx.doi.org/10.15666/aeer/1902_10191031
© 2021, ALÖKI Kft., Budapest, Hungary

Group 8 (Dağdaş NaCl 100 mM): The seedlings were treated with 100 mM NaCl on the 6th day.

Group 9 (Dağdaş cadmium group): The seedlings were treated with 10 mM Cd at the beginning of the 6th day.

Group 10 (Dağdaş NaCl 100 mM + cadmium): The seedlings were treated with 100 mM NaCl and 10 mM Cd at the beginning of the 6th day.

Group 11 (Dağdaş NaCl 200 mM): The seedlings were treated with 200 mM NaCl on the 6th day.

Group 12 (Dağdaş NaCl 200 mM + cadmium): The seedlings were treated with 200 mM NaCl and 10 mM Cd at the beginning of the 6th day.

In our study, each experiment was conducted in triplicate. During the experiment, the location of the containers was randomly changed in a clockwise direction. The wheat seedlings were harvested on the 10th day. After harvesting, the shoot parts of the seedlings were cut into small pieces for some analyses (i.e. CAT, GR and free proline), labelled according to the group number of the seedlings and stored at −80 °C in a deep freezer. Samples were repeatedly prepared three times. The SPSS program was used for statistical analysis. Arithmetic means standard deviations and standard errors of the experimental results were calculated. Duncan's multiple range test was employed to determine the significant differences between means.

Glutathione reductase (GR) activity was measured according to Cakmak and Marschner (1992) and Çakmak (1994). Catalase enzyme activity (CAT) was measured at 240 nm in a spectrophotometer due to the fragmentation rate of H_2O_2. The reaction mixture consists of (1 ml), 50 mM phosphorus buffer (pH 7.6), 0.1 mM EDTA, 100 mM H_2O_2 and enzyme extract (Çakmak and Marschner, 1992). Free proline extraction and determination made according to Bates et al. (1973).

Determination of gene expressions was measured the wheat samples were exposed to cadmium and salt stresses and grown under specific conditions for a certain period. Then, leaf samples were collected after harvest and placed in liquid nitrogen. The samples were stored at −80 °C until RNA analyses were performed. For total RNA isolation and reverse transcription about 1 g of wheat leaves divided into small pieces and taken into 2 ml tube and these analyzes was made considering the work of Ergün et al. (2014).

Quantitative real-time PCR (Q - PCR) Protocol; The Biospeedy™ Relative Count Kit (Turkey) was used to determine the gene expression level in 12 wheat samples exposed to different stress factors. All genes were studied in 3 replicates and 2 ^ - ΔΔCt Method (Livak and Schmittgen, 2001) was used for the experiment.

The kit included target genes of the MYB73 gene encoding putative transcription factor, ERF1 gene encoding ethylene-responsive factor 1, and *T. aestivum* salt response, or TaSRG, gene. Actin was used as the housekeeping gene, which encodes a protein in wheat, to normalize expression levels of target genes. The kit included primers specific to the housekeeping and target genes as well as the enzymes and buffers required for RT - PCR.

The Roche LC 96 (Roche, Switzerland) RT - PCR instrument was employed for all reactions. The reaction contained 1.5 mM $MgCl_2$, 0.2 mM dNTP mix, 1x reaction buffer, 0.1U Fast Start Taq DNA polymerase, 1× EvaGreen, 4 ng/µL of template cDNA and 0.5 µM of each primer. In the instrument, annealing temperatures specific to the primer pairs (*Table 1*) and the optimized reaction cycle temperatures were utilized. During qPCR, melt curve analysis was performed only between 65 °C and 98 °C to

http://www.aloki.hu ● ISSN 1589 1623 (Print) ● ISSN1785 0037 (Online)
DOI: http://dx.doi.org/10.15666/aeer/1902_10191031
© 2021, ALÖKI Kft., Budapest, Hungary

ensure that only the desired product was amplified. qPCR data were analysed by Roche Lightcycler 96 Software 1.1.

Table 1. *Names, code names, sequences and amplicon lengths of the primers used in the study*

Primer Name	Sequence (5′ - 3′)	Annealing Temperature °C	Reference
TaSRG - F (*T. aestivum* salt response gene)	GAAGATGGAGGTCAGGGACA	56	Ergün, Kolukırık, 2014
TaSRG - R	AGCTCTTGCTGAGAGGCTTG		
ActinF	GTCGGTGAAGGGGACTTACA	55	Ergün, Kolukırık, 2014
ActinR	TTCATACAGCAGGCAAGCAC		
ERF1 – F (Ethylene - responsive factor1)	TCCTGTGATGGGTGATGCTA	54	Ergün, Kolukırık, 2014
ERF1 - R	AGGGCATGTCATCAAAGGTC		
MYB73 - F (myeloblastosis oncogene)	GACAGCTTCTGGTCGGAGAC	54	Ergün, Kolukırık, 2014
MYB73 - R	CGACGACGGCGATAAACTAT		

Data Evaluation

The data of the study group were shown as mean ± standard error. The data related to the application groups were analyzed with One-Way Anova in SPSS 22.00 program and the differences between the means were compared with Duncan multiple comparison test (SPSS, 2019). For gene analysis; Arc Stat XLISPPLUS version 3.04 (http://www.stat.umn.edu/arc/software.html) software was employed for PCR data, and the MacAnova (http://www.stat.umn.edu/macanova/) program was employed for variance analysis. Fisher's protected least - significant test was employed to compare the mean threshold cycle values (Ct) ($p < 0.05$).

Results

The obtained results were examined to determine the differences between the control group wheat seedlings (*T. aestivum* L. cv. Konya - 2002 and *T. aestivum* L. cv. Dağdaş - 94) and seedlings exposed to salt and Cd. The CAT and GR activities and proline accumulation in wheat seedlings, as well as RT - PCR analyses of TaMYB73, TaSRG and TaERF1 transcription factors expressed under stress conditions, were investigated.

Effects on Catalase and Glutathione Reductase Activities

The CAT activity in wheat seedlings of the Dağdaş - 94 variety was greater than that of the Konya - 2002 variety ($p \leq 0.01$). Compared to the salt application ($p \leq 0.05$), by the Cd application, the CAT activity increase was greater for the wheat seedlings of the Dağdaş - 94 variety (*Fig. 1*).

http://www.aloki.hu ● ISSN 1589 1623 (Print) ● ISSN1785 0037 (Online)
DOI: http://dx.doi.org/10.15666/aeer/1902_10191031
© 2021, ALÖKI Kft., Budapest, Hungary

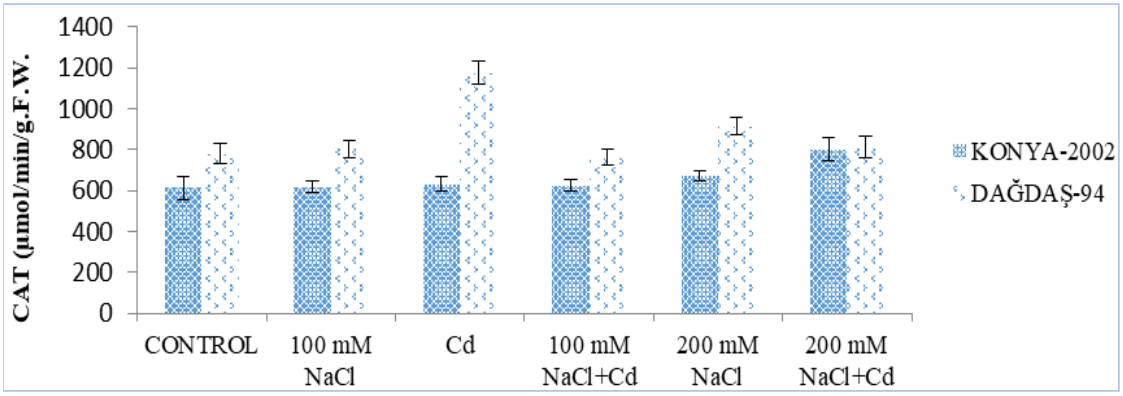


Figure 1. *Changes in the catalase activity of wheat (T. aestivum L. cv. Konya - 2002 and T. aestivum L. cv. Dağdaş - 94) samples grown under 100 mM NaCl, Cd, 100 mM NaCl + Cd, 200 mM NaCl and 200 mM NaCl + Cd conditions (n = 3)*

By applications of 10 mM Cd and 200 mM NaCl + 10 mM Cd compared to the control, the Konya - 2002 seedlings exhibited an ~2 - fold increase in the GR activity. By applications of 10 mM Cd and 200 mM NaCl + 10 mM Cd compared to the control ($p \leq 0.01$), the Dağdaş - 94 seedlings exhibited an ~3 - fold increase in the GR enzyme activity (*Fig. 2*).

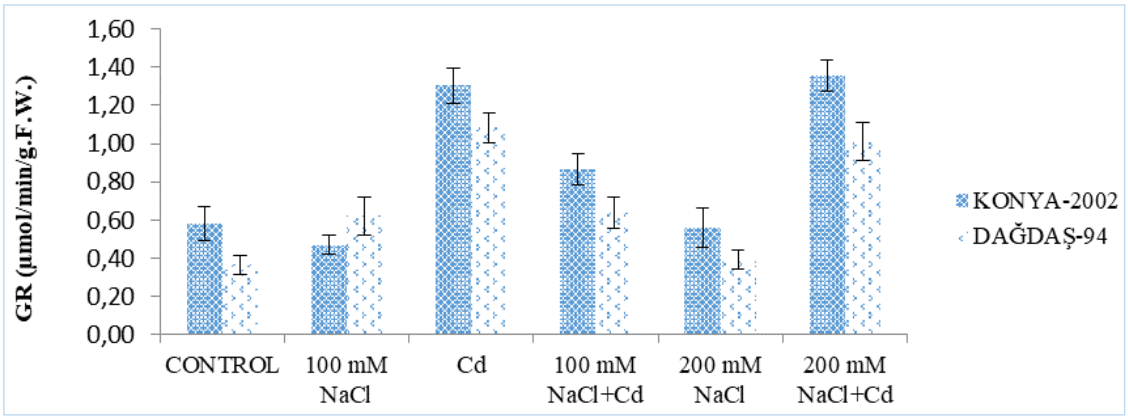


Figure 2. *Changes in the glutathione reductase activity of wheat (T. aestivum L. cv. Konya - 2002 and T. aestivum L. cv. Dağdaş - 94) samples grown under 100 mM NaCl, Cd, 100 mM NaCl + Cd, 200 mM NaCl and 200 mM NaCl + Cd conditions (n = 3)*

Proline Content

The accumulation of proline increased with stress application in both wheat varieties. The amount of proline in wheat seedlings of Konya - 2002 variety increased by 10 times more than the control samples by the application of 200 mM NaCl ($p \leq 0.01$). By the application of 200 mM NaCl + 10 mM Cd compared to the Cd only application, the Konya - 2002 seedlings exhibited an ~11 - fold increase in the proline accumulation. In Dağdaş - 94 seedlings, the proline accumulation increased 3 - fold by the 100 mM NaCl application, 5 - fold by the 100 mM NaCl + Cd application, 8 - fold by the 200 mM NaCl application, 7 - fold by the 200 mM NaCl + Cd application compared to the

http://www.aloki.hu ● ISSN 1589 1623 (Print) ● ISSN1785 0037 (Online)
DOI: http://dx.doi.org/10.15666/aeer/1902_10191031
© 2021, ALÖKI Kft., Budapest, Hungary

control group and Cd only application. Hence, the increase in proline accumulation corresponds to the salt application ($p \leq 0.01$) (*Fig. 3*).

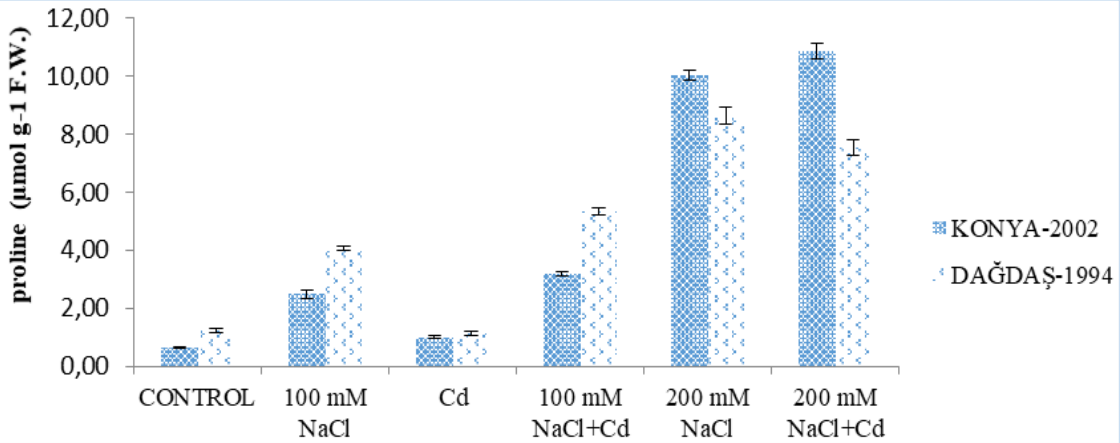


Figure 3. *Changes in the content of free proline in wheat (T. aestivum L. cv. Konya - 2002 and T. aestivum L. cv. Dağdaş - 94) samples grown under 100 mM NaCl, Cd, 100 mM NaCl + Cd, 200 mM NaCl and 200 mM NaCl + Cd conditions (n = 3)*

Gene Expressions and Results

mRNA transcription in *T. aestivum* L. cv. Konya - 2002 and Dağdaş - 94 varieties exposed to salt and heavy metals were examined by quantitative mRNA analyses via RT - PCR. In qPCR, the number of cycles at which DNAs started to undergo logarithmic amplification (Ct) was less than 35, indicative of efficient DNA amplification. As only one temperature corresponded to each gene in the melt curve analysis, the experimental findings were assessed to be positive. The specific melting temperatures of PCR products were 84.00 ± 0.50, 88.00 ± 1.00, 86.00 ± 1.00 and 87 ± 0.50 °C for actin, MYB, ERF and SRG, respectively.

TaMYB73 Gene Results

In this study, the TaMYB73 gene expression in all samples decreased by the application of Cd and NaCl compared to the control. Under control conditions, the TaMYB73 gene expression was ~50% greater in the Konya - 2002 seedlings than in the Dağdaş - 94 seedlings ($p \leq 0.01$) (*Fig. 4*).

TaSRG Gene Results

The TaSRG gene expression is known to be associated with salt tolerance in plants. The increase in the TaSRG expression in Dağdaş - 94 seedlings exposed to low salt concentrations may be associated with the increase in salt tolerance in the relevant variety. Herein, the cadmium salt $CdCl_2$ was used as the heavy metal. The increase in the TaSRG expression in the Konya - 2002 variety by the application of Cd was possibly related to the genes related to Cd stress resistance in the relevant variety. By the comparison of the Konya - 2002 and Dağdaş - 94 varieties of *T. aestivum* L. wheat seedlings, the Dağdaş - 94 seedlings exhibited an ~3 - fold increase in the TaSRG gene expressions under 100 mM NaCl conditions compared to the control. In contrast, gene expression was reduced by 50% in 200 mM salt administration compared to control and

http://www.aloki.hu ● ISSN 1589 1623 (Print) ● ISSN1785 0037 (Online)
DOI: http://dx.doi.org/10.15666/aeer/1902_10191031
© 2021, ALÖKI Kft., Budapest, Hungary

by ~ 90% compared to 100 mM salt administration ($p < 0.01$). By the application of Cd, the SRG rate the Konya - 2002 variety exhibited a 7 - fold greater increased than that observed for the Dağdaş - 94 variety. Herein, the TaSRG ratio decreased by the applications of 100 mM NaCl + 10 mM Cd, 200 mM NaCl and 100 mM NaCl + 10 mM Cd compared to the control in both cultivars ($p \leq 0.01$) (*Fig. 5*).

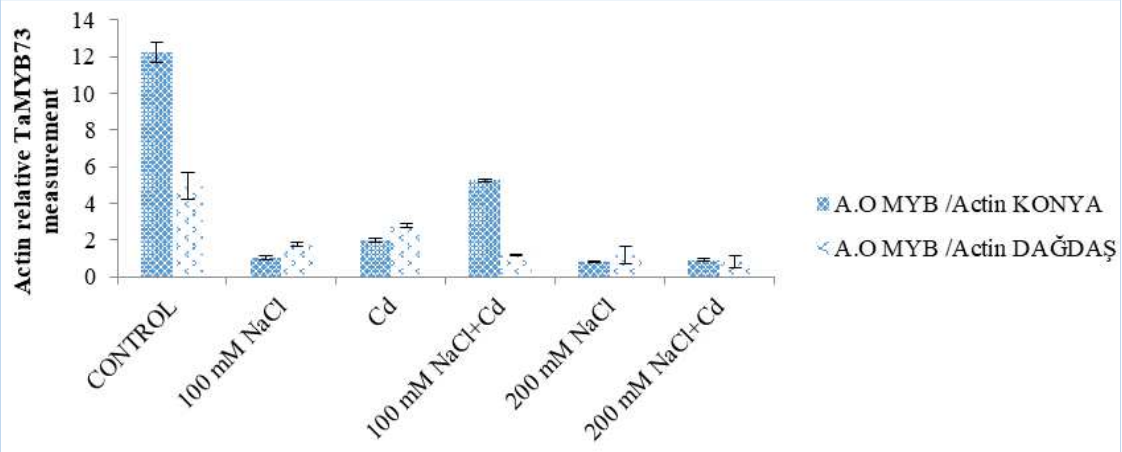


Figure 4. *Changes in the TaMYB73 gene expression in wheat (T. aestivum L. cv. Konya - 2002 and T. aestivum L. cv. Dağdaş - 94) samples grown under 100 mM NaCl, Cd, 100 mM NaCl + Cd, 200 mM NaCl and 200 mM NaCl + Cd conditions (n = 3)*

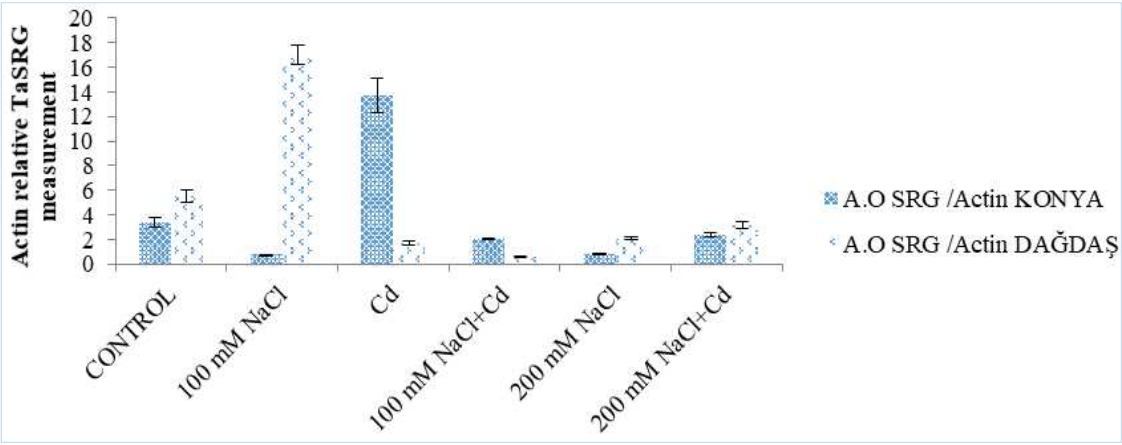


Figure 5. *Changes in the TaSRG gene expression in wheat (T. aestivum L. cv. Konya - 2002 and T. aestivum L. cv. Dağdaş - 94) samples grown under 100 mM NaCl, Cd, 100 mM NaCl + Cd, 200 mM NaCl and 200 mM NaCl + Cd conditions (n = 3)*

TaERF - 1 Gene Results

By the applications of salt, Cd and salt + Cd compared to the control ($p \leq 0.01$), the Konya - 2002 variety exhibited a 0.25 - fold decrease in the TaERF1/actin ratio. Applications of salt and Cd led to the decrease in the TaERF1/actin ratio; however, by the application of 200 mM NaCl + Cd ($p \leq 0.01$), the Dağdaş - 94 variety exhibited an ~3 - fold increase in the TaERF1/actin ratio (*Fig. 6*).

http://www.aloki.hu ● ISSN 1589 1623 (Print) ● ISSN1785 0037 (Online)
DOI: http://dx.doi.org/10.15666/aeer/1902_10191031
© 2021, ALÖKI Kft., Budapest, Hungary

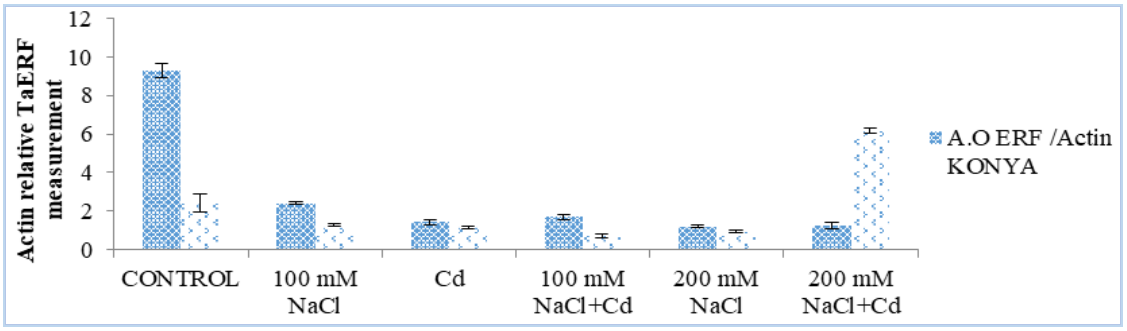


Figure 6. *Changes in the TaERF - 1 gene expression in wheat (T. aestivum L. cv. Konya - 2002 and Dağdaş - 94) samples grown under 100 mM NaCl, Cd, 100 mM NaCl + Cd, 200 mM NaCl and 200 mM NaCl + Cd conditions (n = 3)*

Discussion

It is known, that salinity and heavy metals can cause significant changes in plant expressed genes and metabolism, depending on the plant species, the environment in which they grow. In our study, it was determined that salt and Cd applications in wheat seedlings of Konya - 2002 and Dağdaş - 94 varieties caused changes in CAT and GR activity levels from antioxidant enzymes.

Antioxidant enzyme levels of plants significantly increase due to stress under stress conditions such as salt and heavy metals, and this increase is related to the elimination of antioxidant compounds. Herein, the significant increase in the GR and CAT activities by the applications of NaCl and Cd in both varieties was hypothesized to be related to the removal of free radicals from the environment.

Özçubukçu et al. (2014) have reported the effects of waterlogging (WL) and nitric oxide (NO) in two wheat varieties: Compared to Doğankent seedlings, Ducula - 4 seedlings exhibit a higher CAT activity increase under WL stress, and Ducula - 4 seedlings exhibit an increase in the GR activity under WL - NO conditions, especially at the 48th h and 72nd h.

Glycine, betaine, proline and soluble carbohydrates exhibit osmoregulatory features; therefore, their concentrations increase under abiotic stress conditions such as salinity and temperature (Ergün and Öncel, 2012; Ergün et al., 2014; Özçubukçu et al., 2014). Proline is a hydrophilic amino acid. Its protective function can be achieved by using glycine, betaine and methionine in some plants. Proline is a key osmotic regulator that ensures the integrity of proteins in plants under salt stress (Ergün and Öncel, 2012).

Plants morphologically, physiologically, and biochemically have been reported to adapt to salinity and water scarcity conditions. These changes occur through gene expressions (Rahaie et al., 2010). MYB transcription factors play an important role in abiotic and biotic stress conditions in plants (Wei et al., 2017). In Wei et al. (2017) TaODORANT1, and R2R3-MYB gene was cloned in wheat (*Triticum aestivum* L.). This gene localized in the nucleus. Their results revealed that TaODORANT1 overexpression regulated the expression of stress-related genes and some ROS in response to both salt and drought. Wei et al. (2017) reported that TaODORANT1 positively regulated the plant's tolerance to drought and salt stress.

Under salt stress conditions, the TaMYB73 gene has been reported to stimulate NaCl dehydration and various phytohormones, and the overexpression of the relevant gene

http://www.aloki.hu ● ISSN 1589 1623 (Print) ● ISSN1785 0037 (Online)
DOI: http://dx.doi.org/10.15666/aeer/1902_10191031
© 2021, ALÖKI Kft., Budapest, Hungary

increases the tolerance to salt stress by playing a role in the ionic stress response in *Arabidopsis* (He et al., 2012).

Özçubukçu et al. (2014) have reported that the MYB2 gene expression increases by the application of WL and WL + NO in *T. aestivum* L. cv. Doğankent and *T. aestivum* L. cv. Ducula - 4 wheat seedlings in the first hours of the experiment. MYB is a common transcription factor in plants. The MYB transcription factor has been reported to play a role in plant responses to biotic and abiotic stresses, cell development, signal transfer, etc. (Wang et al., 2016).

The *T. aestivum* salt response gene analysis revealed that the expression of the relevant gene is affected by NaCl, heavy metals and other stress conditions.

Stress - sensitive genes such as SRG genes are involved in the gene expression regulation (Garg and Kumari, 2016). He et al. (2011), have reported that the wheat TaSRG gene acts as a transcription agent in plant varieties and increases tolerance. Also, they have reported that the TaSRG gene function is associated with salt tolerance. Cui et al. (2020) stated that the *Arabidopsis* zinc finger proteins SRG2 and SRG3 are positive regulators of plant immunity.

Salt stress causes the expression of several genes in plants. These genes encode proteins with different functions, osmotic regulators (Tamura et al., 2003), ion channels (Ward and Schroeder, 1994), carriers (Klein et al., 2004), antioxidant and deoxidant proteins and proteins regulated with special transcription factors (He et al., 2011).

Ethylene is a hormone that regulates physiological conditions in plants, such as fruit development, maturation and ageing. Under abiotic and biotic stress conditions, ERF transcription factors regulate gene expressions.

Factors such as salinity, waterlogging and heavy metal stress adversely affect the growth and yield of plants. Plants exhibit various biochemical and physiological adaptations to abiotic stresses (Cheng et al., 2013). Some plants respond to stress conditions by the increase in various gene expressions. ERF1 transcription factors are among those responsible for the adaptation to biotic and abiotic stress. The overexpression of ERF1 has been reported to increase the tolerance to salt and drought in *Arabidopsis* (Cheng et al., 2013). Ethylene Sensitive Factor (ERF) plays a role in a variety of plant growth and stress processes (Zhang et al., 2020). TaERF8, a new member of the ERF family, isolated from wheat. Researchers have shown that TaERF8s play a role in the regulation of wheat growth and development.

Ergün et al. (2014) have investigated the effects of heavy metals and temperature to *T. aestivum* L. cv. Ç - 1252 and Gün - 91 wheat seedlings and reported that the TaMYB73, TaERF1 and TaSRG expressions increase with Cr and temperature, possibly related to the genes regulating Cr and temperature responses in wheat.

Wheat seedlings were exposed to salt and heavy metal stress conditions to determine their effects on the development of wheat seedlings, as well as some physiological and biochemical parameters, and examine the expression of some genes under these conditions. Changes in the growth and development of wheat seedlings due to salt and cadmium were examined. Analysis results revealed that the relevant applications lead to the increase and decrease of some parameters.

The antioxidant enzyme content is known to increase in plants under stress, and these enzymes remove free radicals (e.g. OH^-, H^+ and H_2O_2) from cells. CAT and GR enzyme activities increased by NaCl and Cd applications, and the increase in the Dağdaş - 94 variety was greater than in the Konya - 2002 variety, possibly suggesting that the Dağdaş - 94 variety responds to stress better than the Konya - 2002 variety. The

http://www.aloki.hu ● ISSN 1589 1623 (Print) ● ISSN1785 0037 (Online)
DOI: http://dx.doi.org/10.15666/aeer/1902_10191031
© 2021, ALÖKI Kft., Budapest, Hungary

significant increase in GR and CAT activities and the increase in the relevant enzymes were hypothesized to be associated with the removal of free radicals from the environment.

The accumulation of free proline in wheat seedlings of the Konya - 2002 and Dağdaş - 94 varieties increased by applications of 100 mM NaCl, 100 mM NaCl + cadmium, cadmium, 200 mM NaCl + cadmium and 200 mM NaCl. This result was supported by previous studies in that the proline content in plants increases under all stress conditions. Herein, the proline accumulation increased with the salt concentration for the Konya - 2002 and Dağdaş - 94 wheat seedlings; 4 - fold by the low - concentration salt application; 5 - fold by the 100 mM NaCl application and 10 - fold by 200 mM NaCl and 200 mM NaCl + Cd applications compared to the control. The increased accumulation of free proline was possibly related to stress-induced osmoregulation in the plant. Expression of TaMYB73 and TaERF1 genes in both varieties decreased by heavy metal and NaCl applications compared to the control. By the application of 200 mM NaCl + 10 mM Cd compared to the control, the Dağdaş - 94 variety exhibited a 3 - fold increase in the TaERF gene expression. The Dağdaş - 94 variety of wheat seedlings are resistant to drought. Indeed, the increase in the TaERF1 gene expression by the application of 200 mM NaCl + 10 mM Cd was possibly related to the fact that the TaERF1 gene expression increases the salt tolerance of plants. By the low - concentration salt application compared to the control, the Dağdaş - 94 variety exhibited a 3 - fold increase in the TaSRG gene expression; on the other hand, by the application of Cd compared to the control, the Konya - 2002 variety exhibited a 4 - fold increase in the TaSRG gene expression. On the other hand, the TaSRG ratio decreased by applications of high salt and NaCl + Cd compared to the control.

Conclusion

Abiotic stresses such as salinity and heavy metal stress significantly limit agricultural production. In this study, it is thought that wheat seedlings of Dağdaş - 94 variety are more resistant to salt and cadmium applications than Konya - 2002 variety. Also, the manipulation of salinity tolerance by various genes limits developments in this area. Therefore, more studies are needed to determine enzyme and gene activities, as well as the application of various concentrations to better understand the interactions of salt, cadmium and salt-cadmium interactions.

Acknowledgements. This study is an MSc thesis of Huseyin Dogru and funded by Scientific Research Projects Coordinator (BAP) of Hatay Mustafa Kemal University (17.YL.20).

REFERENCES

[1] Anonym (2020): Kirmizi buğdaylar (Red wheat). – Available at: http://www.tmo.gov.tr/Upload/Document/digerkirmizibugdaylar.pdf. Access date: 12.15.2020.

[2] Bates, L. S., Waldren, R. P., Teare, I. D. (1973): Rapid determination of free proline for water-stress studies. – Plant and Soil 39: 205-207.

[3] Batir, M. B., Candan, F., Büyük, İ. (2016): Determination of the DNA changes in the artichoke seedlings (*Cynara scolymus* L.) subjected to lead and copper stresses. – Plant, Soil and Environment 62: 143-149.

http://www.aloki.hu ● ISSN 1589 1623 (Print) ● ISSN1785 0037 (Online)
DOI: http://dx.doi.org/10.15666/aeer/1902_10191031
© 2021, ALÖKI Kft., Budapest, Hungary

[4] Cakmak, I., Marschner, H. (1992): Magnesium deficiency and high light intensity enhance activities of superoxide dismutase, ascorbate peroxidase, and glutathione reductase in bean leaves. – Plant Physiology 98: 1222-1227.
[5] Cakmak, I. (1994): Activity of ascorbate - dependent H_2O_2 - scavenging enzymes and leaf chlorosis are enhanced in magnesium - and potassium - deficient leaves, but not in phosphorus-deficient leaves. – Journal of Experimental Botany 45: 1259-1266.
[6] Cheng, M. C., Liao, P. M., Kuo, W. W., Lin, T. P. (2013): The Arabidopsis Ethylene Response Factor1 regulates abiotic stress-responsive gene expression by binding to different cis-acting elements in response to different stress signals. – Plant Physiology 162: 1566-1582.
[7] Cui, B., Xu, S., Li, Y., Umbreen, S., Frederickson Matika, D., Yuan, B., Jiang, J., Liu, F., Pan, Q., Loake, G. J. (2020): The arabidopsis zinc finger proteins SRG2 and SRG3 are positive regulators of plant immunity and are differentially regulated by nitric oxide. – New Phytologist, https://doi.org/10.1111/nph.16993.
[8] Doğan, R., Çarpıcı, E. B. (2015): Responses of some durum wheat (*Triticum turgidum* L.) genotypes to salt stress at the germination stage. – Journal of the Faculty of Agriculture Uludağ University 29: 47-55.
[9] Durán, N., Marcato, P. D., De Souza, G. I., Alves, O. L., Esposito, E. (2007): Antibacterial effect of silver nanoparticles produced by fungal process on textile fabrics and their effluent treatment. – Journal of Biomedical Nanotechnology 3: 203-208.
[10] Ergün, N., Öncel, I. (2012): Effects of some heavy metals and heavy metal hormone interactions on wheat (*Triticum aestivum* L. cv. Gun 91) seedlings. – African Journal of Agricultural Research 7: 1518-1523.
[11] Ergün, N., Özçubukçu, S., Kolukirik, M., Temizkan, Ö. (2014): Effects of temperature-heavy metal interactions, antioxidant enzyme activity and gene expression in wheat (*Triticum aestivum* L.) seedling. – Acta Biologica Hungarica 65: 439-450.
[12] Garg, G., Kumari, R. (2016): Functional analysis of plants srg-genes/transmembrane protein (RLKs) under stress condition. – Journal of Bioscience and Agriculture Research 9: 827-836.
[13] He, X., Hou, X., Shen, Y., Huang, Z. (2011): TaSRG, a wheat transcription factor, significantly affects salt tolerance in transgenic rice and *Arabidopsis*. – FEBS Letters 585: 1231-1237.
[14] He, Y., Li, W., Lv, J., Jia, Y., Wang, M., Xia, G. (2012): Ectopic expression of a wheat MYB transcription factor gene, TaMYB73, improves salinity stress tolerance in *Arabidopsis thaliana*. – Journal of Experimental Botany 63: 1511-1522.
[15] Isayenkov, S. V., Maathuis, F. J. (2019): Plant salinity stress: many unanswered questions remain. – Frontiers in Plant Science 10: 1-11.
[16] Klein, M., Geisler, M., Suh, S. J., Kolukısaoğlu, H. U., Azevedo, L., Plaza, S., Curtis, M. D., Richter, A., Weder, B., Schulz, B., Martinoia, E. (2004): Disruption of AtMRP4, a guard cell plasma membrane ABCC-type ABC transporter, leads to deregulation of stomatal opening and increased drought susceptibility. – The Plant Journal 39: 219-236.
[17] Livak, K. J., Schmittgen, T. D. (2001): Analysis of relative gene expression data using real-time quantitative PCR and the2−ΔΔCT method. – Methods 25: 402-408.
[18] Öncel, I., Keleş, Y., Üstün, A. S. (2000): Interactive effects of temperature and heavy metal stress on the growth and some biochemical compounds in wheat seedlings. – Environmental pollution 107: 315-320.
[19] Özçubukçu, S., Ergün, N., Ilhan, E. (2014): Waterlogging and nitric oxide induce gene expression and increase antioxidant enzyme activity in wheat (*Triticum aestivum* L.). – Acta Biologica Hungarica 65: 47-60.
[20] Öztürk, A., Aydin, M. (2017): Physiological characterization of Turkish bread wheat genotypes for resistance to late drought stress. – Turkish Journal of Agriculture and Forestry 41: 414-440.

http://www.aloki.hu ● ISSN 1589 1623 (Print) ● ISSN1785 0037 (Online)
DOI: http://dx.doi.org/10.15666/aeer/1902_10191031
© 2021, ALÖKI Kft., Budapest, Hungary

[21] Rahaie, M., Xue, G. P., Naghavi, M. R., Alizadeh, H., Schenk, P. M. (2010): A MYB gene from wheat (*Triticum aestivum* L.) is up-regulated during salt and drought stresses and differentially regulated between salt-tolerant and sensitive genotypes. – Plant Cell Reports 29: 835-844.
[22] Tamura, T., Hara, K., Yamaguchi, Y., Koizumi, N., Sano, H. (2003): Osmotic stress tolerance of transgenic tobacco expressing a gene encoding a membrane - located receptor-like protein from tobacco plants. – Plant Physiology 131: 454-462.
[23] Tirry, N., Joutey, N. T., Sayel, H., Kouchou, A., Bahafid, W., Asri, M., El Ghachtouli, N. (2018): Screening of plant growth-promoting traits in heavy metals resistant bacteria: prospects in phytoremediation. – Journal of Genetic Engineering and Biotechnology 16: 613-619.
[24] Wang, H., Wang, H., Shao, H., Tang, X. (2016): Recent advances in utilizing transcription factors to improve plant abiotic stress tolerance by transgenic technology. – Frontiers in Plant Science 7: 67.
[25] Ward, J. M., Schroeder, J. I. (1994): Calcium-activated K^+ channels and calcium-induced calcium release by slow vacuolar ion channels in guard cell vacuoles implicated in the control of stomatal closure. – The Plant Cell 6: 669-683.
[26] Wei, Q., Luo, Q., Wang, R., Zhang, F., He, Y., Zhang, Y., Qui, D., Li, K., Chan, J., Yang, G., He, G. (2017): A wheat R2R3-type MYB transcription factor TaODORANT1 positively regulates drought and salt stress responses in transgenic tobacco plants. – Frontiers in Plant Science 8: 1374.
[27] Zhang, L., Liu, P., Wu, J., Qiao, L., Zhao, G., Jia, J., Gao, L., Wang, J. (2020): Identification of a novel ERF gene, TaERF8, associated with plant height and yield in wheat. – BMC Plant Biology 20: 1-12.

http://www.aloki.hu ● ISSN 1589 1623 (Print) ● ISSN1785 0037 (Online)
DOI: http://dx.doi.org/10.15666/aeer/1902_10191031
© 2021, ALÖKI Kft., Budapest, Hungary

IMPACTS OF NITROGEN AND PHOSPHORUS LOADS FROM VARIOUS SOURCES ON THE QUALITY OF SURFACE WATER BODIES IN THE CONTEXT OF CLIMATE CHANGE – CASE STUDY IN POLAND

HAMERLA, A.* – KOŃCZAK, B.

Central Mining Institute Department of Water Protection, Plac Gwarków 1 40-166 Katowice, Poland
(phone: +48-32-259-2292)

**Corresponding author*
e-mail: ahamerla@gig.eu; phone: +48-32-259-2292

(Received 15th Jul 2020; accepted 19th Nov 2020)

Abstract. Climate change has the influence on the occurrence of phenomena such as extreme precipitation, flooding or prolonged rainless periods. The changes in precipitation characteristics have an impact on the nutrient cycle, especially in urban areas. The changes in water management on post mining areas could potentially deepen the problem. The aim of the study was to determine the influence of phosphorus and nitrogen loads from point and dispersed sources onto the water quality of analysed rivers in Poland. The proportion of nutrient loads discharged from different sources was calculated based on the available database, and the concentrations of nitrogen and phosphorus in river waters were analyzed by analytical methods. The results showed that the investment in the water treatment sector is not enough to achieve good status of surface water bodies. The dispersed sources influenced much more the quality of water rivers. The atmospheric deposition is a significant source of nitrogen and may be caused by the progressive changes in the climate. The extreme precipitation increase nitrogen flushed from agricultural systems and will pose greater risks to environmental stability of water. More sophisticated monitoring system of nutrients discharging form different sources may be an opportunity to reduce the pollution in rivers.
Keywords: *water bodies, nutrients, mining areas, atmospheric deposition, agriculture*

Introduction

The climate change is an indisputable phenomenon. Long-term observations of air temperature changes from 1850-1899 to 2001-2005 showed a global increase of 0.76°C (IPCC, 2007) with a tendency to further increase - the average of the 1850-1900 period and the 2003-2012 period is 0.78°C (IPCC, 2013). In addition, the high amplitudes of temperature changes related to the change in surface solar radiation are also observed (Qian et al., 2011), especially in the spring and winter time (Czernecki and Miętus, 2017). This causes the occurrence of extreme phenomena, such as extreme rainfall or on the other hand, extreme drought causing desertification. The global warming and the development of desertification phenomena have a major impact on the natural water cycle. As a result, there are changes in the amount of precipitation, groundwater level, and water levels in rivers and lakes (Malinowski and Skoczko, 2018). The studies of rainless periods were carried out in 1987–2008. Rainless periods in Poland ranged from 9-17 days, but in 2003 and 2008 it was observed that the total length of dry periods was even 101 and 100 days, respectively. The adverse directional changes in the sum of precipitation as well as the increase of the duration of rainless periods, can lead to a drop in the groundwater level. The seasonal variability of groundwater bodies status causes disruption of natural hydraulic continuity between groundwater and river waters

http://www.aloki.hu ● ISSN 1589 1623 (Print) ● ISSN 1785 0037 (Online)
DOI: http://dx.doi.org/10.15666/aeer/1902_10331048
© 2021, ALÖKI Kft., Budapest, Hungary

(Tomalski, 2016). Statistically significant fluctuations in seasonal precipitation are reported in southern Poland. Polish rivers are very sensitive to the fluctuations of various climate-defining variables, with a greater effect being caused by periodic changes of precipitation than similar fluctuations caused by the change in air-temperature and the effectiveness of ground evaporation (Absalon and Matysik, 2016). The fluctuations in the precipitation contribute to the change of the amount of water outflow. The strongest and statistically significant changes in the outflow conditions are observed in the case of rivers drainage basins transformed as a result of human activities, covering industrialized, urbanized and drained areas. In Poland, the regions most transformed are located in the Silesian voivodship. Up to the 1980s high hydrological outflows were observed in the rivers of this region throughout the entire year. After the 1980s, especially during the summer-autumn season lower hydrological outflows were observed as in the case of Kłodnica river (Wrzesiński, 2016). The change of the water regime in the rivers has a deteriorating impact on water quality (Santy et al., 2020).

Despite the implemented multi-million investments involved in reducing the degree of surface water's pollution from anthropogenic sources, the exceeding of permissible concentrations of phosphorus and nitrogen compounds, which is the source of the municipal, industrial and agricultural sectors, is still being identified. The surplus of their load makes it impossible to achieve good status of surface water bodies and to reach the objectives defined in the Water Framework Directive. The problem does not only concern the agricultural catchments but also the highly urbanized areas with a high population concentration. In contrast to the non-urbanized catchments, which show high retention of phosphorus compounds, the urban areas are characterized by rapid transport of nutrients from the catchments to rivers and reservoirs through rainwater (Hobbie et al., 2017). As research has shown (Xia et al., 2016), the impermeable surfaces dominating the urban landscape, from which the sewage is discharged, are the most important factors causing an increase in the concentration of nutrients in surface water bodies. This is mainly due to the small share of wetlands, which play a significant role in removing pollution from the surface waters bodies. As research has shown, among others carried out in Ireland, during which the share of individual sources of pollution in the load discharged from the catchment area was analysed, the main sources of phosphorus come from the sewage treatment plants and agriculture, with large variations across the country – depending on the land use and local hydrogeological conditions (Mockler et al., 2017). Especially the cities climatic conditions and related hydrological conditions have an impact on how pollutants are released and moved. The transport of nitrogen and phosphorus from urban areas to the surface water bodies is closely related to the transport of pollutants in sewage and untreated rainwater. The occurring climate change and prolonged rainless periods result in longer and longer periods of low levels in rivers, which is particularly strongly observed in small watercourses fed from a low-retention urban catchment. The changes in precipitation characteristics will have a strong impact on the nutrient cycle in the catchment areas in the future (Ghane et al., 2016). Since the beginning of the 21st century, many studies have been conducted to model the impact of land use and climate change on nutrients cycling in the catchments, according to the land-cover and land-use change model – LCLUC (Turner and Geoghegan, 2004; Mustard et al., 2012; Jordan et al., 2014). However, as the German studies (Flügel, 2017) convince, the concept of integrated water resource management (IWRM) does not sufficiently take into account the dynamics of processes associated with the nature of the landscape and the associated LULUC model. The authors of the study propose to improve the approach through integrated management

http://www.aloki.hu ● ISSN 1589 1623 (Print) ● ISSN 1785 0037 (Online)
DOI: http://dx.doi.org/10.15666/aeer/1902_10331048
© 2021, ALÖKI Kft., Budapest, Hungary

of land and water resources (ILWRM), which requires consideration of local specificity. It will be of particular importance to take into account the local specificity at strongly transformed areas as in the above-mentioned article on the case of Upper Silesia, where over two hundred years of mining activity has significantly contributed to the change in the hydrological conditions of the area. Mine waters, due to the wide spectrum of pollution, pose a serious problem from an ecological point of view, which is proved by testing physicochemical parameters, and even more by assessing the quality of the surface waters, based on the ecotoxicological indicators (Zgórska et al., 2016). The climate policy limits the extraction of hard coal and reduces the negative impact on the environment, including water resources. This will cause a number of changes, both positive and negative. The inflow of pollutants from the mine waters (not containing nutrients) will be partially limited, while on the other hand, this will reduce the flow of water in the rivers and increase in the concentration of nutrients in the surface waters. In the selected catchment, the share of mine water is significant. For example, in the Rawa 25%, Brynica od zb. Kozłowa Góra 26%, Bytomka as much as 33% of water in the river with an average flow. For low levels of flow, these values exceed 50% – own findings based on information from coal mines. Therefore, it seems unavoidable to include the problem of increasing the concentration of nutrients in the surface waters in the water management plans, prepared for the future for the area after total cessation of hard coal mining. Such plans were adopted, among others, in Germany (Drobniewski et al., 2016), Australia (Everingham et al., 2018), or England (Mayes and Jarvis, 2016).

The aim of the study was to determine the influence of phosphorus and nitrogen loads from point and dispersed sources onto the water quality of analysed rivers in Poland.

Material and methods

The aim of the study was to determine the influence of total phosphorus and total nitrogen loads from point and dispersed sources on the water quality of analysed rivers. For this purpose, the concentrations of phosphorus and nitrogen in selected measurement points within the studied site area were analyzed. Additionally, on the basis of the available data, the amount of nitrogen and phosphorus load discharged into the rivers from point sources (industrial sources, wastewater treatment plants, fishponds) and diffuse sources (agriculture, atmospheric deposition) was determined. A detailed description of the site area, the methodology of collecting samples and analyzing the concentration of nitrogen and phosphorus in the river samples, and calculating the load discharged from each sources are discussed below.

Study area and sampling campaigns

18 Surface Water Bodies (SWB) located in the area of Upper Silesia in southern Poland were analysed. This region is one of the most urbanized and industrialized regions in Europe (*Table 1*). The studies covered both heavily built-up catchments located in urban areas, as well as suburban areas with a significant share of agricultural and forest land. The historical and current industrial activity, especially hard coal mining, has an impact on the quality of the environment of the area, including waters.

Most mining companies discharge the mine waters with high concentrations of chlorides and sulphates, and the level of salinity of the water makes it impossible to achieve environmental goals. The results of the tests on the key parameters of quality and quantity of the mine waters from 53 hard coal mines (active and abandoned) have been

http://www.aloki.hu ● ISSN 1589 1623 (Print) ● ISSN 1785 0037 (Online)
DOI: http://dx.doi.org/10.15666/aeer/1902_10331048
© 2021, ALÖKI Kft., Budapest, Hungary

presented in many publications (Bukowski, 2015; Gzyl et al., 2017; Smith and Sobolewski, 2018).

Table 1. *Characterisation of analysed River Water Bodies*

River Water Bodies (WB)	Accepted concentration related to national legislation (mg/l)		Area (ha)	Average value of water level from multi-year 1986-2016 (m^3/s)		Land use of total catchment area (%)				Mining waters outflow
	N	P		Medium-Low	Medium	Urban & industry	Rural	Forest	Other incl. water	
Potok	3.4	0.2	1.22	0.061	0.124	39	46	15	0	yes
Dokawa	3.2	0.2	4.33	0.081	0.357	14	48	37	1	yes
Gostynia do Starego Koryta	3.2	0.2	6.64	0.334	0.675	15	41	42	2	yes
Tyski Potok	4.6	0.15	2.97	0.149	0.302	44	43	12	1	yes
Bolina	1.7	0.1	2.81	0.184	0.262	39	6	54	1	yes
Dopływ z Mąkołowca	4.6	0.15	1.16	0.060	0.134	13	31	56	0	yes
Rawa	4.6	0.15	7.15	0.813	1.181	86	2	11	1	yes
Szarlejka	1.72	0.08	4.19	0.476	0.692	51	19	29	1	yes
Krzanówka	3.4	0.2	1.70	0.035	0.069	13	86	1	0	no
Lesznica z Jedłownickim	4.6	0.15	8.71	0.619	1.307	36	52	12	0	yes
Jamna	4.6	0.15	2.31	0.124	0.266	37	34	27	2	yes
Kłodnica do Promnej (bez)	4.6	0.15	7.69	0.553	1.016	36	8	55	1	yes
Bielszowicki Potok	4.6	0.15	3.19	0.229	0.421	68	19	12	1	yes
Bytomka	4.6	0.15	14.33	1.691	2.583	49	29	21	1	yes
Drama do Grzybowickiego	4.6	0.15	11.12	0.355	0.551	11	76	13	0	yes
Kłodnica od Promnej	2.4	0.18	4.41	0.942	1.929	68	19	12	1	yes
Lublinica	3.2	0.2	11.86	0.273	0.799	10	40	49	1	no
Brynica od Kozłowej Góry	2.4	0.18	9.31	3.260	5.110	52	42	5	1	yes

Research using the Ecological Risk Assessment and bioindication methods (Bondaruk et al., 2015) was also conducted in the area. The area of Upper Silesia is inhabited by nearly 4 million people. This results in a large amount of municipal sewage discharged, largely treated in the installations with an increased degree of the nutrients removal. The hydrological network of the area includes relatively short streams or source sections of the main rivers. A significant impact on the river regime in most of the analysed catchments has the discharge of mine waters, causing an increase in river flow and a direct impact on the physicochemical parameters of water, including a reduction in nutrient concentrations. Only two of the analysed catchments are outside the direct influence of hard coal mining. *Table 1* presents a brief description of the analysed catchment areas, including characteristic river flows, catchment area, and the land use structure.

The selection of 18 catchments for the study was based on data and assessment of surface water quality, conducted as part of the State Environmental Monitoring in the

http://www.aloki.hu ● ISSN 1589 1623 (Print) ● ISSN 1785 0037 (Online)
DOI: http://dx.doi.org/10.15666/aeer/1902_10331048
© 2021, ALÖKI Kft., Budapest, Hungary

years 2011-2017. Those cases were chosen, where the failure to achieve good status was determined by exceeding the concentration of nutrients at the monitoring points.

The highest rainfall in Poland is in the period between May and October. The rainfall caused run off of nitrogen and phosphorus into the catchment area. Therefore, the samples of the water river were taken in this period. The tests were carried out in three measurement series at the same points in June 2018 (spring fertilizing), August 2018 (summer fertilizing) and October 2018 (autumn fertilizing). In total, 216 analyses were performed for 72 monitoring points, showed on the map below, except that the collection was carried out at least at two points of each of the SWB covered by the study (*Figure 1*).

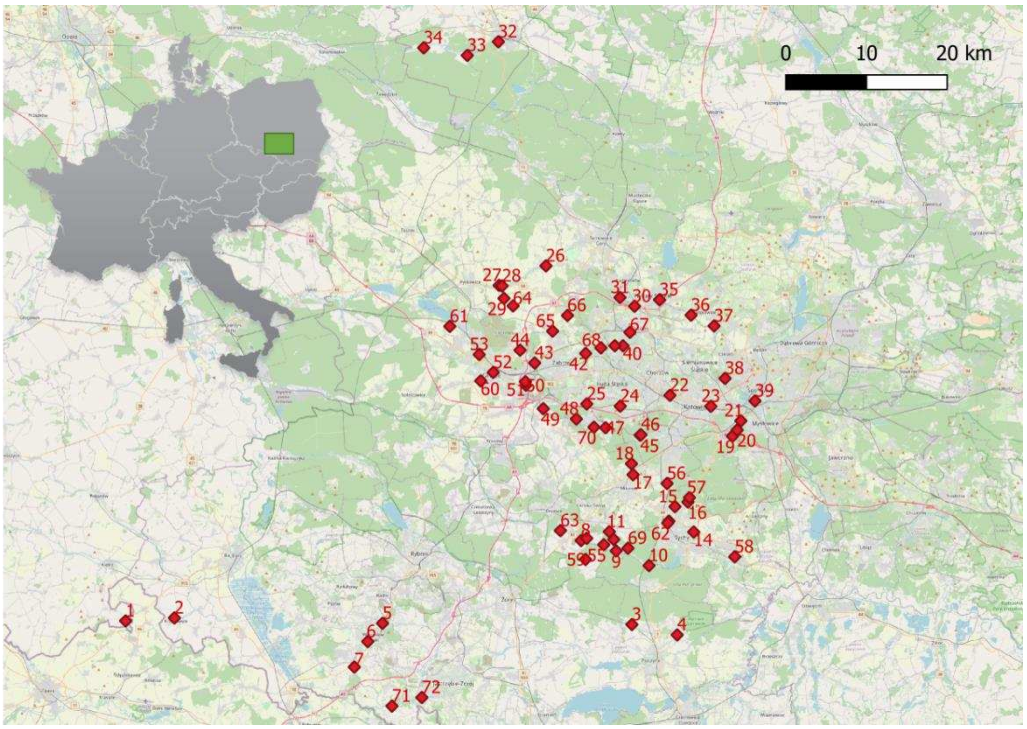


Figure 1. *Monitoring points*

The study was conducted in the rainless period (7 rainless days prior the sampling), for both point and dispersed sources. As part of the study, the determination of total phosphorus and total nitrogen content in the surface waters was performed, and a test of water flow at these points was performed to calculate loads of the tested compounds.

Chemical analysis

Total phosphorus in the water river probes was determined by the ICP-OES method by using emission plasma spectrometer Optima 5300DV (Perkin Elmer company), total nitrogen in the water river probes was determined by high-temperature combustion with chemiluminescence detection by using analyser of nitrogen content TNM-L (Shimadzu company).

Calculation of nitrogen and phosphorus load in the river

The load of nitrogen and phosphorus in the measurement points in the rivers was calculated based on the laboratory results and the values of water flow.

http://www.aloki.hu ● ISSN 1589 1623 (Print) ● ISSN 1785 0037 (Online)
DOI: http://dx.doi.org/10.15666/aeer/1902_10331048
© 2021, ALÖKI Kft., Budapest, Hungary

Calculation of nitrogen and phosphorus load discharged from the point sources

Wastewater Treatment Plants

The loads from the treated sewage were determined based on data from the National Program for Municipal Sewage Treatment (AKPOŚK, 2017), regarding the volume of the discharged treated sewage and value of the pollution indicators. The calculated values of loads were compared with the values of loads determined based on water law permits and the survey data collected as part of the survey from the water and sewage companies (RME, 2014).

Fishponds

The calculations of loads of nitrogen and phosphorus for the identified fishponds were carried out based on the data from water permits regarding the volume of discharges and their timeliness.

The data regarding the concentration of pollutants in waters discharged from fishponds were taken on the base of the literature (Bukacińska et al., 1995; Prądzyńska, 2004; Janicka et al., 2018).

Industrial sources

The loads of nitrogen and phosphorus in the sewage discharging into the watercourses from the identified industrial sources was calculated based on the data from water permits as the volume of discharges (daily, annual), frequency of discharges and permissible concentrations of pollutants in the discharged sewage.

Calculation of nitrogen and phosphorus load discharged from the dispersed sources

The study on identifying pressures from the dispersed sources was conducted based on the methodology proposed by the Institute of Meteorology and Water Management - National Research Institute (IMiGW-PIB, 2013). 3 dispersed sources of nitrogen and phosphorus were identified: agriculture, non-treated sewage and deposition from the atmosphere.

Agriculture – the natural fertilizing

In order to estimate the amount of N, P from the natural fertilizers, it was assumed that the load of nitrogen and phosphorus was equivalent to the load excreted with urine and faeces of farm animals. Firstly, the number of farm animals and the number of Livestock Unit (LSU) (unit conversion of animals assigned to the analysed catchments) was calculated based on statistical data and information obtained from the Animal Identification and Registration System operated by the Agency for Restructuring and Modernisation of Agriculture. The amount of liquid manure and manure produced in the administration unit was determined based on the number of farm animals and the values specified in *Table 7*, which is part of the annex to the Council of Ministers Regulation (CMR, 2005). The composition of manure and liquid manure was adopted in accordance with Pająk and Kowalik (2006). According to the methodology of the Institute of Meteorology and Water Management (2013), the amounts of nitrogen and phosphorus outflow to surface waters were determined assuming that the nitrogen outflow factor is 0.5 and the phosphorus outflow factor is 0.2.

http://www.aloki.hu ● ISSN 1589 1623 (Print) ● ISSN 1785 0037 (Online)
DOI: http://dx.doi.org/10.15666/aeer/1902_10331048
© 2021, ALÖKI Kft., Budapest, Hungary

Agriculture – the mineral fertilizing

In the first step, the nitrogen surplus was determined based on the nitrogen efficiency factor which was assumed at the level of 0.63 according to the data presented by Kopiński (2017). The nitrogen load discharged from the catchment area was calculated by reducing the surplus value of nitrogen and phosphorus load by the value of the base leaching coefficients. The leaching coefficient of nitrogen was determined according to the method described by Ulen et al. (2013). The value of the coefficient was 0.88. Due to the low solubility in a wide pH range, phosphorus is not a very mobile element. Moreover, many regions are deficient in phosphorus. The main mechanism of phosphorus leaching occurs along with surface runoff. About 20% of phosphorus, which is an excess of phosphorus introduced with mineral fertilizers (remaining in the surface layer of the soil), goes to surface waters. The leaching coefficient of phosphorus was determined according to the method described by the Institute of Meteorology and Water Management (2013). The value of the coefficient was 0.2.

Atmospheric deposition

The atmospheric deposition was calculated by multiplying the area of a catchment by the unit load of nitrogen and phosphorus from precipitation per hectare.

The amounts of nitrogen and phosphorus was determined based on reports on the state of the environment (Liana et al., 2017) and the data from rainwater monitoring stations Katowice and Racibórz.

Non-treated sewage sludge

The loads from the non-treated sewage were determined on the base of data from the National Program for Municipal Sewage Treatment (AKPOŚK, 2017), regarding the volume of the discharged non-treated sewage and the values of pollution indicators in the discharged non-treated sewage.

Results and discussion

Nitrogen and phosphorus load from the point sources

Based on the above-described method the loads of total phosphorus and total nitrogen discharged within a year from the point sources (PS) to the individual SWB were calculated (NPS – Load of **N**itrogen from **P**oint **S**ources, PPS - Load of **P**hosphorus from **P**oint **S**ources). The following table shows the results of the calculated load (*Table 2*).

The highest values are directly related to the volume of the municipal sewage discharged from the catchment. Therefore, the largest loads from the point sources come from the highly urbanized catchments. For example, in the Bytomka catchment, there are 7 municipal sewage treatment plants discharging sewage from 3 cities, and the total length of the river is only 19 km. The analysis of average annual flows in the Bytomka catchments in the period from 1970-1992 showed an increase in water flows, despite the fact that rainfall shortages were observed in the period from 1984-1992. The high water flow values at that time was coincided with the maximum demand for water by industrial and municipal services, which resulted in increased amounts of wastewater discharged into these rivers. In the second half of the 1980s, significant discharges of mine waters were also observed, in the case of Bytomka 0.8871 m^3/s of mine waters was dumped, which accounted for over 30% of the average annual flow. The amount of mine water

http://www.aloki.hu ● ISSN 1589 1623 (Print) ● ISSN 1785 0037 (Online)
DOI: http://dx.doi.org/10.15666/aeer/1902_10331048
© 2021, ALÖKI Kft., Budapest, Hungary

discharged has been steadily decreasing since 1990. As a result of the decrease in average annual flows in Bytomka, despite the smaller amount of mine water discharged, their ratio in the average annual flows increased to 40-50%. Such a high ratio of mining waste water in the outflow of these rivers indicates their high impact on their water quality (Absalon and Matysik, 2016). The results showed the high impact of industrial point sources on the quality of water in the highly urbanized catchments (Bolina, Bytomka, Kłodnica do Promnej, Kłodnica od Promnej) (*Table 2*).

Table 2. *Compounds of phosphorus and nitogen loads and total loads of phosphorus and total nitrogen*

River Water Body	Source						Total N	Total P
	Industry		Sewage		Ponds			
	N	P	N	P	N	P		
	kg*10^3/y							
Krzanówka	0	0	0	0	0	0	**0**	**0**
Dokawa	0.1	0.008	0	0	7,209	0.005	**7.3**	**0.013**
Lesznica z Jedłownickim	0	0	56.9	3.7	0	0	**56.9**	**3.7**
Gostynia do starego koryta	0.02	0.002	4.5	1.8	0	0	**4.6**	**1.8**
Potok	0	0	13.7	0.9	0	0	**133.7**	**0.9**
Tyski Potok	0	5.0	0	0	0	0	**0**	**5.0**
Dopływ z Mąkołowca	0	0	0	0	0	0	**0**	**0**
Jamna	0	0	38.3	1.6	0	0	**38.2**	**1.6**
Bolina	21.5	2.1	0	0	0	0	**21.5**	**2.1**
Rawa	0	0	198.8	10.5	0	0	**198.8**	**10.5**
Bielszowicki Potok	1.9	0.2	25.4	1.9	0	0	**27.3**	**2.1**
Drama do Grzybowickiego	4.5	0.4	13.8	0.6	0	0	**18.2**	**1.0**
Szarlejka	0	0.002	70.6	4.7	0	0	**70.6**	**4.7**
Lublinica	0	0	24.4	0.7	0	0	**24.4**	**0.7**
Brynica od zb. Kozłowa Góra	0.2	2.4	181.9	3.5	0	0	**182.1**	**5.9**
Bytomka	1.3	32.5	147.6	1.9	0	0	**148.9**	**34.4**
Kłodnica do Promnej	7.1	0.7	104.3	3.4	0	0	**111.4**	**4.1**
Kłodnica od Promnej	2.1	0.2	116.5	6.9	0	0	**118.6**	**7.1**

In the case of the Rawa River with a length of about 20 km, the calculated total nitrogen load discharged every year from the sewage treatment plant reaches almost 200 t/y (*Table 2*).

The treated sewage caused the increase of nutrient load in the water rivers, especially in catchments of Rawa, Brynica od zb. Kozłowa Góra, Bytomka, Kłodnica do Promnej and Kłodnica od Promnej (*Table 2*), despite the fact that the quality of treated sewage meets the legal requirements (RME, 2014). This phenomenon is especially observed in catchments where climate change causes variation in the water regime. The decreased amount of rainfall has an impact on water resources as well as on water supply and sanitation facilities. During rainless periods low flows in surface waters can be observed and the treated sewage in rivers becomes less diluted causing contamination issues. The increased intensity of rainfall also has a deteriorating impact on water quality.

The following table shows the results of the calculated load for the individual types of dispersed sources. Several SWB have been identified to which untreated sewage is discharged, such as Lesznica z Jedłownickim; Gostynia do starego koryta, Drama do

http://www.aloki.hu ● ISSN 1589 1623 (Print) ● ISSN 1785 0037 (Online)
DOI: http://dx.doi.org/10.15666/aeer/1902_10331048
© 2021, ALÖKI Kft., Budapest, Hungary

Grzybowickiego, Kłodnica od Promnej. The annual nitrogen and phosphorus load from these sources varied respectively between 0.8 – 6.5 MgN/y and 0.1 – 1 MgP/y (*Table 3*).

Table 3. *Load for the individual types of dispersed sources*

Type of nitrogen and phosphorus source	**Mineral Fertilizer**		**Natural Fertilizer**		**Non-treatment sewage**		**Atmospheric deposition**		**Total**	
Water Body	**N**	**P**	**N**	**P**	**N**	**P**	**N**	**P**	**ΣN**	**ΣP**
	kg*10^3/y									
Krzanówka	30.7	1.6	38.6	9.7			14.7	0.2	**84. 0**	**11.5**
Dokawa	43.7	2.0	54.0	13.8			49.0	1.0	**146.8**	**16.9**
Lesznica z Jedłownickim	94.1	4.3	117.1	29.7	6.5	1.0	90.8	1.7	**308.5**	**36.7**
Gostynia do starego koryta	56.1	2.6	69.9	17.7	0.8	0.1	70.9	1.6	**197.7**	**22.1**
Potok	9.2	0.5	14.4	3.7			13.0	0.3	**36.7**	**4.5**
Tyski Potok	40.9	1.2	33.9	8.6			30.2	0.7	**105.0**	**10.5**
Dopływ z Mąkołowca	11.4	0.3	9.5	2.4			11.8	0.3	**32.7**	**3.0**
Jamna	16.4	0.7	20.5	5.2			23.5	0.5	**60.4**	**6.4**
Bolina	3.4	0.2	4.2	1.12			26.2	0.6	**33.7**	**1.8**
Rawa	3.1	0.1	3.8	9.7			69.1	1.5	**76.0**	**2.6**
Bielszowicki Potok	9.8	0.6	15.4	3.9			32.5	0.7	**57.7**	**5.2**
Drama do Grzybowickiego	7.6	0.3	9.5	2.4	0.8	0.1	11.5	0.2	**29.4**	**3.1**
Szarlejka	12.0	0.7	18.9	4.8			40.5	0.9	**71.4**	**6.4**
Lublinica	97.1	4.5	120.9	30.7			117.8	0.3	**335.8**	**37.8**
Brynica od zb. Kozłowa Góra	80.8	3.7	100.6	25.5			89.9	2.0	**271.4**	**31.2**
Bytomka	69.0	4.0	108.5	27.6			139.2	3.1	**316.8**	**34.6**
Kłodnica do Promnej	12.7	0.6	15.8	4.0			77.4	1.6	**105.9**	**6.2**
Kłodnica od Promnej	13.9	0.8	21.8	5.5	1.3	0.2	38.8	0.8	**75.9**	**7.4**

X – no exiting non-treatment sewage

In the case of dispersed sources in the urban catchments, the load related to atmospheric deposition dominates, as well as the load resulting from the runoff of waters contaminated with nitrogen and phosphorus compounds, coming from the natural fertilization used in the agricultural areas and/or the use of mineral fertilizers.

The increase in the amount of nitrogen and phosphorus in the atmospheric precipitation may be caused by the progressive changes in the climate, which affect the plant growth and biochemical cycling. Climate change and nutrient deposition can also have interacting effects. The high amount of nitrogen and phosphorus in precipitation can lead to plant growth potentially enhancing their responsiveness to changes in climate. The results have also showed a great impact of agriculture on the water resources. The precipitation flush mineral fertilizer, manure or liquid manure into water river. It is especially dangerous due to the progressive climate change and more and more frequent occurrence of unfavorable phenomena such as extreme precipitation and flooding. The excess water increase nitrogen flushed from agricultural systems and will pose greater risks to environmental stability of water. The nutrient rich-water are prone to algal blooms which on the other hand are responsible for massive fish kills (Glibert, 2020).

http://www.aloki.hu ● ISSN 1589 1623 (Print) ● ISSN 1785 0037 (Online)
DOI: http://dx.doi.org/10.15666/aeer/1902_10331048
© 2021, ALÖKI Kft., Budapest, Hungary

The following graph presents the share of total nitrogen and total phosphorus in the annual load (*Figure 2*). In most of the analysed cases, the area and dispersed sources are a definitely larger source of this group of pollutants (N_DS – Load of **N**itrogen from **D**ispersed **S**ources, P_DS – Load of **P**hosphorus from **D**ispersed **S**ources). In the case of catchments with a lower degree of urbanization, the role of this type of source is dominant in an unequivocal way.

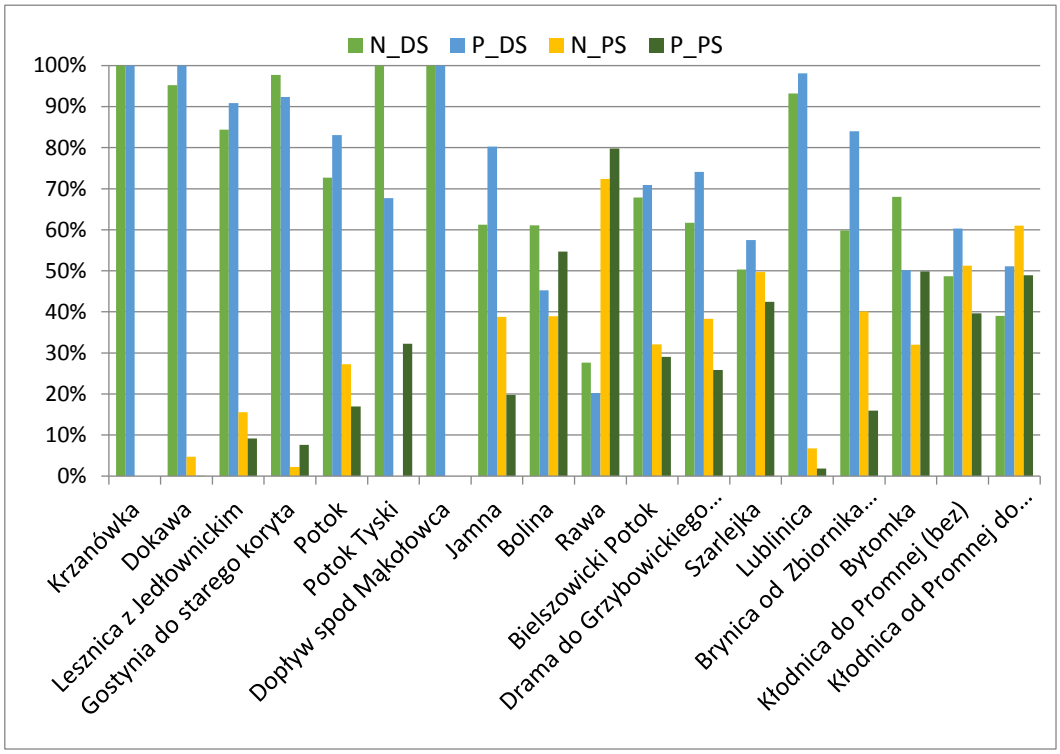


Figure 2. *The share of total nitrogen and total phosphorus in the annual load*

In order to assess how the calculated maximum value of nitrogen and phosphorus loads discharged from all analyzed point sources affect the water quality, a negative scenario was adopted for the analysis. It was assumed that the water flow has low or medium level.

The results showed that in almost all analyzed SWB, the nitrogen and phosphorus loads are too large and exceeds the allowable limit (RME, 2016) (*Table 4*). To determine the degree of necessary reduction of nutrient, the threshold values relevant to the types of individual SWB were adopted. The degree of reduction was defined as the difference between the load discharged to a SWB, and the load that could be the maximum discharged to SWB.

The analysis of results presented in the *Table 4* indicates, that in the case when the nitrogen and phosphorus load will be at maximum allowable level (specified in the water permits) in the scenario with low-medium flow in the watercourses any of the analysed SWB will not obtain a good status. The permissible phosphorus concentration in the analysed watercourses will be exceeded many times. In the event of medium-level flows, the permissible concentrations of pollutants will not be exceeded only in two of the 18 analysed SWB.

http://www.aloki.hu ● ISSN 1589 1623 (Print) ● ISSN 1785 0037 (Online)
DOI: http://dx.doi.org/10.15666/aeer/1902_10331048
© 2021, ALÖKI Kft., Budapest, Hungary

Table 4. *Required degree of reduction of phosphorus and nitrogen compounds*

River Water Body	Limit to good status of WB kg*10^3/y				Real load kg*10^3/y		Requested reduction kg*10^3/y			
	medium flow		medium-low flow				medium flow		medium-low flow	
	N	P	N	P	N	P	N	P	N	P
Potok	32.1	1.6	15.8	0.5	50.4	5.4	**18.3**	**3.8**	**34.6**	**4.9**
Dokawa	55.2	3.4	12.5	0.4	154.1	16.9	**98.8**	**13.5**	**141.5**	**16.5**
Gostynia do starego koryta	104.4	6.4	51.6	1.6	202.3	23.9	**97.9**	**17.5**	**150.6**	**22.3**
Potok Tyski	65.8	3.3	32.4	1.0	105.0	15.5	**39.3**	**12.2**	**72.6**	**14.5**
Bolina	25.6	1.7	18.0	0.6	55.2	3.9	**29.6**	**2.2**	**37.2**	**3.4**
Dopływ spod Mąkołowca	29.2	1.5	13.1	0.4	32.7	3.0	**3.5**	**1.5**	**19.7**	**2.6**
Rawa	257.2	13.0	177.0	5.6	274.8	13.1	**17.6**	**0.1**	**97.8**	**7.5**
Szarlejka	76.4	6.8	52.6	1.7	142.0	11.1	**65.6**	**4.4**	**89.4**	**9.5**
Krzanówka	17.9	0.9	9.1	0.3	84.1	11.5	**66.2**	**10.6**	**75.0**	**11.2**
Lesznica z Jedłownickim	284.6	14.4	134.8	4.3	365.4	40.4	**80.8**	**26.0**	**230.7**	**36.2**
Jamna	57.9	2.9	27.0	0.9	98.7	8.0	**40.8**	**5.1**	**71.7**	**7.2**
Kłodnica do Promnej (bez)	221.2	11.2	120.4	3.8	217.3	10.4	**-3.9**	**-0.9**	**96.9**	**6.6**
Bielszowicki Potok	91.7	4.6	49.9	1.6	85.1	7.3	**-6.6**	**2.7**	**35.2**	**5.7**
Bytomka	562.4	28.5	368.2	11.6	465.7	69.1	**-96.7**	**40.6**	**97.5**	**57.5**
Drama do Grzybowickiego Potoku włącznie	120.0	6.1	77.3	2.4	47.6	4.2	**-72.3**	**-1.8**	**-29.7**	**1.8**
Kłodnica od Promnej do Kozłówki	182.6	13.4	89.2	2.8	194.5	14.5	**11.9**	**1.1**	**105.3**	**11.7**
Lublinica	120.5	7.4	42.2	1.3	360.2	38.5	**239.8**	**31.1**	**318.0**	**37.2**
Brynica od zb. Kozłowa Góra do ujścia	483.8	35.5	308.6	9.7	453.6	37.2	**-30.2**	**1.7**	**144.9**	**27.5**

Conclusions

Due to climate change, nitrogen and phosphorus loads discharged into waters from different sources have a greater impact on the quality of these waters. This is due to the change in the water regime in watercourses. The occurrence of long rainless periods causes the reduction of the flow of water in water courses and as a result of the decrease in average annual flows even when the amount of nitrogen and phosphorus discharged is at the allowable level, their ratio in the average annual flows is too high. Moreover, the forecasting limitation of mine water outflow will cause that water level in selected water bodies to decrease in some cases by more than half. Due to that, it is important in the environmental management plans of the post-mining area to take into account the use of a part of the mine water to perform regulatory functions in the environment.

At the same time, due to the climate change, the occurrence of extreme precipitation, causing flush of a high amount of nutrients from the fertilizing soil should also be considered. The solution to this problem may be intelligent fertilization, which will

http://www.aloki.hu ● ISSN 1589 1623 (Print) ● ISSN 1785 0037 (Online)
DOI: http://dx.doi.org/10.15666/aeer/1902_10331048
© 2021, ALÖKI Kft., Budapest, Hungary

reduce the phenomenon of over-fertilization and discharge of excess nutrients with rainwater to the catchment.

As in the other areas, a significant ratio of the atmospheric deposition in the transfer of nutrients into water bodies was found. In the periods of low water flows, the impact of the dispersed sources of nutrients on water quality is smaller due to the lack of atmospheric precipitation. The share of deposition of these pollutants from the atmosphere is at zero level, and the surface runoff and infiltration from the topsoil layers are negligible. The results show also the impact of the sewage discharged from fishpond on the quality of the water river. This source of pollution has a particular impact on water reservoirs, as the ponds are drained only once a year. It is recommended to pretreat water from fishponds before introducing them into water courses.

The treated wastewater has also an impact on the water quality but the level of nutrient reduction in the sewage treatment plants will no longer be significantly improved, the efforts should be focused on solutions in the catchment area, including the water management and landscaping.

Further analysis should be done taking into account the amount of precipitation and flows in water courses throughout the year. The results of the research would allow to determine the model of the influence of various sources of pollution in the variable flow conditions. This tool would be useful for predicting the impact of nitrogen and phosphorus loads on water bodies quality with regard to the climate change.

Acknowledgements. This work was supported by the Ministry of Science and Higher Education, Republic of Poland (Statutory Activity of the Central Mining Institute in Katowice, Poland. Work no. 14508018-344).

REFERENCES

[1] Absalon, D., Matysik, M. (2016): Zmiany odpływu w silnie zurbanizowanych zlewniach województwa śląskiego. – In: Hejduk, L., Kaznowska, E. (eds.) Hydrologia Zlewni Zurbanizowanych. Monografie Komitetu Gospodarki Wodnej PAN, 39, KGW-PAN, IMGW-PIB, Warszawa.

[2] Bondaruk, J., Janson, E., Wysocka, M., Chałupnik, S. (2015): Identification of hazards for water environment in the Upper Silesian Coal Basin caused by the discharge of salt mine water containing particularly harmful substances and radionuclides. – Journal of Sustainable Mining 14(4): 179-187.

[3] Bukacińska, M., Bukaciński, D., Cygan, J. P., Dobrowolski, K. A. (1995): Natural and economic valorisation of fishponds in Poland. – Foundation IUCN Poland Warszawa; Przyrodniczo-ekonomiczna waloryzacja stawów rybnych w Polsce, Fundacja IUCN Poland Warszawa.

[4] Bukowski, P. (2015): Evaluation of water hazard in hard coal mines in changing conditions of functioning of mining industry in Upper Silesian Coal Basin–USCB (Poland). – Archives of Mining Sciences 60(2): 455-475.

[5] CRE (2015): Regulation of the Council of Ministers of 18 May 2005 amending the regulation on detailed conditions and procedures for granting financial aid for the adaptation of agricultural holdings to the standards of the European Union covered by the rural development plan. – Journal of Laws 93: 780.

[6] Czernecki, B., Miętus, M. (2017): The thermal seasons variability in Poland, 1951–2010. – Theoretical and Applied Climatology 127(1-2): 481-493.

http://www.aloki.hu ● ISSN 1589 1623 (Print) ● ISSN 1785 0037 (Online)
DOI: http://dx.doi.org/10.15666/aeer/1902_10331048
© 2021, ALÖKI Kft., Budapest, Hungary

[7] Drobniewski, M., Balzer, I., Frankenhoff, H., Witthaus, H. (2016): Mine Water Management in the Ruhr coalfield. – Proceedings of the IMWA symposium 2016, IMWA Leipzig (Germany).
[8] Everingham, J. A., Rolfe, J., Lechner, A. M., Kinnear, S., Akbar, D. (2018): A proposal for engaging a stakeholder panel in planning post-mining land uses in Australia's coal-rich tropical savannahs. – Land use policy 79: 397-406.
[9] Flügel, W. A. (2017): River Basin Impact Assessment of Changing Land Use and Climate by Applying the ILWRM Approach in Africa and Asia. – River System Analysis and Management. Springer, Singapore, pp. 85-112.
[10] Ghane, E., Ranaivoson, A. Z., Feyereisen, G. W., Rosen, C. J., Moncrief, J. F. (2016): Comparison of contaminant transport in agricultural drainage water and urban storm water runoff. – PloS one 11(12): e0167834.
[11] Glibert, P. M. (2020): Harmful algae at the complex nexus of eutrophication and climate change. – Harmful Algae 91: 101583.
[12] GUS (2016): CentralStatitical Office. – available on-line: 26.10.2020. https://stat.gov.pl/obszary-tematyczne/rolnictwo-lesnictwo/rolnictwo/.
[13] GUS (2017): CentralStatitical Office. – available on-line: 26.10.2020. https://stat.gov.pl/obszary-tematyczne/rolnictwo-lesnictwo/rolnictwo/.
[14] Gzyl, G., Janson, E., Łabaj, P. (2017): Mine Water Discharges in Upper Silesian Coal Basin (Poland). – In: Bech, J., Bini, C., Pashkevich, M. A. (eds.) Assessment, Restoration and Reclamation of Mining Influenced Soils. Academic Press, pp. 463-486
[15] Hobbie, S. E., Finlay, J. C., Janke, B. D., Nidzgorski, D. A., Millet, D. B., Baker, L. A. (2017): Contrasting nitrogen and phosphorus budgets in urban watersheds and implications for managing urban water pollution. – Proceedings of the National Academy of Sciences 114(16): 4177-4182.
[16] IMiGW-PIB (2013): Developing an analysis of pressures and impacts of the anthropogenic pollution in a detailed approach to all water categories for the purposes of developing update of action programs and water management plans: "Methodology defining procedures for identifying pressures and assessing influences/impacts and the risk of failing to achieve the environmental objectives for all the surface water categories". – data access 12.11.2019.
[17] IPCC (2007): Fourth Assessment Report SPM: Climate Change. – Intergovernmental Panel on Climate Change.
[18] IPCC (2013): Fifth Assessment Report SPM: Climate Change. – Intergovernmental Panel on Climate Change.
[19] Janicka, E., Kanclerz, J., Jany, J., Adamska, A., Murat-Błażejewska, S. (2018): Assessment of water quality and nutrient balance of a small lake in urban landscape–case study of Rusałka lake in the Wielkopolskie Lakeland. – Annals of Warsaw University of Life Sciences–SGGW, Land Reclamation 50(3): 229-239.
[20] Jordan, Y. C., Ghulam, A., Chu, M. L. (2014): Assessing the Impacts of Future Urban Development Patterns and Climate Changes on Total Suspended Sediment Loading in Surface Waters Using Geoinformatics. – Journal of Environmental Informatics 24(2).
[21] Journal of Laws (2016): Regulation of the Minister of Environment of 21 July 2016 on the classification of bodies of surface water and environmental quality standards for priority substances. – Item 118-7.
[22] Kopiński, J. (2017): Ocena zmian efektywności wykorzystania azotu w produkcji rolniczej Polski. – Roczniki Naukowe Stowarzyszenia Ekonomistów Rolnictwa i Agrobiznesu 19(1): 85-91.
[23] KPOŚK (2018): Report on the implementation of the National Program for Urban Waste Water Treatment. – https://dane.gov.pl, available on-line: 26.10.2020.
[24] Liana, E., Błachuta, J., Kolanek, A., Terlecka, E., Pobudejski, M., Miszuk, B., Otop, I., Mazurek, M., Rawa, W. (2017): Monitoring Chemizmu Opadów atmosferycznych i ocena

http://www.aloki.hu ● ISSN 1589 1623 (Print) ● ISSN 1785 0037 (Online)
DOI: http://dx.doi.org/10.15666/aeer/1902_10331048
© 2021, ALÖKI Kft., Budapest, Hungary

depozycji zanieczyszczeń do podłoża w latach 2016-2018. – Inspekcja Ochrony Środowiska, Wrocław.
[25] Malinowski, Ł., Skoczko, I. (2018): Impacts of Climate Change on Hydrological Regime and Water Resources Management of the Narew River in Poland. – Journal of Ecological Engineering 19(4): 167-175.
[26] Mayes, M., Jarvis, A. P. (2016): Mine water outbreak and stability risks: examples and challenges from England and Wales. – Proceedings IMWA 2016, Freiberg Germany, pp. 1078-1083.
[27] Mockler, E. M., Deakin, J., Archbold, M., Gill, L., Daly, D., Bruen, M. (2017): Sources of nitrogen and phosphorus emissions to Irish rivers and coastal waters: estimates from a nutrient load apportionment framework. – Science of the Total Environment 601: 326-339.
[28] Mustard, J. F., Defries, R. S., Fisher, T., Moran, E. (2012): Land-use and land-cover change pathways and impacts. – In: Gutman, G., Janetos, A. C., Justice, C. O., Moran, E. F., Mustard, J. F., Rindfuss, R. R., Skole, D., Turner II, B. L., Cochrane, M. A. (eds.) Land change science. Springer, Dordrecht, pp. 411-429.
[29] Pająk, J. J., Kowalik, B. (2006): Wpływ żywienia i systemu utrzymania zwierząt na ilość i skład odchodów od bydła. – Nawozy i nawożenie 4(29): 7-19.
[30] Prądzyńska, D. (2004): Próba oceny oddziaływania stawów hodowlanych na środowisko przyrodnicze (na przykładzie gminy Malechowo). – Problemy Ecologii Krajobrazu 13: 219-224.
[31] Qian, Ch., Fu, C., Wu, Z. (2011): Changes in the Amplitude of the Temperature Annual Cycle in China and Their Implication for Climate Change Research. – Journal of Climate 24(20): 5292-5302.
[32] RME (2014): Regulation of the Minister of the Environment of 18 November 2014 on the conditions to be met when discharging sewage into waters or into the ground, and on substances particularly harmful to the aquatic environment. – Journal of Laws 2014, item 1800.
[33] RME (2016): Regulation of the Minister of the Environment of July 21, 2016 on the method of classification of the status of the surface water bodies and the environmental quality standards for the priority substances. – Journal of Laws 2016, item 118.
[34] Santy, S., Mujumdar, P., Bala, G. (2020): Potential Impacts of Climate and Land Use Change on the Water Quality of Ganga River around the Industrialized Kanpur Region. – Scientific Reports 10: 9107.
[35] Smith, H. L., Sobolewski, M. (2018): The Saline Water Problem in Upper Silesia. – In: Jasinski, P., Smith, H. L. (eds.) Environmental Regulation in Transforming Economies: The Case of Poland. London, 374p.
[36] Tomalski, P. (2016): Sezonowa zmienność stanów wód podziemnych w dolinie Sokołówki (Łódź). – In: Hejduka, L., Kaznowskiej, E. (eds.) Hydrologia Zlewni Zurbanizowanych. Monografie Komitetu Gospodarki Wodnej PAN, 39, KGW-PAN, IMGW-PIB, Warszawa.
[37] Turner, B. L., Geoghegan, J. (2004): Land-Cover and Land-Use Change (LCLUC) in the Southern Yucatán Peninsular Region (SYPR). – In: Fox, J., Rindfuss, R. R., Walsh, S. J., Mishra, V. (eds.) People and the Environment. Springer, Boston, MA, pp. 31-60.
[38] Ulén, B., Pietrzak, S., Tonderski, K. S. (2013): Samoocena gospodarstw w zakresie zarządzania składnikami nawozowymi i oceny warunków środowiskowych. – Instytut Technologiczno-Przyrodniczy w Falentach.
[39] Wrzesiński, D. (2016): Zmiany reżimu odpływu rzecznego w Polsce. – In: Hejduka, L., Kaznowskiej, E. (eds.) Hydrologia Zlewni Zurbanizowanych. Monografie Komitetu Gospodarki Wodnej PAN, 39, KGW-PAN, IMGW-PIB, Warszawa.
[40] Xia, Y., Ti, C., She, D., Yan, X. (2016): Linking river nutrient concentrations to land use and rainfall in a paddy agriculture–urban area gradient watershed in southeast China. – Science of the Total Environment 566: 1094-1105.

http://www.aloki.hu ● ISSN 1589 1623 (Print) ● ISSN 1785 0037 (Online)
DOI: http://dx.doi.org/10.15666/aeer/1902_10331048
© 2021, ALÖKI Kft., Budapest, Hungary

[41] Yang, Y. Y., Toor, G. S. (2017): Sources and mechanisms of nitrate and orthophosphate transport in urban storm water runoff from residential catchments. – Water research 112: 176-184.
[42] Zgórska, A., Trząski, L., Wiesner, M. (2016): Environmental risk caused by high salinity mine water discharges from active and closed mines located in the Upper Silesian Coal Basin (Poland). – Proceedings IMWA 2016: 85.

APPENDIX

Appendix 1. *Coordinates of monitoring points*

Monitoring points	EPSG 2180	
	X	Y
1	430853	239375
2	436895	239746
3	493580	238931
4	499197	237648
5	462683	239078
6	460855	236824
7	459192	233667
8	487293	249319
9	491638	248035
10	495705	246219
11	490784	250412
12	491339	249446
13	498173	251719
14	501239	250372
15	498921	253510
16	500524	254082
17	493728	257463
18	493534	258810
19	506042	262227
20	506630	262988
21	507091	264122
22	498303	267282
23	503365	265917
24	492138	265936
25	487989	266212
26	482935	283291
27	477130	280880
28	477504	280811
29	477737	279268
30	493913	278294
31	492109	279378
32	477033	311006
33	473184	309322
34	467788	310260
35	497004	279097
36	500914	277192
37	503770	275861
38	505122	269372
39	508834	266584
40	492486	273408
41	491470	273416
42	487858	272459
43	481539	271278
44	479729	272860
45	494603	262345
46	494711	262400
47	490326	263273

http://www.aloki.hu ● ISSN 1589 1623 (Print) ● ISSN 1785 0037 (Online)
DOI: http://dx.doi.org/10.15666/aeer/1902_10331048
© 2021, ALÖKI Kft., Budapest, Hungary

Monitoring points	EPSG 2180	
	X	Y
48	486708	264351
49	482601	265620
50	480446	268525
51	480387	268972
52	476405	270111
53	474664	272324
54	487988	249589
55	490101	248802
56	497937	256374
57	500712	254628
58	506331	247309
59	487841	246978
60	474857	269062
61	471020	275806
62	498032	251486
63	484731	250549
64	478855	278342
65	483763	275214
66	485602	277156
67	493343	275074
68	489744	273151
69	493096	248367
70	488882	263340
71	463857	228842
72	467558	229901

http://www.aloki.hu ● ISSN 1589 1623 (Print) ● ISSN 1785 0037 (Online)
DOI: http://dx.doi.org/10.15666/aeer/1902_10331048
© 2021, ALÖKI Kft., Budapest, Hungary

CHARACTERISTICS AND ASSESSMENT OF THE HEAVY METAL CONTENT OF SOIL AND SPINACH WITH DIFFERENT REMEDIATION

WANG, N.[1,2,3,4*] – WEI, Y.[1,2,3,4] – HE, L. R.[1,2,3,4] – LI, G.[1,2,3,4] – SUN, Y. Y.[1,2,3,4] – LU, N.[1,2,3,4]

[1]*Institute of Land Engineering and Technology, Shaanxi Provincial Land Engineering Construction Group Co., Ltd., Xi'an 710075, China*

[2]*Shaanxi Provincial Land Engineering Construction Group Co., Ltd., Xi'an 710075, China*

[3]*Key Laboratory of Degraded and Unused Land Consolidation Engineering, the Ministry of Natural Resources, Xi'an 710075, China*

[4]*Shaanxi Provincial Land Consolidation Engineering Technology Research Center, Xi'an 710075, China*

[*]*Corresponding author*
e-mail: Na0113@126.com; phone: +86-29-8662-5019

(Received 24th Jul 2020; accepted 19th Nov 2020)

Abstract. In this study, we investigated the effects of different treatments on the physicochemical properties of heavy metal contaminated soil. The total amounts of Hg, inorganic As, Pb, and Cd were determined in a soil-spinach system. The results show that for all of the groups, the soil pH increased by 0.16–1.10, and the inorganic As content of the soil increased by 0.7–6.0 mg/kg. The total content of Hg, Cd, and Pb in soil samples after T1–T7 decreased by 0.8–1.76 mg/kg, 8.0–17.1 mg/kg, and 0.02–0.56 mg/kg, respectively. The largest decreases in total Hg and Cd, at 1.76 mg/kg and 0.93 mg/kg, respectively were seen in group T3. Group T5 had the largest decrease in total Pb content, i.e., by 17.1 mg/kg. After the T1-T7 treatments, the amount of Hg, inorganic As, and Cd in the edible portion of the spinach exceed the National Food Safety Contaminant Limit (GB 2762-2012). However, the order of the risk index of the spinach after the seven treatments of restoration is T1 > T4 > T6 > T2 > T3 > T7 > T5. The risk index of treatment T5 is the lowest, which indicates that 3% cassava straw biochar is better than the other two biochar treatments.
Keywords: *phytoremediation technology, soil-spinach, biochar, hazard index, potential ecological risk index*

Introduction

Soil is the foundation of agricultural production, and it plays an essential role in the quality and safety of the agricultural product. Influenced by parent material (Zhuang et al., 2013; Waterlot et al., 2013), sewage irrigation (Hernandez-Soriano et al., 2012), mining (Wang et al., 2019), and other factors, different kinds of pollutants, especially heavy metals, enter the soil environment through the air, water, and other avenues. According to the 2014 Chinese National Soil Pollution Survey Bulletin, the overall soil environmental quality is not good. The overall standard rate of cultivated soil is 19.4%, and the main pollution type is heavy metal pollution (MEP, 2014). However, due to the lack of arable land in China, the polluted soil is still used for food and other crop production (Xiao et al., 2017). Heavy metal pollution in the soil is highly toxic, persistent, and bioavailable. At present, heavy metal pollution in the soil has become a global problem (Li et al., 2014; Tóth et al., 2016). Compared to other pollutants, heavy metals can accumulate and migrate in the soil and destroy the functionality and balance of the soil ecosystem, seriously affecting human health (Lei et al., 2016) and causing food safety issues (Wuana et al.,

http://www.aloki.hu ● ISSN 1589 1623 (Print) ● ISSN1785 0037 (Online)
DOI: http://dx.doi.org/10.15666/aeer/1902_10491066
© 2021, ALÖKI Kft., Budapest, Hungary

2011). Studies have shown that an excessive intake of Pb can damage the nervous system, the endocrine system, and the immune system (Zhang et al., 2012). When pregnant women are exposed to Pb pollution for a relatively long period of time, the Pb can be transferred from the skeleton of the mother to the body of the fetus at a faster rate, which not only causes certain obstacles to the neural development of the fetus but also affects its future life (Reuben et al., 2017). Long-term exposure to a Cd-polluted environment leads to the risk of lung cancer, renal insufficiency, fractures, and hypertension (Li et al., 2013). In addition, inorganic As is also highly toxic. The intake of large amounts of As strongly interferes with blood vessels and the central nervous system, and it can also lead to gene mutation. When the human body is exposed to As pollution for a long time, it is at risk of lung cancer (Järup, 2003). Compared with pesticides and other organic pollutants, heavy metal pollution has a long-term incubation nature, which undoubtedly increases the difficulty of treating soils that have been polluted with heavy metals. At present, the main methods of remediating heavy metal pollution in farmland include physical remediation, chemical remediation, biological remediation, engineering and technical measures, and agricultural ecological remediation. However, most of these remediation techniques are very expensive, so it is necessary to develop more cost-effective techniques that use low-cost adsorbents (Kailash et al., 2010). At present, the application of soil amendment and the optimization of soil nutrient management have become the most common remediation method. It is generally believed that biochar is the most effective adsorbent for the adsorption of heavy metals and organic pollutants in soil, and it can effectively improve the physical and chemical properties of the soil. In addition, the cost of biochar is relatively low (Klasson et al., 2014; Li et al., 2014).

Biochar is produced by the slow pyrolysis (usually < 700°C) of biological residues in a hypoxic environment (Lehmann and Joseph, 2015). Biochar is a type of insoluble, stable, highly aromatic, and carbon-rich solid substance (Titirici et al., 2007; Tang et al., 2013). The main elements of biochar are carbon, hydrogen, and oxygen, but it is highly enriched in carbon (70%–80%). Biochar is made from a wide range of raw materials, mainly including agricultural and forestry waste, such as wood, straw, fruit shell, organic waste generated by industry, and other urban life waste, such as garbage and sludge (Brick et al., 2010; Chen et al., 2010; Cantrell et al., 2012; Enders et al., 2012). Biochar has a large specific surface area, pore structure, and abundant surface functional groups, which can reduce the bioavailability of heavy metals in soil (Pan et al., 2014). Biochar also improves the activity of soil microorganisms, thus increasing the decomposition and deactivation of harmful substances (Baiamonte et al., 2015; Liu et al., 2016; Abujabhah et al., 2016). Biochar not only has a significant impact on the mitigation of heavy metals in soil, but also directly absorbs the heavy metal ions in the soil, reducing the toxicity of the polluted soils and reducing the toxicity of the plants. In addition, biochar is used in soil improvement (Tang et al., 2013), crop yield increase (Glaser et al., 2002), greenhouse gas emission reduction (Van Zwieten et al., 2009; Woolf et al., 2010; Singh et al., 2012), and the remediation of polluted environments (Sun et al., 2011). Therefore, it has broad application prospects. In recent years, the adsorption of heavy metals by biochar has attracted a great deal of attention, especially in the treatment of heavy metals in sewage (Ahmad et al., 2014; Komkiene et al., 2016) and the remediation of heavy metal contaminated soil (Hossain et al., 2010). For example, Choppala et al. (2012) and others demonstrated that biochar can transform Cr^{6+} into Cr^{3+}, thus reducing the toxicity of Cr. Houben et al. (2013) and others found that the addition of 10% biochar significantly reduces the extractable Cd, Zn, and Pb content of heavy metal contaminated soil by 71%,

http://www.aloki.hu ● ISSN 1589 1623 (Print) ● ISSN1785 0037 (Online)
DOI: http://dx.doi.org/10.15666/aeer/1902_10491066
© 2021, ALÖKI Kft., Budapest, Hungary

87%, and 92%, respectively. Bian et al. (2014) determined that the application of crop straw biochar to paddy soil polluted by heavy metals significantly reduced the absorption of Cd by rice. Lu et al. (2014) found that straw biochar can effectively reduce the concentrations of Cu and Pb in aboveground crops, and bamboo biochar can effectively reduce the concentration of Cd in soil. We believe that the influence of biochar on heavy metals is related to not only the raw materials from which the biochar is made and the amount applied to the soil but also the type of heavy metals. This study shows that biochar can effectively reduce the plant availability and ecological toxicity of heavy metals such as Cd and Pb, and it provides a theoretical basis for the remediation of soil contaminated by heavy metals.

In view of the rapid development of agriculture in China, the production of crop straw is also increasing. However, the common practice in China is to burn the straw remaining in the fields after harvest. According to statistics, the total annual output of crop straw in China is more than 6×10^8 tons, among which the outputs of rice, wheat, and corn straw are about 1.1×10^8, 1.3×10^8, and 2.3×10^8 tons, respectively. At present, 25% of crop straw is burned in the open air after the harvest to remove this crop residue (Shi et al., 2014), of which the smoke is harmful to the air quality and human health (Shen et al., 2016). Therefore, it is necessary to find a new method of crop straw utilization. It is cost-effective to use agricultural plant residues as biochar production materials, making it a renewable waste (Nuithitikul et al., 2010). Cassava, rice, and reed straw are the main agricultural waste plant fibers in China. The preparation of biochar based on this material not only fully utilizes the waste resources but also benefits the environment. Previous studies have focused on the remediation effect of a single type of biochar on heavy metals in soil. In this study, different percentages of cassava straw, rice straw, and reed straw biochar were added to heavy metal contaminated soil. The adsorption efficiency and effectiveness of these three types of biochar on the heavy metals were compared. This study can provide supporting data for the improvement of the resource utilization of crop straw and remediation of heavy metal pollution.

Materials and Methods

Test material

The raw materials used in this study were produced by rice straw, cassava straw and reed straw. The biochar sample used in the study was collected in the region of Fupin County. All the biochar used for the tests were prepared using the temperature control method with an oxygen limiting program. First, the cassava stems, rice stems, and reed stems were washed with clean water and allowed to dry naturally. Second, the air-dried and chopped raw materials were placed into closed iron containers. Each container was filled with N_2 for 10 min, the air was emptied, and they were heated in a preheated muffle furnace with limited oxygen. Finally, the muffle furnace was set to 500°C for 4 h. The closed muffle furnace was allowed to naturally cool to room temperature, and the samples were removed and ground to 100 mesh. The basic properties of the biochar materials are shown in *Table 1*.

The soil used in the tests was collected from the Hg mine in Ankang City, Xunyang County. The soil collected was all 0–20 cm topsoil, which was air-dried in a cool place and sieved through a 5-mm sieve.

http://www.aloki.hu ● ISSN 1589 1623 (Print) ● ISSN1785 0037 (Online)
DOI: http://dx.doi.org/10.15666/aeer/1902_10491066
© 2021, ALÖKI Kft., Budapest, Hungary

Table 1. *Basic physicochemical properties of the materials used in the experiments*

Tested materials	Reed biochar	Cassava biochar	Rice biochar
pH	10.6	11.2	10.9
Organic matter (%)	51	64	57
Conductivity (μS /cm)	677	1313	911
Organic carbon (g/kg)	392.34	591.22	658.21
Ash (%)	15.75	9.85	40.00
C/N	85.07	42.13	30.15
C/H	37.55	39.97	36.77

Note: The values in the table are presented as average values

Biochar SEM images were obtained by FEI Q45 scanning electron microscop (FEI, USA). A CHN elemental analyzer (Flash EA 1112, Thermo Finnigan) was used to determine the carbon (C), hydrogen (H), and nitrogen (N) contents of all biochars.

The pH of the biochar and soil were measured in a 1:10 ratio of biochar suspension in deionized water. The concentrations of Hg and inorganic As were digested by HNO_3-H_2SO_4, after that, atomic fluorescence Spectrometry (AFS-9760) at 253.65 nm was used for the measurement. The concentration of Cd and Pb were digested by HNO_3-H_2O_2-HCl with the ratio of 3:1 (hydrochloric and nitric acids), then using ICP-MS (Agilent 7700e, USA) for their measurement.

In the experiment, 20% parallel samples, GSS9-16 and GSB-26 were used for quality control, and the error was controlled within 5%. The reagents were of excellent grade and the test vessels were soaked in 10% nitric acid for more than 24 h before use.

Design of experiment

The spinach was planted in the temperature room of Qinling field monitoring center, and the indoor temperature range was 23 ~ 28℃. Each basin (18.0 cm in height, 20.0 cm in diameter, and 13.0 in bottom diameter) was filled with 3 kg of soil, and a tray was arranged at the bottom of the basin to prevent the leakage of soil and water. Biochar of a certain quality was applied and mixed with the soil according to the experimental design (*Table 2*). The soil water content was more than 60% of the field water capacity throughout the growth period of the spinach. After 30 days of stabilization, the seeds were planted in the plastic basin in May of 2019, three parallel groups were setup for each remediation method. When the spinach trilobal stage, the seedlings were interspecific to 3 plants.

Table 2. *Test design for the different biochar treatments*

Treatments	Specific operation procedures
T1	The control group. No heavy metal reduction measures were taken.
T2	1% reed biochar added
T3	3% reed biochar added
T4	1% cassava biochar added
T5	3% cassava biochar added
T6	1% rice biochar added
T7	3% rice biochar added

http://www.aloki.hu ● ISSN 1589 1623 (Print) ● ISSN1785 0037 (Online)
DOI: http://dx.doi.org/10.15666/aeer/1902_10491066
© 2021, ALÖKI Kft., Budapest, Hungary

After about 45 days later, soil samples and plant samples were collected, after natural air drying, 50 g of soil samples were ground and passed through nylon screen by quartering method. The upper part of plant samples was collected, washed with tap water, then repeatedly washed with deionized water. After being killed at 105℃ for 0.5 h, dried at 75℃ to constant weight, the soil samples were crushed, passed through 60 mesh nylon screen and bagged for standby.

Data analysis method

SPSS 20.0 was used for statistical analysis, one-way ANOVA was used to compare the treatment, Duncan method was used to analyze the difference significance, and Excel 2010 and sigmaplot 10.0 were used to create the plots. The potential ecological risk index was used to evaluate the soil, and the risk index was used to evaluate the heavy metal content in the spinach.

Evaluation method

Potential ecological risk index method

The potential ecological risk index method was proposed by Swedish scientist Hakanson in 1980. Because it considers the toxicity differences of the different heavy metals and the sensitivity of the environment to heavy metal pollution, this method more accurately expresses the impact of heavy metals on the ecological environment. The calculation equations are as follows:

$$C_f^i = \frac{c_s^i}{c_n^i} \quad \text{(Eq.1)}$$

$$E_r^i = T_r^i \times C_f^i \quad \text{(Eq.2)}$$

$$RI = \sum_{i=1}^{n} E_r^i \quad \text{(Eq.3)}$$

In these equations, C_s^i is the measured value of the sample (mg/kg); C_n^i is the soil background value of Shaanxi Province (mg/kg); T_r^i is the toxicity response coefficient of the i-th heavy metal; E_r^i is the potential ecological risk factor of the i-th heavy metal; RI is the potential ecological risk index of the pollutant; and C_f^i is the pollution coefficient of the i-th heavy metal. The classification of the potential ecological risks is shown in *Table 3*.

Hazard index method

The hazardous impact of heavy metals on human health is the result of a combination of various elements. Therefore, the hazard index (HI) used to conduct a comprehensive evaluation of the health risk of heavy metals to the human body. The calculation equation is as follows:

http://www.aloki.hu ● ISSN 1589 1623 (Print) ● ISSN1785 0037 (Online)
DOI: http://dx.doi.org/10.15666/aeer/1902_10491066
© 2021, ALÖKI Kft., Budapest, Hungary

$$HI = \sum_{i=1}^{4} HQ \quad \text{(Eq.4)}$$

Table 3. *Potential ecological risk assessment and corresponding pollution degree*

Potential ecological risk factors, E_r^i		**Potential ecological risk index, RI**	
Single heavy metal threshold interval	Risk factor classification	Threshold range for multiple metals	Risk index classification
(-∞, 40)	A, Slight ecological harm	(-∞, 150)	1 * ROMAN No risk
[40, 80)	B, Moderate ecological damage	[150, 300)	2 * ROMAN Mild risk
[80, 160)	C, Strong ecological harm	[300, 600)	3 * ROMAN moderate risk
[160, 320)	D, Very strong ecological harm	[600, +∞)	4 * ROMAN Serious risk
[320, +∞)	E, Extreme ecological harm	--	--

In *Eq.(4)*, HQ is the health value of a single heavy metal. If HI∈ (-∞, 1.0], the heavy metals have no negative impact on human health; if HI∈(1.0, 10), the heavy metals may have a relatively negative impact on human health; and if HI∈ [10, + ∞), the heavy metals have a toxic impact on human health.

$$HQ_i = \frac{CID_i}{RfD_i} \quad \text{(Eq.5)}$$

In *Eq.(5)*, CID_i is the daily intake of the heavy metal i (mg/kg·d), and RfD_i is the oral dose of heavy metal i (mg/kg·d). According to the EPA health risk model of the United States, the oral reference doses of Hg, As, Pb, and Cd are 0.0003, 0.0003, 0.004, and 0.001 mg/kg·d, respectively.

$$CID_i = \frac{C_i \times IR \times EF \times ED}{BW \times AT} \quad \text{(Eq.6)}$$

In *Eq.(6)*, C_i is the content of heavy metal i in the edible part of the spinach (mg/kg); IR is the average daily meal of adults, 0.389 kg (person·d); EF is the exposure frequency, 350 d/a; ED is the lifetime exposure time, we use 65 a; BW is the average weight of an adult, 62.7 kg; and the life expectancy in days is 65 × 365 d.

Results and Analysis

Surface characteristics of the biochar

Figure 1 shows picture from a scanning electron microscope of the three types of biochar. As can be seen in *Figure 1*, there are differences among the apparent morphologies of the three types of biochar, which is due to the natural differences in the tissue morphology of the different plants. All three types of biochar have porous structures and large specific surface areas. The biochar of the reed pole is relatively smoother, with some long and narrow filaments and noticeable surface gullies. The structure of the cassava biochar is clear and honeycombed, and the number of

http://www.aloki.hu ● ISSN 1589 1623 (Print) ● ISSN1785 0037 (Online)
DOI: http://dx.doi.org/10.15666/aeer/1902_10491066
© 2021, ALÖKI Kft., Budapest, Hungary

micropores is greater than those of the other biochar. The surface of the rice biochar is rough, and there are many small particles on the surface. The results show that the average pore size of the cassava biochar is 12.08 μm, followed by rice biochar (4.26 μm) and reed biochar (2.53 μm).

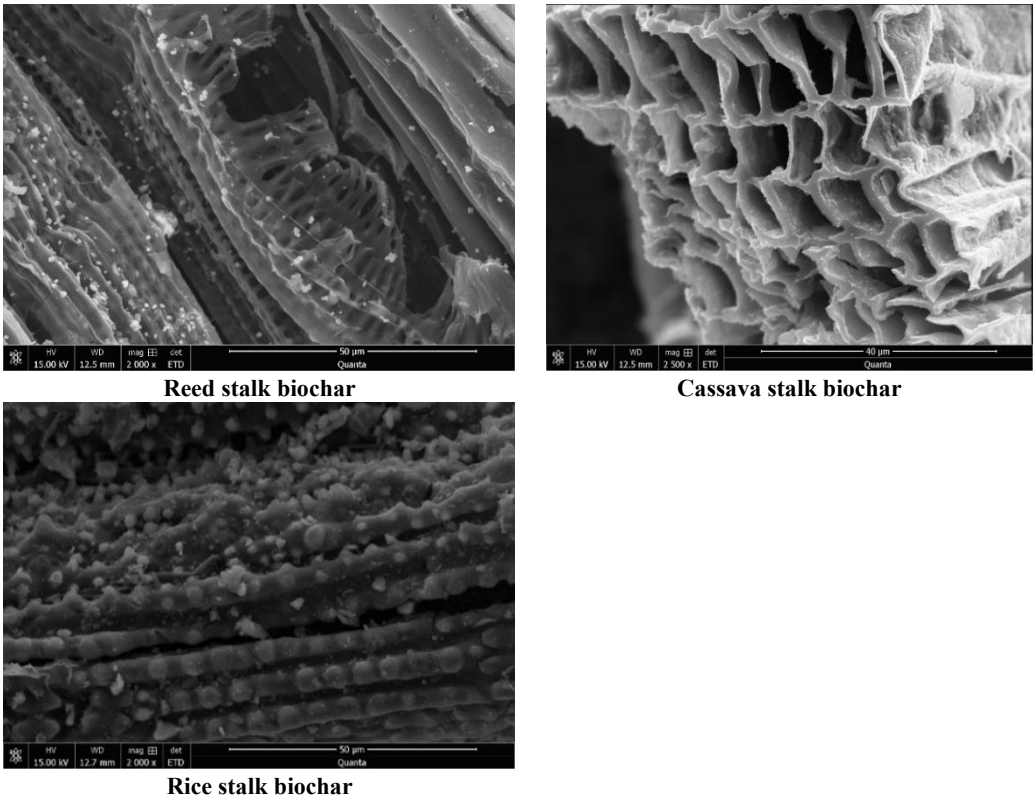


Figure 1. *SEM images of the biochar surfaces*

Analysis and evaluation of the physical and chemical properties and heavy metal content of unrepaired soil

The assessment results of the potential ecological risk factors revealed that the Pb and Cd pollution levels of the soil from the sampling point is level A, i.e., it caused slight harm to the ecological soil environment. The pollution level of inorganic As in the soil is level B, i.e., an intermediate degree of ecological harm; and the Hg pollution level of the soil is level E, i.e., it is very harmful to the ecological soil environment. The potential ecological RI of Hg, Cd, As, and Pb was 2901.59, indicating a serious degree of risk (*Table 4*).

Changes in the organic matter and pH of soil after biochar treatment

The effects of treatments T1–T7 on soil pH and the organic matter are shown in *Figure 2*. As can be seen in *Figure 2*, the pH and organic matter in the soil changed after each treatment. The pH range of the soil before treatment was 6.33–8.46; after the T1–T7 treatments were applied, the pH value of soil increased by 0.16–1.10. The soil organic matter (SOM) content before the treatments were applied ranged from 33.126 to 65.332 g/kg and the change in the SOM content caused by the treatments ranged

http://www.aloki.hu ● ISSN 1589 1623 (Print) ● ISSN1785 0037 (Online)
DOI: http://dx.doi.org/10.15666/aeer/1902_10491066
© 2021, ALÖKI Kft., Budapest, Hungary

from 31.218 to 63.023 g/kg. Specifically, after treatments T2, T6, and T7 were applied, the SOM content increased by 2.10, 1.92, and 2.64 g/kg, respectively; however, for T1, T3, T4, and T5, the SOM content decreased after treatment by 1.91, 2.75, 1.60, and 3.91 g/kg, respectively. The above results show that the pH and organic matter content of the soil changed after the different treatments were applied, but no pattern was revealed in these changes. This could be because the physical and chemical properties of the soil are affected by a variety of factors such as the test temperature and microbial activity.

Table 4. *Evaluation of the heavy metal content of the unamended soil*

Item measured	Average value	Standard value	E_r^i	
			Numerical value	Pollution class
Hg (mg/kg)	5.14±1.35	2.4	2901.59	E
Inorganic As (mg/kg)	75.71±2.76	30	68.21	B
Pb (mg/kg)	94.33±2.69	120	22.04	A
Cd (mg/kg)	0.73±0.33	0.3	28.82	A
pH	6.71±0.85	--	--	--
Organic matter (g/kg)	2.86±0.56	--	--	--
Cation exchange capacity (cmol/kg)	15.96±0.99	--	--	--
RI	--	--	3014.66	IV

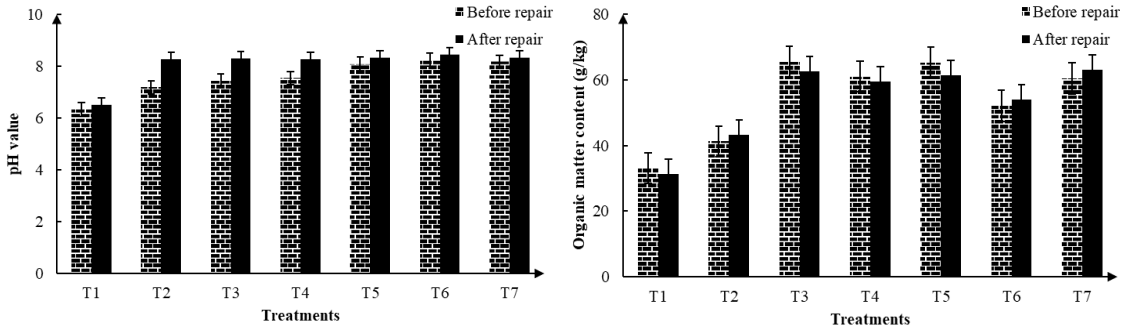


Figure 2. *Changes in the pH value and organic matter content of the soil before and after the different treatments were applied, Error bars represent standard deviation (n =3). The same as below*

Detection and evaluation of the heavy metal content in soil after the different biochar treatments

Characteristics and evaluation of the total Hg content of the soil

The effects of the different remediation treatments on the total Hg content of the soil are shown in *Table 5*. As can be seen in *Table 5*, there is a certain difference in the total Hg content of the soil after treatments T1–T7. Compared with T1, the total Hg content in T2–T7 decreased by 0.97–2.29 mg/kg, and the largest reduction was seen in T3. The results show that the effect of the reed biochar on the total Hg content was the best, and the higher the amount of reed biochar, the stronger its repairing ability. The potential ecological risk assessment index shows that the pollution level of the total Hg content of the soil after treatments T1–T7 were applied was level E. Although the total Hg

http://www.aloki.hu ● ISSN 1589 1623 (Print) ● ISSN1785 0037 (Online)
DOI: http://dx.doi.org/10.15666/aeer/1902_10491066
© 2021, ALÖKI Kft., Budapest, Hungary

content of the soil was lower after treatments T1–T7, it was still high enough to cause serious harm to the ecological soil environment.

Table 5. *Hg content of soil and evaluation of the different treatments (N=3)*

Repair treatments	Mean	E_r^i	
		Value	Pollution level
T1	5.89±0.19	3739.68	E
T2	4.92±0.64	3121.69	E
T3	3.60±0.44	2285.71	E
T4	3.89±0.46	2467.72	E
T5	3.85±0.49	2442.33	E
T6	4.22±0.63	2679.37	E
T7	3.62±0.49	2296.30	E

Note: Every treatment has three parallel (The same as below)

Characteristics and evaluation of the inorganic As content of the soil

The effects of the different remediation treatments on the inorganic As content of the soil are shown in *Table 6*. As can be seen in *Table 6*, compared with T1, after remediation treatments T2–T7 were applied, the inorganic As content of the soil decreased by 0.6-9.8 mg/kg. Among all of the remediation treatments, the inorganic As content of the soil decreased the most after method T3 was applied, with a value of 9.8 mg/kg. The results show that the effect of reed stalk biochar was better than that of the other two materials, and the higher the amount of reed stalk biochar, the better the effect of the remediation. The potential ecological risk assessment index shows that the inorganic As pollution level in the soil after treatments T2 and T3 were applied was level A, i.e., it still causes a slight degree of ecological risk. After treatments T1 and T4–T7 were applied, the pollution level of the inorganic As in the soil was level B. Although the inorganic As content decreased, it still resulted in a moderate degree of harm to the ecological environment.

Table 6. *Inorganic As content and evaluation of the soil after different treatments (N=3)*

Treatment	Mean	E_r^i	
		Value	Pollution level
T1	49.0±3.68	44.14	B
T2	43.2±2.37	38.89	A
T3	39.2±3.12	35.32	A
T4	46.7±3.41	42.07	B
T5	48.4±1.94	43.63	B
T6	47.2±2.16	42.49	B
T7	45.3±3.27	40.84	B

Characteristics and evaluation of the total Pb content of the soil

The total Pb contents of the soil after treatments T1–T7 were applied are shown in *Table 7*. As can be seen in *Table 7*, there is a difference in the total Pb content of the soil after treatments T1–T7 were applied. Compared with method T1, after treatments T2–T7 were applied, the total Pb content of the soil decreased by 10.8–24.1 mg/kg, and

http://www.aloki.hu ● ISSN 1589 1623 (Print) ● ISSN1785 0037 (Online)
DOI: http://dx.doi.org/10.15666/aeer/1902_10491066
© 2021, ALÖKI Kft., Budapest, Hungary

the total Pb content of the soil after T3 was applied decreased by 24.1 mg/kg. The effect of T3 on the recovery of Pb from the soil was better than those of the other treatments, and the higher the content of biochar used, the better the recovery effect. The potential ecological risk index shows that the pollution level of the total Pb in the soil after treatments T1–T7 were applied was level A. Although the total Pb content of the soil after treatments T1-T7 were applied was lower, it was still high enough to cause a slight amount of harm to the ecological soil environment.

Table 7. *Pb content and evaluation of soil after different treatments (N=3)*

Treatment	Mean	E_r^i	
		Value	Pollution level
T1	82.6±13.76	19.30	A
T2	63.1±8.31	14.74	A
T3	58.5±5.99	13.66	A
T4	64.7±3.09	15.11	A
T5	71.8±3.67	16.77	A
T6	63.4±8.49	14.82	A
T7	64.8±3.02	15.13	A

Characteristics and evaluation of the total Cd content of the soil

The total Cd content of the soil after treatments T1–T7 were applied is shown in *Table 8*. As can be seen in *Table 8*, compared with method T1, after treatments T2 and T5 were applied, the Cd content of the soil increased by 0.08 and 0.15 mg/kg, respectively. After treatments T3, T4, and T6 were applied, the Cd content of the soil decreased by 0.20, 0.13, and 0.07 mg/kg, respectively, and the total Cd content of the soil after method T6 was applied decreased more than those of treatments T3 and T4. In general, the remediation effect of each treatment on the Cd in the soil was not significant. The potential ecological risk index shows that the pollution level of the total Cd in the soil after treatments T2 and T5 was level B, i.e., a medium degree of harm to the ecological soil environment. The pollution level of the total Cd in the soil after the other remediation treatments was level A. Although the total Cd content of the soil was low, it was still high enough to cause a slight amount of harm to the ecological soil environment.

Table 8. *Cd content and evaluation of the different repaired soils (N=3)*

Treatment	Mean	E_r^i	
		Value	Pollution levels
T1	0.98±0.09	38.68	A
T2	1.06±0.41	41.97	B
T3	0.78±0.09	30.79	A
T4	0.85±0.05	33.42	A
T5	1.13±0.05	44.74	B
T6	0.91±0.05	36.05	A
T7	0.98±0.07	38.68	A

http://www.aloki.hu ● ISSN 1589 1623 (Print) ● ISSN1785 0037 (Online)
DOI: http://dx.doi.org/10.15666/aeer/1902_10491066
© 2021, ALÖKI Kft., Budapest, Hungary

Changes in the Hg, Pb, Cd and inorganic As content of the soil before and after treatment

Comparisons of the total Hg, Pb, Cd and inorganic As content of the soil before and after the treatments were applied are shown in *Figure 3*. As can be seen in *Figure 3*, the total Hg, Pb, and Cd content of the soil after treatments T1–T7 were applied are lower than those before treatment, with decreases of 0.8–1.76 mg/kg, 8.0–17.1 mg/kg, and 0.02-0.56 mg/kg, respectively. Among all of the groups, the total Hg and Cd content of the soil after T3 was applied show the most improvement, with a decrease of 1.76 mg/kg and 0.93 mg/kg, respectively. After T5 was applied, the total Pb content of the soil decreased the most (17.1 mg/kg). According to the comparison of the specific operation procedures for treatments T1–T7 (*Table 2*), T3 involves the addition of 3% reed biochar, and T5 involves the addition of 3% cassava biochar. Thus, it can be concluded that the addition of 3% reed biochar has a better effect on reducing the total Hg and Cd content of the soil. The addition of 3% cassava biochar can reduce the total Pb in soil. In addition, the inorganic As content of the soil after remediation treatments T2–T7 were applied increased by 0.7–6.0 mg/kg compared with the amounts before remediation. Combined with the results of previous studies (Wei et al., 2016), the pH value in the soil has a significant influence on the effectiveness of available As in the soil. In an acidic environment, the inorganic As in the soil exists in the form of H_3AsO_3. With increasing pH, the inorganic As in the soil is released in the form of dissociation at all levels, which increases the inorganic As content of the soil.

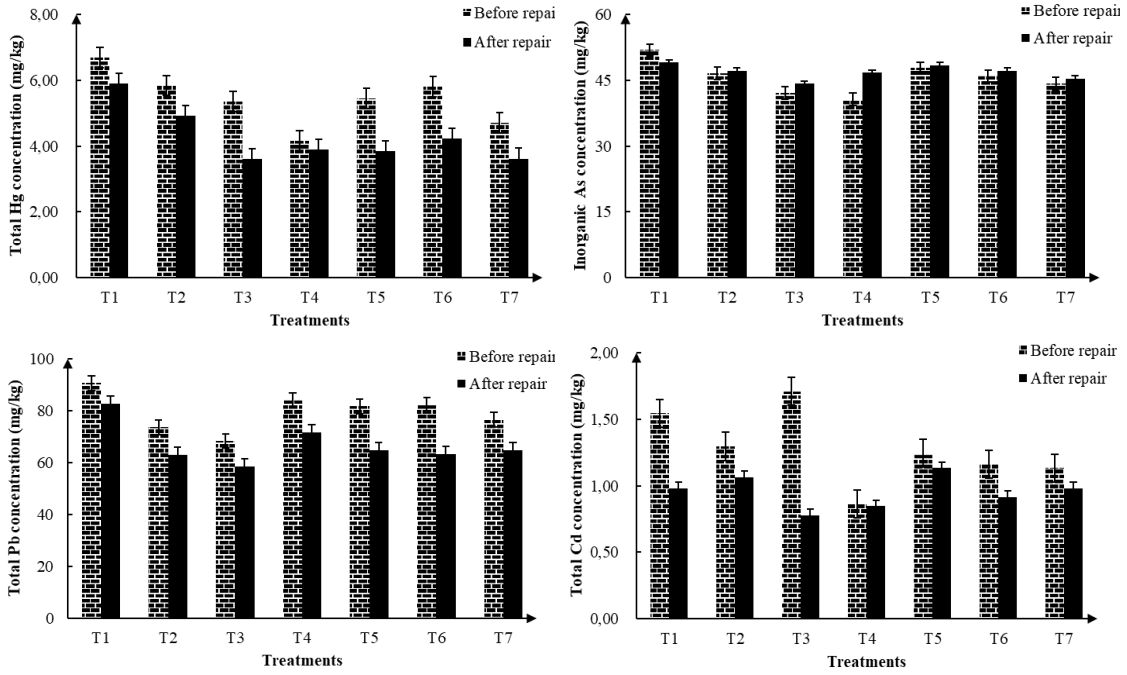


Figure 3. *Changes in the total Hg, Pb, Cd, and inorganic As content of the soil for the different treatments*

http://www.aloki.hu ● ISSN 1589 1623 (Print) ● ISSN1785 0037 (Online)
DOI: http://dx.doi.org/10.15666/aeer/1902_10491066
© 2021, ALÖKI Kft., Budapest, Hungary

Effect and evaluation of the different remediation treatments on the Hg, Pb, Cd, and inorganic As content of spinach

The Hg, Pb, Cd and inorganic As content of the edible parts of spinach after treatments T1–T7 were applied are shown in *Table 9* (Aboveground part). As can be seen in *Table 9*, the average total Hg, Cd, and inorganic As content of the edible part of the spinach after treatments T1–T7 were applied are 0.360–1.059, 0.790–2.605, and 0.540–1.143 mg/kg, respectively. They are all over the threshold of pollutants in foods according to the National Food Safety Standard (GB 2762-2012). The average total Pb content of the edible part of the spinach after treatments T1–T7 was 0.211–1.321 mg/kg. With the exception that the total Pb content of the edible part of the spinach after T1 was slightly higher than the threshold set by GB 2762-2012, the results of the other groups are all below the threshold of the national standard. Among them, the total Pb content of the edible part of the spinach after T1 reached 1.321 mg/kg, which is 1.32 times higher than the limit of pollutants set by GB 2762-2012. Combined with the risk index evaluation, except for T5, the risk index HI of the edible part of the spinach after treatments T1–T7 were applied is greater than 10, which indicates that the total Hg, Pb, Cd and inorganic As content of the spinach have toxic effects on human health. The HI ranking of the edible parts of the spinach follows the order T1–T7 of T1 > T4 > T6 > T2 > T3 > T7 > T5.

Table 9. *Content and evaluation of the total Hg, Pb, Cd, and inorganic As content of the spinach after the different treatments*

Treatment	Total Hg content (mg/kg)	Inorganic As content (mg/kg)	Total Pb content (mg/kg)	Total Cd content (mg/kg)	Hazard index (HI)
T1(control group)	0.759±0.067	2.452±0.376	1.321±0.269	0.783±0.110	12.99
T2	0.737±0.008	2.322±0.302	0.584±0.074	0.872±0.188	12.12
T3	0.468±0.059	2.508±0.131	0.451±0.103	0.908±0.055	11.97
T4	1.059±0.152	1.923±0.265	0.593±0.094	0.965±0.119	12.60
T5	0.482±0.044	0.790±0.020	0.527±0.208	0.759±0.104	7.82
T6	0.360±0.065	2.219±0.511	0.211±0.061	1.143±0.067	12.23
T7	0.851±0.154	2.605±0.222	0.338±0.058	0.540±0.094	10.57
GB 2762-2012	0.01	0.5	1.0	0.2	--

Discussion

It is well known that the pH value is one of the main factors that affects the adsorption of heavy metals. The total Hg, Pb, and Cd content of the soil after remediation treatments T2–T7 were applied were lower than those before the remediation, while the inorganic As content of the soil after remediation was slightly higher than that before remediation. This may be due to the increase in the soil pH caused by the addition of the biochar, which promoted the release of inorganic As into the soil (Hartley et al., 2009). Among the soil properties, the soil pH value has a significant influence on the solubility and form of the metals in soil and plays a vital role in the form of the metals as well as the solubility, migration, and final bioavailability of the minerals (Zeng et al., 2011). In addition, pH value also affects the surface charge of the adsorbent and the ionization adsorption (Yu et al., 2013). Xiao et

http://www.aloki.hu ● ISSN 1589 1623 (Print) ● ISSN1785 0037 (Online)
DOI: http://dx.doi.org/10.15666/aeer/1902_10491066
© 2021, ALÖKI Kft., Budapest, Hungary

al. (2017) pointed out that the degree of the adsorption of the heavy metals onto the biochar is closely related to the acid-base degree of the biochar in addition to the pyrolysis temperature and the ionic strength of the biochar. As the pH value increases, the adsorption of the heavy metals onto the biochar increases significantly. For example, Rahman and Islam (2009) reported that the adsorption capacity of biochar for Cu in solution is very low under acidic conditions, only 28.66%. When the pH value reached 7, the adsorption capacity increased significantly, reaching 83.25%. Kilic et al. (2013) investigated the adsorbtion of Ni and Co in an aqueous solution onto almond shell biochar. The results revealed that when the pH is increased from 2 to 6, the adsorption capacity of the Ni and Co ions increased, and the surface of the adsorbent was negatively charged, which increased the interaction between the Ni (II) and Co (II) and the binding sites. Zeng et al. (2011) found that under acidic conditions, soluble trivalent Cr was reduced to pentavalent Cr, and the mobility and effectiveness of Cr increased with increasing pH. Houben et al. (2013) showed that biochar increased soil pH and reduced the extractability and bioavailability of the Cd, Zn, and Pb in the soil. The positive correlation between the available Cr and the soil pH has also been reported in previous studies (Guo et al., 2017). However, several studies have shown that when the pH exceeds a certain value, the adsorption efficiency of biochar for metal ions decreases, which may be due to the formation of soluble hydroxylation complexes of the metal ions and their competition with the active centers (Sari et al., 2007).

In addition to pH, the organic matter in the soil also affects the availability of the heavy metals. The effect of organic matter on the availability of heavy metals has been widely studied. Studies have shown that as the organic matter content of the soil decreases, the adsorption capacity of the heavy metals in the soil components also decreases (Hettiarachchi et al., 2003; Antoniadis et al., 2008). Bradl (2004) also reported that the organic matter content of the soil is the main characteristic of heavy metal adsorption, and the combination of metal ions and organic matter often reduces the concentration of free heavy metal ions in a soil solution and the toxicity of the heavy metals Abollino et al. (2003). Pichtel et al. (2008) and Gunadasa et al. (2012) determined that as the organic matter content of the soil increases, the Cd content of the plants grown in the soil significantly decreases. Pichtel and Bradway (2008) also pointed out that the addition of organic fertilizer to the soil significantly reduced the bioavailability of Cd. Bolan et al. (2014) and others found that adding organic modifiers to soil contaminated with heavy metals can reduce the mobility of the heavy metals.

In this study, seven different remediation treatments were investigated to determine their impacts on the Hg, inorganic As, Pb, and Cd content of soil and spinach, and their impacts were found to be different. Among them, the risk index of the heavy metals in the spinach after treatments T2–T7 were applied was lower than that of T1, because no biochar was added to T1, while the other factors, e.g., temperature, climate, and water content, were exactly the same as in treatments T2–T7. The risk index of the heavy metals in the spinach was the lowest after method T5 was applied, and the remediation measure taken in method T5 was the addition of 3% cassava stem biochar. The pore diameter of the cassava stem is larger than those of the other types of biochar, which is conducive to the adsorption of heavy metals. However, the pH value of the soil treated using method T5 was higher after the biochar was added. In addition, 3% biochar is higher than 1% biochar, and the application of 3% cassava stem biochar can more effectively remediate the heavy metal pollution in soil and prevent the migration of

http://www.aloki.hu ● ISSN 1589 1623 (Print) ● ISSN1785 0037 (Online)
DOI: http://dx.doi.org/10.15666/aeer/1902_10491066
© 2021, ALÖKI Kft., Budapest, Hungary

heavy metal ions into plants. Compared with treatments T3, T5, and T7, the content of the other heavy metals in the soil after the three remediation treatments were applied were significantly lower than the contents before the remediation, except for inorganic As. The risk index of the heavy metals in the spinach after treatments T3, T5, and T7 were applied was lower than that for treatments T2, T4, and T6. This result shows that the adsorption of heavy metals in soil by biochar decreases as the amount of biochar added increases, and it can effectively inhibit heavy metals from entering plants through bioconcentration. The above results show that cassava stem biochar has a better adsorption effect on heavy metals than the other types of biochar, and the application of biochar can not only improve the physical and chemical properties of soil and decrease the contents of heavy metals but also significantly reduce the risk index of spinach, which is worth promoting in future research and production.

Conclusions

(1) Before remediation, the total Pb and Cd content of the soil indicated slight pollution, the inorganic As content indicated moderate pollution, and the total Hg content indicated extreme pollution. The potential ecological RI of the total Hg, Pb, Cd, and inorganic As was 3014.66, and the pollution level was extremely high, indicating that there was a certain degree of heavy metal pollution in the soil from the collection area (Hg mining area, Xunyang, Ankang).

(2) Compared with the conditions before remediation, the organic matter content and pH value of the soil after remediation treatments T1–T7 were changed. The pH values of the soil increased by 0.16–1.10, indicating that treatments T1–T7 have a certain impact on the physical and chemical properties of the soil.

(3) Compared with the conditions before remediation, after treatments T2–T7 were applied, the inorganic As contents of the soil increased by 0.7–6.0 mg/kg, and after treatments T1–T7 were applied, the total Hg, Cd, and Pb content of the soil decreased by 0.8–1.76 mg/kg, 8.0–17.1 mg/kg, and 0.02–0.56 mg/kg, respectively. After T3 was applied, the total Hg and Cd contents of the soil decreased by 1.76 mg/kg and 0.93 mg/kg, respectively. After T5 was applied, the total Pb content of the soil decreased the most, i.e., by 17.1 mg/kg.

(4) After treatments T1–T7 were applied, the average total Hg, Cd and inorganic As content of the edible part of the spinach were 0.360–1.059, 0.540–1.143 and 0.790-2.605mg/kg, respectively, which exceeds GB 2762-2012. After method T1, the total Pb content of the edible part of the spinach was 1.321 mg/kg, which exceeds GB 2762-2012. The amount of Pb pollutants in the spinach was 1.32 times the limit of GB 2762-2012. In addition, the risk index of the spinach after treatments T1–T7 were applied is greater than 10, which indicates that the crops in the soil collection area (Ankang, Xunyang Hg mining area) are more likely to cause harm to human health, and more attention should be paid to farming in this area.

(5) All in all, biochar can improve soil physical properties and heavy metal content, and significantly reduce the risk index of spinach edible parts, which is worthy of popularization and application. However, in the study, the remediation effect of biochar on heavy metals is not obvious. In the later research, we should focus on the properties of different raw materials and the adsorption mechanism of heavy metals.

http://www.aloki.hu ● ISSN 1589 1623 (Print) ● ISSN1785 0037 (Online)
DOI: http://dx.doi.org/10.15666/aeer/1902_10491066
© 2021, ALÖKI Kft., Budapest, Hungary

Acknowledgments. Financial support was provided by the Research Project of Shaanxi Provincial Land Engineering Construction Group in China (DJNY2021-18). We thank LetPub (www.letpub.com) for its linguistic assistance during the preparation of this manuscript.

REFERENCES

[1] Abollino, O., Aceto, M., Malandrino, M., Sarzanini, C., Mentasti, E. (2003): Adsorption of heavy metals on Na-montmorillonite. Effect of pH and organic substances. – Water Research 37(7): 1619-1627.

[2] Abujabhah, I. S., Bound, S., Doyle, R. B., Bowman, J. P. (2016): Effects of biochar and compost amendments on soil physico-chemical properties and the total community within a temperate agricultural soil. – Applied Soil Ecology 98: 243-253.

[3] Ahmad, M., Rajapaksha, A. U., Lim, J. E., Zhang, M., Bolan, N., Mohan, D., Vithanage, M., Lee, S. S., Ok, Y. S. (2014): Biochar as a sorbent for contaminant management in soil and water: a review. – Chemosphere 99: 19-33.

[4] Antoniadis, V., Robinson, J. S., Alloway, B. J. (2008): Effects of short-term pH fluctuations on cadmium, nickel, lead, and zinc availability to ryegrass in a sewage sludge-amended field. – Chemosphere 71(4): 759-764.

[5] Baiamonte, G., de Pasquale, C., Marsala, V., Cimó, G., Alonzo, G., Crescimanno, G., Conte, P. (2015): Structure alteration of a sandy-clay soil by biochar amendments. – Journal of soil & sediments 15: 816-824.

[6] Bian, R., Joseph, S., Cui, L., Pan, G., Li, L., Liu, X., Zhang, A., Rutlidge, H., Wong, S., Chia, C., Marjo, C., Gong, B., Munroe, P., Donne, S. (2014): A three-year experiment confirms continuous immobilization of cadmium and lead in contaminated paddy field with biochar amendment. – Journal of Hazardous Materials 272: 121-128.

[7] Bolan, N., Kunhikrishnan, A., Thangarajan, R., Kumpiene, J., Park, J., Makino, T., Kirkham, M. B., Scheckel, K. (2014): Remediation of heavy metal(loid)s contaminated soils–to mobilize or to immobilize? – Journal of Hazardous Materials 266: 141-166.

[8] Bradl, H. B. (2004): Adsorption of heavy metal ions on soils and soils constituents. – Journal of Colloid & Interface Science 277(1): 1-18.

[9] Brick, S., Lyutse, S. (2010): Biochar: Assessing the promise and risks to guide US policy. – Natural Resources Defense Council. USA. http://www. nrdc. org/energy/files/biochar_paper.

[10] Cantrell, K. B., Hunt, P. G., Uchimiya, M., Novak, J. M., Ro, K. S. (2012): Impact of pyrolysis temperature and manure source on physicochemical characteristics of biochar. – Bioresource Technology 107: 419-428.

[11] Chen, B., Chen, Z., Lv, S. (2010): A novel magnetic biochar efficiently sorbs organic pollutants and phosphate. – Bioresource Technology 102(2): 716-723.

[12] Choppala, G. K., Bolan, N. S., Megharaj, M., Chen, Z., Naidu, R. (2012): The influence of biochar and black carbon on reduction and bioavailability of chromate in soils. – Journal of Environmental Quality 41(4): 1175-1184.

[13] Enders, A., Hanley, K., Whitman, T., Joseph, S., Lehmann, J. (2012): Characterization of biochars to evaluate recalcitrance and agronomic performance. – Bioresource Technology 114: 644-653.

[14] Glaser, B., Lehmann, J., Zech, W. (2002): Ameliorating physical and chemical properties of highly weathered soils in the tropics with charcoal - a review. – Biology & Fertility of Soils 35: 219-230.

[15] Gunadasa, H., Yapa, P. I., Nissanka, S. P., Perera, S. P. (2012): Remediation of Pb/Cd contaminated forest soils by compost and mycorrhizae: will it be a solution to the forest dieback. – In International Conference on Future Environment and Energy 28: 139-144.

[16] Guo, X., Li, H., Chen, H. (2017): The effects of biochar and intercropping on the Cd, Cr and Zn speciation in soils and plant uptake bymachilus pauhoi. – Bulletin of

http://www.aloki.hu ● ISSN 1589 1623 (Print) ● ISSN1785 0037 (Online)
DOI: http://dx.doi.org/10.15666/aeer/1902_10491066
© 2021, ALÖKI Kft., Budapest, Hungary

Environmental Contamination & Toxicology 98(4): 1-8.
[17] Hakanson, L. (1980): An ecological risk index for aquatic pollution control. A sedimentological approach. – Water Research 14(8): 975-1001.
[18] Hartley, W., Dickinson, N. M., Riby, P., Lepp, N. W. (2009): Arsenic mobility in brownfield soils amended with green waste compost or biochar and planted with Miscanthus. – Environmental Pollution 157(10): 2654-2662.
[19] Hernandez-Soriano, M. C., Jimenez-Lopez, J. C. (2012): Effects of soil water content and organic matter addition on the speciation and bioavailability of heavy metals. – Science of Total Environment 423: 55-61.
[20] Hettiarachchi, G. M., Ryan, J. A., Chaney, R. L., La Fleur, C. M. (2003): Sorption and desorption of cadmium by different fractions of biosolids-amended soils. – Journal of Environment Quality 32(5): 1684-1693.
[21] Hossain, M. K., Strezov, V., Chan, K. Y., Nelson, P. F. (2010): Agronomic properties of wastewater sludge biochar and bioavailability of metals in production of cherry tomato (*Lycopersicon esculentum*). – Chemosphere 78(9): 1167-1171.
[22] Houben, D., Evrard, L., Sonnet, P. (2013): Mobility, bioavailability and pH-dependent leaching of cadmium, zinc and lead in a contaminated soil amended with biochar. – Chemosphere 92(11): 1450-1457.
[23] Järup, L. (2003): Hazards of heavy metal contamination. – Brit Med Bull. 68: 167-182.
[24] Kailash, D., Dharmendra, P., Anil, V. (2010): Low cost adsorbents for heavy metal removal from wastewater: a review. – Research Journal of Chemistry & Environment 14(1): 100-103.
[25] Kılıc, M., Kırbıyık, C., Çepelioğullar, Ö., Pütün, A. E. (2013): Adsorption of heavy metal ions from aqueous solutions by bio-char, a by-product of pyrolysis. – Applied Surface Science 283(15): 856-862.
[26] Klasson, K. T., Uchimiya, M., Lima, I. M. (2014): Uncovering surface area and micropores in almond shell biochars by rainwater wash. – Chemosphere 111: 129-134.
[27] Komkiene, J., Baltrenaite, E. (2016): Biochar as adsorbent for removal of heavy metal ions [Cadmium(II), Copper(II), Lead(II), Zinc(II)] from aqueous phase. – International Journal of Environmental Science & Technology 13(2): 471-482.
[28] Lehmann, J., Joseph, S. (2015): Biochar for Environmental Management: Science, Technology and Implementation. – Science and Technology 25(1): 15801-15811.
[29] Lei, K., Giubilato, E., Critto, A., Pan, H. Y., Lin, C. Y. (2016): Contamination and human health risk of lead in soils around lead/zinc smelting areas in China. – Environmental science and pollution research international 23(13): 13128-13136.
[30] Li, Z. Y., Ma, Z. W., van der Kuijp, T. J., Yuan, Z. W., Huang, L. (2013): A review of soil heavy metal pollution from mines in China: pollution and health risk assessment. – Science of Total Environment 468-469: 843-853.
[31] Li, J. F., Li, Y. M., Wu, Y. L., Zheng, M. Y. (2014): A comparison of biochars from lignin, cellulose and wood as the sorbent to an aromatic pollutant. – Journal of Hazardous Materials 280: 450-457.
[32] Liu, Y. X., Lu, H. H., Yang, S. M., Wang, Y. F. (2016): Impacts of biochar addition on rice yield and soil properties in a cold waterlogged paddy for two crop seasons. – Field Crops Research 191: 161-167.
[33] Lu, K. P., Yang, X., Shen, J. J., Robinson, B., Huang, H. G., Liu, D., Bolan, N., Pei, J. C., Wang, H. L. (2014): Effect of bamboo and rice straw biochars on the bioavailability of Cd, Cu, Pb and Zn to Sedum plumbizincicola. – Agriculture, Ecosystems and Environment 191: 124-132.
[34] MEP (2014): China soil pollution survey communique in Chinese. – Ministry of Environmental Protection (in Chinese).
[35] Nuithitikul, K., Srikhun, S., Hirunpraditkoon, S. (2010): Influences of pyrolysis condition and acid treatment on properties of durian peel-based activated carbon. – Bioresource Technology 101(1): 426-429.

http://www.aloki.hu ● ISSN 1589 1623 (Print) ● ISSN1785 0037 (Online)
DOI: http://dx.doi.org/10.15666/aeer/1902_10491066
© 2021, ALÖKI Kft., Budapest, Hungary

[36] Pan, J. J., Jiang, J., Xu, R. K. (2014): Removal of Cr (VI) from aqueous solutions by Na_2SO_3/$FeSO_4$ combined with peanut straw biochar. – Chemosphere 101: 71-76.
[37] Pichtel, J., Bradway, D. J. (2008): Conventional crops and organic amendments for Pb, Cd and Zn treatment at a severely contaminated site. – Bioresource Technology 99(5): 1242-1251.
[38] Rahman, M. S., Islam, M. R. (2009): Effects of pH on isotherms modeling for Cu (II) ions adsorption using maple wood sawdust. – Chemical Engineering Journal 149(1-3): 273-280.
[39] Reuben, A., Caspi, A., Belsky, D. W., Broadbent, J., Harrington, H., Sugden, K., Houts, R. M., Ramrakha, S., Poulton, R., Moffitt, T. E. (2017): Association of childhood blood lead levels with cognitive function and socioeconomic status at age 38 years and with IQ change and socioeconomic mobility between childhood and adulthood. – JAMA 317(12): 1244-1251.
[40] Sarı, A., Tuzen, M., Uluözlü, Ö. D., Soylak, M. (2007): Biosorption of Pb (II) and Ni (II) from aqueous solution by lichen (*Cladonia furcata*) biomass. – Biochemical Engineering Journal 37(2): 151-158.
[41] Shen, X., Huang, D. Y., Ren, X. F., Zhu, H. H., Wang, S., Xu, C., He, Y. B., Luo, Z. C., Zhu, Q. H. (2016): Phytoavailability of Cd and Pb in crop straw biochar-amended soil is related to the heavy metal content of both biochar and soil. – Journal of Environmental Management 168: 245-251.
[42] Shi, T., Liu, Y., Zhang, L., Hao, L., Gao, Z. (2014): Burning in agricultural landscapes: an emerging natural and human issue in China. – Landscape Ecology 29(10): 1785-1798.
[43] Singh, B. P., Cowie, A. L., Smernik, R. J. (2012): Biochar carbon stability in a clayey soil as a function of feedstock and pyrolysis temperature. – Environmental Science & Technology 46: 11770-11778.
[44] Sun, K., Keiluweit, M., Kleber, M., Pan, Z., Xing, B. (2011): Sorption of fluorinated herbicides to plant biomass-derived biochars as a function of molecular structure. – Bioresource Technology 102(21): 9897-9903.
[45] Tang, J., Zhu, W., Kookana, R., Katayama, A. (2013): Characteristics of biochar and its application in remediation of contaminated soil. – Journal of Bioence & Bioengineering 116(6): 653-659.
[46] Titirici, M. M., Thomas, A., Yu, S. H., Müller, J-O., Antonietti, M. (2007): A direct synthesis of mesoporous carbons with bicontinuous pore morphology from crude plant material by hydrothermal carbonization. – Chemistry of Materials 19(17): 4205-4212.
[47] Tóth, G., Hermann, T., Szatmári, G., Pásztor, L. (2016): Maps of heavy metals in the soils of the European Union and proposed priority areas for detailed assessment. – Science of Total Environment 565: 1054-1062.
[48] Van Zwieten, L., Singh, B. P., Joseph, S. D., Kimber, S., Cowie, A. L. (2009): Biochar and emission of non-CO_2 greenhouse gases from soil. – In: Lehmann, J., Joseph, S. (eds.) Biochar for environmental management science and technology, pp. 227-249.
[49] Wang, N., Han, J. C., Wei, Y., Li, G., Sun, Y. (2019): Potential Ecological Risk and Health Risk Assessment of Heavy Metals and Metalloid in Soil around Xunyang Mining Areas. – Sustainability 11(18): 4828.
[50] Waterlot, C., Bidar, G., Pelfréne, A., Roussel, H., Fourrier, H., Douay, F. (2013): Contamination, fractionation and availability of metals in urban soils in the vicinity of former lead and zinc smelters. – Pedosphere 23(2): 143-159.
[51] Wei, M., Chen, J., Wang, X. (2016): Removal of arsenic and cadmium with sequential soil washing techniques using Na_2EDTA, oxalic and phosphoric acid: optimization conditions, removal effectiveness and ecological risks. – Chemosphere 156: 252-261.
[52] Woolf, D., Amonette, J. E., Street-Perrott, F. A., Lehmann, J., Joseph, S. (2010): Sustainable biochar to mitigate global climate change. – Nature Communications 1: 56.
[53] Wuana, R. A., Okieimen, F. E. (2011): Heavy metals in contaminated soils: a review of sources, chemistry, risks and best available strategies for remediation. – ISRN Ecology:

http://www.aloki.hu ● ISSN 1589 1623 (Print) ● ISSN1785 0037 (Online)
DOI: http://dx.doi.org/10.15666/aeer/1902_10491066
© 2021, ALÖKI Kft., Budapest, Hungary

402647.
[54] Xiao, R., Wang, S., Li, R., Wang, J. J., Zhang, Z. (2017): Soil heavy metal contamination and health risks associated with artisanal gold mining in Tongguan, Shaanxi, China. – Ecotoxicology and Environmental Safety 141: 17-24.
[55] Xiao, Y., Xue, Y., Gao, F., Mosa, A. (2017): Sorption of heavy metal ions onto crayfish shell biochar: effect of pyrolysis temperature, pH and ionic strength. – Journal of the Taiwan Institute of Chemical Engineers 80: 114-121.
[56] Yu, J. X., Wang, L. Y., Chi, R. A., Zhang, Y. F., Xu, Z. G., Guo, J. (2013): Competitive adsorption of Pb^{2+} and Cd^{2+} on magnetic modified sugarcane bagasse prepared by two simple steps. – Applied Surface Science 268: 163-170.
[57] Zeng, F., Ali, S., Zhang, H., Ouyang, Y., Qiu, B., Wu, F., Zhang, G. (2011): The influence of pH and organic matter content in paddy soil on heavy metal availability and their uptake by rice plants. – Environmental Pollution 159(1): 84-91.
[58] Zhang, X., Yang, L., Li, Y., Li, H., Wang, W., Ye, B. (2012): Impacts of lead/zinc mining and smelting on the environment and human health in China. – Environmental Monitoring & Assessment 184(4): 2261-2273.
[59] Zhuang, P., Li, Z. A., Zou, B., Xia, H. P., Wang, G. (2013): Heavy metal contamination in soil and soybean near the Dabaoshan Mine, South China. – Pedosphere 23(3): 298-304.

http://www.aloki.hu ● ISSN 1589 1623 (Print) ● ISSN1785 0037 (Online)
DOI: http://dx.doi.org/10.15666/aeer/1902_10491066
© 2021, ALÖKI Kft., Budapest, Hungary

BIOMASS AND SPATIAL DISTRIBUTION ESTIMATES OF HAIRTAIL (*TRICHIURUS JAPONICUS*) IN THE NORTHERN WATERS OF TAIWAN

KANG, M.[1] – HUANG, H.[2] – FAJARYANTI, R.[1] – YE, H.[2] – ZHANG, H.[3] – LIU, J.[4*]

[1]*Department of Maritime Police and Production System/Institute of Marine Industry, Gyeongsang National University, Tongyeong 53064, Republic of Korea*

[2]*Fisheries Research Institute, Council of Agriculture, Keelung 20246, Taiwan*

[3]*Yangtze River Fisheries Research Institute, Chinese Academy of Fishery Sciences, Wuhan 430223, China*

[4]*Department of Fishery Production and Management, National Kaohsiung University of Science and Technology, Sanmin District, Kaohsiung City 80778, Taiwan*

[*]*Corresponding author*
e-mail: ljm0723@nkust.edu.tw; phone: +886-90-666-8656

(Received 13th Aug 2020; accepted 22nd Oct 2020)

Abstract. In the East China Sea, the population structure of hairtail has varied for the last 20–30 years because of high intensity of fishing pressure. Therefore, for the sustainable management of hairtail, a conservative measure is required on the basis of scientific research. Acoustic transect line survey was conducted from 10 to 17 Dec 2019 in the northern sea of Taiwan along with 7 pole and line fishing and 1 trawl sampling to estimate the biomass and spatial distributional characteristics of hairtail. Two fishing gears had very different results. Thus, for hairtail allocation, three interpretation scenarios of low, medium, and high in total backscatter were considered. Consequently, the hairtail biomass in three scenarios were to be 5286 (30%), 7048 (40%), and 8810 tons (50%), respectively. Acoustic data from a long coastal line and three lines at a similar location were extracted to examine fish distributional characteristics. Lastly interpolated water temperature and salinity with backscatters were compared. This study can support in designing an integrated acoustic trawl survey next year, as well as the sustainable hairtail resource management.
Keywords: *hairtail, biomass, fish school property, water temperature, fishing gear*

Introduction

Largehead hairtail (*Trichiurus japonicus*) is widely distributed throughout the tropical and temperate regions of the world and commonly inhabit in muddy sand bottoms of the continental shelf. It is one of the most commercially and ecologically important fish species in Taiwan, Korea, Japan, and China (Kim and Rho, 2002; Liu et al., 2009). It is characterized by extensive migration, year-around long spawning period, and a slow growing species with a life span of up to nine years. It is a long and slender fish and a swimbladder-bearing, and feeds on crustaceans and a variety of small fishes including its own juvenile. It serves as one of the top predators in the ecosystem (Wu, 1991; Duarte and Garc, 1999; Froese and Pauly, 2019). In the East China Sea, it is a primary fish species incorporating a large proportion of the fishery productivity. In particular, it is an important commercial marine species in Taiwanese fisheries.

The East China Sea is one of the typical over-exploited ecosystems in the world where a number of fish populations are overfished. Hairtail has been extensively exploited since

http://www.aloki.hu ● ISSN 1589 1623 (Print) ● ISSN 1785 0037 (Online)
DOI: http://dx.doi.org/10.15666/aeer/1902_10671083
© 2021, ALÖKI Kft., Budapest, Hungary

the 1950s in the East China Sea, its annual catch in Taiwan was approximately 16,000 tons in recent years. For targeting hairtail in northeastern water off Taiwan, the main fishing season is from September to December, sometimes until January or February of the following year. Because of high intensity of fishing pressure and overfishing, the population structure of hairtail has been varied for the last 20–30 years. It has had a declining trend in hairtail population and its mean population age (Zhou et al., 2002; Panhwar et al., 2018). Therefore, for the sustainable management of hairtail, a conservative measure is required on the basis of scientific research. First of all, reliable estimates of the biomass and spatial distribution of hairtail are important prerequisites. Meanwhile, the changes in spatial distribution of fish can have a significant impact on species interactions. The spatial distributional property of fish is closely connected to fish population since its elements have a positive relationship with fish population (Hutchings, 1996; Reuchlin-Hugenholtz et al., 2015). Thus, the spatial distributional information has a considerable potential to enhance hairtail resource management plans. Fisheries managers can take steps such as biomass limit or certain time period of fishing ban to attain the maintenance of a healthy and productive population of commercially exploited hairtail.

To understand the spatial distribution and biomass of fishery resources, scientific echosounders have been widely used globally (Zhang et al., 2014; Kang et al., 2015; Park et al., 2016). Using an echosounder has great advantages. It covers relatively a wide area in a short time, and produces accurate and precise acoustic data that lead to valuable information on fish abundance and their distributional properties throughout water columns (Simmonds and MacLennan, 2005). To date, the estimation of the biomass and spatial distribution of hairtail off northern Taiwan had not been studied. In Taiwan, a few studies using an echosounder have been done. A couple of studies were to detect gas plume images on the mud volcano a 38 kHz echo sounder to understand the distribution of relevant gas emissions (Hsu et al., 2013) and to realize the intensity of gas emissions and the magnitude of tremors in relation to tidal range (Hsu et al., 2018). For targeting marine fauna in water column, some research was done. For example, acoustic sound scattering layers and their moving speed in northeastern Taiwan were observed using a 38 kHz echosounder (Lee et al., 2011), anchovy larvae were detected by a 200 kHz commercial echosounder to associate with environmental factors (Lee et al., 1995), and commercially important fish species such as skipjack, round scad, horse mackerel, anchovy and larval fish were acoustically and statistically identified using a 420 kHz echosounder (Lu and Lee, 1995). However, there was no study for aiming hairtail using an echosounder. It is the first time to conduct an acoustic survey for targeting hairtail in Taiwan. We hope that the result of this study can assist in designing a next acoustic survey for a better management of the species. The objective of this study is to estimate the biomass and spatial distributional characteristics of hairtail in the northern water of Taiwan.

Materials and Methods

Field survey

Acoustic transect line survey was conducted from 10 Dec 2019 to 17 Dec 2019 in the northern sea of Taiwan. It included 13 parallel transect lines (*Fig. 1*). The green line was entire voyage line. An average transect line was 7.5 nm and a total survey area was 238.2 nm^2. Acoustic data were collected on RV Fishery Research 2 (340 tons) using a

http://www.aloki.hu ● ISSN 1589 1623 (Print) ● ISSN 1785 0037 (Online)
DOI: http://dx.doi.org/10.15666/aeer/1902_10671083
© 2021, ALÖKI Kft., Budapest, Hungary

calibrated scientific echosounder with three frequencies (Simrad EK60, 38, 120, and 200 kHz). Three transducers had the same norminal beam width of 7°. The sounder sampled the water column at ping rate of 3.3 Hz with a pulse duration of 0.256 ms.

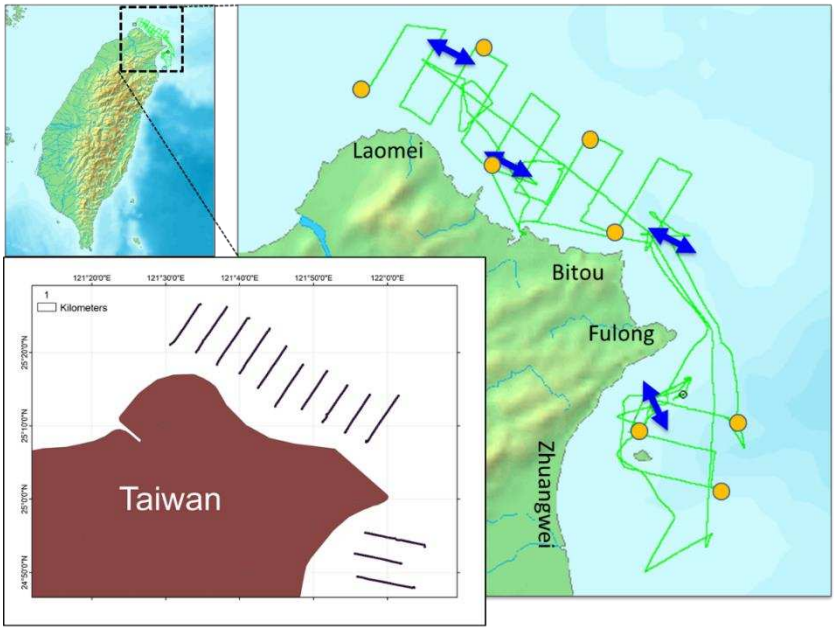


Figure 1. *Survey area including entire voyage line (green line), biological sampling sites (dark blue arrow), and CTD sites (yellow circle). The bottom panel shows 13 transect lines*

The conductivity, temperature, depth sensor (CTD, SBE 911plus, Sea-Bird Scientific) was used to obtain oceanographic information. A total of 8 CTD profiles were recorded. Four CTD stations were located close to the coast (start of the transect line) and other 4 stations were near offshore (end of the transect line). The descent and ascent speeds of the CTD measurement were not more than 1 m/s, and only ascending data were used. The vertical resolution was approximately 0.3 m.

The biological sampling such as pole and line fishing and trawling was performed in concurrent with acoustic survey (*Fig. 1*). For trawl gear, head rope was 8.4 m, ground rope was 10.0 m, and side rope was 45.5 m. The mesh size of the cod-end was 30 mm. The towing speed was 6 m/s. For pole and line fishing, hooks were reached near sea bottom in daytime and approximately 50 m in nighttime, respectively. The bait was sliced saury. The detail biological sampling such as the time, duration, catch weight, and fishing gear are shown in *Table 1*. Seven pole and line fishings were conducted while only one trawling was performed. The duration of trawl was one hour and average duration of pole and line fishing was 5 hours 57 minutes. The caught samples were separated by fish species and the total weight of each species was weighed. Total length and body weight of each species, with snout-anus length for only hairtail species, in representative sampled numbers were measured.

Data processing

Acoustic raw data (38 kHz) of the echosounder were processed using the Echoview ver. 10 (Echoview Software Pty Ltd). The minimum threshold of the volume back scattering strength (S_V) was set as of −75 dB. To eliminate noise signals by ring down

http://www.aloki.hu ● ISSN 1589 1623 (Print) ● ISSN 1785 0037 (Online)
DOI: http://dx.doi.org/10.15666/aeer/1902_10671083
© 2021, ALÖKI Kft., Budapest, Hungary

and surface bubbles, features of the 'threshold offset' and 'line pick' in Echoview were used. To define the seabed line, a 'best bottom candidate algorithm' was applied, and then visually inspected and edited. On S_V echogram, attenuated signals were often observed. The attenuated signal removal algorithm described in Ryan et al. (2015) was applied to set attenuated signals as no-data. It differentiates and adjusts pings which present an attenuated signal when compared to surrounding pings. To increase signal to noise ratio, background noise removal algorithm introduced in de Robertis and Higginbottom (2007) was used. It calculates the background noise for each ping and subtracts it from each data point (Echoview, 2020).

Table 1. *Date, time, total catch and fishing gear of biological sampling*

No	Date	Start time	End time	Duration	Total catch (kg)	Gear type
1	10 Dec	18:13	23:20	5:07	9.7	Pole and line
2	13 Dec	18:02	0:00	5:58	13.2	Pole and line
3	14 Dec	13:24	14:24	1:00	9.1	Trawl
4	14 Dec	15:00	18:00	3:00	8.1	Pole and line
5	14 Dec	18:00	23:00	5:00	21.4	Pole and line
6	16 Dec	16:55	23:00	6:05	0.9	Pole and line
7	17 Dec	6:31	18:00	11:29	3.8	Pole and line
8	17 Dec	18:00	23:00	5:00	5.0	Pole and line

For estimating the hairtail biomass, NASC (Nautical Area Scattering Coefficient, dB re m^2/nm^2) of cell (500 m in horizontal and 250 m in vertical which was deeper than seabed) in transect lines was exported. Acoustic data on the transect line for estimating the hairtail biomass were collected during daytime. Except for 13 transect lines, three voyage lines at a similar location off from Bitou to Fulong (Gongliao District) and relatively one long voyage line off from Laomei to Zhuangwei were selected to understand the fish distributional characteristics (*Fig. 1*). The former line was named as 'three lines' and the latter line was called as 'coastal line'. In especial, information on hotspot where fish are aggregated on the coastal line is beneficial for fishery resources management. To examine the fish distributional characteristics, NASC of a cell (500 m horizontally and 10 m vertically) in three lines and coastal line was exported, respectively.

Hairtail biomass estimation

To estimate hairtail biomass, first of all, the hairtail biomass (ton) per transect line (Bt) was calculated using the *equation (1)*.

$$Bt = \frac{\overline{S_{At}} \cdot \frac{\overline{W}}{1000} \cdot A_t}{4 \cdot \pi \cdot 10^{\frac{\overline{TS}}{10}}} \quad \text{(Eq.1)}$$

where $\overline{S_{At}}$ (m^2/nm^2) is the mean return acoustic signal, that is the linear domain of NASC for transect t, A_t is per transect survey area (nm^2), $\overline{TS}$ is mean target strength (dB re m^2) of hairtail and $\overline{W}$ is mean weight of hairtail (kg). The target strength (TS) for hairtail was adapted from Zhao (2006).

$$TS = 20 \log La - 68.3 \quad \text{(Eq.2)}$$

http://www.aloki.hu ● ISSN 1589 1623 (Print) ● ISSN 1785 0037 (Online)
DOI: http://dx.doi.org/10.15666/aeer/1902_10671083
© 2021, ALÖKI Kft., Budapest, Hungary

where, La is anal length (cm). By applying the average anal length (21.8 cm) of hairtail from the pole and line fishings and trawling, the TS of hairtail became −41.5 dB. The average body weight of hairtail from biological samplings was 187.1 g.

$$Biomass = \sum_{i=1}^{n} Bt_i \quad \text{(Eq.3)}$$

The per-transect biomass (Bt_i) was summed to give an estimate of biomass for the total survey area. To calculate the area based on a transect line, the length of transect line and distance between two lines were estimated using Google earth (Google). Sampling variance was computed using *equation (4) and (5)*, and is a measure of survey repeatability, showing variability between transect lines (Jolly and Hampton, 1990). If a fish aggregation is densely distributed in one or two transect lines, the sampling variance will be high.

$$\overline{(S_A)_i} = \frac{\sum_{i=1}^{n}(S_A)_i \cdot L_i}{\sum_{i=1}^{n} L_i} \quad \text{(Eq.4)}$$

$$Var\overline{(S_A)_i} = \frac{1}{n \cdot (n-1)} \frac{[\sum_{i=1}^{n}(L_i)^2 [\overline{(S_A)_i} - \overline{S_A}]]^2}{[\sum_{i=1}^{n} L_i]^2} \quad \text{(Eq.5)}$$

where $\overline{(S_A)_i}$ is the mean S_A for transect line i, L_i is the length of transect line i, and n is the total number of transect lines.

Fish distributional characteristics

Fish aggregations were observed on the coastal line which was recorded from 23:23 on 16 Dec 2019 to 04:51 on 17 Dec 2019. The fish school detection module imbedded the SHAPES (the shoal analysis and patch estimation system) algorithm in the Echoview was applied (Coetzee, 2000; Echoview, 2020). Two minimum thresholds (−75 dB and −70 dB) were used. The fish schools were determined by defining the boundaries of fish school like regions. Properties of these regions were examined to extract diverse characteristics of the fish schools such as S_V, thickness, length, distributional depth, area, center of mass, inertia, and aggregation index. Various studies were conducted using the characteristics of detected fish schools (Barange, 1994; Scalabrin et al., 1996; Diner, 2001; Urmy et al., 2012; Kang et al., 2016; Echoview, 2020). The description and computation of the fish school characteristics can be referred in the above references. In particular, the center of mass (CM) is the average of all depths sampled by weighting with their S_V values. Inertia (I) is a metric of the spread of backscatter, and it increases when more backscatter is farther away from the CM. The aggregation index (AI) is a metric of the aggregation of backscatter. When backscatter is uniformly distributed, AI will be low; when backscatter is formed in dense clusters, it will be higher.

$$\mathrm{CM} = \frac{\int z Sv(z)}{\int Sv(z)} \quad \text{(Eq.6)}$$

$$\mathrm{I} = \frac{\int (z-CM)^2 Sv(z) dz}{\int Sv(z) dz} \quad \text{(Eq.7)}$$

$$\mathrm{AI} = \frac{\int Sv(z)^2 dz}{(\int Sv(z) dz)^2} \quad \text{(Eq.8)}$$

http://www.aloki.hu ● ISSN 1589 1623 (Print) ● ISSN 1785 0037 (Online)
DOI: http://dx.doi.org/10.15666/aeer/1902_10671083
© 2021, ALÖKI Kft., Budapest, Hungary

where z is the depth (m) of a sample in the region. $S_V(z)$ is the sample volume backscattering coefficient at z.

Statistical analysis

Three lines, which were located in a similar location, were divided into outer line, middle line, and inner line on the basis of their positions. Outer line, middle line and inner line were collected from 23:14, 13 Dec to 01:25, 14 Dec, from 01:43, 17 Dec to 02:54, 17 Dec, and from 03:26, 15 Dec to 05:00, 15 Dec, respectively. The locations of three lines were very close each other. However, their collected times were different although they all were recorded at night. To examine whether the acoustic backscatters among three lines were same or not, one-way analysis of variance (ANOVA) along with post-hoc test was applied. To determine whether significant differences of fish distributional characteristics existed between two threshold values applied, a nonparametric test (Mann-Whitney U test) was performed. Statistical analyses were performed using SPSS ver. 19 (IBM).

Interpolation of water temperature and salinity

Kriging interpolation method in Surfer ver. 8.01 (Golden Software, LLC) was used to visualize the vertical profile of temperature and salinity. Default setting properties of the Kriging interpolation was applied. Its fundamental principle is depending upon the values of adjacent variables, using its exhibit variogram, which is a description of the surface's roughness based quantitatively and statistically, to reflect the inner connection among regionalized variables, and combined with the original data to estimate regional unknown sampling point value. It is a sort of optimal unbiased estimation method (Xiao et al., 2016).

Results

Catch from biological sampling

Surprisingly, only hairtail species was caught by 7 pole and line fishings. Averaged total length, averaged body weight, and averaged snout-anus length were 732.7 mm, 193.1 g, and 236.9 mm, respectively. Averaged total lengths in day time and night time were 742.9 and 727.6 mm, respectively. Averaged snout-anus lengths in day time and night time were 206.3 mm and 197.4 mm, respectively (*Table 2*). From one trawling, hairtail accounted for 7% out of total caught weight. Averaged snout-anus length and averaged body weight were 199.6 mm and 115.5 g, respectively. In addition, no acoustic raw data was recorded during the last biological sampling time (18:00–23:00, 17 Dec).

Hairtail biomass estimation

By the pole and line fishing, only hairtail was caught, and by trawling only 7% of hairtail from total catch was confirmed (*Table 3*). Two different fishing gears had very different results. Thus, it was extremely difficult to determine how much backscatter should be allocated for hairtail species. Inevitably, an assumption with regard to the allocation of hairtail should be made to estimate its biomass. Three interpretation scenarios of low, medium, high such as 30%, 40%, and 50% of total backscatter were considered. Acoustic survey data was echointegrated for each three interpretation scenario using *equations (1) – (3)*. As a result, the hairtail biomass in three interpretation

http://www.aloki.hu ● ISSN 1589 1623 (Print) ● ISSN 1785 0037 (Online)
DOI: http://dx.doi.org/10.15666/aeer/1902_10671083
© 2021, ALÖKI Kft., Budapest, Hungary

scenarios were estimated 5,286 tons (30%), 7,048 tons (40%), and 8,810 tons (50%), respectively (*Table 4*). The sampling variance calculated using *equation (4) and (5)* was 0.4.

Table 2. *Total length, snout-anus length, and body weight of pole and line fishing samples*

Date	Time	Total length (mm)			Snout-anus length (mm)			Body weight (g)		
		Mean	Min	Max	Mean	Min	Max	Mean	Min	Max
10/12/2019	Night	722.4	633	825	225.9	195.1	262.1	164.8	94	238
13/12/2019	Night	700.9	480	927	221.9	173.8	288.0	159.5	71	288
13/12/2019	Night	709.7	552	880	231.6	177.3	302.8	175.9	84	348
14/12/2019	Day	769.2	673	869	258.3	203.2	335.0	240.5	110	464
14/12/2019	Day	797.7	728	918	260.8	224.6	306.5	257.7	159	406
14/12/2019	Night	706.3	612	834	219.3	191.4	282.4	163.0	91	322
14/12/2019	Night	713.1	570	845	227.7	175.4	276.3	172.3	100	346
16/12/2019	Night	805.0	775	860	282.4	247.6	310.0	314.8	172	415
17/12/2019	Day	698.8	620	795	221.9	199.6	254.3	155.7	106	263
17/12/2019	Day	706.1	631	775	227.2	197.9	260.7	158.8	101	231
17/12/2019	Night	702.9	585	792	219.1	185.6	244.8	145.3	99	212
17/12/2019	Night	760.3	730	801	246.9	232.5	258.1	208.8	160	272
Average value		732.7	632.4	843.4	236.9	200.3	281.8	193.1	112.3	317.1

Table 3. *Caught weight by trawling based on fish species and their percentages. Note that it is shown above 5% of total weight*

Common name	Caught weight (g)	Percentage of total weight (%)
Japanese jack mackerel	2671.5	27.2
Horsehead tilefish	1001.9	10.2
Yellow-spotted skate	705.5	7.2
Hairtail	692.9	7.0
Japanese goatfish	673.8	6.9
Silver pomfret	643.2	6.5
Spotted moray	636.2	6.5

Table 4. *Estimated hairtail biomass per transect line in three interpretation scenarios*

Line	NASC (m^2/nm^2)	Area (nm^2)	Biomass (ton)	30% scenario	40% scenario	50% scenario
T1	65.9	25.2	350	105	140	175
T2	105.5	18.5	413	124	165	207
T3	203.1	19.1	820	246	328	410
T4	61.5	18.1	235	71	94	118
T5	80.2	20.5	347	104	139	173
T6	71.6	19.1	289	87	116	144
T7	177.5	14.6	546	164	218	273
T8	224.6	13.8	653	196	261	326
T9	188.9	15.0	597	179	239	299
T10	631.5	13.1	1,744	523	698	872
T11	635.1	21.5	2,885	865	1,154	1,442
T12	113.4	21.9	525	158	210	263
T13	2167.1	17.9	8,216	2,465	3,286	4,108

http://www.aloki.hu ● ISSN 1589 1623 (Print) ● ISSN 1785 0037 (Online)
DOI: http://dx.doi.org/10.15666/aeer/1902_10671083
© 2021, ALÖKI Kft., Budapest, Hungary

Thematic map of NASC is shown in *Fig. 2*. East part off Keelung city presented rather high NASC than in west part. In particular, the last transect line off Yilan county (below 24°50'N) had the highest NASC. The 9th and 10th transect lines off Gongliao district and the 11th transect line off Yilan county occurred high NASC.

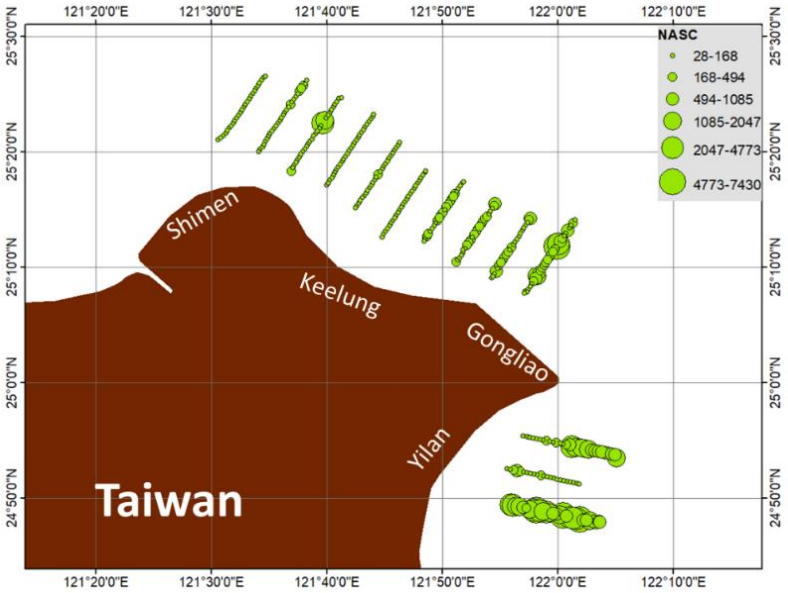


Figure 2. *Thematic map of NASC values in 500 m intervals. Circle size is proportional to the value of NASC*

Fish distributional characteristics: coastal line

Large and dense fish aggregations were observed based on the echogram curtain and the horizontal NASC map of the coastal line (*Fig. 3*). In particular, high NASC was found below 25°N (marked arrow in the *Fig. 3*). Acoustic data were collected at night so that a number of fish aggregations were inspected (*Fig. 3A*). Note that the long thin layers in black on the echogram curtain were echoes of second bottom signal which were processed as no-data. High NASC values were observed around off Gongliao and Yilan (25°10'N−25°50'N, *Fig. 3B*). The peak of NASC in vertical was at 70 m depth. NASC values gradually increased from water surface to 70 m and decreased as water depth became deeper (*Fig. 3C*).

Metrics of fish distributional characteristics on the coastal line is graphed using boxplots and is presented in *Fig. 4*. Between two thresholds, mean S_V and aggregation index seemed to be different. Applying −70 dB of threshold, averaged mean S_V was −64.9 dB, mean thickness was 15.4 m, mean distributional depth was 65.1 m, mean length was 2201.2 m, mean center of mass was 64.9 m, mean inertia was 143.4 m^2, and mean aggregation index was 8E-05 m^{-1}. By using −75 dB of threshold, averaged mean S_V was −68.2 dB, mean thickness was 14.6 m, mean distributional depth was 60.2 m, mean length was 2312.7 m, mean center of mass was 59.8 m, mean inertia was 129.1 m^2, and mean aggregation index was 1.4E-03 m^{-1}. Seventy-five percentage of fish aggregation was distributed below 85 m, their thickness was smaller than 16 m, and their length was shorter than 1542 m. Half of fish aggregation had 32–79 m of the center of mass, 6–70 m^2 of inertial, and 1E-05–2.1E-04 m^{-1} of aggregation index. All fish distributional

http://www.aloki.hu ● ISSN 1589 1623 (Print) ● ISSN 1785 0037 (Online)
DOI: http://dx.doi.org/10.15666/aeer/1902_10671083
© 2021, ALÖKI Kft., Budapest, Hungary

characteristics between two threshold values had no significant difference except for Sv (Mann–Whitney, P=0.00, n=65). This means that a study on the distributional characteristics of hairtail can use either −70 or −75 dB threshold value.

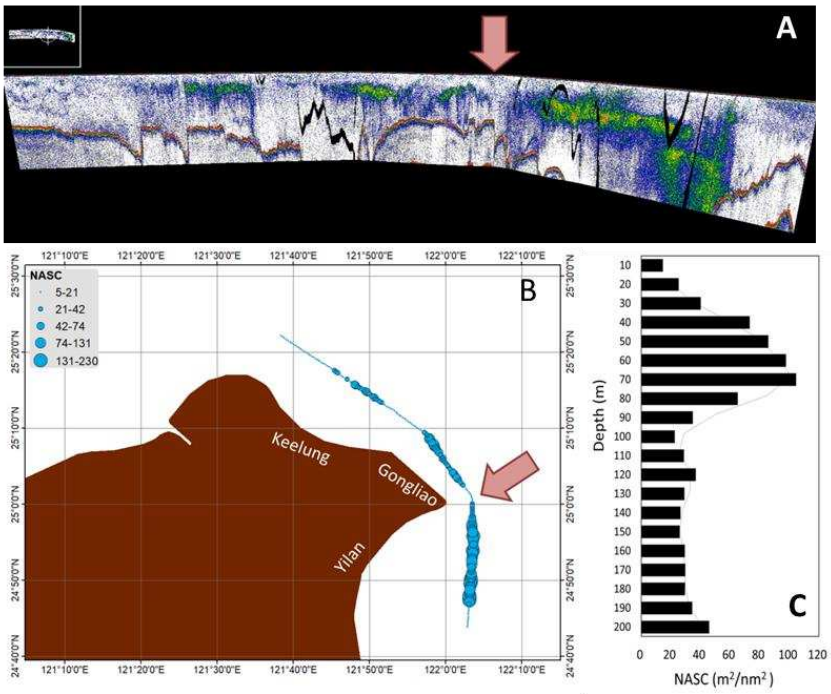


Figure 3. *The echogram curtain A, the horizontal NASC map B, and vertical distribution of NASC C of the coastal line. Arrow means the change of vessel voyage direction and assists to compare A and B. The line C is moving averaged line*

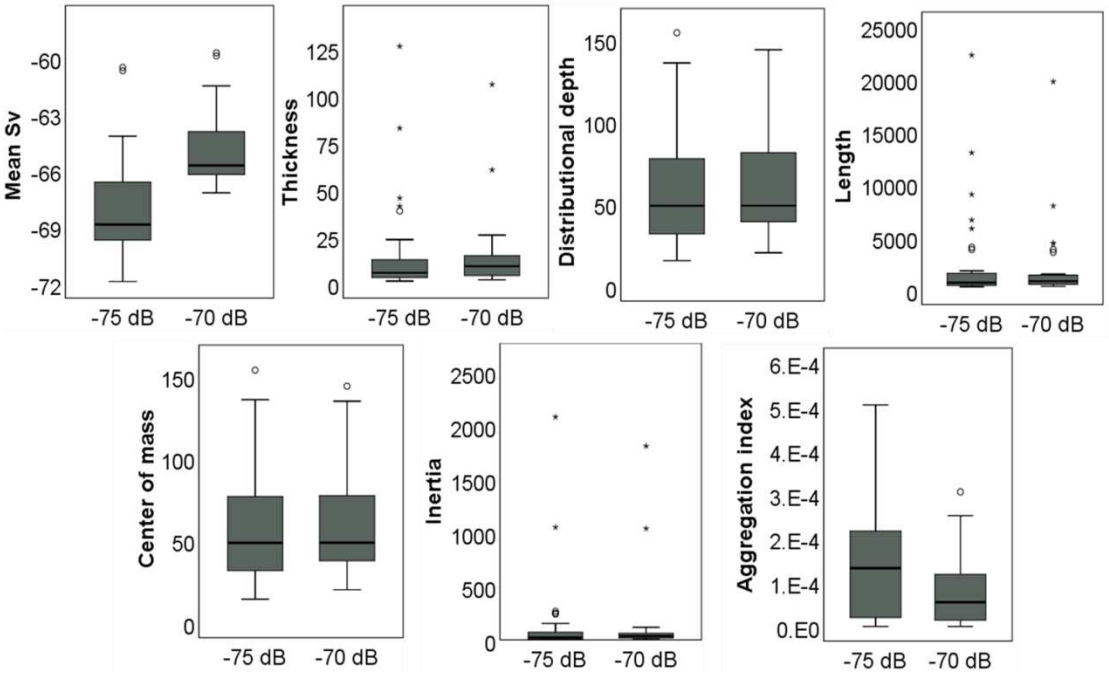


Figure 4. *Metrics of fish distributional characteristics in coastal line using box plots*

http://www.aloki.hu ● ISSN 1589 1623 (Print) ● ISSN 1785 0037 (Online)
DOI: http://dx.doi.org/10.15666/aeer/1902_10671083
© 2021, ALÖKI Kft., Budapest, Hungary

Fish distributional characteristics: three lines

The horizontal NASC map and the echogram curtains of three lines are shown in *Fig. 5*. The location of three lines was simply confirmed (*Fig. 5A*). Overall the highest NASC was observed on the outer line, the second highest NASC was on the middle line, and lowest NASC was on the inner line (*Fig. 5B*). Short and small black parts on the echogram curtain were removed noise marks and processed also as no-data (*Fig. 5C*). The long thin layers in black were echoes of the second bottom signal and processed as no-data (*Fig. 5D and 5E*). Each echogram curtain started top-left part of voyage track. Overall, strong echo signals occurred in outer and middle lines. The vertical distribution of NASC is shown in *Fig. 6*. The average NASC at outer line, middle line, and inner line were 63.1 m^2/nm^2, 30.1 m^2/nm^2, and 8.6 m^2/nm^2, respectively. Overall inner line had very low NASC throughout the water column. The middle line had 50 m peak of NASC while the outer line had 50, 90, and 140 m peaks although the highest peak occurred at 50 m.

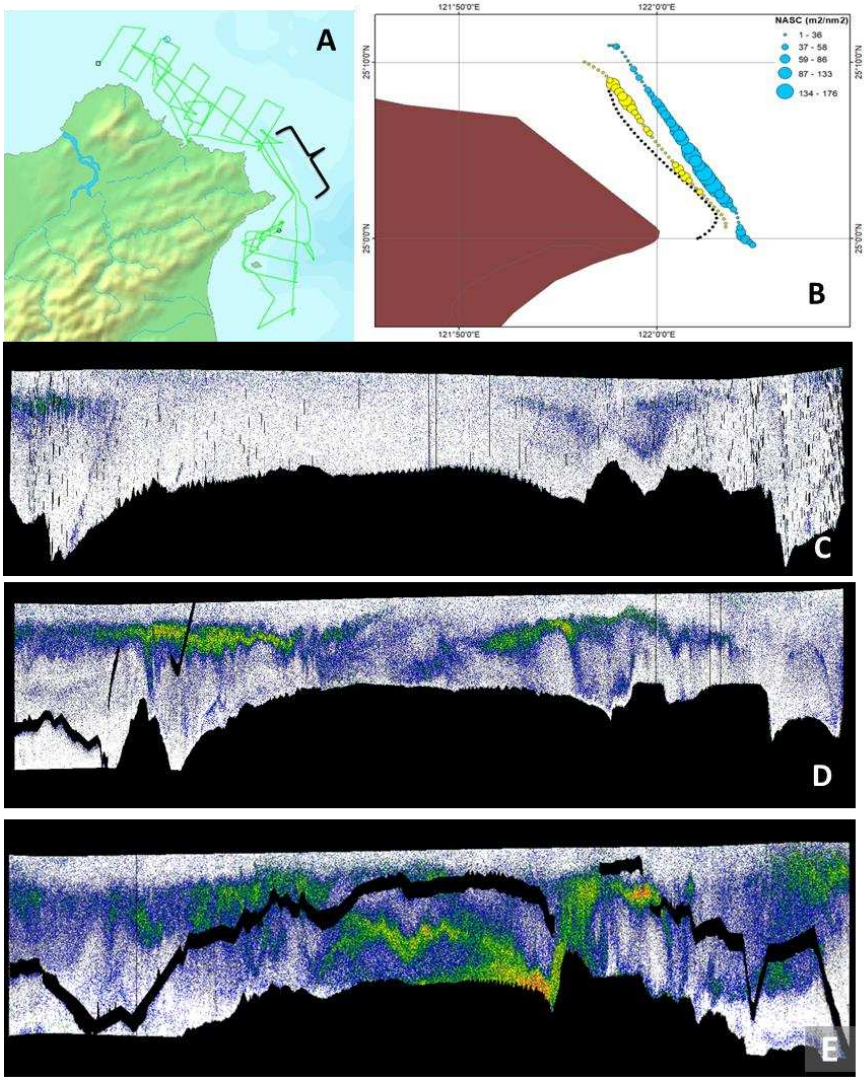


Figure 5. *Three lines on entire voyage line A, the horizontal NASC map of three lines B and the echogram curtains of inner line C, that of middle line D, and that of outline E*

http://www.aloki.hu ● ISSN 1589 1623 (Print) ● ISSN 1785 0037 (Online)
DOI: http://dx.doi.org/10.15666/aeer/1902_10671083
© 2021, ALÖKI Kft., Budapest, Hungary

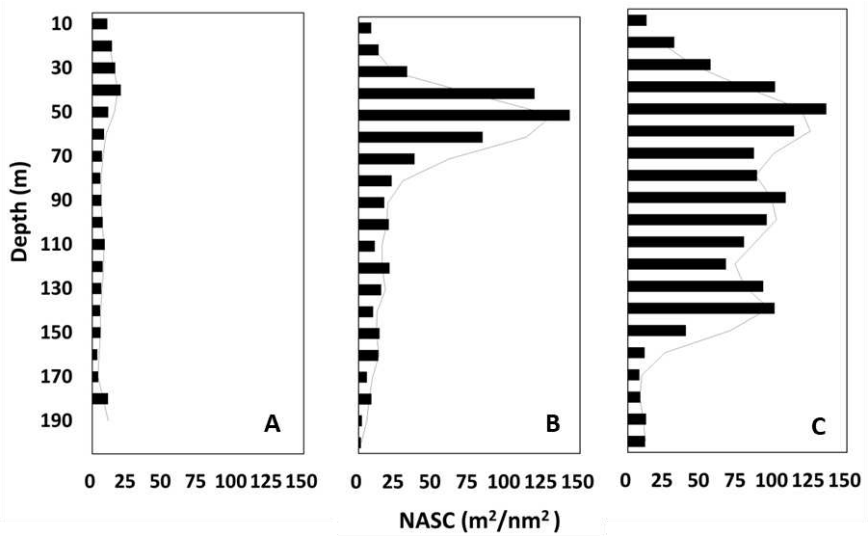


Figure 6. *Vertical distribution of three lines such as outer line A, middle line B, and inner line C*

Marine environmental property

Interpolated water temperature with NASC and interpolated salinity with that are shown in *Fig. 7*. The range of water temperature in 1–5 CTD stations was approximately 16–19°C up to 150 m deep, while that in 6–8 CTD stations was about 16–23°C. It was difficult to mention that rather high water temperature (20–23°C) would have influenced to high NASC. However, higher NASC on horizontal map (*Fig. 2*) was observed on the 6 and 8 CTD station. Slightly low salinity (34–34.2 psu) was observed near water surface in 1 to 3 CTD stations and up to 100 m deep at the 5th CTD station. In regard to the comparison between NASC and water temperature in vertical, high NASC values with 17–21°C in 50–100 m deep and 15–16°C in 160–200 m depth were observed in 6–8 stations. In 1–5 stations, high NASC with 18–19°C occurred in 50 m depth.

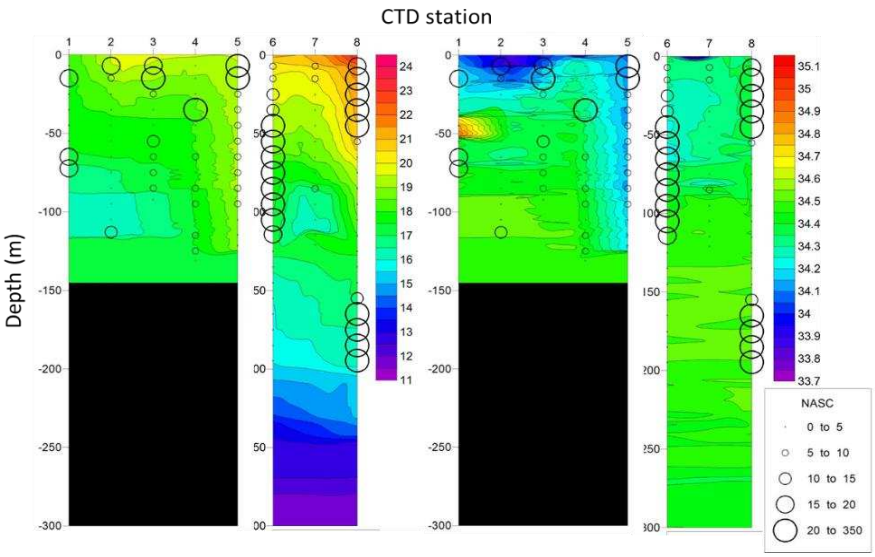


Figure 7. *Interpolated water temperature with NASC (left) and interpolated salinity with NASC (right)*

http://www.aloki.hu ● ISSN 1589 1623 (Print) ● ISSN 1785 0037 (Online)
DOI: http://dx.doi.org/10.15666/aeer/1902_10671083
© 2021, ALÖKI Kft., Budapest, Hungary

Discussion

Target strength of hairtail

TS of hairtail in this study was referred from Zhao (2006) which used juvenile hairtails whose anal lengths ranged from 60 to 120 mm with the mean of 90 mm, and measured *in situ* TS at night time. Tomiyasu et al. (2016) reported that hairtail was observed more than 60° swimming angle in 57.8% of experiment time (consecutive 3 days) with a peak of 77°. They also measured *ex situ* TS in response to swimming angle, and resulted in −47 dB of mean TS between 0–30° of body angle, −54.7 dB between 30–60°, −55.7 dB between 60–90°. It is well known that hairtail feed actively at night time. The foraging behavior causes great diverse swimming angles of hairtail, leading to various TS values. In consideration with these aspects, TS in this study would have not been accurate, although there are not many available and reliable TS for the species. For hairtail resource management, acoustic survey in day time is reliable since their movements and foraging activities at night are dynamic. For accurate biomass estimation of hairtail, reliable TS from hairtail aggregations during a daytime acoustic survey should be obtained although it is not easy to collect those data.

Spatial distribution of hairtail

Hairtail spawn almost year around with two dominant spawning periods such as autumn (November–December) and spring (March–April) in the East China Sea. They ordinarily spawn pelagic eggs in inshore areas and their larvae move to nearshore water. They maturate at age 1 and can live until age 9 in the East China Sea. In particular, hail, in the coastal area off Zhejiang Province of China, undergo seasonal migration from nearshore water to offshore water in the depth around 60–100 m for overwintering. Namely, they move back and forth between nearshore water for spawning and offshore water for overwintering (Ye and Rosenberg, 1991; Shih et al., 2011; Sun et al., 2020). Overall in this study, there was not clear observation that NASC of hairtail in nearshore water was higher than that in offshore water (*Figs. 2 and 5*). However, it is well known that Guisan Island, which is located very close to inshore, is a hotspot for hairtail spawning area. Average total length of hairtail from two different biological samplings in this study was 703.4 mm which was adult. It could be assumed that high NASC distribution in 10, 11, and 13 transect lines around Guisan Island indicated dense spawning hairtail aggregations. On the basis of knowledge on spatial distributional characteristics of hairtail, a design for next acoustic survey such as length, interval, and location of transect line and so forth can be improved. In addition, coastal water is through activities on land that increase delivery of nutrients to the sea. The consequence of food availability for population dynamics and migration of fish have an effect on their growth and a better chance to avoid from predators (Bailey and Houde, 1989).

Hairtail resource management

Global hairtail harvests are 1,217,280 tons in 2017 and annually around 1,250,000 tons between 2013 and 2017 (FAO, 2017). In particular, the total catch of this species in 2019 was 43,479 tons in Republic of Korea (Fisheries statistics, 2020) and that in 2018 was 16,058 tons in Taiwan. In the East China Sea, the hairtail is one of the most important species in commercial and ecological. They are caught primarily by demersal trawl and trivially by set net, gill net and longline. In Taiwan, because hairtail fishery is not under the total allowable catch system, it does not produce long-term scientific data which are

http://www.aloki.hu ● ISSN 1589 1623 (Print) ● ISSN 1785 0037 (Online)
DOI: http://dx.doi.org/10.15666/aeer/1902_10671083
© 2021, ALÖKI Kft., Budapest, Hungary

significant to its resource management and relevant policy formation. As a result, this fishery is exposed a danger of an overfishing issue. The average body length from catch has gradually been decreased, and the species has been matured at relatively younger age due to the heavy fishing pressure (Du et al., 1988; Ji et al., 2019). Accordingly, knowledge on the population and distribution of hairtail is beneficial to facilitate its sustainable exploitation. It is of interest to fisheries scientists and resource managers to understand the status of hairtail stock as accurate as possible in the East China Sea, especially water around Taiwan. In this study, three interpretation scenarios of hailtail allocation in total backscatter were not the best. However, the utilization of acoustic system in extensive areas can expeditiously define fish stocks to estimate the fish biomass efficiently (Simmonds and MacLennan, 2005). Thus, an integrated acoustic trawl survey along with sufficient number of trawls would be a promising tool for aiding useful and feasible measures of hairtail resource. In consideration with results from this study, an integrated acoustic trawl survey will be performed in every month from September, 2020 to March 2021. The transect lines will be divided in northwestern part of Keelung (25.25°N–25.20°N and 121.50°E–121.90°E), region around Guisan Island (24.75°N–25.00°N and 121.75°E–122.15°E), and region off Gongliao (25.15°N–25.3°N and 122.15°E–122.35°E). Sufficient number of trawls will be conducted along with pole and line fishing as the secondary option.

Environmental influence to hairtail

The continental shelf of the South and East China Seas is one of the greatest habitats in the surrounding waters of the Western North Pacific. In the northeastern waters of Taiwan, the Kuroshio Current runs nearby the 200 m isobaths mainly during winter season, and away from it during summer season. On the other hand, the China Coastal Current, which flows southward from Bohai sea to the Taiwan Strait and into the South China Sea, strongly interacted with Kuroshio Current in winter. The intensity of Kuroshio Current and China Coastal Current is a predominant element that leads to marine environmental changes in this study area (Lu and Lee, 2014). In consideration with this aspect, the water temperature in 6–8 CTD stations, in which was strongly affected by the Kuroshio Current, was higher than that in 1–5 stations. Water temperature affects growth, feeding, and breeding of fish, and alters the aptness of marine habitats. Accordingly, it brings in modification in the abundance and distribution of fish species (Wood and McDonald, 2008). Environmental variables, for example water temperature, salinity, and chlorophyll et cetera, affect the timing and duration of the fish reproduction, as well as the abundance and distribution of their preys. The interactions among the variables are complicated and difficult to be isolated (Seo and Kim, 1999; Liu and Gan, 2012). Future studies need to assess how environmental elements may attribute feasible interactions between spatial distribution and preys of hairtail, in particular spawning adult. In addition, the trends of variation in catch number and population of hairtail might be due to fluctuations in the intensities of the Kuroshio Current and China Coastal Current. The relationship between two currrents and hairtail abundance would be an interesting topic for future studies.

Biological sampling gear

All fishing gears are, to the extent, selective and catch individuals in species, body length, and age composition that deviate from their true composition in nature (Wileman et al., 1996; Suuronen, 2005). Humphries et al. (2019) compared two fishing gear types:

http://www.aloki.hu ● ISSN 1589 1623 (Print) ● ISSN 1785 0037 (Online)
DOI: http://dx.doi.org/10.15666/aeer/1902_10671083
© 2021, ALÖKI Kft., Budapest, Hungary

spearguns and handlines, and reported that both gears caught high diversity of fish, but spearguns removed more species and handline catches had a wider range of fish sizes than Spearguns. Food and Agriculture Organization (FAO) reported general overview on fishing gear selectivity (Thompson and Yami, 1983). For example, by using 6 bottom drag nets (Bobbin trawl, Pair Trawl, Light trawl, Scottish seine, Danish seine, and Nephrops trawl), the percentages of different species caught from 6 drag nets varied considerably. It indicates that different types of trawls are selective in different ways although their performance also differed. Pole and line fishing is one of extremely species selective gears, and in general it does not take any other fishes except for the intended species. On the other hand, demersal fish trawl is less selective gear although the mesh size is a key element for fishing species selectivity. For acoustic survey for estimating hairtail biomass, a less selective fishing gear such as trawl would be appropriate. In this study, only one trawl was conducted yet pole and line fishing confirmed the existence of hailtail in the study area. In fact, wind and waves in the northern off Taiwan were very bad in December 2020 so that it was very difficult to carry out a trawl. Also, it was the first time to conduct a trawl in northern water using the RV Fisheries Research 2 for a short amount of preparation. To improve the accuracy of the hairtail resource assessment, a multi-species selective fishing gear such as trawl with an appropriate number of trawl stations will be adapted in next survey.

Conclusion

To estimate the biomass and spatial distributional characteristics of hairtail, an acoustic transect line survey, in concurrent with 7 pole and line fishing and 1 trawl sampling, was conducted from 10 to 17 Dec 2019 in the northern sea of Taiwan. The hairtail biomass, under three scenarios such as low, medium, and high of acoustic backscatter allocation, were to be 5286 (30%), 7048 (40%), and 8810 tons (50%), respectively. For horizontal distribution of hairtail, east part off Keelung city presented rather high NASC than in west part, in particular waters off Yilan county (below 24°50'N) had the highest NASC. Using acoustic data from a long coastal line and three lines at a very similar location, 75% of fish aggregation occurred below 85 m, their thickness was smaller than 16 m, and their length was shorter than 1542 m. The average NASC at outer line, middle line, and inner line were 63.1 m^2/nm^2, 30.1 m^2/nm^2, and 8.6 m^2/nm^2. The statistical analysis revealed significant difference between all three line groups. Lastly, high NASC occurred in the range of 15–21°C in 50–200 m depth. The result of this study will support in designing an integrated acoustic trawl survey next year.

Acknowledgements. We thank the reviewers who improved the manuscript through their comments. This work was supported by the National Research Foundation of Korea (NRF) grant funded by the Korea government (MSIT) (No. NRF-2018R1A2B6005666).

Data availability. All data sets used in this paper are available upon request with a reasonable reason from the first author (mk@gnu.ac.kr).

REFERENCES

[1] Bailey, K. M., Houde, E. D. (1989): Predation on eggs and larvae of marine fishes and the recruitment problem. – Advances in Marine Biology 25: 1-83.

http://www.aloki.hu ● ISSN 1589 1623 (Print) ● ISSN 1785 0037 (Online)
DOI: http://dx.doi.org/10.15666/aeer/1902_10671083
© 2021, ALÖKI Kft., Budapest, Hungary

[2] Barange, M. (1994): Acoustic identification, classification and structure of biological patchiness on the edge of the Agulhas Bank and its relation to frontal features. – African Journal of Marine Science 14: 333-347.
[3] Coetzee, J. (2000): Use of a shoal analysis and patch estimation system (SHAPES) to characterize sardine schools. – Aquatic Living Resources 13: 1-10.
[4] De Robertis, A., Higginbottom, I. (2007): A post-processing technique for estimation of signal-to-noise ratio and removal of echosounder background noise. – ICES Journal of Marine Science 64: 1282-1291.
[5] Diner, N. (2001): Correction on school geometry and density: approach based on acoustic image simulation. – Aquatic Living Resources 14: 211-222.
[6] Du, J. R., Li, F. Z., Lin, S. D., Zhang, Q. D. (1988): On age and growth of hairtail, *Trichiurus Haumela* (Forskal) in western Taiwan Strait. – Journal of Oceanography in Taiwan Strait 7: 339-346. (In Chinese with English abstract).
[7] Duarte, L. O., Garc, C. B. (1999): Diet of the mutton snapper *Lutjanus analis* (Cuvier) from the Gulf of Salamanca, Colombia, Caribbean Sea. – Bulletin of Marine Science 65: 453-465.
[8] Echoview. (2020): Help File for Echoview. – Available at https://support.echoview.com/. [Accessed 1 May 2020].
[9] FAO. (2017): FAO Yearbook, fishery and aquaculture statistics. – Rome.
[10] Fisheries Statistics. (2020): Ministry of Oceans and Fisheries website. – Available at http://www.fips.go.kr/p/S020304/#. [Accessed 6 May 2020].
[11] Froese, R., Pauly, D. (2019): Fish Base. World Wide Web electronic publication. – Available at http://www.fishbase.org. [Accessed 6 May 2020].
[12] Hsu, S. K., Wang, S. Y., Liao, Y. C., Yang, T. F., Jan, S., Lin, J. Y., Chen, S. C. (2013): Tide-modulated gas emissions and tremors off SW Taiwan. – Earth and Planetary Science Letters 369-370: 98-107.
[13] Hsu, S. K., Lin, S. S., Wang, S. Y., Tsai, S. H., Doo, W. B., Chen, S. C., Lin, J. Y., Yeh, Y. C., Wang, H. F., Su, C. S. (2018): Seabed gas emissions and submarine landslides off SW Taiwan. – Terrestrial, Atmospheric and Oceanic Sciences 29: 7-15.
[14] Humphries, A. T., Kelvin, D. G., Carvalho, P. G., Yulianto, I., Artawijaya, T., Campbell, S. J. (2019): Catch composition and selectivity of fishing gears in a multi-species Indonesian coral reef fishery front. – Marine Science 6: 1-9.
[15] Hutchings, J. A. (1996): Spatial and temporal variation in the density of northern cod and a review of hypotheses for the stock's collapse. – The Canadian Journal of Fisheries and Aquatic Sciences 53(5): 943-962.
[16] Ji, Y., Liu, Q., Liao, B., Zhang, Q., Han, Y. (2019): Estimating biological reference points for Largehead hairtail (*Trichiurus lepturus*) fishery in the Yellow Sea and Bohai Sea. – Acta Oceanologica Sinica 38: 20-26.
[17] Jolly, G. M., Hamptom, I. (1990): Stratified random transect design for acoustic surveys of fish stocks. – The Canadian Journal of Fisheries and Aquatic Sciences 47: 1282-1291.
[18] Kang, M., Seo, Y. I., Oh, T. Y., Lee, K., Jang, C. S. (2015): Estimating the biomass of anchovy species off the coast of Tongyeong and Yeosu in South Korea in the spring and winter of 2013 and 2014. – Journal of the Korean Society of Fisheries Technology 51: 86-93.
[19] Kang, M., Zhang, H., Seo, Y. I., Oh, T. Y., Jo, H. S. (2016): Exploratory study for acoustical species identification of anchovies in the South Sea of South Korea. – Thalassas: International Journal of Marine Science 32(1): 1-10.
[20] Kim, S. H., Rho, H. K. (2002): The fluctuation of fishing grounds of hairtail, *Trichiurus lepturus* in the Cheju strait by the distribution of feeding biomass. – Journal of the Korean Society of Fisheries Technology 38: 1-10.
[21] Lee, M. A., Lee, K. T., Shiah, G. Y. (1995): Environmental factors associated with the formation of larval anchovy fishing grounds in the coastal waters of southwest Taiwan. – Marine Biology 121: 621-625.

http://www.aloki.hu ● ISSN 1589 1623 (Print) ● ISSN 1785 0037 (Online)
DOI: http://dx.doi.org/10.15666/aeer/1902_10671083
© 2021, ALÖKI Kft., Budapest, Hungary

[22] Lee, M. A., Chao, M. H., Weng, J. S., Lan, Y. C., Lu, H. J. (2011): Diel distribution and movement of sound scattering layer in Kuroshio waters, northeastern Taiwan. – Journal of Marine Science and Technology 19: 253-258.
[23] Liu, Y., Cheng, J., Chen, Y. (2009): A spatial analysis of trophic composition: a case study of hairtail (*Trichiurus japonicus*) in the East China Sea. – Hydrobiologia 632: 79-90.
[24] Liu, Z., Gan, J. (2012): Variability of the Kuroshio in the East China Sea derived from satellite altimetry data. – Deep-Sea Research I 59: 25-36.
[25] Lu, H. J., Lee, K. T. (1995): Species identification of fish shoals from echograms by an echo-signal image processing system. – Fisheries Research 24: 99-111.
[26] Lu, H. J., Lee, K. T. (2014): Changes in the fish species composition in the coastal zones of the Kuroshio Current and China coastal Current during periods of climate change: Observations from the set-net fishery (1993–2011). – Fisheries Research 155: 103-113.
[27] Panhwar, S. K., Dong, Z. Y., Gao, T., Wang, P., Han, Z., Wang, Z., Wang, Y. (2018): Decadal population traits and fishery of Largehead hairtail, *Trichiurus lepturus* (Linnaeus, 1758) in the East China Sea. – Pakistan Journal of Zoology 50(1).
[28] Park, Y., Seo, Y. I., Oh, T. Y., Lee, K., Zhang, H., Kang, M. (2016): Anchovy distributional properties by time and location: using acoustic data from a primary trawl survey in the South Sea of South Korea. – Journal of Marine Science and Technology 24(4): 864-875.
[29] Reuchlin-Hugenholtz, E., Shackell, N. L., Hutchings, J. A. (2015): The potential for spatial distribution indices to signal thresholds in marine fish biomass. – PLoS ONE 10(3): e0120500.
[30] Ryan, T. E., Downie, R. A., Kloser, R. J., Keith, G. (2015): Reducing bias due to noise and attenuation in open-ocean echo integration data. – ICES Journal of Marine Science 72(8): 2482-2493.
[31] Scalabrin, C., Diner, N., Weill, A., Hillion, A., Mouchot, M. C. (1996): Narrowband acoustic identification of monospecific fish shoals. – ICES Journal of Marine Science 53: 181-188.
[32] Seo, Y. J., Kim, D. S. (1999): Distribution of anchovy school catched by the lift net and environmental factors in the Kamak Bay 1. Relation between distribution of anchovy school and temperature and salinity. – Journal of the Korean Society of Fisheries Technology 35: 267-276.
[33] Shih, N. T., Hsu, K. C., Ni, I. H. (2011): Age, growth and reproduction of cutlassfishes *Trichiurus* spp. in the southern East China Sea. – Journal of Applied Ichthyology 27: 1307-1315.
[34] Simmonds, J., MacLennan, D. N. (2005): Fisheries Acoustics: Theory and Practice, 2nd edition. – Wiley-Blackwell Publishing Inc, New York.
[35] Sun, P., Chen, Q., Fu, C., Zhu, W., Li, J., Zhang, C., Yu, H., Sun, R., Xi, Y., Tian, Y. (2020): Daily growth of young-of-the-year largehead hairtail (*Trichiurus japonicus*) in relation to environmental variables in the East China Sea. – Journal of Marine Systems 201: 103243.
[36] Suuronen, P. (2005): Mortality of fish escaping trawl gears. – FAO Fisheries Technical Paper 478, Rome.
[37] Thompson, D. B., Ben-Yami, M. (1983): Fishing gear selectivity and performance. – A Preparatory Meeting for the FAO World Conference on Fisheries Management and Development, FAO Fisheries Report 289: 215-470.
[38] Tomiyasu, M., Kao, W. Y., Abe, K., Minami, K., Hirose, T., Ogawa, M., Miyashita, K. (2016): The relationship between body angle and target strength of ribbonfish (*Trichiurus japonicus*) displaying a vertical swimming motion. – ICES Journal of Marine Science 73: 2049-2057.
[39] Urmy, S. S., Horne, J. K., Barbee, D. H. (2012): Measuring the vertical distributional variability of pelagic fauna in Monterey Bay. – ICES Journal of Marine Science 69(2): 184-196.

http://www.aloki.hu ● ISSN 1589 1623 (Print) ● ISSN 1785 0037 (Online)
DOI: http://dx.doi.org/10.15666/aeer/1902_10671083
© 2021, ALÖKI Kft., Budapest, Hungary

[40] Wileman, D. A., Ferro, R. S. T., Fonteyne, R., Millar, R. B. (1996): Manual of methods of measuring the selectivity of towed fishing gears. – ICES Cooperative Research Report 215: pp 132.
[41] Wood, C. M., McDonald, D. G. (2008): Global Warming: Implications for Freshwater and Marine Fish. – Society for Experimental Biology Seminar Series, Cambridge University Press, Wootten.
[42] Wu, C. (1991): Distribution of young Hairtail in Zhejiang coastal waters. – Journal of Zhejiang College of Fisheries 10: 21-29.
[43] Xiao, Y., Gu, X., Yin, S., Shao, J., Cui, Y., Zhang, Q., Niu, Y. (2016): Geostatistical interpolation model selection based on ArcGIS and spatio-temporal variability analysis of groundwater level in piedmont plains, northwest China. – Springerplus 5: 425.
[44] Ye, Y., Rosenberg, A. A. (1991): A study of the dynamics and management of the hairtail fishery, *Trichiurus haumela*, in the East China Sea. – Aquatic Living Resources 4: 65-75.
[45] Zhang, H., Wang, C. Y., Yang, D. G., Du, H., Wei, Q. W., Kang, M. (2014): Spatial distribution and habitat choice of adult Chinese sturgeon (*Acipenser sinensis* Gray, 1835) downstream of Gezhouba Dam, Yangtze River, China. – Journal of Applied Ichthyology 30: 1483-1491.
[46] Zhao, X. (2006): In situ target-strength measurement of young hairtail (*Trichiurus haumela*) in the Yellow Sea. – ICES Journal of Marine Science 63: 46-51.
[47] Zhou, Y. D., Xu, H. X., Liu, Z. F. (2002): A study of stock structure of hairtail *Trichiurus haumela* in the East China Sea. – Journal of Zhejiang Ocean University 21: 315-320.

http://www.aloki.hu ● ISSN 1589 1623 (Print) ● ISSN 1785 0037 (Online)
DOI: http://dx.doi.org/10.15666/aeer/1902_10671083
© 2021, ALÖKI Kft., Budapest, Hungary

OCCURRENCE OF MICROPLASTICS AND TRACE METALS IN FISH AND SHRIMP FROM SONGKHLA LAKE, THAILAND DURING THE COVID-19 PANDEMIC

PRADIT, S.[1,2*] – NOPPRADIT, P.[1,2] – GOH, B. P.[1,2] – SORNPLANG, K.[1,2] – ONG, M. C.[3,4] – TOWATANA, P.[1,2*]

[1]*Marine and Coastal Resources Institute, Faculty of Environmental Management, Prince of Songkla University, Songkhla 90110, Thailand*

[2]*Coastal Oceanography and Climate Change Research Center, Prince of Songkla University, Hat Yai, Songkhla 90110, Thailand*

[3]*Faculty of Science and Marine Environment, Universiti Malaysia Terengganu, 21030 Kuala Nerus, Terengganu, Malaysia*

[4]*Ocean Pollution and Ecotoxicology Research Group, Universiti Malaysia Terengganu, 21030 Kuala Nerus, Terengganu, Malaysia*

**Corresponding authors*
e-mail: siriporn.pra@psu.ac.th and prawit.t@psu.ac.th

(Received 27th Aug 2020; accepted 8th Feb 2021)

Abstract. The study was carried out in the beginning of May, 2020 during the COVID-19 pandemic lockdown period in Thailand. This study reported on the occurrence of microplastic debris in stomachs of fish (Arius maculatus) and shrimps (*Parapenaeopsis hardwickii* and *Metapenaeus brevicornis*) from Songkhla Lake. The average occurrences of microplastic pieces per stomach in fish and shrimps according to 10% digested KOH reagent were 2.73 ± 0.15, 4.11 ± 1.12 and 3.78 ± 1.12, respectively. The most common shape of microplastics in fish and shrimp was fiber. Black was the most frequent color found followed by blue, white and red. Microplastic size found in this study ranged from 150 μm to 5 mm and 70% of microplastic size was less than 1 mm. Five polymer types were reported including polyester, rayon, polyvinyl alcohol, polyethylene and paint. It is worth noting that textile fiber also appeared in stomachs of fish and shrimp. It might have been caused by the fact that during the lockdown period people change their way of life such as doing more laundry thus, releasing more cloth fibers (microplastics) into sewer and lake. This study found anomalous correlation coefficients between the number of microplastic particles in the organisms' stomachs and most of the metal concentrations in their tissues.
Keywords: *marine debris, polymer, sediment, pollution, FTIR*

Introduction

Marine plastic waste is the origin of microplastics floating in the sea which is considered to be a global marine pollution problem. Plastics are the most common type of marine debris, constituting between 60% and 80% of all such waste and over 90% of all floating particles (Gordon, 2006). Thailand is ranked as the 6th largest in the world for marine waste disposal and therefore, plastic and marine wastes in the marine and coastal ecosystems are critical problems that need to be urgently resolved. Microplastics are of concern especially because they can be ingested by a variety of marine organisms, and possibly be also transferred along the food web (Setälä et al., 2014). This is similar to other environmental problems caused by other types of pollution since

http://www.aloki.hu ● ISSN 1589 1623 (Print) ● ISSN 1785 0037 (Online)
DOI: http://dx.doi.org/10.15666/aeer/1902_10851106
© 2021, ALÖKI Kft., Budapest, Hungary

marine contamination caused by plastic waste and the microplastics floating in the sea definitely generate threat affecting various marine animals.

Microplastics are generally described as small plastic particles that have the common dimension of less than 5 mm in diameter (Cole et al., 2011; GESAMP, 2015). Microplastics in the marine environment are typically found as pellets, fragments, or fibers and consist of diverse polymers (Hidalgo-Ruz et al., 2012). Some microplastics are denser than seawater and expected to sink to the seafloor. These include polyamide, polyester, polyvinyl chloride and acrylic. Others are lighter than seawater and are often found floating at the surface, including polyethylene, polypropylene, and polystyrene. When plastics enter the ocean, the rate of degradation and persistence of plastics varies by polymer, shape, density, and the purpose of the plastic itself (Eriksen et al., 2014). Over the last 40 years, microplastics have been observed in the stomach contents of marine organisms from invertebrates to mammals (Cole et al., 2014; Jabeen et al.; 2017; Li et al., 2016; Pozo et al., 2019; Rocha-Santos and Duarte, 2015). Ingestion may occur directly due to misidentification of indiscriminate consumption of microplastics for feeding (Ory et al., 2017). These organisms can either ingest microplastics as food, whether unintentionally capturing them while filter or deposit feeding or mistaking them for prey when foraging, or even by ingesting organisms of lower trophic levels containing these particles, i.e. trophic transfer (GESAMP, 2015). Potential consequences of microplastic ingestion include physical damage of the gastrointestinal tract of fish and the creation of a false sensation of satiation, which could result in fish mortality from starvation (Cole et al., 2013; Nadal et al., 2016; Possatto et al., 2011). Microplastic accumulation in organisms has the potential to cause a lot of adverse effects, including mortality, reduction of feeding activity, inhibition of growth and immunity and development of endocrine disruption, oxidative stress, neurotransmission dysfunction and even genotoxicity (Lu et al., 2016). Discarded fishing nets and line made of plastic are also a source of microplastics in the environment (Andrady, 2011) due to accidental loss or careless handling by the commercial fishing industry (Gilman, 2015). Over time this material will fragment into smaller pieces due to weathering and biodegradation (Sivan, 2011).

As the toxicity of microplastic is considered based on chemical characteristics, microplastics can absorb the added chemicals (plastic additives) of the production process to get the color and properties of plastic products matching the needs of the market. Furthermore, microplastics have the ability to absorb persistent organic pollutants (POPs) or heavy metals dissolved in seawater. Microplastics and co-contaminants have the potential to affect fishery business and sustainability representing another pressure to already threat fish stocks (Hutchings and Reynolds, 2004). Therefore, microplastics seem like to be the carriers of those toxins into the aquatic animals that consume microplastics. Marine organisms could accumulate heavy metals and their metal concentrations provide a time-integrated degree of metal availability, over long periods of time depending on the metal species (Rainbow, 2002). For example, Cd may be a carcinogen and Pb can damage blood circulation (Arnich et al., 2012). The uptake of microplastic and absorbed co-contaminants by caught fish represents a risk to human health as these contaminants may transfer to fish tissue and eventually humans through consumption. Over time, plastic particles contaminate the marine ecosystem and the food chain, including foodstuffs intended for human consumption (Lusher et al., 2013). Accumulation of plastic debris in Thailand's coastal ecosystems has been studied at numerous locations (Pradit et al., 2020). However,

http://www.aloki.hu ● ISSN 1589 1623 (Print) ● ISSN 1785 0037 (Online)
DOI: http://dx.doi.org/10.15666/aeer/1902_10851106
© 2021, ALÖKI Kft., Budapest, Hungary

relatively little is known about microplastics in biota, especially in Songkhla lake, unique lagoon in Thailand and one of 117 lagoonal lakes in the world. Studies of microplastic contamination in Thailand were conducted on economic fish in the lower Gulf of Thailand (Azad et al., 2018) on sessile invertebrates in the eastern coast of Thailand (Thushari et al., 2017), on green mussels sold in fresh markets (Goh et al., 2019) and in sediment from sand and mud beaches in Libong Island, Thailand (Pradit et al., 2020). They found that microplastic contamination was present everywhere.

The Songkhla Lake is a shallow coastal lagoon located in the southern part of Thailand and occupies approximately 1,042 km^2. The lake is divided into 4 sections; Thale Noi, Inner Section, Middle Section and Outer Section. The salinity ranges from fresh water in Thale Noi to saline water in the outer section. The Outer Section is connected to the Gulf of Thailand through a deep and narrow outlet at Songkhla City. The Outer Songkhla Lake has several major rivers flowing into the lake such as Samrong, U-tapao and Pawong Canals. Each canal has different activities releasing large amounts of pollutants to the outer Songkhla Lake before flowing into the Gulf of Thailand that is the southern part of the South China Sea. Thus, outer Songkhla Lake acts as a sink receiving wastes from the activities of the upstream area. Important canals in the outer section are a) Samrong Canal, a short canal located in dense population b) Pawong Canal 5.5 km long and both sides of the canal are covered with the mangrove trees and c) U-taphao Canal, the main source of freshwater with the approximate length of 130 km.

According to the COVID-19 pandemic situation, the first infected person in Thailand was found in January 2020 and led to lockdown and curfew measures throughout the country. Songkhla Province and Songkhla Communicable Disease Committee imposed several orders to solve the problem of extensive and rapid outbreak of the disease, e.g. strictly limiting the numbers of people entering and leaving Songkhla Province, implementing the complete lockdown and curfew measures of the whole province during the disease outbreak (March until May 2020). Thus, all the tourism and other business activities were not allowed. This extensively and intensively affected the entire area of Songkhla Province in all the private and government sectors as well as the livelihoods of people in communities around Songkhla Province and Lake resulting in changing their regular way of life to be the new normal one.

In this study, we investigated microplastic presence in stomachs of catfish species (*Arius maculatus*) and two shrimp species (*Parapenaeopsis hardwickii* and *Metapenaeus brevicornis*) which were widely consumed by the people around Songkhla lake**.** Catfish (*Arius maculatus*) is one of the benthic fishes living in Songkhla Lake and it is abundant during the rainy season until the end of the rainy season when the water becomes less salty**.** Therefore, it can be said that this fish likes to live in water that has relatively low salinity**.** It prefers to feed on the group of benthic animals such as crustaceans, crabs as its staple food (Angsupanich et al., 2005). Yellow shrimp (*Metapenaeus brevicornis*) is abundant almost the whole year in the outer lake**.** Its characteristic is different from other shrimp species in that its skin is yellow and turns strong dark yellow during breeding season**.** Hence, this small shrimp is sometimes commonly known as yellow shrimp and has economic value especially in Songkhla lake since it has good taste, thin shell, soft texture and is suitable for many types of cooking resulting in good prices and needed by local markets and nearby countries such as Malaysia and Singapore. Spear shrimp (*Parapenaeopsis hardwickii*) is another type of marine shrimp with a hard, firm shell suitable for being peeled and it is abundant in Songkhla lake. Its shell is quite hard and coarse, only the meat is chopped and then

http://www.aloki.hu ● ISSN 1589 1623 (Print) ● ISSN 1785 0037 (Online)
DOI: http://dx.doi.org/10.15666/aeer/1902_10851106
© 2021, ALÖKI Kft., Budapest, Hungary

crumpled to make shrimp cakes**.** Thus, both kinds of shrimp and catfish are very valuable and important for fishermen and people around the lake since they can generate quite considerable amount of income for fishermen and are also a very inexpensive source of protein for communities around Songkhla Lake. Therefore, this study aimed to investigate the microplastic accumulation in stomach of common fish (*Arius maculatus*) and shrimp species (*Parapenaeopsis hardwickii* and *Metapenaeus brevicornis*) as well as contamination of trace metals (As, Cd and Pb) in their tissues in Songkhla Lake**.** Furthermore, the studies on the prevention of microplastic and trace metal contamination in some economic aquatic organisms found in outer Songkhla Lake are certainly necessary for providing basic background data and information during the COVID-19 outbreak which will be of great benefit as compared to the data obtained ater COVID-19 pandamic in the future.

Materials and methods

Sample collection

A total of 47 samples (fish and shrimp) from 3 species (*Arius maculatus*, *Parapenaeopsis hardwickii* and *Metapenaeus brevicornis*) sold for a human consumption were collected from the local fish market near Songkhla Lake in Songkhla, Thailand (*Table 1*) in early May 2020 which was a lockdown period of the whole country from COVID-19 pandemic. All the samples were sampling from 2 kg fish and 1 kg shrimp per each species. The numbers of samples used in this study are similar to the published articles by various researchers (Cole et al., 2013; De Witte et al., 2014; Kripa et al., 2014; Van Cauwenberghe and Janssen, 2014) Futhermore, these investigated species are commonly consumpted in the southern part of Thailand. All the samples were randomly collected from the local fresh market and transported back to the laboratory of Marine and Coastal Resources Institute at Prince of Songkla University and stored at -20 °C. Additional sediment and water samples were collected from 3 main canals and one small island in the outer lake namely, U-taphao, Pawong, Samrong Canals and Ko Yoh Island respectively (*Fig. 1*). Thereafter pH of sediment and water were determined by pH meter.

Microplastic recovery from fish and shrimp stomachs

The total amount of microplastic pieces present in each stomach of the total of 47 fish and shrimp samples was determined and described as followed; fish and shrimp samples were defrosted, measured for weight and length; and then dissected to remove the stomach and digestive tract from the body of each sample. Once the dissected stomachs and digestive tract of samples were digested following the alkaline method (Cole et al., 2014; Ding Jin-Feng et al., 2018) each sample was placed in a 250 ml conical flask. Then 150 ml of 10% potassium hydroxide (KOH) solution was carefully added before sealing the flask with aluminum foil and left for 12 h at room temperature for assimilation process. The conical flask was then heated on hotplate at 60 °C for 12 h with 1 to 2 min manual shaking every 2 h interval to remove all the organic matter. The digested solution was then filtered immediately through a Whatman GF/F filter (0.7 mm pore size, 47 mm diameter) using a Millipore filter set. After that, the filter paper was placed into a clean petri dish and heated in an oven at 50 °C to complete dryness and then stored in a petri

http://www.aloki.hu ● ISSN 1589 1623 (Print) ● ISSN 1785 0037 (Online)
DOI: http://dx.doi.org/10.15666/aeer/1902_10851106
© 2021, ALÖKI Kft., Budapest, Hungary

dish for visual identification of microplastic debris. Special care was taken to prevent sample contamination during dissection, extraction, sorting and visual identification.

Table 1. *Weight (g), length (mm) and habitat of fish and shrimp species*

Common name	Species	n	Weight (g)	Length (mm)	Habitat
Catfish	*Arius macalatus*	11	155.63 ± 1.21	21.02 ± 1.17	Demersal
Spear shrimp	*Parapenaeopsis hardwickii*	18	7.45 ± 1.18	8.01 ± 0.05	Pelagic
Yellow shrimp	*Metapenaeus brevicornis*	18	5.01 ± 0.44	7.16 ± 1.15	Pelagic

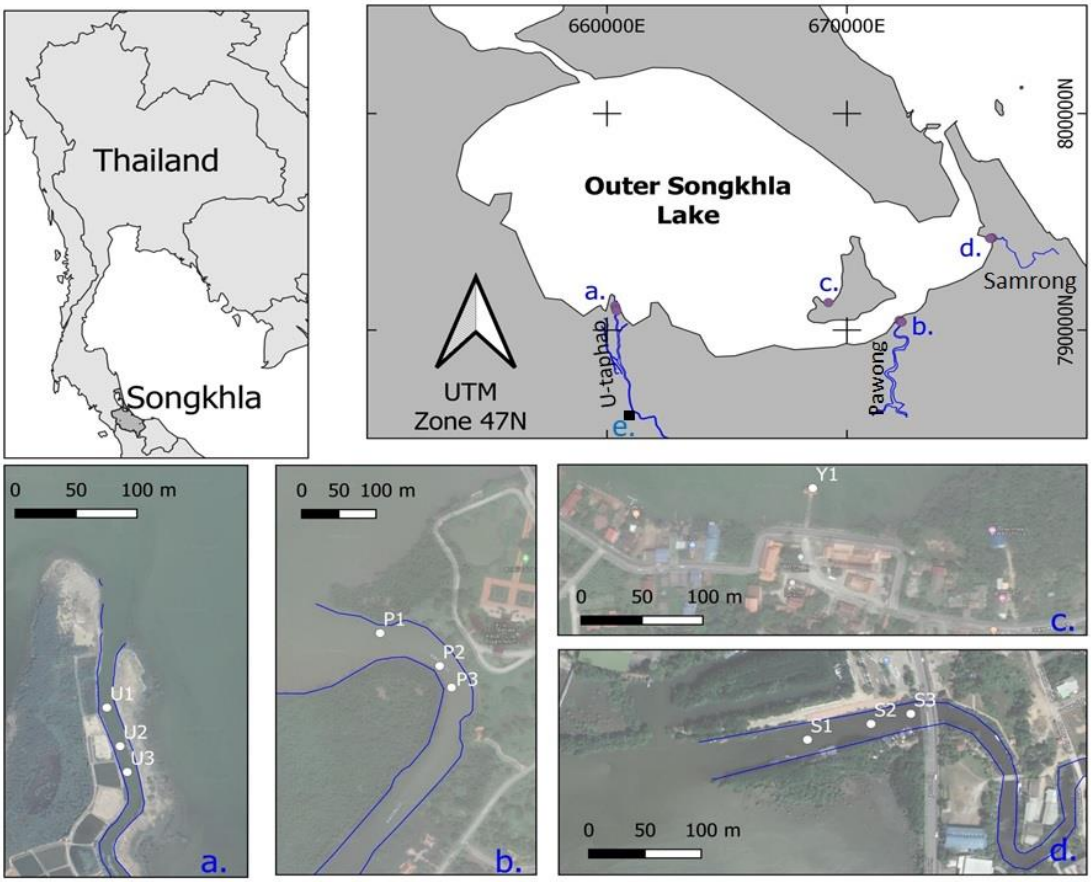


Figure 1. *Sediment and water samples were collected from 3 main canals and one small island in the outer lake namely (a) U-taphao Canal, (b) Pawong Canal, (c) Ko Yoh Island, (d) Somrong Canal and (e) Local market*

Plastic identification

The samples were visually observed under a microscope Olypus SZ, lens 110AL2X-2 with camera Canon EOS 600D and photographed. The morphotypes of microplastic particles were classified into fiber and fragment (Li et al., 2016) and also classified into four sizes, i.e. 150-500 µm, 500 µm-1 mm, 1-1.5 mm and 1.5-5 mm (modified from Karbalaei et al., 2019). The microplastics were assessed visually (Hidalgo-Ruz et al., 2012) to describe length, color and shape (Lusher et al., 2013). Furthermore, the selected microplastic samples were analyzed to identify polymer types with a Bruker

http://www.aloki.hu ● ISSN 1589 1623 (Print) ● ISSN 1785 0037 (Online)
DOI: http://dx.doi.org/10.15666/aeer/1902_10851106
© 2021, ALÖKI Kft., Budapest, Hungary

Lumos Fourier transform infrared (FTIR) microscope using the Attenuated Total Reflectance (ATR) mode to identify their composition. Infrared radiation in the range of 4000 cm^{-1} to 600 cm^{-1} was used. The spectra were identified by comparing with reference polymer spectra in the spectral library obtained from the samples with the Bruker spectrum library. Subsequently, several fibers of the most common ones found in the study were selected to observe microplastic surface using Field Emission Scanning Electron Microscope (FESEM), FEI, Apreo model at the Office of Scientific Instrument and Testing, Prince of Songkla University.

Trace metal determination

The same fish and shrimp samples of the microplastic analysis were randomly selected by using 6 fish of *Arius maculatus*, 6 shrimp of *Parapenaeopsis hardwickii* and 6 shrimp of *Metapenaeus brevicornis* in metal determination and thereafter their tissue and fish livers were dissected. All of them were dried through cold process (freeze dry), ground, sieved, kept in tightly closed polyethylene bags and stored in a desiccator for arsenic (As), cadmium (Cd) and lead (Pb) analyses according to AOAC Official Method (AOAC, 2005). Briefly, the analysis was initialized with the digestion of aquatic samples by weighing about 0.5 g of samples in a test tube, adding 2 ml of HNO_3 (65%, Merck) and digesting in a water bath at a temperature of 95 °C for about 1 h 30 min. Then 0.5 ml H_2O_2 (30%, Merck) was added and further digested in the temperature control water bath for about 30 min, left to cool to room temperature and filtered through Whatman No.1 paper. The volume of the filtrate was adjusted with deionized water to get a volume of 10 ml in volumetric flask and poured into a test tube for analyzation. Determination of trace metal (As, Cd and Pb) concentration was carried out by Inductively Coupled Plasma Optical Emission Spectrometer (ICP-OES), Perkin Elmer Optima, model 4300 DV, equipment located at Central Equipment Division, Faculty of Science, Prince of Songkla University. Additional, trace metals (As, Cd and Pb) determination were applied to the sediment according to AOAC (2005).

Quality control of analysis with standard curve preparation was conducted from standard solution using Multi-Element Calibration Standard. The standard solution was diluted with deionized water to get the concentration at 0 (the value of deionized water), 0.01, 0.05, 0.1, and 1 ppm. Then the standard solution and the volume adjusted filtrates of the digested aquatic samples were analyzed for arsenic, cadmium and lead concentration by measuring absorbance according to AOAC Official Method (AOAC, 2005).

Data analysis

Statistical analysis was used to calculate the minimum, maximum, average and standard deviation by Excel program. Pearson correlation test was performed to found the relationship among number of microplastic pieces found in fish stomach and trace metals in fish tissue and liver. A significance level of 0.05 was considered for all analyses.

Results

Microplastics ingestion by fish and shrimp

Overall, 172 microplastic pieces were recognized from the stomach contents of fish and shrimp (*Table 2*). In particular catfish (*Arius macalatus*) (n = 11) with an average length of 21.02 ± 1.17 cm, and an average weight of 155.63 ± 1.21 g contained 30

http://www.aloki.hu ● ISSN 1589 1623 (Print) ● ISSN 1785 0037 (Online)
DOI: http://dx.doi.org/10.15666/aeer/1902_10851106
© 2021, ALÖKI Kft., Budapest, Hungary

pieces of microplastics in stomachs consisting of 90% fiber and 10% fragment with average occurrence of microplastic debris = 2.73 ± 0.15 pieces/stomach. Spear shrimp (*Parapenaeopsis hardwickii*) (n = 18) with an average length of 8.01 ± 0.05 mm, and an average weight of 7.45 ± 1.18 g had 74 pieces of microplastics in stomachs comprising 100% fiber with average occurrence of microplastic debris = 4.11 ± 1.12 pieces/stomach. Yellow shrimp (*Metapenaeus brevicornis*) (n = 18) had an average length of 7.16 ± 1.15 mm, and an average weight of 5.01 ± 0.44 g and 68 pieces of microplastics in stomachs consisting of 100% fiber with average occurrence of microplastic debris = 3.78 ± 1.12 pieces/stomach.

Table 2. *Summary of microplastics found in stomach of Arius macalatus, Parapenaeopsis hardwickii and Metapenaeus brevicornis*

	***A. macalatus* catfish (n = 11)**	***P. hardwickii* spear shrimp (n = 18)**	***M. brevicornis* yellow shrimp (n = 18)**	**Total (n = 47)**
Number of microplastics (pieces)	30	74	68	172
Mean number of microplastics in stomach	2.73 ± 0.15	4.11 ± 1.12	3.78 ± 1.12	3.54 ± 0.78
Percentage of fiber found	90	100	100	96.67
Percentage of fragment found	10	0	0	3.33

The size of the microplastics in the fish and two types of shrimp (*Fig. 2*) in this study were divided into 4 size intervals. In the catfish, the amount of microplastic debris found in the stomachs in both 0.5-1.0 mm size and 1.5-5.0 mm size was approximately 30%, followed by the 0.15-0.5 mm size (26.67%) and 1.0-1.5 mm size (13.33%). For the spear shrimp (*Parapenaeopsis hardwickii*), the microplastic size was mostly found in 0.5-1.0 mm size (33.78%), followed by 0.15-0.5 mm size (25.68%), 1.5-5 mm size (24.32%) and the least amount found in 1.0-1.5 mm size was 16.22%. For the yellow shrimp (*Metapenaeus brevicornis*) the most common microplastic particles found were in 0.5-1.0 mm size (44.12%), followed by both 0.15-0.5 mm size and 1-1.5 mm size (19.12%) and the smallest amount found was in 1.5-5.0 mm size (17.64%).

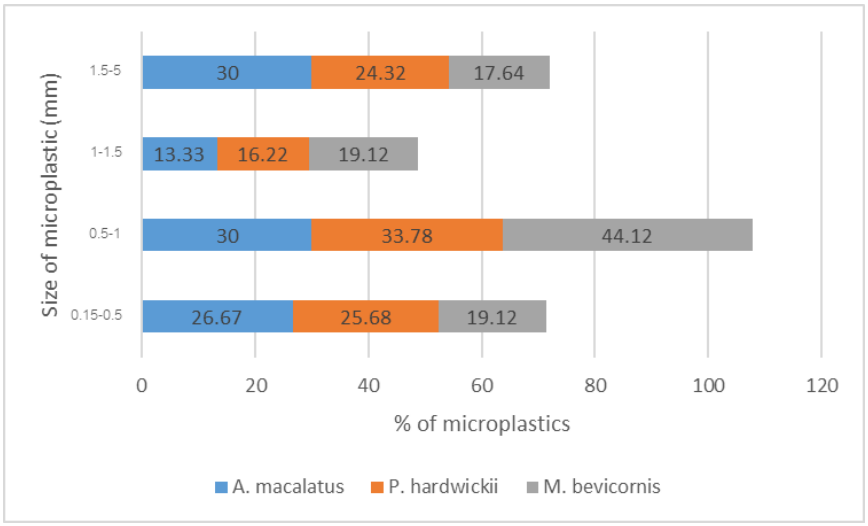


Figure 2. *Size distribution of microplastics in the stomachs of fish (A. macalatus) and shrimp (P. hardwickii and M. brevicornis)*

http://www.aloki.hu ● ISSN 1589 1623 (Print) ● ISSN 1785 0037 (Online)
DOI: http://dx.doi.org/10.15666/aeer/1902_10851106
© 2021, ALÖKI Kft., Budapest, Hungary

The colors of microplastic debris present in both fish and 2 types of shrimp were found in 4 different colors which were black, blue, clear white and red. The color of the debris found was mostly black in the catfish (66%), spear shrimp (*Parapenaeopsis hardwickii*) (56%) and yellow shrimp (*Metapenaeus brevicornis*) (53%), followed by blue, clear white and the least color found was red. The characteristic of microplastic debris found in fish and shrimp is shown in *Figure 3*. In shrimp only fiber was found whereas fish had 90% fiber and 10% fragment.

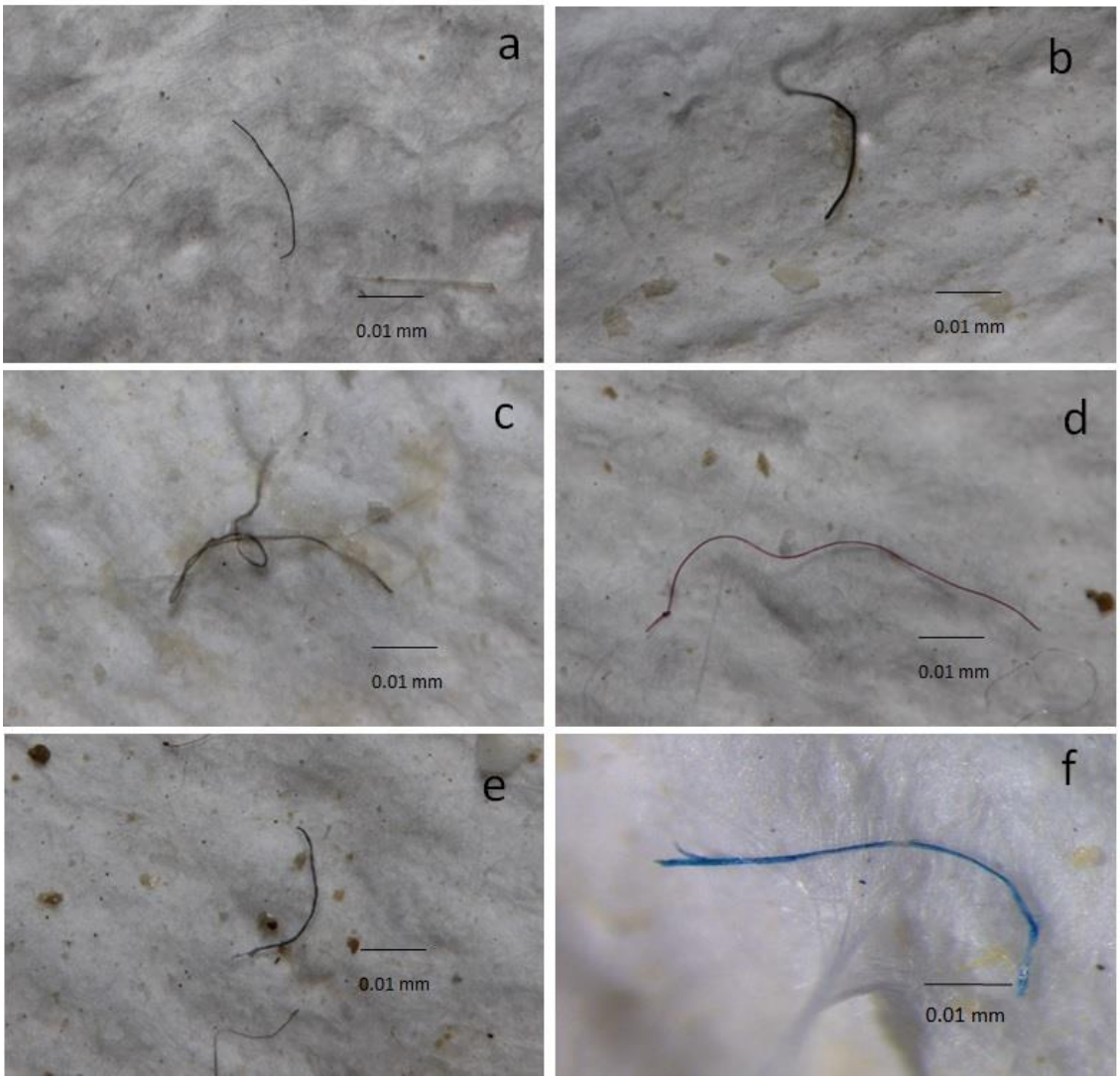


Figure 3. *Selected microplastics found in the stomach contents of shrimps (a-e) and fish (f)*

Polymer type

From the FTIR investigation, five types of the polymers found in this study were rayon, polyester, polyvinyl alcohol, polyethylene and paint. Among those, there were two types of specimens consisting of rayon and polyester fibers (*Fig. 4*) which were found in more than 50% of the samples. Thereafter rayon fibers were selected and coated with gold before investigating by Field Emission Scanning Electron Microscope (FESEM) and the fibers showed the appearance of splits and twists (*Fig. 5*).

http://www.aloki.hu ● ISSN 1589 1623 (Print) ● ISSN 1785 0037 (Online)
DOI: http://dx.doi.org/10.15666/aeer/1902_10851106
© 2021, ALÖKI Kft., Budapest, Hungary

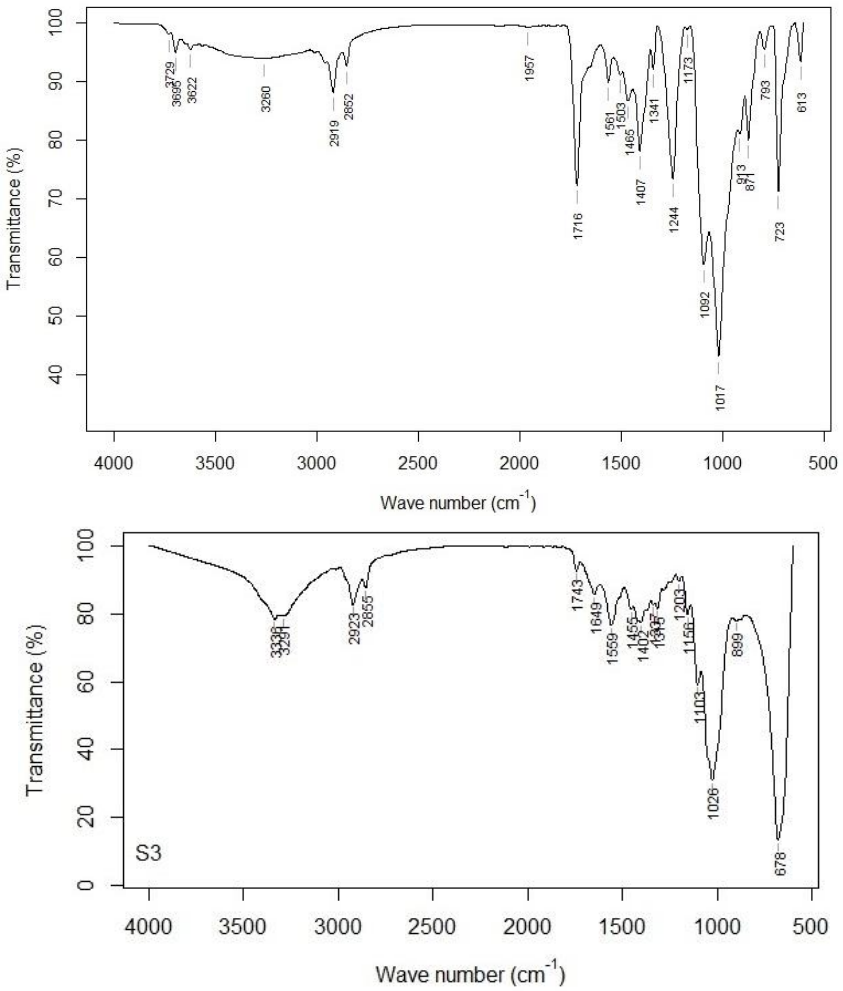


Figure 4. *Top to bottom. Representatives of IR spectra of polyester (top) and rayon (bottom)*

Trace metal concentration in fish and shrimp tissue

Accumulation of trace metals (As, Cd and Pb) in fish *A. macalatus* (tissue and liver) and shrimp (tissue) was shown in *Table 3* and summarized as follows; In *A. macalatus*, the amounts of As in tissue ranged from < dl to 2.73 mg/kg dry weight and < dl to 2.04 mg/kg dry weight of fish liver. The amounts of Cd ranged from < dl to 0.387 mg/kg dry weight of tissue and < dl-1.29 of liver. The amounts of Pb ranged from < dl to 1.58 mg/g dry weight of tissue and < dl-0.727 mg/kg dry weight of liver. In *P. hardwickii*, the amounts of As in tissue ranged from 1.78 to 7.28 mg/kg dry weight. Cd ranged from 0.064 to 0.196 mg/g dry weight of tissue and Pb showed nondetectable level. For *M. brevicornis,* the amounts of As in tissue ranged from 0.97 to 1.83 mg/kg dry weight. Cd ranged from < dl to 2.185 mg/kg and Pb ranged from < dl to 7.69 mg/kg dry weight. Overall, the amounts of As were in order of *P. hardwickii* > *A. macalatus* (tissue) > *A. macalatus* (liver) > *M. brevicornis* for Pb *M. brevicornis* > *A. macalatus* (tissue) > *A. macalatus* (liver) and *M. brevicornis* could not be detected. For Cd *M. brevicornis* > *A. macalatus* (liver). For sediment the concentrations of As, Pb and Cd were 6.214-15.895 mg/g dry weight, 15.335-41.292 mg/g dry weight and 0.01-0.07 mg/g dry weight respectively.

http://www.aloki.hu ● ISSN 1589 1623 (Print) ● ISSN 1785 0037 (Online)
DOI: http://dx.doi.org/10.15666/aeer/1902_10851106
© 2021, ALÖKI Kft., Budapest, Hungary

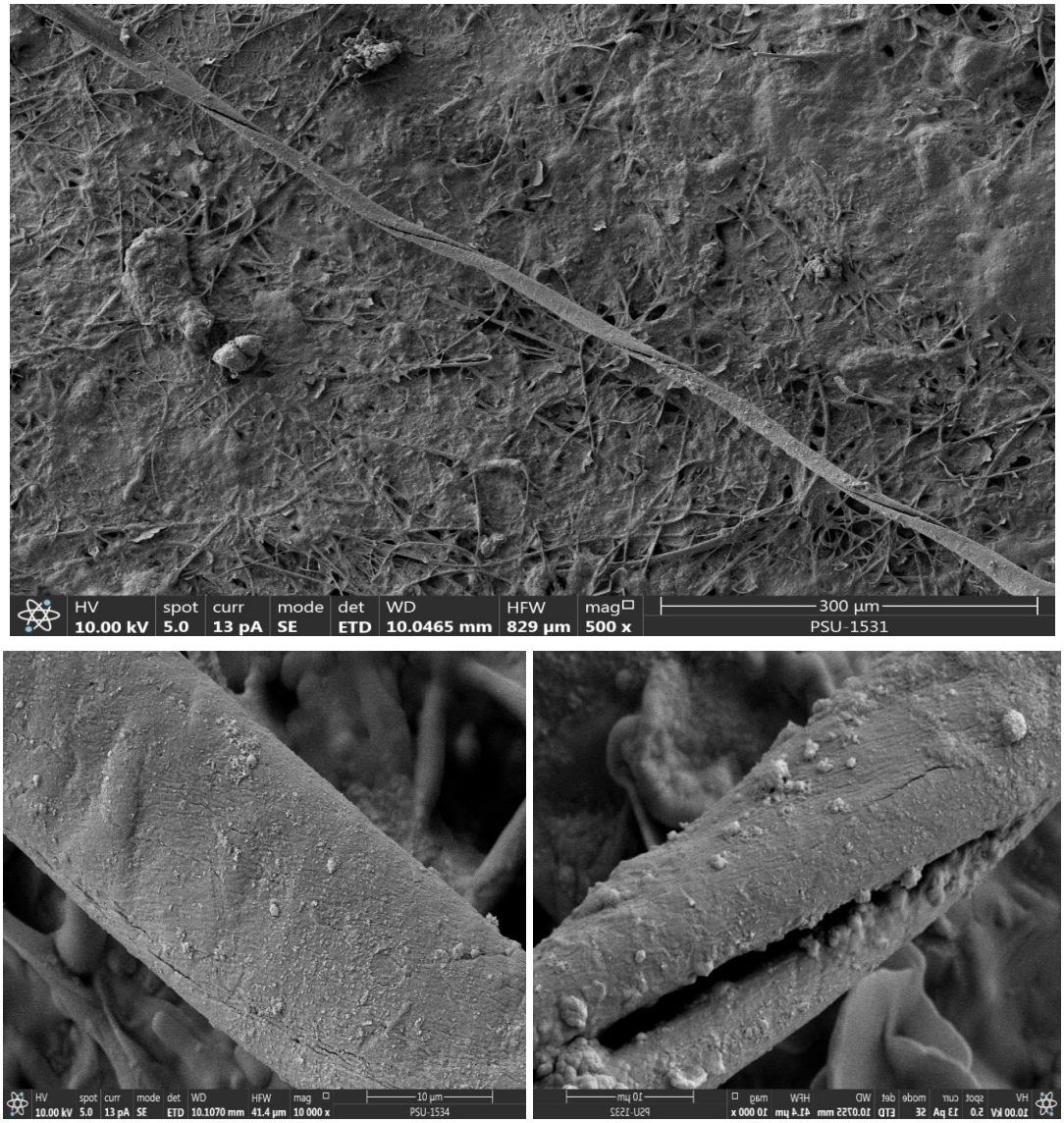


Figure 5. *Top to bottom: FESEM images of the investigated microplastic appearance of rayon fibers. Twist (top), cracks (bottom)*

Table 3. *Concentrations of As, Cd and Pb in fish and shrimp*

Common name	Species	Concentration (mg/kg) (dry weight)		
		As	Cd	Pb
Spear shrimp	*P. hardwickii*	1.78-7.28	0.064-0.196	< dl
Yellow shrimp	*M. brevicornis*	0.97-1.83	< dl-2.185	< dl-7.69
Catfish	*A. macalatus* (tissue)	< dl-2.73	< dl-0.387	< dl-1.58
	A. macalatus (liver)	< dl-2.04	< dl-0.727	< dl-1.29

dl = detection limit

Discussion

This study is the first report of microplastic debris found in two marine shrimp species (*P. hardwickii* and *M. Brevicornis*) and tropical demersal fish (*A. macalatus*) in

http://www.aloki.hu ● ISSN 1589 1623 (Print) ● ISSN 1785 0037 (Online)
DOI: http://dx.doi.org/10.15666/aeer/1902_10851106
© 2021, ALÖKI Kft., Budapest, Hungary

Songkhla Lake, Southern Thailand. It revealed that the majority of microplastic particles were mostly fibers which were expected to be derived from 2 main sources: 1) clothing, apparel and 2) fishing net or fixed fishing gear which decomposed into smaller debris, floated around and eventually accumulated on the sea floor and lake. Five types of the found microplastics included polyester, rayon fiber, polyvinyl alcohol, polyethylene and paint. It is very interesting that the type of microplastics found in shrimp and fish have fibers from clothing since the properties of the most commonly used fabrics made from polyester fibers are wrinkle free textile for making men's and women's clothing with easy care and durable properties. It is also popular to mix polyester fibers with other fibers, such as rayon, silk, cotton, linin, wool, etc. It is possible that during the outbreak of COVID-19 (lock down period), most people stayed at home and worked from home, which resulted in more clothes washing and a great amounts of fibers (clothing lint) caused by washing activities drained to sewers down to canals, entering the water in the lake and eventually contaminating soil and aquatic animals. There was also a possibility that the polyester fibers found would come from the washing of cloth face masks since Thai government issued a "must wear face mask" order while people left home during the outbreak of COVID-19 (March - June 2020). They mostly wore cloth face masks instead of the paper ones because they were very expensive and not available during the outbreak of COVID-19. The cloth masks are washable and needed to be washed every time people wear them. Thus, there is a chance that the fibers will be released during the washing activity. Cloth masks are mostly made from mixture of cotton and polyester. Rayon particles may originate from clothing lint from laundry. The evaluation of microplastic release caused by textile washing processes (more than 6 million microfibers of woven polyester from 5-kg washing load) conducted by De Falco et al. (2018) clearly supported our aforementioned observation. Thus, it is about time for a new generation of washing machines with one more filter layer to remove microplastic debris of the water drained from the washing machines before releasing to the sewer since considerable microplastic debris is definitely drained to the environment each time of doing laundry by washing machines.

From the FTIR spectra in *Figure 4*, the spectrum shows the characteristics functional vibration of polyester (*Fig. 4* top) as seen at the vibration band of carbonyl group (C = O) at 1718 cm^{-1} and ester group (C-O-C) at 1244 cm^{-1} (Koto and Soegijono, 2019). Rayon (*Fig. 4* bottom) is known as an artificial textile. It is made from natural resources such as wood and agricultural plants that are composed to regenerate and purify as cellulose fiber. The chemical structure of rayon is similar to cellulose chemical structure that basically has a lower molecular weight. From the rayon FTIR spectrum, the absorption band of hydroxyl group (-OH) in the cellulose structure at the wave number about 3390 cm^{-1} and C-H stretching at 2850-2930 cm^{-1} are clearly observed (Song et al., 2012). The vibration of C-O-C in the cellulose structure is observed at the wave number of 1100-1200 cm^{-1}. Moreover, -OH bending from water adsorption and C-H planar bending are shown at the adsorption peaks of 1650 cm^{-1} and 1390 cm^{-1}, respectively (Auta et al., 2017).

In addition, Songkhla Lake has quite a few fishing tools including stationary fishing gears such as standing trap, set bag and moving gear such as gill net. Thus, there is a chance that the fragments of the broken fishing nets will float and accumulate in the water surface in the outer Songkhla Lake with an outlet to the lower Gulf of Thailand. The sea water from the Gulf of Thailand will flow into Songkhla Lake through the lake

http://www.aloki.hu ● ISSN 1589 1623 (Print) ● ISSN 1785 0037 (Online)
DOI: http://dx.doi.org/10.15666/aeer/1902_10851106
© 2021, ALÖKI Kft., Budapest, Hungary

mouth during high tide and transport suspended particles including microplastics from the lake to the Gulf of Thailand during low tide. The colored fragments might come out from the broken paint from the fishing boat parking on the lake. Paint, polyester and nylon, which are common raw materials of ropes, fishing nets, fish baskets, bags and coatings used in sea may contribute to the accumulation of microplastic debris in marine organism (Thushari et al., 2017). Comparing the studies of Fang et al. (2019) on the economic fish in China, more types of polymers were found than in our studies. Their study found that the polymer types of microplastics across species could be divided into eight categories, including polypropylene (PP), polyamide (PA), polyethylene (PE), polystyrene (PS), polyethylene terephthalate (PET), polyvinyl chloride (PVC), polyacrylonitrile (PAN) and others. Potential consequences of microplastic ingestion include physical damage of the gastrointestinal track of fish and the creation of a false sensation of satiation, which could result in fish mortality from starvation (Cole et al., 2013; Nadal et al., 2016; Possatto et al., 2011). Moreover, a weakening of the olfactory senses of fish were also observed as a consequence of microplastic ingestion (Jovanović, 2017). Occurrence of plastic debris in gastrointestinal tracts of organisms could be due to trophic transfer of smaller species being prey for higher trophic organisms (Farrell and Nelson, 2013). Once microplastics enter the marine food web, they could be passed up the food chain to higher predators, including humans (Cole et al., 2011).

From the study of microplastic types in sandy soil on the beach in the lower southern part of Thailand (Kreekainut et al., 2019), there were 6 types of microplastics and polyethylene terephthalate (PET) was the most abundant, followed by polyethylene (PE), polyvinyl chloride (PVC), polypropylene (PP), polystyrene (PS) and polyamide (PA). The most common fibers with black and white colors were observed. Furthermore, from the previous study of microplastics in sediment on the beach of Libong Island, Trang Province located in the southwestern sea of Thailand by Pradit et al. (2020), there were 6 types of microplastics including polyvinyl chloride (PVC), polypropylene (PP), nylon, polyethylene (PE), polyester, polyacrylate (PA) and polymer with a structure similar to ethylene propylene diene monomer (EPDM) rubber, the microplastic colors found were white, blue and red. Surprisingly, from the aforementioned studies of both teams, no rayon fiber has been reported in the sandy areas. It is possible that rayon fibers are lightweight and drift with the currents into the open sea and eventually enter into the bodies of aquatic animals which were also reported in Azad et al. (2018) that textile fibers were found in the stomachs of fish. Currently there are no available published data on microplastics in the water of Songkhla Lake or in the seawater of the Gulf coast of the lower south of Thailand. However, the microplastic study in the coastal waters of Terengganu State, Malaysia, which borders the southern region of Thailand conducted by Amin et al. (2020) revealed that the majority of microplastic particles found were fibers and fragments with fibers constituting a majority and the total concentration of microplastics was the greatest at station nearshore (9 particles/l). The increased concentrations of plastics near shore was in part, explained by the large number of fiber content, which were mostly identified as polypropylene (PP), polyethylene terephthalate (PET), polyethylene (PE), polyamide (PA) (nylon), acrylic, and polyvinyl alcohol (PVA) (Browne et al., 2011; Claessens et al., 2013; Sun et al., 2018).

The amounts of microplastic particles that accumulated in the stomachs of both fish and shrimp in this study were higher than in those study conducted by Azad et al.

http://www.aloki.hu ● ISSN 1589 1623 (Print) ● ISSN 1785 0037 (Online)
DOI: http://dx.doi.org/10.15666/aeer/1902_10851106
© 2021, ALÖKI Kft., Budapest, Hungary

(2018) which investigated fish in the lower Gulf of Thailand in the coast of Songkhla Province. They found average occurrence of plastic particles in the pelagic fish (1.75 pieces/stomach) higher than that of demarsal fish (0.97 pieces/stomach) by approximately two times. This was very interesting since this study found the amounts of microplastic debris accumulated in the stomatchs of fish and shrimp higher than those of the study conducted before the outbreak of COVID-19 pandemic by Azad et al. (2018) by approximately 3 times. It is possible that since this study area (Songkhla Lake) is a semi-closed area, the floating microplastic particles accumulate in the lake more than those in the open sea, and it may be the COVID-19 outbreak (lockdown period) that changed the people way of life, for example, by staying longer at home, doing more laundry, releasing more cloth fibers into sewer and lake. As compared with the study of Hossain et al. (2020), investigating microplastic contamination in two shrimp species (Tiger shrimp and Brown shrimp) in the north of the Bay of Bengal revealed that the amounts of microplastic occurrence were similar to our study. However, according to our study, only spear shrimp (*P. hardwickii*) had more microplastic particles per stomach, which can probably be attributed to the different types of shrimp and environment between the two study sites. The shape of the microplastic particles found in both types of shrimp were 100% fibers and 90% fibers were also found in fish in which the fibers were both short pieces and coiled pieces.

In reality, fibers can naturally be folded or twisted or bundled into an aggregate. Thus, reducing their overall size and potentially increasing their bioavailability (Desforges et al., 2015). Some shrimps and fish larvae can feed on prey items which can reach lengths of up to 1.54 mm (Baier and Purcell, 1997). Shrimp are typically eaten without the removal of the gastrointestinal tract and thus microplastics therein could be transferred to humans via food chain (Hossain el al., 2020). Surface morphology of microplastics can change significantly through degradation in the environment caused by surface abrasion (Karbalaei et al., 2019) e.g. *Figure 4* shows appearance of clear twist and crack on the surface of fiber. Inorganic and organic contaminants can absorb into pores or cracks of microplastics (Kowalski et al., 2016). However, fouling or biofouling may increase the density of these polymers (Moret-Ferguson et al., 2010; Karami, 2017) causing them to sink and become available for demersal feeders. It is interesting that *Figure 4* showing photos of microplastic debris possesses cracks. These cracks probably have potential capability to accumulate trace metals or other pollutants through these crack openings and therefore over time the floating fiber fragments have the chance to be the source of trace metals or other toxic substances.

Comparing the concentration of trace metals in fish and sediment before and during the outbreak of COVID-19 in the Songkhla Lake region was conducted (*Table 4*). As expected, the concentrations of As, Cd and Pb in the sediment before COVID-19 pandemic were slightly higher than those during COVID-19. According to sediment quality guideline such as USEPA (1989), the concentration of As classified as heavily polluted is less than 8 mg/kg dry weight whereas Pb values of less than 40 mg/kg dry weight during COVID-19 is classified as nonpolluted. Although the concentration of As during COVID-19 was less than that of before COVID-19 but still in a serious situation. The leakage from acid mine drainage of the tailings associated with arsenopyrite of the abandoned tin mines surrounding the Songkhla Lake Watershed is probably responsible for the high concentrations of As in sediment in the study area.

Surprisingly, no significant difference of As, Cd and Pb concentrations of fish livers, fish and shrimp tissue was found between before and during the COVID-19,

http://www.aloki.hu ● ISSN 1589 1623 (Print) ● ISSN 1785 0037 (Online)
DOI: http://dx.doi.org/10.15666/aeer/1902_10851106
© 2021, ALÖKI Kft., Budapest, Hungary

even though there was no activity of factories, companies and tourism industries performing during the 3-month lockdown and curfew measures and it was not concordant with the aforementioned chemical signature of metal concentrations of the sediment before and during COVID-19. This was probably caused by the higher retention time of the fish and shrimp exposed to the metal contaminated water during the lockdown period since less or no fishing activity was performed and therefore it provided longer time for the fish and shrimp to accumulate metals in their body before they were caught by fishermen. The longer retention time of exposing to the metal contaminated water would definitely raise the low metal concentrations of the fish and shrimp tissue to the same orders of magnitude of metal concentrations as those during COVID-19. In addition, all the factories and companies stopped working during the COVID-19 outbreak and the release of the amount of waste water, trace metals and other contaminants from their activities were expected to decrease. Thus, the amounts of metals and other pollutants present in the lake were the amounts that had been formerly accumulated.

The outer section of the lake is thus a vulnerable area regarding the mobility of As combining both important riverine inputs and reduced sediment conditions prompting mobilization of As (Pradit et al., 2010). In fish, trace metals may be concentrated at different levels in different organs of the body and may present in different forms (Pradit et al., 2010). High levels of arsenic are encountered in marine fish, but arsenic is predominantly present in nontoxic arsenobetaine form (De Gieter et al., 2002; Baeyens et al., 2009). It is worth noting that the pH in the water and sediment increased as expected since most of the people were detained at home and therefore, there were more clothes washing. The water from washing clothes with detergent has normally high alkaline components consisting of ions of OH^-, CO_3^{2-}, HCO_3^- of calcium, sodium, magnesium, potassium and ammonia. This base condition from laundry activity was certainly responsible for raising the pH in both water and sediment.

Table 4. *Comparison of concentration of trace metal (mg/g dry weight) and pH before and during COVID-19 in Songkhla Lake*

Situation	Species	As	Cd	Pb	pHsed	pHwat	Reference
Before COVID	*A macalatus* (T)	1.86-7.25	< dl-0.37	0.06-0.19			Pradit et al., 2010
	A macalatus (L)	1.35-1.96	0.039-0.47	0.75-1.80			Pradit et al., 2010
	Sediment	0.8-70.7	0.1-2.4	8.2-13.1			Pradit et al., 2010
	Sediment	7.0-30.0	0.14-0.92	19.0-66.0	7.00-7.50	7.00-8.20	Pradit et al., 2013
	Sediment	11.33-15.11	-	11.99-14.03	7.00-7.50	-	Aunjangwang,2014
	Sediment	18.55-24.41	-	38.35-59.35	6.78-7.21	-	Baruddin, 2017
	Sediment	20.35-50.50	0.01-0.18	48.8-78.8	6.71-7.53	7.03-7.85	Pradit et al., 2018
	Sediment	14.90-58.10	0.07-0.11	38.9-79.7	6.71-9.00	7.07-9.49	Pradit et al., 2019
During COVID	*A. macalatus* (T)	< dl-2.73	< dl-0.39	< dl-1.58			This study
	A. macalatus (L)	< dl-2.04	< dl-0.73	< dl-1.29			This study
	P. hardwickii	1.78-7.28	0.06-0.20	< dl			This study
	M. brevicornis	0.97-1.83	< dl-2.19	< dl-7.69			This study
	Sediment	6.21-15.90	0.01-0.07	15.34-41.29	8.04-8.76	7.89-8.72	This study

T = tissue, L = liver, dl = detection limit, sed = sediment, wat = water

From the previous studies, it was well known that microplastic particles have a potential to absorb the cations such as metal ions and persistent organic pollutants (POPs)

http://www.aloki.hu ● ISSN 1589 1623 (Print) ● ISSN 1785 0037 (Online)
DOI: http://dx.doi.org/10.15666/aeer/1902_10851106
© 2021, ALÖKI Kft., Budapest, Hungary

dissolved in water and thus, they can act like contaminant scavengers and carriers certainly posing a hazardous risk on aquatic animals, food webs and food security. Hence, the more microplastic pieces are present in the stomachs or gastrointestinal tracts of aquatic animals, the higher metal concentrations in animal tissue are. Surprisingly, from determining the correlation coefficient between numbers of microplastic particles found in fish stomachs and trace metal concentrations in fish fillets and their livers revealed that the numbers of microplastic particles had negative correlation coefficients with all the metal concentrations in fish tissue and liver ($r = -0.904$, -0.469, -0.415 and -0.373) ($p < 0.05$) except As (*Table 5*). A similar trend was also observed in spear shrimp. However, fairly low positive correlation coefficients between the numbers of microplastic particles and metal concentrations were observed in yellow shrimp. This chemical signature was probably caused by the microplastic debris present in fish and shrimp in our study possessing less or no ability of absorbing trace metal ions. This is not congruent with most previous studies. The possible explanation for this anomalous finding was that the microplastics present in the stomachs of fish and shrimp in our study were probably new born microplastic particles and therefore, had very little or no ability of metal absorbing metal ions. Over time, there were biofouling accumulation on these microplastic pieces resulting in increasing their metal absorbing ability. Thus, the metal absorbing ability of microplastic debris increases with age (*Fig. 6*). Furthermore, the study of biofouling is a source of metal pollution conducted by Bighiu et al. (2017) supporting our aforementioned explanation. Hence, normally the moderate or high positive correlation coefficients between the numbers of mature and old microplastic particles and metal concentrations were mostly found in the previous studies whereas the fairly low positive to negative correlation coefficients were observed in the new or young microplastic debris of our study.

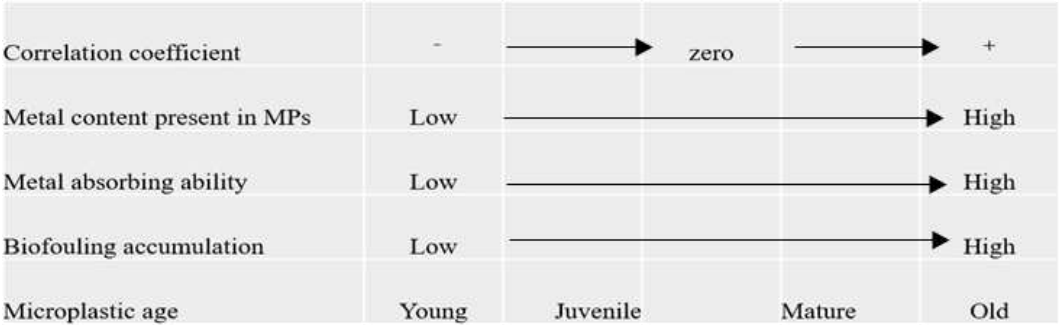


Figure 6. *Diagram of chemical property of microplastic change with time*

From calculating numbers of microplastic pieces per gram of body wet weight in this study (*Table 6*), it was found that *M. brevicornis* shrimp had microplastic occurrence of 0.76 ± 0.48 pieces/g (wet weight) and *P. hardwickii* shrimp possessed 0.55 ± 1.19 pieces/g (wet weight). This was well agreed with the study in brown shrimp, *Crangon crangon*, a commercially important crustacean in the eastern Atlantic and Mediterranean Sea, microplastic were found an average of 0.68 ± 0.55 pieces/g (wet weight) (Devriese et al., 2015). For the fish (*A. macalatus*) in this study, the amount of microplastic pieces found was 0.018 ± 0.27 pieces/g (wet weight), which was less than that of shrimp and fish from other areas. For example, as compared to that in *Scomber japonicus* (Güven et al., 2017) it was estimated at approximately 0.33 pieces/g (wet weight), in Engraulis ringens it was

http://www.aloki.hu ● ISSN 1589 1623 (Print) ● ISSN 1785 0037 (Online)
DOI: http://dx.doi.org/10.15666/aeer/1902_10851106
© 2021, ALÖKI Kft., Budapest, Hungary

0.057 pieces/g (wet weight). However, when compared to mussels (Goh et al., 2019), both shrimp and fish from this study, the microplastic pieces found were much less amounts. Factors influencing microplastic consumption are feeding strategy and environmental prevalence that are primary drivers for microplastic consumption. Generally, lower trophic level organisms appear to ingest more microplastics due to feeding strategy (Walkinshaw et al., 2020). Calculating the weight of microplastic pieces found in fish and shrimp in our study using the consumption rate of meat, fish or seafood of 85 g/person/day (Puangsuwan, 2014) it was found that there was an opportunity for Thai consumers to get microplastic pieces from shrimp and fish consumption between 1.53-64.6 pieces/day. Hence, this means that microplastic contamination currently occurs in brackish water food chain and jeopardizes Thai food security since Songkhla Lake is the biggest lake of Thailand and one of the most significant food sources of the people in lower south of Thailand.

Recently, the information on health risks through the intake of trace metals has been led to a potential interest of the consumers (Barone et al., 2015). Trace metals like As (inorganic) have long time exposure that leads to the occurrence of skin, vascular, nervous system disorders, birth defects, reproductive problems, and finally, people with prolonged exposure to As tend to develop some form of cancer (Bosch et al., 2016). Cd may be a carcinogen and Pb can damage blood circulation (Rahman et al., 2012; Arnich et al., 2012).

Table 5. *Correlation coefficients (R) at $p < 0.05$ between number of microplastic (MPs) found in fish stomachs and trace metals (mg/kg dry weight) in (a) catfish tissue and liver, (b) spear shrimp and (c) yellow shrimp*

(a) Catfish	MPs	Weight	Length	As_T	Cd_T	Pb_T	As_L	Cd_L	Pb_L
MPs	1								
weight	0.498	1							
length	0.427	**0.982**	1						
As_T	0.494	-0.173	-0.181	1					
Cd_T	-0.373	0.022	0.043	**-0.921**	1				
Pb_T	-0.415	0.015	0.026	**-0.947**	**0.995**	1			
As_L	0.513	0.595	0.472	0.081	-0.309	-0.265	1		
Cd_L	**-0.904**	-0.735	-0.687	-0.248	0.232	0.266	-0.680	1	
Pb_L	-0.469	-0.254	-0.220	-0.284	0.379	0.375	-0.724	0.650	1

(b) Spear shrimp	MPs	weight	length	As	Cd
MPs	1				
weight	0.631	1			
length	**0.862**	0.508	1		
As	-0.167	-0.214	0.312	1	
Cd	-0.223	-0.269	0.286	**0.981**	1

(c) Yellow shrimp	MPs	weight	length	As	Cd
MPs	1				
weight	-0.179	1			
length	0.029	**0.821**	1		
As	0.638	-0.385	-0.352	1	
Cd	0.314	-0.031	-0.413	0.211	1

Significant results are highlighted. MPs = microplastics, T = tissue, L = liver

http://www.aloki.hu ● ISSN 1589 1623 (Print) ● ISSN 1785 0037 (Online)
DOI: http://dx.doi.org/10.15666/aeer/1902_10851106
© 2021, ALÖKI Kft., Budapest, Hungary

Table 6. *Numbers of microplastic pieces per gram of body wet weight of marine organisms*

Species	Common name	Number of microplastic	References
P. hardwickii	Spear shrimp	0.55 ± 1.19	This study
M. brevicornis	Yellow shrimp	0.76 ± 0.48	This study
A. macalatus	Catfish	0.018 ± 0.27	This study
Scomber japonicus	Fish	0.33	Güven et al., 2017
Engraulis ringens	Peruvian anchovy	0.057	Ory et al., 2018
Perna viridis	Green mussel	21.10 ± 0.15	Goh et al., 2019
Crangon crangon	Brown shrimp	0.68 ± 0.55	Devriese et al., 2015

Conclusion

The main content of this study was to investigate gastric microplastic and trace metal content (As, Cd and Pb) in tissues of the dominant aquatic organisms in outer Songkhla Lake, which were the catfish and two shrimps, that microplastic pieces were found. The accumulated fiber types and their polymer types were derived from the main component of clothing and fishing gear. During the study period, the COVID-19 outbreak with the government lockdown order, there was no inter-provincial travel and no activity of both private and government organizations for approximately 3 months. Thus, this certainly changed the people's lifestyle by staying at home and working from home, resulting in more laundry activities, releasing more cloth fibers into the drain water and finally entering the Songkhla Lake. Thus, it is recommended that new generation of washing machines should be installed with one more filter layer to get rid of microplastic debris in drain water from the washing machines before releasing to sewer since substantial microplastic debris is definitely drained to the environment each time of doing laundry by washing machines. From most of the previous studies, normally the numbers of microplastic particles present in the stomachs of aquatic organisms should have moderate to high positive correlation coefficients with most of the metal concentrations in their tissues. In fact, this study showed the negative correlation coefficients with all the metal concentrations in fish tissue and liver except for As. A similar trend was also observed in spear shrimp but fairly low positive correlation coefficients between the numbers of microplastic particles and metal concentrations were observed in yellow shrimp. This anomalous chemical signature was probably caused by the microplastics present in the stomachs of fish and shrimp in our study were probably new born microplastic particles and therefore, had very little or no ability of absorbing metal ions. Over time, there was biofouling accumulation on these microplastic pieces resulting in increasing their metal absorbing ability. Thus, the metal absorbing ability of microplastic debris increases with age. Normally the moderate or high positive correlation coefficients between the numbers of mature and old microplastic particles and metal concentrations in organisms were mostly found in the previous studies whereas the fairly low positive to negative correlation coefficients were observed in the new or young microplastic debris of this study. However, there should be studies to monitor the amounts of microplastic pieces in other aquatic animals additionally, since they probably pose potential harmful effects on the health of aquatic organisms, ecosystems and humans.

Acknowledgements. This paper was fully supported by Faculty of Environmental Management Research Fund 2020 (code ENV6304125c), Prince of Songkla University. We thank the anonymous reviewers for their careful reading of our manuscript and their comments.

http://www.aloki.hu ● ISSN 1589 1623 (Print) ● ISSN 1785 0037 (Online)
DOI: http://dx.doi.org/10.15666/aeer/1902_10851106
© 2021, ALÖKI Kft., Budapest, Hungary

REFERENCES

[1] Amin, M. R., Sohaimi, E. S., Anuar, S. T., Bachok, Z. (2020): Microplastic ingestion by zooplankton in Terengganu coastal waters, southern South China Sea. – Marine Pollution Bulletin 150: 110616.

[2] Andrady, A. L. (2011): Microplastics in the marine environment. – Marine Pollution Bulletin 62: 1596-1605.

[3] Angsupanich, S., Somsak, S., Phrommoon, J. (2005): Stomach contents of the catfishes Osteogeneiosus militaris (Linnaeus, 1758) and Arius maculatus (Thunberg, 1792) in the Songkhla Lake. – Songklanakarin Journal of Science and Technology 27: 391-402.

[4] AOAC (2005): Official Methods of Analysis of AOAC International. 18th Ed. – In: Horwitz, W., Latimer, G. W. (eds.) Metals and Other Elements. AOAC, Gaithersburg, Maryland.

[5] Arnich, N., Sirot, V., Rivière, G., Jean, J., Noël, L., Guérin, T., Leblanc, J.-C. (2012): Dietary exposure to trace elements and health risk assessment in the 2nd French Total Diet Study. – Food and Chemical Toxicology 50: 2432-2449.

[6] Aunjangwang, N. (2014): Contamination of arsenic and lead in sediment of U-Taphao Canal. – PhD thesis, Prince of Songkla University, Songkla.

[7] Auta, R., Adamus, G., Kwiecien, M., Radecka, I., Hooley, P. (2017): Production and characterization of bacterial cellulose before and after enzymatic hydrolysis. – Journal of Biotechnology 16: 470-482.

[8] Azad, S. M. O., Towatana, P., Pradit, S., Goh, P. B., Hue, H. T. T., Jualaong, S. (2018): First evidence of existence of microplastics in stomach of some commercial fishes in the lower Gulf of Thailand. – Applied Ecology and Environmental Research 16: 7345-7360.

[9] Baeyens, W., Gao, Y., Galan, S. De, Bilau, M., Larebeke, N. Van, Leermakers, M. (2009): Dietary exposure to total and toxic arsenic in Belgium: importance of arsenic speciation in North Sea fish. – Molecular Nutrition & Food Research 53: 558-565.

[10] Baier, C., Purcell, J. (1997): Trophic interactions of chaetognaths, larval fish, and zooplankton in the South Atlantic Bight. – Marine Ecology Progress Series 146: 43-53.

[11] Barone, G., Storelli, A., Garofalo, R., Busco, V. P., Quaglia, N. C., Centrone, G., Storelli, M. M. (2015): Assessment of mercury and cadmium via seafood consumption in Italy: estimated dietary intake (EWI) and target hazard quotient (THQ). – Food Additives & Contaminants Part A 32: 1277-1286.

[12] Baruddin, N. A., Shazili, N. A. M., Pradit, S. (2017): Sequential extraction analysis of heavy metals in relation to bioaccumulation in mangrove, Rhizophora mucronata from Kelantan Delta, Malaysia. – AACL Bioflux 10: 172-181.

[13] Bighiu, M. A., Eriksson-Wiklund, A. K., Eklund, B. (2010): Biofouling of leisure boats as a source of metal pollution. – Environ Sci Pollut Res 24: 997-1006.

[14] Bosch, A. C., O'Neill, B., Sigge, G. O., Kerwath, S. E., Hoffman, L. C. (2016): Heavy metals in marine fish meat and consumer health: a review. – Journal of the Science of Food and Agriculture 96: 32-48.

[15] Browne, M. A., Crump, P., Niven, S. J., Teuten, E., Tonkin, A., Galloway, T., Thompson, R. (2011): Accumulation of microplastic on shorelines worldwide: sources and sinks. – Environmental Science & Technology 45: 9175-9179.

[16] Claessens, M., Cauwenberghe, L. Van, Vandegehuchte, M. B., Janssen, C. R. (2013): New techniques for the detection of microplastics in sediments and field collected organisms. – Marine Pollution Bulletin 70: 227-233.

http://www.aloki.hu ● ISSN 1589 1623 (Print) ● ISSN 1785 0037 (Online)
DOI: http://dx.doi.org/10.15666/aeer/1902_10851106
© 2021, ALÖKI Kft., Budapest, Hungary

[17] Cole, M., Lindeque, P., Fileman, E., Halsband, C., Goodhead, R., Moger, J., Galloway, T. S. (2013): Microplastic ingestion by zooplankton. – Environmental Science & Technology 47: 6646-6655.
[18] Cole, M., Lindeque, P., Halsband, C., Galloway, T. S. (2011): Microplastics as contaminants in the marine environment: a review. – Marine Pollution Bulletin 62: 2588-2597.
[19] Cole, M., Webb, H., Lindeque, P. K., Fileman, E. S., Halsband, C., Galloway, T. S. (2014): Isolation of microplastics in biota-rich seawater samples and marine organisms. – Scientific Reports 4: 4528.
[20] De Falco, F., Gullo, M. P., Gentile, G., Di Pace, E., Cocca, M., Gelabert, L., Brouta-Agnesa, M., Rovira, A., Escudero, R., Villalba, R., Mossotti, R., Montarsolo, A., Gavignano, S., Tonin, C., Avella, M. (2018): Evaluation of microplastic release cause by textile washing processes of synthetic fabrics. – Environ Pollut 236: 916-925.
[21] De Gieter, M., Leermakers, M., Ryssen, R. Van, Noyen, J., Goeyens, L., Baeyens, W. (2002): Total and toxic arsenic levels in North Sea fish. – Archives of Environmental Contamination and Toxicology 43: 406-417.
[22] De Witte, B., Devriese, L., Bekaet, K., Hoffman, S., Vandermeersch, G., Cooreman, K. (2004): Quality assessment of the blue mussel (Mytilus edulis): comparison between commercial and wild types. – Mar. Pollut. Bull. 85(1): 146-155.
[23] Desforges, J.-P. W., Galbraith, M., Ross, P. S. (2015): Ingestion of microplastics by zooplankton in the Northeast Pacific Ocean. – Archives of Environmental Contamination and Toxicology 69: 320-330.
[24] Devriese, L. I., Meulen, M. D. van der, Maes, T., Bekaert, K., Paul-Pont, I., Frère, L., Robbens, J., Vethaak, A. D. (2015): Microplastic contamination in brown shrimp (Crangon crangon, Linnaeus 1758) from coastal waters of the Southern North Sea and Channel area. – Marine Pollution Bulletin 98: 179-187.
[25] Ding, J.-F., Li, J.-X., Sun, C.-J., He, C.-F., Jiang, F.-H., Gao, F.-L., Zheng, L. (2018): Separation and identification of microplastics in digestive system of bivalves. – Chinese Journal of Analytical Chemistry 46: 690-697.
[26] Eriksen, M., Lebreton, L. C. M., Carson, H. S., Thiel, M., Moore, C. J., Borerro, J. C., Galgani, F., Ryan, P. G., Reisser, J. (2014): Plastic pollution in the world's oceans: more than 5 trillion plastic pieces weighing over 250,000 tons afloat at sea. – PLoS ONE 9: e111913.
[27] Fang, C., Zheng, R., Chen, H., Hong, F., Lin, L., Lin, H., Guo, H., Bailey, C., Segner, H., Mu, J., Bo, J. (2019): Comparison of microplastic contamination in fish and bivalves from two major cities in Fujian province, China and the implications for human health. – Aquaculture 512: 734322.
[28] Farrell, P., Nelson, K. (2013): Trophic level transfer of microplastic: Mytilus edulis (L.) to Carcinus maenas (L.). – Environmental Pollution 177: 1-3.
[29] GESAMP (2015): Sources, Fate and Effects of Microplastics in the Marine Environment: A Global Assessment. – GESAMP, London.
[30] Gilman, E. (2015): Status of international monitoring and management of abandoned, lost and discarded fishing gear and ghost fishing. – Marine Policy 60: 225-239.
[31] Goh, P., Pradit, S., Towatana, P., Khokkiatiwong, S., Azad, S. (2019): Microplastics in green mussel Perna viridis from Singhanakorn District, Songkhla Province, Thailand. – Proceedings of the 34th AUAP Annual Conference 2019 Climate Change Adaptation. The Challenging Role of Higher Education Institutions, pp. 19-23.

http://www.aloki.hu ● ISSN 1589 1623 (Print) ● ISSN 1785 0037 (Online)
DOI: http://dx.doi.org/10.15666/aeer/1902_10851106
© 2021, ALÖKI Kft., Budapest, Hungary

[32] Gordon, M. (2006): Eliminating Land-Based Discharges of Marine Debris in California: A Plan of Action from the Plastic Debris Project. – California Coastal Commission, California.
[33] Güven, O., Gökdağ, K., Jovanović, B., Kıdeyş, A. E. (2017): Microplastic litter composition of the Turkish territorial waters of the Mediterranean Sea, and its occurrence in the gastrointestinal tract of fish. – Environmental Pollution 223: 286-294.
[34] Hidalgo-Ruz, V., Gutow, L., Thompson, R. C., Thiel, M. (2012): Microplastics in the marine environment: a review of the methods used for identification and quantification. – Environmental Science & Technology 46: 3060-3075.
[35] Hossain, M. S., Rahman, M. S., Uddin, M. N., Sharifuzzaman, S. M., Chowdhury, S. R., Sarker, S., Nawaz Chowdhury, M. S. (2020): Microplastic contamination in Penaeid shrimp from the Northern Bay of Bengal. – Chemosphere 238: 124688.
[36] Hutchings, J. A., Reynolds, J. D. (2004): Marine fish population collapse: consequences for recovery and extinction risk. – Bioscience 54: 297-309.
[37] Jabeen, K., Su, L., Li, J., Yang, D., Tong, C., Mu, J., Shi, H. (2017): Microplastics and mesoplastics in fish from coastal and fresh waters of China. – Environmental Pollution 221: 141-149.
[38] Jovanović, B. (2017): Ingestion of microplastics by fish and its potential consequences from a physical perspective. – Integrated Environmental Assessment and Management 13: 510-515.
[39] Karami, A. (2017): Gaps in aquatic toxicological studies of microplastics. – Chemosphere 184: 841-848.
[40] Karbalaei, S., Golieskardi, A., Hamzah, H. B., Abdulwahid, S., Hanachi, P., Walker, T. R., Karami, A. (2019): Abundance and characteristics of microplastics in commercial marine fish from Malaysia. – Marine Pollution Bulletin 148: 5-15.
[41] Koto, N., Soegijono, B. (2019): Effect of rice husk ash filler of resistance against of high-speed projectile impact on polyester-fiberglass double panel composites. – Journal of Physics Conference Series 1191: 012058.
[42] Kowalski, N., Reichardt, A. M., Waniek, J. J. (2016): Sinking rates of microplastics and potential implications of their alteration by physical, biological, and chemical factors. – Marine Pollution Bulletin 109: 310-319.
[43] Kreekrinut, T., Puttapreecha, R., Suksuwan, R., Tangjai, R., Saisahat, R. (2019): The contamination of microplatics in Sediment beach area, Lower Gulf of Thailand. – https://dmcr.go.th/detailLib/4536.
[44] Kripa, V., Nair, P. G., Dhanya, A. M., Pravitha, V. P., Abhilash, K. S., Mohammed, A. A., Vijayan, D., Vishnu, P. G., Mohan, G., Anil Kumar, P. S., Khambadker, L. R., Prema, D. (2014): Microplastics in the gut of anchovies caught from the mud bank area of Alappuzha, Kerala. – Mar. Fish. Inf. Serv. Tech. Ext. Ser. 219: 27-28.
[45] Li, J., Qu, X., Su, L., Zhang, W., Yang, D., Kolandhasamy, P., Li, D., Shi, H. (2016): Microplastics in mussels along the coastal waters of China. – Environmental Pollution 214: 177-184.
[46] Lu, Y., Zhang, Y., Deng, Y., Jiang, W., Zhao, Y., Geng, J., Ding, L., Ren, H. (2016): Uptake and accumulation of polystyrene microplastics in zebrafish (Danio rerio) and toxic effects in liver. – Environmental Science & Technology 50: 4054-4060.
[47] Lusher, A. L., McHugh, M., Thompson, R. C. (2013): Occurrence of microplastics in the gastrointestinal tract of pelagic and demersal fish from the English Channel. – Marine Pollution Bulletin 67: 94-99.

http://www.aloki.hu ● ISSN 1589 1623 (Print) ● ISSN 1785 0037 (Online)
DOI: http://dx.doi.org/10.15666/aeer/1902_10851106
© 2021, ALÖKI Kft., Budapest, Hungary

[48] Morét-Ferguson, S., Law, K. L., Proskurowski, G., Murphy, E. K., Peacock, E. E., Reddy, C. M. (2010): The size, mass, and composition of plastic debris in the western North Atlantic Ocean. – Marine Pollution Bulletin 60: 1873-1878.
[49] Nadal, M. A., Alomar, C., Deudero, S. (2016): High levels of microplastic ingestion by the semipelagic fish bogue Boops boops (L.) around the Balearic Islands. – Environmental Pollution 214: 517-523.
[50] Ory, N. C., Sobral, P., Ferreira, J. L., Thiel, M. (2017): Amberstripe scad Decapterus muroadsi (Carangidae) fish ingest blue microplastics resembling their copepod prey along the coast of Rapa Nui (Easter Island) in the South Pacific subtropical gyre. – Science of The Total Environment 586: 430-437.
[51] Possatto, F. E., Barletta, M., Costa, M. F., Ivar do Sul, J. A., Dantas, D. V. (2011): Plastic debris ingestion by marine catfish: an unexpected fisheries impact. – Marine Pollution Bulletin 62: 1098-1102.
[52] Pozo, K., Gomez, V., Torres, M., Vera, L., Nuñez, D., Oyarzún, P., Mendoza, G., Clarke, B., Fossi, M. C., Baini, M., Přibylová, P., Klánová, J. (2019): Presence and characterization of microplastics in fish of commercial importance from the Biobío region in central Chile. – Marine Pollution Bulletin 140: 315-319.
[53] Pradit, S., Wattayakorn, G., Angsupanich, S., Baeyens, W., Leermakers, M. (2010): Distribution of trace elements in sediments and biota of Songkhla Lake, Southern Thailand. – Water, Air, and Soil Pollution 206: 155-174.
[54] Pradit, S., Gao, Y., Faiboon, A., Galan, S. De, Baeyens, W., Leermakers, M. (2013): Application of DET (diffusive equilibrium in thin films) and DGT (diffusive gradients in thin films) techniques in the study of the mobility of sediment-bound metals in the outer section of Songkhla Lake, Southern Thailand. – Environmental Monitoring and Assessment 185: 4207-4220.
[55] Pradit, S., Shazili, N. A. M., Pattaratumrong, M. S., Chotikarn, P., Kobkeatthawin, T., Yucharoen, M., Towatana, P. (2018): Accumulation of trace metals in mangrove plant Soneratia Caseoralis in Songkhla Lake, Thailand. – Applied Ecology and Environmental Research 16(4): 4081-4095.
[56] Pradit, S., Mohamed Shazili, N. A., Pattaratumrong, M. S., Chotikarn, P., Yucharoen, M., Towatana, P. (2019): Chemical fractionation of trace elements in mangrove sediments from the Songkhla Lake, Thailand using BCR technique. – ScienceAsia 45: 465.
[57] Pradit, S., Towatana, P., Nitiratsuwan, T., Jualaong, S., Jirajarus, M., Sornplang, K., Noppradit, P., Darakai, Y., Weerawong, C. (2020): Occurrence of microplastics on beach sediment at Libong, a pristine island in Andaman Sea, Thailand. – ScienceAsia 46: 336.
[58] Puangsuwan, S. (2014): Heavy metal concentration in tuna from Ninety East Ridge. – Master thesis, Prince of Songkla University, Songkhla.
[59] Rahman, M. S., Molla, A. H., Saha, N., Rahman, A. (2012): Study on heavy metals levels and its risk assessment in some edible fishes from Bangshi River, Savar, Dhaka, Bangladesh. – Food Chemistry 134: 1847-1854.
[60] Rainbow, P. S. (2002): Trace metal concentrations in aquatic invertebrates: why and so what? – Environmental Pollution 120: 497-507.
[61] Rocha-Santos, T., Duarte, A. C. (2015): A critical overview of the analytical approaches to the occurrence, the fate and the behavior of microplastics in the environment. – TrAC Trends in Analytical Chemistry 65: 47-53.
[62] Setälä, O., Fleming-Lehtinen, V., Lehtiniemi, M. (2014): Ingestion and transfer of microplastics in the planktonic food web. – Environmental Pollution 185: 77-83.

http://www.aloki.hu ● ISSN 1589 1623 (Print) ● ISSN 1785 0037 (Online)
DOI: http://dx.doi.org/10.15666/aeer/1902_10851106
© 2021, ALÖKI Kft., Budapest, Hungary

[63] Sivan, A. (2011): New perspectives in plastic biodegradation. – Current Opinion in Biotechnology 22: 422-426.
[64] Song, J., Birbach, N. L., Hinestroza, J. P. (2012): Deposition of silver nanoparticles on cellulosic fibers via stabilization of carboxymethyl groups. – Cellulose 19: 411-424.
[65] Sun, X., Liang, J., Zhu, M., Zhao, Y., Zhang, B. (2018): Microplastics in seawater and zooplankton from the Yellow Sea. – Environmental Pollution 242: 585-595.
[66] Thushari, G. G. N., Senevirathna, J. D. M., Yakupitiyage, A., Chavanich, S. (2017): Effects of microplastics on sessile invertebrates in the eastern coast of Thailand: an approach to coastal zone conservation. – Marine Pollution Bulletin 124: 349-355.
[67] US EPA (1989): Assessing Human Health Risks from Chemically Contaminated Fish and Shellfish. A Guidance Manual. – EPA-503/8-89-002. EPA, Washington, DC.
[68] Van Cauwenberghe, L., Janssen, C. R. (2014): Microplastics in bivalves cultured for human consumption. – Environ. Pollut. 193: 65-70.
[69] Walkinshaw, C., Lindeque, P. K., Thompson, R., Tolhurst, T., Cole, M. (2020): Microplastics and seafood: lower trophic organisms at highest risk of contamination. – Ecotoxicology and Environmental Safety 190: 110066.

http://www.aloki.hu ● ISSN 1589 1623 (Print) ● ISSN 1785 0037 (Online)
DOI: http://dx.doi.org/10.15666/aeer/1902_10851106
© 2021, ALÖKI Kft., Budapest, Hungary

THE INTRODUCTION OF AN ADDITIVE MODELING METHOD RESPONSIVE TO TEMPERATURE AND PRECIPITATION VARIABLES, AND ITS APPLICATIONS TO ESTIMATE THE FOREST STAND BIOMASS OF *PICEA* SPP. OF EURASIA

SHOBAIRI, S. O. R.[1*] – USOLTSEV, V. A.[2,3] – TSEPORDEY, I. S.[3]

[1]*Research Center of Forestry Remote Sensing & Information Engineering, Central South University of Forestry and Technology, Changsha 410004, China*

[2]*Faculty of Forestry, Ural State Forest Engineering University, Sibirskiy Trakt, 37, 620100 Yekaterinburg, Russia*
(e-mail: usoltsev50@mail.ru)

[3]*Botanical Garden of Ural Branch of RAS, Department of Forest Productivity, ul. 8 Marta, 202a, 620144 Yekaterinburg, Russia*
(e-mail: common@botgard.uran.ru)

**Corresponding author*
e-mail: Omidshobeyri214@gmail.com

(Received 30th Aug 2020; accepted 30th Nov 2020)

Abstract. This article was the first attempt of modeling changes in the additive component composition of 900 spruce stands' (genus *Picea* sp.) biomass (t/ha), according to the trans-Eurasian hydrothermal gradients of Eurasia using the database compiled on the structure of harvest biomass. This study found that the biomass of all components increases with higher mean January temperature, regardless of mean annual precipitation, but any increase in precipitation leads to a decrease in biomass of all the components. For the first time, trans-Eurasian patterns of changes in the biomass of all components of spruce stands in the climate gradients were obtained due to the authors' first database on the biomass of forest-forming species in Eurasia. In contrast to previously published regional and transcontinental weakly adequate or unreliable regularities that are not additive in the biomass component composition and depersonalized in the species composition, in the proposed additive models for spruce, the contribution of climate variables to the explanation of biomass variability was 9%. The importance of selecting the correct structure of the developed model is shown.
Keywords: *climate change, additive biomass equations, January mean temperature, mean annual precipitation, regression models, biological productivity*

Abbreviations: *A* = stand age, years; *V* = stem volume, m^3 per ha; *N* = tree density, 1000/ha; *Tm* = mean January temperature, °C; *PRm* = mean annual precipitation, mm; *Pi* = biomass of *i*-th component, t per ha; involving: *Pt* = total (above- and belowground); *Pa* = aboveground; *Pr* = root; *Pc* = crown; *Ps* = stem over bark; *Pw* = stem without bark; *Pbk* = bark only; *Pf* = foliage; *Pb* = branches

Introduction

Since 1850 to the present, the amount of greenhouse gases in the atmosphere has doubled, threatening the planet with catastrophic climate change (Fatichi et al., 2019). At the UN climate summit in Paris in December 2015, 196 countries committed themselves to reducing CO_2 emissions and preventing annual temperatures from rising by more than 2 °C by the end of the century. Forest ecosystems, as sinks of atmospheric carbon, play an important role in this perspective. The ability of forests to remove carbon from the atmosphere and produce organic matter is the basis of their functioning

http://www.aloki.hu ● ISSN 1589 1623 (Print) ● ISSN 1785 0037 (Online)
DOI: http://dx.doi.org/10.15666/aeer/1902_11071122
© 2021, ALÖKI Kft., Budapest, Hungary

(Dylis, 1978). This decrease in the concentration of CO_2 in the atmosphere can be achieved due to the increase of carbon stock in vegetative cover by means of effective forest management. On the other hand, climate change has a significant impact on the biological productivity of vegetation, which in turn affects the transformation of the cycle of organic matter and gas exchange in the biosphere (Golubyatnikov and Denisenko, 2009).

Temperature and precipitation are the most informative climatic factors that determine not only the radial annual growth of tree stems, but also the biological productivity of forest stands (DeLucia et al., 2000; Ni et al., 2001; Stegen et al., 2011; D'Aprile et al., 2015; Fang et al., 2016). Numerous studies of stochastic relationships of biological productivity of stands with temperature and precipitation were carried out at the regional level for indices, depersonalized by age and morphology of stands, and at the global level even without considering the species composition (Lieth, 1974; Anderson et al., 2006; Keeling and Phillips, 2007; Huston and Wolverton, 2009). Analysis of the results of such studies revealed significant contradictions and uncertainties associated with the assessment of the dependence of these indices on temperature and precipitation using both empirical and functional models (Eggers et al., 2008; Shuman, Shugart, 2009; Poudel et al., 2011; Han et al., 2018). Contradictory results were obtained even within a single region, while the influence of the same climatic factors on the biological production of stands of certain tree species (genera) in the Trans-Eurasian climatic gradients of temperature and precipitation is still unknown, since the available information is fragmentary and contradictory (Strömgren and Linder, 2002; Wilmking et al., 2004; Stegen et al., 2011; Fu et al., 2017). It was concluded that biomass–climate models developed at restricted geographic/climatic scales may not hold at broader scales and trans-continental levels (Stegen et al., 2011).

In the development of such not harmonized empirical models, the additivity of component composition is not provided, according to which the total biomass of components (stems, branches, needles, roots) obtained by component equations would be equal to the value of biomass obtained by the common equation (Dong et al., 2015). The influence of climatic changes on the biomass of a tree species in the format of additive models in accordance with transcontinental hydrothermal gradients has not been studied at all.

The purpose of this study is to develop a model of changes in the additive component composition of the *Picea* spp. stand biomass on the trans-Eurasian gradients of the mean January temperature and mean annual precipitation. At the same time, we intend to answer two questions: (1) to design an additive system of equations for the components of spruce stands biomass, including independent variables such as, stand dendrometric indices and hydrothermal indices inherent to ecoregions of Eurasia and compare their adequacy characteristics with the same initial equations; it is assumed that the newly constructed system of equations will be more advanced in relation to the previously calculated system based on the same harvest data (Usoltsev et al., 2019) and (2) to design 3-D dependences of biomass, additive in its components, on the climatic indices of ecoregions, combined recursively with the age, tree density and volume stock inherent to the same ecoregions. Previously, mixed models of spruce stand biomass in Eurasia were reported, including both the mentioned dendrometric variables and dummy variables as independent variables (Usoltsev et al., 2018), which encode the model's belonging to different ecoregions. It was shown that regional biomass models had significant shifts relative to ecoregions. In this study, regional shifts in the biomass

http://www.aloki.hu ● ISSN 1589 1623 (Print) ● ISSN 1785 0037 (Online)
DOI: http://dx.doi.org/10.15666/aeer/1902_11071122
© 2021, ALÖKI Kft., Budapest, Hungary

models are quantified not by dummy variables, but by temperature and precipitation indices that are characteristic of all the ecoregions of Eurasia.

Materials and experimental methods

In the modeling process the compiled Russian database on biomass of forest-forming species of Eurasia was used (Usoltsev, 2010, 2013). The data are taken from it in the amount of 900 sample plots with the harvest biomass and dendrometric indices of the *Picea* spp. forest stands (t per ha). The distribution of the number of sample plots by species and countries is shown in *Table 1*.

Table 1. *Distribution of 900 sample areas with definitions of spruce stands biomass (t/ha) by species and countries*

Species	Country	Number of sample plots
Picea abies (L.) H. Karst.	Austria, Belarus, Belgium, Bulgaria, Czech Republic, Denmark, Estonia, Finland, France, Germany, Italy, Latvia, Lithuania, Norway, Russia, Slovakia, Sweden, Ukraine	486
P. jezoensis (S.&Z.) Carrièr	China, Russia	190
P. obovata L.	Russia	144
P. schrenkiana F. & C.A. Mey.	Kazakhstan, China	58
P. sitchensis (Bong.) Carrière	Great Britain, Ireland	12
P. purpurea Masters	China	4
P. orientalis Link	Georgia, Russia	4
P. koraiensis Nakai	Japan	2

Each sample plot on which the biomass determination was performed is positioned relatively to the isolines of the mean January temperature (*Fig. 1*) and relatively to the isolines of mean annual precipitation (*Fig. 2*). The main pool of our harvest data on forest biomass in Eurasia was obtained since 1970s to 1990s, and the climate maps used cover the period of the late 1990s and early 2000s. Some discrepancy between the two time periods may cause possible biases in the results obtained, but for such a small time difference in the initial data, the inclusion of compensatory mechanisms or phenological shifts in forest communities is unlikely (Anderegg et al., 2019; DeLeo et al., 2020).

The matrix of harvest data is then compiled in a matrix, in which values of biomass component and dendrometric indices of forest stands are joint with the corresponding values of mean January temperature and precipitation. Its fragment is shown in *Table 2*.

The matrix was used as a source of data in the subsequent regression analysis, and recursive equations (Draper and Smith, 1973) for the different components of the stand biomass were derived:

$$N = \exp\{2.7655 - 0.9244(\ln A) + 2.6507[\ln(Tm + 40)] - 0.5396[\ln(Tm + 40)]^2 - 0.1918(\ln PRm);\ adj R^2 = 0.554;\ SE = 0.65 \quad \text{(Eq.1)}$$

$$\downarrow$$

$$V = \exp\{-1.0382 + 1.4781(\ln A) - 0.6992(\ln N) + 0.2501(\ln A)(\ln N) - 2.6771[\ln(Tm + 40)] + 0.8389[\ln(Tm + 40)]^2 - 0.0121(\ln PRm);\ adjR^2 = 0.645;\ SE = 0.85 \quad \text{(Eq.2)}$$

$$\downarrow$$

$$Pi = \exp\{a_0 + a_1(\ln A) + a_2(\ln V) + a_3(\ln N) + a_4(\ln A)(\ln N) + a_5[\ln(Tm + 40)] + a_6[\ln(Tm + 40)]^2 + a_7(\ln PRm)\} \quad \text{(Eq.3)}$$

http://www.aloki.hu ● ISSN 1589 1623 (Print) ● ISSN 1785 0037 (Online)
DOI: http://dx.doi.org/10.15666/aeer/1902_11071122
© 2021, ALÖKI Kft., Budapest, Hungary

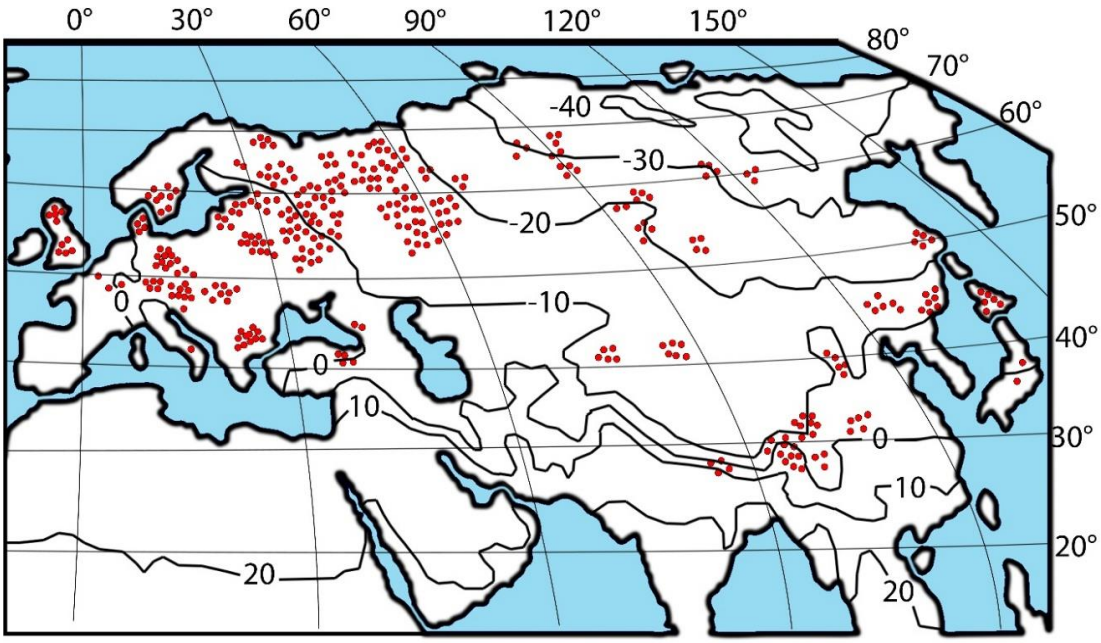


Figure 1. *Distribution of 900 sample plots with harvest biomass (t per ha) of spruce stands (genus Picea sp.) on the map of the mean temperature in January, °C (marked by numbers) (World Weather Maps, 2007)*

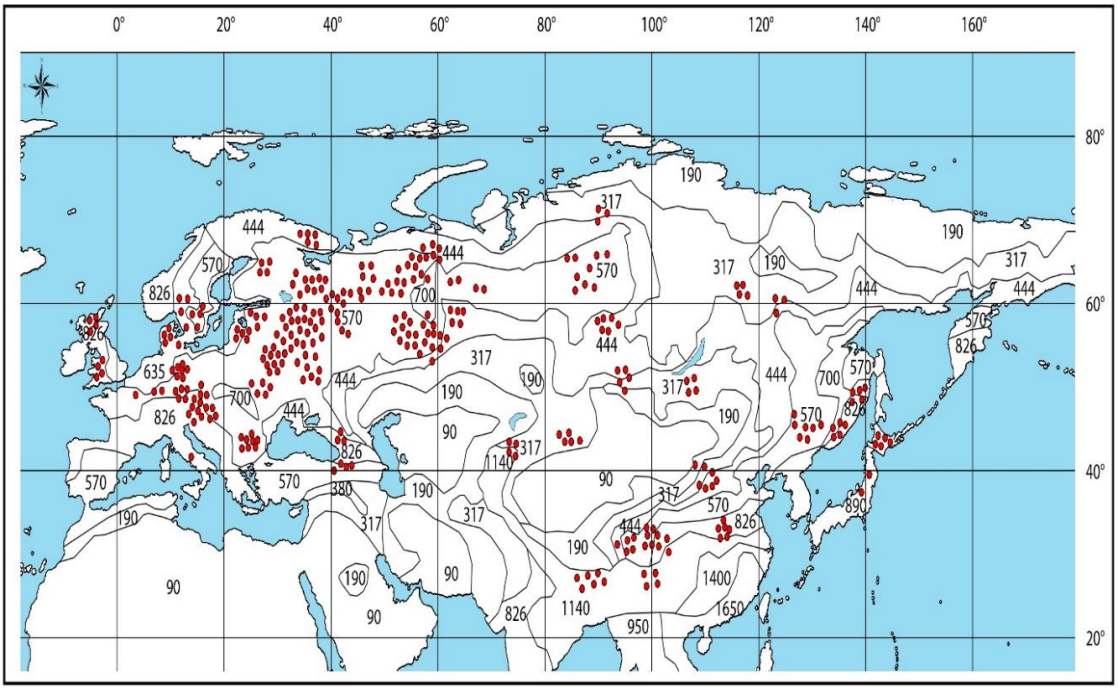


Figure 2. *Distribution of 900 sample plots with harvest biomass (t per ha) of spruce stands (genus Picea sp.) on the map of mean annual precipitation, mm (marked by numbers) (World Weather Maps, 2007, http://www.mapmost.com/world-precipitation-map/free-world-precipitation-map/)*

http://www.aloki.hu ● ISSN 1589 1623 (Print) ● ISSN 1785 0037 (Online)
DOI: http://dx.doi.org/10.15666/aeer/1902_11071122
© 2021, ALÖKI Kft., Budapest, Hungary

Table 2. *A fragment of the original matrix of 900 experimental biomass data representing Picea spp. used for the construction of additive models*

Country	Species	N°	E°	*Tm*	*PRm*	*A*	*N*	*V*	*Ps*	*Pbk*	*Pb*	*Pf*	*Pa*	*Pr*	References
Estonia	*Picea abies* (L.) H.Karst.	58°00’	27°30’	-8	600	51	1.1	240	105.5	10.6	24.6	11.7	141.8	45.8	Kõlli and Kährik, 1970
Estonia	*P. abies*	58°00’	27°30’	-8	600	84	0.608	287	130.1	10.1	26.6	13.8	170.5	64.6	Kõlli and Kährik, 1970
France	*P. abies*	48°12’	7°11’	0	635	92	0.568	614	234.1	19.1	19.5	9.2	262.8	44.5	Persson et al., 2000
France	*P. abies*	48°10’	6°40’	0	635	85	0.475	900	359.4	16.3	47.9	20.8	428.1	61.6	Ranger et al., 1992
The Ukraine	*P. abies*	48°45’	24°30’	-4	700	20	16.523	127	43.1	7.5	10.6	8.4	62.1	38.6	Pasternak and Chernyavskii, 1977
Byelorussia	*P. abies*	53°20’	30°50’	-7	570	90	0.504	455	222.8	18	36.4	31.0	290.2	61.9	Yurkevich et al., 1975
Belgium	*P. abies*	50°02’	5°16’	2	730	55	1.065	449	167.9	11.6	16.6	16.1	200.6	70.0	Kestemont et al., 1977
Bulgaria	*P. abies*	43°00’	23°30’	-3	570	90	0.385	773	296.4	28.9	58.6	45.4	400.4	119.3	Grozeva et al., 1986
Germany	*P. abies*	51°49’	9°35’	-2	600	34	1.49	281	105.1	8.4	18.7	18.9	142.7	34.6	Ellenberg et al., 1986
Russia	*P. abies*	62°00’	34°00’	-12	570	180	1.159	376	163.8	15.7	18.5	9.6	191.9	36.0	Shcherbakov and Zaitseva, 1971
Russia	*P. abies*	62°00’	34°00’	-12	570	160	2.733	310	134.4	12.3	16.5	9.6	160.5	29.6	Shcherbakov and Zaitseva, 1971
Russia	*P. obovata* (Ledeb.) Loudon	56°13’	92°19’	-20	317	25	14.000	119	42.2	5.8	11.5	5.2	58.9	14.5	Vedrova et al., 2000
Russia	*P. jezoensis* (SIEBOLD & ZUCC.)	44°00’	132°00’	-12	826	180	0.735	410	188.4	23.8	41.7	7.69	237.8	42.4	Sapozhnikov et al., 1993
Russia	*P. jezoensis*	44°00’	132°00’	-12	826	180	0.753	364	195.3	19.5	30.3	7.6	233.2	43.9	Sapozhnikov et al., 1993
China	*P. purpurea* Masters	31°30’	103°32’	-10	826	40	0.933	137	72	8.46	28.8	15.5	116.3	27.9	Jiang, 1986
China	*P. purpurea*	31°30’	103°32’	-10	826	49	0.642	124	65	7.64	20.7	13.4	99.1	20.9	Jiang, 1986

http://www.aloki.hu ● ISSN 1589 1623 (Print) ● ISSN 1785 0037 (Online)
DOI: http://dx.doi.org/10.15666/aeer/1902_11071122
© 2021, ALÖKI Kft., Budapest, Hungary

We used a schematic map of the contours of the mean January temperature, rather than the mean annual temperature, as warming is most pronounced in the cold half of the year (Golubyatnikov and Denisenko, 2009; Laing and Binyamin, 2013). F. Schwarz (1899) showed at his time, the air temperature in the period from January to March to be decisive for the growth of trees is twice as strong as the precipitation in the period from May to June. Since the mean January temperature in the northern limit of Eurasia has negative values, the corresponding independent variable is modified to the form ($Tm + 40$) which may be subjected to logarithmic procedure. All the necessary calculations were carried out in Statgraphics software (http://www.statgraphics.com/) with the use of a logarithm correction, by Baskerville (1972).

The first of the questions mentioned above can be answered by calculating the additive biomass equations, the structure of which is represented by *Equation 3* in the recursive system shown above. According to the structure of the disaggregating model of the three-step additive system (Tang et al., 2000; Dong et al., 2015), the total biomass estimated from the initial equation is divided into component ones according to the scheme presented in *Figure 3*.

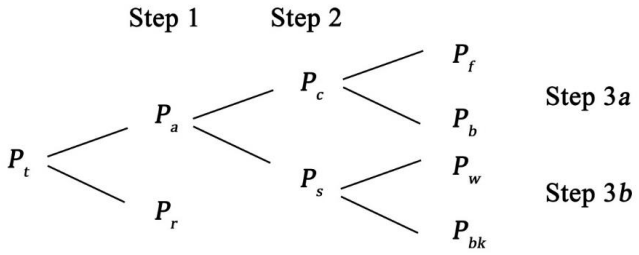


Figure 3. *The pattern of disaggregating three-step proportional weighting additive model*

The second question is answered by sequentially tabulating *Equations 1* and *2* and combining the results with the additive system of biomass equations (*Eq. 3*). As a result, we obtain 3-D dependences of biomass, additive in its components, on the climatic indices in trans-Eurasian gradients, combined recursively with the age, tree density and volume stock data calculated according to *Equations 1* and *2*.

Results and analysis

The results of calculating *Equation 3* for different biomass components are shown in *Table 3*. These equations are modified to additive form according to the above-mentioned algorithm (*Fig. 3*), that was quantified earlier by Dong et al. (2015), and the final form of the transcontinental additive model of component composition of spruce biomass is shown in *Table 4*.

To compare the adequacy indices of the initial and additive equations, both of them are tabulated on the actual mass-forming parameters of the database, and the obtained calculated values of biomass are compared with the actual values. The comparing is fulfilled using the determination coefficient. The results of the comparison are shown in *Table 5*. The ratio of the actual values and the values obtained by the calculation using the initial and additive models of forest stand biomass (*Fig. 4*), shows the degree of correlation of these indices and the absence of visible differences in the structure of residual dispersions obtained of the two models.

http://www.aloki.hu ● ISSN 1589 1623 (Print) ● ISSN 1785 0037 (Online)
DOI: http://dx.doi.org/10.15666/aeer/1902_11071122
© 2021, ALÖKI Kft., Budapest, Hungary

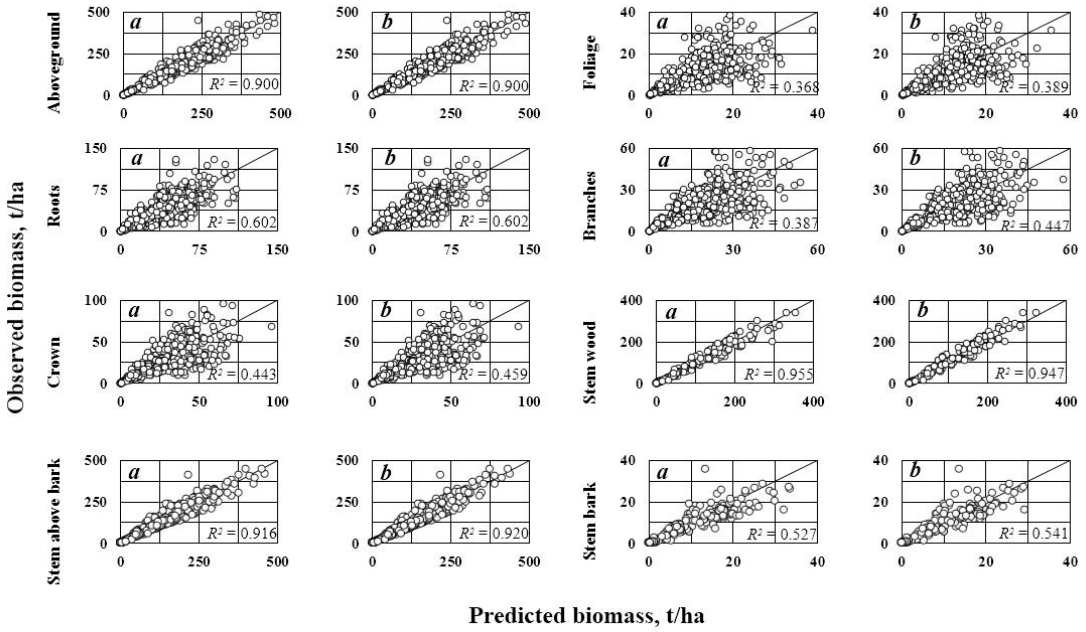


Figure 4. *The ratio of the actual values and the values obtained by calculating the initial (a) and additive (b) models of the biomass of spruce stands*

The results of tabulating the equations in the sequence (1), (2) and (3) represent a rather cumbersome table. We took from it the values of component composition of spruce biomass for the age of 100 years and built figures of their dependence on temperature and precipitation (*Fig. 5*).

Discussion

When comparing the disaggregating method (1) for the additivity of biomass components with the previously proposed aggregating method (2) (Parresol, 1999), Dong and co-authors (Dong et al., 2015) found slightly better adequacy indices of the former in relation to the latter. They explained this phenomenon by the fact that in the second method, aggregation occurs from the tree component equations to the subtotals and then to the total one. The component equations for the biomass of foliage and branches are characterized by the largest residual dispersion, when they are subsequently combined and transferred to the subtotal (crown biomass) and then to the total (above- and belowground biomass), the residual dispersion accumulates. According to the first method, the total equation has the smallest residual variance with respect to the subtotal and tree component levels, and as a result of dividing this total equation into the component ones, accumulations of residual variance does not occur. Although the component equations for foliage and branches calculated using both the first and second methods are characterized by lower determination indices in relation to the total equations, their "binding" to the total equation calculated using the first method, as a result of component disaggregation, serves as a factor limiting the residual variance.

We can see in the data in *Table 5* that of the eight component and subtotal equations, in five cases the determination indices for the first method are greater than for the second one, in two cases they are equal, and only in one case the determination index

http://www.aloki.hu ● ISSN 1589 1623 (Print) ● ISSN 1785 0037 (Online)
DOI: http://dx.doi.org/10.15666/aeer/1902_11071122
© 2021, ALÖKI Kft., Budapest, Hungary

for the first method is less than for the second one. Apparently, in this case, the factor limiting the residual variance appears in the case of the disaggregating method, but this does not happen when calculating the initial (non-additive) equations.

After the publication of the results of calculating additive equations for spruce biomass (Usoltsev et al., 2019), a detailed meaningful analysis of the harvest data was performed. The independent variable as synergy $[\ln(Tm + 40)]\cdot(\ln PRm)$ was removed from the equation structure, since it was not statistically significant at 0.05 for most biomass components, but an additional independent variable was introduced in the form of synergy $(\ln A)(\ln N)$. As a result of correcting the structure of the equations, the coefficients of determination shown in *Table 3* turned out to be higher in relation to those in the previously published version (Usoltsev et al., 2019), namely: for the mass of roots, crown, stem over bark, foliage, branches, stem without bark and bark were 0.7, 0.9, 0.1, 0.7, 1.1, 0.1 and 0.7%, respectively.

Table 3. *The characteristics of the initial regression equations (Eq. 3)*

Biomass components	**Regression coefficients of the model**						
P_t	2.5949	$A^{-0.0566}$	$V^{0.8706}$	$N^{-0.0634}$	$A^{0.0236 (\ln N)}$		
Step 1							
P_a	1.0712	$A^{-0.0501}$	$V^{0.8642}$	$N^{-0.0533}$	$A^{0.0222 (\ln N)}$		
P_r	3.2417	$A^{-0.0022}$	$V^{0.8411}$	$N^{-0.0757}$	$A^{0.0309 (\ln N)}$		
Step 2							
P_c	0.6593	$A^{-0.2440}$	$V^{0.7177}$	$N^{-0.1673}$	$A^{0.0899 (\ln N)}$		
P_s	0.3552	$A^{0.0399}$	$V^{0.9688}$	$N^{-0.1400}$	$A^{0.0403 (\ln N)}$		
Step 3a							
P_f	-1.1338	$A^{-0.2717}$	$V^{0.6321}$	$N^{-0.1895}$	$A^{0.1105 (\ln N)}$		
P_b	0.1374	$A^{-0.1848}$	$V^{0.8140}$	$N^{-0.1546}$	$A^{0.0853 (\ln N)}$		
Step 3b							
P_w	-1.9166	$A^{0.0857}$	$V^{0.9811}$	$N^{0.0097}$	$A^{-0.0070 (\ln N)}$		
P_{bk}	-2.7983	$A^{0.1292}$	$V^{0.8037}$	$N^{0.0495}$	$A^{0.0092 (\ln N)}$		
Biomass components	**Regression coefficients of the model**					***adjR²***	***SE***
P_t	$(Tm + 40)^{-0.2054}$	$(Tm + 40)^{0.0299 \ln(Tm+40)}$	$PRm^{-0.2585}$			0.974	0.23
Step 1							
P_a	$(Tm + 40)^{-0.0887}$	$(Tm + 40)^{0.0322 \ln(Tm+40)}$	$PRm^{-0.1223}$			0.974	0.20
P_r	$(Tm + 40)^{-0.7179}$	$(Tm + 40)^{0.6587 \ln(Tm+40)}$	$PRm^{-0.4122}$			0.920	0.40
Step 2							
P_c	$(Tm + 40)^{0.6943}$	$(Tm + 40)^{-0.1013 \ln(Tm+40)}$	$PRm^{-0.2084}$			0.823	0.41
P_s	$(Tm + 40)^{-0.3422}$	$(Tm + 40)^{0.0641 \ln(Tm+40)}$	$PRm^{-0.1281}$			0.987	0.16
Step 3a							
P_f	$(Tm + 40)^{-0.3297}$	$(Tm + 40)^{-0.0292 \ln(Tm+40)}$	$PRm^{0.0751}$			0.707	0.49
P_b	$(Tm + 40)^{0.5843}$	$(Tm + 40)^{-0.0932 \ln(Tm+40)}$	$PRm^{-0.2797}$			0.828	0.47
Step 3b							
P_w	$(Tm + 40)^{0.2977}$	$(Tm + 40)^{-0.0422 \ln(Tm+40)}$	$PRm^{0.0244}$			0.990	0.15
P_{bk}	$(Tm + 40)^{-0.1173}$	$(Tm + 40)^{-0.0088 \ln(Tm+40)}$	$PRm^{0.1051}$			0.941	0.31

http://www.aloki.hu ● ISSN 1589 1623 (Print) ● ISSN 1785 0037 (Online)
DOI: http://dx.doi.org/10.15666/aeer/1902_11071122
© 2021, ALÖKI Kft., Budapest, Hungary

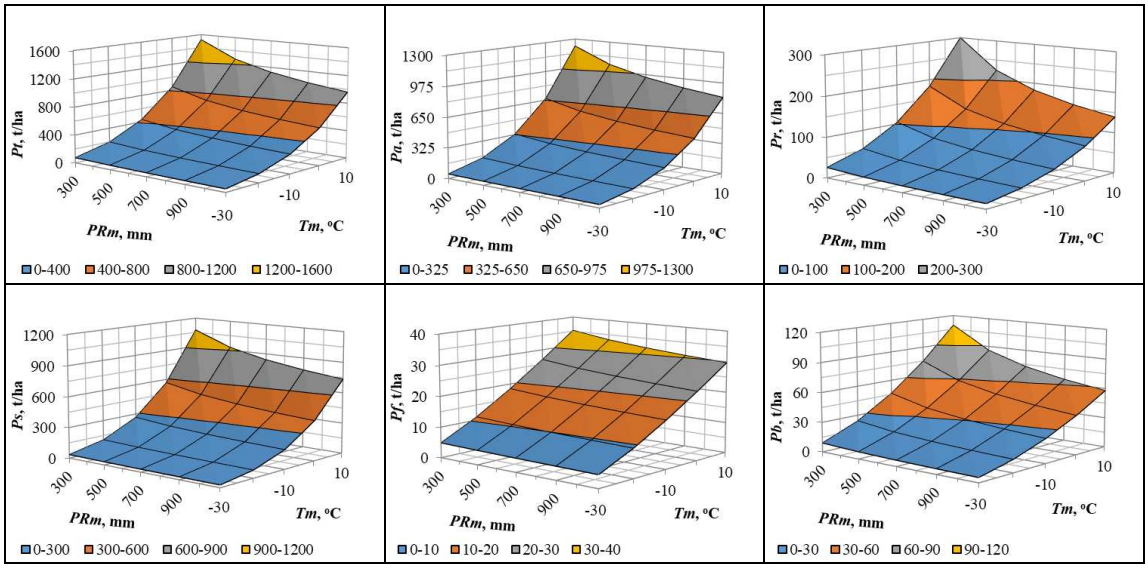


Figure 5. *Dependence of spruce forest biomass upon the mean January temperature (Tm) and the mean annual precipitation (PRm)*

Table 4. *Three-step additive model of component composition of spruce stand biomass, implemented on the principle of proportional weighing*

$$Pt = 13.3955\, A^{-0.0566} V^{0.8706} N^{-0.0634} N^{0.0236(\ln A)} (Tm+40)^{-0.2054} (Tm+40)^{0.0299(\ln(Tm+40))} PRm^{-0.2585}$$

Step 1	$Pa = \frac{1}{1+7.4724\, A^{0.0731} V^{-0.0408} N^{-0.0148} N^{0.0090(\ln A)} (Tm+40)^{-0.9556} (Tm+40)^{0.0937(\ln(Tm+40))} PRm^{-0.2033}} \times Pt$
	$Pr = \frac{1}{1+0.1338\, A^{-0.0731} V^{0.0408} N^{0.0148} N^{-0.0090(\ln A)} (Tm+40)^{0.9556} (Tm+40)^{-0.0937(\ln(Tm+40))} PRm^{0.2033}} \times Pt$
Step 2	$Pc = \frac{1}{1+1.8924\, A^{0.3496} V^{0.2112} N^{0.2452} N^{-0.0949(\ln A)} (Tm+40)^{-2.0323} (Tm+40)^{0.3826(\ln(Tm+40))} PRm^{0.0537}} \times Pa$
	$Ps = \frac{1}{1+0.5284\, A^{-0.3496} V^{-0.2112} N^{-0.2452} N^{0.0949(\ln A)} (Tm+40)^{2.0323} (Tm+40)^{-0.3826(\ln(Tm+40))} PRm^{-0.0537}} \times Pa$
Step 3*a*	$Pf = \frac{1}{1+0.4428\, A^{0.2413} V^{0.1495} N^{0.1485} N^{-0.0490(\ln A)} (Tm+40)^{0.0954} (Tm+40)^{-0.0370(\ln(Tm+40))} PRm^{-0.0812}} \times Pc$
	$Pb = \frac{1}{1+2.2583\, A^{-0.2413} V^{-0.1495} N^{-0.1485} N^{0.0490(\ln A)} (Tm+40)^{-0.0954} (Tm+40)^{0.0370(\ln(Tm+40))} PRm^{0.0812}} \times Pc$
Step 3*b*	$Pw = \frac{1}{1+11.9129\, A^{-0.0364} V^{-0.1786} N^{-0.1663} N^{0.0620(\ln A)} (Tm+40)^{-1.5134} (Tm+40)^{0.2563(\ln(Tm+40))} PRm^{-0.2055}} \times Ps$
	$Pbk = \frac{1}{1+0.0839\, A^{0.0364} V^{0.1786} N^{0.1663} N^{-0.0620(\ln A)} (Tm+40)^{1.5134} (Tm+40)^{-0.2563(\ln(Tm+40))} PRm^{0.2055}} \times Ps$

The lack of the synergy (ln*A*)(ln*N*) in the structure of previously published equations (Usoltsev et al., 2019) led to the fact that the residual variance, not explained by dendrometric variables, passed as "noise" to the variance explained by climate variables and reduced it. As a result of the modification of the equations, the level of variance explained by climate variables increased from 7 to 9%. This is, of course, a small percentage, but we can probably consider it acceptable if we take into account that ecologists today are able to explain no more than 10% of the variability of the phenomena observed in experiments (Møller and Jennions, 2002).

http://www.aloki.hu ● ISSN 1589 1623 (Print) ● ISSN 1785 0037 (Online)
DOI: http://dx.doi.org/10.15666/aeer/1902_11071122
© 2021, ALÖKI Kft., Budapest, Hungary

Modification of the equation structure also increased the coefficients of determination when comparing the original and additive equations on the harvest data, especially for the needle and crown biomass (compare *Tables 5* and *6*).

Table 5. *Comparison of adequacy indices of initial and additive equations of spruce biomass*

Coefficient of determination adjusted	**Biomass components**								
	Pt	***Pa***	***Pr***	***Ps***	***Pw***	***Pbk***	***Pc***	***Pb***	***Pf***
Initial equations									
$adjR^2$	0.886	0.900	0.602	**0.916**	0.955	**0.527**	**0.443**	**0.387**	**0.368**
Additive equations									
$adjR^2$	0.886	0.900	0.602	**0.920**	0.947	**0.541**	**0.459**	**0.447**	**0.389**

Table 6. *Comparison of coefficients of determination of the initial and additive equations of Picea forest biomass (Usoltsev et al., 2019)*

Coefficient of determination adjusted	**Biomass components**								
	Pt	***Pa***	***Pr***	***Ps***	***Pw***	***Pbk***	***Pc***	***Pb***	***Pf***
Initial equations									
$adjR^2$	0.883	**0.898**	0.595	**0.912**	0.956	**0.533**	**0.410**	**0.363**	**0.249**
Additive equations									
$adjR^2$	0.883	**0.899**	0.595	**0.919**	0.947	**0.541**	**0.448**	**0.443**	**0.349**

As it can be seen in *Figure 5,* all the biomass components change with temperature and precipitation gradients according to one common scheme, but in different ratios. The common pattern for all the components: regardless of the level of precipitation, when January temperature rises, the biomass of all components monotonically increases, but any increase in precipitation leads to a decrease in biomass. This is consistent with an increase of the relative radial increment, impersonal in species composition in boreal forests in Canada as the mean annual temperature increases (Miao and Li, 2011). But the dynamics of the radial increase due to the increase in precipitation, regardless of the mean annual temperature, according to the pattern by Miao and Li (2011) is directly opposite to ours.

According to the principle of limiting factors by Liebig (1840), Shelford and Metcalf (1913), plant growth is limited by an environmental factor that is at a minimum relative to a certain "norm". It is known that the variability of the annual ring width and biological productivity of stands is largely determined by the cycles of solar activity and the amount of incoming solar radiation (Douglas, 1919; Kostin, 1961; Budyko, 1977). However, in conditions of excessive moisture, where the limiting factor is the lack of oxygen in the soil, the cyclical growth is largely due to the hydrological regime of the rhizosphere (Olenin, 1982). At the other extreme, namely, the lack of moisture in steppe conditions, the tree sensitivity to precipitation increases, that is expressed in growing variability in the width of the annual rings (Ricklefs, 1979).

In some habitats, elevated temperatures can lead to stress from water scarcity and, consequently, to a decrease in biomass (Wilmking et al., 2004; Stegen et al., 2011). An increase in temperature can have a positive effect on plant productivity, provided that

http://www.aloki.hu ● ISSN 1589 1623 (Print) ● ISSN 1785 0037 (Online)
DOI: http://dx.doi.org/10.15666/aeer/1902_11071122
© 2021, ALÖKI Kft., Budapest, Hungary

the water supply does not decrease at a higher temperature (Yang, 2005; Boivenue and Running, 2006). This was confirmed by the results of studies fulfilled in slash pine plantations in the United States, where it was found that an increase in annual precipitation by 300 mm practically does not change the leaf area index (LAI), which is in the range of 6 to 7. However, a decrease in precipitation by 300 mm causes stress, which reduces the LAI to 4 (Bracho et al., 2012).

The published results of the functional models "forest productivity-climate" are quite contradictory. Chertov (2010) believes that in the process of global warming, forest productivity increases. For the Mediterranean climate zone, it has been suggested that climate change may increase forest productivity by 12-14% and carbon storage by 23-31% over the next 50 years (Eggers et al., 2008). For the forests of Sweden, an average regional temperature increase of 4 °C over the next 100 years is expected to increase annual forest productivity by 33% (Poudel et al., 2011). At the same time, it was found that a 2 °C temperature increase over 200 years will not significantly affect forest biomass in the Eurasian boreal forests (Shuman and Shugart, 2009). The largest biomass reserves in the zone of moderate forests were found at moderately low temperatures and moderately heavy precipitation (Keith et al., 2009).

The dependence of the radial growth of European spruce, Scots pine, and European beech trees on climate and soil water balance was studied using data from 24 sample plots in Saxony (Germany) for the period from 1951 to 2006 (Röhle et al., 2010). For each tree species, the relation of growth with 30 independent variables characterizing precipitation, air temperature, and soil water balance for different months was analyzed, which explained from 50 to 57% of the total variability of growth. By combining the obtained models with climate forecast data, it was shown that environmental conditions for spruce become more unfavorable over time, which leads to a gradual decrease in growth. For pine and beech, the negative impact of climate on radial growth could not be detected until 2100 (Röhle et al., 2010).

For the entire American continent from Canada in the North to the South of Chile (from 55°N to 41°S), positive dependences of aboveground biomass of stands depersonalized by species composition and morphological structure on average annual precipitation were established (R^2 = 0.37-0.39). The relationship of biomass with the average annual temperature in tropical rainforests is positive (R^2 = 0.13), and in forests with excessive moisture is negative, but not statistically significant (R^2 = 0.02). In total, climate variables explain a small, and in many cases not statistically significant (R^2 = 0.02–0.03) share of forest stand biomass variability (Stegen et al., 2011).

When using the data of 56,000 sample plots in Germany and 576,000 ones in the United States, depersonalized by species composition and morphological structure of stands, it was found that an increase in the average annual temperature in Germany causes an increase, and in the United States causes a decrease in their productivity. Growing precipitation in the United States causes increased productivity, and in Germany there is an optimal level of annual precipitation (about 1000 mm), beyond which additional precipitation is counterproductive (Zeller et al., 2018).

Within the territory of China, from the taiga zone in the North to the subequatorial zone in the South, when the average annual temperature increases from -2 to 14 °C, the LAI in spruce and fir stands decreases from 20 to 4, and a similar decrease was found in pine stands (Luo, 1996). In the same temperature range, net primary production (NPP) in spruce and fir stands increases, more intensively in regions of increased moisture supply. As the average annual precipitation increases from 400 to 1400 mm, the NPP of

http://www.aloki.hu ● ISSN 1589 1623 (Print) ● ISSN 1785 0037 (Online)
DOI: http://dx.doi.org/10.15666/aeer/1902_11071122
© 2021, ALÖKI Kft., Budapest, Hungary

these stands increases in warm regions and decreases in cold ones (Luo, 1996). A similar propeller-shaped 3-D pattern was shown for the growth of pine forests in the swamp soils of Central Siberia (Glebov and Litvinenko, 1976). In contrast to *Picea-Abies* spp. stands, in *Larix* spp., *Pinus tabuliformis* Carr., and *Pinus koraiensis* Siebold & Zucc., the NPP increases as both the average annual temperature and the average annual precipitation increase (Luo, 1996; Fang et al., 2016). In contrast to the above-named species, the dependence of the NPP of Chinese fir (*Cunninghamia lanceolata* (Lamb.) Hook.) on temperatures and precipitation under the same conditions, is represented by a dome-capped 3-D surface (Luo, 1996).

In another study, based on data from 1,340 sample plots established in six forest biomes for the main forest-forming species in China (Ni et al., 2001), positive NPP dependences on average annual precipitation ($R^2 = 0.42$-0.86), slightly less pronounced on average annual temperature ($R^2 = 0.31$-0.60), and the least pronounced on potential evapotranspiration ($R^2 = 0.24$-0.50) are revealed. In contrast, for the southern United States, in the predictive model of potential stand productivity, temperature and precipitation were less informative than actual evapotranspiration (Manogaran, 1974).

Studies have shown that growing temperature increases the availability of soil nitrogen, and together with a longer vegetation season, this leads to an increase in tree biomass (Strömgren, Kinder, 2002). However, forest ecosystem responses to habitat include not only hydrothermal conditions, it is also difficult to account for genetically regulated changes at the physiological level. Therefore, models built on a biological basis actually have a correlative basis (Schulze, 2000). Changes in the stand NPP under the influence of annual temperatures are strongly influenced by the biodiversity index (Paquette et al., 2018). Therefore, the greatest uncertainties in assessing the impact of climate on forest biomass are typical for subtropical forests formed by hundreds of tree species in different proportions (Fu et al., 2017).

Thus, published local and regional models of forest stand productivity due to climate variables show contradictory results and do not give any knowledge of the global impact of climate shifts on forest productivity. The published trans-continental models are depersonalized by species composition and morphology of stands and show either weak or unreliable relationships with climate variables. The influence of climatic changes on the biomass of tree species in the additive format by transcontinental hydrothermal gradients has not been studied.

The creation of our first trans-Eurasian database on the biomass of forest-forming tree species is the reason why here suggested results were the first to obtain additive and statistically significant models of the total component composition of the biomass of spruce stands in Eurasia, including as independent variables both dendrometric indices of stands and climate variables, namely, average annual precipitation and average January temperature. The importance of selecting the correct structure of a developed model, which determines the level of its adequacy and ability to carry a predictive function, is shown. The obtained additive models of spruce stand biomass make them possible to establish quantitative changes in biomass structure due to climatic changes in Eurasia, in particular, due the mean temperature of January and mean annual precipitation.

Conclusions

Thus, the first attempt of modeling changes in the additive component composition of 900 spruce stands (genus *Picea* sp.) biomass (t/ha), according to the trans-Eurasian

http://www.aloki.hu ● ISSN 1589 1623 (Print) ● ISSN 1785 0037 (Online)
DOI: http://dx.doi.org/10.15666/aeer/1902_11071122
© 2021, ALÖKI Kft., Budapest, Hungary

hydrothermal gradients of Eurasia is suggested using the database compiled. It is found that all the biomass components change due to the increase in temperature and precipitation according to the same common scheme, but in different ratios. A common pattern for all components: regardless of the level of precipitation, when January temperature rises, the biomass of all components monotonically increases, but any increase in precipitation leads to a decrease in biomass. The development of such models for the main forest-forming species of Eurasia will make it possible to predict changes in the productivity of the forest cover of Eurasia due to climate change. Since the contribution of climate variables to the explanation of biomass variability of different components is on average only 9%, the proposed regularities are preliminary, and to increase this contribution, a more advanced database, adequate databases on trans-Eurasian temperatures and precipitation, and advanced software are needed.

Acknowledgements. The paper was funded by the Key Laboratory of Forestry Remote Sensing Based Big Data & Ecological Security for Hunan Province, Changsha 410004, China (2016TP1014), as well as according to the programs of current scientific research of the Ural Forest Engineering University and Botanical Garden of the Ural Branch of Russian Academy of Sciences.

REFERENCES

[1] Anderegg, W. R. L., Anderegg, L. D. L., Kerr, K. L., et al. (2019): Widespread drought-induced tree mortality at dry range edges indicates that climate stress exceeds species' compensating mechanisms. – Global Change Biology 25: 3793-3802.
[2] Anderson, K. J., Allen, A. P., Gillooly, J. F., et al. (2006): Temperature-dependence of biomass accumulation rates during secondary succession. – Ecology Letters 9: 673-682.
[3] Baskerville, G. L. (1972): Use of logarithmic regression in the estimation of plant biomass. – Canadian Journal of Forest Research 2: 49-53.
[4] Boivenue, C., Running, S. (2006): Impacts of climate change on natural forest productivity - evidence since the middle of the 20th century. – Global Change Biology 12: 862-882.
[5] Bracho, R., Starr, G., Gholz, H. L., et al. (2012): Controls on carbon dynamics by ecosystem structure and climate for southeastern U.S. slash pine plantations. – Ecological Monographs 82(1): 101-128.
[6] Budyko, M. I. (1977): Global Ecology. – Mysl' Publishing, Moscow (Rus.).
[7] Chertov, O. (2010): Impact of Temperature Increase and Precipitation Alteration at Climate Change on Forest Productivity and Soil Carbon in Boreal Forest Ecosystems in Canada and Russia: Simulation Approach with the EFIMOD Model. – In: Rodriguez-Morales, A., Risquez, A., Echezuria, L. (eds.) Impact of Climate Change on Health and Disease in Latin America. InTech Open Access Publisher, London.
[8] D'Aprile, F., Tapper, N., Marchetti, M. (2015): Forestry under climate change. Is time a tool for sustainable forest management? – Open Journal of Forestry 5: 329-336.
[9] DeLeo, V. L., Menge, D. N. L., Hanks, E. M., et al. (2020): Effects of two centuries of global environmental variation on phenology and physiology of Arabidopsis thaliana. – Global Change Biology 26: 523-538.
[10] DeLucia, E. H., Maherali, H., Carey, E. V. (2000): Climate-driven changes in biomass allocation in pines. – Global Change Biology 6(5): 587-593.
[11] Dong, L., Zhang, L., Li, F. (2015): A three-step proportional weighting system of nonlinear biomass equations. – Forest Science 61(1): 35-45.

http://www.aloki.hu ● ISSN 1589 1623 (Print) ● ISSN 1785 0037 (Online)
DOI: http://dx.doi.org/10.15666/aeer/1902_11071122
© 2021, ALÖKI Kft., Budapest, Hungary

[12] Douglas, A. E. (1919): Climatic Cycles and Trees-Growth. A Study of the Annual Rings of Trees in Relation to Climate and Solar Activity. – Publication No. 289. Carnegie Institution of Washington, Washington.
[13] Draper, N., Smith, H. (1973): Prikladnoy regressionnyi analiz. – Statistika, Moscow. (Translated from: Draper, N., Smith, H. 1966, Applied Regression Analysis. Wiley, New York).
[14] Dylis, N. V. (1978): Fundamentals of Biogeocenology. – Moscow State University Publishing, Moscow (Rus.).
[15] Eggers, J., Lindner, M., Zudin, S., et al. (2008): Impact of changing wood demand, climate and land use on European forest resources and carbon stocks during the 21st century. – Global Change Biology 14: 2288-2303.
[16] Ellenberg, H., Mayer, R., Schauermann, J. (1986): Ökosystemforschung - Ergebnisse des Sollingprojekts: 1966-1986. – Verlag Ulmer, Stuttgart.
[17] Fang, O., Yang Wang, Y., Shao, X. (2016): The effect of climate on the net primary productivity (NPP) of *Pinus koraiensis* in the Changbai Mountains over the past 50 years. – Trees 30: 281-294.
[18] Fatichi, S., Pappas, C., Zscheischler, J., et al. (2019): Modelling carbon sources and sinks in terrestrial vegetation. – New Phytologist 221(2): 652-668.
[19] Fu, L., Lei, X., Hu, Z., Zeng, W., et al. (2017): Integrating regional climate change into allometric equations for estimating tree above-ground biomass of Masson pine in China. – Annals of Forest Science 74(42): 1-15.
[20] Glebov, F. Z., Litvinenko, V. I. (1976): The dynamics of tree ring width in relation to meteorological indices in different types of wetland forests. – Lesovedenie 4: 56-62. (Rus.).
[21] Golubyatnikov, L. L., Denisenko, E. A. (2009): Influence of climatic changes on the vegetation of European Russia. – News of Russian Academy of Sciences, Geographic Series 2: 57-68.
[22] Grozeva, M., Dimitrov, E. P., Dzhorgov, I. (1986): Structure and chemical composition of the biomass in spruce stand from Rila Mountain. – Gorskostopanska Nauka 23(2): 52-58. (Bulg.).
[23] Han, S. H., Kim, S., Li, G., et al. (2018): Effects of warming and precipitation manipulation on fine root dynamics of *Pinus densiflora* Sieb. et Zucc. Seedlings. – Forests 9: 14.
[24] Huston, M. A., Wolverton, S. (2009): The global distribution of net primary production: resolving the paradox. – Ecological Monographs 79(3): 343-377.
[25] Jiang, H. (1986): Biomass and productivity of natural *Picea asperata* forests in close mature. – Acta Phytoecologica et Geobotanica Sinica 10(2): 146-152 (Chin.).
[26] Keeling, H. C., Phillips, O. L. (2007): The global relationship between forest productivity and biomass. – Global Ecology and Biogeography 16: 618-631.
[27] Keith, H., Mackey, B. G., Lindenmayer, D. B. (2009): Re-evaluation of forest biomass carbon stocks and lessons from the world's most carbon-dense forests. – Proceedings of the National Academy of Sciences of the United States of America 106: 11635-11640.
[28] Kestemont, P., Duvigneaud, P., Paulet, E. (1977): Biomase et productivite primaire d'une pessiere a Mirwart (Plantation de *Picea abies*). – In: Duvigneaud, P., Kestemont, P. (eds.)_ Productivite biolodique en Belgique. Duculot, Paris, pp. 161-176.
[29] Kõlli, R., Kährik, R. (1970): Phytomass and net primary production in the forests of the *Fragaria-Hepatica* type. – Transactions of Estonian Agricultural Academy: Soil Regimes and Processes 65: 69-91 (Rus.).
[30] Kostin, S. I. (1961): Solar activity and its influence on the growth of trees and the state of forests in the central part of the forest-steppe of the Russian plain. – Proceedings of the Main Geophysical Observatory named after A. I. Voeikov 111: 108-117. (Rus.).

http://www.aloki.hu ● ISSN 1589 1623 (Print) ● ISSN 1785 0037 (Online)
DOI: http://dx.doi.org/10.15666/aeer/1902_11071122
© 2021, ALÖKI Kft., Budapest, Hungary

[31] Laing, J., Binyamin, J. (2013): Climate change effect on winter temperature and precipitation of Yellowknife, Northwest Territories, Canada from 1943 to 2011. – American Journal of Climate Change 2: 275-283.
[32] Liebig, J. (1840): Die organische Chemie in ihrer Anwendung auf Agricultur und Physiologie. – Verlag Vieweg, Braunschweig (Deutsches Textarchiv http://www.deutschestextarchiv.de/liebig_agricultur_1840. Accessed on 26.11.2019).
[33] Lieth, H. (1974): Modeling of primary productivity of the globe. – Soviet Journal of Ecology 2: 13-23.
[34] Luo, T. X. (1996): Patterns of biological production and its mathematical models for main forest types of China. – PhD Dissertation. Committee of Synthesis Investigation of Natural Resources, Chinese Academy of Sciences, Beijing (in Chinese with English abstract).
[35] Manogaran, C. (1974): Climatic limitations of the potential for tree growth in southern forests. – Forestry Abstracts 35(11): 642.
[36] Miao, Z., Li, C. (2011): Predicting Tree Growth Dynamics of Boreal Forest in Response to Climate Change. – In: Li, C. et al. (eds.) Landscape Ecology in Forest Management and Conservation. Higher Education Press, Beijing and Springer-Verlag, Berlin, pp. 176-205.
[37] Møller, A. P., Jennions, M. D. (2002): How much variance can be explained by ecologists and evolutionary biologists? – Oecologia 132: 492-500.
[38] Ni, J., Zhang, X.-S., Scurlock, J. M. O. (2001: Synthesis and analysis of biomass and net primary productivity in Chinese forests. – Annals of Forest Science 58: 351-384.
[39] Olenin, S. M. (1982): Dynamics of radial growth of stands of pine phytocenoses of the middle taiga subzone of the Pre-Urals. – PhD thesis, Sverdlovsk (Rus.).
[40] Paquette, A., Vayreda, J., Coll, L., et al. (2018): Climate change could negate positive tree diversity effects on forest productivity: a study across five climate types in Spain and Canada. – Ecosystems 21(5): 960-970.
[41] Parresol, B. R. (1999): Assessing tree and stand biomass: a review with examples and critical comparison. – Forest Science 45: 573-593.
[42] Pasternak, P. S., Chernyavskiy, N. V. (1977): Biological productivity of *Fagus-Abies-Picea* young forests. – Forest Management and Forest Agromelioration 49: 27-33 (Rus.).
[43] Persson, T., van Oene, H., Harrison, A. F., et al. (2000): Experimental Sites in the NIPHYS/CANIF Project. – In: Schulze, E.-D. (ed.) Carbon and Nutrient Cycling in European Forest Ecosystems. Springer-Verlag, Berlin, pp. 14-46.
[44] Poudel, B. C., Sathre, R., Gustavsson, L., et al. (2011): Effects of climate change on biomass production and substitution in north-central Sweden. – Biomass and Bioenergy 35(10): 4340-4355.
[45] Ranger, J., Cuirin, G., Bouchon, J., et al. (1992): Biomasse et minéralomasse d'une plantation d'épicéa commun (*Picea abies* Karst.) de forte production dans les Vosges (France). – Annales des Sciences Forestières 49: 651-668.
[46] Ricklefs, R. E. (1979): Fundamentals of Common Ecology. – "Mir" Publishing, Moscow (Translated from: Ricklefs, R. E., 1976, The Economy of Nature: A Textbook in Basic Ecology. Chiron Press, Inc., Portland, OR.
[47] Röhle, H., Gerold, D., Gemballa, R. (2010): Beziehungen zwischen Klima und Zuwachs, dargestellt am Beispiel von Fichte, Kiefer und Buche in Sachsen. – Allgemeine Forst- und Jagdzeitung 181(1/2): 21-35.
[48] Sapozhnikov, A. P., Selivanova, G. A., Il'ina, T. M., et al. (1993): Soil Forming and Peculiarities of Biological Cycle of Matters in Mountain Forests at the Southern Sikhote-Alin'. – Forest Management Institute, Khabarovsk. (Rus.).
[49] Schulze, E.-D. (2000): The Carbon and Nitrogen Cycle of Forest Ecosystems. – In: Schulze, E.-D. (ed.) Carbon and Nutrient Cycling in European Forest Ecosystems. Springer-Verlag, Berlin, pp. 3-13.

http://www.aloki.hu ● ISSN 1589 1623 (Print) ● ISSN 1785 0037 (Online)
DOI: http://dx.doi.org/10.15666/aeer/1902_11071122
© 2021, ALÖKI Kft., Budapest, Hungary

[50] Schwarz, F. (1899): Physiologische Untersuchungen über Dickenwachstum und Holzqualität von *Pinus sylvestris*. – P. Parey, Berlin.
[51] Shcherbakov, N. M., Zaitseva, N. L. (1971): Biometrical Characteristics of Mature Spruce Stands on the South Part of Karelia. – Forest Plant Resources of the Southern Karelia. Karelia Publishing House, Petrozavodsk, pp. 22-40 (Rus.).
[52] Shelford, V. E., Metcalf, C. (1913): Animal communities in temperate America, as illustrated in the Chicago region; a study in animal ecology. – The Geographic Society of Chicago Bulletin 13(5).
[53] Shuman, J. K., Shugart, H. H. (2009): Evaluating the sensitivity of Eurasian forest biomass to climate change using a dynamic vegetation model. – Environmental Research Letters 4(4): 1-7.
[54] Stegen, J. C., Swenson, N. G., Enquist, B. J., et al. (2011): Variation in above-ground forest biomass across broad climatic gradients. – Global Ecology and Biogeography 20(5): 744-754).
[55] Strömgren, M., Linder, S. (2002); Effects of nutrition and soil warming on stemwood production of a boreal Norway spruce stand. – Global Change Biology 8: 1195-1204.
[56] Tang, S., Zhang, H., Xu, H. (2000): Study on establish and estimate method of compatible biomass model. – Scientia Silvae Sinica 36: 19-27 (in Chinese with English abstract).
[57] Usoltsev, V. A. (2013): Forest Biomass and Primary Production Database for Eurasia. CD-Version. The Second Edition, Enlarged and Re-harmonized. – Ural State Forest Engineering University, Yekaterinburg (http://elar.usfeu.ru/handle/123456789/3059).
[58] Usoltsev, V. A. (2010): Biomass and primary production of Eurasia's forests. – Ural Branch of RAS, Yekaterinburg. (http://elar.usfeu.ru/handle/123456789/2606).
[59] Usoltsev, V. A., Shobairi, S. O. R., Chasovskikh, V. P. (2018): Triple harmonization of transcontinental allometric models of *Picea* spp. and *Abies* spp. forest stand biomass. – Ecology, Environment and Conservation 24(4): 1966-1972.
[60] Usoltsev, V., Piernik, A., Osmirko, A., et al. (2019): Forest stand biomass of *Picea* spp.: an additive model that may be related to climate and civilisational changes. – Bulletin of Geography, Socio-Economic Series 45(45): 133-147.
[61] Vedrova, E. F., Spiridonova, L. V., Stakanov, V. D. (2000): Carbon cycle in young forests of main forest-forming species in Siberia. – Lesovedeniye 3: 40-48 (Rus.).
[62] Wilmking, M., Juday, G. P., Barber, V. A., et al. (2004): Recent climate warming forces contrasting growth responses of white spruce at treeline in Alaska through temperature thresholds. – Global Change Biology 10: 1724-1736.
[63] World Weather Maps (2007): https://www.mapsofworld.com/referrals/weather/ – Accessed on 2018-06-15.
[64] Yang, Y. (2005): Factors affecting forest growth and possible effects of climate change in the Taihang Mountains, northern China. – Forestry 79: 135-147.
[65] Yurkevich, I. D., Golod, D. S., Parfenov, V. I. (1975): Problems of Biogeocoenology and Biological Productivity of Spruce Forests in Byelorussia. – Ecologic and Biological Studies of Plant Communities. Nauka i Tekhnika Publishing, Minsk, pp. 14-27 (Rus.).
[66] Zeller, L., Liang, J., Pretzsch, H. (2018): Tree species richness enhances stand productivity while stand structure can have opposite effects, based on forest inventory data from Germany and the United States of America. – Ecosystems 5: 4.

http://www.aloki.hu ● ISSN 1589 1623 (Print) ● ISSN 1785 0037 (Online)
DOI: http://dx.doi.org/10.15666/aeer/1902_11071122
© 2021, ALÖKI Kft., Budapest, Hungary

THE EFFECTS OF EARLY HARVESTING ON THE SEED VIGOUR OF THREE CORN (*ZEA MAYS* L.) HYBRIDS BASED ON GERMINATION CHARACTERISTICS

KONUŞKAN, Ö.[1*] – GÖZÜBENLI, H.[1] – BARUTÇULAR, C.[2] – HOSSAIN, A.[3] – ISLAM, M. S.[4] – EL SABAGH, A.[5,6*]

[1]*Department of Field Crops, Faculty of Agriculture, Mustafa Kemal University, Hatay, Turkey (ORCID: 0000-0003-1135-2346 – Ö. Konuşkan; 0000-0003-4799-5749 – H. Gözübenli)*

[2]*Department of Field Crops, Faculty of Agriculture, Cukurova University, Adana, Turkey (ORCID: 000-0003-3583-9191)*

[3]*Bangladesh Wheat and Maize Research Institute, Dinajpur 5200, Bangladesh (ORCID: 0000-0003-0264-2712)*

[4]*Department of Agronomy, Hajee Mohammad Danesh Science and Technology University, Dinajpur 5200, Bangladesh*

[5]*Department of Field Crops, Faculty of Agriculture, Siirt University, Turkey*

[6]*Department of Agronomy, Faculty of Agriculture, Kafrelsheikh University, Kafr Al Sheikh, Egypt (ORCID: 0000-0002-4241-192X)*

**Corresponding author*
e-mail: aymanelsabagh@gmail.com,okonuskan@mku.edu.tr

(Received 31st Aug 2020; accepted 18th Dec 2020)

Abstract. Time of harvesting in the case of corn is a key factor that contributes to obtain high seed vigour. In the context, the study was conducted at the Agricultural Experimental Area of Mustafa Kemal University, Turkey (36°15' N and 36°30' E), to evaluate the germination characteristics of three corn hybrids including 'Dekalp 6589 (FAO 700)', 'Cadiz (FAO 700)' and 'Bolson (FAO 600)'. In order to use them in the present experiment, seeds of the selected corn were harvested at 5 day intervals, starting from the milking stage (seed harvesting of all corn hybrids was done 30 days after tasseling) to physiological maturity stages. Data on 1000 grain weight (1000-GW), electrical conductivity (EC), germination ratio (GR), germination index (GI), accelerated aging test index (AATI), cold test, cold test germination index (CTGI), and cold test germination time (CTGT) significantly varied among the selected hybrids in response to harvesting at different times. When harvesting was done after 30 days of tasseling the dry matter in cultivar 'Cadiz' showed the lowest, while the cultivar 'Bolson' showed the maximum dry matter. The earliest black layer in the cultivar 'Dekalp 6589' was found after 50 days while in the other two hybrids it was recorded 5 days later (55 days). The techniques of the present study related to evaluation seed vigour by estimating and evaluating germination properties may be used in future research as well as by farmers in field conditions for sustainable corn production in the changing climate.
Keywords: *electrical conductivity germination ratio, germination index, aging test index, cold test*

Introduction

Corn (*Zea mays* L.) is one of the most important cereal crops grown across the globe due to its widespread adaptability (Ranum et al., 2014; FAO, 2018 and Molla et al., 2019). It is widely grown in various soil and climatic conditions due to its contribution and adaptability to other cereals in the world. It is broadly used for food, fodder, fuel, industrial raw materials as well as corn oil (Konuskan et al., 2017; EL Sabagh et al., 2018;

http://www.aloki.hu ● ISSN 1589 1623 (Print) ● ISSN 1785 0037 (Online)
DOI: http://dx.doi.org/10.15666/aeer/1902_11231134
© 2021, ALÖKI Kft., Budapest, Hungary

Maqsood et al., 2020). It is suitable for human consumption due to the presence of unsaturated fatty acids (Abdelaal et al., 2017; Sariyev et al., 2020). Area and production of corn ranks third in world after wheat and rice. Besides these, it can play a glorious role in the economy of the country by feeding malnourished people as well as solving food problems. Therefore, corn should get priority considering the protein malnourishment of the people, because it encompasses more digestible protein than other cereals (Ahamed, 2010; Ahmed et al., 2020; EL Sabagh et al., 2020; Ghosh et al., 2020).

In recent years, numerous studies were devoted to the physiological responses of seed germination and seedlings stages to chilling or osmotic stress (Anosheh et al., 2014), but the ecological responses of the whole growing season remain largely unknown (Tian et al., 2014). Rapid and uniform field emergence is an important factor to achieve high yield to meet the growing demand for food (Rosegrant et al., 1995). Naturally, the plant employs several adaptive measures to cope with harsh environments, such adaptive measures bring about changes or adjustments in the physiological and biochemical processes of the plant (EL Sabagh et al., 2018; Iqbal et al., 2021).

Seed quality is generally reflected by seed vigour that refers to the total properties of seed activities from germination under wider environments for storage longevity of seeds (Gu et al., 2017), that determines the potential for fast and uniform seedling emergence (Woltz and TeKrony, 2001; Mondo et al., 2013), and development of vigorous seedlings under a widespread field conditions (AOSA, 1983, 2002). Generally, low germination speed and high sensibility of seed and seedlings face to various stresses during the germination process, lead to irregular shoot and root growth that ultimately leads to decrease in the productivity (Marcos-Filho, 2005).

Since seed harvesting at the optimum time is the vital factor that involves to achieve high seed vigour. During the maturation process, several morphological and physiological changes occur which are linked with seed vigour. Harvesting at a suitable time is a key factor that contributes to get seeds with high vigour (Gu et al., 2017) through maintaining the optimum quality. Harvesting too early leads to immature seeds that produce poor vigour (Fu et al., 2017). The parameters frequently used are black layer formation, milk line development, seed weight (usually expressed as hundred-seed weight, HSW) and seed moisture content (SMC) (Afuakwa and Crookston, 1984; dos Santos et al., 2005). Both black layer formation and milk-line development stages were found the best seed harvesting time of corn for achieving the maximum high vigour of seeds through maintaining the best physiological quality (Gu et al., 2017). However, several scientists argued that the above-mentioned indicators are not always appropriate since these factors are sometime varied due to genetic makeup of a specific genotype and also their interaction with growing environments (Carter and Poneleit, 1973; Kinittle and Burris, 1976; Ma and Dwyer, 2001). Besides these, in classical breeding studies, selfing can be made only one time in a year. In the tropical and sub-tropical areas, there can be two times a year for selfing and harvesting. However, the seeds should be dried up quickly and sown again after the first self-seed. Thus classical breeding period will be halved.

Considering the above-mentioned limitations, scientists suggested some parameters such as 1000 grain weight (1000-GW), electrical conductivity (EC), germination ratio (GR), germination index (GI), accelerated aging test index (AATI), cold test, cold test germination index (CTGI), and cold test germination time (CTGT) are considered the most widely used parameters for determining seed vigour (ISTA, 2015; Gu et al., 2017), when they achieved maximum weight (also called physiological maturity, PM) (Wych,

http://www.aloki.hu ● ISSN 1589 1623 (Print) ● ISSN 1785 0037 (Online)
DOI: http://dx.doi.org/10.15666/aeer/1902_11231134
© 2021, ALÖKI Kft., Budapest, Hungary

1988; TeKrony and Hunter, 1995). For avoiding elevated stress in seedbed at a minimum acceptable vigour level of ≥ 80%, cold and accelerated aging tests are accurately used to optimize the field emergence of seeds (Woltz and TeKrony, 2001). In the context, the recent study was undertaken to determine the seed vigour of early harvesting of three corn (*Zea mays* L.) hybrids through observing several germination characteristics.

Materials and methods

Location of the research

The current study was conducted at the Agricultural Experimental Area of Mustafa Kemal University, Hatay, Turkey (located at 36°15' N and 36°30' E), during the year 2016, where corn was growing as the main crop. Typical Mediterranean climatic conditions prevail in the region. The soil of research area is clay loam having pH 7.7, where available phosphorus and organic matter content are low.

Experimental procedure

The size of each plot was 4 m in length and 5 m in width including plant stand (Intra row: 70 cm, Inter row: 18 cm). Three hybrid corn, namely 'Dekalp 6589 (FAO 700)', 'Cadiz (FAO 700)', and 'Bolson (FAO 600)' were used as experimental material in this study. Seeds of hybrid corns were sown on 10 April 2016. Before planting, mixed fertilizers including N, P_2O_5, and K_2O at 15-15-15 ratio were applied and mixed into the soil. After the V6 stage, nitrogen was applied at 20 kg ha^{-1} as top-dressing. Plots were irrigated every 10-14 days from June to each cob harvesting time when nearly half of available soil water was consumed. Weed control and other agronomic measurements were done when necessary. When cob silk was determined to 2 cm length, it had been marked. Seeds harvesting of all corn hybrids was done 30 days after tasseling based on specific milk line, black layer and dry matter % of seeds in eight harvesting times (*Table 1*). About 10 cobs were harvested in each harvest time. The cobs were harvested for a few days. Seeds were split in two. Milk-line and dry matter were determined in some of them. The other part started the germination process straight away.

Estimation of the germination characteristics to know seeds vigour of all hybrids

Seed testing was done at the Seed Science Laboratory, Department of Field Crops, Faculty of Agriculture, Mustafa Kemal University, Turkey. All of the seeds were dried under laboratory conditions before starting the seed vigour and germination tests.

The accelerated aging test for all hybrid seeds was conducted according to AOSA (1983). Accelerated unites were placed in germination cabinets at 45 °C for 72 h after which the kernels were removed and subjected to the standard germination and other germination tests (Woltz and TeKrony, 2001). The electrical conductivity (EC) test was performed according to Wang et al. (1994). Measurement of soaked water was performed 72 hrs using a conductivity meter (Model HANNA HI 255 Combined Meter, Germany). Results were expressed in μS cm^{-1} g^{-1} to take account of variability in seed weight among the seed lots.

http://www.aloki.hu ● ISSN 1589 1623 (Print) ● ISSN 1785 0037 (Online)
DOI: http://dx.doi.org/10.15666/aeer/1902_11231134
© 2021, ALÖKI Kft., Budapest, Hungary

Table 1. *Seed harvesting of all corn hybrids were done 30 days after tasseling (DAT) based on specific milk-line (ML), black layer formation and dry matter % of seed*

No of harvesting times	Harvest at following dates after tasseling	Grain maturity stage of all hybrids						Dry matter (DM) (%) of all hybrids		
		Dekalp 6589	Days required for ML & BL	Cadiz	Days required for ML & BL	Bolson	Days required for ML & BL	Dekalp 6589	Cadiz	Bolson
1	19/07/2016	¼ ML	92	-		-		63	-	-
2	23/07/2016	½ ML	97	¼ ML	96	-		68	60	-
3	27/07/2016	¾ ML	102	½ ML	101	¼ ML	100	66	59	61
4	01/08/2016	¾ ML	107	½ ML	106	1/3 ML	105	67	62	66
5	04/08/2016	BL	112	¾ ML	111	¾ ML	110	69	62.5	68
6	08/08/2016	-		1/5 ML	116	BL	115	73	65	71
7	12/08/2016	-		BL	121	-		76	70	77
8	16/08/2016	-		-		-		80	71	77
9	20/08/2016	-		-		-		84	81	82
10	24/08/2016	-		-		-		-	85	82

The seed germination ratio was measured according to ISTA (2008). Twenty-five seeds were placed on three layers of moist, non-toxic, germination paper (Anchor Paper Co., St. Paul, Minn.). The papers were rolled, placed in a plastic container (21.5 × 32.5 × 5.5 cm), and incubated in a dark germinator at 25 °C for 10 days. The incubator (model ES120) was used for the germination test. A seed was considered germinated when the emerging radicle was at least 2 mm long.

Cold test and its estimating procedure

Soil obtained from the top 5 cm of a corn-field at the Agricultural Experimental site of Mustafa Kemal University, Turkey was used for the cold test. The soil was screened through a 5 mm sieve and 450 g dry soils were placed into 19 x 6 x 9.5 cm plastic containers. Four replications of 50 seeds from each treatment were planted in each plastic container and covered with 450 g dry soil. A calculated quantity of prechilled (10 °C) distilled water was added to adjust the moisture content to 70% of water holding capacity (227 ml water). The containers were then covered and incubated at 10 °C in darkness for 7 days. The containers then moved to a 25 °C chamber with an altering light source (12 h light day^{-1}) for 4 days grow-out period and normal seedlings were counted for germination ratio. Seedlings were classified as strong or weak after 7 days as described by Fiala (1987).

Cold germination index

Cold germination index was determined according to Carpici et al. (2009), using the formula:

$$GI = \sum(Gi / Tt) \quad \text{(Eq.1)}$$

where, GI is germination index, Gi is the germinating seeds per day, Tt is counting days of germination time.

http://www.aloki.hu ● ISSN 1589 1623 (Print) ● ISSN 1785 0037 (Online)
DOI: http://dx.doi.org/10.15666/aeer/1902_11231134
© 2021, ALÖKI Kft., Budapest, Hungary

Cold germination time

Cold germination time was recorded according to Ellis and Roberts (1980), using the following formula:

$$MGT = \Sigma(n.D) / \Sigma n \quad \text{(Eq.2)}$$

where, 'n' is the number of newly germinated seeds on each day and 'D' is the day of counting.

Statistical analysis

The data were analyzed by partitioning the total variance with the help of a computer using MSTAT-C program. The treatment means were compared using Duncan's Multiple Range Test (DMRT, 1955).

Results and discussion

Analysis of variance (ANOVA) for germination parameters

Table 2 represents the summary of the analysis of variance (ANOVA) for seed germination characteristics of all three corn cultivars. The result indicated that the lowest dry matter was determined in the Cadiz hybrid, while the highest dry matter was determined in the cultivars of 'Bolson' corn at the first harvesting time (30 days after tasseling). This may be from a different FAO (600) groups of Corn varieties.

Table 2. *Analysis of variance (ANOVA) of some germination parameters*

Sources of variation	DF	1000-GW	EC	GR	GI	AAGI	CT	CTGI	CGT
Corn hybrids (A)	2	1191.3**	799.7**	14.6**	22.2**	84.9**	145.8**	93.7**	58.0**
Harvesting times (B)	8	239.4**	122.5**	127.5**	135.8**	30.9**	21.91**	35.1**	14.9**
A X B	16	19.4**	12.1**	28.2**	29.0**	12.8**	19.18**	25.8**	11.5**
CV (%)		2.50	7.26	5.50	6.97	10.67	7.42	6.11	4.99

*, **Significant at P < 0.05 and P < 0.01 levels respectively. DF: degree of freedom; CV (%): coefficient of variation; 1000-GW: 1000 grain weight; EC: electrical conductivity; GR: germination ratio; GI: germination index; AAGI: accelerating aging test index; CT: cold test; CTGI: cold test germination index; CTGT: cold test germination time

The earliest black layer was found in 'Dekalp 6589' hybrid at 50 days. The black layer was determined at 55 days in other corn hybrids. But the period between flowering and physiological maturity was determined as 15 days in 'Bolson' hybrids, but the others were completed in 20-25 days (*Tables 1* and *2*). The analysis of variance (mean squares) of all investigated properties of germination rate, germination index, germination time, root length and root fresh weight in normal and aging seeds were found to be statistically significant regarding the corn hybrids and harvesting times (*Table 3*). It was also observed that there was a significant difference in the interaction between hybrids and harvesting times. Findings of Kapoor et al. (2010) reported that accelerated aging in cowpea seeds influenced the physiological aspects such as germination percentage and vigour index. Further, the reduction in seed viability, germination rate, and vigour is associated with biochemical changes (for example, decrease in soluble proteins and sugar content) related to seed aging (Rastegar et al., 2011).

http://www.aloki.hu ● ISSN 1589 1623 (Print) ● ISSN 1785 0037 (Online)
DOI: http://dx.doi.org/10.15666/aeer/1902_11231134
© 2021, ALÖKI Kft., Budapest, Hungary

Table 3. *Effects of corn hybrids on 1000-GW, EC, GR, GI, AAGI, CT, CGI and CGT of corn hybrids*

Cultivars	1000-GW	EC	GR	GI	AAGI	CT	CTGI	CTGT
Dekalp 6589	283.2b	10.22b	81.75b	9.31c	6.62b	67.1c	9.05c	4.88a
Cadiz	241.1c	12.78a	87.4a	10.18a	9.32a	91.5a	11.57a	4.28b
Bolson	314.5a	8.53c	82.8b	9.70b	7.08b	75.1b	10.22b	4.30b
LSD (5%)	3.4	0.24	2.54	0.3	0.5	3.29	0.41	0.14

1000-GW: 1000 grain weight; EC: electrical conductivity; GR: germination ratio; GI: germination index; AAGI: accelerating aging test index; CT: cold test
The letters in all parameters are indicating the significant differences according to the DMRT

1000-GW (g) and electrical conductivity (µS cm^{-1} g $^{-1}$)

It was also observed that there was a significant difference between hybrids and harvesting times. After the accelerated aging test, the highest 1000-GW (314.5) was observed in 'Bolson' hybrid at different harvesting times (*Table 3*). However, the highest EC (12.78) was recorded in 'Cadiz' hybrid at different harvesting times (*Table 3*). The highest 1000-GW (315.2) was recorded at the 62th DAT (*Tables 3* and *4*). Electrical Conductivity (EC) was also significantly influenced by the harvesting times in this study. On the other hand, the highest EC value was recorded at the 30th DAT (*Table 4*). Interaction effects of variety x harvesting time on the 1000 GW and electrical conductivity of corn hybrids were also varied significantly (*Table 5*). The maximum 1000-GW (333.7) was recorded at the 58th DAT in 'Bolson' corn hybrid, followed by 62th DAT in same corn hybrid (333.3). Whereas the maximum EC (17.84) was recorded at 30th DAT in 'Bolson' hybrid, followed by 'Dekalp 6589' (16.23) at the same harvesting time (30th DAT) (*Table 5*). The explanation for seed deterioration is that high temperature and moisture content reduce the seed quality and these parameters are the factors to predict the life spans of seeds confirmed by earlier finding of Roberts et al. (1973).

Table 4. *Effects of harvesting times on 1000-GW, EC, GR, GI, AAGI, CT, CGI and CGT of corn hybrids*

Harvest at following DAT	1000-GW (g)	EC (µS cm^{-1} g $^{-1}$)	GR (%)	GI	AAGI	CT (%)	CTGI	CTGT (day)
30th	218.0 f	14.78 a	72.58 d	8.32 d	5.72 f	74.5 c	9.24 cd	4.68 ab
34th	247.1 e	13.43 b	65.33 e	6.95 e	6.63 de	73.2 c	9.93 b	4.50 c
38th	266.1 d	11.17 c	59.30 f	6.21 f	6.41 e	63.4 d	8.96 d	4.79 ab
42th	281.7 c	10.73 c	84.50 c	8.87 d	7.35 c	76.3 c	9.37 cd	4.81 a
46th	286.4 c	11.08 c	91.50 b	10.28 c	7.28 cd	74.2 c	9.52 bc	4.61 bc
50th	298.0 b	9.20 d	97.30 a	11.58 b	8.46 b	89.0 a	11.14 a	4.28 d
54th	294.1 b	8.67 d	86.00 c	10.50 c	9.69 a	82.5 b	11.32 a	4.28 d
58th	309.9 a	7.85 e	99.50 a	12.37 a	8.94 b	86.2 ab	11.43 a	4.14 d
62th	315.2 a	7.71 e	99.80 a	12.48 a	8.59 b	81.8 b	11 60 a	4.28 d
LSD (5%)	5.69	0.62	3.76	0.55	0.67	4.7	0.51	0.18

1000-GW: 1000 grain weight; EC: electrical conductivity; GR: germination ratio; GI: germination index; AAGI: accelerating aging test index; CT: cold test
The letters in all parameters are indicating the significant differences according to the DMRT

Germination time (GT)

A significant variation of GT among treatments of all the corn hybrids was found due to the differences in harvest times (*Table 5*). The mean GT, under conditions providing aging were significant with accelerated aging of corn seed (Kapilan, 2015).

http://www.aloki.hu ● ISSN 1589 1623 (Print) ● ISSN 1785 0037 (Online)
DOI: http://dx.doi.org/10.15666/aeer/1902_11231134
© 2021, ALÖKI Kft., Budapest, Hungary

Table 5. *Interaction effects of corn hybrids x harvesting time on the 1000-GW and electrical conductivity of corn hybrids*

Harvest at following DAT	1000 GW (g)			EC (µS cm^{-1} g^{-1})		
	Dekalp 6589	Cadiz	Bolson	Dekalp 6589	Bolson	Cadiz
30th	202.1 op	178.4 q	273.6 l	16.23 b	17.84 a	10.23 fg
34th	251.5 m	194.2 p	295.6 gh	13.72 c	16.16 b	10.39 ef
38th	288.7 h-k	204.5 o	305.1 e-g	10.15 f-h	14.06 c	9.29 g-j
42th	291.2 h-j	240.8 n	313.1 d-f	10. 00 f-i	13.05 c	9.14 h-k
46th	292.5 hi	240.9 n	325.6 a-c	8.97 l-l	13.85 c	10.43 ef
50th	284.1 i-k	278.9 kl	330.9 ab	9.37 f-j	11.55 d	3.68 o
54th	303.4 fg	259.4 m	319.5 cd	8.11 k-n	11.44 de	6.45 o
58th	314.0 de	282.1 j-l	333.7 a	7.13 no	9.06 i-k	7.38 m-o
62th	321.5 bd	290.9 h-j	333.3 a	8.31 j-m	8.06 l-n	6.75 o
LSD (5%)	9.86			1.07		

1000-GW: 1000 grain weight; EC: electrical conductivity
The letters in all parameters are indicating the significant differences according to the DMRT

Table 6. *Interaction effects of corn hybrids x harvesting times on the germination ratio and germination index of corn hybrids*

Harvest at following DAT	Germination ratio (%)			Germination index		
	Dekalp 6589	Cadiz	Bolson	Dekalp 6589	Cadiz	Bolson
30th	87.2 c	83.5 cd	47.0 i	9.92 de	10.39 cd	4.66 i
34th	75.0 ef	69.0 fg	52.0 i	8.93 fg	7.1 h	4.84 i
38th	50.0 i	66.0 gh	62.0 h	4.75 i	7.15 h	6.73 h
42th	83.5 cd	80.0 de	90.0 bc	8.21 g	8.57 g	9.83 d-f
46th	84.0 cd	95.5 ab	95.0 ab	9.08 e-g	10.15 d	11.59 ab
50th	97.5 a	94.5 ab	100 a	11.26 bc	11.12 bc	12.35 a
54th	60.0 h	99.0 a	99.0 a	6.90 h	12.25 a	12.34 a
58th	99.0 a	99.5 a	100 a	12.22 a	12.44 a	12.48 a
62th	99.5 a	100 a	100 a	12.5 a	12.49 a	12.45 a
LSD (5%)	6.51			0.96		

1000-GW: 1000 grain weight; EC: electrical conductivity
The letters in all parameters are indicating the significant differences according to the DMRT

Germination ratio

Germination ratio (GR) is an important trait that influences the stand establishment and yield of crops. After accelerated aging test, the highest GR (75.25%) was observed in 'Dekalp 6589' hybrid at different harvesting time of corn seeds followed by hybrids 'Cadiz' and 'Bolson' (*Table 6*). The GR was also significantly influenced by the harvesting times in this study. However, the highest GR (78.00%) was recorded at the 40th DAT which was statistically identical with 35th and 55th DAT, while the lowest GR (21.00%) was observed at 30th DAT. The germination ratio of different phenological stages has been reported in several earlier studies (Demir and Mavi, 2004; Demir and Mavi, 2008).

http://www.aloki.hu ● ISSN 1589 1623 (Print) ● ISSN 1785 0037 (Online)
DOI: http://dx.doi.org/10.15666/aeer/1902_11231134
© 2021, ALÖKI Kft., Budapest, Hungary

Germination index (GI)

Corn hybrids faced significant variations in the germination index due to harvest times. The maximum values were determined at 58th and 62nd day in the case of the hybrid 'Dekalp 6589', but no significant differences were detectable between 54 to 62nd harvest of hybrid 'Cadiz' or 46 to 62 days of hybrid 'Bolson' through estimation of GI (*Table 6*). Ghassemi-Golezani et al. (2010) reported that the reduction in germination percent and other indices can be due to physiological and biochemical changes during seed aging.

Accelerated aging test index (AAGI) and cold test (CT)

A significant variation of accelerated aging test index (AAGI) and cold test (CT) among treatments of all corn hybrids were found when grown upto the harvest times (*Table 7*). The AAGI was also significantly influenced by the harvesting times in this study. However, the highest AAGI (9.32a) was recorded in 'Cadiz' hybrid at different harvesting times (*Table 3*), and the highest AAGI (9.69 a) was recorded at the 54th DAT (*Table 4*). The reduction of AAGI with aging seed was due to the increase in respiration in the cell during the process to prevent cell damage as confirmed by earlier findings of Torres and Andrews (2006) and Vashisth and Nagarajan (2009). Among the corn hybrids, the maximum CT (91.5) was documented in the cultivar 'Cadiz', while the highest value (89.0) was observed at the harvesting time of 50th DAT. The rate of deterioration of seeds depends on storage conditions such as temperature, atmospheric moisture and oxygen concentration (confirmed by Walters et al., 2005).

Table 7. *Interaction effects of corn hybrids x harvesting times on the AAGI and CT of corn hybrids*

Harvest at following DAT	AAGI			CT (%)		
	Dekalb 6589	Bolson	Cadiz	Dekalb 6589	Cadiz	Bolson
30th	6.08 g-j	5.64 h-j	5.44 ij	76.0 hi	86.0 c-g	61.5 j
34 th	6.09 g-j	8.26 c-e	5.55 h-j	64.0 j	93.0 a-c	62.5 j
38 th	9.42 d-f	5.19 j	6.62 f-h	48.3 k	89.0 a-e	53.0 k
42 th	5.34 ij	9.29 bc	7.47 d-f	51.0 k	95.0 ab	83.0 d-h
46 th	6.27 g-j	9.56 b	6.03 g-j	38.0 l	96.5 a	88.0 b-f
50 th	6.48 f-i	11.75 a	7.13 e-g	82.0 e-h	97.0 a	88.0 b-f
54 th	9.50 b	10.98 a	8.57 b-d	73.5 i	95.5 ab	78.5 g-i
58 th	6.81 fg	11.33 a	8.69 bc	86.5 c-g	90.5a-d	81.5 e-i
62 th	5.63 h-j	11.89 a	8.26 c-e	84.5 d-g	81.0 e-i	80.0 f-i
LSD (5%)	1.15			8.15		

AAGI: accelerating aging test index; CT: cold test
The letters in all parameters are indicating the significant differences according to the DMRT

Cold test germination index (CTGI), and cold test germination time (CTGT)

A significant difference was observed among the hybrids and harvesting times after the accelerated aging test. The highest CTGI (12.38) was observed in the corn hybrid 'Bolson' at different harvesting times and was recorded at the 54th DAT (*Table 8*). The CTGT was also significantly influenced by the harvesting times in this study. However,

http://www.aloki.hu ● ISSN 1589 1623 (Print) ● ISSN 1785 0037 (Online)
DOI: http://dx.doi.org/10.15666/aeer/1902_11231134
© 2021, ALÖKI Kft., Budapest, Hungary

the highest CTGT (5.92) was recorded in 'Dekalp 6589'hybrid at the 42nd DAT, while the lowest (4.03) was recorded in the hybrid 'Bolson' at 54th DAT (*Table 8*).

Table 8. *Interaction effects of corn hybrids x harvesting times on the CTGI, and CTGT of corn hybrids*

Harvest at following DAT	CTGI			CTGT (day)		
	Dekalp 6589	**Bolson**	**Cadiz**	**Dekalp 6589**	**Bolson**	**Cadiz**
30th	8.68 jk	10.98 e-g	8.06 k-m	5.29 b	4.55 de	4.22 f-j
34th	10.09 g-i	11.43 b-f	8.27 km	4.63 d	4.46 d-f	4.41 d-h
38th	7.38 lm	12.15 ab	7.34 m	5.29 b	4.11 h-j	4.96 c
42th	6.01 n	11.52 a-e	10.57 f-h	5.92 a	4.24 e-j	4.27 e-j
46th	5.96 n	11.23 c-f	11.38 b-f	5.35 b	4.40 d-h	4.08 ij
50th	10.09 hi	11.88 a-d	11.45 b-f	4.43 d-g	4.27 e-j	4.14 g-j
54th	9.40 ij	12.38 a	12.18 ab	4.66 cd	4.03 j	4.15 f-j
58th	11.8 a-e	11.38b-f	11.13 d-f	4.16 f-j	4.08 ij	4.18 f-j
62th	12.05 a-c	11.18 c-f	11.57 a-e	4.16 f-j	4.38 di	4.29 e-j
LSD (5%)	0.89			0.32		

The letters in all parameters are indicating the significant differences according to the DMRT

Conclusion

From the above results and discussion of the present study, it can be concluded that germinating properties such as 1000-GW, EC, GR, GI, AATI, CTGI, and CTGT may be used potentially for the evaluation of seed vigour. Among these tested corn hybrids, seeds harvested from hybrid 'Cadiz' showed the lowest dry matter and the highest other parameters during the first harvesting (20 DAT). Considering the milk-line and black layer formation, the earliest black layer (at 50 DAT) was found in the hybrid 'Dekalp 6589', but for the other two hybrids, the black layer was recorded at 55 DAT, indicating that the seed vigour of hybrid 'Cadiz' is better than that of the others. The techniques of the present study related to evaluation seed vigour by estimating and evaluating germination properties may be useful in future research as well as by farmers' field for sustainable corn production in the changing climate.

Conflict of interests. The authors declare that there is no conflict of interests regarding the publication of this paper.

REFERENCES

[1] Abdelaal, K. A. A., Hafez, Y. M., EL Sabagh, A., Saneoka, H. (2017): Ameliorative effects of Abscisic acid and yeast on morpho-physiological and yield characteristics of maize plant (*Zea mays L.*) under water deficit conditions. – Fresenius Environ. Bull. 26(12): 7372-7383.

[2] Afuakwa, J. J., Crookston, R. K. (1984): Using the kernel milk line to visually monitor grain maturity in maize. – Crop Sci. 24: 687-691. DOI: 10.2135/cropsci1984.0011183X002400040015x.

[3] Ahamed, K. U. (2010): Efficacy of indigenous mulches on the maize-pulse association. – Ph.D. Thesis, Department of Crop Botany, Bangladesh Agricultural University, Mymensingh, Bangladesh.

[4] Ahmed, A., Hossain, A., Amiruzzaman, M., Alam, M. A., Farooq, M., EL Sabagh, A., Kizilgeci, F. (2020): Evaluating Short Stature And High Yielding Maize Hybrids In Multiple Environments Using Gge Biplot And Ammi Models. – Turkish Journal of Field Crops 25(2): 216 -226.

http://www.aloki.hu ● ISSN 1589 1623 (Print) ● ISSN 1785 0037 (Online)
DOI: http://dx.doi.org/10.15666/aeer/1902_11231134
© 2021, ALÖKI Kft., Budapest, Hungary

[5] Anosheh, H. P., Emam, Y., Ashraf, M. (2014): Impact of cycocel on seed germination and growth in some commercial crops under osmotic stress conditions. – Archives of Agron. Soil Sci. 60(9): 1277-1289.
[6] Association of Official Seed Analysts (AOSA) (1983): Seed Vigor Testing Handbook. (Contribution to the Handbook on Seed Testing, 32). – AOSA, Ithaca, NY.
[7] Association of Official Seed Analysts (AOSA) (2002): Seed Vigor Testing Handbook. (Contribution, 32) – AOSA, Ithaca, NY.
[8] Carpici, E. B., Celik, N., Bayram, G. (2009): Effects of salt stress on germination of some maize (*Zea mays* L.) cultivars. – Afr. J. Biotechnol. 8: 4918-4922.
[9] Demir, İ., Mavi, K. (2004): The effect of priming on seedling emergence of differentially matured watermelon (*Citrullus lanatus* (Thunb.) Matsum and Nakai) seeds. – Sci. Hort. 102(4): 467-473.
[10] Demir, İ., Mavi, K. (2008): Effect of salt and osmotic stresses on the germination of pepper seeds of different maturation stages. – Brazilian Arc. Biol. Technol. 51(5): 897-902.
[11] dos Santos, C. T., Dalpasquale, V. A., Scapim, C. A., Braccini, A. L., Krzyzanowski, F. C. (2005): Milk line as an indicator of the harvesting time of three hybrid seeds of corn (*Zea mays* L.). – Braz. Arch. Biol. Tech. 48: 161-170. DOI: 10.1590/S1516-89132005000200001.
[12] EL Sabagh et al. (2020): Maize Adaptability to Heat Stress under Changing Climate. – IntechOpen, London. https://www.intechopen.com/online-first/maize-adaptability-to-heat-stress-under-changing-climate. DOI: 10.5772/intechopen.92396.
[13] EL Sabagh, A., Barutçular, C., Hossain, A., Islam, M. S. (2018): Response of maize hybrids to drought tolerance indices in relation to grain weight. – Frese. Environ. Bull. 27(4): 2476-2482.
[14] Ellis, R. H., Roberts, E. H. (1980): Towards Rational Basis for Testing Seed Quality. – Hebblethwaite, P. D. (ed.) Seed Production. Butterworths, London, pp. 605-635.
[15] FAO (Food and Agriculture Organization) (2018): FAOSTAT, Food Supply. – http://www.fao.org/faostat/en/#data (accessed 2018 Oct 05).
[16] Fiala, F. (1987): Handbook of Vigour Test Methods. – International Seed Testing Association, Zurich.
[17] Fu, H., Cao, D. D., Hu, W. M., Guan, Y. J., Fu, Y. Y., Fang, Y. F., Hu, J. (2017): Studies on optimum harvesting time for hybrid rice seed. – J. Sci. Food Agric. 97: 1124-1133.
[18] Ghassemi-Golezani, K., Khomari, S., Dalili, B., Hosseinzadeh-Mahootchy, B., Chadordooz-Jedi, A. (2010): Effect of seed aging on field performance of winter oil seed rape. – J. Food Agric. Environ. 8(1): 175-178.
[19] Ghosh, D., Brahmachari, K., Skalicky, M., Hossain, A., Sarkar, S., Dinda, N.K., Das, A., Pramanick, B., Moulick, D., Brestic, M., Raza, M.A., Barutcular, C., Fahad, S., Saneoka, H., EL Sabagh, A. (2020): Nutrients Supplementation through Organic Manures Influence the Growth of Weeds and Maize Productivity. – Molecules 25(21):4924. https://doi.org/10.3390/molecules25214924
[20] Gu, R., Li, L., Liang, X., Wang, Y., Fan, T., Wang, Y., Wang, J., Gu, R., Li, L., Liang, X., Wang, Y., Fan, T., Wang, Y. (2017): The ideal harvesting time for seeds of hybrid maize (*Zea mays* L.) XY335 and ZD958 produced in multiple environments. – Sci. Rep. 7: 17537. DOI: 10.1038/s41598-017-16071-4.
[21] Iqbal, A., Iqbal, M.A., Awad, M.F., Nasir, M., EL Sabagh, A., Siddiqui, M.H. (2021): Spatial arrangements and seeding rates influence biomass productivity, nutritional value and economic viability of maize (*Zea mays* L.). – Pak. J. Bot. 53(3). DOI: http://dx.doi.org/10.30848/PJB2021-3(44)
[22] ISTA (2008): International Rules for Seed Testing. – International Seed Testing Association, Bassersdorf.
[23] ISTA (2015): International Rules for Seed Testing. – International Seed Testing Association (ISTA), Zurich.

http://www.aloki.hu ● ISSN 1589 1623 (Print) ● ISSN 1785 0037 (Online)
DOI: http://dx.doi.org/10.15666/aeer/1902_11231134
© 2021, ALÖKI Kft., Budapest, Hungary

[24] Kapilan, R. (2015): Accelerated aging declines the germination characteristics of the maize seeds. – Sch. Acad. J. Biosci. 3(8): 708-711.
[25] Kapoor, N., Arya, A., Siddiqui, M. A., Amir, A., Kumar, H. (2010): Seed deterioration in chickpea (*Cicer arietinum* L.) under accelerated aging. – Asian J. Plant Sci. 9(3): 158-162.
[26] Kinittle, K. H., Burris, J. S. (1976): Effect of kernel maturation on subsequent seedling vigor in maize. – Crop Sci. 16: 851-854. DOI: 10.2135/cropsci1976.0011183X 001600060030x.
[27] Konuskan, O., Konuskan Bozdogan, D., Levai, C. M. (2017): Effect of foliar boron fertilization on chemical propeties and fatty acid composition of corn (*Zea mays* L). – Rev. Chim. (Burcherest) 68(9): 2073-2075.
[28] Ma, B. L., Dwyer, L. M. (2001): Maize kernel moisture, carbon and nitrogen concentrations from silking to physiological maturity. – Can. J. Plant Sci. 81: 225-232. DOI: 10.4141/P00-073.
[29] Maqsood, Q., Abbas, R.N., Iqbal, A.M., Serap, A. K., Iqbal, A., EL Sabagh, A. (2020): Overviewing of weed management practices to reduce weed seed bank and to increase maize yield. – Planta Daninha, 38.
[30] Marcos-Filho, J. (2005): Fisiologia de sementes de plantas cultivadas. – FEALQ, Piracicaba.
[31] Molla, S. H., Sutkhet, N., Ali, M. A., Khan, A. S. M. M. R., Alam, M. R., Hossain, A., Farooq, M., EL Sabagh, A. (2019): Influence of nitrogen application on dry biomass allocation and translocation in two maize varieties under short pre-anthesis and prolonged bracketing flowering periods of drought. – Arch. Agron. Soil Sci. 65(7): 928-944.
[32] Mondo, V. H. V., Cicero, S. M., Dourado-Neto, D., Pupim, T. L., Dias, M. A. N. (2013): Seed vigor and initial growth of corn crop. – J. Seed Sci. 35(1): 64-69.
[33] Ranum, P., Peña-Rosas, J. P., Garcia-Casal, M. N. (2014): Global maize production, utilization, and consumption. – Ann. New York Acad Sci. 1312: 105-112.
[34] Rastegar, Z., Sedghi, M., Khomari, S. (2011): Effects of accelerated aging on soybean seed germination indexes at laboratory conditions. – Not. Sci. Biol. 3: 126.
[35] Roberts, B. E., Payne, P. I.,Osborne, D. J. (1973): Protein synthesis and the viability of rye grains: Loss of activity of protein-synthesizing systems in vitro associated with a loss of viability. – Biochem. J. 131: 275-286.
[36] Rosegrant, M. W., Agcaoili-Sombilla, M., Perez, N. D. (1995): Food, Agriculture and the Environment Discussion Paper 5. Global Food Projections to 2020: Implications for Investment. – IFPRI, Washington, DC.
[37] Sariyev, A., Barutcular, C., Acar, M., Hossain, A., EL Sabagh, A. (2020): Sub-surface drip irrigation in associated with H2O2 improved the productivity of maize under clay-rich soil of Adana, Turkey. – Phyton 89:519.
[38] TeKrony, D. M., Hunter, J. L. (1995): Effect of seed maturation and genotype on seed vigor in maize. – Crop Sci. 35: 857-862. DOI: 10.2135/cropsci1995.0011183 X003500030037x.
[39] Tian, Y., Guan, B., Zhou, D., Yu, J., Li, G., Lou, Y. (2014): Responses of seed germination, seedling growth, and seed yield traits to seed pretreatment in maize (*Zea mays* L.). – Sci. World J. 834630.
[40] Torres, C. A., Andrews, P. K. (2006): Developmental changes in antioxidant metabolites, enzymes and pigments in fruit exocarp of four tomato (*Lycopersicon esculentum* Mill.) genotypes: β-carotene, high pigment-1, ripening inhibitor and Rutgers. – Plant Physiol. Biochem. 44: 11-12.
[41] Vashisth, A., Nagarajan, S. (2009): Germination characteristics of seeds of maize (*Zea mays* L.) exposed to magnetic fields under accelerated ageing condition. – J. Agric. Physics 9: 50-58.

http://www.aloki.hu ● ISSN 1589 1623 (Print) ● ISSN 1785 0037 (Online)
DOI: http://dx.doi.org/10.15666/aeer/1902_11231134
© 2021, ALÖKI Kft., Budapest, Hungary

[42] Walters, C., Hill, L. M., Wheeler, L. J. (2005): Dying while dry: kinetics and mechanisms of deterioration in desiccated organisms. – Integrative and Comparative Biology 45(5): 751-758. https://doi.org/10.1093/icb/45.5.751.
[43] Wang, Y. R., Hampton, J. G., Hill, M. J. (1994): Red clover vigor testing - effects of three test variables. – Seed Sci. Technol. 22: 99-105.
[44] Woltz, J. M., TeKrony, D. M. (2001): Accelerated aging test for corn seed. – Seed Technol. 23: 21-34.
[45] Wych, R. D. (1988): Production of Hybrid Seed Corn. – Sprague, G. F., Dudley, J. W. (eds.) Corn and Corn Improvement. ASA, Madison, WI, pp. 565-607.

http://www.aloki.hu ● ISSN 1589 1623 (Print) ● ISSN 1785 0037 (Online)
DOI: http://dx.doi.org/10.15666/aeer/1902_11231134
© 2021, ALÖKI Kft., Budapest, Hungary

THE EFFECTS OF ANTAGONISTIC BACTERIA AGAINST WHITE MOLD DISEASE AGENT [*SCLEROTINIA SCLEROTIORUM* (LIB.) DE BARY] IN CUCUMBER

BAYRAM, M. – BELGUZAR, S.*

Plant Protection Department, Agricultural Faculty, Tokat Gaziosmanpasa University, Tokat, Turkey

**Corresponding author*
e-mail: sabriye.yazici@gop.edu.tr; phone: +90-356-252-1616; fax: +90-356-252-1488

(Received 13th Sep 2020; accepted 11th Feb 2021)

Abstract. This study was carried out to determine the effects of antagonistic bacteria, which were obtained from the soil rhizosphere and have the strong abilities to dissolve phosphorus and reduce nitrogen, on the white mold disease agent *Sclerotinia sclerotiorum* (Lib.) de Bary. In the study, ten antagonistic bacteria of the genus *Pseudomonas* were used. In the *in vitro* study, the tested antagonistic bacteria suppressed the mycelial growth of *S. sclerotiorum* by 65.49-88.25%. Isolates with a high inhibition rate on mycelial growth were also effective on the viability of the sclerotia of the pathogenic fungus. Five bacterial isolates caused complete sclerotia viability loss for *S. sclerotiorum*. According to the result of the in vitro studies, antagonistic bacterial isolates with strong effects on the pathogenic fungus were selected and assayed in pot studies under greenhouse conditions. In pot studies, single treatments with *Pseudomonas chlororaphis* (R-7) and the dual treatments with *Pseudomonas brassicacearum* + *Pseudomonas chlororaphis* (R-3 + R-7) were the most effective against white mold disease. The results of this study show that these antagonistic bacteria can be used in the biological control of *S. sclerotiorum*. In addition to the in vitro and in vivo studies, it is necessary to determine the performances of antagonistic bacterial isolates, which had the highest effect on white mold disease, in greenhouses and field conditions.
Keywords: *biological control, Sclerotinia sclerotiorum, Pseudomonas brassicacearum, Pseudomonas chlororaphis*

Introduction

Species in *Sclerotinia* genus are soil-borne pathogens that cause significant losses to host plants. *Sclerotinia sclerotiorum* (Lib.) de Bary, causes white mold disease in field crops and vegetables all over the world especially in temperate regions (Ferreira and Boley, 2002). *S. sclerotiorum* is a reported host range of over 500 plant species from 75 families (Saharan and Mehta, 2008). In Turkey, white mold diseases has been reported in various proportions on lettuce (*Lactuca sativa* L.) in Izmir, Manisa and Aydın (Yıldız, 1970), on sunflower (*Helianthus annus* L.) in Thrace Region and Cukurova Region (Yucer, 1980; Cınar and Bicici, 1982), on cucumber (*Cucumis sativus* L.), tomato (*Solanum lycopersicum* L.) and eggplants (*Solanum melongena* L.) in the Eastern Mediterranean Region (Aksay et al., 1991), on cucumber in Tokat and Amasya (Onaran and Yanar, 2004), on lettuce in Canakkale (Turk and Dogu, 2004), on greenhouse tomatoes in the provinces of Hatay, Adana, Mersin and Antalya (Tok and Kurt, 2007), in the sunflower fields of the Pasinler Plain of Erzurum (Tozlu and Demirci, 2008), on cucumbers in the greenhouses of Antalya (Onaran, 2009) and on potato in Hatay province (Kurt et al., 2017).

Sclerotinia sclerotiorum produces lots of mycelia and these mycelia aggregate to form a hard, dark brown or black sclerotia, which are of different sizes and irregular

http://www.aloki.hu ● ISSN 1589 1623 (Print) ● ISSN 1785 0037 (Online)
DOI: http://dx.doi.org/10.15666/aeer/1902_11351147
© 2021, ALÖKI Kft., Budapest, Hungary

shapes. This agent is easily recognized from this sclerotium, which is resistant to unfavorable environmental conditions. *S. sclerotiorum* usually attacks the roots or stem of the host that are in close proximity to the soil. Lesions develop on the stem and gradually surround the roots, and the host plant withers and dies. This fungus can cause complete rotting of seedlings, especially in humid environments (Anonymous, 2008).

This pathogen overwinters as sclerotium in soil, contaminated plant debris or as mycelia. In the spring, sclerotia germinates and forms apothecia in which asci and ascospores are produced. Ascospores are released into the air from the apothecia and infection begins when they land and germinate on host plant (Agrios, 1997). Studies have stated that the sclerotia of this fungus can survive in the soil for more than 5 years (Adams and Ayers, 1979) and that environmental conditions are important in the development of the disease.

Cultural measures, physical control, fumigation of soil and green parts are used in the management of white mold disease (Anonymous, 2008), however, difficulties are experienced in managing the disease as some varieties are susceptible to the pathogen, sclerotia of this fungal pathogen can remain viable or many years and not all of them germinate at the same time and more importantly the pathogen is becoming more resistant to currently available fungicides. Accordingly, different alternative methods to chemical control such as the use of antagonistic bacteria and plant growth promoting rhizobacteria (PGPR) are in demand. These bacteria are densely located around the soil rhizosphere of plant roots and they carry out physiochemical activities in the soil. They are in close relationship with plant roots and directly or indirectly have positive effect the development of the plants. These bacteria can be found in several genera but those in the genus *Pseudomonas* are highly efficacious and can multiply rapidly in the soil rhizosphere and spread to the root. In addition, by protecting the plant from stress, they promote plant root and shoot development, improve yield and protect plants against diseases (Imriz et al., 2014).

Several studies have been conducted by various researchers on the biological control of *Sclerotinia sclerotiorum* (Zazzerini and Tosi, 1985; Bogdanova et al., 1986; Turhan and Grossmann, 1986; Inbar et al., 1996; Aksay et al., 1991; Tuncer and Damdere, 1997; Thaning et al., 2001; Al-Masri et al., 2002; Kamensky et al., 2003; Mansour et al., 2008; El-Kafrawy, 2008; Onaran and Yanar, 2011; Tozlu and Demirci, 2011; Rostami et al., 2013; Tozlu et al., 2016; Abdeljalil et al., 2016; Helmy, 2016; Mun et al., 2019). In the search for alternatives, a number of mycoparasitic fungi grow on sclerotia (Adams, 1990) and *Coniothyrium minitans* was the most investigated fungi on *S. sclerotiorum* (Whipps and Gerlagh, 1992; Budge et al., 1995; McLaren et al., 1996; Whipps et al., 2008) and has become available as a commercial product for sclerotia (Gerlagh et al., 1999). Also, *Gliocladium virens* and *Trichoderma harzianum* have been reported to reduce growth of mycelium and apothecial production of *S. sclerotiorum* (Phillips, 1986; Whipps and Budge, 1990; Srinivasan et al., 2001; Mehta et al., 2012). Among the antagonistic bacteria species tested, *Bacillus subtilis* and *Bacillus cereus* have been reported to reduce germination of sclerotia and cause hyphal death (Zazzerini et al., 1987; Kamal et al., 2015; Sun et al., 2017). Similarly, it has been determined that *Pseudomonas putida* and *P. fluorescens* species reduce the damage caused by *S. sclerotiorum* (Expert and Digat, 1995), and that *Bacillus* spp. and *Pseudomonas* spp. prevent disease development by 75.3% (Soylu et al., 2005). Also, *Serretia plymuthia* was highly effective in inducing complete suppression of apothecial formation and

http://www.aloki.hu ● ISSN 1589 1623 (Print) ● ISSN 1785 0037 (Online)
DOI: http://dx.doi.org/10.15666/aeer/1902_11351147
© 2021, ALÖKI Kft., Budapest, Hungary

strongly inhibited the germination of ascospores (Thaning et al., 2001). Under in vivo conditions, *Burkholderia cepacia,* and *Serratia plymuthica* species (Onaran and Yanar, 2011), *B. subtilis, Serratia* sp., and *P. fluorescens* (Helmy, 2016; El-Kafrawy, 2008), *P. chlororaphis* PA-23 (Savchuck, 2002) species have described to significantly reduce disease development. Studies conducted at the same time have also determined that *B. subtilis, B. thuringiensis, B. amyloliquefaciens, Enterobacter cloacae,* and *P. fluorescens* isolates positively affect plant growth (El-Kafrawy, 2008; Abdeljalil et al., 2016).

The aim of this study was to determine the effects of antagonistic bacteria isolates obtained from tomato production areas in Tokat province on *Sclerotinia sclerotiorum,* which causes white mold disease in cucumbers.

Materials and methods

In the study, 10 antagonistic bacterial isolates with high phosphate-reducing and nitrogen-binding properties, previously isolated from tomato production areas in Tokat province in Turkey and described with biochemical tests and MALDI-TOF technique, were used (*Table 1*). *Sclerotinia sclerotiorum* isolate used in the study was isolated from infected tissues of cucumber plant and identified using morphologically and molecular analysis (PCR).

Tests were carried out in Tokat province of Turkey in 2019. In vitro and in vivo tests were carried out as laboratory test and pot studies, respectively.

Table 1. *Scientific names and codes of antagonistic bacteria used in this study*

Isolate code	Scientific name of the isolate
R-1	*Pseudomonas kilonensis*
R-2	*Pseudomonas monteilii*
R-3	*Pseudomonas brassicacearum*
R-4	*Pseudomonas thivervalensis*
R-5	*Pseudomonas koreensis*
R-6	*Pseudomonas thivervalensis*
R-7	*Pseudomonas chlororaphis*
R-8	*Pseudomonas* sp.
R-9	*Pseudomonas* sp.
R-10	*Pseudomonas thivervalensis*

In vitro tests

Determination of the effects of antagonistic bacteria on the mycelial development of Sclerotinia sclerotiorum

Tryptic soy agar (TSA) was used throughout this study. The antagonistic bacterial isolates grown TSA for 24 h were inoculated in a ring form on the edges of the medium in 90 mm diameter petri dishes. Then, a 5 mm diameter mycelium disc was taken from *S. sclerotiorum* culture and placed in the center of the medium (*Fig. 1*). In the control group, only the pathogen fungus was plated onto the medium without bacteria. Petri dishes were wrapped with Parafilm and left to incubation at 25 °C. The

http://www.aloki.hu ● ISSN 1589 1623 (Print) ● ISSN 1785 0037 (Online)
DOI: http://dx.doi.org/10.15666/aeer/1902_11351147
© 2021, ALÖKI Kft., Budapest, Hungary

experiments were ended when the fungus in the control group completely covered the petri dish and the radial growth of fungi in the control group and petri dishes treated with antagonist bacteria were measured (Tozlu et al., 2016; Kotan, 2017). Inhibition rates (%) were calculated by comparing the measured mycelium diameters. The experiment was repeated twice with five replicates per treatment (Aeron et al., 2011).

$$I\ (\%) = [(C - T) / (C - C_0)] \times 100$$

I: inhibition rate (%); C: mycelial diameter of the pathogen in control; T: mycelial diameter of the pathogen in bacterial treatment; C_0: the diameter of the test fungus agar discs (5 mm).

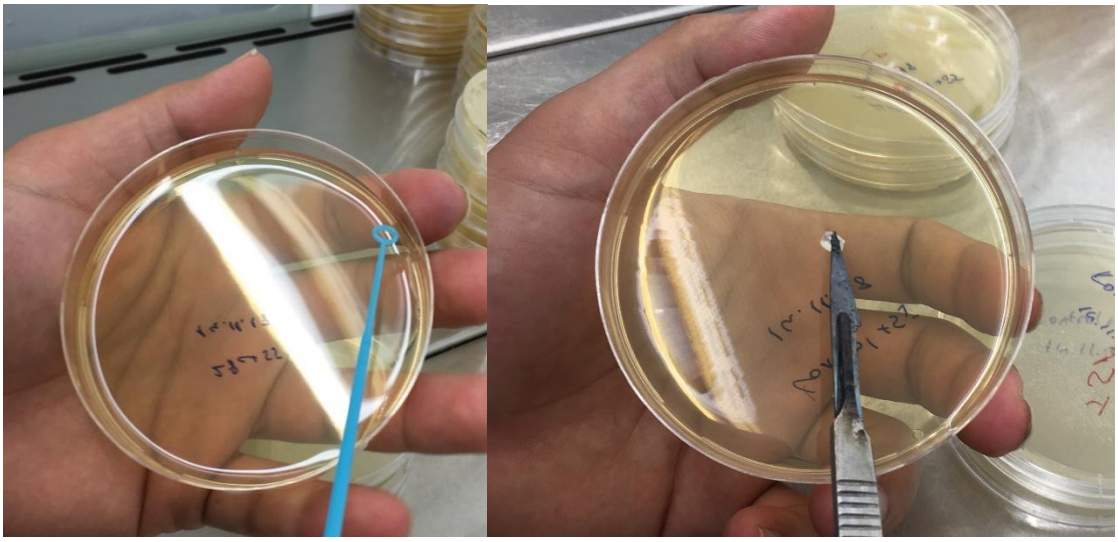


Figure 1. *Inoculation of antagonistic bacteria in a ring form on the edges of the medium-position of mycelium disc from S. sclerotiorum culture in the center of the medium*

Determination of the effects of antagonistic bacteria on germination of Sclerotinia sclerotiorum sclerotia

First the sclerotia of *S. sclerotiorum,* which were developed on Potato Dextrose Agar (PDA) medium for 10 days, were subjected to surface sterilization by immersing in 2% sodium hypochlorite and passing through sterile distilled water three times. The surface-sterilized sclerotia were placed in bacterial suspensions with 10^8 cells/ml density prepared with 10 ml of Luria Bertani Broth (LB) medium. Five sclerotia were used for each antagonistic bacteria isolate, and the treated erlenmeyers were incubated in a rotary incubator at 175 rpm for 24 h. The sclerotia treated with antagonistic bacteria were dissected into two with a scalpel and transferred to the PDA medium and left to incubate at 25 °C for five days. The sclerotia that germinated at the end of the incubation period were considered to be alive and the diameter of mycelium were measured and recorded. For the control group, five sclerotia were placed in LB medium without bacterial isolates. Each treatment in the experiment had three replicates and the study was repeated twice. The effects of the antagonistic bacterial isolates on the survival rates and mycelium growth of sclerotia was determined and compared with the control group (Abdeljalil et al., 2016).

http://www.aloki.hu ● ISSN 1589 1623 (Print) ● ISSN 1785 0037 (Online)
DOI: http://dx.doi.org/10.15666/aeer/1902_11351147
© 2021, ALÖKI Kft., Budapest, Hungary

In vivo test

According to the results obtain in the in vitro test, pot experiments were conducted using single, double and triple combinations of the three antagonistic bacteria isolates which had the highest effect on the pathogen. Dörtel F1 cucumber variety, which is sensitive to pathogen fungus, was used in the study which was conducted under controlled greenhouse conditions. Bacterial isolates that were streaked on King B media and incubated at 28 °C for 48 h. Grown bacterial isolates were suspended in saline (0.85% NaCl), and the density was adjusted to 10^8 cells/ml at 600 nm using spectrophotometer (PG Instrument T60U UV/VIS). Cucumber seedlings were dipped into the prepared suspension and left for 1 h for bacteria colonization and then planted in pots with sterile soil, peat and perlite (1:1:0.5). Seven days after the seedlings were transferred to the pots, a wound with a diameter of 5 mm was opened on the plant stem 4 cm above the soil, then 0.5 ml (10^8 cells/ml) bacterial suspension pipetted was on the wounds. Immediately afterwards, a 5-mm mycelium disc of *S. sclerotiorum* was placed on the opened wound. The inoculated spot was covered with moist cotton and wrapped with plastic film. Positive control group had plants inoculated only with *S. sclerotiorum* (Tozlu et al., 2016). In the negative control group, only water was applied to the plants, and for the chemical control group, Metalaxyl-M + Fludioxonil was applied to the plants at the dose recommended by the producer. Trial coincidence plots were set up two times with 10 replicates according to the trial pattern. Seven days after the application, dead and living plants in the control group and the treatments were counted.

Statistical analyses

The data obtained in the study were analyzed using variance analysis in SPSS statistics 25 package program and the differences between the means were determined with Duncan multiple comparison test at the $p \leq 0.05$ significance level.

Results

In vitro tests

Effects of antagonistic bacteria on the mycelial development of Sclerotinia sclerotiorum

In in vitro studies, ten of the antagonistic bacteria isolates tested showed varying effects ranging between 65.49 and 88.25% on the pathogenic fungus, *S. sclerotiorum*. As can be seen in *Table 2,* it was determined that the effect of all bacterial isolates on the fungus were statistically significant compared to the control group. R-6 coded *Pseudomonas thivervalensis* isolate had the highest (88.25%) effect on fungal pathogen (*Fig. 2*). All of the bacterial isolates tested had an inhibitory effect on the mycelium growth of the fungal pathogen greater than 60% (*Table 2*).

The effect of antagonistic bacteria on the germination of Sclerotinia sclerotiorum sclerotia

In this part of the study, the effect of the bacterial isolates on sclerotia viability was examined and according to the results, sclerotia treated with five isolates (R-1, R-2, R-4, R-5, R8) remained viable while the sclerotia treated with other five isolates (R-3, R-6, R-7, R-9, R-10) were dead. Isolates which were highly efficacious on mycelium

http://www.aloki.hu ● ISSN 1589 1623 (Print) ● ISSN 1785 0037 (Online)
DOI: http://dx.doi.org/10.15666/aeer/1902_11351147
© 2021, ALÖKI Kft., Budapest, Hungary

development were also effective on sclerotia. In addition, R2, R4 and R5 coded antagonists significantly suppressed mycelial growth of sclerotia that did not lose their viability. This situation reveals that these antagonists have fungistatic effects (*Table 3*).

Table 2. *The effects of antagonistic bacteria on the mycelial development of Sclerotinia sclerotiorum*

Codes	Treatments	Diameter of mycelium (mm)	Average effect rate (%)
K	Control	90 a*	0 f
R-1	*Pseudomonas kilonensis*	23.81 cd	73.54 cd
R-2	*Pseudomonas monteilii*	13.46 ef	85.04 ab
R-3	*Pseudomonas brassicacearum*	10.85 f	87.93 a
R-4	*Pseudomonas thivervalensis*	12.40 ef	86.31 ab
R-5	*Pseudomonas koreensis*	15.27 e	83.03 b
R-6	*Pseudomonas thivervalensis*	10.56 f	88.25 a
R-7	*Pseudomonas chlororaphis*	14.71 ef	83.64 ab
R-8	*Pseudomonas* sp.	31.05 b	65.49 e
R-9	*Pseudomonas* sp.	25.86 c	71.26 d
R-10	*Pseudomonas thivervalensis*	20.03 d	77.73 c

*The same letters next to averages in the same column indicate that difference between applications are not significant. (Duncan multiple comparison test, $p \leq 0.05$)

Table 3. *The effect of antagonistic bacteria on Sclerotinia sclerotiorum sclerotia viability*

Codes	Treatments	Sclerotia viability	Diameter of mycelium (mm)
K	Control	Viable	60 a*
R-1	*Pseudomonas kilonensis*	Viable	53.09 b
R-2	*Pseudomonas monteilii*	Viable	21.25 d
R-3	*Pseudomonas brassicacearum*	Dead	0 f
R-4	*Pseudomonas thivervalensis*	Viable	14.27 e
R-5	*Pseudomonas koreensis*	Viable	26.38 cd
R-6	*Pseudomonas thivervalensis*	Dead	0 f
R-7	*Pseudomonas chlororaphis*	Dead	0 f
R-8	*Pseudomonas* sp.	Viable	32.39 c
R-9	*Pseudomonas* sp.	Dead	0 f
R-10	*Pseudomonas thivervalensis*	Dead	0 f

*The same letters next to averages in the same column indicate that difference between applications are not significant. (Duncan multiple comparison test, $p \leq 0.05$)

In vivo test

In vivo tests were conducted with three isolates (R-3, R-6 and R-7) which had the highest effects on the mycelial growth and sclerotia viability of *S. sclerotiorum* in the in vitro studies. Single, double and triple combinations of these three isolates were used. In the evaluation of the applications in the pot study conducted under greenhouse conditions,

http://www.aloki.hu ● ISSN 1589 1623 (Print) ● ISSN 1785 0037 (Online)
DOI: http://dx.doi.org/10.15666/aeer/1902_11351147
© 2021, ALÖKI Kft., Budapest, Hungary

the dead/alive plants were counted. According to the results of the study, 100% death occurred in positive control where only the fungal pathogen was applied, whereas no plant death occurred in negative control and pesticide control applications. In R-3 single application and R-3 + R-6 + R-7 triple combination application, death (50%) occurred in 5 out of 10 plants. In R-6 single application, and R-3 + R-6 and R-6 + R-7 double combination applications, death occurred in 6 out of 10 plants (60%). Among the applications, the highest effect was seen in R-7 single application (*Fig. 3*) and R-3 + R-7 double application. In both applications, while death occurred in 2 out of 10 plants, it was observed that 8 of them were alive and there were no signs of disease or death. It was found that the disease was suppressed by 80% in both applications (*Table 4*).

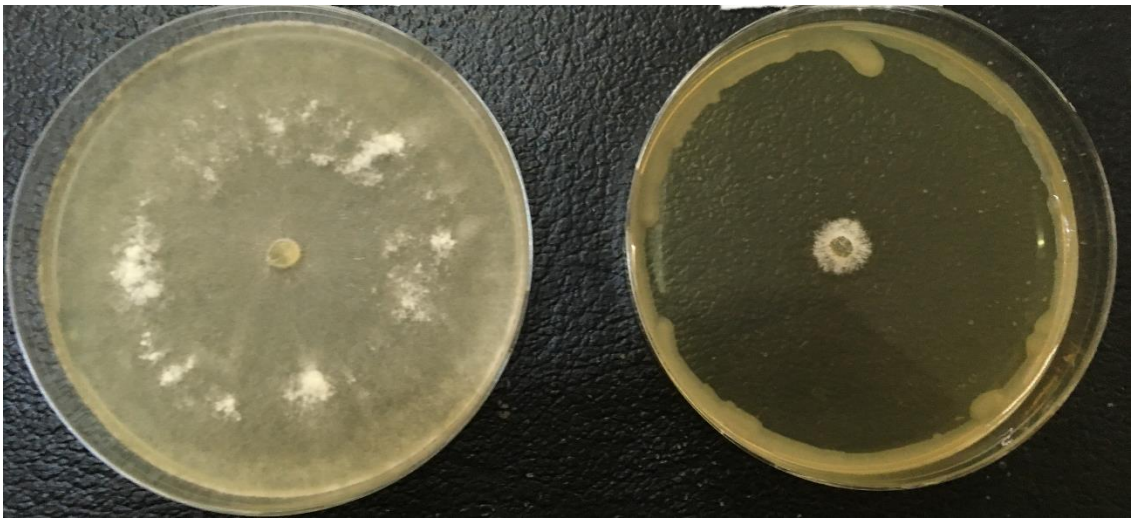


Figure 2. *Effect of R-6 coded Pseudomonas thivervalensis isolate on the mycelial development of S. sclerotiorum*

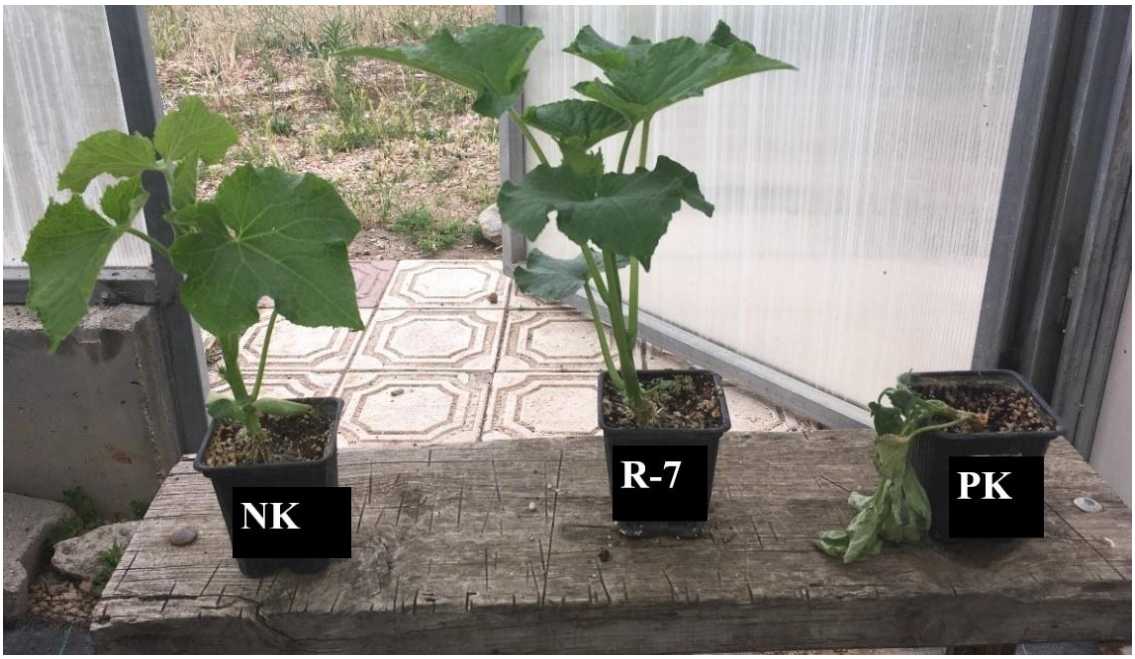


Figure 3. *Differences in plant growth in NK, R-7 and PK treatments*

http://www.aloki.hu ● ISSN 1589 1623 (Print) ● ISSN 1785 0037 (Online)
DOI: http://dx.doi.org/10.15666/aeer/1902_11351147
© 2021, ALÖKI Kft., Budapest, Hungary

Table 4. *The effect of antagonistic bacteria on white rot disease in cucumber plant*

Codes	Treatments	Number of dead plants	Number of live plants	Inhibition rate (%)
PK	*Sclerotinia sclerotiorum* treatment	10	0	0
NK	Treatment with pure water	0	10	100
IK	Metalaxyl-M + Fludioxonil	0	10	100
R-3	*Pseudomonas brassicacearum*	5	5	50
R-6	*Pseudomonas thivervalensis*	6	4	40
R-7	*Pseudomonas chlororaphis*	2	8	80
R-3 + R-6	*Pseudomonas brassicacearum* + *Pseudomonas thivervalensis*	6	4	40
R-3 + R-7	*Pseudomonas brassicacearum* + *Pseudomonas chlororaphis*	2	8	80
R-6 + R-7	*Pseudomonas thivervalensis* + *Pseudomonas chlororaphis*	6	4	40
R-3 + R-6 + R-7	*Pseudomonas brassicacearum* + *Pseudomonas thivervalensis* + *Pseudomonas chlororaphis*	5	5	50

Discussion

Today, in order to increase the quality and yield in plant production and reduce the use of pesticides, the use of antagonistic bacteria against plant diseases and/or plant growth regulating rhizobacteria within the scope of biological control has been an important research topic. Studies with these bacteria show that they are promising in terms of suppressing plant diseases and ensuring healthy plant growth. Although cultural measures, physical and chemical control are used in the management of white mold disease, there are difficulties in managing the disease due to fungicide resistance problem and the survival of sclerotia for many years.

In this study, the effects of antagonistic bacteria which were obtained from the soil rhizosphere and have the high ability to dissolve phosphorus and reduce nitrogen, was determined on the white mold disease agent *Sclerotinia sclerotiorum* (Lib.) de Bary in vitro and in vivo conditions. Our in vitro studies, antagonistic bacteria isolates tested showed varying effects ranging between 65.49-88.25% on *S. sclerotiorum*. And, five bacterial isolates caused complete sclerotia viability loss for *S. sclerotiorum*. Numerous studies similar to our in vitro study have been carried out by various researchers. El-Kafrawy (2008) reported that *Pseudomonas fluorescens* had an antagonistic effect of 69.26% on the radial growth of *S. sclerotiorum* and showed a significant suppressive effect on formation of sclerotia. A study by Helmy (2016) established that *Streptomyces* sp., *Pseudomonas fluorescens* and *Bacillus subtilis* (Bs1) reduced mycelium growth of *S. sclerotiorum* by 72.2%, 68.0, 62.22 respectively. Soylu et al. (2005) examined the antagonistic potential of 113 bacterial isolates against *S. sclerotiorum* in dual petri dishes and reported that *Pseudomonas* spp. AFP104 isolate was 83.3% effective on fungal pathogen. Similarly, study conducted by Onaran and Yanar (2011) showed that 12 of the 23 tested isolates especially *P. putida* and *P. fluorescens* from the genus *Pseudomonas, Paenibacillus macerans*, and *Bacillus pumilis* were highly effective and caused sclerotia death.

In our pot studies, *Pseudomonas chlororaphis* (R-7) and *Pseudomonas brassicacearum* + *Pseudomonas chlororaphis* (R-3 + R-7) were the most effective against white mold disease. It was found that the disease was suppressed by 80% in both applications. Previous studies conducted on the biological control of white mold disease

http://www.aloki.hu ● ISSN 1589 1623 (Print) ● ISSN 1785 0037 (Online)
DOI: http://dx.doi.org/10.15666/aeer/1902_11351147
© 2021, ALÖKI Kft., Budapest, Hungary

have determined that several antagonistic bacteria partially or completely inhibits this fungal agent. Similar to our study, Onaran and Yanar's (2011) study under greenhouse conditions showed that the bacterial isolates tested were effective at 43.20-89.22% on white mold disease with *Burkholderia cepecia* being the most effective. Likewise, Helmy (2016) reported that dipping seedlings into bacterial suspensions of *Bacillus subtilis, B. thuringiensis* and *Streptomyces* sp. prevented the disease severity caused by fungal pathogen by 100% after one week. A greenhouse study determined that *Bacillus subtilis* and *Pseudomonas fluorescens* species prevented white mold disease by 95-100% and 85-90%, respectively when cucumber seedlings were planted in soils treated with these antagonistic bacteria (El-Kafrawy, 2008).

Besides cucumber plants, a study conducted under greenhouse and field conditions for the biological control of *S. sclerotiorum* in canola plant, showed that *P. chlororaphis* (PA-23), *Pseudomonas* sp. (DF-41) significantly suppressed the disease compared to *B. amyloliquefaciens* (BS6) fungicide application. While the rate of stem mold in the canola plants varied between 20-75%, this rate was 5.0-29.6% in *P. chlororaphis* application (Fernando et al., 2007). In addition, Savchuck and Fernando (2004) stressed that the application of *P. chlororaphis* and *P. brassicacearum* at a density of 10^4-10^8 cfu/ml was highly effective on ascospore germination.

Antagonistic bacteria against *S. sclerotiorum* affect the systemic resistance of the host plant. *Pseudomonas* spp., produces numerous antimicrobial compounds such as pyoluteorin, pyrrolnitrin, phenazines, siderophores, cyanide, 2,4-diacetylphloroglucinol (Compant et al., 2005) and enzymes such as cellulose, chitinase, proteases, beta-glucanase (Hernandez-Leon et al., 2015). Similarly, bacterial isolates of *Pseudomonas* spp. DF200 and DF209 which inhibit *S. sclerotiorum* under in vitro conditions produce benzothiazole, cyclohexanol, n-decanal, dimethyl trisulfide, 2-ethyl 1-hexanol, nonanal antifungal organic volatile compounds. In the field, bacteria prevent carpogenic germination of sclerotia and emergence of ascospores (Fernando et al., 2004). It has been reported that *Pseudomonas brassicacearum,* used in the present study, uses hydrogen cyanide (HCN), protease, alginate, sclerocin and lipopeptide molecules, 2,4-diacetylphloroglucinol and antifungal compounds such as cyanide in suppressing *S. sclerotiorum* (Berry et al., 2010, 2014; Ortet et al., 2011; Loewen et al., 2014).

Pseudomonas chlororaphis, also used in this study, is an important biocontrol agent that suppresses *S. sclerotiorum* by producing antibiotics such as phenazine-1-carboxylic acid,2-hydroxyphenazine and pyrrolnitrin (PRN) which causes hyphal lysis, vacuolation and protoplast leakage, hereby preventing sclerotia and spore germination (Savchuck, 2002; Fernando et al., 2007; Zhang et al., 2004a, b; Selin et al., 2010).

Conclusion

In recent years, negatives effects of pesticides used extensively in agricultural areas on both the environment and human health have been reported in many studies. Antagonistic bacteria or plant growth promoting rhizobacteria have the potential to protect against soil-borne pathogens. Biopreparat or biofertilizers made from such microorganisms can be widely used in areas where sustainable organic agriculture. Our study revealed that antagonistic bacterial isolates have the potential to be used as a biological control agent against white rot disease. In this context, the efficacy of the R-7 coded isolate and the R-3 + R-7 coded double combination, which were effective on the agent in both the in vitro and in vivo studies, should also be evaluated under greenhouse and field conditions.

http://www.aloki.hu ● ISSN 1589 1623 (Print) ● ISSN 1785 0037 (Online)
DOI: http://dx.doi.org/10.15666/aeer/1902_11351147
© 2021, ALÖKI Kft., Budapest, Hungary

Acknowledgements. This study was extracted from the first author's master's thesis and was supported by the Tokat Gaziosmanpasa University Scientific Research Projects with the project no 2019/24 in Turkey.

REFERENCES

[1] Abdeljalil, N. O. B., Vallance, S., Gerbore, J., Rey, P., Daami-Remadi, M. (2016): Bio-suppression of *Sclerotinia* stem rot of tomato and biostimulation of plant growth using tomato-associated rhizobacteria. – Journal of Plant Pathology and Microbiology 7(2): 331.

[2] Adams, P. B. (1990): The potential of mycoparasites for biological control of plant diseases. – Annual Review of Phytopathology 28: 59-72.

[3] Adams, P. B., Ayers, W. A. (1979): Ecology of *Sclerotinia Species*. – Phytopathology 69: 896-899.

[4] Aeron, A., Dubey, R. C., Maheshwari, D. K., Pandey, P., Bajpai, V. K., Kang, S. C. (2011): Multifarious activity of bioformulated *Pseudomonas fluorescens* PS1 and biocontrol of *Sclerotinia sclerotiorum* in Indian rapeseed (*Brassica campestris* L.). – Eur. J. Plant Pathology 131(1): 81-93.

[5] Agrios, G. N. (1997): Plant Pathology. – Academic Press, California.

[6] Aksay, A., Bicici, M., Cinar, O. (1991): Determination of Antagonists against *Sclerotinia sclerotiorum* (Lib) De Bary Causal Agent White Mold Disease. – Cukurova University Journal of Agricultural Faculty 6(2): 55-62.

[7] AL-Masri, M. I., Ali-Shtayeh, M. S., Elad, Y., Sharon, A., Tudzynski, P., Barakat, R. (2002): Effect of plant growth regulators on white mold (*Sclerotinia sclerotiorum*) on bean and cucumber. – Journal Phytopathology 150: 481-487.

[8] Anonymous (2008): Agricultural Control, Plant Health. – Republic of Turkey Ministry of Agriculture and Forestry, Ankara, pp. 73-77.

[9] Berry, C., Fernando, W. G. D., Loewen, P. C., de Kievit, T. R. (2010): Lipopeptides are essential for *Pseudomonas* sp. DF41 biocontrol of *Sclerotinia sclerotiorum.* – Canadian Journal of Plant Pathology 16: 93-108.

[10] Berry, C., Nandi, M., Manuel, J., Brassinga, A. K. C., Fernando, W. G. D., Loewen, P. C., de Kievit, T. R. (2014): Characterization of the *Pseudomonas* sp. DF41 quorum sensing locus and its role in fungal antagonism. – Biological Control 69: 82-89. http://dx.doi.org/10.1016/j.biocontrol.2013.11.005.

[11] Bogdanova, V. N., Karadzhova, L. V., Klimenko, T. F. (1986): Use of *Coniothyrum minitans* Cambell as a hyperparasite in controlling the pathogen of white rot of sunflower. – Sel's Kokhozyaistvennaya Biologia 5: 80-84.

[12] Budge, S. P., McQuilken, M. P., Fenlon, J. S., Whipps, J. M. (1995): Use of *Coniothyrium minitans* and *Gliocladium virens* for biological control of *Sclerotinia sclerotiorum* in glasshouse lettuce. – Biological Control 5: 513-522.

[13] Cınar, A., Bicici, M. (1982): Etiology and importance of head rot and root collar and stem blight diseases in sunflower plots in Cukurova. – III. Turkey Phytopathology Congress (12-15 October 1982) Adana, pp. 68-79.

[14] Compant, S., Duffy, B., Nowak, J., Christophe, C., Ait Barka, E. (2005): Use of plant growth-promoting bacteria for biocontrol of plant diseases: principles, mechanisms of action, and future prospects. – Applied and Environmental Microbiology 71(9): 4951-4959.

[15] Elkafrawy, A. (2008): biological control of white rot of cucumber caused by *Sclerotinia sclerotiorum* under greenhouse conditions. – Journal of Agricultural Research 6(1).

[16] Expert, J. M., Digat, B. (1995): Biocontrol of *Sclerotinia* wilt of sunflower by *Pseudomanas fluorescens* and *Pseudomonas putida* strains. – Canadian Journal of Microbiology 41: 685-691.

http://www.aloki.hu ● ISSN 1589 1623 (Print) ● ISSN 1785 0037 (Online)
DOI: http://dx.doi.org/10.15666/aeer/1902_11351147
© 2021, ALÖKI Kft., Budapest, Hungary

[17] Fernando, W. G. D., Nakkeeran, S., Zhang, Y. (2004): Ecofriendly methods in combating *Sclerotinia sclerotiorum* (Lib.) de Bary. – Recent Res. Devel. Environ. Biol. 1: 329-347.
[18] Fernando, W. G. D., Nakkeeran, S., Zhang, Y., Savchuk, S. (2007): Biological control of *Sclerotinia sclerotiorum* (Lib.) de Bary by *Pseudomonas* and *Bacillus* species on canola petals. – Crop Protection 26: 100-107.
[19] Ferreira, S. A., Boley, R. A. (2002): *Sclerotinia sclerotiorum*. – http://www.extento.hawaii.edu/kbase/Crop/Type/s_scler.htm (01.09.2018).
[20] Gerlagh, M., Goossen-van de Geijn, H. M., Fokkema, N. J., Vereijken, P. F. (1999): Long-term biosanitation by application of *Coniotyhrium minitans* on *Sclerotinia sclerotiorum*-infected crops. – Phytopathology 89(2): 141-147.
[21] Helmy, K. G. (2016): Screening potential of some bacterial species and *Trichoderma harzianum* against *Sclerotinia sclerotiorum* on cucumber. – Journal of Plant Protection and Pathology 7(12): 867-872.
[22] Hernandez-Leon, R., Rojas-Solis, D., Contreras-Perez. M., Orozco-Mosqueda, M. C., Macias-Rodriguez, L. L., Reyes-de la Cruz, H., Valencia-Cantero, E., Santoyo, G. (2015): Characterization of the antifungal and plant growth-promoting effects of diffusible and volatile organic compounds produced by *Pseudomonas fluorescens* strains. – Biological Control 81: 83-92.
[23] Imriz, G., Ozdemir, F., Topal, I., Ercan, B., Tas, M. N., Yakısır, E., Okur, O. (2014): Plant growth promoting rhizobacteria and effect mechanisms of PGPR in plant production. – Electronic Microbiology Journal TR. 12: 1-19.
[24] Inbar, J., Menendez, A., Chet, I. (1996): Hyphal Interaction between *Trichoderma harzianum* and *Sclerotinia sclerotiorum* and its role in biological control. – Soil Biology and Biochemistry 28(6): 757-763.
[25] Kamal, M. M., Lindbeck, K. D., Savocchia, S., Ash, G. J. (2015): Biological control of sclerotinia stem rot of canola using antagonistic bacteria. – Plant Pathology 64: 1375-1384.
[26] Kamensky, M., Ovadis, M., Chet, I., Chernin, L. (2003): Soil-borne strain IC14 of *Serratia plymuthica* with multiple mechanisms of antifungal activity provides Biocontrol of *Botrytis cinerea* and *Sclerotinia sclerotiorum* diseases. – Soil Biology and Biochemistry 35: 323-331.
[27] Kotan, R. (2017): Oral presentation. – 6th Entomopathogens and Microbial Control Congress, 14-16 September 2017, Gaziosmanpasa University, Tokat, Turkey.
[28] Kurt, S., Uysal, A., Kara, M., Soylu, S., Soylu, E. M. (2017): Natural infection of potato by *Sclerotinia sclerotiorum* causing stem rot disease in Turkey. – Australasian Plant Disease Notes 12: 39.
[29] Loewen, P. C., Switala, J., Fernando, W. G. D., de Kievit, T. (2014): Genome sequence of *Pseudomonas brassicacearum* DF41. – Genome Announcements 2(3): e00390-14: 1-2.
[30] Mansour, T. A., Nida, Y. A., Patrice, S. (2008): Biological control of *Sclerotinia sclerotiorum* (Lib.) de Bary with *Trichoderma harzianum* and *Bacillus amyloliquefaciens*. – Crop Protection 27: 1354-1359.
[31] McLaren, D. L., Huang, H. C., Rimmer, S. R. (1996): Control of apothecial production of *Sclerotinia sclerotiorum* by *Coniothyrium minitans* and *Talaromyces flavus*. – Plant Disease 80: 1373-1378.
[32] Mehta, N., Hieu, N., Sangwan, M. (2012): Efficacy of various antagonistic isolates and species of against causing white stem rot of mustard. – Journal of Mycology and Plant Pathology 42(2): 244-250.
[33] Mun, B-G., Lee, W-H, Kang, S-M, Lee, S-U, Lee, S-M., Lee, D-Y, Shahid, M., Yun, B-W, Lee, I-J. (2019): *Streptomyces* sp. LH4 promotes plant growth and resistance against *Sclerotinia sclerotiorum* in cucumber via modulation of enzymatic and defense pathways. – Plant Soil. https://doi.org/10.1007/s11104-019-0441-4.
[34] Onaran, A. (2009): Study on the identification, distribution, mycelial compatibility groups pathogenicity and biological control of *Sclerotinia sclerotiorum* (Lib.) de Bary

http://www.aloki.hu ● ISSN 1589 1623 (Print) ● ISSN 1785 0037 (Online)
DOI: http://dx.doi.org/10.15666/aeer/1902_11351147
© 2021, ALÖKI Kft., Budapest, Hungary

(white mold disease of greenhouse grown cucumber) in Antalya Province. – Ph. D. Thesis, Gaziosmanpasa University, Graduate School, Tokat, Turkey.

[35] Onaran, A., Yanar, Y. (2004): Studies on the prevalence of the white rot agent *Sclerotinia sclerotiorum* (Lib.) de Bary in cucumbers in greenhouses in Tokat and Amasya and determination of Mycelium compatibility groups. – Turkey II. Plant Protection Congress, 27-29 August 2007, Isparta.

[36] Onaran, A., Yanar, Y. (2011): Screening bacterial species for antagonistic activities against the *Sclerotinia sclerotiorum* (Lib.) de Bary causal agent of cucumber white mold disease. – African Journal of Biotechnology 10(12): 2223-2229.

[37] Ortet, P., Brakat, M., Lalaouna, D., Fochesato, S., Barbe, V., Vacheria, B., Santaella, C., Heulin, T., Achouak, W. (2011): Complete genome sequence of a beneficial plant root-associated bacterium *Pseudomonas brassicacearum*. – Journal of Bacteriology 193: 3146-3147.

[38] Peter, C., Loewen, J. S., Fernando, W. G. D., de Kievit, T. R. (2014): Genome sequence of *Pseudomonas brassicacearum* DF41. – Genome Announcements 2-3: e00390-14. DOI: 10.1128/ genomeA.00390-14.

[39] Phillips, A. (1986): Factors affecting the parasitic activity of *Gliocladium virens* on sclerotia of *Sclerotinia sclerotiorum* and a note on its host range. – Journal Phytopathology 116(3): 212-220.

[40] Rostami, S., Maleki, M., Shahriari, D. (2013): The Use of *Bacillus amyloliquefaciens* to Control of *Sclerotinia* Stem Rot (*Sclerotinia sclerotiorum*) of Cucumber. – International Journal of Farming and Allied Sciences 2(22): 965-970.

[41] Saharan, G. S., Mehta, N. (2008): Sclerotinia Diseases of Crop Plants: Biology, Ecology and Disease Management. – Springer, Dordrecht.

[42] Savchuk, S. C. (2002): Evaluation of biological control of *Sclerotinia sclerotiorum* on Canola (*Brassica napus*) in the lab, in the greenhouse, and in the field. – Msc. Thesis, University of Manitoba, pp. 49-83.

[43] Savchuk, S., Fernando, W. G. D. (2004): Effect of timing of application and population dynamics on the degree of biological control of *Sclerotinia sclerotiorum* by bacterial antagonists. – FEMS Microbiology Ecology 49: 379-388.

[44] Selin, C., Habibiban, R., Poritsanos, N., Athukorala, S. N. P., Fernando, D., de Kievit, T. R. (2010): Phenasines are not essential for *Pseudomonas chlororaphis* PA23 Biocontrol of *Sclerotinia sclerotiorum*, but do play a role in biofilm formation. – FEMS Microbiology Ecology 71: 73-83.

[45] Soylu, S., Soylu, E. M., Kurt, Ş., Ekici, Ö. K. (2005): Antagonistic potentials of rhizosphere associated bacterial isolated against soil borne diseases of tomato and pepper caused by *Sclerotinia sclerotiorum* and *Rhizoctonia solani*. – Pakistan Journal of Biological Sciences 8(1): 43-48.

[46] Srinivasan, A., Kang, I., Singh, R., Kaur, J. (2001): Evaluation of selected *Trichoderma* isolates against *Sclerotinia sclerotiorum* causing white rot of *Brassica napus* L. – Proc XI International Sclerotinia Workshop, York, UK, pp. 143-144.

[47] Sun, G., Yao, T., Feng, C., Chen, L., Li, J., Wang, L. (2017): Identification and biocontrol potential of antagonistic bacteria strains against *Sclerotinia sclerotiorum* and their growth-promoting effects on *Brassica napus.* – Biological Control 104: 35-43.

[48] Thaning, C., Welch, C. J., Borowıcz, J. J., Hedman, R., Gerhardson, B. (2001): Suppression of *Sclerotinia sclerotiorum* apothecial formation by the soil bacterium *Serratia plymuthica* identification of a chlorinated macrolide as one of the causal agents. – Soil Biology and Biochemistry 33(12-13): 1817-1826.

[49] Tok, F. M., Kurt, S. (2007): Characterization by pathogenicity methods and mycelium compatibility (MUG) of *Sclerotinia sclerotiorum* (Lib.) De Bary isolates obtained from the Mediterranean region greenhouse tomato plants. – Turkey Plant Protection Congress (27-29 August 2007), Isparta.

http://www.aloki.hu ● ISSN 1589 1623 (Print) ● ISSN 1785 0037 (Online)
DOI: http://dx.doi.org/10.15666/aeer/1902_11351147
© 2021, ALÖKI Kft., Budapest, Hungary

[50] Tozlu, E., Demirci, E. (2008): Incidence and characterization of sunflower stem rot disease caused by *Sclerotinia sclerotiorum* and *S. minor* in Pasinler Plain of Erzurum, and reaction of some sunflower cultivars to the pathogens. – Plant Protection Bulletin 48(4): 19-33.
[51] Tozlu, E., Demirci, E. (2011): Determination of potential biocontrol organisms against *Sclerotinia sclerotiorum* and *S. minor* on sunflower. – Anadolu Journal Agricultural Science 26(2): 101-106.
[52] Tozlu, E., Parisa, M., Kotan, M. S., Nadaroglu, H., Kotan, R. (2016): Biological control of *Sclerotinia sclerotiorum* (Lib.) de Bary, the causal agent of white mould disease in red cabbage, by some bacteria. – Plant Protection Science 52(3): 188-198.
[53] Tuncer, F. E., Damdere, H. (1997): Research on the biological control possibilities of the disease of white rot (*Sclerotinia sclerotiorum* (Lib.) De Bary) damaging vegetables in the greenhouses of Antalya Province (final report). – http://www.tagem.gov.tr/projeler/97/bsag/bsagl8.html.
[54] Turhan, G., Grossamann, F. (1986): Investigation of a great number of actinomycete isolates on their antagonistic effects against soil-borne fungal plant pathogens by an improved method. – Journal of Phytopathology 116(3): 193-288.
[55] Türk, M. F., Doğu, M. (2004): Determination of disease incidence and mycelial compatible groups of *Sclerotinia sclerotiorum* in lettuce growing in greenhouses of Canakkale Province. – MKU Journal of Agricultural Faculty 9(1-2): 1-8.
[56] Whipps, J. M., Budge, S. (1990): Screening for sclerotial mycoparasites of *Sclerotinia sclerotiorum*. – Mycological Research 94(5): 607-612.
[57] Whipps, J. M., Gerlagh, M. (1992): Biology of *Coniothyrium minitans* and its potential for use in disease biocontrol. – Mycological Research 96: 897-907.
[58] Whipps, J. M., Sreenivasaprasad, S., Muthumeenakshi, S., Rogers, C. W., Challen, M. P. (2008): Use of *Coniothyrium minitans* as a biocontrol agent and some molecular aspects of sclerotial mycoparasitism. – European Journal Plant Pathology 121: 323-330.
[59] Yıldız, M. (1970): Studies on *Sclerotina* Species, their taxonomy, distribution, degree of damage and pathogenicity in Izmir, Manisa and Aydin Provinces. – Ege University, Journal Agricultural Faculty Serial A 1: 223-235.
[60] Yücer, M. (1980): Studies on The Rate of Diseases, Fungal Factors and Pathogenicity of Sunflowers in the Thrace Region. – İstanbul Province Plant Protection Central Research Enstitute, Serial 14, Ankara.
[61] Zazzerini, A., Tosi, L. (1985): Observations on the antagonistic activity of some fungi and bacteria against *Sclerotinia sclerotiorum* (Lib.) de Bary. – Difesa-delepiante 8(2): 163-168.
[62] Zazzerini, A., Tosi, L., Rossi, S. (1987): Antagonistic effect of *Bacillus* spp. on *Sclerotinia sclerotiorum* Sclerotia. – Phytopathologia Mediterranea 26: 185-187.
[63] Zhang, Y. (2004a): Biocontrol of *Sclerotinia* stem rot of canola by bacterial antagonists and study of biocontrol mechanisms involved. – Msc. Thesis, University Manitoba, Winnipeg.
[64] Zhang, Y., Fernando, W. G. D., Kavitha, K., Nakkeeran, S., Ramarathnam, R. (2004b): Combination of mechanisms in *Pseudomonas chlororaphis* strain PA-23 results in control of multiple pathogens. – Phytopathology 94: 115.

http://www.aloki.hu ● ISSN 1589 1623 (Print) ● ISSN 1785 0037 (Online)
DOI: http://dx.doi.org/10.15666/aeer/1902_11351147
© 2021, ALÖKI Kft., Budapest, Hungary

EFFECTS OF LIGHT CONDITIONS AT DIFFERENT GROWTH STAGES ON GROWTH AND PHOTOSYNTHETIC CHARACTERISTICS OF *PINUS SYLVESTRIS* VAR. *SYLVESTRIFORMIS* SEEDINGS

JIN, H. – QIN, L. W. – LIU, L. J. – CHEN, Q. H. – JIA, X. – DAI, Y. H. – ZHAO, Y.* – YIN, H.*

Jilin Provincial Joint Key Laboratory of Changbai Mountain Biocoenosis and Biodiversity, Changbai Mountain Academy of Sciences, Antu 133613, P. R. China

**Corresponding authors*
e-mail: rjrge26m@163.com; fivecl10jinhui@163.com

(Received 14th Sep 2020; accepted 18th Dec 2020)

Abstract. *Pinus sylvestris* var. *sylvestriformis* is an endemic plant in Changbai Mountain area of China. Five different light levels were simulated and designed with control experiments: full sunlight (CK), light shading (light transmittance was 10%) (LA), light and moderate shading (light transmittance was 20%) (LB), moderate shading (light transmittance was 40%) (LC), and severe shading (light transmittance was 60%) (LD). The optimal light levels and the main physiological and ecological factors affecting photosynthesis in different growth stages were discussed. The results showed that the phenotypic index and photosynthetic physiological and ecological indicators were the highest when the light transmittance was 40%. In the early growth phase, the physiological factors intercellular CO_2 concentration (C_i) and ecological factors transmittance (*Tran*) and air temperature (*Temp*) jointly affected the changes of net photosynthetic rate (P_n). In the peak growth phase, transpiration rate (T_r), air humidity (*RH*), and *Tran* had greater direct positive effects on P_n, and C_i and stomatal conductance (G_s) had direct negative effects on P_n. In the later growth phase, T_r and C_i had large direct positive effects on P_n. The research results could provide important references for the scientific cultivation and popularization of *P. sylvestris* var. *sylvestriformis*.
Keywords: *P. sylvestris var. sylvestriformis, light transmittance, growth phases, the phenotypic index, photosynthetic physiological and ecological indicators*

Introduction

Light is an important environmental factor that affects the growth and development, morphogenesis, regeneration, and distribution of plants (Rozendaal et al., 2006). Plants regulate their growth and development by sensing the changes of light signals in the external environment (Kim et al., 2017). In the weak light environment, the plant's ability to capture light is limited, which restricts the photosynthetic capacity of plants and causes the decrease of photosynthetic rate, but it will increase the content of photosynthetic pigment to increase the ability to capture light energy (Liu et al., 2011). "Trade- off theory" holds that under shading conditions, plants tend to allocate more biomass to the aboveground part and less to the root, which affects water absorption (Smith et al., 1989). In order to cope with different light conditions, plants can increase the utilization of light energy through morphological and physiological plasticity response, so as to avoid the photoinhibition or photodamage, and finally reduce the photosynthetic rate (Duan et al., 2005).

Pinus sylvestris var. *sylvestriformis* is a rare and endangered tree species in Changbai Mountain, China's national first-class protected plant. The natural population of *P. sylvestris* var. *sylvestriformis* is distributed in the northern slope of Changbai Mountain and Changbai Mountain Nature Reserve in China, with a small area of about 200 hm^2.

http://www.aloki.hu ● ISSN 1589 1623 (Print) ● ISSN1785 0037 (Online)
DOI: http://dx.doi.org/10.15666/aeer/1902_11491162
© 2021, ALÖKI Kft., Budapest, Hungary

Because of its straight trunk, beautiful tree shape, and handsome posture, the local people called it "beauty pine." However, in recent years, due to the increase of population, economic development, and environmental damage, the number of *P. sylvestris* var. *sylvestriformis* has become less and less, which has reached the edge of extinction and needs further protection (Bu et al., 1995).

There is a strong correlation between plant growth and light environment heterogeneity, especially light intensity (Bazzaz, 1996). The need and sensitivity of seedlings growth to light are high, so it is often necessary to adopt necessary tending measures according to the response of seedlings to light (Welander and Ottosson, 1998; Wang, 2008). In order to obtain the best light environment for the growth of *P. sylvestris* var. *sylvestriformis* seedlings, so as to take corresponding tending measures, it is particularly important to study and practice the response of *P. sylvestris* var. *sylvestriformis* seedlings to the light environment.

At present, researches on *P. sylvestris* var. *sylvestriformis* mainly involve the population, community and ecological investigation, etc. (Hu et al., 1966; Zhao et al., 2002; Zhao et al., 2017; Jin et al., 2015; Chen et al., 2017). It is not reported to study the growth status of *P. sylvestris* var. *sylvestriformis* and analyze the dynamic changes of leaf photosynthesis in the whole growth period by short- term artificial control of light conditions.

In this experiment, through artificial shading treatment, the growth status and photosynthetic parameters of *P. sylvestris* var. *sylvestriformis* seedlings under different light conditions at different growth stages were observed continuously. The adaptability of *P. sylvestris* var. *sylvestriformis* seedlings to different light conditions was discussed, and the effects of environmental factors on Photosynthesis in different growth phases were analyzed. In order to seek the most suitable light conditions to promote the growth of *P. sylvestris* var. *sylvestriformis* seedlings, and to identify the main physiological and ecological factors that affect the photosynthesis of *P. sylvestris* var. *sylvestriformis* in different growth phases. So as to provide theoretical basis and technical reference for scientific management of *P. sylvestris* var. *sylvestriformis* seedlings.

Materials and methods

Overview of experimental sites

The experimental site is located at Northeast Asia Arboretum of Changbai Mountain Nature Reserve, China, with a geographical location of 128°01' E, 42°22' N, and the altitude of 770-780 m, the climate belongs to the temperate continental monsoon alpine climate. The annual average temperature is 3-7 ℃. The minimum temperature has appeared -44 ℃. The annual sunshine hours are less than 2300 hours. The frost-free period is about 100 days. The annual precipitation is between 700-1400 mm, and 6-9 month accounts for 60-70% (Yin et al., 2017).

Test materials and methods

Materials

Biennial seedlings were planted in the spring of 2016 in the test site, and the test was conducted in May 2018. The shading nets with a light transmittance of 10%, 20%, 40%, and 60% were selected.

http://www.aloki.hu ● ISSN 1589 1623 (Print) ● ISSN1785 0037 (Online)
DOI: http://dx.doi.org/10.15666/aeer/1902_11491162
© 2021, ALÖKI Kft., Budapest, Hungary

Cultivation substrate

The ratio of dark brown loam to river sand was 2: 1. When cultivated, the border was 35 cm high and 120 cm wide.

Experimental methods

There were five treatments in the light environment:
CK control: full sunlight;
LA: light transmittance was 10%;
LB: light transmittance was 20%;
LC: light transmittance was 40%;
LD: light transmittance was 60%.

During the experiment, the maximum light intensity of each treatment was monitored by HOBOU12 environmental factor monitor of American HOBO Onset Company at noon on five sunny days. The light intensity is as follows:
CK control: 112304-128032 lux;
LA: 3313-7594 lux;
LB: 13656-28546 lux;
LC: 45644-69650 lux;
LD: 58762-79364 lux.

Each sunshade was 6 m long, 4 m wide and 2 m high. Each treatment was repeated three times, with 20 plants per repeat. The plant row spacing was 20 cm by 20 cm. The seedling height, ground diameter, and leaf length (maximum leaf length) of *P. sylvestris* var. *sylvestriformis* seedlings were measured in June, July, August, and September, respectively. From May to October, a sunny day was choosing every month, photosynthetic characteristics were measured using an LI- 6400 portable photosynthesis system (American LI- COR Company) between 9 a.m. and 11 a.m. The effective light radiation was set at 1500 lux. The net photosynthetic rate (P_n), stomatal conductance (G_s), transpiration rate (T_r), and intercellular CO_2 concentration (C_i) of *P. sylvestris* var. *sylvestriformis* seedlings of different treatments were measured. Each repeating was measured once, and the data acquisition time was 3 minutes, which would be recorded after it was stable.

During the period from mid-May to October 2019, the HOBOpro automatic temperature and humidity recorder was used to automatically collect the atmospheric temperature and relative humidity during the test period every half an hour.

Data processing and analysis

All data were analyzed by Excel and IBM SPSS statistics software for multiple comparison, significance test, regression analysis, simple correlation analysis and path analysis. The statistical graph was drawn by sigmaplot 14.0. Descriptive statistics were expressed in mean ± SEM and letter notation.

Results and analysis

Changes in temperature and relative humidity

Figure 1 showed course of daily and monthly average temperature and relative humidity in experimental period. The temperature of the experimental area was low in May, with an average monthly temperature of 15.71 ℃, an average monthly relative

http://www.aloki.hu ● ISSN 1589 1623 (Print) ● ISSN1785 0037 (Online)
DOI: http://dx.doi.org/10.15666/aeer/1902_11491162
© 2021, ALÖKI Kft., Budapest, Hungary

humidity of 63.95%, and the air was dry. From June to August, the temperature rose rapidly. From July to August, the temperature reached its highest value. This period was the main rainfall period. The temperature difference between day and night was large. The monthly average temperature was 20.43 ℃ and 19.36 ℃, respectively. The weather was humid and cool. From September to October, the temperature gradually decreased, with the lowest temperature in October. The monthly average temperature was below 10 ℃. The monthly average relative humidity of the air was maintained at about 66%. The weather was dry and cold.

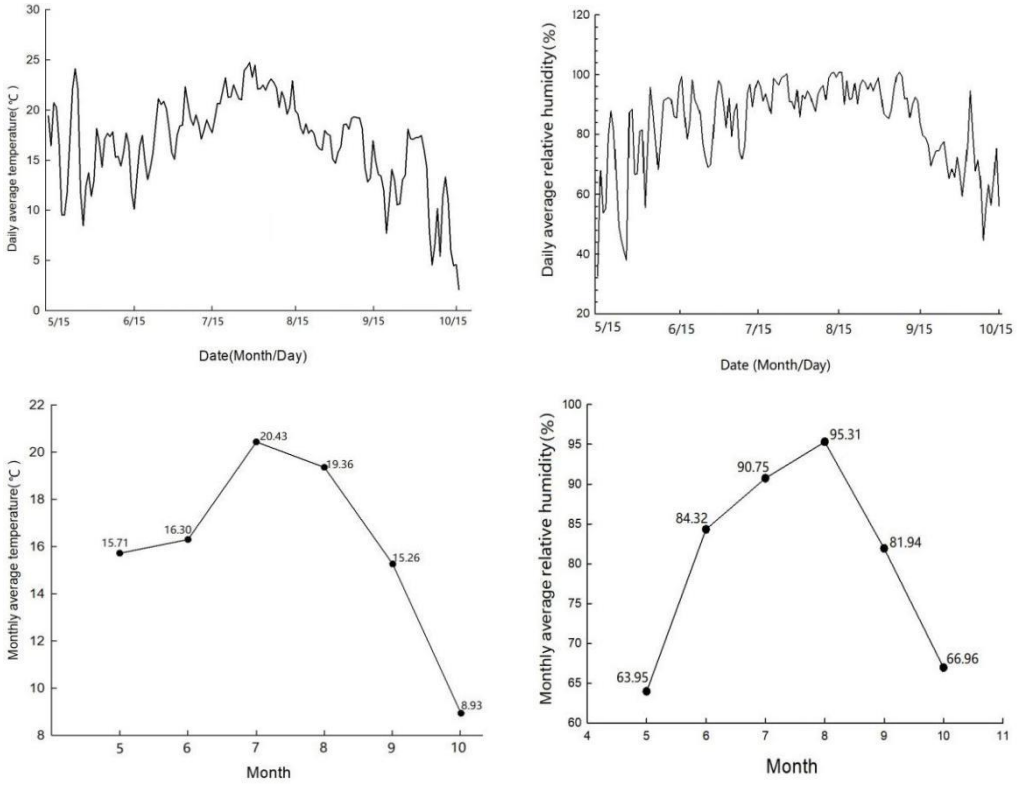


Figure 1. *Course of daily and monthly average temperature and relative humidity in experimental period*

Effects of different light conditions on the growth of P. sylvestris var. sylvestriformis seedlings

Effects of different light conditions on plant height of P. sylvestris var. sylvestriformis seedlings

Table 1 showed the average plant height of each treatment measured in different months. According to the plant height of two adjacent months, the change rate of plant height of different treatments in each month is further calculated. From June to July, plant height change rate of treatment CK was 39.48%, plant height change rate of treatment LA was 14.22%, plant height change rate of treatment LB was 24.46%, plant height change rate of treatment LC was 37.65%, plant height change rate of treatment LD was 42.44%. Based on the change rate of plant height treated with treatment CK, the plant height of *P. sylvestris* var. *sylvestriformis* seedlings decreased by 25.26% after treatment LA,

http://www.aloki.hu ● ISSN 1589 1623 (Print) ● ISSN1785 0037 (Online)
DOI: http://dx.doi.org/10.15666/aeer/1902_11491162
© 2021, ALÖKI Kft., Budapest, Hungary

15.02% after treatment LB, 1.83% after treatment LC than treatment CK, but after treatment LD, the plant height increased by 2.96% than CK. From July to August, based on the change rate of plant height treated with CK, after each treatment, the height of seedlings increased by 4.46%, 4.76%, 19.39%, and 16.70%, respectively, compared with that of treatment CK (full sunlight). From August to September, based on the change rate of plant height treated with CK, the height of seedlings increased by 0.71%, 2.15%, 3.45%, and 1.43% compared with that of treatment CK.

Table 1. *Growth of plant height in different months (cm)*

Tran	June	July	August	September
CK	12.21±2.74a	17.03±2.38ab	19.04±3.02ab	19.42±3.24bc
LA	13.08±1.17a	14.94±1.69b	17.37±1.91b	17.84±1.75c
LB	14.31±1.34a	17.81±1.31a	20.76±0.74a	21.62±0.29ab
LC	11.9±0.06ab	16.38±0.15ab	21.49±1.08a	22.66±1.13a
LD	9.26±0.98b	13.19±0.38c	16.95±0.59b	17.53±0.63c

Note: Lowercase letters in the same column represented significance differences at the $p<0.05$ level

The growth rates of plant height of *P. sylvestris* var. *sylvestriformis* seedlings treated by CK, LA, LB, LC and LD from June to September were 59.05%, 36.39%, 51.08%, 90.42%, and 89.31%, respectively. The growth rate during the growing season was as follows: treatment LC> LD> CK> LD> LA. The plant height of each treatment showed an upward trend during the whole growing season. The plant height of treatment CK, LB, LC, LD increased rapidly in the period of June-July. The plant height of treatment LA increased rapidly in the period of July- August. Each treatment increased slowly in the period of August- September.

Effects of different light conditions on the ground diameter of P. sylvestris var. sylvestriformis seedlings

Table 2 showed the average ground diameter of each treatment measured in different months. According to the ground diameter of two adjacent months, the change rate of the ground diameter of different treatments in each month is further calculated. From June to July, the ground diameter change rate of treatment CK was 19.25%, the ground diameter change rate of treatment LA was 5.57%, the ground diameter change rate of treatment LB was 15.49%, the ground diameter change rate of treatment LC was 21.49%, the ground diameter change rate of treatment LD was 7.34%. Based on the change rate of the ground diameter treated with treatment CK. the ground diameter of *P. sylvestris* var. *sylvestriformis* seedlings decreased by 13.68% after treatment LA, 3.76% after treatment LB, 11.91% after treatment LD than treatment CK, but after treatment LC, the ground diameter increased by 2.24% than treatment CK. From July to August, based on the change rate of the ground diameter treated with CK, the ground diameter of *P. sylvestris* var. *sylvestriformis* seedlings decreased by 9.14% after treatment LA, 4.53% after treatment LB, 0.04% after treatment LC than treatment CK, but after treatment LD, the ground diameter increased by 0.93% than CK. From August to September, the ground diameter seedlings decreased by 1.34% after treatment LA, 0.83% after treatment LB, 0.72% after treatment LC, 3.68% after treatment LD than treatment CK.

http://www.aloki.hu ● ISSN 1589 1623 (Print) ● ISSN1785 0037 (Online)
DOI: http://dx.doi.org/10.15666/aeer/1902_11491162
© 2021, ALÖKI Kft., Budapest, Hungary

Table 2. *Growth of ground diameter in different months (mm)*

Tran	June	July	August	September
CK	3.22±0.56a	3.84±0.67ab	4.37±0.59a	4.48±0.08b
LA	3.05±0.34a	3.22±0.34b	3.37±0.35b	3.50±0.37a
LB	3.55±0.06a	4.10±0.08a	4.48±0.11a	4.63±0.17a
LC	3.35±0.12a	4.07±0.12ab	4.63±0.08a	4.78±0.10a
LD	3.54±0.17a	3.80±0.28ab	4.36±0.33b	4.63±0.47a

Note: Lowercase letters in the same column represented significance differences at the $p<0.05$ level

The growth rates of the ground diameter of *P. sylvestris* var. *sylvestriformis* seedlings treated by CK, LA, LB, LC and LD from June to September were 39.13%, 14.75%, 30.42%, 42.69%, and 30.79%, respectively. The ground diameter of each treatment showed an upward trend during the whole growing season. The ground diameter of treatment CK, LB, LC, LD increased rapidly in the period of June- August and increased slowly in the period of August-September. The ground diameter of treatment LA increased slowly during the whole growing season.

Effects of different light conditions on the leaf length of P. sylvestris var. sylvestriformis seedlings

Table 3 showed the average leaf length of each treatment measured in different months. According to the leaf length of two adjacent months, the change rate of the leaf length of different treatments in each month is further calculated. From June to July, the leaf length change rate of treatment CK was 10.24%, the leaf length change rate of treatment LA was 10.86%, the leaf length change rate of treatment LB was 10.23%, the leaf length change rate of treatment LC was 16.91%, the leaf length change rate of treatment LD was 14.77%. Based on the change rate of the leaf length treated with treatment CK. the leaf length of *P. sylvestris* var. *sylvestriformis* seedlings increased by 0.62% after treatment LA, 6.67% after treatment LC, 4.53% after treatment LD than treatment CK, but after treatment LB, the leaf length decreased by 0.01% than treatment CK. From July to August, the leaf length of seedlings decreased by 13.22% after treatment LA, 2.25% after treatment LD than treatment CK and the leaf length of seedlings increased by 0.69% after treatment LB, 7.70% after treatment LC than treatment CK. From August to September, the leaf length of seedlings increased by 3.56% after treatment LB, 3.90% after treatment LC, 0.79% after treatment LD than treatment CK, but after treatment LA, the leaf length decreased by 0.45% than treatment CK.

Table 3. *Growth of leaf length in different months (cm)*

Tran	June	July	August	September
CK	5.86±0.82b	6.46±0.70c	8.06±0.92bc	8.36±0.72c
LA	6.17±0.09ab	6.84±0.11bc	7.63±0.48c	7.88±0.33c
LB	6.45±0.15ab	7.11±0.12abc	8.92±0.29ab	9.57±0.07b
LC	6.27±0.11ab	7.33±0.21ab	9.71±0.84a	10.45±0.13a
LD	6.77±0.56a	7.77±0.35a	9.52±0.66a	9.95±0.69ab

Note: Lowercase letters in the same column represented significance differences at the $p<0.05$ level

http://www.aloki.hu ● ISSN 1589 1623 (Print) ● ISSN1785 0037 (Online)
DOI: http://dx.doi.org/10.15666/aeer/1902_11491162
© 2021, ALÖKI Kft., Budapest, Hungary

The growth rates of leaf length of *P. sylvestris* var. *sylvestriformis* seedlings treated by CK, LA, LB, LC and LD from June to September were 42.66%, 27.71%, 48.37%, 66.67%, and 46.97%, respectively. The leaf length of each treatment showed an upward trend during the whole growing season. The leaf length of treatment CK, LB, LC, LD increased rapidly in the period of July- August and increased slowly in the period of June-July and August- September. The leaf length of treatment LA increased slowly during the whole growing season.

Growth distribution of P. sylvestris var. sylvestriformis seedlings under different light conditions

Table 4 showed that under the condition of treatment LC, the growth of ground diameter was 1.43 mm, which was the highest under each treatment, and the difference from treatment CK was not significant. The growth of ground diameter was only 0.45 mm under treatment LA, which was the lowest under all treatments. The difference was significant compared with other treatments ($p< 0.05$).

Table 4. *Growth distribution of P. sylvestris var. sylvestriformis seedlings under different light conditions*

Tran	Ground diameter /mm	Plant height /cm	Leaf length /cm
CK	1.16±0.12a	7.22±1.01bc	2.50±0.18bc
LA	0.45±0.03b	4.76±0.21c	1.71±0.14c
LB	1.09±0.11a	7.31±1.23bc	3.12±0.22ab
LC	1.43±0.24a	10.76±1.68a	4.18±0.19a
LD	1.08±0.09a	8.28±0.75ab	3.18±0.28ab

Note: Lowercase letters in the same column represented significance differences at the $p<0.05$ level

Under the condition of treatment LC, the growth of plant height was 10.76 cm, which was the highest under each treatment, and the difference was significant ($p< 0.05$). The growth of plant height was only 4.76 cm under treatment LA, which was the lowest under all treatments, and the difference from treatment LD ($p< 0.05$) was significant.

Under the condition of treatment LC, the growth of leaf length was 4.78 cm, which was the highest under each treatment, and the difference from treatment CK ($p< 0.05$) was significant. The growth of leaf length under treatment LA was 1.71 cm, and the difference from treatment CK was not significant.

Division of growth and development stages of P. sylvestris var. sylvestriformis

After years of continuous observation of plant growth law in Changbai Mountain area, the growth period can be divided into three periods: 1. Early growth phase: from mid-May to the end of June, the plant growth is the fastest; 2. The peak growth period: from the beginning of July to the end of August, the plant growth is slower than the initial growth; 3. The late growth period: from the beginning of September to mid- October, the growth is slow or even stopped.

http://www.aloki.hu ● ISSN 1589 1623 (Print) ● ISSN1785 0037 (Online)
DOI: http://dx.doi.org/10.15666/aeer/1902_11491162
© 2021, ALÖKI Kft., Budapest, Hungary

Changes of leaf photosynthetic parameters in different growth phases

Photosynthetic capacity of P. sylvestris var. sylvestriformis seedlings in different growth phases

It could be seen from *Figure 2* that P_n, G_s, C_i and T_r of *P. sylvestris* var. *sylvestriformis* seedlings under different light conditions could be roughly divided into four stages of "low, rapid rise, stable and decline" in the whole growth phases. Combined with the growth law, growth period division and photosynthesis monitoring of *P. sylvestris* var. *sylvestriformis* seedlings, it was found that the growth and photosynthetic characteristics basically overlapped. Therefore, the seasonal variation of photosynthetic characteristics could accurately reflect the change of its growth cycle.

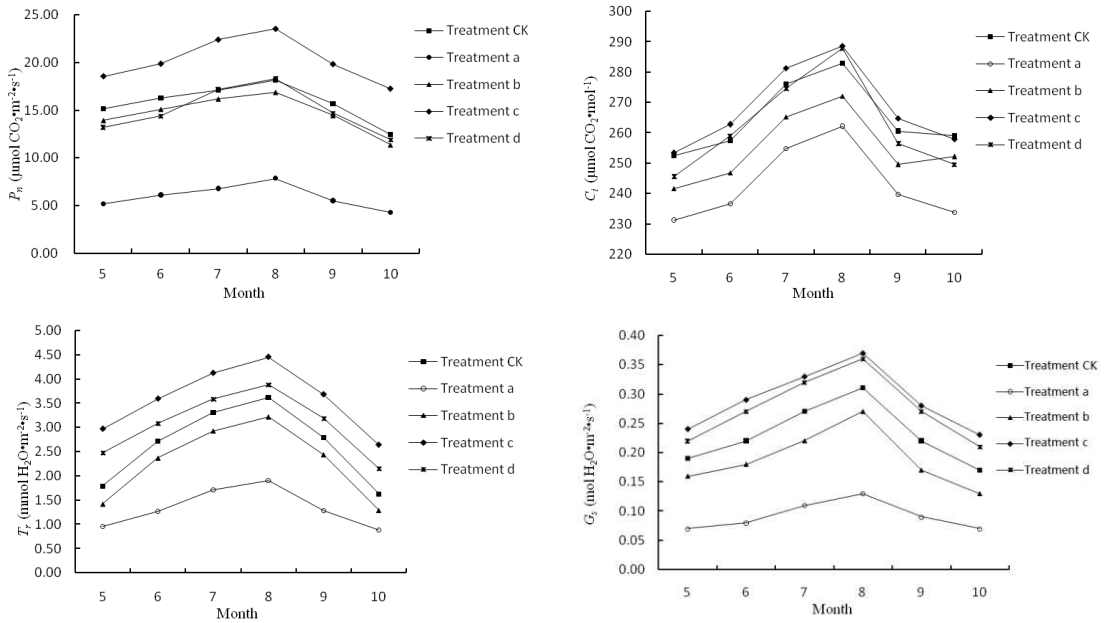


Figure 2. *Variations of P_n, G_s, C_i and T_r in different growth phases*

Photosynthetic capacity of P. sylvestris var. sylvestriformis seedlings under different light conditions

Taking August, where the photosynthetic capacity was the strongest, as an example, the photosynthetic capacity of *P. sylvestris* var. *sylvestriformis* seedlings under different light conditions was listed in *Table 5*. P_n and G_s were treatment LC> LD> CK> LB> LA. Under the condition of treatment LC, P_n and G_s were 23.52 μmol CO_2 m^{-2} s^{-1} and 0.37 mol H_2O m^{-2} s^{-1}, respectively, which were the highest under each treatment. P_n and G_s under treatment LA were only 7.85 μmol CO_2 m^{-2} s^{-1} and 0.13 mol H_2O m^{-2} s^{-1}, which were the lowest under all treatments. The difference was significant compared with other treatments ($p< 0.05$). T_r was treatment LC> LD> CK> LB> LA. Under the condition of treatment LC, T_r was 4.45 mmol H_2O m^{-2} s^{-1}, which was the highest under each treatment, and the difference from treatment CK was significant ($p< 0.05$). T_r was 1.90 mmol H_2O m^{-2} s^{-1} under treatment LA, which was the lowest under all treatments, and the difference was significant compared with other treatments ($p< 0.05$). C_i was treatment LC> LD> CK> LB> LA. C_i was 288.67 μmol CO_2 mol^{-1} under the condition

http://www.aloki.hu ● ISSN 1589 1623 (Print) ● ISSN1785 0037 (Online)
DOI: http://dx.doi.org/10.15666/aeer/1902_11491162
© 2021, ALÖKI Kft., Budapest, Hungary

of treatment LC, which was the highest, and Gs was 262.05 μmol CO_2 mol^{-1} under the condition of treatment LA, which was the lowest in each shading treatment.

Table 5. *Effects of different light conditions on photosynthetic capacity of P. sylvestris var. sylvestriformis seedlings*

Tran	P_n / μmol CO_2 m^{-2} s^{-1}	G_s / mol H_2O m^{-2} s^{-1}	T_r / mmol H_2O m^{-2} s^{-1}	C_i / μmol CO_2 mol^{-1}
CK	18.16±0.76b	0.31±0.04bc	3.62±0.16b	283.02±1.88b
LA	7.85±0.19d	0.13±0.02d	1.90±0.16d	262.05±3.26d
LB	16.87±0.40c	0.27±0.03c	3.22±0.22c	272.14±1.84c
LC	23.52±0.08a	0.37±0.02a	4.45±0.10a	288.67±1.75a
LD	18.32±0.39b	0.36±0.03ab	3.88±0.09b	287.88±0.84a

Note: Lowercase letters in the same column represented significance differences at the $p<0.05$ level

The relationship between photosynthetic rate and main physiological and ecological factors in different growth phases

According to different growth phases, the order of P_n mean value of *P. sylvestris* var. *sylvestriformis* was peak growth phase > early growth phase > later growth phase (*Figure 2*). *Table 6* showed correlation among photosynthetic and environmental factors. The correlation analysis between main physiological factors (G_s, C_i, T_r) and ecological factors (*Tran*, *Temp*, *RH*) and P_n showed that the correlation between P_n and other physiological and ecological factors such as G_s, C_i, T_r, *Tran* reached a significant level of 0.01, The correlation between air temperature and air humidity was not significant, and the correlation between factors was complex.

Table 6. *Correlation among photosynthetic and environmental factors*

Factors	P_n	C_i	G_s	T_r	*Tran*	*Temp*
C_i	0.77**					
G_s	0.91**	0.87**				
T_r	0.90**	0.87**	0.96**			
Tran	0.47**	0.43*	0.49**	0.39*		
Temp	0.33	0.55**	0.43*	0.53**	0.00	
RH	0.32	0.70**	0.48**	0.60**	0.00	0.77**

Note: * represents significant level at 0.05; ** represents significant level at 0.01

In order to further analyze the relationship between P_n and main physiological and ecological factors at different growth phases, path analysis was conducted on each factor (X) and P_n (Y). The weight of each factor influencing P_n was analyzed by path analysis. The results were shown in *Table 7*. The main factors that had great influence on P_n in different growth phases were different. In the early growth phase, physiological factors C_i, ecological factors *Tran* and *Temp* jointly affected the changes of P_n, the most direct effect on P_n was C_i. *Tran* and *Temp* had a greater indirect effect on P_n through C_i. In the peak growth phase, T_r, *RH* and *Tran* had a greater direct positive effect on P_n. C_i and G_s had a direct negative effect on P_n, Tr was the physiological factor that had the greatest

http://www.aloki.hu ● ISSN 1589 1623 (Print) ● ISSN1785 0037 (Online)
DOI: http://dx.doi.org/10.15666/aeer/1902_11491162
© 2021, ALÖKI Kft., Budapest, Hungary

effect on P_n, *Tran* and *RH* were the ecological factors that had the greatest effect on P_n. In the late growth phase, T_r and C_i had a large direct positive effect on P_n, G_s, *Tran* and *Temp* had a direct negative effect on P_n.

Table 7. *Path analysis between the factors and Pn in different growth phases*

Growth phases	Factors	Direct path	Indirect path	Through C_i	Through G_s	Through T_r	Through *Tran*	Through *Temp*	Through *RH*
Early growth phase	C_i	1.214	-0.335	-	-	-	--0.193	-0.141	-
	Tran	-0.290	0.808	0.808	-	-	-	0.000	-
	Temp	-0.356	0.482	0.482	--	-	0.000	-	-
Peak growth phase	C_i	-0.439	1.322	-	-0.645	1.887	0.047	-	0.034
	G_s	-0.675	1.613	-0.419	-	1.970	0.043	-	0.019
	T_r	2.004	1.613	-0.413	-0.664	-	0.040	-	0.014
	RH	0.086	0.013	-0.171	-0.150	0.334	0.000	-	-
	Tran	0.075	0.414	-0.276	-0.385	1.075	-	-	0.000
Later growth phase	C_i	1.082	-0.158	-	-1.640	1.620	-0.073	-0.065	-
	G_s	-1.781	2.757	0.996	-	1.950	-0.056	-0.134	-
	T_r	2.041	-1.119	0.859	-1.701	-	-0.039	-0.237	-
	Tran	-0.104	0.581	0.760	-0.951	0.772	-	0.000	-
	Temp	-0.452	0.699	0.156	-0.529	1.072	0.000	-	-

Discussion

Plant growth is inseparable from sunlight. Light can directly promote the growth and division of plant cells, promote the differentiation of plant tissues and organs, and affect plant growth and development speed (Huang et al., 2020). The results showed that when the light transmittance was 10%, the growth of plant height, ground diameter, and leaf length in the growing season was the lowest in all treatments. The average plant height increment was only 4.76 cm, the average ground diameter increment was only 0.45 mm, and the average leaf length increment was only 1.71 cm. In a different light environment, the *P. sylvestris* var. *sylvestriformis* seedlings showed different growth characteristics. Within a certain range of light intensity, the growth of plants always increased with the increase of light intensity (Welander and Ottosson, 1998; Wen et al., 1999). Some studies also considered that plants grew best at moderate light intensity (Valladares et al., 2000). The result of this experiment was consistent with that. According to the statistical results of phenotypic data, when the light transmittance was 40%, the growth of plant height, ground diameter, and leaf length in the growing season were the highest in all treatments. The average plant height increment was 10.76 cm, the average ground diameter increment was 1.43 mm, and the average leaf length increment was 4.18 cm. Growth indicators such as seedling height growth and ground stem growth under the light condition of 40% light transmittance were higher than other treatments, indicating that the seedlings of *P. sylvestris* var. *sylvestriformis* can promote plant growth under moderate shading treatment. It is consistent with the research results of *Clerodendrum japonicum* seedlings (Huang et al., 2020).

The growth of plant height, leaf length, and ground diameter were three important phenotypic indexes of *P. sylvestris* var. *sylvestriformis* seedlings, combined with

http://www.aloki.hu ● ISSN 1589 1623 (Print) ● ISSN1785 0037 (Online)
DOI: http://dx.doi.org/10.15666/aeer/1902_11491162
© 2021, ALÖKI Kft., Budapest, Hungary

photosynthetic characteristics as four indexes, whose differences could comprehensively reflect the effects of different shading treatments. Excessive shading would restrict the photosynthesis of *P. sylvestris* var. *sylvestriformis* seedlings. Choosing suitable light conditions was more conducive to the growth of seedlings. Some scholars have confirmed that heavy shading is not suitable for seedling growth (Jiang et al., 2017). Therefore, understanding the response of seedlings to different light environments is of great practical significance for studying the succession and ecological restoration of *P. sylvestris* var. *Sylvestriformis* community.

Photosynthesis is the basis of plant material production. It is not only affected by environmental factors, but also closely related to its own growth and development and physiological and ecological characteristics. The continuous changes in environmental temperature and humidity brought about by the growth of plants and the changing of seasons will inevitably cause the photosynthetic characteristics of plants to change with the changing of seasons and growth phases. Under treatment CK, the light transmittance of 20%, the light transmittance of 40%, and light transmittance of 60%, plant height of *P. sylvestris* var. *sylvestriformis* grew rapidly in the period of June-July, and the seedlings could make good use of light energy. When the light transmittance was 10%, the plant height grew slower than that of other treatments in the period of June-July, and the seedlings could not get enough light energy. However, in the period of July-August, when other treatments showed strong light suppression, the seedlings had enough light energy for photosynthesis under 10% light transmittance.

The net photosynthetic rate (P_n) is the result of the comprehensive effect of plant growth and the external environment, and its size restricts the speed of plant growth (Shang et al., 2020). The higher the P_n, the stronger the adaptability of the plant and the more favorable it is for growth. The intercellular CO_2 concentration (C_i) is an important factor affecting plant photosynthesis, and stomata is an important channel that directly affects the exchange of water vapor and CO_2. Excessive closure of stomata will have certain effect on the transpiration of plants and cause certain effects (Yue et al., 2020). P_n, C_i and the transpiration rate (T_r) were LC> LD> Ck> LB> LA, LC treatment was higher than other treatments, and LA treatment was the lowest. It showed that moderate shading could increase the P_n, C_i, and T_r of plants. When excessive shading, the net photosynthetic rate of *P. sylvestris* var. *sylvestriformis* decreased sharply. In addition, the intercellular CO_2 concentration was low, and the degree of stomata opening restricted the transportation of CO_2, the transpiration rate also decreased (Yue et al., 2020).

In the early growth phase, the internal structure and function development of the leaves were not perfect, the stomata of the leaves were partially closed, G_s was still relatively low. P_n of the leaves changed with the change of C_i. This was a regular reflection of the relationship between the two. At this time, P_n was low. In the peak growth phase, the color of leaves gradually changed from light green to thick green, and the internal structure and function of leaves gradually developed and perfected G_s, T_r and C_i were higher. The resistance of water and CO_2 entering and exiting the stomata and photosynthesis was small, which was conducive to the analysis of photosynthesis (Chen et al., 2015). It was worth noting that path analysis showed that *Tran* and *RH* were important ecological factors affecting photosynthesis at this stage. In later growth phase, the growth of *P. sylvestris* var. *sylvestriformis* was slow or even stagnant, and G_s was still an important physiological factor affecting photosynthesis.

http://www.aloki.hu ● ISSN 1589 1623 (Print) ● ISSN1785 0037 (Online)
DOI: http://dx.doi.org/10.15666/aeer/1902_11491162
© 2021, ALÖKI Kft., Budapest, Hungary

Conclusion

There were some differences in the growth of *P. sylvestris* var. *sylvestriformis* seedlings under different shading treatments. Plant height, ground diameter, and leaf length were the most direct reflection of seedling growth and seedling quality. *P. sylvestris* var. *sylvestriformis* showed a good growth trend under the shading condition of 40% light transmittance. Under low light intensity, the light was the limiting factor for seedling growth. Under the condition of insufficient light resources, the growth of plant height, ground diameter, and leaf length in the growing season were all inhibited by a light factor, showing the smallest with significant change, whose growth was inhibited.

Excessive shading or full light was not conducive to the growth of *P. sylvestris* var. *sylvestriformis* seedlings. Excessive shading inhibited the normal progress of photosynthesis and reduced the content of photosynthetic products. under full light conditions, although photosynthesis was the strongest, photoinhibition would appear, Inhibiting the normal progress of photosynthesis. The research results showed that P_n, C_i, and T_r were the highest when light transmittance was 40%.

In conclusion, through the study on the growth status of *P. sylvestris* var. *sylvestriformis* under different light conditions, it was found that moderate light environment could promote the growth of *P. sylvestris* var. *sylvestriformis* seedlings. The phenotypic index and photosynthetic physiological and ecological indicators were the highest when the light transmittance was 40%. It was the best light condition for the growth and ecological adaptation of *P. sylvestris* var. *sylvestriformis* seedlings. Through the observation of photosynthetic characteristics in different growth phases, it was found that the growth of *P. sylvestris* var. *sylvestriformis* and their photosynthetic changes overlapped. In different growth phases, the physiological and ecological factors affecting the photosynthesis of *P. sylvestris* var. *sylvestriformis* were different. In the early growth phase from May to June, the photosynthetic rate of *P. sylvestris* var. *sylvestriformis* increased rapidly, C_i was the decisive factor affecting the photosynthetic rate of *P. sylvestris* var. *sylvestriformis* in this phase, and the light transmittance and air relative temperature were the important environmental factors affecting the photosynthetic rate. In the peak growth phase from July to August, *Tran* and *RH* were the important ecological factors affecting photosynthesis in this phase. In the later growth phase from September to October, the photosynthetic rate gradually decreased. Therefore, in the peak and later growth phases, shade conditions could be used to properly adjust the air temperature and humidity to achieve the optimum temperature and humidity range for photosynthesis, increase the photosynthetic rate of the leaves, promote and extend the growth season of *P. sylvestris* var. *sylvestriformis*.

P. sylvestris var. *sylvestriformis* is unique and rare woody plants in Changbai Mountain of China. The limitation of the number of experimental materials has caused many restrictions on the experiment. In the future, under the premise of limited experimental materials, it is necessary to explore the light response of *P. sylvestris* var. *sylvestriformis* from the perspectives of morphology, anatomy and gene expression. In addition, it is more convincing to analyze the specific mechanism of the influence of light environment on *P. sylvestris* var. *sylvestriformis* from the molecular level.

Acknowledgements. This research was financially supported by the Scientific and Technological Development Project of Jilin Province, China (Grant No. 20180101017JC) (Grant No. 20200201188JC), and the central government guides the local science and technology development fund project Jilin Province basic research special project (Grant No. 202002077JC).

http://www.aloki.hu ● ISSN 1589 1623 (Print) ● ISSN1785 0037 (Online)
DOI: http://dx.doi.org/10.15666/aeer/1902_11491162
© 2021, ALÖKI Kft., Budapest, Hungary

REFERENCES

[1] Bazzaz, F. A. (1996): Plants in changing environments: linking physiological, population, and community ecology. – Cambridge University Press, Britain.
[2] Bu, J., Zou, C. J., Xu, W. D. (1995): Study on the relationship between growth and development and ecological conditions of *Pinus sylvestriformis*. – Journal of Shenyang Teachers College (Natural Science) 3: 47-51.
[3] Chen, Y., Yu, J., Huang, B. (2015): Effects of elevated CO_2 concentration on water relations and photosynthetic responses to drought stress and recovery during rewatering in Tall Fescue. – J Am Soc Hortic Sic 140: 19-26.
[4] Chen, X. L., Li, L., Huang, Y. S. (2017): The growth laws of *Pinus sylvestris* var. *Sylvestriformis* (Takenouchi) Cheng et C. D. Chu. – Shaanxi Forestry Science and Technology 6: 35-37.
[5] Duan, B. L., Lü, Y. W., Yin, C. Y., Li, C. (2005): Morphological and physiological plasticity of woody plant in response to high light and low light. – Chinese Journal of Applied and Environmental Biology 11(2): 238-245.
[6] Hu, Y. M., Xu, W. D., Zheng, Y. R. (1996): Spatial distribution pattern of natural *Pinus sylvestriformis* population with same age. – Journal of Applied Ecology 7(02): 113-116.
[7] Huang, W. Y., Feng, Z. J. (2020): Effect of light intensity on the growth and photosynthetic characteristics of *Clerodendrum japonicum*. – Forestry and Environmental Science 36(04): 96-101.
[8] Jiang, R. F., Liu, Y. H. (2017): Effects of light intensity on photosynthesis and growth characteristics of *Davidia involucrata* seedlings. – Ecological Science 36(05): 114-120.
[9] Jin, H., Zhao, Y., Zhao, W. et al. (2015): Natural population status and endangered mechanism of *Pinus sylvestriformis* in Changbai Mountain. – Journal of Beihua University (Natural Science) 16(5): 661-665.
[10] Kim, J. H., Lee, H. J., Park, C. M. (2017): HOS1 acts as a key modulator of hypocotyl photomorphogenesis. – Plant Signaling & Behavior 12(5): e1315497.
[11] Liu, J. F., Yang, W. J., Jiang, Z. P., Guo, Q. (2011): Effects of shading on photosynthetic characteristics and chlorophyll fluorescence parameters in leaves of the endangered plant *Thuja sutchuenensis*. – Acta Ecologica Sinica 31(20): 5999-6004.
[12] Rozendaal, D. M. A., Hurtado, V. H., Poorter, L. (2006): Plasticity in leaf traits of 38 tropical tree species in response to light: relationships with light demand and adult stature. – Functional Ecology 20(2): 207-216.
[13] Shang, S. J., Wang, Y. J., Wang, N., Yang, J. L., Xu, S., He, X. Y., Chen, W. (2020): Effects of light intensity on physiological and growth characteristics of *Paeonia suffruticosa* var. *papaveracea*. – Chinese Journal of Ecology 39(9): 2963-2973.
[14] Smith, T., Huston, M. (1989): Atheory of the spatial and temporal dynamics of plant communities. – Vegetatio 83(1/2): 49-69.
[15] Valladares, F., Wright, S. J., Lasso, E., Kitajima, K., Pearcy, R. W. (2000): Plastic phenotypic response to light of 16 congeneric shrubs from a panamanian rainforest. – Ecology 81(7): 1925-1936.
[16] Wang, J. M. (2008): Brief analysis of Korean pine plantation translucent tending. – Journal of Heilongjiang Ecological Engineering Vocational College 21(2): 21-22.
[17] Welander, N. T., Ottosson, B. (1998): The influence of shading on growth and morphology in seedlings of *Quercus robur* L. and *Fagus sylvatica* L. – Forest Ecology and Management 107: 117-126.
[18] Wen, D. Z., Kong, G. H., Lin, Z. F., Ye, W. H. (1999): A comparative study on the growth responses to light intensity in seedlings of four subtropical tree species. – Journal of Tropical and Subtropical Botany 7(2): 125-132.
[19] Yin, H., Zhao, Y., Jin, H., Liu, L. J., Zhang, D. W., Bing, G. P., Wang, C., Meng, Q. J. (2017): The experiment of preventing *Thuja koraiensis* cutting seedling frost heaving

http://www.aloki.hu ● ISSN 1589 1623 (Print) ● ISSN1785 0037 (Online)
DOI: http://dx.doi.org/10.15666/aeer/1902_11491162
© 2021, ALÖKI Kft., Budapest, Hungary

damage in Changbai mountain. – Journal of Jilin Forestry Science and Technology 46(3): 1-2.

[20] Yue, G. F., Han, Z. Q., Xue, Z. W. et al. (2020): The effect of different shades on the flowering period and photosynthetic characteristics of *peony*. – Jiangsu Agricultural Sciences 48(17): 166-170.

[21] Zhao, S. J., Yan, K. S., Zhang, H. J. et al. (2002): Investigation report on introduction of Pinus sylvestris. – Hebei Forestry Science and Technology 5: 13-14.

[22] Zhao, Y., Jin, H., Yin, H., et al. (2017): Effects of different exogenous hormones on Seed Germination Ability of *Pinus sylvestriformis*. – Journal of Beihua University (Natural Science) 6: 722-726.

http://www.aloki.hu ● ISSN 1589 1623 (Print) ● ISSN1785 0037 (Online)
DOI: http://dx.doi.org/10.15666/aeer/1902_11491162
© 2021, ALÖKI Kft., Budapest, Hungary

WET NITROGEN DEPOSITION AND CAUSAL FACTORS IN THE FOREST ECOSYSTEMS OF SOUTHEAST TIBET, CHINA

HAN, L.[1] – WANG, G.[2*] – TANG, X. Y.[2]

[1]*Chengdu University of Information Technology, Chengdu 610225, China*

[2]*Institute of Plateau Meteorology, China Meteorological Administration, Chengdu 610072, China*

**Corresponding author*
e-mail: wg800110@aliyun.com

(Received 18th Sep 2020; accepted 21st Dec 2020)

Abstract. A continuous three-year observation (from May 2012 to September 2014) was conducted to characterize the different forms of nitrogen deposition for a forest ecosystem in the southeastern part of the Tibet Plateau in China. Total nitrogen (TN) throughfall deposition varied from 6.9 kg $N \cdot ha^{-1} \cdot yr^{-1}$ to 8.8 kg $N \cdot ha^{-1} \cdot yr^{-1}$ (average: 7.5 kg $N \cdot ha^{-1} \cdot yr^{-1}$). NH_4^+-N was the dominant form of total inorganic nitrogen (TIN) deposition, accounting for 53% of TN deposition in throughfall, while NO_3^--N accounted for 22% and dissolved organic nitrogen accounted for 25%. Seasonal variability indicated that TN deposition peaked in summer. Monthly average temperature was positively correlated with NO_3^--N and TIN deposition ($p < 0.05$), and cumulative precipitation was positively correlated with NO_3^--N, TN, and TIN deposition ($p < 0.05$). Additionally, NH_4^+-N and monthly cumulative precipitation accounted for 90.2% of the variation of the TN deposition flux in the forest throughfall. Thus, elevated deposition of various forms of nitrogen likely threaten forest ecosystems via cumulative precipitation, influenced by average temperature to a lesser extent. Finally, TN deposition in this region is mostly controlled by agricultural activities rather than industrial activities or transportation.
Keywords: *Tibet plateau, observation, total nitrogen, NH_4^+-N content, NO_3^--N content*

Introduction

From 1860 to 2000, nitrogen discharge into the atmosphere increased from 15 Tg $N \cdot yr^{-1}$ to 165 Tg $N \cdot yr^{-1}$ due to human activities (Chen and Mulder, 2007). Rainwater penetration is an important factor that maintains the nutrient balance of forest ecosystems, directly affecting soil moisture distribution and nutrient cycling (Carly-Moses, 2004). In China, total NO_x emissions increased from 8.4 Tg $N \cdot yr^{-1}$ in 1990 to 11.3 Tg $N \cdot yr^{-1}$ in 2000, and total NH_3 emissions increased from 10.8 Tg $N \cdot yr^{-1}$ to 13.6 Tg $N \cdot yr^{-1}$ over the same period (Lu and Tian, 2007). Elevated nitrogen deposition to terrestrial ecosystems may lead to nitrogen saturation and greatly elevate associated ecological risks (Matson et al., 2002), such as the eutrophication of water bodies (Gao et al., 2007), soil acidification (Bouwman et al., 2002), plant nutrient imbalances, and undesirable changes in biodiversity (Stevens et al., 2010). Therefore, a quantitative assessment of nitrogen deposition through rainwater penetration is key in monitoring atmospheric nitrogen deposition received by the forest ecosystem, and is also necessary for understanding the feedback mechanism of the forest ecosystem for atmospheric nitrogen deposition.

Forest ecosystems are commonly nitrogen deficient and sensitive to sharp increases in nitrogen deposition (Aber and Magill, 2004). There has been widespread concern worldwide about the effect of increasing nitrogen deposition in forest ecosystems, and researchers have confirmed that it has resulted in nitrogen saturation in many sites

http://www.aloki.hu ● ISSN 1589 1623 (Print) ● ISSN 1785 0037 (Online)
DOI: http://dx.doi.org/10.15666/aeer/1902_11631176
© 2021, ALÖKI Kft., Budapest, Hungary

(Macdonald et al., 2002; Kristensen et al., 2004; Dise et al., 2009). However, research on nitrogen deposition of forest ecosystems in China has mainly focused on heavily polluted areas (Fan et al., 2009; Fang et al., 2011), resulting in little information on high-altitude forest ecosystems. Known as the third pole, the Qinghai–Tibet Plateau has experienced relatively little interference by human activities. It is also a sensitive area for global environmental change. Thus, there is great need to conduct environmental research in this part of the world, and to explore the impact of increased atmospheric nitrogen on the nitrogen storage of forest soils.

In this study, we systematically studied the wet nitrogen deposition of forest ecosystems in the Nyingchi region of the Qinghai–Tibet Plateau. We used an in situ observation method to measure atmospheric nitrogen deposition. The purpose of this work is to 1) investigate the variation and characteristics of atmospheric nitrogen deposition, 2) derive the general sources of atmospheric nitrogen deposition, and 3) assess the contribution rate of the Qinghai–Tibet Plateau to global climate change.

Materials and methods

Site description

A forested experimental plot was selected at the Southeast Tibet Observation and Research Station for the Alpine Environment, Chinese Academy of Sciences (29°46'N, 94°44'E), near Lulang town, Nyingchi district, Tibet Autonomous Region. The station supports integrated observation and research of alpine environments. The topography is flat and lies 3200 m above sea level.

Nyingchi district has a tropical humid and semi-humid climate that is affected by the warm ocean currents of the Indian Ocean and the Pacific Ocean. Typically, spring is dry and windy, autumn is cool and foggy, summer is short, warm, and sunny, and winter is long and cold. The latter is further characterized by a long frost period, with much of the frost-free days (about 170 days of the year) concentrated in other seasons. The average annual temperature is 12 °C. The average annual rainfall ranges from 600 mm to 800 mm, with 92.4% of the rainfall concentrated during the growing season.

The vegetation type is mature virgin coniferous *Picea abies* forest, with an average age of the dominant tree species of more than 100 years. Other main tree species include *Abies georgei* var. *smithii*, *Picea likiangenses* var. *linzhiensis*, *Pinus yunnanensis*, and *Pinus densata*. The soil in this area is brown forest soil.

Sampling and chemical analyses

A forested plot (30 × 40 m) with flat topography and small spatial heterogeneity was selected at the research station. Rainwater samples were collected using self-made rain collectors, which consisted of a 7-cm-diameter plastic funnel and a 500-ml plastic collecting bottle. Sixteen rain collectors were randomly placed in the plot area, and the average distance of the rain gauges was 3 m. Each collected sample volume did not exceed 100 ml. Samples were collected at irregular intervals, according to the frequency of precipitation, two to three times per month from May to October during 2012–2014. This approach helped assure sample integrity and measurement accuracy. The contents of various forms of nitrogen in the precipitation were determined using an ultraviolet spectrophotometer, flow analyzer, and total organic carbon/total nitrogen (TOC/TN) analyzer (TOC-VCSH TN; Shimadzu, Kyoto, Japan).

http://www.aloki.hu ● ISSN 1589 1623 (Print) ● ISSN 1785 0037 (Online)
DOI: http://dx.doi.org/10.15666/aeer/1902_11631176
© 2021, ALÖKI Kft., Budapest, Hungary

Calculation and statistical analysis

The average values and standard errors of nitrogen deposition flux (kg $N \cdot ha^{-1} \cdot yr^{-1}$) were calculated. The correlation of atmospheric nitrogen wet deposition was analyzed using principal component regression analysis and calculated using SPSS ver. 19.0 (IBM Corp., Armonk, NY, USA).

The monthly cumulative precipitation was used to calculate the monthly nitrogen deposition from forest throughfall. The wet atmospheric nitrogen deposition flux (F) was calculated as:

$$F = (P \times C_i \times 10^{-9}) \div (S \times 10^{-8}) \quad \text{(Eq.1)}$$

where F is the monthly wet nitrogen deposition flux ($kg \cdot ha^{-1}$), P is monthly cumulative precipitation (ml), S is the area of the rainfall collector (cm^2), and C_i is the monthly average concentration of nitrogen in precipitation ($mg \cdot L^{-1}$), including the concentration of total inorganic nitrogen (TIN), TN, NO_3^--N, and NH_4^+-N in precipitation. The standard error was calculated for all results. The linear regression between precipitation/temperature and wet atmospheric nitrogen deposition flux was analyzed using SPSS ver. 19.0, and the level of the significance was verified with the Pearson's χ^2-test.

Results

Variations in annual average temperature and cumulative precipitation

Figure 1 shows the variations in average temperature and monthly cumulative precipitation from May to October during 2011–2014. The average monthly temperature showed similar annual trends among the study years, with maximum values in July and minimum values in January and December. During the study period, the highest monthly temperature was 16.7 °C, the lowest was −4.6 °C, and the average annual temperature was 6.1 °C. By contrast, the cumulative monthly precipitation showed different trends and ranges among the study years. The cumulative annual precipitation from 2011 to 2014 was 631.4 mm, 954.1 mm, 835.6 mm, and 683 mm, respectively.

Characteristics of different forms of wet nitrogen deposition

There were significant differences in the amount of cumulative nitrogen deposition of throughfall among the various forms of nitrogen (*Table 1*). The relative concentrations of the various forms of nitrogen followed the order TN > TIN > NH_4^+-N > NO_3^--N. Notably, the NH_4^+-N deposition flux was significantly smaller than that of TN ($p < 0.05$), whereas the NO_3^--N deposition flux was significantly smaller than those of NH_4^+-N, TIN ($p < 0.05$) and TN ($p < 0.01$).

The average annual cumulative deposition fluxes of NO_3^--N, NH_4^+-N, TIN, and TN in 2012–2014 were 1.41 kg $N \cdot ha^{-1} \cdot yr^{-1}$, 4.06 kg $N \cdot ha^{-1} \cdot yr^{-1}$, 5.47 kg $N \cdot ha^{-1} \cdot yr^{-1}$, and 7.47 kg $N \cdot ha^{-1} \cdot yr^{-1}$, respectively. The proportions of TIN/TN and NH_4^+-N/TIN were 74.43% and 71.12%, respectively. These results indicated that TIN and NH_4^+-N were the main components of TN and TIN deposition, respectively. In addition, there was a significant correlation between the NH_4^+-N and NO_3^--N deposition fluxes ($p < 0.05$).

http://www.aloki.hu ● ISSN 1589 1623 (Print) ● ISSN 1785 0037 (Online)
DOI: http://dx.doi.org/10.15666/aeer/1902_11631176
© 2021, ALÖKI Kft., Budapest, Hungary

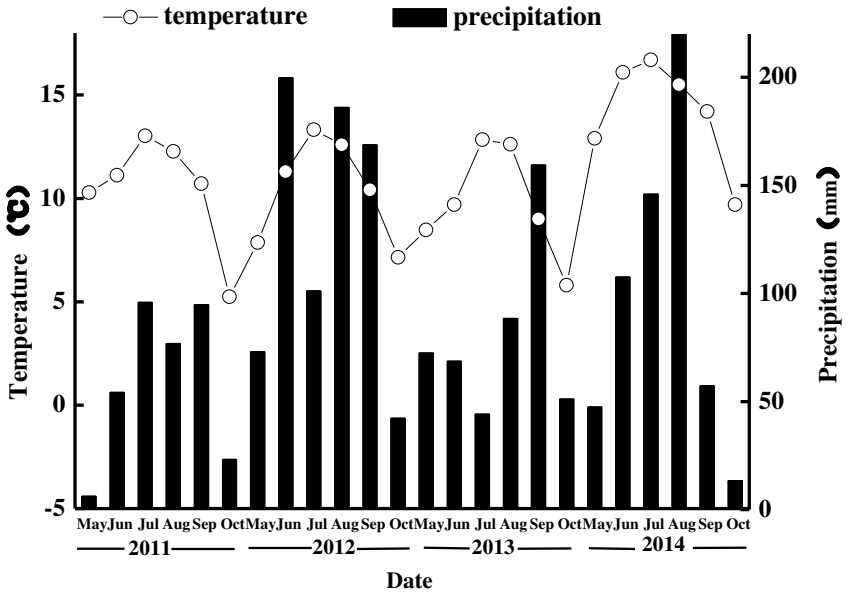


Figure 1. *Monthly variations in temperature and precipitation from 2011 to 2014*

Table 1. *Cumulative nitrogen deposition of throughfall*

Period	Month	NH_4^+-N	NO_3^--N	TIN	TN	NH_4^+-N/NO_3^--N	NH_4^+-N/TIN	TIN/TN
		$kg \cdot hm^{-2} \cdot yr^{-1}$				%		
2012	May	0.08	0.18	0.26	0.47	0.44	30.77	55.32
	June	0.70	0.38	1.08	1.38	1.84	64.81	78.26
	July	0.83	0.76	1.59	1.67	1.09	52.20	95.21
	Aug.	1.88	0.68	2.56	2.83	2.76	73.44	90.46
	Sep.	0.87	0.14	1.01	1.62	6.21	86.14	62.35
	Oct.	0.69	0.06	0.75	0.85	11.50	92.00	88.24
	Average	0.84	0.37	1.21	1.47	2.27	66.56	78.30
2013	May	0.72	0.27	0.99	1.53	2.67	72.51	64.59
	June	1.30	0.10	1.41	2.04	13.00	92.73	68.73
	July	0.54	0.08	0.61	0.72	6.75	87.24	85.77
	Aug.	0.32	0.04	0.36	0.53	8.00	89.24	67.18
	Sep.	0.29	0.23	0.51	1.11	1.26	56.10	46.06
	Oct.	0.27	0.07	0.35	0.97	3.86	78.38	35.73
	Average	0.57	0.13	0.70	1.15	4.38	79.37	61.34
2014	May	1.01	0.23	1.24	1.30	4.39	81.45	95.38
	June	0.99	0.24	1.23	1.71	4.13	80.49	71.93
	July	0.69	0.42	1.11	1.20	1.64	62.16	92.50
	Aug.	0.70	0.64	1.34	1.90	1.09	52.24	70.53
	Sep.	0.31	0.20	0.51	0.58	1.55	60.78	87.93
	Average	0.74	0.35	1.09	1.34	2.11	67.42	83.65

The monthly cumulative nitrogen deposition fluxes exhibited different monthly variation characteristics in 2012–2014 (*Fig. 2*). In 2012 and 2014, the fluxes of TIN and

http://www.aloki.hu ● ISSN 1589 1623 (Print) ● ISSN 1785 0037 (Online)
DOI: http://dx.doi.org/10.15666/aeer/1902_11631176
© 2021, ALÖKI Kft., Budapest, Hungary

TN reached a significant maximum in August ($p < 0.05$). In 2013, the fluxes of TIN and TN reached their maximum values in June ($p < 0.01$). In addition, the TN flux showed inter-annual variations. The cumulative deposition fluxes of TN in 2012, 2013, and 2014 were 8.82 kg $N \cdot ha^{-1} \cdot yr^{-1}$, 6.91 kg $N \cdot ha^{-1} \cdot yr^{-1}$, and 6.69 kg $N \cdot ha^{-1} \cdot yr^{-1}$, respectively. The cumulative deposition flux of TN reached a maximum in late spring or early summer, and accumulated more than 30% of whole years.

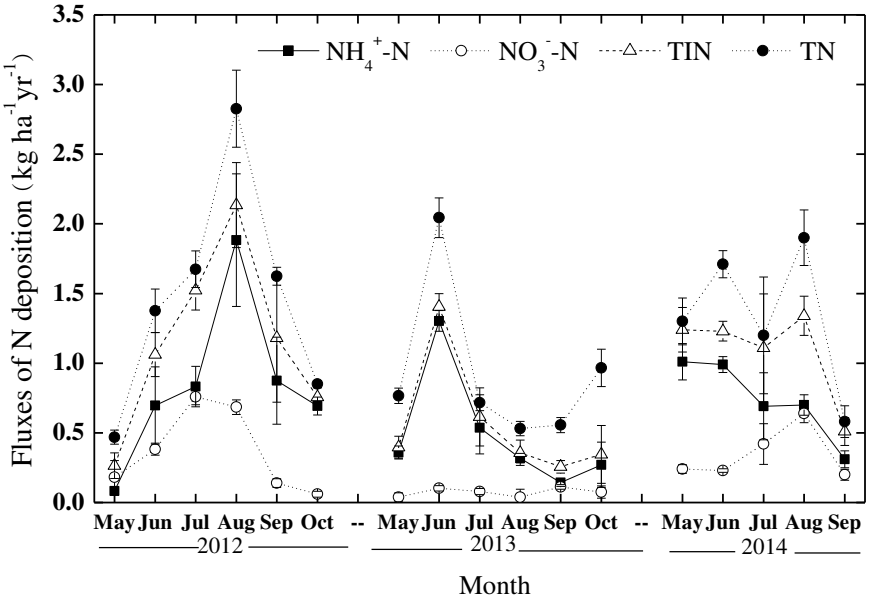


Figure 2. *Monthly variation of different forms nitrogen deposition*

Relationships of different forms of wet nitrogen deposition with temperature and precipitation

The relationship between different forms of wet nitrogen deposition fluxes and monthly average temperature or monthly cumulative precipitation were explored using principal component regression analysis (*Figs. 3* and *4*). The trend of atmospheric nitrogen deposition in 2012–2014 was generally more consistent with monthly cumulative precipitation than with monthly average temperature.

Different forms of monthly nitrogen deposition were positively correlated with mean temperature and cumulative precipitation. NO_3^--N and TIN were significantly correlated with monthly mean temperature ($p < 0.05$), and NO_3^--N, TIN, and TN were significantly correlated with monthly cumulative precipitation ($p < 0.05$). Thus, nitrogen deposition fluxes of forest throughfall in the Nyingchi region from 2012–2014 were affected by both temperature and precipitation, with precipitation having a greater influence.

Considering that nitrogen deposition from forest throughfall is mainly influenced by meteorological factors, the contribution of different forms of nitrogen deposition flux could be derived from the regression analysis results. Monthly cumulative precipitation (x_1) accounted for 28.0% of NO_3^--N deposition (y_1) changes in forest throughfall ($y_1 = 0.002\ x_1 - 0.013$, $R^2 = 0.280$, $p < 0.05$, n = 17). Monthly cumulative precipitation (x_1) accounted for 28.3% of TIN deposition (y_2) changes in forest throughfall ($y_2 = 0.005\ x_1 + 0.303$, $R^2 = 0.283$, $p < 0.05$, n = 17). Finally, NH_4^+-N(x_1) and monthly cumulative precipitation (x_2) accounted for 90.2% of TN deposition (y_3) changes in

http://www.aloki.hu ● ISSN 1589 1623 (Print) ● ISSN 1785 0037 (Online)
DOI: http://dx.doi.org/10.15666/aeer/1902_11631176
© 2021, ALÖKI Kft., Budapest, Hungary

forest throughfall ($y_3 = 1.178\ x_1 + 0.003\ x_2 + 0.057$, $R^2 = 0.902$, $p < 0.01$, n = 17). Thus, cumulative precipitation was the main factor affecting the deposition rates of the various forms of nitrogen from forest throughfall. When combined with environmental factors, cumulative precipitation can more effectively predict nitrogen deposition rates.

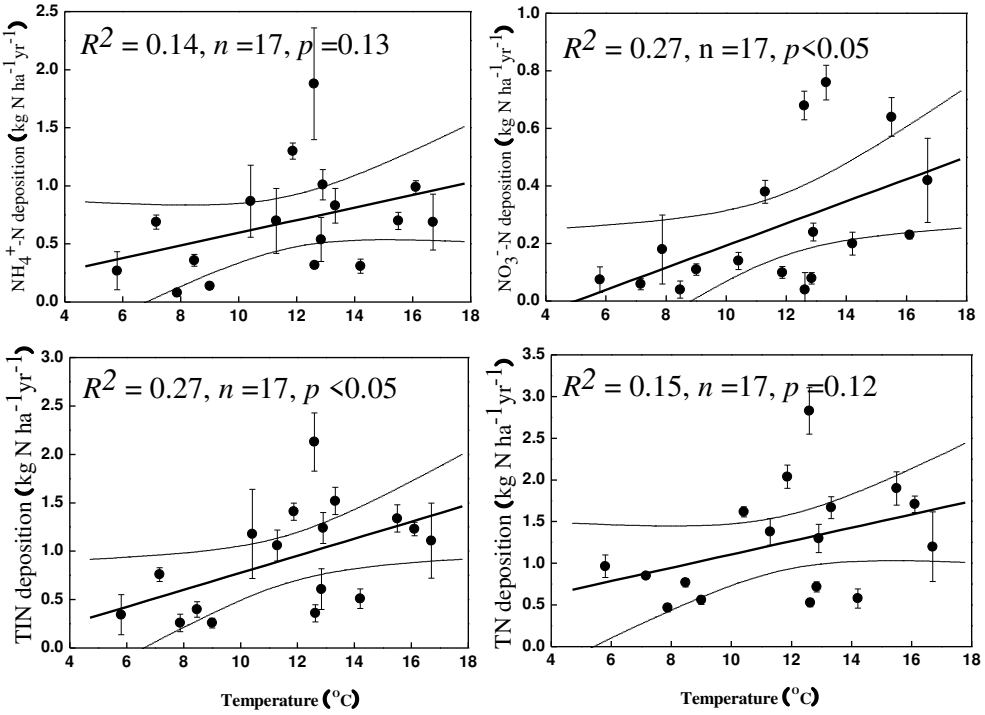


Figure 3. *Principal component regression analysis of nitrogen deposition and temperature*

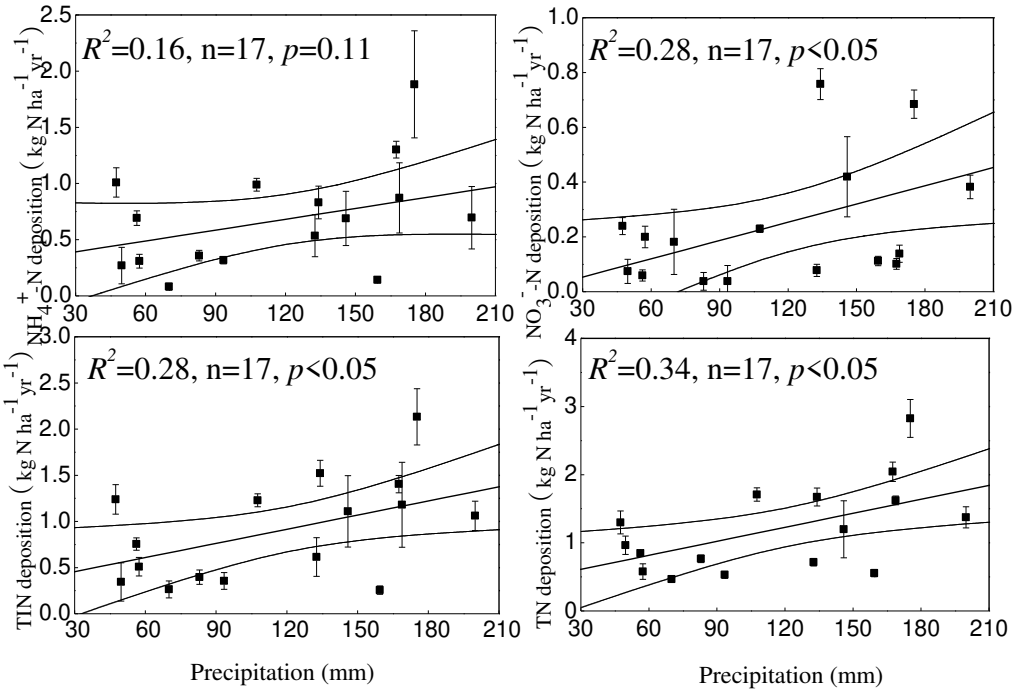


Figure 4. *Principal component regression analysis of nitrogen deposition and precipitation*

http://www.aloki.hu ● ISSN 1589 1623 (Print) ● ISSN 1785 0037 (Online)
DOI: http://dx.doi.org/10.15666/aeer/1902_11631176
© 2021, ALÖKI Kft., Budapest, Hungary

Discussion

Annual variations of different forms of nitrogen deposition

In this study, the average TIN deposition was 5.01 kg $N \cdot ha^{-1} \cdot yr^{-1}$, while the atmospheric TIN deposition fluxes of five forest ecosystems in South China and eight forest ecosystems in East China were 6.6–21.8 $kg \cdot ha^{-1} \cdot yr^{-1}$ and 1.3–29.5 kg $N \cdot ha^{-1} \cdot yr^{-1}$, respectively (Chen and Mulder, 2007). Thus, TIN deposition in the Linzhi area is lower than that in other parts of China. In addition, Jia et al. (2009) measured the average amount of atmospheric TIN wet deposition in 2005–2006 at the Linzhi Tibet Agriculture and Animal Husbandry College ecological station as 2.36 kg $N \cdot ha^{-1} \cdot yr^{-1}$, although plants there produce a leaching effect that causes the rainwater to contain large amounts of dry sediment components (Fenn et al., 1999; Yeon et al., 2014). In the Welsh Highlands, Stecens et al. (1994) measured a deposition flux of TIN in throughfall of 25.1 kg $N \cdot ha^{-1} \cdot yr^{-1}$, half that in precipitation, demonstrating the importance of dry atmospheric nitrogen deposition in precipitation. However, the atmospheric dry deposition flux is affected by micro-meteorology (Thimonier et al., 2005); therefore, the contribution rate of dry deposition to total atmospheric nitrogen deposition in this study was not certain. In some cases, dry atmospheric deposition has accounted for nearly 80% of total nitrogen deposition (Goulding et al., 1998; Fan et al., 2009) in forest ecosystems, while the critical load of atmospheric nitrogen deposition (including dry and wet deposition) in forest ecosystems is 10–20 kg $N \cdot ha^{-1} \cdot yr^{-1}$ (Krupa, 2003).

TIN deposition is present mainly as NH_4^+-N and NO_3^--N. NH_4^+-N is formed from the dissolution of atmospheric NH_3 and scavenging of NH_4^+-N aerosols. The main anthropogenic sources include human and animal excrement, volatilization of fertilizer, and biomass burning, which are closely related with agricultural activities (Prospero et al., 1996). The formation of NO_3^--N is considerably more complex. NO_3^--N is an end-product of a series of gas-phase photochemical and heterogeneous reactions involving NO_x. The major anthropogenic sources include fossil-fuel combustion by power plants and automobiles (Gao et al., 2007). Thus, the NH_4^+-N/NO_3^--N ratio can reflect the relative contribution of reactive nitrogen from industry and transportation, agriculture, and animal husbandry to TIN deposition at a local scale, and can be used to evaluate the degree of industrialization (Larssen et al., 2006; Zhao et al., 2009).

In this study, NH_4^+-N was the dominant form of TIN deposition, although the NH_4^+-N/NO_3^--N ratio varied greatly from 1.0 to 3.1 (average: 2.0; *Table 1*); this range compared well with that of a compiled analysis of Chinese forest ecosystems (Fang et al., 2011). In western China, with a much lower degree of economic development, the NH_4^+-N/NO_3^--N ratio was much higher, reaching 6.0 (Tang et al., 2000), while the NH_4^+-N/NO_3^--N ratio was as low as 0.8 in the more developed regions of East China (Zhang, 2006). Compared to developed countries, the NH_4^+-N/NO_3^--N ratio in our study was much larger than those in highly industrialized areas of New York and Canada, with ratios less than 1.0 (Watmough et al., 2005; Golden and Boyer, 2009) (*Table 2*). The results from our study indicate that NH_4^+-N from agriculture, as well as human and animal excrement, are larger contributors to nitrogen deposition compared to NO_3^--N from fossil fuel combustion in industry and transportation. Therefore, the Nyingchi region is more heavily influenced by agriculture rather than industry or transportation.

http://www.aloki.hu ● ISSN 1589 1623 (Print) ● ISSN 1785 0037 (Online)
DOI: http://dx.doi.org/10.15666/aeer/1902_11631176
© 2021, ALÖKI Kft., Budapest, Hungary

Table 2. *Comparison of bulk nitrogen deposition reported for regional forest ecosystems from different studies*

Forest form	Station		Climate factor		Nitrogen deposition (Kg N·ha^{-1}) yr^{-1}	Study period	Reference
	Latitude	Longitude	Precipitation (mm)	Temperature (°C)			
Sitka spruce	42.3N	72.10W	1120	3.5	8	2001–2002	Zerva, 2005
Sitka spruce	57.29N	4.13W	973	7.7	6.4	1994–1995	Macdonald, 1997
Grassland	45.38N	2.44E	1200	7	80	2002–2004	Allard, 2007
Norway spruce	51.31N	9.34E	1090	6.4	11.8	1993–2001	Borken, 2005
Pine	47N	9.5E	800	7.3	20	1993–1995	Butterbach-Bahl, 2002
Red pine	40N	138E	1076	14.5	30.6	1999–2000	Oura, 2001
Coniferous	43N	72.10W	1120	3.5	7.9	1981–1982	Goodroad, 1984
Sitka spruce	57.29N	4.13W	973	7.7	6.7	1995–1997	Skiba, 1998
Disturbed forest	23.1N	112.1E	1927	21.4	34	2004–2005	Zhang, 2006
Coniferous forest	42.24N	85.24W	890	9.7	6	1995–1996	Ambus, 2006
Breech	51.46N	9.35E	1038	7.2	63.3	1997–1999	Borken, 2002
Tropical forest	9.06N	79.50W	2650	27.4	5	2006–2007	Koehler, 2009
Horsetail pine	27.5N	114.3E	1400	17.9	57	1985–1987	Ma, 1989
Monsoon forest	23.1N	112.1E	1927	21.4	38.4	1998–1999	Zhou, 2001
Larch	45.2N	127.3E	724	2.8	12.89	1980–1982	Liu, 1992
Tropical rainforest	21.6N	101.2E	1557	21.4	8.89	1999	Sha, 2002
Wetland	47.4N	133.3E	600	1.9	7.57	2004–2005	Sun, 2007
Spruce	29.5N	93.3E	700	11.5	3.05	2005–2006	Jia, 2009
Qinghai, China	36.6N	101.8E	400	7.6	2.9 (TIN)	2000	Tang, 2000
Shanghai, China	31.1N	121.8E	1166	16.0	58.1 (TIN)	2006	Zhang, 2006
Chinese forest	23 -50.1N	73.3-135.1E	400-1500	8.0-18.0	16.6 (TIN)	2011	Fang, 2011
New York, USA	40.4N	74.0W	1063	11.5	7.2 (TIN)	2009	Golden, 2009
North–South China	40N	109–128E	467–1771	−5.6–22.1	9.8 (TIN)	2014	Zhan, 2014
Southeast Tibet	29.5N	94.4E	700	11.5	7.47	2014	This study

Casual factors of nitrogen deposition in forest throughfall

The results of this study revealed a significant positive correlation between atmospheric nitrogen deposition and precipitation in forest throughfall, similar to several other studies in China. For example, Fan et al. (2009) found that atmospheric TIN deposition was significantly positively correlated with precipitation in the southeastern forest of China ($p < 0.05$, $R^2 = 0.245$). Zhai et al. (2009) found that the atmospheric TN deposition was significantly positively correlated with precipitation near Taihu Lake, China ($p < 0.05$, $R^2 = 0.501$). Different forms of nitrogen deposition and precipitation can also exhibit linear, logarithmic, or exponential correlations. For example, Zhan and Yu (2014) found that the TIN deposition flux (y) in forest rainfall in eastern China was linearly related to annual average precipitation (x) ($y = 0.02\ x - 6.89$, $R^2 = 0.682$, $p < 0.001$). Yuan et al. (2009) found that the precipitation fluxes of NO_3^--N, NH_4^+-N, and TN in typical areas of Chongqing also showed a significant linear correlation with monthly mean precipitation (NO_3^--N: $y = 0.0106\ x + 0.0408$, $p < 0.05$, $R^2 = 07618$; NH_4^+-N: $y = 0.0186\ x + 0.0359$, $p < 0.05$, $R^2 = 0.7947$; TN: $y = 0.0397\ x_1 + 0.1633$, $p < 0.05$, $R^2 = 0.8451$). However, Xu et al. (2009) found that the nitrogen deposition flux measured in the Yangtze River region of China was logarithmically correlated with monthly average precipitation (NO_3^--N: $y = 0.0818\text{Ln}(x) - 0.0043$, $p < 0.001$, $R^2 = 0.1954$; NH_4^+-N: $y = 0.0797\text{Ln}(x) - 0.0021$, $p < 0.001$, $R^2 = 0.2079$). Furthermore, Jia et al. (2009) found that the nitrogen deposition flux in the Nyingchi region was exponentially related to

http://www.aloki.hu ● ISSN 1589 1623 (Print) ● ISSN 1785 0037 (Online)
DOI: http://dx.doi.org/10.15666/aeer/1902_11631176
© 2021, ALÖKI Kft., Budapest, Hungary

monthly average precipitation (NO_3^--N: $y = 0.0034\ x + 0.2741$, $p < 0.05$, $R^2 = 0.410$; NH_4^+-N: $y = 0.0054\ x + 0.7469$, $p < 0.001$, $R^2 = 0.501$).

In addition, many studies have shown that temperature is closely related to agricultural activities, animal and plant activity, tree burning, and so on (Goulding et al., 1998), such that nitrogen can enter the atmosphere through particles, gases, etc. This is not only the main source of NH_4^+-N and NO_3^--N in precipitation, but also interferes with atmospheric dry deposition of the surface layer of trees in forest ecosystems, which affects the nitrogen deposition flux in forest rainfall (Jin et al., 2006). The atmospheric nitrogen deposition flux in forest rainfall is also related to vegetation type (Bhat et al., 2011), wind direction (Goulding et al., 1998), geographic location (Glatzel, 1990), and so on. Therefore, determining the influencing factors of nitrogen deposition in forest rainfall can contribute to the prediction of atmospheric nitrogen deposition flux and input in the soil of forest ecosystems.

Uncertainty of estimated nitrogen deposition

NH_4^+-N and NO_3^--N are the main nitrogen forms that are readily available for organisms to incorporate into their bodies. Therefore, most researchers have concentrated extensively on their deposition at local and regional scales. However, TIN deposition has been measured using different methods, which causes some confusion in comparing different results, although the patterns within dataset are still useful. In our study, winter measurements of TIN may have been underestimated because snow can be transported by wind before melting. Therefore, further research is required to develop novel techniques to estimate TIN deposition more precisely. Furthermore, organic nitrogen is another ubiquitous component of atmospheric nitrogen deposition. Some studies have found that organic nitrogen deposition can account for 10–30% of wet nitrogen deposition (Neff et al., 2002; Violaki et al., 2010). In Chinese forest ecosystems, Fang et al. (2011) measured organic nitrogen at 7.7 kg $N \cdot ha^{-1} \cdot yr^{-1}$, which constituted 32% of total dissolved nitrogen in precipitation. Additionally, dry nitrogen deposition can contribute an equal or greater proportion of nitrogen than wet deposition (Anatolaki and Tsitouridou, 2007; Lu and Tian, 2007). In North America, dry deposition contributed only 20–46% of wet deposition (Ollinger et al., 1993), whereas dry deposition was up to twice the wet nitrogen deposition in Europe (Kristensen et al., 2004). In China, the average dry deposition was 3.0 kg $N \cdot ha^{-1} \cdot yr^{-1}$ (Lu and Tian, 2007).

Elevated nitrogen deposition can cause acidification and eutrophication and considerably burden various ecosystems (Stevens et al., 2004; Bowman et al., 2006). A report on European forest ecosystems demonstrated that, above a threshold loading of approximately 10 kg $N \cdot ha^{-1} \cdot yr^{-1}$, many sites seemed to be nitrogen saturated (Macdonald et al., 2002; Kristensen et al., 2004; Dise et al., 2009). Fang et al. (2011) noted that elevated nitrogen leaching occurs in forest ecosystems when they receive throughfall TIN deposition of more than 5 kg $N \cdot ha^{-1} \cdot yr^{-1}$. Available evidence suggests that the critical load of nitrogen deposition may be nearly identical, at approximately 10 kg $N \cdot ha^{-1} \cdot yr^{-1}$ (Aber et al., 2003). Thus, forest ecosystems, particularly in the southern range of the North–South Transect of Eastern China are at risk of ecological disaster, because excessive nitrogen deposition could favor the invasion of nitrophilous plants caused by the decrease of nitrogen spatial heterogeneity (Cassidy et al., 2004; Gilliam, 2006). To minimize the deleterious influences of nitrogen deposition on sensitive forest ecosystems, additional reliable methods of measuring total nitrogen deposition are urgently required to develop a better understanding of nitrogen deposition scenarios.

http://www.aloki.hu ● ISSN 1589 1623 (Print) ● ISSN 1785 0037 (Online)
DOI: http://dx.doi.org/10.15666/aeer/1902_11631176
© 2021, ALÖKI Kft., Budapest, Hungary

Conclusions

Southeastern Tibet is a widely forested area and shows a large spatial variation of atmospheric nitrogen deposition, which has evidently increased with global change. Average throughfall TIN deposition and TN deposition were 5.56 kg $N \cdot ha^{-1} \cdot yr^{-1}$ and 7.47 kg $N \cdot ha^{-1} \cdot yr^{-1}$, respectively, and both were significantly correlated with precipitation. TIN deposition was greater than dissolved organic nitrogen deposition in the forest throughfall, indicating that the forest canopy is of paramount importance to the spatial variation of TN deposition. Compared to more developed regions, the higher NH_4^+-N/NO_3^--N ratio (average: 2.0) in this study suggests that TIN deposition is mostly controlled by agricultural activities rather than industrial activities or transportation. This study is valuable to planners and decision-makers in their attempts to curb atmospheric nitrogen emissions, and to evaluate the effects of consequent nitrogen deposition on forest ecosystems. And we will systematically study the dry nitrogen deposition of forest ecosystems in the Nyingchi region of the Qinghai–Tibet Plateau in the future.

Acknowledgments. The authors would like to thank the staff of the Southeast Tibet Observation and Research Station for the Alpine Environment, Chinese Academy of Sciences, for their contribution to field work. We also thank the anonymous reviewers for presenting valuable suggestions to improve this paper.

REFERENCES

[1] Aber, J. D., Magill, A. H. (2004): Chronic nitrogen additions at the Harvard forest (USA): The first 15 years of a nitrogen saturation experiment. – Forest Ecology and Management 196(1): 1-5.

[2] Aber, J. D., Goodale, C. L., Ollinger, S. V., Smith, M., Stoddard, J. L. (2003): Is nitrogen deposition altering the nitrogen status of northeastern forests? – BioScience 53(4): 375-389.

[3] Allard, V., Soussana, J. F., Falcimagne, R., Berbigier, P., Bonnefond, J. M., Ceschia, E., D'hour, P., Hénault, C., Laville, P., Martin, C., Pinarès-Patino, C. (2007): The role of grazing management for the net biome productivity and greenhouse gas budget (CO2, N2O and CH4) of semi-natural grassland. – Agriculture, Ecosystems and Environment 12: 47-58.

[4] Ambus, P., Robertson, G. P. (2006): The effect of increased N deposition on nitrous oxide, methane and carbon dioxide fluxes from unmanaged forest and grassland communities in Michigan. – Biochemistry 79: 315-337.

[5] Anatolaki, C., Tsitouridou, R. (2007): Atmospheric deposition of nitrogen, sulfur and chloride in Thessaloniki, Greece. – Atmospheric Research 85(3): 413-428.

[6] Bhat, S., Jacobs, J. M., Bryant, M. L. (2011): The chemical composition of rainfall and throughfall in five forest communities: a case study in Fort Benning, Georgia. – Water Air Soil Pollut 218: 323-332.

[7] Borken, W., Beese, T. (2005): Control of nitrous oxide emissions in European beech, Norway spruce and Scots pine forests. – Biogeochemistry 76: 141-159.

[8] Borken, W., Beese, F., Brumme, R., Lamersdorf, N. (2002): Long-term reduction in nitrogen and proton inputs did not affect atmospheric methane uptake and nitrous oxide emission from a German spruce forest soil. – Soil Biology & Biochemistry 34: 1815-1819.

http://www.aloki.hu ● ISSN 1589 1623 (Print) ● ISSN 1785 0037 (Online)
DOI: http://dx.doi.org/10.15666/aeer/1902_11631176
© 2021, ALÖKI Kft., Budapest, Hungary

[9] Bouwman, A. F., Boumans, L. J. M., Batjes, N. H. (2002): Estimation of global NH3 volatilization loss from synthetic fertilizers and animal manure applied to arable lands and grasslands. – Global Biogeochemical Cycles 16(2): 8-1-8-14.
[10] Bowman, W. D., Gartner, J. R., Holland, K., Wiedermann, M. (2006): Nitrogen critical loads for alpine vegetation and terrestrial ecosystem response: Are we there yet? – Ecological Applications 16(3): 1183-1193.
[11] Carly-Moses, D. E. (2004): Through fall, stemflow, and canopy interception loss fluxes in a semiarid Sierra Madre Oriental matorral community. – Journal of Arid Environments 58(2): 182-202.
[12] Cassidy, T. M., Fownes, J. H., Harrington, R. A. (2004): Nitrogen limits an invasive perennial shrub in forest understory. – Biological Invasions 6(1): 113-121.
[13] Chen, X. Y., Mulder, J. (2007): Atmospheric deposition of nitrogen at five subtropical forested sites in south China. – Science of the Total Environment 378(3): 317-330.
[14] Dise, N. B., Rothwell, J. J., Gauci, V., Salm, C. V. D., Vries, W. D. (2009): Predicting dissolved inorganic nitrogen leaching in European forests using two independent databases. – Science of the Total Environment 407(5): 1798-1808.
[15] Fan, J. L., Hu, Z. Y., Wang, T. J., Zhou, J., Wu, C. Y. H., Xu, X. (2009): Atmospheric inorganic nitrogen deposition to a typical red soil forestland in southeastern China. – Eniron Monit Assess 159: 241-253.
[16] Fang, Y. T., Gundersen, P., Vogt, R. D., Koba, K., Chen, F. S., Chen, X. Y., Yoh, M. K. (2011): Atmospheric deposition and leaching of nitrogen in Chinese forest ecosystems. – Journal of Forest Research 16(5): 341-350.
[17] Fenn, M. E., Bauder, L. I. D., Quevedo-Nolasco, A., Rodriguez-Frausto, C. (1999): Nitrogen and sulfur deposition and forest nutrient status in the valley of Mexico. – Water, Air and Soil Pollution 133: 155-174.
[18] Gao, Y., Kennish, M. J., Flynn, A. M. (2007): Atmospheric nitrogen deposition to the New Jersey coastal waters and its implications. – Ecological Applications 17(5): 31- 41.
[19] Gilliam, F. S. (2006): Response of the herbaceous layer of forest ecosystems to excess nitrogen deposition. – Journal of Ecology 94(6): 1176-1191.
[20] Glatzel, G. (1990): The nitrogen status of Austrian forest ecosystems as influenced by atmospheric deposition, biomass harvesting and lateral organomass exchange. – Plant and Soil 128: 67-74.
[21] Golden, H. E., Boyer, E. W. (2009): Contemporary estimates of atmospheric nitrogen deposition to the watersheds of New York State, USA. – Environmental Monitoring and Assessment 155(1): 319-339.
[22] Goodroad, L. L., Keeney, D. R., Peterson, L. A. (1984): Nitrous oxide emissions from agricultural soils in Wisconsin, J. – Journal of Environmental Quality 13: 448-453.
[23] Goulding, K. W. T., Bailey, N. J., Bradbury, N. J., Hargreaves, P., Howe, M., Murphy. D. V., Poulton, P. R., Willison, T. W. (1998): Nitrogen deposition and its contribution to nitrogen cycling and associated soil processes. – New Phytologist 139: 49-58.
[24] Jenssen, M., Butterbach-Bahl, K., Hofmann, G., Papen, H. (2002): Exchange of trace gases between soils and the atmospheric in Scots pine forest ecosystems of the Northeastern German lowlands: 2. A novel approach to scale up N2O-and NO-fluxes from forest soils by modeling their relationships to vegetation structure. – Forest Ecology and Management 167: 123-134.
[25] Jia, J. Y., Zhang, Y., Cai, X. B., Li, X. J. (2009): A dynamic change of wet deposition of nitrogen in southeast Tibet taking Linzhi experiment station as an example. – Acta Ecologica Sinica 29(4): 1907-1913.
[26] Jin, L., Shao, M., Zeng, L. M. (2006): Estimation of dry deposition fluxes of major inorganic species by canopy throughfall approach. – Chinese Science Bulletin 51(11): 1333-1337.

http://www.aloki.hu ● ISSN 1589 1623 (Print) ● ISSN 1785 0037 (Online)
DOI: http://dx.doi.org/10.15666/aeer/1902_11631176
© 2021, ALÖKI Kft., Budapest, Hungary

[27] Koehler, B., Corre, M. D., Veldkamp, E., Hans, W., Joseph, W. S. (2009): Immediate and long-term nitrogen oxide emissions from tropical forest soils exposed to elevated nitrogen input. – Global Change Biology 15: 2049-2066.
[28] Kristensen, H. L., Gundersen, P., Callesen, I., Reinds, G. J. (2004): Throughfall nitrogen deposition has different impacts on soil solution nitrate concentration in European coniferous and deciduous forests. – Ecosystems 7(2): 180-192.
[29] Krupa, S. V. (2003): Effects of atmospheric ammonia terrestrial vegetation: a review. – Environ Pollute 124: 179-221.
[30] Larssen, T., Lydersen, E., Tang, D. G., He, Y., Gao, J. X., Liu, H. Y., Duan, L., Seip, H. M., Vogt, R. D., Mulder, J. (2006): Acid rain in China. – Environmental Science and Technology 40(2): 418-425.
[31] Liu, S. R. (1992): Biogeochemical cycling characteristics of Dahurian larch plantation ecosystem. – Chinese Journal of Ecology 11(5): 1-6.
[32] Lu, C. Q., Tian, H. Q. (2007): Spatial and temporal patterns of nitrogen deposition in China: synthesis of observational data. – Journal of Geophysical Research 112(D22).
[33] Ma, X. H. (1989): Effects of rainfall on the nutrient cycling in man-made forests of Cunninghamia lanceolata and Pinus Massoniana. – Acta Ecologica Sinica 9(1): 15-20.
[34] Macdonald, J. A., Skiba. U., Sheppard, L. J., Ball, B., Roberts, J. D., Smith, K. A., Fowler, D. (1997): The effect of nitrogen deposition and seasonal variability on methane oxidation and nitrous oxide emission rates in an uptake spruce plantation and moorland. – Atmospheric Environment 22: 3693-3706.
[35] Macdonald, J. A., Dise, N. B., Matzner, E., Armbruster, M., Forsius, M. (2002): Nitrogen input together with ecosystem nitrogen enrichment predicts nitrate leaching from European forests. – Global Change Biology 8(10): 1028-1033.
[36] Matson, P., Lohse, K. A., Hall, S. J. (2002): The globalization of nitrogen deposition: consequences for terrestrial ecosystems. – Ambio: A Journal of the Human Environment 31(2): 113-119.
[37] Neff, J. C., Holland, E. A., Dentener, F. J., McDowell, W. H., Russell, K. M. (2002): The origin composition and rates of organic nitrogen deposition: a missing piece of the nitrogen cycle? – Biogeochemistry 57(1): 99-136.
[38] Ollinger, S. V., Aber, J. D., Lovett, G. M., Millham, S. E., Lathrop, R. G., Ellis, J. M. (1993): A spatial model of atmospheric deposition for the northeastern U.S. – Ecological Applications 3(3): 459-472.
[39] Oura, N., Shindo, J., Fumoto, T. (2001): Effects of nitrogen deposition on nitrous oxide emission from the forest floor. – Water, Air, and Soil Pollution 130: 673-678.
[40] Prospero, J. M., Barrett, K., Church, T., Dentener, F., Duce, R. A., Galloway, J. N., Levy, H., Moody, J., Quinn, P. (1996): Atmospheric deposition of nutrients to the North Atlantic Basin. – Biogeo-chemistry 35(1): 27-73.
[41] Sha, L. Q., Zheng, Z., Feng, L. Z., Liu, Y. H., Li, M. R. (2002): Biogeochemical cycling of nitrogen at a tropical seasonal Rain forest in XishuangBanna, SW China. – Acta Phytoecologica Sinica 26(6): 689-694.
[42] Skiba, U. M., Sheppard, L. J., Pitcairn, C. E. R., Leith, I., Fowler, D. (1998): Soil nitrous oxide and nitric oxide emissions as indicators of elevated atmospheric N deposition rates in seminatural ecosystems. – Environmental Pollution 102: 457-461.
[43] Stecens, P. A., Norris, D. A., Sparks, T. H., Hodgson, A. L. (1994): The impacts of atmospheric N inputs on throughfall, soil and stream water interactions for different aged forest and moorland catchments in wales. – Water, Air and Soil Pollution 73: 297-317.
[44] Stevens, C. J., Dise, N. B., Mountford, J. O., Gowing, D. J. (2004): Impact of nitrogen deposition on the species richness of grasslands. – Science 303(5665): 1876-1879.
[45] Stevens, C. J., Dupre, C., Dorland, E., Gaudnik, C., Gowing, D. J. G., Bleeker, A., Diekmann, M., Alard, D., Bobbink, R., David Fowler, D. (2010): Nitrogen deposition threatens species richness of grasslands across Europe. – Environmental Pollution 158(9): 2940-2945.

http://www.aloki.hu ● ISSN 1589 1623 (Print) ● ISSN 1785 0037 (Online)
DOI: http://dx.doi.org/10.15666/aeer/1902_11631176
© 2021, ALÖKI Kft., Budapest, Hungary

[46] Sun, Z. G., Liu, J. Q., Wang, J. D. (2007): Study on nitrogen concentration and deposition amount in wet deposition in typical Wetland ecosystem of Sanjing Plain. – System Sciences and Comprehensive Studies in agriculture 23(1): 114-123.
[47] Tang, J., Xue, H. S., Yu, X. L., Cheng, H. B., Ji, J. (2000): The preliminary study on chemical characteristics of precipitation at Mt Waliguan. – Acta Scientiae Circumstantiae 20(4): 420-425.
[48] Thimonier, A., Schmitt, M., Waldner, P., Rihm, B. (2005): Atmospheric deposition on Swiss long-term forest ecosystem research (LWF) plots. – Environmental Monitoring and Assessment 104: 81-118.
[49] Violaki, K., Zarbas, P., Mihalopoulos, N. (2010): Long-term measurements of dissolved organic nitrogen (DON) in atmospheric deposition in the Eastern Mediterranean: fluxes, origin and biogeochemical implications. – Marine Chemistry 120(1): 179-186.
[50] Watmough, S. A., Aherne, J., Alewell, C., Arp, P., Bailey, S., Clair, T., Dillon, P., Duchesne, L., Eimers, C., Fernandez, I. (2005): Sulphate, nitrogen and base cation budgets at 21 forested catchments in Canada, the United States and Europe. – Environmental Monitoring and Assessment 109(1): 1-36.
[51] Xu, Z., Yan, X. Y., Xiong, Z. Q., Xie, Y. X., Xing, G. X., Shi, S. L., Zhu, Z. L. (2009): Spatial and temporal variation of inorganic nitrogen wet deposition to the Yangtze River Delta Region. – China Water Air Soil Pollut 203: 277-289.
[52] Yuan, L., Zhou, X. B., Gu, X. R., Huang, J. G. (2009): Temporal and spatial variation of atmospheric wet nitrogen deposition in typical areas of Chongqing. – Acta Ecologica Sinica 29: 6095-6101.
[53] Zerva, A., Mencuccini, M. (2005): Short-term effects of clearfelling on soil CO2, CH4 and N2O fluxes in a Sitka spruce plantation. – Soil Biology & Biochemistry 37: 2025-2036.
[54] Zhai, S. J., Yang, L. Y., Hu, W. P. (2009): Observations of atmospheric nitrogen and phosphorus deposition during the period of algal bloom formation in Northern Lake Taihu, China. – Environmental Management 44: 542-551.
[55] Zhan, X. Y., Yu, G. R., He, N. P., Fang, H. J., Jia, B. R., Zhou, M., Wang, C. K., Zhang, J. H., Zhao, G. D., Wang, S. L. (2014): Nitrogen deposition and its spatial pattern in main forest ecosystems along north-south transect of Eastern China. – Chinese Geographical Science 24(2): 137-146.
[56] Zhang, X. F. (2006): Atmospheric nitrogen wet deposition and its effects on wetland water environment of Shanghai area. – Chinese Journal of Applied Ecology 17(6): 1099-1102.
[57] Zhao, X., Yan, X. Y., Xiong, Z. Q., Xie, Y. X., Xing, G. X., Shi, S. L., Zhu, Z. L. (2009): Spatial and temporal variation of inorganic nitrogen wet deposition to the Yangtze River Delta Region, China. – Water, Air, and Soil Pollution 203(1): 277-289.
[58] Zhou, G. Y., Yan, J. H. (2001): The influences of regional atmospheric precipitation characteristics and its element inputs on the existence and development of Dinghushan forest ecosystems. – Acta Ecologica Sinica 21(12): 2002-2012.

http://www.aloki.hu ● ISSN 1589 1623 (Print) ● ISSN 1785 0037 (Online)
DOI: http://dx.doi.org/10.15666/aeer/1902_11631176
© 2021, ALÖKI Kft., Budapest, Hungary

APPENDIX



Appendix 1. *Experimental plot*

APPLIED ECOLOGY AND ENVIRONMENTAL RESEARCH 19(2):1163-1176.
http://www.aloki.hu ● ISSN 1589 1623 (Print) ● ISSN 1785 0037 (Online)
DOI: http://dx.doi.org/10.15666/aeer/1902_11631176
© 2021, ALÖKI Kft., Budapest, Hungary

USAGE OF MAGNETIC IRON TO RAISE TOLERANCE OF SOME ORNAMENTAL TREES AND SHRUBS TO SOIL SALINITY IN CASE OF HORSERADISH TREE (*MORINGA OLEIFERA* LAM.)

NOFAL, E. M. S.[1] – KHALAFALLAH, M. M.[1] – SHAHIN, S. M.[2] – MONTASSER, H. M. M. S.[2*]

[1]*Hort. Dept., Fac. Agric., Kafrelsheikh Univ., Egypt*

[2]*Botanical Gards. Res. Dept., Hort. Res. Inst., ARC, Giza, Egypt*

**Corresponding author*
e-mail: heba.montaser78@gmail.com

(Received 20th Sep 2020; accepted 19th Jan 2021)

Abstract. An experiment was performed at Orman Botanical Garden, Giza, Egypt to determine the role of magnetite ore at either 2 or 4 g/pot in reducing the harmful effects of soil salinity on growth and quality of *Moringa oleifera* Lam. grown in soil mixture salinized with a mixture of NaCl and $CaCl_2$ salts at concentrations of 0, 2000, 4000, 6000 and 8000 ppm. The effect of the interaction between salinity and magnetite was also studied. The results indicated that a gradual decrease in survival percentage was observed with the gradual increments in salinity, but it was progressively increased with higher magnetite rates irrespective of salinity concentration. Connecting between magnetite at any dose and salinity up to 4000 ppm gave the highest percentage of survival rate in the two seasons. While, the lowest survival rate was recorded at 8000 ppm, especially in the absence of magnetite. A response similar to that of survival percentage occurred for vegetative and root growth traits, and leaf chemical composition, with few exceptions in both seasons. Thus, it is advised to drench soil mixture with magnetite at 4 g/pot to enhance growth and quality of *Moringa oleifera* transplants under salt stress.
Keywords: *salinity, Moringa oleifera, magnetite, carotenoids, proline*

Introduction

Among many species included in Fam. *Moringaceae* is considered the miracle species having tremendous uses, such as aforestation, alley cropping, medicines, water purification biopesticides, biogas, green manure and gum production, domestic cleaning agent and as a vegetable for their edible roots, young leaves, fruits and seeds, from which oil is often extracted (Aiyelaagbe, 2011). It grows rapidly up to 9-10 m height in poor soil with little care for long periods of drought (McConnachie, 1999). It is originated in India and Pakistan, but is now distributed to most tropical areas as ornamental, fodder, fibrous, malnutrition solving and economic plant (Fahey, 2005; Thurber and Fahey, 2009). It is easily propagated by seeds and stem cuttings, tolerates a wide range of soil conditions, but prefers a neutral to slightly acidic (pH 6.5-7), well drained sandy or loamy soils. It is considered as drought resistant, but water logging sensitive (Suein, 2008).

Regarding salinity tolerance of *Moringa oleifera*, Dos Santos et al. (2011) noticed that the gradual increase in NaCl concentration (0, 25, 50, 100, 200 and 250 mol/m^3) caused a gradual decrement in germination % germination speed index and seedling length. Moreover, Nouman et al. (2012a) reported that moringa seedlings survived up to 3500 ppm NaCl salinity with a slight reduction in its biomass, chlorophyll a, crude protein and mineral concentrations. Activity of superoxide dismutase (SOD) and peroxidase (POD) and Ca, K and Mg concentrations were progressively decreased, but

http://www.aloki.hu ● ISSN 1589 1623 (Print) ● ISSN1785 0037 (Online)
DOI: http://dx.doi.org/10.15666/aeer/1902_11771190
© 2021, ALÖKI Kft., Budapest, Hungary

catalase (CAT), total phenols, chlorophyll b, β-carotene, Na and P concentrations were significantly increased with raising salinity up to 5500 ppm relative to control. Similarly, were those results of Nouman et al. (2012b), Rivas et al. (2013) and Elhag and Abdalla (2014) on *Moringa oleifera*.

The deleterious effects of salinity on ornamentals, such as reduction of plant growth and leaf yellowing, browning of the leaf tips and margins, defoliation, root shortening and may ultimately plant die were previously suggested by Al-Qubaie et al. (2003) on *Bongainvilleaglabra*, *Conocarpus erectus*, *Ficus benghalensis*, *Jasminum azoricum*, *Tamarix articulata* and *Ziziphus spina-christi*, Shahin et al. (2008) on *Ficus macrocarpa*var. Hawaii and *Euonymus Joponica* cv. Mediopicta, Shahin et al. (2013) on *Ficus benjamina cv. Samantha and Schefflera arboricola* cv. Gold Capella, El-Fouly et al. (2015) on *Iris tingitana* cv. Wedgewood, Jose et al. (2016) on *Eucalyptus urophylla* and Shahin et al. (2017) on *Casuarina equisetifolia* and *Eucalyptus rostrata*. However, these harms were minimized by some practical methods, such as those revealed by Moustafa et al. (2017) on *Moringa oleifera* using magnetic iron. The role of magnetite in reducing hazards of salinity was also documented by Abdel-Fattah (2014) on *Jacaranda acutifolia*, Ahmed et al. (2016) on *Acalypha wilkesiana*, Shahin et al. (2018) on *Terminalia arjuna* and El-Sayed et al. (2019) on *Enterolobium contortisiliquum*.

Such trial, however aims to evaluate the role of magnetic iron in reducing the harmful effects of soil salinity on growth and quality of *Moringa oleifera* transplants during rearing period in the nursery.

Materials and methods

The current study was conducted in the full sun the average temperature between (27-38ºC) and the average percentage of humidity 56% at the nursery of Orman Botanical garden, Giza, Egypt throughout the two successive seasons of 2018 and 2019 as an attempt to verify the benefit of magnetite in minimizing the hazards of soil salinity on growth and quality of moringa transplants, and to detect its role in helping these nurslings to grow well under such stress.

Thus, 4-months-old, uniform transplants of the plant at a length of about 30 cm with 3-4 leaves were transplanted on April, 1st for every season to 15-cm-diameter polyethylene black bags (one seedling/bag) filled with about 3.5 kg of sand and clay mixture at equal volume parts (1:1, v/v). The physical and chemical properties of the soil mixture used in the two seasons were determined and illustrated in *Table 1*.

Table 1. *The physical and chemical analysis of the soil mixture used in 2018 and 2019 seasons*

Soil mixture	**Particle size distribution (%):**				**S.P.**	**E.C. (dS/m)**	**pH**	**Cations (meq/l)**			
Sand + Clay (1:1, v/v)	Coarse sand	Fine sand	Silt	Clay				Ca^{++}	Mg^{++}	Na^{+}	K^{+}
	38.6	31.3	20.6	9.5	25	6.5	7.86	17.8	14.2	33.1	0.9
Soil texture	**Anions (meq/l)**				**Macro-and micro-elements (ppm)**						
	HCO_3^-	Cl^-	SO_4^{--}	CO_3	N	P	K	Fe	Zn	Mn	Cu
Sandy clay	2.10	58.40	5.50	0.00	173.10	15.78	361.76	15.80	4.36	8.03	8.81

http://www.aloki.hu ● ISSN 1589 1623 (Print) ● ISSN1785 0037 (Online)
DOI: http://dx.doi.org/10.15666/aeer/1902_11771190
© 2021, ALÖKI Kft., Budapest, Hungary

Immediately before transplanting, the above soil mixture was salinized with an equal mixture of NaCl and $CaCl_2$ pure salts (1:1, by weight) at the concentrations of 0, 2000, 4000, 6000 and 8000 ppm. After planting, however the soil mixture was thoroughly drenched with magnetic iron (Fe_3O_4, 22.5%) secured from Alahram Mining Co., Maadi, Cairo at the rates of 0, 2 and 4 g/plant, as one batch at the beginning of the season. Each level of salinity was combined with each one of magnetic iron to formalize 15 interaction treatments.

The transplants under various experimental treatments were fertilized 3 times during the course of this study with 2 g/transplants of NPK + micro elements chemical fertilizer (Kristalon, 19:19:19) and watered every other day. Furthermore, all the other agricultural practices needed for such plantation were done as usually grower did. A factorial in complete randomized design with 3 replicates, as each one contained 5 seedlings was used in every season (Mead et al., 1993).

Data recorded, at the end of each season (on October, 1st), were: survival (%), plant height (cm), stem diameter (cm), number of leaves/plant, leaf length (cm), the longest root length (cm), root collar diameter (cm), aerial parts and roots fresh and dry weights (g) and salt resistance index as a percentage (SRI %) was calculated from the equation of Wu and Huff (1983) as follows:

$$\text{SRI (\%)} = \text{Mean root length of the longest root in salt treated plant / mean root length of the longest root in control one x 100} \quad \text{(Eq.1)}$$

In addition, the benefit coefficient of magnetite (Fe_3O_4) under various salinity levels as a percentage (B. Coe %) was estimated from the following equation:

$$\text{B. Coe (\%)} = \text{Increase rate in dry matter of treated plant / dry matter of control one x 100.} \quad \text{(Eq.2)}$$

In fresh samples concentrations of photosynthetic pigments (chlorophyll a, b and carotenoids, mg/g f.w.) were determined according to the method of Sumanta et al. (2014), while in dry ones the percentages of nitrogen (Blake, 1965), phosphorus (Luatanab and Olsen, 1965), as well as potassium, sodium and chloride (Jackson, 1973) were measured. Concentration of the free proline (mg/100 g d.w.) was also assessed in dry leaf samples by the method of Batels et al. (1973). The abovementioned constituents were evaluated in the second season only.

Data were then subjected to analysis of variance using the computer program of SAS Institute (2009), followed by Duncan's New Multiple Range t-Test (Steel and Torrie, 1980) for means comparison.

Results

Effect of soil salinity, magnetite and their interaction on vegetative and root growth parameters

Data presented in *Table 2* show that survival % means were descendingly decreased with increasing salinity level to reach the minimum at 8000 ppm level in both seasons, but progressively increased with rising magnetite rate to be maximum at 4 g/plant rate

http://www.aloki.hu ● ISSN 1589 1623 (Print) ● ISSN1785 0037 (Online)
DOI: http://dx.doi.org/10.15666/aeer/1902_11771190
© 2021, ALÖKI Kft., Budapest, Hungary

regardless of salinity level. Combining between any dose of magnetic iron and salinity up to 4000 ppm gave the highest survival percentage in the two seasons. A significant reduction in means of this character was observed when salinity level was elevated to 6000 ppm, but it was still higher than 50% in most cases of both seasons especially in the presence of magnetite. The least records however were attained by 8000 ppm salinity level, even in the presence of Fe_3O_4, but it`s absence greatly reduced means of such trait to 27.4% in the first season and to 00.00% in the second one due to death of the plants.

Table 2. *Effect of salinity levels, magnetite rates and their interactions on survival and height of Moringa oleifera Lam. transplants during 2018 and 2019 seasons*

Fe_3O_4 rate (g/plant) / Salinity level (ppm)	Survival (%)				Plant height (cm)			
	0.00	2 g	4 g	Mean	0.00	2 g	4 g	Mean
	First season; 2018							
0.00	100.00a	100.00a	100.00a	100.00A	94.67d	103.0b	108.9a	102.2A
2000	100.00a	100.00a	100.00a	100.00A	92.00e	98.99c	102.6b	97.86B
4000	89.22b	100.00a	100.00a	96.41B	70.78i	78.93h	88.51f	79.41C
6000	53.17e	70.82d	76.91c	66.97C	62.12j	70.17i	83.11g	71.80D
8000	27.40g	35.17f	40.34f	34.30D	49.00l	55.73k	63.10j	55.95E
Mean	73.96C	81.20B	83.45A		73.71C	81.36B	89.25A	
	Second season; 2019							
0.00	100.00a	100.00a	100.00a	100.00A	86.50e	103.0b	114.4a	101.8A
2000	100.00a	100.00a	100.00a	100.00A	84.83ef	100.1c	102.2bc	95.71B
4000	73.33c	87.20b	100.00a	86.94B	76.67g	83.67f	94.43d	84.92C
6000	41.53f	58.30e	65.80d	55.21C	64.50i	73.90h	87.27e	75.22D
8000	0.00h	34.50g	38.30g	24.27D	0.00l	33.07k	36.10j	23.06E
Mean	62.97C	76.00B	80.82A		62.50C	79.01B	86.89A	

Mean followed by the same letter in a column or row don't differ significantly according to Duncan's New Multiple Range test

A similar trend to that of survival percentage was just obtained regarding plant height (cm), stem diameter (cm), No. leaves/plant, leaf length (cm), root length (cm), root collar diameter (cm), as well as aerial parts and roots fresh and dry weights (g) attributes (*Tables 2, 3, 4, 5 and 6*), as the means of these traits were gradually decreased with increasing salinity levels, but progressively increased with raising magnetic iron rate. The highest averages were also recorded by the concentrations between salinity concentration up to 4000 ppm and any dose of magnetite. Increasing salinity level to 6000 ppm caused a significant reduction in the means of foregoing criteria, with the exception for plants which received Fe_3O_4 at any rate. The minimal values were however acquired by 8000 ppm salinity treatments especially for plants abandoned of magnetic iron.

Salt resistance index (SRI %) and benefit coefficient of magnetite (B. Coe. %).

It is clear from data presented in *Table 7* that percent of salt resistance index was linearly decreased as salinity concentration was increased. Thus, the least SRI value was achieved by 8000 ppm concentration to be 53.54% in the first season and 39.46% in the

http://www.aloki.hu ● ISSN 1589 1623 (Print) ● ISSN1785 0037 (Online)
DOI: http://dx.doi.org/10.15666/aeer/1902_11771190
© 2021, ALÖKI Kft., Budapest, Hungary

second one. Decrement mean of this index to less than 50% really indicates the low tolerance of moringa to salinity higher than 6000 ppm. Magnetite at the rate of 2 g/plant scored the highest percentages of SRI in the two seasons, followed by 4 g/plant rate. Under control treatment, a pronounced decline in the values of this index was acquired with increasing salinity level to be less than 50% in both seasons by 8000 ppm treatment. This confirms that moringa is not able to tolerate salinity higher than 6000 ppm as mentioned before. On the other side, application of Fe_3O_4 improved the means of such index to be higher than 50% even under 8000 ppm treatment, showing the important role of this natural ore in enhancing moringa tolerance to high salinity.

Table 3. *Effect of salinity levels, magnetite rates and their interactions on stem diameter and No. leaves/plant of Moringa oleifera Lam. transplants during 2018 and 2019 seasons*

Fe_3O_4 rate (g/plant) / Salinity level (ppm)	Stem diameter (cm)				No. leaves /plant			
	0.00	2 g	4 g	Mean	0.00	2 g	4 g	Mean
	First season; 2018							
0.00	0.797c	0.870b	0.947a	0.871A	7.07c	8.33b	9.67a	8.36A
2000	0.740d	0.830c	0.890b	0.820B	6.50d	8.50b	9.50a	8.17B
4000	0.683ef	0.737d	0.803c	0.741C	5.67e	7.17c	8.33b	7.06C
6000	0.577g	0.647f	0.693e	0.639D	3.83g	5.67e	6.50d	5.33D
8000	0.477i	0.497i	0.527h	0.500E	3.00h	4.00g	4.83f	3.94E
Mean	0.655C	0.716B	0.772A		5.21C	6.33B	7.77A	
	Second season; 2019							
0.00	0.750de	0.877b	0.930a	0.852A	7.33e	8.67c	9.67a	8.56A
2000	0.740de	0.837bc	0.863b	0.813A	5.33g	9.00c	9.33ab	7.89B
4000	0.660f	0.713e	0.793cd	0.722B	5.67g	7.00ef	8.00d	6.89C
6000	0.547g	0.627f	0.730e	0.634C	4.67h	5.67g	6.67f	5.67D
8000	0.00i	0.353h	0.387h	0.247D	0.00j	3.33i	4.67h	2.67E
Mean	0.539C	0.681B	0.741A		4.60C	6.73B	7.67A	

Mean followed by the same letter in a column or row don't differ significantly according to Duncan's New Multiple Range test

As for the benefit coefficient of magnetite percentage (B. Coe. %), as a real indicator for the advantage of magnetic iron in reducing hazards of salinity, with promoting plant growth, is presented in *Table 7* which exhibits that Fe_3O_4 significantly increased dry matter production of treated plants under the different salinity levels over control in the two seasons. However, the upper hand in the increased means of such coefficient in the first season was for magnetite under 2000 and 6000 ppm salinity treatments, as 31.88 and 31.27% against 15.97% for control, followed by magnetite under 4000 ppm level, while in the second season, that was true for magnetite under 8000 ppm level, which raised the percent of this coefficient to 259.0% versus 27.85% for control. Likewise, a progressive increment was occurred in the means of this coefficient with raising Fe_3O_4 rate. So, the greatest benefit of this ore was recorded in both seasons by 4 g/plant dose. Interaction treatments also encouraged dry matter production as applying Fe_3O_4 at 2 or 4 g/plant caused a significant increase in the production of dry matter over control regardless of salinity level in the two seasons.

http://www.aloki.hu ● ISSN 1589 1623 (Print) ● ISSN1785 0037 (Online)
DOI: http://dx.doi.org/10.15666/aeer/1902_11771190
© 2021, ALÖKI Kft., Budapest, Hungary

Table 4. *Effect of salinity levels, magnetite rates and their interactions on leaf and root length and root callar diameter of Moringa oleifera Lam. transplants during 2018 and 2019 seasons*

Fe_3O_4 rate (g/plant) / Salinity level (ppm)	Leaf length (cm)				Root length (cm)				Root callar diameter (cm)			
	0.00	2 g	4 g	Mean	0.00	2 g	4 g	Mean	0.00	2 g	4 g	Mean
	First season; 2018											
0.00	15.81g	14.94h	16.11fg	15.62C	13.44cd	13.97bc	16.19a	14.53A	1.87de	2.20c	2.37b	2.14B
2000	16.67ef	18.78d	20.50b	18.65A	12.49e	13.07d	14.37b	13.31B	1.80ef	2.40b	2.47b	2.22AB
4000	11.90i	19.45c	21.72a	17.69B	10.92f	11.44f	13.35d	11.91C	1.67fg	2.27b	2.67a	2.27A
6000	10.78j	16.06g	17.23e	14.69D	8.86h	9.93g	10.93f	9.91D	1.50g	1.92de	1.99d	1.80C
8000	9.03l	9.65k	10.80j	9.83E	6.10j	8.20i	9.05h	7.78E	1.27h	1.56g	1.61g	1.48D
Mean	12.84C	15.78B	17.27A		10.36C	11.32B	12.78A		1.62C	2.11B	2.22A	
	Second season; 2019											
0.00	15.55b	16.96a	17.25a	16.59A	12.50c	13.22b	15.36a	13.70A	2.20bc	2.24b	2.57a	2.34A
2000	14.19c	15.15b	17.28a	15.54B	11.44d	11.52d	13.45b	12.14B	2.02d	2.04cd	2.37b	2.14B
4000	13.06d	14.17c	15.25b	14.16C	10.16f	10.78e	13.00c	11.31C	1.79e	1.90de	2.31b	2.00C
6000	11.94e	11.42ef	14.00c	12.45D	8.31h	8.94g	10.03f	9.09D	1.45g	1.58fg	1.74ef	1.59D
8000	0.00h	8.06g	11.33f	6.47E	0.00i	8.11h	8.61gh	5.57E	0.00h	1.43g	1.48g	0.97E
Mean	10.95C	13.15B	15.02A		8.48C	10.51B	12.09A		1.49C	1.84B	2.09A	

Mean followed by the same letter in a column or row don't differ significantly according to Duncan's New Multiple Range test

http://www.aloki.hu ● ISSN 1589 1623 (Print) ● ISSN1785 0037 (Online)
DOI: http://dx.doi.org/10.15666/aeer/1902_11771190
© 2021, ALÖKI Kft., Budapest, Hungary

Table 5. *Effect of salinity levels, magnetite rates and their interactions on aerial parts fresh and dry weights of Moringa oleifera Lam. transplants during 2018 and 2019 seasons*

Fe_3O_4 rate (g/plant) / Salinity level (ppm)	Aerial parts fresh weights (g)				Aerial parts dry weights (g)			
	0.00	2 g	4 g	Mean	0.00	2 g	4 g	Mean
	First season; 2018							
0.00	13.64de	14.17d	19.44a	15.75A	6.37c-e	6.94c	8.48a	7.27A
2000	10.95f	15.19c	17.60b	14.58B	5.15f	6.98c	7.63b	6.59B
4000	9.80g	13.12e	15.44c	12.78C	4.59fg	6.06de	6.74cd	5.80C
6000	8.00h	11.10f	13.35e	10.82D	3.74hi	4.94fg	5.81e	4.83D
8000	6.62i	8.72h	9.98g	8.44E	3.10i	3.89h	4.34gh	3.78E
Mean	9.80C	12.46B	15.16A		4.59C	5.76B	6.60A	
	Second season; 2019							
0.00	11.48e	16.51c	19.75a	15.91A	6.14c	7.37b	9.40a	7.84A
2000	8.54g	16.76c	18.69b	14.66B	4.61d-f	8.18b	8.92a	7.24B
4000	8.88g	13.97d	16.07c	12.98C	4.75de	6.73c	7.64b	6.37C
6000	7.54h	10.88e	13.41d	10.61D	4.05f	5.25d	6.38c	5.23D
8000	0.00i	6.71h	9.54f	5.42E	0.00h	3.25g	4.52ef	2.59E
Mean	7.29C	12.97B	15.49A		3.91C	6.28B	7.37A	

Mean followed by the same letter in a column or row don't differ significantly according to Duncan's New Multiple Range test

Table 6. *Effect of salinity levels, magnetite rates and their interactions on roots fresh and dry weights of Moringa oleifera Lam. transplants during 2018 and 2019 seasons*

Fe_3O_4 rate (g/plant) / Salinity level (ppm)	Roots fresh weights (g)				Roots dry weights (g)			
	0.00	2 g	4 g	Mean	0.00	2 g	4 g	Mean
	First season; 2018							
0.00	13.38e	22.38b	25.78a	20.51A	4.13f	7.99b	10.31a	7.48A
2000	13.81de	22.42b	25.73a	20.65A	4.28f	8.02b	10.25a	7.52A
4000	11.23f	18.97bc	20.39c	16.86B	3.46g	6.73c	8.13b	6.10B
6000	9.23gh	13.28e	15.33d	12.61C	2.85h	4.68e	6.12d	4.55C
8000	7.16j	8.38hi	10.62fg	8.72D	2.20i	2.98h	4.19f	3.13D
Mean	10.96C	17.09B	19.57A		3.38C	6.08B	7.80A	
	Second season; 2019							
0.00	11.63b-d	12.69b	14.03a	12.78A	2.96cd	3.42b	3.89a	3.43A
2000	10.65de	11.05c-e	12.20b	11.30B	2.71de	2.96cd	3.39b	3.02B
4000	9.48fg	10.23ef	11.84bc	10.52B	2.37e-g	2.70de	3.26bc	2.78C
6000	7.70hi	8.43gh	9.03g	8.39C	1.89h	2.25f-h	2.52ef	2.22D
8000	0.00j	7.39hi	7.30i	4.90D	0.00i	1.95h	2.01gh	1.32E
Mean	7.89C	9.96B	10.88A		1.99C	2.66B	3.02A	

Mean followed by the same letter in a column or row don't differ significantly according to Duncan's New Multiple Range test

http://www.aloki.hu ● ISSN 1589 1623 (Print) ● ISSN1785 0037 (Online)
DOI: http://dx.doi.org/10.15666/aeer/1902_11771190
© 2021, ALÖKI Kft., Budapest, Hungary

Table 7. *Effect of salinity levels, magnetite rates and their interactions on resistance index and benefit coefficient of Moringa oleifera Lam. transplants during 2018 and 2019 seasons*

Fe_3O_4 rate (g/plant) / Salinity level (ppm)	Salt resistance index (%)				Benefit coefficient of Fe_3O_4 (%)			
	0.00	2 g	4 g	Mean	0.00	2 g	4 g	Mean
	First season; 2018							
0.00	100.00a	100.00a	100.00a	100.00A	0.00h	9.57g	38.34de	15.97D
2000	93.62b	94.15b	89.23c	92.33B	0.00h	40.97cd	54.67b	31.88A
4000	82.03d	81.97d	82.90d	82.30C	0.00h	35.20e	51.77b	28.99B
6000	65.86f	71.37e	68.11f	68.45D	0.00h	34.74e	59.05a	31.27A
8000	45.39h	58.91g	56.33h	53.54E	0.00h	27.70f	42.57c	23.42C
Mean	77.38C	81.28A	79.61B		0.00C	29.64B	49.28A	
	Second season; 2019							
0.00	100.00a	100.00a	100.00a	100.00A	0.00j	27.67i	53.87f	27.85E
2000	92.09b	88.49c	88.10c	89.56B	0.00j	86.41d	102.5c	62.97B
4000	82.04d	81.89d	85.50c	83.14C	0.00j	40.55h	64.07e	34.87D
6000	66.31e	68.89e	66.22e	67.14D	0.00j	48.95g	63.88e	37.61C
8000	0.00h	62.06f	56.33g	39.46E	0.00j	325.0b	452.0a	259.0A
Mean	68.09C	80.27A	79.23B		0.00C	106.1B	147.3A	

Mean followed by the same letter in a column or row don't differ significantly according to Duncan's New Multiple Range test

Chemical composition of the leaves

It is evident from data presented in *Table 8* that the gradual increase of salinity level resulted a gradual decrease in concentrations of chlorophyll a, b and carotenoids (mg/g f.w.) and the percentages of N and P except for 2000 ppm salinity level that raised P concentration to 0.752% versus 0.657% for control. The opposite was the right in relation to K, Na and Cl percentages as well free proline (mg/100 g d.w.). Which was progressively increased with increasing salinity level.

Magnetite, on the other side, linearly elevated concentrations of the previous constituents as the rate of its application was increased except for N and Na percentages which were adversely affected. Also, Fe_3O_4 at 4 g/plant rate diminished Cl %, whereas 2 g/plant rate increased it.

The highest concentrations of chlorophyll a, b, carotenoids and nitrogen were attained by interacting between either zero or 2000 ppm salinity and magnetic iron, especially at 4 g/plant dose, but the highest percent of phosphorus was obtained from 2000 ppm salinity level + magnetite at either 2 or 4 g/plant. The opposite was the right concerning K, Na, Cl and proline, as their maximal concentrations were obtained by combining between 8000 ppm salinity and magnetite at 2 g/plant in most cases of both seasons.

http://www.aloki.hu ● ISSN 1589 1623 (Print) ● ISSN1785 0037 (Online)
DOI: http://dx.doi.org/10.15666/aeer/1902_11771190
© 2021, ALÖKI Kft., Budapest, Hungary

Table 8. *Effect of salinity levels, magnetite rates and their interactions on some constituent's concentrations in Moringa oleifera Lam. leaves during 2019 seasons*

Fe_3O_4 rate (g/plant) / Salinity level (ppm)	Chlorophyll a (mg/g f.w.)				Chlorophyll b (mg/g f.w.)				Carotenoids (mg/g f.w.)			
	0.00	2 g	4 g	Mean	0.00	2 g	4 g	Mean	0.00	2 g	4 g	Mean
	First season; 2018											
0	2.103g	3.384a	3.219c	2.902A	1.640f	1.837d	2.226a	1.901A	0.733a-c	0.810a	0.796ab	0.780A
2000	2.04g	3.319b	3.110d	2.823B	1.631f	1.755e	2.083b	1.823B	0.734a-c	0.817a	0.781ab	0.777A
4000	1.503h	2.233f	2.467e	2.068C	1.36g	1.640f	1.937c	1.651C	0.697c	0.810a	0.790ab	0.766A
6000	1.299i	2.061g	2.201f	1.854D	1.045i	1.321h	1.375g	1.247D	0.675c	0.724bc	0.733-c	0.711B
8000	0.00j	1.293i	1.358i	1.326E	0.00j	1.039i	1.050i	1.045E	0.000e	0.501d	0.540d	0.521C
Mean	1.736B	2.458A	2.471A		1.423C	1.518B	1.734A		0.71B	0.733A	0.728A	
	N (%)				P (%)				K (%)			
	0.00	2 g	4 g	Mean	0.00	2 g	4 g	Mean	0.00	2 g	4 g	Mean
0	4.250bc	4.250bc	4.310a	4.270A	0.651cd	0.658c	0.663c	0.657B	1.073l	1.163k	1.177k	1.138E
2000	4.230c	4.240c	4.300ab	4.260A	0.649cd	0.726b	0.880a	0.752A	1.328j	1.396i	1.465h	1.396D
4000	3.760f	3.950e	4.070d	3.930B	0.476g	0.617e	0.635d	0.576C	1.670g	1.793f	1.881e	1.781C
6000	3.350h	3.610g	3.780f	3.580C	0.418hi	0.479g	0.521f	0.473D	1.911d	2.013c	2.094b	2.006B
8000	0.000k	2.360j	2.450i	2.410D	0.00j	0.411i	0.429h	0.420E	0.00m	2.133a	2.148a	2.141A
Mean	3.900C	3.680B	3.782A		0.549C	0.578B	0.626A		1.496C	1.700B	1.753A	
	Na (%)				Cl (%)				Proline (mg/100 g f.w.)			
	0.00	2 g	4 g	Mean	0.00	2 g	4 g	Mean	0.00	2 g	4 g	Mean
0	0.859g	0.730j	0.730j	0.773E	1.170g	1.170g	1.100h	1.147E	5.976l	5.910l	5.646m	5.844E
2000	1.013f	0.783i	0.771i	0.856D	0.760e	1.460f	1.430f	1.550D	9.735i	9.315j	9.000k	9.350D
4000	1.079e	0.811h	0.780i	0.890C	2.050d	2.050d	1.790e	1.963C	20.284f	17.391g	17.110h	18.262C
6000	1.303c	1.110d	1.101d	1.171B	2.630a	2.350c	2.310c	2.430B	41.500b	35.581d	31.532e	36.204B
8000	0.000k	1.567a	1.433b	1.500A	0.00i	2.610a	2.500b	2.555A	0.00n	43.610a	38.336c	40.973A
Mean	1.064A	1.000B	0.963C		1.903AB	1.928A	1.826B		19.374C	22.361A	20.325B	

Mean followed by the same letter in a column or row don't differ significantly according to Duncan's New Multiple Range test

http://www.aloki.hu ● ISSN 1589 1623 (Print) ● ISSN1785 0037 (Online)
DOI: http://dx.doi.org/10.15666/aeer/1902_11771190
© 2021, ALÖKI Kft., Budapest, Hungary

Discussion

Effect of soil salinity, magnetite and their interaction on vegetative and root growth parameters

The adverse effects of saline soil on growth may be attributed to either low water uptake due to low potential of soil water (Munns, 2002) or certain ion toxicity (Na^+ and Cl^-) or both (Carter et al., 2005). This fact was emphasized by Elhag and Abdalla (2014) who stated that salinity depresses plant growth via affecting water absorption and biochemical processes such as N, CO_2 assimilation and protein biosynthesis or accumulated high concentration of potentially toxic ions (Na^+ and Cl^-). Jose et al. (2016) ascribed the reduction in growth by salinity to the effect of osmotic stress and the inhibition of cell division rather than cell expansion coupled with the great reduction in photosynthesis. High salinity also leads to leaf abscission due to ion accumulation in the leaves, particularly the oldest ones. Reduction of growth by salinity may be attributed to a decrease in all volume at a constant cell number. Mechanism of salt may result in inhibition of cell division, consequently reduces the rate of plant development (Khan et al., 2009). Jou et al. (2006), however suggested that ATPase participates in the endoplasmic Reticulum-Golgi mediated, protein sorting machinery for both housekeeping function and compartmentalization of excess Na^+ under high salinity. Such truth was aforementioned by Munns (2002) who proposed that salt tolerant plants may have a low rate of Na^+ and Cl^- transport to leaves beside their ability to compartmentalize these ions in vacuoles to prevent their buildup in the cytoplasm or cell walls and thus avoid salt toxicity. The previous results are in accordance with those postulated by Elhag and Abdalla (2014) who found that stem length and No. leaves of 2-months-old moringa transplants were significantly reduced (30 and 40% successively) by the highest NaCl concentration (0.8%). Hence, the 2-months-old moringa transplants can tolerate NaCl concentration up to 0.4%. This tolerance may be attributed to its ability to restrict the transport of toxic Na^+ and Cl^- ions to the shoot at such lower concentration and their accumulation in the older leaves at higher ones to get rid of them by shedding of those older leaves. So, the mechanism of salinity tolerance of moringa may be the avoidance of toxic ions. Likewise, Cassaniti et al. (2013) claimed that brackish water can be commercially used for production of *Chrysanthemum morifolium*, *Dianthus caryophyllus*, *Gerbera jamesonii*, *Hippeastrum vittatum* and *Anthurium andreanum*, up to 2500 ppm. Similarly, were those results of Shahin et al. (2008) on *Ficus macrocarpa* var. Hawaii and *Euonymus Japonica* cv. Mediopicta, Shahin et al. (2013) on *Ficus benjamina* cv. Samanthaand *Schefflera arboricola* cv. Gold Capella, El-Fouly et al. (2015) on *Iris tingitana* cv. Wedgewood, Jose et al. (2016) on *Eucalyptus urophylla* and the hybrid of *E. urophylla* x *E. grandis* Shahin et al. (2017) affirmed that a gradual decrement in vegetative and root growth of both *Casuarina equisetifolia* and *Eucalyptus rostrata* seedlings was observed due to the gradual increment in salinity concentration from 5000 to 15000 ppm.

On the other hand, the positive effect of magnetic iron on growth of plants suffered from salt stress may be due to its role in promoting the uptake of N, P, K and Fe which stimulates plant growth against the toxicity of Na^+ and Cl^- ions that inhibit it. It induces cell metabolism and mitosis of meristematic cells (Barage et al., 2009). It is believed that new protein bands are formed in plants that are treated with Fe_3O_4 and these proteins are responsible for the increased growth (Hozyan and Abdul-Qodos, 2010). Furthermore, it declines the hydration of salt ions and colloids, increasing salt solubility,

http://www.aloki.hu ● ISSN 1589 1623 (Print) ● ISSN1785 0037 (Online)
DOI: http://dx.doi.org/10.15666/aeer/1902_11771190
© 2021, ALÖKI Kft., Budapest, Hungary

and finally leading to leaching such salts from the soil. In the iron atom, there is a number of valence electrons that generates a magnetic field influence on the biochemical processes in plants and renders the roots to exhibit symptoms of magnetism that kills nematodes and injurious bacteria (Yuliando et al., 2016). The aforementioned gains are in harmony with those obtained by Dos Santos et al. (2011) and Nouman et al. (2012b) on *Moringa oleifera* and Moustafa et al. (2017) who pointed out that seedlings length, No. leaves, root length, No. roots and aerial parts and roots fresh and dry weights of *Moringa oleifera* seedling subjected to salinity up to 8000 ppm were improved in response to applying Fe_3O_4 at 2 g/pot. Supporting results for this study were also obtained by Abdel-Fattah (2014) on *Jacaranda acutifolia*, Ahmed et al. (2016) on *Acalypha wilkesiana*, Shahin et al. (2018) on *Terminalia arjuna* and El-Sayed et al. (2019) on elephant`s ear tree.

Salt resistance index (SRI %) and benefit coefficient of magnetite (B. Coe. %).

These results are reasonable because magnetite usually solubilizes and leaches salts from the soil, and this gives roots a chance to penetrate and distribute well through the growing medium, consequently uptake enough water and nutrients necessary for good and healthy growth. On the same line were those results attained by Al-Qubaie et al. (2003) on *Ficus benghalensis*, *Bougainvillea glabra*, *Jasminum azoricum*, *Conocarpus erectus*, *Tamarix articulata* and *Ziziphus spina-christi*, Shahin et al. (2008) on *Ficus macrocarpa* Var. Hawaii and *Euonymus Japonica* cv. Mediopicta, Abdel-Fattah et al. (2012a) on *Ficus retusa*, Abdel-Fattah et al. (2012b) on *Ficus benjamina* and El-Sayed et al. (2019) on *Enterolobium contortisiliquum*.

Chemical composition of the leaves

The previous data showed the effect of the gradual increase of salinity level may be reasonable because salts usually reduces the water potential of soil solution, consequently decreases minerals and water uptake by roots, accompanied by a depression of photosynthesis and enzymes activity (Munns, 2002). It was also remarkable that accumulation of some amino acids and amides in the leaves and roots of salinity-stressed plants may be attributed to *de novo* synthesis by protein sorting machinery and not the result of protein degradation (Jou et al., 2006).

On the other hand, improving constituent's concentrations by magnetic iron may indicate its role in repairing salinity harms by reducing Na^+ and Cl^- toxic ions in the medium, coupled with increasing the free proline formation which improves as a colloid water balance in plant cells (Mostafazadeh et al., 2012). Further, Fe_3O_4 may create a high energy magnetic field in the root medium which may increase the solubility of N, P, K and Fe nutrients and this in turn promotes the absorption of such minerals, improving ultimately plant growth (Yuliando et al., 2016).

These results, showed a similar trend to those of Elhag and Abdalla (2014) and Moustafa et al. (2017) on *Moringa oleifera*, Ahmed et al. (2016) on *Acalypha wilkesiana*, Shahin et al. (2018) on *Terminalia arjuna* and El-Sayed et al. (2019) who observed that chlorophyll a, b, carotenoids and total carbohydrates concentrations were increased in the leaves of *Enterolobium contortisiliquum* under salt stress by application of Fe_3O_4 at either 2 or 4 g/plant.

http://www.aloki.hu ● ISSN 1589 1623 (Print) ● ISSN1785 0037 (Online)
DOI: http://dx.doi.org/10.15666/aeer/1902_11771190
© 2021, ALÖKI Kft., Budapest, Hungary

Conclusion

From the previous findings, it can be proposed to apply magnetic iron at the rate 4 g/plant for enhancing growth and quality of *Moringa oleifera* seedlings under salt stress up to 6000 ppm.

REFERENCES

[1] Abdel-Fattah, G., Shahin, S. M., Khenizy, S. A. M. (2012a): Improving tolerance of *Ficus benjamina* L. plant to saline water stress by VAM (Glomus sp.). – J. Biol. Chem. & Environ. Sci. 7(1): 1-16.

[2] Abdel-Fattah, G., Shahin, S. M., Abdel-Moniem, A. M. (2012b): Could phosphorene help *Ficus retosa* L. plant to tolerate the deleterious effects of saline water? – J. Biol. Chem. & Environ. Sci. 7(1): 17-32.

[3] Abdel-Fattah, G. (2014): The role of magnetic iron and sodium selenate in minimizing soil salt hazards on growth and quality of Jacaranda acutifolia Tumb. & Bionol seedlings. – Sci. J. Flowers & Ornam. Plants 1(3): 187-198.

[4] Ahmed, M., Abdel-Fattah, G., Shahin, S. (2016): The role of magnetic iron in enhancing the ability of Acalypha wilkesiana Müll. Arg. transplants to tolerate soil salinity. – J. Plant Production, Mansoura Univ. 7(3): 379-384.

[5] Aiyelaagbe, I. O. (2011): Nigerian Horticulture: Facing the Challenges of Human Health and Agricultural productivity. – Keynote address Presented at the 29th Annual National Conf. of Hort. Soc. of Nigeria (HORTSON), 24-29 July; pp. 131-148.

[6] Al-Qubaie, A. I., Shahin, S. M., Abdel-Samad, F. A. (2003): Effect of diluted sea water on growth and chemical composition of some ornamental trees and shrubs. – Egypt J. Appl. Sci. 18(8B): 587-601.

[7] Barage, L. F., da Sousa, M. P., Almeida, T. A. (2009): Enterolobium schomburgkii Benth. Seed germination under saline stress and polyamine application. – Revista Braz Plantas Med. 11(1): 1516-1527.

[8] Batels, L. S., Walden, R. P., Teare, T. D. (1973): Rapid determination of free proline under water stress studies. – Plant and Soil 939: 205-207.

[9] Blake, C. A. (1965): Methods of Soil Analysis Part 1 Physical and Mineralogical Properties Including a Statistics of Measurement and Sampling. – Amr. Soc. Agron. Inc. Pub., Wisconsin., U.S.A.

[10] Carter, C. T., Grieve, C. M., Poss, J. A. (2005): Salinity effects on emergence, survival and ion accumulation of Limonium perezii. – J. Plant Nutrition 28: 1243-1257.

[11] Cassniti, C., Romano, D., Hop, M. E., Flowers, T. J. (2013): Growing floricultural crops with brackish water. – Environmental and Experimental Botany 92: 165-175.

[12] Dos Santos, A. R. F., Mann, R., Ferreira, R. A., de Souza Brito, A. (2011): Water pre-hydration as priming for *Moringa oleifera* Lam. seeds under salt stress. – Tropical and Subtropical Agroecosystems 14: 201-207.

[13] El-Fouly, A. S., Abdel-Sattar, M. M., Shahin, S. M. (2015): Effect of different salinity levels, PP-333 treatments and their interaction on growth, flowering, bulbs productivity and chemical composition of Iris tingitana cv. Wedgewood. – J. Agric. Res., Kafr El-Sheikh Univ. 41(1): 347-369.

[14] El-Sayed, M. A., El-Fouly, A. S., Shahin, S. M. (2019): Reducing the harmful effect of saline irrigation water on growth and quality of Enterolobium contortisiliquum (elephant`s ear) seedlings. – Bull Fac. Agric., Cairo. Univ. 70: 267-276.

[15] Elhag, A. Z., Abdalla, M. H. (2014): Investigation of sodium chloride tolerance of Moringa oleifera Lam. transplants. – Universal J. Agric. Res. 2(2): 45-49.

[16] Fahey, J. W. (2005): Moringa oleifera: A review of the medical evidence for its nutritional, therapeutic and prophylactic properties. – Trees for Life J. 1(1): 5.

http://www.aloki.hu ● ISSN 1589 1623 (Print) ● ISSN1785 0037 (Online)
DOI: http://dx.doi.org/10.15666/aeer/1902_11771190
© 2021, ALÖKI Kft., Budapest, Hungary

[17] Hozyan, M., Abdul-Qodos, A. (2010): Irrigation with magnetized water enhances growth, chemical constituent and yield of chickpea (*Cicer arietinum* L.). – Agric. and Biol. J. of Amer. 1(4): 671-676.
[18] Jackson, M. H. (1973): Soil Chemical Analysis. – Prentice-Hall of India Private Limited M-97, New Delhi, India, 498p.
[19] Jose, A. C., Silva, N. C. N., Faria, J. M., Pereira, W. V. (2016): Influence of osmotic conditioning of Eucalyptus spp. seeds in the tolerance to salt stress. – J. Seed Sci. 38(4): 329-334.
[20] Jou, Y., Chiang, C., Jauh, G., Yen, H. (2006): Functional characterization of ice plant, on AAA-type ATPase associated with the endoplasmic reticulum-Golgi network, and its role in adaptation to salt stress. – Plant Physiol. 141(1): 135-146.
[21] Khan, G. S., Khan, Z. H., Imran, J., Quraishi, M. U., Yaqoob, S., Khan, S. H. (2009): Effect of salinity on germination and growth of some forest tree species at seedling growth. – J. Agric. Res. 47(3): 271-279.
[22] Luatanab, F. S., Olsen, S. R. (1965): Test of an ascorbic acid method for determining phosphorus in water and $NaHCO_3$ extracts from soil. – Soil Sci. Soc. Amer. Proc. 29: 677-678.
[23] McConnachie, G. L., Folkard, G. K., Mtawali, M. A., Sutherland, J. P. (1999): Field trails of appropriate hydraulic flocculation processes. – Water Res. 33(6): 1425-1434.
[24] Mead, R., Curnow, R. N., Harted, A. M. (1993): Statistical Methods in Agriculture and Experimental Biology. – 2nd Ed., Chapman & Hall Ltd., London, 335p.
[25] Mostafazadeh, B., Khoshrovesh, M., Mousove, S. F., Kiani, A. R. (2012): Effects of magnetized water on soil chemical components underneath trick irrigation. – Amer. Soc. of Civil Engineers: http://dx.doi.org/10.1061/(ASCE) IR. 1943-4774.0000513.
[26] Moustafa, H. E. B., Abdel-Fattah, G., Shahin, S. M. (2017): Germination of Moringa oleifera Lam seeds under salinity conditions in the presence of magnetic iron. – J. Biol. Chem. & Environ. Sci. 12(3): 551-566.
[27] Munns, R. (2002): Comparative physiology of salt and water stress. – Plant Cell and Environment 25: 239-250.
[28] Nouman, W., Siddiqui, M. T., Basra, S. M., Afzal, I., Rehman, H. (2012a): Enhancement of emergence potential and stand establishments of *Moringa oleifera* Lam. by seed priming. – Turk J. Agric. For. 36: 227-235.
[29] Nouman, W., Siddiqui, M. T., Basra, S. M., Afzal, I., Rehman, H. (2012b): Response of *Moringa oleifera* to saline conditions. – Inter. J. Agric. & Biol. 14(5): 757-762.
[30] Rivas, R., Oliveira, M. T., Santos, M. G. (2013): Three cycles of water deficit from seed to young plants of Moringa oleifera woody species improves stress tolerance. – Plant Physiol. & Biochem. 63(1): 200-208.
[31] SAS Institute. (2009): SAS/STAT User`s Guides Statistics. – Vers. 6.04, 4th Ed., SAS Institute Inc. Cary, N.C., USA.
[32] Shahin, S. M., Naglaa, E. Y., Mahmoud, A. M. A., El-Feky, A. H. (2008): How far diluted sea water can be used for irrigation of some pot plants. – Proc. 9th Inter. Conf. on Dry Land Development, 7-10 Nov., Organized by IDDC, Alex., Egypt, pp. 363-372.
[33] Shahin, S. M., El-Fouly, A. S., Abdel-Sattar, M. M. (2013): Response of F. benjamina L. cv. Samantha and Schefflera arboricola Endl cv. Gold Copella plants cultivated in two different growing media to salinity of irrigation water. – J. Biol. Chem. & Environ. Sci. 8(2): 201-218.
[34] Shahin, S. M., Ahmed, M., Tawila, A. S. (2017): Effect of saline irrigation water on growth and quality of *Casuarina equisetifolia* L. and Eucalyptus rostrata Schlecht plants grown in some soils of Egypt. – Middle East J. Appl. Sci. 7(3): 460-471.
[35] Shahin, S. M., Aly, A. M., Helaly, A. A. E. (2018): Germination of Indian almond (Terminal arjuna Roxb.) seeds as affected by soil salinity in presence or absence of magnetic iron. – J. Plant Production, Mansoura Univ. 9(4): 417-422.

http://www.aloki.hu ● ISSN 1589 1623 (Print) ● ISSN1785 0037 (Online)
DOI: http://dx.doi.org/10.15666/aeer/1902_11771190
© 2021, ALÖKI Kft., Budapest, Hungary

[36] Steel, R. G. D., Torrie, J. H. (1980): Principles and Procedures of Statistics. – McGrow Hill Book Co., Inc., New York, pp. 377-400.
[37] Suein, W. A. (2008): Moringa oleifera climate, using Moringa oleifera as a source for production of bio-diesel from perennials. – A report by Agric. and Food Dept., Government of Western Australia, 5p.
[38] Sumanta, N., Haque, C. I., Nishika, J., Suprakash, R. (2014): Spectrophotometric analysis of chlorophyllous and carotenoids from commonly grown fern sp. by using various extracting solvents. – Research J. Chem. Sci. 4(9): 63-69.
[39] Thurber, M. D., Fahey, J. W. (2009): Adoption of Moringa oleifera to combat under nutrition viewed through the lens of the "Diffusion of Innovations" theory. – Ecol. Food. Nutr. 48: 212-225.
[40] Wu, L., Huff, D. R. (1983): Characteristics of creeping bentgrass clones (*Agrostis stolonifera* L.) from a salinity tolerant population after surviving drought stress. – HostScience 18(6): 883-885.
[41] Yuliando, A., Astuti, B., Amalia, S. R. (2016): Enhancement of iron content in spinach plants stimulated by magnetic nano particles. – Proc. 3rd Inter Conf. on Advanced Materials Science and Technology (ICAMST), 19 April; 205p., available at: http//doi.org./10.1063/1.4945554.

http://www.aloki.hu ● ISSN 1589 1623 (Print) ● ISSN1785 0037 (Online)
DOI: http://dx.doi.org/10.15666/aeer/1902_11771190
© 2021, ALÖKI Kft., Budapest, Hungary

USAGE OF MAGNETIC IRON TO RAISE TOLERANCE OF SOME ORNAMENTAL TREES AND SHRUBS TO SOIL SALINITY IN CASE OF CHINA ROSE (*HIBISCUS ROSA-SINENSIS* L.)

NOFAL, E. M. S.[1] – KHALAFALLAH, M. M.[1] – SHAHIN, S. M.[2] – MONTASSER, H. M. M. S.[2*]

[1]*Hort. Dept., Fac. Agric., Kafrelsheikh Univ., Kafr El Sheikh, Egypt*

[2]*Botanical Gards. Res. Dept., Hort. Res. Inst., ARC, Giza, Egypt*

**Corresponding author*
e-mail: heba.montaser78@gmail.com

(Received 20th Sep 2020; accepted 19th Jan 2021)

Abstract. An investigation was conducted at Orman Botanical Garden, Giza, Egypt to reveal the role of magnetite at 2 or 4 g/pot in reducing the harmful effects of NaCl + $CaCl_2$ salt mixture added to the soil mixture at various concentrations, on growth and quality of Chinese hibiscus transplants. Interaction effect was also studied. The results showed that hibiscus transplants attained 100% survival, even at 8000 ppm salinity level and the absence of magnetic iron. However, means of the different vegetative and root characteristics were progressively decreased as the concentration of salinity was increased scoring minimal values at the highest concentration. The opposite was true regarding magnetite treatments. A marked improvement in growth was also acquired by the different interaction treatments with superiority of combining between any level of salinity and the high rate of magnetite. The percentage of salt resistance index exhibited a descending decrement with salinity level increment, but it was, generally higher than 50% even at the high salinity level. A similar trend was obtained regarding leaf chemical composition, with few exceptions in both seasons. Accordingly, it is advised to apply magnetite at 4 g/pot rates to saline soil for better growth of *Hibiscus rosa-sinensis* L. transplants.
Keywords: *Hibiscus rosa-sinensis L., soil salinity, magnetic iron, chemical composition*

Introduction

China Rose or Chinese hibiscus (*Hibiscus rosa-sinensis* L.) Fam. Malvaceae is one of the most beautiful, evergreen flowering shrubs used widely for landscape in Egypt. It is a large shrub, grow up to 5-7 m height, leaves usually simple ovate to 8-10 cm long, not lobed but toothed or nearly entire. It is native to subtropical and tropical areas as an ornamental plant for its glossy, flourish leaves and very large flowers that are born solitary in many colors on the leaf axils, for hedging and also glasshouses for summer bloom. It is easily propagated by cuttings, grafting and layering (Bailey, 1976).

Concerning its tolerance to salinity, Kratsch et al. (2008) categorized such ornamental shrub as sensitive to salinity, due to its tolerance of salts up to 650 ppm. On the other side, Mcfarland et al. (2014) found that it can tolerate soil salinity up to 2500 ppm, but can tolerate salinity of irrigation water up to 1250 ppm only. So, it considered moderately sensitive to salts. Moreover, Khafagy et al. (2013) reported that it can tolerate the low level of diluted seawater (10%), but higher levels (up to 40%) gradually decreased all growth characters. That was documented by Ahmed (2017) who revealed that soil salinity higher than 2000 ppm clearly depressed it growth and flowering.

Many salinity disorders, such as plant growth reduction, delay flowering, decrease flower quality, tip and marginal leaf burn as a result of Na and Cl accumulation, and finally decreasing of aesthetical value of the plant were explored before by Mahmoud et al. (2008) on *Dovyalis caffra* and *Lantana camara*, Cassaniti et al. (2013) on

http://www.aloki.hu ● ISSN 1589 1623 (Print) ● ISSN 1785 0037 (Online)
DOI: http://dx.doi.org/10.15666/aeer/1902_11911202
© 2021, ALÖKI Kft., Budapest, Hungary

Chrysanthemum morifolium, *Dianthus cartophyllus*, *Gerberra jamesonii*, *Hippeastrum vittatum* and *Anthurium andreanum*, Shahin et al. (2014) on tall fescue (*Festuca arundinacea* var. Festoria), El-Shewaikh et al. (2015) on areca (*Dypsis lutescens*), El-Sayed et al. (2015) on saltbush (*Atriplex halimus*) and Shahin et al. (2017) on *Casuarina equisetifolia* and *Eucalyptus rostrata*. However, these disorders were corrected by some applicable ways elicited by Ahmed et al. (2011) on roselle (*Hibiscus sabdariffa*) Khafagy et al. (2013) and Ahmed (2017) on *H. rosa-sinensis*, Abdel-Fattah (2014) on *Jacaranda acutifolia*, Ahmed et al. (2016) on *Acalypha wilkesiana* and El-Sayed et al. (2019) on *Enterolobium contortisiliquum*.

The purpose of this trial was to evaluate the role of magnetite in alleviating injury of soil salinity on growth and aesthetical performance of Chinese hibiscus during rearing in the nursery.

Materials and methods

In order to find out the function of magnetic iron to mitigate damage of salinized soils on growth and flowering of China rose transplants an experiment was consummated under the full sun, temperature between (27-38°c) the average percentage of humidity is 56% throughout the course of study at nursery of Orman Botanical Garden, Giza, Egypt during 2018 and 2019 consecutive seasons to determine the importance of this natural ore in enhancing growth of this plant under such stress.

Therefore, 4-months-old, uniform transplants of China rose of 17-18 cm height, carrying about 8-9 leaves were planted on April, 1st for each season in 15-cm-diameter polyethylene black bags (one transplant/bag) filled with about 3.5 kg of sand and clay mixture at equal volume parts (1:1, v/v). The physical and chemical properties of the soil mixture used in both seasons were measured and listed in *Table 1*.

Table 1. *The physical and chemical analysis of the soil mixture used in 2018 and 2019 seasons*

Soil mixture	**Particle size distribution (%)**				**S.P.**	**E.C. (dS/m)**	**pH**	**Cations (meq/l)**			
Sand + Clay (1:1, v/v)	Coarse sand	Fine sand	Silt	Clay				Ca^{++}	Mg^{++}	Na^{+}	K^{+}
	38.6	31.3	20.6	9.5	25	6.5	7.86	17.8	14.2	33.1	0.9
Soil texture	**Anions (meq/l)**				**Macro-and micro-elements (ppm)**						
	HCO_3^-	Cl^-	SO_4^{--}	CO_3	N	P	K	Fe	Zn	Mn	Cu
Sandy clay	2.10	58.40	5.50	0.00	173.10	15.78	361.76	15.80	4.36	8.03	8.81

Immediately before planting, the soil mixture was salinized with a mixture of NaCl and $CaCl_2$ pure salts at equal weight parts (1:1, g/g) at the concentrations of 0, 2000, 4000, 6000 and 8000 ppm, while after planting the soil mixture was well mixed with magnetic iron ore (Fe_3O_4, 22.5%) obtained from Alahram Mining Co., Maadi, Cairo at the rates of 0, 2 and 4 g/plant, added as one batch at the commencing of the season. Salinity and magnetite treatments were connected factorially to create fifteen interactions.

During the course of the study, the plants under the different experimental treatments were fertilized 3 times with 2 g/plant of a compound chemical fertilizer (NPK + microelements i.e., Kristalon 19: 19: 19) and watered day by day. Besides, the various agricultural practices required for such plantation were carried out whenever needed. A factorial experiment based

http://www.aloki.hu ● ISSN 1589 1623 (Print) ● ISSN 1785 0037 (Online)
DOI: http://dx.doi.org/10.15666/aeer/1902_11911202
© 2021, ALÖKI Kft., Budapest, Hungary

on a complete randomized design was accomplished in the two seasons, replicated thrice with five transplants for each replicate (Mead et al., 1993). The magnetite treatments represented the main factor and salinity levels represented the sub-factor.

At the end of each season (on October, 1st), the following data were recorded: survival (%), plant height (cm), stem diameter (cm), number of branches/plant, number of leaves/plant, leaf area (cm^2) using a planimeter, root length (cm), aerial parts and roots fresh and dry weights (g) after removing the soil under running water then lefts to dry and salt resistance index as a percentage (SRI %) which was estimated from the equation of Wu and Huff (1983) as follows:

$$\text{SRI (\%)} = \frac{\text{Mean root length of the longest root in salt treated plant}}{\text{mean root length of the longest root in control one}} \times 100$$

Furthermore, the benefit coefficient of magnetite (Fe_3O_4) under various salinity levels as a percentage (B. Coe %) was calculated from the following equation:

$$\text{B. Coe (\%)} = \frac{\text{Increase rate in dry matter of treated plant}}{\text{dry matter of control one}} \times 100$$

In the second season only, concentrations of photosynthetic pigments (chlorophyll a, b and carotenoids, mg/g f.w.) were assessed in fresh leaf samples using the method of Sumanta et al. (2014), whereas in dry ones, the percentages of nitrogen, phosphorus as well as potassium, sodium and chloride were measured according to the methods of Blake (1965), Luatanab and Olsen (1965) and Jackson (1973), consecutively. Proline concentration (g/100 g d.w.) was evaluated in dry leaf sample using the method of Batels et al. (1973).

Data were statistically analyzed using the computer program of SAS Institute (2009) and Duncan's New Multiple Range to compare among means of treatments (Steel and Torrie, 1980).

Results

Effect of soil salinity, magnetite and their interaction on vegetative and root growth parameters

It is obvious from data presented in *Table 2* that no mortality was occurred among transplants subjected to salinity concentration up to 8000 ppm, giving 100% survival % in the two seasons, although (*Tables 3-6*) means of plant height (cm) stem diameter (cm), No. branches and leaves / plant, leaf area (cm^2), root length (cm) and aerial parts and roots fresh and dry weights (g) were progressively declined with increasing salinity level to become the least at 8000 ppm concentration in both seasons. On the contrary, a gradual elevating in values of the previously stated traits was occurred as the rate of Fe_3O_4 was raised. Therefore, the utmost high means were attained by 4 g/pot rate in the two seasons. Interacting between salinity treatments and magnetite rates recorded also a marked improvement in averages of all vegetative and root growth characters mentioned above irrespective of salinity concentration. However, combining between salinity levels and 4 g magnetic iron/pot dose fulfilled higher records than salinity levels + 2 g/pot magnetite combination in most cases of both seasons.

http://www.aloki.hu ● ISSN 1589 1623 (Print) ● ISSN 1785 0037 (Online)
DOI: http://dx.doi.org/10.15666/aeer/1902_11911202
© 2021, ALÖKI Kft., Budapest, Hungary

Table 2. *Effect of salinity levels, magnetite rates and their interactions on survival and height of Hibiscus rosa-sinensis L. plant during 2018 and 2019 seasons*

Fe_3O_4 rate (g/plant) / Salinity level (ppm)	Survival (%)				Plant height (cm)			
	0.00	2 g	4 g	Mean	0.00	2 g	4 g	Mean
	First season 2018							
0.00	100.00a	100.00a	100.00a	100.00A	37.00g	45.00c	55.43a	45.81A
2000	100.00a	100.00a	100.00a	100.00A	38.53f	42.30d	47.07b	42.63B
4000	100.00a	100.00a	100.00a	100.00A	35.83h	39.30ef	42.80d	39.31C
6000	100.00a	100.00a	100.00a	100.00A	34.13i	37.07g	40.17e	37.12D
8000	100.00a	100.00a	100.00a	100.00A	31.00j	33.27i	36.48gh	33.58E
Mean	100.00 A	100.00 A	100.00 A	–	35.30C	39.39B	44.39A	–
	Second season 2019							
0.00	100.00a	100.00a	100.00a	100.00A	36.33d	40.00b	47.07a	41.13A
2000	100.00a	100.00a	100.00a	100.00A	32.10g	38.00c	40.90b	37.00B
4000	100.00a	100.00a	100.00a	100.00A	29.87h	35.33d	37.53c	34.24C
6000	100.00a	100.00a	100.00a	100.00A	27.77i	32.63f	33.90e	31.43D
8000	100.00a	100.00a	100.00a	100.00A	25.67j	28.87hi	31.13g	28.56E
Mean	100.00 A	100.00 A	100.00 A	–	30.35C	34.97B	38.11A	–

Mean followed by the same letter in a column or row do not differ significantly according to Duncan's new multiple range test

Table 3. *Effect of salinity levels, magnetite rates and their interactions on stem diameter and No. branches/plant of Hibiscus rosa-sinensis L. plant during 2018 and 2019 seasons*

Fe_3O_4 rate (g/plant) / Salinity level (ppm)	Stem diameter (cm)				No. branches/plant			
	0.00	2 g	4 g	Mean	0.00	2 g	4 g	Mean
	First season 2018							
0.00	0.500fg	0.667ab	0.700a	0.622A	2.67cd	3.00c	4.00a	3.22A
2000	0.467g	0.567de	0.633bc	0.556B	2.67cd	3.00c	3.50b	3.06B
4000	0.600cd	0.600cd	0.600cd	0.600A	2.67cd	3.00c	3.00c	2.89B
6000	0.533ef	0.567de	0.600cd	0.567B	2.33de	2.67cd	2.67cd	2.56C
8000	0.533ef	0.533ef	0.567de	0.544B	1.67f	1.67f	2.00ef	1.78D
Mean	0.427C	0.587B	0.620A	–	2.40C	2.67B	3.03A	–
	Second season 2019							
0.00	0.410fg	0.557b	0.613a	0.527A	1.67g	2.33e	2.67cd	2.22C
2000	0.387g	0.463de	0.513c	0.454BC	2.00f	3.00b	3.33a	2.78A
4000	0.470de	0.477cd	0.467de	0.471B	1.67g	2.83bc	3.00b	2.50B
6000	0.437d-f	0.433ef	0.440d-f	0.437CD	1.63g	2.67cd	2.83bc	2.38BC
8000	0.440d-f	0.407fg	0.417fg	0.421D	1.27h	1.83fg	2.44de	1.84D
Mean	0.429C	0.467B	0.490A	–	1.65C	2.53B	2.85A	–

Mean followed by the same letter in a column or row do not differ significantly according to Duncan's new multiple range test

http://www.aloki.hu ● ISSN 1589 1623 (Print) ● ISSN 1785 0037 (Online)
DOI: http://dx.doi.org/10.15666/aeer/1902_11911202
© 2021, ALÖKI Kft., Budapest, Hungary

Table 4. *Effect of salinity levels, magnetite rates and their interactions on leaf and root length and root callar diameter of Hibiscus rosa-sinensis L. plant during 2018 and 2019 seasons*

Fe_3O_4 rate (g/plant) / Salinity level (ppm)	No. leaves/plant				Leaf area (cm^2)				Root length (cm)			
	0.00	2 g	4 g	Mean	0.00	2 g	4 g	Mean	0.00	2 g	4 g	Mean
	First season 2018											
0.00	33.67e	42.33b	48.67a	41.56A	28.40cd	30.77b	33.57a	30.91A	33.33e	36.40c	40.67a	36.80A
2000	32.67e	39.37c	42.03b	38.02B	27.40de	29.53c	33.23a	30.06B	32.03e	35.00d	38.50b	35.18B
4000	29.07f	34.43e	37.10d	33.53C	25.37f	27.20de	30.97b	27.84C	27.77g	30.63f	32.87e	30.42C
6000	24.77g	29.03f	34.27f	29.36D	22.50h	23.97g	26.90e	24.46D	24.37i	26.40h	28.60g	26.46D
8000	20.67h	23.03g	30.17f	24.62E	20.00i	21.70h	24.17fg	21.96E	19.70k	21.60j	23.43i	21.58E
Mean	28.17C	33.64B	38.45A	–	24.73C	26.63B	29.77A	–	27.44C	30.01B	32.81A	–
	Second season 2019											
0.00	32.40cd	36.60b	40.87a	36.62A	33.00d	39.43b	41.60a	38.01A	19.33h	22.73de	31.00a	24.36A
2000	29.10e	33.80c	35.47b	32.79B	29.47f	32.80d	37.27c	33.18B	17.40ij	21.20fg	27.07b	21.89B
4000	26.43f	31.33d	32.50cd	30.09C	24.43ij	28.90f	33.20d	28.84C	16.80j	20.10gh	25.50c	20.80C
6000	24.47g	27.93e	29.17e	27.19D	23.93j	27.00gh	30.93e	27.29D	16.10jk	19.27h	23.77d	19.71D
8000	21.83h	24.83g	26.47f	24.38E	21.33k	25.77hi	28.10fg	25.07E	15.03k	17.70i	21.80ef	18.18E
Mean	26.85C	30.90B	32.89A	–	26.43C	30.78B	34.22A	–	17.60C	20.20B	25.83A	–

Mean followed by the same letter in a column or row do not differ significantly according to Duncan's new multiple range test

Table 5. *Effect of salinity levels, magnetite rates and their interactions on aerial parts fresh and dry weights of Hibiscus rosa-sinensis L. plant during 2018 and 2019 seasons*

Fe_3O_4 rate (g/plant) / Salinity level (ppm)	Aerial parts fresh weights (g)				Aerial parts dry weights (g)			
	0.00	2 g	4 g	Mean	0.00	2 g	4 g	Mean
	First season 2018							
0.00	42.27d	47.10b	52.20a	47.19A	12.40d	13.80b	17.43a	15.54A
2000	37.67e	41.53d	44.33c	41.18B	10.76d	12.18c	14.37b	12.44B
4000	35.10g	34.60f	38.70e	36.13C	9.70e	10.10de	12.90c	10.90C
6000	26.90h	28.43h	32.07g	29.13D	7.50g	8.37f	10.43de	8.77D
8000	20.57j	21.03j	24.00i	21.87E	5.43h	6.07h	8.00fg	6.50E
Mean	32.50C	34.54B	38.26A	–	9.16C	10.10B	12.63A	–
	Second season 2019							
0.00	23.97d	25.93c	32.17a	27.36A	8.80ef	9.87cd	12.67a	10.44A
2000	21.53e	24.07d	27.87b	24.49B	8.13fg	9.27de	11.63b	9.68B
4000	19.40f	21.80e	25.17cd	22.12C	7.14h	8.23fg	10.53c	8.63C
6000	16.40g	19.17f	22.10e	19.22D	5.80jk	7.00hi	9.30e	7.37D
8000	13.83h	16.73g	19.87f	16.81E	4.90k	6.10ij	7.63gh	6.21E
Mean	19.03C	21.54B	25.43A	–	6.95C	8.09B	10.35A	–

Mean followed by the same letter in a column or row do not differ significantly according to Duncan's new multiple range test

Salt resistance index (SRI %) and benefit coefficient of magnetite (B. coe. %)

As shown in *Table 7,* a progressive decrease in the percentages of salt resistance index was acquired due to the gradual increment in salinity concentration to reach the least values by 8000 ppm level in the two seasons. However, these values were higher

http://www.aloki.hu ● ISSN 1589 1623 (Print) ● ISSN 1785 0037 (Online)
DOI: http://dx.doi.org/10.15666/aeer/1902_11911202
© 2021, ALÖKI Kft., Budapest, Hungary

than 50% at such high concentration (8000 ppm); 58.78% in the first season and 75.14% in the second one pointing to the good tolerance of Chinese hibiscus to soil salinity up to 8000 ppm. On the other side, adding Fe_3O_4 was found to be out of order, especially at 4 g/pot rate, which gave means for such index closely near to those of control ones. The rates of 2 g/pot, however, slightly improved the percent of this index in the 1st season, whilst in the second one, caused a significant increase in it. Moreover, combining between magnetite (especially at 4 g/pot dose) and various salinity levels was worthless compared to control treatment in the two seasons. Thus, application of Fe_3O_4 may be unvalued to improve resistance of Chinese hibiscus to soil salinity. This result may be unexpected and deserve more investigation to confirm it.

The opposite was the right concerning the benefit coefficient of magnetite percentages (*Table 7*) that cleared a great benefit for applying of Fe_3O_4 in production of dry matter, especially at the high salinity concentration (8000 ppm) in the first season and at 4000, 6000 and 8000 ppm concentrations in the second one. In addition, drenching the soil mixture with magnetic iron at the rate of 4 g/pot attained the highest benefit for dry matter formation in both seasons, followed by 2 g/pot rate relative to control treatment. Results of the combined treatments in the first season were fluctuated except for 8000 ppm level + magnetite at any rate combination which showed higher benefit than other combinations. In the second season, all combinations cleared more advantage than control ones giving heaviest dry matter at all.

Table 6. *Effect of salinity levels, magnetite rates and their interactions on roots fresh and dry weights of Hibiscus rosa-sinensis L. plant during 2018 and 2019 seasons*

Fe_3O_4 rate (g/plant) / Salinity level (ppm)	Roots fresh weights (g)				Roots dry weights (g)			
	0.00	**2 g**	**4 g**	**Mean**	**0.00**	**2 g**	**4 g**	**Mean**
	First season 2018							
0.00	13.97d	16.80b	17.57a	16.11A	6.20ef	7.07c	8.40a	7.22A
2000	13.00e	15.77c	16.53b	15.10B	5.73g	6.57de	7.87b	6.72B
4000	11.27g	13.87d	13.97d	13.03C	5.00h	5.80fg	6.70cd	5.83C
6000	9.80h	11.70fg	12.10f	11.20D	4.37i	4.90h	5.87fg	5.04D
8000	8.07i	9.77h	10.10h	9.31E	3.57j	4.13j	4.83h	4.18E
Mean	11.22C	13.58B	14.05A	–	4.97C	5.69B	6.73A	–
	Second season 2019							
0.00	5.40e	6.47cd	9.53a	7.13A	3.43d-f	3.70b-d	4.53a	3.89A
2000	4.90ef	6.07d	8.37b	3.45B	3.07gh	3.60c-e	3.90b	3.52B
4000	4.70ef	5.80de	7.88bc	6.13C	2.83hi	3.33e-g	3.73bc	3.30C
6000	4.50f	5.60de	7.03c	5.71D	2.70ij	3.10gh	3.30fg	3.03D
8000	4.20g	5.01e	6.40cd	5.20E	2.43j	2.87hi	3.00h	2.77E
Mean	4.74C	5.79B	7.84A	–	2.89C	3.32B	3.69A	–

Mean followed by the same letter in a column or row do not differ significantly according to Duncan's new multiple range test

Chemical composition of the leaves

As shown in *Table 8,* concentrations of chlorophyll a, b and carotenoids (mg/g. f. w.) and the percentages of N, P and K exhibited a gradual decrease as a result of the progressive increment in salinity level, whereas Na and Cl percentages and proline

http://www.aloki.hu ● ISSN 1589 1623 (Print) ● ISSN 1785 0037 (Online)
DOI: http://dx.doi.org/10.15666/aeer/1902_11911202
© 2021, ALÖKI Kft., Budapest, Hungary

(mg/100 g d. w.) were linearly increased. On the other hand, drenching the soil mixture with magnetite successively raised chlorophyll a, b, N, P and K concentrations as the rate of magnetite was increased, but concentrations of carotenoids, Na, Cl and proline were cumulatively declined. Generally, the combining between salinity level up to 4000 ppm and magnetic iron at the rate of 4 g/plant recorded the utmost high concentrations of chlorophyll a, b, N, P and K, but that was true for carotenoids when plants grown in no salinized soil mixture and abandoned of Fe_3O_4, and for Na, Cl and proline constituents when plants cultured in soil mixture which received 8000 ppm salinity level in the absence of Fe_3O_4.

The results pronouncedly clear that magnetite application markedly reduced Na^+ and Cl^- toxic ions leading to mitigating their deleterious effects on growth and performance of Chinese hibiscus plants. As Na and Cl concentration was decreased by raising Fe_3O_4 rate the concentration of proline was diminished due to alleviating salt stress.

Table 7. *Effect of salinity levels, magnetite rates and their interactions on resistance index and benefit coefficient of Hibiscus rosa-sinensis L. plant during 2018 and 2019 seasons*

Fe_3O_4 rate (g/plant) / Salinity level (ppm)	Resistance index (%)				Benefit coefficient of Fe_3O_4			
	0.00	**2 g**	**4 g**	**Mean**	**0.00**	**2 g**	**4 g**	**Mean**
	First season 2018							
0.00	100.00a	100.00a	100.00a	100.00A	0.00g	11.41e	40.50b	17.80B
2000	96.33b	96.28b	94.69b	95.76B	0.00g	13.48d	33.93c	15.51C
4000	83.44c	84.25c	84.18c	83.96C	0.00g	7.83f	33.59c	13.81D
6000	73.24d	72.78de	70.40e	72.14D	0.00g	11.88de	39.84b	17.24B
8000	59.16f	59.43f	57.75f	58.78E	0.00g	12.02de	47.38a	19.80A
Mean	82.43AB	82.55A	81.40B	–	0.00C	11.32B	39.05A	–
	Second season 2019							
0.00	100.00a	100.00a	100.00a	100.00A	0.00g	12.15h	43.90d	18.68C
2000	66.60h	93.22b	87.70cd	82.51C	0.00g	13.93gh	42.84d	18.92C
4000	86.88cd	88.38c	82.54e	85.93B	0.00g	15.38g	47.68c	21.02B
6000	83.24e	84.74de	77.13f	81.71C	0.00g	19.71f	59.78a	26.50A
8000	78.16f	76.55f	70.71g	75.14D	0.00g	24.51e	55.94b	26.82A
Mean	83.97B	88.58A	83.62B	–	0.00C	17.14B	50.03A	–

Mean followed by the same letter in a column or row do not differ significantly according to Duncan's New Multiple Range test

Discussion

Effect of soil salinity, magnetite and their interaction on vegetative and root growth parameters

From the previous results it was notice that the adverse effects of saline soil on growth may be attributed to either low water uptake due to low potential of soil water (Munns, 2002) or certain ion toxicity (Na^+ and Cl^-) or both (Carter et al., 2005). This fact was emphasized by Elhag and Abdalla (2014) who stated that salinity depresses plant growth via affecting water absorption and biochemical processes such as N, CO_2 assimilation and protein biosynthesis or accumulated high concentration of potentially toxic ions (Na^+ and Cl^-). Jose et al. (2016) ascribed the reduction in growth by salinity

http://www.aloki.hu ● ISSN 1589 1623 (Print) ● ISSN 1785 0037 (Online)
DOI: http://dx.doi.org/10.15666/aeer/1902_11911202
© 2021, ALÖKI Kft., Budapest, Hungary

to the effect of osmotic stress and the inhibition of cell division rather than cell expansion coupled with the great reduction in photosynthesis. High salinity also leads to leaf abscission due to ion accumulation in the leaves, particularly the oldest ones. Reduction of growth by salinity may be attributed to a decrease in all volume at a constant cell number. Mechanism of salt may result in inhibition of cell division, consequently reduces the rate of plant development (Khan et al., 2009). Jou et al. (2006), however suggested that ATPase participates in the endoplasmic reticulum-Golgi mediated, protein sorting machinery for both housekeeping function and compartmentalization of excess Na^+ under high salinity.

Table 8. *Effect of salinity levels, magnetite rates and their interactions on some constituent's concentrations in the leaves of Hibiscus rosa-sinensis L. plants during 2019 seasons*

Fe3O4 rate (g/plant) / Salinity level (ppm)	Chlorophyll a (mg/g f.w.)				Chlorophyll b (mg/g f.w.)				Carotenoids (mg/g f.w.)			
	0.00	**2 g**	**4 g**	**Mean**	**0.00**	**2 g**	**4 g**	**Mean**	**0.00**	**2 g**	**4 g**	**Mean**
	First season 2018											
0.00	2.320d	2.673b	3.040a	2.678A	0.887cd	1.006b	1.163a	1.019A	0.819a	0.533c	0.537c	0.630A
2000	1.765h	2.135f	2.669b	2.190B	0.794ef	0.845de	1.056b	0.898B	0.658b	0.494d	0.461e	0.538B
4000	1.512j	2.258e	2.605c	2.125C	0.687g	0.799ef	0.932c	0.806C	0.447e	0.410fg	0.418f	0.425C
6000	1.450c	1.610i	1.821i	1.627D	0.689g	0.743fg	0.940c	0.791C	0.450e	0.381gh	0.394fg	0.408D
8000	0.675n	0.811m	1.062l	0.849E	0.553h	0.680g	0.710g	0.648D	0.387gh	0.359h	0.380gh	0.375E
Mean	1.545C	1.898B	2.239A	–	0.722C	0.815B	0.960A	–	0.552A	0.436B	0.438B	–
	N (%)				P (%)				K (%)			
	0.00	2 g	4 g	Mean	0.00	2 g	4 g	Mean	0.00	2 g	4 g	Mean
0.00	3.475d	3.861b	4.147a	3.828A	0.829a	0.843a	0.854a	0.842A	1.696e	1.983b	2.012a	1.897A
2000	3.088g	3.187e	3.501c	3.259B	0.753b	0.758b	0.775b	0.762B	1.552f	1.753d	1.892c	1.732B
4000	2.779i	2.891h	3.153f	2.941C	0.599d	0.671c	0.698c	0.656C	1.208j	1.394h	1.534g	1.380C
6000	2.303l	2.376k	2.575j	2.418D	0.493e	0.550d	0.563d	0.535D	1.087k	1.223j	1.350i	1.220E
8000	1.843o	1.873n	1.991m	1.902E	0.392f	0.456e	0.457e	0.435E	1.879c	0.980l	1.080k	1.313D
Mean	2.698C	2.838B	3.073A	–	0.613B	0.656A	0.669A	–	1.484B	1.467C	1.574A	–
	Na (%)				Cl (%)				Proline (mg/100 g f.w.)			
	0.00	2 g	4 g	Mean	0.00	2 g	4 g	Mean	0.00	2 g	4 g	Mean
0.00	0.812h	0.796h	0.730i	0.779E	1.460h	1.460h	1.490h	1.470E	53.23k	49.12l	45.48m	49.27E
2000	0.933g	0.914g	0.813h	0.887D	1.780f	1.670g	1.500h	1.650D	68.16h	64.83i	64.77i	65.92D
4000	1.120f	1.118f	1.108f	1.115C	2.050d	1.830f	1.620g	1.830C	74.32g	65.35i	62.49j	67.39C
6000	1.543b	1.416d	1.133ef	1.364B	2.360b	2.050d	1.830f	2.080B	89.19d	79.73e	76.36f	81.76B
8000	1.850a	1.481c	1.154e	1.495A	2.590a	2.230c	1.950e	2.260A	129.50a	113.61b	99.91c	114.34A
Mean	1.252A	1.145B	0.988C	–	2.050A	1.850B	1.680C	–	82.88A	74.53B	69.80C	–

Means followed by the same letter is a column or row do not differ significantly according to Duncan's new multiple range test

Likewise, Cassaniti et al. (2013) claimed that brackish water can be commercially used for production of *Chrysanthemum morifolium*, *Dianthus caryophyllus*, *Gerbera jamesonii*, *Hippeastrum vittatum* and *Anthurium andreanum*, but saline water higher than 2500 ppm concentration reduced their growth, delayed flowering and decreased flower quality. Similarly, were those results of Shahin et al. (2008) on *Ficus macrocarpa* var. Hawaii and *Euonymus Japonica* cv. Mediopicta, Shahin et al. (2013) on *Ficus benjamina* cv. *Samantha and Schefflera arboricola* cv. Gold Capella, El-Fouly et al. (2015) on *Iris tingitana* cv. Wedgewood, Jose et al. (2016) on *Eucalyptus urophylla* and the hybrid of *E. urophylla* x *E. grandis*.

On the other hand, the positive effect of magnetic iron on growth of plants suffered from salt stress may be due to its role in promoting the uptake of N, P, K and Fe which

http://www.aloki.hu ● ISSN 1589 1623 (Print) ● ISSN 1785 0037 (Online)
DOI: http://dx.doi.org/10.15666/aeer/1902_11911202
© 2021, ALÖKI Kft., Budapest, Hungary

stimulate plant growth against the toxicity of Na^+ and Cl^- ions that inhibit it. It induces cell metabolism and mitosis of meristematic cells (Barage et al., 2009). It is believed that new protein bands are formed in plants that are treated with Fe_3O_4 and these proteins are responsible for the increased growth (Hozyan and Abdul-Qodos, 2010). Furthermore, it declines the hydration of salt ions and colloids, increasing salt solubility, and finally leading to leaching such salts from the soil. So, it is successfully used to reclaim soils with high cations and anions, such as Ca, Na, Cl and HCO_3 (Mostafazadeh et al., 2012). In the iron atom, there is a number of valence electrons that generates a magnetic field influence on the biochemical processes in plants and renders the roots to exhibit symptoms of magnetism that kills nematodes and injurious bacteria (Yuliando et al., 2016). Supporting results for those of this study were also obtained by Abdel Fattah (2014) on *Jacaranda ocutifolia*, Ahmed et al. (2016) on *Acalypha wilkesiana*, Shahin et al. (2018) on *Terminalia arjuna* and El-Sayed et al. (2019) on elephant`s ear tree.

Salt resistance index (SRI%) and benefit coefficient of magnetite (B. coe.%)

Such gains may be reasonable, as they indicate the role of magnetic in alleviating salt hazards and promoting dry matter production. These results are reasonable because magnetite usually solubilizes and leaches salts from the soil, and this gives roots a chance to penetrate and distribute well through the growing medium, consequently uptake enough water and nutrients necessary for good and healthy growth. On the same line were those results attained by Al-Qubaie et al. (2003) on *Ficus benghalensis*, *Bougainvillea glabra*, *Jasminum azoricum*, *Conocarpus erectus*, *Tamarix articulata* and *Ziziphus spina-christi*, Shahin et al. (2008) on *Ficus macrocarpa* var. Hawaii and *Euonymus Japonica* cv. Mediopicta, Abdel-Fattah et al. (2012a) on *Ficus retusa*, Abdel Fattah et al. (2012b) on *Ficus benjamina* and El-Sayed et al. (2019) *Enterolobium contortisiliquum.*

Chemical composition of the leaves

This may be reasonable because salts usually reduces the water potential of soil solution, consequently decrease minerals and water uptake by roots, accompanied by a depression of photosynthesis and enzymes activity (Munns, 2002). It was also remarkable that accumulation of some amino acids and amides in the leaves and roots of salinity-stressed plants may be attributed to *de novo* synthesis by protein sorting machinery and not the result of protein degradation (Jou et al., 2006).

These results, are similar trend to those of Elhag and Abdalla (2014) and Moustafa et al. (2017) on *Moringa oleifera*, Ahmed et al. (2016) on *Acalypha wilkesiana*, Shahin et al. (2018) on *Terminalia arjuna* and El-Sayed et al. (2019) who observed that chlorophyll a, b, carotenoids and total carbohydrates concentrations were increased in the leaves of *Enterolobium contortisiliquum* under salt stress by application of Fe_3O_4 at either 2 or 4 g/pot.

Conclusion

Hence, it can be recommended to drench the soil mixture, in which hibiscus of China plants are grown with 4 g/pot of magnetic iron (Fe_3O_4) to improve their growth and aesthetic value under salt stress during rearing in the nursery.

It is recommended to use transplants of different ages growing under higher dose of salinity.

http://www.aloki.hu ● ISSN 1589 1623 (Print) ● ISSN 1785 0037 (Online)
DOI: http://dx.doi.org/10.15666/aeer/1902_11911202
© 2021, ALÖKI Kft., Budapest, Hungary

REFERENCES

[1] Abdel-Fattah, G. H., Shahin, S. M., Khenizy, S. A. M. (2012a). Improving tolerance of Ficus benjamina L. plant to saline water stress by VAM (Glomus sp.). – J. Biol. Chem. & Environ. Sci. 7(1): 1-16.

[2] Abdel-Fattah, G. H. (2014): The role of magnetic iron and sodium salenate in minimizing soil salt hazards on growth and quality of Jacaranda acutifolia Humb. & Bionol seedlings. – Sci. J. Flowers & Ornam. Plants 1(3): 187-198.

[3] Abdel-Fattah, G. H., Shahin, S. M., Abdel-Moniem, A. M. (2012b). Could phosphorene help Ficus retosa L. plant to tolerate the deleterious effects of saline water? – J. Biol. Chem. & Environ. Sci. 7(1): 17-32.

[4] Ahmed, M., A. (2017): Effect of salinity ($NaCl + CaCl_2$) and some soil additions on growth, flowering and chemical composition of rose of China (Hibiscus rosa-sinensis L.) plant. – Middle East J. Agric. Res. 6(2): 302-314.

[5] Ahmed, Y. M., Shalaby, E. A., Shanan, N. T. (2011): The use of organic and inorganic cultures in improving vegetative growth, yield characters and antioxidant activity of roselle plants (Hibiscus sabdariffa L.). – African J. Biotech.,10(11): 1988-1996.

[6] Ahmed, M., A., Abdel-Fattah, G. H., Shahin, S. M. (2016): The role of magnetic iron in enhancing the ability of Acalypha wilkesiana Mull. Arg. transplants to tolerate soil salinity. – J. Plant Production, Mansoura Univ. 7(3): 379-384.

[7] Al-Qubaie, A. I., Shahin, S. M., Abdel-Samad, F. A. (2003): Effect of diluted sea water on growth and chemical composition of some ornamental trees and shrubs. – Egypt J. Appl. Sci. 18(8 B): 587-601.

[8] Bailey, L. H. (1976): Hortus. – Macmillan Publishing Co., Inc., New York.

[9] Barage, L. F., da Sousa, M. P., Almeida, T. A. (2009): Enterolobium schomburgkii Benth. Seed germination under saline stress and polyamine application. – Revista Braz Plantas Med. 11(1): 1516-1527.

[10] Batels, L. S., Walden, R. P., Teare, T. D. (1973): Rapid determination of free proline under water stress studies. – Plant and Soil 939: 205-207.

[11] Blake, C. A. (1965): Methods of Soil Analysis Part 1 Physical and Mineralogical Properties Including a Statistics of Measurement and Sampling. – Amr. Soc. Agron. Inc. Pub., Madison, WI.

[12] Carter, C. T., Grieve, C. M., Poss, J. A. (2005): Salinity effects on emergence, survival and ion accumulation of Limonium perezii. – J. Plant Nutrition 28: 1243-1257.

[13] Cassniti, C., Romano, D., Hop, M. E., Flowers, T. J. (2013): Growing floricultural crops with brackish water. – Environmental and Experimental Botany 92: 165-175.

[14] El-Fouly, A. S., Abdel-Sattar, M. M., Shahin, S. M. (2015): Effect of different salinity levels, PP-333 treatments and their interaction on growth, flowering, bulbs productivity and chemical composition of Iris tingitana cv. Wedgewood. – J. Agric. Res. Kafr El-Sheikh Univ. 41(1): 347-369.

[15] Elhag, A. Z., Abdalla, M. H. (2014): Investigation of sodium chloride tolerance of Moringa oleifera Lam. transplants. – Universal J. Agric. Res. 2(2): 45-49.

[16] El-Sayed, B. A., Shahin, S. M., El-Tayeb, H. F. (2015): Response of saltbush (Atriplex halimus L.) plants to salinity and type of growing media. – Scientific J. Flowers & Ornam. Plants 2(1): 135-148.

[17] El-Sayed, M. A., El-Fouly, Amal, S., A., Shahin, S. M. (2019): Reducing the harmful effect of saline irrigation water on growth and quality of Enterolobium contortisiliquum (Elephant`s ear) seedlings. – Bull, Fac. Agric. Cairo. Univ. 70: 267-276.

[18] El-Shewaikh, Y. M. E., Khenizy, S. A. M., El-Deeb, E. E. A. (2015): Effect of some physiological treatments on areca seedlings. B. Effect of irrigation with saline water on areca (Dypsis lutescens Wendl.) seedlings. – J. Biol, Chem., & Environ. Sci. 10(4): 297-308.

http://www.aloki.hu ● ISSN 1589 1623 (Print) ● ISSN 1785 0037 (Online)
DOI: http://dx.doi.org/10.15666/aeer/1902_11911202
© 2021, ALÖKI Kft., Budapest, Hungary

[19] Hozyan, M., Abdul-Qodos, A. (2010): Irrigation with magnetized water enhances growth, chemical constituent and yield of chickpea (Cicer arietinum L.). – Agric. and Biol. J. of Amer. 1(4): 671-676.
[20] Jackson, M. H. (1973): Soil Chemical Analysis. – Prentice-Hall of India Private Limited, New Delhi.
[21] Jose, A. C., Silva, N. C. N., Faria, J. M., Pereira, W. V. (2016): Influence of osmotic conditioning of Eucalyptus spp. seeds in the tolerance to salt stress. – J. Seed Sci. 38(4): 329-334.
[22] Jou, Y., Chiang, C., Jauh, G., Yen, H. (2006): Functional characterization of ice plant, on AAA-type ATPase associated with the endoplasmic reticulum-Golgi network, and its role in adaptation to salt stress. – Plant Physiol. 141(1): 135-146.
[23] Khafagy, M. A., Abdalla, M. Y. A., Hussein, H. A. A., Ahmed, S. A. M. (2013): Response of Hibiscus rosa-sinensis L. to the interactive effect of seawater salinity and ascorbic acid. – J. Plant Production Mansoura Univ. 4(1): 51-78.
[24] Khan, G. S., Khan, Z. H., Imran, J., Quraishi, M. U., Yaqoob, S., Khan, S. H. (2009): Effect of salinity on germination and growth of some forest tree species at seedling growth. – J. Agric. Res. 47(3): 271-279.
[25] Kratsch, H., Olsen, S., Rupp, L., Cardon, G., Heflebower, R. (2008): Soil Salinity and Ornamental Plant Selection. – Horticulture Utah State Univ., Cooperative Extension, Logan, pp. 2-8.
[26] Luatanab, F. S., Olsen, S. R. (1965): Test of an ascorbic acid method for determining phosphorus in water and $NaHCO_3$ extracts from soil. – Soil Sci. Soc. Amer. Proc. 29: 677-678.
[27] Mahmoud, A. M. A., Ahmed, S. S., El-Feky, A. H. (2008): Effect of diluted sea water on growth and chemical composition of two ornamental hedges grown in some soils of Egypt. – J. Agric. Res. Kafr El-Sheikh Univ. 34(2): 522-535.
[28] Mcfarland, M. L., Provin, T. L., Redmon, L. A., Boellstorff, D. E., McDonald, A. K., Stem, L. A., Wherley, B. G. (2014): An Index of Salinity and Boron Tolerance of Common Native and Introduced Plant Species in Texas. – Texas A & M AgriLife Extension Service, College Station, Texas.
[29] Mead, R., Curnow, R. N., Harted, A. M. (1993): Statistical Methods in Agriculture and Experimental Biology. 2nd Ed. – Chapman & Hall Ltd., London.
[30] Mostafazadeh, B., Khoshrovesh, M., Mousove, S. F., Kiani, A. R. (2012): Effects of Magnetized Water on Soil Chemical Components Underneath Trick Irrigation. – Amer. Soc. of Civil Engineers. Reston, VA. http://dx.doi.org/10.1061/(ASCE) IR. 1943-4774.0000513.
[31] Moustafa, H. E. B., Abdel-Fattah, G. H., Shahin, S. M. (2017): Germination of Moringa oleifera Lam seeds under salinity conditions in the presence of magnetic iron. – J. Biol. Chem. & Environ. Sci. 12(3): 551-566.
[32] Munns, R. (2002): Comparative physiology of salt and water stress. – Plant Cell and Environment 25: 239-250.
[33] SAS Institute (2009): SAS/STAT User's Guides Statistics. Vers. 6.04, 4th Ed. – SAS Institute Inc. Cary, N. C., USA.
[34] Shahin, S. M., Eliwa, Naglaa, Y., Mahmoud, A. M. A., El-Feky, A. H. (2008): How far diluted sea water can be used for irrigation of some pot plants. – Proc. 9th Inter. Conf. on Dry Land Development, 7-10 Nov., Organized by IDDC, Alex., Egypt, pp. 363-372.
[35] Shahin, S. M., El-Fouly, A. S., Abdel-Sattar, M. M. (2013): Response of F. benjamina L. cv. Samantha and Schefflera arboricola Endl cv. Gold Copella plants cultivated in two different growing media to salinity of irrigation water. – J. Biol. Chem. & Environ. Sci. 8(2): 201-218.
[36] Shahin, S. M., El-Sayed, B. A., El-Tayeb, H. F. (2014): Impact of irrigation with saline water on growth, quality and chemical composition of tall fescue turf (Festuca

http://www.aloki.hu ● ISSN 1589 1623 (Print) ● ISSN 1785 0037 (Online)
DOI: http://dx.doi.org/10.15666/aeer/1902_11911202
© 2021, ALÖKI Kft., Budapest, Hungary

arundinacea Schreb. var. Festorina). – Scientific J. Flowers & Ornam. Plants 1(2): 137-144.

[37] Shahin, S. M., Ahmed, M. A., Tawila, A. S. (2017): Effect of saline irrigation water on growth and quality of *Casuarina equistifolia* L. and *Eucalyptus rostrata* Schlecht plants grown in some soils of Egypt. – Middle East J. Appl. Sci. 7(3): 460-471.

[38] Shahin, S. M., Aly, A. M., Helaly, A. A. E. (2018): Germination of Indian almond (Terminal arjuna Roxb.) seeds as affected by soil salinity in presence or absence of magnetic iron. – J. Plant Production, Mansoura Univ. 9(4): 417-422.

[39] Steel, R. G. D., Torrie, J. H. (1980): Principles and Procedures of Statistics. – McGraw Hill Book Co., Inc., New York, pp. 377-400.

[40] Sumanta, N., Haque, C. I., Nishika, J., Suprakash, R. (2014): Spectrophotometric analysis of chlorophyllous and carotenoids from commonly grown fern sp. by using various extracting solvents. – Research J. Chem. Sci. 4(9): 63-69.

[41] Wu, L., Huff, D. R. (1983): Characteristics of creeping bent grass clones (Agrostis stolonifera L.) from a salinity tolerant population after surviving drought stress. – Hort Science 18(6): 883-885.

[42] Yuliando, A., Astuti, B., Amalia, S. R. (2016): Enhancement of iron content in spinach plants stimulated by magnetic nano particles. – Proc. 3rd Inter Conf. on Advanced Materials Science and Technology (ICAMST), 19 April, 2016. http//doi.org./10.1063/1.4945554.

http://www.aloki.hu ● ISSN 1589 1623 (Print) ● ISSN 1785 0037 (Online)
DOI: http://dx.doi.org/10.15666/aeer/1902_11911202
© 2021, ALÖKI Kft., Budapest, Hungary

INFLUENCE OF SOIL AND WEATHER FACTORS ON THE GERMINATION OF DRY SOWN RAIN-FED CROPS ON THE SEMI ARID TRACTS OF TAMIL NADU, INDIA

VIJAYAPRABHAKAR, A.[1*] – VIJAYAKUMAR, E.[2] – SRIDEVI KRISHNAVENI, T.R.[1] – JAYANTHI, C.[3]

[1]*Institute of Agriculture, Tamil Nadu Agricultural University, Kumulur, Tiruchirappalli 621712, Tamil Nadu, India*

[2]*Department of Genetics and Plant Breeding, Tamil Nadu Agricultural University, Coimbatore 641003, Tamil Nadu, India*

[3]*Department of Agronomy, Tamil Nadu Agricultural University, Coimbatore 641003, Tamil Nadu, India*

**Corresponding author*
e-mail: a.vijayp@ymail.com; phone: +91-959-767-2655

(Received 10th Oct 2020; accepted 19th Jan 2021)

Abstract. In rain-fed farming, crop failure and the low stands are the common problem due to poor germination of dry sown crops due to insufficient soil moisture. This leads to heavy losses of inputs, energy and time of the farmers. To address this, an investigation was made on the germination of major dry land pulses, oil seeds and fiber crops over three different locations of Northern Tamil Nadu, India during 2016-17 and 2017-18 growing periods with the objective of assessing the germination behavior of dry sown rain-fed crops to reduce germination failure. The experiment with test crops (C_1: Blackgram, C_2: Greengram, C_3: Cowpea, C_4: Groundnut, C_5: Sesame, C_6: Cotton, C_7: Redgram) was laid out in randomized block design and observations were made on germination. According to the results, germination of sesame was higher under deficit rainfall and in saline soils with negative and positive correlations exhibiting soil moisture and soil salinity, respectively. The germination of groundnut and pulses showed poor germination under deficit soil moisture condition indicating positive correlation with soil moisture. Over different locations, sesame, cotton and cowpea gave higher mean germination under favorable condition. Raising sesame, cotton and cowpea as alternate crops or including as essential component in cropping system helps to overcome the germination failure in the study area of Northern Tamil Nadu.
Keywords: *crop failure, alternative crops, dry seeding, soil moisture, salinity*

Introduction

Seed germination is the most important stage and a complex process of plant's lifecycle (Bewley et al., 2013). This is a more vulnerable stage than any other stages of crop growth and development (Villalobos et al., 2016). Germination of seeds is highly essential for achieving a successful crop establishment, especially under dry land condition, since it determines the crop stand and consequently yield (Heikal et al., 1982). The poor or failure in germination is frequently occurring under field level, which leads heavy economic losses to the farmers by re-sowing. The total economic impact in monetary terms and the overall area reseeded for major crops on national and global level remain unknown (Lamichhane et al., 2018).

In rain-fed agriculture, uncertainty in rainfall distribution is a common constrain to crop production, where dry sowing is commonly practiced before the onset of monsoon, which is difficult to be predicted due climate change and the same influence applies for the distribution of crops (Hooftman et al., 2016) and their establishment. In this

http://www.aloki.hu ● ISSN 1589 1623 (Print) ● ISSN 1785 0037 (Online)
DOI: http://dx.doi.org/10.15666/aeer/1902_12031220
© 2021, ALÖKI Kft., Budapest, Hungary

condition, early sowing causes poor establishment due to the soil moisture deficit for uniform germination and emergence (Bodner et al., 2015). The poor crop stand leads to inefficiency in utilizing available soil moisture due to excess soil moisture evaporation (Bozso et al., 2008) and runoff during rainy period (Bodner et al., 2015). Ultimately germination failure causes seed and household food insecurity (Mucioki et al., 2018). The same water deficit condition restricts the decision-making process of a farmer on reseeding by difficulties in practicality of accessing the field (e.g. a deficit of soil moisture does not allow a prompt re-seeding), economic reasons (the difference between the profit and cost with and without re-seeding), availability of working time (for a prompt intervention) and resource availability (e.g. seed availability, seeder) (Lamichhane et al., 2018). Hence, knowledge on dry sown crops' germination is essential to reduce germination failure under moisture deficit condition. Even though many investigations were made on the germination of various plant species in relation to environmental factors worldwide, only few literatures are available on the germination of field crops under controlled environment condition.

Addressing this knowledge gap in the germination of field crops under dry sowing, the investigation was carried out in three different locations representing three agro climatic zones of Tamil Nadu, India, which produce variety of crops from the 5.36 M ha of rain-fed area from total cultivable area of 8.16 M ha (TN Govt., 2015). Crop failure is a common problem in the region due to poor germination and crop stand (TN Govt., 2015) due to prolonged dry spell. The total estimated value of food crop production losses alone was Rs. 2770 crore (79.7%) from 8.68 lakh hectare. Hence, it is essential to overcome the crop failure by developing effective technologies. As part of this objective, this extensive study was made on the germination rate of different dry crops to access the possibility of maximum germination between the dry land crops to ensure the optimum crop stand by better germination immediately after sowing. The test crops were selected from the major pulses, oil seeds and fiber crops cultivated in the study zones (*Fig. 1*) (Western Zone, North Western Zone and North Eastern Zone) of Northern Tamil Nadu. Groundnut and blackgram accounted for 75% of total area and the rest of the area (25%) was occupied by cotton, redgram, cowpea, greengram and sesame cultivation (*Fig. 2*). These crops were used as test crops and the germination was analyzed with the following objectives: i) To find out the crops having higher germination sown under dry condition ii) To understand the relationship between the germination and environmental factors in rain-fed ecosystem and iii) To study the interactions between the crop germination and different environments.

Materials and methods

Location

A field experiment was conducted across three different agro climatic zones of Tamil Nadu namely Western Zone, North Western Zone and North Eastern Zone to study the germination pattern of major dry crops under rain-fed ecosystems during the period of 2016-17 and 2017-18. In the western zone of Tamil Nadu, the experimental field of Eastern farm, Tamil Nadu Agricultural University is geographically situated at 11°0' North latitude and 76°9' East longitude at an altitude of 426.7 m above MSL (*Fig. 1*). In the North Western Agro-climatic Zone of Tamil Nadu, the experimental field of Regional Research Station, Paiyur is geographically located at 12°21' North latitude and 78°18' East longitude at an altitude of 490 m above MSL (*Fig. 1*). In the North Eastern Agro-climatic Zone, the

http://www.aloki.hu ● ISSN 1589 1623 (Print) ● ISSN 1785 0037 (Online)
DOI: http://dx.doi.org/10.15666/aeer/1902_12031220
© 2021, ALÖKI Kft., Budapest, Hungary

experimental field of Agricultural Research Station, Virinjipuram is situated at 12°.5' North latitude and 79°.0' East longitude at an altitude of 231 m above MSL (*Fig. 1*).

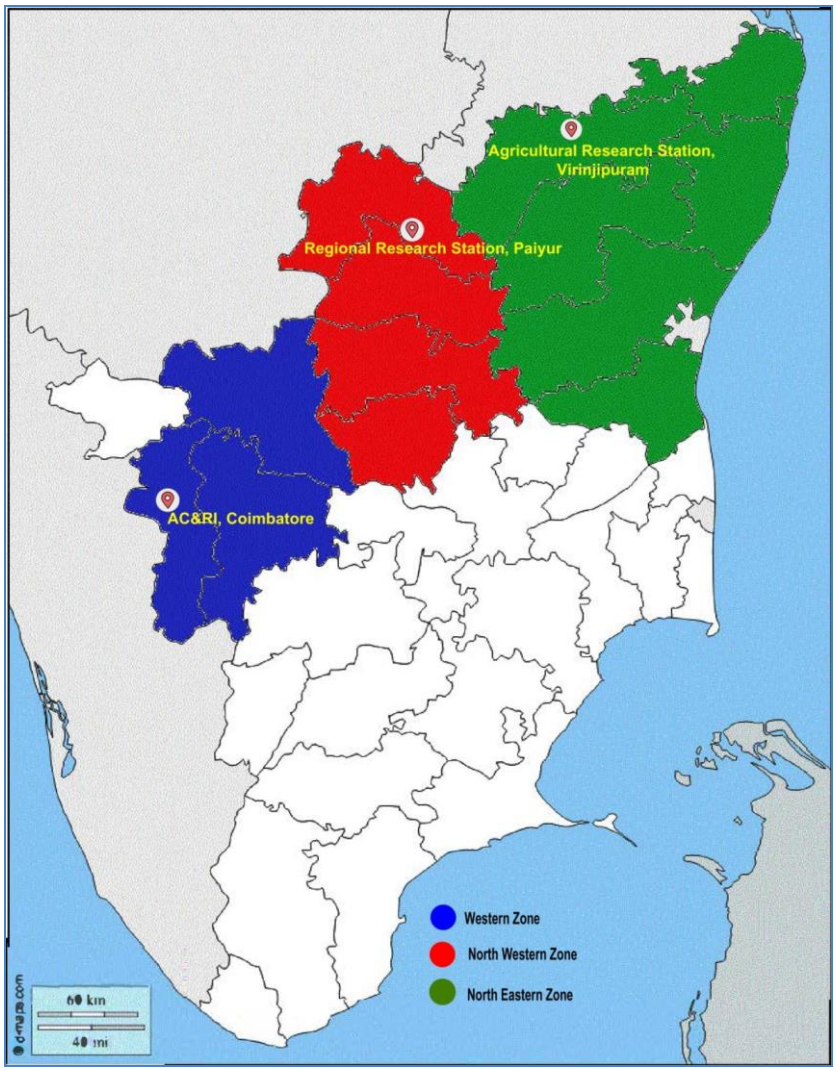


Figure 1. *Experimental locations zone wise in northern part of Tamil Nadu, India*

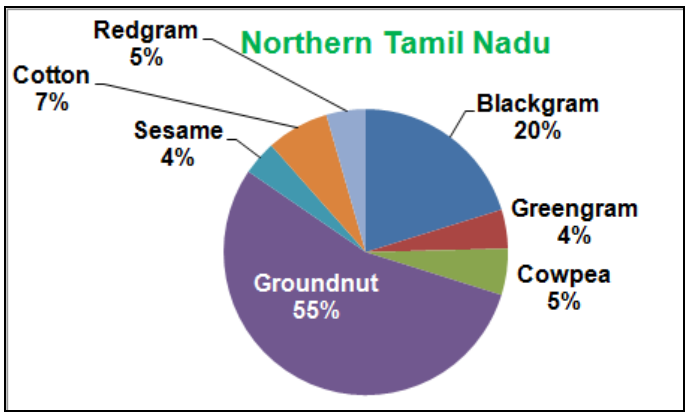


Figure 2. *Proportion of test crops cultivation area under rain-fed condition in the study zones of Northern Tamil Nadu, India*

http://www.aloki.hu ● ISSN 1589 1623 (Print) ● ISSN 1785 0037 (Online)
DOI: http://dx.doi.org/10.15666/aeer/1902_12031220
© 2021, ALÖKI Kft., Budapest, Hungary

Climate and soil

In all the three locations, five soil samples at 15 cm depth were collected at random in the experimental field before laying out the experiment during both year and the composite soil sample was obtained by quartering method and processed for analyzing physico-chemical characteristics of the soil. The soil characteristics are presented in *Table 1a*. The long-term average annual rainfall is 720.8 mm, 918 mm and 860 mm at Coimbatore, Paiyur and Virinjipuram, respectively. The weather condition of the different locations was observed and mean values of the first 10 days of sowing were summarized in the *Table 1b* and the rainfall details were given in *Figure 3*.

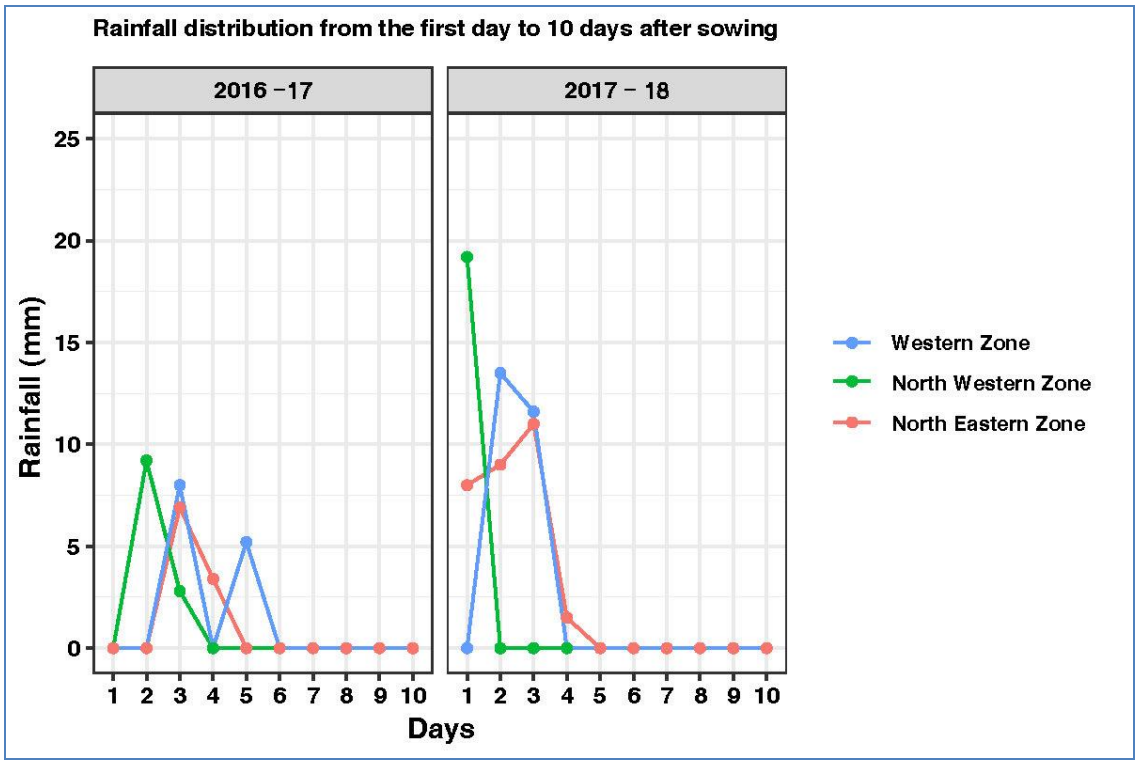


Figure 3. *Rainfall distribution from sowing to 10 days after sowing at experimental locations*

Table 1a. *Soil condition of experiment locations*

Soil characteristics	2016-17			2017-18		
	WZ	NWZ	NEZ	WZ	NWZ	NEZ
Soil nitrogen (kg/ha)	331	198	279	336	198	285
Soil phosphorus (kg/ha)	17.4	16.5	15.7	17.5	16.8	15.2
Soil potassium (kg/ha)	611	249	273	613	256	276
Soil organic matter (%)	0.38	0.32	0.41	0.38	0.32	0.41
Clay (%)	35.63	9.36	23.78	35.63	9.36	23.78
Silt (%)	9.95	24.25	13.65	9.95	24.25	13.65
Sand (%)	54.42	66.39	62.57	54.42	66.39	62.57
Soil pH	8.3	6.1	7.8	8.3	6.1	7.8
Soil EC (ds/m)	1.75	0.26	0.22	1.75	0.26	0.22

http://www.aloki.hu ● ISSN 1589 1623 (Print) ● ISSN 1785 0037 (Online)
DOI: http://dx.doi.org/10.15666/aeer/1902_12031220
© 2021, ALÖKI Kft., Budapest, Hungary

Table 1b. *Weather condition of experiment locations from the first receipt of rainfall to 10 days after sowing*

Weather parameters	2016-17			2017-18		
	WZ	NWZ	NEZ	WZ	NWZ	NEZ
Rainfall (mm)	13.2	12.0	10.3	25.1	19.2	29.5
Soil Moisture %	23.5	18.5	22.8	30.4	26.4	44.7
Maximum Temperature (°C)	31.7	32.71	33.12	31.31	31.06	32.01
Minimum Temperature (°C)	23.4	24.56	23.92	23.67	23.19	23.34
Relative humidity (%)	84.3	79.63	82.61	71.11	74.97	84.29
Wind speed (km/hr)	14.3	12.65	7.56	12.41	8.51	2.39
Solar radiation (cal/cm^2/day)	341.76	362.18	395.7	319.03	284.82	438.91

Crop and variety

The crops and varieties used for the experiment were blackgram (*Vigna mungo*) - Co (Coimbatore) 6, greengram (*Vigna radiata*) - Co (Coimbatore) 8, cowpea (*Vigna unguiculata*) -VBN (Vamban) 1, groundnut (*Arachis hypogaea*) - TMV (Tindivanam) 13), sesame (*Arachis hypogaea*) - TMV (Tindivanam) 7, cotton (*Gossypium hirsutum*) - Co (Coimbatore) 14 and redgram (*Cajanus cajan*) - CO (Rg) [Coimbatore (Redgram)] 7.

Methodology

An experiment was conducted with Randomized block design and replicated thrice. The seven different test crops (C_1: Blackgram, C_2: Greengram, C_3: Cowpea, C_4: Groundnut, C_5: Sesame, C_6: Cotton, C_7: Redgram) were randomly allotted in each replication.

The layout consisted of 21 experimental plots in three replications having 7 plots in each replication and different test crops were allocated randomly in each replication. Ridges and furrow were formed with the spacing of 45 cm for redgram and cotton, and 30 cm for blackgram, greengram, cowpea, groundnut and sesame. The gross plot size was 4.7 m × 2.3 m (10.81 m^2) and net plot size was 3.9 m × 1.5 m (5.85 m^2). Recommended quantity of seeds weighed and counted in Nos. and sown by dibbling method with recommended spacing. The spacing was adopted as 30 × 10 cm for blackgram, greengram, groundnut and sesame; 30×15 cm for cowpea; 45 × 15 for cotton and 45 × 30 for redgram. Likewise, sowing depth were 2 cm, 2 cm, 2.5 cm, 3 cm, 0.5 cm, 2 cm and 2 cm for blackgram, cowpea, groundnut, sesame, cotton and redgram respectively. The sowing was carried out before the onset of monsoon at each location. The recommended dose of fertilizer was applied to each treatment individually as per recommendation given in the crop production guide 2014 of TNAU. Germination of various crops individually accounted from the first receipt of rainfall after sowing to 10 DAS and germination percentage of crops were calculated for all three locations. The rainfall distribution from the date of sowing to 10 DAS are presented in *Figure 3*.

Soil moisture content was estimated from the date of sowing to 10 days after sowing by gravimetric method. For that samples were collected and oven dried at 105 °C for attaining a constant weight to account dry weight and *Equation 1* was used to calculate the soil moisture content and computed as average for the first 10 days of sowing and presented in *Table 1b*.

http://www.aloki.hu ● ISSN 1589 1623 (Print) ● ISSN 1785 0037 (Online)
DOI: http://dx.doi.org/10.15666/aeer/1902_12031220
© 2021, ALÖKI Kft., Budapest, Hungary

$$\text{Soil moisture}\,(\%) = \frac{\text{Fresh weight}\,(g) - \text{dry weight}\,(g)}{\text{Dry weight}\,(g)} \qquad \text{(Eq.1)}$$

Statistical analysis

The seed germination and soil moisture computed data was subjected to statistical scrutiny as per the procedure given by Gomez and Gomez (1984). The germination, soil and weather data collected from experiment locations were pooled and used for Pearson's correlation test and correlation coefficient value between 0.5 to 1 considered as strong correlation. The graphical representation done by language R, version 4.0.1 was used with package of corrplot (Taiyun and Viliam, 2017). To assess the germination stability over three different locations, AMMI biplot analysis was carried out with agricolae package version 1.4.0 (Menduburu and Yaseen, 2020) in R version 4.0.1.

Results

Germination percentage of dry sown crops at different agro climatic zones

In Western Zone, during 2016-17, the highest Germination Percentage (GP) was recorded in sesame (96.2%), followed by cotton and cowpea were accounted higher GP of 87.7 and 74 respectively. GP of cowpea was comparable with redgram (73.4%), blackgram (70.3%) and greengram (69.8%). The lowest GP was recorded in groundnut as 58.2 (*Table 2*). Similarly, during 2017-18, the same trend was observed; the sesame (S_5) recorded the highest GP of 96.5. Next to this, cotton (S_6) and cowpea (S_3) gave higher GP of 87.2 and 83.2 respectively and these were on par with each other. Greengram (S_2) was recorded 76.1% of germination and comparable with blackgram (75.1%). The lowest GP was observed in groundnut (S_4) as 66.8.

In North Western Zone, the highest germination (90%) was recorded in sesame, followed by greengram (86%), cotton (81.7%), blackgram (81.4%) and redgram (80.7%) during 2016-17. The cowpea and groundnut alone recorded lesser than 80% germination as 74.0% and the lowest of 71.9%, respectively (*Table 2*). For the duration of 2017-18, the highest germination was observed in greengram (95.3%) and it was comparable with cowpea (S_3), blackgram (S_1) and groundnut (S_4). The germination of cotton was comparable with groundnut. The lowest germination was recorded in sesame (S_5) as 68.3% (*Table 2*).

In 2016-17, the highest GP was recorded in sesame as 90.6%. Followed by cotton, redgram, cowpea, greengram, groundnut and blackgram in the case of which the recorded GP was of 82.3, 79.9, 79.5, 78.5, 78.1 and 76.4, respectively and these were comparable with each other (*Table 2*). During 2017-18, in the case of cowpea (S_3) a higher GP of 91.1 was recorded and this was comparable with the germination of groundnut (S_4), cotton (S_6), blackgram (S_1) and greengram (S_2). The lowest germination was observed in sesame (S_5) as 73.1% (*Table 2*).

Influence of weather and soil moisture on germination percentage of dry sown crops

The correlation test results between germination percentage and weather factors were presented in *Table 3*. The GP of blackgram, greengram, cowpea, groundnut, cotton and redgram exhibited strong positive correlation with soil moisture. Meanwhile, sesame exhibited negative non-significant correlation with soil moisture at germination stage.

http://www.aloki.hu ● ISSN 1589 1623 (Print) ● ISSN 1785 0037 (Online)
DOI: http://dx.doi.org/10.15666/aeer/1902_12031220
© 2021, ALÖKI Kft., Budapest, Hungary

Likewise, non-significant positive correlation was observed between rainfall and blackgram, greengram, cowpea, groundnut, cotton and redgram; and negative non-significant correlation was observed with sesame. The relationship between GP and temperature, relative humidity and solar radiation was non-significant. Wind speed exhibited strong positive correlation with germination of sesame and it was negative non-significant with blackgram, greengram, cowpea, groundnut, cotton and redgram (*Table 3*).

Table 2. *Germination percentage of rainfed dry sown crops at various agro climatic zones of Tamil Nadu*

Crop	2016-17			2017-18		
	WZ	NWZ	NEZ	WZ	NWZ	NEZ
BG	70.3±0.835 ^{de}	81.4±0.669 ^{cd}	76.4±1.185 ^{e}	75.1±1.513 ^{e}	94.3±0.781 ^{a}	90.3±0.754 ^{ab}
GG	69.8±0.722 ^{e}	86.1±0.941 ^{b}	78.5±1.216 ^{cd}	76.1±1.411 ^{e}	95.2±1.244 ^{a}	89.6±0.577 ^{ab}
CP	74.0±1.763 ^{c}	79.7±0.679 ^{d}	79.5±0.487 ^{cd}	83.2±2.316 ^{c}	95.2±0.700 ^{a}	91.2±1.676 ^{a}
GN	58.2±2.061 ^{f}	71.9±0.623 ^{e}	78.1±0.742 ^{d}	66.8±1.189 ^{f}	94.0±1.393 ^{a}	90.9±1.803 ^{a}
SM	96.2±0.024 ^{a}	90.0±0.699 ^{a}	90.6±1.011 ^{a}	96.6±0.769 ^{a}	68.3±1.519 ^{c}	73.1±1.732 ^{c}
CT	87.7±1.626 ^{b}	81.7±0.420 ^{c}	82.3±1.201 ^{b}	87.2±1.452 ^{b}	89.7±1.885 ^{b}	90.3±2.030 ^{a}
RG	73.4±1.258 ^{cd}	80.7±1.036 ^{cd}	79.9±0.801 ^{c}	79.8±1.302 ^{d}	88.4±1.192 ^{b}	86.6±1.272 ^{b}
SEd	2.2	2.6	2.8	2.7	2.1	2.4
CD (P=0.05)	4.3	5.2	5.7	5.6	4.4	4.8

Values presented in table are the mean of three replicates. Values fallowed by ± values are standard deviation of the germination and same lower-case letters are not significantly different among different crop germination percentage. BG – Blackgram; GG – Greengram; CP – Cowpea; GN – Groundnut; SM – Sesame; CT – Cotton; RG – Redgram

Table 3. *Correlation between the germination of dry sown crops with soil moisture and weather factors*

Crop	Soil moisture (%)	Rainfall (mm)	Temp. (°C)	RH (%)	Wind speed (km/hr)	Solar radiation (cal/cm2/day)
BG	0.63**	0.19 ^{NS}	-0.30 ^{NS}	-0.13 ^{NS}	-0.67 ^{NS}	0.005 ^{NS}
GG	0.55**	0.15 ^{NS}	-0.14 ^{NS}	-0.16 ^{NS}	-0.59 ^{NS}	-0.014 ^{NS}
CP	0.64*	0.27 ^{NS}	-0.49 ^{NS}	-0.32 ^{NS}	-0.64 ^{NS}	-0.103 ^{NS}
GN	0.55*	0.11 ^{NS}	-0.20 ^{NS}	-0.03 ^{NS}	-0.82 ^{NS}	0.156 ^{NS}
SM	-0.48 ^{NS}	-0.10 ^{NS}	0.39 ^{NS}	-0.02 ^{NS}	0.72**	-0.041 ^{NS}
CT	0.57**	0.29 ^{NS}	-0.78 ^{NS}	-0.08 ^{NS}	-0.31 ^{NS}	-0.123 ^{NS}
RG	0.66**	0.28 ^{NS}	-0.31 ^{NS}	-0.28 ^{NS}	-0.69 ^{NS}	0.005 ^{NS}

Correlation co-efficient 1% = 0.57, 5% = 0.43
*Significant at 5% level. **Significant at 1% level. NS: Non significant

Influence of soil factors on germination percentage of dry sown crops

The results of correlation between soil factors and germination percentage were presented in *Table 4*. Germination of sesame exhibited positive correlation with soil nutrients (Nitrogen, Phosphorus and Potassium), clay content, soil pH and Ec at initial stage of germination. Likewise, cotton also positively correlated with soil nutrients (Nitrogen, Phosphorus and Potassium), soil organic matter, clay content, soil pH and Ec. In other side, sesame and cotton exhibited non-significant negative correlation with silt and sand content of soil. Germination of blackgram, greengram, cowpea, groundnut and

http://www.aloki.hu ● ISSN 1589 1623 (Print) ● ISSN 1785 0037 (Online)
DOI: http://dx.doi.org/10.15666/aeer/1902_12031220
© 2021, ALÖKI Kft., Budapest, Hungary

redgram expressed non-significant negative correlation with soil nutrients (Nitrogen, Phosphorus and Potassium), soil organic matter, clay content, soil pH and Ec. Meanwhile, these crops expressed significant positive correlation with silt and sand content of soil.

Table 4. *Correlation between the germination of dry sown crops with soil factors*

Crop	Soil N	Soil P_2O_5	Soil K_2O	Soil OM	Clay	Silt	Sand	Soil pH	Soil EC (dS/m)
BG	-0.67 ^{NS}	-0.46 ^{NS}	-0.71 ^{NS}	.0.34 ^{NS}	-0.71 ^{NS}	0.65**	0.74**	-0.64 ^{NS}	-0.69 ^{NS}
GG	-0.79 ^{NS}	-0.46 ^{NS}	-0.79 ^{NS}	-0.45 ^{NS}	-0.82 ^{NS}	0.77**	0.84**	-0.75 ^{NS}	-0.76 ^{NS}
CP	-0.43 ^{NS}	-0.32 ^{NS}	-0.48 ^{NS}	-0.21 ^{NS}	-0.47 ^{NS}	0.42 ^{NS}	0.50*	-0.41^{NS}	-0.48^{NS}
GN	-0.57 ^{NS}	-0.63 ^{NS}	-0.77 ^{NS}	-0.10 ^{NS}	-0.62 ^{NS}	0.51*	0.72**	-0.49^{NS}	-0.78^{NS}
SM	0.58**	0.49*	0.67**	0.22 ^{NS}	0.61**	-0.54 ^{NS}	-0.67 ^{NS}	0.53*	0.66**
CT	0.19 ^{NS}	0.05 ^{NS}	0.18 ^{NS}	0.09 ^{NS}	0.18 ^{NS}	-0.16 ^{NS}	-0.18 ^{NS}	0.16 ^{NS}	0.16 ^{NS}
RG	-0.53 ^{NS}	-0.44 ^{NS}	-0.62 ^{NS}	-0.21 ^{NS}	-0.58 ^{NS}	0.51*	0.62**	-0.49 ^{NS}	-0.62 ^{NS}

Correlation co-efficient 1% = 0.57, 5% = 0.43
*Significant at 5% level. **Significant at 1% level. NS: Non significant

Stability of germination percentage across the different environments

From the AMMMI stability analysis, redgram (C_1) was considered to be stable over different environments and it was followed by cowpea (C_3), greengram (C_2) and blackgram (C_1). Though these crops are stable over environments, they are considered as least contributors for the crop × environment interactions. Cotton (C_6), Sesame (C_5) and Groundnut (C_4) were prognosticated to be unstable crops over environment, but they contributed most for the crop germination × environment interactions.

Among the Environments, E5 (NWZ, 2017-18) had the highest score on PC1 axis and higher mean germination, which is considered as more unstable environment. Whereas E2 (NWZ, 2016-17) and E3 (NEZ, 2016-17) had the lowest scores on PC1 axis and they are prognosticated to be more stable environments.

AMMI biplot PC1 vs PC2 shows the stability of environments and crops as well as crop × environment interactions. The crop redgram (C_7) is considered to be the stable crop over the environments. Environments E3 (NEZ, 2016-17) and E4 (WZ, 2017-18) gave stable performance for all the crops. The crop sesame (C_5) performed better in Environments E1 (WZ, 2016-17), E2 (NWZ, 2016-17), E3 (NEZ, 2016-17), E4 (WZ, 2017-18). Cotton (C6) has the highest overall mean among the crops and over the environments.

Discussion

Germination performance of test crops

Western zones

The increased GP of sesame and cotton (*Table 2*) was due to the sufficiency in mean available soil moisture (23.5%) up to 10 DAS from the first receipt of rainfall to imbibe the seeds through hydration and initiation of metabolic activity (Obroucheva, 2017). In this same moisture condition, GP of blackgram, greengram, cowpea, groundnut and redgram was reduced 27%, 27.4%, 23% and 23.7% respectively over the Germination Percentage of sesame (*Fig. 4*) during 2016-17 and the same trend was followed in 2017-18 (*Table 2*). This was due to the sensitivity of legume crops to the soil salt concentration by accumulating higher salt (Keating and Fisher, 1985) from the saline soil, which lead to reduced water uptake osmotically or imbalance in nutrient uptake

http://www.aloki.hu ● ISSN 1589 1623 (Print) ● ISSN 1785 0037 (Online)
DOI: http://dx.doi.org/10.15666/aeer/1902_12031220
© 2021, ALÖKI Kft., Budapest, Hungary

ionically and then affect the metabolic and enzyme activity during the germination process (Bewley et al., 2013). This was in line with the findings of Dash and Panda (2001), who observed reduced germination of greengram, blackgram and cowpea in saline soils. Among the legume crops, cowpea performed relatively better germination; it might be due to the little higher tolerance to salinity by accumulating low salts (Keating and Fisher, 1985) than other legume crops. The lowest germination of groundnut was might be the reason of relatively higher sensitiveness to the soil salinity. This is in line with the findings of Shalhevet et al. (1969), who observed 50% reduced germination of groundnut in saline soil over control. In this saline condition, higher germination of sesame and cotton was representing the tolerance to salinity against other crops. This agreed with the findings of Eynard et al. (2005), who reported, semi tolerance of sesame and tolerance of cotton to soil salinity. Similarly, Yousif et al. (1972) reported that, sesame shows high tolerance to soil salinity at germination stage than in other growth and development stages. This tolerance may be the reason of osmotic adjustment by accumulation of compatible solutes and regulatory mechanism for ion transport (Ashraf and Harris, 2004).

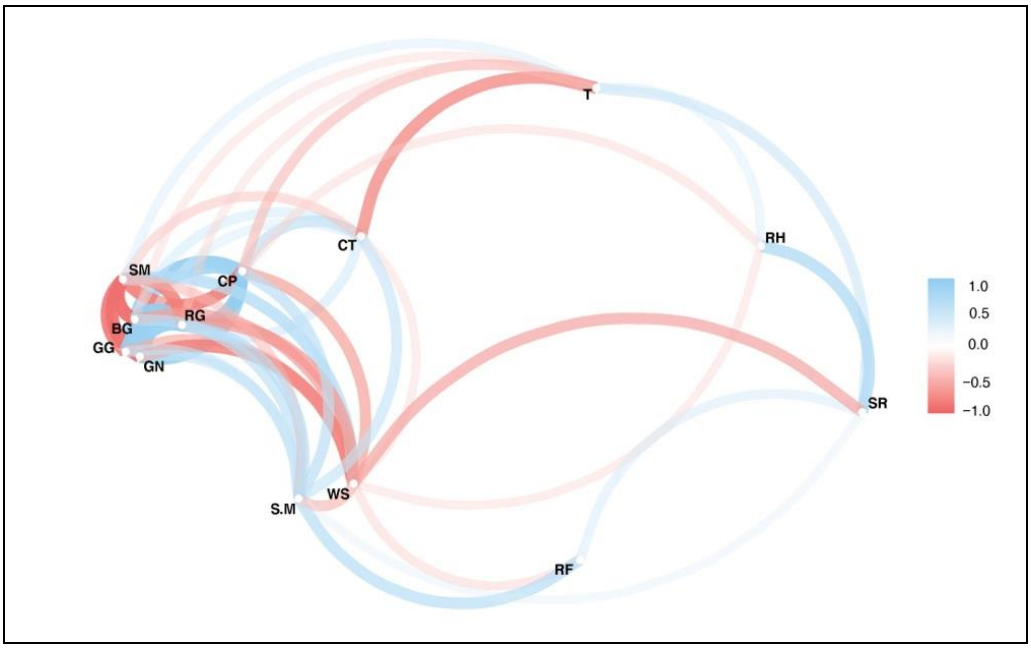


Figure 4. *Correlation network between the germination percentage of test crops and climatic factors. BG: Blackgram; GG: Greengram; CP: Cowpea; GN: Groundnut; SM: Sesame; CT: Cotton; RG: Redgram; S.M: Soil Moisture (%);RF: Rainfall (mm); T: Temperature (°C); RH:Relative humidity (%); WS: Wind speed (km/hr); SR: Solar radiation (cal/cm^2/day)*

North western zones

During 2016-17, increased germination of sesame (*Table 2*) with mean soil moisture of 18.5% shows its ability to germinate under scarce soil moisture condition due to the quick imbibitions by lower water need of small size seeds (Wu and Du, 2007) to initiate the metabolic activities of germination. These results agree with the findings of Kaya (2008), who reported that small seeds show lower water uptake than bold seeds in chickpea. The poor germination of cowpea and groundnut (*Table 2*) was due to

http://www.aloki.hu ● ISSN 1589 1623 (Print) ● ISSN 1785 0037 (Online)
DOI: http://dx.doi.org/10.15666/aeer/1902_12031220
© 2021, ALÖKI Kft., Budapest, Hungary

insufficient soil moisture to imbibe the seeds, since bold seeds can uptake more water for germination over small seeds (Kaya et al., 2008). In contradiction, Gómez (2004) reported as bold seeds have more germination rate compared to small seeds due to its more reserve. But, it is decided by ecological external factors such as rainfall, soil moisture, temperature etc., (Parker et al., 2006).

Like seed size, depth of sowing also might be contributed to significant difference between the crops GP (Amini et al., 2015). Shallow sowing of sesame seeds (1.5 cm) might be the reason for increased germination (Florentine et al., 2016) due to effectiveness of soil moisture and other physical properties of soil (Xu et al., 2017). The increased sowing depth of cowpea and groundnut reduced the germination over other crops under dry sowing condition due to restriction for soil moisture availability to imbibe the seeds (Dinelli et al., 2013). This is against the findings of Schillinger et al. (2017), who reported sowing at greater depth is generally practiced to reach adequate soil moisture for germination. But, this concept may vary in different ecological condition (Lamichhane et al., 2018) like rainfed agro ecosystems, where dry seeding is practiced before the onset of monsoon. If, rainfall is not sufficient to moist the sowing depth of any crops will lead to germination failure by partial imbibitions due to soil moisture deficit.

During, 2017-18 the highest germination was observed in greengram and it was comparable with cowpea (S_3), blackgram (S_1) and groundnut (S_4) (*Table 2*). The increased germination of these crops might be the reason of increased mean soil moisture (26.4%) by higher rainfall than in the previous cropping season and boldness of these seeds might gave higher germination potential with sufficient moisture condition over small seeds (Erskine, 1996). In addition to this, native soil of red sandy loam contains less clay facilitating germination better by offering favorable environment (Prasad, 2017) to blackgram, greengram, cowpea and groundnut and the same decreased the germination of cotton. The lowest GP was observed in sesame (S_5) as 68.3 due to high intense rainfall (19.2 mm within 8 h) immediately after sowing, which dispersed the small sesame seeds by exerting long floating time (Sarneel, 2013) in beds and got run off due to shallow sowing of sesame seeds and soil characteristics (Tekiela and Barney, 2013) as poor clay content of native soil (high sand) may have reduced the stickiness of seeds and favored seed displacement.

North eastern zone

Similar to NWZ, germination of sesame was increased (*Table 2*) with soil moisture content of 22.8% with lower rainfall of 10.3 mm during 2016-17 and the next year (2017-18) germination decreased (*Table 2*) due to increased soil moisture of 44.7% by heavy rainfall (29.5 mm) over the first 3 days of sowing. This intense excessive rainfall might have dispersed the small sesame seeds (Sarneel, 2013) and water saturation reduced the germination due to reduced oxygen concentration (Tian and Arihara, 2003), which is necessary for respiration. Germination of redgram, greengram, cowpea, blackgram and groundnut was lesser (*Table 2*) than 80% due to insufficient moisture (22.8%) to imbibe the bold seeds (Dinelli et al., 2013) and higher sowing depth during 2016-17. Interestingly, except groundnut these GPs were lower than the germination observed with 15.5% soil moisture at NWZ during 2016-17. This was might be the negative effect of native soil pH (7.8) on seed germination biological systems (Basto et al., 2013). Next year GP increased in cowpea, groundnut, cotton, blackgram, greengram and redgram (*Table 2*) by more than 80% due to its greater germination potential under optimum soil moisture condition of 44.7% (Gomez, 2004).

http://www.aloki.hu ● ISSN 1589 1623 (Print) ● ISSN 1785 0037 (Online)
DOI: http://dx.doi.org/10.15666/aeer/1902_12031220
© 2021, ALÖKI Kft., Budapest, Hungary

Influence of weather and soil moisture on germination

Except sesame, all the crops showed significant positive correlation with soil moisture (*Fig. 4*) due to increased seed size, which required high soil moisture for imbibitions of the seed completely (Kaya et al., 2008) to activate the metabolic process of germination. Statistically, soil moisture alone caused significant positive influence on germination of blackgram, greengram, cowpea, groundnut, cotton and redgram (*Fig. 4*). This was in line with the findings of Bewley et al. (2013) who reported, decreasing soil moisture potential reduces water uptake for imbibitions and germination got reduced. It might be assumed that the failure of live seeds to germinate under insufficient moisture condition (Evans and Therington, 1990), which is not sufficient to species specific hydration level of seeds (Hadas and Stibbe, 1973).

Germination of these crops excluding sesame expressed negative relationship with temperature (Tang and Chen, 2017) and wind speed (*Fig. 4*) (Jacobson, 1998), which might be the reason of increased temperature and wind speed leads evaporation demand in atmosphere and subsequently reduced soil moisture (Rao, 2008). Similarly, Dove (2010) stated that, a warmer climate may increase evaporation and decrease soil moisture, which would negatively affect germination. Most of the research dealt with the relationship between germination and soil temperature and fewer reports are available on atmospheric temperature. The atmospheric temperature indirectly influences germination of seeds by altering the soil temperature, which can influence germination through initiating enzyme activities and promoting germination under optimum condition or inhibit the germination by above the optimum level (Mohamed et al., 1988) through the synthesis of hormones involved in seed germination (Xu et al., 2017).

Against to these results, correlation between germination of sesame and soil moisture percentage is non-significant and expressed negative correlation in the analysis (*Fig. 4*). This implies that, deficit soil moisture is not a limiting factor for sesame germination at all three environments, since it gave maximum germination with 18.5% soil moisture at NWZ. The negative relationship between sesame germination and soil moisture was due to the poor germination under increased soil moisture by oxygen deficit (Tian and Arihara, 2003). This was in line with findings of Fawusi and Agboola (1980), who reported reduced germination of millets with increased soil moisture percentage due to inhibition of seed respiration by limited oxygen. Likely, germination of sesame negatively correlated with rainfall and relative humidity. This was due to the positive relationship between the soil moisture and rainfall and reduced soil moisture loss by evaporation due to higher relative humidity (Salvucci, 2012). Sesame germination positively correlated with temperature and wind speed; negatively correlated with soil moisture, rainfall and relative humidity (*Fig. 4*), which might have increased wind speed and temperature, decreased the excess soil moisture by evaporation and saved the seed from stagnation and provided sufficient oxygen (Tian and Arihara, 2003). Influence of solar radiation was non-significant with GP of all the test crops.

Influence of soil factors on germination

From the results, except for sesame and cotton, all crops showed negative correlation with soil nitrogen, phosphorus, potassium, organic matter, clay content, soil pH and EC (*Fig. 5*). This was due to the sensitivity of legume crops to soil salinity (Mass and Hoffman, 1977) and high concentration of soil nutrients may have decreased the germination rate by reduced imbibitions (Durrant and Mash, 1989) due to the lower

http://www.aloki.hu ● ISSN 1589 1623 (Print) ● ISSN 1785 0037 (Online)
DOI: http://dx.doi.org/10.15666/aeer/1902_12031220
© 2021, ALÖKI Kft., Budapest, Hungary

water potential at soil portion around the seed (Hegarty, 1976). These findings agree with Luzuriaga et al. (2006), who reported, decreased germination under increased soil salinity, pH and soil nutrient concentration in various studies. Likewise, positive correlation was observed with soil silt and sand content (*Fig. 5*). Sand content expressed positive correlation with germination of blackgram, greengram, cowpea, groundnut and redgram (Jepsen et al., 2011). The sand and silt content might have helped to avoid water stagnation by providing better aeration and drainage facility, which helps the exchange of more oxygen (Benvenuti, 2003).

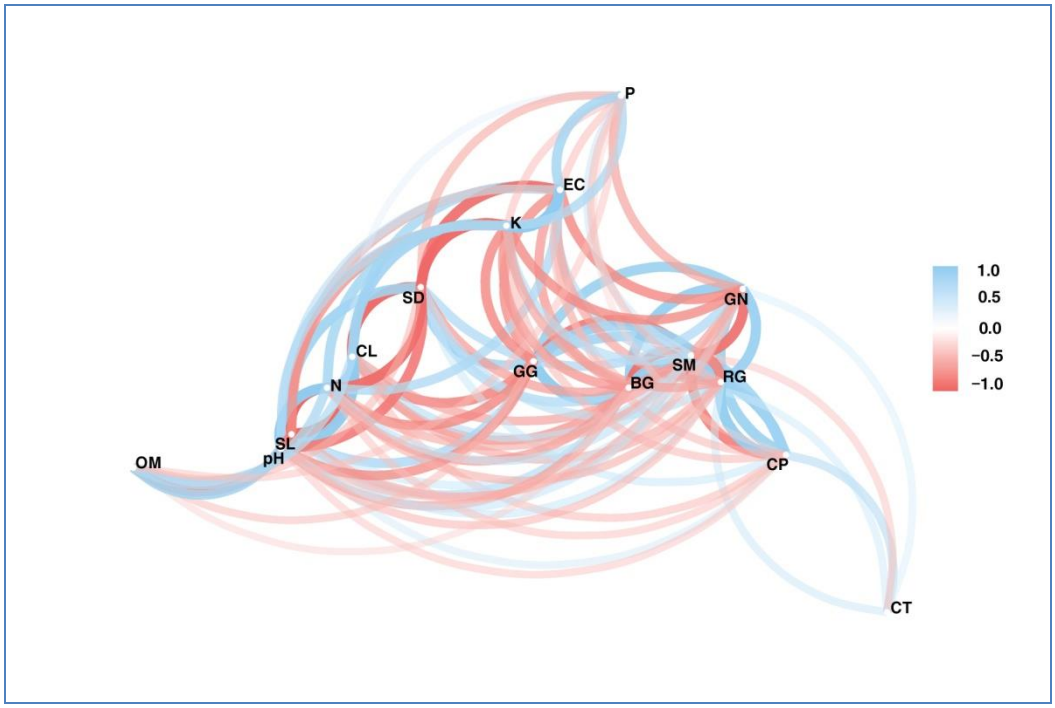


Figure 5. *Correlation network between the germination percentage of test crops and soil factors {BG: Blackgram; GG: Greengram; CP: Cowpea; GN: Groundnut; SM: Sesame; CT: Cotton; RG: Redgram; N: Soil Nitrogen (kg/ha); P: Soil Phosphorus (kg/ha); K: Soil Potassium (kg/ha); OM: Soil organic matter(%); CL: Clay (%); SL: Silt (%); SD: Sand (%); pH: Soil PH;EC: Soil Ec (dS/m)*

Sesame and cotton show positive relationship with soil nitrogen, phosphorus and potassium, soil organic matter, clay content, soil pH and EC (*Fig. 5*) due to the tolerance for high salt concentration (Eynar et al., 2012), on the other hand it shows negative correlation with silt and sand content, which easily allows the sesame seeds to disperse under high rainfall (Sarneel, 2013) and reduces the imbibitions of cotton seeds by quick water loss more than clay soil (Michael, 2008).

Stability of germination percentage across the different environments

Redgram (C_7) was considered to be stable over different environments and it was followed by cowpea (C_3), greengram (C_2) and blackgram (C_1). Though these crops are stable over environments, they are considered as least contributors for the Crop × Environment interactions (*Figs. 6* and *8*). Stability of redgram over different environment was due to the suitability with wide range of soil types without water stagnation and

http://www.aloki.hu ● ISSN 1589 1623 (Print) ● ISSN 1785 0037 (Online)
DOI: http://dx.doi.org/10.15666/aeer/1902_12031220
© 2021, ALÖKI Kft., Budapest, Hungary

moderate saline tolerance (Saxena, 2010). Likewise, redgram is a suitable crop for moisture stress environment due to large food reserve to survive under drought condition and also have in-built compensation mechanism for survival (Saxena, 2008).

Cotton (C_6), Sesame (C_5) and Groundnut (C_4) were prognosticated to be unstable crops over environment, but they contributed most for the Crop × Environment interactions (*Figs. 6* and *8*). This was due to the significant influence of environmental factors, such as soil texture and rainfall. Apart from the soil salinity, the fine soil texture (higher clay content) of WZ and NEZ recorded higher cotton germination over NWZ and increased rainfall significantly increased the germination of cotton (Sehgal, 1991). The increased rainfall immediately after sowing might be the reason for reduced germination of sesame due to lack of oxygen (Tian and Arihara, 2003) and seed dispersal (Sarneel, 2013) at the same time germination was increased under soil moisture deficit condition (Zech-Matterne et al., 2015). Similarly, Van Rheenen (1979) stated that, sesame grow on relatively dry, light and well drained soils and excessive rainfall may limit the sesame production. The higher interaction of groundnut germination with the environment was due to the positive impact of rainfall, soil moisture (Ramakrishna et al., 2006) and negative impact of increased soil clay content (Ayalew, 2015) and salt concentration (Shalhevet et al., 1969). Cotton (C_6), sesame (C_5) and cowpea (C_3) performed above the overall mean and are considered to adapt at all the environments and therefore, generalists based on the standard performance at all the locations.

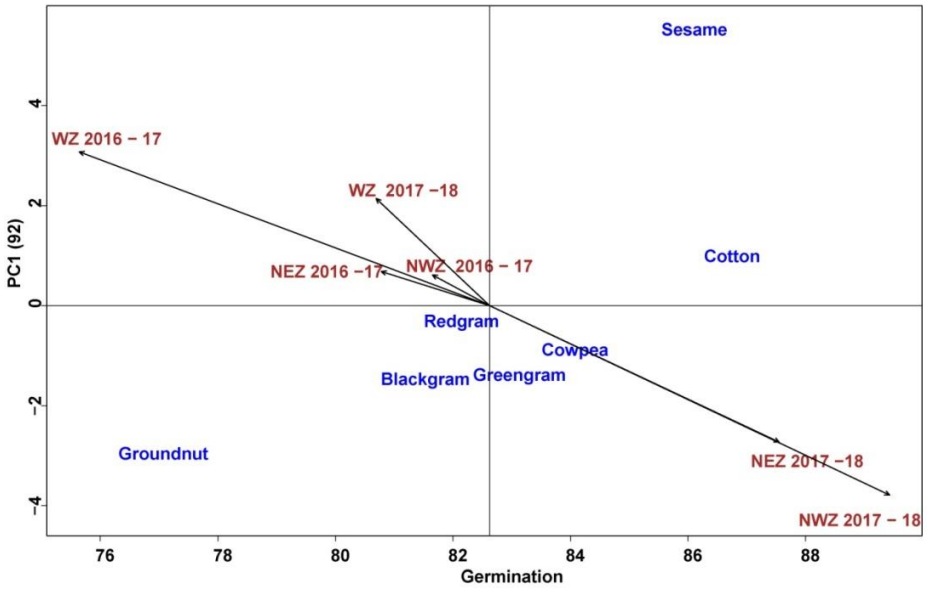


Figure 6. *AMMI biplot showing the main and interaction (PC1) effects of both crops and environments on germination percentage. An estimate of the Crop Environment interaction effect for a specific Crop–environment combination is the product of their corresponding interaction PC1 scores*

Among the Environments, E5 (NWZ, 2017-18) had the highest score on PC1 axis and higher mean germination which is considered as a more unstable environment (*Figs. 7* and 8). Because, intense rainfall of 19.2 mm within 8 h is not possible at all time. Whereas E2 (NWZ, 2016-17) and E3 (NEZ, 2016-17) had the lowest scores on PC1 axis and they are prognosticated to be more stable environments. AMMI biplot PC1 vs PC2

http://www.aloki.hu ● ISSN 1589 1623 (Print) ● ISSN 1785 0037 (Online)
DOI: http://dx.doi.org/10.15666/aeer/1902_12031220
© 2021, ALÖKI Kft., Budapest, Hungary

(*Fig. 7*) shows the stability of environments and crops as well as crop germination X Environment interactions. The crop redgram (C_7) is considered to be the stable crop over the environments. Environments E3 (NEZ, 2016-17) and E4 (WZ, 2017-18) gave stable performance for all the crops. The crop sesame (C_5) performed better in Environments E1 (WZ, 2016-17), E2 (NWZ, 2016-17), E3 (NEZ, 2016-17), and E4 (WZ, 2017-18). Cotton (C_6) has the highest overall mean among the crops and over the environments. So, it is considered as the crop which is adapted to all the environments.

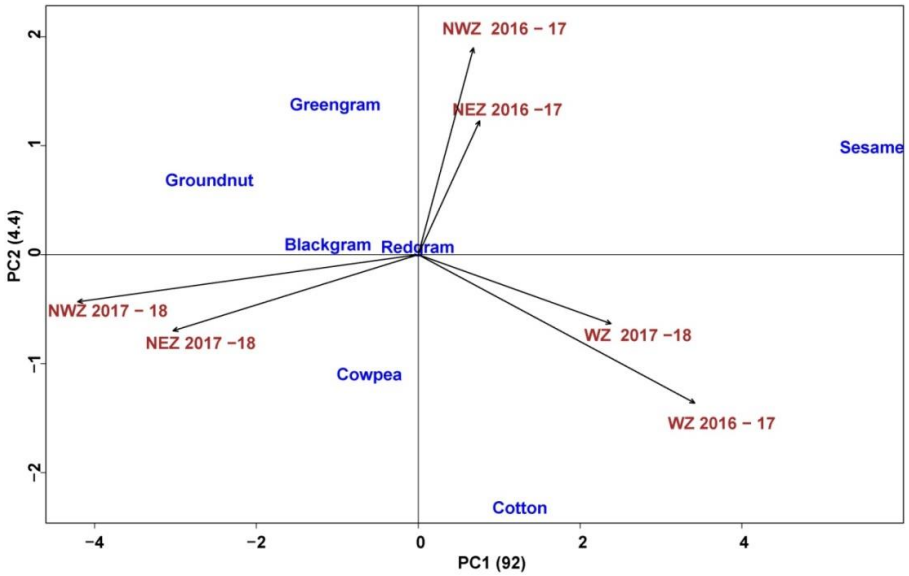


Figure 7. *AMMI biplot analysis showing the mega-environments and their respective crops with higher germination*

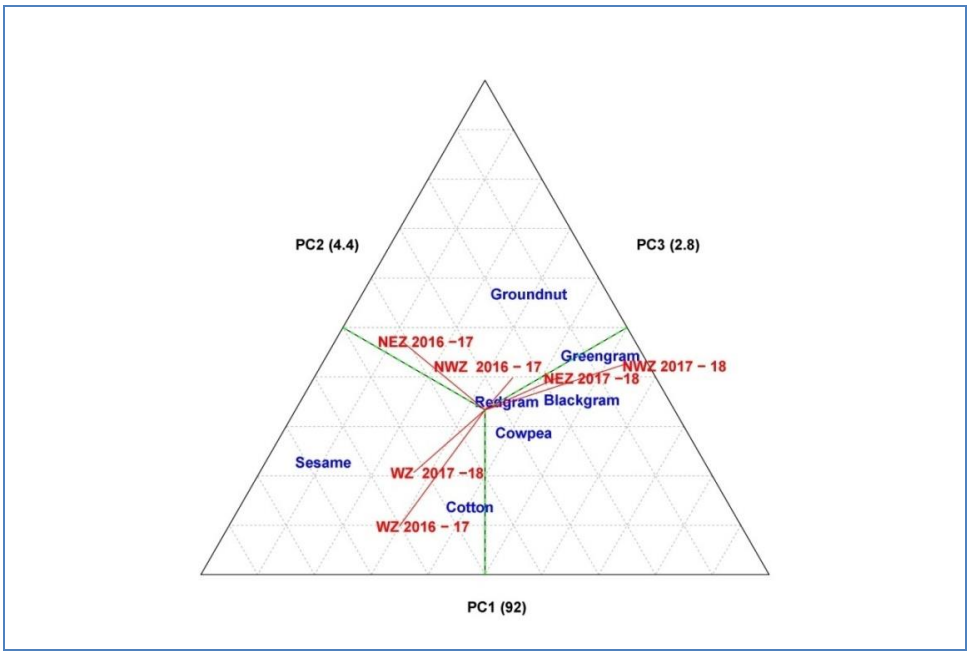


Figure 8. *AMMI 1 triplot for germination percentage of test crops and environments using crops and environmental scores*

http://www.aloki.hu ● ISSN 1589 1623 (Print) ● ISSN 1785 0037 (Online)
DOI: http://dx.doi.org/10.15666/aeer/1902_12031220
© 2021, ALÖKI Kft., Budapest, Hungary

Conclusion

From the results and detailed discussion, among the dry sown crops used to cultivate in Northern Tamil Nadu (India), sesame and cotton gave better germination under soil moisture deficit condition and saline soils compared to blackgram, greengram, cowpea and groundnut. These crops (blackgram, greengram, cowpea and groundnut) gave good germination under sufficient soil moisture and salinity free soil condition. Mean time excessive intensive rainfall reduced the germination of sesame under sandy soil condition not in the clay dominated soil. Soil contains higher nutrients (N, P and K), clay encouraged the germination of sesame and cotton, simultaneously reduced the germination of blackgram, greengram, cowpea and groundnut. Over different locations, sesame, cotton and cowpea gave mean higher germination. These crops responded positively to favourable soil and weather condition. Redgram, blackgram, greengram and groundnut gave stable response with poor interaction with environmental condition. Farmers of these zones (WZ, NWZ and NEZ) may be advised to include sesame, cotton and cowpea in cropping system as resilient crop in order to reduce the germination failure with optimum crop stand. These findings strongly recommend to carry out experiments with various field crops like cereals, millets to assess the germination under rainfed sowing. Likewise, investigation on germination of field crops in relation to days interval between rainfed sowing and first receipt of rainfall after sowing is highly needed to dry land farmers to take decision on selecting crops which can survive under aberrant rainfall condition. These findings may directly help farming community to select appropriate crops for dry seeding under rainfed condition.

Acknowledgments. Authors are thankful to former Director of Directorate of Crop Management, Tamil Nadu Agricultural University, who gave permission and helped technically to conduct this extensive study over different research stations situated in Tamil Nadu. Also, authors are grateful for the support given by faculties and farm workers of Regional Research Station, Paiyur; Agricultural Research Station, Virinjipuram and Department of Agronomy, TNAU, Coimbatore.

REFERENCES

[1] Amini, V., Zaefarian, F., Rezvani, M. (2015): Interspecific variations in seed germination and seedling emergence of three Setaria species. – Brazilian J of Bot 38(3): 539-45. https://doi.org/10.1007/s40415-015-0158-6.
[2] Ashraf, M. P., Harris, P. J. (2004): Potential biochemical indicators of salinity tolerance in plants. – Plant Sci 166(1): 3-16. https://doi.org/10.1016/j.plantsci.2003.10.024.
[3] Ayalew, G. (2015): A geographic information system based physical land suitability evaluation to groundnut and sweet potato in east Amhara, Highlands of Ethiopia. – J of Biol, Agri and Healthcare 5(1).
[4] Basto, S., Dorca-Fornell, C., Thompson, K., Rees, M. (2013): Effect of pH buffer solutions on seed germination of Hypericum pulchrum, Campanula rotundifolia and Scabiosa columbaria. – Seed Sci and Tech 41(2): 298-302. https://doi.org/10.15258/sst.2013.41.2.12.
[5] Benvenuti, S. (2003): Soil texture involvement in germination and emergence of buried weed seeds. – Agron J 95(1): 191-198. https://doi.org/10.2134/agronj2003.1910.
[6] Bewley, J. D., Bradford, K., Hilhorst, H., Nonogaki, H. (2013): Seeds: Physiology of Development, Germination and Dormancy. 3rd Ed. – Springer, New York.

http://www.aloki.hu ● ISSN 1589 1623 (Print) ● ISSN 1785 0037 (Online)
DOI: http://dx.doi.org/10.15666/aeer/1902_12031220
© 2021, ALÖKI Kft., Budapest, Hungary

[7] Bodner, G., Nakhforoosh, A., Kaul, H. P. (2015): Management of crop water under drought: a review. – Agron Sustain Dev 35(2): 401-442. https://doi.org/10.1007/s13593-015-0283-4.
[8] Bozso, G., Pal-Molnar, E., Hetenyi, M. (2008): Relations of pH and mineral composition in salt-affected lacustrine profiles. – Cereal Res Commun 36: 1463-6. https://www.jstor.org/stable/90002991.
[9] Dash, M., Panda, S. K. (1988): Salt stress induced changes in growth and enzyme activities in germinating Phaseolus mungo seeds. – Biol Plantarum 44(4): 587-9. https://doi.org/10.1023/A: 1013750905746.
[10] Dinelli, G., Marotti, I., Catizone, P., Bosi, S., Tanveer, A., Abbas, R., Pavlovic, D. (2013): Germination ecology of Ambrosia artemisiifolia L. and Ambrosia trifida L. biotypes suspected of glyphosate resistance. – Open Life Sci 8(3): 286-96. https://doi.org/10.2478/s11535-013-0135-z.
[11] Dove, N. (2010): The Effect of Increasing Temperature on Germination of Native Plant Species in the North Woods Region. – University of Vermont, Burlington, VT.
[12] Durrant, M. J., Mash, S. J. (1989): Stimulation of sugarbeet hypocotyls extension with potassium nitrate. – Annals of App Biol 115: 367-374. https://doi.org/10.1111/j.1744-7348.1989.tb03395.x.
[13] Erskine, W. (1996): Seed-size effects on lentil (*Lens culinaris)* yield potential and adaption to temperature and rainfall in West Asia. – J Agric Sci (Camb.) 126: 335-341. https://doi.org/10.1017/S002185960007489X.
[14] Evans, C. E., Etherington, J. R. (1990): The effect of soil water potential on seed germination of some British plants. – New Phytol 115: 539-548. https://doi.org/10.1111/j.1469-8137.1990.tb00482.x.
[15] Eynard. A., Lal, R., Wiebe, K. (2005): Crop response in salt-affected soils. – J of Sust Agri 27(1): 5-50. https://doi.org/10.1300/J064v27n01_03.
[16] Fawusi, M. O., Agboola, A. A. (1980): Soil Moisture requirements for germination of sorghum, millet, tomato, and Celosia 1. – Agron J 72(2): 353-7. https://doi.org/10.2134/agronj1980.00021962007200020023x.
[17] Florentine, S. K., Weller, S., Graz, P. F. (2016): Influence of selected environmental factors on seed germination and seedling survival of the arid zone invasive species tobacco bush (Nicotiana glauca R. Graham). – The Rangeland J 38(4): 417-25. https://doi.org/10.1071/RJ16022.
[18] Gomez, J. M. (2004): Bigger is not always better: conflicting selective pressures on seed size in Quercus ilex. – Evolution 58(1): 71-80. https://doi.org/10.1111/j.0014-3820.2004.tb01574.x.
[19] Gomez, K. A., Gomez, A. A. (1984): Statistical Procedures for Agricultural Research. 2nd Ed. – John Wiley and Sons, New York.
[20] Hadas, A., Stibbe, E. (1973): Analysis of Water Uptake and Growth Patterns of Seedlings of Four Species Prior to Emergence. – In: Hadas, A. et al. (eds.) Physical Aspects of Soil Water and Salts in Ecosystems. Ecol. Stud. Vol. 4. Springer, Berlin, pp. 97-106. https://doi.org/10.1007/978-3-642-65523-4_11.
[21] Hegarty, T. W. (1976): Effects of fertilizer on the seedling emergence of vegetable crops. – J Sci Fd Agric 27: 962-968. https://doi.org/10.1002/jsfa.2740271014.
[22] Heikal, M. M., Shaddad, M. A., Ahmed, M. (1982): Effect of water stress and gibberellic acid on germination of flax, sesame and onion seeds. – Biologia Plantarum 24(2): 124-9. https://doi.org/10.1007/BF02902858.
[23] Hooftman, D. A., Edwards, B., Bullock, J. M. (2016): Reductions in connectivity and habitat quality drive local extinctions in a plant diversity hotspot. – Ecography 39(6): 583-592. https://doi.org/10.1111/ecog.01503.
[24] Jacobson, M. Z. (1999): Effects of soil moisture on temperatures, winds, and pollutant concentrations in Los Angeles. – J App Meteorol 38(5): 607-616. https://doi.org/10.1175/1520-0450(1999)038<0607:EOSMOT>2.0.CO;2.

http://www.aloki.hu ● ISSN 1589 1623 (Print) ● ISSN 1785 0037 (Online)
DOI: http://dx.doi.org/10.15666/aeer/1902_12031220
© 2021, ALÖKI Kft., Budapest, Hungary

[25] Jepsen, J. K., Henning, R. R., Nyathi, B. (2006): Generative propagation of Jatropha curcas L. on Kalahari sand. – The Jatropha System. https://jatropha.pro/genarative-propagation-of-jatropha-curcas-l-on-kalahari-sand/.
[26] Kaya, M., Kaya, G., Kaya, M. D., Atak, M., Saglam, S. K., Khawar, M., Ciftci, C. Y. (2008): Interaction between seed size and NaCl on germination and early seedling growth of some Turkish cultivars of chickpea (Cicer arietinum L.). – J of Zhejiang Univ Sci B 9(5): 371. https://doi.org/10.1631/jzus.B0720268.
[27] Keating, B. A., Fisher, M. J. (1985): Comparative tolerance of tropical grain legumes to salinity. – Aust J Agric Res 36: 373-83. https://doi.org/10.1071/AR9850373.
[28] Lamichhane, J. R., Debaeke, P., Steinberg, C., You, M. P., Barbetti, M. J., Aubertot, J. N. (2018): Abiotic and biotic factors affecting crop seed germination and seedling emergence: a conceptual framework. – Plant and Soil 432(1-2): 1-28. https://doi.org/10.1007/s11104-018-3780-9.
[29] Luzuriaga, A. L., Escudero, A., Pérez-Garcia, F. (2006): Environmental maternal effects on seed morphology and germination in Sinapis arvensis (Cruciferae). – Weed Res 46: 163-174. https://doi.org/10.1111/j.1365-3180.2006.00496.x.
[30] Maas, E. V., Hoffman, G. J. (1977): Crop salt tolerance current assessment. – J. of the Irrigation and Drainage Division 103(2): 115-34.
[31] Mendiburu, F., Yaseen, M. (2020): Agricolae: Statistical Procedures for Agricultural Research. R Package Version 1.4.0. – https://myaseen208.github.io/agricolae/https://cran.r-project.org/package=agricolae.
[32] Michael, A. M. (2009): Irrigation: Theory and Practice, 2nd Edition. – Vikas Publishing House, Noida.
[33] Mohamed, H. A., Clark, J. A., Ong, C. K. (1988): Genotypic differences in the temperature responses of tropical crops: I. Germination characteristics of groundnut (Arachis hypogaea L.) and pearl millet (Pennisetum typhoides S. & H.). – J. of Exp Bot 39(8): 1121-8. https://doi.org/10.1093/jxb/39.8.1121.
[34] Mucioki, M., Pelletier, B., Johns, T., Muhammad, L. W., Hickey, G. M. (2018): On developing a scale to measure chronic household seed insecurity in semi-arid Kenya and the implications for food security policy. – Food Security 10(3): 571-87. https://doi.org/10.1007/s12571-018-0807-2.
[35] Obroucheva, N. V., Sinkevich, I. A., Lityagina, S. V., Novikova, G. V. (2017): Water relations in germinating seeds. – Russian J of Plant Physiol 64(4): 625-33. https://doi.org/10.1134/S102144371703013X.
[36] Parker, W. C., Noland, T. L., Morneault, A. E. (2006): The effects of seed mass on germination, seedling emergence, and early seedling growth of eastern white pine (Pinus strobus L.). – New Forests 32(1): 33-49. https://doi.org/10.1007/s11056-005-3391-1.
[37] Prasad, R. (2017): Text Book of Field Crop Production: Food Grain Crop. Vol. 1. – Indian Council of Agricultural Research, New Delhi. pp. 248-320.
[38] Ramakrishna, A., Tam, H. M., Wani, S. P., Long, T. D. (2006): Effect of mulch on soil temperature, moisture, weed infestation and yield of groundnut in northern Vietnam. – Field crops Res 95(2-3): 115-25. https://doi.org/10.1016/j.fcr.2005.01.030.
[39] Rao, P. (2008): Agricultural Meteorology. – PHI Learning, New Delhi.
[40] Salvucci, G. D., Gentine, P. (2013): Emergent relation between surface vapor conductance and relative humidity profiles yields evaporation rates from weather data. – Proceedings of the National Academy of Sciences 110(16): 6287-91. https://doi.org/10.1073/pnas.1215844110.
[41] Sarneel, J. M. (2013): The dispersal capacity of vegetative propagules of riparian fen species. – Hydrobiologia 710: 219-225. https://doi.org/10.1007/s10750-012-1022-3.
[42] Saxena, K. B. (2008): World's First CMS Pigeonpea Hybrid Commercialized. – ICRISAT, Patancheru.
[43] Saxena, K. B., Mula, M. G., Sugui, F. P., Layaoen, H. L., Domoguen, R. L., Pascua, M. E., Mula, R. P., Dar, W. D., Gowda, C. L. L., Kumar, R. V., et al. (2010): Pigeonpea: A

http://www.aloki.hu ● ISSN 1589 1623 (Print) ● ISSN 1785 0037 (Online)
DOI: http://dx.doi.org/10.15666/aeer/1902_12031220
© 2021, ALÖKI Kft., Budapest, Hungary

Resilient Crop for the Philippine Drylands. Information Bulletin No. 85. – International Crops Research Institute for the Semi-Arid Tropics, Patancheru.

[44] Schillinger, W. F., Schofstoll, S. E., Smith, T. A., Jacobsen, J. A. (2017): Laboratory method to evaluate wheat seedling emergence from deep planting depths. – Agron J 109: 2004-2010. https://doi.org/10.2134/agronj2016.12.0715.

[45] Sehgal, J. L. (1991): Soil-site suitability evaluation for cotton. – Agropedology 1: 49-63.

[46] Shalhevet, J., Reiniger, P., Shimshi, D. (1969): Peanut Response to Uniform and Non-niform Soil Salinity. – Agron J 61: 384-387. https://doi.org/ 10.2134/agronj1969.00021962006100030015x.

[47] Taiyun, W., Viliam, S. (2017): R package "corrplot": Visualization of a Correlation Matrix (Version 0.84). – https://github.com/taiyun/corrplot.

[48] Tang, C., Chen, D. (2017): Interaction between soil moisture and air temperature in the Mississippi River Basin. – J Water Resource Prot 9(10): 1119-1131. https://doi.org/10.4236/jwarp.2017.910073.

[49] Tekiela, D. R., Barney, J. N. (2013): Quantifying Microstegium vimineum seed movement by non-riparian water dispersal using an ultraviolet-marking based recapture method. – PLoS ONE 8(9): e63811. https://doi.org/10.1371/journal.pone.0063811.

[50] Tian, X., Joji, A. (2003): Response of sesame (Sesamum indicum L.) to low oxygen concentration during germination. – Plant Production Sci 6(2): 126-131. https://doi.org/10.1626/pps.6.126.

[51] TN Govt. (2015): Vision (2023), Government of Tamil Nadu. – http://www.spc.tn.gov.in/pdfs/TN_Vision_2023.pdf.

[52] Van Rheenen, H. A. (1979): Soil moisture and growth of sesame. – Plant and Soil 53(3): 277-85. https://doi.org/10.1007/BF02277862.

[53] Villalobos, F. J., Orgaz, F., Fereres, E. (2016): Sowing and Planting. – In: Villalobos, F. J., Fereres, E. (eds.) Principles of Agronomy for Sustainable Agriculture. Springer International Publishing, Cham, pp. 217-227.

[54] Wu, G., Du, G. (2007): Germination is related to seed mass in grasses (Poaceae) of the eastern Qinghai-Tibetan Plateau, China. – Nordic J of Bot 25(5-6): 361-5.

[55] Xu, H., Su, W., Di Zhang, L. S. (2017): Influence of environmental factors on Cucumis melo L. var. agrestis Naud. seed germination and seedling emergence. – PLoS ONE 12(6). https://doi.org/10.1016/j.fcr.2005.01.030.

[56] Yousif, Y. H., Bingham, F. T., Yermanos, D. M. (1972): Growth, mineral composition, and seed oil of sesame (Sesamum indicum L.) as affected by NaCl. – Soil Sci Soci of America J 36(3): 450-453. https://doi.org/10.2136/sssaj1972.03615995003600030025x.

[57] Zech-Matterne, V., Tengberg, M., Van Andringa, W. (2015): Sesamum indicum L.(sesame) in 2nd century BC Pompeii, Southwest Italy, and a review of early sesame finds in Asia and Europe. – Vegetation History and Archaeo Bot 24(6): 673-81. https://doi.org/10.1007/s00334-015-0521-3.

http://www.aloki.hu ● ISSN 1589 1623 (Print) ● ISSN 1785 0037 (Online)
DOI: http://dx.doi.org/10.15666/aeer/1902_12031220
© 2021, ALÖKI Kft., Budapest, Hungary

EFFECTS OF ERICOID MYCORRHIZAL FUNGI OR DARK SEPTATE ENDOPHYTIC FUNGI ON THE SECONDARY METABOLITE OF *RHODODENDRON PSEUDOCHRYSANTHUM* (*R. MORII*) SEEDLINGS

LIN, L.-C.[1*] – LIN, C.-Y.[2] – LIN, W.-R.[3] – TUNG, Y.-T.[4*] – WU, J.-H.[2*]

[1]*Department of Forestry and Natural Resources, National Chiayi University, Chiayi 600, Taiwan*
(phone: +886-5-271-7474; fax: +886-5-271-7467)

[2]*Department of Forestry, National Chung Hsing University, Taichung 402, Taiwan*

[3]*Bioresource Collection and Research Center (BCRC), Food Industry Research and Development Institute (FIRDI), Hsinchu 300, Taiwan*

[4]*Graduate Institute of Metabolism and Obesity Sciences, Taipei Medical University, Taipei 110, Taiwan*

[*]*Corresponding authors*
e-mail: linerm@mail.ncyu.edu.tw; f91625059@tmu.edu.tw; eric@nchu.edu.tw

(Received 12th Oct 2020; accepted 21st Dec 2020)

Abstract. We investigated the effects of ericoid mycorrhizal fungi (ERMFs) or dark septate endophytic fungi (DSEFs) on secondary metabolite production and growth promotion of *Rhododendron pseudochrysanthum*. The strains Rf9 (*Cryptosporiopsis* sp.) and Rf32 (*Cryptosporiopsis* sp.) were isolated from *Rhododendron formosanum*, whereas strains Rp7 *(Phialocephala fortinii*), Rp9 (Hyaloscyphaceae sp.), and Rp28 *(Phialocephala fortinii*) were isolated from *R. pseudochrysanthum* (*R. morii*). We studied their molecular relationships using phylogenetic analysis and divided these five strains into three groups (*Cryptosporiopsis* sp., *Phialocephala fortinii*, and Hyaloscyphaceae sp.). We found that strains Rf9 and Rf32 belonged to ERMFs, which form a hyphal complex with *R. pseudochrysanthum*, whereas strains Rp7, Rp9, and Rp28 belonged to DSEFs, which form microsclerotia on *R. pseudochrysanthum*. The endophytic fungi can promote the growth of *R. pseudochrysanthum* seedlings, and the total fresh weight of inoculated seedlings was higher than that of the control seedlings. In addition, the phytochemical profile showed that the methanolic extract of Rp7-inoculated seedlings had the highest content of rutin, hyperoside, quercitrin, and (2*R*,3*S*)-catechin among all inoculated seedlings. In conclusion, DSEFs and ERMFs promoted the growth response and secondary metabolite production of *R. pseudochrysanthum* seedlings.
Keywords: *ericoid mycorrhiza, dark septate endophyte, growth response, phytochemical, Rhododendron pseudochrysanthum*

Introduction

Rhododendron is a large genus of the family Ericaceae (Yang et al., 1999; Wu et al., 2003) with approximately 1,200 native *Rhododendron* species reported worldwide (Chamberlain et al., 1996). Both low and high elevations in Taiwan show a wide distribution of *Rhododendron*, and 15 indigenous species have been identified (Tseng and Lu, 2003), with most of their leaf extracts exhibiting excellent antioxidant activities (Lin et al., 2014a). Mycorrhizae are root associations synthesized between plants and fungi; 98% of all plant species have symbiotic fungal partners associated with their root systems (Bonfante and Genre, 2010). Mycorrhizal associations present in various forms are ubiquitous in nature and play crucial roles in plant nutrition and nutrient cycling. They

http://www.aloki.hu ● ISSN 1589 1623 (Print) ● ISSN 1785 0037 (Online)
DOI: http://dx.doi.org/10.15666/aeer/1902_12211232
© 2021, ALÖKI Kft., Budapest, Hungary

also influence the structure and dynamics of the plant communities within which they exist (Cairney and Meharg, 2003). The species of the family Ericaceae can form ericoid mycorrhizae (ERM) with ericoid mycorrhizal fungi (ERMFs) (Davies et al., 2003), which help their host plants gain more nutrients under stressful conditions (Schmid et al., 1995; Rice and Currah, 2001; Piercey et al., 2002; Lin et al., 2011). Therefore, ERM improves the host plants' competitiveness at the ecosystem level (Michelsen et al., 1996). In addition, ericaceous plants are frequently associated with dark septate endophytic fungi (DSEFs), which are also beneficial to host plants to obtain nutrients (Jumpponen and Trappe, 1998).

Recent studies have demonstrated the ability of mycorrhizal fungi and DSEFs to enhance secondary metabolite contents of their host plants. For instance, arbuscular mycorrhizal fungi could increase the berberine content in *Phellodendron chinense* (Zhou and Fan, 2007); moreover, DSEF (EF-37) could promote the growth and increase flavonoid content in its host plant, *Saussurea involucrate* (Wu et al., 2010). *Rhododendron* species contain numerous antioxidative phenolic compounds that could be developed into pharmaceutical products (Qiang et al., 2011). Of 10 common indigenous *Rhododendron* species in Taiwan, *Rhododendron pseudochrysanthum* (*R. morii*) has demonstrated the most efficient antioxidant activities (Lin et al., 2014a). Although ERMFs and DSEFs promote growth, survival, and competition in *Rhododendron* species, no research has focused on the growth response and phytochemical profile of *Rhododendron* seedlings with ERMFs or DSEFs to the best of our knowledge. Therefore, we assessed the effect of five varieties of endophytic fungi (mycorrhiza or dark septate) on plant biomass and its ability to produce secondary metabolites of *R. pseudochrysanthum* in this study.

Material and Methods

Seeds

R. pseudochrysanthum seeds were collected from the Alishan Forest Recreation Area in Chiayi City, Taiwan (longitude, 120°48′3″E; latitude, 23°31′10″N; altitude, 2,189 m). The seeds were obtained from the capsule of *R. pseudochrysanthum*. The average fresh weight of per hundred seeds was 27.3 ± 1.8 mg.

Endophytic fungi

We used five strains of endophytic fungi in this study: Strains Rf9 and Rf32 are ericoid mycorrhizal fungi, capable of forming ericoid mycorrhiza with Formosan rhododendron (Lin et al., 2011), and strains Rp7, Rp9, and Rp28 from *R. pseudochrysanthum* (Lin et al., 2014b). For inoculation, these five strains were transferred to 2% malt extract agar (2% MEA: malt extract, 20 g/L; agar, 15 g/L) plates and incubated in growth chambers at 23°C after 21 days.

DNA extraction, sequencing and phylogenetic analysis

Total DNA was extracted from the mycelium using the cetyl trimethyl ammonium bromide (CTAB) method (Doyle and Doyle, 1990). The rDNA ITS region was amplified with the primers V9G and LR1 (Vilgalys and Hester, 1990; De Hoog and van den Ende, 1998). An ABI PRISM 3730 Genetic Analyzer (PE Applied Biosystems, Foster City, CA, USA) was used to directly sequence PCR products. Sequence data for the ITS regions

http://www.aloki.hu ● ISSN 1589 1623 (Print) ● ISSN 1785 0037 (Online)
DOI: http://dx.doi.org/10.15666/aeer/1902_12211232
© 2021, ALÖKI Kft., Budapest, Hungary

was compared with sequences deposited in NCBI GenBank by BLAST, using the default settings. We assigned names to the sequences according to the following criteria: (1) sequence identity of ≥98.0%; (2) ≥1.0% separations from the next closest species; (3) ≥95.0% sequence coverage for the matching sequence; and (4) matching sequence published in a peer-reviewed journal article or submitted by the culture collection centers (CLSI, 2008).

Pure resynthesis and growth responses

Pure resynthesis was performed using the method of Dalpé (Dalpé, 1986; Lin et al., 2011; Okane et al., 2012). with some modifications. After surface cleaning, *R. formosanum* seeds were sterilized in 30% hydrogen peroxide solution for 90 s, rinsed three times in sterilized distilled water, and then incubated in 9-cm petri dishes containing 1% water agar for germination. Germinated seedlings were transplanted to modified Mitchell and Read medium (NH_4Cl, 32 mg/L; $CaCl_2 \cdot 7H_2O$, 43.5 mg/L; $MgSO_4 \cdot 7H_2O$, 10 mg/L; KCl, 5.5 mg/L; $FeCl_3$, 3.75 mg/L; sucrose, 2 g/L; KH_2PO_4, 210 mg/L; pyridoxine, 100 μg/L; thiamine, 100 μg/L; agar, 10 g/L). When the germinated seedlings had two cotyledons, all aseptic seedlings were inoculated with Rf9, Rf32, Rp7, Rp9, and Rp28 strains, whereas no inoculated seedlings were used as the control. A growth chamber was used to grow all the seedlings (22 °C, 65% relative humidity, and 16 h of light with a maximum illumination of 5000 lux). The seedlings were carefully removed from their substrate after incubation for 12 months to measure the effects of all treatments on the growth performance of seedlings. Each treatment had four replicates, and the fresh weight was measured.

Morphology of root association

The roots of all treatments were sampled and cleaned with water (Upson et al., 2007). A stereomicroscope was used to observe root morphology (Usuki and Narisawa, 2005). The roots were cleaned in 10% KOH for 24 h, washed in dH_2O, acidified in 10% HCl for 1 h, and stained by transferring to 0.05% aniline blue (aniline blue, 0.25 g; dH_2O, 25 mL; lactic acid, 475 mL) for 1 h and then to the destaining solution (dH_2O, 25 mL; lactic acid, 475 mL) for 2 h. They were then mounted on microscope slides in lactoglycerol (lactic acid:glycerol:dH_2O = 14:1:1, v/v/v) (Hutton et al., 1994).

Extraction, isolation, and quantification

The extraction and isolation of secondary metabolites from *R. pseudochrysanthum* shoots were performed using our previously reported method (Lin et al., 2014a). Each fresh sample was chopped into small pieces, and secondary metabolites were extracted using methanol by soaking the samples two times for one week at room temperature (25 °C). The resulting methanolic extracts were decanted and filtered using Whatman No. 1 filter paper. After concentrating the filtrates in a rotary evaporator, they were lyophilized. The phytochemicals of each sample were quantified through high-performance liquid chromatography (HPLC) on a Jasco PU-2080 instrument (Tokyo, Japan) with a 250 mm length × 4.6 mm i.d. and a 5-μm Supelco RP-amide column (Bellefonte, PA, USA). The mobile phase consisted of solvents A and B comprising 100% MeOH and ultrapure water, respectively. The elution conditions were 0–10 min of 30–36% A followed by 10–50 min of 36–72% A, all at a flow rate of 0.75 mL/min, on a Jasco MD-2010 photodiode array detector (Tokyo, Japan) at a 280 nm

http://www.aloki.hu ● ISSN 1589 1623 (Print) ● ISSN 1785 0037 (Online)
DOI: http://dx.doi.org/10.15666/aeer/1902_12211232
© 2021, ALÖKI Kft., Budapest, Hungary

wavelength. In total, we isolated and identified six specific phytochemicals, namely, (2*R*,3*S*)-catechin, (2*R*,3*R*)-dihydromyricetin 3-*O*-*β*-L-arabinopyranoside, (2*R*,3*R*)-taxifolin 3-*O*-*β*-L-arabinopyranoside, rutin, hyperoside, and quercitrin (Lin et al., 2014a). In addition, standard stock solutions of compounds were prepared in methanol, filtered through Millipore filters (0.45 μm), and appropriately diluted to obtain the desired concentrations in the quantification range for preparing the calibration curve for quantifying these phytochemicals in *R. pseudochrysanthum* shoots. The calibration graphs were plotted after the linear regression of the peak areas versus concentrations.

Statistical analysis

All statistical analyses were performed using the software Statistical Package for the Social Science (SPSS 12.0) (Chicago, IL, USA) for Windows. The significance of difference was calculated using the Tukey's test, and statistical significance was set at $p < 0.05$.

Results and Discussion

Phylogenetic analysis

According to previous ecological studies of endophytic fungi, 90%–95% ITS sequence similarity is often used as a species boundary in fungi (Arnold et al., 2009; Okane et al., 2012). The query coverage and maximum identity of endophytes isolated from *Rhododendron* with their most closely related fungal ITS sequences in GenBank are presented in *Table 1*. In European rhododendrons roots had been demonstrated frequent interactions between ERMFs and dark septate endophytes (DSE) and a morphological continuum between ERM and DSE associations (Vohník and Albrechtová, 2011). Among the five endophytic fungi used in this study (*Fig. 1*), the strains Rp7 and Rp28 were isolated from *R. pseudochrysanthum* and closed to *Phialocephala fortinii*. *P. fortinii*, a DSEF (Lukešová et al., 2015), has been frequently isolated from ericaceous plants (Hambleton and Currah, 1997). In addition, the strain Rp9 was closed to Hyaloscyphaceae sp. with 97% ITS sequence similarity (*Table 1*). Rf9 and Rf32 were closely related to *Cryptosporiopsis* and *Pezicula*; however, *Cryptosporiopsis* species are anamorphs of ascomycetes in the genera *Pezicula* and *Neofabraea* (*Dermataceae*) (Sigler et al., 2005). Thus, both Rf9 and Rf32 were still closely related to *Cryptosporiopsis*.

Table 1. *Endophytes isolated from Rhododendron species in Taiwan*

Isolates	GenBank sequences			
	Blast results	Accession No.	Query coverage	Maximum identity
Rf9	*Cryptosporiopsis* sp.	JF519423	99%	94%
Rf32	*Cryptosporiopsis* sp.	JF519423	99%	94%
Rp7	*Phialocephala fortinii*	EU882733	99%	98%
Rp9	Hyaloscyphaceae sp.	AB986449	98%	97%
Rp28	*Phialocephala fortinii*	EU882733	99%	98%

GenBank accession number of the rDNA ITS sequence of the isolates used in this study and the query coverage and maximum identity with their most closely related fungal ITS sequences in GenBank are given

http://www.aloki.hu ● ISSN 1589 1623 (Print) ● ISSN 1785 0037 (Online)
DOI: http://dx.doi.org/10.15666/aeer/1902_12211232
© 2021, ALÖKI Kft., Budapest, Hungary

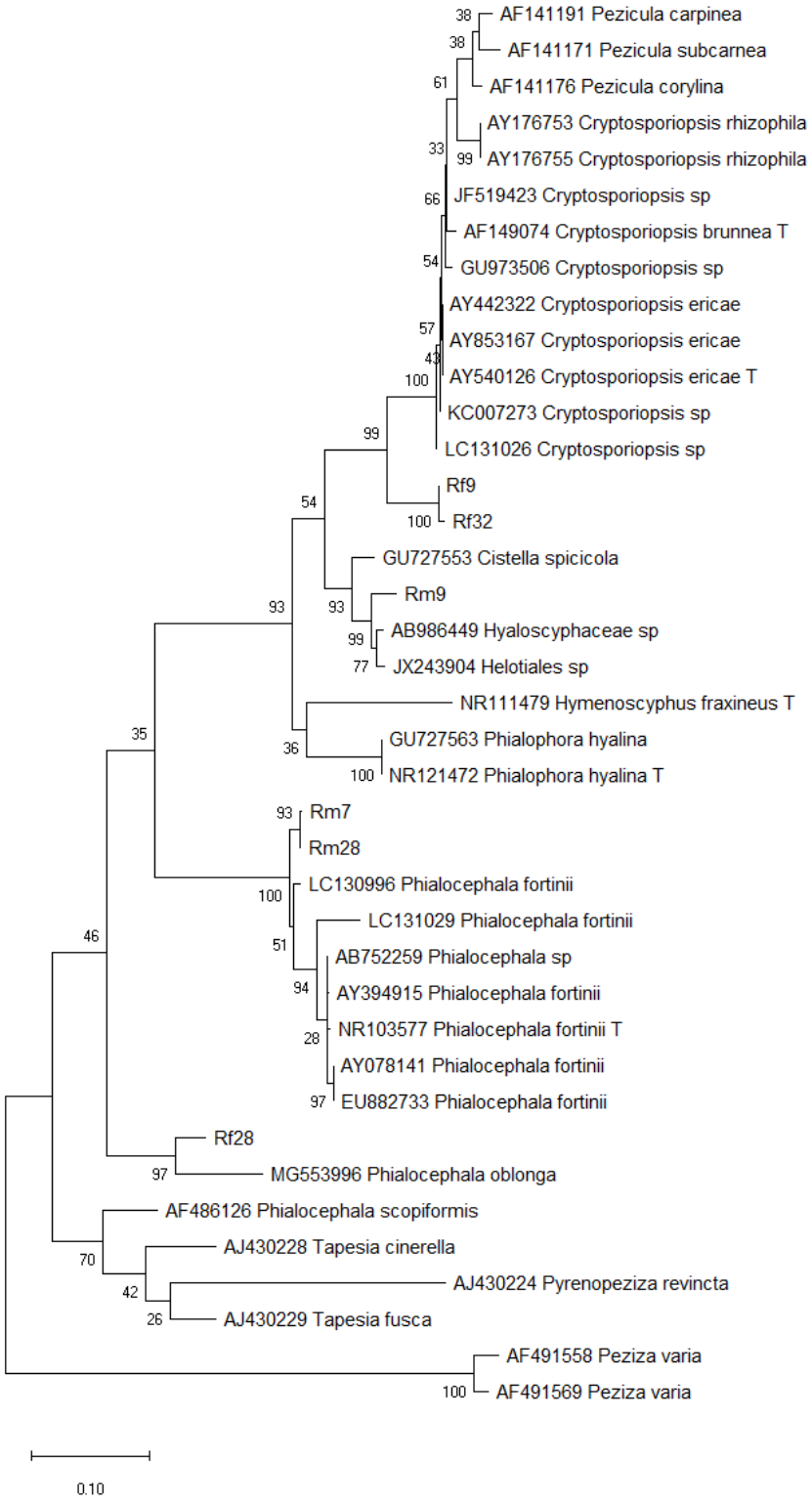


Figure 1. *Maximum likelihood phylogenetic tree based on internal transcribed spacer rDNA sequence data from these two endophytes, including fungal species from GenBank with high sequence similarities. T = sequence from Ex-type or type isolate. Isolates Rp7 and Rp28 clustered with Phialocephala fortinii with high bootstrap values (ML = 100%). Rp9 was identified as Hyaloscyphaceae sp.; isolates Rf9 and Rf32 were closely related to Cryptosporiopsis*

http://www.aloki.hu ● ISSN 1589 1623 (Print) ● ISSN 1785 0037 (Online)
DOI: http://dx.doi.org/10.15666/aeer/1902_12211232
© 2021, ALÖKI Kft., Budapest, Hungary

Morphology and colonization of R. pseudochrysanthum in resynthesized seedlings

Rhododendron seedlings are a slow-growing species and must have ERMFs to promote their growth (Lin et al., 2011, 2019, 2020; Okane et al., 2012; Wei et al., 2016, 2020). All resynthesized seedlings survived after 12 months of incubation (*Fig. 2*). The root-related features of all treatments were observed under light microscopy (*Fig. 3*). Seedlings inoculated with Rf9 and Rf32 grew well (*Fig. 2A,B*). Brown root associations were identified using stereomicroscopy (*Fig. 3A,C*), with specific ERMF characteristics of the hyphal complex observed in the stained roots (*Fig. 3B,D*). Similarly, *Fig. 2C–E* illustrates that Rp7-, Rp9-, and Rp28-inoculated seedlings also grew well; however, dark brown (*Fig. 3E*), light brown (*Fig. 3G*), and black root associations (*Fig. 3I*) were observed by stereomicroscopy. Moreover, specific DSEF characteristics of melanized (*Fig. 3F*), hyaline (*Fig. 3H*), and melanized and hyaline microsclerotia-like structures (*Fig. 3J*) were found in the stained roots of Rp7-, Rp9-, and Rp28-inoculated seedlings, respectively. The control seedlings were smaller than all those of the inoculated groups as expected (*Fig. 2F*), and light microscopy showed hyaline roots before (*Fig. 3K*) and after staining (*Fig. 3L*).

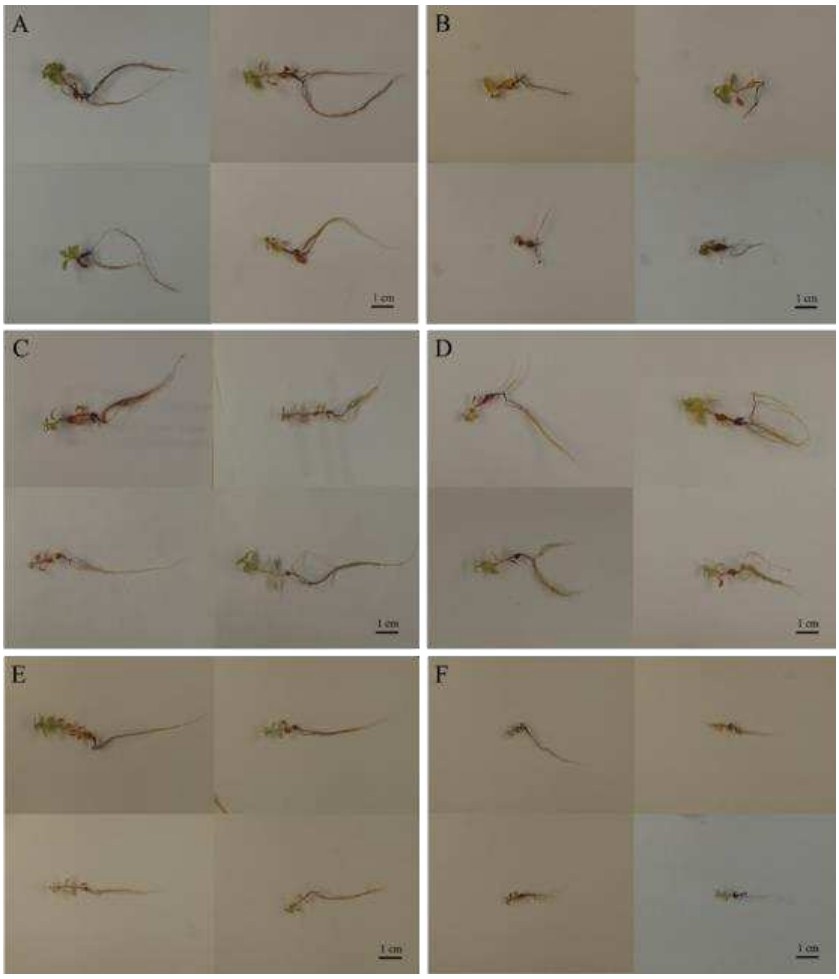


Figure 2. *Morphology of mycorrhizal synthesis of Rhododendron pseudochrysanthum seedlings after 12 months of incubation. A, Rf9-inoculation. B, Rf32-inoculation. C, Rp7-inoculation. D, Rp9 inoculation. E, Rp28-inoculation. F, control*

http://www.aloki.hu ● ISSN 1589 1623 (Print) ● ISSN 1785 0037 (Online)
DOI: http://dx.doi.org/10.15666/aeer/1902_12211232
© 2021, ALÖKI Kft., Budapest, Hungary

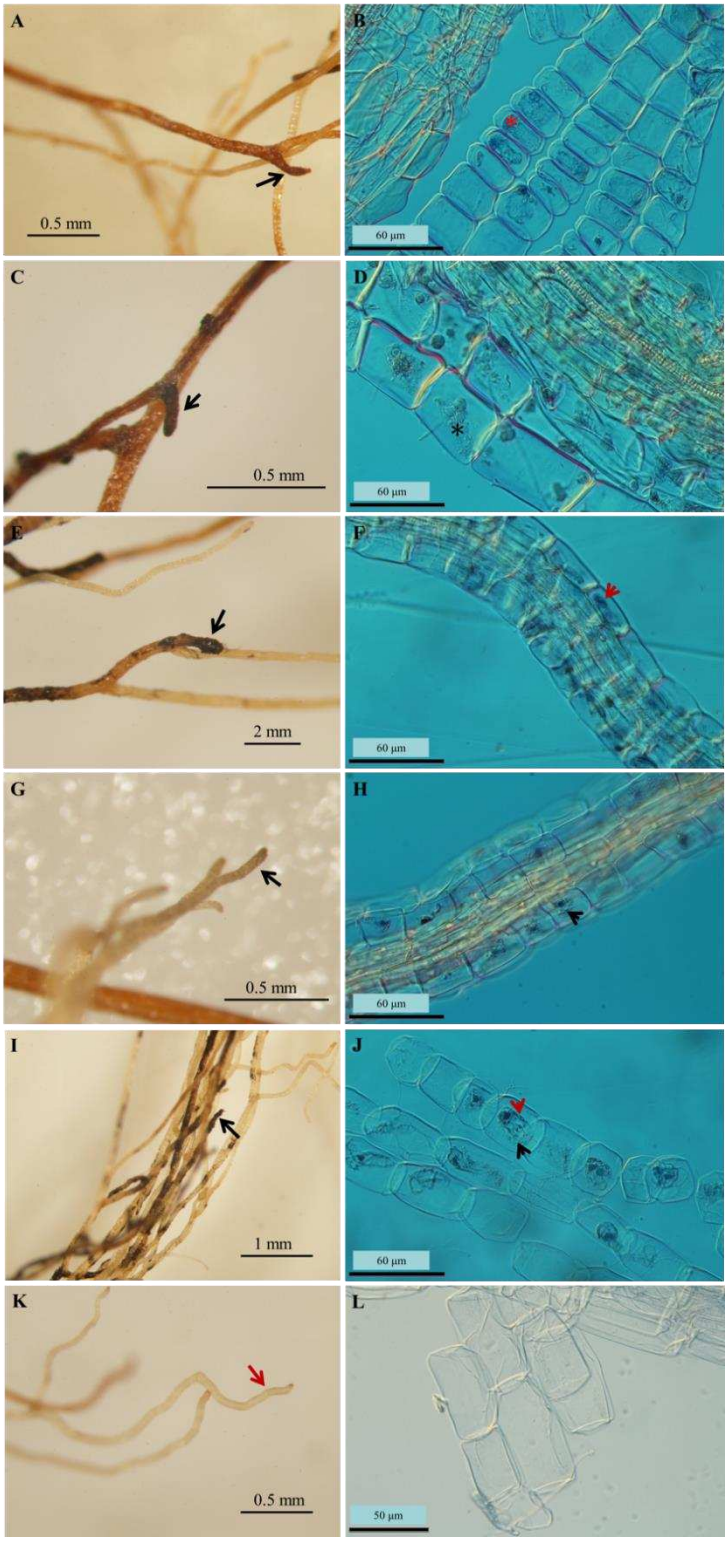


Figure 3. *Root association and stain of Rhododendron pseudochrysanthum seedlings after 12 months incubation. A and B, Rf9 inoculation. C and D, Rf32 inoculation. E and F, Rp7 inoculation. G and H, Rp9 inoculation. I and J, Rp28 inoculation. K and L, control. Red ✻: hyphae complex, black ✻: hyphae complex-like, red arrowhead: melanized microsclerotia-like, black arrowhead: hyaline microsclerotia-like, black arrow: root association, and red arrow: root*

http://www.aloki.hu ● ISSN 1589 1623 (Print) ● ISSN 1785 0037 (Online)
DOI: http://dx.doi.org/10.15666/aeer/1902_12211232
© 2021, ALÖKI Kft., Budapest, Hungary

Growth responses of R. pseudochrysanthum

The results of growth responses indicated that all treated seedlings showed a positive effect after incubation for 12 months as demonstrated in *Fig. 2*. The Rp9 inoculation had the highest average shoot fresh weight; this value then decreased in the following order: Rp28 inoculation > Rp7 inoculation > Rf9 inoculation > Rf32 inoculation > and control (*Table 2*). By contrast, after the 12-month incubation, the seedlings' average root fresh weight decreased in the following order: Rp28 inoculation > Rp7 inoculation > Rp9 inoculation > Rf9 inoculation > Rf32 inoculation > control. Moreover, the average total fresh weight of all inoculations was significantly greater than that of the control as given in *Table 2*.

Table 2. *Fresh weight of Rhododendron pseudochrysanthum seedlings with different treatments after 12-month incubation*

Treatment	Fresh weight (mg)			S/R
	Shoot	Root	Total	
Control	6.5 ± 0.5^{a}	2.0 ± 0.6^{a}	8.5 ± 1.0^{a}	4.2 ± 1.1^{ab}
Rf9	16.5 ± 1.2^{ab}	7.5 ± 2.4^{abc}	24.0 ± 3.4^{b}	2.9 ± 0.8^{ab}
Rf32	16.3 ± 2.5^{ab}	3.3 ± 0.8^{ab}	19.5 ± 3.2^{ab}	5.8 ± 1.1^{b}
Rp7	16.8 ± 3.8^{ab}	9.5 ± 1.4^{c}	26.3 ± 3.0^{b}	2.1 ± 0.8^{a}
Rp9	17.3 ± 2.1^{b}	9.3 ± 1.3^{bc}	26.5 ± 0.9^{b}	2.1 ± 0.4^{a}
Rp28	17.0 ± 2.3^{b}	10.0 ± 0.8^{c}	27.0 ± 1.8^{b}	1.8 ± 0.4^{a}

All values are means ± standard error (n = 4). Different superscript letters (a, b, c) within a column indicate significant difference at $p < 0.05$

The composition and content of secondary metabolites

As previously reported *Rhododendron* species are rich in antioxidative phytochemicals, especially flavonoids (Jung et al., 2007; Nirmala and Ramanathan, 2011; Qiang et al., 2011). *R. pseudochrysanthum* exhibits the best antioxidant activity of the 10 indigenous *Rhododendron* species in Taiwan. We isolated and identified the following six specific phytochemicals from wild-type *R. pseudochrysanthum* leaves in our previous study: (2*R*,3*S*)-catechin (1), (2*R*,3*R*)-dihydromyricetin 3-*O*-*β*-L-arabinopyranoside (2), (2*R*,3*R*)-taxifolin 3-*O*-*β*-L-arabinopyranoside (3), rutin (4), hyperoside (5), and quercitrin (6) (Lin et al., 2014a). However, the chemical compositions of these phytochemicals were different between all inoculated seedlings and the control as well as from each other after the 12-month incubation as shown in *Fig. 4*. Few weak signals were observed in the HPLC profile of the control group. The control seedlings only get basic nutrients and are less irritating to plants, so there are almost no secondary metabolites. All mycorrhizal seedlings of *R. pseudochrysanthum* exhibited stronger signals in HPLC profiles compared with the control seedlings, especially for the peaks of rutin, hyperoside, and quercitrin. Moreover, the Rf32 strain is good at promoting plant growth. But this is not conducive to promoting the secondary metabolites of plants. Therefore, the secondary metabolites of *R. pseudochrysanthum* seedlings are affected by mycorrhiza.

In addition, the phytochemical level of seedlings inoculated with DSEFs was higher than that of seedlings inoculated with ERMFs. The phytochemicals (2*R*,3*S*)-catechin and (2*R*,3*R*)-taxifolin 3-*O*-*β*-L-arabinopyranoside were only detected in Rp7-inoculated seedlings. Moreover, six quantitative analytes in various methanolic extracts of

http://www.aloki.hu ● ISSN 1589 1623 (Print) ● ISSN 1785 0037 (Online)
DOI: http://dx.doi.org/10.15666/aeer/1902_12211232
© 2021, ALÖKI Kft., Budapest, Hungary

R. pseudochrysanthum seedlings were determined through HPLC. Among all treatments, the extract of Rp7-inoculated seedlings exhibited the highest phytochemical content as shown in *Table 3*. The contents of (2*R*,3*S*)-catechin, rutin, hyperoside, and quercitrin were 27.2 ± 2.4, 136.5 ± 20.6, 23.6 ± 2.3, and 55.4 ± 6.5 μg per milligram of methanolic extract, respectively. By contrast, these phytochemicals were almost not detected in the control sample.

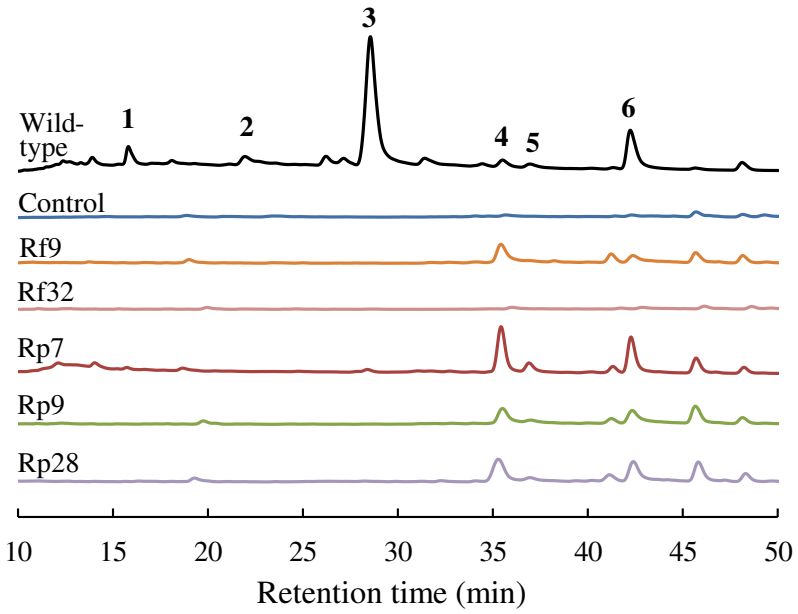


Figure 4. *HPLC profiles of methanolic extracts from Rhododendron pseudochrysanthum seedlings inoculated with different ericoid mycorrhizal fungi.* ***1****: (2R,3S)-catechin,* ***2****: (2R,3R)-dihydromyricetin 3-O-β-L-arabinopyranoside,* ***3****: (2R,3R)-taxifolin 3-O-β-L-arabinopyranoside,* ***4****: rutin,* ***5****: hyperoside, and* ***6****: quercitrin*

Table 3. *Contents of major phytochemicals from the methanolic extracts of Rhododendron pseudochrysanthum seedlings inoculated with various ericoid mycorrhizal fungi and dark septate endophytic fungi*

Treatment	Phytochemical content (μg/mg of methanolic extract)					
	1	**2**	**3**	**4**	**5**	**6**
Control	ND*	ND	ND	Trace	Trace	ND
Rf9	ND	ND	ND	53.3±11.5	Trace	19.0±3.2
Rf32	ND	ND	ND	Trace	Trace	Trace
Rp7	27.2±2.4	ND	Trace	136.5±20.6	23.6±2.3	55.4±6.5
Rp9	ND	ND	ND	51.2±11.7	14.2±1.4	31.1±5.8
Rp28	ND	ND	ND	44.8±10.9	11.8±1.9	26.1±3.6

Results area mean ± standard deviation (n = 3). *ND: Not detected

The ubiquitous mycorrhizal associations are essential for plant nutrition and nutrient cycling (Schmid et al., 1995; Cairney and Meharg, 2003; Gibson and Mitchell, 2005; Johansson, 2011; Lin et al., 2011). The five strains (Rf9, Rf32, Rp7, Rp9, and Rp28) used in this study were demonstrated to belong to Helotiales. Rf9 and Rf32 and Rp7, Pp9, and Rp28 were ERMFs and DSEFs, respectively. All of them demonstrated a significant

http://www.aloki.hu ● ISSN 1589 1623 (Print) ● ISSN 1785 0037 (Online)
DOI: http://dx.doi.org/10.15666/aeer/1902_12211232
© 2021, ALÖKI Kft., Budapest, Hungary

increase in fresh weight by 129%–212% compared with the control group. This result revealed that the growth of *R. pseudochrysanthum* seedlings could be improved by inoculation with all given DSEFs and ERMFs. These results are similar to those observed in *R. formosanum* (Lin et al., 2011), *R. ovatum* (Lin et al., 2019) and *R. Kanehirae* (Lin et al., 2020). Moreover, the Rf32-inoculated seedlings exhibited the highest value of shoot/root ratio (S/R; 5.8 ± 2.2), whereas Rp7-inoculated (2.1 ± 1.6) and Rp9-inoculated (2.1 ± 0.9) seedlings exhibited the smallest S/R among all treatments.

Similar to that of other researchers, our results also indicated that DSEFs and ERMFs remarkably affected the composition and content of the secondary metabolites of *R. pseudochrysanthum*. Previous reports demonstrated that mycorrhizal fungi, such as arbuscular mycorrhizae and DSEFs, not only promoted the growth of host plants (Johansson, 2001; Sigler et al., 2005; Lin et al., 2011) but also affected the content of secondary metabolites (Ponce et al., 2004; Zhou and Fan, 2007; Wu et al., 2010). Moreover, Martino et al. (2000) indicated that the different fungal strains had functional diversity. Similarly, the phytochemical content of host seedlings was also dependent on the fungal strains among the five endophytic fungi used in the present study. Considerable diversity was observed in the content of secondary metabolites of *R. pseudochrysanthum* seedlings inoculated with different strains of endophytic fungi.

Conclusion

Fungal strains Rf9 and Rf32 could form ERM with *Rhododendron pseudochrysanthum* and Rp7, Rp9, and Rp28 could form DSE with their host plants. Our study results showed that all of these inoculated seedlings showed a positive effect on growth response. In addition, the phytochemical composition and content of *R. pseudochrysanthum* was significantly influenced by these five stains. After the 12-month incubation, the DSEF Rp7 had the highest antioxidative phytochemical content in their host seedlings. Accordingly, the endophytic fungi used in our study, DSEF Rp7 had the best performance for promote the content of secondary metabolites of *R. pseudochrysanthum* seedlings.

REFERENCES

[1] Arnold, A. E., Miadlikowska, J., Higgins, K. L., Sarvate, S. D., Gugger, P., Way, A., Hosfstetter, V., Kauff, F., Lutzoni, F. (2009): A phylogenetic estimation of tropic transition networks for ascomycetous fungi: are lichens cradles of symbiotrophic fungal diversification? – Syst. Biol. 58: 283-297.

[2] Bonfante, P., Genre, A. (2010): Mechanisms underlying beneficial plant–fungus interactions in mycorrhizal symbiosis. – Nat. Commun. 1: 48.

[3] Cairney, J. W. G., Meharg, A. A. (2003): Ericoid mycorrhiza: a partnership that exploits harsh edaphic conditions. – Eur. J. Soil Sci. 54: 735-740.

[4] Chamberlain, D. F., Hyam, R., Argent, G., Fairweather, G., Walter, K. S. (1996): The genus *Rhododendron*: its classification and synonymy. – Royal Botanic Garden Edinburgh, Edinburgh.

[5] CLSI (2008): Interpretive criteria for identification of bacteria and fungi by DNA target sequencing; approved guideline. – Clinical and Laboratory Standards Institute, Wayne, PA.

[6] Dalpé, Y. (1986): Axenic synthesis of ericoid mycorrhiza in *Vaccinium angustifoliurn* Ait. by *Oidiodendron* species. – New Phytol. 103: 391-396.

http://www.aloki.hu ● ISSN 1589 1623 (Print) ● ISSN 1785 0037 (Online)
DOI: http://dx.doi.org/10.15666/aeer/1902_12211232
© 2021, ALÖKI Kft., Budapest, Hungary

[7] Davies, P. W., Mclean, C. B., Bell, T. L. (2003): Root survey and isolation of fungi from alpine epacrids (Ericaceae). – Australas. Mycol. 22(1): 4-10.
[8] De Hoog, G. S., van den Ende, A. H. G. G. (1998): Molecular diagnostics of clinical strains of filamentous basidiomycetes. – Mycoses 41(5-6): 183-189.
[9] Doyle, J. J., Doyle, J. L. (1990): Isolation of plant DNA from fresh tissue. – Focus 12: 13-15.
[10] Gibson, B. R., Mitchell, D. T. (2005): Influence of pH on copper and zinc sensitivity of ericoid mycobionts *in vitro*. – Mycorrhiza 15: 231-234.
[11] Hambleton, S., Currah, R. S. (1997): Fungal endophytes from the roots of alpine and boreal Ericaceae. – Can. J. Bot. 75: 1570-1581.
[12] Hutton, B. J., Dixon, K. W., Sivasithamparam, K. (1994): Ericoid endophytes of Western Australian heaths (Epacridaceae). – New Phytol. 127: 557-566.
[13] Johansson, M. (2001): Fungal associations of Danish *Calluna vulgaris* roots with special reference to ericoid mycorrhiza. – Plant Soil 231: 225-232.
[14] Jumpponen, A., Trappe, J. M. (1998): Dark septate endophytes, a review of facultative biotrophic root-colonizing fungi. – New Phytol. 140: 295-310.
[15] Jung, S. J., Kim, D. H., Hong, Y. H., Lee, J. H., Song, H. N., Rho, Y. D. (2007): Flavonoids from the flower of *Rhododendron yedoense* var. *poukhanense* and their antioxidant activities. – Arch. Pharm. Res. 30: 146-150.
[16] Lin, L. C., Lee, M. J., Chen, J. L. (2011): Decomposition of organic matter by the ericoid mycorrhizal endophytes of Formosan rhododendron (*Rhododendron formosanum* Hemsl.). – Mycorrhiza 21: 331-339.
[17] Lin, C. Y., Lin, L. C., Ho, S. T., Tung, Y. T., Tseng, Y. H., Wu, J. H. (2014a): Antioxidant activities and phytochemicals of leaf extracts from 10 native *Rhododendron* species in Taiwan. – Evid-Based Compl. Alt.
[18] Lin, L. C., Chang, L. H., Liao, I. K., Lee, T. M., Tseng, T. Y. (2014b): Morphology and endophytes of root-fungus association of *Rhododendron pseudochrysanthum* (*R. morii*) in Alishan area. – Taiwan J. Biodivers. 16(3): 253-262. [In Chinese].
[19] Lin, L. C., Ye, Y. S., Lin, W. R. (2019): Characteristics of root cultivable endophytic fungi from *Rhododendron ovatum* Planch. – Brazilian Journal of Microbiology 50: 185-193.
[20] Lin, L. C., Lin, W. R., Hsu, Y. C., Pan, H. Y. (2020): Influences of three *Oidiodendron maius* isolates and two inorganic nitrogen sources on the growth of *Rhododendron kanehirae*. – Hortic. Sci. Technol. 38(5): 742-753.
[21] Lukešová, T., Kohout, P., Větrovský, T., Vohník, M. (2015): The potential of dark septate endophytes to form root symbioses with ectomycorrhizal and ericoid mycorrhizal middle European forest plants. – PLoS One 10(4): e0124752.
[22] Martino, E., Turnau, K., Girlanda, M., Bonfante, P., Perotto, S. (2000): Ericoid mycorrhizal fungi from heavy metals polluted soils: their identification and growth in the presence of heavy metals. – Mycol. Res. 104: 338-344.
[23] Michelsen, A., Schmidt, I. K., Jonasson, S., Quarmby, C., Sleep, D. (1996): Leaf ^{15}N abundance of subarctic plants provides field evidence that ericoid, ectomycorrhizal and non- and arbuscular mycorrhizal species access different sources of soil nitrogen. – Oecologia 105: 53-63.
[24] Nirmala, P., Ramanathan, M. (2011): Effect of kaempferol on lipid peroxidation and antioxidant status in 1,2-dimethyl hydrazine induced colorectal carcinoma in rats. – Eur. J. Pharmacol. 654: 75-79.
[25] Okane, I., Srikitikulchai, P., Tabuchi, Y., Sivichai, S., Nakagirl, A. (2012): Recognition and characterization of four Thai xylariaceous fungi inhabiting various tropical foliages as endophytes by DNA sequences and host plant preference. – Mycoscience 53: 122-132.
[26] Piercey, M. M., Thormann, M. N., Currah, R. S. (2002): Saprobic characteristics of three fungal taxa from ericalean roots and their association with the roots of *Rhododendron groenlandicum* and *Picea mariana* in culture. – Mycorrhiza 12: 175-180.

http://www.aloki.hu ● ISSN 1589 1623 (Print) ● ISSN 1785 0037 (Online)
DOI: http://dx.doi.org/10.15666/aeer/1902_12211232
© 2021, ALÖKI Kft., Budapest, Hungary

[27] Ponce, M. A., Scervino, J. M., Erra-Balsells, R., Ocampo, J. A., Godeas, A. M. (2004): Flavonoids from shoots and roots of *Trifolium repens* (white clover) grown in presence or absence of the arbuscular mycorrhizal fungus *Glomus intraradices*. – Phytochemistry 65: 1925-1930.
[28] Qiang, Y., Zhou, B., Gao, K. (2011): Chemical constituents of plants from the genus *Rhododendron*. – Chem. Biodivers. 8(5): 792-815.
[29] Rice, A. V., Currah, R. S. (2001): Physiological and morphological variation in *Oidiodendron maius*. – Mycotaxon 79: 383-396.
[30] Schmid, E., Oberwinkler, F., Gomez, L. D. (1995): Light and electron microscopy of a host-fungus interaction in the roots of some epiphytic ferns from Costa Rica. – Can. J. Bot. 73: 991-996.
[31] Sigler, L., Allan, T., Lim, S. R., Berch, S., Berbee, M. (2005): Two new *Cryptosporiopsis* species from roots of ericaceous hosts in western North America. – Stud. Mycol. 53: 53-62.
[32] Tseng, Y. H., Lu, S. Y. (2003): Introduction of *Rhododendron* spp. in the field. – Nat. Conserv. Quart. 43: 18-30. [In Chinese].
[33] Upson, R., Read, D. J., Newsham, K. K. (2007): Widespread association between the ericoid mycorrhizal fungus *Rhizoscyphus ericae* and a leafy liverwort in the maritime and sub-Antarctic. – New Phytol. 176: 460-471.
[34] Usuki, F., Narisawa, K. (2005): Formation of structures resembling ericoid mycorrhizas by the root endophytic fungus *Heteroconium chaetospora* within roots of *Rhododendron obtusum* var. *kaempferi*. – Mycorrhiza 15: 61-64.
[35] Vilgalys, R., Hester, M. (1990): Rapid genetic identification and mapping of enzymatically amplified ribosomal DNA from several *Cryptococcus* species. – J. Bacteriol. 172: 4238-4246.
[36] Vohník, M., Albrechtová, J. (2011): The co-occurrence and morphological continuum between ericoid mycorrhiza and dark septate endophytes in roots of six European *Rhododendron* species. – Folia Geobot. 46: 373-386.
[37] Wei, X., Chen, J., Zhang, C., Pan, D. (2016): A new *Oidiodendron maius* strain isolated from *Rhododendron fortunei* and its effects on nitrogen uptake and plant growth. – Front. Microbiol. 7: 1327.
[38] Wei, X., Chen, J., Zhang, C., Liu, H., Zheng, X., Mu, J. (2020): Ericoid mycorrhizal fungus enhances microcutting rooting of *Rhododendron fortunei* and subsequent growth. – Hortic. Res. 7: 140.
[39] Wu, Z. Y., Lu, A. M., Tang, Y. C., Chen, Z. D., Li, D. Z. (2003): The Families and Genera of Angiosperms in China. – Sci. Press, Beijing.
[40] Wu, L., Lv, Y., Meng, Z., Chen, J., Guo, S. X. (2010): The promoting role of an isolate of dark-septate fungus on its host plant *Saussurea involucrata* Kar. et Kir. – Mycorrhiza 20: 127-135.
[41] Yang, H. B., Fang, R. C., Jin, C. L. (1999): Ericaceae. – In: Fang (ed.) Flora Reipublicae Popularis Sinicae. Sci. Press, Beijing.
[42] Zhou, J. H., Fan, J. H. (2007): Effects of AM fungi on the berberine content in *Phellodendron chinense* seedings. – North. Horticult. 12: 25-27. [In Chinese].

http://www.aloki.hu ● ISSN 1589 1623 (Print) ● ISSN 1785 0037 (Online)
DOI: http://dx.doi.org/10.15666/aeer/1902_12211232
© 2021, ALÖKI Kft., Budapest, Hungary

UTILIZATION OF PAPER WASTES FOR CELLULOLYTIC ENZYME PRODUCTION BY *ASPERGILLUS NIGER* STRAIN 13A AND USING THE BIOORGANIC MATERIALS IN THE BIOCONTROL OF FUSARIUM WILT OF CUCUMBER (*CUCUMIS SATIVUS* L.)

BELAL, E. B.[1] – SHALABY, M. E.[1] – EL-SAID, R. A. R.[2] – ABDELRAZEK, M. A. S.[3] – EBRAHIM, A. E. E.[2*] – GAD, W. A.[4]

[1]*Agricultural Botany Department, Agricultural Microbiology, Faculty of Agriculture, Kafrelsheikh University, Kafr El-Sheikh, Egypt*

[2]*Biological and Ecological Department, Faculty of Home Economic, Al-Azhar University, Tanta, Egypt*

[3]*Department of Chemistry and Toxicity of Pesticides, Faculty of Agriculture, Kafrelsheikh University, Kafr El-Sheikh, Egypt*

[4]*Central Laboratory, Kafr El-Sheikh Company for Water and Wastewater, Kafr El-Sheikh, Egypt*

**Corresponding author*
e-mail: alzahraa_ibrahim16@yahoo.com; phone: +20-10-2053-2190

(Received 15th Sep 2020; accepted 21st Dec 2020)

Abstract. The main purpose of this study is maximizing the utilization of paper waste material and decrease its harmful effect. Eleven fungal isolates were selected and tested to assess their cellulolytic potential. The isolates13A which were isolated from immature compost showed the highest Cellulolytic Index values 0.47 mm. According to the morphological characteristics and the 18S rRNA gene sequence, the isolate13A was identified as *Aspergillus niger* strain13A. The effect of pH and temperature on growth of *Aspergillus niger* strain13A and its production of cellulase were investigated, the optimal culture conditions was recorded at pH 6.0 after 6 days of incubation at 35 °C. Under optimal conditions various paper waste materials were used for enzyme production under submerged and solid-state fermentation. Maximum production of cellulase by *Aspergillus niger* strain13A was shown using kraft brown bags and cardboard under solid state fermentation. *Aspergillus niger* strain13A exhibited also good degradability for a mixture of kraft, cardboard, foolscap and printout paper, under solid state fermentation resulting in the production of bioorganic material. Results of this study showed that treatment of soil with bioorganic materials demnstrarting high effectiveness in controlling Fusarium wilt of cucumber (*Cucumis sativus* L.) could be considered as promising alternative to chemical fungicides.
Keywords: *waste paper, cellulase, solid-state fermentation, Aspergillus niger, biological control*

Introduction

In recent years, solid wastes (MSW) generated by industrial, commercial, domestic and agricultural activities, have become serious environment issues (Joshi et al., 2017). Among all solid waste, waste paper represents 10-39% of global solid waste, where the annual world output of these wastes is nearly 400-1000 million tons per year (Edjabou et al., 2015; Neelamegam et al., 2018; Ozola et al., 2019). Paper waste is defined as waste generally comprised of newspaper, printout paper, packing paper, advertising paper, newspaper and cardboard (Fonoll et al., 2016). Almost all waste paper, especially

http://www.aloki.hu ● ISSN 1589 1623 (Print) ● ISSN 1785 0037 (Online)
DOI: http://dx.doi.org/10.15666/aeer/1902_12331246
© 2021, ALÖKI Kft., Budapest, Hungary

in developing countries, is usually disposed of by landfilling or incineration leading to the formation of leachate and greenhouse gases causing more environmental pollution and loss of cellulose resources (Saferi and Yusof, 2013; Su et al., 2017). As renewable and abundant resources, many reports have been focused on the conversion of paper waste into value-added products such as bioethanol, cellulase enzymes and mixed with other organic materials for co-composting (Fonoll et al., 2016).

Paper products are made from fibers of plant origin, especially wood. Paper wastes materials are mainly composed of cellulose 40-80%, hemicellulose 5-15% and slight amounts of lignin (Sun and Cheng, 2002). This rich content of cellulose gives these wastes a significant potential as cheaper fermentation substrates for cellulase production compared with avicel and carboxymethylcellulose. Enzymatic hydrolysis of cellulose in waste paper produces glucose, which is also used in the biofuel production process (Wu and Cheng, 2005; Zapata et al., 2018).

In nature, cellulolytic microorganisms play an important role in biodegradation process of lignocellulosic materials. Cellulase enzymes belong to the glycoside hydrolase family and are capable of hydrolyzing cellulose materials and related oligosaccharides into glucose and other monoproducts (Lynd et al., 2002; Peciulyte, 2007; Sukharnikov et al., 2012). This multi-enzyme complexes, include three enzymes, namely: endo-1,4-β-D-glucanase, EC 3.2.1.4 (CMCase), exo-1,4-β-D-glucanase, EC 3.2.1.91 (cellodextrinase), β-glucosidase, EC 3.2.1.21 (cellobiase) (Dashtban et al., 2009). Cellulolytic enzymes are the third largest industrial enzymes worldwide due to their applications in many industrial fields such as food, paper and pulp, textile and detergent industry, feed additives paper recycling, waste water treatment, organic acids, bio-ethanol, etc.

The main problem for industrial application of this enzyme is the high- cost and low yield of the production. Therefore, the use of low-cost fermentation technologies as well as developing hyper producing microbial strains to utilize cheaper substrates can help to reduce the production cost as well as to achieve environmental sustainability (Kurup et al., 2005; Singhania, 2009). Several microorganisms can use lignocellulosic wastes as their growth medium to produce cellulolytic enzymes. Filamentous fungi are generally known to be a good source for cellulases due to their ability of decomposing lignocellulose materials, extracellular release, higher yields production of enzymes compared to other microbes and ability to produce complete enzyme complex (Lee and Koo, 2001). Many fungal species including *Aspergillus* sp, *Trichoderma* sp and *Penicillium* sp. (Bansal et al., 2012; Prasanna et al., 2016; Ellilä et al., 2017) are used to produce cellulolytic enzymes especially Aspergillus *ornatus* (Toor and Ilyas, 2014), *Aspergillus niger* and *Rhizopus* sp. (Baig and Saleem, 2012; Santos et al., 2016). Fungal production of cellulases is carried out by both submerged fermentation (SmF) and solid state (SSF) fermentation (Bansal et al., 2012; Lodha et al., 2020).

F. oxysporum is a soil-borne plant pathogen, accountable for vascular wilts in a wide range of economical plants, this disease spreads widely and takes place, nearly all the cucumber plant regions in the world. *Fusarium* wilt has already become one of the most destructive diseases in commercial production of cucumber (Ye et al., 2004).

Biological control using antagonistic microbes to minimize the use of chemicals has become important in recent years (Khan and Khan, 2001).

This study is focused on bio-utilization of paper wastes for cellulolytic enzyme production using submerged and solid-state fermentation techniques as well as using the bioorganic materials in controlling *Fusarium* wilt of cucumber (*C. sativus* L.).

http://www.aloki.hu ● ISSN 1589 1623 (Print) ● ISSN 1785 0037 (Online)
DOI: http://dx.doi.org/10.15666/aeer/1902_12331246
© 2021, ALÖKI Kft., Budapest, Hungary

Materials and methods

Media

The following media were used: Czapek's dox medium (CDA), potato dextrose agar (PDA) and potato dextrose without agar (PDB) (Nasr et al., 2011), mineral salt medium (MSl) described by Cunha et al. (2012) and contained (w/v): 0.14% $(NH_4)_2SO_4$, 0.20% KH_2PO_4, 0.03% $CaCl_2$, 0.02% $MgSO_47H_2O$, 0.50% peptone, 0.20% yeast extract, 0.03% urea, 0.10% Tween 80, and 0.10% of salt solution (5 mg/L $FeSO_47H_2O$, 1.6 mg/L, $MnSO_4H_2O$, 1.4 mg/L $ZnSO_47H_2O$, and 2.0 mg/L $CoCl_2$) and mineral salt medium +1.5% agar (MSA). All media are of high chemical purity products of DIFCO, Becton Dickinson and Company, USA.

Selection and preparation of raw material

Newspaper, coated cardboard, kraft brown bags, corrugated cardboard, foolscap and A4 printout paper sheets of 80 g were selected for the cellulase production and these wastes were collected from the different areas of Kafr El-Sheikh Governorate: Kafr El-Sheikh University Colleges, houses and supermarkets. All wastepaper material and Whatman No. 1 filter paper were cut into small pieces and dried in a hot-air oven to reduce the moisture content; substrates were then milled to obtain the powder form.

Sample collection

Isolation samples of 500 g (ml) were collected in sterile plastic containers from two localities which serve as their natural habitat for cellulose-degrading fungi, four samples were obtained from Kafr El-Sheikh University farms: (A1) mature compost, (A2) immature compost, (A3) cow dung and (A4) old degraded tree. As well as three samples, (B1) primary effluent mud (B2) wastewater from the sedimentation reservoir, (B3) paper wastes were collected from the paper factory located in Tanta city - Gharbia Governorate in Egypt as shown in *Figure 1*.

Isolation, purification and screening of cellulolytic fungi

Isolation was performed by serial dilution method, 100 µl of each dilution was spread on plates containing MSA medium supplemented with 1% carboxymethyl cellulose (CMC) as a sole source of carbon and incubated at room temperature for 4 days. Morphologically dissimilar single fungal colonies were isolated and further purified by repeated culturing on the same media to obtain a pure culture and then stocked at 4 °C on PDA slant in refrigerator for further studies.

Cellulolytic isolates were screened by clearance test using Congo red staining method as described by Teather and Wood (1982). Cellulolytic fungal isolates were selected on the basis of the diameter of the clear zone surrounding the colonies, hydrolysis zone could be observed only around colonies of the active fungal isolates. Cellulolytic activity on CMC agar was recorded as the Cellulolytic Index (CI) which was recorded as hydrolysis ratios = clear zone diameter / growth diameter (Khokhar et al., 2012).

Identification

All selected fungal isolates were identified on the basis of morphological characteristics. Mycelia morphology characteristics such as surface appearance, texture, reverse and pigmentation were determined on the CDA and PDA plates after incubation

http://www.aloki.hu ● ISSN 1589 1623 (Print) ● ISSN 1785 0037 (Online)
DOI: http://dx.doi.org/10.15666/aeer/1902_12331246
© 2021, ALÖKI Kft., Budapest, Hungary

at 25 °C for 4 and 7 days. Microscopic characterization, spore shape, color and conidiophores shape were examined under light microscope.

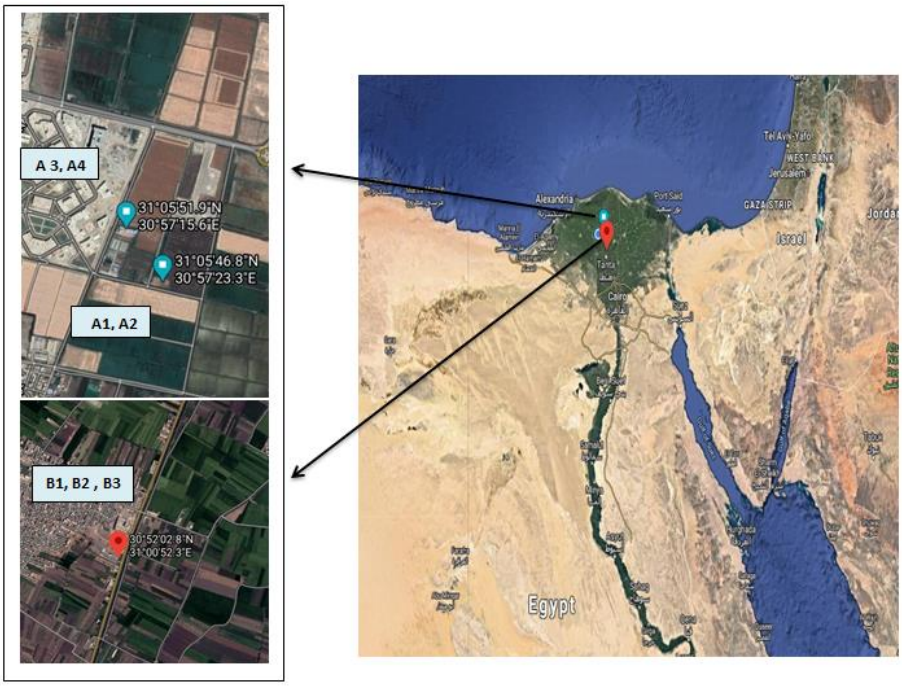


Figure 1. *The sampling location: A1, A2, A3 and A4 at Kafr El-Sheikh University farms. B1, B2 and B3 at Tanta city - Gharbia Governorate in Egypt*

The efficient cellulolytic fungus identification encoded 13A was completed according to molecular biology techniques. For molecular identification, fungal mycelium from a 3 days old culture in potatoes dextrose broth (PDB) was harvested using Whatman No. 1 filter paper. The total genomic DNA was extracted using CTAB protocol (Benito et al., 1993). DNA of the fungal isolate was amplified by polymerase chain reaction (PCR) at Sigma Scientific Services. The identification was achieved by comparing the contiguous DNA sequence with data from the reference and type strains available in public databases of Gen Bank using the BLAST program (National Centre for Biotechnology Information). (http://www.ncbi.nlm.nih.Gov/BLAST). The obtained nucleotide sequences were aligned using ARB to construct the phylogenetic tree using the neighbor-joining method based on Jukes Cantor Model and the isolate was registered in Gen Bank (Eida et al., 2018).

Effect of pH and temperature on A. niger strain 13A growth and cellulases production

Production of cellulolytic enzymes was performed by SmF method in a 250 mL Erlenmeyer flasks. All flask contained 100 ml of MSL medium supplemented with 1% carboxymethyl cellulose as a sole source of carbon. After sterilizing medium was inoculated with 3 ml of 1×10^6 *A. niger* strain 13A spore suspension. To determine the optimum pH the experiment was carried out at pH levels (4, 5, 6, 7 and 8), and the culture was incubated at room temperature for 6 days. Optimal temperature was

http://www.aloki.hu ● ISSN 1589 1623 (Print) ● ISSN 1785 0037 (Online)
DOI: http://dx.doi.org/10.15666/aeer/1902_12331246
© 2021, ALÖKI Kft., Budapest, Hungary

determined by adjusting MSL medium at pH 6.0 and incubating cultures at different temperature values (20, 25, 30, 35, 40, 45 and 50 °C) for 6 days.

Bio-utilization of different paper waste materials

The production of cellulolytic enzymes using waste paper was carried out at the optimal fermentation parameters under Smf and SSF. For SmF, fifty ml of MSL medium was applied containing 1% from each prepared raw-material or CMC as a control. SSF was carried out in fermentation medium, containing 5 g of each prepared raw-material or Whatman No. 1 filter paper as a control, moistened with 7.5 ml nutrient salt solution. All flasks were inoculated with 3 ml of 1×10^6 fungus spore suspension and incubated at 35 °C for 14 days.

Enzyme extraction

For extraction of cellulases in the SmF process, fungal cultures were filtered through a two layered woven gauze, while in SSF the enzyme was extracted by adding 50 mL of 0.05 M citrate buffer (pH 4.8) on SSF culture-flasks and shaken at 120 rpm for 1 h to separate and suspend the extracellular enzymes in the buffer. The whole contents were then filtered as in the case of SmF. The culture filtrate thus obtained was centrifuged for 20 min at 7000 rpm to separate the biomass, and the supernatant was analyzed to determine the cellulolytic productivity (Imran et al., 2017).

Analytical methods

FP-ase and CMC-ase activities were determined using IUPAC methods as described by Ghose (1987). Reducing sugar concentration was estimated by dinitrosalicylic acid (DNS) method using glucose as the standard (Miller, 1959).

Estimation of fungal growth

The mycelial dry weight of biomass (g) was determined by washing the fungal filtrate mycelium and biomass pellet obtained from centrifugation process and drying it at 80 °C for 24 h (Belal, 2003).

Assay of biocontrol agents

A. niger strain 13A was evaluated for their ability to inhibit *Fusarium* oxysporum in dual culture as described by Martyn and Stack (1990) and Tapwal et al. (2005). The radial mycelial growth of the pathogen was recorded after 10 days of incubation and inhibition percent in mycelial growth was calculated as: inhibition Percent = Control – Treatment / Control × 100**.**

Biodegradation of paper wastes mixture to produce biomass (bioorganic materials) for the suppression of Fusarium wilt of cucumber

Dry-milled paper wastes, kraft brown bags, cardboard, foolscap and printout paper were mixed well with ratio of 1:1:1:1 and placed in two glass boxes. This mixture was moistened in a ratio of 1 g: 3 ml of MSL medium without the addition of any carbon source, as well as moistened when needed under sterile conditions. One of the two boxes was treated with 1×10^6 spore suspension of *A. niger* strain 13A while the other was not treated. The two boxes were incubated at the optimal growth conditions for 42 days, on

http://www.aloki.hu ● ISSN 1589 1623 (Print) ● ISSN 1785 0037 (Online)
DOI: http://dx.doi.org/10.15666/aeer/1902_12331246
© 2021, ALÖKI Kft., Budapest, Hungary

the other hand, the produced biomass (bioprorganic materials) was used for soil treatment (at a rate of 2%) for controlling Fusarium wilt of cucumber *(Cucumis sativus* L.*)* (Belal, 2008). Soil was inoculated with *Fusarium oxysporum*, as described by Belal et al. (1996).

Calculation of the infection severity

The incidence and the severity of the disease were calculated according to Ahmed (2010) from the beginning of the disease symptoms on the studied plants weekly after 17 days of planting until the end of the study (45 days).

Statistical analysis

All experiments were carried out using completely randomized design and data were analyzed by one-way analysis of variance (ANOVAs), except for bio-utilization of different paper waste materials experiment was analyzed by two-way analysis of variance (ANOVAs). The means comparison was done using Duncan's multiple range test and least significant difference (LSD) at $P \leq 0.05$. All statistical calculations were carried out using statistical program, SPSS, version, 20.

Results and discussion

Isolation and screening of fungi with cellulolytic production

Seven samples were collected from different locates for the isolation of highly efficient cellulose degrading fungi. Twenty-three fungal strains were isolated, out of which 11 fungal isolates were selected based on morphological dissimilarities and tested to assess the celluloes-hydrolisis ability on MSA medium containing 1% CMC as sole carbon source as tabulated in *Table 1.* All tested isolates showed Cellulolytic Index (CI) ranging from 0.0 to 0.47 mm. High CI values of 0.47 mm was showed by the isolate encoded 13A which was isolated from immature compost. this isolate was selected as a potential cellulase producing isolate for further studies**.**

Table 1. *Hydrolysis ratio of carboxymethycellulose (CMC) by fungal genera incubated at 25 °C for 4 days*

Isolation source	Fungal genera	Growth diameter (mm)	Growth diameter + clear zone (mm)	Clear zone (mm)	CI
Wastewater	*Penicillium* sp	20.33	26.66	6.33	0.31^{b}
Degraded tree	*Trichoderma* sp,	77.00	90.00	13.0	0.17^{d}
	Cladosporium sp	30.33	35.33	5.00	0.16^{d}
Primary effluent mud	*Penicillium* sp	18.00	20.00	2.00	0.11^{d}
Mature compost	*Fusarium* sp	29.66	42.33	10.7	0.34^{b}
	Trichoderma sp,	71.88	90.00	18.1	0.25^{b}
Paper wastes	*Rhizopus* sp.	90.00	90.00	00.0	0.00^{e}
Immature compost	***Aspergillus niger***	**61.33**	**90.00**	**28.7**	**0.47^{a}**
	Aspergillus flavus	88.33	90.00	1.67	0.02^{e}
Cow dung	*Mucor* sp.	90.00	90.00	00.0	0.00^{e}
	Alternaria sp.	25.66	25.66	00.0	0.00^{e}

Values having the same letter within a column are not significantly different according to Duncan multiple range test ($P \leq 0.05$). Bold values indicate the highest Cellulolytic Index

http://www.aloki.hu ● ISSN 1589 1623 (Print) ● ISSN 1785 0037 (Online)
DOI: http://dx.doi.org/10.15666/aeer/1902_12331246
© 2021, ALÖKI Kft., Budapest, Hungary

Identification

All selected isolates were preliminary classified based on the morphological and the microscopical characteristics. Eleven isolates were identified as *Trichoderma* sp, *Penicillium* sp., *Rhizopus* sp., *Mucor* sp., *Aspergillus niger*, *Fusarium* sp. *Aspergillus* sp. *Cladosporium* sp, *Aspergillus flavus*, *Penicillium* sp. and *Alternaria* sp. Fungi are known to excrete a large number of cellulolytic enzymes for commercial production (Imran et al., 2016).

The most efficient isolate 13 A was confirmed and identified based on molecular approach following 18Sr DNA sequencing. This isolate was found to be closely similar to *Aspergillus niger*, thus identified as A. *niger*. This sequence has been recorded in NCBI GenBank with an accession No. SFC101821 with the name of *A. niger* strain 13A. Phylogenetic tree showed in *Figure 2* was constructed by neighbor-joining method using nucleotide evolutional model based on synonymous and non-synonymous nucleotide substitutions. *Aspergillus niger* is known to be a good producer of cellulolytic enzymes perhaps due to its high cellulase productivity and safe use in industry. Our results are in agreement with previous findings of researchers, such as Juhasz et al. (2003) and Abdullah et al. (2016). Therefore, *Aspergillus niger* strain 13A was selected as efficient producer for extracellular cellulases for further studies.

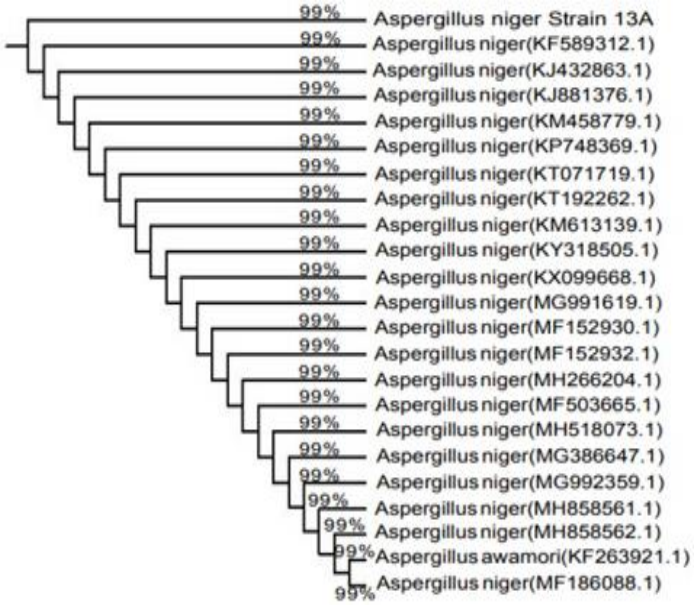


Figure 2. *Phylogenetic tree derived from 18S ribosomal DNA gene sequence of Aspergillus niger (SFC101821) and sequences of the closest phylogenetic neighbors obtained by NCBI BLAST*

Effect of pH and temperature on A. niger strain 13A growth and cellulases production

Environmental factors have an important influence on the microbial growth, production activity and their degradation ability of organic material. Factors like pH and temperature, have an important effect on the microbial degradation of paper wastes and so these conditions must be considered when the biodegradability of paper wastes is tested (Belal, 2008) therefore temperature and pH factors were optimized to determine the optimal conditions for growth and maximum levels of cellulase production.

http://www.aloki.hu ● ISSN 1589 1623 (Print) ● ISSN 1785 0037 (Online)
DOI: http://dx.doi.org/10.15666/aeer/1902_12331246
© 2021, ALÖKI Kft., Budapest, Hungary

Optimum pH

The effect of pH on *A. niger* strain 13A growth and their cellulase production is shown in *Table 2.* Generally, the obtained results showed that the optimum pH for *A. niger* strain 13A was pH 6.0. The maximum mycelial dry weight was 0.37 ± 0.026 g/100 ml as well as the maximum production of CMC-ase and FP-ase were 1.24 ± 0.049 and 0.27 ± 0.025 IU/ml respectively. Fungus growth and FP-ase production showed stability at pH 6.0-7.0, a further increase in the optimal pH decreased the growth and cellulase productivity. The enzyme production reduced drastically at pH 9.0, this decreasing at higher pH may be due to proteolytic inhibition of the cellulase. slightly acidic pH is preferred for cellulase production by *A. niger* (Dutt and Kumar, 2014).

Table 2. *Effect of pH on A. niger strain 13A growth and cellulase production*

pH	Mycelial dry weight (g/100 ml)	CMC-ase IU/ml	FP-ase IU/ml
4.0	0.21 ± 0.02^{c}	0.82 ± 0.018^{d}	0.13 ± 0.01^{c}
5.0	0.32 ± 0.025^{a}	1.07 ± 0.074^{b}	0.18 ± 0.042^{b}
6.0	0.37 ± 0.026^{a}	1.24 ± 0.049^{a}	0.27 ± 0.025^{a}
7.0	0.29 ± 0.35^{b}	0.94 ± 0.011^{c}	0.25 ± 0.026^{a}
8.0	0.20 ± 0.025^{c}	0.36 ± 0.093^{e}	0.15 ± 0.093^{c}
9.0	0.13 ± 0.021^{d}	0.04 ± 0.028^{f}	0.08 ± 0.041^{d}

Values having the same letter within a column are not significantly different according to Duncan multiple range test ($P \leq 0.05$)

Optimum temperature

The influence of different temperatures on *A. niger* strain 13A growth and their cellulase production is shown in *Table 3.* The highest yield of mycelial dry weight (0.51 ± 0.025 g/100 ml) as well as the maximum productivity of CMC-ase (1.21 ± 0.041 IU/ml) FP-ase (0.44 ± 0.060 IU/ml) was obtained when *A. niger* strain 13A was grown at 35 °C and the initial pH was 6.0. An increase in incubation temperature to 35 °C decrease fungus growth and enzyme production. Our results are in agreement with previous findings of researchers, such as Sohail et al. (2009) and Nasr et al. (2011) who reported that the optimum temperature for cellulase production by the fungus might lie between 27 and 35 °C. The decrease of cellulase production levels at lower temperature may be due to the depressed transport of cellulose across the cells, causing reduced yield of cellulase production (Dutt and Kumar, 2014).

Bio-utilization of different paper waste materials

Aspergillus niger strain 13A was used under the optimal growth conditions with the aim of utilization of paper waste materials as a sole carbon source for cellulase production under submerged (SmF) and solid-state fermentation (SSF).

The obtained results were illustrated in *Figure 3;* the general trend of substrate degradation with *A. niger* strain 13A under both of SmF and SSF was CMC (SmF control) > filter paper (SSF control) > kraft brown bags > cardboard > foolscap > printout paper > newspapers and coated cardboard. The highest production of cellulase by *A. niger* strain 13A was obtained by using kraft

http://www.aloki.hu ● ISSN 1589 1623 (Print) ● ISSN 1785 0037 (Online)
DOI: http://dx.doi.org/10.15666/aeer/1902_12331246
© 2021, ALÖKI Kft., Budapest, Hungary

brown bags as a carbon source in both SSF (CMC-ase was 0.813 ± 0.067 IU/ml, FP-ase was 0.25 ± 0.05 IU/ml) and SmF (CMC-ase was 0.36 ± 0.11 IU/ml, FP-ase was 0.090 ± 0.02 IU/ml). As well as cardboard substrate gave the highest cellulase production in both SSF (CMC-ase was 0.72 ± 0.016 IU/ml, FP-ase was 0.24 ± 0.017 IU/ml) and SmF (CMC-ase was 0.43 ± 0.076 IU/ml, FP-ase was 0.16 ± 0.008 IU/ml). On the other hand, newspaper and coated cardboard exhibited the lowest enzyme production.

Table 3. *The effect of temperature on A. niger strain 13A growth and cellulase production*

Temperature (°C)	Mycelial dry weight (g/100ml)	CMC-ase IU/ml	FP-ase IU/ml
20	0.32 ± 0.021^{d}	0.40 ± 0.028^{f}	0.08 ± 0.05^{e}
25	0.39 ± 0.020^{cb}	0.54 ± 0.026^{e}	0.23 ± 0.012^{c}
30	0.42 ± 0.034^{b}	0.93 ± 0.057^{c}	0.36 ± 0.021^{b}
35	0.51 ± 0.025^{a}	1.21 ± 0.041^{a}	0.44 ± 0.060^{a}
40	0.46 ± 0.036^{b}	1.09 ± 0.015^{b}	0.26 ± 0.039^{c}
45	0.26 ± 0.047^{e}	0.61 ± 0.032^{d}	0.15 ± 0.092^{d}
50	0.22 ± 0.031^{e}	0.33 ± 0.026^{g}	0.006 ± 0.065^{e}

Values having the same letter within a column are not significantly different according to Duncan multiple range test ($P \leq 0.05$)

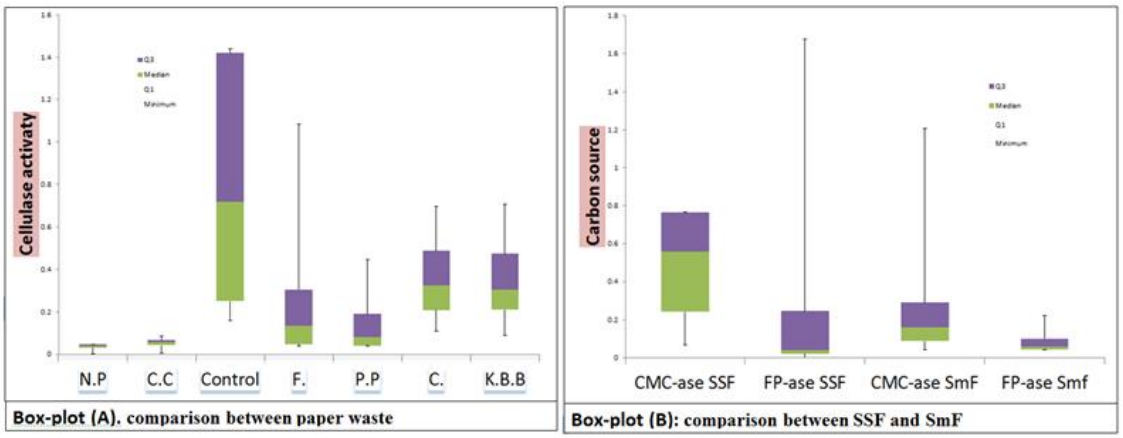


Figure 3. *Using paper waste (PW) as a sole source of carbon for cellulase production by Aspergillus niger strain 13A under submerged and solid-state fermentation. Box-plot (A) illustrated that no significant difference between KBB and C on cellulase production under SmF and Smf, low significant difference * between F and P.P., N.P and CC were outliter. Box-plot (B) illustrated high significant difference ** between SSF and SmF as well as between CMC-ase and FP-ase productivity under both SSF and SmF. Kraft brown bags (KBB), cardboard (C), foolscap (F), printout paper (P.P) newspapers (N.P) and coated cardboard (C.C)*

Kraft brown bags and cardboard contain about 60-70% cellulose, 10-20% hemicellulose, and they have a high content of lignin about 5-10% on the other hand office paper contains about 70% cellulose and 4% lignin. Newspaper production is made from paper with high recycled fibre or paper, which contains about 40-55% cellulose, 25-40% hemicellulose, and 18-30% lignin (López Alvarez et al., 2009;

http://www.aloki.hu ● ISSN 1589 1623 (Print) ● ISSN 1785 0037 (Online)
DOI: http://dx.doi.org/10.15666/aeer/1902_12331246
© 2021, ALÖKI Kft., Budapest, Hungary

Gonzalez-Estrella et al., 2017; Li et al., 2020). Although a high cellulose and low lignin content of printing paper and foolscap compared with other type of papers, brown bags and cardboard were found favorable sources of carbon for cellulolytic *A. niger* strain 13A. These results may be depending on a high lignin content of newspaper and coated cardboard in addition to quantity and type of pigment and ink and other contaminants included with using paper materials. Cummings and Stewart (1994) reported that the presence of ink reduced the rate of cellulose solubilization as well as inhibited the biodegradation process.

The obtained results also showed the highest production of cellulase by *A. niger* strain 13A was exhibited under SSF compared with SmF for all kinds of paper waste. On the other hand, the CMC-ase production was higher than the FP-ase production for all wastes under both SSF and SmF. SSF has many advantages over SmF such as low-cost, and higher yield of enzymes and productivity, absence of free water and control of bacterial contamination, therefore it is a more suitable technique for the production of fungal enzymes (Bansal et al., 2012; Lodha et al., 2020).

Assay of biocontrol agents

The experiment between *Aspergillus niger* strain 13A and *Fusarium oxysporum* showed noticeable inhibitory effect on the pathogen. The inhibition rate of *Aspergillus niger* strain 13A ranged from 63.27 to 78.5%.

Biodegradation of paper wastes mixture to produce biomass (bioorganic materials) for the suppression Fusarium wilt in cucumber

The four best carbon sources of waste paper materials have been mixed well and used as a mass multiplication substrate for *A. niger* strain 13A to evaluate it is efficacy against the cucumber *(Cucumis sativus L.)* wilt pathogen. A mixture of waste materials exhibited complete degradation after 42 days and the color of wastepaper mixture was converted to black which is the color of *Aspergillus niger*; this process produces biomass called bioorganic materials. Under greenhouse conditions, application of the bioorganic materials to soil infested artificially with *F. oxysporum, Table 4* and *Figure 4,* exhibited their efficacy to control *Fusarium* wilt and increased survival of plants.

The results also showed that the use of *A. niger*-bioorganic materials had demonstrated high efficiency in reducing the disease incidence and disease severity of Fusarium wilt infection. While the incidence and disease severity of *A. niger*-bioorganic materials were 44% and 26% respectively, with the efficiency 37.97 and 55.85, in the control treatment (*F. Oxysporum* and *F. oxysporum* + untreated mixture) incidence and disease severity were 71.33, 60% and 72, 61%, respectively. Sen et al. (1993) and Vibha (2011) reported that *A. niger* is a potential biocontrol agent for soil borne pathogens. The antagonistic interaction of *A. niger* with the disease may be due to production of antibiotics, overgrowth and hyper-parasitism. Abed et al. (2019) referred to the use of *T. harzianum*, *T. viride*, and *Glomus mosseae* having a significant effect in reducing the disease incidence of Fusarium wilt of cucumber with the efficiency of 43.54, 39.11 and 65.18%, respectively. Also, Ahmed (2010) found that *Pseudomonas fluorescens* No.3 and *Serratia marcensens* No.2 had completely prevented the Fusarium wilt disease incidence. Compared to the previous reports, *A. niger* strain13A is considered a promising biological control agent.

http://www.aloki.hu ● ISSN 1589 1623 (Print) ● ISSN 1785 0037 (Online)
DOI: http://dx.doi.org/10.15666/aeer/1902_12331246
© 2021, ALÖKI Kft., Budapest, Hungary

Table 4. *Effect of A. niger-bioorganic materials and its efficiency in controlling the Fusarium wilt of cucumber (Cucumis sativus L.)*

Treatments	Pre-emergence damping-off (%)	Post-emergence damping-off (%)	Survival of plants (%)	Disease incidence (%)	Disease severity (%)	Efficiency in reduction infection (%)	Efficiency in reduction severity (%)
Control (uninoculated)	8[a]	0[a]	92[a]	0	0	0	0
F. oxysporum	25[c]	25[b]	50[c]	71.33[b]	60b	0	0
F. oxysporum + untreated mixture	25[c]	20[b]	45[c]	72[a]	61a	0	0
A. niger + *F. Oxysporum*	16[b]	0[a]	84[b]	44[c]	26c	37.97	55.85

Values having the same letter within a column are not significantly different according to Duncan multiple range test ($P \leq 0.05$). Each number represents an average of three replicates with eight plants in each replicate

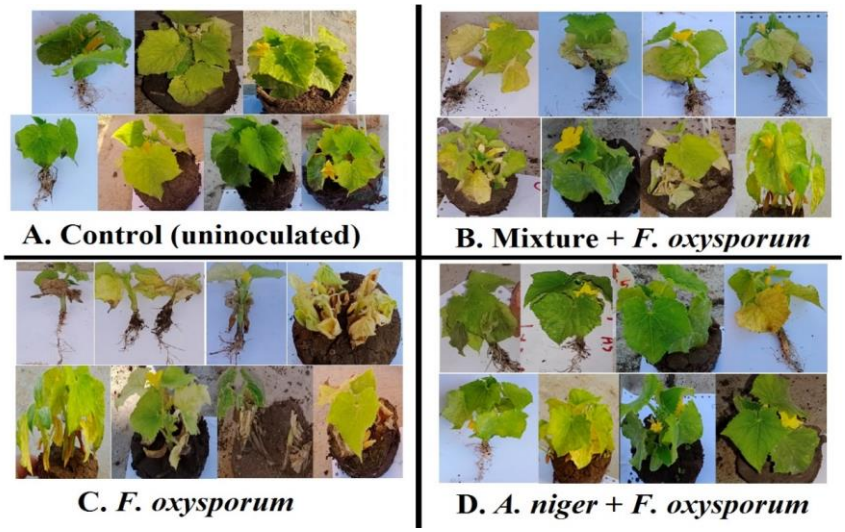


Figure 4. *Biocontrol of Fusarium wilt of cucumber by the bioorganic materials*

Conclusion

Successful experiments have been made to convert paper waste (PW) materials into high-value-added products. Kraft brown bags, cardboard, foolscap, printout paper, newspapers and coated cardboard which are some of the paper wastes used in this study as a fermentation substrate produced a good amount of cellulolytic enzyme by *Asperigillus niger* strain 13A under solid state fermentation. In addition, using *A. niger*-bioorganic material exhibited efficiency in controlling Fusarium wilt in cucumber. The application of these results may help in limiting the effect of environmental pollution caused by paper waste materials and fungicides.

This study recommends the utilization of paper wastes as a renewable resource of cellulosic constituents to consolidate a cleaner environment and to produce valuable materials. On the other hand, the use of *A. niger* as a biological control agent needs further study and evaluation.

Acknowledgements. The authors gratefully acknowledge Kafr El-sheikh University and Al-Azhar University, Egypt for supporting this work.

http://www.aloki.hu ● ISSN 1589 1623 (Print) ● ISSN 1785 0037 (Online)
DOI: http://dx.doi.org/10.15666/aeer/1902_12331246
© 2021, ALÖKI Kft., Budapest, Hungary

REFERENCES

[1] Abdullah, J. J., Greetham, D., Pensupa, N., Tucker, G. A., Du, C. (2016): Optimizing cellulase production from municipal solid waste (MSW) using solid state fermentation (SSF). – Journal of Fundamentals of Renewable Energy and Applications 6(3): 1-10.

[2] Abed, J. M., Farhan, T. A., Kadhum, A. A., Abed, M. M., Zaki, N. A., Edbeib, M. F. (2019): Effect of some biocontrol factors and their efficacy in resistance to Fusarium wilt disease caused by *Fusarium oxysporum* F. sp. *Cucumerinum* on Cucumber plant under open field conditions. – International Conference on Biosci. and Medi. Engin. AIP Conf. Proc. 2155: 020031-1–020031-5.

[3] Ahmed, G. A. (2010): Controlling of Fusarium wilt of cucumber by antagonistic bacteria. – Journal of Life Sciences 4(7): 16-21.

[4] Baig, S., Saleem, M. (2012): Production and characterization of cellulases of *Aspergillus niger* by using rice husk and saw dust as substrates. – Pakistan Journal of Botany 44: 377-382.

[5] Bansal, N., Tewari, R., Soni, R., Soni, S. K. (2012): Production of cellulases from *Aspergillus niger* NS-2 in solid state fermentation on agricultural and kitchen waste residues. – Waste Management 32: 1341-1346.

[6] Belal, E. B. A. (2003): Investigation on the biodegradation of polyesters by isolated mesophilic microbes. – Dissertation, Technical University Braunschweig.

[7] Belal, E. B. (2008): Biodegradation of wastepaper by *Trichoderma viride* and using the bioprocessed materials in biocontrol of damping-off of pea caused by *Pythium debaryanum*. – J. Agric. Res., Kafrelsheikh Univ. 34(3): 567-587.

[8] Belal, E. B., Gabr, M., El-Gremi, S., Ibrahim, M. E. (1996): Interaction between Antagonistic Microorganisms and certain soil-borne pathogens of soybean in relation to *Bradyrhizobium japonicum*. – J. Agric. Res. Tanta Univ. 22(4): 451-459.

[9] Benito, C., Figueiras, A., Zaragoza, C., Gallego, F., De La Pena, A. (1993): Rapid identifi-cation of Triticeae genotypes from single seeds using the polymerase chain reaction. – Plant Mol. Biol. 21(1): 181-183.

[10] Cummings, S. P., Stewart, C. S. (1994): Newsparer as substrate for cellulolytic landfill bacteria. – J. Appl. Bacteriol. 76: 196-202.

[11] Cunha, M. N., Esperança, T. C., Zangirolami, A. C., Badino, C. S. (2012): Farinas Sequential solid-state and submerged cultivation of *Aspergillus niger* on sugarcane bagasse for the production of cellulose. – Bioresource Technology 112: 270-274271.

[12] Dashtban, M., Schraft, H., Qin, W. (2009): Fungal bioconversion of lignocellulosic residues; opportunities & perspectives. – International Journal of Biological Sciences 5(6): 578.

[13] Dutt, d., Kumar, A. (2014): Optimization of cellulase production under solid-state fermentation by *Aspergillus flavus* (AT-2) and *Aspergillus niger* (AT-3) and its impact on stickies and ink particle size of sorted office paper. – Cellulose Chem. Technol. 48: 285-298.

[14] Edjabou, M. E., Jensen, M. B., Gotze, R., Pivnenko, K., Petersen, C., Scheutz, C., Astrup, T. F. (2015): Municipal solid waste composition: sampling methodology, statistical analyses, and case study evaluation. – Waste Manag. 36: 12-23.

[15] Eida, M. F., Darwesh, O. M., Matter, I. A. (2018): Cultivation of oleaginous microalgae Scenedesmus obliquus on secondary treated municipal wastewater as growth medium for biodiesel production. – J. Ecol. Engin. 19(5): 38-51.

[16] El-Hassan, S. A., Gowen, S. R. (2006): Formulation and delivery of the bacterial antagonist *Bacillus subtilis* for management of lentil vascular wilt caused by *Fusarium oxysporum* f. sp. - lentis. – Phytopathol.154: 148-155.

[17] Ellilä, S., Fonseca, L., Uchima, C., Cota, J., Goldman, G. H., Saloheimo, M., Sacon, V., Siika-aho, M. (2017): Development of a low-cost cellulase production process using

http://www.aloki.hu ● ISSN 1589 1623 (Print) ● ISSN 1785 0037 (Online)
DOI: http://dx.doi.org/10.15666/aeer/1902_12331246
© 2021, ALÖKI Kft., Budapest, Hungary

Trichoderma reesei for Brazilian biorefineries. – Biotechnology for Biofuels 10(30): 1-17.

[18] Fonoll, X., Astals, S., Dosta, J., Mata-Alvarez, J. (2016): Impact of paper and cardboard suppression on OFMSW anaerobic digestion. – Waste Manag. 56: 100-105.

[19] Ghose, T. K. (1987): Measurement of cellulase activities. – Pure Appl Chem 59: 257-268.

[20] Gonzalez-Estrella, J., Asato, C. M., Jerke, A. C., Stone, J. J., Gilcrease, P. C. (2017): Effect of structural carbohydrates and lignin content on the anaerobic digestion of paper and paper board materials by anaerobic granular sludge. – Biotechnol. Bioeng. 114(5): 951-960.

[21] Imran, M., Anwar, Z., Irshad, M., Asad, M. J., Ashfaq, H. (2016): Cellulase production from species of fungi and bacteria from agricultural wastes and its utilization in industry: a review. – Advances in Enzyme Research 4(2): 44-55.

[22] Joshi, G., Naithani, S., Varshney, V. K., Bisht, S. S., Rana, V. (2017): Potential use of waste paper for the synthesis of cyanoethyl cellulose: a cleaner production approach towards sustainable environment management. – Journal of Cleaner Production 142: 3759-3768.

[23] Juhasz, T., Kozma, K., Szengyel, Z., Reczey, K. (2003): Production of beta glucosidase in mixed culture of *Aspergillus niger* BKMF 1305 and *Trichoderma reesei* RUT-C30. – Food Technol. Biotechnol. 41: 49-53.

[24] Khan, M. R., Khan, S. M. (2001): Biomanagement of *Fusarium* wilt of tomato by the soil application for certain phosphorus solubilizing microorganism. – Int J Pest Manag. 47: 227-231.

[25] Khokhar, I., Haider, M. S., Mushtaq, S., Mukhtar, I. (2012): Isolation and screening of highly cellulolytic filamentous fungi. – J. Appl. Sci. Environ. Manage. 16(3): 223 – 226.

[26] Kurup, S. C., Snishamol, R., Nagendra, C., Prabhu, G. (2005): Cellulase production by native bacteria using water hyacinth as substrate under solid state fermentation. – Malay. J Microbiol. 1(2): 25-29.

[27] Lee, S. M., Koo, Y. M. (2001): Pilot-scale production of cellulase using *T. reesei* rut C-30 in fed-batch mode. – J. Microbial Biotechnol. 11: 229- 233.

[28] Li, W., Khalid, H., Amin, F. R., Zhang, H., Dai, Z., Chen, C., Liu, G. (2020): Biomethane production characteristics, kinetic analysis, and energy potential of different paper wastes in anaerobic digestion. – Renewable Energy 157: 1081-1088.

[29] Lodha, A., Pawar, S., Rathod, V. (2020): Optimised cellulase production from fungal co-culture of *Trichoderma reesei* NCIM 1186 and *Penicillium citrinum* NCIM 768 under solid state fermentation. – Journal of Environmental Chemical Engineering 8: 1-6.

[30] López Alvarez, J. V., Aguilar Larrucea, M., Arraiza Bermúdez, P., León Chicote, B. (2009): Biodegradation of paper waste under controlled composting conditions. – Waste Management 29: 1514-1519.

[31] Lynd, L. R., Weimer, P. J., Van Zy, W. H., Pretorius, I. S. (2002): microbial cellulose utilization: fundamentals and biotechnology. – Microbiol Mol Biolo Reviews 66: 506-577.

[32] Martyn, R. D., Stack, J. P. (1990): Biological Control of Soil Borne Plant Pathogens by Antagonistic Fungi. – In: Baudoin, A. B. A. M. (ed.) Laboratory Exercises in Plant Pathology. Scientific Publisher, Jodhpur. pp 64-74.

[33] Miller, G. L. (1959): Use of dinitrosalicylic acid reagent for determination of reducing sugar. – Anal. Chem. 31: 426-429.

[34] Nasr, S., Hussein, N. A., Abozaid, A. A., Al-salemi, F. A. (2011): Cellulose production by two fungal strains isolated from Taif in Saudi Arabia. – J. Agric. Sci. 19(1): 171-178.

[35] Neelamegam, A., Al-Battashi, H., Al-Bahry, S., Nallusamy, S. (2018): Biorefinery production of poly-3-hydroxybutyrate using waste office paper hydrolysate as feedstock for microbial fermentation. – Journal of Biotechnology 265: 25-30.

[36] Ozola, Z. U., Vesere, R., Kalnins, S. N., Blumberga, D. (2019): Paper waste recycling. Circular economy aspects. – Environmental and Climate Technologies 23(3): 260-273.

http://www.aloki.hu ● ISSN 1589 1623 (Print) ● ISSN 1785 0037 (Online)
DOI: http://dx.doi.org/10.15666/aeer/1902_12331246
© 2021, ALÖKI Kft., Budapest, Hungary

[37] Prasanna, H. N., Ramanjaneyulu, G., Rajasekhar, Reddy, B. (2016): Optimization of cellulase production by *Penicillium* sp. – Biotech. 6(162): 1-11.
[38] Saferi, S.K., Yusof, Y. (2013): A review: natural fiber as reinforcement in waste paper recycling and its processing methods. – Appl. Mech. Mater. 315: 443-447.
[39] Santos, T. C., Arbreu Filho, G., Brito, A. R., Pires, A. J., Bonomo, R. C., Franco, M. (2016): Production and characterization of cellulolytic enzymes by *Aspergillus niger* and *Rhizopus* sp. By solid state fermentation of prickly pear. – Revista Caatinga 29: 222-233.
[40] Sen, B., Sharma, J., Asalmol, M. N., Chattopadhyay, C., Patibanda, A. K. (1993): *Aspergillus niger* - a potential biocontrol agent for soil borne pathogens. – Ind. Phytopath. 46(3): 275-278.
[41] Singhania, R. R., Patel, A. K., Soccol, C. R., Pandey, A. (2009): Recent advances in solid-state fermentation. – Biochemical Engineering Journal 44(1): 13-18.
[42] Sohail, M., Siddiqi, R., Ahmad, A., Khan, S. A. (2009): Cellulase production from *Aspergillus niger* MS82: effect of temperature and pH. – New Biotechnology 25(6): 437-441.
[43] Su, H., Zhu, P., Zhang, L., Zhou, F., Li, G., Li, T., Li, Q., Wang, R., Sun, C., Wong. (2017): Waste to wealth: a sustainable and flexible supercapacitor based on office waste paper electrodes. – Journal of Electroanalytical Chemistry 786: 28-34.
[44] Sukharnikov, L. O., Alahuhta, M., Brunecky, R., Upadhyay, A., Himmel, M. E., Lunin, V. V., Zhulin, I. B. (2012): Sequence, structure, and evolution of cellulases in glycoside hydrolase family 48. – J. Biol. Chem. 287(49): 41068-41077.
[45] Sun, Y., Cheng, J. (2002): Hydrolysis of lignocellulosic materials for ethanol production: a review. – Bioresource Technology 83: 1-11.
[46] Tapwal, A., Sharma, Y. P., Lakhanpal, T. N. (2005): Use of biocontrol agents against white root rot of apple. – J. Mycol. Plant Pathol. 35:67-69.
[47] Teather, R. M., Wood, P. J. (1982): Use of congo red-polysacharide interactions in enumeration and characterization of cellulolytic bacteria in the bovine rumen. – Appl. Environm. Microbiol. 43(4): 777-780.
[48] Toor, Y., Ilyas, U. (2014): Optimization of cellulase production by *Aspergillus ornatus* by the solid state fermentation of Cicer arietinum. – American Journal of Research 2: 125-141.
[49] Vibha (2011): Evaluation of fungal and bacterial bioagents against *Rhizoctonia solani* on *Solanum melongena* L. – Archives of Phytopathology and Plant Protection 44(8): 743-750.
[50] Wu, C-c., Cheng, C. (2005): A study of the hydrolysis of waste paper cellulose with a vertically hanging immobilized cellulase reactor and the reuse of the immobilized cellulase. – Journal of the Chinese Chemical Society 52: 85-95 85
[51] Ye, S. F., Yu, J. Q., Peng, Y. H., Zheng, J. H., Zou, Y. (2004): Incidence of Fusarium wilt in *Cucumis sativus* L. is promoted by cinnamic acid, an autotoxin in root exudates. – Plant and Soil 263: 143-150.
[52] Zapata, C. B., Yang, C., Yeh, S., Ogden, J., Kleeman, M. J. (2018): Low-carbon energy generates public health savings in California. – Atmos. Chem. Phys. 18: 4817-4830.

http://www.aloki.hu ● ISSN 1589 1623 (Print) ● ISSN 1785 0037 (Online)
DOI: http://dx.doi.org/10.15666/aeer/1902_12331246
© 2021, ALÖKI Kft., Budapest, Hungary

POTENTIAL SIDE-EFFECTS OF A FERTILIZER ON GROWTH, BIOCHEMICAL COMPOSITION AND BIOMARKER RESPONSES OF THE GREY WORM (*APORRECTODEA CALIGINOSA* SAVIGNY, 1826)

HALAIMIA, S.[1] – TINE, S.[1,2] – TINE-DJEBBAR, F.[1,2*] – SOLTANI, N.[2]

[1]*Laboratory of Water and Environment, University of Tebessa, Tebessa, Algeria*

[2]*Laboratory of Applied Animal Biology, University Badji Mokhtar, Annaba, Algeria*

**Corresponding author*
e-mail: fouzia.djebbar@univ-tebessa.dz

(Received 20th Oct 2020; accepted 19th Jan 2021)

Abstract. Earthworms are a major component of soil fauna communities in most ecosystems and comprise a large proportion of macro fauna biomass. They play multiple roles in soil heath. Earthworms represent one of the most important biological indicators in the terrestrial environment. However, they are exposed to agrochemicals used to increase crop yield. The present study was conducted to assess the potential hazards of a complete fertilizer (NPK), commonly used in agriculture, on juveniles of *Aporrectodea caliginosa* Savigny, 1826 an abundant species in the region of Tebessa (Northeast Algeria)**.** The fertilizer was tested at different doses ranging between 400 and 1200 mg on juvenile earthworm under laboratory conditions. Growth, biochemical composition (lipid, protein, and carbohydrate content) and four selected biomarkers of oxidative stress (glutathione peroxidase, lactate dehydrogenase, glutathione S-Transferase and glutathione) were examined weekly during an exposure of four weeks. The earthworm mortality was monitored after 4 weeks of exposure. The LD_{25}, LD_{50} and LC_{90} values were 518.9, 644.9 and 996.4 mg, respectively. The tested fertilizer (LD_{25} and LD_{50}) showed inhibitory effects on the growth of *A. caliginosa*. Moreover, it resulted in a significant reduction in the energy reserves as evidenced by a reduction in carbohydrate, lipid and protein amounts. Lastly, enzymatic assays revealed a stimulation of the detoxification system traduced by an increase in glutathione peroxidase, lactate dehydrogenase and glutathione S- Transferase activities and a decrease in glutathione rate compared to control series. Overall results indicate that application of the fertilizer tested could have harmful effects on earthworms.

Keywords: *ecosystem engineers, NPK fertilizer, growth rate, energy reserves, detoxification system, oxidative stress*

Introduction

In order to increase crop yield, pesticides and fertilizers are now being used in higher quantities than in the past (Gill and Garg, 2014; Băcanu et al., 2019). When these agrochemicals enter the soil, they may disturb the soil ecosystems by impairing the physical, chemical and biological components specially the non-target beneficial microorganisms and earthworms (Edwards and Bohlen, 1992). Indiscriminate use of these products has led to many negative effects such as loss of top soil due to pollution by fertilizers, weedicides and pesticides, as well as magnification of chemicals in food chains and food webs (Shruthi et al., 2017). They are also responsible for extensive soil air and water pollution, and affect not only the target organisms, but also the non-targeted species such as earthworms. They constitute more than 80% of the invertebrate biomass in most of the agroecosystems of the world (Yasmin and D'Souza, 2010) and contribute to a number of soil properties, such as soil structure, porosity, water

http://www.aloki.hu ● ISSN 1589 1623 (Print) ● ISSN 1785 0037 (Online)
DOI: http://dx.doi.org/10.15666/aeer/1902_12471266
© 2021, ALÖKI Kft., Budapest, Hungary

retention, cationic exchange and pH buffering capacity (Lal, 2004). Due to their beneficial role in the agroecosystem, earthworms are used as indicator species for monitoring the impact of pollutants, changes in soil structure and agricultural practices (Yasmin and D'Souza, 2010). Earthworms recognized as 'ecosystem engineers' are naturally in contact with the solid and aqueous phases of the soil, ingest large amounts of soil and are therefore directly exposed to contaminants, industrial activities and atmospheric deposition. However, their diversity, density and biomass are strongly influenced by soil management (Gill and Garg, 2014). Pelosi et al. (2014) reported that earthworms are affected at all levels of the organism; changed individual behaviors, disrupted metabolism and enzyme activities, increased individual mortality, reduced fertility, retardation of growth and reproduction. Several studies have been carried out on the toxic impact of some pesticides on soil organisms, especially earthworms, although little research has been done on the toxicity of different fertilizers to earthworms in a soil profile (Yahyaabadi et al., 2018). A number of studies have found the positive effects of fertilizers on earthworms and their populations (Estevez et al., 1996; Curry et al., 2008). Few researchers also emphasized the negative effects of chemical fertilizers on earthworms (Tindaon et al., 2011; Bhattacharya and Sahu, 2014). Both beneficial (Callaham et al., 2003) and harmful effects (Marhan and Scheu, 2005) of inorganic fertilizers on earthworm populations have been reported from different agroecosystems. Several studies were conducted on the toxicity of NPK using earthworms as test animal by Paper contact method (Abbiramy and Ross, 2013a, b; Bhattacharya and Sahu, 2016). But very few studies were conducted to test the toxicity of NPK on the soil ecosystem. The use of biochemical biomarkers to investigate the contaminant toxicity, metabolization, and detoxification in earthworms is nowadays becoming a current practice (Denoyelle, 2007; Reinecke and Reinecke, 2007). The importance of antioxidant enzymes is generally emphasized in the prevention of oxidative stresses by scavenging of reactive oxygen species (ROS) (Lijun et al., 2005). The antioxidant system comprises several enzymes such as superoxide dismutase (SOD), catalase (CAT), and guaiacol peroxidase (GPx). Superoxide radicals that are generated are converted to H_2O_2 by the action of SOD, and the accumulation of H_2O_2 is prevented in the cell by CAT and GPx.

Our objective was to assess the potential hazards of a balanced fertilizer (NPK), widely used in agriculture, against *Aporrectodea caliginosa* an abundant earthworm species in Tébessa area (Northeast Algeria) (Bouazdia and Habes, 2017) and used as bioindicator of soil contamination. Thus, the fertilizer was tested on survival, growth, biochemical composition of the whole body and also on two selected environmental stress biomarkers (GPx and LDH). The purpose of this study was to obtain more comprehensive understanding of the effects of the fertilizers on earthworm, and to provide more information about the potential ecological risk agrochemicals on the soil ecosystem particularly beneficial and non-target fauna. The information obtained from this study is considered critical, as it will provide a foundation for risk assessment.

Materials and methods

Earthworm collection and soil properties

Earthworm populations were sampled at the end of autumn, which is known to be a period of great earthworm activity (Bouché, 1972). Population samples of the endogenic juvenile's earthworm's *A. caliginosa* L. were collected by hand from the region of El

http://www.aloki.hu ● ISSN 1589 1623 (Print) ● ISSN 1785 0037 (Online)
DOI: http://dx.doi.org/10.15666/aeer/1902_12471266
© 2021, ALÖKI Kft., Budapest, Hungary

Merdja, located at 4.5 Km northeast of the city of Tebessa (northeastern Algeria) (35°25'N, 8°10'E; elevation: 830 m a.s.l.). 40-cm-depth block of soil was excavated and earthworms were hand-sorted according to the method of Bouché (1972) from an upland non-irrigated paddy field which had no record of input of agrochemicals. After collection, the earthworms were cultured for 7 days of adaptation (Mekahlia et al., 2016) at their native soil. The experiment was maintained at 60 ± 2% soil moisture and 25 ± 2 °C soil temperature. The physical and chemical properties of the soil are shown in *Table 1*.

Table 1. *Physical and chemical properties of the soil*

Properties	Results
Texture	clay
pH	8.68 ± 0.01
Electronic conductivity	335.5 ± 3.5 µsm/cm
Organic matter	11.86 ± 0.4%
CaCO3	24.25 ± 0.75%

Then, they were categorized into three age classes (juveniles, immature and adults) on the basis of size and presence or absence of genital papilla and clitellium (Bhattacharya and Sahu, 2016). Earthworms are considered sub-adult if they have a full tubercula pubertatis but no clitellum and adult if they are clitellate (Sims and Gerard, 1999). They are considered juvenile if they have neither tubercula pubertatis nor clitellum (Pelosi, 2008).

Fertilizer and treatment

Inorganic fertilizer was supplied from Agricultural Services Directorate of Tebessa area. Mixtures containing all the three principal nutrients (N, P and K) are termed complete fertilizers. NPK fertilizer contains: 15% N + 15% P_2O_5 + 15% K_2O. The studies carried out in plastic containers of 20 × 10 × 7 cm (length × width × depth), were set up each with 500 gm of native soil. Before the initiation of the exposure test, earthworms were rinsed in tap water and moved to Petri dishes on moist filter paper to void their gut contents.

Serial amounts of the dry powder (400 to 1200 mg) were prepared (*Fig. 1A*). These were added to the soil surface and then mixed thoroughly with enough water to ensure a homogeneous mixture (*Fig. 1B*). For the control treatment, distilled water was used. The test was carried out with 4 replicates each containing 10 earthworms per dose. The tested fertilizer was replaced weekly using the same concentration. The mortality was monitored by counting the number of dead earthworms at the end of different time periods (1st, 2nd, 3rd, and 4th week) and Finney's probit method was followed to calculate LD_{25}, LD_{50} and LD_{90} values.

Earthworms were considered dead if they showed any of the following statuses: disappeared, lacking movement and no response to a definite tactile stimulus (Zheng et al., 2016). The choice of doses was made according to studies of Shruthi et al. (2017) and on the basis of the high mortality rate observed after treatment with the recommended agricultural dose (RAD corresponding to LD_{90}).

http://www.aloki.hu ● ISSN 1589 1623 (Print) ● ISSN 1785 0037 (Online)
DOI: http://dx.doi.org/10.15666/aeer/1902_12471266
© 2021, ALÖKI Kft., Budapest, Hungary

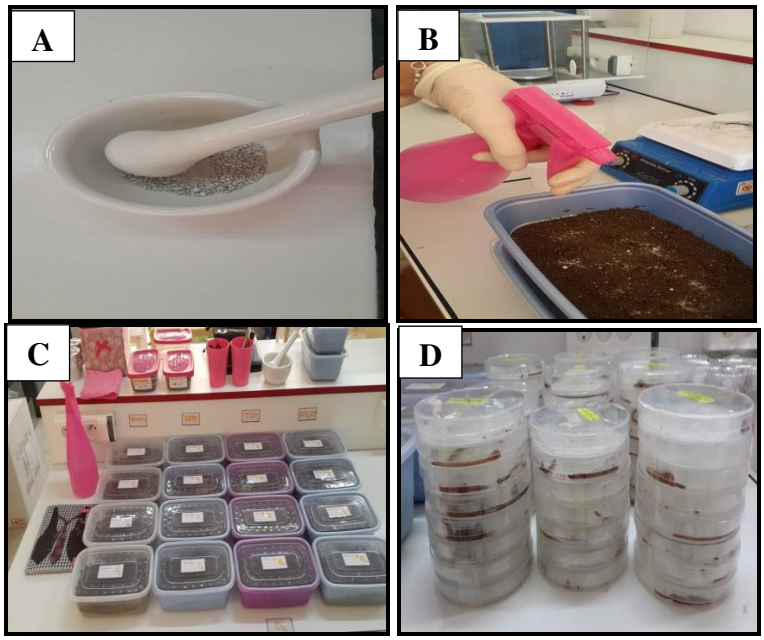


Figure 1. *Experimental protocol. (A) Preparation of fertilizer (powder). (B) Treatment of the soil. (C) Earthworm rearing and treatment. (D) Voiding of the earthworm*

Performance test

Ten individual earthworms were added to each plastic container and the sets were subdivided as follows; five plastic containers were applied for a control test with only water and 10 others were treated with two doses of NPK, corresponding to the LD_{25} and LD_{50} respectively (*Fig. 1C*). During the test period, earthworms were separated from the test substrate, counted, cleaned with deionized water and blotted with filter paper. Then, they were weighed on weeks 1, 2, 3, and 4, using an electro-balance. All the replicates were examined on each sampling date and the worms then replaced in the containers.

The weights of earthworms in each concentration reported from the various exposure periods were then used to calculate the growth inhibition as follows Shi et al. (2007):

$$GIn = (W_0 - W_t/W_0) \times 100 \quad \text{(Eq.1)}$$

where *GIn* is the growth inhibition for dose group *n*, W_0 is the weight on day 0 and W_t is the weight after *t* days of exposure.

Specific growth rates for a specific interval (SGR) were calculated by the formula:

$$SGRn = (\ln Wj - \ln Wi)/(tj - ti) \quad \text{(Eq.2)}$$

where SGRn is the specific growth rate for a specific interval for dose group n from day i to j, Wi is the weight on day i and Wj is the weight after j days of exposure (OECD, 2006).

Determination of biochemical composition

Specimens of both treated (LD_{25} and LD_{50}) and control earthworms removed from the soil, were cleaned with deionized water, and moved to Petri dishes on moist filter

http://www.aloki.hu ● ISSN 1589 1623 (Print) ● ISSN 1785 0037 (Online)
DOI: http://dx.doi.org/10.15666/aeer/1902_12471266
© 2021, ALÖKI Kft., Budapest, Hungary

paper to void their gut contents (*Fig. 1D*). One earthworm was selected from each container to determine biochemical composition at the tested period (i.e., at 1st, 2nd, 3rd, and 4th week).

The main components (proteins, carbohydrates and lipids) were extracted following the procedure of Shibko et al. (1967). Fragments of the body (50 mg) were extracted in 1 ml of TCA (20%). In brief, quantification of proteins was carried following the Coomassie Brilliant Blue G-250 dye-binding method of Bradford (1976) with bovine serum albumin as a standard. The absorbance was measured at 595 nm. Carbohydrates were determined as described by Duchateau and Florkin (1959) using anthrone as reagent and glucose as standard. Lipids were measured by the vanillin method of Goldsworthy (1972) and the table oil (99% triglycerides) used as a standard. Data were expressed in µg per mg of fresh tissue and assays conducted with 3 replicates per treatment.

Glutathione peroxidase assay (GPx)

The same sample preparation protocol was followed for the biomarkers assay. GPx assay was performed according to Flohe and Gunzler (1984). Fragments of the body (50 mg) of control and treated earthworm (LD_{25} and LD_{50}) were homogenized in 1 ml of phosphate buffer (pH 7.8). The homogenate was centrifuged (3000 rpm for 10 min), and the supernatant was recovered as an enzyme source. The assay was performed on an aliquot of 200 µl of supernatant added to 400 µl of the GSH solution (0.2 mM, pH 10). Absorbance reading was performed after 5 min at 412 nm. Data were expressed in µM per min per mg of protein and assays conducted with 3 replicates per treatment.

Lactate dehydrogenase assay (LDH)

The determination was based on the conversion of lactate to pyruvate or pyruvate to lactate. The assay of LDH was conducted according to the method of Hill and Levi (1954) as previously described (Sifi and Soltani, 2019) using NAD (nicotinamide adenine dinucleotide) as substrate. Fragments of the body (50 mg) of control and treated earthworm (LD_{25} and LD_{50}) were homogenized in 1 ml of Tris/HCl (0.1 M, pH 7.2). The homogenate was centrifuged (3000 rpm for 5 min) and then the supernatant recovered for use as enzyme source. The assay was performed with 50 µl of supernatant added to 675 µl of substrate buffer (0.2 M, pH 10) and 50 µl of NAD solution. The absorbance reading was done every minute for 5 min at 340 nm. Data was expressed in µM per min per mg of protein and assays conducted with 3 replicates per treatment.

Glutathione S-transferase assay (GST)

The assay of GST was carried out according to Habig et al. (1974) previously described (Dris et al., 2017) with use of GSH (5 mM). Fragments of the body (50 mg) of control and treated earthworm (LD_{25} and LD_{50}) were homogenized in 1 ml phosphate buffer (0.1 M, pH 6). The homogenate was centrifuged (14000 rpm for 30 min). 200 µl of the resulting supernatant was added to 1.2 ml of the mixture GSH-CDNB in phosphate buffer (0.1, pH 7). Changes in absorbance were measured at 340 nm every minute for a period of 5 min. Data was expressed in nM per min per mg of protein and assays conducted with 3 replicates per treatment.

http://www.aloki.hu ● ISSN 1589 1623 (Print) ● ISSN 1785 0037 (Online)
DOI: http://dx.doi.org/10.15666/aeer/1902_12471266
© 2021, ALÖKI Kft., Budapest, Hungary

Glutathione assay (GSH)

The assay of GSH was conducted according to the method of Weckberker and Cory (1988) previously used (Maiza et al., 2013). Fragments of the body (50 mg) of control and treated earthworm (LD_{25} and LD_{50}) were homogenized in 1 ml of EDTA (0.02 M, pH 6). The homogenate was subjected to a deproteinization with sulfosalysilic acid (SSA) at 0.25%. The optical density was measured at 412 nm. Data were expressed in μM per mg of protein and assays conducted with 3 replicates per treatment.

Statistical analysis

Data are presented as a mean value ± SEM (standard error mean) in each treatment group. The normality of data was verified using the Kolmogorov-Smirnov test, and the homogeneity of variances was checked by Levene's test. Comparison of the experimental groups was tested by analysis of variance (ANOVA), and means were tested for statistical significance by a post hoc Tukey's honestly significant difference test. The statistical tests were performed using GraphPad Prism, version 7.00 (GraphPad Software, San Diego, CA, USA), where $p < 0.05$ indicates a statistically significant difference.

Results

Effect on juvenile earthworm

Different doses of NPK fertilizer: 400, 500, 600, and 1200 mg were applied on juvenile earthworm of *A. caliginosa* exhibited toxicity. The mortality was scored at 4weeks after treatment. There was a wide variation in toxicity of NPK on juvenile earthworm with respect to dose conducted in five replicates. About 6% mortality of earthworms were recorded when they were exposed to 400 mg of NPK in all the five replicates. The mortality increased to 24% when they were exposed to 500 mg of NPK followed by 40% at 600 mg, and 96% of the juvenile earthworms died at 1200 mg of NPK. Lethal doses (LD_{25}, LD_{50} and LD_{90}) values with 95% confidence limit for juvenile earthworm were of 518.9, 644.9 and 996.4 mg respectively (*Table 2*). No mortality was reported in control series.

Table 2. *Toxicity test for A. caliginosa exposed to different doses of NPK*

Doses (mg)	Mortality (%)	LD_{25} (95% FL)	LD_{50} (95% FL)	LD_{90} (95% FL)	HillSlope	R^2
400	6.00 ± 4.80 a	**518.9** (479.1 to 557.3)	**644.9** (598.6 to 710.8)	**996.4** (801.2 to 1284)	0.507	0.99
500	24.00 ± 4.80 b					
600	40.00 ± 4.00 b					
1200	43.00 ± 9.08 c					

Effect on growth

Specific growth rate of earthworms is shown in *Figure 2A,* positive Specific growth rate means the weight of earthworms increased, and negative ones represent growth inhibition of earthworms at specific intervals. The SGR of the earthworms in both dose-treated during all the exposure intervals exposed to NPK were negative. With the time increase, the specific growth rates decreased at all tested periods: 0-1 week (F_2,

http://www.aloki.hu ● ISSN 1589 1623 (Print) ● ISSN 1785 0037 (Online)
DOI: http://dx.doi.org/10.15666/aeer/1902_12471266
© 2021, ALÖKI Kft., Budapest, Hungary

$_{12}$ = 46.53; p < 0.001), 1-2 week ($F_{2,12}$ = 18.57; p < 0.001), 2-3 week ($F_{2,\ 12}$ = 17.95; p < 0.001) and 3-4 week ($F_{2,\ 12}$ = 103.3; p < 0.001).

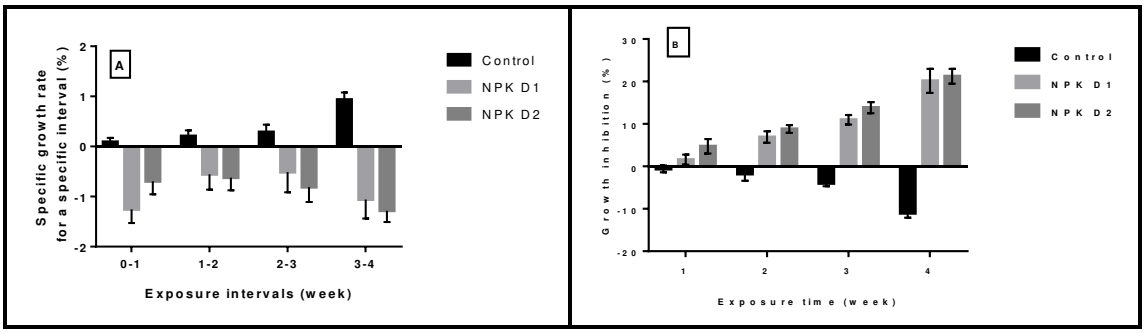


Figure 2. *Effects of fertilizer administrated at two doses on specific growth rate (%) (A) and growth inhibition (%) (B) in juvenile of A. caliginosa (mean ± SEM, n = 5 repeats, each containing 10 individuals)*

The growth inhibition of earthworms at 1, 2, 3, and 4 weeks for the two doses of fertilizer are shown in *Figure 2B*. Under the experimental conditions used here, the growth inhibition for the controls was negative. The fertilizer showed inhibitory effects on the gain of weight at the first ($F_{2,12}$ = 21.39 : p < 0.001), the second ($F_{2,12}$ = 88.64 : p < 0.001), the third ($F_{2,12}$ = 393.3 : p < 0.001: p < 0.001) and the fourth week ($F_{2,12}$ = 409.3 : p < 0.001) with a dose relationship at the first (Dose 1 vs Dose 2: p = 0.0059) and the third week (Dose 1 vs Dose 2: p = 0.0032).

Effects on biochemical components

Changes in main biochemical components (lipids, carbohydrates and proteins) were determined in whole body of *A. caliginosa* juveniles at different times of exposure (1st week, 2nd week, 3rd week and 4th week) to tested doses (500 and 600 mg) (*Figs. 3, 4* and *5*).

According to ANOVA test, results showed a significant decrease (p < 0.001) in the lipid contents in both treated series (Dose 1 and Dose 2) as compared to controls during all tested exposure time with a dose-response relationship: 1st week ($F_{2,\ 6}$ = 38.36; p < 0.001), 2nd week ($F_{2,\ 6}$ = 363.1; p < 0.001), 3rd week ($F_{2,\ 6}$ = 69.09; p < 0.001) and 4th week ($F_{2,\ 6}$ = 4609; p < 0.001).

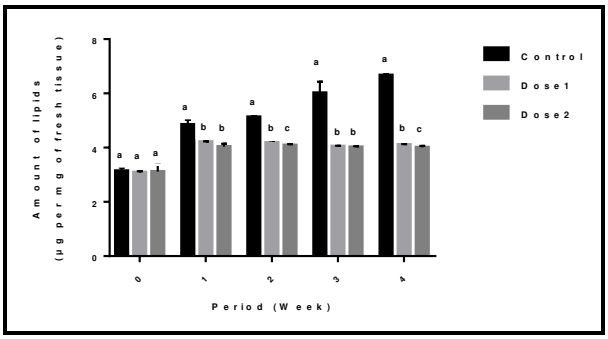


Figure 3. *Effects of fertilizer applied at two doses on amounts (µg per mg of fresh tissue) of lipids in juvenile of A. caliginosa during the exposure period (mean ± SEM, n = 3 repeats each containing 50 mg of fresh tissue). The different lowercase letters indicate significant differences at the same time based on Tukey's HSD test (p < 0.05)*

http://www.aloki.hu ● ISSN 1589 1623 (Print) ● ISSN 1785 0037 (Online)
DOI: http://dx.doi.org/10.15666/aeer/1902_12471266
© 2021, ALÖKI Kft., Budapest, Hungary

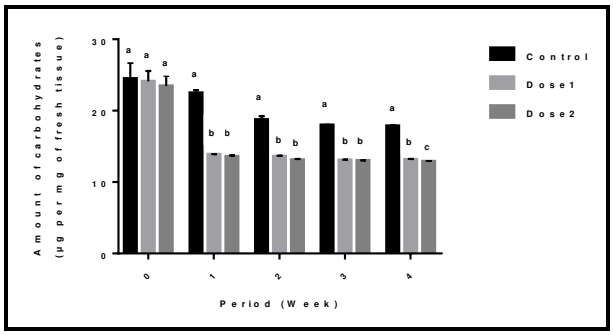


Figure 4. *Effects of fertilizer applied at two doses on amounts (µg per mg of fresh tissue) of carbohydrates in juvenile of A. caliginosa during the exposure period (mean ± SEM, n = 3 pools each containing 50 mg of fresh tissue). The different lowercase letters indicate significant differences at the same time based on Tukey's HSD test (p < 0.05)*

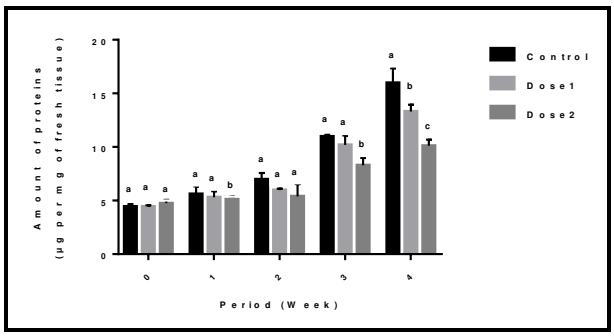


Figure 5. *Effects of fertilizer applied at two doses on amounts (µg per mg of fresh tissue) of proteins in juvenile of A. caliginosa during the exposure period (mean ± SEM, n = 3 repeats each containing 50 mg of fresh tissue). The different lowercase letters indicate significant differences at the same time based on Tukey's HSD test (p < 0.05)*

The carbohydrate contents decreased significantly at the 1st ($F_{2, 6} = 1247$, $p < 0.001$), the 2nd ($F_{2,6} = 324.3$; $p < 0.001$) and the 3rd week ($F_{2, 6} = 28509$; $p < 0.001$) without dose-response relationship and at the 4th week ($F_{2, 6} = 4218$; $p < 0.001$) with a dose-response relationship (Dose 1 vs Dose 2 : $p = 0.035$).

Lastly, concerning the protein rates, results showed a significant decrease at 1st week ($F_{2, 6} = 5.23$, $p = 0.048$) and 3rd week ($F_{2, 6} = 13.48$; $p = 0.006$) with the highest dose (Dose 2) and at 4th week ($F_{2, 6} = 29.16$; $p < 0.001$) with a dose-response relationship (Dose 1 vs Dose 2; $p = 0.014$).

Effects on biomarkers

Results of the specific activities of antioxidant defense enzyme (GPx, LDH and GST) and a cofactor GSH in *A. caliginosa* are summarized in *Figures 6, 7, 8* and *9*. They show that values are very similar in different tested periods. GPx activity increased significantly with the two doses at the first (Control vs Dose 1: $p = 0.038$; Control vs Dose 2: $p = 0.017$) and the fourth week (Control vs Dose 1: $p = 0.033$; Control vs Dose 2: $p = 0.013$) without dose-response relationship. At the third week, an activation of GPx was observed with the highest dose (Dose 2) ($p = 0.024$). No effect of the NPK was reported with the two doses applied ($P > 0.05$) at the second week.

http://www.aloki.hu ● ISSN 1589 1623 (Print) ● ISSN 1785 0037 (Online)
DOI: http://dx.doi.org/10.15666/aeer/1902_12471266
© 2021, ALÖKI Kft., Budapest, Hungary

Concerning LDH activity, a significant increase was observed in first, second, third and fourth week with the highest dose compared to controls ($p = 0.002$; 0.001; 0.002 and 0.005 respectively). No effect of the product was reported with the lowest applied dose ($P > 0.05$) in all tested periods.

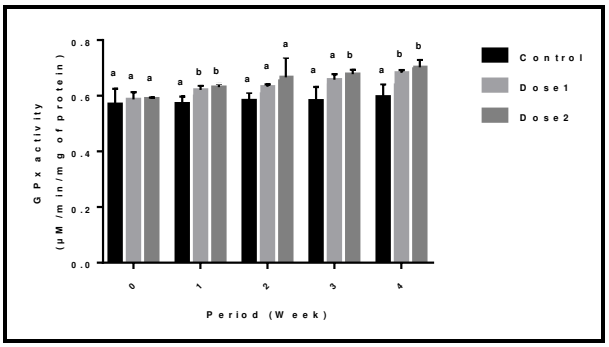


Figure 6. *Effects of fertilizer applied at two doses on GPx activity (µm/min/mg of protein) in juvenile of A. caliginosa during the exposure period (mean ± SEM, n = 3 repeats each containing 50 mg of fresh tissue). The different lowercase letters indicate significant differences at the same time based on Tukey's HSD test ($p < 0.05$)*

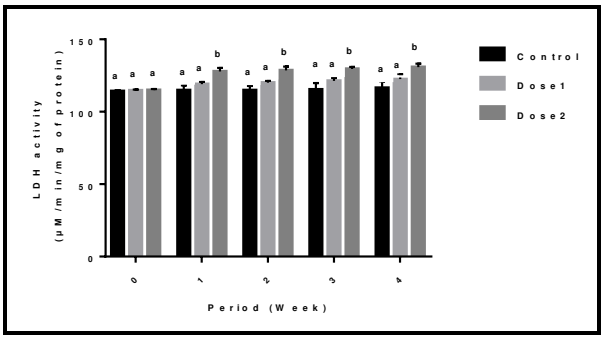


Figure 7. *Effects of fertilizer applied at two doses on LDH activity (µM/min/mg of protein) in juvenile of A. caliginosa during the exposure period (mean ± SEM, n = 3 pools each containing 50 mg of fresh tissue). The different lowercase letters indicate significant differences at the same time based on Tukey's HSD test ($p < 0.05$)*

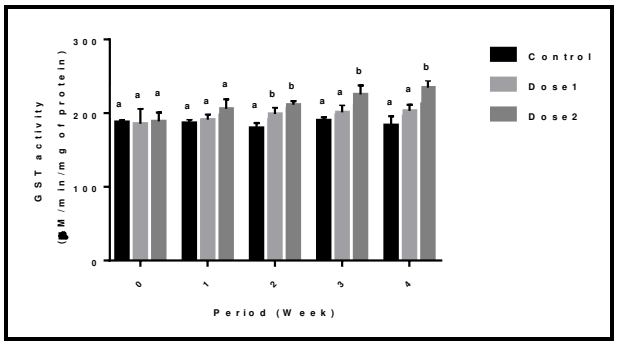


Figure 8. *Effects of fertilizer applied at two doses on GST activity (nM/min/mg of protein) in juvenile of A. caliginosa during the exposure period (mean ± SEM, n = 3 repeats each containing 50 mg of fresh tissue). The different lowercase letters indicate significant differences at the same time based on Tukey's HSD test ($p < 0.05$)*

http://www.aloki.hu ● ISSN 1589 1623 (Print) ● ISSN 1785 0037 (Online)
DOI: http://dx.doi.org/10.15666/aeer/1902_12471266
© 2021, ALÖKI Kft., Budapest, Hungary

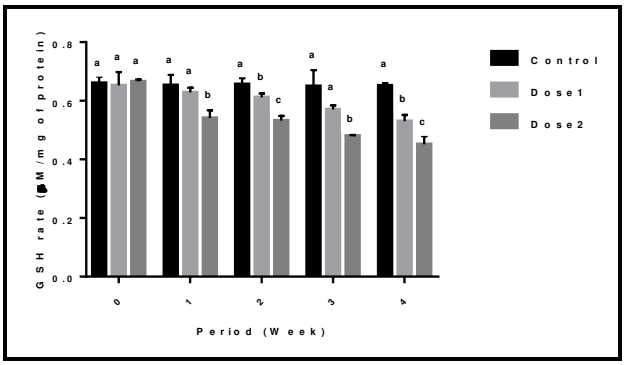


Figure 9. *Effects of fertilizer applied at two doses on GSH rate (µM/mg of protein) in juvenile of A. caliginosa during the exposure period (mean ± SEM, n = 3 pools each containing 50 mg of fresh tissue). The different lowercase letters indicate significant differences at the same time based on Tukey's HSD test ($p < 0.05$)*

Results of the specific activity of GST in *A. caliginosa* exposed to two doses of NPK fertilizer showed a significant increase in GST activity at the second month with two tested doses (Control vs Dose 1: $p = 0.038$; Control vs Dose 2: $p = 0.0039$) and the third (Control vs Dose 2: $p = 0.009$; Dose 1 vs Dose 2: $p = 0.046$) and the fourth month with the highest dose (Control vs Dose 2: $p = 0.002$; Dose 1 vs Dose 2: $p = 0.023$) respectively as compared to control series.

Finally, our results showed a significant decrease in the rate of GSH in the treated series at the first (Control vs Dose 2: $p = 0.005$; Dose 1 vs Dose 2: $p = 0.01$) and the third month with the highest dose (Control vs Dose 2: $p = 0.001$; Dose 1 vs Dose 2: $p = 0.037$) as compared to control series respectively. In addition, we note a significant decrease of GSH rate at the second (Control vs Dose 1: $p = 0.041$; Control vs Dose 2: $p = 0.0003$; Dose 1 vs Dose 2: $p = 0.003$) and the fourth month (Control vs Dose 1: $p = 0.0009$; Control vs Dose 2: $p < 0.0001$; Dose 1 vs Dose 2: $p = 0.008$) with the two tested doses as compared to control series.

Discussion

Effects on juvenile earthworm

Mortality, growth inhibition and biochemical responses are typical indicators for assessing the toxic effects of chemicals on earthworms (Shi et al., 2007; Wu et al., 2011). Study found that the juvenile, immature and adult worms of *Drawida willsi* survived in soil containing up to 250, 370 and 490 mg/kg of NPK respectively. But 100% mortality of juveniles were recorded when worms were exposed to concentration of 490 mg/kg of NPK. However, at a concentration of 640 mg/kg and 730 mg/kg, 96% of immature and 92% of adult mortality was observed respectively. Gradually the mortality increased with the increase of doses (Bhattacharya and Sahu, 2016).

The result of this study further demonstrates that the inorganic mineral fertilizer can also be toxic to earthworms when contacted directly (Abbiramy et al., 2013a). The results of Shruthi et al. (2017) revealed that, when the food material was incorporated with various inorganic fertilizers, there was wide variation among the treatments with respect to mortality of adult and juvenile *Eudrilus eugeniae* earthworms ranging from

http://www.aloki.hu ● ISSN 1589 1623 (Print) ● ISSN 1785 0037 (Online)
DOI: http://dx.doi.org/10.15666/aeer/1902_12471266
© 2021, ALÖKI Kft., Budapest, Hungary

0.00 to 100 per cent. Little information has been generated on the toxicity of inorganic fertilizers to earthworms in sugarcane and agricultural eco-system (Shruthi et al., 2017).

Effects on growth

Earthworms provide key soil functions that favor many positive ecosystem services. These services are important for agroecosystem sustainability but can be degraded by intensive cultural practices (Pelosi et al., 2014). The biggest threat to soil health is pesticides and synthetic chemicals including fertilizers (Miglani and Bisht, 2019). The presence of contaminants in soil may cause stress to the individual which can divert energy from reproduction, burrowing activity and growth (Pelosi et al., 2014). The use of body mass change as a biomarker is thought to be ecologically relevant, as high losses in body mass are thought to lead to negative effects on survival and reproduction (Dittbrenner et al., 2010). These biomass changes could be a good indicator of chemical stress and link chemical effects to energy dynamics and, ultimately, to growth inhibition (Shi et al., 2007; Wu et al., 2012).

Several studies demonstrated that the application of chemical fertilizers as pulverization or powder can have negative effect on earthworm populations (Reinecke and Reineke, 2004; Rai et al., 2014). Weight loss appears to be a valuable indicator of physiological stress, related to the degree of intoxication and time of exposure (Van Gestel et al., 1995; Frampton et al., 2006). Our results showed an inhibitory effect of fertilizer on the gain of weight of *A. caliginosa* juvenile. Some studies have shown that growth of earthworms appeared to be more severely affected at juvenile stage than at adult stage (Zhou et al., 2008). It is reported that the use of inorganic fertilizer influences the biomass of earthworms (Lalthanzara and Ramanujam, 2010). The harmful effect of inorganic fertilizers has been reported to be due to its strong acidic and toxic effect of ammonia on earthworms (Donahue, 2001). It can be interpreted as indication of general health (Olvera-Velona et al., 2008). Robert (2008) reported that nitrogen containing fertilizers like NPK fertilizer are repellant to snails and insects. According to him, the fertilizer act as a repellant by inhibiting feeding and disrupting growth. El-Deeb et al. (2017), showed that three types of NPK fertilizers (high nitrogen, high phosphorus and balanced) treatment can influence *Biomphalaria alexandrina* snail growth, while Ragab and Shoukry (2006) reported that sublethal concentrations of urea had a stronger effect on the growth rate of the same species than sublethal concentrations of ammonium nitrate. Meanwhile, Abdel-Hamid et al. (1998) observed that urea and ammonium nitrate reduced the growth of juvenile *B. alexandrina* snails. Wu et al. (2020) reported that soil pH due to the increasing N fertilizer applications had significant inhibitory effects on the growth of *E. foetida* earthworms. Specific growth and growth inhibition rates in all BDE-47-treated groups of *E. foetida* were significantly different from those of the controls (Xu et al., 2015).

The SGR of this earthworm in almost all the treatments during all the exposure intervals exposed to perfluorooctane sulphonate and perfluorooctanoic acid were negative (Zheng et al., 2016). Growth inhibition of earthworms exposed to lindane and deltamethrin treated soil were significantly higher than those of the controls appeared to be time-dependent, with longer exposure duration resulting in higher inhibition (Shi et al., 2007). Choo and Baker (1998) found that endosulfan and fenamiphos significantly reduced the weight of *Aporrectodea trapezoids* juvenile. Zhou et al. (2006) have reported that the weight of the earthworms was a more sensitive index compared to the mortality in indicating toxic effects of acetochlor and methamidophos. Helling et al.

http://www.aloki.hu ● ISSN 1589 1623 (Print) ● ISSN 1785 0037 (Online)
DOI: http://dx.doi.org/10.15666/aeer/1902_12471266
© 2021, ALÖKI Kft., Budapest, Hungary

(2000) tested in laboratory the effect of copperoxychloride, while Yasmin and D'Souza (2007) investigated the impact of three pesticides, carbendazim, glyphosate and dimethoate on *Eisenia fetida* and found a significant reduction in the earthworm growth in a dose-dependent manner.

Effects on biochemical composition

Edwards (1985) reported that the dry matter of an earthworm body contains 60 to 70% protein, 7 to 10% fat, 8 to 20% carbohydrate, 2.3% minerals and variety of vitamins. Biochemical parameters in organisms exposed to toxic contaminants have been used as biomarkers and may be considered an important diagnostic tool to assess the exposure and effects of xenobiotics (McLoughlin et al., 2000). Changes in energy reserves and/or energy consumption have been used as biomarkers of toxic stress (Świątek and Bednarska, 2019). During stress, organisms need more energy to detoxify, biotransform and excrete the toxicants with the view of minimizing the toxic effects (Khalil, 2016). Very little work has been done to test the effect of fertilizers on the biochemical profile of earthworms.

Lipids play extremely important roles in the normal function of a cell. They not only serve as highly reduced storage form of energy, but they also play an intimate role in the structure of cell membranes and the organelles found in the cell (Kandil et al., 2009). Indeed, lipids are the preferred energy fuel offered to tissues when needed after carbohydrates. During periods of chronic stress, they also constitute another source of energy (Padmaja and Rao, 1994). In our study, a decrease in total lipids was noted in *A. caliginosa* earthworm treated with NPK fertilizer compared to control earthworm.

Carbohydrates are the first energy source mobilized by organisms under toxic stress (Moolman et al., 2007). Thus, it could be suggested that the body fat of earthworms contains the enzyme system necessary to convert glucose into fatty acid and glycerol and that these in turn would be incorporated into neutral phospholipids, triglycerides and phosphatidylcholines which are involved in the growth of the organism (Mosleh et al., 2003). In our research, the tested fertilizer, NPK caused a significant reduction in the energy reserves as evidenced by a reduction in carbohydrate rates. Hence, the adverse effect of atrazine on glucose levels of earthworms may contribute to the reduction of their growth rate (Mosleh et al., 2003). It should be noted that the evolution of glucose level from chlorfluazuron over the test period could be a result of activation of phosphorylase and glucose-6-phosphatase, as reported by Koundinya and Ramamurthi (1979). The exposure of *E. andrei* earthworm to Zn caused an increase in energy consumption at the cellular level, reflecting the relatively high energy demand of responding to toxic stress, but no effect was observed at the whole body level (Świątek and Bednarska, 2019). Some factors such as contamination by metals and soil characteristics influence glycogen, protein and lipid content in *A. caliginosa* with a 50% depletion of energy reserves (Beaumelle et al., 2014).

Protein content is considered to be the building material and involved in the alteration of almost every physiological function. It is always proportional to the growth of worm (Shankerappa, 2013). The protein content of earthworms shows considerable variability between different species and between different experimental treatments in the same species, possibly due to variability in the extent of gut inclusion (Sun and Jiang, 2017). Our experiment showed a significant decrease in protein rates in *A. caliginosa* treated with NPK fertilizer. A lower concentration of soluble protein in treated worms with pesticides suggests that physiological compensatory mechanisms were activated to

http://www.aloki.hu ● ISSN 1589 1623 (Print) ● ISSN 1785 0037 (Online)
DOI: http://dx.doi.org/10.15666/aeer/1902_12471266
© 2021, ALÖKI Kft., Budapest, Hungary

provide intermediates for deriving energy (Mosleh et al., 2003). Because it appears that the lower growth rate of worms may be a result of lower food intake, the reduction in protein content may be due to a catabolism of protein in response to worm energy demand, as suggested for an isopod in response to parathion (Ribeiro et al., 2001). Other studies have looked at the decrease in protein content and enzyme activities in response to agrochemicals (Ismail et al., 1997). In contrast, protein content increased significantly after exposure with TSP and the mixture in *L. terrestris* and no effect of sekator was reported (Mekahlia et al., 2016). This increase might indicate physiological adaptability to compensate stress and the development of cellular defenses induced by the pesticide and phosphate fertilizer impact. Furthermore, protein accumulation could be necessary to restore enzymes or lost in tissue necrosis induced by sekator or TSP exposure (Mosleh et al., 2006). Similarly, Mosleh et al. (2006) observed changes in protein content among aquatic worms *Tubifex tubifex* exposed to copper.

Effects on biomarker responses

The concept of a biomarker as a biological response to a chemical that indicates the degree of exposure or toxic effect is of considerable importance in environmental toxicology (Peakall, 1994). Although the activity of antioxidant enzymes may be increased or inhibited under chemical stress, there is, however, no general rule for the different enzymes (Nmaduka et al., 2018). Earthworm biomarkers have shown promise in various applications. Biomarker responses are of interest because they integrate a wide array of environmental, toxicological and ecological factors that control and modulate exposure contaminants (Arnaud et al., 2000).

Hence, biomarker responses (GPx and LDH activities) were used for evaluating the oxidative stress of earthworm *A. caliginosa* after short-term exposures to NPK.

LDH is involved in the metabolism of carbohydrates in cells and plays a key role in maintaining the balance between the catabolism and anabolism of carbohydrates (Chen et al., 2001). In a stressful environment, LDH converts pyruvate into lactate, which in turn leads to the enhanced concentration of carboxylic acid (lactic acid) in tissues and hemolymph. The results showed that LDH activity increased in response to increased concentrations of fertilizer. Such elevation of enzyme activity could be a result of the increased synthesis of particular enzymes to defend against insecticidal stress and to increase the sources of energy production through the breakdown of energy-rich nucleotides and amino acids (Mosleh et al., 2003). A similar result was obtained for lymphocytes in a report by Liu et al. (2001). The study of Mekahlia et al. (2016) revealed that sekator and triple superphosphate fertilizer, TSP induced the biomarker responses, which was proportional to exposure time and administered dose. A significant increase in the activity of LDH was observed in *Deroceras reticulatum* exposed to Caselio fertilizer (Abd-El Azeem and Sheir, 2018). In addition, a significant increase has been reported in the LDH activity in the land snails (*Eobania vermiculata*) exposed to methomyl (Khalil, 2016).

GPx is another enzyme that can remove H_2O_2 in organisms by using reduced glutathione as a hydrogen donor. The enzymes of the glutathione redox cycle, comprising GPx and GST, play a protective role against oxidative stress (Van der Oost et al., 2003). In our study, a significant increase in GPx activity was found in *A. caliginosa* exposed to NPK fertilizer. The increase in antioxidant enzyme GPx may be an important indicator of the detoxification capacity of the earthworm (Maity et al., 2018). Interestingly, same as our results, a previous study on earthworms (Wang et al.,

http://www.aloki.hu ● ISSN 1589 1623 (Print) ● ISSN 1785 0037 (Online)
DOI: http://dx.doi.org/10.15666/aeer/1902_12471266
© 2021, ALÖKI Kft., Budapest, Hungary

2016) also found that GPx activity was induced by naphthenic acids after 1 d but inhibited after 14 d of exposure. The reasons might be that (i) GPx activity was inhibited by excessive ROS in cells; and (ii) large amounts of glutathione (GSH) were consumed to remove ROS (Cao et al., 2017). While a slight inhibition was observed in GPx activity with high phosphorus fertilizer treatment, a marked induction was obtained in GPx activity after the second week with high nitrogen fertilizer treatment (El-Deeb et al., 2017). Elumalai et al. (2007) indicate that a combined effect of different trace elements induces GST and GPx activity in the whole body tissue of *A. caliginosa* for the increased demand of organisms to eliminate trace elements and manage peroxidative damage by reducing the level of peroxides.

Glutathione S-transferase (GST) is a phase II detoxification enzyme modulated by xenobiotics and thus has been suggested for use as a biomarker indicative of environmental contaminant exposure (Gunderson et al., 2016). GST activity is required for the maintenance of homeostasis of the internal environment (Maity et al., 2018). It aims to combine reduced glutathione (GSH) on electrophilic compounds to facilitate their elimination (Ketterer et al., 1983). By conjugation, GST neutralizes many xenobiotics and endogenous metabolites (Hayes et al., 2005), which seems to be a possible explanation for the reduced GSH content. Interestingly, the induction of GST and GPx activity that can be correlated to the reduction in the GSH level leads to depletion in cellular antioxidant status (Radu et al., 2010). GSH deficiency might be due to the faster rate of GSH consumption for scavenging free radicals non-enzymatically or in a reaction catalyzed by GPx through the oxidation of two molecules of GSH to a molecule of GSSG (oxidized glutathione) (Van der Oost et al., 2003).

In the study of Mekahlia et al. (2016), the biomarker responses (GSH, and GST activity) were used for evaluating the oxidative stress of earthworm *L. terrestris* after short-term exposures to TSP and sekator. The data indicated high sensitivity of biomarkers and the changes in the GST and GSH levels reflect the oxidative stress in the earthworm. Xue et al. (2009) and Maity et al. (2008) mentioned that increased levels of GST were seen in earthworms after exposure to tetrabromobisphenol and lead, respectively. Further, Aly and Schröder (2008) showed that the GST conjugation rate in *Eisenia foetida* varied using two different herbicides namely fenoxaprop and metolachlor.

Conclusion

Soil organisms are exposed to a wide variety of environmental pollutants. Earthworms are significantly influenced by environmental stress, and because of their sensitive metabolic and physiological changes. The results obtained showed that the NPK fertilizer inhibited the increase in weight of *A. caliginosa*, which could be due to the repulsion of the contaminated food. This fertilizer also reduced content of proteins, lipids and carbohydrates in the whole body and caused the activation of the system of detoxification, traduced by an increase of the specific activity of GPx, LDH and GST and a decrease of GSH. Earthworms are useful as test organisms to assess the toxicity of chemical stressors.

Further experiments are warranted to evaluate if these effects will occur in other organisms and can cause chronic effects after more prolonged exposure as well as on other resistance mechanisms mainly detoxification enzymes, histological changes, reproduction and residue accumulation in earthworms.

http://www.aloki.hu ● ISSN 1589 1623 (Print) ● ISSN 1785 0037 (Online)
DOI: http://dx.doi.org/10.15666/aeer/1902_12471266
© 2021, ALÖKI Kft., Budapest, Hungary

Acknowledgements. This study was supported by the National Fund for Scientific Research to Pr. N. Soltani (Laboratory of Applied Animal Biology, Badji Mokhtar University, Annaba) and the Ministry of High Education and Scientific Research of Algeria (PRFU Project to Dr. S. Tine).

REFERENCES

[1] Abbiramy, K. S. K., Ross, P. R. (2013a): Determination of acute toxicity of NPK fertilizers to *Eisenia foetida* using a simple paper contact method. – Int. J. Sci. Res. 2(2): 415-417.

[2] Abbiramy, K. S. K., Ross, P. R. (2013b): Validation of tropical artificial soil ecotoxicological studies on Eisenia foetida against combine fertilizers. – Int. J. Innovative. Res. Studies. 2(7): 212-227.

[3] Abd-El Azeem, H. H., Sheir, S. K. (2018): Impacts of the plant fertilizer, Caselio on the slug, *Deroceras reticulatum* (Gastropoda, Stylommatophora): laboratory studies. – Res. J. Pharm. Biol. Chem. Sci. 9(1): 386-396.

[4] Abdel-Hamid, A. Z., Farrag, E., Rizk, M., Omar, M., Mantawy, M. M. E. (1998): Effect of nitrogen, sulpher and phosphorus containing fertilizers and organophosphorus insecticide on reproduction of *Biomphalaria alexandrina* snails. – Egypt. J. Pharm. Scie. 38: 147-158.

[5] Aly, M. A., Schröder, P. (2008): Effect of herbicides on glutathione S-transferases in the earthworm, *Eisenia fetida*. – Environ. Sci. Poll. Res. Inter. 15: 143-149.

[6] Arnaud, A. C., Saint-Denis, M., Narbonne, J. F., Soler, P., Ribera, D. (2000): Influences of different standardized test methods on biochemical responses in the earthworm *Eisenia fetida*. – Soil. Biol & Biochem. 32(1): 67-73. DOI: 10.1016/S0038-0717(99)00130-3.

[7] Băcanu, C. S., Cristina, S. D., Iuliana Manuela, D. I., Silvius, S. (2019): Agricultural production, soil quality and fertilizer used in Braila County, Romania. – Res. Agr. Agron. 9. DOI: 10.5171/2019.970358.

[8] Beaumelle, L., Lamy, I., Cheviron, N., Hedde, M. (2014): Is there a relationship between earthworm energy reserves and metal availability after exposure to field-contaminated soils? – Environ. Poll. 191: 182-189.

[9] Bhattacharya, A., Sahu, S. K. (2014): Lethal effect of urea on soil biota: a laboratory study on earthworm (*Drawida willsi*). – J. Biodivers. Environ. Sci. 4(6): 64-72.

[10] Bhattacharya, A., Sahu, S. K. (2016): Acute toxicity of NPK fertilizer on soil ecosystem using earthworm, *Drawida willsi* as a test specimen. – Int. J. Adv. Pharm. Biol. Chem. 5(3): 233-238.

[11] Bouazdia, K., Habes, D. (2017): Earthworm species identified in the region of Tebessa (Eastern Algeria). – Int. J. Zool. Res. 13: 38-44. DOI: 10.3923/ijzr.2017.38.44.

[12] Bouché, M. B. (1972): Lombriciens de France: écologie et systématique. – Institut national de la recherche agronomique, Paris.

[13] Bradford, M. (1976): A rapid and sensitive method for the quantitation microgram quantities of protein utilizing the principle of protein-dye binding. – Anal. Biochem. 72: 248-254.

[14] Callaham, M. A., Blair, J. M., Todd, T. C., Kitchen, D. J., Whiles, M. R. (2003): Macroinvertebrates in North American tallgrass prairie soils: effects of fire, mowing, and fertilization on density and biomass. – Soil. Biol. Biochem. 35: 1079-1093. DOI: 10.1016/S0038-0717(03)00153-6.

[15] Cao, W., Li, M., Wu, T., Feng, F., Feng, T., Xu, Y., Sun, C. (2017): αMSH prevents ROS-induced apoptosis by inhibiting Foxo1/mTORC2 in mice adipose tissue. – Oncotarget. 8(25): 40872-40884. DOI: 10.18632/oncotarget.16606.

[16] Chen, K., Liu, Q., Xie, L., Sharp, P. A., Wang, D. I. (2001): Engineering of a mammalian cell line for reduction of lactate formation and high monoclonal antibody production. – Biotech. Bioeng. 72(1): 55-61.

http://www.aloki.hu ● ISSN 1589 1623 (Print) ● ISSN 1785 0037 (Online)
DOI: http://dx.doi.org/10.15666/aeer/1902_12471266
© 2021, ALÖKI Kft., Budapest, Hungary

[17] Choo, L. P. D., Baker, G. H. (1998): Influence of four commonly used pesticides on the survival, growth, and reproduction of the earthworm *Aporrectodea trapezoides* (Lumbricidae). – Aust. J. Agr. Res. 49(8): 1297-1303. DOI: 10.1071/A98021.
[18] Curry, J. P., Dohert, P., Purvis, G., Schmidt, O. (2008): Relationships between earthworm populations and management intensity in cattle-grazed pastures in Ireland. – Appl. Soil. Ecol. 39: 58-64. DOI: 10.1016/j.apsoil.2007.11.005.
[19] Denoyelle, R., Rault M., Mazzia C., Mascle O., Capowiez Y. 2007. Cholinesterase activity as a biomarker of pesticide exposure in Allolobophora chlorotica earthworms living in apple orchards under different management strategies. – Envir. Toxicol. Chem. 26(12): 2644-2649. DOI: 10.1897/06-355.1.
[20] Dittbrenner, N., Triebskorn, R., Moser, I., Capowiez, Y. (2010): Physiological and behavioural effects of imidacloprid on two ecologically relevant earthworm species (*Lumbricus terrestris* and *Aporrectodea caliginosa*). – Ecotox. 19: 1567-1573. DOI: 10.1007/s10646-010-0542-8.
[21] Donahue, S. (2001): Agricultural management effects on earthworm populations. – Soil. Qual. Tech. Note. 11: 1-8.
[22] Dris, D., Tine-Djebbar, F., Bouabida, H., Soltani, N. (2017): Chemical composition and activity of an *Ocimum basilicum* essential oil on *Culex pipiens* larvae: toxicological, biometrical and biochemical. – South African Journal of Botany. 113: 362-369.
[23] Duchateau, G., Florkin, M. (1959): Sur la tréhalosémie des insectes et sa signification. – Arch. Insect. Biochem. Physiol. 67: 306-314.
[24] Edwards, C. A. (1985): Production of feed protein from animal waste by earthworms. – Phil. Trans. R. Soc. Lon. B. 310: 299-307.
[25] Edwards, C. A., Bohlen, P. J. (1992): The effects of toxic chemicals on earthworms. – Rev. Environ. Contam. Toxicol. 125: 23-99.
[26] El-Deeb, F., Mohamed-Assem, S. M., Hasheesh, W. S. H., Hussein, R. M. A., Sayed, S. S. M. (2017): Biomarkers of oxidative stress in *Biomphalaria alexandrina* snails for assessing the effects of certain inorganic fertilisers. – Mollusc. Res. 37(4): 289-294. DOI: 10.1080/13235818.2017.1357783.
[27] Elumalai, M., Antunes, C., Guillhermino, L. (2007): Enzymatic biomarkers in the crab *Carcinus maenas* from Minho River estuary (NW Portugal) exposed to zinc and mercury. – Chemosphere. 66(7): 1249-1255.
[28] Estevez, B., N'Dayegamiye, A., Coderre, D. (1996): The effect on earthworm abundance and selected soil properties after 14 years of solid cattle manure and NPK Mg fertilizer application. – Can. J. Soil. Sci. 76: 351-355.
[29] Flohe, L., Gunzler, W. A. (1984): Analysis of glutathione peroxidase. – Methods. Enzymol. 105: 114-21.
[30] Frampton, G. K., Jansch, S., Cott-Fordsmand, S. J. J., Rombke, J., Van den Brink, P. J. (2006): Effects of pesticides on soil invertebrates in laboratory studies: a review and analysis using species sensitivity distributions. – Envir. Toxicol. Chem. 25(9): 2480-2489. DOI: 10.1897/05-438r.1.
[31] Gill, H. K., Garg, H. (2014): Pesticide: environmental impacts and management strategies. – Pestic. Toxic. Asp. 8: 187-230. DOI: 10.5772/57399.
[32] Goldsworthy, A. C., Mordue, W., Guthkelch, J. (1972): Studies on insect adipokinetic hormones. – Gen. Comp. Endocrinol. 18(3): 545-551. DOI: 10.1016/0016-6480(72)90034-2.
[33] Gunderson, M. P., Pickett, M. A., Martin, J. T., Hulse, E. J., Smith, S. S., Smith, L. A., Campbell, R. M., Lower, R. H., Boggs, A. S., Guillette, L. J. (2016): Variations in hepatic biomarkers in American alligators (*Alligator mississippiensis*) from three sites in Florida, USA. – Chemosphere. 155: 180-1.
[34] Habig, W. H., Pabst, M. J., Jakoby, W. B. (1974): Glutathione S-Tranferases: the first enzymatic step in mercapturic acid formation. – J. Biol. Chem. 249: 7130-7139.

http://www.aloki.hu ● ISSN 1589 1623 (Print) ● ISSN 1785 0037 (Online)
DOI: http://dx.doi.org/10.15666/aeer/1902_12471266
© 2021, ALÖKI Kft., Budapest, Hungary

[35] Hayes, J. D., Flanagan, J. U., Jowsey, I. R. (2005): Glutathione transferases. – Annu. Rev. Pharmacol. Toxicol. 45: 51-88.
[36] Helling, B., Reinecke, S. A., Reinecke, A. J. (2000): Effects of the fungicide copper oxychloride on the growth and reproduction of *Eisenia fetida* (Oligochaeta). – Ecotoxicol. Environ. Safety. 46(1): 108-116. DOI: 10.1006/eesa.1999.1880.
[37] Hill, B. R., Levi, C. (1954): Elevation of a serum component in neoplastic disease. – Cancer. Res. 14: 513-515.
[38] Ismail, S. M., Ahmed, Y. M., Mosleh, Y. Y., Ahmed, T. M. (1997): The activities of some proteins and protein related enzymes of earthworms as biomarker for atrazine exposure. – Toxicol. Environ. Chem. 63: 141-148. DOI: 10.1080/02772249709358524.
[39] Kandil, M. A., El-Deeb, H. I., Mobarak, S. A., Eweis, E. A. (2009): Biochemical impacts of methomyl and abamectin and their binary mixtures with acetylsalicylic acid against the land snails *Eobania vermiculata* and *Monacha obstructa*. – Z. Gesamte Exp. Med. 135: 545-561.
[40] Ketterer, B., Coles, B., Meyer, D. J. (1983): The role of glutathione in detoxication. – Environ. Health Perspect. 49: 59-69.
[41] Khalil, A. M. (2016): Impact of methomyl lannate on physiological parameters of the land snail Eobania vermiculata. – J. Basic. Appl. Zool. 74: 1-7.
[42] Koundinya, P. R., Ramamurthi, R. (1979): Effect of organophosphate pesticide Sumithion (Fenitrothion) on some aspects of carbohydrate metabolism in a freshwater fish, *Sarotherodon* (Tilapia) *mossambicus* (Peters). – Experientia. 35(12): 1632-1633.
[43] Lal, R. (2004): Soil carbon sequestration to migrate climate change. – Geoderma 123: 1-22. DOI: 10.1016/j.geoderma.2004.01.032.
[44] Lalthanzara, H., Ramanujam, S. N. (2010): Effect of fertilizer (NPK) on earthworm population in the agro-forestry system of Mizoram India. – Sci. Vis. 10(4): 159-167.
[45] Lijun, L., Xuemei, L., Yaping, G., Enbo, M. (2005): Activity of the enzymes of the antioxidative system in cadmium-treated Oxya chinensis (Orthoptera Acridoidae). – Envir. Toxicol. Pharmacol. 20(3): 412-416. DOI: 10.1016/j.etap.2005.04.001.
[46] Liu, M. T., Armstrong, D., Hamilton, T. A., Lane. (2001): Expression of Mig (monokine induced by interferon-γ) is important in T lymphocyte recruitment and host defense following viral infection of the central nervous system. – J. Immunol. 166: 1790-1795. DOI: 10.4049/jimmunol.166.3.1790.
[47] Maity, S., Roy, S., Chaudhury, S., Bhattacharya, S. (2008): Antioxidant responses of the earthworm *Lampito mauritii* exposed to Pb and Zn contaminated soil. – Environ. Poll. 151: 1-7.
[48] Maity, S., Poráčová, J., Dey, P., Vašková, J., Vaško, L., Sedlák, V., Blaščáková, M. M. (2018): Antioxidant responses in the earthworm Aporrectodea caliginosa of eastern Slovakia: application of principal component analysis as a tool to identify metal contaminated areas. – Environ. Monitor. Assess. 190(1): 21. DOI: 10.1007/s10661-017-6377-5.
[49] Maiza, R. (2013): Sublethal effects on reproduction and biomarkers by spinosad and indoxacarb in cockroaches *Blattella germanica*. – Bull. Insectol. 66(1): 11-20.
[50] Marhan, S., Scheu, S. (2005): The influence of mineral and organic fertilizers on the growth of the endogenic earthworm *Octolasion tyrtaeum* (Savigny). – Pedobiologia 49(3): 239-249. DOI: 10.1016/j.pedobi.2004.11.002.
[51] McLoughlin, N., Yin, D., Maltby, L., Wood, R. M., Yu, H. (2000): Evaluation of sensitivity and specificity of two crustacean biochemical biomarkers. – Environ. Toxicol. Chem. 19(8): 2085-2092. DOI: 10.1002/etc.5620190818.
[52] Mekahlia, M. N., Tine, S., Amieur, H., Salhi, H. (2016): In vitro biomarker responses of earthworm Lumbricus terrestris exposed to herbicide Sekator and phosphate fertilizer. – Water. Air. Soil. Pollut. 227: 15. DOI: 10.1007/s11270-015-2712-z.
[53] Miglani, R., Bisht, S. S. (2019): World of earthworms with pesticides and insecticides. – Interdiscip. Toxicol. 12: 71-82. DOI: 10.2478/intox-2019-0008.

http://www.aloki.hu ● ISSN 1589 1623 (Print) ● ISSN 1785 0037 (Online)
DOI: http://dx.doi.org/10.15666/aeer/1902_12471266
© 2021, ALÖKI Kft., Budapest, Hungary

[54] Moolman, L., Van Vuren, J. H. J., Wepener, V. (2007): Comparative studies on the uptake and effects of cadmium and zinc on the cellular energy allocation of two freshwater gastropods. – Ecotox. Environ. Safe. 68: 443-450. https://doi.org/10.1016/j.ecoenv.2006.12.017.

[55] Mosleh, Y. M., Saad, M. M., Ismail, M. T. A., Ahmed, Y. M. (2003): Comparative Toxicity and Biochemical responses of certain pesticides to the mature earthworm *Aporrectodea caliginosa* under laboratory conditions. – Environ. Toxicol. 18(5): 338-346. DOI: 10.1002/tox.10134.

[56] Mosleh, Y. Y., Paris-Palacios, S., Biagianti-Risbourg, S. (2006): Metallothioneins induction and antioxidative response in aquatic worms *Tubifex tubifex* (Oligochaeta, Tubificidae) exposed to copper. – Chemosphere. 64(1): 121-128. DOI: 10.1016/j.chemosphere. 2005.10.045.

[57] Nmaduka, N. J., Samuel, U. C., Akudo, O. C. (2018): Biomarkers in Achatina achatina as ecological risk assessment models of mining activities. – Res. J. Environ. Toxicol. 12: 63-72.

[58] OECD (2006): Guideline for Testing of Chemicals Test 201: Freshwater Alga and Cyanobacteria, Growth Inhibition Test. – Organization for Economic Cooperation and Development (OECD), Paris.

[59] Olvera-Velona, A., Capowiez, Y., Mascle, O., Ortiz-Hernandez, L., Benoit, P. (2008): Assessment of the toxicity of ethylparthion to earthworms (*Aporrectodea caliginosa*) using behavioural, physiological and biochemical markers. – Appl. Soil. Ecol. 40(3): 476-483. DOI: 10.1016/j.apsoil.2008.07.002.

[60] Padmaja, R. J., Rao, M. B. (1994): Effect of an organochlorine and three organophosphate pesticides on glucose, glycogen, lipid, and protein contents in tissues of the freshwater snail *Bellamya dissimilis* (moiler). – Bull. Environ. Contam. Toxicol. 53: 142-148.

[61] Peakall, D. B. (1994): The role of biomarkers in environmental assessment (1). Introduction. – Ecotoxicol. 3(3): 157-160.

[62] Pelosi, C. (2008): Modelisation de la dynamique d'une population de vers de terre *Lumbricus terrestris* au champ. – PhD thesis, l'Institut des Sciences et Industries du Vivant et de l'Environnement (Agro Paris Tech), France.

[63] Pelosi, C., Barot, S., Capowiez, Y., Hedde, M., Vandenbulcke, F. (2014): Pesticides and earthworms: a review. – Agro. Sustain. Dev. 34(1): 199-228. DOI: 10.1007/s13593-013-0151-z.

[64] Radu, M., Munteanu, M. C., Petrache, S., Serban, A. I., Dinu, D., Hermenean, A., Sima, C., Dinischiotu, A. (2010): Depletion of intracellular glutathione and increased lipid peroxidation mediate cytotoxicity of hematite nanoparticles in MRC-5 cells. – Acta. Biochim. Pol. 57: 355-360.

[65] Ragab, F. M. A., Shoukry, N. M. (2006): Influence of certain fertilizers on the activity of some molluscicides against *Biomphalaria alexandrina* and *Lymnaea natalensis* snails. – J. Egypt Soc. Parasitol. 36(3): 959-977.

[66] Rai, N., Ashiya, P., Rathore, D. S. (2014): Comparative study of the effect of chemical fertilizers and organic fertilizers on *Eisenia foetida*. – Int. J. Innov. Res. Sci. 3(5): 12991-12998.

[67] Reinecke, A. J., Reinecke, S. A. (2004): Earthworm as Test Organisms in Ecotoxicological Assessment of Toxicant Impacts on Ecosystems. – In: Edwards, C. A. (ed.) Earthworm Ecology, CRC Press LLC: Boca Raton, FL, pp. 299-320.

[68] Reinecke, S. A., Reinecke, A. J. (2007): The impact of organophosphate pesticides in orchards on earthworms in the Western Cape, South Africa. – Ecotoxicol. Envir. Safe. 66(2): 244-251. DOI: 10.1016/j.ecoenv.2005.10.006.

[69] Ribeiro, S., Sousa, J. P., Nogueira, A. J. A., Soares, A. M. V. M. (2001): Effect of endosulfan and parathion on energy reserves and physiological parameters of the

http://www.aloki.hu ● ISSN 1589 1623 (Print) ● ISSN 1785 0037 (Online)
DOI: http://dx.doi.org/10.15666/aeer/1902_12471266
© 2021, ALÖKI Kft., Budapest, Hungary

terrestrial isopod *Porcellio dilatatus*. – Ecotoxicol. Environ. Saf. 49(2): 131-138. DOI: 10.1006/eesa.2001.2045.

[70] Robert, J. B. (2008): Environmental horticulture. Institute of Food and Agriculture Sciences, University of Florida, Gainesville, Florida. – Organic. Farming. 326: 11-12.

[71] Shankerappa, S. (2013): Chemical composition like protein, lipid and glycogen of local three species of earthworms of Gulbarga city, Karnataka India. – Inter. J. Adv. Res. Tech. 2(7): 73-97.

[72] Shi, Y., Shi, Y., Wang, X., Lu, Y., Yan, S. (2007): Comparative effects of lindane and deltamethrin on mortality, growth, and cellulose activity in earthworms (*Eisenia fetida*). – Pestic. Biochem. Physiol. 89: 31-38. DOI: 10.1016/j.pestbp.2007.02.005.

[73] Shibko, S., Koivistoinen, P., Tratnyek, C. A., Newhall, A. R., Friedman, L. (1967): A method for sequential quantitative separation and determination of protein, RNA, DNA, Lipid, and Glycogen from a single rat liver homogenate or from a subcellular fraction. – Anal. Biochem. 19: 514-528.

[74] Shruthi, N., Biradar, A. P., Muzammil, S. (2017): Toxic effect of inorganic fertilizers to earthworms (*Eudrilus eugeniae*). – J. Entomol. Zool. Stud. 5(6): 1135-1137.

[75] Sifi, K., Soltani, N. (2019): Seasonal changes of two biomarkers of oxidative stress (LDH, MDA) in the edible mollusc *Donax trunculus* (Mollusca: Bivalvia) from the Gulf of Annaba (Algeria): correlation with carbohydrate and lipid contents. – Mollusc. Res. 39(1): 44-52.

[76] Sims, R. W., Gerard, B. M. (1999): Earthworms. Notes for the identification of British Species. Synopses of the British Fauna (New Series) No 31 (Revised). – Published for the Linnean Society of London and The Estuarine and Coastal Sciences Association by the Field Studies Council, Shrewsbury.

[77] Sun, Z., Jiang, H. (2017): Nutritive Evaluation of Earthworms as Human Food. – In: Mikkola, H. (ed.) Future Foods. IntechOpen, London, pp.128-141. DOI: 10.5772/intechopen.70271.

[78] Świątek, M., Bednarska, A. J. (2019): Energy reserves and respiration rate in the earthworm *Eisenia andrei* after exposure to zinc in nanoparticle or ionic form Zuzanna. – Environ. Sci. Poll. Res. 26: 24933-24945.

[79] Tindaon, F., Benckiser, G., Ottow, C. G. (2011): Side effects of nitrification inhibitors on non-target microbial processes in soils. – J. Trop. Soils. 16: 7-16. DOI: 10.5400/jts.2011.16.1.7.

[80] Van der Oost, R., Beyer, J., Vermeulen, N. (2003): Fish bioaccumulation and biomarkers in environmental risk assessment: a review. – Environm. Toxicol. Pharmacol. 13: 57-149.

[81] Van Gestel, C. A. M., Zaal, J., Dirven-Van Breemen, E. M., Baerselman, R. (1995): Comparison of two test methods for determining the effects of pesticides on earthworm reproduction. – Acta. Zool. Fennica. 196: 278-283.

[82] Wang, J., Cao, X., Chai, L., Liao, J., Huang, Y., Tang, X. (2016): Oxidative damage of naphthenic acids on the *Eisenia fetida* earthworm. – Environ. Toxicol. 31: 1337-1343.

[83] Weckberker, G., Cory, J. G. (1988): Ribonucleotide reductase activity and growth of glutathione-depleted mouse leukemial 1210 cells in vitro. – Cancer lettres. 40: 257-264.

[84] Wu, S. J., Wu, E. M., Qiu, L. Q., Zhong, W. H., Chen, J. M. (2011): Effects of phenanthrene on the mortality, growth, and anti-oxidant system of earthworms (*Eisenia fetida*) under laboratory conditions. – Chemosphere 83(4): 429-434.

[85] Wu, S. J., Zhang, H. X., Zhao, S. L., Wang, J. L., Li, H. L., Chen, J. M. (2012): Biomarker responses of earthworms (*Eisenia fetida*) exposed to phenanthrene and pyrene both singly and combined in microcosms. – Chemosphere. 87(4): 285-293.

[86] Wu, J., Ren, Z., Zhang, C., Motelica-Heino, M., Deng, T., Wang, H., Dai, J. (2020): Effects of soil acid stress on the survival, growth, reproduction, antioxidant enzyme activities, and protein contents in earthworm (*Eisenia fetida*). – Environ. Scie. Pol. Res. 27: 33419-33428.

http://www.aloki.hu ● ISSN 1589 1623 (Print) ● ISSN 1785 0037 (Online)
DOI: http://dx.doi.org/10.15666/aeer/1902_12471266
© 2021, ALÖKI Kft., Budapest, Hungary

[87] Xu, X. B., Shi, Y. J., Lu, Y. L., Zheng, X. Q., Ritchie, R. J. (2015): Growth inhibition and altered gene transcript levels in earthworms (*Eisenia fetida*) exposed to 2,2',4,4'-tetrabromodiphenyl ether. – Arch Environ Contam Toxicol. DOI: 10.1007/s00244-014-0125-4.

[88] Xue, Y. G., Gu, X. Y., Wang, X. R., Sun, C., Xu, X. H., Sun, J., Zhang, B. G. (2009): The hydroxyl radical generation and oxidative stress for the earthworm *Eisenia fetida* exposed to tetrabromobisphenol A. – Ecotoxicology. 18: 693-699.

[89] Yahyaabadi, M., Hamidian, A. H., Ashrafi, S. (2018): Dynamics of earthworm species at different depths of orchard soil receiving organic or chemical fertilizer amendments. – Eurasian. J. Soil. Sci. 7: 318-325. DOI: 10.18393/ejss.454506.

[90] Yasmin, S., D'Souza, D. (2007): Effect of pesticides on the reproductive output of *Eisenia fetida*. – Bul. Envir. Contam. Toxicol. 79(5): 529-532. DOI: 10.1007/s00128-007-9269-5.

[91] Yasmin, S., D'Souza, D. (2010): Effects of pesticides on the growth and reproduction of earthworm: a review. – Appl. Environ. Soil. Sci. 9. DOI: 10.1155/2010/678360.

[92] Zheng, X. Q., Shi, Y. J., Lu, Y. L., Xu, X. B. (2016): Growth inhibition and DNA damage in the earthworm (*Eisenia fetida*) exposed to perfluorooctane sulphonate and perfluorooctanoic acid. – Chemistry and Ecology. DOI: 10.1080/02757540.2015.1116524.

[93] Zhou, Q. X., Zhang, Q. R., Liang, J. D. (2006): Toxic effects of acetochlor and methamidophos on earthworm *Eisenia fetida* in phaiozem, northeast China. – J. Envir. Sci. 18(4): 741-745.

[94] Zhou, S., Duan, C., Wang, X., Michelle, W. H. G., Yu, Z., Fu, H. (2008): Assessing cypermethrin-contaminated soil with three different earthworm test methods. – J. Envir. Sci. 20(11): 1381-1385. DOI: 10.1016/S1001-0742(08)62236-6.

http://www.aloki.hu ● ISSN 1589 1623 (Print) ● ISSN 1785 0037 (Online)
DOI: http://dx.doi.org/10.15666/aeer/1902_12471266
© 2021, ALÖKI Kft., Budapest, Hungary

INFLUENCE OF Ca^{2+}, Mg^{2+} AND Fe^{3+} ON THE ACTIVITY OF AMYLASES AND PROTEASES DURING AEROBIC GRANULATION

KOŃCZAK, B.

Department of Water Protection, Central Mining Institute, Pl. Gwarków 1, 40-166 Katowice, Poland
(e-mail: bkonczak@gig.eu; phone: +48-32-259-2628; fax: +48-32-259-2154)

(Received 21st Oct 2020; accepted 21st Dec 2020)

Abstract. The article presents the results of studies on amylase and protease activity in different fractions of extracellular polymeric substances of granular sludge. The research showed that most of the enzymes are stored in the fraction of tightly-bound extracellular polymers and in pellets. The activity of enzymes is influenced by the presence of divalent and trivalent cations. The highest protease activity of 4 $\mu mol^{x} min^{-1}$ was observed in the presence of Ca^{2+} and the lowest of 0.5 $\mu mol^{x} min^{-1}$ in the presence of Fe^{3+}. Protease activity in the system without cation addition was almost two times lower than in the all-cation-fed system. The highest activity of extracellular enzymes was observed at day 7 of granulation. The maximum value of amylase activity was 30 $\mu mol_{maltose}{}^{x} g_{starch}{}^{-1 x} min^{-1}$. The presence of Ca^{2+} is crucial for the processes of cell adhesion. Ca^{2+} plays a role in the regulation of proteolytic enzyme activity and thus on the growth rate of granules. The study also showed a change in enzyme activity during a single cycle of operation in the granular sludge sequencing batch reactor. The highest enzyme activity was observed at the end of the aeration cycle.
Keywords: *aerobic granule, enzymes, extracellular polymeric substances, cations*

Introduction

Due to numerous advantages, such as reduced space and, low energy requirements as well as a high efficiency in wastewater treatment (Pronk et al., 2015; Nancharaiah et al., 2019), the technology based on aerobic granular sludge is becoming increasingly popular (Liu and Tay, 2004). The results of researches to date indicate that the process of sludge granulation is initiated by physical factors such as increased aeration intensity, reduced sedimentation time, or increased rate of sewage discharge from the reactor (Morgenroth et al., 1997; Arrojo et al., 2004, 2007; Liu et al., 2010b; Wojnowska-Baryła et al., 2010). All these factors cause microbial stress and therefore affect the increased secretion of extracellular polymeric substances (EPS) by microorganisms to protect themselves in activated sludge. Extracellular polymeric substances (proteins, polysaccharides, eDNA) take part in the processes of bacterial cell adhesion (Zhang et al., 2018) and biofilm and granule formation (Liu et al., 2010a, 2020).

The physical strength of the sludge granules is a key factor that provides the long-term stable operation of granular biomass reactors (Zhu et al., 2015). There are very few literature reports in which the strength of granules is analysed (Nor-Anuar et al., 2012; de Graff et al., 2018; Czarnota et al., 2020). Kończak et al. (2014) stated that an increase in the density of granules and improvement of their sedimentation properties can be achieved by dosing Ca^{2+} and Mg^{2+} cations. However, the mechanisms that determine this process are unknown.

In turn, Hamiruddin et al. (2019) reported that extracellular polymeric substances (EPS) play a key role in maintaining the granular form and stability of the granules. Felz (2019) indicated that EPS play multiple roles in granules, ranging from the initiation of

http://www.aloki.hu ● ISSN 1589 1623 (Print) ● ISSN 1785 0037 (Online)
DOI: http://dx.doi.org/10.15666/aeer/1902_12671277
© 2021, ALÖKI Kft., Budapest, Hungary

granulation processes to the protection of granule co-forming micro-organisms and as a source of nutrients and stores of extracellular enzymes. As extracellular polymeric substances are a mixture of many compounds, therefore are difficult to analyse and quantify (Jiao et al., 2010). Due to that the knowledge about the structure of EPS matrix are still largely unknown.

The functioning of the EPS matrix also depends on the bivalent and trivalent metal cations present in the wastewater, especially Ca^{2+} and Mg^{2+} cations (Kończak and Miksch, 2011, 2012; Felz et al., 2016).

Therefore, this article focuses on the study of changes in the activity of extracellular enzymes in the presence of bivalent and trivalent metal cations. The research is a contribution to the development of knowledge on the processes occurring in the EPS matrix under the influence of extracellular enzymes. The available literature reports mostly concentrated on the role of extracellular enzymes in the process of maintaining granule form and activity of microorganisms during the storing process at 4°C (Adav et al., 2008). It was observed that a high activity of proteolytic enzymes caused the degradation of extracellular proteins, whereas only slight degradation of polysaccharides occurred. Subsequent research has shown that polysaccharides are a structural material, whereas proteins are a carbon and energy reservoir released due to the activity of proteolytic enzymes (Bae et al., 1995; Ng, 2002; Martinez et al., 2004; Zeng et al., 2007; Wang et al., 2007, 2008; Caudan et al., 2014; Ding et al., 2015). Due to the digest of protein by proteolytic enzymes, the low molecular weight polypeptides are found in the supernatant. This allows smaller fragments of proteins to diffuse into the granule, feeding the micro-organisms in deeper layers with nutrients, which allows them to remain active (van der Berg et al., 2020). Hydrolytic enzymes can also actively participate in cell adhesion processes (Burgess and Pletschke, 2008), similarly to the invasion of bacterial cells in the human body and the creation of a biofilm that covers the tissues. The hydrolytic enzymes digest the tissues, revealing the receptor areas, which makes it possible for bacteria to adhere to the tissues of the infected organism (Lipka and Boratynski, 2010). The role of enzymes in the regulation of biomass growth had previously been studied for the conventional sewage treatment plant and wastewater treatment system based on biofilm (Weissbrodt et al., 2013; Hassard et al., 2016) but never for the aerobic granular sludge system.

The estimation of enzyme activity during biogranulation could help us to clarify the hypothetical roles of enzymes in aerobic granules formation process and their role in the biological distribution of excess extracellular polymeric substances.

The paper presents innovative results of studies concerning changes in protease and amylase activity during the formation of aerobic granular sludge in the presence of Ca^{2+}, Mg^{2+} and Fe^{3+} cations.

Materials and experimental methods

Laboratory tests

Laboratory tests were carried out in six sequential reactors (GSSBR, Granular Sludge Sequencing Batch Reactor) with a capacity of 2 L and the following dimensions: height: 565 mm, internal diameter: 83.5 mm. The sludge inoculum was the activated sludge taken from the sewage treatment plant in Gliwice (Poland). Synthetic wastewater of the following system was cyclical introduced to the reactor (3 cycles per day): 0.75 g/l CH_3COONa (Stanlab, p.a.), 0.1 g/l NH_4Cl (Stanlab, p.a.) and 0.075 g/l KH_2PO_4

http://www.aloki.hu ● ISSN 1589 1623 (Print) ● ISSN 1785 0037 (Online)
DOI: http://dx.doi.org/10.15666/aeer/1902_12671277
© 2021, ALÖKI Kft., Budapest, Hungary

(Stanlab, p.a.). Individual or mixed compound doses were fed to the reactors: 0.016 g/l $CaCl_2$ (Stanlab, p.a.), 0.05 g/l $MgCl_2$ (Stanlab, p.a.), 0.02 g/l $FeCl_3$ (Stanlab, p.a.). The reactors' operating cycle included: feeding (3 min), aeration (170 min), sedimentation (3 min), discharge (3 min) and idle period (1 min). The air bubbles for aeration were supplied through an air diffuser at the reactors bottom.

EPS extraction and concentration measurement

The methodology described in previous studies was applied for the EPS extraction (Kończak et al., 2014). The samples were used to extract the loosely bound extracellular polymeric substances (LB-EPS) and the fraction of tightly bound extracellular polymers marked as TB-EPS. The LB-EPS fraction was obtained by centrifuging granules at 2,000 g for 15 minutes and filtering the separated liquid through a cellulose acetate filter with 45 μm pore diameter. The TB-EPS was obtained by extraction with cation exchange resin, followed by centrifugation at 20,000 g for 20 minutes and filtration of the resulting liquid. The residue from the centrifugation (a fraction of pellets) was also used in the research.

The content of polysaccharides was determined using the Dubois method (Dubois et al., 1956). The protein content was determined by using Quant-iT™ Protein Assay Kit (Thermo Fisher Sc.).

Enzyme activity analyses

Measurements of enzyme activity were conducted by the colorimetric method using the Genesys 5 Spectronic spectrophotometer. Enzyme activity was measured in three repetitions and the obtained values were averaged. The blank was prepared simultaneously with the samples, adding the homogenate after the enzyme reaction was interrupted. The enzyme activity was tested on the same day that the extraction of extracellular polymers was performed. This study examined the activity of enzymes contained in the supernatant fraction (LB-EPS), the tightly-bound granule fraction (TB-EPS), and pellets (P-EPS). The measurement of the rate of the catalysed reaction enables the determination of the enzyme activity. The Enzyme Commission of the International Union of Biochemistry has introduced the concept of an international standard unit 'U' to ease the comparison of the activity of enzyme preparations. This unit represents the amount of enzyme that catalyses the transformation of 1μmole of the substrate or a specific part of it, in 1 minute, under optimal conditions. The standard unit is μmol/min (Worsfold, 1995).

Protease activity determinants

General proteolytic activity was determined on the basis of the methodology proposed by Stygar (2008). 0.15 ml of azocasein solution and 0.05 ml of the sample were introduced into 0.2 ml of Tris-HCl buffer. Samples were incubated for one hour at 30ºC. Enzymatic reactions were interrupted by adding 0.3 ml TCA. After 15 minutes of protein precipitation, the samples were centrifuged for 10 minutes at 10,000 g, then extinction at 366 nm was measured within 10 minutes.

The total proteolytic activity for a given sample was expressed in standard Units of Activity (U), with the difference of 0.001 in the value of absorbance reading between the reference and the test sample being considered as 1 U.

http://www.aloki.hu ● ISSN 1589 1623 (Print) ● ISSN 1785 0037 (Online)
DOI: http://dx.doi.org/10.15666/aeer/1902_12671277
© 2021, ALÖKI Kft., Budapest, Hungary

In the case of a reference sample, an appropriate amount of buffer was added instead of the enzyme. The blank test for the enzyme was prepared by mixing the enzyme, TCA, and azocasein in that order. The unit of activity (U) is the amount of the enzyme that causes a change in absorbance of 0.01 under given reaction conditions.

Amylase activity determinations

Amylase activity was determined using the modified Bernfeld method (Bernfeld, 1955). Tubes containing 0.5 ml of 1% starch solution were preincubated for 5 minutes at 30ºC. Then 0.1 ml of the sample was added, mixed with Vortex, and incubated for one hour at 30ºC. Termination of the enzymatic reaction was performed by adding 1 ml of 3,5-dinitrosalicylic acid reagent and boiling it in boiling water for 10 minutes. Samples were cooled and 1.5 ml of distilled water was added. After a minimum of 10 minutes (but maximum before 1 hour) extinction at 540 nm light wavelength was read. The calibration curve for maltose with a 3,5-dinitrosalicylic acid reagent was prepared for solutions of maltose at concentrations between 0.2 and 2.0 mg in the sample. Using the calibration curve for maltose, the concentration of the released maltose was determined, and the specific α-amylase activity was then calculated according to the formula (*Eq.1*), expressed in μmoles of released maltose per 1 g of starch and per 1 minute.

$$A_{amylase} = \frac{c \cdot V}{B \cdot t} \left[\frac{\mu mol\ maltose}{g\ starch \cdot min}\right] \quad \text{(Eq.1)}$$

where:
A – activity ($\mu mol_{maltose}$ x g_{starch}^{-1} x min^{-1}),
c – concentration of released maltose ($\mu mol_{maltose}$ x ml^{-1}),
V – volume of reaction mixture (ml),
B – amount of starch in the reaction mixture (g),
t – incubation time (min)

Statistical analysis

Statistical analyses were performed in Statistica 13 (TIBCO Software) ($p \leq 0.05$). Averages and standard deviations were calculated.

Results and discussion

The results showed that during granulation the activity of proteases contained in the supernatant is low and remains in the range of 0.5 – 1 μmol x min^{-1}. No correlation was found between changes in protease activity in the LB-EPS fraction (loosely bound EPS) and the type of bivalent or trivalent cation dosed (*Fig. 1a*). The proteases contained in the TB-EPS fraction (tightly bound EPS) showed much higher activity. Zhang et al. (2015) reported that a fraction of tightly-bound extracellular polymeric substances (TB-EPS) can also capture extracellular catalytic enzymes and keep them close to cells (Li et al., 2008; Zhang et al., 2015). Similar results were presented by Dube and Guiot (2019), who reported that catabolic enzymes are stored in the EPS matrix, which makes the extracellular envelope capable of extracellular catabolic reactions, which is an advantage for both conventional activated sludge and anaerobic granular activated sludge.

This study has shown that Ca^{2+} and Mg^{2+} cations have a significant role in binding enzymes to the TB-EPS matrix. In all tested fractions of EPS matrix proteases showed

http://www.aloki.hu ● ISSN 1589 1623 (Print) ● ISSN 1785 0037 (Online)
DOI: http://dx.doi.org/10.15666/aeer/1902_12671277
© 2021, ALÖKI Kft., Budapest, Hungary

the highest activity in the presence of Ca^{2+} cations. In the case of Fe^{3+} cation, no increase in protease activity was observed. At the same time, it was found that the variability of protease activity is related to the initiation of granules formation and further development process of granules. In the first days of granulation (up to the 7th day), it was observed the increase in protease activity from 3 μmol ^{x} min^{-1} to 6 μmol ^{x} min^{-1} in the Ca-fed reactor. In the system, where Mg^{2+} cation was dosed on the 7th day, an inconsiderable increase of activity was observed, whereas in the system where Fe^{3+} was dosed, no increase in protease activity was observed. From the 20th day, the protease activity stabilized at the level of 4 μmol ^{x} min^{-1} and 3.5 μmol ^{x} min^{-1}, respectively for the system where Ca^{2+} and Mg^{2+} were dosed (*Fig. 1b*).

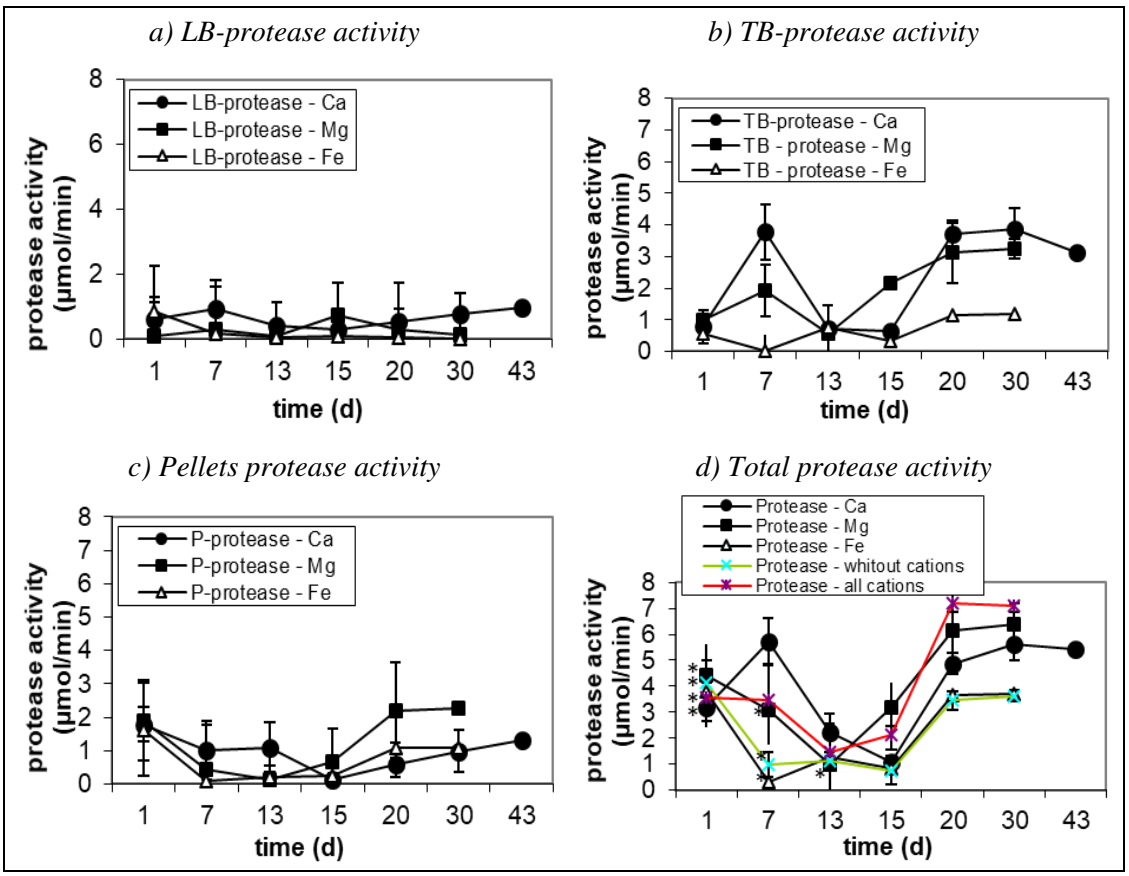


Figure 1. *The influence of Ca^{2+}, Mg^{2+} and Fe^{3} on the change of protease activity a) in LB-EPS-fraction (loosely bound EPS, b) in TB-EPS-fraction (tightly bound EPS), c) in P-EPS (EPS in pellets) and on the change of the total protease activity (d) (vertical bars – standard deviation, * - no statistical significance, p<0.05)*

The research showed no statistically significant differences between the activity of protease in the cation-fed systems and in the control system (without cations addition) during the first 7th days of granulation ($p<0.05$). The statistically significant differences were observed from the 13th days of granulation till the end of granulation process, except Mg-fed system ($p<0.05$). In the Mg-fed system the statistically significant differences in the protease activity was observed from 15th days of granulation (*Fig. 1d*) ($p<0.05$).

http://www.aloki.hu ● ISSN 1589 1623 (Print) ● ISSN 1785 0037 (Online)
DOI: http://dx.doi.org/10.15666/aeer/1902_12671277
© 2021, ALÖKI Kft., Budapest, Hungary

Previous results show that the time of granule formation in laboratory conditions is about 20-30 days and granules reach from 3 mm to even 29 mm (Kończak et al., 2014). Changes in the activity of extracellular proteases in the initial days of the granulation process are the result of the self-immobilisation of microorganisms form the activated sludge. From the 20th day of the process, when the granules reach their maximum size, the enzyme activity stabilises and remains at a high level close to the maximum. The diffusion of substrates into the granule is limited by the size of the granules (Liu et al., 2005; Li and Chróst, 2006; Li et al., 2008; Dube and Guiot, 2019). The storage of enzymes in the EPS matrix helps to maintain the stability of the sludge granules (regulation of granule size through degradation of excess organic compounds) and to nourish the microorganisms inside the granule (diffusion of low-molecular substrates into the granule).

Moreover, it was found that proteases in the TB fraction are most active in the presence of Ca^{2+} and in the system where all cations were dosed. The activity of proteases in the system where Ca^{2+} cation was dosed on the 7th day was 6 $\mu mol^{x} min^{-1}$, then on the 15th day it decreased to 1 $\mu mol^{x} min^{-1}$, which was related to changes in the structure of forming granules. From the 30th day, it remained at 5-5.5 $\mu mol^{x} min^{-1}$. The fluctuations of protease activity in the all cations-fed system ranged from 1.3 $\mu mol^{x} min^{-1}$ on the 13th day to 7.5 $\mu mol^{x} min^{-1}$ on the 20th day of the granulation process. It was found that bivalent and trivalent cations participate in the activation of extracellular proteases. The protease activity in the control system, where no cations were dosed, was almost twice as low as in the system to which all cations were dosed (*Fig. 1d*).

The main function of extracellular proteases is an enzymatic digestion of the intercellular matrix components. The results of the research indicate that the extracellular matrix proteases are involved in the process of its reconstruction.

As in the case of proteases, the amylase activity was lower in the LB-fraction than in the other fractions (*Figure 2a*). The highest amylase activity was observed in TB-fraction and pellets (*Fig. 2b and c*). From the 3rd day of the biogranulation process, the amylase activity started to increase rapidly, reaching a peak on the 7th day. From this point, the activity dropped quickly and started to remain stable at the initial value (*Figure 2*).

Additional, in the previous research, it was found that polysaccharides are not degraded during granulation (Kończak et al., 2014) so that they can form a three-dimensional network to make stable of the granular form of sludge.

The amylase activity was statistically significant highest in the presence of Mg^{2+} ($p \leq 0.05$). On the 7th day of the process, in the control system to which all cations were dosed the activity of amylases reached 30 $\mu mol_{maltose}{}^{x} g_{starch}{}^{-1}{}^{x} min^{-1}$. However, in the system without cations, the maximum amylase activity was only 6 $\mu mol_{maltose}{}^{x} g_{starch}{}^{-1}{}^{x} min^{-1}$. Starting from the 13th day of the process, it was observed that amylase activity in the TB-fraction, in the presence of Ca^{2+}, was higher than in the presence of other cations. Therefore, it was found that Ca^{2+} and Mg^{2+} cations, as well as Fe^{3+} cations, affect the increase in amylase activity (*Fig. 2d*).

The research showed no statistically significant differences between the activity of protease in the cation-fed systems and in the control system (without cations addition) during the first 3rd days of granulation ($p<0.05$). The statistically significant differences were observed from the 7th days of granulation till the end of granulation process, except Mg and Fe-fed systems ($p<0.05$). In the Mg and Fe-fed systems no statistically significant differences in the protease activity was observed in 20th and 23th days of granulation (*Fig. 2d*) ($p<0.05$).

http://www.aloki.hu ● ISSN 1589 1623 (Print) ● ISSN 1785 0037 (Online)
DOI: http://dx.doi.org/10.15666/aeer/1902_12671277
© 2021, ALÖKI Kft., Budapest, Hungary

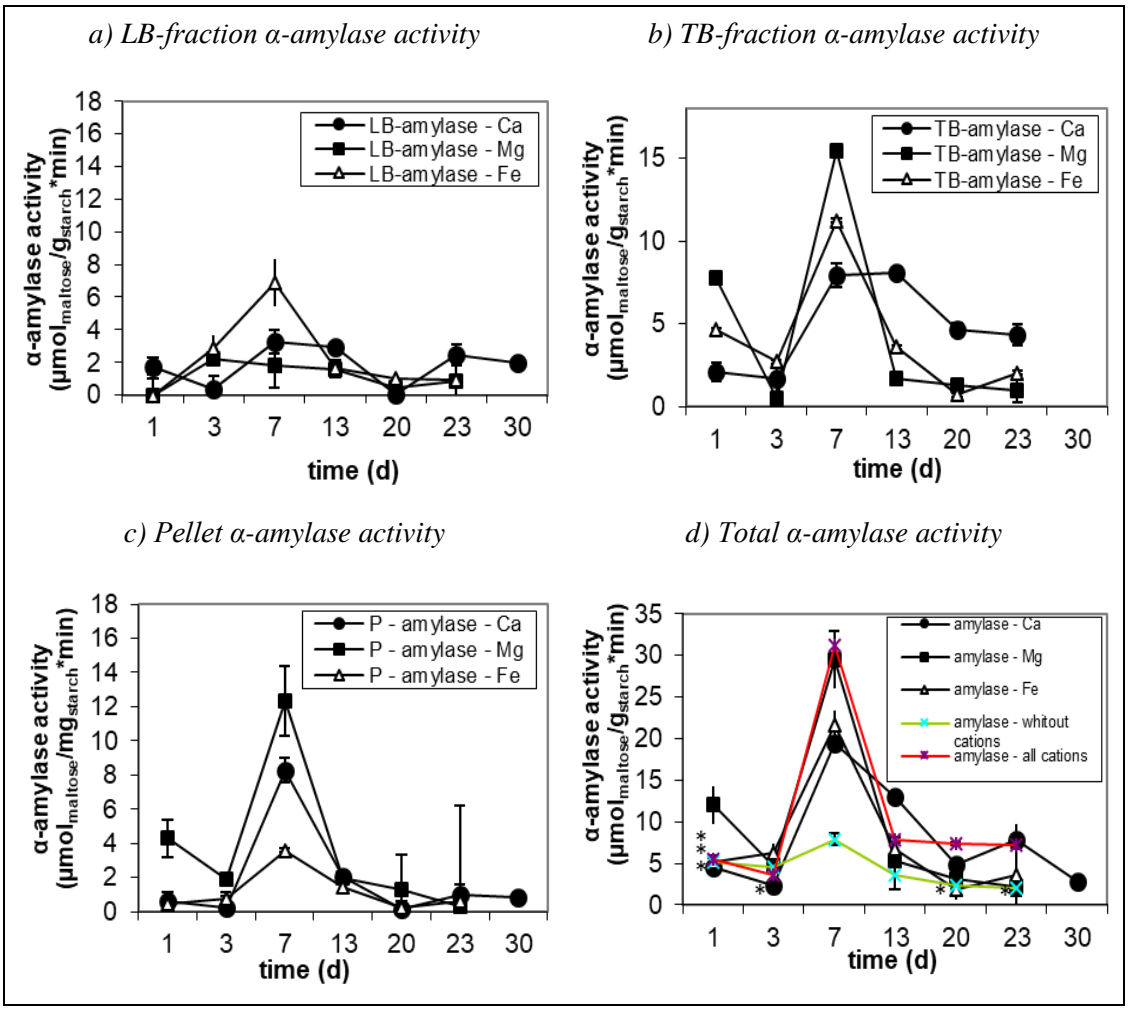


Figure 2. *The influence of Ca^{2+}, Mg^{2+} and Fe^{3+} on the change of amylase activity a) in LB-EPS fraction, b) in TB-EPS fraction, c) in P-EPS fraction (pellets) and on the change of the total amylase activity (d) (vertical bars – standard deviation, * - no statistical significance, $p<0.05$)*

The analysis of the activity of proteases and amylases during a single cycle of operation of a reactor with granulated biomass showed the increase of the activity of pellets amylase (P-amylase) and TB-amylase under substrate deficiency conditions, i.e. from 34 minutes of aeration. At the same time, it was observed that the amount of secreted polysaccharides in the TB-fraction (PS-TB) increased from ca. 5 mg/g_{VSS} (VSS – volatile suspdended solids) to 15 mg/g_{VSS} and the content of PS in LB-fraction of EPS was almost the same (ca. 2 mg/g_{VSS}). It was therefore concluded that under substrate deficiency conditions, microorganisms activate amylases, which participate in extracellular catabolic processes (*Fig. 3a*).

The activity of proteases stored in the TB-EPS fraction and pellets (P-EPS) increased from 94 minutes of the wastewater aeration process. No changes in protease activity were observed in the LB-EPS. The concentration of polypeptides in both LB-EPS and in the TB-EPS fraction increased with the aeration time (*Fig. 3b*).

http://www.aloki.hu ● ISSN 1589 1623 (Print) ● ISSN 1785 0037 (Online)
DOI: http://dx.doi.org/10.15666/aeer/1902_12671277
© 2021, ALÖKI Kft., Budapest, Hungary

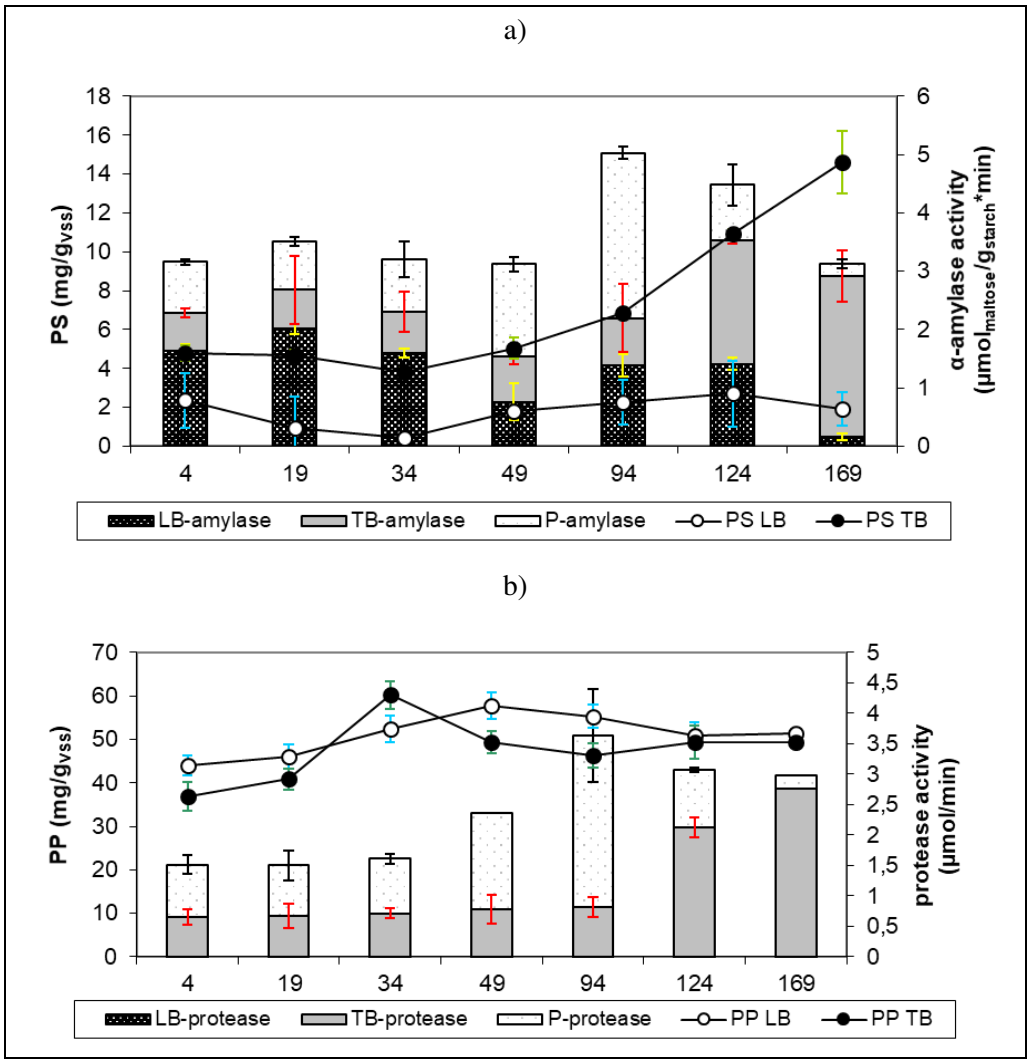


Figure 3. *Dynamics of changes in amylase and protease activity during a single reactor cycle with granular sludge (30th day of the granulation). Explanations: PP – polypeptides, LB – loosely-bound, PS – polysaccharides, TB – tightly-bound, P – pellets. *vertical bars – standard deviation*

Conclusion

The extracellular hydrolytic enzymes are stored mainly in the fraction of tightly-bound extracellular polymeric substances and play an important role in regulating of the granulation process. The research has shown that under substrate deficiency conditions, microorganisms activate amylases, which participate in extracellular catabolic processes.

The extracellular enzymes are responsible for regulating the content of proteins and polysaccharides in granules. The activity of enzymes is related to the presence of bivalent and trivalent metal ions, which are activators of proteases and amylases present in fractions of tightly-bound polymers.

Extracellular enzymes show the highest activity in the presence of Ca^{2+} cation and in systems to which Ca^{2+}, Mg^{2+} and Fe^{3+} cations are simultaneously dosed. Fe^{3+} cation is the weakest activator of extracellular enzymes.

http://www.aloki.hu ● ISSN 1589 1623 (Print) ● ISSN 1785 0037 (Online)
DOI: http://dx.doi.org/10.15666/aeer/1902_12671277
© 2021, ALÖKI Kft., Budapest, Hungary

The results show that there is a need to further expand the knowledge on the role of extracellular enzymes in the processes of active sludge granulation under aerobic conditions, which will contribute significantly to understanding the mechanisms of this process.

The research is a contribution to the knowledge of the processes occurring in the EPS matrix under the influence of extracellular enzymes. An increase in protease activity in the first phase of granulation (up to the 7th day), especially in the presence of Ca^{2+} showed the importance of this cation in the processes of regulation of proteolytic enzymes activity. Ca^{2+} play the special role in the processes of cell adhesion and control of granule growth. The research need to be continued to determine the relationship between cations addition and the process of cell adhesion during aerobic granulation process.

Acknowledgements. This work was supported by the Polish Ministry of Science and Higher Education in the framework of the research work [No 111 580 18-340], in the Central Mining Institute in Poland.

REFERENCES

[1] Adav, S. S., Lee, D. J., Tay, J. H. (2008): Extracellular polymeric substances and structural stability of aerobic granule. – J. Wat. Res. 42: 1644-1650.

[2] Arrojo, B., Mosquera-Corral, A., Garrido, J. M., Mendez, R. (2004): Aerobic granulation with industrial waste-water in sequencing batch reactors. – Wat. Res. 38: 3389-3399.

[3] Arrojo, B., Vazquez Padin, J. R., Figueroa, M., Mosquera-Corral, A., Campos, J. L., Mendez, R. (2007): Rectors of biomass granular – more efficiency in less space (in spanish: Reactores de biomasa granular - más capacidad en menos espacio). – Tecnologia de agua 287: 31-39.

[4] Bae, B.-U., Shin, H.-S., Paik, B.-Ch., Chung, J.-Ch. (1995): Re-activation characteristics of preserved anaerobic granular sludges. – Bioresour. Technol. 53: 231-235.

[5] Bernfeld, P. (1955): α-, β-amylases. – In: Colwick, S. P., Kaplan, N. O. (eds.) Methods in enzymology. Academic Press, New York, pp. 149-158.

[6] Burgess, J. E., Pletschke, B. I. (2008): Hydrolytic enzymes in sewage sludge treatment: A mini-review. – Water SA 34(3): 343-349.

[7] Caudan, C., Filali, A., Spérandio, M., Girbal-Neuhauser, E. (2014): Multiple EPS interactions involved in the cohesion and structure of aerobic granules. – Chemosphere 117: 262-270.

[8] Czarnota, J., Masłoń, A., Zdeb, M., Łagód, G. (2020): Powdered Ceramsite and Powdered Limestone Use in Aerobic Granular Sludge Technology. – Molecules 25(2): 386.

[9] de Graaf, D. R., van Dijk, E. J. H., van Loosdrecht, M. C. M., Pronk, M. (2018): Strength characterization of full-scale aerobic granular sludge. – Env Technol. 41(13): 1637-1647.

[10] Ding, Z., Bourven, I., Guibaud, G., van Hullebusch, E. D., Panico, A., Pirozzi, F., Esposito, G. (2015): Role of extracellular polymeric substances (EPS) production in bioaggregation: application to wastewater treatment. – Appl. Microbiol. Biotechnol. 99(23): 9883-9905.

[11] Dube, Ch. D., Guiot, S. R. (2019): Characterization of the protein fraction of the extracellular polymeric substances of three anaerobic granular sludges. – AMB Express 9: 23.

[12] Dubois, M. K., Gilles, J. K., Hamilton, J. K., Rebers, P. A., Smith, F. (1956): Colorimetric Method for Determination of Sugars and Related Substances. – Anal. Chem. 28: 350-352.

[13] Felz, S., Al-Zuhairy, S., Aarstad, O. A., van Loosdrecht, M. C. M., Lin, Y. M. (2016): Extraction of structural extracellular polymeric substances from aerobic granular sludge. – J Vis Exp. 115: 54534.

http://www.aloki.hu ● ISSN 1589 1623 (Print) ● ISSN 1785 0037 (Online)
DOI: http://dx.doi.org/10.15666/aeer/1902_12671277
© 2021, ALÖKI Kft., Budapest, Hungary

[14] Felz, S., Vermeulen, S., van Loosdrecht, M. C. M., Lin, Y. M. (2019): Chemical characterization methods for the analysis of structural extracellular polymeric substances (EPS). – Water Res. 157: 201-208.
[15] Hamiruddin, N. A., Awang, N. A., Shaaban, M. G. (2019): The performance of extracellular polymeric substance (EPS) on stability of aerobic granular sludge (AGS). – CEER 29(3): 060-069.
[16] Hassard, F., Biddle, J., Cartmell, E., Stephenson, T. (2016): Biosolids recycling impact on biofilm extracellular enzyme activity and performance of hybrid rotating biological reactors. – Process Saf. Environ. Prot. 103: 69-75.
[17] Jiao, Y., Cody, G. D., Harding, A. K., Wilmes, P., Schrenk, M., Wheeler, K. E., Banfiled, J. F., Thelen, M. P. (2010): Characterization of Extracellular Polymeric Substances from Acidophilic Microbial Biofilms. – App. Environ. Microbiol. 76(9): 2916-2922.
[18] Kończak, B., Miksch, K. (2011): Influence of Ca^{2+}, Mg^{2+} and Fe^{3+} on granular sludge formation. – Chem. Eng. 90/11: 2002-2005.
[19] Kończak, B., Miksch, K. (2012): Distribution of extracellular polymeric substances and their role in aerobic granule formation. – Chem. Process Eng. 33(4): 679-688.
[20] Kończak, B., Karcz, J., Miksch, K. (2014): Influence of Calcium, Magnesium, and Iron Ions on Aerobic Granulation. – Appl. Biochem. Biotechnol. 174: 2910-2918.
[21] Li, Y., Chróst, R. J. (2006): Microbial enzymatic activities in aerobic activated sludge model reactors. – Enzym. Microb. Technol. 39: 568-572.
[22] Li, Y., Liu, Y., Shen, L., Chen, F. (2008): DO diffusion profile in aerobic granule and its microbiological implications. – Enzyme Microb. Technol. 43(4-5): 349-354.
[23] Lipka, D., Boratyński, J. (2010): Metalproteinase MMP. The structure and function. (in polish: Metaloproteinazy MMP. Struktura i funkcja). – J. Postępy Hig. Med. Dośw. 62: 328-336.
[24] Liu, Y., Tay, J. H. (2004): State of the art of biogranulation technology for wastewater treatment. – Biotechnol. Adv. 22: 533-563.
[25] Liu, Y.-Q., Liu, Y., Tay, J-H. (2005): Relationship between size and mass transfer resistance in aerobic granules. – Lett. Appl. Microbiol. 40(5): 312-315.
[26] Liu, L., Gao, D. W., Zhang, M., Fu, Y. (2010a): Comparison of Ca^{2+} and Mg^{2+} enhancing aerobic granulation in SBR. – J. Hazard. Mater. 181: 382-387.
[27] Liu, T.-Q., Moy, B., Kong, Y.-H., Tay, J.-H. (2010b): Formation, physical characteristic and microbial structure of aerobic granules in pilot-scale sequencing batch reactor for Real wastewater treatment. – Enzyme Microb. Technol. 46: 520-525.
[28] Liu, Y., Shan, R., Chen, G., Liu, L. (2020): Linking flow velocity-regulated EPS production with early-stage biofilm formation in drinking water distribution systems. – Water Supply 20(4): 1253-1263.
[29] Martinez, F. O., Lema, J., Mendez, R., Cuervo-Lopez, F., Gomez, J. (2004): Role of exopolymeric protein on the settleability of nitrifying sludges. – Bioresour. Technol. 94: 43-48.
[30] Morgenroth, E., Sherden, T., van Loosdrecht, M. C. M., Heijnen, J. J., Wilder, P. A. (1997): Aerobic granular sludge in a sequencing batch reactor. – Wat. Res. 31: 3191-3194.
[31] Nancharaiah, V. Y., Sarvajith, M., Krishna Mohan, T. V. (2019): Aerobic Granular Sludge: The Future of Wastewater Treatment. – Current science 117(3): 395-404.
[32] Ng, P. H. (2002): Storage stability of aerobic granules cultivated in aerobic granular sludge blanket reactor. – Master Thesis Nanyang Technological University, Singapore.
[33] Nor-Anuar, A., Ujang, Z., van Loosdrecht, M. C. M., de Kreuk, M. K., Olsson, G. (2012): Strength characteristics of aerobic granular sludge. – Water Sci Technol 65(2): 309-316.
[34] Pronk, M., de Kreuk, M. K., de Bruin, B., Kamminga, P., Kleerebezem, R., van Loosdrecht, M. C. (2015): Full scale performance of the aerobic granular sludge process for sewage treatment. – Water Res. 1(84): 207-17.

http://www.aloki.hu ● ISSN 1589 1623 (Print) ● ISSN 1785 0037 (Online)
DOI: http://dx.doi.org/10.15666/aeer/1902_12671277
© 2021, ALÖKI Kft., Budapest, Hungary

[35] Stygar, D. (2008): Digestive and glucose metabolism enzymes in the caterpillars of successive generations Cameraria Ohridella (Lepidoptera: Gracillariide). – PhD Thesis, The Silesian University, Katowice, Poland.
[36] van der Berg, L., Kirkland, C. M., Seymour, J. D., Codd, S. L., van Loosdrecht, M. C. M., de Kreuk, M. K. (2020): Heterogeneous diffusion in aerobic granular sludge. – Biotech. Bioeng. 117(12): 3809-3819.
[37] Wang, Z. W., Liu, Y., Tay, J.-H. (2007): Biodegradability of extracellular polymeric substances produced by aerobic granules. – Microbiol. Biotechnol. 74: 462-466.
[38] Wang, X., Zhang, H., Yang, F., Wang, Y., Gao, M. (2008): Long-term storage and subsequent reactivation of aerobic granules. – Bioresour. Technol. 99: 8304-8309.
[39] Weissbrodt, D. G., Neu, T. R., Kuhlicke, U., Rappaz, Y., Holliger, Ch. (2013): Assessment of bacterial and structural dynamics in aerobic granular biofilms. – Front. Microbiol. 4(175): 1-18.
[40] Wojnowska-Baryła, I., Cydzik-Kwiatkowska, A., Szatkowski, M., Gutowski, Ł. (2010): Granulation of activated sludge in SBR reactor. – Biotechnologia 1(88): 161-169.
[41] Worsfold, J. (1995): Classification and chemical characteristics of immobilized enzymes. – Pure & Appl. Chem. 67(4): 597-600.
[42] Zeng, P., Zhuang, W. Q., Tay, S. T. L., Tay, J. H. (2007): The influence of storage on the morphology and physiology of phthalic acid-degrading aerobic granules. – Chemosphere 69: 1751-1757.
[43] Zhang, P., Shen, Y., Guo, J. S., Li, C., Wang, H., Chen, Y. P., Yan, P., Yang, J. X., Fang, F. (2015): Extracellular protein analysis of activated sludge and their functions in wastewater treatment plant by shotgun proteomics. – Sci Rep. 5: 12041.
[44] Zhang, H., Jia, Y., Khanal, S. K., Lu, H., Fang, H., Zhao, Q. (2018): Understanding the Role of Extracellular Polymeric Substances on Ciprofloxacin Adsorption in Aerobic Sludge, Anaerobic Sludge, and Sulfate-Reducing Bacteria Sludge Systems. – Environ. Sci. Technol. 52(11): 6476-6486.
[45] Zhu, L., Zhou, J., Lv, M., Yu, H., Zhao, H., Xu, X. (2015): Specific component comparison of extracellular polymeric substances (EPS) in flocs and granular sludge using EEM and SDS-PAGE. – Chemosphere 121: 26-32.

http://www.aloki.hu ● ISSN 1589 1623 (Print) ● ISSN 1785 0037 (Online)
DOI: http://dx.doi.org/10.15666/aeer/1902_12671277
© 2021, ALÖKI Kft., Budapest, Hungary

EFFECT OF HUMIC ACID COMBINED WITH FERTILIZER ON THE IMPROVEMENT OF SALINE-ALKALI LAND AND COTTON GROWTH

HU, Y. W. [1,2] – LI, Q. K.* [1,2] – SONG, C. J. [1,2] – JIN, X. H. [1,2]

[1]*Yellow River Institute of Hydraulic Research, Zhengzhou, China*

[2]*Key Laboratory of the Loess Plateau Soil Erosion and Water Loss Process and Control, Zhengzhou, China*

**Corresponding author*
e-mail: luckdog3699@163.com

(Received 26th Oct 2020; accepted 21st Dec 2020)

Abstract. The effect of humic acid combined with fertilizer is an important basis for improving the soil's ecological environment. Therefore, this study is aimed at investigating the effect of the combined application of humic acid and fertilizer on the physicochemical properties of saline-alkali soil, cotton growth, and nutrient utilization in an arid area. The random field block test method was adopted, and biochemical humic acid (BHA), ammoniated humic acid (AHA), and microbial activated humic acid (MHA) were used as experimental materials. Soil pH, electrical conductivity (EC), water-soluble cation content, soluble nitrogen content, available phosphorus content, cotton biomass, and yield were determined. The results showed that humic acid combined with fertilizer had no obvious effect on the pH of the salinized soil. However, the addition of three types of humic acid showed a certain reduction effect on soil EC, water-soluble Na^+ and K^+ content, and sodium adsorption ratio (SAR), affecting the soil depth of 0-40 cm. In addition, the content of available phosphorus in soil could be increased by adding three humic acids, among which MHA was the best. The addition of humic acid could significantly improve the yield of cotton, but there was no significant difference between the three.
Keywords: *biochemical humic acid, ammoniated humic acid, microbial activated humic acid, soil fertility, cotton yield*

Introduction

Cotton cultivation in Xinjiang plays an important role in China's cotton production (Yang et al., 2019). In 2019, the area sown with cotton in Xinjiang was 2540.5 thousand hectares, and its total cotton output was 5.889 million tons, accounting for 76.1% and 84.9% of the national total, respectively (Li et al., 2020). Due to scarce rainfall and intense evaporation, 37.72% of cultivated land in Xinjiang is endangered by saline-alkali conditions (Xiao et al., 2019). Excessive salt ions and alkaline environment in saline-alkali soil cause the loss of nitrogen fertilizer volatilization, leading to cotton nutritional disorders, and thus affecting the growth and yield of cotton (He et al., 2020). Therefore, the fertilization of cotton in saline-alkali land should be determined not only based on the nutrient demand of cotton, but also the amelioration of saline-alkali land and the improvement of soil fertility.

Humic acid is a kind of organic polymer active material, which has been widely used in many fields (Ciarkowska et al., 2017; Dehghani et al., 2018; Xie et al., 2019). Studies have shown that humic acid itself can be used as an organic fertilizer to increase soil fertility (Zhang et al., 2019a). Fawzy et al. (2010) found that increasing humic acid application could improve the vegetative growth of bean plants and improve the yield and quality of beans. Fan et al. (2014) pointed out that the chlorophyll content and

http://www.aloki.hu ● ISSN 1589 1623 (Print) ● ISSN 1785 0037 (Online)
DOI: http://dx.doi.org/10.15666/aeer/1902_12791294
© 2021, ALÖKI Kft., Budapest, Hungary

chloroplast ultrastructure of chrysanthemum were significantly improved after applying humic acid on the leaves compared with that after applying common chemical fertilizer. Selladurai and Purakayastha (2016) found that there was no significant difference between humic acid and fertilizer in yield, N, P, K content, absorption, and utilization efficiency. Li et al. (2019) showed that humic acid increased soil nutrient content, including total nitrogen, total phosphorus, total potassium, available nitrogen, available phosphorus, available potassium, and organic matter, showing the greatest effect in the third year. As a soil conditioner, humic acid can also change the composition of soil ions (Abe et al., 2011), promote the formation of soil aggregates (Liu et al., 2019), increase soil permeability (Khaled and Fawy, 2011), and accelerate the leaching and irrigation of soil surface salts and alkalis (Zhao et al., 2017). Humic acid can also activate soil phosphorus, improve the supply of phosphorus in saline-alkali soil, and promote the absorption and utilization of phosphorus by crops (He et al., 2011; Ifansyah, 2014). In addition, humic acid can regulate root morphogenesis and promote osmotic regulation of substance accumulation and nutrient absorption of crops (Asli and Neumann, 2010; Jindo et al., 2012).

The above studies indicate that humic acid plays a positive role in ameliorating saline-alkali soil and improving nutrient utilization efficiency. However, at present, the sources of humic acid are complex, and different sources of humic acid have great differences in chemical composition, structure, and properties, and their improvement effects on different types of saline-alkali soil are not the same (Erhayem and Sohn, 2014; Türkmen et al., 2004). The effects of different humic acids and chemical fertilizers on the improvement of saline-alkali land and crop growth are less studied. Therefore, 3 kinds of humic acids from different sources were used as the material in this study. Through field experiments, the effects of humic acids combined with fertilizers on soil physicochemical properties, cotton growth, and nutrient utilization in Xinjiang saline-alkali land were discussed, so as to clarify the application effects of different humic acids combined with fertilizers in saline-alkali land in inland arid areas.

Materials and methods

The study area and test materials

The experiment was conducted in Baotouhu Farm (41°39'N, 85°48'E) in Korla, Xinjiang, China in 2016. This region is a typical inland arid climate type, with annual precipitation of 53.5-62.5 mm, evaporation of 2270-2785 mm, average temperature of 11.2 ℃, annual sunshine number of 3035.7 h, wind speed of 2.36 $m \cdot s^{-1}$, and frost-free period of 145-242 days. Before the experiment, the physical and chemical properties of the initial soil were determined. The soil in the study area (0-40 cm) was sandy loam (64.27% sand, 32.83% silt, 2.9% clay), soil bulk density was 1.70 $g \cdot cm^{-3}$, saturated water content was 0.398 $cm^3\ cm^{-3}$, wilting coefficient was 0.050 $cm^3 \cdot cm^{-3}$, field water capacity was 0.196 $cm^3 \cdot cm^{-3}$, organic matter content was 10.7 g kg^{-1}, total nitrogen was 0.61 $g \cdot kg^{-1}$, available phosphorus was 18.64 $mg \cdot kg^{-1}$, available potassium was 233 $mg \cdot kg^{-1}$, pH was 8.27, and electroconductibility (EC) was 5.47 $ds \cdot m^{-1}$. The tested cotton variety was No. 43 of Zhonglu Institute. The tested fertilizer urea (N, 46.4%) and superphosphate (P_2O_5, 14%) was purchased from the market. The 3 humic acids were all provided by Beijing Aojia Ecological Agriculture Co., LTD., including biochemical humic acid (BHA), ammoniated humic acid (AHA), and microbial activated humic acid (MHA). The basic physicochemical properties of the 3 humic acids are shown in *Table 1*.

http://www.aloki.hu ● ISSN 1589 1623 (Print) ● ISSN 1785 0037 (Online)
DOI: http://dx.doi.org/10.15666/aeer/1902_12791294
© 2021, ALÖKI Kft., Budapest, Hungary

Table 1. *Basic physicochemical properties of humic acid material*

Tested material	Organic matter (%)	Humic acid (%)	Total nitrogen ($g \cdot kg^{-1}$)	Total phosphorus ($g \cdot kg^{-1}$)	Total potassium ($g \cdot kg^{-1}$)	pH
BHA	70	40	1.8	11.8	19.8	9.72
AHA	50	40	47.1	11.9	0.9	9.89
MHA	50	40	25.1	16.2	2.2	8.35

Experimental design

Using the field test method, 6 treatments were set as follows:

1. -N (only phosphorus fertilizer, no nitrogen fertilizer)
2. -P (only nitrogen fertilizer, no phosphorus fertilizer)
3. NP (nitrogen and phosphate fertilizer)
4. BHA + NP (BHA combined with nitrogen and phosphate fertilizer)
5. AHA + NP (AHA combined with nitrogen and phosphorus fertilizer)
6. MHA + NP (MHA combined with nitrogen and phosphate fertilizer)

Each treatment area was 30 m^2 (6 m long and 5 m wide), with 3 replicates, arranged in random groups. A one-time application of urea (420 $kg \cdot hm^{-2}$) and superphosphate (643 $kg \cdot hm^{-2}$) was as base fertilizer, and three humic acids were applied at 1500 $kg \cdot hm^{-2}$. Considering the high content of available potassium in the test soil, potassium fertilizer was not applied in the field.

Cotton was planted by drip irrigation under the film. The experimental field was sown on April 20, 2016, with a film and two pipes arranged in four rows. The plant spacing was 10 cm, the narrow row spacing was 20 cm, the wide row spacing was 50 cm, and the film spacing was 40 cm. The prevention and control of diseases, pests, and weeds during cotton growth and water management were equivalent to conventional production fields. The irrigation quota of cotton growth period was 5250 $m^3 \cdot hm^{-2}$, the irrigation period was 7-10 days, and the total irrigation time was 10 times. Aphids and red spiders were prevented at stage 14 in BBCH scale and cotton bollworms were prevented at stage 61 in BBCH scale for cotton.

Investigate items and methods

The chlorophyll content of functional leaves was measured by SPAD-50-Puls portable chlorophyll meter at stages 56 and 75 in BBCH scale for cotton. At stage 105 in BBCH scale, three uniformly robust fields with an area of 6.67 m^2 were selected, the number of bolls with a diameter greater than 2 cm were recorded, 100 bolls were selected to be weighed in each test area, so as to calculate the cotton yield (Liang et al., 2019). Four plants of cotton were taken in each experimental plot, and the root, stem, leaf, and bell were determined by the drying method (Tan et al., 2018). The dried cotton plants were crushed for the determination of nitrogen and phosphorus content. The plant samples were digested with concentrated H_2SO_4-H_2O_2, total nitrogen was determined by the Kjeldahl method, and total phosphorus was determined by the vanadium-molybdenum yellow colorimetric method (Sudiarto et al., 2019). Soil samples (100 g, three replicates) were taken from soil layers of 0-10 cm, 10-20 cm, and 20-40 cm respectively to determine the contents of pH, EC, the contents of water-soluble K^+, Na^+,

http://www.aloki.hu ● ISSN 1589 1623 (Print) ● ISSN 1785 0037 (Online)
DOI: http://dx.doi.org/10.15666/aeer/1902_12791294
© 2021, ALÖKI Kft., Budapest, Hungary

Ca^{2+}, and Mg^{2+}, NO_3^--N, NH_4^+-N, and soluble total nitrogen (TSN) as well as available phosphorus. Soil pH was determined by pH meter method, soil electroconductibility (EC) was determined by electroconductibility meter method, water-soluble Ca^{2+} and Mg^{2+} were determined by atomic absorption spectrophotometry method, and water-soluble K^+ and Na^+ were determined by flame photometry method (Sharpley, 1991). NO_3^--N was determined by UV spectrophotometer method, NH_4^+-N by indophenol blue colorimetric method, and TSN by alkaline potassium persulfate oxidation method (Margot et al., 1994). The content of available phosphorus in soil was determined by 0.5 $mol \cdot L^{-1}$ $NaHCO_3$ extraction and molybdenum-antimony resistance colorimetric method (Zhang et al., 2019b).

Data processing and analysis

Microsoft Excel 2016 and SPSS 22.0 statistical software were used for data processing and statistical analysis, and the least significant difference (LSD) method ($\alpha = 0.05$) was used for multiple comparison.

Xing et al. (2010) proposed the calculation method of soil soluble organic nitrogen (SON):

$$SON = TSN - (NH_4^+ - N + NO_3^- - N) \quad \text{(Eq.1)}$$

where TSN is soil soluble total nitrogen.

Mahdy (2011) used the calculation formula of soil sodium adsorption ratio (SAR):

$$SAR = \frac{\left[Na^+\right]}{\sqrt{\frac{\left[Ca^{2+}\right]+\left[Mg^{2+}\right]}{2}}} \quad \text{(Eq.2)}$$

Zhang et al. (2016) and Wang et al. (2019) proposed the calculation method of apparent availability of nitrogen (phosphorus) fertilizer, nitrogen (phosphorus) agronomic efficiency, and nitrogen (phosphorus) partial productivity.

$$AAN = \frac{NUF - NUD}{NUA} \times 100\% \quad \text{(Eq.3)}$$

$$AAP = \frac{PUF - PUD}{PUA} \times 100\% \quad \text{(Eq.4)}$$

$$NAE = \frac{Y_F - Y_{DN}}{NUA} \quad \text{(Eq.5)}$$

$$PAE = \frac{Y_F - Y_{DP}}{PUA} \quad \text{(Eq.6)}$$

$$NPP = \frac{Y_F}{NUA} \quad \text{(Eq.7)}$$

http://www.aloki.hu ● ISSN 1589 1623 (Print) ● ISSN 1785 0037 (Online)
DOI: http://dx.doi.org/10.15666/aeer/1902_12791294
© 2021, ALÖKI Kft., Budapest, Hungary

$$PPP = \frac{Y_F}{PUA} \quad \text{(Eq.8)}$$

where AAN and AAP represent the apparent availability of nitrogen (phosphorus) fertilizer (%), NUF and PUF represent the amounts of nitrogen (phosphorus) uptake in the fertilized area (kg), NUD and PUD represent the amounts of nitrogen (phosphorus) uptake in nitrogen (phosphorus) deficient area (kg), and NUA and PUA represent the amounts of nitrogen (phosphorus) nutrient application (kg). NAE and PAE represent nitrogen (phosphorus) agronomic efficiency ($kg \cdot kg^{-1}$), Y_F represents fertilized area yield, Y_{DN} and Y_{DP} represent nitrogen (phosphorus) deficient area yields. NPP and PPP represent nitrogen (phosphorus) partial productivity ($kg \cdot kg^{-1}$).

Results

The effect of humic acid combined with fertilizer on soil pH

The pH value directly affects many chemical reactions in the soil. In 0-40 cm soil layer, pH value showed a trend of gradual increase with soil depth (*Fig. 1*). Compared with the control group (NP) without humic acid, the application of 3 kinds of humic acid materials had no significant effect on the pH value of the soil at 0-10 cm, 10-20 cm, and 20-40 cm soil layers. However, compared with the three humic acid materials, the pH value of the soil treated with BHA in the 0-10cm soil layer was lower than that of AHA and MHA (*Fig.1A*), the pH value of the soil treated with MHA in the 10-20 cm soil layer was lower than that of AHA (*Fig.1B*), and there was no significant difference between the three test materials in the 20-40 cm soil layer (*Fig. 1C*).

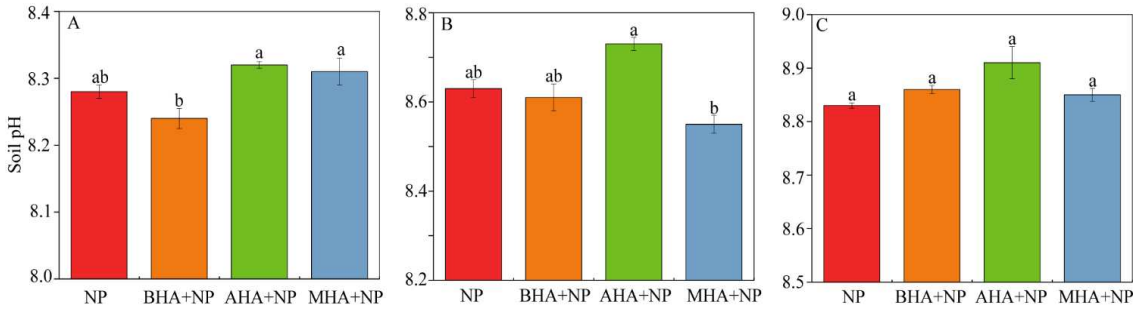


Figure 1. *Influence of humic acid combined with fertilizer on soil pH. A, B, and C represent soil layers 0-10 cm, 10-20 cm, and 20-40 cm, respectively. "NP" represents nitrogen and phosphate fertilizer, "BHA + NP" represents biochemical humic acid combined with nitrogen and phosphate fertilizer, "AHA + NP" represents ammoniated humic acid combined with nitrogen and phosphorus fertilizer), and "MHA + NP" represents microbial activated humic acid combined with nitrogen and phosphate fertilizer. The error lines represent the standard variance, and different lowercase letters represent significant differences among treatments in the same soil layer ($P < 0.05$)*

The effect of humic acid combined with fertilizer on soil electric conductivity

As a saline-alkali soil improvement agent, humic acid had a certain effect on electroconductibility (EC) of 0-40 cm soil layer (*Fig. 2*). Compared with control (NP), the EC values of 0-10 cm soil layer treated by BHA, AHA and MHA decreased by

http://www.aloki.hu ● ISSN 1589 1623 (Print) ● ISSN 1785 0037 (Online)
DOI: http://dx.doi.org/10.15666/aeer/1902_12791294
© 2021, ALÖKI Kft., Budapest, Hungary

27.4%, 26.3%, and 21.4% respectively (*Fig. 2A*), the EC values of 10-20 soil layer decreased by 23.8%, 21.9%, and 12.7% respectively (*Fig. 2B*), and the EC values of 20-40 cm soil layer decreased by 20.9%, 131%, and 8.8% respectively (*Fig. 2C*). Compared with NP, BHA in the three soil layers all showed significant differences, while AHA and MAH only showed significant differences in the 0-10 cm soil layer.

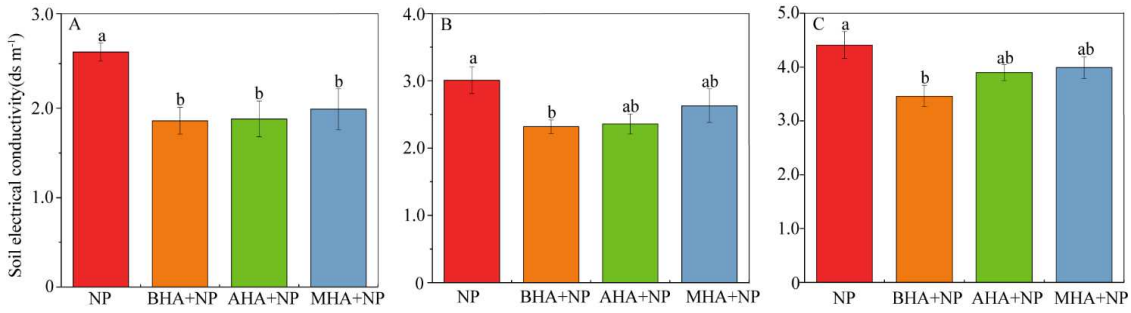


Figure 2. *Influence of humic acid combined with fertilizer on soil electric conductivity. A, B, and C represent soil layers 0-10 cm, 10-20 cm, and 20-40 cm, respectively. "NP" represents nitrogen and phosphate fertilizer, "BHA + NP" represents biochemical humic acid combined with nitrogen and phosphate fertilizer, "AHA + NP" represents ammoniated humic acid combined with nitrogen and phosphorus fertilizer), and "MHA + NP" represents microbial activated humic acid combined with nitrogen and phosphate fertilizer. The error lines represent the standard variance, and different lowercase letters represent significant differences among treatments in the same soil layer ($P < 0.05$)*

The effect of humic acid combined with fertilizer on soil cation composition and SAR

Soil salinization is the process of adsorption of sodium ions by soil colloid and the exchange of cations between the solid phase and liquid phase, and sodium adsorption ratio (SAR) is an important indicator of soil alkalinization. Compared with NP, the combination of humic acid and fertilizer had no significant effect on the content of water-soluble Ca^{2+} and Mg^{2+} in the 0-40 cm soil layer, but reduced the content of water-soluble K^+ and Na^+ by 5.5-40.0% and 12.8-22.0%, respectively. Among the three humic acid materials, the content of water-soluble Ca^{2+} and Mg^{2+} in the 0-10 cm soil layer treated by MHA was significantly higher than that of BHA and AHA, and there was no significant difference in the soil layer below 10 cm. The content of water-soluble K^+ in the 20-40 cm soil layer treated by AHA was significantly higher than that of BHA and MHA. However, there was no significant difference in the content of water-soluble Na^+ among the three materials in any soil layer. The combination of three humic acids and fertilizers can significantly reduce the SAR of 0-40 cm soil layer by 7.7-22.7%. However, there was no significant difference between different humic acid materials (*Table 2*).

The effect of humic acid combined with fertilizer on soil soluble nitrogen content

Soil inorganic nitrogen mainly includes nitrate nitrogen (NO_3^--N) and ammonium nitrogen (NH_4^+-N). Compared with NP, the content of NO_3^--N in the 0-40 cm soil layer at the maturity stage of cotton treated with BHA, AHA and MHA decreased by 9.9-28.1%, 18.0-78.6% and 37.6-66.2%, respectively, especially the AHA and MHA humic acid treatment showed the greatest reduction (*Table 3*). The influence of NH4 + -N

http://www.aloki.hu ● ISSN 1589 1623 (Print) ● ISSN 1785 0037 (Online)
DOI: http://dx.doi.org/10.15666/aeer/1902_12791294
© 2021, ALÖKI Kft., Budapest, Hungary

content in soil treated with MHA was not significant, but the NH_4^+-N content in soil treated with MHA was significantly increased in 0-10 cm and 20-40 cm soil layers (*Table 3*).

Table 2. *Effects of humic acid combined with fertilizer on soil water-soluble cation composition and SAR*

Soil layer (cm)	Treatment	Cation content (cmol·kg^{-1})				SAR
		K^+	Na^+	Ca^{2+}	Mg^{2+}	
0-10	NP	6.16a	20.86a	4.9ab	1.68ab	11.5a
	BHA + NP	5.60ab	18.20b	4.34b	1.54b	10.61b
	AHA + NP	5.18b	16.80b	4.20b	1.40b	10.04b
	MHA + NP	4.90b	16.80b	5.32a	1.82a	8.89b
10-20	NP	4.90a	45.50a	5.04a	1.96a	24.32a
	BHA + NP	2.94b	38.92b	4.76a	1.96a	21.23b
	AHA + NP	3.78b	37.66b	4.62a	2.10a	20.54b
	MHA + NP	4.06b	38.36b	4.76a	1.96a	20.93b
20-40	NP	3.64a	61.18a	6.44a	2.10a	29.61a
	BHA + NP	3.08b	52.64b	6.02a	2.24a	25.90b
	AHA + NP	3.44a	53.20b	6.16a	2.52a	25.54b
	MHA + NP	3.08b	47.74b	6.30a	2.38a	22.92b

"NP" represents nitrogen and phosphate fertilizer, "BHA + NP" represents biochemical humic acid combined with nitrogen and phosphate fertilizer, "AHA + NP" represents ammoniated humic acid combined with nitrogen and phosphorus fertilizer), and "MHA + NP" represents microbial activated humic acid combined with nitrogen and phosphate fertilizer. Different lowercase letters represent significant differences among treatments in the same soil layer ($P < 0.05$)

Table 3. *Effects of humic acid combined with fertilizer on soil soluble nitrogen content (mg·kg^{-1})*

Soil layer (cm)	Treatment	NH_4^+-N	NO_3^--N	SON	TSN
0-10	NP	1.68b	7.52a	9.03b	17.42b
	BHA + NP	2.24ab	6.76ab	10.18b	19.42b
	AHA + NP	2.03ab	6.15b	14.54a	22.89a
	MHA + NP	2.41a	4.68c	14.70a	22.33a
10-20	NP	1.79ab	6.13a	9.87b	18.72a
	BHA + NP	1.41b	6.41b	11.68a	18.89a
	AHA + NP	2.08a	1.83c	7.45b	11.76c
	MHA + NP	1.93a	2.07c	12.13b	14.73d
20-40	NP	1.27bc	13.14a	7.44b	21.51a
	BHA + NP	1.15c	10.54b	9.63a	21.58a
	AHA + NP	1.57b	2.81d	6.98b	12.39c
	MHA + NP	1.78a	5.12c	9.75a	15.76d

SON and TSN represent soil soluble organic nitrogen and soluble total nitrogen respectively. "NP" represents nitrogen and phosphate fertilizer, "BHA + NP" represents biochemical humic acid combined with nitrogen and phosphate fertilizer, "AHA + NP" represents ammoniated humic acid combined with nitrogen and phosphorus fertilizer), and "MHA + NP" represents microbial activated humic acid combined with nitrogen and phosphate fertilizer. Different lowercase letters represent significant differences among treatments in the same soil layer ($P < 0.05$)

http://www.aloki.hu ● ISSN 1589 1623 (Print) ● ISSN 1785 0037 (Online)
DOI: http://dx.doi.org/10.15666/aeer/1902_12791294
© 2021, ALÖKI Kft., Budapest, Hungary

The analysis results of soluble organic nitrogen (SON) showed that the SON content in the 10-20 cm and 20-40 cm soil layers treated with BHA was significantly higher than NP content, while that in the 0-10 cm soil layer treated with AHA was significantly higher than NP content, and that in the 0-10 cm and 20-40 cm soil layers treated with MHA was significantly higher than NP content (*Table 3*). Thus, the application of humic acid has the effect of increasing SON content, and the depth of BHA and MHA in the season of application reaches 40 cm soil layer, while AHA only has a significant effect at 0-10 cm soil layer.

Soil soluble total nitrogen (TSN) is the sum of NO_3^--N, NH_4^+-N, and SON. The TSN content of BHA and NP in the 0-40 cm soil layer was not significantly different, while the TSN content of AHA and MHA in the 0-10 cm soil layer was significantly higher than NP, and the TSN content of AHA and MHA in the 0-10 cm soil layer was significantly lower than NP. Among the three humic acids, BHA in 0-10 cm soil layer was lower than AHA and MHA, and there is no significant difference between the latter two. The TSN content in the 10-40 cm soil layer was manifested as BHA > MHA > AHA, and the difference between the three treatments was significant.

The effect of humic acid combined with fertilizer on soil available phosphorus content

The content of available phosphorus in 0-40 cm soil significantly decreased with the increase of soil depth (*Fig. 3*). The combination of humic acid and fertilizer significantly increased the available phosphorus content in soil layers 0-10 cm and 20-40 cm by 17.9-73.4%, and 62.3-98.4%, respectively (*Fig. 3A* and *C*), but the available phosphorus content in soil layers 10-20 cm showed no obvious advantage (*Fig. 3B*). The content of available phosphorus in soil under MHA treatment was the highest in all 3 soil layers and was significantly higher in 0-10 cm soil layer than other treatments.

The effect of humic acid combined with fertilizer on chlorophyll content and biomass of cotton

No application of nitrogen fertilizer or phosphorus fertilizer had no significant effect on the chlorophyll content of cotton functional leaves at the flowering and boll period, but it significantly reduced the total biomass of cotton. The combination of humic acid and fertilizer effectively increased the chlorophyll content of functional leaves by 6.7-8.4% compared with NP, but the difference between the three humic acid materials was not significant. In addition, the combined application of BHA, AHA, and MHA increased the total biomass of cotton by 9.2%, 19.3%, and 11.6%, respectively, compared with NP (*Table 4*). The analysis of biomass distribution of different parts of cotton plants showed that nitrogen deficiency mainly affected the biomass of leaves, stems, and bolls, phosphorus deficiency mainly affected the biomass of leaves and bolls, and humic acid combined with nitrogen and phosphorus mainly promoted the biomass of leaves and bolls.

The effect of humic acid combined with fertilizer on yield and components of cotton

Under the condition of soil fertility, only nitrogen or phosphorus fertilizer could significantly reduce cotton yield. Compared with the application of nitrogen and phosphorus fertilizer (NP), the yield of cotton increased by 15.9%, 15.9%, and 14.1% respectively with the addition of BHA, AHA, and MHA. However, the yield of cotton among the three humic acid treatments was almost the same (*Table 5*). Through the analysis

http://www.aloki.hu ● ISSN 1589 1623 (Print) ● ISSN 1785 0037 (Online)
DOI: http://dx.doi.org/10.15666/aeer/1902_12791294
© 2021, ALÖKI Kft., Budapest, Hungary

of the components of cotton yield, it was found that the deficiency of nitrogen supply in saline-alkali land had a significant effect on the number of effective bolls per plant and the weight of a single boll. The deficiency of phosphorus supply mainly affected the weight of single boll. The increase of cotton yield with BHA and AHA was mainly due to the increase of the number of effective bolls per plant, while the combination of MHA and chemical fertilizer had a significant effect on the weight of a single boll.

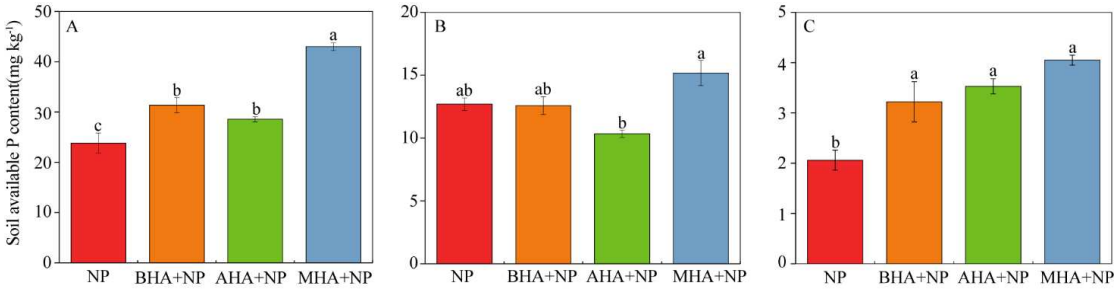


Figure 3. *Influence of humic acid combined with fertilizer on soil available phosphorus content. A, B and C represent soil layers 0-10 cm, 10-20 cm and 20-40 cm, respectively. "NP" represents nitrogen and phosphate fertilizer, "BHA + NP" represents biochemical humic acid combined with nitrogen and phosphate fertilizer, "AHA + NP" represents ammoniated humic acid combined with nitrogen and phosphorus fertilizer), and "MHA + NP" represents microbial activated humic acid combined with nitrogen and phosphate fertilizer. The error lines represent the standard variance, and different lowercase letters represent significant differences among treatments in the same soil layer ($P < 0.05$)*

Table 4. *Effects of humic acid combined with fertilizer on chlorophyll content and biomass of cotton*

Treatment	SPAD	Biomass (t hm^{-2})				
		Root	Stem	Leaf	boll	Total biomass
-N	54.75b	0.62ab	3.91c	7.21c	14.29d	26.03c
-P	56.84ab	0.64ab	4.46b	6.81c	15.38c	27.29c
NP	55.65b	0.69a	4.10bc	8.41b	19.23b	32.43b
BHA + NP	60.34a	0.71a	4.23b	9.12ab	21.35a	35.41ab
AHA + NP	59.76a	0.59b	5.48a	11.73a	20.88a	38.68a
MHA + NP	59.39a	0.69a	4.40b	10.55a	20.55a	36.19ab

"-N" represents only phosphorus fertilizer, no nitrogen fertilizer, "-P" represents only nitrogen fertilizer, no phosphorus fertilizer, "NP" represents nitrogen and phosphate fertilizer, "BHA + NP" represents biochemical humic acid combined with nitrogen and phosphate fertilizer, "AHA + NP" represents ammoniated humic acid combined with nitrogen and phosphorus fertilizer), and "MHA + NP" represents microbial activated humic acid combined with nitrogen and phosphate fertilizer. Different lowercase letters represent significant differences among treatments in the same soil layer ($P < 0.05$)

The effect of humic acid combined with fertilizer on absorption and utilization of nitrogen and phosphorus in cotton

The nitrogen and phosphorus utilization rates of cotton with combined application of humic acid and fertilizer increased by 42.0-105.8% and 52.7-112.7%, respectively, with significant differences. Among the three tested humic acid materials,

http://www.aloki.hu ● ISSN 1589 1623 (Print) ● ISSN 1785 0037 (Online)
DOI: http://dx.doi.org/10.15666/aeer/1902_12791294
© 2021, ALÖKI Kft., Budapest, Hungary

AHA > MHA > BHA (*Table 6*). Compared with NP, the agronomic efficiency of nitrogen and phosphorus increased by 29.6-51.9% and 47.2-71.7%, respectively, after the combination of humic acid and fertilizer. The agronomic efficiency of BHA combined with fertilizer was the highest, which indicated that the application of BHA was more conducive to the improvement of unit nutrient yield. The partial productivity of nitrogen and phosphate fertilizer treated with humic acid was significantly higher than that of the control group, but there was no significant difference among the three humic acid materials.

Table 5. *Effects of humic acid combined with fertilizer on yield and components of cotton*

Treatment	Yield components		Yield (kg hm^{-2})
	Effective bolls per plant	Single boll weight (g)	
-N	5.87d	5.93d	4212d
-P	6.96cd	6.04d	4623c
NP	7.39bc	6.50b	5387b
BHA + NP	9.15a	6.23c	6241a
AHA + NP	8.61a	6.21c	6243a
MHA + NP	8.46ab	6.70a	6147a

"-N" represents only phosphorus fertilizer, no nitrogen fertilizer, "-P" represents only nitrogen fertilizer, no phosphorus fertilizer, "NP" represents nitrogen and phosphate fertilizer, "BHA + NP" represents biochemical humic acid combined with nitrogen and phosphate fertilizer, "AHA + NP" represents ammoniated humic acid combined with nitrogen and phosphorus fertilizer), and "MHA + NP" represents microbial activated humic acid combined with nitrogen and phosphate fertilizer. Different lowercase letters represent significant differences among treatments in the same soil layer ($P < 0.05$)

Table 6. *Effects of humic acid combined with fertilizer on cotton nutrient utilization*

Treatment	Nutrient apparent use efficiency (%)		Agronomic efficiency of fertilizer (kg kg^{-1})		Partial fertilizer productivity (kg kg^{-1})	
	N	P	N	P	N	P
NP	13.8c	11.0c	8.1c	12.7c	38.3b	83.2b
BHA + NP	19.6b	16.8b	12.3a	21.8a	44.2a	96.5a
AHA + NP	28.4a	23.4a	11.2ab	19.8a	44.3a	96.3a
MHA + NP	20.8b	21.7a	10.5b	18.3b	43.5a	94.8a

"NP" represents nitrogen and phosphate fertilizer, "BHA + NP" represents biochemical humic acid combined with nitrogen and phosphate fertilizer, "AHA + NP" represents ammoniated humic acid combined with nitrogen and phosphorus fertilizer), and "MHA + NP" represents microbial activated humic acid combined with nitrogen and phosphate fertilizer. Different lowercase letters represent significant differences among treatments in the same soil layer ($P < 0.05$)

Discussion

The combination of humic acid and fertilizer can improve soil physicochemical properties

According to some analyses, because humic acid is an organic acid, it can combine with cations in the soil to form humate, and then form a buffer system of mutual transformation between humic acid and humate, so it can play a role in regulating soil pH (Boguta et al., 2019). However, in our study, the effect of the three humic acid

http://www.aloki.hu ● ISSN 1589 1623 (Print) ● ISSN 1785 0037 (Online)
DOI: http://dx.doi.org/10.15666/aeer/1902_12791294
© 2021, ALÖKI Kft., Budapest, Hungary

materials on soil pH was not significant (*Fig. 1*), which may be related to the high pH value and of the short period of humic acid materials in this test, or the application of humic acid materials may increase the buffer strength of the soil (Zeng et al., 2013).

Our results showed that the application of the three humic acid materials had a significant reduction in soil EC value, water-soluble Na^+ and K^+ content, and SAR (*Fig. 2; Table 2*), which were similar to the research results of Wang et al. (2016). The reason is that humic acid is a kind of colloid with negative electricity, which can absorb the univalent cation, promote the formation of soil aggregates and increase the permeability of the soil, and accelerating the leaching of salt and alkali on the surface of the soil (Zhao et al., 2017). It is also possible that the hydroxyl and carboxyl functional groups of humic acid condense with calcium ions in the soil, forming soil aggregates through the physiological action of crop roots, thus improving the soil structure and facilitating the leaching of salts (Yonebayashi and Hattori, 1988). In this study, in the 0-40 cm soil layer, the EC value treated with BHA was lower than that of AHA and MHA (*Fig. 2*), which may be related to the fact that BHA is biochemical humic acid, with more active groups and large exchange capacity of salt ions (Zhang and Zhang, 2014). There were no significant differences among the three humic acid materials in the influence of soil water-soluble Na^+ and K^+ content and SAR (*Table 2*). Compared with NP, the contents of water-soluble Ca^{2+} and Mg^{2+} in soil treated with three humic acids were not significantly different, but the contents of water-soluble Ca^{2+} and Mg^{2+} in 0-10 cm soil layer treated with MHA was significantly higher than that of BHA and AHA (*Table 2*), and the reasons remain to be further analyzed.

Through the analysis of the differences of the nitrogen content of various forms in the soil, it was found that the content of NO_3^--N in the soil layer 0-40 cm after humic acid application significantly decreased, while the content of NH_4^+-N and SON increased (*Table 3*). The content of TSN increased in 0-10 cm soil layer with the humic acid application, but it was lower in the soil layer below 10 cm than that in the control, which was similar to the results of Tan et al. (1972). The influence of humic acid on the form of soil nitrogen may be related to the that the carboxyl group and phenolic hydroxyl group of humic acid can react with the amide group of urea to form humic acid urea complex, and the carboxyl group of humic acid can combine with ammonium to form ammonium humate (Aquino et al., 2011). It is also possible that humic acid can stimulate root growth and promote the uptake of nitrogen by crops (Jindo et al., 2012). In farmland, soluble organic nitrogen mainly comes from the humification of organic matter and microbial decomposition (Zang et al., 2000). Humic acid, as an organic modifier, increases the content of soil organic matter on the one hand (Jiménez-González et al., 2019), and on the other hand provides more carbon sources for microorganisms, which has a stimulating effect on the decomposition of soil organic matter (Singh et al., 2019), which may also be the reason why humic acid application improves the content of soil soluble organic nitrogen (Xing et al., 2010). Among the three humic acid materials, mineral humic acid had the best effect in reducing the content of NO_3^--N in soil and increasing the content of NH_4^+-N. The effect of BHA and MHA on increasing the content of SON was as deep as 40 cm soil layer in the application season, while the effect of AHA was only significant in 0-10 cm soil layer. There was no significant difference in the TSN content between BHA and NP in 0-40 cm soil layer, while the TSN content of AHA and MHA in 0-10 cm soil layer was significantly higher than that of NP, and that in soil layer below 10 cm is significantly lower than that in NP (*Table 3*). The results of the significant increase of TSN content

http://www.aloki.hu ● ISSN 1589 1623 (Print) ● ISSN 1785 0037 (Online)
DOI: http://dx.doi.org/10.15666/aeer/1902_12791294
© 2021, ALÖKI Kft., Budapest, Hungary

of mineral source humic acid in 0-10 cm soil layer were mainly due to the increase of SON content, while the results of the decrease of TSN in 10-20 cm and 20-40 cm soil layer were mainly due to the decrease of NO_3^--N content. The decrease of NO_3^--N content is beneficial to the reduction of nitrogen leaching loss and the alleviation of groundwater pollution. The increase of NH_4^+-N and SON content is beneficial to the fixation of soil nitrogen and has a positive effect on the satisfaction of nitrogen nutrition demand in the later growth stage of cotton. It can be seen that the effect of mineral humic acid on nitrogenous fertilizer is better than that of biochemical humic acid.

Relevant research results showed that after humic acid was applied into the soil, it could combine with Ca^{2+} in the soil and reduce Ca-P precipitation (Perassi and Borgnino, 2014). The hydroxyl functional group of humic acid can react with phosphoric acid to form water-soluble phosphorus humic acid and humic acid ammonium phosphorus (Cimrin and Yilmaz, 2005). Wang et al. (2020) found that the available phosphorus content in the soil treated with additional humic acid was significantly higher than that treated with phosphate fertilizer alone, and the fixation rate of soil to phosphorus was reduced. This study also drew a similar conclusion that humic acid could improve the content of soil available phosphorus to a certain extent, and the effect of MHA was the most significant (*Table 4*).

The three humic acid materials all showed a certain effect on the improvement of saline-alkali soil, but the influence degree of different materials on the physical and chemical properties of soil was different. The reason for the difference is that humic acid is a kind of mixture composed of various compounds with different molecular weights. Humic acid raw materials from different origins and different sources have different processing and activation technologies, and their active humic acid content, functional group type, quantity, and activity are different (Wang et al., 2016). In addition, it also may be that the contents of organic matter, total nitrogen, and total potassium of the three humic acid materials vary greatly (*Table 1*), even though the availability of the materials as the total nutrients is limited in season, which led to the different effects of the materials on the physical and chemical properties of saline and alkaline land.

The combination of humic acid and fertilizer promote the growth and development of plants, and increase the yield and nutrient absorption and utilization of cotton

Humic acid can obviously promote the absorption of N, P, and K nutrients in plants, effectively improve the agronomic traits of crops, increase the yield of crops, and promote the absorption and utilization of nutrients in crop plants (Fawzy et al., 2010). In our study, the synergistic effect of humic acid was mainly reflected in the significant improvement of chlorophyll content, biomass, yield, apparent fertilizer utilization rate, and agronomic efficiency of cotton. The increase of chlorophyll content may be related to the application of humic acid promoting the absorption of Mg^{2+} or Fe^{2+} (Mackowiak et al., 2001). This study showed that different humic acid materials could improve cotton biomass in different degrees under the same nutrient input, and AHA treatment reached a significant level, which was similar to the results (Atiyeh et al., 2002). This may be because mineral humic acid can promote the activities of polyphenol oxidase, catalase, and invertase, etc. The enhancement of the enzyme activity speeds up the metabolic process of cotton, thus promoting the growth of cotton (Arancon et al., 2006). Compared with NP, the yield of cotton treated with additional humic acid increased by 14.1-15.9%, but there was no significant difference between the three humic acid

http://www.aloki.hu ● ISSN 1589 1623 (Print) ● ISSN 1785 0037 (Online)
DOI: http://dx.doi.org/10.15666/aeer/1902_12791294
© 2021, ALÖKI Kft., Budapest, Hungary

materials on the yield (*Table 5*). Compared with NP, the utilization rate of nitrogen and phosphorus fertilizer in cotton treated with humic acid increased by 42.0-104.2% and 11.7-55.0%, respectively, and the AHA treatment had the best effect of increasing the utilization rate of nitrogen and phosphorus fertilizer (*Table 6*). The combination of humic acid and fertilizer can improve yield and nutrient utilization. On the one hand, it is related to the improvement of physical and chemical properties of saline-alkali soil by humic acid, which reduces the harm of saline-alkali to crops and creates a more favorable soil environment for the growth of cotton. In addition, humic acid has the function of activating nitrogen and phosphorus and improves the availability of nitrogen and phosphorus (Allison, 2006; Khaled and Fawy, 2011). On the other hand, it may be related to the fact that humic acid can stimulate root growth and development of crops, increase root length, root mass, and root activity, and thus contribute to the improvement of root absorption capacity (Hatami et al., 2018; Jindo et al., 2012).

Conclusions

The effect of a combination of humic acid and fertilizer on saline-alkali land improvement is remarkable. Compared with single fertilizer application, electrical conductivity (EC), water soluble Na^+ and K^+, content and SAR of soil treated with additional humic acid decreased significantly. BHA had the best effect on reducing soil EC, but there was no significant difference among the three humic acid materials in reducing the content of Na^+ and K^+ and the effect of SAR. The content of soluble organic nitrogen in soil could be improved to some extent by applying humic acid, and the BHA and MHA acted at a depth of 40 cm. The content of available phosphorus in soil could be significantly increased by 18.7-101.5% by applying humic acid, among which the MHA effect was the best. The effect of three humic acid materials on the growth and yield of cotton was not obvious but compared with the control treatment with the same nutrient fertilizer. The chlorophyll content and biomass of flowering and boll stage functional leaves of cotton with additional humic acid were significantly increased, the cotton yield increased by 15%, and cotton nitrogen and phosphorus fertilizer use efficiency increased by 42.0-105.8% and 52.7-112.7%, respectively. To sum up, the application of different humic acid materials on saline-alkali land has different effects on soil physical and chemical properties, but the overall effect of improving saline-alkali land and increasing cotton yield is significant. However, due to the short period of this experiment, the medium and long-term effects of different humic acids on soil physical and chemical properties and crop growth need to be further studied.

Acknowledgements. This work was supported by the Central Public Welfare Scientific Research Basic Scientific Research and Special Funds (HKY-JBYW-2020-13 and HKY-JBYW- 2018-04).

REFERENCES

[1] Abe, T., Kobayashi, S., Kobayashi, M. (2011): Aggregation of colloidal silica particles in the presence of fulvic acid, humic acid, or alginate: effects of ionic composition. – Colloids and Surfaces A: Physicochemical and Engineering Aspects 379: 21-26.

[2] Allison, S. D. (2006): Soil minerals and humic acids alter enzyme stability: implications for ecosystem processes. – Biogeochemistry 81: 361-373.

http://www.aloki.hu ● ISSN 1589 1623 (Print) ● ISSN 1785 0037 (Online)
DOI: http://dx.doi.org/10.15666/aeer/1902_12791294
© 2021, ALÖKI Kft., Budapest, Hungary

[3] Aquino, A. J., Tunega, D., Pašalić, H., Schaumann, G. E., Haberhauer, G., Gerzabek, M. H., Lischka, H. (2011): Study of solvent effect on the stability of water bridge-linked carboxyl groups in humic acid models. – Geoderma 169: 20-26.
[4] Arancon, N. Q., Edwards, C. A., Lee, S., Byrne, R. (2006): Effects of humic acids from vermicomposts on plant growth. – European Journal of Soil Biology 42: S65-S69.
[5] Asli, S., Neumann, P. M. (2010): Rhizosphere humic acid interacts with root cell walls to reduce hydraulic conductivity and plant development. – Plant and Soil 336: 313-322.
[6] Atiyeh, R. M., Lee, S., Edwards, C. A., Arancon, N. Q., Metzger, J. D. (2002): The influence of humic acids derived from earthworm-processed organic wastes on plant growth. – Bioresource technology 84(1): 7-14.
[7] Boguta, P., D'Orazio, V., Senesi, N., Sokołowska, Z., Szewczuk-Karpisz, K. (2019): Insight into the interaction mechanism of iron ions with soil humic acids. The effect of the pH and chemical properties of humic acids. – Journal of Environmental Management 245: 367-374.
[8] Ciarkowska, K., Sołek-Podwika, K., Filipek-Mazur, B., Tabak, M. (2017): Comparative effects of lignite-derived humic acids and FYM on soil properties and vegetable yield. – Geoderma 303: 85-92.
[9] Cimrin, K. M., Yilmaz, I. (2005): Humic acid applications to lettuce do not improve yield but do improve phosphorus availability. – Acta Agriculturae Scandinavica, Section B-Soil & Plant Science 55(1): 58-63.
[10] Dehghani, M. H., Zarei, A., Mesdaghinia, A., et al. (2018): Production and application of a treated bentonite-chitosan composite for the efficient removal of humic acid from aqueous solution. – Chemical Engineering Research and Design 140: 102-115.
[11] Erhayem, M., Sohn, M. (2014): Effect of humic acid source on humic acid adsorption onto titanium dioxide nanoparticles. – Science of the Total Environment 470: 92-98.
[12] Fan, H. M., Wang, X. W., Sun, X., Li, Y. Y., Sun, X. Z., Zheng, C. S. (2014): Effects of humic acid derived from sediments on growth, photosynthesis and chloroplast ultrastructure in chrysanthemum. – Scientia Horticulturae 177: 118-123.
[13] Fawzy, Z., Abd El-Baky, M., Mahmoud, R. (2010): Response of snap bean plants to mineral fertilizers and humic acid application. – Research Journal of Agriculture and Biological Sciences 6: 169-175.
[14] Hatami, E., Shokouhian, A. A., Ghanbari, A. R., Naseri, L. A. (2018): Alleviating salt stress in almond rootstocks using of humic acid. – Scientia Horticulturae 237: 296-302.
[15] He, Z., Olk, D. C., Cade-Menun, B. J. (2011): Forms and lability of phosphorus in humic acid fractions of hord silt loam soil. – Soil Science Society of America Journal 75: 1712-1722.
[16] He, K., He, G., Wang, C. P., Zhang, H. P., Xu, Y., Wang, S. M., Kong, Y. Z., Zhou, G. K., Hu, R. B. (2020): Biochar amendment ameliorates soil properties and promotes Miscanthus growth in a coastal saline-alkali soil. – Applied Soil Ecology 155: 103674.
[17] Ifansyah, H. (2014): Soil pH and solubility of aluminum, iron, and phosphorus in ultisols: the roles of humic acid. – Jurnal Tanah Tropika 18: 203-208.
[18] Jiménez-González, M. A., Álvarez, A. M., Carral, P., Almendros, G. (2019): Chemometric assessment of soil organic matter storage and quality from humic acid infrared spectra. – Science of The Total Environment 685: 1160-1168.
[19] Jindo, K., Martim, S. A., Navarro, E. C., Pérez-Alfocea, F., Hernandez, T., Garcia, C., Aguiar, N. O., Canellas, L. P. (2012): Root growth promotion by humic acids from composted and non-composted urban organic wastes. – Plant and Soil 353: 209-220.
[20] Khaled, H., Fawy, H. A. (2011): Effect of different levels of humic acids on the nutrient content, plant growth, and soil properties under conditions of salinity. – Soil and Water Research 6: 21-29.
[21] Li, Y., Fang, F., Wei, J. L., Wu, X. B., Cui, R. Z., Li, G. S., Zheng, F. L., Tan, D. S. (2019): Humic acid fertilizer improved soil properties and soil microbial diversity of continuous cropping peanut: a three-year experiment. – Scientific Reports 9(1): 12014.

http://www.aloki.hu ● ISSN 1589 1623 (Print) ● ISSN 1785 0037 (Online)
DOI: http://dx.doi.org/10.15666/aeer/1902_12791294
© 2021, ALÖKI Kft., Budapest, Hungary

[22] Li, N., Lin, H. X., Wang, T. X., Li, Y., Liu, Y., Chen, X. G., Hu, X. T. (2020): Impact of climate change on cotton growth and yields in Xinjiang, China. – Field Crops Research 247: 107590.
[23] Liang, J. P., Shi, W. J., He, Z. J., Pang, L. N., Zhang, Y. C. (2019): Effects of poly-γ-glutamic acid on water use efficiency, cotton yield, and fiber quality in the sandy soil of southern Xinjiang, China. – Agricultural Water Management 218: 48-59.
[24] Liu, M. L., Wang, C., Wang, F. Y., Xie, Y. J. (2019): Maize (*Zea mays*) growth and nutrient uptake following integrated improvement of vermicompost and humic acid fertilizer on coastal saline soil. – Applied Soil Ecology 142: 147-154.
[25] Mackowiak, C. L., Grossl, P. R., Bugbee, B. G. (2001): Beneficial effects of humic acid on micronutrient availability to wheat. – Soil Science Society of America Journal 65: 1744-1750.
[26] Mahdy, A. M. (2011): Soil properties and wheat growth and nutrients as affected by compost amendment under saline water irrigation. – Pedosphere 21(6): 773-781.
[27] Margot, A., Flaschel, E., Renken, A. (1994): Continuous monitoring of enzymatic whey protein hydrolysis. Correlation of base consumption with soluble nitrogen content. – Process Biochemistry 29(4): 257-262.
[28] Perassi, I., Borgnino, L. (2014): Adsorption and surface precipitation of phosphate onto $CaCO_3$–montmorillonite: effect of pH, ionic strength and competition with humic acid. – Geoderma 232: 600-608.
[29] Selladurai, R., Purakayastha, T. J. (2016): Effect of humic acid multinutrient fertilizers on yield and nutrient use efficiency of potato. – Journal of Plant Nutrition 39(7): 949-956.
[30] Sharpley, A. N. (1991): Effect of soil pH on cation and anion solubility. – Communications in Soil Science and Plant Analysis 22(9): 827-841.
[31] Singh, S., Kumar, V., Singh, S., Singh, J. (2019): Influence of humic acid, iron and copper on microbial degradation of fungicide Carbendazim. – Biocatalysis and Agricultural Biotechnology 20: 101196.
[32] Sudiarto, S. I. A., Renggaman, A., Choi, H. L. (2019): Floating aquatic plants for total nitrogen and phosphorus removal from treated swine wastewater and their biomass characteristics. – Journal of Environmental Management 231: 763-769.
[33] Tan, K. H., Beaty, E. R., McCreery, R. A., Powell, J. D. (1972): Humic-Fulvic acid content in soils as related to ley clipping management and fertilization. – Soil Science Society of America Journal 36(4): 565-567.
[34] Tan, S., Wang, Q. J., Zhang, J. H., Chen, Y., Shan, Y. Y., Xu, D. (2018): Performance of AquaCrop model for cotton growth simulation under film-mulched drip irrigation in southern Xinjiang, China. – Agricultural Water Management 196: 99-113.
[35] Türkmen, Ö., Dursun, A., Turan, M., et al. (2004): Calcium and humic acid affect seed germination, growth, and nutrient content of tomato (Lycopersicon esculentum L.) seedlings under saline soil conditions. – Acta Agriculturae Scandinavica, Section B - Soil & Plant Science 53(3): 168-174.
[36] Wang, F. Y., Wang, C., Liu, Q. Q., Jin, S. J., Xie, J. Y. (2016): Improve effect of humic acid, earthworm protein fertilizer and vermicompost on coastal saline soils. – Journal of China Agricultural University 20(5): 89-94. (in Chinese with English abstract)
[37] Wang, Q. Z., Wang, Y., Sun, Z. M., Liu, J., Niu, S. B., Xue, C., Ma, W. Q. (2019): Amelioration effect of humic acid on saline-alkali soil. – Chinese Journal of Applied Ecology 30(4): 1227-1234 (in Chinese with English abstract).
[38] Wang, M., Liu, S., Zhang, S., Zhang, Q., Mu, K., Chen, Q. (2020): Effect of potassium humate and phosphate fertilizer application method on soil phosphate mobility. – Journal of Agricultural Resources and Environment 37(2): 209-215.
[39] Xiao, Y. S., Peng, F. T., Zhang, Y. F., Wang, J., Zhuge, Y. P., Zhang, S. S., Gao, H. F. (2019): Effect of bag-controlled release fertilizer on nitrogen loss, greenhouse gas emissions, and nitrogen applied amount in peach production. – Journal of Cleaner Production 234: 258-274.

http://www.aloki.hu ● ISSN 1589 1623 (Print) ● ISSN 1785 0037 (Online)
DOI: http://dx.doi.org/10.15666/aeer/1902_12791294
© 2021, ALÖKI Kft., Budapest, Hungary

[40] Xie, W. Q., Gong, Y. X., Yu, K. X. (2019): An efficient headspace gas chromatographic technique for determining humic acid content in fertilizer. – Journal of Chromatography A 1596: 194-198.
[41] Xing, S. H., Chen, C. R., Zhou, B. Q., Zhang, H., Nang, Z. M., Xu, Z. H. (2010): Soil soluble organic nitrogen and active microbial characteristics under adjacent coniferous and broadleaf plantation forests. – Journal of Soils and Sediments 10(4): 748-757.
[42] Yang, Y. L., Chen, M. Z., Tian, J. S., Xiao, F., Xu, S. Z., Zuo, W. Q., Zhang, W. F. (2019): Improved photosynthetic capacity during the mid- and late reproductive stages contributed to increased cotton yield across four breeding eras in Xinjiang, China. – Field Crops Research 240: 177-184.
[43] Yonebayashi, K., Hattori, T. (1988): Chemical and biological studies on environmental humic acids. – Soil Science and Plant Nutrition 34(4): 571-584.
[44] Zang, X., van Heemst, J. D., Dria, K. J., Hatcher, P. G. (2000): Encapsulation of protein in humic acid from a histosol as an explanation for the occurrence of organic nitrogen in soil and sediment. – Organic Geochemistry 31(7-8): 679-695.
[45] Zeng, W. A., Zeng, M., Zhou, H., Lei, M., Hu, L. Q. (2013): Improvement of alkaline tobacco field soil by combined application of humic acid and ferric sulfate. – Journal of Soil and Water Conservation 27(03): 170-173 (in Chinese with English abstract).
[46] Zhang, Y. P., Zhang, X. Z. (2014): Extraction and characterization of biotechnology humic acid of fermented furfural residue. – Journal of Anhui Agricultural Science 42: 9752-9754 (in Chinese with English abstract).
[47] Zhang, M., Xiao, H. J., Zhao, H., An, J. Y., Qin, S., Gou, J. L., Hu, G. (2016): Responses of dry matter, nitrogen accumulation and distribution and nitrogen utilization of pepper to new-type fertilizers in Guizhou yellow soil. – Chinese Journal of Applied Ecology 27(9): 2983-2990 (in Chinese with English abstract).
[48] Zhang, Q., Li, Y., Xing, J. J., Brookes, P. C., Xu, J. M. (2019a): Soil available phosphorus content drives the spatial distribution of archaeal communities along elevation in acidic terrace paddy soils. – Science of The Total Environment 658: 723-731.
[49] Zhang, S. Q., Liang, Y., Li, W., Lin, Z. A., Li, Y. T., Hu, S. W. (2019b): Effects of urea enhanced with different weathered coal-derived humic acid components on maize yield and fate of fertilizer nitrogen. – Journal of Integrative Agriculture 18(3): 656-666.
[50] Zhao, S. X., Chen, Z. L., Shen, J. M., Kang, J., Shen, Y. Q. (2017): Leaching mechanisms of constituents from fly ash under the influence of humic acid. – Journal of Hazardous Materials 321: 647-660.

http://www.aloki.hu ● ISSN 1589 1623 (Print) ● ISSN 1785 0037 (Online)
DOI: http://dx.doi.org/10.15666/aeer/1902_12791294
© 2021, ALÖKI Kft., Budapest, Hungary

BIODEGRADATION OF 4-CHLORO-2-METHYLPHENOXYACETIC ACID BY ENDOPHYTIC FUNGUS *PHOMOPSIS* SP. IN LIQUID MEDIUM AND SOIL

WANG, Y.[1,2‡] – FENG, G.[1‡] – LI, H.[1] – DU, L.[3*] – ZENG, D.[1*]

[1]*Institute of Pesticide and Environmental Toxicology, Guangxi University Nanning 530004, PR China*

[2]*Guangxi Key Laboratory of Biology for Crop Diseases and Insect Pests, Plant Protection Research Institute, Guangxi Academy of Agricultural Sciences, Nanning 530005, PR China*

[3]*College of Chemistry and Chemical Engineering, Guangxi University Nanning 530004, PR China*

[‡]*These authors contributed equally to this work.*

[*]*Corresponding authors*
e-mail: dulily9@163.com (Du, L.) or zengdq550@163.com (Zeng, D.)
phone/fax: +86-771-323-1584

(Received 27th Oct 2020; accepted 27th Jan 2021)

Abstract. An endophytic fungus strain, newly isolated from *Psidium guajava* (common guava), could effectively degrade 4-chloro-2-methylphenoxyacetic acid (MCPA). According to the analysis of its phenotypic feature and ITS rDNA gene sequence, the isolated strain was identified as *Phomopsis* sp. and named E41. The influencing factors including medium pH, temperature, and initial concentration of MCPA affecting the degradation of MCPA by this strain were optimized in this study. The maximum biodegradation rate of 86.89% was obtained after inoculation for 7 days under the optimal conditions with MCPA concentration of 50 mg/L, temperature 30 °C and a pH of 6. The metabolite 4-chloro-2-methylphenol was detected by using gas chromatography-mass spectrometry (GC-MS). In the bioremediation experiment, the biodegradation of MCPA was significantly enhanced in all soils with the presence of the strain E41. These results suggested that the strain E41 may have potential value for the bioremediation of MCPA-contaminated environment.
Keywords: *phenoxy acid herbicide, Psidium guajava, microbe, decompose, bioremediation*

Introduction

4-chloro-2-methylphenoxyacetic acid (MCPA), a phenoxy acid herbicide, was registered for the control of annual and perennial post-emergence broad-leaf weeds in agricultural field. MCPA is relatively soluble in water, weakly sorbed by soil, where it is highly mobile in soil, which gives rise to high leaching risk into surface water and groundwater (Cabrera et al., 2011; Önneby et al., 2014). MCPA has been frequently detected in surface water, groundwater and well water in many countries. Some studies have reported that this phenoxy acid herbicide could cause endocrine disturbance for humans and animals although it has relatively slight toxicity (Bukowska et al., 2008; Salvo et al., 2015). For these reasons, the European Community and US Environmental Protection Agency have classified MCPA as priority pollutant (Sanchis et al., 2014). Therefore, it is necessary to develop effective ways to accelerate the decrease and elimination of MCPA residue in environment.

http://www.aloki.hu ● ISSN 1589 1623 (Print) ● ISSN 1785 0037 (Online)
DOI: http://dx.doi.org/10.15666/aeer/1902_12951307
© 2021, ALÖKI Kft., Budapest, Hungary

Previous studies have shown that degradation by microbes is regarded as an effective method in the removal of MCPA residue for the environment (Verma et al., 2014; Wu et al., 2017). However, only a few bacteria and fungi were isolated to utilize MCPA as sole carbon source for growth due to its antibacterial properties (Tan et al., 2013; Xiang et al., 2020; Zhang et al., 2020). It is essential to screen more excellent MCPA-degrading microbes with high environmental tolerance. The endophytic microbes as a valuable microbial resource reside in internal tissues of living plants without causing apparent symptoms of infection and have mutualism effect on plants. It has been demonstrated that endophytes play a crucial role in host plant for the adaptation to the polluted environment (Khan et al., 2014). Many endophytic microbes have been successfully isolated from different plants with pollutant-degrading activities (Sun et al., 2014a,b; Zhu et al., 2016). Recently, several endophytic bacteria have been reported to degrade herbicides including simazine, glyphosate and quinclorac (Ozawa et al., 2004; Liu et al., 2014). Up to now, no MCPA-degrading endophytic microbe has been reported.

In this work, an endophytic fungus with the ability to degrade MCPA was isolated from leaves of *Psidium guajava* grown in Nanning city of south China and then was identified by morphological and molecular analysis. The effect factors on degradation efficiency were also optimized by single-factor optimization test. The metabolic fate of MCPA was deducted according to the identification of metabolites by gas chromatography-mass spectrometry (GC-MS). The soil bioremediation experiment was carried out to evaluate its potential in the remediation of MCPA-contaminated soil. To our knowledge, it is the first report on the biodegradation of MCPA by endophyte isolated from *Psidium guajava*.

Materials and methods

Chemicals and solutions

MCPA (98% purity) was purchased from Dr. Ehrenstorfer GmbH (Augsburg, Germany). Acetonitrile and methanol were HPLC grade (Fisher Scientific Company, USA) and other reagents were analytical grade (National Pharmaceutical Group Corporation, China). Unless otherwise stated, deionized water was used in all of the experiments.

The mineral salt medium (MSM) was composed of (g/L) NH_4NO_3 1.0, K_2HPO_4 1.5, KH_2PO_4 0.5, NaCl 1.0, $MgSO_4 \cdot 7H_2O$ 0.1, and $FeSO_4$ 0.025. The potato dextrose (PD) medium was prepared by containing 200 g/L potato extract and 20 g/L D-glucose. The composition of Luria–Bertani (LB) medium contained (g/L): yeast extract 5, tryptone 10, NaCl 10. Solid media were prepared by adding 1.5% (w/v) agar into the above liquid media.

Psidium guajava was collected at July when the leaf was fully unfolded and grew well nearby warehouse of the factory producing MCPA in Nanning city of south China (22°35′15.29″N, 108°13′1.26″E) for at least 5 years. The stems and leaves were placed into labelled plastic bags, then immediately transported to the laboratory for use.

Isolation of MCPA-degrading endophytic fungi

The surface of samples (stems and leaves) was sterilized by immersing into 75% ethanol for 2–3 min, and 0.1% mercuric chloride for 5 min. Then the sterilized samples were washed three times with sterile water for 2 min and cut into pieces (approximately

http://www.aloki.hu ● ISSN 1589 1623 (Print) ● ISSN 1785 0037 (Online)
DOI: http://dx.doi.org/10.15666/aeer/1902_12951307
© 2021, ALÖKI Kft., Budapest, Hungary

1×2 cm) with a sterilized blade. To verify whether the sterilization process was successful, aliquots of the final washing sterile water were spread onto LB agar plate and incubated at 28 ºC. The sterilization process was considered successful if no colony was found on agar plate after inoculation.

After sterilization, 1 g samples were ground with 10 mL sterile water using a sterilized mortar and pestle, and then the samples were stepwise diluted to 10^{-2} and 10^{-3}. 100 μL diluted solution was spread onto MSM agar plate containing 500 mg/L MCPA and then incubated at 28 ºC. Isolates exhibiting distinct colonial morphologies were isolated and purified by repeated streaking on PD agar plate.

Identification of endophytic fungus

According to the results of screening experiment, a strain named E41 was selected for further analysis. After strain E41 was incubated on PD agar plate at 28 ºC for 7 days, the morphological feature was observed. The ITS sequence of strain E41 was extracted, purified and amplified by polymerase chain reaction (PCR) with universal fungal primers of ITS1 (5′-TCCGTAGGTGAACCTGCGG-3′) and ITS4 (5′-TCCTCCGCTTATTGATATGC-3′) (Song et al., 2013). The PCR condition was as follows: denaturation at 95 ºC for 5 min, 35 cycles with each consisting of 95 ºC for 30 s, 55 ºC for 30 s and 72 ºC for 1 min, and a final extension at 72 ºC for 10 min. The PCR product was verified and purified by agarose gel electrophoresis, and then sequenced in Shanghai Invitrogen Biological Technology Co., Ltd. The sequence was compared with the published sequences in GenBank using BLAST program on the National Centre for Biotechnology Information (NCBI) website (http://www.ncbi.nlm.nih.gov). The partial ITS gene sequences of the isolate and related fungi were then aligned and processed to produce an unrooted phylogenetic tree using the neighbor-joining method with MEGA software package (Tamura et al., 2011).

Biodegradation of MCPA in MSM

A MCPA-degrading strain designated as E41 was used for inoculum preparation and cultured in a 250-mL Erlenmeyer flask containing 100 mL PD medium supplemented with 50 mg/L MCPA. After incubation for 3 days, the strain was collected by centrifugation at 12000 rpm for 2 min and washed three times with MSM to remove the remaining PD medium. Then, the biomass (0.55 g dr w/L) was seeded into 100 mL MSM supplemented with 50 mg/L MCPA as the only carbon source.

In order to study the optimal degradation condition of MCPA by this strain, single-factor test was designed under different conditions including pH (4–9), temperature (20–40 ºC), and initial concentration of MCPA (25–100 mg/L). All samples in triplicate were incubated at 28 ºC in a rotary shaker (150 rpm).

Samples were periodically collected to determine MCPA concentration and fungal biomass. 5 mL culture solution was collected, followed by the addition of 5 mL acetonitrile and 2 g NaCl. After shaking at 150 rpm for 2 h, 2 mL supernatant was taken, added with 0.2 g $MgSO_4$, vortexed for 1 min, and centrifuged at 4000 rpm for 2 min. The solution was then filtered through an organic membrane prior to the analysis of MPCA residue by high-performance liquid chromatograph (HPLC). The biomass of strain E41 was measured by dry weight of mycelium (in grams per liter).

http://www.aloki.hu ● ISSN 1589 1623 (Print) ● ISSN 1785 0037 (Online)
DOI: http://dx.doi.org/10.15666/aeer/1902_12951307
© 2021, ALÖKI Kft., Budapest, Hungary

Determination of degradation products

During the biodegradation experiment in MSM under the optimal conditions, 10 mL culture solution was collected and centrifuged at 12000 rpm for 2 min to remove the proteins. The supernatant was mixed with 30 mL acetonitrile to extract the degradation products. Then 8 g NaCl was added to make the mixed solution separate into two layers. Finally, the upper layer was taken, dewatered, dried and re-dissolved before the detection by GC-MS (Zertal et al., 2004).

The degradation products of MCPA were detected by an Agilent 7890N/5975 GC-MS equipped with HP-5MS capillary column (30 m×0.25 mm i.d., 0.25 μm film). The temperature program was as follows: the column was held initially at 40 °C for 5 min, raised with 10 °C/min to 200 °C, held at 200 °C for 1 min, ramped with 10 °C/min to 280 °C, and then held at 280 °C for 8 min. Analyses were performed in splitless mode at 220 ºC. The transfer line temperature was set at 250 ºC, and the ion source was operated at 70 eV and 250 ºC. Full scans were obtained by scanning from 100 to 500 m/z. Helium was used as a carrier gas with a flow rate of 1.5 mL/min.

Bioremediation of MCPA in soil

The bioremediation experiment with this fungus strain was carried out in soils. Soil sample was sterilized three times by autoclaving for 1 h at 121 ºC. The stock solution of MCPA was added to 500 g sterile soil with a final concentration of 2.5 mg/kg. After mixing and solvent evaporation, the microbial suspension was introduced into the soil with the final biomass of approximately 1 g per 100 g soil. In order to study the dissipation rate of MCPA under abiotic condition, the sample of sterile soil without the added fungus was kept as control. The water content in soil samples was adjusted to 50% of the maximum water-holding capacity by the addition of sterile deionized water. All soil samples were incubated at 30 ºC in a dark thermostatic chamber. During the incubation period, sterile deionized water was added to the soil treatments to compensate for any water loss exceeding 5% of the initial amount added. Periodically, samples of soil treatments were aseptically removed for the determination of MCPA concentration.

Soil samples were mixed with 40 mL acetonitrile for 6 h by shaking at 150 rpm, added with 5 g NaCl, and vortexed for 1 min. After centrifugation at 4000 rpm for 5 min, 30 mL supernatant was taken, added with 3 g $MgSO_4$, vortexed for 1 min, and centrifuged at 4000 rpm for 5 min. Then, 20 mL supernatant was collected, transferred into a 50-mL rotating steam bottle, rotated to dryness at 40 °C, and dissolved in 2 mL acetonitrile. Finally, the solution was filtered through an organic membrane before the determination of MCPA concentration by HPLC.

Determination of MCPA

The MCPA residue was detected by an Agilent 1260 HPLC equipped with a UV detector and ZORBAX Eclipse XDB C_{18} column (250 mm×4.6 mm i.d., 5 μm). A mixture of methanol and water with 0.2% acetic acid (60:40, v/v) was used as mobile phase with a flow rate of 1 mL/min. The detection wavelength was 230 nm and the injection volume was 20 μL with column temperature at 30 ºC. The degradation rate was calculated by regression using a first-order reaction model (*equation 1*):

$$C_t = C_0 \times e^{-kt} \quad \text{(Eq.1)}$$

http://www.aloki.hu ● ISSN 1589 1623 (Print) ● ISSN 1785 0037 (Online)
DOI: http://dx.doi.org/10.15666/aeer/1902_12951307
© 2021, ALÖKI Kft., Budapest, Hungary

where C_0 (mg/L) is the initial concentration of MCPA, C_t (mg/L) is the MCPA concentration at time t (d) and k is the degradation rate (day^{-1}). The half-life was calculated as *equation (2)* (Tortella et al., 2010):

$$t_{1/2} = \ln(2)/k \quad \text{(Eq.2)}$$

Statistical analysis

The data were calculated using Excel 2010 and then analyzed with the SPSS 22.0 software and Origin 9.0 software. The statistical significance of differences was performed with the one-way analysis of variance (ANOVA) by Tukey's test. Differences were considered significant at p values < 0.05.

Results and Discussion

Isolation and identification of fungus

As the result of the screening process, thirteen fungus strains were isolated and purified from *Psidium guajava* by streaking plate method. Among the isolated strains, primary experiments showed that the degradation rates of MCPA were below 30% by 12 fungus strains. Thus, a strain named E41 was selected for further detailed research due to its relatively high MCPA-degrading ability. This strain could utilize MCPA as the sole carbon source and energy source for its growth in MSM.

Morphological feature was used to identify strain E41. On PD agar plate, strain E41 was full of the whole plate at the seventh day with the growth rate of 0.64 cm/d. After incubation for 7 days at 28 °C (*Fig. 1*), the colony approximately 5 cm in semidiameter was dark brown with white villous on both sides, and grew radially with similar annual wheel-like boundaries. The thickness of the center was basically the same as that of the edge, and the edge of the colony was in an irregular shape.

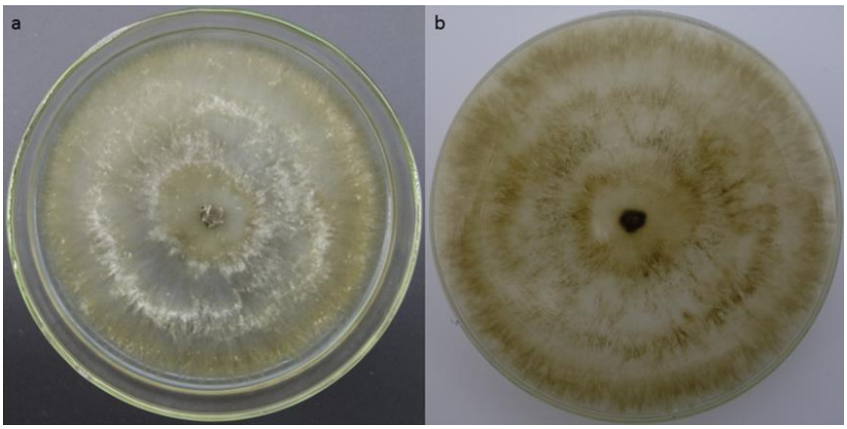


Figure 1. *Colonies on PD agar plate in 9-cm petri dish after incubation for 7 days, the front side (a), and the reverse side (b)*

Due to the lack of sporulation, identification of strain E41 was further performed by the analysis of ITS sequence. The ITS gene sequence with 555 bps was deposited in GenBank database under accession number KY797680. Analysis of partial ITS rDNA

http://www.aloki.hu ● ISSN 1589 1623 (Print) ● ISSN 1785 0037 (Online)
DOI: http://dx.doi.org/10.15666/aeer/1902_12951307
© 2021, ALÖKI Kft., Budapest, Hungary

sequence showed that strain E41 was closely related to the species of fungus *Phomopsis* sp. (GenBank Accession No. GU066614.1, GU066605.1, KX953471.1, GU066629.1, and GU066607.1). To identify the phylogeny of strain E41, strains from different genera were chosen to construct a phylogenetic tree based on ITS sequence using MEGA 6.0 (*Fig. 2*). Phylogenetic tree showed that strain E41 exhibited 99% similarity to *Phomopsis* sp. (GenBank Accession No. GU066614.1).

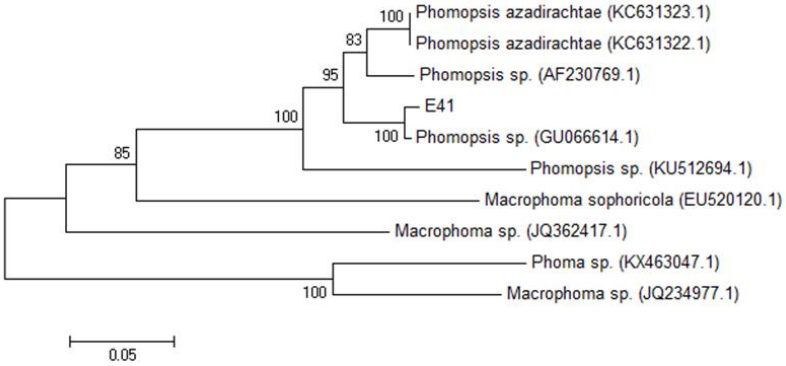


Figure 2. *Phylogenetic tree of strain E41 and related by the neighbor-joining approach. Bootstrap values obtained with 1000 repetitions are indicated as percentage at all branches*

According to the results of phenotypic feature and ITS gene sequence, strain E41 was identified as *Phomopsis* sp. Previous reports have demonstrated that members of endophyte *Phomopsis* sp. have the potential ability to degrade organic pollutants such as 4-hydroxybenzoic acid (Chen et al., 2011), N-heterocyclic indole (Chen et al., 2013a), ferulic acid (Xie and Dai, 2015), and soil resveratrol (Wang et al., 2019) and have the potential application to the ecological remediation of long-term cropping soil (Chen et al., 2013b). At present, many bacteria and fungi capable of degrading phenoxy acid herbicide have been isolated from various environments (Wu et al., 2017; Xiao et al., 2017; Zhang et al., 2020; Sheng et al., 2020). However, there are few reports on the degradation of MCPA by endophytic fungi. This study was the first report about MCPA-degrading endophytic fungus and expanded the application range of endophytic fungus in the field of environmental pollution remediation.

Biodegradation of MCPA in MSM

The effect of pH values on the degradation of MCPA by strain E41 was investigated and the result was shown in *Fig. 3a*. Observed from *Fig. 3a*, strain E41 could degrade MCPA in a range of pH 4–9 with the biodegradation rate from 60.69% to 89.21%. Many studies also demonstrated that biodegradation of organic pollutants was depended on the initial pH (Wang and Xie, 2012; Lin et al., 2014; Yu et al., 2015). Compared with *Cupriavidus campinensis* BJ71 and *Achromobacter* sp. LZ35, strain E41 showed a wider pH range to phenoxy acid herbicide (Han et al., 2015; Xia et al., 2017). The biodegradation rate of MCPA reached the maximum value at optimal pH 6. Meanwhile, the degradation rate of MCPA by strain E41 was not affected significantly in the pH range of 5–7. These results showed that strain E41 was more efficient to degrade MCPA in weak acid and neutral conditions. The similar pH condition was previously reported on the biodegradation of phenoxy acid herbicide (Greer et al., 1990; Byunghoon et al., 2003; Wu et al., 2017).

http://www.aloki.hu ● ISSN 1589 1623 (Print) ● ISSN 1785 0037 (Online)
DOI: http://dx.doi.org/10.15666/aeer/1902_12951307
© 2021, ALÖKI Kft., Budapest, Hungary

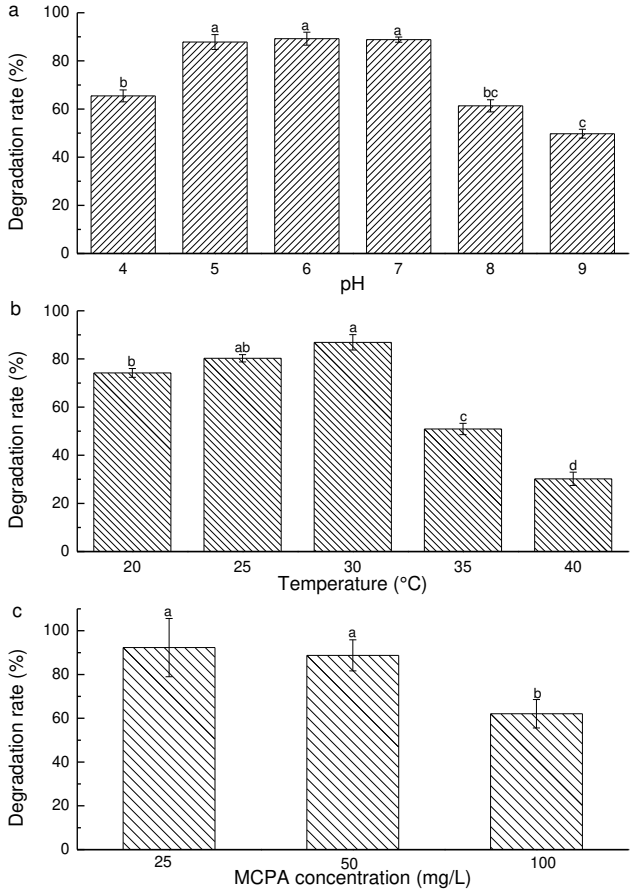


Figure 3. *The effect of different conditions on MCPA degradation by strain E41. (a) Effect of pH on the removal of MCPA, (b) effect of temperature on the removal of MCPA, (c) Effect of initial concentration on the removal of MCPA. The columns marked by different letters indicate significantly different from each other. Error bars represent the standard deviation of three replicates*

Temperature was an important factor on the biodegradation of organic pollutant in MSM (Yu et al., 2005; Song et al., 2013; Liu et al., 2016). The degradation rate of MCPA by strain E41 was investigated at the temperature from 20 to 40 °C and the result was illustrated in *Fig. 3b*. The biodegradation rates at 20, 25, 30, 35, and 40 °C were 74.19, 80.29, 86.89, 50.92, and 30.21% after incubation with strain E41 for 7 days, respectively. The degradation rate of MCPA gradually increased at 20–30 °C, but significantly decreased at 40 °C. The optimal temperature was 30 °C for the degradation of MCPA by strain E41. The temperature condition of strain E41 for MCPA degradation were similar to those previous findings on the biodegradation of phenoxy acid herbicide (Han et al., 2015; Samir et al., 2015; Xia et al., 2017; Xiao et al., 2017).

The biodegradation experiments were carried out with the initial MCPA concentration from 25 to 100 mg/L at 30 °C and pH 6, while the corresponding degradation rates were 92.31, 88.75, and 62.08% in MSM with strain E41, respectively (*Fig. 3c*). This result indicated that the initial concentration of MCPA above 100 mg/L could inhibit the degradation capacity of strain E41. This finding was consistent with the report of Chen et al. (2011), who demonstrated that 4-hydroxybenzoic acid in high concentrations could inhibit the growth of endophytic fungus *Phomopsis liquidambari* in vitro. Similarly, Wu

http://www.aloki.hu ● ISSN 1589 1623 (Print) ● ISSN 1785 0037 (Online)
DOI: http://dx.doi.org/10.15666/aeer/1902_12951307
© 2021, ALÖKI Kft., Budapest, Hungary

et al. (2017) reported that the degradation of 2,4-dichlorophenoxyacetic acid by *Cupriavidus gilardii* T-1 was inhibited with increasing concentrations.

The MCPA residue and biomass of strain E41 under optimal conditions were periodically determined during degradation process (*Fig. 4*). Observed from *Fig. 4*, the MCPA residue was gradually decreasing and the fungal biomass was contrarily increasing with the increase of incubation time. The degradation rate of MCPA was up to 99.80% after incubation with strain E41 for 14 days. Meanwhile, the degradation of MCPA was associated with a concomitant increase in fungal biomass up to 4.19 g dry wt/L in MSM culture. This result indicated that strain E41 could utilize MCPA as the sole carbon source for its growth and effectively degrade MCPA. In previous report, ninety fungus strains belonging to ten taxonomic groups were used to degrade phenoxy acid herbicides in liquid medium. However, only two of the species attained a dissipation potential of about 50% within 5 days (Vroumsia et al., 2005). In this study, strain E41 showed a potential ability to degrade MCPA herbicide.

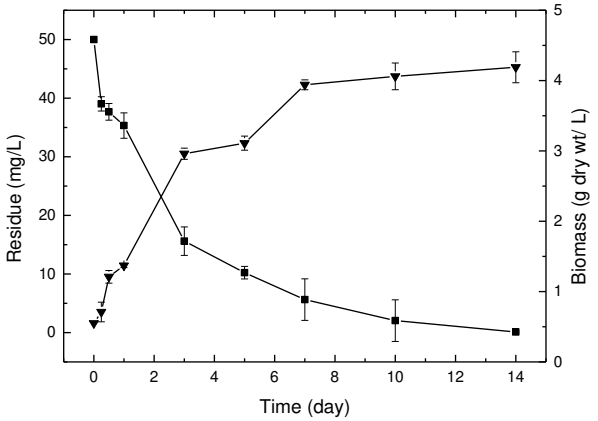


Figure 4. *The degradation kinetics of MCPA (square) and biomass of strain E41 (triangle) in MSM. Error bars represent the standard deviation of three replicates*

Degradation products and pathway of MCPA

The degradation products of MCPA in MSM culture were extracted and identified by GC-MS. A metabolite was observed with retention time of 15.77 min in *Fig. 5a*. By comparison with the National Institute of Standards and Technology (NIST, USA) library database, the metabolite was identified as 4-chloro-2-methylphenol and its mass spectrogram was illustrated in *Fig. 5b* with characteristic fragment ion peaks at m/z 142.0, 107.0 and 77.0. The metabolite was also reported in direct photolysis of MCPA (Zertal et al., 1999; Costa et al., 2013). In previous report, MCPA degraded by most bacteria was demonstrated to be initiated by the oxidative cleavage of the ether bond producing 4-chloro-2-methylphenol, subsequent hydroxylated to catechol, and finally underwent ring-cleavage (Häggblom, 1992). Ring hydroxylation was also an important metabolic route in the biodegradation of MCPA by fungi. *Aspergillus niger* could metabolize MCPA to a variety of hydroxylated products (Evangelista et al., 2010). However, catechol was undetermined in this study, which indicated the degradation pathway of MCPA by strain E41 was different with these microbes. The hypothetical biodegradation pathway of MCPA by strain E41 in MSM was illustrated in *Fig. 6*.

http://www.aloki.hu ● ISSN 1589 1623 (Print) ● ISSN 1785 0037 (Online)
DOI: http://dx.doi.org/10.15666/aeer/1902_12951307
© 2021, ALÖKI Kft., Budapest, Hungary

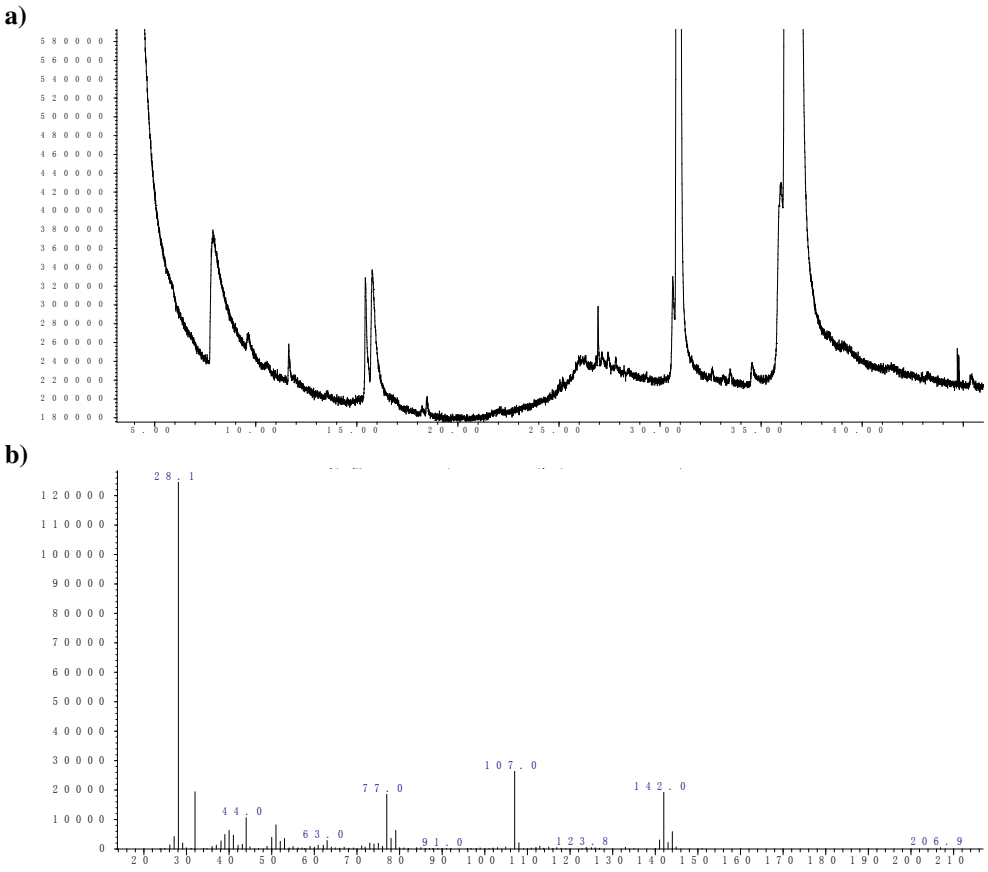


Figure 5. *The total ion chromatogram (a) and mass spectrogram (b) of the metabolite by GC-MS*

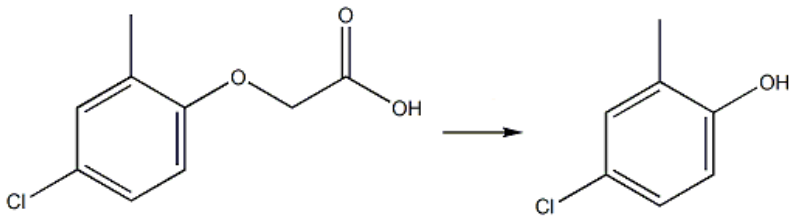


Figure 6. *Hypothetical biodegradation pathway of MCPA by strain E41 in MSM*

The amount of this metabolite was also detected during the biodegradation process. The amount of 4-chloro-2-methylphenol increased to 12.18 mg/L until 5 days of incubation and then decreased to 6.73 mg/L at 14 days, probably due to the hydroxylation and its own degradation (Bojanowska-Czajka et al., 2006). Finally, the metabolite was not detected in the culture medium after 21 days of incubation. These results indicated that the added MCPA in MSM was completely degraded by strain E41 without any accumulative metabolites at the end of incubation.

Biodegradation of MCPA in soil

To investigate the bioremediation of MCPA in contaminated soils by strain E41, the biodegradation experiment was performed in soils with initial MCPA concentration of

http://www.aloki.hu ● ISSN 1589 1623 (Print) ● ISSN 1785 0037 (Online)
DOI: http://dx.doi.org/10.15666/aeer/1902_12951307
© 2021, ALÖKI Kft., Budapest, Hungary

2.5 mg/kg, and the analytic results were shown in *Table 1*. The results showed that the half-lives of MCAP were 12.84, 2.07, 27.73, and 2.73 d in non-sterile soil, non-sterile soil+strain E41, sterile soil, and sterile soil+strain E41, respectively. The MCPA in non-sterile soil degraded faster than that in sterile soil, which showed that the indigenous microbes in soil probably played a role in MCPA degradation. After inoculated with strain E41, the degradation of MCPA was 6.2 and 10.2 times faster than that in non-sterile soil and sterile soil. It was obvious that the biodegradation of MCPA was significantly enhanced in soils with the presence of strain E41. Attaining highly efficient degradation strain was critical to the bioremediation of environmental pollutants and the usefulness of bioaugmentation with pesticide-degrading microorganisms in the clean-up of polluted soil was proven some years ago. Endophytic fungi have the capability to degrade organic compounds, decompose environmental contaminants, and improve the soil microenvironment (Ortega et al., 2020). Previous studies have demonstrated that *Phomopsis* sp. could accelerate leaf litter decomposition, soil phenol transformation, and biodegrade soil resvertrol (Chen et al., 2013b; Wang et al., 2019). The result in our study indicated that endophyte *Phomopsis* sp. E41 was a valuable microbial resource for potential applications in agricultural soil. However, it was noticeable that this result was mere an academic observation and further experiments should be conducted as to its large-scale applicability.

Table 1. *Degradation dynamics of MCPA by strain E41 in different soils*

Soil treatment	Equation	Correlation coefficient (R^2)	Half-life (day)
non-sterile soil	$y = 2.2196e^{-0.054x}$	$R^2 = 0.8080$	12.84
non-sterile soil+E41	$y = 4.2441e^{-0.335x}$	$R^2 = 0.8609$	2.07
sterile soil	$y = 2.4031e^{-0.025x}$	$R^2 = 0.9521$	27.73
sterile soil+E41	$y = 3.5932e^{-0.254x}$	$R^2 = 0.8331$	2.73

Conclusion

An entophytic fungus strain E41 could degrade MCPA in liquid medium and soil. The optimal degradation conditions for MCPA by strain E41 were at 30 ºC and pH 6–7. The main metabolite was 4-chloro-2-methylphenol. The strain *Phomopsis* sp. used to remove and detoxify the MCPA contamination in practice needs to be investigated in detail in the future, for instance, degradation mechanism and the effect factors on the bioremediation of MCPA in soil.

Acknowledgements. This work was supported by National Natural Science Foundation of P.R. China (No. 31660524, 31760522), the Special Fund for Agro-scientific Research in the Public Interest, P.R. China (No. 201203098), and Guangxi Natural Science Foundation (No. 2017GXNSFAA198140).

Declaration of interest statement. No potential conflict of interests was reported by the authors.

REFERENCES

[1] Bojanowska-Czajka, A., Drzewicz, P., Kozyra, C., Nałęcz-Jawecki, G., Sawicki, J., Szostek, B., Trojanowicz, M. (2006): Radiolytic degradation of herbicide 4-chloro-2-

http://www.aloki.hu ● ISSN 1589 1623 (Print) ● ISSN 1785 0037 (Online)
DOI: http://dx.doi.org/10.15666/aeer/1902_12951307
© 2021, ALÖKI Kft., Budapest, Hungary

methyl phenoxyacetic acid (MCPA) by γ-radiation for environmental protection. – Ecotoxicology and Environmental Safety 65(2): 265-277.

[2] Bukowska, B., Rychlik, B., Krokosz, A., Michałowicz, J. (2008): Phenoxyherbicides induce production of free radicals in human erythrocytes: oxidation of dichlorodihydrofluorescine and dihydrorhodamine 123 by 2,4-D-Na and MCPA-Na. – Food and Chemical Toxicology 46(1): 359-367.

[3] Byunghoon, K., Han, M., Cho, S., Ahn, S., Lim, S.-P., Yoo, S. (2003): Statistical optimization for biodegradation of 2,4-dichlorophenoxyacetic acid by soil isolated bacterium. – Korean Journal of Microbiology and Biotechnology 31(1): 83-89.

[4] Cabrera, A., Cox, L., Spokas, K. A., Celis, R., Hermosín, M. C., Cornejo, J., Koskinen, W. C. (2011): Comparative sorption and leaching study of the herbicides fluometuron and 4-chloro-2-methylphenoxyacetic acid (MCPA) in a soil amended with biochars and other sorbents. – Journal of Agricultural and Food Chemistry 59(23): 12550-12560.

[5] Chen, Y., Peng, Y., Dai, C.-C., Ju, Q. (2011): Biodegradation of 4-hydroxybenzoic acid by *Phomopsis liquidambari*. – Applied Soil Ecology 51: 102-110.

[6] Chen, Y., Xie, X.-G., Ren, C.-G., Dai, C.-C. (2013a): Degradation of N-heterocyclic indole by a novel endophytic fungus *Phomopsis liquidambari*. – Bioresource Technology 129: 568-574.

[7] Chen, Y., Wang, H.-W., Li, L., Dai, C.-C. (2013b): The potential application of the endophyte *Phomopsis liquidambari* to the ecological remediation of long-term cropping soil. – Applied Soil Ecology 67: 20-26.

[8] Costa, C., Maia, S., Silva, P., Garrido, J., Borges, F., Garrido, E. M. (2013): Photostabilization of phenoxyacetic acid herbicides MCPA and mecoprop by hydroxypropyl-*β*-cyclodextrin. – International Journal of Photoenergy 2013: 542783.

[9] Evangelista, S., Cooper, D. G., Yargeau, V. (2010): The effect of structure and a secondary carbon source on the microbial degradation of chlorophenoxy acids. – Chemosphere 79(11): 1084-1088.

[10] Greer, C. W., Hawari, J., Samson, R. (1990): Influence of environmental factors on 2,4-dichlorophenoxyacetic acid degradation by *Pseudomonas cepacia* isolated from peat. – Archives of Microbiology 154(4): 317-322.

[11] Häggblom, M. M. (1992): Microbial breakdown of halogenated aromatic pesticides and related compounds. – FEMS Microbiology Reviews 103(1): 29-72.

[12] Han, L., Zhao, D., Li, C. (2015): Isolation and 2,4-D-degrading characteristics of *Cupriavidus campinensis* BJ71. – Brazilian Journal of Microbiology 46(2): 433-441.

[13] Khan, Z., Roman, D., Kintz, T., delas Alas, M., Yap, R., Doty, S. (2014): Degradation, phytoprotection and phytoremediation of phenanthrene by endophyte *Pseudomonas putida*, PD1. – Environmental Science & Technology 48(20): 12221-12228.

[14] Lin, M., Hu, X., Chen, W., Wang, H., Wang, C. (2014): Biodegradation of phenanthrene by *Pseudomonas* sp. BZ-3, isolated from crude oil contaminated soil. – International Biodeterioration & Biodegradation 94: 176-181.

[15] Liu, M., Luo, K., Wang, Y., Zeng, A., Zhou, X., Luo, F., Bai, L. (2014): Isolation, identification and characteristics of an endophytic quinclorac degrading bacterium *Bacillus megaterium* Q3. – PLoS ONE 9(9): e108012.

[16] Liu, Z., Xie, W., Li, D., Peng, Y., Li, Z., Liu, S. (2016): Biodegradation of phenol by bacteria strain *Acinetobacter calcoaceticus* PA isolated from phenolic wastewater. – International Journal of Environmental Research and Public Health 13(3): 300.

[17] Marriott, M. W., Smejkal, C. W., Lappin-Scott, H. M. (2000): Biodegradation of mixtures of chlorophenoxyalkanoic acid herbicides by *Alcaligenes denitrificans*. – Journal of Industrial Microbiology & Biotechnology 25(5): 255-259.

[18] Önneby, K., Håkansson, S., Pizzul, L., Stenström, J. (2014): Reduced leaching of the herbicide MCPA after bioaugmentation with formulated and stored *Sphingobium* sp. – Biodegradation 25(2): 291-300.

http://www.aloki.hu ● ISSN 1589 1623 (Print) ● ISSN 1785 0037 (Online)
DOI: http://dx.doi.org/10.15666/aeer/1902_12951307
© 2021, ALÖKI Kft., Budapest, Hungary

[19] Ortega, H. E., Torres-Mendoza, D., Cubilla-Rios, L. (2020): Patents on endophytic fungi for agriculture and bio- and phytoremediation applications. – Microorganisms 8: 1237.
[20] Ozawa, T., Yoshida, R., Wakashiro, Y., Hase, H. (2004): Improvement of simazine degradation by inoculation of corn and soybean plants with rhizobacteria. – Soil Science and Plant Nutrition 50(8): 1295-1299.
[21] Salvo, L. M., Malucelli, M. I. C., da Silva, J. R. M. C., Alberton, G. C., De Assis, H. C. S. (2015): Toxicity assessment of 2,4-D and MCPA herbicides in primary culture of fish hepatic cells. – Journal of Environmental Science and Health Part B-Pesticides Food Contaminants and Agricultural Wastes 50(7): 449-455.
[22] Samir, R., Essam, T., Ragab, Y., Hashem, A. (2015): Enhanced photocatalytic–biological degradation of 2,4 dichlorophenoxyacetic acid. – Bulletin of Faculty of Pharmacy, Cairo University 53(2): 77-82.
[23] Sanchis, S., Polo, A. M., Tobajas, M., Rodriguez, J. J., Mohedano, A. F. (2014): Strategies to evaluate biodegradability: application to chlorinated herbicides. – Environmental Science and Pollution Research 21(16): 9445-9452.
[24] Song, J., Gu, J., Zhai, Y., Wu, W., Wang, H., Ruan, Z., Shi, Y., Yan, Y. (2013): Biodegradation of nicosulfuron by a *Talaromyces flavus* LZM1. – Bioresource Technology 140: 243-248.
[25] Sun, K., Liu, J., Gao, Y., Jin, L., Gu, Y., Wang, W. (2014a): Isolation, plant colonization potential, and phenanthrene degradation performance of the endophytic bacterium *Pseudomonas* sp. Ph6-*gfp*. – Scientific Reports 4: 5462.
[26] Sun, K., Liu, J., Jin, L., Gao, Y. (2014b): Utilizing pyrene-degrading endophytic bacteria to reduce the risk of plant pyrene contamination. – Plant and Soil 374(1): 251-262.
[27] Tamura, K., Peterson, D., Peterson, N., Stecher, G., Nei, M., Kumar, S. (2011): MEGA5: molecular evolutionary genetics analysis using maximum likelihood, evolutionary distance, and maximum parsimony methods. – Molecular Biology and Evolution 28(10): 2731-2739.
[28] Tan, L., Hu, Q., Xiong, X., Su, X., Huang, Y., Jiang, Z., Zhou, Q., Zhao, S., Zeng, W. (2013): Isolation and characterization of a novel 2-methyl-4-chlorophenoxyacetic acid-degrading *Enterobacter* sp. strain SE08. – Ecotoxicology and Environmental Safety 96: 198-204.
[29] Tortella, G. R., Rubilar, O., Cea, M., Wulff, C., Martínez, O., Diez, M. C. (2010): Biostimulation of agricultural biobeds with npk fertilizer on chlorpyrifos degradation to avoid soil and water contamination. – Journal of Soil Science and Plant Nutrition 10(4): 464-475.
[30] Verma, J. P., Jaiswal, D. K., Sagar, R. (2014): Pesticide relevance and their microbial degradation: a-state-of-art. – Reviews in Environmental Science and Bio/Technology 13(4): 429-466.
[31] Vroumsia, T., Steiman, R., Seigle-Murandi, F., Benoit-Guyod, J.-L. (2005): Fungal bioconversion of 2,4-dichlorophenoxyacetic acid (2,4-D) and 2,4-dichlorophenol (2,4-DCP). – Chemosphere 60(10): 1471-1480.
[32] Wang, Q., Xie, S. (2012): Isolation and characterization of a high-efficiency soil atrazine-degrading *Arthrobacter* sp. strain. – International Biodeterioration & Biodegradation 71: 61-66.
[33] Wang, H. W., Sun, K., Guan, Y. X., Qiu, M. H., Zhang, L., Dai, C. C. (2019): Fungal endophyte Phomopsis liquidambari biodegrades soil resveratrol: a potential allelochemical in peanut monocropping systems. – Journal of the Science of Food and Agriculture 99(13): 5899-5909.
[34] Wu, X., Wang, W., Liu, J., Pan, D., Tu, X., Lv, P., Wang, Y., Cao, H., Wang, Y., Hua, R. (2017): Rapid biodegradation of the herbicide 2,4-dichlorophenoxyacetic acid by *Cupriavidus gilardii* T-1. – Journal of Agricultural and Food Chemistry 65(18): 3711-3720.

http://www.aloki.hu ● ISSN 1589 1623 (Print) ● ISSN 1785 0037 (Online)
DOI: http://dx.doi.org/10.15666/aeer/1902_12951307
© 2021, ALÖKI Kft., Budapest, Hungary

[35] Xia, Z.-Y., Zhang, L., Zhao, Y., Yan, X., Li, S.-P., Gu, T., Jiang, J.-D. (2017): Biodegradation of the herbicide 2,4-dichlorophenoxyacetic acid by a new isolated strain of *Achromobacter* sp. LZ35. – Current Microbiology 74(2): 193-202.
[36] Xiang, S., Lin, R., Shang, H., Xu, Y., Zhang, Z., Wu, X., Zong, F. (2020): Efficient degradation of phenoxyalkanoic acid herbicides by the alkali-tolerant *Cupriavidus oxalaticus* strain X32. – Journal of Agricultural and Food Chemistry 68(12): 3786-3795.
[37] Xiao, L., Jia, H.-F., Jeong, I.-H., Ahn, Y.-J., Zhu, Y.-Z. (2017): Isolation and characterization of 2,4-D butyl ester degrading *Acinetobacter* sp. ZX02 from a Chinese ginger cultivated soil. – Journal of Agricultural and Food Chemistry 65(34): 7345-7351.
[38] Xie, X.-G., Dai, C.-C. (2015): Degradation of a model pollutant ferulic acid by the endophytic fungus *Phomopsis liquidambari*. – Bioresource Technology 179: 35-42.
[39] Yu, Y. L., Wang, X., Luo, Y. M., Yang, J. F., Yu, J. Q., Fan, D. F. (2005): Fungal degradation of metsulfuron-methyl in pure cultures and soil. – Chemosphere 60(4): 460-466.
[40] Yu, F., Fu, R., Xie, Y., Chen, W. (2015): Isolation and characterization of polyacrylamide-degrading bacteria from dewatered sludge. – International Journal of Environmental Research and Public Health 12(4): 4214-4230.
[41] Zertal, A., Sehili, T., Boule, P. (1999): Phototransformation of 4-chloro-2-methylphenoxy acetic acid (MCPA). – Zeitschrift Fur Physikalische Chemie 213: 87-92.
[42] Zertal, A., Molnár-Gábor, D., Malouki, M. A., Sehili, T., Boule, P. (2004): Photocatalytic transformation of 4-chloro-2-methylphenoxyacetic acid (MCPA) on several kinds of TiO_2. – Applied Catalysis B: Environmental 49(2): 83-89.
[43] Zhang, L., Hang, P., Zhou, X.-Y., Qiao, W.-J., Jiang, J.-D. (2020): Enantioselective catabolism of the two enantiomers of the phenoxyalkanoic acid herbicide dichlorprop by *Sphingopyxis* sp. DBS4. – Journal of Agricultural and Food Chemistry 68(26): 6967-6976.
[44] Zhu, X., Jin, L., Sun, K., Li, S., Ling, W., Li, X. (2016): Potential of endophytic bacterium *Paenibacillus* sp. PHE-3 isolated from *Plantago asiatica* L. for reduction of PAH contamination in plant tissues. – International Journal of Environmental Research and Public Health 13(7): 633.

http://www.aloki.hu ● ISSN 1589 1623 (Print) ● ISSN 1785 0037 (Online)
DOI: http://dx.doi.org/10.15666/aeer/1902_12951307
© 2021, ALÖKI Kft., Budapest, Hungary

DIVERSIFIED CLIMATE RESILIENT PECAN (*CARYA ILLINOINENSIS* (WANGENH.) K. KOCH) BASED SUSTAINABLE AGROFORESTRY IMPROVES LIVELIHOOD AND RETURNS IN INDIAN HIMALAYA

YADAV, R. P.* – BISHT, J. K. – MONDAL, T. – MEENA, V. S. – PANDEY, B. M. – MISHRA, P. K. – PATTANAYAK, A. – KANT, L.

ICAR-Vivekananda Parvatiya Krishi Anusandhan sansthan, Almora-263601, Uttarakhand, India

**Corresponding author*
e-mail: rams34052@gmail.com

(Received .3rd Nov 2020; accepted 8th Feb 2021)

Abstract. Mono-cropping systems are prone to increasing climate variability leading to biotic and abiotic pressure, which results in a risk of failure. Therefore, a diversified pecan-based agroforestry experiment was conducted (2010-2016) with an aim to enhance productivity, profitability and resilience over sole cropping (without pecan) in the rainfed ecosystem of the Indian Himalaya. It was hypothesized that integration of seasonal crops in the alleys of pecan trees will improve production, livelihood and returns due to diversified output. Four cropping systems, *viz*. FM–L, FM–W, S–L and S–W were evaluated under pecan and sole cropping. Between two situations, wheat equivalent grain yield (WEGY) and production efficiency (PE) were significantly higher in sole cropping (15.06 & 16.3%) as compared to under pecan. Among cropping systems WEGY was significantly higher in S–W ranging between 4.9 and 51.4% compared to other cropping systems. S–W system was also significantly more productive. In 2016 fruit, wood, litter fall and C stock were recorded as 1.11, 21.31, 8.44 and 46.50 t ha^{-1} for pecan, respectively. The grain productivity of crops was positively correlated with rainfall. The gross returns was threefold with pecan as compared to sole cropping (1345.9 \$ ha^{-1}) concerning 2016. Irrespective of growing situations S-W (3629.2 \$ ha^{-1}) cropping system provided maximum gross returns in year 2016. Hence, it is concluded that pecan-based agroforestry is more profitable in terms of economics, diversified output and ecological balance.
Keywords: *agri-horticulture, cropping system, mono-cropping, productivity, wheat equivalent grain yield*

Introduction

Globally, land and water are two of the most prominent resources for the growth and survival of humans (Schneider et al., 2011) and smart farming is need of the hour for social upliftment (Wolfert et al., 2017; Namatsheve et al., 2020). The land-use systems that strive escalating climatic vulnerabilities ensuring resilience are significant to enhance livelihood security and economic return with climate change mitigation and adaptation strategies (Yadav et al., 2016a; González-Esquivel et al., 2020; Orr et al., 2020). Agroforestry systems (AFS) which are sustainable in nature and provide diversified outputs, viz. fruits, food, timber, fuel wood, nuts and spices are pervasive globally (Adane et al., 2019). Food production for consumption and income generating potential of fruit tree based agroforestry attracts farming community than other trees to plant on the farm (Bellow et al., 2008a; Yadav et al., 2015a; Mondal et al., 2020). These AFS being a form of integrated land management (Leakey, 2010) increase resilience to climate change (Kalaugher et al., 2017; Yadav et al., 2017, 2019; Yasin et al., 2018), enhance efficiency of natural resources, and total factor productivity and mitigate food insecurity (Thangata et al., 2002). Fruit tree based agroforestry is more profitable due to uniform income

http://www.aloki.hu ● ISSN 1589 1623 (Print) ● ISSN 1785 0037 (Online)
DOI: http://dx.doi.org/10.15666/aeer/1902_13091323
© 2021, ALÖKI Kft., Budapest, Hungary

distribution round the year, besides higher returns on inputs compared to mono-cropping (Yadav et al., 2018a). The extrinsic and intrinsic variables are taken into account to adopt the agroforestry innovations (Meijer et al., 2015) and for climate and food security tasks, agroforestry is one of the identified solution.

In Himalayan region, fruit based agroforestry is more appropriate livelihood option because of congenial climate for horticulture crops. In these fruit based AFS in spite of reduced yields of some annual crops compared to sole-cropping, it is economically more rewarding with higher gross returns (GR) and overall system productivity, i.e. fruit tree + annual crop. Complex interactions between system components and environment are responsible for varying increase and decrease in yields of annual crops under AFS (Bellow et al., 2008b). Performance of the fruit based agroforestry depends on crop (type, variety), trees type and climatic conditions of the area (Yadav et al., 2017, 2018b).

In the Himalayan region, most of the inhabitants depend on yields of crops, viz. finger millet, lentil, wheat, soybean besides other crops for subsistence. Fruit and vegetable crops are income earning cash crops besides domestic consumption. Fruit trees are popular among inhabitants of the region and found many on the farming lands. In entire Himalayan region, fruit based agroforestry is distributed in the form of scattered fruit trees on farming lands, including agricultural crops in orchards and home gardens (Yadav et al., 2016b, 2018c). In the area most common fruit trees are mango (*Mangifera indica*), citrus (Citrus spp.), pear (*Pyrus communis*), plum (*Prunus domestica*), apple (*Malus domestica*), apricot (*Prunus armeniaca*), peach (*Prunus persica*), walnut (*Juglans regia*), pecan (*Carya illinoinensis*) and aonla (*Emblica officinalis*) with other various species in smaller number (Yadav et al., 2016b; GoUK, 2020). The source of earnings for livelihood of the inhabitants is produce of these fruit trees besides livestock in the Himalayan region. Hence, fruit based agroforestry is an alternate land management option that can lead to improved income, production and stability for rainfed marginal lands which have low, unstable and uneconomic production.

The evaluation of fruit tree based agroforestry in Himalayan region will offer options to resource poor small farmers in similar hill agriculture ecosystems. The superiority of mixed cropping compared to sole cropping has been established (Bellow, 2004; Hossain et al., 2014) and land equivalent ratio (LER) >1.0 has been demonstrated (Li et al., 1999; Rahman et al., 2014). Fruit trees on farming land enjoys popularity and provides direct cash as well as indirect ecological benefits (Gaba et al., 2015; Yadav et al., 2019) which leads its acceptability and greater adoption (Parrotta et al., 2015). Fruit based agroforestry interests for sustainability in relation to disease and pest control (Simon et al., 2015), economic efficiency (Duru et al., 2015) and carbon neutral farming. Research on pecan with annual agricultural crops to optimize system yield is scarce. Considering the potential of fruit tree based agroforestry in the region, we evaluated different cropping systems (CS) for (i) their yields potential, (ii) characterization of productivity and (iii) gross returns with and without pecan (sole cropping).

Materials and methods

Experimental site

The study was conducted at the experimental farm, Hawalbagh (29°36′N; 79°40′E) of the ICAR-Vivekananda Parvatiya Krishi Anusandhan Sansthan, Almora located at an altitude of 1250 m above sea level. Annual mean temperature was 18.3 °C with mean maximum of 26.2 °C and mean minimum of 10.5 °C during the crop growth period of

http://www.aloki.hu ● ISSN 1589 1623 (Print) ● ISSN 1785 0037 (Online)
DOI: http://dx.doi.org/10.15666/aeer/1902_13091323
© 2021, ALÖKI Kft., Budapest, Hungary

seven years (2010-2016). The mean annual rainfall was 973.7 mm with 81 mean number of rainy days majority (70%) of which during June to September. Mean annual relative humidity, evaporation and sunshine hours were 70.7%, 2.4 mm day^{-1} and 6.5 h day^{-1}, respectively (*Table 1*).

Table 1. *Mean meteorological parameters received during the study period (2010-2016)*

Year	Temperature (°C)		Rainfall (mm)	Number of rainy days	Evaporation (mm day^{-1})	Sunshine (h)	Mean relative humidity (%)
	Maximum	Minimum					
2010	26.8	10.8	1369.5	87	2.5	6.7	70.9
2011	25.6	10.6	1088.0	90	2.2	6.4	71.6
2012	26.2	10.0	849.4	87	2.5	6.4	67.8
2013	26.1	10.8	1005.2	90	2.4	6.3	70.9
2014	25.8	9.8	943.3	68	2.4	6.3	73.7
2015	25.9	10.6	667.9	73	2.3	6.1	73.7
2016	27.0	10.6	892.8	71	2.7	7.0	66.3

Experimental design and treatments

In the present investigation four cropping systems: (i) finger millet {(FM) *Eluesine coracana*}–lentil {(L) *Lens esculentum*}, (ii) finger millet {(FM) *Eluesine coracana*}–wheat {(W) *Triticum aestivum*}, (iii) soybean {(S) *Glysine max*}–lentil {(L) (*Lens esculentum*} and (iv) soybean {(S) *Glysine max*)}–wheat {(W) *Triticum aestivum*} were evaluated. Soybean and finger millet were grown in *kharif* season (June-September) and wheat and lentil were grown in *rabi* season (October-May). The pecan plantation was of 22 years old and planted at a spacing of 6 m × 6 m with a density of 277 trees ha^{-1}. These cropping systems were examined in two growing situation (GS) (i) under pecan and (ii) sole cropping (without pecan) in rainfed (irrigation was not provided) ecosystem. The experiment was laid out in Factorial Randomized Block Design (FRBD) with three replications for each treatment.

Crop management

The experimentation period for this study was of seven years from 2010 to 2016. The crops, viz. soybean (VL *Soya* 63), finger millet (VL *Mandua* 324), wheat (VL *Gehun* 804) and lentil (VL *Masoor* 126) were grown with recommended dose of NPK (20:80:40; 40:20:20; 60:40:20 and 20:60:40, respectively) in rainfed condition. Urea, single super phosphate (SSP) and muriate of potash (MOP) was used to apply mineral N, P and K fertilization, respectively. The NPK was applied as basal dose in soybean and lentil, however, in wheat and finger millet nitrogen was applied in two equal splits at the time of field preparation, and after four weeks of sowing (*Table 2*). The gross plot size was 21.6 m^2 (5.4 m × 4.0 m).

Cropping system productivity

The grain and straw/stover yield (t ha^{-1}) for the annual agricultural crops and growth parameters {girth (cm), height (cm)}, yield {fruit (t ha^{-1}) and pruned material (t ha^{-1})} and accumulation of biomass (t ha^{-1}), biomass C (t ha^{-1}) and litter fall (t ha^{-1}) were recorded for the pecan. Wheat equivalent grain yield (WEGY) calculated by multiplying the grain

http://www.aloki.hu ● ISSN 1589 1623 (Print) ● ISSN 1785 0037 (Online)
DOI: http://dx.doi.org/10.15666/aeer/1902_13091323
© 2021, ALÖKI Kft., Budapest, Hungary

yields of crops with their respective minimum support price (MSP), the value obtained so were divided with MSP of wheat. The PE was measured by dividing individual crop yield to number of days taken to harvest.

Table 2. *Details of experiment and agronomic management during 2010-2016*

Experimentation period	2010 to 2016 (Seven years)			
Growing situation (GS)	Under pecan (*Carya illinoinensis*)		Sole cropping	
Cropping systems (CS)	*Kharif*		*Rabi*	
(i)	Finger millet (*Eluesine coracana*)		Lentil (*Lens esculentum*)	
(ii)	Finger millet		Wheat (*Triticum aestivum*)	
(iii)	Soybean (*Glysine max*)		Lentil	
(iv)	Soybean		Wheat	
Crops	Finger millet (FM)	Lentil (L)	Wheat (W)	Soybean(S)
Crop varieties	VL *Mandua* 324	VL *Masoor* 126	VL *Gehun* 804	VL *Soya* 63
Seed rate (kg ha^{-1})	10	35	100	75
Row distance (cm)	25	25	23	45
Sowing time	June	October	October	June
Fertilizer applied ($N-P_2O_5-K_2O$ kg ha^{-1})	40:20:20	20:60:40	60:40:20	20:80:40
Maturity time (days)	105-135	168	164-178	121
Harvesting time	October	April/May	April/May	October
Experimental design	Factorial randomized block design			
Replication	03			

Gross returns

The grain and straw/stover yield of crops (soybean, finger millet, wheat and lentil) and pecan (fruit and fuel wood) were converted in monetary terms; resultant total returns were considered as gross returns. The gross return was converted into $ based on the prevailing exchange rate of INR (Indian rupees) 75.9 for each $.

Statistical analysis

Statistical analysis suggested by Gomez and Gomez (1984) was used to analyze the data in factorial randomized block design. JMP version 9.0.1 was used to measure analysis of variance. Means of growing situation, cropping systems and interaction, if any were compared at the 5% level of significance ($p < 0.05$) using least significant difference (LSD).

Results and discussions

Cropping system yield

The results depicted in *Table 3* revealed that among growing situation significantly higher (15%) annual grain yield was obtained in sole cropping (3.67 t ha^{-1}) compared to under pecan (3.19 t ha^{-1}). Likewise, during *kharif* and *rabi* higher (21.5 and 7.7%) grain

http://www.aloki.hu ● ISSN 1589 1623 (Print) ● ISSN 1785 0037 (Online)
DOI: http://dx.doi.org/10.15666/aeer/1902_13091323
© 2021, ALÖKI Kft., Budapest, Hungary

yield was recorded in sole cropping than under pecan (1.63 and 1.56 t ha^{-1}), respectively. Among different cropping systems significantly 16.4, 47.2 and 73.9% higher annual grain yield was recorded from S-W system compared to FM-W, S-L and FM-L cropping systems, respectively. Similarly, ranging from 27.7 to 29.3% and 7.7 to 152% higher grain yield was obtained during *kharif* and *rabi* from S-W system compared to remaining systems, respectively except for S-L system during *kharif*.

Table 3. *Mean (2010-2016) grain yield under growing situation and different cropping systems*

Treatments	Mean grain yield (t ha^{-1})		
	Kharif **(finger millet/soybean)**	***Rabi*** **(lentil/ wheat)**	**Total (*kharif+rabi*)**
A. Growing situation (GS)			
(i) Under pecan	1.63 b	1.56 b	3.19 b
(ii) Sole cropping	1.98 a	1.68 a	3.67 a
LSD (P <0.05)	0.10	0.11	0.18
B. Cropping system (CS)			
(i) Finger millet-lentil	1.59 b	0.94 c	2.53 d
(ii) Finger millet-wheat	1.57 b	2.20 b	3.78 b
(iii) Soybean-lentil	2.03 a	0.96 c	2.99 c
(iv)Soybean-wheat	2.03 a	2.37 a	4.40 a
LSD (P <0.05)	0.14	0.16	0.26
GS × CS (P <0.05)	NS	NS	NS

Ghosh et al. (2016) and Panday et al. (2018) under rainfed situation in similar type of cropping systems confirmed almost similar results for wheat and soybean yields in Himalayan region. However, these studies were in sole cropping systems and present study was includes pecan in addition to wheat-soybean cropping. Qin et al. (2015) also reported similar findings for soybean yield under rainfed conditions. S-W cropping system recorded 4.93 t ha^{-1} mean grain yield in a long term (21 years old) experiment under irrigated situation (Choudhary et al., 2018) which was a little higher than present study in Himalaya. However, soybean grain yield (2.0 t ha^{-1}) was almost similar but wheat grain yield (2.93 t ha^{-1}) was higher than present study. The grain yield under pecan and sole cropping during *kharif* (R^2 = 0.63 & 0.32), *rabi* (R^2 = 0.003 & 0.069) and annual grain productivity (R^2 = 0.54 & 0.25) showed positive relationship with annual rainfall (*Fig. 1*).

The presence of fruit trees significantly reduced the grain yield of crops under different cropping systems compared to sole crop. This reduction in grain yields may be due to competitive effect for water, nutrients and light besides shading of fruit trees (Yadav et al., 2014b, 2015b). In similar type of study Hossain et al. (2014) reported that under fruit (mango, guava and olive) based agroforestry fruit yield of tomato was significantly lower (10.26-23.47 t ha^{-1}) than in sole cropping (34.06 t ha^{-1}) condition in Bangladesh. The yields of fava bean and maize under fruit trees reduced up to 34% in Guatemala and it was correlated with competition for water, nutrients and light (Bellow, 2004).

http://www.aloki.hu ● ISSN 1589 1623 (Print) ● ISSN 1785 0037 (Online)
DOI: http://dx.doi.org/10.15666/aeer/1902_13091323
© 2021, ALÖKI Kft., Budapest, Hungary

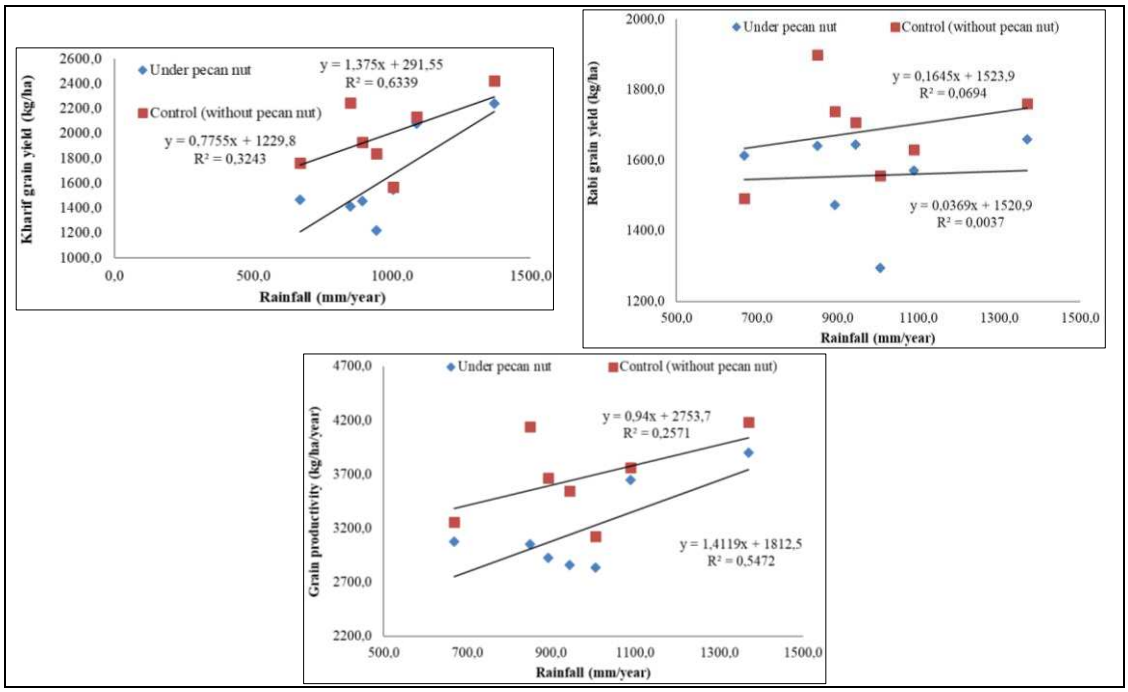


Figure 1. *Linear relationship between kharif (rainy season), rabi (winter season) and annual grain yield (with pecan and sole cropping) with yearly rainfall*

Wheat equivalent grain yield (WEGY)

The *Fig. 2a* revealed that annual WEGY in sole cropping was significantly higher (15%) compared to yield under pecan (4.25 t ha^{-1}). The WEGY during *kharif* and *rabi* also followed the similar trend and was significant high (21.9 and 8.6%) in sole cropping compared to under pecan (2.15 and 2.09 t ha^{-1}), respectively (*Fig. 2b*). The interaction between growing season and growing situation was non-significant (*Fig. 2c*). S-W system recorded 4.9, 46.2 and 51.4% higher WEGY compared to S-L, FM-W and FM-L cropping systems, respectively (*Fig. 2d*). Likewise, the WEGY in S-W system was higher ranging from 96.9 to 99.4% and 7.7 to 15.6% during *kharif* and *rabi*, respectively than other cropping systems (*Fig. 2e*).

The interaction effect of year with growing situation and cropping systems (*Fig. 2f*) was significant ($P < 0.01$) for WEGY. The WEGY of S-W system (5.54 t ha^{-1}) was higher (4.9-51.4%) than other cropping systems in rainfed situation. In Himalayan region, Panday et al. (2018) also reported lesser (4.71 t ha^{-1}) WEGY of S-W cropping system in a nine-year-old experiment under rainfed situation. Similar results also confirmed under rainfed situation by other researchers (Bhattacharyya et al., 2010; Qin et al., 2015). Whole model of actual versus predicted WEGY (*Fig. 2g*) was significant ($P < 0.01$; $R^2 = 0.85$).

Production efficiency (PE)

The mean PE was significantly higher in sole cropping (26.36 kg $ha^{-1}day^{-1}$) compared to under pecan (22.67 kg $ha^{-1}day^{-1}$) irrespective of cropping systems (*Table 4*). The similar trend was also followed during *kharif* and *rabi* season and mean PE was significantly high (13.52 and 9.15 kg $ha^{-1}day^{-1}$) in sole cropping as compared to under pecan (16.47 and 9.90 kg $ha^{-1}day^{-1}$), respectively. Among cropping systems, S-W system recorded significantly higher (17.9, 36.2 and 62.5%) grain PE in comparison to FM-W,

http://www.aloki.hu ● ISSN 1589 1623 (Print) ● ISSN 1785 0037 (Online)
DOI: http://dx.doi.org/10.15666/aeer/1902_13091323
© 2021, ALÖKI Kft., Budapest, Hungary

S-L and FM-L systems, respectively. In the present study, the production efficiency was higher than the research findings of Panday et al. (2018) from S-W cropping system in Indian Himalayas.

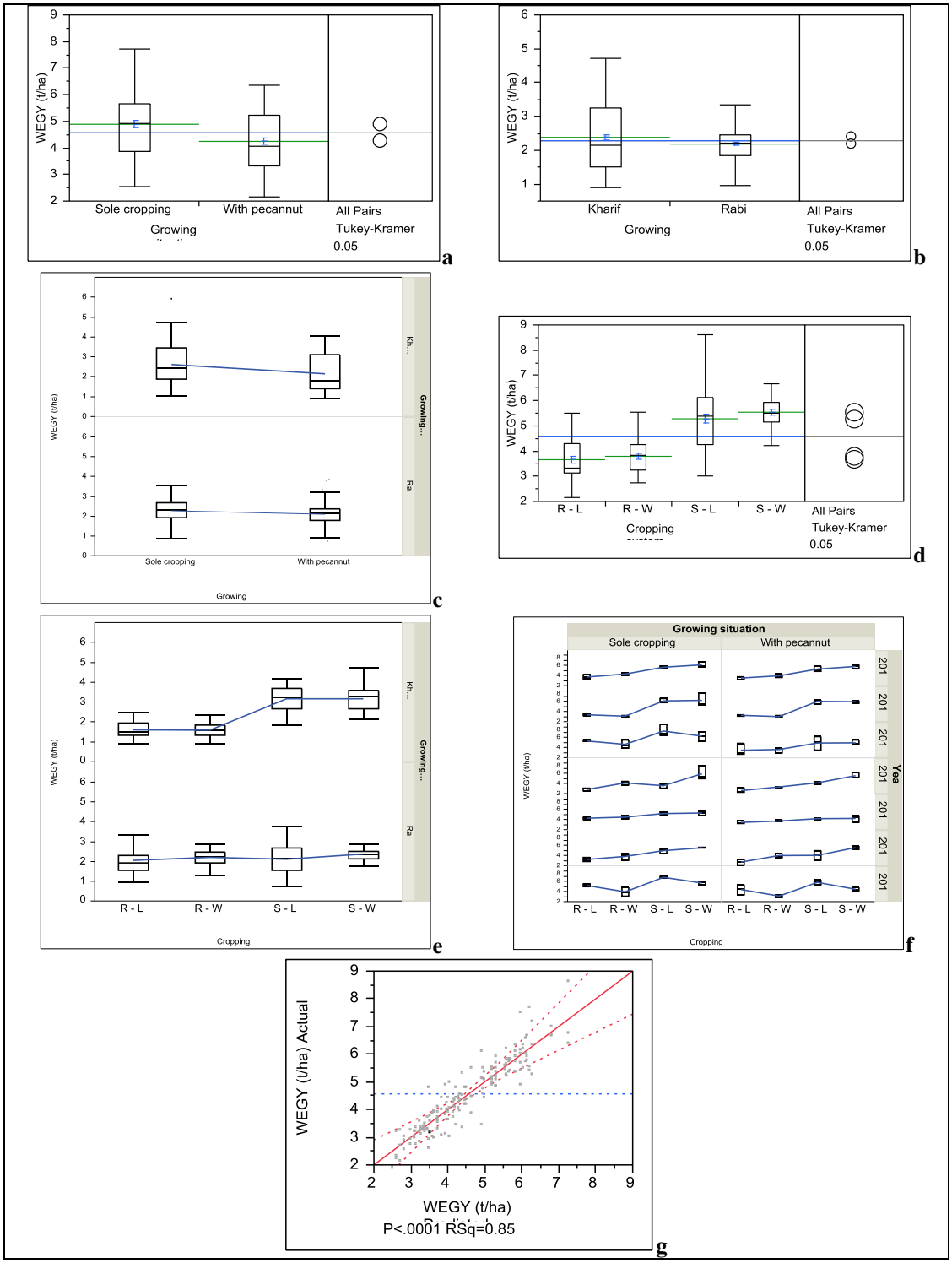


Figure 2. *Effect of (a) growing situations (kharif + rabi) (b) growing season (c) growing situation × growing season (d) cropping systems (kharif + rabi) (e) growing season × cropping systems (f) year wise with growing situation and cropping system (kharif + rabi) (g) whole model actual versus predicted wheat equivalent grain yield (WEGY)*

http://www.aloki.hu ● ISSN 1589 1623 (Print) ● ISSN 1785 0037 (Online)
DOI: http://dx.doi.org/10.15666/aeer/1902_13091323
© 2021, ALÖKI Kft., Budapest, Hungary

Table 4. *Production efficiency (2010-2016) of crops under growing situation and different cropping systems*

Treatments	Production efficiency (kg ha^{-1}day^{-1})		
	Kharif **(Finger millet/soybean)**	***Rabi*** **(lentil/wheat)**	**Total (*kharif+rabi*)**
A. Growing situation (GS)			
(i) Under pecan	13.52 b	9.15 b	22.67 b
(ii) Sole cropping	16.47 a	9.90 a	26.36 a
LSD (P <0.05)	0.85	0.66	1.31
B. Cropping system (CS)			
(i) Finger millet-lentil	13.28 b	5.59 c	18.87 d
(ii) Finger millet-wheat	13.13 b	12.89 b	26.02 b
(iii) Soybean-lentil	16.77 a	5.74 c	22.52 c
(iv) Soybean-wheat	16.78 a	13.88 a	30.67 a
LSD (P <0.05)	1.19	0.93	1.86
GS × CS (P <0.05)	NS	NS	NS

Likewise, mean grain PE was recorded significantly higher in S-W system (16.78 kg ha^{-1}day^{-1}) compared to FM-L (13.28 kg ha^{-1}day^{-1}) and FM-W (13.13 kg ha^{-1}day^{-1}) however it was at par in S-L cropping system (16.77 kg ha^{-1}day^{-1}) in *kharif* season. During *rabi* season, significantly higher mean grain PE was also recorded in S-W system (13.88 kg ha^{-1}day^{-1}) compared to FM-W (12.89 kg ha^{-1}day^{-1}), S-L (5.74 kg ha^{-1}day^{-1}) and least under FM-L (5.59 kg ha^{-1}day^{-1}) cropping systems during *rabi* season. Whole model for production efficiency actual versus predicted (*Fig. 3*) was significant (P <0.01; R^2 = 0.87).

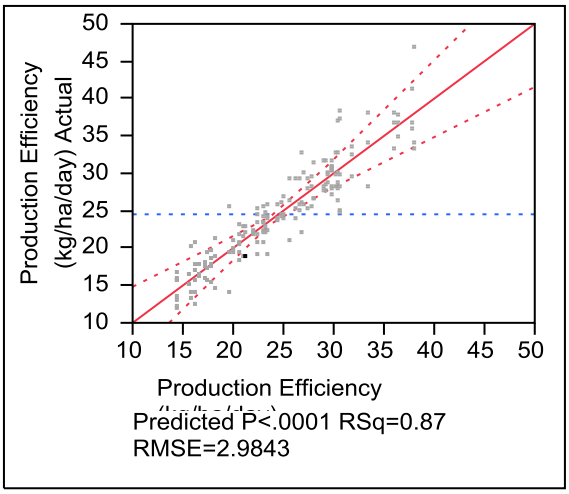


Figure 3. *Whole model of production efficiency actual versus predicted*

Gross returns (GR)

The gross returns was significantly two and four fold higher under pecan compared to sole cropping ($933.9 and $1345.9) during year 2010 and 2016, respectively (*Table 5*). The crops contribution in gross returns reduced from 43.6% during 2010 to 20.2% during

http://www.aloki.hu ● ISSN 1589 1623 (Print) ● ISSN 1785 0037 (Online)
DOI: http://dx.doi.org/10.15666/aeer/1902_13091323
© 2021, ALÖKI Kft., Budapest, Hungary

2016, whereas contribution of pecan increased from 46.4% during 2010 to 79.8% during 2016. During 2010 S-W system recorded 23.9, 25.1 and 29.1% more gross returns in comparisons to S-L, FM-W and FM-L cropping systems, respectively. Likewise, during 2016 among cropping systems, 2.52, 5.5 and 20.5% higher gross returns was recorded from S-W system compared to S-L, FM-L and FM-W systems, respectively. The crops and pecan accounted for 52.7-63.7% and 33.9-47.3% gross returns during 2010. Similarly, during 2016 crops and pecan contributed ranging from 33.1 to 40.65% and 59.4 to 66.9% in gross returns. The contribution of crops decreased whereas pecan contribution increased in gross returns of different cropping systems during 2016 compared to during 2010.

Table 5. *Gross returns (2010 and 2016) under growing situation and different cropping systems*

Treatments	Gross returns ($ ha^{-1})					
	Year 2010			Year 2016		
	Crop	Pecan nut	Total	Crop	Pecan nut	Total
A. Growing situation (GS)						
(i) Under pecan	874.3 b (43.6%)	1130.8 (46.4%)	2005.2 a	1104.0 b (20.2%)	4362.0 (79.8%)	5466.0 a
(ii) Sole cropping	933.9 a	-	933.9 b	1345.9 a	-	1345.9 b
LSD (P <0.05)	56.8	-	104.5	105.0	-	183.7
B. Cropping system (CS)						
(i) Finger millet-lentil	710.3 c (52.7%)	636.5 (47.3%)	1346.8 b	1137.5 b (33.1%)	2304.1 a (66.9%)	3441.7 a
(ii) Finger millet-wheat	918.2 b (66.1%)	471.4 (33.9%)	1389.6 b	1007.8 b (33.4%)	2005.2 b (66.5%)	3013.1 b
(iii) Soybean-lentil	880.4 b (62.7%)	522.6 (37.3%)	1403.0 b	1435.5 a (40.6%)	2104.4 a (59.4%)	3539.9 a
(iv) Soybean-wheat	1107.4 a (63.7%)	631.2 (36.3%)	1738.7 a	1318.9 a (36.3%)	2310.2 a (63.7%)	3629.2 a
LSD (P <0.05)	80.4	NS	147.8	148.5	210.1	259.8
GS × CS (P <0.05)	NS	NS	NS	NS	NS	NS

In Himalayan region, the research findings of Panday et al. (2018) confirmed the gross return ($1092.2) from soybean-wheat system, which was lower to this study under rainfed situation. Similar type of result was confirmed for gross returns from maize-wheat cropping system under rainfed situation (Sharma et al., 2017). The gross returns of year 2010 and 2016 (*Fig. 4*) with growing situation and cropping system was significant (P <0.01).

The findings of the present study reveals that fruit based AFS have provided more gross returns compared to cropping without fruit trees. The net returns and benefit was almost double in mango + tomato and guava + tomato agroforestry compared to pure cropping of tomato in Bangladesh (Hossain et al., 2014). In South Ethiopia, Anshiso et al. (2017) also reported that the net present value of fruit-tree based agroforestry practice was two, five and four times higher than ginger, sequential mono-cropping of maize with sweet potato and taro with teff. Similar findings that AFS are financially more beneficial and productive than pure cropping (without tree component) have been reported by Ajayi et al. (2009) in Zambia, Getahun (2012) and Adane et al. (2019) in Ethiopia and Yadav

http://www.aloki.hu ● ISSN 1589 1623 (Print) ● ISSN 1785 0037 (Online)
DOI: http://dx.doi.org/10.15666/aeer/1902_13091323
© 2021, ALÖKI Kft., Budapest, Hungary

et al. (2018a,b) in Indian Himalaya. The whole model of gross returns actual versus predicted (*Fig. 5*) was significant ($P < 0.01$; $R^2 = 0.99$).

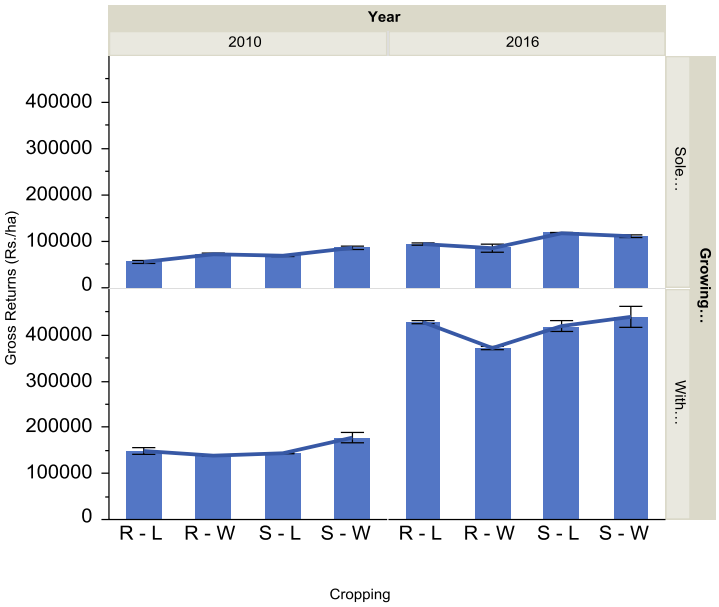


Figure 4. *Gross returns according to cropping system, growing situation and year wise*

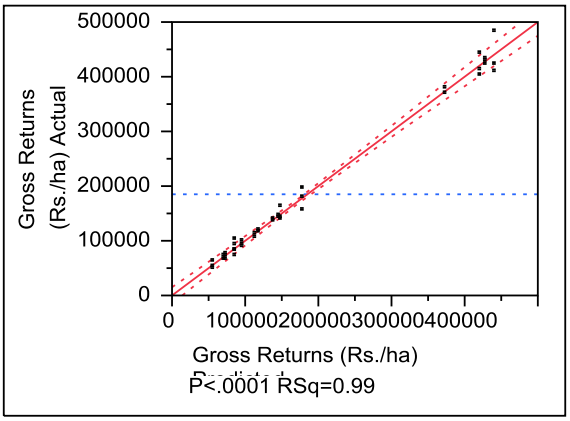


Figure 5. *Whole model of gross returns actual versus predicted*

Growth and yield of pecan

The girth and height of pecan were increased from 56.94 cm and 9.15 m per plant in the year of 2010 (when the experiment was initiated) to 76.18 cm and 10.69 m per plant, respectively at the end of the experimentation in the year of 2016 (*Fig. 6*). Likewise, wood and fruit yields were 11.70 and 0.81 t ha^{-1} in 2010 and 21.31 and 1.11 t ha^{-1}, respectively in the year of 2016. Crown spread was increased from 6.13 m/plant in 2010 to 7.29 m/plant in 2016. Similarly, in the year 2010 the litter fall and biomass C were 1.96 and 23.88 t/ha which increased to 8.44 and 46.50 t ha^{-1}, respectively in the year of 2016.

The linear increase in the growth parameters (girth and height) of pecan during experimentation period (2010-2016) helped to improve yields (wood and fruits) and

http://www.aloki.hu ● ISSN 1589 1623 (Print) ● ISSN 1785 0037 (Online)
DOI: http://dx.doi.org/10.15666/aeer/1902_13091323
© 2021, ALÖKI Kft., Budapest, Hungary

accumulation of more litter, biomass and biomass C stock. This supported to enhance profitability in economic terms besides ecological benefits. Stem diameter at breast height (DBH) of pecan increased linearly with time, hulled nut production ranged from 0.05 to 1.60 t ha^{-1} with 35 to 74 trees ha^{-1} in a stands of 72 years of age (average) and production of woody material improved the profitability of pecan-based system (Aries et al., 2006). In this present study, the gross returns are higher in pecan-based cropping system. Besides pecan, also help in improving soil properties via litter fall and meet the subsistence requirements of the farming community.

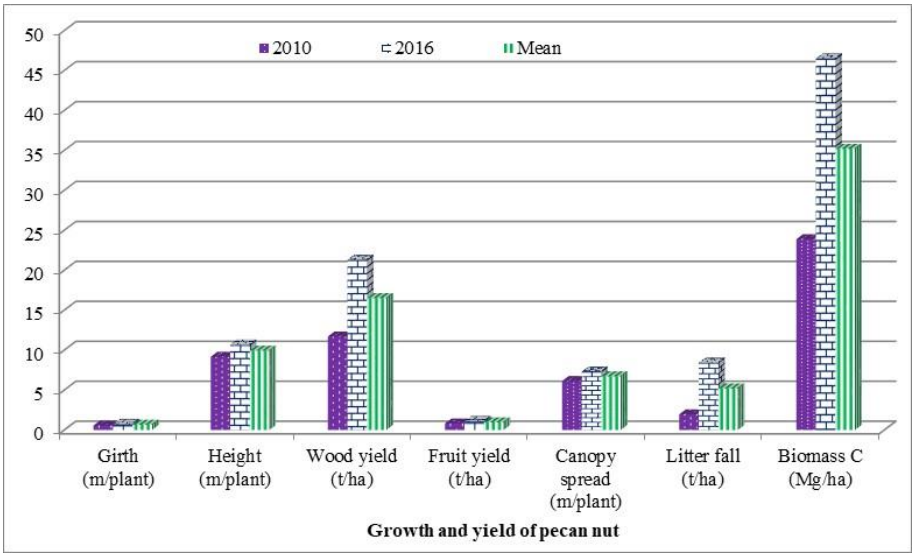


Figure 6. *Girth, height, wood yield, fruit yield, canopy spread, litter fall and biomass C (2010 and 2016) of pecan in rainfed pecan-based agroforestry system*

Conclusions

The results from this study indicated that sole cropping situation is more productive as compared to under pecan in terms of crop yield, wheat equivalent yield and production efficiency. Higher crop yield, wheat equivalent yield and production efficiency was obtained from S-W cropping system, hence, it is a suitable cropping system Indian Himalaya. However, from economic point of view the cropping under pecan was more remunerative to the farmers of rainfed situation. S-W system was provided highest gross returns followed by S-L, FM-L and FM-W cropping systems. Diversified output the farmers obtain from agroforestry such as food, fruit, pruned material as firewood, nuts etc. ensure livelihood security at inaccessible hill location. Litter fall from fruit trees enhance soil inherent capacity through decomposition that improves the soil structure and fertility. The fruit tree based agroforestry increases livelihood security, productivity and profitability of farmers. Besides pecan being a fruit tree, improve climate resilience via capturing atmospheric CO_2 in its tissues and store in the form of C for the long term. However, attempts on nutrient returns via litter fall and fruit production predictions required strengthening investment for spreading pecan plantation. Hence, pecan-based agroforestry is economically more viable and climate resilient option for the rainfed areas of the hill farming community in Himalayas.

http://www.aloki.hu ● ISSN 1589 1623 (Print) ● ISSN 1785 0037 (Online)
DOI: http://dx.doi.org/10.15666/aeer/1902_13091323
© 2021, ALÖKI Kft., Budapest, Hungary

Acknowledgements. Authors acknowledge the support received from Director of ICAR-Vivekananda Parvatiya Krishi Anusandhan Sansthan, Almora for providing necessary facilities and field staff for carrying out field activity during the course of investigation.

REFERENCES

[1] Adane, F., Legesse, A., Weldeamanuel, T., Belay, T. (2019): The contribution of a fruit tree-based agroforestry system for household income to smallholder farmers in Dale District, Sidama Zone, Southern Ethiopia. – Advances in Plants and Agriculture Research 9(1): 78-84.

[2] Ajayi, O. C., Akinnifesi, F. K., Sileshi, G., Kanjipite, W. (2009): Labour inputs and financial profitability of conventional and agroforestry-based soil fertility management practices in Zambia. – Agrekon 48(3): 276-292.

[3] Anshiso, A., Woldeamanuel, T., Asfaw, Z. (2017): Financial analysis of fruit tree based agroforestry practice in Hadero Tunto Zuria Woreda, Kembata Tembaro Zone, South Ethiopia. – Research Journal of Finance and Accounting 8(3): 72-80.

[4] Aries, A., Reid, W., Brauer, D. (2006): Production and economics of native pecan silvopastures in central United States. – Agroforestry Systems 66(3): 205-215.

[5] Bellow, J. G. (2004): Fruit-tree-based agroforestry in the western highlands of Guatemala. – Dissertation, University of Florida, Gainesville, FL, USA.

[6] Bellow, J. G., Hudson, R. F., Nair, P. K. R. (2008a): Adoption potential of fruit-tree-based agroforestry on small farms in the subtropical highlands. – Agroforestry Systems 73: 23-36.

[7] Bellow, J. G., Nair, P. K. R., Martin, T. A. (2008b): Tree-crop interactions in fruit tree based agroforestry systems in the western highlands of Guatemala: component yields and system performance. – In: Jose, S., Gordon, A. M. (eds.) Towards Agroforestry Design. Advances in Agroforstry, Vol 4, Springer, Dordrecht.

[8] Bhattacharyya, R., Pandey, A. K., Gopinath, K. A., Mina, B. L., Bisht, J. K., Bhatt, J. C. (2016): Fertilization and crop residue addition impacts on yield sustainability under a rainfed maize-wheat system in the Himalayas. – Proceedings of National Academy of Sciences India, Section B Biological Sciences 86: 21-32.

[9] Choudhary, M., Panday, S. C., Meena, V. S., Singh, S., Yadav, R. P., Mahanta, D., Mondal, T., Mishra, P. K., Bisht, J. K., Pattanayak, A. (2018): Long-term effects of organic manure and inorganic fertilization on sustainability and chemical soil quality indicators of soybean-wheat cropping system in the Indian mid-Himalayas. – Agriculture, Ecosystems and Environment 257: 38-46.

[10] Duru, M., Therond, O., Fares, M. (2015): Designing agroecological transitions: a review. – Agronomy for Sustainable Development 35: 1237-1257.

[11] Gaba, S., Lescourret, F., Boudsocq, S., Enjalbert, J., Hinsinger, P., Journet, E., Navas, M., Wery, J., Louarn, G., Malezieux, E., Pelzer, E., Prudent, M., Ozier-Lafontaine, H. (2015): Multiple cropping systems as drivers for providing multiple ecosystem services: from concepts to design. – Agronomy for Sustainable Development 35: 607-623.

[12] Getahun, K. M. (2012): Economic analysis and determinants of fruit tree based agroforestry system in Wondo district, Ethiopia: comparative analysis with monocropping systems. – M.Sc. thesis, Wondo Genet College of Forestry and Natural Resources, Hawassa University, Ethiopia.

[13] Ghosh, B. N., Meena, V. S., Alam, N. M., Dogra, P., Bhattacharyya, R., Sharma, N. K., Mishra, P. K. (2016): Impact of conservation practices on soil aggregation and the carbon management index after seven years of maize–wheat cropping system in the Indian Himalayas. – Agriculture Ecosystem Environment 216: 247-257.

[14] Gomez, K. A., Gomez, A. A. (1984): Statistical Procedures for Agricultural Research, 2nd edition. – ISBN: 978-0-471-87092-0, 704p.

http://www.aloki.hu ● ISSN 1589 1623 (Print) ● ISSN 1785 0037 (Online)
DOI: http://dx.doi.org/10.15666/aeer/1902_13091323
© 2021, ALÖKI Kft., Budapest, Hungary

[15] González-Esquivel, C. E., Camacho-Moreno, E., Larrondo-Posadas, L., Sum-Rojas, C., León-Cifuentes, W. E., Vital-Peralta, E., Astier, M., López-Ridaura, S. (2020): Sustainability of agroecological interventions in small scale farming systems in the Western Highlands of Guatemala. – International Journal of Agricultural Sustainability 18(4): 285-299.
[16] Government of Uttarakhand. (2020): State Profile. – Department of Horticulture, Government of Uttarakhand, India. Accessed on January 21, 2020.
[17] Hossain, J., Ahamed, T., Hasnat, M. Z., Karim, D. (2014): Screening of tomato varieties for fruit tree based agroforestry system. – International Journal of Agricultural Research, Innovation and Technology 4(2): 61-69.
[18] Kalaugher, E., Beukes, P., Bornman, J. F., Clark, A., Campbell, D. I. (2017): Modelling farm-level adaptation of temperate, pasture-based dairy farms to climate change. – Agricultural system 153: 53-68.
[19] Leakey, R. R. B. (2010): Should we be growing more trees on farms to enhance the sustainability of agriculture and increase resilience to climate change. – Special Report, ISTF News, USA.
[20] Li, L., Yang, S., Li, X., Zhang, F., Christie, P., Li, L., Yang, S. C., Li, X. L., Zhang, F. S. (1999): Interspecific complementary and competitive interactions between intercropped maize and faba bean. – Plant and Soil 212: 105-114.
[21] Meijer, S. S., Catacutan, D., Ajayi, O. C., Sileshi, G. W., Nieuwenhuis, M. (2015): The role of knowledge, attitudes and perceptions in the uptake of agricultural and agroforestry innovations among smallholder farmers in sub-Saharan Africa. – International Journal of Agricultural Sustainability 13(1): 40-54.
[22] Mondal, T., Yadav, R. P., Meena, V. S., Choudhary, M., Nath, S., Bisht, J. K., Mishra, P. K., Arya, S. K., Pattanayak, A. (2020): Biomass yield and nutrient content of dual purpose wheat in the fruit based cropping system in the North-Western mid-Himalaya ecosystem, India. – Field Crops Research 247:107700. doi: 10.1016/j.fcr.2019.107700.
[23] Namatsheve, T., Cardinael, R., Corbeels, M., Chikowo, R. (2020): Productivity and biological N_2-fixation in cereal-cowpea intercropping systems in sub-Saharan Africa. A review. – Agronomy for Sustainable Development 40: 30. https://doi.org/10.1007/s13593-020-00629-0.
[24] Orr, A., Tiba, Z., Congrave, J., Porázik, P., Dejen, A., Hassen, S. (2020): Smallholder commercialization and climate change: a simulation game for teff in South Wollo, Ethiopia. – International Journal of Agricultural Sustainability. doi: 10.1080/14735903.2020.1792735.
[25] Panday, S. C., Choudhary, M., Singh, S., Meena, V. S., Mahanta, D., Yadav, R. P., Pattanayak, A., Bisht, J. K. (2018): Increasing farmer's income and water use efficiency as affected by long-term fertilization under a rainfed and supplementary irrigation in a soybean-wheat cropping system of Indian mid-Himalaya. – Field Crops Research 219: 214-221.
[26] Parrotta, J. A., de Pryck, J. D., Obiri, B. D., Padoch, C., Powell, B., Sandbrook, C., Agarwal, B., Ickowitz, A., Jeary, K., Serban, A., Sunderland, T. C. H., Tran, N. T. (2015): The historical, environmental and socio-economic context of forests and tree-based systems for food security and nutrition. – In: Forests, Trees and Landscapes for Food Security and Nutrition. A Global Assessment Report. https://www.researchgate.net/publication/276950253
[27] Qin, W., Wang, D., Guo, X., Yang, T., Oenema, O. (2015): Productivity and sustainability of rainfed wheat-soybean system in the North China Plain: results from a long-term experiment and crop modelling. – Scientific Reports 5: 17514.
[28] Rahman, G. M. M., Wadud, M. A., Shahjahan, M., Jewel, K. N. A. (2014): Fruit tree based agroforestry practices in char land farming system. – Journal of Agroforestry and Environment 8(1): 1-6.

http://www.aloki.hu ● ISSN 1589 1623 (Print) ● ISSN 1785 0037 (Online)
DOI: http://dx.doi.org/10.15666/aeer/1902_13091323
© 2021, ALÖKI Kft., Budapest, Hungary

[29] Schneider, U. A., Havlik, P., Schmid, E., Valin, H., Mosnier, A., Obersteiner, A., Bottcher, H., Skalsky, R., Balkovik, J., Sauer, T., Fritz, Z. (2011): Impacts of population growth, economic development, and technical change on global food production and consumption. – Agricultural System 104: 204-215.

[30] Sharma, N. K., Singh, R. J., Mandal, D., Kumar, A., Alam, N. M., Keesstra, S. (2017): Increasing farmer's income and reducing soil erosion using intercropping in rainfed maize-wheat rotation of Himalaya, India. – Agriculture Ecosystem and Environment 247: 43-53.

[31] Simon, S., Lesueur-Jannoyer, M., Plénet, D., Lauri, P., le Bellec, F. (2015): Design of innovative orchards: proposal of an adapted conceptual framework. – 5th Intern Symp for Farm Syst Design. 7-10 September 2015, Montpellier, France.

[32] Thangata, P. H., Hildebrand, P. E., Gladwin, C. H. (2002): Modeling agroforestry adoption and household decision making in Malawi. – African studies quarterly 6(1): 271-293.

[33] Wolfert, S., Ge, L., Verdouw, C., Bogaardt, M. (2017): Big Data in Smart Farming–A review. – Agricultural System 153: 69-80.

[34] Yadav, R. P., Bana, O. P. S., Kaushal, R., Rajput, P. R. (2014): Effect of pruning in jatropha (*Jatropha curcas* linn.) and fertility levels in wheat on performance of agrisilviculture system in Tarai region of Uttarakhand. – Indian J. of Agroforestry 16(2): 68-72.

[35] Yadav, R. P., Bisht, J. K., Pandey, B. M. (2015a): Aboveground biomass and carbon stock of fruit tree based land use systems in Indian Himalaya. – The Ecoscan 9(3-4): 779-783.

[36] Yadav, R. P., Bana, O. P. S., Kaushal, R., Rajput, P. R. (2015b): Growth analysis and yield of wheat in agrisilviculture system in Tarai region of north-west India. – Indian Forester 141(3): 313-318.

[37] Yadav, R. P., Bisht, J. K., Pandey, B. M., Kumar, A., Pattanayak, A. (2016a): Cutting management versus biomass and carbon stock of oak under high density plantation in Central Himalaya, India. – Applied Ecology & Environmental Research 14(3): 207-214.

[38] Yadav, R. P., Gupta, B., Bhutia, P. L., Bisht, J. K. (2016b): Socioeconomics and sources of livelihood security in Central Himalaya, India: a case study. – International Journal of Sustainable Development & World Ecology 24(6): 545-553.

[39] Yadav, R. P., Bisht, J. K., Bhatt, J. C. (2017): Biomass, carbon stock under different production systems in the mid hills of Indian Himalaya. – Tropical Ecology 58(1): 15-21.

[40] Yadav, R. P., Gupta, B., Bhutia, P. L., Bisht, J. K. (2018a): Sustainable agroforestry systems for livelihood security and their economic appraisal in Indian Himalayas. – Economic Affairs 63(3): 01-07.

[41] Yadav, R. P., Bisht, J. K., Mondal, T., Meena, V. S., Choudhary, M. (2018b): Peach based horti-pastoral system of forage production on marginal land in Indian Himalaya. – Indian Journal of Agroforestry 20(2): 63-67.

[42] Yadav, R. P., Gupta, B., Bhutia, P. L., Bisht, J. K., Pattanayak, A. (2018c): Sustainable agroforestry systems and their structural components as livelihood options along elevation gradient in central Himalaya. – Biological Agriculture & Horticulture 35(2): 73-95.

[43] Yadav, R. P., Gupta, B., Bhutia, P. L., Bisht, J. K., Pattanayak, A., Meena, V. S., Choudhary, M., Tiwari, P. (2019): Biomass and carbon budgeting of sustainable agroforestry systems as ecosystem service in Indian Himalayas. – International Journal of Sustainable Development & World Ecology 26(5): 460-470.

[44] Yasin, G., Nawaz, M. F., Siddiqui, M. T., Niazi, N. K. (2018): Biomass, carbon stocks and CO2 sequestration in three different aged irrigated *Populus deltoides* Bartr. Ex Marsh. bund planting agroforestry systems. – Applied Ecology and Environmental Research 16(5): 6239-6252.

http://www.aloki.hu ● ISSN 1589 1623 (Print) ● ISSN 1785 0037 (Online)
DOI: http://dx.doi.org/10.15666/aeer/1902_13091323
© 2021, ALÖKI Kft., Budapest, Hungary

APPENDIX



Appendix 1. *Photo plate of experiments area during (a) kharif and (b) rabi season*

http://www.aloki.hu ● ISSN 1589 1623 (Print) ● ISSN 1785 0037 (Online)
DOI: http://dx.doi.org/10.15666/aeer/1902_13091323
© 2021, ALÖKI Kft., Budapest, Hungary

YIELD AND FATTY ACID COMPOSITION OF BLACK CUMIN (*Nigella sativa* L.) POPULATIONS COLLECTED FROM REGIONS UNDER DIFFERENT ECOLOGICAL CONDITIONS

CAN, M.[1*] – KATAR, D.[2] – KATAR, N.[3] – BAGCI, M.[4] – SUBASI, I.[4]

[1]*Agriculture and Forestry Provincial Directorate, Uşak, Turkey*

[2]*Eskisehir Osmangazi University, Faculty of Agriculture, Eskisehir, Turkey*

[3]*Agriculture and Forestry Provincial Directorate, Eskisehir, Turkey*

[4]*Dept. of Oilseeds Breeding, Central Research Institute for Field Crops, Ankara, Turkey*

[*]*Corresponding author*
e-mail: mustafican@gmail.com; phone: +90-276-231-1504; fax: +90-276-231-1500

(Received 3rd Nov 2020; accepted 8th Feb 2021)

Abstract. This study aimed to reveal the effect of different genotypes (population and variety) on yield, yield components and quality parameters of black cumin (*Nigella sativa* L.). The experiment was carried out in the Aegean Region of Turkey in two vegetation seasons of 2017 and 2018. In the study, four black cumin populations (Uşak, Hatay, Diyarbakır and Burdur) obtained from Turkey's different regions as well as Çameli variety were used. The plant materials had been cultivated in a randomized complete block design with three replications. Results showed that there were statistically significant differences among genotypes in terms of all parameters examined except for fixed oil ratio. The mean seed yield varied between 0.34-0.86 t ha^{-1} in 2017 and 0.10-0.31 t ha^{-1} in 2018. The seed and fixed oil yields were higher for Çameli, Hatay and Diyarbakır genotypes. The percentages of linoleic and oleic acid of genotypes varied in a range of 55.85-57.67% and 21.05-22.59%, respectively. There was no significant difference among genotypes in terms of linoleic acid content. However, a significant difference was found among genotypes in terms of oleic acid content and the oleic acid content was higher in the black cumin populations than the Çameli variety.
Keywords: *genotypes, fixed oil, linoleic acid, oleic acid, palmitic acid*

Introduction

Black cumin (*Nigella sativa* L.), one of the most important species belonging to Ranunculaceae family, is an annual herbaceous medicinal plant (Thilakarathna et al., 2018). It is a plant distributed within the natural flora of Eastern Mediterranean, Southern Europe and Central Asia (Wajs et al., 2008). There are 12 species (*Nigella orientalis* L., *Nigella sativa* L., *N. oxypetala* L., *N. latisecta* P.H. Davis, *N. segetalis* Bieb., *N. arvensis* L., *N. damascena* L., *N. elata* Boiss., *N. nigellastrum* (L.) Willk., *N. unguicularis* (Lam.) Spenner ve *N. lancifolia* Hub. -Mor.) of Nigella genus in the flora of Turkey. However, only *N. sativa* and *N. damascena* are cultivated in different regions of Turkey (Toncer and Kizil, 2004; Baydar, 2013).

Black cumin is known as one of the cultivated plants that have been used for different purposes since ancient times. Its seeds and oil have been used in traditional medicine for hundreds of years, especially in Asia and Africa. In today's medicine, its seeds are used in the treatment of different diseases due to their stimulating effect. In the future, it is thought that its seeds and oil will occupy an important place in alternative medicine due to its protective effect in both the treatment of and in the prevention of various diseases (Abdolrahimi et al., 2012). The part of the plant used in food and alternative medicine is its

http://www.aloki.hu ● ISSN 1589 1623 (Print) ● ISSN 1785 0037 (Online)
DOI: http://dx.doi.org/10.15666/aeer/1902_13251336
© 2021, ALÖKI Kft., Budapest, Hungary

seed (Gun, 2012). Black cumin seeds have been used as a spice for many years in many parts of the world, especially in the Middle East and India (Kara et al., 2015; Thilakarathna et al., 2018).

In addition, these seeds have been used in the food industry to decorate bakery products and add taste and flavor to the products. Fixed oils and essential oils from black cumin seeds are an important source of raw materials for the pharmaceutical and cosmetics industry (Hussain et al., 2009). The seeds of the plant have been used in folk medicine for thousands of years in the treatment of asthma, cough, bronchitis, headache, rheumatism, fever, flu, eczema. Seeds are also used in the treatment of obesity, kidney disorders, digestive diseases and in the regulation of blood circulation (Abdolrahimi et al., 2012; Thilakarathna et al., 2018).

Fixed oil and essential oils of black cumin in alternative medicine systems in recent years; It is used to take advantage of the activities of antibacterial, antifungal, cholesterol regulating, antitumor, calming, soothing, pain relief, lowering blood sugar, antiemetic and relaxing smooth muscles (Nivkavar et al., 2003). Studies conducted on black cumin showed that its seeds have essential oils (0.30-0.60%), fixed oils (35-40%), proteins (16-21%), amino acids, saponins, alkaloids, tannins, fibers (5.5%), carbohydrates (35%) minerals (1.79-3.44%), thymoquinone (a phenolic compound found in essential oil), ascorbic acid (vitamin C), thiamine, niacin, pyridoxine and folic acid (Hussain et al., 2009; Ghamarnia et al., 2012; Gullu and Avci, 2013; Shaker et al., 2014).

It is known that thymoquinone, an important bioactive substance of black cumin, has an anti-carcinogenic effect (Padhye et al., 2008). Most of the researchers stated that the fixed oil rate of black cumin varies between 25% and 40% (Sener et al., 1985; Ustun et al., 1990; Nergiz and Otles, 1993; Ghorbanli et al., 2000; Matthaus and Ozcan, 2011; Kara et al., 2015). When the fatty acid composition of the oil was examined, it was seen that approximately 84-85% of the oil consisted of oleic (27%) and linoleic (57%) acids. In addition, black cumin oil contains low rates of eicosadienoic, arachidonic and linolenic acid, known as unsaturated fatty acids. Fixed oil of black cumin seeds has also saturated fatty acids such as myristic, palmitic and stearic acid (Gullu and Avci, 2013). Amin et al. (2010) reported that the major fatty acids of black cumin oil was linoleic acid (50.2%), oleic acid (19.9%), margaric acid (10.3%), cis-11,14-eicosadienoic acid (7.7%) and stearic acid (2.5%). Sener et al. (1985) stated that the fixed oil of black cumin seeds contains 0.26% lauric, 1.06% myristic, 20.4% palmitic, 1.56% stearic, 4.75% oleic, 64.6% linoleic and 7.18% arachidonic acid.

As it is known, many factors are effective in the growth and development of plants (Katar and Katar, 2017). These factors are generally divided into two as intrinsic and extrinsic factors (Janina, 2003). Intrinsic factors are controlled by the genetic makeup of plants (Franz, 1993). Therefore, the growth and development performances of plants with various inherited characteristics differ with the effect of their genes (Hussain et al., 2006).

Black cumin is generally cultivated under dry farming conditions. Growing black cumin under these conditions often results in low seed yield and quality losses due to limited rainfall, the requirement to compete with weeds, etc. İt can vary yield and quality due to variation in genetic and ecological influence in different regions cultivated of black cumin. Thus, geographical and genetic diversity are extremely important in respect to yield and quality characteristics of black cumin. One of the most crucial factors to achieve higher yield and quality in agriculture is the selection of suitable genotype adapted to the region. Native plant populations generally adapt better to regional conditions. Therefore, it should be determined the yield and quality potential of these populations under various ecological

http://www.aloki.hu ● ISSN 1589 1623 (Print) ● ISSN 1785 0037 (Online)
DOI: http://dx.doi.org/10.15666/aeer/1902_13251336
© 2021, ALÖKI Kft., Budapest, Hungary

conditions. The effect of black cumin genotypes on yield, yield components and quality characters was examined by some researchers (Nickavar et al., 2003; Abdolrahimi et al., 2012; Hosseinia et al., 2018). However, each of these studies was conducted with different genotypes under different ecological conditions.

Therefore, in this study conducted in Turkey where black cumin production increasingly in recent years, ıt was aimed to reveal the performances of different black cumin genotypes (population and variety) in terms of yield, yield components and quality parameters.

Material and methods

Experimental location

The experiments were carried out under the ecological conditions of Uşak province located in the Aegean Region of Turkey during 2017 and 2018 growing seasons. Uşak province is located between 38° 12 'and 39° 50' N latitudes and 28° 48' and 29° 57' E longitudes with 907 m altitude. Location of the working area was shown in *Figure 1*.



Figure 1. *Locations of genotypes collected and study region in map of Turkey (1: Çameli, 2: Uşak, 3: Hatay, 4: Diyarbakır, 5: Burdur, sr: study region)*

Climatic data of the experimental site

The climate of the Usak province has a transition characteristic between the Aegean and Central Anatolia regions. The climate is warm and temperate in Usak. The winter months are much rainier than the summer months in province. The province was characterized by semi-arid climate with a mean annual precipitation of 567 mm and mean temperature of 12.5°C. In the growing period at the experimental site, total precipitation is 269.3 mm in 2017 and 336.2 mm in 2018. For the same growing period (March-August) at the experimental site, the total rainfall for long years is 216.3 mm. April 2018 precipitation (6.4 mm) was very low compared to the same month in 2017 (62.9 mm). Mean air temperatures were 17.3°C, 18.4°C and 16.9°C during the cropping period in 2017, 2018 and long years, respectively. In addition, the mean relative humidity values were 54.4%, 55.6% and 57.4% during the cropping periods in 2017, 2018 and long years, respectively (*Table 1*).

http://www.aloki.hu ● ISSN 1589 1623 (Print) ● ISSN 1785 0037 (Online)
DOI: http://dx.doi.org/10.15666/aeer/1902_13251336
© 2021, ALÖKI Kft., Budapest, Hungary

Table 1. *Meteorological data of the experiment location*

Climatic factors	Years	Months						Mean/Sum
		March	April	May	June	July	August	
Total Precipitation (mm)	2017	37.1	62.9	100.2	42.3	1.2	25.6	269.3
	2018	76.8	6.4	102.4	54.6	58.2	37.8	336.2
	LYA*	54.6	61.6	46.2	25.8	17.2	10.9	216.3
Mean Temperature (°C)	2017	8.3	11.1	15.1	20.1	25.1	24.0	17.3
	2018	9.3	15.4	17.2	20.2	23.7	24.3	18.4
	LYA	6.4	11.0	15.7	20.3	24.0	24.1	16.9
Mean Relative Humidity (%)	2017	59.7	56.4	61.9	58.7	41.4	48.2	54.4
	2018	67.6	47.5	61.5	59.4	49.3	48.0	55.6
	LYA	67.1	64.0	61.1	55.1	48.9	48.2	57.4

*LYA: Long-years average (1986-2016)

Soil properties

The soil samples (0-30 cm depth) were taken from various parts of the experimental area and the collected soil samples were homogeneously mixed. Then, the mixed soil samples were analyzed to determine physicochemical properties of soil. The results indicated that the soils were clay-loam with pH 7.81-7.88 and 9.9-11.4% lime. Furthermore, it was found that the soil contains low organic matter (0.88-1.71%), low P_2O_5 (2.46-1.20 kg ha^{-1}) and high K_2O (340-360 kg ha^{-1}). The soil, in which the second year of the experiment was conducted, contains more organic matter than the soil of first year. However, it contains slightly more lime than the soil of first year (*Table 2*).

Table 2. *Some physical and chemical characteristics of the experimental soil*

Years	Texture	Lime (%)	Available phosphorus (P_2O_5) (kg ha^{-1})	Available potassium (K_2O) (kg ha^{-1})	pH	Organic matter (%)
2017	Clay-Loam	9.9	2.46	340	7.81	0.88
2018	Clay-Loam	11.4	1.20	360	7.88	1.71

Experimental conditions

In the study, four populations obtained from farmers in Turkey's Usak, Hatay, Diyarbakır and Burdur provinces and Cameli variety obtained from Transitional Zone Agrıcultural Research Institute, Turkey were used as plant material. Location of collected genotypes was marked in *Figure 1*. The experimental design was a randomized complete block design with three replications. Seeds were sown by hand, with 25 cm row spacing on plots of 5 m^2 harvest area (1 m width x 5 m length) on 25 March of 2017 and 22 March of 2018. Seeding was performed with a seeding rate of 15 kg ha^{-1} and sowing depth of 2-3 cm (Hussain et al., 2009; Haj Seyed Hadi et al., 2012; Kara et al., 2015). Each plot was 5 m length and consisted of 4 rows. In both years, it was done by hand when weed control of the experimental area was need. No irrigation was applied. The experimental plots were fertilized with a dose of 50 kg N and 30 kg P_2O_5 per ha (Hussain et al., 2009; Tuncturk et al., 2011; Ghamarnia et al., 2012). A photograph of the study area was presented in *Figure 2*. At the harvest, two border rows of the plots and 0.5 m from each side were excluded to eliminate border effects and then the plants in the plots were harvested by hand on the dates indicated in *Table 3*.

http://www.aloki.hu ● ISSN 1589 1623 (Print) ● ISSN 1785 0037 (Online)
DOI: http://dx.doi.org/10.15666/aeer/1902_13251336
© 2021, ALÖKI Kft., Budapest, Hungary



Figure 2. *A photo of the experimental area*

Table 3. *Harvest times of black cumin genotypes*

Genotypes	2017	2018
Çameli	13.08.2017	11.08.2018
Uşak	12.08.2017	11.08.2018
Hatay	05.08.2017	04.08.2018
Diyarbakır	29.07.2017	28.07.2018
Burdur	12.08.2017	11.08.2018

Fixed oil

The oil contents and compositions were determined in the laboratories of the Central Research Institute for Field Crops of the Ministry of Agriculture and Forestry, in Ankara, Turkey. Determination of the oil contents was performed following the method of Matthäus and Brühl (2001), with some modifications. Next, 5 grams of whole seeds were milled in a Foss KN 195 Knifetec laboratory mill (Hillerød, Denmark). Afterwards, the extraction was performed for 3 h in a Soxhlet extractor (Soxtherm 2000 automatic, Gerhardt, Germany) with hexane. After extraction, the solvent was evaporated at 103°C for 2.5 h, cooled for 30 min in a desiccator, and weighed. The seed oil content was reported as the mass percent (crude oil weight (g)/ground seeds weight (g) × 100). For determination of the fatty acid compositions, 0.1 g of oil was dissolved in 10 mL n-hexane, to which 0.5 mL 2 N potassium hydroxide/methanol solution was added, and it was incubated for 30 min at room temperature. The fatty acids were esterified as methyl esters and placed to a Shimadzu AOC-20i automatic Injector (Kyoto, Japan) (split ratio 1:100). The methyl ester phase was analyzed using a Shimadzu GC-2010 system equipped with a Teknokroma capillary column (Barcelona, Spain) (100 m × 0.25 mm and 0.2 μm) and FID detector. Helium was used as carrier gas at a flow rate of 0.94 mL/min. The injector and detector temperature was 250°C. The column was programmed with the following temperature regime: hold at 140°C for 5 min, ramp to 240°C at 4°C/min, and hold at 240°C for 20 min. Fatty acid methyl esters (FAMEs) were identified by comparison of their retention times with those of the reference standards (Restek FAME Mix 37). The fatty acid content was calculated based on the peak area ratio and expressed as g fatty acid/100 g of oil.

http://www.aloki.hu ● ISSN 1589 1623 (Print) ● ISSN 1785 0037 (Online)
DOI: http://dx.doi.org/10.15666/aeer/1902_13251336
© 2021, ALÖKI Kft., Budapest, Hungary

Statistical analysis

With randomized complete block design, analytical data collected with three replications of each treatment were subjected to analysis of variance using SPSS statistical software program, and differences among mean values were compared via the Tukey (Tukey's Honest Significant Difference test) test.

Results

The plant heights of black cumin genotypes varied according to genotypes, years and genotype by year interaction. In compared to genotypes, maximum plant heights (39.17, 38.84, 38.15 and 36.45 cm) were counted on the genotypes of Burdur, Cameli, Hatay and Usak, respectively. Mean plant height value in the first year (46.80 cm) were higher than that of the second year (25.75 cm) (*Table 4*).

The number of branches per plant of black cumin genotypes varied according to genotypes and genotype by year interaction. By comparing mean values of genotypes, the highest numbers of branches per plant (3.74 and 3.22) were obtained from the genotypes of Cameli and Usak, respectively. As it can be seen from *Table 4*, statistical significant differences were not observed between years for the numbers of branches per plant. In 2017, the highest number of branches per plant was determined in Usak (3.40), Hatay (3.37) and Cameli (3.08) genotypes in the same group, while in 2018 it was determined in Cameli (4.40) genotype (*Table 4*).

The capsule number values of genotypes varied according to genotypes, years and genotype by year interaction. According to the two-year mean, the number of capsules per plant ranged from 3.24 to 4.45 and the highest values were determined in Cameli and Burdur genotypes. According to the mean of genotypes, the number of capsules per plant was 4.74 in 2017 and 3.02 in 2018. According to the genotype by year interaction values, the highest values were determined in Burdur (5.43) and Hatay (5.03) genotypes in 2017, while it was obtained from Çameli genotype (4.43) in 2018 (*Table 4*).

The genotypes, years, and genotype by year interaction had a significant effect on seed weight per capsule. As the mean of genotypes, the seed weight per capsule was 0.23 g in 2017 and 0.12 g in 2018. As the mean of two-year, the seed weight per capsule ranged from 0.13 to 0.21 g and the highest values were determined in Hatay and Çameli genotypes. Considering the values of genotype by year interaction, the highest values in 2017 were obtained from Hatay (0.28 g) and Uşak (0.25 g) genotypes. On the other hand, in 2018, the second year of the study, the highest values were obtained from Hatay (0.14 g), Çameli (0.14 g), Uşak (0.11 g) and Burdur (0.11 g) genotypes (*Table 4*).

Only a significant difference among genotypes was detected in terms of 1000 seed weight. As the mean of two-year, 1000 seed weight values ranged between 1.98-2.39 g and the highest values were obtained from Hatay (2.39 g), Uşak (2.19 g) and Diyarbakır (2.14 g) genotypes (*Table 4*).

The genotypes, years, and genotype by year interaction had a significant effect on seed yield (t ha^{-1}). While mean seed yield was 0.67 t ha^{-1} in 2017, it was 0.23 t ha^{-1} in 2018. As the mean of two-year, the seed yield ranged from 0.30 to 0.55 t ha^{-1} and the highest values were determined in Hatay (0.55 t ha^{-1}), Çameli (0.52 t ha^{-1}) and Diyarbakır (0.48 t ha^{-1}) genotypes. Considering the genotype values with the year interaction, the highest values in 2017 were obtained from Diyarbakır, Hatay and Çameli genotypes as 0.86 t ha^{-1}, 0.79 t ha^{-1} and 0.75 t ha^{-1} respectively (*Table 4*). On the

http://www.aloki.hu ● ISSN 1589 1623 (Print) ● ISSN 1785 0037 (Online)
DOI: http://dx.doi.org/10.15666/aeer/1902_13251336
© 2021, ALÖKI Kft., Budapest, Hungary

other hand, the highest values in 2018 were obtained from the Hatay, Çameli and Burdur genotypes as 0.31 t ha^{-1}, 0.30 t ha^{-1} and 0.26 t ha^{-1} respectively (*Table 4*).

Table 4. *Yield, yield components and fixed oil rate of black cumin genotypes*

Genotypes	Plant height (cm)			Number of branches per plant		
	2017	2018	Mean	2017	2018	Mean
Çameli	49.50 a	28.17 a	38.84 a	3.08 ab	4.40 a	3.74 a
Uşak	47.90 a	25.00 ab	36.45 a	3.40 a	3.03 b	3.22 a
Hatay	50.97 a	25.33 ab	38.15 a	3.37 a	2.20 c	2.79 b
Diyarbakır	34.93 b	22.60 b	28.77 b	2.78 b	2.30 c	2.54 b
Burdur	50.70 a	27.63 a	39.17 a	2.85 b	2.71 bc	2.78 b
Mean	46.80 A	25.75 B	36.27	3.10	2.93	3.01
CV (%)	32.48			21.59		
Year	**			ns		
Genotypes	**			**		
Y x G	**			**		
Genotypes	**Number of capsule per plant**			**Seed weight per capsule (g)**		
	2017	**2018**	**Mean**	**2017**	**2018**	**Mean**
Çameli	4.47 bc	4.43 a	4.45 a	0.23 bc	0.14 a	0.19 ab
Uşak	4.55 bc	3.47 b	4.01 b	0.25 ab	0.11 ab	0.18 bc
Hatay	5.03 ab	2.23 c	3.63 bc	0.28 a	0.14 a	0.21 a
Diyarbakır	4.20 c	2.28 c	3.24 c	0.18 c	0.08 c	0.13 d
Burdur	5.43 a	2.67 c	4.05 ab	0.20 c	0.11 ab	0.16 cd
Mean	4.74 A	3.02 B	3.88	0.23 A	0.12 B	0.17
CV (%)	29.15			35.29		
Year	**			**		
Genotypes	**			**		
Y x G	**			**		
Genotypes	**1000 seed weight (g)**			**Seed yield (t ha^{-1})**		
	2017	**2018**	**Mean**	**2017**	**2018**	**Mean**
Çameli	1.89	2.16	2.03 b	0.75 a	0.30 a	0.52 a
Uşak	2.08	2.29	2.19 ab	0.59 b	0.20 b	0.39 b
Hatay	2.47	2.31	2.39 a	0.79 a	0.31 a	0.55 a
Diyarbakır	2.20	2.07	2.14 ab	0.86 a	0.10 c	0.48 a
Burdur	2.03	1.92	1.98 b	0.34 c	0.26 a	0.30 c
Mean	2.13	2.15	2.14	0.67 A	0.23 B	0.45
CV (%)	10.24			59.54		
Year	ns			**		
Genotypes	**			**		
Y x G	ns			**		
Genotypes	**Fixed oil rate (%)**			**Fixed oil yield (L ha^{-1})**		
	2017	**2018**	**Mean**	**2017**	**2018**	**Mean**
Çameli	33.62 ab	34.95 a	34.29	250.00 a	104.20 a	177.1 a
Uşak	32.34 b	33.01 a	32.68	190.20 b	65.10 c	127.7 b
Hatay	31.34 b	33.15 a	32.25	249.10 a	97.00 a	173.1 a
Diyarbakır	31.54 b	34.46 a	33.00	272.00 a	34.50 d	153.3 a
Burdur	35.55 a	31.37 a	33.46	120.10 c	81.10 b	100.6 c
Mean	32.88	33.39	33.13	216.30 A	76.40 B	146.3
CV (%)	6.71			57.49		
Year	ns			**		
Genotypes	ns			**		
Y x G	*			**		

*: P<0.05, **: P<0.01, Y: Year, G: Genotypes, ns: Not significant, CV: Coefficient of variation. Means in the same columns followed by the different small letters and in the same rows followed by the different capital letters are significantly different as statistically

http://www.aloki.hu ● ISSN 1589 1623 (Print) ● ISSN 1785 0037 (Online)
DOI: http://dx.doi.org/10.15666/aeer/1902_13251336
© 2021, ALÖKI Kft., Budapest, Hungary

No statistically significant difference was determined among the fixed oil rates of black cumin genotypes used in this study. Genotype by year interaction had a significant effect on fixed oil rate. The highest fixed oil rates were determined in Burdur (35.55%) and Çameli (33.62%) genotypes in 2017. No statistically significant difference was found among genotypes in terms of fixed oil rate in 2018. The fixed oil rate of 33.13% was determined as the mean value of two-year and genotypes (*Table 4*).

The genotypes, years, and genotype by year interaction had a significant effect on fixed oil yield (L ha^{-1}). While mean fixed oil yield was 216.30 L ha^{-1} in 2017, It was 76.40 L ha^{-1} in 2018. As the mean of two-year, the fixed oil yield ranged from 100.6 to 177.1 L ha^{-1} and the highest value were determined in Çameli (177.1 L ha^{-1}), Hatay (173.1 L ha^{-1}) and Diyarbakır (153.3 L ha^{-1}) genotypes. Diyarbakır, Hatay and Çameli genotypes were the genotypes with the highest fixed oil yield in 2017. On the other hand, the highest fixed oil yield in 2018 was obtained from the Çameli and Hatay genotypes as 104.20 L ha^{-1} and 97.00 L ha^{-1}, respectively (*Table 4*).

The content of total unsaturated fatty acids (palmitoleic, oleic, linoleic, arachidonic, linolenic and cis-11,14-eicosadienoic) of black cumin genotypes ranged from 81.03% to 82.41%, whereas saturated fatty acids (caproic, palmitic and stearic) were 16.26-17.27%. In addition, linoleic (55.85-57.67%), oleic (21.05-22.59%) and palmitic (11.16-12.24%) were found to be the major fatty acids. The highest linoleic acid content was obtained from the Çameli variety (57.67%). However, no significant difference was found among genotypes in terms of linoleic acid content. On the other hand, the oleic acid content of the Çameli variety was significantly lower than the other genotypes. In addition, the four populations examined in the study were not significantly different in terms of oleic acid content (*Table 5*).

Table 5. *Fatty acids components of black cumin genotypes*

Fatty acids (%)	Genotypes					Mean	
	Çameli	Uşak	Hatay	Diyarbakır	Burdur		
Caproic Acid (C6:0)	1.74	2.08	1.22	1.90	1.53	1.70	n.s.
Palmitic Acid (C16:0)	11.16	11.32	11.98	11.25	12.24	11.59	n.s.
Palmitoleic Acid (C16:1)	0.15	-	0.15	-	0.16	0.15	n.s.
Stearic Acid (C18:0)	3.36	3.55	3.42	3.34	3.50	3.44	n.s.
Oleic Acid (C18:1n9c)	21.05 b	21.94 ab	22.59 a	21.72 ab	21.85 ab	21.83	*
Linoleic Acid (C18:2n6c)	57.67	56.43	55.85	56.85	56.14	56.59	n.s.
Arachidonic Acid (20:4. ω-6)	0.21	-	0.21	0.19	0.20	0.20	n.s.
Linolenic Acid (C18:3n6)	0.32	0.30	0.30	0.31	0.29	0.30	n.s.
Cis-11.14-Eicosadienoic Acid (C20:2)	3.01 a	3.08 a	2.62 b	3.08 a	2.39 ab	2.83	**
Total	98.65	98.71	98.34	98.63	98.29		

*: P<0.05, **: P<0.01, n.s.: Not significant. Means in the same rows followed by the different small letters are significantly different as statistically

Discussion

Yield and yield components

As the environmental conditions move away from the ideal conditions for optimum growth and development of each plant; yield and quality losses increase (Amin et al., 2010; Goksoy et al., 2019). The variation in yield and yield components detected in the study depending on the years can be explained by the extreme drought experienced in April 2018. Since the seeds sowed on March 22, 2018 were faced with an extreme

http://www.aloki.hu ● ISSN 1589 1623 (Print) ● ISSN 1785 0037 (Online)
DOI: http://dx.doi.org/10.15666/aeer/1902_13251336
© 2021, ALÖKI Kft., Budapest, Hungary

drought immediately after emergence (in April), the initial growth and development of the plants were limited. Although the precipitation returned to normal in the following months, this growth and development retardation experienced in April caused the values obtained in 2018 to be lower compared to 2017. Also, the variation in the yield and yield components due to genotypes can be attributed to the difference in the genetic makeup of the plant materials used in the study.

Different yield response of cultivars/varietis from one environment to another is called genotype by environment (GEI) interaction (Goksoy et al., 2019). The fact that genotypes showed different values in yield and yield components in 2017 and 2018 can be explained by the response of genotypes to changing climatic conditions. Genotypes were negatively affected by drought in 2018, resulting in a decrease in yield and yield components. It was stated that the seed yield and components of black cumin decreased rapidly due to the increasing water stress during the growth periods in semi-arid climatic conditions (Ghamarnia and Jalili, 2013). In addition, Sadeghi (2009) reported that there was a positive correlation between seed yield and aboveground biomass. In the study, seed yields of black cumin genotypes varied according to years and genotypes. This difference between two years can be explained by the extreme drought in April 2018. This drought negatively affected the growth performance of the plant during the first development period and caused significant decreases in the values of the yield and yield components in 2018. The yield difference detected among genotypes can be attributed to the different inherited make up of genotypes. The Hatay and Diyarbakır populations used in the study and obtained from warmer regions are more early populations than the others (*Table 3*). It has been reported that yield of early genotypes may be higher due to their better use of available moisture in semi-arid and arid climatic conditions in a study conducted on wheat genotypes (Ludwig and Asseng, 2010). D'Antuono et al. (2002) reported that the main factor reducing yield for black cumin genotypes seemed low vegetative growth. These results were lower than those of Ozel et al. (2009), Tuncturk et al. (2012) and Kara et al. (2015). These differences are thought to be due to probably variations in genotype, environmental conditions, agronomic practices. In addition, it has been reported that the environmental conditions during pollination determine the number of capsules and branches (Sadeghi, 2009).

Fixed oil rate

There was no difference in fixed oil rate between the two years in which the study was conducted. This showed that the plant materials used in the study were not very different from each other in terms of genetic inheritance that determined the oil content. Matthaus and Ozcan (2011) determined that the fixed oil rate of black cumin seeds vary between 30.4% and 36.4%. Kara et al. (2015) reported that the fixed oil rates of black cumin populations collected from the Burdur, Tokat, Uşak, Eskişehir and Antalya provinces were 24.5%, 30.6%, 30.5%, 25.6% and 30.4%, respectively. Results from this study are similar with the Matthaus and Ozcan (2011) findings but was higher than Kara et al. (2015). Differing findings among studies in terms of fixed oil rate can be probably due to genotype, growing, localities, climatic and environmental conditions (Matthaus and Ozcan, 2011; Hendawy et al., 2012).

Fatty acid compositions

While the variation of linoleic acid among genotypes is 3.26%, the variation of oleic acid is 7.32%. The variation in palmitic acid, which is another major fatty acid, was

http://www.aloki.hu ● ISSN 1589 1623 (Print) ● ISSN 1785 0037 (Online)
DOI: http://dx.doi.org/10.15666/aeer/1902_13251336
© 2021, ALÖKI Kft., Budapest, Hungary

found to be 9.68%. That is, genotypes showed the highest variation in palmitic acid in terms of fatty acid composition. It is desired that palmitic, which is a saturated fatty acid in terms of fat quality, is low and oleic acid, which is a monounsaturated fatty acid, is also high. While Çameli genotype stood out in terms of low palmitic acid, the variation among Çameli (78.72%), Usak (78.37%), Hatay (78.44%) and Diyarbakır (78.57%) genotype was very low in terms of the sum of oleic and linoleic acids. As a result, genotypes were generally found to be similar in terms of fatty acid composition. Ustun et al. (1990) reported that the linoleic acid contents of black cumin seeds collected from the Kutahya, Denizli and Konya provinces were 61.84%, 62.53%, and 58.38%, respectively. Also, Matthaus and Ozcan (2011) determined that the linoleic acid contents of black cumin seeds vary between 56.7% and 58.9%. Some researchers have found that the oleic acid contents of black cumin seeds vary between 18.7% and 23.7% (Ustun et al., 1990; Matthaus and Ozcan, 2011). The differences among the fatty acid composition reported in previous studies and the values obtained in this study can be explained by the different climatic conditions of the regions where the experiments carried out, as well as the difference among the genotypes studied (Amin et al., 2010; Gullu and Avci, 2013).

Conclusions

According to the results of this study that with five genotypes obtained from different regions of Turkey conducted two years, yield and its components of black cumin were significantly affected by plant genotypes. On the other hand, no significant difference was found among the genotypes in terms of linoleic acid (the major fatty acid) content. However, genotypes differed significantly in terms of oleic acid (the second fatty acid) content. The oleic acid content of the Çameli variety was significantly lower than the other genotypes. Considering the results of this study conducted under Turkey's Uşak ecological conditions, Hatay, Çameli and Diyarbakır genotypes can be recommended for the region in terms of high seed and oil yield. When the composition of oil as well as the yield of black cumin was evaluated together, the favorite genotypes were Hatay and Diyarbakır genotypes. İt is thought that the results obtained from this research will be a data especially for future black cumin breeding studies. Considering that the effects of climate change will be felt more in the future, it would be extremely beneficial to test different black cumin populations (native) more in terms of traits such as competition with weeds, drought resistance and cold resistance under dry farming conditions. Therefore, it should be to increase the breeding studies on black cumin plant.

REFERENCES

[1] Abdolrahimi, B., Mehdikhani, P., Hassanzadeh Gort Tappe, A. (2012): The effect of harvest index, yield and yield component of three varieties of black cumin (*Nigella sativa* L.) in different planting densities. – International Journal of AgriScience 2(1): 93-101.

[2] Amin, S., Mir Showkat, R., Kohli, K., Ali, B., Ali, M. (2010): A study of the chemical composition of black cumin oil and its effect on penetration enhancement from transdermal formulations. – Natural Product Research 24(12): 1151-7.

[3] Baydar, H. (2013): Medical, aromatic and delightful plants science and technology. – Suleyman Demirel University, Publication No: 51, Isparta, Turkey.

http://www.aloki.hu ● ISSN 1589 1623 (Print) ● ISSN 1785 0037 (Online)
DOI: http://dx.doi.org/10.15666/aeer/1902_13251336
© 2021, ALÖKI Kft., Budapest, Hungary

[4] D'Antuono, L. F., Moretti, A., Antonio, F. S. (2002): Seed yield, yield components, oil content and essential oil content and composition of *Nigella sativa* L. and *Nigella damascena* L. – Industrial Crops and Products 15: 59-69.
[5] Franz, C. H. (1993): Genetics. – In: Hay, R. K. M., Waterman, P. G. (eds.) Volatile Oil Crops. London: Longman Group UK Limited.
[6] Ghamarnia, H., Khosravy, H., Sepehri, S. (2012): Yield and water use efficiency of (*Nigella sativa* L.) under different irrigation treatments in semi-arid region in the west of Iran. – Journal of Medicinal Plants Research 4(16): 1612-1616.
[7] Ghamarnia, H., Jalili, Z. (2013): Water stress effects on different black cumin (*Nigella sativa* L.) components in a semi-arid region. – Int. J. of Agronomy and Plant Production 4(4): 753-762.
[8] Ghorbanli, M., Babai, A., Sepehr, M. F. (2000): The effect of water stress on the seed oil of *Nigella sativa* L. – Journal Essential Oil Research 12: 36-38.
[9] Goksoy, A. T., Sincik, M., Erdogmus, M., Ergin, M., Aytac, S., Gumuscu, G., Gunduz, O., Keles, R., Bayram, G., Senyigit, E. (2019): The parametric and non-parametric stability analyses for interpreting genotype by environment interaction of some soybean genotypes. – Turk Journal Field Crops 24(1): 28-38.
[10] Gullu, E. B., Avci, G. (2013): Thymoquinone: The bioactive component of *Nigella sativa*. – Kocatepe Veterinary Journal 6(1): 51-61.
[11] Gun, M. (2012): Holly seed: *Nigella sativa* (black cumin). Some knowledge corresponding to *Nigella sativa*'s therapy ailment. – Mersin University School of Medicine Lokman Hekim Journal of History of Medicine and Folk Medicine 2(1): 43-46.
[12] Haj Seyed Hadi, M., Darzi, M. T., Ghandehari, Z. (2012): Effect of irrigation treatment and Azospirillum inoculation on yield and yield component of black cumin (*Nigella sativa* L.). – Journal Medicinal Plants Research 6(30): 4553-4561.
[13] Hendawy, S. F., El-Sherbeny, S. E., Hussein, M. S., Khalid, K. A., Ghazal, G. M. (2012): Response of two species of black cumin to foliar spray treatments. – Australian J. of Basic and Applied Sciences 6(10): 636-642.
[14] Hosseinia, S. S., Nadjafia, F., Asarehb, M. H., Rezadoost, H. (2018): Morphological and yield related traits, essential oil and oil production of different landraces of black cumin (*Nigella sativa*) in Iran. – Scientia Horticulturae 233: 1-8.
[15] Hussain, A., Anjum, F., Rab, A., Sajid, M. (2006): Effects of nitrogen on the growth and yield of asparagus (*Asparagus officinalis*). – Journal of Agricultural and Biological Science 2: 41-47.
[16] Hussain, A., Nadeem, A., Ashraf, I., Awan, M. (2009): Effect of weed competion periods on the growth and yield of black cumin (*Nigella sativa* L.). – Pakistan Journal of Weed Science Research 15(1): 71-81.
[17] Janina, M. S. (2003): *Melissa officinalis*. – The Int. J. Aromatherapy 10: 132-139.
[18] Kara, N., Katar, D., Baydar, H. (2015): Yield and quality of black cumin (*Nigella sativa* L.) populations: The effect of ecological conditions. – Turkish Journal of Field Crops 20(1): 9-14.
[19] Katar, D., Katar, N. (2017): Effect of sowing rates in different row spacing on the yield and yield components of false flax (*Camelina sativa* (L.) Crantz). – Journal of Agricultural Faculty of Gaziosmanpasa University 34(1): 76-85.
[20] Ludwig, F., Asseng, S. (2010): Potential benefits of early vigor and changes in phenology in wheat to adapt to warmer and drier climates. – Agriculture Systems 103: 127-136.
[21] Matthäus, B., Brühl, L. (2001): Comparison of different methods for the determination of the oil content in oilseeds. – Journal of the American Oil Chemists' Society 78(1): 95-102.
[22] Matthaus, B., Ozcan, M. M. (2011): Fatty acids, tocopherol, and sterol contents of some *Nigella* species seed oil. – Czech J. Food Science 29(2): 145-150.
[23] Nergiz, C., Otles, S. (1993): Chemical composition of *Nigella sativa* L. seeds. – Food Chemistry 48: 259-261.

http://www.aloki.hu ● ISSN 1589 1623 (Print) ● ISSN 1785 0037 (Online)
DOI: http://dx.doi.org/10.15666/aeer/1902_13251336
© 2021, ALÖKI Kft., Budapest, Hungary

[24] Nickavar, B., Mojab, F., Javidnia, K., Amoli, M. A. R. (2003): Chemical composition of the fixed and volatile oils of *Nigella sativa* L. from Iran. – Zeitschrift fur Naturforschung 58(9-10): 629-631.
[25] Ozel, A., Demirel, U., Guler, I., Erden, K. (2009): Effect of different row spacing and seeding rate on black cumin (*Nigella sativa* L.) yields and some agricultural characters. – Harran Uni. J. of Agriculture Faculty 13(1): 17-25. (in Turkish).
[26] Padhye, S., Banerjee, S., Ahmad, A., Mohammad, R., Sarkar, F. H. (2008): From here to eternity-the secret of pharaohs: Therapeutic potential of black cumin seeds and beyond. – Cancer Ther. 6(b): 495-510.
[27] Sadeghi, S., Rahnavard, A., Ashrafi, Z. Y. (2009): Study importance of sowing date and plant density effect on black cumin yield. – Botany Research International 2(2): 94-98.
[28] Sener, B., Kusmenoğlu, S., Mutlugil, A., Bingol, F. (1985): A study with the seed of *Nigella sativa*. – Gazi Uni. J. of Pharmacy Faculty 2(1): 1-8.
[29] Shaker, A. H., Jamal, A. T., Sajid, O. M. (2014): Effect of watery and alcoholic medicinal plants extractions on in-vitro ruminant digestibility. – KSU Doga Bil. Derg. 17(3): 30-33.
[30] Thilakarathna, R. C. N., Madhusankha, G. D. M. P., Navaratne, S. B. (2018): Morphological characteristics of black cumin (*Nigella sativa*) seeds. – Chemistry Research Journal 3(3): 40-45.
[31] Toncer, O., Kizil, S. (2004): Effect of seed rate on agronomic and technologic characters of *Nigella sativa* L. – International Journal of Agriculture & Biology 3: 529-532.
[32] Tuncturk, R., Tuncturk, M., Ciftci, V. (2012): The effects of varying nitrogen doses on yield and some yield components of black cumin (*Nigella sativa* L.). – Advances in Environmental Biology 6(2): 855-858.
[33] Ustun, G., Kent, L., Cekin, N., Civelekoglu, H. (1990): Investigation on the technological properties of *Nigella sativa* (black cumin) seed oil. – J. American Oil Chemical Society 67: 958-960.
[34] Wajs, A., Bonikowski, R., Kalemba, D. (2008): Composition of essential oil from seeds of *Nigella sativa* L. cultivated in Poland. – Flavour and Fragrance Journal 23: 126-132.

http://www.aloki.hu ● ISSN 1589 1623 (Print) ● ISSN 1785 0037 (Online)
DOI: http://dx.doi.org/10.15666/aeer/1902_13251336
© 2021, ALÖKI Kft., Budapest, Hungary

SALINE-ALKALINE SOIL BACTERIAL COMMUNITY STRUCTURE AND DIVERSITY ANALYSIS UNDER DIFFERENT PATTERNS OF LAND-USE IN A LAKE WETLAND IN SONGNEN PLAIN, CHINA

SHI, C. Q.[1,2] – LI, Y.[3] – YU, S. P.[1*] – HU, B. Z.[1,2] – GUO, H.[1] – JIN, L.[4] – CONG, D. L.[1] – MENG, B.[1] – DING, J. N.[1] – LIANG, X. W.[1]

[1]*Heilongjiang Province Key Laboratory of Cold Region Wetland Ecology and Environment Research, Harbin University, Harbin 150086, Heilongjiang Province, P. R. China*

[2]*College of Life Science, Northeast Agricultural University, Harbin 150038, Heilongjiang Province, P. R. China*

[3]*College of Resource and Environment, Northeast Agricultural University, Harbin 150038, Heilongjiang Province, P. R. China*

[4]*Plant Nutriention and Resources Institute, Beijing Academy of Agriculture and Forestry Sciences, Beijing 100097, Heilongjiang Province, P. R. China*

[*]*Corresponding author*
e-mail: wetlands1972@126.com; phone: +86-0451-8662-3372

(Received 5th Nov 2020; accepted 8th Feb 2021)

Abstract. In this study, the saline-alkaline soil samples were collected from Gudahu Wetland in Songnen Plain, China, in May (dry season) and July (rainy season), 2018. The soil bacterial community structure and diversity in the original meadow, lake dam, cropland, and woodland were analyzed using high-throughput sequencing technology. The results showed that Proteobacteria were the dominant bacterial phylum during the two seasons. Except for an unclassified group at the generic level, *Pseudomonas* showed the highest relative abundance. The lake dam's soil bacterial community diversity was the lowest, followed by the original meadow, while those of cropland and woodland were higher. The soil bacterial community structures differed among the four land-use patterns. Cropland and woodland showed the highest differences in soil bacterial community structure compared to the original meadow than the lake dam. In contrast to cropland and woodland, soil bulk density, electrical conductivity, and pH had a higher impact on the bacterial community diversities of the original meadow and the lake dam. Dam construction, cultivation, and afforestation in the saline-alkaline lake wetland of Songnen Plain changed the physicochemical properties of soil from the original meadow. It affected the bacterial community structure and diversity.
Keywords: *soil microbe, high-throughput sequencing, saline-alkaline wetland, seasonal changes*

Introduction

Soil alkalization or salinization is a type of soil degradation, which poses a severe threat to ecosystems across the globe since it adversely affects plant growth and microbial function (Yan et al., 2015; Liu et al., 2016). The total area of saline land has reached 950 million ha of land worldwide (Zhang et al., 2005). Songnen Plain in northeast China is one of the three largest sodic-saline areas globally due to significant alkalization of soil, and > 3.2 million ha land is affected by high salt content (Bian et al., 2008; Wang et al., 2009). The primary factors causing soil salinization and alkalization are a) natural environmental factors, such as geology and geomorphology, soil matrix, climate, hydrology and rainfall, and b) human interferences, such as road construction,

http://www.aloki.hu ● ISSN 1589 1623 (Print) ● ISSN 1785 0037 (Online)
DOI: http://dx.doi.org/10.15666/aeer/1902_13371352
© 2021, ALÖKI Kft., Budapest, Hungary

embankment construction, reservoir engineering, and overgrazing. Soil degradation, has adverse effects on the ecological environment, agriculture, and husbandry; it degenerates a large grassland area (Shang et al., 2003; Wan et al., 2003; Wang et al., 2009; Zhou et al., 2011).

Soil microbiota is a crucial component of the ecosystem, which participates in distinct ecological processes, such as organic matter decomposition, nutrient transformation, and pollutant degradation (Foti et al., 2007; Griffiths and Laurent, 2013; Zhao et al., 2015). Environmental changes influence the community structure and diversity of soil microbiota, and they serve as an indicator of soil's ecological environment (Hansel et al., 2008; Canfora et al., 2014; Zhang et al., 2018; Liu et al., 2020). Multiple environmental factors, such as land-use patterns (Peng et al., 2017), vegetation types (Zak et al., 2003; Jin et al., 2017; Deng et al., 2018; Li et al., 2018a), and soil nutrient condition (Li et al., 2018b) influences the diversity of soil microbiota. Several physicochemical factors, such as pH, soil electrical conductivity (EC), soil moisture, and so on, also play crucial roles in deriving the diversity of microbial community structure. Microbial diversity is affected by pH (Shen et al., 2013; Li et al., 2018c; Fan and Wu, 2020) as a high pH substantially mitigates the microbial growth, culminating in decreased diversity of microbial community (Zhang and Feng, 2008; Chu et al., 2017). Apart from pH, soil's EC is also a crucial physicochemical component that influences microbial activity, biomass, and community structure (Yan et al., 2015). EC also alters bacterial community structure under alkaline conditions in saline-alkaline soil (Wang et al., 2020). Soil moisture affects oxygen content and regulates the type, activity, and growth of microbes (Yan et al., 2015; Zhang et al., 2016; Zou et al., 2018), substantially influencing the microbial community structure.

The soil nutrient content, permeability of saline-alkaline wetland soil, and soil microbes' diversity are also low (Niu et al., 2017). However, only a few studies have explored the structure and diversity of soil microbial communities in saline-alkaline wetland environment (Gandhi et al., 2018), particularly in different seasons and land-use conditions. Systematic analysis of soil microbial community structure dynamics and diversity could provide significant data for wetland protection in different seasons. The Gudahu Wetland is a typical representative of the permanent saline lake in the Songnen Plain lake wetland, where artificial interferences pose a significant threat to the soil environment. In this study, the saline-alkaline soils in different land-use patterns of the Gudahu Wetland were analyzed. A total of 24 soil samples were collected during May and July, 2018, and analyzed using high-throughput sequencing technology to elucidate the structure and diversity of the soil microbial community and associated influencing factors. The objective of this study was i) to reveal the characteristics of the soil microbial community in saline-alkaline wetland, and ii) to provide scientific data for studying microbial biodiversity in the saline-alkaline wetland in the cold and arid areas of northeast China. Additionally, reference and theoretical guidance for the protection and rational utilization of saline-alkaline wetland and strategies for returning farmland to wetland were suggested in this study.

Materials and methods

Study area description

Gudahu Wetland is located in the middle of Songnen Plain, Anda City, Heilongjiang Province, China. It occupies a total of 4, 850.1 ha area, which is 8.2 km long (south to

http://www.aloki.hu ● ISSN 1589 1623 (Print) ● ISSN 1785 0037 (Online)
DOI: http://dx.doi.org/10.15666/aeer/1902_13371352
© 2021, ALÖKI Kft., Budapest, Hungary

north 46°19′31″-46°23′58″N), and 8 km wide (west to east 125°28′06″-125°34′34″E), This wetland has a continental monsoon climate, and it experiences low annual rainfall and high evaporation rate. In this wetland, spring and autumn seasons are accompanied by frequent strong winds, summers with torridity, and winters with cold-dry weather. The annual average temperature is 3.2℃. Under such climatic conditions, most plants start growing in May and flourish in July. Gudahu Wetland is a typical inland plain and permanently saline lake wetland, and it includes most of the Qingken Lake area, and herbaceous swamp and marshy meadow, with a 99.1% wetland rate. This region is surrounded by cropland and woodland.

Soil sample collection

Soil samples were collected from the original meadow (O), lake dam (L), cropland (C), and woodland (W) on May 30, 2018 (dry season) and July 30, 2018 (rainy season). Three quadrats were set for each soil type. 200 g soil was sampled from four vertices and center points at a depth of 5-10 cm below the ground surface, each quadrat (20 m × 20 m) using a ring knife (Φ=4 cm). The impurities from the soil samples were removed, and purified samples were thoroughly mixed. 50 g portion of the soil sample was retained, and 2 g was put into an appropriately labeled tube containing microbial DNA preservation solution (TinyGene, Shanghai, China). The remaining soil was used for physicochemical analysis at low temperatures (-20°C) at the laboratory. The geographical coordinates, altitude, and dominant plant species in the sampling area were recorded (*Table 1*).

Table 1. *Details of soil samples collected in Gudahu Wetland in Songnen Plain, China*

Type	Sample	Longitude	Latitude	Altitude	Dominant plants in May	Dominant plants in July
O	O1	125°28'17.34"E	46°20'30.42"N	149.4 m	*Suaeda glauca, Puccinellia tenuiflora, Kochia scoparia*	*Artemisia anethifolia*, *Suaeda glauca*, *Kochia scoparia*
	O2	125°34'09.18"E	46°22'55.07"N	144.2 m		
	O3	125°32'27.41"E	46°23'46.96"N	148.2 m		
L	L1	125°29'02.95"E	46°23'09.05"N	142.9 m	*Phragmites australis, Artemisia selengensis, Chenopodium album, Ixeris chinensis*	*Phragmites australis, Artemisia selengensis*, *Aster pekinensis, Setaria viridis, Plantago asiatica*
	L2	125°29'45.57"E	46°23'50.52"N	146.3 m		
	L3	125°30'26.90"E	46°23'56.60"N	143.6 m		
C	C1	125°28'56.66"E	46°23'20.79"N	145.5 m	*Zea mays, Equisetum arvense*	*Zea mays*, *Solanum nigrum*, *Echinochloa crus-galli, Amethystea caerulea*
	C2	125°27'59.95"E	46°22'33.69"N	144.3 m		
	C3	125°27'43.59"E	46°22'11.95"N	149.1 m		
W	W1	125°28'56.42"E	46°23'33.93"N	152.0 m	*Populus simonii*, *Leymus chinensis, Potentilla chinensis, Artemisia scoparia, Kochia scoparia, Chloris virgata*	*Populus simonii*, *Leymus chinensis*, *Potentilla chinensis, Artemisia scoparia, Kochia scoparia, Digitaria ciliaris* var. *chrysoblephara*
	W2	125°30'16.64"E	46°23'57.24"N	157.5 m		
	W3	125°31'42.96"E	46°23'53.22"N	154.7 m		

Note: O (original meadow), L (lake dam), C (cropland), and W (woodland) were the four land-use patterns in Gudahu Wetland in Songnen Plain, China. Identical soil samples were collected from the same location during May and July, 2018. The identification of dominant plant species was based on the "Flora of China" (Wu et al., 2013)

Determination of soil's physicochemical properties

The physicochemical properties of 24 soil samples were determined as described previously by Bao (2007) and Yu et al. (2020). Ring knife (Φ=4 cm) method was used

http://www.aloki.hu ● ISSN 1589 1623 (Print) ● ISSN 1785 0037 (Online)
DOI: http://dx.doi.org/10.15666/aeer/1902_13371352
© 2021, ALÖKI Kft., Budapest, Hungary

to determine soil bulk density (BD), drying method (105°C) for soil moisture (M), electrical conductivity meter (DDS-307A, RER, Shanghai) method for soil EC, pH meter (INESA PHS-3C, Shanghai) method for soil pH, TOC analyzer (Multi N/C2100, Analytik-Jena, Germany) method for total organic carbon (TOC), Semi-Micro Kjeldahl Method for total N (TN), alkaline hydrolysis diffusion method for available N (AN), Mo-Sb anti spectrophotometric method for total P (TP) and available P (AP), flame photometer method for total K (TK) and available K (AK), were used. Each index was measured three times.

Soil bacteria genomic DNA extraction and PCR amplification

Bacterial DNA was extracted using the MIO-BIO Power Soil DNA Isolation Kit (QIAGEN, Germany), as per manufacture's instructions. Specific primers (515F 5'-GTGCCAGCMGCCGCGGTAA-3' and 926R 5'-CCGTCAATTCMTTTGAGTT-3') were used to amplify the 16S rRNA V4-V5 region of the soil bacteria. Amplicon sequencing was performed using the Illumina MiSeq platform at TinyGene Technologies, Inc. (Shanghai, China).

Statistical analysis

The pair-end reads obtained from DNA of bacterial soil samples were distinguished using barcode. To extract effective sequences, all the sequences were quality controlled and filtered as described previously by Liu et al. (2012) and Zhao et al. (2018). All data were submitted into the NCBI Sequence Read Archive database (Accession number: PRJNA615241). The effective sequences were merged based on the overlaps and subsequently quality controlled and filtered to obtain the optimized sequences of soil bacteria. The relative abundance information of each OTU in each sample was computed using the UPARSE pipeline (Edgar, 2013) to cluster the optimized sequences into operational taxonomic units (OTUs) at 97% similarity. QIIME (version 1.8.0) software (Caporaso et al., 2010) was used to analyze factors representing the diversity of the bacterial community in each sample, including the Chao1 and Shannon index and rarefaction curves. Venn diagrams were drawn using the VennDiagram package version 1.6.20 (Chen, 2018) in R (version 3.4.1) software (R Core Team, 2017). Histograms depicting the community structure at the phyletic and generic levels of relative abundance were generated using Office Excel 2010. The pheatmap package version 1.0.12 (Kolde, 2019) in R (v3.4.1) software (R Core Team, 2017) analyzed and displayed the bacterial community similarity at the OTU level based on the unweighted UniFrac algorithm. The correlation between the bacterial communities and soil's physicochemical properties were analyzed using Canoco for Windows (version 4.54) software with the redundancy analysis (RDA) method. Monte Carlo permutation tests were used to determine significance (number of permutations=999). CanoDraw for Windows (version 4.13) was used for drawing. SPSS Statistics for Windows (version 17.0, SPSS Inc. Chicago, IL, USA) was used to test the differences in physicochemical properties, the richness and diversity indexes of bacterial communities and the relative abundance of dominant phyla using Duncan's multiple range test and t-test ($P < 0.05$ represent significant difference and $P < 0.01$ represent very significant difference), also, to analyze the correlation between the dominant bacterial phyla and soil's physicochemical properties using Pearson correlation analysis ($P < 0.05$ represent significant correlation and $P < 0.01$ represent very significant correlation).

http://www.aloki.hu ● ISSN 1589 1623 (Print) ● ISSN 1785 0037 (Online)
DOI: http://dx.doi.org/10.15666/aeer/1902_13371352
© 2021, ALÖKI Kft., Budapest, Hungary

Results

Physicochemical properties of soil

Out of all the land-use patterns, the BD of L was the highest due to the compaction of lake dam soil (*Table 2*), and that of C was the lowest due to plowing. The M of C was the highest in May. M of L and C either increased significantly ($P < 0.05$) in July. The EC of W was lowest, and the EC of L and C showed a significant ($P < 0.05$) decrease in July. The pH for each soil type was higher than 7, and the pH of O was the highest. The pH of L increased significantly ($P < 0.05$) in July, and that for C decreased significantly ($P < 0.05$). Due to fertilization, the contents of soil nutrients (TOC, TN, TK, and so on) in C were significantly ($P < 0.05$) higher than those of W, L, and O. The changes in the contents of C and W soil nutrients were more significant in July than L and O.

Table 2. *Physicochemical properties of soil in Gudahu Wetland in Songnen Plain, China in May and July*

Index	May				July			
	O	L	C	W	O	L	C	W
BD (g/cm^3)	1.48±0.05 bB	1.87±0.07 aA	1.04±0.10 cC	1.38±0.03 bB	1.47±0.06 bB	1.93±0.05 aA	1.22±0.06 cC	1.41±0.05 bB
M (%)	13.09±1.53 bB	16.32±1.09 bB **	22.60±1.92 aA *	13.33±2.66 bB	16.50±1.95 bB	23.85±1.43 aA **	26.38±1.08 aA *	18.52±2.03 bB
EC (ms/cm)	3.43±0.79 bAB	4.61±0.86 abA *	5.28±0.33 aA **	1.77±0.56 cB	3.64±0.60 aA	2.21±0.50 bcAB *	3.15±0.68 abAB **	1.56±0.44 cB
pH	9.12±0.11 aA	8.14±0.10 bB *	8.00±0.15 bB *	8.15±0.06 bB	9.09±0.10 aA	8.48±0.13 bB *	7.69±0.11 cC *	8.39±0.15 bB
TOC (g/kg)	3.51±0.19 dD	7.78±0.65 cC	24.18±2.10 aA *	16.27±1.27 bB **	3.84±0.33 dC	7.37±0.34 cC	33.76±3.10 aA *	24.61±2.04 bB **
TN (g/kg)	0.68±0.02 cC **	1.17±0.02 bB **	2.24±0.15 aA **	1.06±0.05 bB **	1.02±0.06 cC **	0.89±0.03 dD **	3.16±0.04 aA **	2.68±0.05 bB **
AN (mg/kg)	18.53±1.55 dC **	38.33±7.07 cC	111.37±4.69 aA **	85.63±12.42 bB **	27.17±1.48 cC **	50.96±5.14 bB	133.83±4.71 aA **	124.17±7.68 aA **
TP (g/kg)	0.03±0.01 bB	0.04±0.01 bB	0.23±0.03 aA	0.05±0.01 bB	0.02±0.01 cB	0.05±0.01 bB	0.25±0.03 aA	0.06±0.01 bB
AP (mg/kg)	3.77±0.28 cBC **	2.87±0.48 cC	30.31±7.03 aA	13.33±1.86 bB	5.14±0.18 cC **	3.11±0.03 cC	42.08±3.91 aA	15.05±2.02 bB
TK (g/kg)	1.66±0.10 cC	1.88±0.13b BC	3.14±0.08 aA *	1.98±0.03 bB *	1.54±0.13 dC	1.91±0.14 cB	2.88±0.10 aA *	2.14±0.08 bB *
AK (mg/kg)	122.49±9.12 dC	143.20±8.36 cBC **	265.27±8.41 aA **	166.81±10.33 bB **	137.28±11.65 dD	233.35±20.08 cC **	327.72±14.29 aA **	274.55±12.28 bB **

Note: O (original meadow), L (lake dam), C (cropland), and W (woodland) in the table head were the four land-use patterns in Gudahu Wetland in Songnen Plain, China. BD, bulk density, M, moisture, EC, electrical conductivity, TOC, total organic carbon, TN, total N, AN, available N, TP, total P, AP, available P, TK, total K, AK, available K. Data represent means±standard deviation. The different lowercase letters represent significant differences ($P < 0.05$) and the different capital letters represent very significant differences ($P < 0.01$) between the sampling sites at the same sampling time using Duncan's multiple range test. T-test was used to evaluate the differences between different sampling times for the same sampling sites. * represents significant differences ($P < 0.05$) and ** represents significant differences ($P < 0.01$)

Sequencing of soil bacterial samples

At the 97% similarity level, most bacterial samples' rarefaction curve tended to be flat (*Fig. 1*). It indicated that increased sequencing depth did not increase the number of new OTUs. The OTU coverage of the bacterial sample was close to saturation, and it

http://www.aloki.hu ● ISSN 1589 1623 (Print) ● ISSN 1785 0037 (Online)
DOI: http://dx.doi.org/10.15666/aeer/1902_13371352
© 2021, ALÖKI Kft., Budapest, Hungary

could reflect the microbial community structure of the saline-alkaline soil samples. In general, the OTU numbers of O and L were lower than those of C and W in the dry season, but these OTU numbers gradually converged in the rainy season.

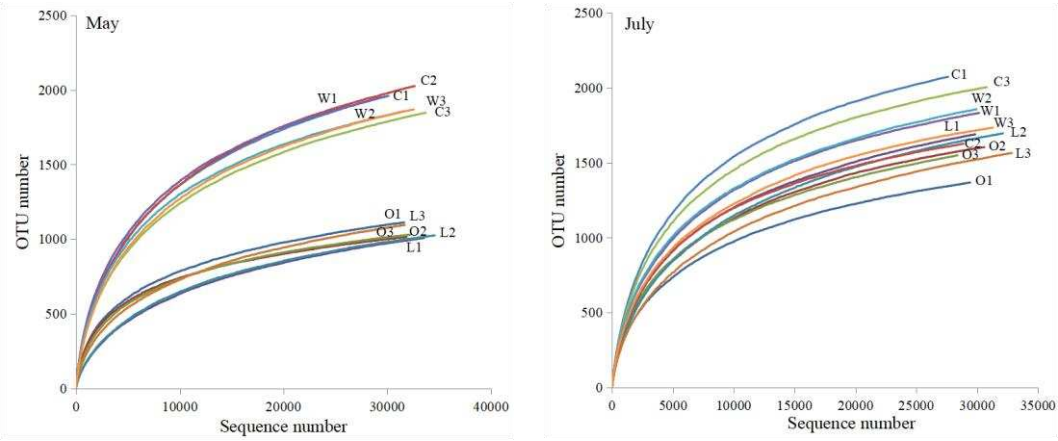


Figure 1. *Rarefaction curve of bacterial soil samples at the 97% similarity level. Note: O (original meadow), L (lake dam), C (cropland), and W (woodland) were the four land-use patterns in Gudahu Wetland in Songnen Plain, China*

A total of 3,847 and 4,148 OTUs were observed in May and July, respectively (*Fig. 2*). A total of 3,489 core OTUs were found in May and July, which accounted for 90.69% and 84.11% of the total number of OTUs in May and July, respectively. At the two sampling times, there were 494 core OTUs in May and 707 in July. The OTU number of C was higher, and O was smallest than other land-use patterns, but the number of unique OTUs of O was the highest of all the land-use patterns.

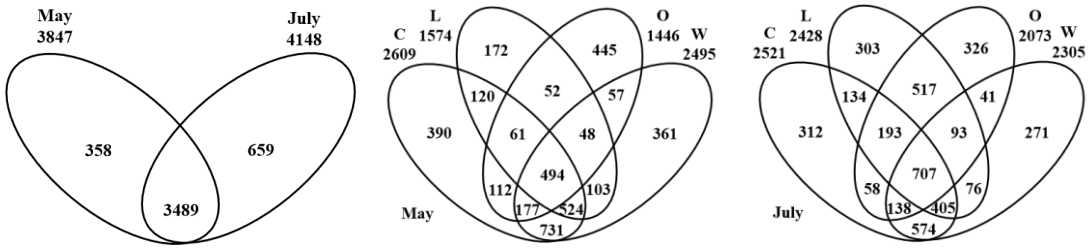


Figure 2. *Venn diagram of OTU numbers of bacterial soil samples at the 97% similarity level. Note: O (original meadow), L (lake dam), C (cropland), and W (woodland) were the four land-use patterns in Gudahu Wetland in Songnen Plain, China*

Soil bacterial community structure

As per the histogram representing the relative abundance of soil bacterial community compositions at the phyletic level (*Fig. 3*), 17 bacterial phyletic level groups (excluding groups with relative abundance < 0.5%) were observed in May. With the highest relative abundance, Proteobacteria (61.68% in L and 30.99% in C) was found to be the dominant soil bacterial group in May. The relative abundance of Acidobacteria in C was 18.28%, and the lowest was 2.90% in L. The relative abundance of Chlorofloxi in L was

http://www.aloki.hu ● ISSN 1589 1623 (Print) ● ISSN 1785 0037 (Online)
DOI: http://dx.doi.org/10.15666/aeer/1902_13371352
© 2021, ALÖKI Kft., Budapest, Hungary

20.01%, but only 4.93% in O, and the relative abundance of Gemmatimonadetes in O was 18.27%, lowest was 0.91% in L.

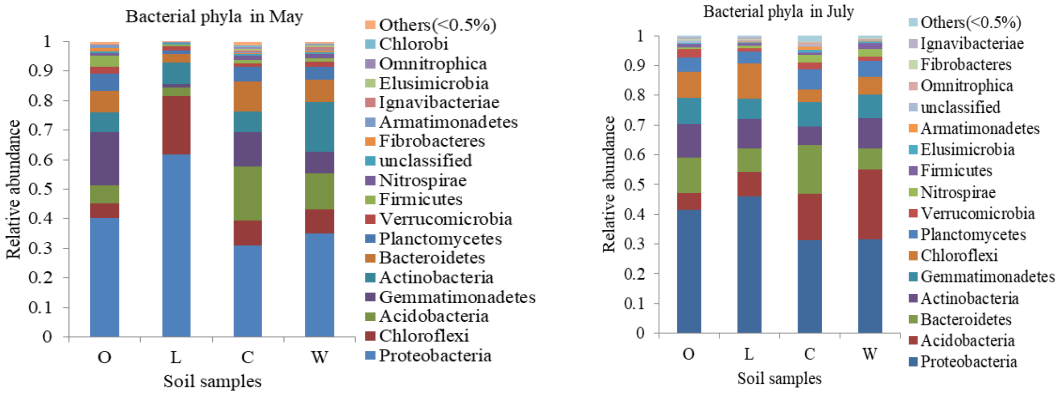


Figure 3. *Soil bacterial community compositions at the phyletic level. Note: O (original meadow), L (lake dam), C (cropland), and W (woodland) were the four land-use patterns in Gudahu Wetland in Songnen Plain, China*

A total of 16 phyletic level groups with relative abundance > 0.5% were observed in July. Proteobacteria was still the dominant group with a relative abundance of 45.86% in L and close to 31% in C and W (*Fig. 3*). The total relative abundance of Proteobacteria in July and May was not significantly ($P > 0.05$) different. The relative abundance of Acidobacteria in W was 23.51%, very significantly ($P < 0.01$) higher than May, however, it was only 5.7% in O. The relative abundance of Bacteroides in C was 16.41% and Actinobacteria in L, O, and W was around 10%. In general, the top ten phyla with higher relative abundance in different seasons were the same, although the relative abundance was different.

A total of 21 and 36 generic level groups of soil bacteria (except those with relative abundance < 0.5%) were observed in May and July, respectively, and a large number of unclassified groups were also observed (*Fig. 4*). In May, the number of unclassified genera in C reached 71.03% and >50% in each soil type in July.

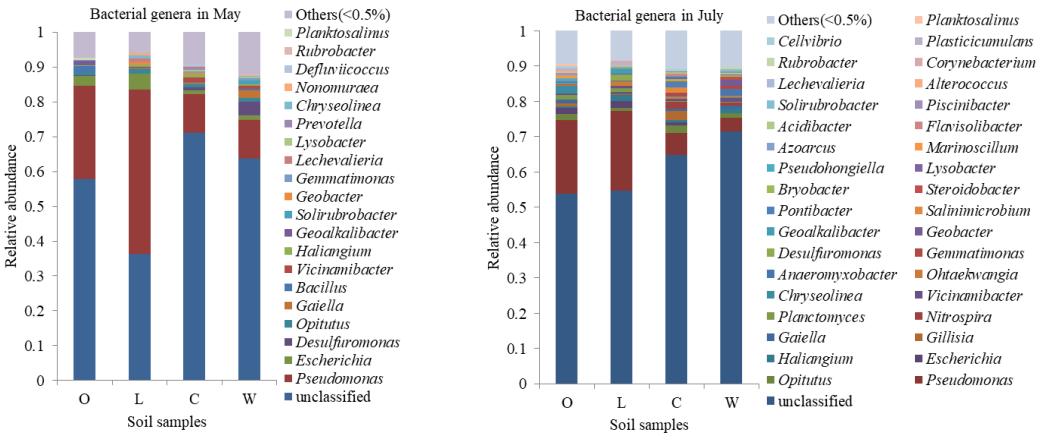


Figure 4. *Soil bacterial community compositions at the generic level. Note: O (original meadow), L (lake dam), C (cropland), and W (woodland) were the four land-use patterns in Gudahu Wetland in Songnen Plain, China*

http://www.aloki.hu ● ISSN 1589 1623 (Print) ● ISSN 1785 0037 (Online)
DOI: http://dx.doi.org/10.15666/aeer/1902_13371352
© 2021, ALÖKI Kft., Budapest, Hungary

In May, *Pseudomonas* (47.43% in L) belonging to Proteobacteria showed the highest relative abundance, followed by *Escherichia* (4.40% in L), *Desulfuromonas* (3.92% in W), and *Opitutus* (1.36% in L). The relative abundance of *Geoalkalibacter* was 1.42% in O, but < 0.1% in the other land-use patterns and *Planktosalinus* were found only in O (0.58%).

In July also, *Pseudomonas* showed the highest relative abundance (22.54% in L and 20.98% in O), followed by *Opitutus* (2.04% in C), *Escherichia* (1.20% in L), and *Haliangium* (1.70% in L). The relative abundance of *Geoalkalibacter* was 1.39% in L, and *Planktosalinus* in O was more than 0.5%, both of which were very low or absent in other soil types.

Soil bacterial community diversity

The bacterial community richness of O and L, and the diversity of L in May were lower than that in July (*Table 3*). It suggested that the bacterial community of O and L were more sensitive to seasonal changes. In May, the richness of O and L was very significantly ($P < 0.01$) lower than that of C and W, however, in July, this difference was not very significant ($0.01 < P < 0.05$). In both seasons, the bacterial community diversity of L was the lowest, followed by O, while that of C and W was higher.

Table 3. *Bacterial community richness and diversity indexes of soil in Gudahu Wetland in Songnen Plain, China in May and July*

Type	Chao1 index		Shannon index	
	May	July	May	July
O	1334.33±107.93 bB **	1879.53±139.26 bA **	4.541±0.413 bB	5.268±0.346 bAB
L	1367.91±78.86 bB **	2071.02±54.24 abA **	3.357±0.660 cC *	5.158±0.400 bB *
C	2407.73±101.63 aA	2272.04±268.88 aA	5.786±0.110 aA	6.084±0.310 aA
W	2349.85±110.11 aA	2198.30±108.81 abA	5.801±0.301 aA	6.032±0.091 aAB

Note: O (original meadow), L (lake dam), C (cropland), and W (woodland) in the table first column are the four land-use patterns in Gudahu Wetland in Songnen Plain, China. Data represent means±standard deviation. The different lowercase letters represent significant differences ($P < 0.05$) and the different capital letters represent very significant differences ($P < 0.01$) between the sampling sites at the same sampling time using Duncan's multiple range test. T-test was used to evaluate the differences between different sampling times for the same sampling sites. * represents significant differences ($P < 0.05$) and ** represents significant differences ($P < 0.01$)

Similarity analysis of bacterial community

Based on the unweighted UniFrac algorithm, the bacterial community similarity of the four soil types in different seasons was determined at the OTU level. Out of the four land-use patterns, O was the first to be separated, which indicated that O was quite different from the others in terms of bacterial species composition (*Fig. 5*). Subsequently, L was separated, while C and W were the closest in bacterial species composition. It indicated that the bacterial community similarity of C and W was different from that of O, besides, different land-use patterns in Gudahu Wetland altered the original bacterial community structure of the original meadow soil.

http://www.aloki.hu ● ISSN 1589 1623 (Print) ● ISSN 1785 0037 (Online)
DOI: http://dx.doi.org/10.15666/aeer/1902_13371352
© 2021, ALÖKI Kft., Budapest, Hungary

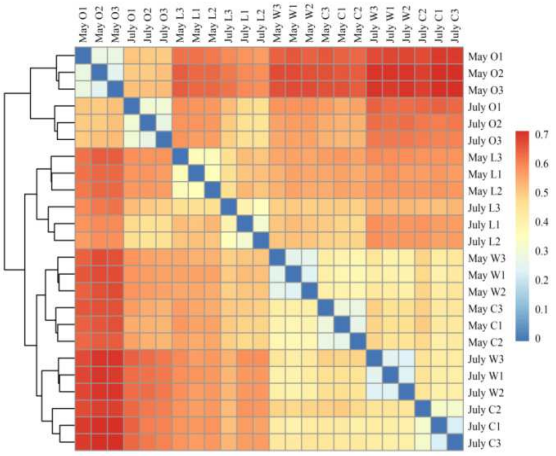


Figure 5. *Heatmap of soil bacterial community similarity analysis based on the unweighted Unifrac algorithm. Note: O (original meadow), L (lake dam), C (cropland), and W (woodland) were the four land-use patterns in Gudahu Wetland in Songnen Plain, China. Three soil samples were collected from each of these land-use patterns. The dark blue color indicates the small differences, while the deep red color indicates the low similarity*

Correlation between bacterial community and soil's physicochemical properties

The RDA results were depicted in *Fig. 6*. The distance between C, W, and O on the first ordination axis was relatively low; however, L was separated from the other land-use patterns in May. C and W were close on the second ordination axis and were separated from O. It indicated that the soil bacterial community of C and W was identical at the phyletic level, but remarkably different from O and L. In July, the four soil types were divided on the first two ordination axes, indicating the four soil types were different in the bacterial communities at the phyletic level.

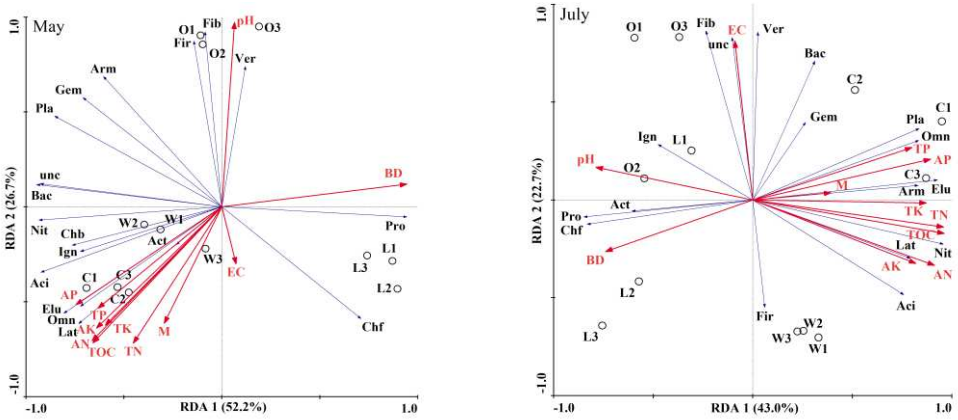


Figure 6. *Redundancy analysis of bacterial communities (phyletic level) and soil's physiochemical properties. Note: O (original meadow), L (lake dam), C (cropland), and W (woodland) were the four land-use patterns in Gudahu Wetland in Songnen Plain, China. Three soil samples were collected from each of these land-use patterns. The abbreviation of bacterial phylum in this figure is the first three letters of Latin name in Figure 3, where Chf is Chlorofloxi, Chb is Chlorobi, and unc is unclassified. BD, bulk density, M, moisture, EC, electrical conductivity, TOC, total organic carbon, TN, total N, AN, available N, TP, total P, AP, available P, TK, total K, AK, available K*

http://www.aloki.hu ● ISSN 1589 1623 (Print) ● ISSN 1785 0037 (Online)
DOI: http://dx.doi.org/10.15666/aeer/1902_13371352
© 2021, ALÖKI Kft., Budapest, Hungary

At the phyletic level of bacteria, BD and pH were very significantly ($P < 0.01$) correlated to bacterial communities in May. A high correlation was observed between BD and L, pH and O. In July, BD, pH, and EC were very significantly ($P < 0.01$) correlated to bacterial communities. BD and pH had higher correlations with O and L. Besides, EC was found to be correlated with O. In general, BD, EC and pH showed a higher impact on the bacterial communities of O and L, while soil nutrients (TOC, TN, AK, and so on) and M showed a higher impact on C and W, but the impact was not statistically significant.

BD was negatively correlated with most bacterial phyla (*Fig. 6*). When integrated with Pearson correlation analysis outcomes between dominant phyla and soil's physicochemical properties (*Table 4*), BD showed a significant ($P < 0.05$) or very significant ($P < 0.01$) impact on phyla, such as Proteobacteria, Chlorofloxi. However, its impact differed with seasons. M and EC showed no significant ($P > 0.05$) effect on the dominant phyla except for Actinobacteria. However, pH showed a significant ($P < 0.05$) positive correlation with Gemmatimonades and Actinobacteria in different seasons. Except for Gemmatimonades, soil nutrients significantly ($P < 0.05$) affected bacterial phyla, such as Acidobacteria and Bacteroidetes (positive), or Chlorofloxi and Proteobacteria (negative). Out of the eleven soil physicochemical indexes analyzed in this study, soil nutrients remarkably impacted most of the bacterial phyla, especially on the rainy season, it showed the extensive impact. In contrast, BD, M, EC and pH primarily impacted individual dominant phylum to a different extent.

Table 4. *Pearson correlation analysis between soil's physicochemical properties and top six soil bacterial phyla in Gudahu Wetland in Songnen Plain, China*

Season	Phylum	BD	M	EC	pH	TOC	TN	AN	TP	AP	TK	AK
May	Proteobacteria	0.854**	-	+	-	-	-	-	-	-0.602*	-	-
	Chlorofloxi	0.648*	+	+	-	-	+	-	-	-	-	-
	Acidobacteria	-0.928**	+	+	-	0.867**	0.728**	0.870**	0.840**	0.924**	0.830**	0.867**
	Gemmatimonades	-	+	+	0.662*	-	-	-	+	+	+	+
	Actinobacteria	-	-	-0.700*	-	+	-	+	-	+	-	-
	Bacteroidetes	-0.920**	+	+	+	+	+	+	0.661*	0.734**	0.597*	0.617*
July	Proteobacteria	0.673*	-	+	+	-0.751**	-0.817**	-0.741**	-	-0.652*	-	-
	Acidobacteria	-	+	-	-	0.738**	0.757**	0.821**	+	+	+	0.644*
	Bacteroidetes	-	+	+	-	+	+	+	0.667*	0.627*	+	+
	Actinobacteria	-	-0.641*	-	0.641*	-0.627*	-	-	-0.724**	-0.685*	-0.661*	-0.613*
	Gemmatimonades	-	-	+	+	+	+	+	+	+	+	-
	Chlorofloxi	0.822**	-	-	+	-0.748**	-0.829**	-0.721**	-0.625*	-0.765**	-0.654*	-

Note: BD, bulk density, M, moisture, EC, electrical conductivity, TOC, total organic carbon, TN, total N, AN, available N, TP, total P, AP, available P, TK, total K, AK, available K. The data in the table are correlation coefficients. * represents significant correlation ($P < 0.05$); ** represents very significant correlation ($P < 0.01$); + represents positive correlation and - represents negative correlation

Discussion

Characteristics of soil bacterial community structure of Gudahu Wetland

In this study, although the relative abundance of bacteria altered with seasons, Proteobacteria, Chlorofloxi, and Acidobacteria were highly dominant in the saline-alkaline soil bacterial communities in the soil samples from Gudahu Wetland. These

http://www.aloki.hu ● ISSN 1589 1623 (Print) ● ISSN 1785 0037 (Online)
DOI: http://dx.doi.org/10.15666/aeer/1902_13371352
© 2021, ALÖKI Kft., Budapest, Hungary

results were in line with Ma and Gong's (2013) study, except for the relative abundance of Firmicutes, which was relatively low. Proteobacteria have high adaptability and widely distributed across different environments. Besides, Proteobacteria play a crucial role in the ecosystem (Su et al., 2006; Zhao et al., 2018; Shao et al., 2019; Wang et al., 2020). In Gudahu Wetland's saline-alkaline soil, Proteobacteria showed the highest relative abundance in different seasons, demonstrating its high adaptability. Chlorofloxi is found in seafloor sediments, temperate grasslands, and alpine meadows (Krzmarzick et al., 2012). Hug et al. (2013) reported that Chloroflexi was the most abundant and highly diverse in the aquifer sediments. In this study, the relative abundance of Chlorofloxi in L was relatively high, which might be related to the excavation of soil from the lake during the dam construction. Acidobacteria, commonly occurring phylum in the natural environment (Dedysh and Damsté, 2018), is actively involved in the degradation of plant cellulose and other macromolecular polymers. However, species occurring in this phylum are difficult to culture (Wei et al., 2018). In this study, Acidobacteria in C and W showed high relative abundance, which might be correlated to the accumulation of a high amount of cellulose in plant litter, such as straw and leaves.

As per a previous study, many unclassified genera are present in saline-alkaline wetland soil (Liu et al., 2016). Similar observations were made in this study as well. It indicated that saline-alkaline wetland soil could be a potential source of novel species. Besides, *Pseudomonas*, which is a widely occurring bacteria in soil and actively involved in removing environmental pollutants (Kimura et al., 2018; Wang et al., 2019), showed the higheat relative abundance in this study. *Geoalkalibacter* were isolated from soda lakes and were identified as a potential alkaliphilic representative (Zavarzina et al., 2006). In this study, *Geoalkalibacter* were found in O and L of Gudahu Wetland. *Planktosalinus* of Bacteroidetes were found in Xiaochaidan salt lake in Qaidam Basin in China (Zhong et al., 2016), which could also be considered a representative group of O in Gudahu Wetland. *Planktosalinus* showed a relative abundance of 0.5% in O.

Factors impacting the bacterial communities of Gudahu Wetland soil

Soil microbial community structure and diversity exhibit seasonal variations (Zhao et al., 2018; Yang et al., 2020). Zhang and Feng (2008) proposed that the number of saline-alkaline soil microbiota in Songnen Plain increased with increasing temperature. In this study, the total OTU numbers of the four soil types in May were lower than those in July. The bacterial community richness of O and L, and the diversity of L increased significantly, with the changes in season, however, C and W did not show any significant changes. It showed that altered soil bacterial communities of O and L were remarkably affected by seasonal changes.

The land-use pattern is crucial factor in determining the microbial community composition of wetland soil (Pei et al., 2009; Chi et al., 2018). Apart from O, human disturbances affected L, C, and W soil types in Gudahu Wetland differently in different periods. Cultivation and fertilization had remarkable effects on C. When soil nutrient content was high, the bacterial OTU number was the highest, and the richness and diversity of the bacterial community were relatively higher. Besides, afforestation improves microbial diversity (Qin et al., 2017). In this study, the bacterial community of W was similar to that of C but more diverse than O and L.

Saline-alkaline soil is generally afflicted with degradation, and plant diversity associated with different land-use patterns substantially affects the degradation process

http://www.aloki.hu ● ISSN 1589 1623 (Print) ● ISSN 1785 0037 (Online)
DOI: http://dx.doi.org/10.15666/aeer/1902_13371352
© 2021, ALÖKI Kft., Budapest, Hungary

of soil (Peng et al., 2017). In C, cultivation and fertilization increased the nutrient content, but reduced plant diversity, also, afforestation increased plant diversity and soil fertility, but dam construction reduced soil fertility and altered soil texture. O had the lowest bacterial OTUs, and the highest number of unique OTUs, besides, its bacterial community was significantly different from the other three soil types. It showed that artificial disturbance, dam construction, cultivation, and afforestation altered the original meadow's soil bacterial community in Gudahu Wetland.

The physicochemical properties of saline-alkaline wetland soil affected soil microbial composition and diversity (Niu et al., 2017). In this study, BD, M, EC and pH had significant effects on individual dominant bacterial phyla. Soil pH significantly impacts the diversity of soil microbial communities (Shen et al., 2013; Li et al., 2018c; Fan and Wu, 2020). High pH generally decreases the diversity of soil microbial communities (Zhang and Feng, 2008; Chu et al., 2017). Wang et al. (2020) reported that soil EC is a key factor that drives the composition of the bacterial community under alkaline conditions in the saline-alkaline soil of Songnen Plain. This study also showed that pH and EC significantly affected bacterial communities, especially in O and L. At the phyletic level, pH significantly affected Gemmatimonadetes and Actinobacteria, while EC significantly affected only Actinobacteria, in contrast, to the previous study by Canfora et al. (2014). The influence of soil moisture on microorganisms was also very significant. Soil moisture can regulate the soil's oxygen content, and regulate the type, activity, and growth of microbes in the soil. Furthermore, excessively high or low water content found to be detrimental for bacterial growth (Yan et al., 2015; Zhang et al., 2016; Zou et al., 2018). However, in this study, the Gudahu Wetland soil had a low M with no significant seasonal changes. Besides, no significant differences were observed between O and W. Apart from Actinobacteria, M had no significant impact on the bacterial community at the phyletic level. Soil nutrients showed significant effects on bacterial communities (Hansel et al., 2008). In this study, soil nutrients affected multiple bacterial phyla, especially in the rainy season, but the impact was not significant as that of BD, pH, and EC. Li et al. (2018b) showed that the relative abundance of Actinobacteria was negatively correlated to AP and AK, and the impact was significant in July, in line with the outcomes of this study. Concurrently, Li et al. (2018b) showed that AN and AP did not significantly affect Proteobacteria, whereas AK significantly influenced Chlorofloxi, not in line with the current study.

Suggestions for rational land-use

Saline-alkaline soil is ecologically fragile and prone to further degradation (Zhang and Feng, 2008). Vegetation restoration can not only improve the quality of saline-alkaline soil (Ravindran et al., 2007), but also improve the degraded wetland soil environment and improve the diversity of plants and soil microbes (Shao et al., 2019). In the process of returning farmland to wetland around Gudahu Wetland, we should not only consider the physicochemical properties of the soil, but also refer to the differences in soil microbial community structure, which has an important significance in guiding the choice of the plants used to return farmland to wetland. This study on the structure and diversity of soil bacterial communities of four land-use patterns showed that the bacterial community of C was similar to that of W, but different from that of O. Afforestation improves soil microbial diversity and soil fertility (Kaiser et al., 2016; Qin et al., 2017; Yang et al., 2019), and restore saline-alkaline soil ecology (Zhang et al., 2005). Thus, to protect the biodiversity of wetland and return farmland to wetland

http://www.aloki.hu ● ISSN 1589 1623 (Print) ● ISSN 1785 0037 (Online)
DOI: http://dx.doi.org/10.15666/aeer/1902_13371352
© 2021, ALÖKI Kft., Budapest, Hungary

effectively, we suggest that trees should be planted in the cropland and lake dam, to increase the woodland area. It will prevent the gradual degradation of the saline-alkaline soil, and enhance the ecological and economic benefits.

Conclusion

Proteobacteria was the dominant bacterial phylum of Gudahu saline-alkaline wetland soil in the dry and rainy seasons. Numerous unclassified genera were observed in the soil samples of Gudahu Wetland, which indicates that it is a potential source for new bacterial species. The bacterial community diversity of cropland and woodland was higher than the original meadow, the lowest diversity found in the lake dam soil. Dam construction, agriculture and forestry changed the structure and diversity of the original meadow's soil bacterial community, and agriculture and forestry had a more significant influence than dam construction. BD, EC and pH had significant effects on the soil bacterial community, especially that of the original meadow and lake dam. Soil nutrients (TOC, TN, AK, and so on) and M had no significant effect on the soil bacterial community, particularly in cropland and woodland. BD, M, EC and pH showed significant effects on individual dominant phyla, whereas soil nutrients had more extensive effects on dominant phyla. Different land-use patterns altered the physicochemical properties of saline-alkaline soil and affected the soil bacterial community's structure and diversity. Based on the outcomes of the current study, we suggest that afforestation of cropland and lake dam areas can effectively return farmland to wetland in Gudahu Wetland and prevent the degradation of the saline-alkaline soil of Songnen Plain. Our future studies will focus on microbial function in saline-alkaline soil, to improve the microbial application to prevent and control soil degradation in the saline-alkaline wetland.

Acknowledgements. This work was funded by Teaching Reform Project of Higher Education in Heilongjiang Province [SJGZ20190034], Heilongjiang Province Key Laboratory of Cold Region Wetland Ecology and Environment Research Laboratory Open Project [201905], Heilongjiang Province Key Laboratory of Cold Region Wetland Ecology and Environment Research Laboratory Open Project [201906], National Natural Science Foundation of China [41977095] and China-Norway International Collaboration Project “Sinagrain Ⅱ” [CHN-17/0019].

REFERENCES

[1] Bao, S. (2007): Soil Agro-chemistrical Analysis, 3rd ed. – China Agriculture Press, Beijing.
[2] Bian, J., Tang, J., Lin, N. (2008): Relationship between saline-alkali soil formation and neotectonic movement in Songnen Plain, China. – Environmental Geology (Berlin) 55(7): 1421-1429.
[3] Canfora, L., Bacci, G., Pinzari, F., Papa, G. L., Dazzi, C., Benedetti, A. (2014): Salinity and bacterial diversity: to what extent does the concentration of salt affect the bacterial community in a saline soil? – Plos One 9(9): 1-15.
[4] Caporaso, J. G., Kuczynski, J., Stombaugh, J., Bittinger, K., Bushman, F. D., Costello, E. K., Fierer, N., Peña, A. G., Goodrich, J. K., Gordon, J. I., Huttley, G. A., Kelley, S. T., Knights, D., Koenig, J. E., Ley, R. E., Lozupone, C. A., McDonald, D., Muegge, B. D., Pirrung, M., Reeder, J., Sevinsky, J. R., Turnbaugh, P. J., Walters, W. A., Widmann, J., Yatsunenko, T., Zaneveld, J., Knight, R. (2010): QIIME allows analysis of high-throughput community sequencing data. – Nature Methods 7(5): 335-336.

http://www.aloki.hu ● ISSN 1589 1623 (Print) ● ISSN 1785 0037 (Online)
DOI: http://dx.doi.org/10.15666/aeer/1902_13371352
© 2021, ALÖKI Kft., Budapest, Hungary

[5] Chen, H. (2018): Generate high-resolution Venn and Euler plots. – URL https://CRAN.R-project.org/package=VennDiagram.
[6] Chi, Q., Wu, D., Wang, Y., Sun, G. (2018): Research on soil microbial community structure of different forest-wetland ecotones in Xiaoxing'an Mountain. – Forest Engineering 34(3): 6-13, 18.
[7] Chu, H., Wang, Y., Shi, Y., Lv, X., Zhu, Y., Han, X. (2017): Current status and development trend of soil microbial biogeography. – Bulletin of Chinese Academy Sciences 32(6): 585-592.
[8] Dedysh, S. N., Damsté, J. S. S. (2018): Acidobacteria. – John Wiley & Sons, Ltd., Hoboken.
[9] Deng, J., Zhu, W., Zhou, Y., Yin, Y., Bai, X., Zhang, H., Zhang, Y., Qin, S. (2018): Effects of different land use patterns on the soil microbial community diversity in montane region of eastern Liaoning Province, China. – Chinese Journal of Applied Ecology 29(7): 2269-2276.
[10] Edgar, R. C. (2013): UPARSE: highly accurate OTU sequences from microbial ampliconreads. – Nature Methods 10: 996-998.
[11] Fan, W., Wu, J. (2020): Short-term effects of returning granulated straw on soil microbial community and organic carbon fractions in dryland farming. – The Journal of Microbiology 58(8): 657-667.
[12] Foti, M., Sorokin, D. Y., Lomans, B., Mussman, M., Zacharova, E. E., Pimenov, N., Kuenen, J. G., Muyzr, G. (2007): Diversity, activity, and abundance of sulfate-reducing bacteria in saline and hypersaline soda lakes. – Applied & Environmental Microbiology 73(7): 2093-2100.
[13] Gandhi, J. K., Tatu, K., Kamboj, R. D. (2018): A review of studies on bacterial and fungal diversity in wetland ecosystems. – Research & Reviews: A Journal of Microbiology and Virology 8(1): 25-38.
[14] Griffiths, B. S., Laurent, P. (2013): Insights into the resistance and resilience of the soil microbial community. – FEMS Microbiology Reviews 37(2): 112-129.
[15] Hansel, C. M., Fendorf, S., Jardine, P. M., Francis, C. A. (2008): Changes in bacterial and archaeal community structure and functional diversity along a geochemically variable soil profile. – Applied and Environmental Microbiology 74(5): 1620-1633.
[16] Hug, L. A., Castelle, C. J., Wrighton, K. C., Thomsa, B. C., Sharon, I., Frischkorn, K. R., Williams, K. H., Trige, S. G., Banfied, J. F. (2013): Community genomic analyses constrain the distribution of metabolic traits across the Chloroflexi phylum and indicate roles in sediment carbon cycling. – Microbiome 1(1): 22.
[17] Jin, Y., Wu, Z., Tan, F., Zhang, Y. (2017): Study on functional diversity of soil microorganism in different mangrove plants based on Biolog-Eco Technology. – Ecology and Environmental Sciences 26(8): 1292-1300.
[18] Kaiser, K., Wemheuer, B., Korolkow, V., Wemheuer, F., Nacke, H., Schöning, I., Schrumpf, M., Daniel, R. (2016): Driving forces of soil bacterial community structure, diversity, and function in temperate grasslands and forests. – Scientific Reports 6(1): 33696.
[19] Kimura, N., Watanabe, T., Suenaga, H., Fujihara, H., Futagami, T., Goto, M., Hanada, S., Hirose, L. (2018): *Pseudomonas furukawaii* sp. nov. a polychlorinated biphenyl-degrading bacterium isolated from biphenyl-contaminated soil in Japan. – International Journal of Systematic and Evolutionary Microbiology 68(5): 1429-1435.
[20] Kolde, R. (2019): pheatmap: Pretty Heatmaps. – URL https://CRAN.R-project.org/package=pheatmap.
[21] Krzmarzick, M. J., Crary, B. B., Harding, J. J., Oyerinde, O. O., Leri, A. C., Myneni, S. C. B., Novak, P. J. (2012): Natural niche for organohalide - respiring Chloroflexi. – Applied & Environmental Microbiology 78(2): 393-401.
[22] Li, Y., Yang, X., Qin, L., Lv, G., He, X., Zhang, X. (2018a): The bacterial diversity and community structures in rhizosphere soil of two halophytes, *Lycium ruthenicum* and *Kalidium capsicum*. – Acta Ecologica Sinica 38(9): 3118-3131.

http://www.aloki.hu ● ISSN 1589 1623 (Print) ● ISSN 1785 0037 (Online)
DOI: http://dx.doi.org/10.15666/aeer/1902_13371352
© 2021, ALÖKI Kft., Budapest, Hungary

[23] Li, J., Hou, H., Wang, C., Zhang, S., Ma, J., Ding, Z., Huang, L., Dong, J., Yang, Y. (2018b): Soil bacteria diversity of reclaimed soil based on High Throughput Sequencing. – Environmental Science & Technology 41(12): 148-157.
[24] Li, S., Ma, D., Zang, S., Wang, L., Sun, H. (2018c): Structural and functional characteristics of soil microbial community in the Songjiang wetland under different interferences. – Acta Ecologica Sinica 38(22): 7979-7989.
[25] Liu, B., Yuan, J., Yiu, S., Li, Z., Xie, Y., Chen, Y., Shi, Y., Zhang, H., Li, Y., Lam, T., Luo, R. (2012): COPE: an accurate *k*-mer-based pair-end reads connection tool to facilitate genome assembly. – Bioinformatics 28(22): 2870-2874.
[26] Liu, W., Zhang, W., Liu, G., Zhang, Y., Zhang, G. (2016): Microbial diversity in the saline-alkali soil of a coastal *Tamarix chinensis* woodland at Bohai bay, China. – Journal of Arid Land 8(2): 284-292.
[27] Liu, F., Mo, X., Kong, W., Song, Y. (2020): Soil bacterial diversity, structure, and function of *Suaeda salsa* in rhizosphere and non-rhizosphere soils in various habitats in the Yellow River Delta, China. – Science of The Total Environment 740: 140144.
[28] Ma, B., Gong, J. (2013): A meta-analysis of the publicly available bacterial and archaeal sequence diversity in saline soils. – World Journal of Microbiology and Biotechnology 29(12): 2325-2334.
[29] Niu, S., Long, Y., Li, Y., Da, W., Hu, S., Li, W., Zhu, X., Kong, W. (2017): Microbial diversity in saline alkali soil from Hexi Corridor analyzed by Illumina MiSeq High-throughput Sequencing system. – Microbiology China 44(9): 2067-2078.
[30] Pei, X., Xu, Y., Wei, W. (2009): A Review on soil microorganisms in wetland ecosystem. – Wetland Science 7(2): 181-186.
[31] Peng, M., Jia, H., Wang, Q. (2017): The effect of land use on bacterial communities in saline-alkali soil. – Current Microbiology 74(3): 325-333.
[32] Qin, H., Li, C., Ren, Q. (2017): Effects of different land use patterns on soil bacterial and fungal biodiversity in the hydro-fluctuation zone of the Three Gorges Reservoir region. – Acta Ecologica Sinica 37(10): 3494-3504.
[33] R Core Team. (2017): R: A language and environment for statistical computing. – R Foundation for Statistical Computing, Vienna, Austria. URL http://www.R-project.org/.
[34] Ravindran, K. C., Venkatesan, K., Balakrishnan, V. (2007): Restoration of saline land by halophytes for Indian soils. – Soil Biology and Biochemistry 39(10): 2661-2664.
[35] Shang, Z., Gao, Q., Dong, M. (2003): Impacts of grazing on the alkalinized-salinized meadow steppe ecosystem in the Songnen Plain, China - a simulation study. – Plant and Soil 249(2): 237-251.
[36] Shao, Y., Cao, S., Liu, C., Luo, M. (2019): Bacterial diversity in soils of Nanniwan wetland based on high-through put sequencing. – Journal of Arid Land Resources and Environment 33(2): 158-163.
[37] Shen, C., Xiong, J., Zhang, H., Feng, Y., Lin, X., Li, X., Liang, W., Chu, H. (2013): Soil pH drives the spatial distribution of bacterial communities along elevation on Changbai Mountain. – Soil Biology & Biochemistry 57: 204-211.
[38] Su, Y., Li, H., Li, J., Yu, Y., Chen, B. (2006): Investigation on bacterial diversity of deep-sea sediments from Pacific Arctic. – Chinese High Technology Letters 16(7): 752-756.
[39] Wan, Z., Yu, S., Wang, H., Sun, G. (2003): The types and characteristics of inland saline-alkaline wetland in Songnen Plain. – Wetland Science 1(2): 141-146.
[40] Wang, L., Seki, K., Miyazaki, T., Ishihama, Y. (2009): The causes of soil alkalinization in the Songnen Plain of Northeast China. – Paddy and Water Environment 7(3): 259-270.
[41] Wang, M., Wang, Z., Yu, L., Zhang, C., Bi, J., Sun, J. (2019): *Pseudomonas qingdaonensis* sp. nov., an aflatoxin-degrading bacterium, isolated from peanut rhizospheric soil. – Archives of Microbiology 201(5): 673-678.
[42] Wang, S., Sun, L., Ling, N., Zhu, C., Chi, F., Li, W., Hao, X., Zhang, W., Bian, J., Chen, L., Wei, D. (2020): Exploring soil factors determining composition and structure of the

http://www.aloki.hu ● ISSN 1589 1623 (Print) ● ISSN 1785 0037 (Online)
DOI: http://dx.doi.org/10.15666/aeer/1902_13371352
© 2021, ALÖKI Kft., Budapest, Hungary

bacterial communities in saline-alkali soils of Songnen Plain. – Frontiers in Microbiology 10: 2902.

[43] Wei, Z., Li, Y., Jiang, W., Liao, X. (2018): Diversity of Acidobacteria in rhizosphere soils of common trees in Wuxi. – Chinese Journal of Ecology 37(9): 2649-2656.

[44] Wu, Z., Raven, P. H., Hong, D. (2013): Flora of China. – Science Press, Beijing.

[45] Yan, N., Marschner, P., Cao, W., Zuo, C., Qin, W. (2015): Influence of salinity and water content on soil microorganisms. – International Soil and Water Conservation Research 3(4): 316-323.

[46] Yang, W., Ren, Q., Li, C., Song, H., Yuan, Z., Ma, W., Cui, Y., Wang, C. (2019): Dynamic changes in soil microbial biomass carbon, nitrogen and phosphorus of *Taxodium distichum* and *Salix matsudana* plantation in the hydro-fluctuation belt of the Three Gorges Reservoir Region. – Acta Ecologica Sinica 39(5): 1496-1506.

[47] Yang, Z., Wang, Y., Wu, Z., Ren, L., Ma, Y. (2020): Microbial community structure and seasonal variations in mudflat sediments of Sansha Bay, China. – Applied Ecology and Environmental Research 18(1): 987-1000.

[48] Yu, S., Shi, C., Hu, B., Ding, J., Meng, B., Yang, C. (2020): Analysis of microbial community structure and diversity of saline soil in Gudahu Wetland. – Acta Ecologica Sinica 40(11): 3764-3775.

[49] Zak, D. R., Holmes, W. E., White, D. C., Peacock, A. D., Tilman, D. (2003): Plant diversity, soil microbial communities, and ecosystem function: are there any links? – Ecology 84(8): 2042-2050.

[50] Zavarzina, D. G., Kolganova, T. V., Boulygina, E. S., Kostrikina, N. A., Tourova, T. P., Zavarzin, G. A. (2006): *Geoalkalibacter ferrihydriticus* gen. nov. sp. nov. the first alkaliphilic representative of the family *Geobacteraceae*, isolated from a soda lake. – Microbiology 75(6): 673-682.

[51] Zhang, J., Zhang, X., Zhou, J., Liu, G., Li, D. (2005): World resources of saline soil and main amelioration measures. – Research of Soil and Water Conservation 12(6): 28-31.

[52] Zhang, W., Feng, Y. (2008): Distribution of soil microorganism and their relations with soil factors of saline-alkaline grasslands in Songnen Plain. – Grassland and Turf 3: 7-11.

[53] Zhang, Q., Huang, X., Guo, X. (2016): Analysis of the characteristics of rhizosphere bacterial diversity from plants with different water level gradients based on T-RFLP. – Acta Ecologica Sinica 36(14): 4518-4530.

[54] Zhang, Q., Wakelin, S. A., Liang, Y., Chu, G. (2018): Soil microbial activity and community structure as affected by exposure to chloride and chloride-sulfate salts. – Journal of Arid Land 10(5): 737-749.

[55] Zhao, C., Xie, H., Xu, J., Xu, X., Zhang, J., Hu, Z., Liu, C., Liang, S., Wang, Q., Wang, J. (2015): Bacterial community variation and microbial mechanism of triclosan (tcs) removal by constructed wetlands with different types of plants. – Science of The Total Environment 505: 633-639.

[56] Zhao, M., Yin, C., Li, C., Zhong, S., Yu, K., Fang, S. (2018): Using Miseq sequencing to analyze seasonal soil microbial community dynamics in reclaimed *Scirpus mariqueter* coastal wetlands. – Journal of Shanghai Ocean University 27(5): 718-727.

[57] Zhong, Z., Liu, Y., Wang, F., Zhou, Y., Liu, H., Liu, Q., Liu, Z. (2016): *Planktosalinus lacus* gen. nov., sp. nov., a member of the family Flavobacteriaceae isolated from a salt lake. – International Journal of Systematic and Evolutionary Microbiology 66(5): 2084-2089.

[58] Zhou, D., Li, Q., Song, Y., Wang, X. (2011): Salinizaion-alkalization of *Leymus chinensis* glassland in Songnen Plain of Northeast China. – Chinese Journal of Applied Ecology 22: 1423-1430.

[59] Zou, F., Wu, X., Zhang, W., Ma, Y., Liu, Y., Wu, L. (2018): Responses of soil microbial functional traits to seasonal water level changes in a typical wetland of the Poyang Lake. – Acta Ecologica Sinica 38(11): 3838-3847.

http://www.aloki.hu ● ISSN 1589 1623 (Print) ● ISSN 1785 0037 (Online)
DOI: http://dx.doi.org/10.15666/aeer/1902_13371352
© 2021, ALÖKI Kft., Budapest, Hungary

POST-SPILL ECOLOGICAL HEALTH ASSESSMENT AT THE SOUTHERN COAST OF MACTAN ISLAND, PHILIPPINES USING MULTIMETRIC PHYTOPLANKTON INDEX FOR BIOTIC INTEGRITY

EDULLANTES, B.* – SAÑOZA, W. – VARGAS, C. – SANGUTAN, S. – POCONG, M. – SILAPAN, J.

Department of Biology and Environmental Science, College of Science, University of the Philippines Cebu, Lahug, Cebu City, Cebu 6000, Philippines

**Corresponding author*
e-mail: bedullantes@up.edu.ph; phone: +63-32-233-398

(Received 9th Nov 2020; accepted 8th Feb 2021)

Abstract. Evaluation of ecological health status after an oil spill is crucial for effective restoration measures of the affected aquatic ecosystems. In this study, we applied a multimetric phytoplankton index for biotic integrity (MPI-BI) to assess the ecological health status of the southern coast of Mactan Island, Philippines after 8, 12, 24, and 30 months from the MV Thomas Aquinas spill incident in August 2013. Phytoplankton community analysis revealed (1) no difference in abundance, richness, and diversity between affected and reference sites, (2) increasing trend of diversity over time after the spill, and (3) higher remotely-sensed chlorophyll *a* level in affected sites. Phytoplankton relative abundance, diversity, and trophic state were used to derive MPI-BI. Based on MPI-BI, the health status of the affected sites was generally in good condition 8 – 30 months after. A time-series analysis of remotely-sensed and meteorological parameters showed no difference between pre and post spill conditions, except for chlorophyll *a* and particulate organic carbon. Generally, the health status of the coastal water may be affected by the oil spillage as indicated by the increased trophic state after the spill but may be recovering from the oil spill stress.
Keywords: *phytoplankton community, bioindicator, oil spill impact, multivariate analysis, remote sensing application*

Introduction

Discharge of oils into marine ecosystems due to accidental spillage has been a major environmental issue for several decades and a major contributor to the instability of the marine ecosystem worldwide (Farrington, 2013). Oil spill events disturb the complex ecological interactions that subsequently decrease the integrity of water quality to support aquatic life (Farrington, 2014). Similar to any other anthropogenic perturbations, these incidents also degrade the sustainable human use of the coastal ecosystems resulting in the economic loss (García Pérez, 2003; Surís-Regueiro et al., 2007). It is, therefore, crucial to assess the ecological health status of aquatic ecosystems after an oil spill to provide information for effective restoration measures (IMO/UNEP, 2009). Biological indicators have been used as the main tool for ecological health assessment after the spill (e.g. Gesteira and Dauvin, 2000; Bolognesi et al., 2006). These are quantifiable biological features that are sensitive to environmental perturbation. Most assessments are often concentrated on oil spill impacts in the coastal, mangrove, and sublittoral areas where the effect is very much noticeable as compared to the pelagic and planktonic organisms (Parsons et al., 2015).

Phytoplankton is a diverse group of microscopic, single-celled organisms that are ubiquitous in aquatic environments (Reynolds, 2006). Their ecological role of providing energy to the next trophic level (Falkowski, 2012) may be disrupted when a high level

http://www.aloki.hu ● ISSN 1589 1623 (Print) ● ISSN 1785 0037 (Online)
DOI: http://dx.doi.org/10.15666/aeer/1902_13531370
© 2021, ALÖKI Kft., Budapest, Hungary

of spilled oil floats at the upper layer of the water column (Gin et al., 2001). The presence of oil can cause a fairly rapid and marked reduction in the abundance of certain species, and possibly a proliferation of other species (Hallare et al., 2011; Ozhan et al., 2014). The sensitivity of phytoplankton to anthropogenic pressures makes them a reliable biological indicator of the ecological health status of an aquatic environment (Verlecar et al., 2006). Phytoplankton diversity indices and the other single biotic index methods have been used to assess aquatic ecological health status (El-Sheekh et al., 2000; Suderman and Thistle, 2004; Hallare et al., 2011). Although these methods are easier and faster to perform, they are incomprehensive and incomplete because they reflect limited information of environmental changes (Teng et al., 2014). The ecological health status entails pressure-independent assessment and can be attained by using pressure-specific multimetric indices (Barbour et al., 2000). The multimetric approach typically involves two phases: (1) development phase where metrics are selected, calibrated and aggregate into an index, and (2) evaluation phase where the index is used to assesses ecological condition at sites and evaluate impairment (Barbour et al., 2000). This approach can be used to determine the ecological health status of coastal waters that are exposed to anthropogenic perturbations like oil spills.

Chlorophyll *a* is a vital component of phytoplankton primary production and is often used as a measure to indirectly estimate the biomass. Measurement of the chlorophyll *a* concentration (*Chl a*) is also important monitoring the phytoplankton distribution in seawater surface to understand wide-scoped biological processes. Large-scale observations of *Chl a* can be conducted in near real-time by satellite remote sensing compared to laboratory analysis and traditional ship surveys that are limited to small spatiotemporal coverage and are time-consuming (Behrenfeld and Falkowski, 1997). Satellite remote sensing has been used in a recent study to evaluate whether the *Chl a* was affected by the Deepwater Horizon oil spill in the northern Gulf of Mexico over a multi-year time period (Li et al., 2019).

The collision between MV St. Thomas Aquinas and MV Sulpicio Express Siete in August 2013 discharged 20,000 liters of diesel, 120,000 liters of bunker or crude oil, and 20,000 liters of lube oil into the coastal waters in Talisay, Cebu, Philippines. The leaked oil was carried by the southwest monsoon winds to the coastal areas in the southern part of Mactan Island. This contaminated the fishing grounds, aquaculture ponds, and beaches of the affected areas. Previous studies have documented the impact of this oil spill on mangrove communities (Sadaba and Niego, 2016), bacterial composition (Bensig et al., 2014), and zooplankton abundance (Flores et al., 2020). No studies have been published yet that assess the phytoplankton communities after the oil spill incident.

This study aimed to assess the ecological health status of the southern coastal waters of Mactan Island after the MV Thomas Aquinas oil spill incidence using a multimetric phytoplankton index. Working under the overall hypothesis that the ecological health status declines after the oil spill, we focused on answering three research questions: (1) How does the phytoplankton community structure in affected sites differ in a reference condition after the spill incident? (2) What is the post-spill health status in the affected sites based on the multimetric phytoplankton index for biotic integrity? (3) Does the oil spill cause the post-spill pattern of phytoplankton in the affected sites? In this paper, we described patterns of variation in phytoplankton community structure in the oil spill affected areas using multivariate analysis. The correlative trends were used to identify significant variables for the development of the multimetric phytoplankton index to

http://www.aloki.hu ● ISSN 1589 1623 (Print) ● ISSN 1785 0037 (Online)
DOI: http://dx.doi.org/10.15666/aeer/1902_13531370
© 2021, ALÖKI Kft., Budapest, Hungary

assess the affected sites' ecological health status after the spill. Finally, we analyzed available meteorological data and remotely sensed data to examine whether the pattern in the phytoplankton-based health status is caused by the oil spill or by natural variability caused by meteorological conditions.

Methodology

Study sites

Three sites off the coast of southern Mactan Island, Philippines were selected in terms of the extent of MV Thomas Aquinas oil spill impact (*Fig. 1*). These were the coastal areas in Alegria (S1; 10°14'56.43"N, 123°58'4.79"E), Calawisan (S2; 10°16'20.23"N, 123°55'2.90"E) and Day-as (S3; 10°15'17.23"N, 123°55'28.90"E), which were identified to have low, mid and high oil spill impact status, respectively (Bensig et al., 2014; Flores et al., 2020). The offshore water in Dalaguete was chosen as a reference site (Ref; 9°45'57.34"N, 123°33'2.60"E). Ref was not affected by the oil spill, and it has similar features with the affected sites in Mactan, i.e. presence of fringing mangroves and seagrass meadows. Ref is about 97 km away from the oil spill affected areas.

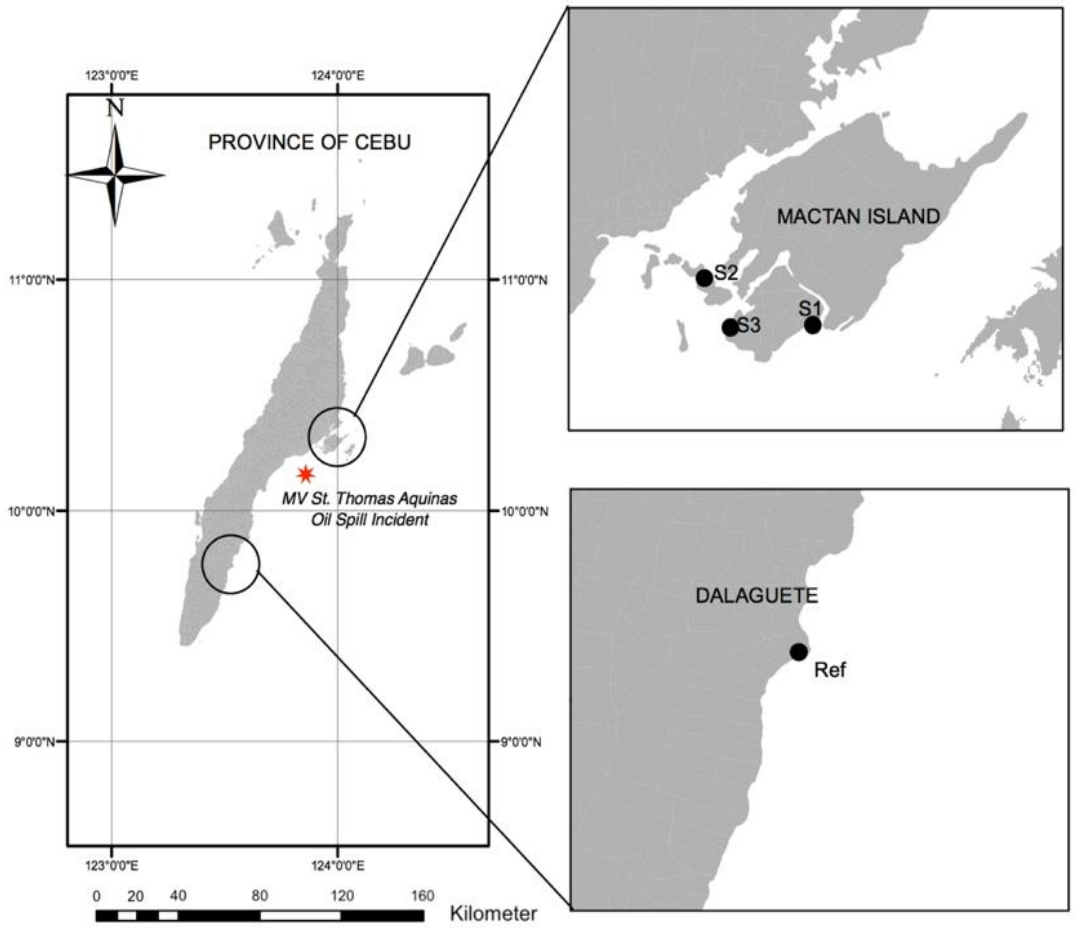


Figure 1. *The sampling sites in Barangays Alegria (S1), Calawisan (S2), and Day-as (S3) in Mactan Island, and the reference site (Ref) in Dalaguete, Cebu, Philippines*

http://www.aloki.hu ● ISSN 1589 1623 (Print) ● ISSN 1785 0037 (Online)
DOI: http://dx.doi.org/10.15666/aeer/1902_13531370
© 2021, ALÖKI Kft., Budapest, Hungary

Sampling

In each site, three random points were established for water sampling. The samplings were conducted in May and August 2014, August 2015, and March 2016 (8, 12, 24, and 30 months after the oil spill, respectively). The water samples were collected at 0.5 m below the surface. The samples were placed into 1 L sample bottles and were preserved immediately with 5 mL of Lugol's solution, and were brought to the laboratory for analysis.

Phytoplankton community structure analysis

Water samples were set aside for at least 24 h to allow phytoplankton to settle at the bottom. Subsequently, 0.9 L sample was carefully siphoned from the surface. The remaining 0.l L concentrated algal sample was homogenized before 1 mL aliquot of the sample was subjected for enumeration of the phytoplankton under a compound light microscope. The drop-count method was used to examine the aliquot one to two drops at a time following the protocol of Verlecar and Desai (2004). The species were identified and verified using the AlgalBase (Guiry and Guiry, 2016). Abundance, relative abundance, diversity indices at the species level (*Eq.1 to Eq.7*) were included in the quantitative description of the phytoplankton community structure of the study sites (*Table 1*).

Table 1. *Description of the different metrics of the phytoplankton community structure*

Metrics	Equations/Unit	
Total Abundance (ind L^{-1})	N = total # of individuals	(Eq.1)
Relative abundance of diatoms (%)	Dia = # of diatoms *100 / N	(Eq.2)
Relative abundance of dinoflagellates (%)	$Dino$= # of dinoflagellates *100 / N	(Eq.3)
Relative abundance of cyanobacteria (%)	Cya = # of cyanobacteria *100 / N	(Eq.4)
Species Richness [b]	S = # of species	(Eq.5)
Shannon's diversity index [b]	$H' = -\Sigma(n_i/N)\ln(n_i/N)$ [a]	(Eq.6)
Pielou's evenness [b]	J = H'/ log(S)	(Eq.7)
Phytoplankton biomass [c]	*Chl a*, mg m^{-3}	

[a] n_i is the number of individuals of the ith group in the sample
[b] calculated using the vegan package in R (Oksanen et al., 2019)
[c] chlorophyll a as proxy, which is extracted from Aqua-MODIS monthly Level- 3 estimates as described below

Principal Component Analysis (PCA) was used to explore the pattern of variation of phytoplankton community structure using the matrix that contains 48 observations (3 sampling points x 4 sites x 4 sampling dates) and 8 phytoplankton variables (as listed in *Table 1*). The data were log-transformed to normalize the data distribution. Kolmogorov-Smirnov test was used to determine the normality of the data. The data were centered since the variables were measured in the different scale and were standardized because PCA is sensitive to the relative scaling of the original variable. The relationship between the eight phytoplankton variables was determined using the Pearson correlation coefficients. The resulting correlation matrix was used to extract the principal axes, and only those axes that explained significantly the total variance were selected for

http://www.aloki.hu ● ISSN 1589 1623 (Print) ● ISSN 1785 0037 (Online)
DOI: http://dx.doi.org/10.15666/aeer/1902_13531370
© 2021, ALÖKI Kft., Budapest, Hungary

interpretation. ANOVA and pairwise comparison using t-test were used to test differences between the reference and affected sites.

Derivation of Multimetric Phytoplankton Index for Biotic Integrity (MPI-BI)

The results of the PCA was used to select variables that best illustrated the variation captured by each axis. Variables whose loadings were higher than 0.45 were selected for the development of the Multimetric Phytoplankton Index for Biotic Integrity (MPI-BI). Each of the selected variables was used to compute for the Ecological Quality Ratio (EQR) using *Eq.8*. For phytoplankton biomass data, EQR was calculated using *Eq.9*. The range of the EQR scores was set from 0 to 1. The MPI-BI score was computed by averaging all the EQR scores at each sampling point (*Eq.10*). A higher MPI-BI score indicates better health of the affected the site. MPI-BI were then compared among oil spill affected sites.

$$EQR_i = x_i \text{ in affected site} / x_i \text{ in reference site} \quad \text{(Eq.8)}$$

$$EQR_j = x_j \text{ in reference site} / x_j \text{ in affected site} \quad \text{(Eq.9)}$$

$$\text{MPI-BI} = \Sigma EQR_i / \text{no. of metrics} \quad \text{(Eq.10)}$$

where x is the observed value of the variable in an affected site i and reference j.

Assessment of meteorological and satellite-based data

Aqua-MODIS monthly Level- 3 estimates of chlorophyll *a* (*Chl a*, mg m^{-3}), particulate organic carbon (*POC*, mg m^{-3}), sea surface temperature (*SST*, deg C), and photosynthetically active radiation (*PAR*, einstein m^{-2} d^{-1}) were obtained from NASA Distributed Active Archive Center (http://oceancolor.gsfc.nasa.gov/). The spatial resolution of these data was 4 km^2, and temporal resolution was monthly from 2012-2015. Monthly estimates of *Chl a*, *POC*, *SST*, and *PAR* in all the study sites were extracted using SeaDAS software version 7.3.2 (Baith et al., 2006; https://seadas.gsfc.nasa.gov/). All remotely sensed data in the affected sites were pooled and reported as mean mean ± SE. Air temperature (*AT*, deg C), relative humidity (*RH*, %), precipitation (*P*, mm), and mean sea level pressure (*MSLP*, hpa) were obtained from Philippine Atmospheric Geophysical and Astronomical Services Administration (PAGASA) – Department of Science and Technology (DOST). These meteorological data were measured in the Mactan station. The temporal resolution of this data was daily from 2012-2015. Monthly average values of these meteorological parameters were computed and reported as mean ± SEM. PCA was also applied to examine the variability of the monthly estimates of remotely sensed and meteorological parameters using the matrix that contains 48 observations (12 months x 4 years) and 8 parameters.

Data processing and analysis

Descriptive statistics were determined to summarize the collected data. All averaged values were reported as mean ± SEM. PCA, ANOVA, Pearson correlation, and Welch t-test were carried out using the *stat* R package (R Core Team, 2019).

http://www.aloki.hu ● ISSN 1589 1623 (Print) ● ISSN 1785 0037 (Online)
DOI: http://dx.doi.org/10.15666/aeer/1902_13531370
© 2021, ALÖKI Kft., Budapest, Hungary

Data wrangling and visualization were implemented in R version 3.3.2 (R Core Team, 2019) software using the following packages: *tidyverse* (Wickham et al., 2019), *maps* (Becker et al., 2018), *raster* (Hijmans, 2020), and *ggthemes* (Arnold, 2019).

Results

Pattern of variation in phytoplankton community structure

The affected sites revealed the dominance of three major taxonomic groups – diatoms dominated with pooled mean relative abundance of 62.0 ± 8.4%, 54.3 ± 7.8%, 83.6 ± 2.5%, and 50.4 ± 11.0% after 8, 12, 24 and 30 months from the oil spill incident, respectively; followed by dinoflagellates (25.5 ± 7.6%, 32.6 ± 7.7%, 10.8 ± 2.5%, and 46.38 ± 12.0%, respectively); and then by cyanobacteria (12.5 ± 7.5%, 13.1 ± 6.0%, 2.6 ± 0.8%, and 2.0 ± 0.8%, respectively).

For all samples in affected sites, diatoms were comprised of five classes, i.e. Bacillariophyceae (17 orders, 28 families, 64 genera, and 124 species), Coscinodiscophyceae (7 orders, 9 families, 11 genera, and 13 species), Mediophyceae (6 orders and families, and 8 genera and species), Biddulphiophycidae (2 genera, and 4 species), and Fragilariophyceae (1 species); dinoflagellates were represented by two classes (Dinophyceae (7 orders, 16 families, 23 genera, and 33 species) and Noctilucophyceae (1 species); and cyanobacteria were composed by class Cyanophyceae (5 orders and families, 6 genera and 7 species). Several diatoms (9 orders, 13 families, 36 genera, and 74 species), dinoflagellates (2 orders, 5 families, 10 genera, and 15 species), and cyanobacteria (3 orders and families, 4 genera, and 5 species) are present in affected sites and not found in the reference site. However, 6 diatom species and none of the dinoflagellate and cyanobacteria in the reference site were absent in the affected sites.

ANOVA showed a significant difference in the relative abundance of diatoms (*Dia*), dinoflagellates (*Dino*), and cyanobacteria (*Cya*), Pielou's evenness (*J*), and phytoplankton biomass (*Chl a*) among sites (*Table 2*). Pairwise comparisons using t-tests confirmed the significant difference in these parameters between the reference and affected sites after a certain period from the oil spill incident (*Fig. 2*). Among these site-specific parameters, *Chl a* in all affected sites were significantly higher than the values in the reference condition, suggesting that this parameter is pressure-specific. A significant temporal variation was observed in *Cya*, *S* (species richness), and *H* (Shannon's diversity index) that showed to increase after 8 – 24 months from the spill (*Table 2*). A two-way ANOVA revealed evidence of a significant interaction effect between spatial and temporal scales at which the *N* (total abundance), *Dino*, *Cya*, and *Chl a* were sampled (*Table 2*).

We applied PCA to obtain further information on the pattern of variation in phytoplankton community structure. *Fig. 3* shows the progressive decline of principal components' (PC) eigenvalues and the proportion of explained variances. The last four PCs represented a small proportion of the total variance (< 6.5%) and were not included in the interpretation. Four significant PC axes were obtained and revealed that PC1 – PC4 explained 39.1%, 22.6%, 15.4%, and 9.4% of the total variance, respectively. These PCs accounted for 86.5% of the total variance explained, while 13.5% of the variance remained unexplained. *Fig. 4* illustrates the projections of the phytoplankton variables of the reference and affected sites 8, 12, 24, and 30 months after the spill.

http://www.aloki.hu ● ISSN 1589 1623 (Print) ● ISSN 1785 0037 (Online)
DOI: http://dx.doi.org/10.15666/aeer/1902_13531370
© 2021, ALÖKI Kft., Budapest, Hungary

Table 2. *Summary statistics of the analysis of variance (ANOVA) conducted to examine the spatial and temporal variation in total abundance of phytoplankton (N), relative abundance of diatoms (Dia), dinoflagellates (Dino), and cyanobacteria (Cya), species richness (S), Shannon's diversity index (H), Pielou's evenness (J), and phytoplankton biomass (Chl a)*

ANOVA Models	Terms	df	Sum Sq.	Mean Sq.	F value	p-value	
N ~ Site x Date	Site	3	1132406.25	377468.75	1.00	0.40	
	Date	1	3533.75	3533.75	0.01	0.92	
	Site:Date	3	4545894.63	1515298.21	4.02	0.01	*
	Residuals	40	15083963.29	377099.08			
Dia ~ Site x Date	Site	3	13452.61	4484.20	12.47	<0.01	*
	Date	1	390.42	390.42	1.09	0.30	
	Site:Date	3	1797.76	599.25	1.67	0.19	
	Residuals	40	14386.37	359.66			
Dino ~Site x Date	Site	3	12251.86	4083.95	11.71	<0.01	*
	Date	1	0.39	0.39	<0.01	0.97	
	Site:Date	3	3120.00	1040.00	2.98	0.04	*
	Residuals	40	13954.76	348.87			
Cya ~ Site x Date	Site	3	2937.16	979.05	22.66	<0.01	*
	Date	1	616.42	616.42	14.27	<0.01	*
	Site:Date	3	2882.67	960.89	22.24	<0.01	*
	Residuals	40	1727.89	43.20			
S ~ Site x Date	Site	3	768.90	256.30	1.92	0.14	
	Date	1	6042.16	6042.16	45.19	<0.01	*
	Site:Date	3	342.04	114.01	0.85	0.47	
	Residuals	40	5347.88	133.70			
H ~ Site x Date	Site	3	1.06	0.35	0.69	0.56	
	Date	1	7.39	7.39	14.44	<0.01	*
	Site:Date	3	3.78	1.26	2.46	0.08	
	Residuals	40	20.46	0.51			
J ~ Site x Date	Site	3	0.19	0.06	3.65	0.02	*
	Date	1	0.05	0.05	2.85	0.10	
	Site:Date	3	0.13	0.04	2.49	0.07	
	Residuals	40	0.70	0.02			
Chl a ~ Site x Date	Site	3	1.69	0.56	27.38	<0.01	*
	Date	1	0.03	0.03	1.39	0.25	
	Site:Date	3	0.35	0.12	5.65	<0.01	*
	Residuals	40	0.82	0.02			

Notes: asterisk * indicates significance at 95% confidence interval

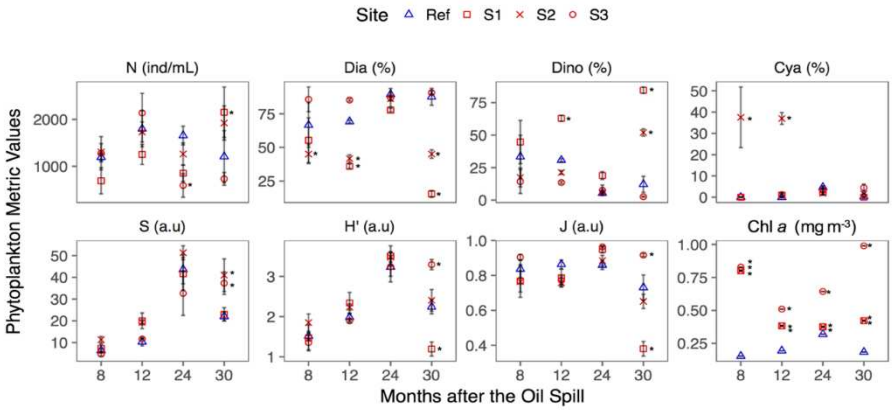


Figure 2. *Variation of (A) total phytoplankton biomass, relative abundance of (B) diatoms, (C) dinoflagellates, (D) cyanobacteria, (E) species richness, (F) Shannon's diversity index, (G) species evenness, and (H) chlorophyll a levels (mean ± SE) in the reference and affected sites after 8 - 30 months from the oil spill incident. An asterisk (*) indicates a significant difference ($p<0.05$) to the mean value in the reference site*

http://www.aloki.hu ● ISSN 1589 1623 (Print) ● ISSN 1785 0037 (Online)
DOI: http://dx.doi.org/10.15666/aeer/1902_13531370
© 2021, ALÖKI Kft., Budapest, Hungary

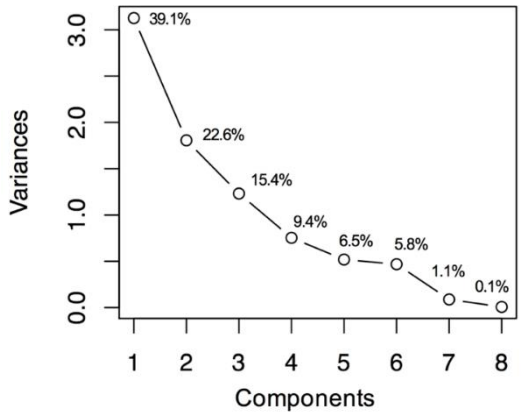


Figure 3. *Scree plot of the percent of variance explained by each principal component*

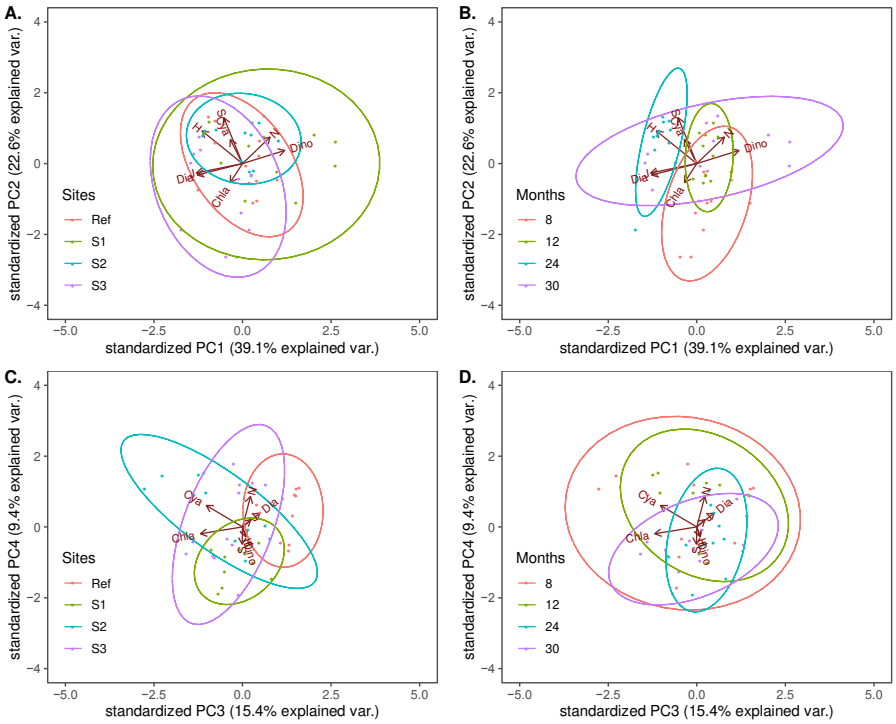


Figure 4. *Projection of the eight phytoplankton variables on the (A – B) PC1 and PC2 axes, and (C - D) PC3 and PC4 axes. Ellipses (95% confidence) represent the projections of the variables sampled in reference and affected sites after 8 – 30 months from the oil spill*

Fig. 5 shows the temporal changes in PC eigenvalues between reference and affected sites. PC1 relates to the relative abundance of phytoplankton as it best explained the variability of *Dia*, *Dino*, and *J* with Pearson correlation coefficients (*r*) of 0.48, -0.45, and 0.49, respectively. This suggests that *Dia* and *J* decrease with increasing PC1 eigenvalues, while *Dino* increase with decreasing PC1 eigenvalues. PC2, on the other hand, relates to the phytoplankton diversity as the variability of *S* and *H'* were best explained by this axis. Both variables had a positive correlation with PC2 eigenvalues with *r* values of 0.64 and 0.45, respectively. PC3 was negatively related to *Chl a* (r = -0.71) and is related to the trophic state. PC4 was positively related to *N* (r = 0.66) and *Cya* (r = 0.46).

http://www.aloki.hu ● ISSN 1589 1623 (Print) ● ISSN 1785 0037 (Online)
DOI: http://dx.doi.org/10.15666/aeer/1902_13531370
© 2021, ALÖKI Kft., Budapest, Hungary

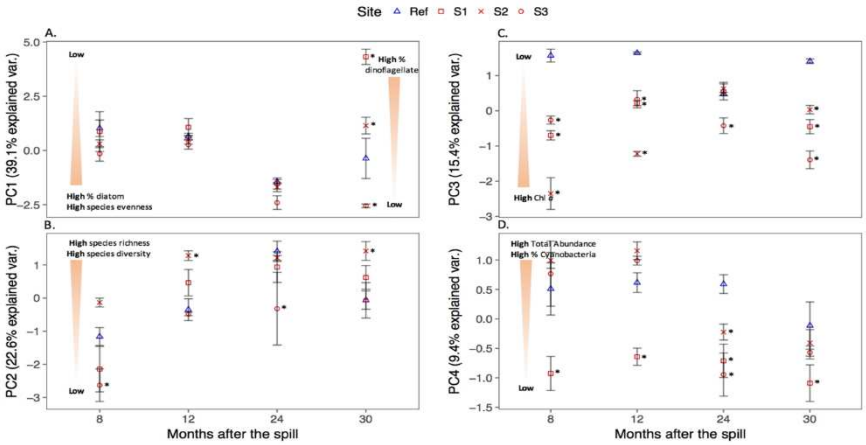


Figure 5. *Variation of the PC1 – PC4 eigenvalues (mean ± SE; A – D, respectively) in the reference and affected sites after 8 - 30 months from the oil spill incident. An asterisk (*) indicates a significant difference ($p<0.05$) to the mean value in the reference site*

ANOVA showed significant spatial variation in PC1, PC2, PC3, and PC4 axes, but only PC2 and PC4 axes did vary significantly (*Table 3*). *Fig. 5* displayed the significant difference in the PC eigenvalues between the reference and affected sites after a certain period from the oil spill incident. The findings suggest that the relative abundance of phytoplankton and trophic state differ across sites, while diversity varies both spatially and temporally. PC3 eigenvalues in the Ref vary significantly to the values in S1, S2, and S3 after 8, 12, and 30 months from the spill, suggesting a higher trophic state in the oil spill affected sites. Also, PC2 eigenvalues observed in 8 months were significantly different from the observations in 12, 24 and 30 months after the oil spill, implying a higher phytoplankton diversity within these periods.

Table 3. *Summary statistics of the analysis of variance (ANOVA) conducted to examine the spatial and temporal variation in PC1 to PC4 axes and in Multimetric Phytoplankton Index for Biotic Integrity (MPI-BI)*

ANOVA Models	Terms	df	Sum Sq.	Mean Sq.	F value	p-value	
PC1 ~ Site x Date	Site	3	34.51	11.50	5.67	<0.01	*
	Date	1	4.19	4.19	2.07	0.16	
	Site:Date	3	27.17	9.06	4.47	0.01	*
	Residuals	40	81.12	2.03			
PC2 ~ Site x Date	Site	3	19.89	6.63	6.20	<0.01	*
	Date	1	20.95	20.95	19.60	<0.01	*
	Site:Date	3	1.32	0.44	0.41	0.75	
	Residuals	40	42.74	1.07			
PC3 ~ Site x Date	Site	3	28.26	9.42	27.33	<0.01	*
	Date	1	0.35	0.35	1.03	0.32	
	Site:Date	3	15.49	5.16	14.98	<0.01	*
	Residuals	40	13.79	0.34			
PC4 ~ Site x Date	Site	3	12.22	4.07	15.18	<0.01	*
	Date	1	8.68	8.68	32.36	<0.01	*
	Site:Date	3	3.79	1.26	4.71	0.01	*
	Residuals	40	10.73	0.27			
MPI-BI ~ Site x Date	Site	3	0.77	0.26	21.04	<0.01	*
	Date	1	<0.01	<0.01	0.18	0.68	
	Site:Date	3	0.03	0.01	0.73	0.54	
	Residuals	40	0.49	0.01			

Notes: asterisk * indicates significance at 95% confidence interval

http://www.aloki.hu ● ISSN 1589 1623 (Print) ● ISSN 1785 0037 (Online)
DOI: http://dx.doi.org/10.15666/aeer/1902_13531370
© 2021, ALÖKI Kft., Budapest, Hungary

PCA was successfully demonstrated in this study as a useful and effective tool to decrease the number of phytoplankton parameters to explain the variation observed between the reference and affected sites after 8 – 30 months from the spill. The reduction of the number of variables did not impair the quality of the information in this study as the PCA agrees with the previous analysis. The PCA results revealed that the variation in the observations can be best explained by the phytoplankton relative abundance (*Dia*, *Dino*, and *J*), phytoplankton diversity (*S* and *H*), and trophic state (*Chl a*). All these parameters were site-specific, but only the trophic state showed pressure-specificity.

Assessment of health status using MPI-IB

Based on the PCA results, the variables that explained the variation captured by each axis were selected. Out of eight components, PC1, PC2, and PC3 were selected as they provide a meaningful explanation of the variability of phytoplankton relative abundance, diversity, and trophic state, respectively. The variables that significantly correlated with each of the selected PC were extracted. Only six out of eight variables met this requirement and were retained for the development of MPI-BI. Each metric represents a unique biological feature and plays a distinct role in the MPI-IB. For instance, diatom dominated in oil spill affected sites, and hence, the relative abundance of diatom deserves attention when assessing the ecological health status of coastal water after the oil spill. These metrics represent ecological quality changes and can explain the degree of stress after the oil spill. In each of these variables, the Ecological Quality Ratio (EQR) was computed to determine the degree of departure of the metric value in the affected site from the value in the reference site. These scores were averaged to determine MPI-BI scores. The MPI-BI range was equally divided into 5 ecological health status: (1) High (0.81 – 1.0), (2) Good (0.61 – 0.80), (3) Moderate (0.41 – 0.60), (4) Poor (0.21 – 0.40), and, (5) Bad (0 – 0.20). The high condition indicates that the environment is characterised by low trophic state due to low chlorophyll *a* levels, and high species richness and evenness that results in high diversity. At the other extreme, bad condition indicates environment with high trophic state due to high chlorophyll *a* levels, and low biodiversity due to low richness and uneven distribution of phytoplankton. MPI-BI scores of the affected sites were generally above 0.6, suggesting that the health status of the affected sites were in good to high condition after 8 – 30 months from the oil spill incident (*Fig. 6*). Variation in MPI-BI was evident spatially but not temporally (*Table 3*).

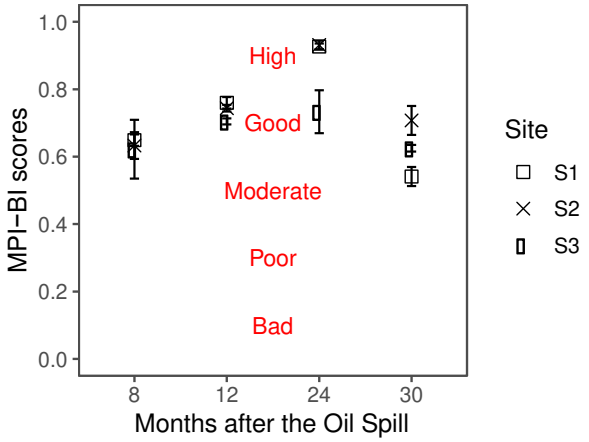


Figure 6. *Multimetric phytoplankton index for biotic integrity (mean ± SE) in affected sites after 8 - 30 months from the oil spill incident*

http://www.aloki.hu ● ISSN 1589 1623 (Print) ● ISSN 1785 0037 (Online)
DOI: http://dx.doi.org/10.15666/aeer/1902_13531370
© 2021, ALÖKI Kft., Budapest, Hungary

Time series analysis of environmental parameters before and after the spill

Earlier analysis revealed that *Chl a* is pressure specific. Hence, we used *Chl a* to indicate trophic status changes in the southern coast of Mactan before and after the spill. We also correlated *Chl a* to other environmental parameters to determine whether the changes in the trophic status can be attributed to the oil spill or to natural conditions in the environment. However, this study does not give a claim on the direct nor the isolated effect of oil spill on the *Chl a* changes. Instead, this study attempted to estimate, based on the evidence gathered, the trend of *Chl a* before and after the oil spill considering the role of other environmental and meteorological factors such as the particulate organic carbon (*POC*), photosynthetically active radiation (*PAR*), sea surface temperature (*SST*), air temperature (*AT*), relative humidity (*RH*), precipitation (*P*), and mean sea level pressure (*MSLP*). These factors may play different roles in the variation of *Chl a*.

Fig. 7 shows the temporal patterns of *Chl a* and the other environmental parameters. One-way ANOVA showed significant monthly and seasonal variations of all the parameters ($p < 0.05$). Based on the pooled means in pre spill (1 – 18 months before the spill) and post spill (1 – 26 months after the spill) conditions, higher *Chl a* and *POC* were observed after the oil spill incident ($p<0.01$), while the other parameters showed no significant difference before and after the oil spill. This suggests a possible contribution of the oil spill impact to the changes of *Chl a* and *POC* in the affected sites.

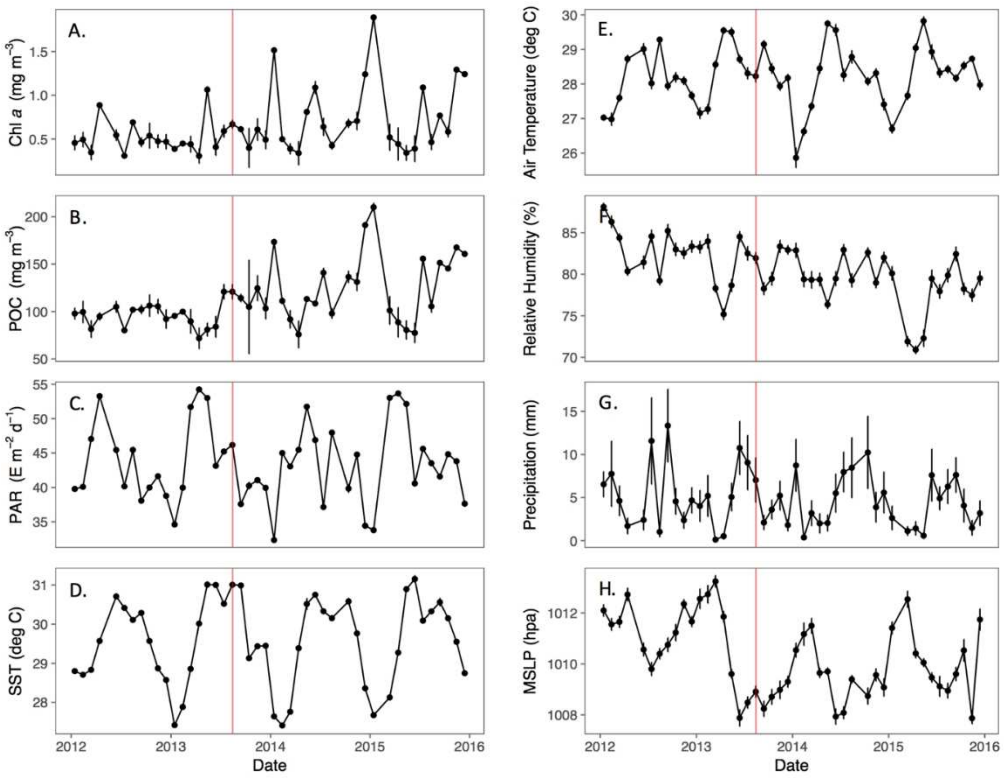


Figure 7. *Temporal variation of (A) chlorophyll a level, (B) particulate organic carbon, (C) photosynthetically active radiation, (D) sea surface temperature, (E) air temperature, (F) relative humidity, (G) precipitation, and (H) mean sea level pressure. Remotely sensed estimates (A – D) are reported as pooled mean (mean ± SE) of the observed values in the affected sites. Meteorological data (E – H) from PAGASA-DOST are reported as monthly average (mean ± SE) of the values collected in the Mactan Station. The vertical line indicates the date of oil spill incidence*

http://www.aloki.hu ● ISSN 1589 1623 (Print) ● ISSN 1785 0037 (Online)
DOI: http://dx.doi.org/10.15666/aeer/1902_13531370
© 2021, ALÖKI Kft., Budapest, Hungary

Based on the Pearson correlation analysis, *Chl a* was positively correlated to *AT* ($r = 0.45$) and *PAR* ($r = 0.46$) in the pre spill condition. However, it was negatively correlated to both parameters ($r = -0.42$ and -0.52, respectively) in post spill condition. A positive correlation between *Chl a* and *POC* ($r = 0.88$) was also observed in the post spill condition.

We also used PCA to explore further the variability of the environmental parameters before and after the spill. About 91.3% of the total variance was explained by the first four PC axes as shown in the projections of the environmental parameters before and after the spill on different PC axes in *Fig. 8*. PC1 and PC2 relate to hydrographic and meteorological conditions. PC1 explained 38.9% of the total variance and significantly explained the variability of air temperature and photosynthetically active radiation with Pearson correlation coefficients (r) of 0.48 and 0.5, respectively. PC2 explained 27.2% of the total variance and was related to mean sea level pressure and sea surface temperature ($r = 0.60$ and -0.51, respectively). Both components did not significantly vary before and after the spill ($p > 0.05$). On the other hand, PC3 and PC4 are related to the trophic condition as it best explained the variability of *Chla* with r value of 0.57 and -0.47, respectively. PC3 was also positively related to particulate organic carbon ($r = 0.49$). There were significant differences in PC3 and PC4 between pre and post spill conditions ($p < 0.01$), suggesting a possible shift in trophic status in the southern coast of Mactan Island after the oil spill incidence.

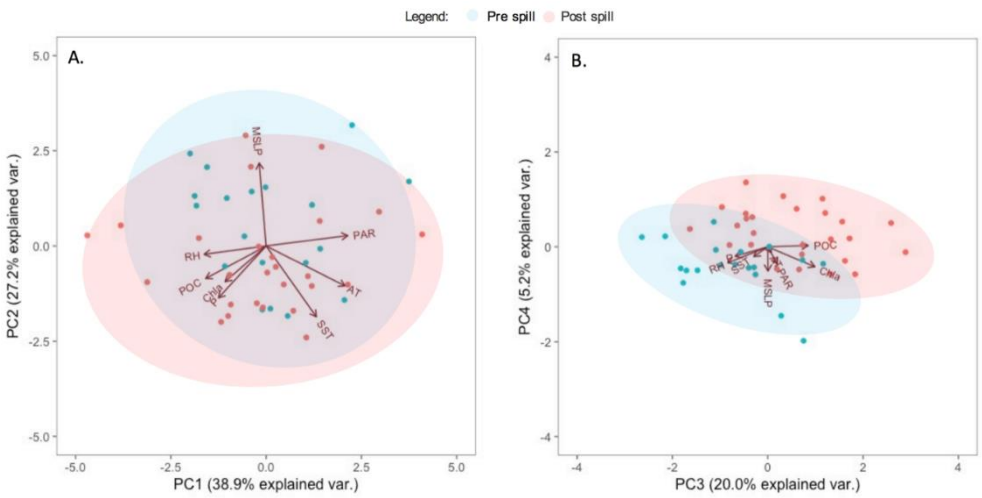


Figure 8. *Projection of the chlorophyll a level (Chl a), particulate organic carbon (POC), photosynthetically active radiation (PAR), sea surface temperature (SST), air temperature (AT), relative humidity (RH), precipitation (P), and mean sea level pressure (MSLP) on the (A) PC1 and PC2, and (B) PC3 and PC4 axes. Ellipses (95% confidence) represent the projections of the variables in pre spill and post spill conditions*

Discussion

The affected sites had an increase in one or more taxonomic groups, changing the phytoplankton community composition. Certain phytoplankton genera dominate during an oil-spill event, which could be used as indicators of the marine phytoplankton community stressed by oil components (Hallare et al., 2011). Three of them (i.e. *Chaetoceros*, *Rhizosolenia*, and *Skeletonema*) were present in the affected sites.

http://www.aloki.hu ● ISSN 1589 1623 (Print) ● ISSN 1785 0037 (Online)
DOI: http://dx.doi.org/10.15666/aeer/1902_13531370
© 2021, ALÖKI Kft., Budapest, Hungary

Results also showed the dominance of diatoms and dinoflagellates in affected sites. Diatoms proliferated dominantly relative to dinoflagellates in more highly affected site. Unlike dinoflagellates, diatoms have been demonstrated to possess the ability to use oil as a carbon source even at low concentrations to propagate colonizing an area affected by oil spillage (El-Sheekh et al., 2000). They also possess silica frustules that protect them from acute lethal effects of oil compared to the other naked phytoplankton (Ikavalko et al., 2005). Conversely, some studies show that diatom growth is suppressed during the oil spill and laboratory experiments (Harrison et al., 1986; Lee and Page, 1997) because the structure of diatoms allows them to absorb hydrocarbons more readily thereby enabling subsequent toxicity as well as hindering reproduction (Kustenko, 1981). Centric diatoms (e.g. *Coscinodiscus, Rhizosolenia, Skeletonema*) predominates pennate diatoms (e.g. *Navicula, Nitzschia, Pleurosigma*) due to the fact that the latter are more sensitive to pollutants (Perez et al., 2010). However, this was not observed in the affected sites since centric diatoms were found at very low densities.

The findings also suggest that phytoplankton communities in affected and reference sites after 8 – 30 months from the spill had relatively similar abundance and richness, which results in no variation in the diversity. The result suggests no apparent change in phytoplankton communities from the reference condition throughout the investigated period. However, remotely sensed chlorophyll *a* estimates in the affected sites were higher than in the reference site, suggesting higher phytoplankton biomass and hence a higher trophic state in the oil spill affected sites. Existing studies on the effect of oil spill towards phytoplankton communities showed unclear and contradictory results – e.g. no change in the number of planktonic population (Johansson et al., 1980; Khalaf et al., 2006), reduction in the density, the number of species, diversity and ecophysiological indices (Batten et al., 1998), and proliferation of phytoplankton (Hallare et al., 2011) in an oil spill affected site.

Temporal variation was demonstrated in phytoplankton diversity, where it showed a significant increasing trend after the spill. These findings suggest a possible shift in taxonomic groups that change the composition of the phytoplankton community, subsequently increasing the phytoplankton diversity and possibly the biomass after the spill incidence.

One limitation in our *in situ* assessment of composition is that it is biased not only on the armored or those with tests but the sampling is also biased on those net phytoplankton that is usually in the microphytoplankton size. The phytoplankton or the autotrophic bacteria and phytoplankton smaller than 20 microns are not captured in the analysis. Another limitation of the assessment is the condition that the southern coast of Mactan is chronically exposed also to oil being a navigational route of ships while the reference is not that might contribute to the variation observed between the sites.

Oil spill affected sites may return to their reference condition just within two weeks (Johansson et al., 1980) or more than six months (Spooner, 1977) after the oil spill. Recovery of an affected site is greatly influenced by a myriad of factors such as coastal topography, water-body characteristics, oil composition, and its fate, and also abiotic and biotic factors. It is possible that the spilled oil had already been dispersed by spreading, emulsification, dissolution, evaporation, sedimentation, adsorption (Bartha and Atlas, 1977), photo-oxidation (Lacaze and de Naïde, 1976), and bacterial degradation (McGenity et al., 2012; Bensig et al., 2014). However, the recovery of phytoplankton communities after the occurrence of the oil spill cannot be inferred from the findings due to the absence of pre oil spill data.

http://www.aloki.hu ● ISSN 1589 1623 (Print) ● ISSN 1785 0037 (Online)
DOI: http://dx.doi.org/10.15666/aeer/1902_13531370
© 2021, ALÖKI Kft., Budapest, Hungary

The observed differences in *Chl a* and *POC* between pre and post spill condition suggest a possible contribution of the oil spill impact to the changes of trophic state in the affected coastal water of Mactan Island. The correlative patterns of the environmental parameters to the changes of *Chl a* showed to differ between pre and post spill conditions. This may suggest possible interactive effects of the oil spill and meteorological factors on the variability of *Chl a*. It is also possible that the change in the *Chl a* after the oil spill may not be due to its interaction with environmental parameters but could be the previous events that happened in the area, i.e oil spill incidence. For instance, the variability of *Chl a* in areas with natural disturbance is not affected by the seasonal change of *SST* but is mainly dependent on the current action of the ecosystem such as nutrients and chemical composition of the area (Nababan et al., 2016). In this case, the probability of contributing to the oil spill changed the chemical composition of the area and may lead to the effect of the oil on the affected coastal waters.

Time-series analysis showed that there was a change in the monthly distribution of *Chl a* in the affected area. No significant change was observed during first five months of the oil spill when compared to the previous years of the same months, respectively. However, a significant increase occurred 6 months after the oil spill. There was a lag time before significant changes in the *Chl a* was observed. The time interval of this study confirmed the findings of Sheng et al. (2011) that *Chl a* increase at an average of 6 months. In other studies, an increase in *Chl a* was observed after 5.5 months (Vargo et al., 1982), 7 months (Riaux-Gobin, 1985), and 9 months (Sheng et al., 2011). While there was no change in *Chl a* in this study during the first five months of the oil spill, findings suggest the decrease of *Chl a* for about 2 weeks (Lee et al., 2009) while, in other study, for about 7 weeks (Wang, 2015).

Increase of the phytoplankton in a time interval is possibly due to the oil weathering in the area and the decreased zooplankton primarily feeding to the phytoplankton (Lee et al., 2009). It has also been proven that zooplankton decreased significantly after the oil spill and maybe the reason for lesser herbivory in the area (Johansson et al., 1980). Also, the chance of the increased bacteria feeding the oil, as evidenced by increased nitrogen products of bacterial metabolism, enhanced the possibility of removing oil fractions in the area (Banks, 2003). Sheng et al. (2011) stated that the short-lived increase of phytoplankton may be the roles of reduced grazing pressure, decomposition of dead organisms, competitive and tolerant phytoplankton, and stimulating effect of oil to phytoplankton.

Surprisingly, there was still evidence of *Chl a* increase in the affected area even after the span of 18, 28, and 29 months. This observation is speculated to be a result of the long term effect of the oil spill. It is likely that long term changes in the *Chl a* may be attributed to the oil spill residue that may still be present in the underlying sediment of the affected coastal waters. Duan et al. (2018) observed the presence of the residual oil in the sediment at Bay Jimmy five years after the oil spill. They observed after the oil spill that there is a significant increase in concentrations of polycyclic aromatic hydrocarbons (PAH), n-alkenes, and total petroleum hydrocarbon. A number of studies have demonstrated the negative effect of PAH on the phytoplankton biomass (Pelletier et al., 2006; Kamalanathan et al., 2018). Degradation of these oil spill residue components may provide a potential source of carbon for phytoplankton growth and productivity, which may explain the long term increase of *Chl a*. However, this hypothesis is impossible to test due to a lack of continuous field measurements.

http://www.aloki.hu ● ISSN 1589 1623 (Print) ● ISSN 1785 0037 (Online)
DOI: http://dx.doi.org/10.15666/aeer/1902_13531370
© 2021, ALÖKI Kft., Budapest, Hungary

Conclusion

This study evaluated the multimetric phytoplankton-based ecological health status of the coastal water of Mactan Island after 8 – 30 months from the oil spill incidence. The important findings of this study were as follows: (1) Phytoplankton community structure in affected and reference sites did not differ in abundance and richness that resulted in no variation in the diversity between sites. However, the difference in abundance between sites can be significantly different depending on the dates. Furthermore, the dominance of the major taxonomic groups had shifted that changes the phytoplankton community composition, subsequently increasing the phytoplankton diversity over time after the spill incidence. Higher chlorophyll *a* was observed in oil spill affected sites. (2) Multivariate analysis showed that the observed spatial and temporal variation can be best explained by phytoplankton relative abundance diversity and trophic state, which can be used to determine the MPI-BI. Based on the MPI-BI scores, the health status of the affected sites after 8 – 30 months from the oil spill incident was generally in good condition. (3) A time-series analysis of chlorophyll *a* concentration revealed the difference between pre and post spill conditions that may suggest the effect of oil spill on the trophic state in the affected coastal water. Overall, the health status of the affected coastal water may be affected by oil as indicated by the increased level of chlorophyll *a* in the post spill condition. However, the affected coastal water may also undergo a certain level of recovery from the oil spill stress as suggested by the similarity of the phytoplankton community structure to the reference site. Further study is recommended to evaluate the long term chronic effects of oil spill on phytoplankton community and primary productivity, but this requires continuous field measurements to verify the cause of the changes.

Acknowledgements. We would like to thank the University of the Philippines Cebu (Creative Work and Research Grant) for the funding. We also thank Monique Eloise Mercado for sharing the meteorological data collected from PAGASA-DOST.

REFERENCES

[1] Arnold, J. B. (2019): ggthemes: Extra Themes, Scales and Geoms for 'ggplot2'. – R package version 4.2.0.
[2] Baith, K., Lindsay, R., Fu, G., McClain, C. R. (2001): SeaDAS, a data analysis system for ocean-color satellite sensors. – EOS Transactions American Geophysical Union 82: 202.
[3] Banks, S. (2003): SeaWiFS satellite monitoring of oil spill impact on primary production in the Galápagos Marine Reserve. – Marine Pollution Bulletin 47(7): 325-330.
[4] Barbour, M. T., Swietlik, W. F., Jackson, S. K., Courtemanch, D. L., Davies, S. P., Yoder, C. O. (2000): Measuring the attainment of biological integrity in the USA: a critical element of ecological integrity. – Hydrobiologia 422/423: 453-464.
[5] Bartha, R., Atlas, R. M. (1977): The Microbiology of Aquatic Oil Spills. – Advances in Applied Microbiology 22: 225-266.
[6] Batten, S. D., Allen, R. J. S., Wotton, C. O. M. (1998): The effects of the Sea Empress oil spill on the plankton of the Southern Irish Sea. – Marine Pollution Bulletin 36(10): 764-774.
[7] Becker, R. A., Wilks, A., Brownrigg, R., Minka, T. P., Deckmyn, A. (2018): maps: Draw Geographical Maps. – R package version 3.3.0.
[8] Behrenfeld, M. J., Falkowski, P. G. (1997): Photosynthetic rates derived from satellite-based chlorophyll concentration. – Limnology and Oceanography 42: 1-20.

http://www.aloki.hu ● ISSN 1589 1623 (Print) ● ISSN 1785 0037 (Online)
DOI: http://dx.doi.org/10.15666/aeer/1902_13531370
© 2021, ALÖKI Kft., Budapest, Hungary

[9] Bensig, E. O., Edullantes, B., Silapan, J. R., Narsico, J. T. (2014): Oil degrading and heterotrophic bacteria composition in the oil-spilled affected mangrove forest sediment in Mactan Island, Central Philippines. – International Journal of Biosciences 5(8): 141-146.
[10] Bolognesi, C., Perrone, E., Roggieri, P., Sciutto, A. (2006): Bioindicators in monitoring long term genotoxic impact of oil spill: Haven case study. – Marine Environmental Research 62: S287-S291.
[11] Duan, J., Liu, W., Zhao, X., Han, Y., O'Reilly, S., Zhao, D. (2018): Study of residual oil in Bay Jimmy sediment 5 years after the Deepwater Horizon oil spill: persistence of sediment retained oil hydrocarbons and effect of dispersants on desorption. – Science of the Total Environment 618: 1244-1253.
[12] El-Sheekh, M. M., El-Naggar, A. H., Osman, M. E. H., Haieder, A. (2000): Comparative Studies on the Green Algae *Chlorella homosphaera and Chlorella vulgaris* with Respect to Oil Pollution in the River Nile. – Water, Air, and Soil Pollution 124(1-2): 187-204.
[13] Falkowski, P. (2012): Ocean science: The power of plankton. – Nature 483(7387): S17-S20.
[14] Farrington, J. W. (2013): Oil Pollution in the Marine Environment I: Inputs, Big Spills, Small Spills, and Dribbles. – Environment: Science and Policy for Sustainable Development 55(6): 3-13.
[15] Farrington, J. W. (2014): Oil Pollution in the Marine Environment II: Fates and Effects of Oil Spills. – Environment: Science and Policy for Sustainable Development 56(4): 16-31.
[16] Flores, M. J., Silapan, J., Edullantes, B. (2020): Effect of the MV Saint Thomas Aquinas on zooplankton composition and abundance in Mactan Island, Cebu, the Philippines. – Journal of Nature Studies 19(1): 105-119.
[17] García Pérez, J. D. (2003): Early socio-political and environmental consequences of the Prestige oil spill in Galicia. – Disasters 27(3): 207-23.
[18] Gesteira, J. L. G., Dauvin, J. C. (2000): Amphipods are Good Bioindicators of the Impact of Oil Spills on Soft-Bottom Macrobenthic Communities. – Marine Pollution Bulletin 40(11): 1017-1027.
[19] Gin, K. Y. H., Kamrul Huda, M., Kiat Lim, W., Tkalich, P. (2001): An Oil Spill–Food Chain Interaction Model for Coastal Waters. – Marine Pollution Bulletin 42(7): 590-597.
[20] Guiry, M. D., Guiry, G. M. (2016): AlgaeBase. – World-wide electronic publication, National University of Ireland, Galwa, http://www.algaebase.org.
[21] Hallare, A. V, Lasafin, K. J. A., Magallanes, J. R. (2011): Shift in Phytoplankton Community Structure in a Tropical Marine Reserve Before and After a Major Oil Spill Event. – International Journal Environmental Research 5(3): 651-660.
[22] Harrison, P. J., Cochlan, W. P., Acreman, J. C., Parsons, T. R., Thompson, P. A., Dovey, H. M., Xiaolin, C. (1986): The effects of crude oil and Corexit 9527 on marine phytoplankton in an experimental enclosure. – Marine Environmental Research 18(2): 93-109.
[23] Hijmans, R. J. (2020): raster: Geographic Data Analysis and Modeling. – R package version 3.3-13.
[24] Ikavalko, J., Gerdes, B., Hiukka, R. (2005): Effects of crude oil on arctic sea ice biota, an experimental study. – Phycologia 44: 48-58.
[25] International Maritime Organization, United Nations (2009): IMO/UNEP guidance manual on the assessment and restoration of environmental damage following marine oil spills. – Environment Programme, International Maritime Organization.
[26] Johansson, S., Larsson, U., Boehm, P. (1980): The Thesis oil spill impact on the pelagic ecosystem. – Marine Pollution Bulletin 11(10): 284-293.
[27] Kamalanathan, M., Xu, C., Schwehr, K., Bretherton, L., Beaver, M., Doyle, S. M., Genzer, J., Hillhouse, J., Sylvan, J. B., Santschi, P. (2018): Extracellular enzyme activity profile in a chemically enhanced water accommodated fraction of surrogate oil: toward understanding microbial activities after the Deepwater Horizon oil spill. – Frontiers in Microbiology 9: 798.

http://www.aloki.hu ● ISSN 1589 1623 (Print) ● ISSN 1785 0037 (Online)
DOI: http://dx.doi.org/10.15666/aeer/1902_13531370
© 2021, ALÖKI Kft., Budapest, Hungary

[28] Khalaf, G., Nakhlé, K., Abboud-Abi Saab, M., Tronczynski, J., Mouawad, R., Fakhri, M. (2006): Preliminary results of the oil spill impact on Lebanese coastal waters. – Lebanese Science Journal 7(2): 135-153.
[29] Kustenko, N. G. (1981): Effect of low oil concentrations on Spermatogonangii and Auxospores in three species of marine diatoms. – Okeanologiya/Oceanology (Moscow) 21: 366-369.
[30] Lacaze, J. C., Villedon de Naïde, O. (1976): Influence of illumination on phytotoxicity of crude oil. – Marine Pollution Bulletin 7(4): 73-76.
[31] Lee, R. F., Page, D. S. (1997): Petroleum hydrocarbons and their effects in subtidal regions after major oil spills. – Marine Pollution Bulletin 34(11): 928-940.
[32] Lee, C. I., Kim, M. C., Kim, H. C. (2009): Temporal variation of chlorophyll a concentration in the coastal waters affected by the Hebei Spirit oil spill in the West Sea of Korea. – Marine Pollution Bulletin 58(4): 496-502.
[33] Li, Y., Hu, C., Quigg, A., Gao, H. (2019): Potential influence of the Deepwater Horizon oil spill on phytoplankton primary productivity in the northern Gulf of Mexico. – Environmental Research Letters 14: 094018.
[34] McGenity, T. J., Folwell, B. D., McKew, B. A., Sanni, G. O. (2012): Marine crude-oil biodegradation: a central role for interspecies interactions. – Aquatic biosystems 8(1): 10.
[35] Nababan, B., Rosyadi, N., Manurung, D., Natih, N. M., Hakim, R. (2016): The Seasonal Variability of Sea Surface Temperature and Chlorophyll-a Concentration in the South of Makassar Strait. – Procedia Environmental Sciences 33: 583-599.
[36] NASA Goddard Space Flight Center, Ocean Biology Processing Group (2014): Sea-viewing Wide Field-of-view Sensor (SeaWiFS) Ocean Color Data. – NASA OB.DAAC, Greenbelt, MD, USA. http://doi.org/10.5067/ORBVIEW-2/SEAWIFS_OC.2014.0. Accessed 2018/10/21. Maintained by NASA Ocean Biology Distibuted Active Archive Center (OB.DAAC), Goddard Space Flight Center, Greenbelt MD.
[37] Oksanen, J., Blanchet, F. G., Friendly, M., Kindt, R., Legendre, P., McGlinn, D., Minchin, P. R., O'Hara, R. B., Simpson, G. L., Solymos, P., Stevens, M. H., Szoecs, E., Wagner, H. (2019): vegan: Community Ecology Package. – R package version 2.5-6.
[38] Ozhan, K., Parsons, M. L., Bargu, S. (2014): How Were Phytoplankton Affected by the Deepwater Horizon Oil Spill? – BioScience 64(9): 829-836.
[39] Parsons, M. L., Morrison, W., Rabalais, N. N., Turner, R. E., Tyre, K. N. (2015): Phytoplankton and the Macondo oil spill: A comparison of the 2010 phytoplankton assemblage to baseline conditions on the Louisiana shelf. – Environmental pollution 207: 152-60.
[40] Pelletier, E., Sargian, P., Payet, J., Demers, S. (2006): Ecotoxicological effects of combined UVB and organic contaminants in coastal waters: a review. – Photochemistry and Photobioliology 82: 981-93.
[41] Perez, P., Fernandez, E., Beiras, R. (2010): Fuel toxicity on Isochrysis galbana and a coastal phytoplankton assemblage: Growth rate vs. variable fluorescence. – Ecotoxicology and Environmental Safety 73(3): 254-261.
[42] R Core Team (2019): R: A language and environment for statistical computing. – R Foundation for Statistical Computing, Vienna, Austria. https://www.R-project.org/.
[43] Reynolds, C. S. (2006): Ecology of phytoplankton. – Cambridge: Cambridge University Press.
[44] Riaux-Gobin, C. (1985): Long-term changes in microphytobenthos in a Brittany estuary after the ”Amoco Cadiz” oil spill. – Marine Ecology Progress Series 24: 51-56.
[45] Sadaba, R., Niego, A. G. (2016): Assessment on the effects of an oil spill in the mangroves of Cordova, Cebu, Philippines. – The Malaysian Forester 79(1&2): 144-156.
[46] Sheng, Y., Tang, D., Pan, G. (2011): Phytoplankton bloom over the Northwest Shelf of Australia after the Montara oil spill in 2009. – Geomatics, Natural Hazards and Risk 2(4): 329-347.
[47] Spooner, M. F. (1977): Oil spill in Hong Kong. – Marine Pollution Bulletin 8(3): 62-65.

http://www.aloki.hu ● ISSN 1589 1623 (Print) ● ISSN 1785 0037 (Online)
DOI: http://dx.doi.org/10.15666/aeer/1902_13531370
© 2021, ALÖKI Kft., Budapest, Hungary

[48] Suderman, K., Thistle, D. (2004): The relative impacts of spills of two alternative fuels on the microalgae of a sandy site: a microcosm study. – Marine Pollution Bulletin 49(5): 473-478.
[49] Surís-Regueiro, J. C., Garza-Gil, M. D., Varela-Lafuente, M. M. (2007): The Prestige oil spill and its economic impact on the Galician fishing sector. – Disasters 31(2): 201-215.
[50] Teng, L., Zhang, B., Liu, X., Bai, C., Zhang, J., Tan, D., Huang, P. (2014): Development and Use of a Phytoplankton-Index of Biotic Integrity to Assess Yongjiang River Ecosystem Health. – Polish Journal of Environmental Studies 23(3): 901-908.
[51] Vargo, G., Hutchins, M., Almquist, G. (1982): The effect of low, chronic levels of no. 2 fuel oil on natural phytoplankton assemblages in microcosms: 1. Species composition and seasonal succession. – Marine Environmental Research 6(4): 245-264.
[52] Verlecar, X. N., Desai, S. (2004): Phytoplankton Identification Manual. – First Dona Paula, Goa: National Institute of Oceanography.
[53] Verlecar, X. N., Desai, S. R., Sarkar, A., Dalal, S. G. (2006): Biological indicators in relation to coastal pollution along Karnataka coast, India. – Water Research 40(17): 3304-3312.
[54] Wang, D. (2015): Remote Sensing-Based Study on the Temporal Variations in Chlorophyll-a Concentration After Confo Oil Spill in Bohai Sea. – Journal of the Indian Society of Remote Sensing 43(1): 133-142.
[55] Wickham, H., Averick, M., Bryan, J., Chang, W., D'Agostino McGowan, L., François, R., Grolemund, G., Hayes, A., Henry, L., Hester, J., Kuhn, M., Pedersen, T. L., Miller, E., Milton Bache, S., Müller, K., Ooms, J., Robinson, D., Paige Seidel, D., Spinu, V., Takahashi, K., Vaughan, D., Wilke, C., Woo, K., Yutani, H. (2019): Welcome to the tidyverse. – Journal of Open Source Software 4(43): 1686.

http://www.aloki.hu ● ISSN 1589 1623 (Print) ● ISSN 1785 0037 (Online)
DOI: http://dx.doi.org/10.15666/aeer/1902_13531370
© 2021, ALÖKI Kft., Budapest, Hungary

SPATIAL AND TEMPORAL CHANGES OF VEGETATION COVER IN CHINA BASED ON MODIS NDVI

KASORO, F. R.[1] – YAN, L.[1*] – ZHANG, W.[2*] – ASANTE-BADU, B.[1]

[1]*College of Resources and Environment Sciences, Jilin Agricultural University, Changchun, PR China*

[2]*Research Center for Total Emission Control and Trading of CAEP, Chinese Academy for Environmental Planning, Beijing 100000, China*

**Corresponding authors*
e-mail/phone/fax: yanlijau@163.com/+86-155-2686-6351; lunwen201906@163.com

(Received 17th Nov 2020; accepted 8th Feb 2021)

Abstract. Vegetation in China experienced serious threat from several driving forces such as population growth and anthropogenic activities. Real-time mapping and assessment of yearly vegetation cover is vital to understand environmental conditions. Here, we examined the trend of vegetation cover changes in China over a 15-year period using remote sensed data. To achieve this, we reclassified the Normalized Difference Vegetation Index (NDVI) values into four classes: No, Low, Medium, and High covers and proceeded to vegetation change detection. The results indicated a difference in values at each level. At the national level, there is an increase in vegetation cover as reflected by High cover class with 41.03% in 2015. At the regional level, the most significant changes were determined in the south where the rate of green cover was declining by -63622.3 km^2 from 2000 to 2015 in the High cover class. Vegetation cover changes varied from province to province. Some provinces showed a reduction in vegetation cover such as Guangdong; whereas Xinjiang experienced an increase (*Tables A1* and *A2*). The findings of this study provide further information on China's vegetation cover and will also serve as reference for future research.
Keywords: *remote sensing, satellites, monitoring, forest, environment*

Introduction

In the past decades, the Earth has experienced fast population growth which has led to a rise in demand and supply for consumer goods and products thereby leading to an overuse of natural resources from the ecosystem (Hutchinson, 1969; FAO, 1997; Li et al., 2013b; Obienusi et al., 2014). Consequently, this has exerted significant pressure on the ecosystem which in turn has led to a series of environmental issues such as soil erosion from water runoff (Arima et al., 2005), pollution through industrial emission of hazardous substances (Caldas et al., 2007) or soil degradation from intensive use of pesticides (Pacheco and Poccard-Chapuis, 2012) and fertilizers (Kaimowitz and Angelsen, 1998). Furthermore, issues of deforestation (resulting from excessive logging, bush fire, agricultural activities, urbanization) (Islam et al., 2018; Lambin, 1994), energy generation (Ratcliffe, 1984; Sasaki and Takahara, 2011) and tourism (Burden and Randerson, 1972; Kerbiriou et al., 2008; Lucas-Borja et al., 2011) are high. All these activities lead to a reduction in the quantity and quality of natural resources available in the ecosystem (Vitousek et al., 1997). Globally, research has proven that vegetation cover that has undergone pressure from anthropogenic activities is more significant than vegetation without pressure (Zubair, 2006; Jacinthe and Lal, 2006; Wang et al., 2014). In addition, changes in vegetation cover have a more important

http://www.aloki.hu ● ISSN 1589 1623 (Print) ● ISSN 1785 0037 (Online)
DOI: http://dx.doi.org/10.15666/aeer/1902_13711390
© 2021, ALÖKI Kft., Budapest, Hungary

effect on the ecosystem than changes in climatic factors (Jensen, 1996) and China is equally affected by these pressures on the ecosystem.

China is a leading country in technology, industrial development and has the largest population over the world (United Nations, 2017). From the 1970s, the country has undoubtedly undergone rapid economic expansions and urbanization (Wang, 2010) and has managed to take a great number of its population out of poverty. According to Yan et al. (2017), China's population explosion has led an alarming expansion of urban areas from 17.92% in 1978 to 57.35% in 2016 and was projected by the National Bureau of Statistics of the People's Republic of China to reach 60% in 2020. Despite the great benefit behind the development of China, the effect of the development on the ecosystem has caused an alarming degradation level. For instance, mining projects have negatively affected the vegetation and contributed to spatial changes in Pingshuo opencast coal mining located in Shanxi province (Zhang et al., 2019). In addition, some research have observed deficit in ecosystem resources and an important green land transformation in built up areas, agricultural land, opencast mining, and barren land which have largely influenced the decrease in vegetation cover (Zhang et al., 2007; Wang, 2010).

Owing to the complex situation of vegetation cover changes in China, the government implemented several laws and policies on ecosystem protection mainly for vegetation conservation. According to some studies, the country has financed several projects with the amount of 354 billion Yuan from 1999 to 2003 and with 1636 billion Yuan for environmental restoration and protection from the year 2003 to 2008 (Kauppi et al., 2006; Piao et al., 2009; Liang et al., 2018). The results of all these attempts have been positive in several provinces with a significant vegetation growth and reduction of degradation of the ecosystem. Nevertheless, permanent monitoring and mapping of vegetation cover dynamic at different scales is important in order to predict the future state, understand and assess the development and changes that occur as a consequence of human activities (Bozkaya et al., 2015; Gu et al., 2016; Weng, 2001; Mao et al., 2011; Mu et al., 2012; Mooney et al., 2013; Sterling et al., 2013).

Several methods were applied in some studies for analyzing the trend of vegetation cover and were mainly based on traditional surface measurement methods with a mandatory field observation (Liu et al., 2018). These methods have good precision, however, they showed limitations due to high cost and the results are often personal to the data collector (Wei et al., 2006) when the study is on a large scale (Lu, 2006; Bao et al., 2014; Zhou et al., 2015). Therefore, other methods have emerged such as remote sensing with the benefits of brief sampling time, dynamic data, wide scale cover, spectral resolution, and minimal costs (Gillespie et al., 2018; Zoungrana et al., 2018). Remote sensing becomes a method widely adopted and applied in land survey and vegetation cover analysis because of its ability to offer multi-spatial and temporal crop cover changes (Zhang and Wu, 2015). Furthermore, it has been given free access on earth data with a great amelioration on methods analysis (Gutman et al., 2013).

Recently, there has been growing interest in the use of Moderate Resolution Imaging Spectroradiometer (MODIS) NDVI data for land cover analysis and monitoring especially vegetation cover (Beck et al., 2006; Lunetta et al., 2006; Jacquin et al., 2010; Louise et al., 2014; Usman et al., 2015; Zoungrana et al., 2018). MODIS NDVI products have been mostly used in studies over large surface areas compared to other NDVI products such as VEGETATION instrument on Satellite Pour l'Observation de la Terre (SPOT VGT) and National Oceanic Aeronautic Administration Advanced Very

http://www.aloki.hu ● ISSN 1589 1623 (Print) ● ISSN 1785 0037 (Online)
DOI: http://dx.doi.org/10.15666/aeer/1902_13711390
© 2021, ALÖKI Kft., Budapest, Hungary

High-Resolution Radiometer (NOAA-AVHRR) NDVI (Fensholt and Sandholt, 2005; Fensholt et al., 2006). They have high-sensitivity radiometric information in 36 spectral bands allowing in-depth perception of the changes that happened in the different components of land cover (Wang et al., 2013). In addition, they have three different spatial resolutions which are 250 m, 500 m and 1000 m making it possible to achieve studies at different scales (Skole et al., 1997; Janetos and Justice, 2000). Since MODIS NDVI products provide spatial resolution, surface anisotropy, calibration, atmosphere correction, grid protection, vegetation sensitivity and cloud detection, they are considered as one of the most sophisticated remote sensing data images and mostly used in land cover monitoring (Yan et al., 2013). Furthermore, the NDVI contained in the MODIS data is described as a quantitative index which explains the health of vegetation cover by using the near infrared and visible band (Carlson and Ripley, 1997) and it is among the most applied indices for monitoring changes in vegetation cover (Scanlon et al., 2002; Yang et al., 2012; Zhang et al., 2018).

Investigations carried out by several authors (Liping et al., 2018; Xu et al., 2018), applied remote sensing techniques to assess the global trend of vegetation cover changes, including China. Their findings showed how remote sensing is a reliable method to understand land cover changes by providing accurate information on vegetation changes. Going further, numerous studies have used vegetation indices to detect the vegetation cover changes which were limited to either provincial or regional levels in China (Mu et al., 2012; Li et al., 2013b; Zhang et al., 2017). However, few of them have assessed the spatial and temporal changes in vegetation at three levels in China using MODIS NDVI time series. Therefore, our study provides useful information on vegetation cover trend for provincial, regional, and national levels.

Thus, the current research attempts to assess spatial and temporal changes of vegetation cover throughout China using MODIS NDVI data products over a 15-year period from 2000 to 2015. As a move in this direction, we hope that this research could be used as a starting point for further studies which intense will help local policymakers in environmental sustainability.

Review of literature

Vegetation cover is considered as a key constituent of the ecosystem and covers almost 70% of the earth land cover (Arellano et al., 2015; Veraverbeke et al., 2012; Zhou et al., 2015; Peng et al., 2015). It plays a major role in biogeochemical and hydrological cycles. Additionally, it connects with others natural constituents of the environment such as soil, water, and the atmosphere (Piao et al., 2003). Several environmental services and functions such as carbon sequestration, water and soil sustentation, air purification, and preservation of biodiversity are provided by vegetation which is important for all living things on the earth (Sheram, 1993; Wang et al., 2012). Vegetation cover is also an indicator of any change that occurs in the ecosystem (Lambin and Strahler, 1994). Furthermore, vegetation is one of the key elements in climate change mitigation and the reduction of greenhouse gases (Caputo, 2009; Moroni, 2013) and portrays an important function in the conservation and regulation of environmental quality (Piao et al., 2011; Peng et al., 2012; Yan et al., 2017).

http://www.aloki.hu ● ISSN 1589 1623 (Print) ● ISSN 1785 0037 (Online)
DOI: http://dx.doi.org/10.15666/aeer/1902_13711390
© 2021, ALÖKI Kft., Budapest, Hungary

Materials and methods

Description of the study area

The study was conducted in the People's Republic of China (PRC) which is the third largest country in the world with 9.6 million km² with almost 21% of the global population. China is located in the east side of Asia, between 73°33'E-135°05'E and 3°51'N-53°33'N (*Fig. 1*).

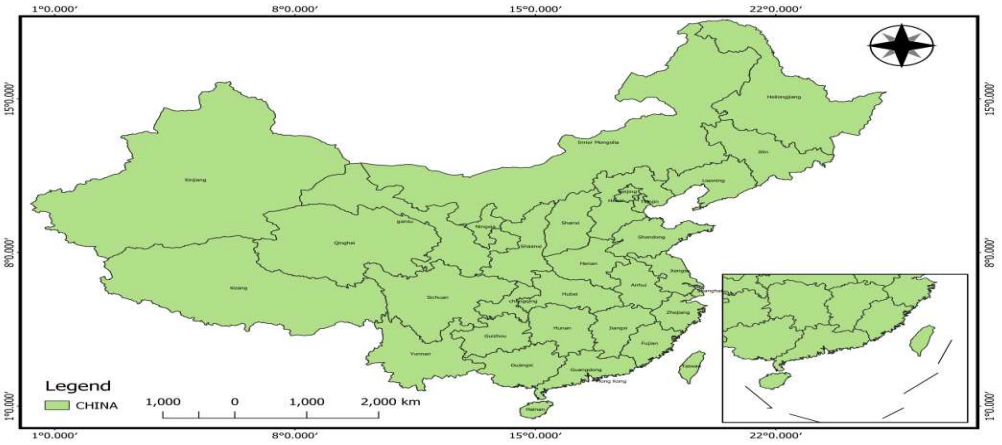


Figure 1. *Overview of the study area*

China is covered by mountains, plateaus, valleys, plains and hills. The administrative subdivision of China is as follows: 4 municipalities, 5 autonomous regions and 23 provinces, as well as Macao and Hong Kong which are considered as special territories.

The study area has four main agro-climatic zones: the semi-humid zone and the humid zone in the southern and southwestern part of China, the arid zone in the western and northwestern, and the semi-arid zone in the central. Heavy rainy season extends in the northern part from June to September and in the southern part from April to August.

The average annual rainfall is estimated at 645 mm but may reach 1000 to 2000 mm in the southeast and southwest coastal regions. The research area has an abundant sunlight and radiation estimated between 3200 and 3300 h. China has a very diverse flora and is considered as one of the countries with the richest vegetation on the planet.

Our study was conducted on three scales: the national, regional, and provincial levels as described in *Table 1*. *Table 1* shows the description of different China's regions. The Special Territory of Macao was not analyzed as part of this research due to a lack of information and data.

Data source

In this research, the data used to assess the trends in vegetation in China over a fifteen-year period was MODIS NDVI data (MODND1M). The selected MODIS NDVI data was obtained from the web interface http://www.gscloud.cn./ and was presented by the satellite in a gridded appearance with a sinusoidal or periodic projection. The spatial resolution of the collected data was 500 m with a temporal resolution of 32 days.

The selected data of the years 2000, 2005, 2010, and 2015 were collected during summer in June because vegetation cover is usually varying accordingly to seasonal

http://www.aloki.hu ● ISSN 1589 1623 (Print) ● ISSN 1785 0037 (Online)
DOI: http://dx.doi.org/10.15666/aeer/1902_13711390
© 2021, ALÖKI Kft., Budapest, Hungary

factors which is favorable to generate a better reflectance in that period of the year, marked by the growing season in China.

Table 1. *Description of regions and provinces with their climate and terrain information*

Regions	Provinces	Climate	Topography
N	Inner Mongolia, Beijing, Tianjin, Shanxi, and Hebei	Semi-humid continental monsoon	Mountains, plains, and plateaus
E	Anhui, Fujian, Jiangxi, Jiangsu, Shandong, Shanghai, Taiwan, and Zhejiang	Subtropical monsoon humid	Plains, hills, and mountains
N-E	Jilin Heilongjiang, and Shenyang	Temperate continental monsoon	Mountains and hills
N-W	Xinjiang, Qinghai, Gansu, Shaanxi, and Ningxia	Semi-humid continental monsoon	Mountains and plateaus
S	Hong Kong, Hainan, Guangdong, and Guangxi	Subtropical and tropical monsoon	Hills, plains, mountains, and plateaus
S-W	Sichuan, Yunnan, Guizhou, Chongqing and Xizang	Subtropical wet monsoon	Hills, mountains, and plateaus
S-C	Hubei, Hunan, and Henan	Subtropical monsoon	Mountains and plains

N is north; E is east; N-E is northeast; N-W is northwest; S is south; S-W is southwest; S-C: south central

Data analysis

The selected MODIS NDVI data from the years 2000, 2005, 2010 and 2015 were clipped, extracted from all China (provinces and regions), projected with the Xian 1981 coordinate system using ArcGIS 10.5 software. Moreover, the reclassification of the images was performed based on the NDVI value of each pixel into four classes No, Low, Medium and High cover, respectively (Hashim et al., 2019; Sahebjalal and Dashtekian, 2013). The NDVI value is estimated between -1 and + 1, the highest value showed a greener cover and the lowest for a barren land, urbanized or water areas (Madonsela et al., 2018). The NDVI is often determined with the following formula (*Eq. 1*) by Tucker (1979):

$$\mathrm{NDVI} = \frac{(\mathrm{NIR}-\mathrm{RED})}{(\mathrm{NIR}+\mathrm{RED})} \quad \text{(Eq.1)}$$

where *RED* is the value of reflectance of red band and *NIR* is the near infrared band.

As described in *Table 2*, the NDVI values for the study area range from 0.1 to 0.9. Thus, after the reclassification of the NDVI images for the years 2000, 2005, 2010 and 2015, the new land cover maps for the different corresponding years were produced using ArcGIS 10.5 and QGIS 3.

Vegetation cover change analysis

Change detection images time series is a remote sensing method applied to estimate and locate changes occurred in a study area. This method is mainly established on the comparison of the spectral change of the image between two time periods (*Eqs. 3* and *4*).

http://www.aloki.hu ● ISSN 1589 1623 (Print) ● ISSN 1785 0037 (Online)
DOI: http://dx.doi.org/10.15666/aeer/1902_13711390
© 2021, ALÖKI Kft., Budapest, Hungary

It is widely used and is very useful for vegetation cover change studies (Lu et al., 2004; Coppin et al., 2004; Kashaigili et al., 2006).

Table 2. *NDVI density classes*

Vegetation classes	Description	Vegetation cover (NDVI)
No vegetation	Barren land, built up areas, road network and water	< 0.1
Low vegetation	Shrub land	0.1 -0.3
Medium vegetation	Grassland and agriculture land	0.3 - 0.6
High vegetation	Forest land	0.6- 0.9

In this research, change detection analysis was conducted to understand the trend of spatial variations in vegetation cover in fifteen years.

As a result, the trend of change of each class and year were calculated in km² and then converted to percentages (%) as shown in *Equation 2*. The results obtained helped to detect and identify changes occurred in China on three different scales. The percentage rate of each class was calculated by:

$$n = \frac{A*100}{S} \quad \text{(Eq.2)}$$

where n was the percentage rate of each class, A was surface area of each class and S was the total surface area in km^2.

Percent area change between the two periods (2000 and 2015) was calculated according to the following equation:

$$PAC = \left(\Delta A/_T\right) * 100 \quad \text{(Eq.3)}$$

where PAC corresponds to the Percent area change, ΔA was the value of the final and initial years (a_2-$a_{1)}$, and T was total area of the study area.

Percent annual rate (PAR) of change was estimated by the formula:

$$PAR = \left(\Delta A/_T * 100\right)/n \quad \text{(Eq.4)}$$

where n denote the number of years between the initial and final years

Results

Spatial variation of vegetation coverage classes from 2000 to 2015 at national level

Following the NDVI density classes in *Table 2*, the spatial and temporal changes of vegetation cover were revealed from the year 2000 to 2015. As shown in *Table 3*, the results demonstrated that in 2000, 17.75% of the land cover in China was found to be in No cover class (barren land, water, road network, and built-up areas). Notwithstanding, in 2005, 2010 and 2015 of the same class, results showed a change of 17.43%, 15.50% and 15.15%, respectively. The Low class characterized by shrub land experienced a saw-tooth dynamic, increase, and decrease during the fifteen years of study with 21.21% in 2000 and 20.72% in 2015, respectively. However, the Medium and High

http://www.aloki.hu ● ISSN 1589 1623 (Print) ● ISSN 1785 0037 (Online)
DOI: http://dx.doi.org/10.15666/aeer/1902_13711390
© 2021, ALÖKI Kft., Budapest, Hungary

classes showed a significant rise in the area of vegetation with 22.60% in 2000 and 23.10% in 2015, and 38.44% in 2000 and 41.03% in 2015, respectively.

The results in *Table 3* indicate the change in vegetation cover area from 2000 to 2015. It showed that the No cover and Low cover classes lost 2.61% and 0.49% respectively, i.e., -248679.97 km² and -46629.71 km² of surface area. In contrast, the Medium and High classes gained a 0.61% and 2.36% respectively, i.e., 48259.71 km² and 246341.28 km². All these results may reveal that forests and grasslands have increased slightly while barren land or shrub lands areas have decreased. Further information is also demonstrated in *Figure 2*.

Table 3. *Evolution of vegetation cover from 2000 to 2015*

Types of vegetation	Spatial area cover								Change area (2000-2015)		The annual rate of change (2000-2015)
	2000		2005		2010		2015				
	Area (km²)	%	Area (km²)	%	Area (km²)	%	Area (km²)	%	Area (km²)	PAC	km²/year
No	1693988	17.75	1662832	17.43	1479306	15.5	1445309	15.15	-248679	2.61	0.17
Low	2023697	21.21	2024872	21.22	2063100	21.62	1977067	20.72	-46630	0.49	0.03
Medium	2156018	22.6	2241893	23.49	2296709	24.07	2204278	23.1	48259.7	0.61	0.04
High	3668111	38.44	3613107	37.86	3702681	38.8	3914452	41.03	246341	2.36	0.16

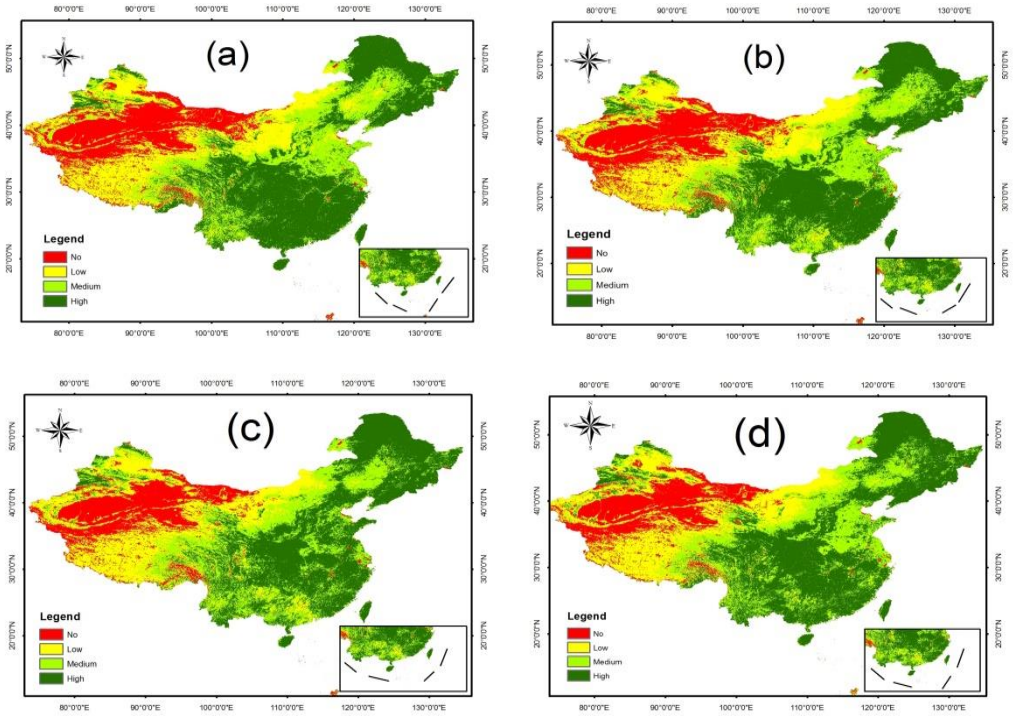


Figure 2. *The vegetation cover maps for the year (a) 2000, (b) 2005, (c)2010 and (d) 2015*

Spatial and temporal trend analysis (2000-2015)

Trend in changes of vegetation cover over the period of 2000 to 2015 at regional level

Table 4 shows variation of vegetation cover over 2000 through 2005 and 2005 through 2010. The findings for 2000 to 2005, showed that the southwestern and the

http://www.aloki.hu ● ISSN 1589 1623 (Print) ● ISSN 1785 0037 (Online)
DOI: http://dx.doi.org/10.15666/aeer/1902_13711390
© 2021, ALÖKI Kft., Budapest, Hungary

southern were highest in values in terms of No cover class with 44946.27 km^2 and 1080 km^2 respectively. However, in the northwestern and northern regions there were reduction of No cover class areas for the same period with -43528.9 km^2 and -34278 km^2. In addition, for the same period the results revealed a significant decrease in High cover class in the south-central region with -21475.5 km^2.

Similarly, the results of the 2005-2010 are presented in the same *Table 4*. It was observed that most regions such as the northern, northwestern and southwestern the amount of No cover areas were significantly reduced hence these could be converted to Low, Medium or High cover classes. Obviously, most of the regions revealed an increase in vegetation cover; with the exception of southern and southwestern regions which detected a decrease in High cover with -21391.9 km^2 and -226147 km^2, accordingly.

Comparing the results of both 2000-2005 and 2005-2010 in *Table 4,* the study reveals that from 2000 to 2010, there was positive improvement of vegetation cover areas in most of the regions, even though, there were few instances where reduction occurred.

Table 4. *Statistics of vegetation cover from 2000 to 2005 and from 2005 to 2010 at regional scale*

Regions	2000-2005				2005-2010			
	No	Low	Medium	High	No	Low	Medium	High
N	-34278	-14262	-11363	60002	-44479.5	-77161.9	-14455.6	136124
E	938	-5345	-12127	16466	-377.18	3111.15	-84532.8	81834.82
NE	-475.84	-8659.63	-8158.72	18307.48	-457.81	6193.9	-86495.7	92139.94
NW	-43528.9	18753.2	17384.88	7393.1	-94915.9	-38133.2	106460.2	26577.35
S	1080.18	40403.64	133853.6	-175378	760.43	7248.51	13367.62	-21391.9
SW	44946.27	-32154.7	-52470.7	39676.16	-44307.1	143808.6	126592.7	-226147
SC	162.92	2529.1	18776.07	-21475.5	250.42	5457.88	6139.24	437.12

The statistic of vegetation changes is estimated from 2010 to 2015 and from 2000 to 2015 at regional level in China (*Table 5*). Based on the results of 2010 to 2015, the northwestern, northern and southern regions experienced a reduction in No cover areas with -7846.14 km^2, -4070.48 km^2, -1686.47 km^2; whereas the southwestern and northeastern had an increase in No cover areas with 24165.9 km^2 and 2608.59 km^2. Our findings also showed that in High cover class, that is, southern and the southwestern regions there were significant increment in vegetation from 2010 to 2015.

Table 5. *Statistics of vegetation cover from 2010 to 2015 and from 2000 to 2015 at regional scale*

Regions	2010-2015				2000-2015			
	No	Low	Medium	High	No	Low	Medium	High
N	-4070.48	24106.01	34693.1	-54749.9	-82827.5	-67318	8874.36	141376.1
E	572.62	744.32	121306.7	-122686	1133.58	-1489.59	24647.34	-24384.9
NE	2608.59	-235.53	11289.59	-14179.7	1674.94	-15089.1	-83364.9	96267.69
NW	-7846.14	11572.6	-77238.5	73420	-146291	-7807.24	46606.58	107390.5
S	-1686.47	-40159.1	-91273.5	133147.3	154.14	7493.07	55947.63	-63622.3
SW	24165.9	-76033.4	-101014	201258.7	-23526.7	35620.57	-26891.6	14787.68
SC	590.23	-6027.38	9805.71	-4366.68	1003.57	1959.6	22442.54	-25405.1

http://www.aloki.hu ● ISSN 1589 1623 (Print) ● ISSN 1785 0037 (Online)
DOI: http://dx.doi.org/10.15666/aeer/1902_13711390
© 2021, ALÖKI Kft., Budapest, Hungary

From 2000 to 2015, the results of the study illustrated that there was a general decrease of No cover areas in the northern, southwestern and northwestern regions; while High cover areas showed a significant improvement over the fifteen years (*Table 5*). This may be as a result of the efforts made by the local and central governments to improve forest. On the contrary, the southern, eastern and south central regions recorded a reduction in vegetation cover with -63622.3 km^2, -24384.9 km^2 and -25405.1 km^2, respectively. The results can be concluded as having experienced a saw-tooth trend in each class of vegetation for the fifteen years study period.

Trend in changes of vegetation cover over the period of 2000 to 2015 at provincial level

Table A1 shows the changes in vegetation areas from 2000 to 2005 for each municipalities, autonomous cities and provinces of China. The results revealed that vegetation cover decreased, as shown in the High cover class, in some provinces such as Heilongjiang, Henan, Guangxi, and Qinghai with -16550.09 km^2, -12110.08 km^2, -131949.5 km^2, -12105.383 km^2, accordingly. However, other provincial levels demonstrated an increase of green vegetation during the same period. For instance, Inner Mongolia, Hebei, Sichuan, and Gansu with 17822.12 km^2, 26496 km^2, 29867.89 km^2, and 9522.64 km^2, respectively.

Similarly, changes in vegetation for the years 2005 to 2010 were produced and presented in *Table A1*. The data shows that numerous municipalities, autonomous cities and provinces which demonstrated a decrease in vegetation in previous years (2000-2005) had a significant increase in High cover class; for example Heilongjiang, Henan and Anhui. Furthermore, most provinces experienced significant reduction in No cover areas such as Xizang and Qinghai with -48234.65 km^2 and -21019.3 km^2. Nevertheless, most of provinces indicated an obvious change in both No and High cover classes.

For the years 2010-2015, our findings show that No cover class representing barren lands or built-up areas have escalated in Heilongjiang, Qinghai and Gansu with 212.41 km^2, 4932.93 km^2, and 3985 km^2; whereas most of the provinces reveal an increase in vegetation cover as referred to High cover class (*Table A2*).

In general, the results indicated an improvement in vegetation cover for many provinces; for instance Xinjiang, Heilongjiang, Jilin, Liaoning, Shaanxi and Gansu over the period of study. Even though there were huge reclamation of vegetation, provinces like Guangxi, Guangdong, Fujian, Jiangxi, Hunan, and Hubei showed degradation of forest zones mainly located in eastern and southern China as shown in *Table A2*.

Discussion

The continuous estimation and analysis of vegetation cover changes at different scales is a crucial tool for an in-depths understanding of the changes that happened in the ecosystem. This aims to establish a link with all ecosystem components and to acknowledge the driving factors that caused these changes. As aforementioned, remote sensing data has been demonstrated to be one of the best and widely applied methods used in several studies to assess changes in vegetation cover and the ecosystem (Guo et al., 2016; Lyon et al., 1998; Jia et al., 2014).

At the national level, the findings demonstrated that vegetation cover areas have risen throughout China. The analysis of vegetation trends revealed that in 2000, the vegetation cover was less dense than that observed in 2015 with 38.44% and 41.03%, respectively (*Table 3*). These changes are mainly reflected by the conversion in areas

http://www.aloki.hu ● ISSN 1589 1623 (Print) ● ISSN 1785 0037 (Online)
DOI: http://dx.doi.org/10.15666/aeer/1902_13711390
© 2021, ALÖKI Kft., Budapest, Hungary

from the No and Low cover classes to Medium or High cover classes in 2015 (*Table 3*). The slight evolution of forest land by 2.36% (*Table 3*) observed during the study period may be the results of greater efforts undertaken by the central government to conduct environmental restoration projects, particularly to increase green vegetation throughout the country. These results are consistent with studies (Xu et al., 2018) who indicated that 83.34% of China's territory are experiencing a general increase in vegetation due to environmental restoration projects. Recently, the 9th National Forest Inventories (NFI) revealed that there was an increase of forest lands (National Forestry and Grassland Administration, 2019). Similarly, Liang et al. (2018) indicated a rise in forest areas with 3.60 million ha over the 25 years of study (1982-2006) or 0.15 million ha/year. Besides these successes, the government has also promulgated a series of laws aimed at strengthening environmental restoration and management measures (Chunmei and Zhaolan, 2010; Sims, 1999; Zhang et al., 2007). For example, the Environmental Protection Law which has been formed to lead to ecological protection while industrial development will still be undertaken (Zwierzchowski and Rott-Pietrzyk, 2020; Mu et al., 2014).

Further, several other green building projects have been implemented such as "Pastureland to Grassland", "Shelterbelt", and "Grain to Green" with the same goal of improving vegetation conditions and to reduce human pressure on the ecosystem (Bennett and Smith, 2017; Xu et al., 2017). With the establishment of these projects, a significant change of forest areas has been recorded in the different zones where they have been carried out in China (Zhang et al., 2018; Li et al., 2018). Additionally, the growth in forest lands detected in these study areas may be as a result of climate change experienced in recent years around the globe including China. The contribution of climate change was explained by various authors that global warming has favored the lengthening of the vegetative season and also has increased the photosynthesis capacity of plants in non-arid areas. This has greatly influenced the growth in forests, grassland and the reduction of barren areas (Niemand et al., 2005; Piao et al., 2007, 2008; Arellano et al., 2015; Xu et al., 2014). Contradictorily, some authors declared a decrease in vegetation cover. According to Cao et al. (2011) vegetation lost in China has been intensified because of the unchecked reforestation projects. This lost is due to the fact that they do not take into account local conditions (pedology, hydrology or climate factors) and the use of unsuitable tree species in the regions which could not adapt to soil or weather conditions.

At regional level, the results (*Table 5*) indicated that the southern, south-central, and eastern regions have decreased in vegetation cover areas, over the fifteen years, with -63622.3 km^2, -25405.1 km^2, and -24384.9 km^2, respectively. Even though some studies indicated an increase in vegetation cover in these regions as a results of vegetation restoration projects (Wang et al., 2015). These three regions are among the most urbanized, populated, and developed regions in China. Therefore, the intense activities occurring may be due to changes in vegetation cover. For instance, a progressive reduction in green areas in the eastern were detected in *Tables 4* and *5*. These results are consistent with studies carried out by several authors in the eastern region. They noted that the excessive resource utilization, the conversion of forest to cropland and the increase in built-up areas have greatly impacted the urban and non-urban forest areas (Fan et al., 2015; Song et al., 2018; Zhang and Huang, 2019). Furthermore, studies showed that the high rate of population density increase of this region, with 503 persons

http://www.aloki.hu ● ISSN 1589 1623 (Print) ● ISSN 1785 0037 (Online)
DOI: http://dx.doi.org/10.15666/aeer/1902_13711390
© 2021, ALÖKI Kft., Budapest, Hungary

per km^2 in 2000 to 566 persons per km^2 in 2010, has also contributed the decrease in vegetation areas (Yu et al., 2018).

In addition, topography and climate may also act as driving forces for vegetation change. Topography influences vegetation distribution and density (Xin and Xu, 2007; Pan et al., 2003). As mentioned previously in *Table 1*, China has various terrain structure such as plains and plateaus which may be the cause of fast vegetation degradation. According to Zhao et al. (2014), forest lands are more dense in the upper terrain than in lower elevation. These low elevations facilitate access to human-being for resources extraction which might result to fast vegetation alteration in the east, south and south-central regions of our study area. Furthermore, several studies have stated that changes in climate conditions in China plays a crucial role in vegetation distribution. This is mainly due to the fact that temperature and precipitation changes with time and hence have great impact on vegetation cover growth in several regions, including the southern and eastern China's regions (Wang et al., 2019; Xu et al., 2014).

In contrast, the north, northeast, and northwest regions showed significant growth of vegetation cover over the fifteen years period, with 141376.1 km^2, 96267.69 km^2, and 107390.5 km^2, accordingly. Our findings agree with ShengPei et al. (2011) and Wei et al. (2018) who carried out studies on vegetation cover in the northwestern of China from 1982 to 2006 and 2000 to 2010, respectively. The increase in vegetation was illustrated with a rise in NDVI values over the study period due to barren lands reduction by 40,925 km^2 and forest improvement of 10% (ShengPei et al., 2011). Going further, both research indicated that grassland and forestland expansion in the northwestern China, was as a consequence of the Three-North Shelterbelt, Return Cultivated Land for Forest Land and Grass Land Projects.

At the provincial level, the results of 34 provinces, including autonomous cities and municipalities, were shown in *Tables A1* and *A2* with a constant five-year interval. The results depicted an obvious difference in each province. From the year 2000 to 2015, High cover areas evolved slightly in Xinjiang, Inner Mongolia, Gansu, Yunnan and Shandong provinces, with 40239.77 km^2, 60650.32 km^2, 33835.56 km^2, 39962.94 km^2, and 33020.3 km^2, respectively as indicated in *Table A2*. Additionally, some provinces such as Guangdong, Guangxi and Jiangxi showed irregular changes or a reduction in vegetation cover over the 15-year period. Our results are in conformity with a study carried out by Hu et al., (2019) and Zhang et al. (2020). Their results showed that Guangdong, Guangxi and Jiangxi had decreased in green cover; whereas in Inner Mongolia and Yunnan there was an increase. However, other studies indicated that Jiangxi has demonstrated a slight increase of vegetation due to reforestation projects, and a significant forest loss in Inner Mongolia due to rainfall and temperature change (Xu et al., 2014; Song et al., 2018).

Studies have explained the cause of vegetation cover change at provincial level in China as a consequence of various factors such as migration and population growth. Most of these studies are focused on human activities due to the rapid development that occurs in China since their economic reform. These factors influenced land use change in several ways. In China, the migration of population from rural to urban regions has brought about a significant increase in population density. This has also led to demand for land and raw materials causing a decrease in urban forests areas and grasslands (Walker et al., 2000; Barbieri and Carr, 2005; Carr, 2009; Zhou et al., 2014), and the degradation of ecosystems resources (Wang et al., 2014; Liu et al., 2014). For example, it was indicated that Guangdong province experienced a rapid growth of population

http://www.aloki.hu ● ISSN 1589 1623 (Print) ● ISSN 1785 0037 (Online)
DOI: http://dx.doi.org/10.15666/aeer/1902_13711390
© 2021, ALÖKI Kft., Budapest, Hungary

mainly attributed to fast economic expansion and geographical conditions which has impacted vegetation cover growth in suburban areas (Li et al., 2013a). In addition, an investigation conducted in Guangxi province also illustrated that population growth has influenced the transition of forestland and grassland to urban areas from 1990 to 2017 (Hu et al., 2019). Therefore, these examples show how human activities are the key to drastic vegetation cover loss in some provinces or municipalities in China.

It has also been shown that vegetation and weather conditions are interrelated (Xia et al., 2007). To be more precise, vegetation is sensitive to microclimate variations, thus this may have probably contributed to the vegetation cover changes of each province where there were changes depicted in High cover class.

Conclusion

Ecosystem health is determined by vegetation cover conditions. Therefore, providing information on the vegetation cover changes constitute an important and fundamental guideline for monitoring the environment. Implementation of effective laws with the purpose of protecting the vegetation from anthropogenic pressure as well as from natural pressure is vital. This research determined the spatial and temporal evolution trend of the vegetation cover in China by using MODIS NDVI data over a period of fifteen years. The study indicated a general trend of vegetation cover at national level in terms of increase in forestland and grasslands. Notwithstanding, the reduction of vegetation cover observed within the study area (regional and provincial levels) may be the results of several driving factors such as rapid population growth, climatic change, urbanization and fast development that occurred in China which need deeper investigations. The results of this study constitute a reference point for future research and a decision-making tool for ecosystems management and restoration. Future research should therefore focus on: (i) a more in-depth study of China's vegetation cover using other satellite products and classification methods which can provide the current and future vegetations conditions and in situ observations. (ii) More research of the driving factors that induce vegetation cover changes at three different levels. (iii) at the provincial level, local policymakers ought to strengthen environmental laws and measures in order to maintain vegetation recovery where there were rise in forest areas, for instance Xinjiang and Yunnan. (iv) However, Guangdong and Guangxi (with huge vegetation loss) need to implement more restoration projects which will essentially focus on forest growth.

Acknowledgements. The authors would like to acknowledge the National Key R&D Program of China (2017YFD0201804 and 2016YFD0200403) for their financial support.

REFERENCES

[1] Arellano, P., Tansey, K., Balzter, H., Boyd, D. S. (2015): Detecting the effects of hydrocarbon pollution in the Amazon forest using hyperspectral satellite images. – Environmental Pollution 205: 225-239.

[2] Arima, E. Y., Walker, R. T., Perz, S. G., Caldas, M. (2005): Loggers and forest fragmentation: Behavioral models of road building in the Amazon basin. – Annals of the Association of American Geographers 95: 525-541.

http://www.aloki.hu ● ISSN 1589 1623 (Print) ● ISSN 1785 0037 (Online)
DOI: http://dx.doi.org/10.15666/aeer/1902_13711390
© 2021, ALÖKI Kft., Budapest, Hungary

[3] Bao, G., Qin, Z., Bao, Y., Zhou, Y., Li, W., Sanjjav, A. (2014): NDVI-based long-term vegetation dynamics and its response to climatic change in the Mongolian Plateau. – Remote Sensing 6: 8337-8358.
[4] Barbieri, A. F., Carr, D. L. (2005): Gender-specific out-migration, deforestation and urbanization in the Ecuadorian Amazon. – Global and Planetary Change 47: 99-110.
[5] Beck, P. S., Atzberger, C., Høgda, K. A., Johansen, B., Skidmore, A. K. (2006): Improved monitoring of vegetation dynamics at very high latitudes: a new method using MODIS NDVI. – Remote sensing of Environment 100: 321-334.
[6] Bennett, M. M., Smith, L. C. (2017): Advances in using multitemporal night-time lights satellite imagery to detect, estimate, and monitor socioeconomic dynamics. – Remote Sensing of Environment 192: 176-197.
[7] Bozkaya, A. G., Balcik, F. B., Goksel, C., Esbah, H. (2015): Forecasting land-cover growth using remotely sensed data: a case study of the Igneada protection area in Turkey. – Environmental Monitoring and Assessment 187: 59.
[8] Burden, R., Randerson, P. (1972): Quantitative studies of the effects of human trampling on vegetation as an aid to the management of semi-natural areas. – Journal of Applied Ecology 439-457.
[9] Caldas, M., Walker, R., Arima, E., Perz, S., Aldrich, S., Simmons, C. (2007): Theorizing land cover and land use change: the peasant economy of Amazonian deforestation. – Annals of the Association of American Geographers 97: 86-110.
[10] Cao, S., Chen, L., Shankman, D., Wang, C., Wang, X., Zhang, H. (2011): Excessive reliance on afforestation in China's arid and semi-arid regions: lessons in ecological restoration. – Earth-Science Reviews 104: 240-245.
[11] Caputo, J. (2009): Sustainable Forest Biomass: Promoting Renewable Energy and Forest Stewardship. – EESI, Washington, DC.
[12] Carlson, T. N., Ripley, D. A. (1997): On the relation between NDVI, fractional vegetation cover, and leaf area index. – Remote Sensing of Environment 62: 241-252.
[13] Carr, D. (2009): Population and deforestation: why rural migration matters. – Progress in Human Geography 33: 355-378.
[14] Chunmei, W., Zhaolan, L. (2010): Environmental policies in China over the past 10 years: progress, problems and prospects. – Procedia Environmental Sciences 2: 1701-1712.
[15] Coppin, P., Jonckheere, I., Nackaerts, K., Muys, B., Lambin, E. 2004. Review ArticleDigital change detection methods in ecosystem monitoring: a review. – International Journal of Remote Sensing 25: 1565-1596.
[16] Fan, J., Liu, J., Zhang, X., Cumtb, B. (2015): Urbanization effect on regional household energy consumption in China. – China Population Resources Environment 1: 55-60.
[17] FAO (1997): Estimating Biomass and Biomass Change in Tropical Forests. – FAO, Rome.
[18] Fensholt, R., Sandholt, I. (2005): Evaluation of MODIS and NOAA AVHRR vegetation indices with in situ measurements in a semi-arid environment. – International Journal of Remote Sensing 26: 2561-2594.
[19] Fensholt, R., Sandholt, I., Stisen, S. (2006): Evaluating MODIS, MERIS, and VEGETATION vegetation indices using in situ measurements in a semiarid environment. – IEEE Transactions on Geoscience and Remote Sensing 44: 1774-1786.
[20] Gillespie, T. W., Ostermann-Kelm, S., Dong, C., Willis, K. S., Okin, G. S., Macdonald, G. M. (2018): Monitoring changes of NDVI in protected areas of southern California. – Ecological Indicators 88: 485-494.
[21] Gu, X., Li, W., Wang, L. 2016. Understanding vegetation changes in northern China and Mongolia with change vector analysis. – SpringerPlus 5: 1780.
[22] Guo, H., Huang, Y., Li, X. (2016): Dynamic changes of fractional vegetation cover along the mainstream of the Tarim River. – Journal of Desert Research 36: 1472-1480.

http://www.aloki.hu ● ISSN 1589 1623 (Print) ● ISSN 1785 0037 (Online)
DOI: http://dx.doi.org/10.15666/aeer/1902_13711390
© 2021, ALÖKI Kft., Budapest, Hungary

[23] Gutman, G., Huang, C., Chander, G., Noojipady, P., Masek, J. G. (2013): Assessment of the NASA–USGS global land survey (GLS) datasets. – Remote Sensing of Environment 134: 249-265.
[24] Hashim, H., Abd Latif, Z., Adnan, N. A. (2019): Urban vegetation classification with NDVI threshold value method with very high resolution (VHR) PLEIADES Imagery. Int. Arch. Photogramm. – Remote Sens. Spat. Inf. Sci. 237-240.
[25] Hu, Y., Zhen, L., Zhuang, D. (2019): Assessment of land-use and land-cover change in Guangxi, China. – Scientific Reports 9: 1-13.
[26] Hutchinson, J. (1969): Population and Food Supply. – Cambridge University Press, Cambridge.
[27] Islam, K., Jashimuddin, M., Nath, B., Nath, T. K. (2018): Land use classification and change detection by using multi-temporal remotely sensed imagery: the case of Chunati wildlife sanctuary, Bangladesh. – The Egyptian Journal of Remote Sensing and Space Science 21: 37-47.
[28] Jacinthe, P.-A., Lal, R. (2006): Spatial variability of soil properties and trace gas fluxes in reclaimed mine land of southeastern Ohio. – Geoderma 136: 598-608.
[29] Jacquin, A., Sheeren, D., Lacombe, J.-P. (2010): Vegetation cover degradation assessment in Madagascar savanna based on trend analysis of MODIS NDVI time series. – International Journal of Applied Earth Observation and Geoinformation 12: S3-S10.
[30] Janetos, A., Justice, C. (2000): Land cover and global productivity: a measurement strategy for the NASA programme. – International Journal of Remote Sensing 21: 1491-1512.
[31] Jensen, J. R. (1996): Introductory Digital Image Processing: A Remote Sensing Perspective. – Prentice-Hall Inc, Upper Saddle River, NJ.
[32] Jia, Y., Yu, G., He, N., Zhan, X., Fang, H., Sheng, W., Zuo, Y., Zhang, D., Wang, Q. (2014): Spatial and decadal variations in inorganic nitrogen wet deposition in China induced by human activity. – Scientific Reports 4: 1-7.
[33] Kaimowitz, D., Angelsen, A. (1998): Economic Models of Tropical Deforestation: A Review. – CIFOR, Bogor.
[34] Kashaigili, J. J., Mbilinyi, B. P., MCcartney, M., Mwanuzi, F. L. (2006): Dynamics of Usangu plains wetlands: use of remote sensing and GIS as management decision tools. – Physics and Chemistry of the Earth, Parts A/B/C 31: 967-975.
[35] Kauppi, P. E., Ausubel, J. H., Fang, J., Mather, A. S., Sedjo, R. A., Waggoner, P. E. (2006): Returning forests analyzed with the forest identity. – Proceedings of the National Academy of Sciences 103: 17574-17579.
[36] Kerbiriou, C., Leviol, I., Jiguet, F., Julliard, R. (2008): The impact of human frequentation on coastal vegetation in a biosphere reserve. – Journal of Environmental Management 88: 715-728.
[37] Lambin, E. F. (1994): Modelling Deforestation Processes. A Review. – Research Report, Joint Research Center, Institute for Remote Sensing Applications; European Space Agency, Luxembourg.
[38] Lambin, E. F., Strahler, A. H. (1994): Indicators of land-cover change for change-vector analysis in multitemporal space at coarse spatial scales. – International Journal of Remote Sensing 15: 2099-2119.
[39] Li, C., Kuang, Y., Huang, N., Zhang, C. (2013a): The long-term relationship between population growth and vegetation cover: an empirical analysis based on the panel data of 21 cities in Guangdong province, China. – International Journal of Environmental Research and Public Health 10: 660-677.
[40] Li, X., Zhang, B., Jin, Z. (2013b): Dynamic monitoring of vegetation coverage change in Hedong Area of Gansu based on MODIS-NDVI. – Research of Soil and Water Conservation 20: 112-115+307.

http://www.aloki.hu ● ISSN 1589 1623 (Print) ● ISSN 1785 0037 (Online)
DOI: http://dx.doi.org/10.15666/aeer/1902_13711390
© 2021, ALÖKI Kft., Budapest, Hungary

[41] Li, D., Xu, D., Wang, Z., You, X., Zhang, X., Song, A. (2018): The dynamics of sand-stabilization services in Inner Mongolia, China from 1981 to 2010 and its relationship with climate change and human activities. – Ecological Indicators 88: 351-360.
[42] Liang, L., Chen, F., Shi, L., Niu, S. (2018): NDVI-derived forest area change and its driving factors in China. – PloS ONE 13.
[43] Liping, C., Yujun, S., Saeed, S. (2018): Monitoring and predicting land use and land cover changes using remote sensing and GIS techniques—a case study of a hilly area, Jiangle, China. – PloS ONE 13.
[44] Liu, X., Ma, L., Li, X., Ai, B., Li, S., He, Z. (2014): Simulating urban growth by integrating landscape expansion index (LEI) and cellular automata. – International Journal of Geographical Information Science 28: 148-163.
[45] Liu, H., Zheng, L., Yin, S. (2018): Multi-perspective analysis of vegetation cover changes and driving factors of long time series based on climate and terrain data in Hanjiang River Basin, China. – Arabian Journal of Geosciences 11: 509.
[46] Louise, L., Agnès, B., Danny, L. S. (2014): Regional analysis of crop and natural vegetation in West Africa based on NDVI metrics. – 2014 IEEE Geoscience and Remote Sensing Symposium, IEEE 5107-5110.
[47] Lu, D. (2006): The potential and challenge of remote sensing-based biomass estimation. – International Journal of Remote Sensing 27: 1297-1328.
[48] Lu, D., Mausel, P., Brondizio, E., Moran, E. (2004): Change detection techniques. – International Journal of Remote Sensing 25: 2365-2401.
[49] Lucas-Borja, M., Bastida, F., Moreno, J., Nicolás, C., Andres, M., Lopez, F., del cerro, A. (2011): The effects of human trampling on the microbiological properties of soil and vegetation in Mediterranean mountain areas. – Land Degradation & Development 22: 383-394.
[50] Lunetta, R. S., Knight, J. F., Ediriwickrema, J., Lyon, J. G., Worthy, L. D. (2006): Land-cover change detection using multi-temporal MODIS NDVI data. – Remote Sensing of Environment 105: 142-154.
[51] Lyon, J. G., Yuan, D., Lunetta, R. S., Elvidge, C. D. (1998): A change detection experiment using vegetation indices. – Photogrammetric Engineering and Remote Sensing 64: 143-150.
[52] Madonsela, S., Cho, M. A., Ramoelo, A., Mutanga, O., Naidoo, L. (2018): Estimating tree species diversity in the savannah using NDVI and woody canopy cover. – International Journal of Applied Earth Observation and Geoinformation 66: 106-115.
[53] Mao, D., Wang, Z., Song, K., Liu, D., Zhang, B., Zhang, S., Luo, L., Zhang, C. (2011): The vegetation NDVI variation and its responses to climate change and LUCC from 1982 to 2006 year in northeast permafrost region. – China Environmental Science 31: 283-292.
[54] Mooney, H. A., Duraiappah, A., Larigauderie, A. (2013): Evolution of natural and social science interactions in global change research programs. – Proceedings of the National Academy of Sciences 110: 3665-3672.
[55] Moroni, M. (2013): Simple models of the role of forests and wood products in greenhouse gas mitigation. – Australian Forestry 76: 50-57.
[56] Mu, S., Li, J., Chen, Y., Gang, C., Zhou, W., Ju, W. (2012): Spatial differences of variations of vegetation coverage in Inner Mongolia during 2001–2010. – Acta Geographica Sinica 67: 1255-1268.
[57] Mu, Z., Bu, S., Xue, B. (2014): Environmental legislation in China: achievements, challenges and trends. – Sustainability 6: 8967-8979.
[58] National Forestry and Grassland Administration (2019): Forest Resources in China: The 9th National Forest Inventory. – NFGA, Beijing.
[59] Niemand, C., Köstner, B., Prasse, H., Grünwald, T., Bernhofer, C. (2005): Relating tree phenology with annual carbon fluxes at Tharandt forest. – Meteorologische Zeitschrift 14: 197-202.

http://www.aloki.hu ● ISSN 1589 1623 (Print) ● ISSN 1785 0037 (Online)
DOI: http://dx.doi.org/10.15666/aeer/1902_13711390
© 2021, ALÖKI Kft., Budapest, Hungary

[60] Obienusi, E., Ekezie, M., Onwuka, S. (2014): Investigating the place of population increase and level of income earning in food security a study of yam supply in Awka urban, Anambra state of Nigeria. – J. Nat. Sci. Res 11: 11-21.
[61] Pacheco, P., Poccard-Chapuis, R. (2012): The complex evolution of cattle ranching development amid market integration and policy shifts in the Brazilian Amazon. – Annals of the Association of American Geographers 102: 1366-1390.
[62] Pan, Y., Li, X., Gong, P., He, C., Shi, P., Pu, R. (2003): An integrative classification of vegetation in China based on NOAA AVHRR and vegetation-climate indices of the Holdridge life zone. – International Journal of Remote Sensing 24: 1009-1027.
[63] Peng, D., Zhang, B., Liu, L., Fang, H., Chen, D., Hu, Y., Liu, L. (2012): Characteristics and drivers of global NDVI-based FPAR from 1982 to 2006. – Global Biogeochemical Cycles 26.
[64] Peng, J., Li, Y., Tian, L., Liu, Y., Wang, Y. (2015): Vegetation dynamics and associated driving forces in Eastern China during 1999–2008. – Remote Sensing 7: 13641-13663.
[65] Piao, S., Fang, J., Zhou, L., Guo, Q., Henderson, M., Ji, W., Li, Y., Tao, S. (2003): Interannual variations of monthly and seasonal normalized difference vegetation index (NDVI) in China from 1982 to 1999. – Journal of Geophysical Research: Atmospheres 108. DOI: 10.1029/2002JD002848.
[66] Piao, S., Friedlingstein, P., Ciais, P., Viovy, N., Demarty, J. (2007): Growing season extension and its impact on terrestrial carbon cycle in the Northern Hemisphere over the past 2 decades. – Global Biogeochemical Cycles 21. DOI: 10.1029/2006gb002888.
[67] Piao, S., Ciais, P., Friedlingstein, P., Peylin, P., Reichstein, M., Luyssaert, S., Margolis, H., Fang, J., Barr, A., Chen, A. (2008): Net carbon dioxide losses of northern ecosystems in response to autumn warming. – Nature 451: 49-52.
[68] Piao, S., Fang, J., Ciais, P., Peylin, P., Huang, Y., Sitch, S., Wang, T. (2009): The carbon balance of terrestrial ecosystems in China. – Nature 458: 1009-1013.
[69] Piao, S., Wang, X., Ciais, P., Zhu, B., Wang, T., Liu, J. (2011): Changes in satellite-derived vegetation growth trend in temperate and boreal Eurasia from 1982 to 2006. – Global Change Biology 17: 3228-3239.
[70] Ratcliffe, D. A. (1984): Post-medieval and recent changes in British vegetation: the culmination of human influence. – New Phytologist 98: 73-100.
[71] Sahebjalal, E., Dashtekian, K. (2013): Analysis of land use-land covers changes using normalized difference vegetation index (NDVI) differencing and classification methods. – African Journal of Agricultural Research 8: 4614-4622.
[72] Sasaki, N., Takahara, H. (2011): Late Holocene human impact on the vegetation around Mizorogaike Pond in northern Kyoto Basin, Japan: a comparison of pollen and charcoal records with archaeological and historical data. – Journal of Archaeological Science 38: 1199-1208.
[73] Scanlon, T. M., Albertson, J. D., Caylor, K. K., Williams, C. A. (2002): Determining land surface fractional cover from NDVI and rainfall time series for a savanna ecosystem. – Remote Sensing of Environment 82: 376-388.
[74] Shengpei, D., Zhang, B., Haijun, W., Yamin, W., Lingxia, G., Xingmei, W., Dan, L. (2011): Vegetation cover change and the driving factors over northwest China. – Journal of Arid Land 3: 25-33.
[75] Sheram, K. (1993): The Environmental Data Book: A Guide to Statistics on the Environment and Development. – World Bank, Washington, DC.
[76] Shu, W., Ximing, Y. (2018): How China's Grain-for-Green Project Contributes to Farmers' Income Growth. – China Economist 13: 88-102.
[77] Sims, H. (1999): One-fifth of the sky: China's environmental stewardship. – World Development 27: 1227-1245.

http://www.aloki.hu ● ISSN 1589 1623 (Print) ● ISSN 1785 0037 (Online)
DOI: http://dx.doi.org/10.15666/aeer/1902_13711390
© 2021, ALÖKI Kft., Budapest, Hungary

[78] Skole, D., Justice, C., Townshend, J., Janetos, A. (1997): A land cover change monitoring program: strategy for an international effort. – Mitigation and Adaptation Strategies for Global Change 2: 157-175.
[79] Song, X.-P., Hansen, M. C., Stehman, S. V., Potapov, P. V., Tyukavina, A., Vermote, E. F., Townshend, J. R. (2018): Global land change from 1982 to 2016. – Nature 560: 639-643.
[80] Sterling, S. M., Ducharne, A., Polcher, J. (2013): The impact of global land-cover change on the terrestrial water cycle. – Nature Climate Change 3: 385-390.
[81] Tucker, C. J. (1979): Red and photographic infrared linear combinations for monitoring vegetation. – Remote Sensing of Environment 8: 127-150.
[82] United Nations (2017): World Urbanization Prospects: The 2017 Revision. – UN Department of Economic and Social Affairs Population Division, New York.
[83] Usman, M., Liedl, R., Shahid, M., Abbas, A. (2015): Land use/land cover classification and its change detection using multi-temporal MODIS NDVI data. – Journal of Geographical Sciences 25: 1479-1506.
[84] Veraverbeke, S., Gitas, I., Katagis, T., Polychronaki, A., Somers, B., Goossens, R. (2012): Assessing post-fire vegetation recovery using red–near infrared vegetation indices: accounting for background and vegetation variability. – ISPRS Journal of Photogrammetry and Remote Sensing 68: 28-39.
[85] Vitousek, P. M., Mooney, H. A., Lubchenco, J., Melillo, J. M. (1997): Human domination of Earth's ecosystems. – Science 277: 494-499.
[86] Walker, R., Moran, E., Anselin, L. (2000): Deforestation and cattle ranching in the Brazilian Amazon: external capital and household processes. – World Development 28: 683-699.
[87] Wang, L. (2010): The changes of China's environmental policies in the latest 30 years. – Procedia Environmental Sciences 2: 1206-1212.
[88] Wang, G., Han, L., Tang, X., Jin, Z. (2012): Temporal and spatial variation of vegetation in the Jinsha River basin. – Resources and Environment in the Yangtze Basin 21: 1191-1196.
[89] Wang, J., Yan, Q., Liu, Z., Luo, C. (2013): Analysis on the change of vegetation coverage in Qinghai province from 2000 to 2012. – ISPRS - International Archives of the Photogrammetry, Remote Sensing and Spatial Information Sciences 1: 121-126.
[90] Wang, S., Ma, H., Zhao, Y. (2014): Exploring the relationship between urbanization and the eco-environment—a case study of Beijing–Tianjin–Hebei region. – Ecological Indicators 45: 171-183.
[91] Wang, J., Wang, K., Zhang, M., Zhang, C. (2015): Impacts of climate change and human activities on vegetation cover in hilly southern China. – Ecological Engineering 81: 451-461.
[92] Wang, W., Li, C., Shu, J., Chen, W. (2019): Changes of vegetation in southern China. – Science China Earth Sciences 62: 1316-1328.
[93] Wei, Q., Qingke, Z., Xuexia, Z. (2006): Review of vegetation covering and its measuring and calculating method. – Journal of Northwest Sci-Tech University of Agriculture and Forestry.
[94] Wei, X., Wang, S., Wang, Y. (2018): Spatial and temporal change of fractional vegetation cover in North-western China from 2000 to 2010. – Geological Journal 53: 427-434.
[95] Weng, Q. (2001): Modeling urban growth effects on surface runoff with the integration of remote sensing and GIS. – Environmental Management 28: 737-748.
[96] Xia, K., Zhang, L., Yang, J. (2007): Correlation analysis between land cover change and climate change in Zhejiang province. – Geoinformatics 2007: Geospatial Information Science, International Society for Optics and Photonics 675339. https://doi.org/10.1117/12.763556.

http://www.aloki.hu ● ISSN 1589 1623 (Print) ● ISSN 1785 0037 (Online)
DOI: http://dx.doi.org/10.15666/aeer/1902_13711390
© 2021, ALÖKI Kft., Budapest, Hungary

[97] Xin, Z., Xu, J. (2007): Spatial and temporal evolution of vegetation cover in the Loess Plateau and its response to climate change. – Progress in Natural Science 17: 770-778.
[98] Xu, G., Zhang, H., Chen, B., Zhang, H., Innes, J. L., Wang, G., Yan, J., Zheng, Y., Zhu, Z., Myneni, R. B. (2014): Changes in vegetation growth dynamics and relations with climate over China's landmass from 1982 to 2011. – Remote Sensing 6: 3263-3283.
[99] Xu, G., Zhang, J., Li, P., Li, Z., Lu, K., Wang, X., Wang, F., Cheng, Y., Wang, B. (2018): Vegetation restoration projects and their influence on runoff and sediment in China. – Ecological Indicators 95: 233-241.
[100] Xu, W., Xiao, Y., Zhang, J., Yang, W., Zhang, L., Hull, V., Wang, Z., Zheng, H., Liu, J., Polasky, S. (2017): Strengthening protected areas for biodiversity and ecosystem services in China. – Proceedings of the National Academy of Sciences 114: 1601-1606.
[101] Yan, J., Qiao, M., Zhou, H., Zhou, S., Lou, L., Song, P. (2013): Vegetation dynamics in Ili River valley of Xinjiang based on MODIS/NDVI. – Arid Land Geography 36: 512-519.
[102] Yan, L., He, R., Kašanin-Grubin, M., Luo, G., Peng, H., Qiu, J. (2017): The dynamic change of vegetation cover and associated driving forces in Nanxiong Basin, China. – Sustainability 9: 443.
[103] Yang, J., Weisberg, P. J., Bristow, N. A. (2012): Landsat remote sensing approaches for monitoring long-term tree cover dynamics in semi-arid woodlands: comparison of vegetation indices and spectral mixture analysis. – Remote Sensing of Environment 119: 62-71.
[104] Yu, S., Zhang, Z., Liu, F. (2018): Monitoring population evolution in China using time-series DMSP/OLS nightlight imagery. – Remote Sensing 10: 194.
[105] Zhang, X., Wu, B. (2015): A temporal transformation method of fractional vegetation cover derived from high and moderate resolution remote sensing data. – Acta Ecologica Sinica 35: 1155-1164.
[106] Zhang, K., Zongguo, W., Liying, P. (2007): Environmental policies in China: evolvement, features and evaluation. – China Population, resources and Environment 17: 1-7.
[107] Zhang, H. K., Roy, D. P., Yan, L., Li, Z., Huang, H., Vermote, E., Skakun, S., Roger, J.-C. (2018): Characterization of Sentinel-2A and Landsat-8 top of atmosphere, surface, and nadir BRDF adjusted reflectance and NDVI differences. – Remote Sensing of Environment 215: 482-494.
[108] Zhang, M., Wang, J., Li, S. (2019): Tempo-spatial changes and main anthropogenic influence factors of vegetation fractional coverage in a large-scale opencast coal mine area from 1992 to 2015. – Journal of Cleaner Production 232: 940-952.
[109] Zhang, X., Xie, H., Shi, J., Lv, T., Zhou, C., Liu, W. (2020): Assessing changes in ecosystem service values in response to land cover dynamics in Jiangxi Province, China. – International Journal of Environmental Research and Public Health 17: 3018.
[110] Zhang, Y., Li, L., Wang, H., Zhang, Y., Wang, N., Chen, J. (2017): Land surface phenology of northeast China during 2000–2015: temporal changes and relationships with climate changes. – Environmental Monitoring and Assessment 189: 1-13.
[111] Zhao, Y., Tomita, M., Hara, K., Fujihara, M., Yang, Y., Da, L. (2014): Effects of topography on status and changes in land-cover patterns, Chongqing City, China. – Landscape and Ecological Engineering 10: 125-135.
[112] Zhou, P., Wen, A.-B., Yan, D.-C., Shi, Z.-L., Guo, J., Ju, Z.-S., Zhang, Y.-L. (2014): Changes in land use and agricultural production structure before and after the implementation of grain for green program in Western China—taking two typical counties as examples. – Journal of Mountain Science 11: 526-534.
[113] Zhou, Y., Zhang, L., Fensholt, R., Wang, K., Vitkovskaya, I., Tian, F. (2015): Climate contributions to vegetation variations in central Asian drylands: pre- and post-USSR collapse. – Remote Sensing 7: 2449-2470.

http://www.aloki.hu ● ISSN 1589 1623 (Print) ● ISSN 1785 0037 (Online)
DOI: http://dx.doi.org/10.15666/aeer/1902_13711390
© 2021, ALÖKI Kft., Budapest, Hungary

[114] Zoungrana, B. J., Conrad, C., Thiel, M., Amekudzi, L. K., Da, E. D. (2018): MODIS NDVI trends and fractional land cover change for improved assessments of vegetation degradation in Burkina Faso, West Africa. – Journal of Arid Environments 153: 66-75.
[115] Zubair, A. O. (2006): Change Detection in Land Use and Land Cover Using Remote Sensing Data and GIS (A Case Study of Ilorin and Its Environs in Kwara State). – Department of Geography, University of Ibadan, Ibadan.
[116] Zwierzchowski, J., Rott-Pietrzyk, E. (2020): Polish and Chinese approach to environmental law. – Suleyman Demirel University Bulletin: Social Sciences 53(2): 27-34. https://doi.org/10.47344/sdubss.v53i2.324.

APPENDIX

Table A1. *Changes in area (km^2) from 2000 to 2005, 2005 to 2010*

Name	2000-2005				2005-2010			
	No	Low	Medium	High	No	Low	Medium	High
Heilongjiang	-442.40	-1747.15	18753.16	-16550.09	-95.97	-1144.1	-70506.3	71728.14
Xinjiang	-47162.31	31766.51	12741.53	2649.54	-47201.6	19249.5	16391.93	11568.58
Shanxi	-16.71	-15189.92	3569.34	11628.23	-4.04	-12958.4	-29346.8	42323.52
Ningxia	-631.85	-4478.22	4442.97	667.71	-136.76	-11225.6	8722.93	2633.98
Xizang/Tibet	46199.99	-28344.07	-23913.4	6048.23	-48234.7	100793.5	10842.93	-63409.4
Shandong	251.80	-4595.31	-6807	11144.23	-279.46	-1492.56	-83462.4	85234.22
Henan	16.07	452.16	11659.68	-12110.09	-29.92	-2323.64	-50309.3	52665.27
Jiangsu	363.00	-208.49	-11185.44	11031.65	34.8	-43.72	-21661	21670.19
Anhui	125.93	-226.86	5559.98	-5446.39	-182.77	-490.43	-22344.6	23011.32
Hubei	153.06	-304.57	-1777.19	1931.10	-62.26	792.71	16790.71	-17525.8
Zhejiang	46.60	-68.93	1516.89	-1494.33	-49.35	90.75	1757.22	-1805.17
Jiangxi	213.95	-322.11	-86.87	196.08	134.86	3587.46	27145.11	-30882.7
Hunan	-6.20	2291.51	8875.59	-11296.57	342.59	7078.8	27397.34	-34702.4
Yunnan	-1888.43	-4481.52	-506.52	6890.59	1754.63	1728.58	1226.77	-4726.41
Guizhou	6.85	2021.74	-1904.66	-130.28	150.72	19252.47	39936.64	-59346.4
Fujian	41.97	38.75	-0.74	-74.82	-70.16	1423.74	14081.94	-15447
Guangxi	888.00	32108.96	98851.28	-131949.50	-20.68	-5589.91	-1409.89	7096.68
Guangdong	136.54	8050.20	29427.39	-37621.76	852.67	12941.94	18220.42	-32027.1
Hainan	-18.70	186.76	5245.4	-5414.57	1.6	-158.35	-3484.54	3637.03
Jilin	-32.04	-5450.71	10057.7	-4573.86	-174.66	-4835.4	-19300.3	24316.98
Liaoning	-1.41	-1461.77	-36969.58	39431.44	-187.18	-214.41	3310.83	-3905.18
Tianjin	19.23	-778.30	-1388.13	2152.95	-158.83	-328.89	-1411.51	1899.26
Qinghai	11719.82	11268.25	-10881.05	-12105.38	-21019.3	-9917.38	49879.89	-18944.7
Gansu	-7407.15	-3054.56	951.13	9522.65	-26529.2	-2404.88	24418.53	4503.09
Shaanxi	-47.46	-16748.66	10130.3	6658.58	-29.13	-33834.8	7046.97	26816.39
Inner Mongolia	-34301.31	14762.72	1812.44	17822.12	-44058.3	-60784.6	50980.47	53875.95
Chongqing	2.89	327.47	2674.28	-3000.27	-13.22	340.47	4227.67	-4558.19
Hebei	18.62	-12998.94	-13510.15	26496.00	-255	-3069.34	-30688.9	34010.23
Shanghai	-5.98	-18.11	-1147.94	1168.62	9.67	-13.58	-465.92	470.65
Beijing	2.62	-57.70	-1846.63	1902.68	-3.29	-20.72	-3988.85	4015.03
Taiwan	-26.75	56.00	24.55	-58.72	-47.16	49.49	416.76	-416.67
Hongkong	1.351	57.712	329.48	-391.917	-0.16	54.83	41.63	-98.45
Sichuan	624.97	-1678.27	-28820.41	29867.89	2035.47	21693.52	70358.69	-94106.9

http://www.aloki.hu ● ISSN 1589 1623 (Print) ● ISSN 1785 0037 (Online)
DOI: http://dx.doi.org/10.15666/aeer/1902_13711390
© 2021, ALÖKI Kft., Budapest, Hungary

Table A2. *Changes in area (km^2) from 2010 to 2015, 2000 to 2015*

Name	2010-2015				2000-2015			
	No	Low	Medium	High	No	Low	Medium	High
Heilongjiang	2172.41	167.39	12155.2	-14501.6	1634.04	-2723.86	-39598	40676.42
Xinjiang	-16776.2	13102.49	-22356.9	26021.66	-111140	64118.5	6776.54	40239.77
Shanxi	137.13	-352.69	1505.63	-1291.82	116.38	-28501	-24271.8	52659.93
Ningxia	-1.82	4703.63	-3871.3	-828.46	-770.42	-11000.2	9294.6	2473.23
Xizang/Tibet	-18018	-27100.6	999.95	44125.17	-20052.7	45348.91	-12070.5	-13236
Shandong	150.76	281.27	62873.39	-63298.1	123.1	-5806.61	-27396	33080.3
Henan	49.1	1860.06	42811.16	-44724.3	35.25	-11.42	4161.54	-4169.11
Jiangsu	-259.75	522.17	31182.57	-31451.5	138.05	269.96	-1663.83	1250.32
Anhui	517.91	395.41	19603.06	-20518.3	461.07	-321.87	2818.43	-2953.38
Hubei	597.98	642.68	-5794.74	4551.63	688.78	1130.83	9218.78	-11043
Zhejiang	56.96	2351.72	15420.1	-17827.2	54.21	2373.54	18694.2	-21126.7
Jiangxi	-248.68	-2687.82	-13028.8	15827.39	100.13	577.54	14029.43	-14859.2
Hunan	-56.85	-8530.12	-27210.7	35805.99	279.54	840.19	9062.22	-10193
Yunnan	-1570.17	-11133.4	-25082.1	37798.76	-1703.97	-13886.3	-24361.9	39962.94
Guizhou	-108.19	-16112.1	-27172.3	43409.79	49.38	5162.09	10859.71	-16066.9
Fujian	164.7	-178.55	3708.83	-3692.23	136.5	1283.94	17790.02	-19214.1
Guangxi	-724.41	-20401.4	-55497.6	76644.96	142.91	6117.66	41943.75	-48207.9
Guangdong	-973.57	-19628	-34425.4	55027.56	15.63	1364.16	13222.4	-14621.3
Hainan	12.69	-16.17	-981.69	989.09	-4.41	12.24	779.17	-788.45
Jilin	150.05	-217.4	7559.64	-8009.3	-56.65	-10503.5	-1682.91	11733.82
Liaoning	286.14	-185.51	-8425.25	8331.2	97.55	-1861.69	-42084	43857.46
Tianjin	44.23	162.45	2109.44	-2315.72	-95.36	-944.74	-690.2	1736.5
Qinghai	4932.93	-5473.31	-30939.1	31482.33	-4366.54	-4122.44	8059.72	432.26
Gansu	3985.31	-4839.22	-18947.8	19809.82	-29951	-10298.7	6421.88	33835.56
Shaanxi	13.67	4079	-1123.42	-3065.35	-62.92	-46504.4	16053.85	30409.63
Inner Mongolia	-4360.36	23823.58	-8432.35	-11047.8	-82720	-22198.3	44360.56	60650.32
Chongqing	159.43	-609.48	-3388.02	3831.53	149.1	58.46	3513.93	-3726.93
Hebei	108.07	439.03	34632.26	-35177.5	-128.3	-15629.3	-9566.81	25328.69
Shanghai	-14.26	24.16	1141.94	-1151.99	-10.57	-7.53	-471.92	487.28
Beijing	0.45	33.64	4878.13	-4917.05	-0.22	-44.78	-957.35	1000.66
Taiwan	204.99	35.96	405.67	-647.03	131.09	141.45	846.98	-1122.43
Hongkong	-1.19	-113.53	-368.81	485.68	0	-0.99	2.31	-4.69
Sichuan	-4628.94	-21077.8	-46371.1	72093.5	-1968.5	-1062.59	-4832.8	7854.5

http://www.aloki.hu ● ISSN 1589 1623 (Print) ● ISSN 1785 0037 (Online)
DOI: http://dx.doi.org/10.15666/aeer/1902_13711390
© 2021, ALÖKI Kft., Budapest, Hungary

A NEW SOYBEAN NDVI DATA-BASED PARTITIONING ALGORITHM FOR FERTILIZATION MANAGEMENT ZONING

CHEN, H. – WANG, X.* – ZHANG, W. – WANG, X. Z. – DI, X. D. – QI, L. Q.

College of Engineering, Heilongjiang Bayi Agricultural University, Daqing 163319, China (phone: +86-4596-819-216)

**Corresponding author*
e-mail: 7455663@qq.com; phone: +86-138-3696-1962

(Received 17th Nov 2020; accepted 8th Feb 2021)

Abstract. With the broad application of management zoning, various partitioning algorithms are used for this purpose. The K-means algorithm is the most widely used method with the best performance. We proposed a model-based partitioning algorithm based on the K-means algorithm that does not need to process all the data in each computational iteration and thus is able to improve the management zoning speed. We constructed a calculation model for management zone partitioning using 2000 normalized difference vegetation index (NDVI) values. This model was then used to partition the next 2000 points of NDVI data acquired, and the model was updated after each 2000 NDVI values until the management zoning computation was completed for the entire field. Based on both internal evaluation indicators (the sum of squared errors (SSE) and silhouette coefficient (SC)) and external evaluation indicators (the Rand index (RI) and homogeneity), we compared the clustering performance of the two algorithms in management zone partitioning and found that when the amount of NDVI data reaches 8000 values, the proposed method achieves a management zone partition result similar to that of the conventional K-means algorithm but is faster. This advantage becomes increasingly profound as the data volume increases.
Keywords: *K-means, model-based algorithm, SSE, silhouette coefficient, Rand index, homogeneity*

Introduction

Heilongjiang Province is a major production area of high-quality soybeans in China. With the expansion of soybean acreage, the amount of chemical fertilizer applications has increased, which has in turn raised operating costs and decreased the quality of cultivated land. A large quantity of unutilized fertilizer can cause soil compaction in the field and damage soil microbial communities, thus severely hindering the sustainable development of agriculture. With the continuous development of precision agriculture, management zoning has been extensively investigated. Management zoning refers to the division of cultivated land into different management units based on the differentiation of various features, such as soil properties, the growth of crops, the crop yield, and terrain, so that the features of interest are similar within each unit but differ markedly between them. Through management zoning, differentiated fertilization schemes can be applied, which helps improve fertilizer use efficiency, protect the environment and quality of arable land and achieve the sustainable use of agricultural resources (Lopes et al., 2012; Koenig et al., 2015). Management zoning is an important foundation for the development of precision agriculture and has been thoroughly studied. Currently, the data sources for management zoning mainly include soil fertility, soil conductivity, soil texture, terrain, the crop yield, and crop canopy spectral information (Johnson et al., 2003; Flowers et al., 2005). Zoning based on soil fertility and terrain has been the most common practice, with relatively high accuracy. However, such approaches are time consuming and labor intensive, and the timing tends to be poor. Additionally, when

http://www.aloki.hu ● ISSN 1589 1623 (Print) ● ISSN 1785 0037 (Online)
DOI: http://dx.doi.org/10.15666/aeer/1902_13911405
© 2021, ALÖKI Kft., Budapest, Hungary

making measurements, it is difficult to determine the appropriate spacing, making it impossible to use these methods to zone large areas. In addition, such methods are associated with a high risk of machine-derived damage to the crop in the measurement process. Yield-based zoning methods cannot be performed in real time, as yield data are often not readily available. Satellite remote sensing-based zoning methods can be simultaneously performed in real time over a large area and rapidly generate high-resolution images and data. However, remote sensing data is geometrically and radiometrically distorted, with poor periodicity, stability, and repeatability; thus, complex data processing is needed, and the cost of generating the images is high.

The reflections of light of specific wavelength bands from plants in different growth states differ significantly. From these reflections, crop canopy spectral information can be collected through active remote sensing to estimate the growth status of crops. This technique does not rely on external light sources and can be applied at any time to rapidly acquire data in a timely manner. The normalized difference vegetation index (NDVI) data obtained through spectral detection techniques can be used to help evaluate crop growth, nutritional status, potential yield, and the impacts of pests and diseases (Jiang et al., 2006). The NDVI data that reflect the crop growth status facilitate the zoned management of crops, so that differentiated fertilization can be applied according to the growth of the crops.

Studies in the field of precision agriculture have focused on the use of management zoning to conduct differentiated fertilization management. NDVI-based management zoning is essentially a clustering process involving NDVI data. Clustering, an important part of data mining and machine learning, is the division of datasets into multiple clusters so that the data in the same cluster are similar and the data in different clusters are different. In the case of management zoning, each cluster represents a management zone. Unlike classification, clustering is a typical unsupervised learning method that does not require the labeling of data in advance (Barlow, 1989). There are many algorithms for data clustering, such as the K-means (MacQueen, 1967), hierarchical clustering (Johnson, 1967), DBSCAN (Ester et al., 1996) and fuzzy C-means (Bezdek et al., 1984). Among them, the K-means algorithm is one of the most well-known, simplest, and best clustering algorithms (Saxena et al., 2017).

Liu and Wang (2019) applied the K-means clustering algorithm for the management zoning of corn and concluded that it was the best algorithm for the NDVI data collected by GreenSeeker. However, during each clustering iteration in the K-means algorithm, all the data have to be processed to update the centroid (mean) of the data of each class. Therefore, as the data volume increases, the computational speed declines. The current clustering algorithms are faster than the previous algorithms for management zoning applications, but with the growing data volume to be processed, clustering computations face potential limitations. NDVI data are classified as a data stream, which represents an "unbounded" sequence of observations (Lu, 2005), i.e., an open time series of data with an ever-increasing data volume. Such data require a fast clustering algorithm dedicated to processing the incoming data stream.

In this study, we aim to propose a model-based partitioning algorithm for soybean fertilization management zoning that does not perform computations on all NDVI data but updates the model with data at certain intervals. Further, we aim to use the model to process the subsequent data to improve the management zoning speed.

http://www.aloki.hu ● ISSN 1589 1623 (Print) ● ISSN 1785 0037 (Online)
DOI: http://dx.doi.org/10.15666/aeer/1902_13911405
© 2021, ALÖKI Kft., Budapest, Hungary

Materials and methods

Experimental site

The experimental site (*Fig. 1*) was located at Zhaoguang Farm, a state-owned mechanized farm affiliated with the Land Reclamation Bureau of Heilongjiang Province, China. Standardized production operations, mostly with large-scale agricultural equipment, were used in the experiment. Zhaoguang Farm (126°26'-127°6' E, 47°54'-48°12' N) is located in the center of Bei'an city, to the east of Kedong County in Heilongjiang Province and at the edge of the southern foot of the Xiaoxing'an Mountains. The area is located at moderate to high latitudes and has a cold-temperature monsoon climate. The average annual temperature is 0.5 °C, the frost-free period is 120 days, annual rainfall totals 570 mm, and the average annual sunshine duration is over 2700 hours (Liu and Wang, 2019). The overall climate is characterized by dry and windy springs, hot and rainy summers, quickly cooling autumns with early frost, and long and cold winters. The region has four types of soil, namely, brown soil, black soil, meadow soil and bog soil, of which black soil covers 57.4% of the total area of arable land. This experiment was conducted at the 12-3 plot of Station 17 of the 4th Management District of Zhaoguang Farm, which is 34 ha in area. The soil type in this area is black soil. The area is planted with soybeans, with two lines per ridge (1.1 m in width). The soybean variety is Heihe 43, the amount of fertilizer applied is 105 kg/ha, and the ratio of N and P in fertilizer is 1:1.3. Plot 12-3 was unobstructed, thus supporting the accuracy requirements of the received GPS signals. The data were acquired on Jun 22, 2019.



Figure 1. *Experimental site (Zhaoguang Farm, China)*

Data collection and processing

Soybean canopy NDVI data were acquired with a ground-based remote sensing detection platform consisting of six GreenSeeker plant canopy spectrum analyzers (Trimble, U.S.), a GPS receiver (Model AG332, Trimble, U.S.) and a controller area network (CAN) data logger. The soybean canopy NDVI data were acquired with GreenSeeker plant canopy spectrum analyzers, each of which was equipped with narrow-band red light (660 nm) and near-infrared light (770 nm) LEDs as active light sources, and next-generation optical sensors from NTech were used to acquire plant

http://www.aloki.hu ● ISSN 1589 1623 (Print) ● ISSN 1785 0037 (Online)
DOI: http://dx.doi.org/10.15666/aeer/1902_13911405
© 2021, ALÖKI Kft., Budapest, Hungary

canopy reflectance spectra at the two aforementioned bands, with a measurement area of 61 cm±10 cm (width) × 1.5 cm±0.5 cm (length). During the measurement process, the probe of the spectrometer sensor was directed vertically downward and maintained at approximately 80 cm above the canopy. GreenSeeker is currently the most widely used agricultural spectrum sensor. For example, John Deere's GreenStar high-clearance adjustable sprayer uses GreenSeeker to control the application of liquid fertilizer so that smart, real-time and adjustable fertilization operations can be performed. The GreenSeeker sensor does not rely on sunlight and can work around the clock because it is unaffected by atmospheric and soil reflections. Additionally, the sensor provides a fast measurement speed and accurate data and can estimate the plant growth status in real time. Therefore, the sensor overcomes the shortcomings of poor timeliness, damage to crops and a high workload for large-scale measurements; moreover, unlike passive hyperspectral remote sensing, it does not require an external light source (Jiang et al., 2019). Applications of GreenSeeker in nutritional diagnosis, yield prediction and management zoning for many crops, such as wheat and corn, have been extensively investigated. For example, Sharp et al. (2004) demonstrated that it is feasible to determine the NDVI for the management zoning of cotton through GreenSeeker data. *Fig. 2* shows the ground-based remote sensing detection platform used for the acquisition of soybean canopy NDVI data and the corresponding control box used in this study.



(a) (b)

Figure 2. *Ground-based remote sensing detection platform for the acquisition of soybean canopy NDVI data. (a) Data acquisition site; (b) Interior of the remote sensing platform control box*

The Trimble GPS receiver (Model AG332) uses the ultimate choice technique and is the most advanced high-performance dual-frequency receiver available; it provides centimeter-level measurement accuracy and has a position information updating frequency of 1 Hz. The data acquisition frequency of GreenSeeker was also 1 Hz in this study. The acquired data were analyzed and recorded through the CAN data logger. *Table 1* shows the details of some representative data collected during the test.

In this study, we used Python and ArcGIS for data processing. We compiled the model-based partitioning algorithm program using the Scikit-learn library in Python. Scikit-learn is a machine learning tool library based on Python that includes many simple and efficient data mining and analysis tools. We used ArcGIS, which is an excellent geographic information processing software, to plot the fertilization management zones.

http://www.aloki.hu ● ISSN 1589 1623 (Print) ● ISSN 1785 0037 (Online)
DOI: http://dx.doi.org/10.15666/aeer/1902_13911405
© 2021, ALÖKI Kft., Budapest, Hungary

Table 1. *Details of the acquired data (partial)*

Date	Time	Longitude	Latitude	Mean NDVI
2019-6-22	12:36:31	126.6747136	48.0562793	0.650
2019-6-22	12:36:32	126.6747353	48.0562942	0.667
2019-6-22	12:36:33	126.6747584	48.0563087	0.650
2019-6-22	12:36:34	126.6747819	48.0563236	0.637
2019-6-22	12:36:35	126.6748047	48.0563384	0.658
2019-6-22	12:36:36	126.6748265	48.0563530	0.682
2019-6-22	12:36:37	126.6748489	48.0563684	0.706
2019-6-22	12:36:38	126.6748721	48.0563838	0.674
2019-6-22	12:36:39	126.6748942	48.0563986	0.659
2019-6-22	12:36:40	126.6749157	48.0564132	0.647

Fertilization management zoning method

K-means algorithm

The K-means algorithm, which was proposed by MacQueen in 1967, is a commonly used and effective clustering algorithm classified as an unsupervised machine learning method. In the past three decades, this algorithm has been used in most clustering algorithm-related studies. Later, many new clustering algorithms were developed or modified based on this algorithm (Fahad et al., 2014). During implementation, the K-means algorithm divides the data objects into K (defined by the user) clusters, each of which has a center (also called the centroid or mean) to which the distance of each of the data objects is calculated. The data object with the shortest distance to the center of a certain cluster is then assigned to that cluster. The clustering process is iterative, and the Euclidean distances between the data points and cluster centers are continuously optimized. For the set of data points $X= [x_1, \cdots, x_N]$, the K-means algorithm presents k divisions of dataset X. If $[C_1, \cdots, C_K]$ represents the centers of the K clusters, then we have the following function (*Eq. 1*):

$$V = \sum_{i=1}^{K} \sum_{x_j \in Xi} \left\| x_j - C_i \right\|^2 \qquad \text{(Eq.1)}$$

where K is the number of partitions, X_i is a data point in the ith partition, x_j is a data point in the data point set, and C_i is the cluster center of the ith partition.

The K-means algorithm is a method that constantly searches for the minimum value of the above function (Huang et al., 2006; Jing et al., 2007).

Determination of the number of clusters K using the elbow method

The K-means algorithm minimizes the squared error between a data point and data center, and this minimization process is encompassed in the objective function. The sum of squared errors (SSE) between the center of each cluster and the data points in the cluster is called the distortion. In a cluster, the lower the distortion is, the closer the cluster members are to each other; the higher the distortion is, the looser the cluster structure. As the number of classes increases, the distortion decreases, but for data with a certain degree of distinction, the distortion is greatly reduced when a certain critical point is reached. Then, the decrease becomes gradual. The critical point can be

http://www.aloki.hu ● ISSN 1589 1623 (Print) ● ISSN 1785 0037 (Online)
DOI: http://dx.doi.org/10.15666/aeer/1902_13911405
© 2021, ALÖKI Kft., Budapest, Hungary

considered a point where good clustering performance is displayed. Based on the above-described principle, the elbow method calculates the mean distortion to determine the optimum number of clusters (K). The mean distortion is calculated using the following formula (*Eq.2*):

$$MD = \frac{\sum_{p \in C_i} |p - m_i|^2}{n} \quad \text{(Eq.2)}$$

where *MD* is the mean distortion, *Ci* is the dataset of the ith partition, p represents a certain piece of data in the ith partition, m_i is the center of the C_i partition, and n is the data volume of the ith partition.

Model-based algorithm

The proposed algorithm is based on the K-means clustering algorithm. The number of clusters (K) is set by the user, and the centers of clusters are randomly set by the algorithm. Then, the distances between the data points and cluster center are calculated, and the data points are clustered based on the minimum distance. The calculation is iteratively performed to update cluster centers, and when the accuracy requirements are met and 2000 data points are processed, a clustering model is constructed based on the cluster centers. Subsequently, without updating the cluster centers, the established clustering model is used to perform the clustering calculations, and when 2000 data points have been processed, the clustering model is updated. Similarly, in data intervals of 2000 points, the clustering model is updated until all the data are clustered. The flow chart of the proposed algorithm is shown in *Fig. 3*.

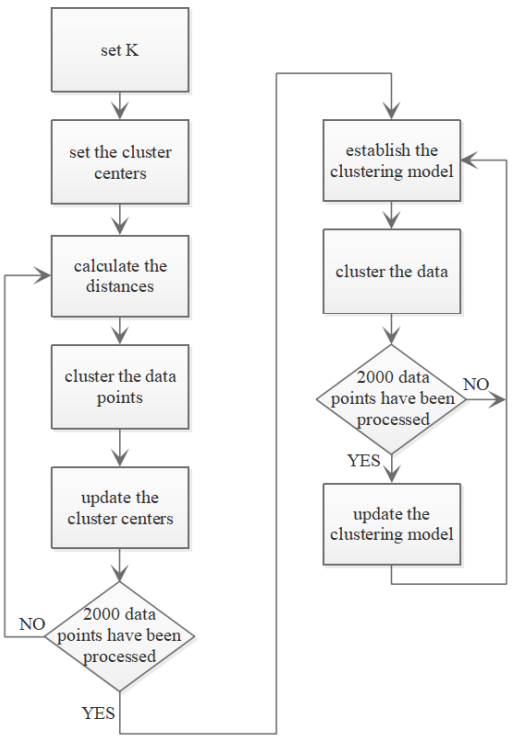


Figure 3. *Flow chart of model-based algorithm*

http://www.aloki.hu ● ISSN 1589 1623 (Print) ● ISSN 1785 0037 (Online)
DOI: http://dx.doi.org/10.15666/aeer/1902_13911405
© 2021, ALÖKI Kft., Budapest, Hungary

Evaluation of clustering performance

Two kinds of evaluation indicators are commonly used to assess clustering performance: internal evaluation indicators and external evaluation indicators. Internal evaluation indicators are able to assess clustering performance without comparing the clustering result with the ideal result, and external evaluation indicators have to rely on comparing the clustering result with the ideal clustering result (Amigó et al., 2009). To avoid the limitations of a single evaluation method and obtain accurate results, we use both internal and external evaluation indicators. Notably, the clustering result obtained through the K-means algorithm is used as the ideal clustering result to assess clustering performance with external indicators.

The SSE is used as an indicator for the evaluation of unsupervised clustering results. This parameter can be used to assess clustering performance without a comparison database (ideal clustering result). The purpose of the K-means algorithm is to find a solution that divides a dataset into K clusters, where the data in the same cluster are similar, the data from different clusters are different and each data point has a minimized SSE relative to the corresponding cluster center. The SSE is a common indicator of clustering quality. For the same number of clusters (K), the lower the SSE is, the higher the clustering quality. In terms of principles, the SSE evaluation method is similar to the elbow method. The calculation formula of the SSE is given as *Eq. 3*.

$$SSE = \sum_{i=1}^{K} \sum_{p \in C_i} \left| p - m_i \right|^2 \quad \text{(Eq.3)}$$

where *SSE* is the sum of squared errors, *K* is the number of partitions, C_i is the dataset of the ith partition, *p* represents certain data points in the partition, and m_i is the center of partition C_i.

The silhouette coefficient (SC) (Rousseeuw, 1987), which was proposed by Rousseeuw in 1986, is an internal evaluation indicator for unsupervised clustering based on two factors: cohesion and separation. This variable can be used to evaluate different clustering algorithms based on a given dataset and the effects of different methods of operation of the same clustering algorithm on the partitioning result.

In the samples, the average distance from each data point (i) to the other samples in the same cluster is defined as a(i), and accordingly, the average distance from each data point (i) to the other samples in cluster C_j is defined as B_{ij}. Therefore, b(i)= min[B_{i1}, B_{i2}, ..., B_{ik}]. The lower the value of a(i) is, the stronger the association of the sample data point (i) with the corresponding cluster is, so a(i) is called the intracluster dissimilarity for sample data point (i). The higher the value of b(i) is, the weaker the association of sample data point (i) with other clusters is, so b(i) is called the intercluster dissimilarity for sample data point (i). The SC-based partitioning algorithm was proposed to estimate the number of clusters (Azimi et al., 2017; Ünlü and Xanthopoulos, 2019). The definitions of a(i), b(i), and SC can be found in the following formula (*Eq. 4*):

$$SC(i) = \frac{b(i) - a(i)}{max\{a(i), b(i)\}} \quad \text{(Eq.4)}$$

http://www.aloki.hu ● ISSN 1589 1623 (Print) ● ISSN 1785 0037 (Online)
DOI: http://dx.doi.org/10.15666/aeer/1902_13911405
© 2021, ALÖKI Kft., Budapest, Hungary

In the equation, -1 ≤ SC (i) ≤ 1; a(i) represents the compactness of the cluster to which (i) belongs, and the lower the a(i) value is, the more compact the points are in the cluster; and b(i) represents the degree of separation of (i) and the other clusters, and the higher the b(i) value is, the more separated (i) is from the other clusters (Han et al., 2011) However, when SC (i) < 0, (i) is closer to the samples in other clusters than to those in the same cluster. This situation is not ideal in actual clustering and should be avoided.

The clustering process can be regarded as a series of decision-making processes in which it is determined whether each pair of data points in the dataset should be assigned to the same cluster. In this process, the Rand index (RI) (Hubert and Arabie, 1985; Vinh et al., 2010) is used to measure the accuracy of decisions. Assuming that U is the ideal cluster set and that V is the clustering result, four statistical measures are established as follows: a is the number of datapoint pairs that fall in the same cluster in both U and V; b is the number of datapoint pairs that fall in the same cluster in U but not in V; c is the number of datapoint pairs that fall in the same cluster in V but not in U; and d is the number of datapoint pairs that do not fall in the same cluster in U and V. Then, RI is defined according to *Eq. 5*.

$$RI = \frac{a+d}{a+b+c+d} \tag{Eq.5}$$

The *RI* values are in the range of [0,1]. When the clustering result perfectly matches the ideal clustering result, *RI* is 1. However, the *RI* value cannot guarantee a value of 0 in the case of random clustering, so the adjusted Rand index (ARI) (Yeung and Ruzzo, 2001; Steinley, 2004) is introduced to address this issue and is defined in *Eq. 6*.

$$ARI = \frac{RI - E[RI]}{\max(RI) - E[RI]} \tag{Eq.6}$$

where *ARI* is the adjusted Rand index, *RI* is the Rand index, *E*[*RI*] is the expected value of the *RI*, and max(*RI*) is the maximum value of the *RI*.

Homogeneity is an external evaluation indicator used to assess clustering performance based on conditional entropy analysis. Specifically, data from the same cluster should be from the same class (Hirschberg and Rosenberg, 2007). This parameter is defined in *Eq. 7*.

$$H = 1 - \frac{\sum_{c,k} n_{c,k} \log \frac{n_{c,k}}{n_k}}{\sum_c n_c \log \frac{n_c}{D}} \tag{Eq.7}$$

where *H* is the homogeneity, n_c is the number of data points in class *c*, n_k is the number of data points in partition *k*, $n_{c,k}$ is the number of data points present in class c and cluster *K* at the same time, and *D* is the number of data points in the dataset.

http://www.aloki.hu ● ISSN 1589 1623 (Print) ● ISSN 1785 0037 (Online)
DOI: http://dx.doi.org/10.15666/aeer/1902_13911405
© 2021, ALÖKI Kft., Budapest, Hungary

Results and discussion

Calculation of the number of management zones K

Using the elbow method, we calculate the mean distortion and plot the changes. As shown in *Fig. 4*, for the soybean NDVI data, when the number of partitions K is greater than 2, the mean distortion does not decrease significantly and is characterized by a smooth curve, indicating that a number greater than 2 is reasonable for the number of management zones based on the acquired soybean NDVI data. As the number of management zones increases, the requirements for working machinery that can provide variable-rate fertilization increase, which inevitably increases the related costs; thus, many methods and machines are impractical in actual agricultural production activities. Therefore, it is necessary to choose a suitable number of management zones with the optimal zoning accuracy and best comprehensive economic benefits. In this study, we determined that the number of fertilization management zones should be 4 based on the fertilization site conditions and experience.

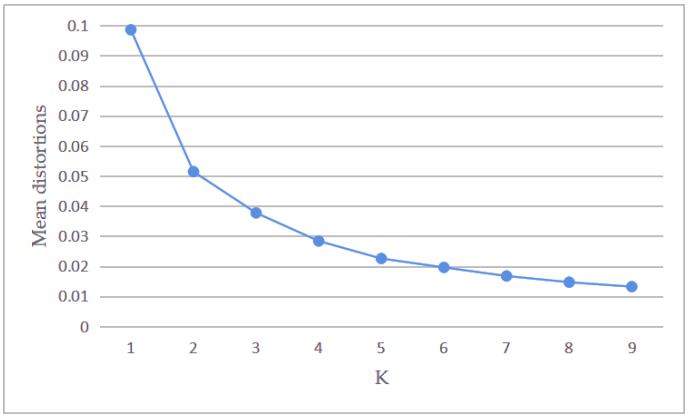


Figure 4. *Mean distortions*

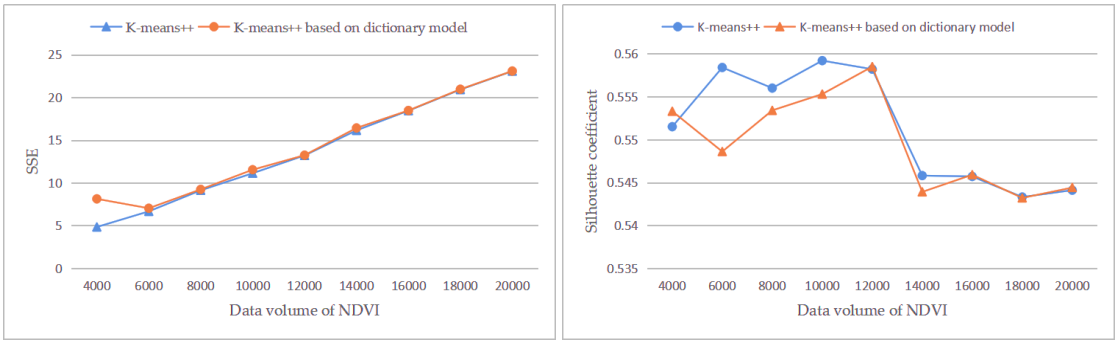
Comparison of the K-means algorithm and model-based algorithm

We compiled the K-means algorithm and the model-based algorithm programs through the Scikit-learn library and obtained the management zoning results from the two algorithms. We also compiled the program to evaluate the clustering performance of the two algorithms, and based on the results of the evaluation of clustering performance, we plotted the changes in the internal evaluation indicators (SSE and SC) for different data volumes, as shown in *Fig. 5*.

The SSE is a commonly used internal evaluation index of the clustering effect and reflects the degree of aggregation of the data points in a cluster to the clustering centroid and thus the clustering performance, as demonstrated in previous studies (Chayangkoon and Srivihok, 2016; Zhang and Zhou, 2018). A comparison of the SSE values of the K-means algorithm and the model-based algorithm shows that when 4000 data points are processed, the SSE values of the K-means algorithm and the model-based algorithm are 4.83 and 8.12, respectively, indicating that the K-means algorithm outperforms the model-based algorithm. When the volume of processed data reaches 6000 data points, the SSE values of the K-means algorithm and model-based algorithm are 6.65 and 7.02, respectively, indicating that the two algorithms perform similarly. When the volume of

http://www.aloki.hu ● ISSN 1589 1623 (Print) ● ISSN 1785 0037 (Online)
DOI: http://dx.doi.org/10.15666/aeer/1902_13911405
© 2021, ALÖKI Kft., Budapest, Hungary

processed data surpasses 6000 data points, the SSE value of the model-based algorithm using partial data is as low as that of the K-means clustering algorithm using all the data; i.e., the model-based algorithm, using less data, can perform as well as the K-means algorithm using more data.

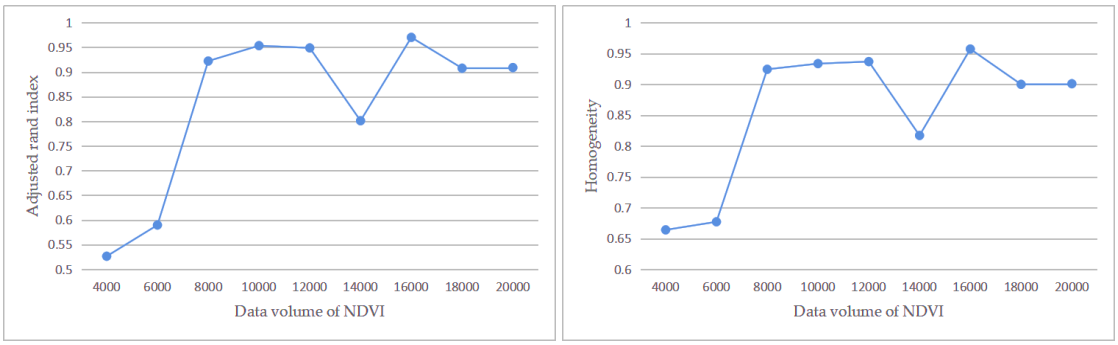


(a) (b)

Figure 5. *Changes in the internal evaluation indicators with the data volume. (a) Comparison of the SSE values of the two algorithms; (b) Comparison of the SC values of the two algorithms*

The SC is another commonly used internal evaluation indicator of clustering performance, and it reflects the degree of closeness of data points to the center of the cluster to which they belong and the degree of remoteness of data points to centers of other clusters. To obtain good clustering results, the points within a cluster should be close to each other but distant from the data points in other clusters. In previous studies (Hasanzadeh-Mofrad and Rezvanian, 2018; Dinh et al., 2019), the SC value was used to assess the quality of different clustering methods. A comparison of the SC values of the K-means algorithm and the model-based algorithm shows that when the volume of processed data reaches 8000 data points, the SC values of the two algorithms are very similar. This result is similar to that for the SSE, indicating that the clustering performance of the model-based algorithm using partial data is similar to that of the K-means algorithm using all the data.

A comparison of the changes in the external evaluation indicators (ARI and homogeneity) of the clustering performance with the data volume is shown in *Fig. 6*.



(a) (b)

Figure 6. *Changes in the external evaluation indicators with the data volume. (a) ARI changes; (b) Homogeneity changes*

http://www.aloki.hu ● ISSN 1589 1623 (Print) ● ISSN 1785 0037 (Online)
DOI: http://dx.doi.org/10.15666/aeer/1902_13911405
© 2021, ALÖKI Kft., Budapest, Hungary

The ARI is an improved external evaluation indicator of the RI indicator for clustering performance, and it reflects the correctness of the clustering result through the similarity of two different clustering results. Previously, the ARI evaluation method was used to assess the stability of five clustering methods in evaluating the clustering of single-cell RNA-seq data, and good results were achieved (Duò et al., 2018). In this study, in calculating the ARI, we treat the clustering result of the K-means algorithm as the ideal result for the model-based algorithm and find that when the data volume reaches 8000 data points, the ARI value is 0.92 and stabilizes at approximately 0.95 as the volume of data increases. Thus, after the data volume reaches 8000 data points, the clustering performance results of the two algorithms are similar. When the data volume reaches 14,000 data points, the ARI decreases to 0.80, indicating that the accuracy of the clustering model is unstable and fluctuates, which will be examined further in future studies.

In previous studies (SanJuan and Ibekwe-SanJuan, 2006; Mohammadrezapour et al., 2020), homogeneity was used to evaluate the clustering performance and proven to be effective. In this study, we also use the homogeneity indicator to evaluate the clustering results and find that when the data volume reaches 8000 data points, the homogeneity value is 0.93. Thus, when the data volume reaches 8000 data points, high clustering accuracy is achieved. When the data volumes are 4000 and 6000 data points, the homogeneity values are 0.66 and 0.67, respectively. Therefore, for these data volumes, the clustering accuracy is not high. When the data volume reaches 14,000 data points, the homogeneity value decreases to 0.82; this trend is similar to that for the ARI, indicating that the model accuracy is not stable.

We used ArcGIS to plot the fertilization management zones. We interpolated the NDVI data for crop growth based on geographical information (latitude and longitude) and generated fertilization management zones based on the above-described clustering results for the soybean NDVI data. Then, we plotted the results, as shown in *Fig. 7*.

A comparison of the management zones obtained using the K-means algorithm and the model-based algorithm shows that for a data volume of 4000 data points, the two zoning methods differ significantly, and the SSE values of the two methods differ significantly. These findings are consistent with the results of actual management zoning. The difference in SC is slight. The values of the two external evaluation indicators, RI and homogeneity, are 0.53 and 0.67, respectively, indicating that the results based on the two methods differ significantly and that the zoning accuracy of the model-based algorithm is poor. When the data volume reaches 6000 data points, the two methods differ slightly in terms of management zoning, with slight differences in the internal evaluation indicators (SSE and SC). Additionally, the values of the two external evaluation indicators, RI and homogeneity, are 0.59 and 0.68, respectively. When the data volume reaches 8000 data points or more, the two methods show no difference in terms of management zoning, with minimal differences in the internal evaluation indicators (SSE and SC). In this case, the values of the two external evaluation indicators, RI and homogeneity, are 0.92 and 0.93, respectively. These results indicate that the zoning results based on the K-means algorithm and the model-based algorithm show minimal differences and that the model-based algorithm achieves a high accuracy when the result of the K-means algorithm is used as the ideal clustering result.

http://www.aloki.hu ● ISSN 1589 1623 (Print) ● ISSN 1785 0037 (Online)
DOI: http://dx.doi.org/10.15666/aeer/1902_13911405
© 2021, ALÖKI Kft., Budapest, Hungary

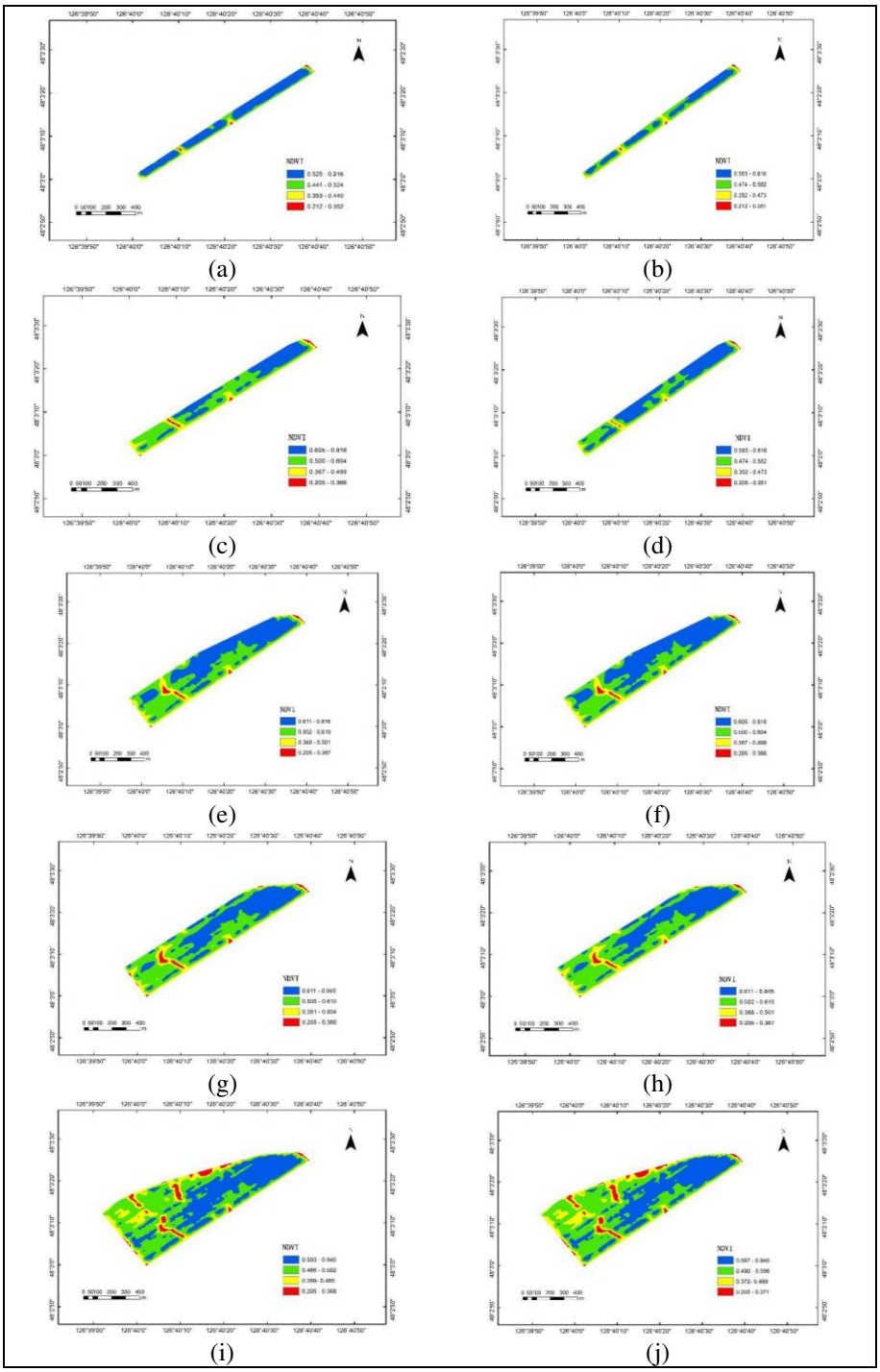


Figure 7. *Comparison of the management zones obtained using the K-means algorithm and the model-based algorithm. (a) K-means algorithm when the data volume reaches 4000 data points; (b) model-based algorithm when the data volume reaches 4000 data points; (c) K-means algorithm when the data volume reaches 6000 data points; (d) model-based algorithm when the data volume reaches 6000 data points; (e) K-means algorithm when the data volume reaches 8000 data points; (f) model-based algorithm when the data volume reaches 8000 data points; (g) K-means algorithm when the data volume reaches 10,000 data points; (h) model-based algorithm when the data volume reaches 10,000 data points; (i) K-means algorithm when the data volume reaches 18,000 data points; (j) model-based algorithm when the data volume reaches 18,000 data points*

http://www.aloki.hu ● ISSN 1589 1623 (Print) ● ISSN 1785 0037 (Online)
DOI: http://dx.doi.org/10.15666/aeer/1902_13911405
© 2021, ALÖKI Kft., Budapest, Hungary

Conclusions

In this study, we investigated partitioning algorithms for soybean fertilization management zoning by acquiring soybean NDVI data through a ground-based remote sensing detection platform and proposed a model-based algorithm based on the K-means clustering algorithm. With NDVI data acquired from an entire soybean field as the partitioning data sample and the K-means and model-based algorithms compiled in Python, we comparatively analyzed the produced fertilization management zoning charts and the corresponding internal and external evaluation indicators. When the data volume reached 8000 data points, the model-based algorithm produced SSE and SC values similar to those of the K-means algorithm. Additionally, the ARI and homogeneity values were high (approximately 0.95 for both) when the clustering result of the K-means clustering algorithm was used as the ideal clustering result, indicating that the model-based algorithm differs from the traditional K-means algorithm when the volume of sample data is below 8000 data points and does not differ from the traditional K-means algorithm when the volume of sample data is 8000 data points or more but is faster. This advantage becomes increasingly profound as the data volume increases.

Subsequent research will further improve the model-based algorithm, reduce computation time, improve the operational efficiency, establish a reasonable fertilization model based on the NDVI, calculate the recommended amount of fertilizer, and compare the difference in the recommended amount of fertilizer between the model-based algorithm and other algorithms.

Acknowledgements. This research was funded by the National Soybean Industry Technology System (No. CARS-04-PS32), the Heilongjiang Bayi Agricultural University Support Program for San Heng San Zong (ZRCPY202014), and the Heilongjiang Farms & Land Reclamation Administration Support Project (2019HKQNJTG0015).

REFERENCES

[1] Amigó, E., Gonzalo, J., Artiles, J., Verdejo, F. (2009): A comparison of extrinsic clustering evaluation metrics based on formal constraints. – Information retrieval 12: 461-486.

[2] Azimi, R., Ghayekhloo, M., Ghofrani, M., Sajedi, H. (2017): A novel clustering algorithm based on data transformation approaches. – Expert Systems with Applications 76: 59-70.

[3] Barlow, H. B. (1989): Unsupervised learning. – Neural computation 1: 295-311.

[4] Bezdek, J. C., Ehrlich, R., Full, W. (1984): FCM: The fuzzy c-means clustering algorithm. – Computers 10: 191-203.

[5] Chayangkoon, N., Srivihok, A. (2016): Two step clustering model for K-means algorithm. – Proceedings of the Fifth International Conference on Network, Communication and Computing, pp. 213-217.

[6] Dinh, D.-T., Fujinami, T., Huynh, V.-N. (2019): Estimating the optimal number of clusters in categorical data clustering by silhouette coefficient. – International Symposium on Knowledge and Systems Sciences, Springer, pp. 1-17.

[7] Duò, A., Robinson, M. D., Soneson, C. (2018): A systematic performance evaluation of clustering methods for single-cell RNA-seq data. – FResearch 7.

[8] Ester, M., Kriegel, H.-P., Sander, J., Xu, X. (1996): A density-based algorithm for discovering clusters in large spatial databases with noise. – KDD-96 Proceedings, pp. 226-231.

http://www.aloki.hu ● ISSN 1589 1623 (Print) ● ISSN 1785 0037 (Online)
DOI: http://dx.doi.org/10.15666/aeer/1902_13911405
© 2021, ALÖKI Kft., Budapest, Hungary

[9] Fahad, A., Alshatri, N., Tari, Z., Alamri, A., Khalil, I., Zomaya, A. Y., Foufou, S., Bouras, A. (2014): A survey of clustering algorithms for big data: Taxonomy and empirical analysis. – IEEE transactions on emerging topics in computing 2: 267-279.
[10] Flowers, M., Weisz, R., White, J. G. (2005): Yield-Based Management Zones and Grid Sampling Strategies: Describing Soil Test and Nutrient Variability. – Agronomy Journal 97: 968-982.
[11] Han, J., Pei, J., Kamber, M. (2011): Data mining: concepts and techniques. – Elsevier.
[12] Hasanzadeh-Mofrad, M., Rezvanian, A. (2018): Learning automata clustering. – Journal of computational science 24: 379-388.
[13] Hirschberg, J. B., Rosenberg, A. (2007): V-Measure: a conditional entropy-based external cluster evaluation. – Proceedings of EMNLP, Columbia University.
[14] Huang, S., Chen, Z., Yu, Y., Ma, W.-Y. (2006): Multitype features co-selection for web document clustering. – IEEE Transactions on Knowledge Data Engineering 18: 448-459.
[15] Hubert, L., Arabie, P. (1985): Comparing partitions. – Journal of classification 2: 193-218.
[16] Jiang, Z., Huete, A. R., Chen, J., Chen, Y., Li, J., Yan, G., Zhang, X. (2006): Analysis of NDVI and scaled difference vegetation index retrievals of vegetation fraction. – Remote sensing of environment 101: 366-378.
[17] Jiang, R., Wang, P., Xu, Y., Zhou, Z., Luo, X., Lan, Y. J. S. (2019): A Novel Illumination Compensation Technique for Multi-Spectral Imaging in NDVI Detection. – Sensors 19: 1859.
[18] Jing, L., Ng, M. K., Huang, J. Z. (2007): An entropy weighting k-means algorithm for subspace clustering of high-dimensional sparse data. – IEEE Transactions on knowledge data engineering 19: 1026-1041.
[19] Johnson, S. C. (1967): Hierarchical clustering schemes. – Psychometrika 32: 241-254.
[20] Johnson, C. K., Mortensen, D. A., Wienhold, B. J., Shanahan, J. F., Doran, J. W. (2003): Site-specific management zones based on soil electrical conductivity in a semiarid cropping system. – Agronomy journal 95: 303-315.
[21] Koenig, K., Höfle, B., Hämmerle, M., Jarmer, T., Siegmann, B., Lilienthal, H. (2015): Comparative classification analysis of post-harvest growth detection from terrestrial LiDAR point clouds in precision agriculture. – ISPRS Journal of Photogrammetry and Remote Sensing 104: 112-125.
[22] Liu, H., Wang, X. (2019): Assessing ndvi spatial pattern related to management zones. – Applied Ecology and Environmental Research 17: 6269-6285.
[23] Lopes, F. B., Silva, M. C. D., Miyagi, E. S., Fioravanti, M., Facó, O., Guimarães, R. F., de C. Júnior, O. A., McManus, C. M. (2012): Spatialization of climate, physical and socioeconomic factors that affect the dairy goat production in Brazil and their impact on animal breeding decisions. – Pesquisa Veterinária Brasileira 32: 1073-1081.
[24] Lu, Y.-H. (2005): Mining data streams using clustering. – International Conference on Machine Learning and Cybernetics, IEEE, pp. 2079-2083.
[25] Macqueen, J. (1967): Some methods for classification and analysis of multivariate observations. – Proceedings of the fifth Berkeley symposium on mathematical statistics and probability, Oakland, CA, USA, pp. 281-297.
[26] Mohammadrezapour, O., Kisi, O., Pourahmad, F. (2020): Fuzzy c-means and K-means clustering with genetic algorithm for identification of homogeneous regions of groundwater quality. – Neural Computing Applications 32: 3763-3775.
[27] Rousseeuw, P. J. (1987): Silhouettes: a graphical aid to the interpretation and validation of cluster analysis. – Journal of computational applied mathematics 20: 53-65.
[28] Sanjuan, E., Ibekwe-Sanjuan, F. (2006): Text mining without document context. – Information Processing & Management 42: 1532-1552.
[29] Saxena, A., Prasad, M., Gupta, A., Bharill, N., Patel, O. P., Tiwari, A., Er, M. J., Ding, W., Lin, C.-T. (2017): A review of clustering techniques and developments. – Neurocomputing 267: 664-681.

http://www.aloki.hu ● ISSN 1589 1623 (Print) ● ISSN 1785 0037 (Online)
DOI: http://dx.doi.org/10.15666/aeer/1902_13911405
© 2021, ALÖKI Kft., Budapest, Hungary

[30] Sharp, T., Evans, G., Salvador, A. (2004): Weekly NDVI relationships to height, nodes and productivity index for low, medium, and high cotton productivity zones. – Proceedings of the Beltwide Cotton Conferences: 2048.
[31] Steinley, D. (2004): Properties of the Hubert-Arable Adjusted Rand Index. – Psychological methods 9: 386.
[32] Ünlü, R., Xanthopoulos, P. (2019): Estimating the number of clusters in a dataset via consensus clustering. – Expert Systems with Applications 125: 33-39.
[33] Vinh, N. X., Epps, J., Bailey, J. (2010): Information theoretic measures for clusterings comparison: Variants, properties, normalization and correction for chance. – The Journal of Machine Learning Research 11: 2837-2854.
[34] Yeung, K. Y., Ruzzo, W. L. (2001): Details of the adjusted rand index and clustering algorithms, supplement to the paper an empirical study on principal component analysis for clustering gene expression data. – Bioinformatics 17: 763-774.
[35] Zhang, H., Zhou, X. (2018): A novel clustering algorithm combining niche genetic algorithm with canopy and K-means. – International Conference on Artificial Intelligence and Big Data (ICAIBD), IEEE, pp. 26-32.

http://www.aloki.hu ● ISSN 1589 1623 (Print) ● ISSN 1785 0037 (Online)
DOI: http://dx.doi.org/10.15666/aeer/1902_13911405
© 2021, ALÖKI Kft., Budapest, Hungary

CHEMICAL AND MOLECULAR CHARACTERIZATION OF ANATOLIAN SAGE (*Salvia fruticosa* Mill.) POPULATIONS DISTRIBUTED NATURALLY IN SOUTHWESTERN AEGEAN

ELMAS, S.[1*] – ARABACI, O.[2] – AKPINAR, E.[3] – HASANCEBI, S.[3] – ZEYBEK, A.[1]

[1]*Department of Biology, Faculty of Science, Mugla Sitki Kocman University, Mugla, Turkey*

[2]*Department of Field Crops, Faculty of Agriculture, Adnan Menderes University, Aydin, Turkey*

[3]*Department of Genetics and Bioengineering, Faculty of Engineering, Trakya University, Edirne, Turkey*

[*]*Corresponding author*
e-mail: sinemelmas@hotmail.com.tr; phone: +90-554-867-10-96

(Received 17th Nov 2020; accepted 27th Jan 2021)

Abstract. This study was carried out to determine the chemical, and molecular characterizations of *Salvia fruticosa* Mill. (Anatolian sage) populations distributed naturally in Mugla province. Plant materials were collected in June 2017 and 2018 from 30 different locations, in comprising districts of Mugla including Mentese (4), Ula (6), Koycegiz (1), Marmaris (11), Ortaca (2), Fethiye (2), Dalaman (2), and Milas (2). Thirty plants were collected from each population. The study showed the following rates: essential oil in the leaf, 0.34–3.76%; essential oil in the haulm, 0.01–0.23%; and total essential oil, 0.22–2.80%. Genetic variation among the populations was determined by RAPD (Random Amplified Polymorphic DNA) molecular markers. In total, 150 bands were obtained from gel electrophoresis, and the populations were separated into two main clusters by evaluating these bands. Chemical and genetic profiles of *Salvia fruticosa* Mill. populations were determined to be compatible with each other in hierarchical clustering analysis and the created dendrograms. The different essential oil rates and components determined in the of them confirmed the genetic variation in each population.
Keywords: *hydrodistillation, essential oils, RAPD-PCR, hierarchical cluster analysis, dendrogram*

Introduction

The Lamiaceae family is cosmopolitan, and many species of this family have economic and medicinal importance. It is more widespread in the Mediterranean region, and in Turkey's flora, it is represented by 46 genera and 725 species (Guner et al., 2001; Elmas, 2019a). Among these, the genus *Salvia* is known in Turkish as "island tea," and it has been known for its pharmacological importance since ancient times (Altindal, 2019). The dried leaves of *Salvia fruticosa* Mill., which are economically important, are used as herbal tea or for the production of essential oil. The leaves are prepared as infusions or decoctions and consumed as tea. Water distillation from the leaves yields a colorless or light-yellow oil called *Oleum Salviae trilobae*, which is rich in 1,8-cineole components (Elmas, 2019a).

Salvia fruticosa Mill., which has been used for many years utilized collection from flora, has an important place in both domestic and foreign trade. In Turkey, the average sage production was 299 tonnes in the 2014–2018 period. Mugla province is important for sage cultivation and export; in Mugla, the amount of average sage production was recorded as 18.4 tonnes in 2014–2018 (TUIK, 2019).

Controlled use of economic interests and plant resources is essential for the protection of biodiversity, but many factors, such as irregular construction, intense grazing and

http://www.aloki.hu ● ISSN 1589 1623 (Print) ● ISSN1785 0037 (Online)
DOI: http://dx.doi.org/10.15666/aeer/1902_14071421
© 2021, ALÖKI Kft., Budapest, Hungary

unintentional harvests–where many plant species are distributed naturally–can reduce the populations of these species and jeopardize their continuity. It has been reported that *Salvia fruticosa* Mill. is classified as vulnerable (Elmas, 2019a). Therefore, there is an immediate need to assess the diversity of natural populations that are economically and medically valuable due to such potential threats (Bacu et al., 2005). Molecular markers, especially polymerase chain reaction (PCR)-based genetic markers, are suitable tools for identifying genetic diversity among populations. Of these, the RAPD marker is one of the simplest and most common methods used to determine the genetic similarity and diversity of populations. In addition, it has many advantages such as not needing the sequence data, ability to work with small quantity of DNA, short testing timeframe and quick results, as well as low cost (Wang et al., 2011).

The study, it was aimed to determine the structure of populations using chemical and molecular markers in *Salvia fruticosa* Mill. populations, which are naturally distributed in the Mugla province, Turkey, to determine the gene pools of populations and differences between them. This study can be taken as a reference to provide genetic data to the gene banks to be established in the future and reach populations with superior genotypes and phenotypes in breeding programs. This, in turn, will contribute to the development of suitable varieties for breeding and the desired product needs of enterprises.

Materials and Methods

In the study, *Salvia fruticosa* Mill., which is naturally distributed in the Turkey's province of Mugla was used as a plant material to investigate some of its chemical and molecular properties. The samples were collected at the end of the flowering period in June 2017 and 2018, plant materials were collected from 30 different locations in districts of Mugla including Mentese (4), Ula (6), Koycegiz (1), Marmaris (11), Ortaca (2), Fethiye (2), Dalaman (2), and Milas (2). Thirty plant materials were collected from each population. The coordinates, location, altitude of the places where *Salvia fruticosa* Mill. was collected are given in *Table 1*. These coordinates were already determined by a previous study (Elmas et al., 2019b).

Chemical Studies

In the study, essential oil rates (%) components and their rates (%) were determined as chemical properties.

After separating the dried plant samples into leaves and haulms, the hydro-distillation method was used to determine the essential oil rates. These rates were found volumetrically with the Neo-Clevenger apparatus (Electro-Mag) in the drog leaves and haulms (Wichtl, 1971). The gas chromatography–mass spectrometry (GC-MS) method was used for determination of essential oil components. GC–MS analyses were realized a Shimadzu (Japan) GC-2010 Plus Shimadzu GCMS-QP2010 SE (Detector) spectrometer using a Restek Rx-5Sil MS column (30 m× 0.25 mm× 0.25 um) (Catalog Number: Restek 1362). For GC–MS detection, an El system, with ionization energy of 70 eV, was used. Helium was the carrier gas, at a flow rate of 1.0 ml/min. Injector and MS transfer line temperatures were set at 250 °C and 250 °C, respectively. Diluted samples (1/10 in acetone, v/v) of 1.0 μL were injected in the split (1:10 split) mode.

http://www.aloki.hu ● ISSN 1589 1623 (Print) ● ISSN1785 0037 (Online)
DOI: http://dx.doi.org/10.15666/aeer/1902_14071421
© 2021, ALÖKI Kft., Budapest, Hungary

Table 1. *The coordinates, locations and altitudes of where Salvia fruticosa Mill. populations were collected*

Population Number	Coordinates	Locations	Altitude
1	37°09'02.2"N 28°25'16.5"E	Yenikoy, Mentese/Mugla	734
2	37°08'44.7"N 28°25'10.6"E	Yenikoy, Mentese/Mugla	772
3	37°05'38.0"N 28°22'11.1"E	Ula, Mugla	411
4	37°04'50.6"N 28°26'11.6"E	Ula, Mugla	613
5	37°04'49.4"N 28°26'10.6"E	Yesilova, Ula/Mugla	147
6	37°03'33.0"N 28°26'25.5"E	Yesilova, Ula/Mugla	68
7	37°03'31.0"N 28°26'21.8"E	Elmali, Ula/Mugla	77
8	37°02'52.0"N 28°17'17.1"E	Kuyucak, Mentese/Mugla	83
9	37°02'51.0"N 28°16'05.4"E	Kiransahili, Mentese/Mugla	162
10	37°00'39.4"N 28°20'21.0"E	Gokce, Ula/Mugla	75
11	37°00'44.5"N 28°19'28.1"E	Cetibeli, Marmaris/Mugla	112
12	36°59'25.4"N 28°17'25.4"E	Cetibeli, Marmaris/Mugla	295
13	36°58'41.6"N 28°16'54.5"E	Camlikoy, Marmaris/Mugla	65
14	36°58'59.1"N 28°15'37.1"E	Camlikoy, Marmaris/Mugla	5
15	36°58'43.6"N 28°14'54.9"E	Camlikoy, Marmaris/Mugla	105
16	36°58'16.2"N 28°16'09.3"E	Camlikoy, Marmaris/Mugla	23
17	36°55'55.6"N 28°14'12.8"E	Karaca, Marmaris/Mugla	248
18	36°56'34.1"N 28°13'25.3"E	Karaca, Marmaris/Mugla	95
19	36°53'51.6"N 28°16'04.2"E	Beldibi, Marmaris/Mugla	287
20	36°52'44.0"N 28°14'41.8"E	Marmaris, Mugla	259
21	36°52'22.301"N 28°14'38.323"E	Armutalan, Marmaris/Mugla	183
22	36°53'37.7"N 28°35'19.5"E	Sultaniye, Koycegiz/Mugla	26
23	36°43'59.4"N 28°40'51.4"E	Sarigerme, Ortaca/Mugla	99
24	36°43'35.2"N 28°51'39.8"E	Serefler, Dalaman/Mugla	238
25	36°47'36.9"N 28°39'42.7"E	Dalyan, Ortaca/Mugla	3
26	37°6'17.584 "N 27°54'36.224"E	Cakiralan, Milas/Mugla	290
27	37°2'37.912 "N 27°54'21.589"E	Turkevleri, Milas/Mugla	43
28	36°46'18.336 "N 28°55'47"E	Gocek, Fethiye/Mugla	182
29	36°48'35.831"N 28°56'11.49"E	Akarca, Dalaman/Mugla	256
30	36°45'39.452"N 28°58'23.139"E	Gocek, Fethiye/Mugla	199

Molecular Studies

DNA isolation

While starting the isolation, the tissues were dissected with the help of a homogenizer (Retsch MM400) using liquid nitrogen. Instead of Falcon tubes, 2 ml sample tubes were used and the prepared solution was added to the disrupted tissues and mixed in a homogenizer for 1 minute. In addition, the amount of NaCl in the homogenization buffer was used as 4M instead of 6M. In collecting DNA, centrifuge was used instead of glass pipette and the washing step was repeated 2 times. Genomic DNAs (gDNA) were extracted from the drog leaves of *Salvia fruticosa* Mill. for the DNA isolation, the extraction method described in Aljanabi et al.'s (1999) was modified and applied.

http://www.aloki.hu ● ISSN 1589 1623 (Print) ● ISSN1785 0037 (Online)
DOI: http://dx.doi.org/10.15666/aeer/1902_14071421
© 2021, ALÖKI Kft., Budapest, Hungary

Determination of DNA quantity and quality

Concentration of gDNAs were detected as ng/µl by spectrophotometer (OPTIZEN NanoQ). The quality of gDNAs were observed on agarose gel (0.8%). Agarose gel electrophoresis (Invitrogen Ultrapure Agarose, Catalog number: 16500500) was carried out for 1 hour at 100 V, 80 mA. Following this, the DNA quality of the samples was monitored under ultraviolet (UV) light on a gel imaging device.

Molecular marker analyses

gDNAs from the leaves of *Salvia fruticosa* Mill. was used for molecular analysis. In RAPD analysis, 15 RAPD primers (*Table 2*) which is high polymorphic for *Salvia* were selected from reported studies. As a result of the literature search for molecular marker analysis, RAPD markers–which are the most polymorphic for *Salvia* species–were employed (Skoula et al., 1999; Javan et al., 2012).

Table 2. *All primers used in the Salvia fruticosa Mill. molecular analysis, the number of bands formed by the band generating primers, and band sizes*

Primers	Name of primers	5'-Base Sequence-3'	Numbers of bands	Bands size
1	OPA-03	AGT CAG CCA C	19	250-3000 bp
2	OPA-04	AAT CGG GCT G	19	450-3000 bp
3	OPA-05	AGG GGT CTT G	8	300-3000 bp
4	OPA-06	GGT CCC TGA C	0	-
5	OPA-07	GAA ACG GGT G	18	200-3000 bp
6	OPB-01	GTT TCG CTC C	0	-
7	OPB-02	TGA TCC CTG G	0	-
8	OPB-03	CAT CCC CCA G	0	-
9	OPB-04	GGA CTG GAG T	0	-
10	OPB-05	TGC GCC CTT C	15	600-3000 bp
11	OPD-02	GGA CCC AAC C	14	550-2500 bp
12	OPD-03	GTC GCC GTC A	12	300-3000 bp
13	OPD-05	TGA GCG GAC A	10	300-3000 bp
14	OPD-08	GTG TGC CCC A	16	250-3000 bp
15	OPD-11	AGC GCC ATT G	19	450-3000 bp
Total			150	

PCR reactions performed in total 25 µl PCR reaction 1x PCR buffer, 30 ng of genomic DNA, 1 unit Taq DNA polymerase, 2 mM $MgCl_2$, O.2 mM each dATP, dCTP, dGTP, dTTP and 0.15 mM RAPD primer. Amplification was performed in Mycycler thermocycler (Biorad T100) as follows; 3 min at 94°C, 1 min at 94°C, 1 min at 50, 55, 60°C (depending on the annealing temperature), 1 min at 72°C for 40 cycles with 10 min final extension at 72°C. PCR reactions were analysed by 1.5% agarose gel.

Evaluation of Data

Ten out of the 15 primers shown in *Table 2* yielded reproducible and reliable amplified DNA products. These amplified DNA fragments were evaluated for genetic diversity of *Salvia fruticosa* Mill. The amplified RAPD bands were scored as 1 or 0 depending on the presence or absence on gel to create the excel tables. Populations and primers were entered using the GenAlex 6.5 software (Peakall and Smouse, 2012). With the unweighted pair group method with arithmetic mean (UPGMA) method, a genetic proximity-distance dendrogram as standardized by Nei (1978) was created. Hierarchical

http://www.aloki.hu ● ISSN 1589 1623 (Print) ● ISSN1785 0037 (Online)
DOI: http://dx.doi.org/10.15666/aeer/1902_14071421
© 2021, ALÖKI Kft., Budapest, Hungary

clustering analysis and dendrogram were generated by SPSS Statistics v 22 program; these showed the proximity and distance between the populations in terms of chemical components examined.

Results and Discussion

Chemical Results

As shown in *Table 3*, the average essential oil rate of leaves in the populations varied in the range of 0.34–3.76%, the average essential oil rate of the haulm was 0.01–0.23%, and the average total essential oil rate was 0.22–2.80%. The essential oil rates of the *Salvia fruticosa* Mill. species determined in the study are compatible with those determined by Karousou and Kokkini (1997), Mossi et al. (2011), and Karik (2015).

Table 3. *Average values of essential oil rates of Salvia fruticosa Mill. in 2017 and 2018*

Populations	The Rates of Essential Oil in The Leaf (%)	The Rates of Essential Oil in The Haulm (%)	The Total Rates of Essential Oil (%)
1.P	0.56	0.03	0.28
2.P	0.34	0.03	0.22
3.P	2.75	0.19	1.98
4.P	2.67	0.18	1.24
5.P	2.92	0.16	1.95
6.P	3.76	0.20	1.99
7.P	2.29	0.10	1.24
8.P	2.99	0.05	1.42
9.P	2.55	0.01	1.45
10.P	2.48	0.04	1.30
11.P	2.20	0.05	1.27
12.P	1.93	0.02	1.06
13.P	2.97	0.03	1.62
14.P	2.26	0.08	1.30
15.P	3.09	0.09	1.91
16.P	1.97	0.07	1.46
17.P	2.49	0.09	1.36
18.P	2.96	0.13	1.70
19.P	3.39	0.20	2.80
20.P	2.21	0.13	1.37
21.P	2.18	0.09	1.31
22.P	3.38	0.13	1.88
23.P	2.93	0.15	1.48
24.P	2.62	0.06	1.64
25.P	3.14	0.17	1.81
26.P	2.93	0.08	1.43
27.P	2.89	0.23	1.79
28.P	2.81	0.22	1.70
29.P	2.72	0.13	1.39
30.P	2.77	0.19	1.24
Average	**2.57**	**0.11**	**1.49**
S.D.	**0.7**	**0.06**	**0.48**

The components of essential oils in *Salvia fruticosa* Mill. populations collected from flora in 2017 and 2018 were determined using the GC-MS method, and their average components and distribution according to the populations are given in *Table 4*. The rates

http://www.aloki.hu ● ISSN 1589 1623 (Print) ● ISSN1785 0037 (Online)
DOI: http://dx.doi.org/10.15666/aeer/1902_14071421
© 2021, ALÖKI Kft., Budapest, Hungary

of 1,8-cineole, camphor, camphene, α-pinene–some of the major essential oil components of *Salvia fruticosa* Mill. –determined by GC-MS analysis showed wide variation among the populations, and the results are compatible with those of Bayram (2001), Uysal (2015), and Karik (2015), who previously studied this species.

Table 4. *Average of principal chemical components of Salvia fruticosa Mill. populations collected in 2017 and 2018 and distribution by population (%)*

Populations	α-Humulene	α-Pinene	α-Thujone	1,8-Cineole	β-Pinene	Camphene	Camphor	Trans β-Caryophyllene	Caryophyllene oxide	Cymol	β-Myrcene	Thujene-α
1.P	3.98	30.46	0.0	38.72	3.56	1.17	1.09	0.88	1.96	0.0	1.51	0.37
2.P	3.72	19.93	0.08	24.62	17.82	0.88	2.24	0.78	1.29	1.07	1.78	0.38
3.P	1.43	5.26	0.50	59.90	3.62	0.54	1.15	2.57	15.00	0.24	6.79	0.26
4.P	1.26	4.88	1.76	59.38	3.55	1.21	2.63	3.56	0.55	0.58	2.43	0.15
5.P	0.62	4.78	2.88	50.65	6.86	1.82	6.26	2.68	0.45	0.58	2.67	0.45
6.P	0.67	4.32	3.47	58.40	6.91	1.02	3.73	3.63	0.40	0.44	3.07	0.32
7.P	1.17	5.46	1.54	53.58	6.02	2.45	5.17	2.49	0.56	0.64	3.77	0.22
8.P	2.00	3.81	1.69	45.16	4.75	2.03	8.52	2.90	0.64	0.55	2.46	0.12
9.P	0.87	4.99	3.55	55.75	5.99	1.25	2.77	2.66	0.38	0.59	3.41	0.20
10.P	1.26	6.85	1.22	53.21	7.83	2.77	3.85	7.95	0.43	0.29	1.90	0.30
11.P	1.04	6.01	1.12	53.75	7.19	2.85	5.27	4.05	0.48	0.57	2.57	0.16
12.P	1.00	5.39	1.03	58.14	2.99	0.58	1.03	4.20	0.52	0.69	4.02	0.23
13.P	0.60	5.33	0.92	56.13	7.56	2.57	4.52	2.33	0.46	0.41	4.60	0.28
14.P	1.32	5.54	0.47	59.83	8.80	0.51	1.54	2.36	0.55	0.45	3.11	0.30
15.P	0.68	5.95	1.04	50.61	4.68	4.50	9.03	2.92	0.37	0.41	2.68	0.12
16.P	1.01	5.37	0.59	49.39	3.51	3.99	9.68	2.75	0.38	0.59	5.10	0.15
17.P	1.42	5.59	0.66	54.58	7.46	1.94	3.76	4.03	0.50	0.11	3.66	0.11
18.P	1.28	5.22	0.79	58.99	7.60	1.58	2.75	1.68	0.34	0.40	2.90	0.29
19.P	0.72	4.32	1.14	61.01	3.61	1.05	2.24	3.63	0.45	0.28	2.54	0.10
20.P	1.05	5.11	0.83	60.15	6.18	1.26	2.91	4.54	0.51	0.27	3.26	0.22
21.P	1.41	5.24	0.63	59.27	3.38	1.15	1.63	4.31	0.48	0.49	6.72	0.30
22.P	0.54	4.82	3.91	56.31	6.38	1.51	2.71	2.35	0.56	0.54	3.79	0.45
23.P	0.81	4.41	4.02	57.38	5.98	1.18	2.17	2.93	0.39	0.56	4.69	0.32
24.P	0.6	4.68	2.55	54.97	5.29	2.24	7.4	1.80	0.50	0.31	3.7	0.12
25.P	0.7	4.37	3.61	57.82	6.58	0.88	2.4	4.01	0.36	0.44	6.2	0.33
26.P	1.0	5.44	0.64	62.47	6.77	1.08	2.3	2.59	0.42	0.57	7.4	0.15
27.P	1.0	5.03	2.52	57.31	6.23	1.74	4.8	3.61	0.52	0.59	5.6	0.16
28.P	1.2	4.47	2.44	60.52	6.78	1.39	2.9	2.10	0.28	0.52	5.7	0.33
29.P	1.5	4.03	1.82	59.76	6.06	1.30	8.1	3.41	0.41	0.57	5.0	0.15
30.P	0.9	5.06	2.92	58.89	6.47	1.67	4.0	1.68	0.23	0.73	4.9	0.32
Av.	**1.23**	**6.40**	**1.68**	**54.89**	**6.21**	**1.67**	**3.95**	**3.05**	**1.01**	**0.48**	**3.93**	**0.25**
S.D.	**0.79**	**5.33**	**1.21**	**7.64**	**2.70**	**0.94**	**2.47**	**1.34**	**2.66**	**0.20**	**1.59**	**0.10**

Table 5 shows the relationships between populations in terms of essential oil components. For the clustering analysis, it was determined that the populations were separated into two main clusters and subclusters within them.

http://www.aloki.hu ● ISSN 1589 1623 (Print) ● ISSN1785 0037 (Online)
DOI: http://dx.doi.org/10.15666/aeer/1902_14071421
© 2021, ALÖKI Kft., Budapest, Hungary

Table 5. *Hierarchical clustering analysis showing the relationships between genotypes in terms of chemical properties of Salvia fruticosa Mill. (Squared Euclidean Distance)*

Populations	1.P	2.P	3.P	4.P	5.P	6.P	7.P	8.P	9.P	10.P	11.P	12.P	13.P	14.P	15.P	16.P	17.P	18.P	19.P	20.P	21.P	22.P	23.P	24.P	25.P	26.P	27.P	28.P	29.P	30.P
1.P	**0.0**																													
2.P	516.2	**0.0**																												
3.P	1291.9	1885.4	**0.0**																											
4.P	1108.4	1660.2	235.9	**0.0**																										
5.P	876.0	1075.9	365.9	104.5	**0.0**																									
6.P	1130.2	1543.1	262.0	17.7	69.2	**0.0**																								
7.P	896.3	1220.0	288.2	51.2	15.2	35.3	**0.0**																							
8.P	824.6	905.9	504.7	242.0	47.9	211.8	91.0	**0.0**																						
9.P	990.8	1371.0	269.4	26.3	40.6	11.4	17.4	159.6	**0.0**																					
10.P	858.8	1155.9	343.5	84.8	53.5	64.1	42.2	132.7	57.4	**0.0**																				
11.P	882.1	1190.0	305.3	57.4	22.3	38.0	7.6	98.5	29.0	19.3	**0.0**																			
12.P	1036.6	1582.5	224.2	10.6	114.1	34.6	57.1	238.3	35.2	81.8	62.8	**0.0**																		
13.P	991.4	1341.7	262.6	42.5	49.4	24.3	15.1	155.0	25.3	51.7	14.9	45.4	**0.0**																	
14.P	1111.5	1542.2	250.7	33.7	121.5	23.9	66.1	288.7	40.1	90.4	63.1	42.6	33.0	**0.0**																
15.P	838.9	1120.6	398.0	133.4	28.6	116.9	33.8	43.1	91.3	73.7	34.5	143.1	67.9	175.8	**0.0**															
16.P	854.6	1119.7	412.3	167.9	45.5	153.6	51.6	36.4	119.7	108.9	62.1	166.9	91.6	220.1	10.1	**0.0**														
17.P	918.3	1236.6	274.7	44.4	34.8	27.8	10.2	126.4	20.9	23.2	5.8	43.2	9.0	39.8	61.0	86.1	**0.0**													
18.P	1081.8	1513.9	251.7	22.4	92.3	15.9	42.1	238.1	27.4	79.3	42.2	34.1	16.9	5.7	129.3	169.0	27.0	**0.0**												
19.P	1206.1	1791.5	236.0	4.5	142.3	27.0	77.5	295.9	46.3	110.0	81.2	14.7	54.9	33.6	170.6	208.1	63.1	25.8	**0.0**											
20.P	1141.5	1644.7	237.4	10.9	114.0	14.3	56.3	265.7	35.1	70.8	51.8	19.6	30.3	14.7	145.2	183.2	34.7	11.9	10.0	**0.0**										
21.P	1107.6	1669.3	215.1	23.0	138.7	43.6	69.3	273.2	50.1	103.8	79.6	9.8	47.2	47.8	162.3	175.8	53.8	41.1	23.3	22.8	**0.0**									
22.P	1033.2	1414.4	269.2	31.7	49.1	12.5	24.8	181.6	2.1	71.4	40.0	45.0	31.7	41.8	106.5	136.2	30.3	30.8	51.2	39.6	56.3	**0.0**								
23.P	1097.0	1511.7	260.8	27.3	70.8	12.2	37.8	215.3	6.5	83.8	55.1	38.1	39.3	40.1	132.7	159.7	39.2	32.9	42.7	34.1	43.0	3.2	**0.0**							
24.P	1019.5	1455.9	311.7	57.9	43.0	55.4	26.6	121.8	38.2	103.7	51.0	80.3	57.8	115.3	51.3	62.8	59.5	80.7	85.1	84.2	90.3	40.7	50.0	**0.0**						
25.P	1117.7	1665.1	243.4	25.4	108.8	39.5	61.1	232.6	33.2	113.6	84.3	21.8	64.7	81.1	144.2	154.1	66.9	65.3	36.4	46.1	20.9	35.7	24.7	52.0	**0.0**					
26.P	1250.8	**1968.2**	229.8	42.8	218.2	81.5	127.3	382.4	95.8	197.9	151.4	40.0	99.5	85.5	234.0	246.0	122.2	76.3	35.1	52.9	20.8	96.3	75.9	113.2	36.6	**0.0**				
27.P	1058.6	1608.8	246.6	24.7	86.3	40.9	41.4	187.9	35.3	98.9	61.3	27.2	49.6	85.9	95.1	103.1	54.5	61.0	38.8	45.1	26.4	40.8	36.1	27.0	9.4	41.6	**0.0**			
28.P	1204.8	1822.2	238.8	19.8	143.3	41.8	78.0	294.4	46.3	151.9	104.6	29.6	69.4	65.6	173.3	190.9	84.5	51.3	23.1	38.2	22.9	44.5	31.9	58.6	13.8	14.9	18.3	**0.0**		
29.P	1232.5	1858.6	280.9	52.5	148.6	78.8	92.1	243.0	96.6	161.3	107.4	65.5	86.6	128.8	126.5	133.0	106.3	95.1	56.4	71.0	59.4	106.4	99.7	59.5	52.9	55.6	26.5	45.9	**0.0**	
30.P	1110.3	1687.4	252.2	18.7	102.4	33.8	51.5	234.8	30.4	127.4	77.5	32.0	54.7	68.0	126.7	144.5	66.9	47.4	29.8	41.3	32.4	30.1	24.8	30.9	13.3	32.8	9.8	5.5	40.7	**0.0**

http://www.aloki.hu ● ISSN 1589 1623 (Print) ● ISSN1785 0037 (Online)
DOI: http://dx.doi.org/10.15666/aeer/1902_14071421
© 2021, ALÖKI Kft., Budapest, Hungary

As illustrated in *Figure 1,* yellow-marked populations 1 and 2 formed the first cluster, while red-marked populations 5, 7, 8, 10, 11, 13, 15, 16, and 17 and blue-marked populations 3, 4, 6, 9, 12, 14, 18, 19, 20, 21, 22, 23, 24, 25, 26, 27, 28, 29, and 30 formed the second cluster. In the dendrogram in *Figure 2*, it is shown that populations 1 and 2 from Yenikoy are distinctly separated from other populations and form a spontaneous cluster. The populations closest to each other in terms of the proportions of the components are populations 9 and 22 (Euclidean distance: 2.1). Following this, the closest populations were determined as 22 (Koycegiz) and 23 (Ortaca) and 4 (Ula) and 19 (Marmaris; Euclidean distances: 3.2 and 4.5, respectively). As a result of the hierarchical clustering analysis, the most distant populations were identified as populations 2 (Yenikoy) and 26 (Milas; Euclidean distance: 1,968.2). The next farthest populations were 2 (Yenikoy) and 3 (Ula) and 2 and 29 (Dalaman; Euclidean distances: 1,885.4 and 1,858.6, respectively). While populations from Fethiye (28 and 30), Milas (26 and 27), Ortaca (23 and 25), and Dalaman (24 and 29) were clustered tightly, it was determined that populations from Marmaris, Ula, and Mentese were distributed in separate subsets.

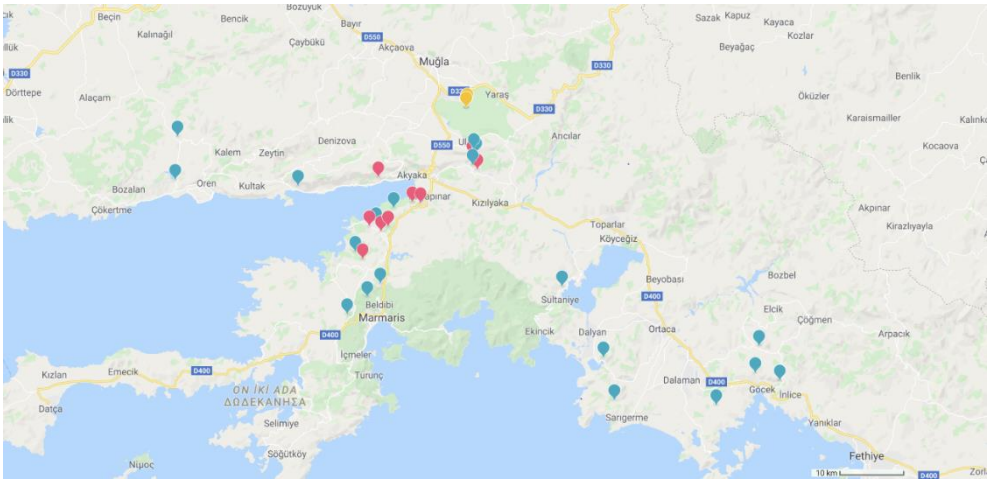


Figure 1. *Map image of clusters of Salvia fruticosa Mill. populations according to chemical markers*

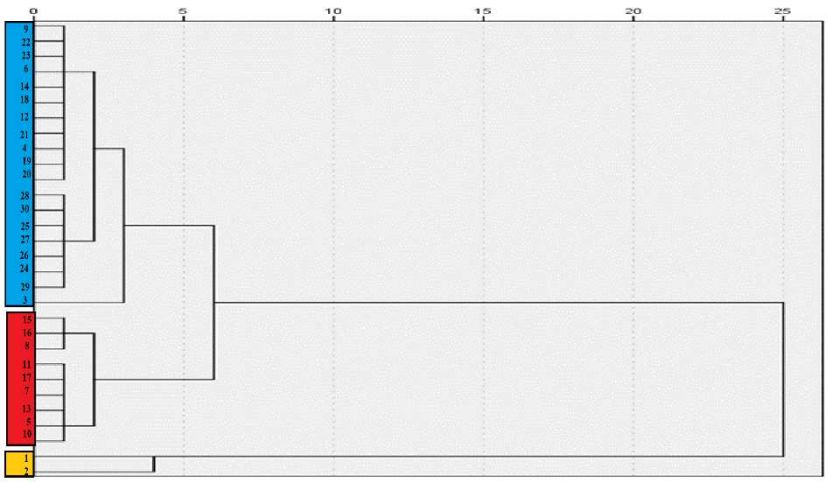


Figure 2. *Dendogram of the relationships between populations in terms of rates of chemical components of Salvia fruticosa Mill.*

http://www.aloki.hu ● ISSN 1589 1623 (Print) ● ISSN1785 0037 (Online)
DOI: http://dx.doi.org/10.15666/aeer/1902_14071421
© 2021, ALÖKI Kft., Budapest, Hungary

Molecular Marker Analysis

The amplified products from RAPD loci from each sample were separated by gel electrophoresis. In total 150 DNA bands were produced and evaluated. The bands were scored as 1 or 0 according to the presence and absence of bands. The agarose gel images of RAPD-PCR analysis with isolated DNA from the leaves of Salvia fruticosa Mill. are given in *Figure 3*.

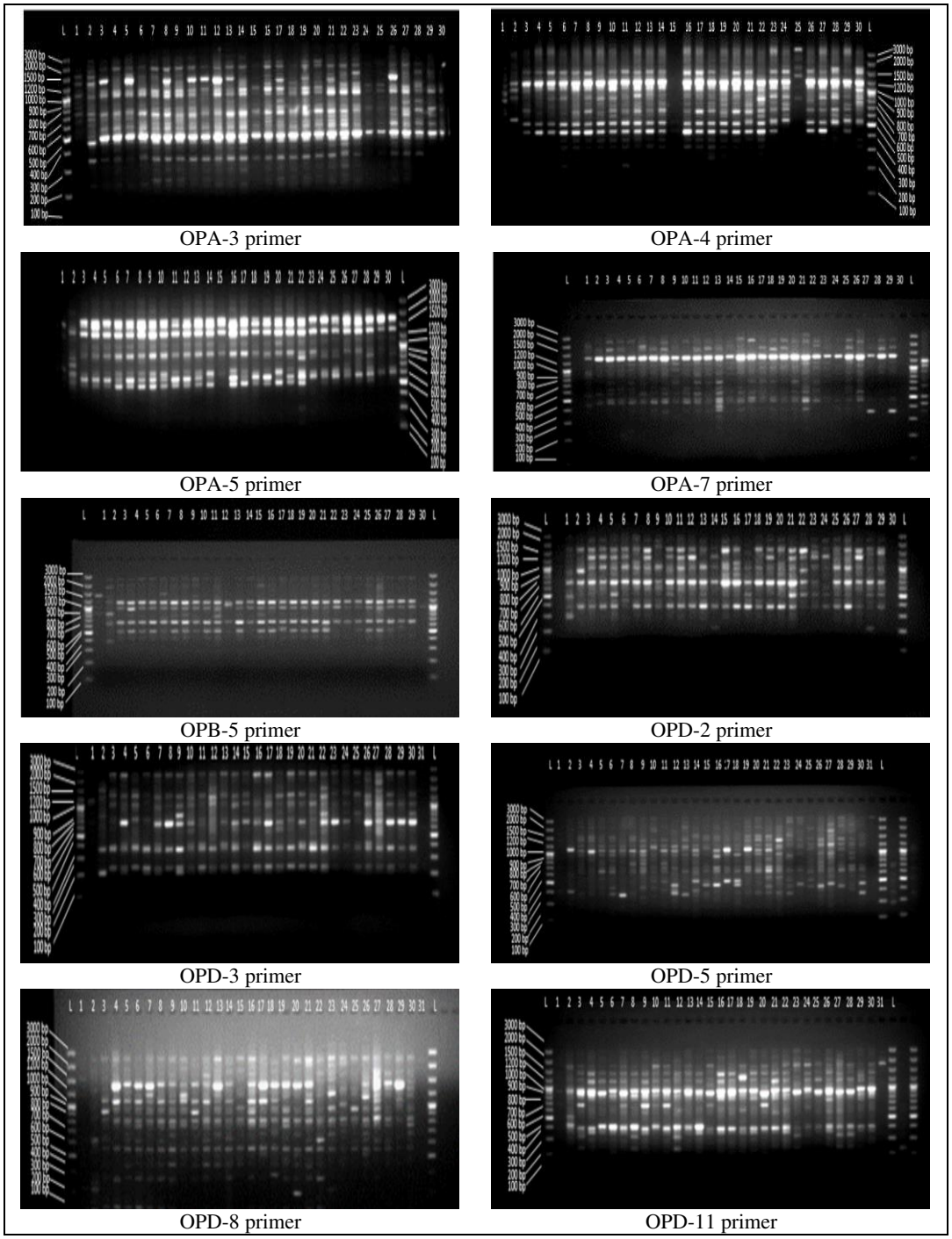


Figure 3. *Agarose gel images of RAPD-PCR products obtained from drog leaf with primers*

http://www.aloki.hu ● ISSN 1589 1623 (Print) ● ISSN1785 0037 (Online)
DOI: http://dx.doi.org/10.15666/aeer/1902_14071421
© 2021, ALÖKI Kft., Budapest, Hungary

The values showing genetic relationships among *Salvia fruticosa* Mill. populations collected from nature in the Mugla region are given in *Table 6*. In addition, dendrograms showing genetic relationships between populations are given in *Figure 4*. As a result of the analyses illustrated in *Figure 4*, it is shown that populations are genetically divided into two main clusters.

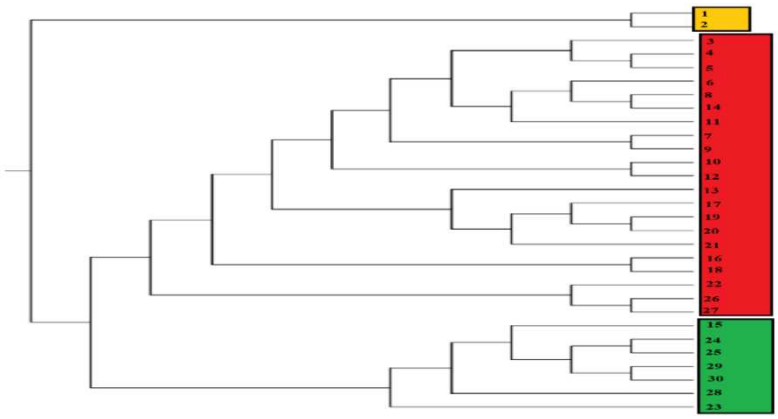


Figure 4. *Dendrogram showing the genetic relationship between Salvia fruticosa Mill. populations*

As shown in *Figure 5*, yellow-marked populations 1 and 2 formed the first cluster, while green-marked populations 15, 23, 24, 25, 28, 29, and 30 and red-marked populations 3, 4, 5, 6, 7, 8, 9, 10, 11, 12, 13, 14, 16, 17, 18, 19, 20, 21, 22, 26, and 27 formed the second cluster. In the UPGMA dendrogram in *Figure 4*, it can be observed that populations 1 and 2 from Yenikoy are distinctly separate from the other populations. The genetic distances of the populations are as follows: Fethiye and Marmaris, 32.3–48.8%; Fethiye and Ula, 33.2–45.5%; Fethiye and Ortaca, 30.4–44.4%; Fethiye and Dalaman, 22.3–38.2%; Fethiye and Mentese, 40.2–64.6%; Fethiye and Milas, 34.2–39.2%; and Fethiye and Koycegiz, 40.2–41.2%. The genetic distance between populations 28 and 30 collected from Fethiye is 27.6%. The distance between the Marmaris and Mentese populations is 16.5–83.4%, that of Marmaris and Ortaca is 30.4–59.5%, that of Marmaris and Koycegiz is 28.5–59.5%, that of Marmaris and Dalaman is 32.3–55.8%, that of Marmaris and Ula is 17.3–48.8%, and that of Marmaris and Milas is 26.7–47.7%. The genetic distance of the Marmaris populations is 15.7–59.5%. As shown in *Table 6*, the most genetically distant populations were determined as 1 (Yenikoy) and 22 (Sultaniye, Koycegiz; genetic distance value: 0.88), followed by populations 2 (Yenikoy) and 20 (Marmaris) and 1 (Yenikoy) and 21 (Marmaris; genetic distance value of both: 0.83).

The genetically closest populations were populations 4 and 5, both collected from Ula (genetic distance value: 0.14). The next closest populations were populations 19 and 20 (Marmaris; genetic distance value: 0.15). Skoula et al. (1999) used the RAPD-PCR method to search the effect of genotype on the chemical profile of the *Salvia fruticosa* Mill. species and determined that there is genetic diversity both within and between populations; the same finding was evident in our study. In their research, the different essential oil rates and component's rates determined in the populations confirmed the genetic variability in each population. Skoula et al.'s (1999) results are compatible with the results obtained in our study.

http://www.aloki.hu ● ISSN 1589 1623 (Print) ● ISSN1785 0037 (Online)
DOI: http://dx.doi.org/10.15666/aeer/1902_14071421
© 2021, ALÖKI Kft., Budapest, Hungary

Table 6. *Genetic distance matrix between Salvia fruticosa Mill. genotypes*

Pop.	1	2	3	4	5	6	7	8	9	10	11	12	13	14	15	16	17	18	19	20	21	22	23	24	25	26	27	28	29	30
1	1.00																													
2	0.44	1.00																												
3	0.53	0.63	1.00																											
4	0.63	0.65	0.19	1.00																										
5	0.57	0.59	0.20	**0.14**	1.00																									
6	0.74	0.63	0.30	0.18	0.24	1.00																								
7	0.64	0.67	0.29	0.17	0.23	0.25	1.00																							
8	0.72	0.64	0.17	0.18	0.19	0.18	0.24	1.00																						
9	0.74	0.80	0.38	0.24	0.29	0.23	0.22	0.25	1.00																					
10	0.65	0.63	0.34	0.30	0.37	0.24	0.25	0.22	0.30	1.00																				
11	0.59	0.70	0.24	0.22	0.23	0.22	0.21	0.19	0.24	0.27	1.00																			
12	0.78	0.75	0.33	0.25	0.26	0.20	0.34	0.21	0.25	0.25	0.28	1.00																		
13	0.72	0.75	0.39	0.24	0.26	0.29	0.24	0.28	0.29	0.27	0.24	0.30	1.00																	
14	0.72	0.72	0.29	0.17	0.24	0.20	0.24	0.16	0.25	0.25	0.21	0.24	0.24	1.00																
15	0.36	0.60	0.40	0.42	0.41	0.48	0.33	0.47	0.46	0.42	0.33	0.59	0.41	0.45	1.00															
16	0.75	0.75	0.43	0.33	0.40	0.31	0.30	0.32	0.24	0.29	0.32	0.32	0.40	0.24	0.49	1.00														
17	0.72	0.75	0.33	0.25	0.32	0.31	0.26	0.30	0.33	0.31	0.24	0.32	0.30	0.23	0.41	0.28	1.00													
18	0.63	0.80	0.36	0.32	0.43	0.34	0.33	0.37	0.38	0.34	0.29	0.35	0.33	0.27	0.34	0.29	0.24	1.00												
19	0.67	0.72	0.27	0.29	0.34	0.31	0.28	0.28	0.31	0.29	0.23	0.34	0.26	0.28	0.39	0.32	0.18	0.29	1.00											
20	0.74	0.83	0.36	0.30	0.35	0.34	0.24	0.29	0.26	0.30	0.27	0.37	0.24	0.20	0.36	0.27	0.18	0.26	0.15	1.00										
21	0.83	0.77	0.28	0.30	0.31	0.30	0.27	0.24	0.32	0.24	0.27	0.33	0.27	0.25	0.44	0.29	0.22	0.36	0.17	0.21	1.00									
22	**0.88**	0.78	0.52	0.37	0.46	0.31	0.38	0.40	0.31	0.37	0.42	0.36	0.30	0.32	0.59	0.42	0.32	0.39	0.28	0.31	0.35	1.00								
23	0.53	0.68	0.46	0.53	0.54	0.48	0.45	0.45	0.55	0.44	0.49	0.49	0.54	0.47	0.40	0.47	0.47	0.40	0.49	0.46	0.44	0.41	1.00							
24	0.44	0.53	0.36	0.40	0.41	0.42	0.43	0.37	0.48	0.36	0.39	0.47	0.43	0.41	0.32	0.49	0.41	0.40	0.41	0.40	0.42	0.43	0.32	1.00						
25	0.40	0.51	0.40	0.42	0.39	0.48	0.45	0.45	0.51	0.51	0.39	0.59	0.47	0.47	0.30	0.59	0.49	0.51	0.49	0.48	0.46	0.52	0.42	0.23	1.00					
26	0.74	0.68	0.40	0.30	0.31	0.32	0.33	0.35	0.34	0.32	0.37	0.29	0.29	0.29	0.42	0.35	0.33	0.38	0.31	0.26	0.30	0.27	0.38	0.34	0.40	1.00				
27	0.70	0.72	0.33	0.31	0.38	0.33	0.44	0.28	0.45	0.33	0.42	0.28	0.40	0.32	0.47	0.42	0.40	0.41	0.40	0.37	0.31	0.36	0.31	0.39	0.43	0.25	1.00			
28	0.59	0.64	0.39	0.41	0.40	0.45	0.44	0.40	0.45	0.39	0.44	0.42	0.40	0.44	0.43	0.46	0.48	0.43	0.40	0.39	0.47	0.40	0.41	0.29	0.39	0.35	0.34	1.00		
29	0.47	0.59	0.45	0.39	0.38	0.52	0.36	0.48	0.47	0.41	0.46	0.55	0.40	0.40	0.33	0.44	0.44	0.39	0.40	0.37	0.39	0.48	0.43	0.29	0.33	0.29	0.40	0.38	1.00	
30	0.48	0.53	0.40	0.34	0.35	0.40	0.33	0.41	0.40	0.40	0.35	0.47	0.37	0.37	0.32	0.47	0.37	0.42	0.37	0.34	0.40	0.41	0.44	0.23	0.30	0.34	0.39	0.27	0.22	1.00

http://www.aloki.hu ● ISSN 1589 1623 (Print) ● ISSN1785 0037 (Online)
DOI: http://dx.doi.org/10.15666/aeer/1902_14071421
© 2021, ALÖKI Kft., Budapest, Hungary

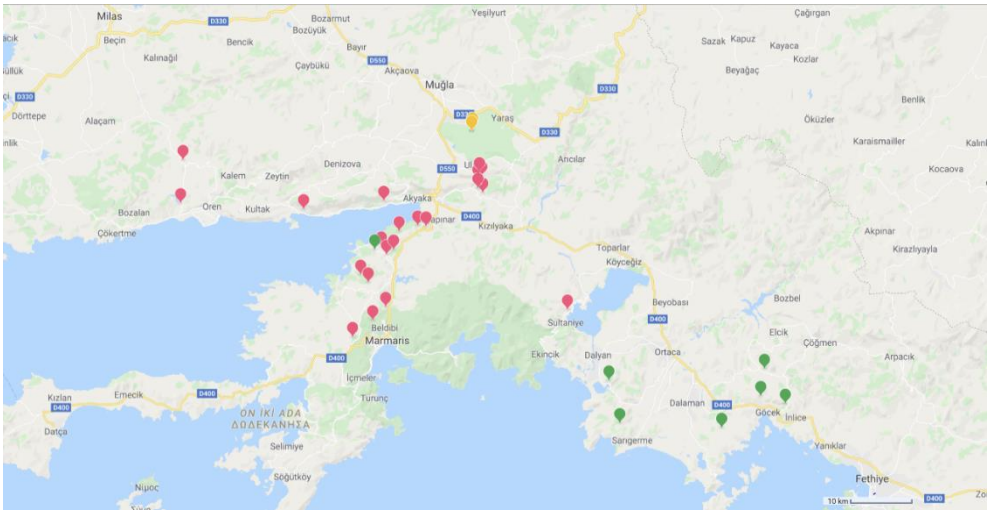


Figure 5. *Map image of clusters of Salvia fruticosa Mill. populations according to molecular markers*

In another study carried out in Mugla province, Altindal (2019) determined the genetic relationships in natural sage populations collected from the Fethiye, Gocek, Dalaman, Koycegiz, Yerkesik, Dalyan, Marmaris, and Bodrum districts. In the dendrogram, Dalyan, Koycegiz, Marmaris, and Bodrum were in the first group, while Gocek, Dalaman, and Fethiye formed the second group; the sages belonging to the Yerkesik region formed a spontaneous group. The highest genetic similarity rate was determined in the Koycegiz and Bodrum populations and the lowest between the Yerkesik and Bodrum populations. The molecular method used by Altindal (2019) to determine genetic relationships is different from that in our study, but the dendrogram in which the genetic relationships are shown is similar to ours.

Conclusion

In this study on *Salvia fruticosa* Mill., which has a natural distribution in Mugla province, it was determined that there is wide chemical and genetic variation both within and among the populations. In the study, while within-population differences essential oil rates and components were determined by comparing them with the mean values of that population, differences between populations were determined by comparing the essential oil ratios in other populations and their mean value of components and by molecular analyses. In hierarchical clustering analysis and dendrogram, chemical and genetic profiles of *Salvia fruticosa* Mill. populations were found to be compatible with each other.

The differences between dendrograms may be due to a number of complex linkages, such as gene expression between phenotypes and genotypes, as well as the morphological and chemical characteristics of plants, which may change with the environment and gene exchange between species during natural selection. In the study, the genetic proximity of populations that are geographically close to each other showed that there was gene flow between populations (Skoula et al., 1999). The different rates and components of essential oils determined in the populations also confirmed that there is genetic variability in each population.

http://www.aloki.hu ● ISSN 1589 1623 (Print) ● ISSN1785 0037 (Online)
DOI: http://dx.doi.org/10.15666/aeer/1902_14071421
© 2021, ALÖKI Kft., Budapest, Hungary

The chemical properties of medicinal and aromatic plants may vary depending on their genetic profile, and the geographical and climatic conditions in which they distributed naturally. In this study, *Salvia fruticosa* Mill. both essential oil rates and components showed wide variation in populations. Different biotic (bacteria, fungus, virus, etc.) and abiotic stress factors (drought, salinity, radiation, light, low or high temperatures, nutrient deficiencies, etc.), which were reported to cause changes in the chemical structure of the *Salvia fruticosa* Mill. plant in previous studies, may be the reason for the wide variation in chemical properties among the populations in this study (Arikat et al., 2004; Chrysargyris et al., 2016) In previous studies carried out on *Salvia fruticosa Mill.* it has been reported that the plant produces anatomical, physiological and morphological changes in its structure as well as changes in its chemical structure in order to overwhelm these factors that cause stress. The reason for the wide variation in the rates and components of *Salvia fruticosa* Mill. essential oil among the populations may be due to genetic characteristics, environmental, climatic conditions and the effect of each of different stress factors or a combination of all these factors.

Salvia fruticosa Mill. populations, which have a natural distribution in Mugla province, have been used extensively in folk medicine for many years and provide additional income to local people, who collect and sell the plants (Karik, 2015). However, many factors, such as irregular construction, intense grazing, and unconscious harvests in Mugla province–where many plant species are distributed naturally–can cause reduced populations of these species and jeopardize their continuity. The degradation or disintegration of these natural populations may lead to differentiation in the genetic structure of populations due to gene flow and genetic drift between species (Hatmaker et al., 2018). To prevent a possible genetic erosion, a gene database should be determined using molecular methods for economically valuable, endemic, and endangered species; furthermore, gene banks should be set up, and genetic resources of these species should be protected (Altindal, 2019).

Production of superior genotypes that will provide economic benefits by determining and manipulating genetic and chemical diversity can be beneficial for economic development. *Salvia fruticosa* Mill. is a species of high medicinal and economic value, so it is important to investigate its utilizability and sustainability in future studies. Characterization of the diversity of essential oils of *Salvia fruticosa* Mill. and the comparison of molecular characterization can contribute to the opportunity to grow homogeneous plant material with desired commercial characteristics such as stable essential oil profile. This study will provide insight into the future studies to obtain superior genotypes and to benefit from them in commercial breeding studies. In future studies on *Salvia fruticosa* Mill. it is recommended to investigate genetic differences and identify agriculturally important genes using different molecular markers (ISSR, SSR etc.) together with chemical and morphological characteristic analyzes.

The limitations of the study are as follows:

1. Soil analysis of the locations where *Salvia fruticosa* Mill. populations were collected was not performed. Therefore, other than genetic diversity, the cause of the wide variation in the population and between populations may be related to many ecological factors, including soil structure, temperature, precipitation, sunshine duration and intensity, altitude, drought, and salinity.

2. The study was conducted at the end of the flowering period of *Salvia fruticosa* Mill., and in each population, the plant material collection hours were different. In previous

http://www.aloki.hu ● ISSN 1589 1623 (Print) ● ISSN1785 0037 (Online)
DOI: http://dx.doi.org/10.15666/aeer/1902_14071421
© 2021, ALÖKI Kft., Budapest, Hungary

studies, the highest essential oil rates of *Salvia fruticosa* Mill. was reported in May–June, before flowering or at the beginning of flowering, and at noon when the active components reached their peaks. In addition, various factors affect the yield and quality of the essential oil of the plants, including the age of the plant; climatic, seasonal, and geographical conditions; harvest time of the plant; drying methods; part of the plant; and distillation technique (Altindal, 2019).

Acknowledgments. This article was developed from a doctoral thesis titled '*Determination of Morphological, Chemical and Molecular Characterization of Salvia fruticosa Mill. Populations Distributed in Mugla Province Naturally*'. The project was supported by Mugla Sitki Kocman University Scientific Research Projects Unit, project number 17/213. It was also presented as an oral paper at the 2nd International Congress on Agriculture, Environment and Health at Adnan Menderes University and 1st International Symposium on Biodiversity Research at Canakkale Onsekiz Mart University.

REFERENCES

[1] Aljanabi, S. M., Forget, L., Dookun, A. (1999): An improved and rapid protocol for the isolation of polysaccharide-and polyphenol-free sugarcane DNA. – Plant Molecular Biology Reporter 17(3): 281-282.

[2] Altindal, D. (2019): Determination of genetic diversity of natural sage populations in Mugla region of Turkey. – International Journal of Environmental Science and Technology 16(9): 5219-5226.

[3] Arikat, N. A., Jawad, F. M., Karam, N. S., Shibli, R. A. (2004): Micropropagation and accumulation of essential oils in wild sage (*Salvia fruticosa* Mill.). – Scientia Horticulturae 100(1-4): 193-202.

[4] Bacu, A., Konkjika, E., Mullaj, A. (2005): Molecular characterization of *Salvia officinalis* and *Salvia triloba* grown in Albania. – Albanian Journal of Natural and Technical Sciences (1), X (17): 65-71.

[5] Bayram, E. (2001): A study on selecting suitable types of the Anatolia sage (*Salvia fruticosa* Mill.) in the flora of western Anatolia. – Turkish Journal of Agriculture and Forestry 25(6): 351-357. (in Turkish).

[6] Chrysargyris, A., Laoutari, S., Litskas, V. D., Stavrinides, M. C., Tzortzakis, N. (2016): Effects of water stress on lavender and sage biomass production, essential oil composition and biocidal properties against *Tetranychus urticae* (Koch). – Scientia horticulturae 213: 96-103.

[7] Elmas, S. (2019a): Determination of morphological, chemical and molecular characterization of *Salvia fruticosa* Mill. populations distributed in Mugla province naturally. – Mugla Sitki Kocman University, Institute of Science Department of Biology, PhD Thesis, Mugla, Turkey. (in Turkish).

[8] Elmas, S., Arabacı, O., Zeybek, A. (2019b): Determination of some agricultural characteristics and essential oil amounts of *Salvia fruticosa* Mill. populations in Mugla province. – Mediterranean Agricultural Sciences 32(2): 243-249. (in Turkish).

[9] Guner, A., Ozhatay, N., Ekim, T., Baser, K. H. C. (2001): Flora of Turkey and the east Aegean Islands. – Edinburgh University Press, Edinburgh.

[10] Hatmaker, E. A., Staton, M. E., Dattilo, A. J., Hadziabdic, D., Rinehart, T. A., Schilling, E. E., Trigiano, R. N., Wadl, P. A. (2018): Population structure and genetic diversity within the endangered species *Pityopsis ruthii* (Asteraceae). – Frontiers in Plant Science 9: 943.

[11] Javan, Z. S., Rahmani, F., Heidari, R. (2012): Assessment of genetic variation of genus' *Salvia*' by RAPD and ISSR markers. – Australian Journal of Crop Science 6(6): 1068.

http://www.aloki.hu ● ISSN 1589 1623 (Print) ● ISSN1785 0037 (Online)
DOI: http://dx.doi.org/10.15666/aeer/1902_14071421
© 2021, ALÖKI Kft., Budapest, Hungary

[12] Karik, U. (2015): Some Morpholocigal, Yield and Quality Characteristics of Anatolian Sage (*Salvia fruticosa* Mill.) Populations in Aegean and West Mediterranean Region. – Journal of Tekirdag Agricultural Faculty 12(2): 32. (in Turkish).
[13] Karousou, R., Kokkini, S. (1997): Distribution and clinal variation of *Salvia fruticosa* Mill. (Labiatae) on the island of Crete (Greece). – Willdenowia 27(1-2): 113-120.
[14] Mossi, A. J., Cansian, R. L., Paroul, N., Toniazzo, G., Oliveira, J. V., Pierozan, M. K., Pauletti, G., Rota, L., Santos, A. C. A., Serafini, L. A. (2011): Morphological characterisation and agronomical parameters of different species of *Salvia* sp.(Lamiaceae). – Brazilian Journal of Biology 71(1): 121-129.
[15] Nei, M. (1978): Estimation of average heterozygosity and genetic distance from a small number of individuals. – Genetics 89(3): 583-590.
[16] Peakall, R., Smouse, P. E. (2012): GenAlEx 6.5: Genetic analysis in Excel. Population genetic software for teaching and research-an update. – Bioinformatics 28(19): 2537-2539.
[17] Skoula, M., El Hilali, I., Makris, A. M. (1999): Evaluation of the genetic diversity of *Salvia fruticosa* Mill. clones using RAPD markers and comparison with the essential oil profiles. – Biochemical Systematics and Ecology 27(6): 559-568.
[18] TUIK. (2019): Foreign Trade Statistics. – Available at: https://biruni.tuik.gov.tr/disticaretapp/disticaret.zul?param1=25&param2=0&sitcrev=0&isicrev=0&sayac=5802, (Accessed December 03.2019).
[19] Uysal, F. (2015): Determining superior genotypes by selective breeding of Anatolian sage (*Salvia fruticosa* Mill.) populations in the flora of Antalya. – Akdeniz University Institute of Science Department of Field Crops, PhD Thesis, Antalya, Turkey. (in Turkish).
[20] Wang, M., Li, J., Zhang, L., Yang, R. W., Ding, C. B., Zhou, Y. H., Yin, Z. Q. (2011): Genetic diversity among *Salvia miltiorrhiza* Bunge and related species using morphological traits and RAPD markers. – Journal of Medicinal Plants Research 5(13): 2687-2694.
[21] Wichtl, M. (1971): Die fharmakognostisch-Chemische Analyse. – Gehaltsbestimmung von Drogen (und Zubereitungen) mit atherischem 1: 263-281. (in German).

http://www.aloki.hu ● ISSN 1589 1623 (Print) ● ISSN1785 0037 (Online)
DOI: http://dx.doi.org/10.15666/aeer/1902_14071421
© 2021, ALÖKI Kft., Budapest, Hungary

MICROORGANISM VARIABILITY OF THE SOIL AND THE INHIBITION OF THE BANANA FUSARIUM WILT BY STRAW ADDITION COMBINED WITH FLOODING

FAN, P.[#] – CHENG, J.[#] – RUAN, Y.[*]

Hainan Key Laboratory for Sustainable Utilization of Tropical Bio-resources, College of Tropical Crops, Hainan University, Haikou 570228, PR China

[#]These authors contributed equally to this work

**Corresponding author*
e-mail: ruanyunze1974@hainanu.edu.cn

(Received 18th Nov 2020; accepted 27th Jan 2021)

Abstract. Straw addition combined with flooding is a form of the Reductive Soil Disinfestation（RSD） which can effectively prevent soil-borne diseases to some extent. However, little is known about the continuous effects of straw addition combined with flooding on the key culturable microbes and the pathogen *Fusarium oxysporum* in soils susceptible to banana Fusarium wilt (BFW). We studied the effects of continuous cropping (CK), fallow (FW), flooding (RSD-FD) and straw addition combined with flooding (RSD-FS) treatments for 0-120 days on soil properties and the dominant culturable microorganisms. Compared to CK, RSD-FS treatment had the lowest incidence of BFW; RSD-FS treatments significantly increased soil pH, but soil Eh and the number of *Fusarium Oxysporum*, culturable bacteria and fungi decreased significantly after flooding (30 days). The bacteria genera *Agrobacterium*, *Enterobacter*, *Aeromonas*, and the fungal genera *Trichoderma*, *Penicillium* and *Myxoflagella* increased with the time of flooding; while the bacteria genera *Pseudoxanthomonas*, *Sphingomonas* and *Leckercia*, decreased first and then increased; Interestingly, the bacterial genera *Bacillus* and *Brevibacterium*, and the fungal genera *Phoma*, *Coprinus* and *Filamentous* could not be cultured after flooding (30 days). Therefore, RSD-FS treatment could change the microbial flora and increase the general inhibition of the highly susceptible banana soil.
Keywords: *Fusarium oxysporum, reductive soil disinfestation, species composition, Leckercia, Trichoderma*

Introduction

Bananas (*Musa nana* Lour) are the main source of food and income for many people in the tropics and subtropics (FAOSTAT, 2017). Today nearly 50% of the world's banana production is made up of the Cavendish (Musa Aaa) variety, which is susceptible to the current widespread pathogenic strain of *Fusarium oxysporum f. sp. tropical Race 4 (Foc TR4)*, which causes banana fusarium wilt that is threatening banana production worldwide (Mostert et al., 2017). There is no commercially effective way to control *Foc TR4* (Ploetz, 2015). Even though some *Foc TR4* resistant varieties such as *Goldfinger* and *Taiwanese GCTCV somaclones* (Hwang and Ko, 2004) have also been produced, their yields are nowhere near as high as that of the Cavendish variety, so continued large-scale production of bananas depends on agronomic management of the fusarium wilt disease.

Reductive Soil Disinfestation (RSD) was an effective method to suppress various types of soil-borne diseases in various crops (Messiha et al., 2007), that was interpreted to add a lot of easily decomposed organic materials, irrigation, film mulching or flooding to block gas exchange with the atmosphere, quickly creating strong reduction

http://www.aloki.hu ● ISSN 1589 1623 (Print) ● ISSN 1785 0037 (Online)
DOI: http://dx.doi.org/10.15666/aeer/1902_14231436
© 2021, ALÖKI Kft., Budapest, Hungary

environment of soil, killing soil-borne pathogens in a short period of time (Liu et al., 2019; Larkin and Griffin, 2007). Crop straw is rich in organic carbon and essential nutrient elements, which can promote soil organic matter accumulation, improve soil physical and chemical properties and increase soil fertility (Franzluebbers, 2002; Rasool et al., 2008; Surekha et al., 2003), which could make up for the shortcomings that flooding tends to promote soil erosion and degradation (Alkhaibari et al., 2018). It was also observed that the anaerobic soil formed by straw addition combined with flooding could drive microbial factors, improve soil microbial community and inactivate pathogens, thus inhibit the growth of *F. oxysporum* and prevent the occurrence of banana wilt (Wen et al., 2016). Previous studies have reported that combined flooding with 2% (w/w) maize (Zea mays) straw could significantly decrease the population of *F. oxysporum* and the relative abundances of fungi such as *Chaetomium spp.* and *Penicillium spp*, but significantly increased pH and the relative abundances of bacteria belonging to the phylum Bacteroidetes, Acidobacteria and Planctomycetes, which that was beneficial to the disease suppression (Huang et al., 2015). Recent reports also studied the RSD effecting on cucumber damping-off diseased, and the result showed that the potential benefit species which were negatively correlated with disease incidence and positively associated with the change of the soil environment, such as bacterial order *Sphingobacteriales* and fungal order *Sordariales* was significantly increased and led to the soil more disease-suppressive and beneficial to the soil nutrient cycling and banana growth (Liu et al., 2019).

key microorganism's dynamic in a disease-suppressed banana soil and their potential relation to the soil-borne pathogens and soil environments during and after the straw addition combined with flooding remains are poorly understood. Therefore, we conducted a greenhouse pot experiment to identify the dynamic changes of the abundance of cultivable pathogen *F. oxysporum* and the dominant cultivable bacteria and fungus and microbial community, and their relationship with the RSD-soil properties from 0 to 120 days by straw addition combined with flooding to provide the theoretical guidance for the controlling of banana fusarium wilt.

Materials and Methods

Experimental design and soil

The soil was come from the banana fields which have continuously cropped for seven years, and the incidence of banana fusarium wilt was 50% higher. The basic properties of the soil were as follows: organic matter 10.98 $g \cdot kg^{-1}$, alkali-hydrolyzed nitrogen 23.71 $mg \cdot kg^{-1}$, available phosphorus 102.55 $mg \cdot kg^{-1}$, available potassium 237.15 $mg \cdot kg^{-1}$, pH 6.5, *F. oxysporum* count 2×104 $CFU \cdot kg^{-1}$. The greenhouse culture experiment was conducted from June 1, 2019, to December 27, 2019, in Ledong County, Hainan Province, China. The location was 18°42′N, 108°48′E. The experiment consisted of four treatments: continuous cropping (CK), fallow (FW), flooding (RSD-FS), straw addition combined with flooding (RSD-FS), 10 repetitions per treatments, and 5.5 kg of 2 mm sieved soil in each pot which is 23.5 cm diameter and 20 cm height, 110 g rice straw which crushed by micro-pulverize, after the rice straw and the soil were mixed and homogenized, the soil in the basin was kept smooth and filled with water until the soil was saturated. The test period was 120 days, and 30 days was the interval. The soil samples were collected 4 times, and the submergence depth of each treatment was 3 cm. After flooding, the next generation

http://www.aloki.hu ● ISSN 1589 1623 (Print) ● ISSN 1785 0037 (Online)
DOI: http://dx.doi.org/10.15666/aeer/1902_14231436
© 2021, ALÖKI Kft., Budapest, Hungary

banana was planted after the flooding over, and the incidence of banana fusarium wilt was calculated after 3 months. Before planting the next banana, 55 g bio-organic fertilizer was followed in each pot. The bio-organic fertilizer was acquired from Jiangsu Huarun Earth Fertilizer Co., Ltd. The banana variety is 'Brazil', which was provided by the experimental research base of Heat Science Academy of Danzhou Campus of Hainan University. Rice (Nanjing 2728 Yinnuo) Straw was taken in 2018 at the local rice fields.

Soil collection and properties

After removing the dead branches and leaves from the soil surface layer, 10 soil columns with a depth of 5-10 cm and a diameter of 2 cm were randomly collected with a soil drill, with the center of the pot plant circle as the center, mix the remaining soil into a sample. After homogenizing the soil samples, the samples were divided into three parts. One part of the soil was air-dried naturally, then the soil was sieved through 2 mm sieve to determine the physical and chemical properties of the soil, one part of the soil was stored in a 4 °C refrigerator for picking up single strains of soil. Soil pH and Eh was determined using a soil-to-water ratio of 1:2.5 (w/v). The exchangeable ammonia (NH_4^+-N) and nitrate (NO_3^--N) in the soil was extracted with 2 M KCl (w/v, 1:5) and determined on a Continuous flow analyzer (Foss Tecator, Hillerød, Denmark).

Determination of the number of culturable microorganisms in soil

The number of F. oxysporum, bacteria, fungi and actinomycetes in the soil was determined by the plate dilution coating method (Ben-David and Davidson, 2014). The culturable F. oxysporum were counted using the improved Komada 2 medium at 28 °C for 96 h (Komada, 1975). The bacteria were cultured in Luria-Bertani (LB) medium at 30 °C for 24 h (Macwilliams and Liao, 2006), and the fungi were cultured in Martin medium at 28 °C for 72 h (Martin, 1981), the number expressed as colony forming unit (CFU) per gram of dry soil.

Isolation and identification of culturable bacteria and fungi

Isolation of single bacterial strain from microbial community using LB medium. Martin medium is used to isolate individual fungal strains from the microbial community. According to the manufacturer's instructions, single-strain DNA is extracted from the purified culture using a bacterial Genomic DNA Extraction Kit (DP302) (Tiangen biotech (Beijing) Co., Ltd.) and Fungi Genomic DNA Extraction Kit Fungal genomic (D2300) (Beijing Suolaibao Technology Co., Ltd.). The primer pair 27F(5'-AGAGTTT-GATCCTGGCTCAG-3') and 1492R(5'-GGTTACCTTGTTACGACTT-3') was selected to amplify the 16S rRNA gene (Yu et al., 2013). The primer pair ITS1(5'-TCCGTAGGTGAACCTGCGG-3') and ITS4(5'-TCCTCCGCTTATTGATATGC-3') were used for the fungal ITS1 gene (Schoch et al., 2012) 18. We established a 50-μl of reaction solution including 25 μl of TaKaRa Ex Taq® Premix (Takara Bio Inc., Japen), 0.5 μl of each primer (10 μM), 4 μl of template DNA, and 20 μl of sterile water. Cycling conditions were as follows: 95 °C for 10 min polymerase activation, followed by 45 cycles of denaturation at 95 °C for 30 s, annealing at 55 °C (bacteria) and 50 °C (fungi) for 45 s, and extension at 72 °C for 60 s used the Bio-Rad Bole PCR T100. The purified PCR product was analyzed with the Illumina MiSeq platform at Personal Biotechnology Co., Ltd. (Shanghai, China).

http://www.aloki.hu ● ISSN 1589 1623 (Print) ● ISSN 1785 0037 (Online)
DOI: http://dx.doi.org/10.15666/aeer/1902_14231436
© 2021, ALÖKI Kft., Budapest, Hungary

Taxonomy assignment was performed using BLASTP (Version 2.2.28+, http://blast.ncbi.nlm.nih.gov/Blast.cgi) by aligning non-redundant gene catalogs against NCBI database (Altschul et al., 1997).

Statistical analysis

The test data was processed and plotted with Microsoft Excel 2016. Variance analysis and Pearson correlation analysis were carried out with SPSS 20.0 (IBM Corporation, USA). Multiple comparisons were conducted with Least-significant-difference (LSD) at a $p = 0.05$ level.

Results

Soil properties and Fusarium wilt disease influenced by straw addition combined with flooding

RSD-FS treatment (straw addition combined with flooding) significantly affected soil Eh, ammonium and nitrate contents ($p < 0.01$) (*Table A1*). Compared with CK treatment and FW treatment, soil Eh and ammonium in soil treated with RSD-FD and RSD-FS significantly decreased after the 30th day of flooding, while the soil nitrate and pH significantly increased, after that, the trend gradually eased with the extension of flooding time ($p < 0.05$) (*Fig. 1*). Pearson correlation showed that flooding duration was positively correlated with soil pH and ammonium content, but negatively correlated with Eh and nitrate nitrogen content by the RSD-FS treatment ($p < 0.01$) (*Table 1*).

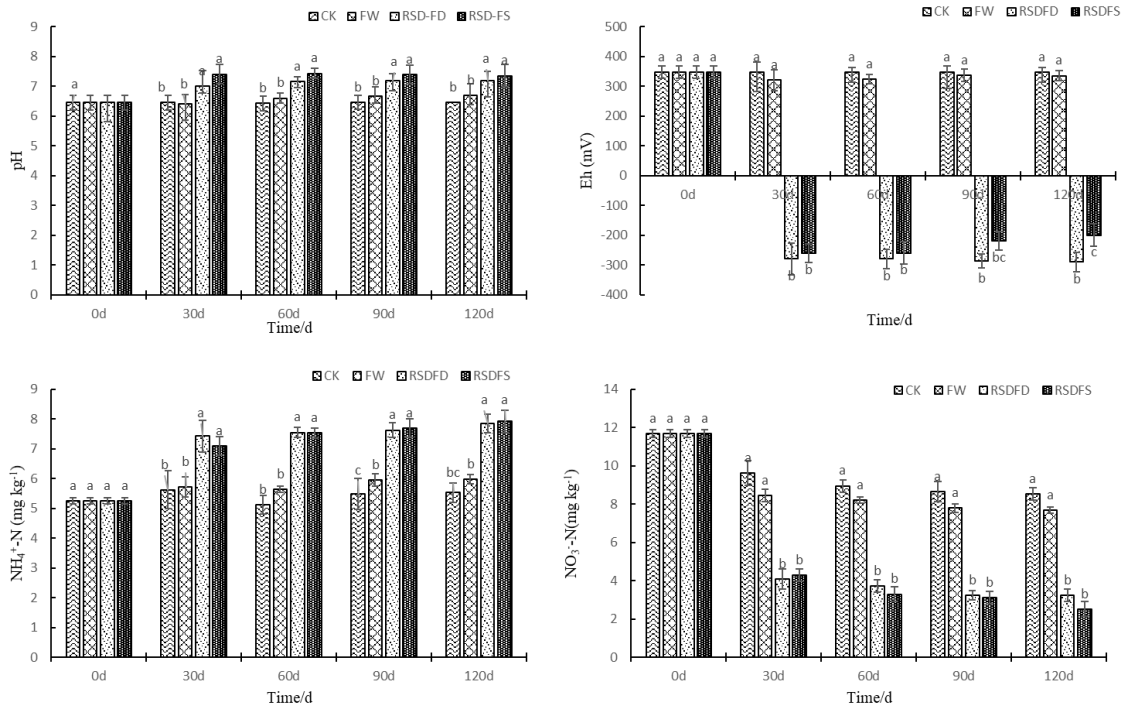


Figure 1. *Effects of straw addition combined with flooding on soil Eh, pH, ammonium and nitrate contents. CK: continuous cropping; FW: Fallow; RSD-FD: Flooding; RSD-FS: Flooding + Straw. Error bars indicate standard error (n = 3). Different small letters indicate a significant difference among treatments at the 0.05 level*

http://www.aloki.hu ● ISSN 1589 1623 (Print) ● ISSN 1785 0037 (Online)
DOI: http://dx.doi.org/10.15666/aeer/1902_14231436
© 2021, ALÖKI Kft., Budapest, Hungary

In addition, CK treatment has the highest incidence of banana fusarium wilt (BFW), and followed by FW treatment (*Fig. 2*). Compared with CK and FW treatments the incidence of BFW with RSD-FS and RSD-FD was significantly lower ($p < 0.05$), 50% and 37.5% lower than CK, respectively.

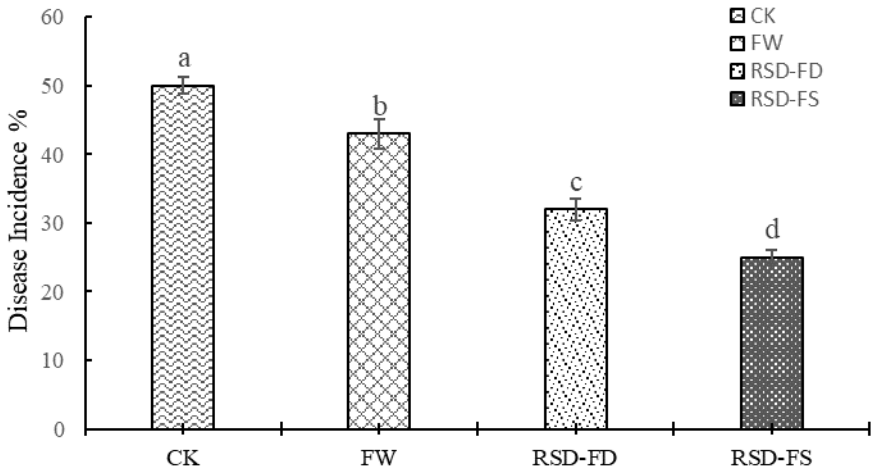


Figure 2. *Incidence of banana Fusarium wilt of the next generation banana after flooding. CK: continuous cropping; FW: Fallow; RSD-FD: Flooding; RSD-FS: Flooding + Straw. Error bars indicate standard error (n = 3). Different small letters indicate a significant difference among treatments at the 0.05 level*

The number of culturable microorganisms under straw addition combined with flooding

Both fallow and flooding could significantly reduce the number of soil *F. oxysporum*. Moreover, the number of soil *F. oxysporum* flooding treatments (RSD-FD and RSD-FS) was significantly lower than fallow treatments and became stable after (90 days) ($p < 0.05$). However, both of RSD-FD and RSD-FS treatments was significantly lower after the 30th day than other treatments and lasted until the 120th day. On the 90th day, FW, RSD-FD, and RSD-FS treatments significantly decreased than CK treatment 18.33%, 60% and 62.25% ($p < 0.05$), respectively. RSD-FS treatment significantly decreased to 4.2×10^3 CFU g^{-1} (dry soil). The results of variance analysis showed that straw addition combined with flooding significantly affected the number of *F. oxysporum* ($F = 3238.1$, $p < 0.01$) (*Table A1*), and the Pearson correlation analysis showed that the number of *F. oxysporum* decreased with the increase of flooding time ($p < 0.01$) (*Table 1*).

Compared with CK treatment, the number of culturable bacteria after 60 days was significantly lower under other treatments (*Fig. 3b*) ($p < 0.05$), and all treatments tended to stabilize to the120th day. In general, the number of bacteria in soil under RSD-FS treatment was the lowest, followed by RSD-FD and FW treatment.

There was no significant change in the number of culturable fungi in CK and FW treatments. Compared with CK and FW treatment, the number of culturable fungi in the soil under flooding treatment (RSD-FS and RSD-FS) after the 30th day was significantly reduced, while the number of culturable fungi was the lowest after flooding to the 60th day, the culturable fungi in RSD-FD and RSD-FS treatments were 46.84% and 17.72% of the control, respectively, and tended to stabilize to120th day (*Fig. 3c*) ($p < 0.05$). The results of

http://www.aloki.hu ● ISSN 1589 1623 (Print) ● ISSN 1785 0037 (Online)
DOI: http://dx.doi.org/10.15666/aeer/1902_14231436
© 2021, ALÖKI Kft., Budapest, Hungary

variance analysis showed that Straw addition combined with flooding significantly affected the number of culturable bacteria ($F = 351.49$, $p < 0.01$) and the number of culturable fungi ($F = 244.72$, $p < 0.01$) (*Table A1*), and the correlation analysis shows that both of them decrease with the increase of flooding time (*Table 1*) ($p < 0.05$).

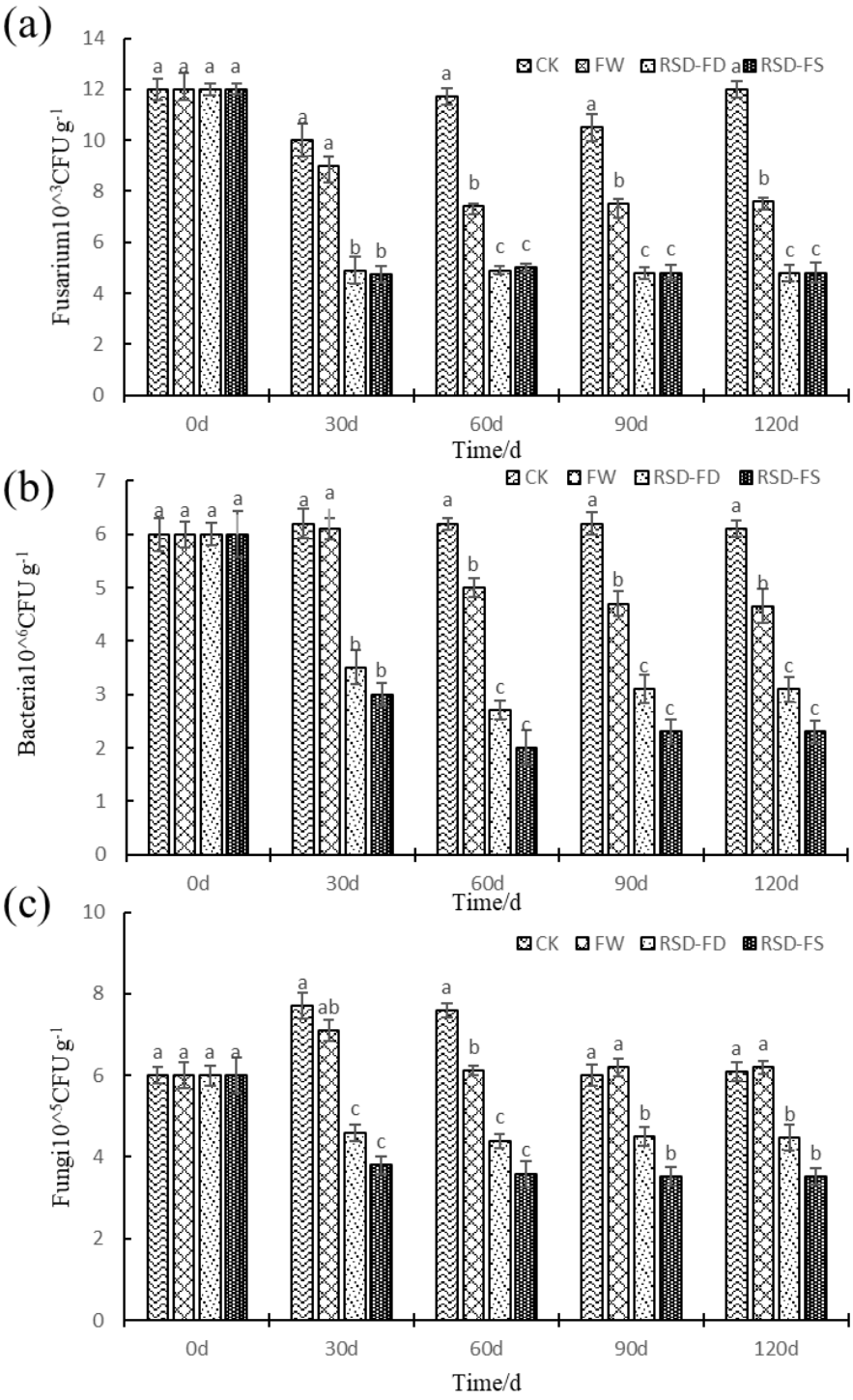


Figure 3. *Effects of straw addition combined with flooding on the number of F. oxysporum (a), bacteria (b) and fungi (c). CK: continuous cropping; FW: Fallow; RSD-FD: Flooding; RSD-FS: Flooding + Straw. Error bars indicate standard error (n = 3). Different small letters indicate a significant difference among treatments at the 0.05 level. CFU, colony forming unit*

http://www.aloki.hu ● ISSN 1589 1623 (Print) ● ISSN 1785 0037 (Online)
DOI: http://dx.doi.org/10.15666/aeer/1902_14231436
© 2021, ALÖKI Kft., Budapest, Hungary

Table 1. *Pearson correlation analysis of investigation parameters*

	Time	**pH**	**Eh**	**NH_4^+—N**	**NO_3^-—N**	***F. oxysporum* CFU**
Time	—	0.68**	-0.59	0.87**	-0.81**	-0.71**
***F. oxysporum* CFU**	-0.71**	-0.99**	0.87**	-0.96**	0.98**	—
Bacteria CFU	-0.78**	-0.97**	0.79**	-0.98**	0.99**	0.97**
Fungus CFU	-0.74**	-0.99**	0.84**	-0.97**	0.99**	0.99**
Bacterial genera						
Bacillus	-0.71**	-0.99**	0.86**	-0.96**	0.99**	1.00**
Lysine Bacillus	-0.89**	—	—	—	0.57*	0.48
Pseudoxanthomonas	0.69**	—	—	—	—	0.01
Oligomonas	-0.95**	-0.83**	0.67**	-0.96**	0.92**	0.84**
Sphingomonas	0.61**	—	—	—	—	—
Agrobacterium	—	—	—	—	—	—
Leckercia	0.84**	—	—	—	—	—
Enterobacter	0.38	0.92**	-0.80**	0.78**	-0.85**	-0.92**
Aeromonas	-0.75**	-0.16	—	—	0.34**	0.17**
Brevibacterium	-0.71**	-0.99**	0.86**	-0.96**	0.99**	1.00**
Fungal genus						
Aspegillus	-0.99**	-0.72**	0.61	-0.89**	0.84**	0.74**
Trichoderma	0.81**	0.97**	-0.86**	0.99**	-1.00**	-0.99**
Penicillium	0.98**	0.79**	-0.65**	0.93**	-0.89**	-0.80**
Penicillium	0.89**	0.94**	-0.80**	1.00**	-0.99**	-0.95**
Fusarium	-0.78**	-0.97**	0.85 **	-0.98**	0.99**	0.99**
Myxoflagella	0.97**	0.82**	-0.67**	0.95**	-0.91**	-0.83**
Trametes	0.97**	0.68**	-0.52*	0.86**	-0.80**	-0.68**
Phoma	-0.71**	-0.99**	0.86**	-0.96**	0.99**	1.00**
Coprinus	-0.71**	-0.99**	0.86**	-0.96**	0.99**	1.00**
Filamentous	-0.71**	-0.99**	0.86**	-0.96**	0.99**	1.00 **

Time: the day of flooding; * and ** were significantly correlated at 0.05 and 0.01 levels, respectively

Changes in the dominant soil culturable microorganisms by straw addition combined with flooding

A total of 298 strains of bacteria and 376 strains of fungi were screened and identified. The bacteria belong to 4 phyla 7 classes, 12 orders, 22 families, 22 genera, and the fungi belong to 2 phyla, 3 classes, 7 orders, 15 families and 17 genera. After flooding 120 days, the total number of bacteria and fungi were 216 and 245 respectively, and the total number of bacteria and fungi decreased by 82 and 131 respectively, compared to unflood (*Tables A2 and A3*).

RSD-FS treatment had obvious changes of soil culturable microorganisms (*Fig. 4*). For bacteria genera, *Bacillus* and *Brevibacterium* could not be cultivated after flooding 30 days; lysine *Bacillus* finally dying out after flooding 90 days; The genus *pseudoxanthomonas* decreased at first and then increased after flooding 60-120 days; The *Agrobacterium* increased first and then decreased, and decreased slowly after

http://www.aloki.hu ● ISSN 1589 1623 (Print) ● ISSN 1785 0037 (Online)
DOI: http://dx.doi.org/10.15666/aeer/1902_14231436
© 2021, ALÖKI Kft., Budapest, Hungary

60 days; The *Leckercia* showed a trend of decreasing first and then increasing, and the increase was gradually slowed down from flooding 60 to 120 day; *Enterobacter* had a tendency of increasing first and then decreasing, and the decreasing range became larger gradually after 60 days of flooding. The *Aeromonas* increased first and then decreased, and decreased gradually after 60 days of flooding (*Fig. 4a*).

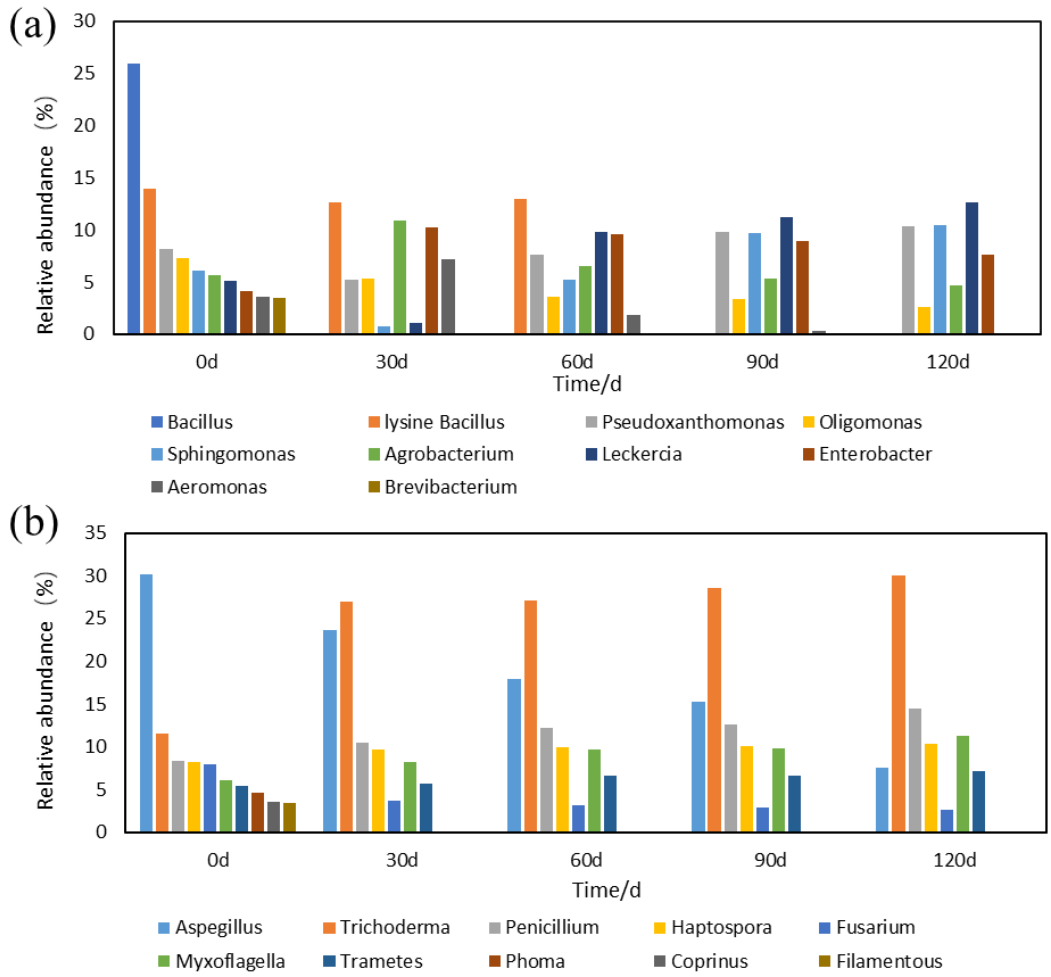


Figure 4. *TOP10 cultivable bacterial (a) and (b) fungal genera dynamic changes in flooded soil with straw addition*

The dominant fungi of *Phoma*, *Coprinus* and *Filamentous* could not be cultured after flooding 30 days; The relative abundance of *Aspegillus* before flooding was the highest, which decreased by 7.61% at 120 days after flooding; The relative abundance of *Trichoderma* showed a continuous increasing trend, and the maximum increase was 15.45% at 30 days after flooding; The relative abundance of *Penicillium* showed an increasing trend, and the maximum increase was 2.2% after 30 days of flooding. The *Fusarium* abundance showed a decreasing trend, the biggest decrease was 0.5% after 60 days of flooding. The *Myxoflagella* abundance showed an increasing trend, and the maximum increase was 2.08% after 30 days of flooding; The *Trametes* abundance showed an increasing trend, and the maximum increase was 0.88% after 60 days of flooding (*Fig. 4b*).

http://www.aloki.hu ● ISSN 1589 1623 (Print) ● ISSN 1785 0037 (Online)
DOI: http://dx.doi.org/10.15666/aeer/1902_14231436
© 2021, ALÖKI Kft., Budapest, Hungary

Relationship between Fusarium oxysporum and dominant microorganisms and soil properties after RSD-FS treatment

The number of soils *F. oxysporum* was negatively correlated with soil pH and ammonium ($p < 0.01$), but positively correlated with soil Eh and nitrate. In addition, there was a significant correlation between the number of *F. oxysporum* and the number of the dominant culturable bacteria and fungi in the soil. Such as, the dominant bacterial genera including of Bacillus, stenotrophomonas, aeromonas, brevibacterium, and the dominant genera Aspergillus, Fusarium, Phoma, Coprinus and Filamentous, there was a significant positive correlation between the number of cultural *F. oxysporum* ($p < 0.01$), this indicated that these microflora might be the potential harmful microorganisms; However, there was a significant negative correlation between the number of *Enterobacter*, *Trichoderma*, *Penicillium*, *Myxosporea*, *Trametes* and the number of *F. oxysporum* ($p < 0.01$), and these genera groups might be potential beneficial microorganisms. Besides *Enterobacter*, flooding time was significantly correlated with other dominant bacteria and fungi ($p < 0.01$), while soil pH, Eh, the contents of ammonium and nitrate were almost correlated with the potential beneficial and harmful microorganisms ($p < 0.01$) (*Table 1*).

Discussion

Our results provided evidence that straw addition combined with flooding could reduce the incidence of banana fusarium wilt effectively, and change the biological and abiotic characteristics of the susceptible soil. And this pattern is consistent with previously reported that the Reductive Soil Disinfestation (RED) method in preventing soilborne diseases (Liu et al., 2019; Huang et al., 2015)

It is well known that there is a direct positive correlation between the number of soil pathogen *F. oxysporum* and the severity of the disease (Shen et al., 2014, 2019). With or without Straw, flooding for 30 days significantly reduced the number of *F. oxysporum*, and the trend remained the same after 30 days until 120 days (*Fig. 1*). This suggests that flooding measures played a relatively more important role, and could be interpreted as providing unfavorable conditions for the growth of *F. oxysporum* (Huang et al., 2015). Straw returning as potential fertility of soil, can provide carbon and nitrogen sources for soil microorganisms in the process of flooding (Dong et al., 2018). However, it was found that the shredded straw could form larger pore structure in a waterlogged environment, which provided living space for fungal chlamydospores (Jang et al., 2018). It suggested that straw addition might be beneficial to the survival of pathogens. Previous studies have shown that an increase in bacteria or fungi diversity contributes to a decrease in *F. oxysporum* (Wang et al., 2015). This could be explained by an increase in bacterial diversity that reinforces the general inhibition, expands the array of nutrient acquisition strategies, and increases the likelihood of a strong competitor to the *F. oxysporum*. Although the flooding measures in this study reduced the number and diversity of culturable bacteria and fungi in the soil, the reduction in the number of *F. oxysporum* was even greater, the results showed that the possible negative effects of flooding and Straw addition could be offset by the effect of disease control. It should be noted that fallow is ineffective because the *F. oxysporum* usually persists in the soil for more than 20 years (Stotzky and Torrence Martin, 1963). Although fallow can also reduce the number and incidence of *F. oxysporum* but the effect of fallow is far less than that of flooding.

http://www.aloki.hu ● ISSN 1589 1623 (Print) ● ISSN 1785 0037 (Online)
DOI: http://dx.doi.org/10.15666/aeer/1902_14231436
© 2021, ALÖKI Kft., Budapest, Hungary

The importance of microbial populations for disease suppression has been demonstrated by the loss of support in soil sterilization (Noble and Coventry, 2005). Microbes which occupy most part of farmland soil is more likely to participate in environmental activities, and to some extent affect the distribution of soil microbes, but the mechanism is still unknown. Before the treatment of fallow, the dominant bacterial genera were *Bacillus*, *Pseudoxanthomonas*, *Sphingomonas* and *Agrobacterium*. This result was consistent with that of (Yang et al., 2020). At the same time, *Penicillium* and *Aspergillus* are the most dominant species in the fungal community, and *Fusarium* was abundant, which are basically consistent with the previous results (Lee and Kim, 2020). Our results showed that the structure of soil microbial community under straw addition combined with flooding treatment changed significantly, *Leckerciaas* replaced *Bacillus* to become the new dominant bacteria genus; *Trichoderma* replaced *Aspergillus* to become the new dominant fungal genus. The largely application of *Trichoderma* strains with biocontrol and plant growth-promoting capacities that highly suppressed the pathogen *F. oxysporum* (Bunbury-Blanchette and Walker, 2019; Martínez-Medina et al., 2014; Xiong et al., 2017). For example, *Trichoderma* strains can take advantage of limited living space to grow and reproduce quickly and capture water and nutrients (López-Mondéjar and Pascual, 2011), also can secrete a few bacteriostatic chemical substances to wait (Saravanakumar et al., 2016). Lee and Kim (2020) pointed out that the *Leckercia* genus has a strong survival ability in harsh environment, and was insensitive to environmental changes, so it is more suitable than aerobic microorganisms in the application of the promotion. It is suggested that the inhibition of straw addition combined with flooding may be explained as, *Trichoderma spp*. and *Leckercia spp*. may be able to compete for space and nutrients in the presence of limited resources, these two dominant groups will play a great role in the biocontrol of *F. oxysporum* in the future.

The modification of soil physical and chemical characteristics plays an important role in control of banana Fusarium wilt (Hong et al.,2020). Many previous studies reported that the severity of banana Fusarium wilt was negatively correlated with soil pH (Shen et al., 2014, 2019), and the which was consistent with the results of this study and other result that significantly increased the pH level by reductive soil disinfestation (Huang et al., 2015; Liu et al., 2016). Soil pH changes with the input of material (carbon source, nitrogen source, etc.), and affects other abiotic and biological properties of the soil (Brady and Weil, 2004). For example, soil pH directly affects soil nutrient availability, especially for oxidation and reduction sensitive micronutrient (Dhungana and Crumbliss, 2005); pH is strongly positively correlated with bacterial diversity and abundance. Bacterial diversity can double between pH 4 and 8 (Rousk et al., 2010) 38. While many studies have shown the effect of pH on *F. oxysporum*, our understanding of this relationship is still incomplete. For each combination of soil conditions and management systems, it is assumed that there is an optimal pH for plant growth and disease suppression. The relationship between pH and inhibition needs to be studied in the field to better understand these complex interactions. Interestingly, we found that no matter whether straw was added or not, the nitrate content decreased with the increase of flooding time, while the ammonium decreased. This may be related to the enhancement of nitrate uptake in banana by flooding or the inhibition of nitrification in flooded and anoxic environment. In addition, the correlation analysis further indicated that soil pH, Eh, ammonium and nitrate content might be the key physical and chemical factors impact the potential beneficial and harmful microbe associated with *F. oxysporum* (*Table 1*).

http://www.aloki.hu ● ISSN 1589 1623 (Print) ● ISSN 1785 0037 (Online)
DOI: http://dx.doi.org/10.15666/aeer/1902_14231436
© 2021, ALÖKI Kft., Budapest, Hungary

Conclusions

The incidence of banana fusarium wilt by straw-adding combined with flooding was significantly lower than that by single flooding and other non-flooding treatments (continuous cropping and fallow). Flooding and Straw addition method significantly reduced the amount of the pathogen *F. oxysporum*, culturable bacteria and fungi in the soil. It also increased the soil pH and reduced Eh and nitrate nitrogen levels after straw-adding combined flooding. A remarkable shift has happened in microbial community by the straw-adding combined flooding. When the flooding was doner, the key genus Leckercia took the place of the genus Bacillus, and the key genus Trichoderma took the place of the genus Aspergillus. Further studies (e.g., secreted antagonists) on the interactions of these two dominant species with pathogens will be needed. To sum up, the measures of flooding combined with straw addition can just offset the shortage of a single measure, which makes the banana fusarium wilt prevention and control achieve optimistic results.

Acknowledgements. This research was financially supported by National Natural Science Foundation of China (31672239), National Key Basic Research Program of China (2015CB150503).

REFERENCES

[1] Alkhaibari, A. M., Maffeis, T., Bull, J. C., Butt, T. M. (2018): Combined use of the entomopathogenic fungus, Metarhizium brunneum, and the mosquito predator, Toxorhynchites brevipalpis, for control of mosquito larvae: is this a risky biocontrol strategy? – Journal of Invertebrate Pathology 153: 38-50.

[2] Altschul, S. F., Madden, T. L., Schäffer, A. A., Zhang, J., Zhang, Z., Miller, W., Lipman, D. J. (1997): Gapped BLAST and PSI-BLAST: a new generation of protein database search programs. – Nucleic Acids Research 25(17): 3389-3402.

[3] Ben-David, A., Davidson, C. E. (2014): Estimation method for serial dilution experiments. – Journal of Microbiological Methods 107: 214-221.

[4] Brady, N. C., Weil, R. R. (2004): Elements of the Nature and Properties of Soils. – Journal of Microbiological Methods 278.

[5] Bunbury-Blanchette, A. L., Walker, A. K. (2019): Trichoderma species show biocontrol potential in dual culture and greenhouse bioassays against Fusarium basal rot of onion. – Biological Control 130: 127-135.

[6] Dhungana, S., Crumbliss, A. L. (2005): Coordination chemistry and redox processes in siderophore-mediated iron transport. – Geomicrobiology Journal 22(3-4): 87-98.

[7] Dong, L., Linghu, W., Zhao, D., Mou, Y., Hu, B., Asiri, Abdullah, M., Alamry, K. A., Xu, D. (2018): Performance of biochar derived from rice straw for removal of Ni (II) in batch experiments. – Water Science and Technology 77: 824-834.

[8] Food and Agriculture Organization of the United Nations (FAOSTAT) (2017): Data of crop production (2016-12-08) [2017-04-02]. – http://www.fao.org/faostat/en/#data/QC.

[9] Franzluebbers, A. J. (2002): Soil organic matter stratification ratio as an indicator of soil quality. – Soil and Tillage Research 66(2): 95-106.

[10] Hong, S., Jv, H., Lu, M., Wang, B., Zhao, Y., Ruan, Y. (2020): Significant decline in banana Fusarium wilt disease is associated with soil microbiome reconstruction under chilli pepper-banana rotation. – European Journal of Soil Biology 97: 103154.

[11] Huang, X., Liu, L., Wen, T., Zhu, R., Zhang, J., Cai, Z. (2015): Illumina MiSeq investigations on the changes of microbial community in the Fusarium oxysporum f. sp.

http://www.aloki.hu ● ISSN 1589 1623 (Print) ● ISSN 1785 0037 (Online)
DOI: http://dx.doi.org/10.15666/aeer/1902_14231436
© 2021, ALÖKI Kft., Budapest, Hungary

cubense infected soil during and after reductive soil disinfestation. – Microbiological Research 181: 33-42.
[12] Hwang, S. C., Ko, W. H. (2004): Cavendish banana cultivars resistant to fusarium wilt acquired through somaclonal variation in Taiwan. – Plant Disease 88(6): 580-588.
[13] Jang, J., Mirana, W., Divine, S. D., Nawaz, M., Shahzad, A., Woo, S. H., Lee, D. S. (2018): Rice straw-based biochar beads for the removal of radioactive strontium from aqueous solution. – Science of the Total Environment 615: 698-707.
[14] Komada, H. (1975): Development of a selective medium for quantitative isolation of Fusarium oxysporum from natural soil. – Review of Plant Protection Research 8: 114-124.
[15] Larkin, R. P., Griffin, T. S. (2007): Control of soilborne potato diseases using Brassica green manures. – Crop Protection 6: 1067-1077.
[16] Lee, H., Ahmad, R., Kim, J. (2020): Alginate to simulate biofouling in submerged fluidized ceramic membrane reactor: effect of solution pH and ionic strength. – Bioresource Technology 302: 122813.
[17] Liu, L., Kong, J., Cui, H., Zhang, J., Wang, F., Cai, Z., Huang, X. (2016): Relationships of decomposability and C/N ratio in different types of organic matter with suppression of Fusarium oxysporum and microbial communities during reductive soil disinfestation. – Biological Control 101: 103-113.
[18] Liu, L., Huang, X., Zhao, J., Zhang, J., Caia, Z. (2019): Characterizing the key agents in a disease-suppressed soil managed by reductive soil disinfestation. – Applied and Environmental Microbiology 85(7): e02992-18.
[19] López-Mondéjar, R., Ros, M., Pascual, J. A. (2011): Mycoparasitism-related genes expression of Trichoderma harzianum isolates to evaluate their efficacy as biological control agent. – Biological Control 56(1): 59-66.
[20] Macwilliams, M. P., Liao, M.-K. (2006): Luria Broth (LB) and Luria Agar (LA) Media and Their Uses Protocol. – American Society for Microbiology, Washington, DC.
[21] Martin, G. R. (1981): Isolation of a pluripotent cell line from early mouse embryos cultured in medium conditioned by teratocarcinoma stem cells. – Proceedings of the National Academy of Sciences of the United States of America 78(12): 7634-7638.
[22] Martínez-Medina, A., Del Mar Alguacil, M., Pascual, J. A., Van Wees, S. C. M. (2014): Phytohormone profiles induced by trichoderma isolates correspond with their biocontrol and plant growth-promoting activity on melon plants. – Journal of Chemical Ecology 40(7): 804-15.
[23] Messiha, N. A. S., Van Diepeningen, A. D., Wenneker, M., Van Beuningen, A. R., Janse, J. D., Coenen, T. G. C., Termorshuizen, A. J., Van Bruggen, A. H. C., Blok, W. J. (2007): Biological Soil Disinfestation (BSD), a new control method for potato brown rot, caused by Ralstonia solanacearum race 3 biovar 2. – European Journal of Plant Pathology 177(4): 403-415.
[24] Mostert, D., Molina, A. B., Daniells, J., Fourie, G., Hermanto, C., Chao, C. P., Fabregar, E., Sinohin, V. G., Masdek, N., Thangavelu, R., Li, C., Yi, G., Mostert, L.,Viljoen, A. (2017): The distribution and host range of the banana Fusarium wilt fungus, Fusarium oxysporum f. sp. cubense, in Asia. – Plos one 12(7): e0181630.
[25] Noble, R., Coventry, E. (2005): Suppression of soil-borne plant diseases with composts: a review. – Biocontrol Science and Technology 15(1): 3-20.
[26] Ploetz, R. C. (2015): Management of Fusarium wilt of banana: a review with special reference to tropical race 4. – Crop Protection 73: 7-15.
[27] Rasool, R., Kukal, S. S., Hira, G. S. (2008): Soil organic carbon and physical properties as affected by long-term application of FYM and inorganic fertilizers in maize-wheat system. – Soil and Tillage Research 101: 31-36.
[28] Rousk, J., Bååth, E., Brookes, P. C., Lauber, C. L., Lozupone, C., Caporaso, J. G., Knight, R., Fierer, N. (2010): Soil bacterial and fungal communities across a pH gradient in an arable soil. – ISME Journal 4: 1340-1351.

http://www.aloki.hu ● ISSN 1589 1623 (Print) ● ISSN 1785 0037 (Online)
DOI: http://dx.doi.org/10.15666/aeer/1902_14231436
© 2021, ALÖKI Kft., Budapest, Hungary

[29] Saravanakumar, K., Yu, C., Dou, K., Wang, M., Li, Y., Chen, J. (2016): Synergistic effect of Trichoderma-derived antifungal metabolites and cell wall degrading enzymes on enhanced biocontrol of Fusarium oxysporum f. sp. cucumerinum. – Biological Control 94: 37-46.
[30] Schoch, C. L. et al. (2012): Nuclear ribosomal internal transcribed spacer (ITS) region as a universal DNA barcode marker for Fungi. – Proceedings of the National Academy of Sciences of the United States of America 109: 6241-6246.
[31] Shen, Z., Wang, D., Ruan, Y., Xue, C., Zhang, J., Li, R., Shen, Q. (2014): Deep 16S rRNA pyrosequencing reveals a bacterial community associated with banana Fusarium wilt disease suppression induced by bio-organic fertilizer application. – PLoS One 9(5): 1-10.
[32] Shen, Z., Xue, C., Penton, C. R., Thomashow, L. S., Zhang, N., Wang, B., Ruan, Y., Li, R., Shen, Q. (2019): Suppression of banana Panama disease induced by soil microbiome reconstruction through an integrated agricultural strategy. – Soil Biology and Biochemistry 128: 164-174.
[33] Stotzky, G., Torrence Martin, R. (1963): Soil mineralogy in relation to the spread of fusarium wilt of banana in central America. – Plant and Soil 18(3): 317-337.
[34] Surekha, K., Padma Kumari, A. P., Narayana Reddy, M., Satyanarayana, K., Sta Cruz, P. C. (2003): Crop residue management to sustain soil fertility and irrigated rice yields. – Nutrient Cycling in Agroecosystems 67(2): 145-154.
[35] Wang, B., Li, R., Ruan, Y., Ou, Ya., Zhao, Y., Shen, Q. (2015): Pineapple-banana rotation reduced the amount of Fusarium oxysporum more than maize-banana rotation mainly through modulating fungal communities. – Soil Biology and Biochemistry 86: 77-86.
[36] Wen, T., Huang, X., Zhang, J., Cai, Z. (2016): Effects of biological soil disinfestation and water regime on suppressing Artemisia selengensis root rot pathogens. – Journal of Soils and Sediments 16(1): 215-225.
[37] Xiong, W., Guo, S., Jousset, A., Zhao, Q., Wu, H., Li, R., Kowalchuk, G. A., Shen, Qi. (2017): Bio-fertilizer application induces soil suppressiveness against Fusarium wilt disease by reshaping the soil microbiome. – Soil Biology and Biochemistry 114: 238-247.
[38] Yang, F., Huai, W. X., Zeng, Y. H. (2020): New dynamic two-layer model for predicting depth-averaged velocity in open channel flows with rigid submerged canopies of different densities. – Advances in Water Resources 138: 103553.
[39] Yu, J., Zhou, X. F., Yang, S. J., Liu, W. H., Hu, X. F. (2013): Design and application of specific 16S rDNA-targeted primers for assessing endophytic diversity in Dendrobium officinale using nested PCR-DGGE. – Applied Microbiology and Biotechnology 97(22): 9825-9836.

APPENDIX

Table A1. *Analysis of variance of investigated parameters*

	Treatment	Time	Treatment × Time
pH	3.58*	1.55	1.17
Eh	30.86**	14.75**	5.07**
NH_4^+—N	69.75**	30.31**	2.45*
NO_3^-—N	76874.4**	51949.2**	3394.23**
F. oxysporum CFU	25745.2**	29635.3**	3238.1**
Bacteria CFU	5471.78**	1509.1**	351.49**
Fungus CFU	1585.98**	259.5**	244.72**

* and ** were significantly different at 0.05 and 0.01 levels, respectively

http://www.aloki.hu ● ISSN 1589 1623 (Print) ● ISSN 1785 0037 (Online)
DOI: http://dx.doi.org/10.15666/aeer/1902_14231436
© 2021, ALÖKI Kft., Budapest, Hungary

Table A2. *Changes of bacterial population during flooding cycle*

Time (d)	Total number	Phyla	Classes	Orders	Families	Genera
0	298	4	7	12	15	22
30	223	2	4	6	10	12
60	218	2	4	6	10	11
90	201	2	4	6	10	11
120	216	2	4	6	10	10

Table A3. *changes of fungal population during flooding cycle*

Time (d)	Total number	Phyla	Classes	Orders	Families	Genera
0	376	2	3	7	15	17
30	266	1	2	4	7	9
60	215	1	2	4	7	9
90	265	1	2	4	7	9
120	245	1	2	4	7	9

http://www.aloki.hu ● ISSN 1589 1623 (Print) ● ISSN 1785 0037 (Online)
DOI: http://dx.doi.org/10.15666/aeer/1902_14231436
© 2021, ALÖKI Kft., Budapest, Hungary

CHARACTERISTICS OF THE BACTERIAL COMMUNITY-STRUCTURE AND MICROBIAL DIVERSITY OF ACTIVATED SLUDGE UNDERGOING DIFFERENT TEMPERATURE CONDITIONS IN PLATEAU AREAS BASED ON A^2O PROCESSES

ZONG, Y. C.[1,2] – LI, Y. W.[2] – HUANG, D. C.[2] – HAO, K. Y.[2] – LU, G. H.[1,2*]

[1]*Res. Institute of Tibet Plateau Ecology, Tibet Agriculture & Animal Husbandry University, Linzhi 860000, China*

[2]*Water Conservancy Project & Civil Engineering College, Tibet Agriculture & Animal Husbandry University, Linzhi 860000, China*

**Corresponding author*
e-mail: ghlu@hhu.edu.cn

(Received 19th Nov 2020; accepted 8th Feb 2021)

Abstract. In this study, laboratory-scale A^2O wastewater treatment was performed in Linzhi at an altitude of 3000 m. Water temperatures were maintained at four operating conditions (25, 20, 15, and 10 °C). We analyzed the community structure of phylum, class, order, family, genus and species of bacteria isolated from activated sludge by 16SrRNA sequencing technology. The bacteria within the sludge showed significant differences at varying temperatures ($P < 0.05$). A significant correlation between the number of bacteria in anaerobic tanks and anoxic tanks also occurred. Significant differences in bacterial abundance were also observed and differed from those of previously reported superior community categories and proportions. Correlation analysis of environmental factors and colony structure further confirmed the association between temperature and colony structure ($P < 0.05$). The removal rates of TP, TN, NH_3-N, and COD were all affected by the sample community structure. The variety of colony structure including nitrifying bacteria, denitrifying bacteria, phosphorus accumulating bacteria and other bacteria differed, but their proportions were relatively low. Heatmaps were used to identify species sensitive to temperature, TP, TN, NH_3-N, COD. Amongst the common dominant bacteria, Bacteroidetes_bacterium_OLB10 was significantly affected by temperature. Other common dominant bacteria that temperature were related to metagenome_g__Gordonia, unclassified_f__Burkholderiaceae, uncultured_bacterium_g__norank_f__Saprospiraceae.
Keywords: *Tibet, temperature,16SrRNA sequencing, Sewage treatment, dominant bacteria*

Introduction

As the third pole, the Qinghai-Tibet Plateau has an average altitude of more than 4000 m. The high altitude creates unique environmental conditions of high cold and low air pressure. In recent years, Tibet has amassed a large number of urban sewage treatment plants, but their operating conditions are unsatisfactory, mainly due to the poor effects of nitrogen and phosphorus removal because of the unique environment conditions (Zong et al., 2019a).

According to measurements, the summer water temperature in Changdu City at an altitude of 3500 m is 12.2~18.5 °C (Zhai et al., 2012) compared to the water temperature of Linzhi City at an altitude of 3000 m is -1~15 °C (Chen et al., 2018a). But temperature has been greatly improved through technical treatment, and the current water temperature is about 10.8~22.5 °C. Studies have shown that the water temperature in Tibet is low, which impacts the microbial structure of the sewage treatment system and the effects of nitrogen and phosphorus removal (Zong et al., 2019b). Tian et al.

http://www.aloki.hu ● ISSN 1589 1623 (Print) ● ISSN 1785 0037 (Online)
DOI: http://dx.doi.org/10.15666/aeer/1902_14371455
© 2021, ALÖKI Kft., Budapest, Hungary

(2015) identified 51,880 genus microorganisms from the activated sludge ecosystem of municipal sewage treatment plants using the anaerobic-anoxic-Oxic (A^2O), including Proteus, Bacteroides, Nitrospira and Green Campylobacter as the dominant bacteria. In view of the large differences in microbial colony structures at different water temperatures, numerous studies on water temperature and microbial structure have been performed. Using biological aerated filters, Dou and colleagues (Nasha and Lin, 2016) reported that when the temperature was lower than 18 °C (low temperature), the removal rate of COD and NH_3-N of the biological aerated filters were less than 60%. The structure of the flora in the tank was simple, and the density of the flora decreased. The activity and quantity of enriched phosphorus accumulating bacteria showed a decreasing trend at increasing temperatures, but when the temperature decreased, the activity of phosphorus accumulating bacteria Acinetobacter enhanced its phosphorus removal effect (Fang et al., 2011). Ma et al. (2020) assessed induced temperature periodic changes. They found that the activity a50nd relative abundance of ammonia oxidizing bacteria, nitrite oxidizing bacteria, and anammox bacteria, were dominated by Candidatus Brocadia at low temperatures, which changed following periodic temperature shocks. The formation of dissolved organic nitrogen was also influenced by both microbial activity and microbial community structure (Liao et al., 2019). The performance and stabilization of biological wastewater treatment systems are also closely related to the microbial community structure, variations in which are driven by temperature (Chen et al., 2017). Decreased temperatures result in significant reductions in microbiome diversity, and the alpha diversity of the active community (Paul et al., 2020). Upon analysis of the capacity of nitrogen removal and the spatial distribution of microbial communities at low temperatures, it was shown that low temperatures inhibit nitrogen removal (Paul et al., 2020). It is therefore clear that temperature changes impact microbial structure in wastewater treatment processes and the quality of wastewater treatment water.

Microbial composition and changes in A^2O processes under different temperature conditions are typical characteristics of the community structure. This must be explored to fully understand microbial response mechanisms under the influence of plateau environmental factors, and provides a theoretical system for sewage biological treatment systems affected by plateau environmental factors. In this study, we selected the A^2O system as a typical sewage treatment process to analyze the influence of temperature conditions. We assessed community structure characteristics and their alterations in anoxic and Oxic regions to explore the microbial response mechanisms influenced by plateau environmental factors.

Materials and methods

The A^2O system was selected as a typical sewage treatment process. Microbial structure characteristics were explored to investigate the influence of low temperature at a range of environmental factors. We further explored the performance of experimental scale A^2O processes in response to a range of plateau environmental factors.

Experimental setup

Laboratory-scale A^2O sewage treatment devices were produced from Plexiglas. Each device had an effective volume of 210 L and was divided into 3 compartments; (1) an anaerobic tank; (2) an anoxic tank; (3) an Oxic tank. The volume ratio of the three

http://www.aloki.hu ● ISSN 1589 1623 (Print) ● ISSN 1785 0037 (Online)
DOI: http://dx.doi.org/10.15666/aeer/1902_14371455
© 2021, ALÖKI Kft., Budapest, Hungary

regions were 35:58:117, and the effective volume of the sedimentation tank was 39 L. Both the anaerobic and anoxic tank were equipped with a stirring device at a stirring speed of 50 rpm. The Oxic tank was equipped with an aeration head for the oxygen supply. A peristaltic pump was used to control the inlet water, return sludge and nitrification liquid. To ensure constant temperatures in the test, a constant temperature circulator was used to control the water temperature. Each tank wall had a sampling port. The specific device processes are shown in *Figure 1*.

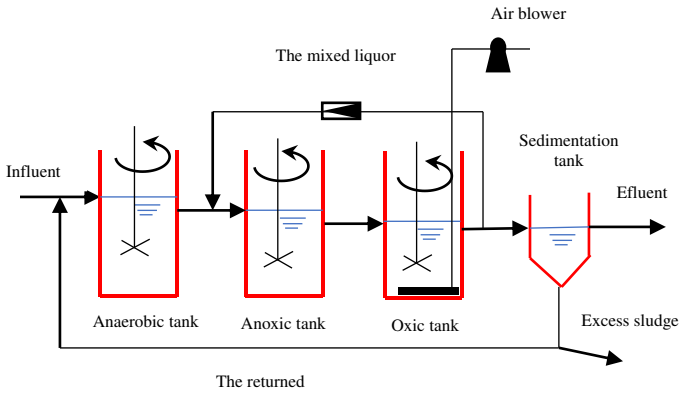


Figure 1. *Schematic of A^{2}O process*

After 35 days of activated sludge culture, the temperature was controlled at 20.0 °C, the SV_{30} was 34%, and the MLSS was 4325 mg/L. We used urban sewage in Linzhi City as the test water, the quality status of which is shown in *Table 1*.

Table 1. *Quality indicators of sewage*

Time (h)	Potential of hydrogen	Chemical oxygen demand (mg/L)	Total nitrogen (mg/L)	Total phosphorous (mg/L)
0	8.87	530.62	153.630	8.595
24	8.94	460.34	186.775	12.810
48	9.00	302.99	156.600	14.325
72	8.97	168.04	215.250	2.970
96	8.97	273.38	116.850	8.820
120	9.04	223.59	72.630	3.990
144	8.90	177.76	38.725	6.510
168	8.93	92.95	63.750	2.075
192	8.87	143.18	57.810	3.030
216	8.79	376.23	105.030	8.235
240	8.98	398.09	110.940	4.778
264	8.81	222.80	111.210	2.610
288	8.87	342.15	89.856	7.675

A^{2}O operation

A^{2}O processes at each temperature were investigated. The designed inlet flow rate was 10.0 ± 0.1L/s. The Oxic tank had a dissolved oxygen content of 2 mg/L. The

http://www.aloki.hu ● ISSN 1589 1623 (Print) ● ISSN 1785 0037 (Online)
DOI: http://dx.doi.org/10.15666/aeer/1902_14371455
© 2021, ALÖKI Kft., Budapest, Hungary

hydraulic retention time was 21.0 ± 0.2 h, the anaerobic tank residence time: anoxic tank residence time: and Oxic tank residence time were 35:58:117. The reflux ratio of the mixed solution was RI = 200%. The reflux ratio of the sludge was R = 100%. Both the mixed solution and sludge were continuously refluxed. Changes in dissolved oxygen were achieved through altering the levels of blown aeration. Controls were set to four levels of 25 °C, 20 °C, 15 °C, and 10 °C. 72 h after the temperature reached the design value, water quality samples were collected at intervals of 24 h, and sludge samples were collected after 288 h of test operation for microbial community structure analysis.

Results and discussion

Microbiological indicators were compared using SPSS 20.0(IBM, Inc., Armonk, NY, USA) and are expressed as the mean ± standard deviation (SD). A one-way analysis of variance (ANOVA, R. A. Fisher, UK) to assess significant differences. $P < 0.05$ (Simon et al., 1989) indicated significant differences between samples.

Anaerobic, anoxic and Oxic tank sludge were sampled at each temperature and 16SrRNA sequencing was performed.

Basic information

Taxonomic analysis of the domain, kingdom, phylum, class, order, family, genus and species of each sample were assessed. Operational Taxonomic Units (OTU) were identified using the Silva database. The statistical results of specific samples are shown in *Table 2,* temp stands for temperature condition, and ana represents anaerobic tank, ano represents anoxic tank, and Oxic represents Oxic tank, and 10, 15, 20, 25 correspond to 10 °C, 15 °C, 20 °C, 25 °C respectively.

Table 2. *Sample information*

Sample	Domain	Kingdom	Phylum	Class	Order	Family	Genus	Species	OTU
temp_ana_25	1	1	20	35	97	188	376	533	734
temp_ana_20	1	1	27	52	126	234	477	707	969
temp_ana_15	1	1	29	56	134	241	505	757	1067
temp_ana_10	1	1	30	54	131	239	453	664	898
temp_ano_25	1	1	24	41	103	198	413	607	849
temp_ano_20	1	1	27	47	123	235	491	712	970
temp_ano_15	1	1	29	53	131	242	493	745	1028
temp_ano_10	1	1	28	52	129	239	455	675	908
temp_Oxic_25	1	1	27	44	103	194	394	567	772
temp_Oxic_20	1	1	27	50	126	238	471	678	911
temp_Oxic_15	1	1	26	43	102	193	379	560	758
temp_Oxic_10	1	1	27	49	121	225	426	625	837

Only a single Domain and Kingdom were investigated through sequencing, and Phylum ∈ (20,30), Class ∈ (35,56), Order ∈ (97,134), Family ∈ (188,242), Genus ∈ (376,505), Species ∈ (533,757), OTU ∈ (734,1067), and the corresponding genealogical values were significantly lower than those stated in the literature. On Phylum level, values were similar to the 24 reported by Sun et al. (2019), but were lower than the

http://www.aloki.hu ● ISSN 1589 1623 (Print) ● ISSN 1785 0037 (Online)
DOI: http://dx.doi.org/10.15666/aeer/1902_14371455
© 2021, ALÖKI Kft., Budapest, Hungary

value of 51 recorded by Tian et al. (2015). On Genus level, the values were also lower than the Tian study (Tian et al., 2015). The value of the test 800 was low. On OTU level, the values (924~1363) were comparable to Wen et al. (2015) in the SBR process, but exceeded those of Jin and other researchers (Jin et al., 2017; Zhang et al., 2019a; Fan et al., 2018). Upon measurement of the A/O processes, the Oxic tank had low OTU values. Previous studies suggest that the temperature on Phylum, Class, Order, and Family levels significantly influence the number of species ($P < 0.05$). Compared to previous studies, we observed large differences in the number of microbial species, particularly at the temperature of the plateau, variations in which significantly influenced the number of bacteria on Phylum, Class, Order, and Family levels. In addition, correlation analysis revealed significant differences in the number of species of phylum, phylum, order, family, genus and species at each temperature ($P < 0.05$). The number of phylum, phylum, order, family, genus and species also differed. A significant correlation between the anaerobic tank and anoxic tank were observed ($P < 0.05$). No significant correlation between the Oxic tank and the above two reactors ($P \geq 0.05$) were observed. There were no obvious correlations between the number of genus, order, family, genus and species ($P \geq 0.05$).

Alpha diversity analysis

The Alpha diversity comprises the diversity index and the differences between index groups. Community richness refers to the number of species in the community, and its common indicators are chao and ace. Community evenness refers to the distribution of the number of individuals of all species in a community or environment, and its common indicators is Simpson. Community diversity refers to the general term for the complexity of all biological species and their genetic variation and ecosystems in a certain time and in a certain area, and its common indicators is shannoneven. T tests were performed to detect significant correlations between the two groups. The diversity index of each sample is shown in *Table 3*.

Table 3. *Alpha diversity statistics table*

Sample	Shannoneven	Ace	Chao	Coverage	Simpson
temp_ana_25	0.686311	678.636	672.000	0.996	0.063589
temp_ana_20	0.700519	867.345	904.167	0.996	0.028344
temp_ana_15	0.643979	902.975	912.556	0.996	0.023550
temp_ana_10	0.613907	866.421	892.741	0.994	0.064387
temp_Oxic_25	0.619765	720.442	726.797	0.996	0.045108
temp_Oxic_20	0.656817	839.848	839.318	0.995	0.032669
temp_Oxic_15	0.688048	925.187	882.961	0.995	0.062754
temp_Oxic_10	0.661908	816.326	844.380	0.995	0.087890
temp_ano_25	0.710761	785.327	818.406	0.996	0.042694
temp_ano_20	0.645525	884.870	911.405	0.996	0.029929
temp_ano_15	0.626017	910.082	875.190	0.995	0.032413
temp_ano_10	0.689180	876.520	862.011	0.994	0.063279

The community coverage (Wang et al., 2019) has an overage coefficient of 0.994~0.996, with all exceeding 0.990. The sample sequencing coverage was good,

http://www.aloki.hu ● ISSN 1589 1623 (Print) ● ISSN 1785 0037 (Online)
DOI: http://dx.doi.org/10.15666/aeer/1902_14371455
© 2021, ALÖKI Kft., Budapest, Hungary

meaning the probability that the sample sequence not being detected was extremely low. The ace coefficient of community richness was 678.6~925.2 which was comparable to previous studies (Chen et al., 2018b; Zhang et al., 2019). Ace values were 1300~2200 and 1038~1159. Low levels of community uniformity were observed with a Shannon coefficient of 0.613907~0.710761, which was lower than previously reported values (Li et al., 2014). The community diversity measured as the Simpson coefficient was 0.02355~0.08789 in previous studies (Zhang et al., 2019b). The Shannon coefficient was 0.935-0.976 which was comparable to Chen et al. (2018b) who reported values of 0.835.

Upon assessment of the four operating conditions: excluding operating conditions of 10 °C and 20 °C, there were significant differences in the ace coefficient of community richness between each of the operating conditions ($P \leq 0.05$). There were significant differences in the number of species except for at 10 °C and 20 °C. The community diversity measured through the Simpson coefficient differed between 10 °C and 20 °C, 10 °C and 15 °C, and 20 °C and 25 °C ($P < 0.05$); Significance analysis of the community richness chao coefficient revealed significant differences between 10 °C and 15 °C, 20 °C and 25 °C, and 15 °C and 25 °C ($P < 0.05$). The Simpson even coefficient of community uniformity also showed significant differences between 10 °C and 20 °C, 10 °C and 20 °C, and 20 °C and 25 °C ($P < 0.05$). Under the four groups of working conditions, there are were one or more significant differences in community richness, community diversity or community uniformity, suggesting that temperature significantly influences colony structure. Differences in community richness from the Oxic to anoxic tank, oxygen tank and anaerobic tank, and anoxic tank and anaerobic tank were observed. The community diversity varied in both the anaerobic and anoxic tank, anaerobic tank and Oxic tank, and anoxic tank and Oxic tank. Differences in community uniformity were observed upon comparison of anaerobic and anoxic, anoxic and Oxic, and anaerobic and Oxic tanks.

Community composition analysis

The RDPClassifier was used for classification statistics of the three reactors under each of the operating conditions in the order of Domain, Kingdom, Phylum, Class, Order, Family, and Genus. We further focused on the analysis of fungus function at the Genus level, and analyzed each sample. The composition of the middle population when including community with an abundance greater than 1% of different classification levels showed only a single bacteria at the domain analysis level and no rank_d__Bacteria at the Kingdom analysis level.

Analysis of the characteristics of colony structure on Phylum level

Figure 2 shows that shared dominant communities on Phylum level were Proteobacteria, Bacteroidetes, Actinobacteria, Firmicutes, and Chloroflexi. A total of 31 Phyla were obtained. The abundance of five of the Phyla were 94.31-99.04% in the anaerobic and anoxic tanks. The Oxic tank showed a decreasing trend as the temperature decreased. More abundant Phylum and Firmicutes were observed compared to the literature (Cydzik-Kwiatkowska et al., 2016).

The abundance of Proteobacteria (27.58%~46.22) represented a relatively high proportion of organic matter-degrading bacteria. The abundance of Proteobacteria in anaerobic tanks, anoxic tanks, and Oxic tanks gradually decreased, whilst the abundance of Proteobacteria increased. The most abundant Phylum are consistent with

http://www.aloki.hu ● ISSN 1589 1623 (Print) ● ISSN 1785 0037 (Online)
DOI: http://dx.doi.org/10.15666/aeer/1902_14371455
© 2021, ALÖKI Kft., Budapest, Hungary

previous studies (Cydzik-Kwiatkowska et al., 2016), but the corresponding abundance was lower than previously reported (Muszyński et al., 2015). The abundance of Bacteroidetes was 21.93%~38.25%. This obligate anaerobic phylum can promote the utilization of nitrogen-containing substances and the hydrolysis of macromolecular organic substances. The Oxic tanks had a significantly higher abundance than anaerobic and anoxic tanks. Bacteroidetes were more abundant than those reported by Juretschko et al. (2002) and Kong et al. (2007). The values obtained were low; the abundance of Actinobacteria were 12.33%-25.14% in heterotrophic Oxic phylum, and its change in abundance suggested that the concentration of the anoxic tank exceeded that of the anaerobic tank and oxygen tank. The abundance of Firmicutes was 4.52% to 12.74%. These are denitrifying bacteria that are mainly present in anoxic conditions. Their abundance in the anaerobic tank was higher, and the abundance of Firmicutes was higher than that reported by Beer et al. (2006), but lower than that reported by Wong et al. (2005). The abundance of Chloroflexi was 1.04%~6.26%. These are Oxic sulphur bacteria the abundance of which decreases in anoxic and Oxic tanks as temperature decreases.

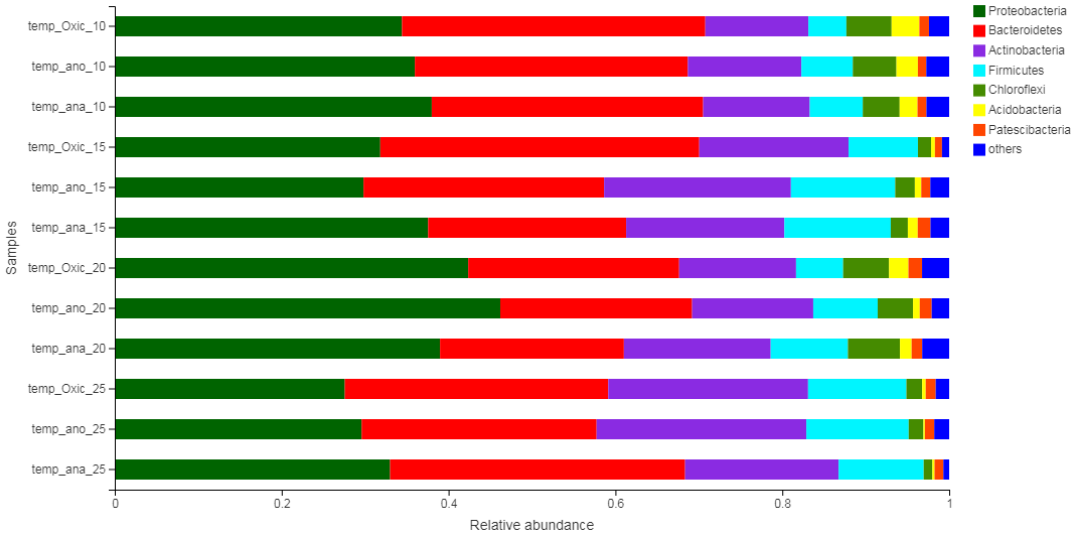


Figure 2. *Community composition on Phylum level*

The abundance of Proteobacteria, Actinobacteria, Firmicutes and Chloroflexi all differed according to temperature ($P \leq 0.05$). Of these four dominant bacteria, the Phylum number had a significant effect, but the dominant strains on Phylum level showed no significant differences under different reactors.

Analysis of the characteristics of colony structure on Class level

Figure 3 shows the five classes of Bacteroidia, Gammaproteobacteria, Actinobacteria, Alphaproteobacteria, Clostridia. A total of 66 Classes were obtained. The abundance of 5 classes were 84.96-94.23% which showed a decreasing trend in the anoxic tank as temperature decreased. These findings were comparable to previous studies (Cydzik-Kwiatkowska et al., 2016) excluding the β-proteobacteria values. These findings also differed to Kang et al. (2019) in terms of the type and proportion of dominant strains.

http://www.aloki.hu ● ISSN 1589 1623 (Print) ● ISSN 1785 0037 (Online)
DOI: http://dx.doi.org/10.15666/aeer/1902_14371455
© 2021, ALÖKI Kft., Budapest, Hungary

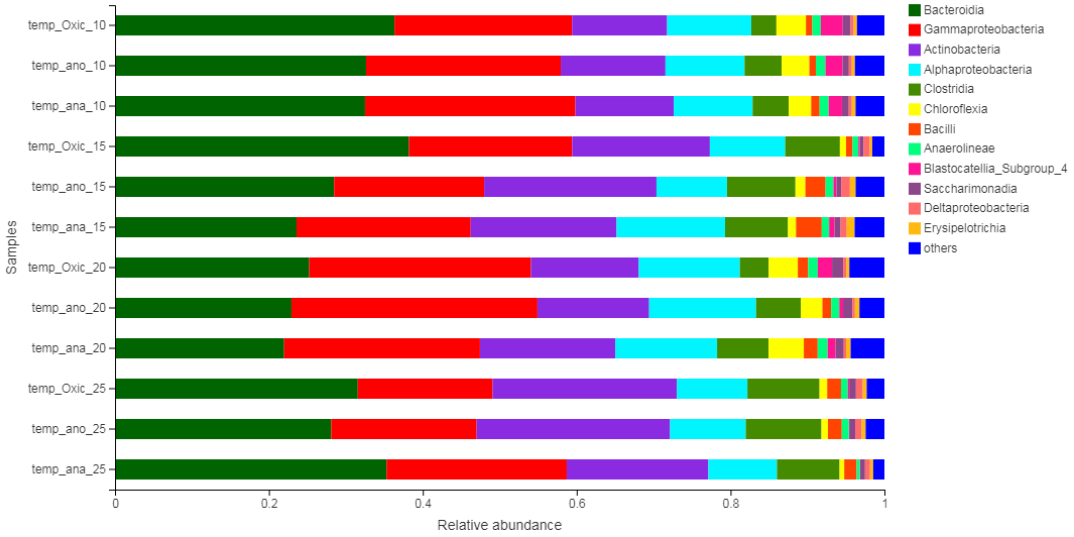


Figure 3. *Community composition on Class level*

Gammaproteobacteria and Alphaproteobacteria belong to the Proteobacteria phylum and represent denitrifying bacteria. The abundance of Alphaproteobacteria and Gammaproteobacteria were higher than the literature (Muszyński et al., 2015), whilst the abundance of Bataproteobacteria were higher than reported by Nielsen et al. (2012), Wong et al. (2005) and Schmid et al. (2003) Clostridia belongs to the Chloroflexi, which varies greatly in different reactors under different working conditions. The abundance of Actinobacteria (12.33-25.14%) was higher than Zhang et al. (2018). The change interval was smaller than Chen et al. (2017) and the abundance of Bacteroidia was larger than Zhang et al. (2018).

Gammaproteobacteria, Actinobacteria, Clostridia were the three dominant bacteria that showed significant differences ($P \leq 0.05$) under different temperature conditions. In addition, Chloroflexia (0.61-4.61%) and Anaerolineae (0.42 -1.30%) showed changes in abundance at different temperatures ($P \leq 0.05$). Whilst temperature has a significant effect on the number of the above five bacterial community, there no significant differences observed as a result of the different reactors ($P > 0.05$).

Analysis of the colony structure on Order level

Figure 4 shows that under the above working conditions, the predominant bacterium order were Betaproteobacteriales, Sphingobacteriales, Chitinophagales, Xanthomonadales, Clostridiales, Microtrichales, Propionibacteriales, Corynebacteriales, Sphingomonadales, Rhizobiales, and Rhodobacterales. A total of 168 Orders were obtained. The abundance of 11 Orders were 71.93-86.24%. In addition, the abundance of seven orders of Thermomicrobiales, Bacteroidales, Micrococcales, Lactobacillales, Caulobacterales, Pseudomonadales, and Solirubrobacterales varied greatly. This accounted for 6.77-13.36% of all bacteria that were sensitive to temperature changes.

The analysis showed that: Microtrichales, Propionibacteriales, Corynebacteriales, Micrococcales, Solirubrobacterales belong to the Actinobacteria. The abundance of Microtrichales and Corynebacteriales were relatively stable, the abundance of Propionibacteriales increased at increasing temperature, and Micrococcales and Solirubrobacterales were relatively unstable at different temperature conditions.

http://www.aloki.hu ● ISSN 1589 1623 (Print) ● ISSN 1785 0037 (Online)
DOI: http://dx.doi.org/10.15666/aeer/1902_14371455
© 2021, ALÖKI Kft., Budapest, Hungary

Sphingobacteriales, Chitinophagales, and Bacteroidales belong to the Bacteroidetes. Sphingobacteriales decreased with increasing temperature and were more abundant in the Oxic tank compared to other reactors. Chitinophagales, Bacteroidales are unstable with changes in temperature changes and showed a correlation. Clostridiales, Lactobacillales and Erysipelotrichales belong to the Firmicutes; Betaproteobacteriales, Xanthomonadales, Sphingomonadales, Rhizobiales, Rhodobacterales, Caulobacterales, Pseudomonadales belong to the Proteobacteria. Amongst them, Betaproteobacteriales were more abundant than those of other well-characterised anaerobic bacteria. The proportions of Caulobacterales and Pseudomonadales in anaerobic and anoxic tanks were higher. Betaproteobacteriales tended to increase with increasing temperatures in each reactor and were higher in anaerobic tanks. Xanthomonadales were higher in Oxic tanks and increased with temperature Sphingomonadales and Rhizobiales did not change with temperature or according to the reactor. Rhodobacterales showed an increasing trend with increasing temperature in each reactor. Thermomicrobiales belong to the Chloroflexi, which was greatly affected by temperature, including at 25 °C. All three reactors were lower (less than 1%), the Oxic tank was slightly higher than 1% in the anoxic tank and the anaerobic tank at 15 °C.

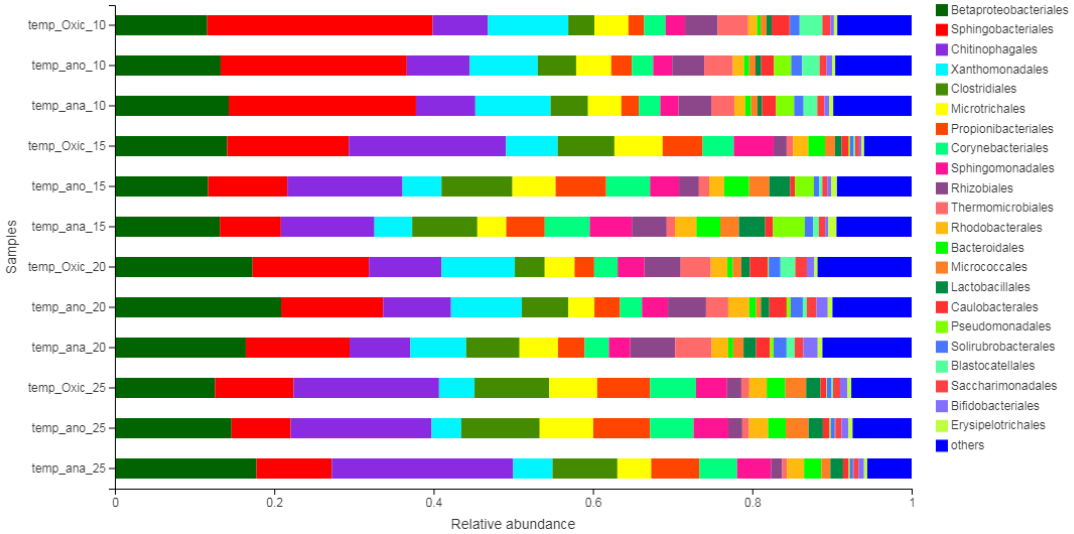


Figure 4. *Community composition on order level*

A total of 8 common dominant bacterial orders of Sphingobacteriales, Chitinophagales, Xanthomonadales, Clostridiales, Propionibacteriales, Corynebacteriales, Sphingomonadales, Rhizobiales showed significant differences under temperature conditions ($P \leq 0.05$), and Thermomicrobiales (0.61-4.60%), Bacteroidales (0.47-3.14%), Caulobacterales (0.63-2.25%), Solirubrobacterales (0.41-1.58%) showed an altered abundance under temperature conditions ($P \leq 0.05$). Temperature therefore had a significant effect on these four bacteria. The predominant strains on order level showed no significant differences in each reactor ($P > 0.05$).

Analysis of the characteristics of colony structure on Family level

Figure 5 shows that the dominant family were AKYH767, Burkholderiaceae, Saprospiraceae, Microtrichaceae, Propionibacteriaceae, Sphingomonadaceae,

http://www.aloki.hu ● ISSN 1589 1623 (Print) ● ISSN 1785 0037 (Online)
DOI: http://dx.doi.org/10.15666/aeer/1902_14371455
© 2021, ALÖKI Kft., Budapest, Hungary

Xanthomonadaceae, Rhodanobacteraceae, Chitinophagaceae, Nocardiaceae, Rhodobacteraceae, and Peptostreptococaceae. A total of 325 Families were obtained. The abundance of 5 Families were 54.98-72.41%, which were the dominant Families in the plateau environment. The composition of the dominant bacteria in previous studies (Yang et al., 2017) lack Comamon-adaceae, Nitrospiraceae, Sinobacteraceae, Hyphomicrobiaceae, and Chromatiaceae. It was also important to note that the abundance of nine Families of JG30-KF-CM45, Rhizobiaceae, Clostridiaceae_1, Christensenellaceae, Carnobacteriaceae, Caulobacteraceae, Hydrogenophilaceae, Microbacteriaceae, and Moraxellaceae varied greatly and were more sensitive to temperature.

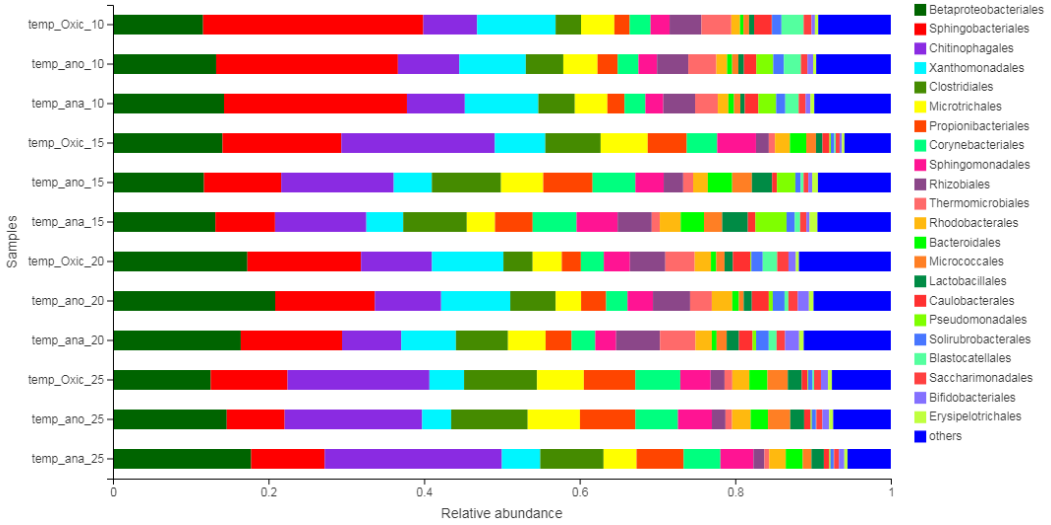


Figure 5. *Community composition on family level*

In addition, Microtrichaceae, Propionibacteriaceae, Nocardiaceae, and Microbacteriaceae belong to Actinobacteria, the abundance of which increased with temperature and were higher in the Oxic tank. AKYH767, Saprospiraceae, and Chitinophagaceae belong to Bacteroidetes, and the abundance of AKYH767 increased with temperature. The Oxic tank showed higher levels of these bacteria than other reactors. The abundance of Saprospiraceae showed an increasing trend with increasing temperature and the Oxic tank was superior to other reactors. The abundance of Chitinophagaceae showed a downward trend with increasing temperature. The reactor was relatively balanced; Peptostreptococcaceae, Clostridiaceae_1, Christensenellaceae, and Carnobacteriaceae belong to the Firmicutes family. The abundance of anaerobic tanks of Peptostreptococcaceae were significantly higher than other reactors. Clostridiaceae_1, Christensenellaceae, Carnobacteriaceae, ceca Xanthomonadaceae, Rhodanobacteraceae, Rhodobacteraceae, Rhizobiaceae, Caulobacteraceae, Hydrogenophilaceae, and Moraxellaceae belong to the Proteobacteria, amongst which Burkholderiaceae and Hydrogenophilaceae belong to Betaproteobacteriales, which are polyphosphate bacteria. JG30-KF-i45 belongs to the Chloroflex and Chloroflexi.

AKYH767, Saprospiraceae, Microtrichaceae, Propionibacteriaceae, Sphingomonadaceae, Xanthomonadaceae, Rhodanobacteraceae, Chitinophagaceae, Nocardiaceae, Rhodobacteraceae were then the 10 common dominant bacteria under temperature conditions $P \leq 0.05$). JG30-KF-CM45 (0.42-3.56%), Rhizobiaceae (0.62-2.84%), Clostridiaceae_1 (0.77-2.27%), Christensenellaceae (0.26-3.03%),

http://www.aloki.hu ● ISSN 1589 1623 (Print) ● ISSN 1785 0037 (Online)
DOI: http://dx.doi.org/10.15666/aeer/1902_14371455
© 2021, ALÖKI Kft., Budapest, Hungary

Caulobacteraceae (0.63-2.13%), and Hydrogenophilaceae (0.52-2.89%) showed changes in abundance according to temperature ($P \leq 0.05$). The abundance of Peptostreptococcaceae significantly differed between the reactors ($P \leq 0.05$). No other significant differences between bacteria in different reactors were observed ($P > 0.05$).

Analysis of the characteristics of colony structure on Genus level

Figure 6 shows that the common dominant bacterial genus were norank_f__AKYH767, norank_f__Saprospiraceae, unclassified_f__Burkholderiaceae, Ottowia, IMCC26207, Novosphingobium, Gordonia, Romboutsia octabacterium. A total of 719 Genus were obtained. The abundance of 8 Genus were 33.33-53.11%, which represent the dominant genus in the plateau environment. The dominant bacteria on genus level reported in previous studies (Yang et al., 2017; Chen et al., 2017) were relatively different, excluding Pseudomonas that were similar (Tian et al., 2015; Kang et al., 2019). The dominant bacterial community differed to these studies.

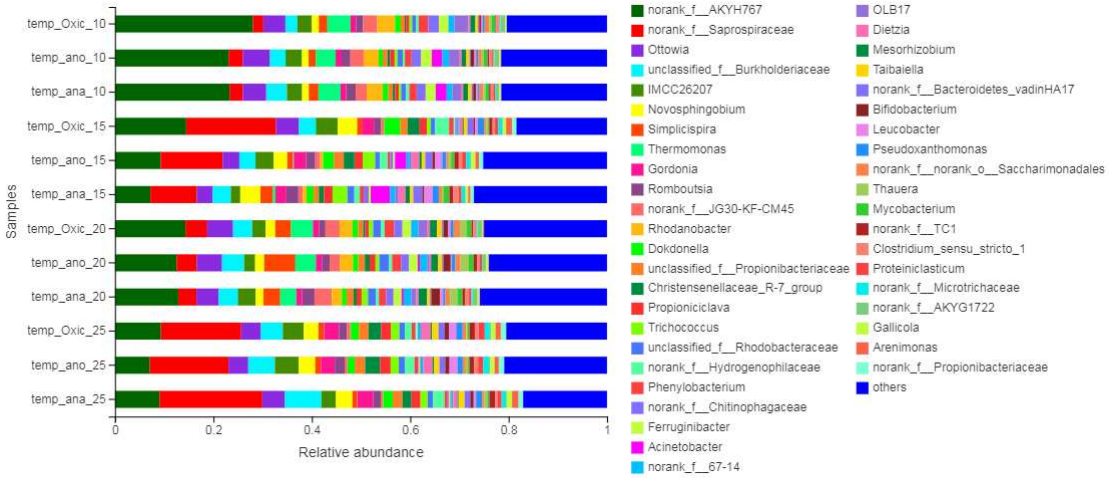


Figure 6. *Community composition on genus level*

Thermomonas, Simplicispira, norank_f__JG30-KF-CM45, Rhodanobacter, Dokdonella, unclassified_f__Propionibacteriaceae, Christensenellaceae_R-7_group, Propioniciclava, Trichococcus, norank_f__Hydrogenophilaceae, unclassified_f__ Large (total abundance 15.33-28.97%) were more sensitive to temperature changes.

Norank_f__AKYH767, norank_f__Saprospiraceae, Ferruginibacter, norank_f__Chitinophagaceae belong to the Bacteroidetes, and these four genera of bacteria vary greatly under temperature conditions; Christensenellaceae_R-7_group, Romboutsia, Trichococcus belong to the Firmicutes. Romboutsia did not significantly change between temperature and reactor. Christensenellaceae_R-7_group increased with increasing temperature, and the abundance of Trichococcus decreased with increasing temperature. Ottowia, unclassified_f__Burkholderiaceae, Novosphingobium, Thermomonas, Simplicispira, Rhodanobacter, Dokdonella, Simplicispira, unclassified_f__Burkholderiaceae, norank_f__Hydrogenophilaceae, norank_f__Hydrogenophilaceae, unclassified_f__ Ottowia belong to Betaproteobacteriales as phosphorus-accumulating bacteria. The corresponding proportion in the Oxic tank was significantly higher than other reactors.

http://www.aloki.hu ● ISSN 1589 1623 (Print) ● ISSN 1785 0037 (Online)
DOI: http://dx.doi.org/10.15666/aeer/1902_14371455
© 2021, ALÖKI Kft., Budapest, Hungary

Norank_f__JG30-KF-CM45 belongs to the Chloroflexi, which was greatly affected by the temperature conditions, the anoxic tank and the anaerobic tank.

The abundance of six common dominant genera of norank_f__AKYH767, norank_f__Saprospiraceae, Novosphingobium, Thermomonas, Simplicispira, and Gordonia significantly differed under different temperature conditions ($P \leq 0.05$). These included Norank_f__JG30- KF-CM45 (0.42-3.56%), Rhodanobacter (0.03-4.70%), Dokdonella (0.82-3.27%), unclassified_f__Propionibacteriaceae (0.79-2.11%), Christensenellaceae_R-7_group (0.25-3.01%), Propioniciclava (0.71-2.17%), Trichococcus (0.47-3.04%), norank_f__Hydrogenophilaceae (0.43-2.86%), Phenylobacterium (0.52-1.93%), Ferruginibacter (0.28-2.16%), norank_f__Chitinophagaceae (0.17-2.22%). There were significant differences at each temperature ($P \leq 0.05$). The abundance of the genus-level dominant Genus Romboutsia significantly differed between the reactors ($P \leq 0.05$). There were no significant differences between the other bacteria in the different reactors ($P > 0.05$).

Analysis of the characteristics of colony structure on Species level

From *Figure 7,* the common dominant bacteria genus under the above working conditions were Bacteroidetes_bacterium_OLB10, metagenium_g__Gordordium, uncultured_bacterium_g__norank_f__Saprospiraceae, unclassified_f__Burkholderiaceae, uncultured_bacterium_g__IMCC26207, unclassified_g__Novosphingobium, and uncultured_bacterium_g__Romboutsia. A total of 1178 Species were obtained. The abundance of 7 Species were 28.11-47.98%, which were the dominant strain in the plateau environment. Unclassified_g__Ottowia, unclassified_g__Simplicispira, uncultured_gamma_proteobacterium_g__Dokdonella, uncultured_Xanthomonadaceae_bacterium_g__Rhodanobacter, unclassified_f__Propionibacteriaceae, uncultured_bacterium_g__Propioniciclava, metagenome_g__Trichococcus, unclassified_g__norank_f__Hydrogenophilaceae, unclassified_f__Rhodobacteraceae, uncultured_bacterium_g__Phenylobacterium, uncultured_Comamonadaceae_bacterium_g__Ottowia, unclassified_g__Christensenellaceae_R-7_group, unclassified_g__Ferruginibacter, uncultured_bacterium_g__Thermomonas, metagenome_g__norank_f__JG30-KF-CM45 showed highly changes in abundance, and were abundant (17.43-25.99%), and more sensitive to temperature changes.

Uncultured_bacterium_g__IMCC26207, unclassified_f__Propionibacteriaceae, metagenome_g__Gordonia, uncultured_bacterium_g__Propioniciclava belong to the Actinobacteria phylum. The abundance of uncultured_bacterium_g__IMCC26207 and metagenome_g__Gordonia increased as temperature increased. Unclassified_f__Propionibacteriaceae, uncultured_bacterium_g__Propioniciclava also increased at increasing temperature and were significantly superior to the other two reactors in the anoxic tank. Uncultured_bacterium_g__norank_f__Saprospiraceae、Bacteroidetes_bacterium_OLB10、unclassified_g__Ferruginibacter are belong to Bacteroidetes. Uncultured_bacterium_g__norank_f__Saprospiraceae and Bacteroidetes_bacterium_OLB10 also increased at increasing temperature and were significantly superior to the other two reactors in the Oxic tank. Unclassified_g__Ferruginibacter showed a downward trend at increasing temperatures. Uncultured_bacterium_g__Romboutsia, metagenome_g__Trichococcus,

http://www.aloki.hu ● ISSN 1589 1623 (Print) ● ISSN 1785 0037 (Online)
DOI: http://dx.doi.org/10.15666/aeer/1902_14371455
© 2021, ALÖKI Kft., Budapest, Hungary

unclassified_g__Christensenellaceae_R-7_group belong to Firmicutes, And metagenome_g__Trichococcus、uncultured_bacterium_g__Romboutsia decreased as temperature increased, at were highest in the anaerobic tank. The abundance of unclassified_g__Christensenellaceae_R-7_group increased with temperature. Unclassified_f__Burkholderiaceae, unclassified_g__Novosphingobium, unclassified_g__Ottowia, unclassified_f__Rhodobacteraceae, uncultured_Xanthomonadaceae_bacterium_g__Rhodanobacter, unclassified_g__Simplicispira, uncultured_gamma_proteobacterium_g__Dokdonella, unclassified_g__norank_f__Hydrogenophilaceae, uncultured_Comamonadaceae_bacterium_g__Ottowia, uncultured_bacterium_g__Phenylobacterium, uncultured_bacterium_g__Thermomonas belongs Proteobacteria, wherein unclassified_f__Burkholderiaceae, unclassified_g__Ottowia, unclassified_g__norank_f__Hydrogenophilaceae, unclassified_g__Simplicispira, uncultured_Comamonadaceae_bacterium_g__Ottowia belonging to Betaproteobacteriales of PAOs; metagenome_g__norank_f__JG30-KF-CM45, uncultured_Chloroflexi_bacterium_g__norank_f__AKYG1722, unclassified_g__norank_f__JG30-KF-CM45, metagenome_g__norank_f__JG30-KF-CM45 belong to Chloroflexi and showed fluctuations at different temperatures.

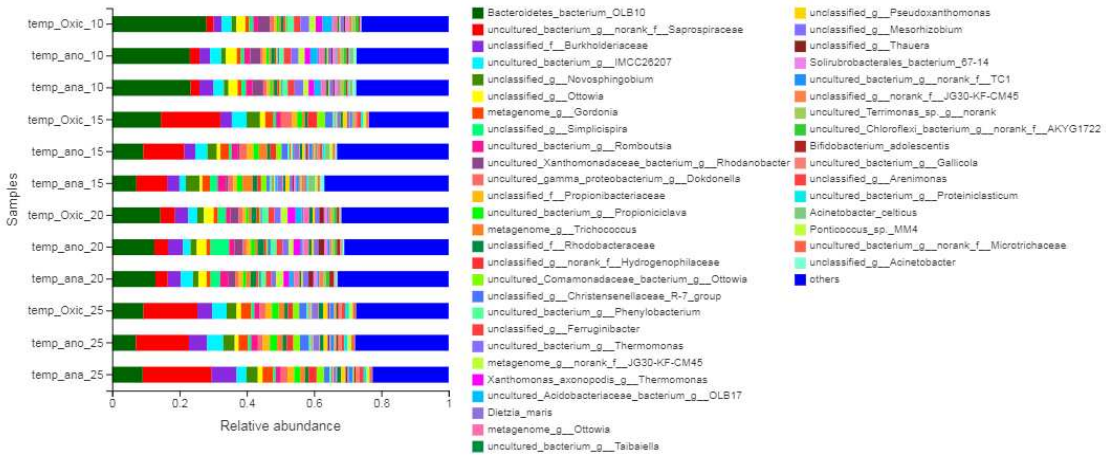


Figure 7. *Community composition on species level*

Bacteroidetes_bacterium_OLB10, uncultured_bacterium_g__norank_f__Saprospiraceae, unclassified_g__Novosphingobium, unclassified_g__Ottowia, metagenome_g__Gordonia showed significant changes in abundance (5.52%), uncultured_Xanthomonadaceae_bacterium_g__Rhodanobacter (0.03-3.62%), uncultured_gamma_proteobacterium_g__Dokdonella (0.79-3.27%), unclassified_f__Propionibacteriaceae (0.79-2.11%), uncultured_bacterium_g__Propioniciclava (0.70-2.14%), unclassified_g__norank_f__Hydrogenophilaceae (0.43-2.86%), uncultured_Comamonadaceae_bacterium_g__Ottowia (0.36-2.32%), unclassified_g__Christensenellaceae_R-7_group (0.22-2.68%), uncultured_bacterium_g__Phenylobacterium (0.51-1.92%), uncultured_bacterium_g__Thermomonas (0.00-2.67%), metagenome_g__norank_f__JG30-KF-CM45 (0.17-2.25%). These data suggest that

http://www.aloki.hu ● ISSN 1589 1623 (Print) ● ISSN 1785 0037 (Online)
DOI: http://dx.doi.org/10.15666/aeer/1902_14371455
© 2021, ALÖKI Kft., Budapest, Hungary

temperature has a significant effect on all these bacteria. The abundance of the dominant bacteria uncultured_bacterium_g__Romboutsia at the species level significantly differed between the reactors ($P \leq 0.05$). There were no significant differences between other dominant bacteria in different reactors ($P > 0.05$).

Relationship between A^2O process colony structure and environmental factors

Correlation analysis of the environmental factors and colony structure were performed through RDA/CCA analysis, which carries out regression analysis on the community structure and environmental factors at different temperature to reflect the relationship between the community structure and environmental factors. The microbial classification level is Species, environment. The factors corresponding to temperature, TN, TP, NH_3-N and COD were assessed. Given the purpose of the experiment design, CCA analysis was performed for the anaerobic tank, anoxic tank and Oxic tank.

From *Figure 8,* CCA analysis showed that the correlation coefficients r of temperature, TN, TP, NH_3-N, and COD were 0.9555, -0.7292, -0.7916, 0.77882, and 0.5565, respectively. Significance analysis showed that the correlation between temperature and the samples was significant ($p < 0.05$), suggesting that environmental factors show a significant relationship to sample colony structure. The removal rate of TP, TN, NH_3-N, and COD were affected by the sample community structure. The degree of impact was sequentially weakened. The interpretation degree of RDA1 and RDA2 were 78.47% and 7.86% respectively.

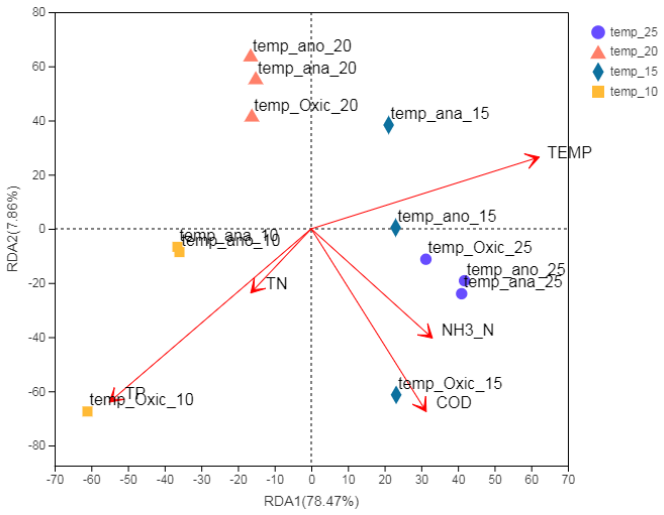


Figure 8. *CCA analysis*

We used correlation Heatmaps to analyze the relationship between different species and environmental variables. To assess the correlation between microorganisms and environmental variables (temperature, TN, TP, NH_3-N, and COD) samples were classified according to the top 50 species.

Figure 9 shows that: On species level, temperature is significantly related to the species of Bacteroidetes_bacterium_OLB10, Dietzia_maris, Ponticoccus_sp._MM4, unclassified_f__Sphingomonadaceae, unclassified_g__Arenimonas, unclassified_g__Christensenellaceae_R-7_group, unclassified_g__Pseudoxanthomonas,

http://www.aloki.hu ● ISSN 1589 1623 (Print) ● ISSN 1785 0037 (Online)
DOI: http://dx.doi.org/10.15666/aeer/1902_14371455
© 2021, ALÖKI Kft., Budapest, Hungary

unclassified_g__norank_f__Hydrogenophilaceae, uncultured_Xanthomonadaceae_bacterium_g__Rhodanobacter, uncultured_bacterium_g__Gallicola, uncultured_bacterium_g__Proteiniclasticum, uncultured_bacterium_g__Thermomonas, uncultured_bacterium_g__norank_f__Microtrichaceae. Temperature also significantly influenced related species including metagenome_g__Gordonia, unclassified_f__Burkholderiaceae, unclassified_f__Propionibacteriaceae, uncultured_Acidobacteriaceae_bacterium_g__OLB17, uncultured_bacterium_g__Taibaiella, uncultured_bacterium_g__norank_f__Saprospiraceae, and uncultured_bacterium_g__norank_f__TC1. TN correlated to the absence of certain bacterial species. TP was significantly associated with species of Bacteroidetes_bacterium_OLB10, metagenome_g__Trichococcus, unclassified_f__Propionibacteriaceae, uncultured_bacterium_g__norank_f__TC1. TP was significantly related to unclassified_f__Burkholderiaceae, unclassified_f__Rhodobacteracea E. NH_3-N was significantly related to uncultured_gamma_proteobacterium_g__Dokdonella. COD was significantly associated with Solirubrobacterales_bacterium_67-14, Xanthomonas_axonopodis_g__Thermomonas, unclassified_f__Rhizobiaceae, unclassified_f__Rhodobacteraceae, unclassified_g__Mesorhizobium, unclassified_g__Ottowia, unclassified_g__Thauera, uncultured_Chloroflexi_bacterium_g__norank_f__AKYG1722, uncultured_bacterium_g__Phenylobacterium, uncultured_gamma_proteobacterium_g__Dokdonella. Extremely relevant bacteria and COD species included Bifidobacterium_adolescentis, metagenome_g__Ottowia, and uncultured_bacterium_g__Simplicispira.

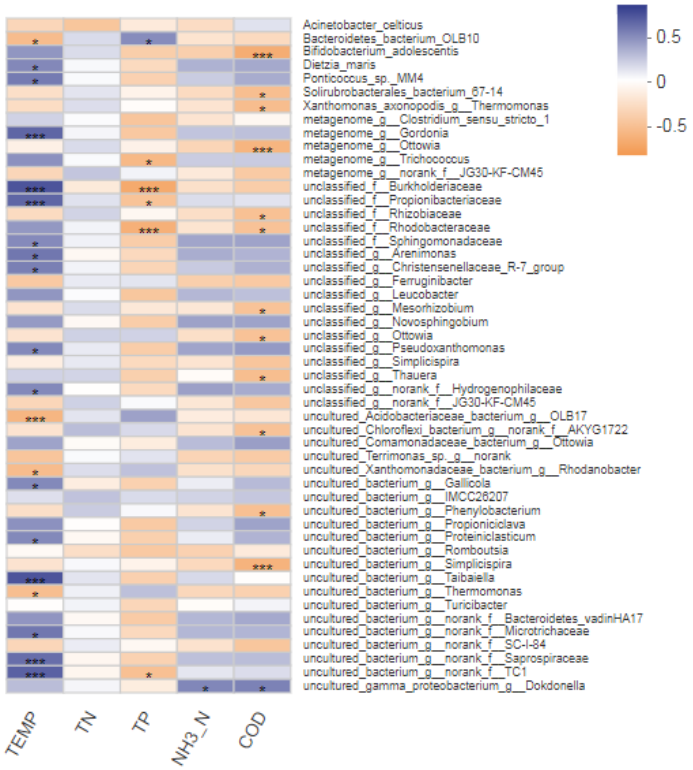


Figure 9. *Correlation heatmap*

http://www.aloki.hu ● ISSN 1589 1623 (Print) ● ISSN 1785 0037 (Online)
DOI: http://dx.doi.org/10.15666/aeer/1902_14371455
© 2021, ALÖKI Kft., Budapest, Hungary

Conclusions

Using 16SrRNA gene sequencing and correlation analysis, the differences in bacterial communities in anaerobic, anoxic and Oxic tanks under four temperature conditions were analyzed based on species number, diversity, composition, and Heatmaps of the sequenced samples.

(1) Sequencing analysis revealed that the number of species on phylum, Class, order, family, genus and species level in the high-in situ samples were lower than those previously reported and varied according to the working conditions of the three reactors. There were significant differences in community number at the phylum, class, order, family, genus and species level. A significant correlation was observed between the number of community on phylum, Class, order, family, genus and species level ($P \leq 0.05$). However, no obvious correlation between temperature and the number of phylum, class, order, family, genus and species of each tank were observed.

(2) Alpha diversity analysis showed that the community richness, community uniformity, and community diversity under high in situ temperatures differed to those reported in the literature. T tests showed that, excluding 10 °C and 20 °C, significant differences exist in the number of community according to working conditions. Community diversity coefficients were also significantly different between 10 °C and 20 °C, 10 °C and 15 °C, and 20 °C and 25 °C. The community richness chao coefficient was significantly different between the three groups of operating conditions at 10 °C and 15 °C, 20 °C and 25 °C, and 15 °C and 25 °C. The Simpsoneven coefficient of community uniformity showed that at 10 °C, there were significant differences between the three groups of operating conditions at 20 °C, 10 °C and 20 °C, 20 °C and 25 °C. Significance analysis of the three reactors showed no significant differences in the community numbers in the different reactors.

(3) We assessed the community composition of the three reactors under different temperature conditions on Phylum, Class, Order, Family, Genus, and species level. The common dominant community on each level were analyzed and their response to temperature were assessed.

(4) Using the CCA chart to further verify that temperature is an important factor that influences the composition of the colony structure, and using the correlation heatmap to analyze the species that are significantly related to temperature, our analysis showed that the abundance of 13 species were related to temperature. In total, 7 species showed a significant correlation; TN significantly correlated were not observed; 4 species correlated with TP, 2 of which showed a high correlation; 1 species significantly correlated with NH_3-N; a single species significantly correlated with COD.

Based on these analyses, the A^2O species structure in high-in situ correlated with temperature in terms of species number, Alpha diversity, and dominant species composition. The dominant bacteria that were significantly related to temperature at the species level were Bacteroidetes_bacterium_OLB10. The dominant bacteria with an extremely significant correlation were unclassified_f__Burkholderiaceae, uncultured_bacterium_g__norank_f__Saprospiraceae, metagenome_g_Gordonia. The dominant bacteria with significant TP removal rates were Bacteroidetes_bacterium_OLB10. The dominant bacteria with extremely significant TP removal rates were unclassified_fae. bacteria. Follow-up work will continue to advance in the identification of bacterial functions, functional genes, metabolic pathways, and COG.

http://www.aloki.hu ● ISSN 1589 1623 (Print) ● ISSN 1785 0037 (Online)
DOI: http://dx.doi.org/10.15666/aeer/1902_14371455
© 2021, ALÖKI Kft., Budapest, Hungary

Acknowledgements. The study was supported by the National Natural Science Foundation of China (NO. 51868069, 51769034), Natural Science Foundation of Tibet (NO. XZ 2018 ZR G-20), the Program for Scientific Research Innovation Team in Colleges and Universities of Tibet Autonomous Region.

REFERENCES

[1] Beer, M., Stratton, H. M., Griffiths, P. C., Seviour, R. J. (2006): Which are the polyphosphate accumulating organisms in full-scale activated sludge enhanced biological phosphate removal systems in Australia? – Journal of Applied Microbiology 100(2): 233-243.

[2] Chen, H., Chang, S. (2017): Impact of temperatures on microbial community structures of sewage sludge biological hydrolysis. – Bioresource Technology 245: 502-510.

[3] Chen, Y., Lan. S., Wang, L., et al. (2017): A review: driving factors and regulation strategies of microbial community structure and dynamics in wastewater treatment systems. – Chemosphere 174.

[4] Chen, X., Hao, K., Su, D., Zong, Y. (2018a). Characteristic study on wastewater treatment in high altitude area by A2/O process. – China Technology of Water Treatment 44(2):93-96.

[5] Chen, C., Ouyang, W., Huang, S., Peng, X. (2018b): Microbial community composition in a simultaneous nitrification and denitrification bioreactor for domestic wastewater treatment. – IOP Conference Series: Earth and Environmental Science 112(1): 012007.

[6] Cydzik-Kwiatkowska, A., Zielińska, M. (2016): Bacterial communities in full-scale wastewater treatment systems. – World Journal of Microbiology and Biotechnology 32(4): 66.

[7] Fan, X. Y., Gao, J. F., Pan, K. L., Li, D. C., Dai, H. H., Li, X. (2018): Functional genera, potential pathogens and predicted antibiotic resistance genes in 16 full-scale wastewater treatment plants treating different types of wastewater. – Bioresource Technology 268: 97-106.

[8] Fang, Z., Sun, P., Zhong, X., Jiang, T. (2011): Effect of water temperature on the microbial community in an enhanced biological phosphorus removal system. – Acta Scientiae Circumstantiae 31(5): 941-947.

[9] Jin, X., Zhao, Z., Qin, Z., et al. (2017): Distribution and degradation of organic matter with different molecular weight in an A2O treatment system. – Applied Water Science 7(7): 3497-3502.

[10] Juretschko, S., Loy, A., Lehner, A., Wagner, M. (2002): The microbial community composition of a nitrifying-denitrifying activated sludge from an industrial sewage treatment plant analyzed by the full-cycle rRNA approach. – Systematic and Applied Microbiology 25(1): 84.

[11] Kang, A. J., Munz, G., Yuan, Q. (2019): Influence of pH control on material characteristics, bacterial community composition and BNR performance of mature aerobic granules. – Process Safety and Environmental Protection 124: 158-166.

[12] Kong, Y., Xia, Y., Nielsen, J. L., Nielsen, P. H. (2007): Structure and function of the microbial community in a full-scale enhanced biological phosphorus removal plant. – Microbiology 153(12): 4061-4073.

[13] Li, G., Song, J., Li, X., Zhang, S., Tao, L., Zhang, C. (2014): Metabolic characteristics and functional diversity of carbon source in microflora of ponds with recirculating aquaculture system. – Agricultural Science & Technology 15(2): 278-282: 299.

[14] Liao, K., Hu, H., Ma, S., Ren, H. (2019): Effect of microbial activity and microbial community structure on the formation of dissolved organic nitrogen (DON) and bioavailable DON driven by low temperatures. – Water Research 159.

http://www.aloki.hu ● ISSN 1589 1623 (Print) ● ISSN 1785 0037 (Online)
DOI: http://dx.doi.org/10.15666/aeer/1902_14371455
© 2021, ALÖKI Kft., Budapest, Hungary

[15] Ma, X., Zhao, B., Zhang, X., Xie, F., Cui, Y., Li, H., Yue, X. (2020): Effect of periodic temperature shock on nitrogen removal performance and microbial community structure in plug-flow microaerobic sludge blanket. – Chemosphere 241: 124934.
[16] Muszyński, A., Tabernacka, A., Miłobędzka, A. (2015): Long-term dynamics of the microbial community in a full-scale wastewater treatment plant. – International Biodeterioration & Biodegradation 100: 44-51.
[17] Nasha, D., Lin, W. (2016): Microbial community structure and the performance of biological aerated filter under different temperatures. – Chinese Journal of Environmental Engineering 10(6): 2800-2806.
[18] Nielsen, P. H., Saunders, A. M., Hansen, A. A., Larsen, P., Nielsen, J. L. (2012): Microbial communities involved in enhanced biological phosphorus removal from wastewater—a model system in environmental biotechnology. – Current Opinion in Biotechnology 23(3): 452-459.
[19] Paul, G., McAteer, A. Trego, C., Thorn, C., Mahony, T., Abram, F., O'Flaherty, V. (2020): Reactor configuration influences microbial community structure during high-rate, low-temperature anaerobic treatment of dairy wastewater. – Bioresource Technology 307.
[20] Schmid, M., Thill, A., Purkhold, U., Walcher, M., Bottero, J. Y., Ginestet, P., ... Wagner, M. (2003): Characterization of activated sludge flocs by confocal laser scanning microscopy and image analysis. – Water Research 37(9): 2043-2052.
[21] Simon, S. D., Lesage, J. P. (1989): Assessing the accuracy of ANOVA calculations in statistical software. – Computational Statistics Data Analysis 8(3): 325-332.
[22] Sun, F. L., Fan, L. L., Wang, Y. S., Huang, L. Y. (2019): Metagenomic analysis of the inhibitory effect of chromium on microbial communities and removal efficiency in A2O sludge. – Journal of Hazardous Materials 368: 523-529.
[23] Tian, M., Zhao, F., Shen, X., Chu, K., Wang, J., Chen, S. (2015): The first metagenome of activated sludge from full-scale anaerobic/anoxic/oxic (a2o) nitrogen and phosphorus removal reactor using illumina sequencing. – Journal of Environmental Sciences 35: 181-190.
[24] Wang, X., Gao, M., Wang, Y., Yang, Y., Gang, J., Fu, G., Wang, L. (2019): Effect of on-line Na Cl O backwashing on microbial communities in an inverted A2O-MBR system. – Chinese Journal of Environmental Science 40(7): 3208-3215.
[25] Wen, Y., Wang, X., Lin, C. (2015): Bacterial community dynamics in an activated sludge system based on Miseq sequencingMiseq. – Chinese Journal of Environmental Engineering 9(11): 5225-5230.
[26] Wong, M. T., Mino, T., Seviour, R. J., Onuki, M., Liu, W. T. (2005): In situ identification and characterization of the microbial community structure of full-scale enhanced biological phosphorous removal plants in Japan. – Water Research 39(13): 2901-2914.
[27] Yang, Q., Zhao, H., Du, B. (2017): Bacteria and bacteriophage communities in bulking and non-bulking activated sludge in full-scale municipal wastewater treatment systems. – Biochemical Engineering Journal 119: 101-111.
[28] Zhai, J., Chen, M., Xiao, H., Chen, Z. (2012): Solar preheating/biological contact oxidation/compound constructed wetland for treatment of sewage from Tibet Plateau area. – China Water & Wastewater 28(2): 42-45.
[29] Zhang, B., Xu, X., Zhu, L. (2018): Activated sludge bacterial communities of typical wastewater treatment plants: distinct genera identification and metabolic potential differential analysis. – AMB Express 8(1): 184.
[30] Zhang, X.-H., Jiang Bo, Zhang Wen-Wu, et al. (2019a): Microbial community diversity of activated sludge from municipal wastewater treatment plants in Beijing-Tianjin-Hebei region. – Microbiology China 46(8): 1896-1906.
[31] Zhang, L., Zhang, M., Guo, J., Zheng, J., Chen, Z., Zhang, H. (2019b): Effects of K+ salinity on the sludge activity and the microbial community structure of an A2O process. – Chemosphere 235: 805-813.

http://www.aloki.hu ● ISSN 1589 1623 (Print) ● ISSN 1785 0037 (Online)
DOI: http://dx.doi.org/10.15666/aeer/1902_14371455
© 2021, ALÖKI Kft., Budapest, Hungary

[32] Zong, Y. C., Hao, K. Y., Li, Y. W., Lu, G. H., Huang, D. C. (2019a). Nitrogen and phosphorous removal of pilot-scale anaerobic-anoxic-aerobic process under plateau environmental factors. – Applied Ecology and Environmental Research 17(5): 12213-12226.

[33] Zong, Y., Li, Y., Hao, K., Lu, G., Huang, D. (2019b). Influence of transient change of water temperature on pilot-scale anaerobic-anoxic-oxic process under plateau environmental factors. – Applied Ecology and Environmental Research 17(5) 12191-12202.

http://www.aloki.hu ● ISSN 1589 1623 (Print) ● ISSN 1785 0037 (Online)
DOI: http://dx.doi.org/10.15666/aeer/1902_14371455
© 2021, ALÖKI Kft., Budapest, Hungary

EVALUATION OF GROWING STOCK, BIOMASS AND SOIL CARBONS AND THEIR ASSOCIATION WITH A DIAMETER: A CASE STUDY FROM A PLANTED CHIR PINE (*PINUS ROXBURGHII*) FOREST

KHAN, I.[1#] – HAYAT, U.[2#*] – MUJAHID, A.[3] – MAJID, A.[1] – CHAUDHARY, A.[4] – BADSHAH, M. T.[3] – HUANG, J.[1]

[1]*School of Soil and Water Conservation, Beijing Forestry University, 100083 Beijing, China (e-mails: inamkhan.1325@gmail.com, abdulmajid3637@gmail.com, jiankunhuang@yahoo.com)*

[2]*Sino-France Joint Laboratory for Invasive Forest Pests in Eurasia, School of Forestry, Beijing Forestry University, 100083 Beijing, China*

[3]*Department of Forest Management, School of Forestry, Beijing Forestry University, 100083 Beijing, China (e-mails: forester37101@outlook.com, badshahgi90@gmail.com)*

[4]*Department of Forestry and Range Management, University of Agriculture, Faisalabad, Pakistan (e-mail: aroojch533@gmail.com)*

#These authors have contributed equally to this work

**Corresponding author*
e-mail: oomarcassi6116@gmail.com; phone: + 92-30-4429-1135, + 86-188-1139-2885

(Received 20th Nov 2020; accepted 27th Jan 2021)

Abstract. The statistical association between the capacity for carbon sequestration and planted *Pinus roxburghii* tree diameter classes are not recorded in Pakistan. Through the forest inventory approach, a comprehensive study was conducted in planted *P. roxburghii* forest in Pakistan's Swat Hindu Kush area to determine the carbon stock (CS) of a live tree, forest floor and soil (SOC) and their association with three diameter classes (6-22, 23-40, 41-60 cm). The results specified that stem density had a polynomial relation with the diameter (R2 = -0.54), while tree height had a linear relationship with the diameter (R2 = 0.73). Association of tree volume, stem biomass, total tree biomass with basal area against diameter classes were positively linear [(R2 = 0.86, 0.80, 0.80) for DBH (41-60 cm)]. As the diameter increases, grass CS reduced while litter and deadwood CS increased significantly. Association of diameter classes with (SOC) at various depths was negatively linearly correlated [R2 = -0.99; for DBH (41-60 cm)], while the topsoil layer (0-20 cm) SOC rose significantly with increase in diameter class. With the increase in tree diameter, the tree age increased definitively (R2 = 0.99). An increase in diameter class ultimately increased CS amount, and the trend was as follows: live tree > soil > forest floor. This study significantly demonstrated the diameter relationship with the tree, forest floor and soil CS of planted *P. roxburghii* forest.

Keywords: *Pinus roxburghii, afforestation, inventory, biomass carbon, carbon stock (CS), soil bulk density (SBD), SOC, Swat, Pakistan*

Introduction

Global climate change is a burning issue within the scientific community because of accelerating carbon dioxide concentration in the atmosphere due to various human activities. The rapid social activities and industrialization increase the carbon contents

http://www.aloki.hu ● ISSN 1589 1623 (Print) ● ISSN 1785 0037 (Online)
DOI: http://dx.doi.org/10.15666/aeer/1902_14571472
© 2021, ALÖKI Kft., Budapest, Hungary

in the atmosphere, causing global warming and climate change (Sharma et al., 2011). According to the Intergovernmental Panel on Climate Change report 2018, the Earth's average temperature by 1.5 °C until now is considered to accelerate probably to 3 °C increase of the end of this century (Delmotte et al., 2018).

According to the Kyoto Protocol, the UNFCC acknowledges the forest, a potential tool to palliate and stabilize the carbon concentration (Ahmad et al., 2014b). Forest restoration is an essential tool that significantly countervails atmospheric carbon emanations (Laurance, 2007). Unfortunately, due to the forest restoration scheme's vague apprehension, the real latent of forest biomass has been halted (Holl and Zahawi, 2014). Planted forests are essential mitigation tools for the climate. Many studies have revealed that thick plantations have higher carbon stocks (Bonner et al., 2013), while some reported that the carbon stocks ratio is higher for naturally regenerated secondary forests (Chrsquo et al., 2011). However, forest carbon accumulation capacity is higher for thick planted forests than regenerated forests stand, which also rendered the application of prudish silvicultural management (Baishya et al., 2009). Forest soil can also be used as a significant sink for storing an immense volume of carbon in the form of soil organic materials that can help mitigate global climate change (Ullah et al., 2019).

As a core proposition, afforestation enhances the earth's organic carbon stock by growing plant litter in the soil. Soil carbon sequestration is a long-term, cost-effective and efficient approach for enhancing soil characteristics and quality (Li et al., 2013). Tree plantations had an ambivalent role in ecosystem services in the past. Their production function has functioned the growing demands for wood products efficiently (Bauhus et al., 2010). Many ecological resources improved where plantations were developed on the deteriorated or former property (Cossalter and Pye-Smith, 2003).

The capacity of forest plantations to store carbon throughout the Globe is about 3.8% (FAO, 2006), but overall, this small percentage of storage capacity plays a vital role in mitigating and fight against climate change (Canadell et al., 2007). Generally, natural forests have more potential for storing biomass than forest plantations per hectare (Pan et al., 2004). However, natural forests have decreased from 46% to 28% of the Earth's terrestrial ecosystems (Winjum and Schroeder, 1997). The measurement of biomass and carbon stock is essential to calculate the forest carbon potential in the region. The evaluation of biomass and carbon stock needs forest inventory data in sampled plots of different pools, i.e., aboveground biomass, belowground biomass, soil organic carbon, deadwood carbon and forest floor (litter/twigs) (Nizami et al., 2009; Sullivan et al., 2017).

Previously, different types of study have been conducted for the estimation of carbon stock in different forest types of Pakistan (Nizami, 2012; Ahmad and Nizami, 2015; Ahmad et al., 2014a; Amir et al., 2019); most of the study in Pakistan have been conducted in the natural forests of Pakistan. Some of the reviews regarding forest carbon in planted Bela forests and irrigated plantation in Punjab province, Pakistan is available (Saeed et al., 2016; Arif et al., 2017). There is a lack of information to estimate annual carbon sequestration potential in planted Chir pine forests in Pakistan.

For the first time in Pakistan, this study outlines the carbon stock in respective carbon pools in the planted Chir pine forests. We hypothesized that the young planted conifer forest and its soil are essential sources to sink and store the atmosphere's carbon, just like the natural forest. The main aims of the present study were to determine the tree biomass and carbon stock and their association with three different

http://www.aloki.hu ● ISSN 1589 1623 (Print) ● ISSN 1785 0037 (Online)
DOI: http://dx.doi.org/10.15666/aeer/1902_14571472
© 2021, ALÖKI Kft., Budapest, Hungary

diameter classes (6-22, 23-40, 41-60 cm) of planted *P. roxburghii* forest; to determine the forest cover (grasses, litter and deadwood) carbon stock and their association with three different diameter classes, to determine the soil carbon stock (SOC) and their association with three different diameter classes at various depths (0-20, 21-40, 41-60, 61-80 cm); and to find out the association of tree diameter with tree age.

Materials and methods

Study zone

The current study was carried out in Dureshkhela village of district swat (Latitude and Longitude 34.7933°N and 72.2889°E, respectively) KPK, Pakistan (*Fig. 1; Table A1*), from April 2017 to May 2017. The elevation ranges from 914.4 to 1118.6 m. The area receives 1000-1200 mm annual average precipitation, as recorded by Saidu Sharif metrological station. The minimum and maximum average temperatures vary from 5 to 38 °C, as evident from the data recorded in December and June by the meteorological station of Saidu Sharif; mainly area occupied by the mountain ranges and weather is just like the closest area "Kumrat valley, Hindu Kush Region, Pakistan" (Ahmad and Nizami, 2015).

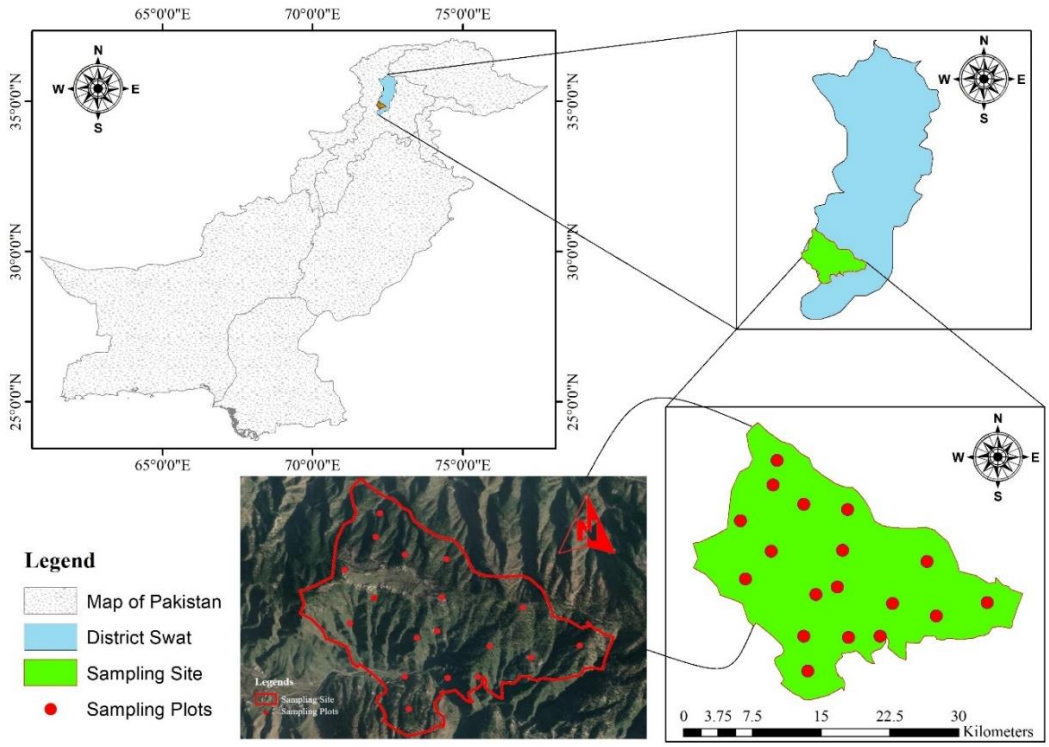


Figure 1. *Location of study area of Swat in Northwest Pakistan*

Research design and data source

The data was collected through forest inventory (*Fig. 2*). 18 square-shaped sampling plots (0.1 ha each) were randomly selected to cover the total area of 262 ha. The data collected from those sampling plots were tree height (m) using 'Spiegel relay scope,' DBH (cm) using 'Vernier caliper,' latitude and longitude of each plot using 'GPS device.'

http://www.aloki.hu ● ISSN 1589 1623 (Print) ● ISSN 1785 0037 (Online)
DOI: http://dx.doi.org/10.15666/aeer/1902_14571472
© 2021, ALÖKI Kft., Budapest, Hungary

For investigating soil organic carbon, by following the IPCC guideline, soil samples from the four different layers of soil (0-20 cm, 21-40 cm, 41-60 cm and 61-80 cm) with a thickness level of 20 cm each were collected using soil auger. For soil samples analysis for finding the soil organic carbons, the core method was adopted (Gross and Harrison, 2018), and analysis was carried out in the "Soil Testing and Conservation Lab, Rawalpindi, Pakistan."

For investigating shrub, herb, grasses, deadwood, and litter layer biomass, the subplot or quadrates of 1 m × 1 m were selected, and the data was recorded. Samples for each layer were selected and weighed fresh in the field with weighing balance and then placed in plastic bags and later dried in the oven at 72 °C for 48 h.

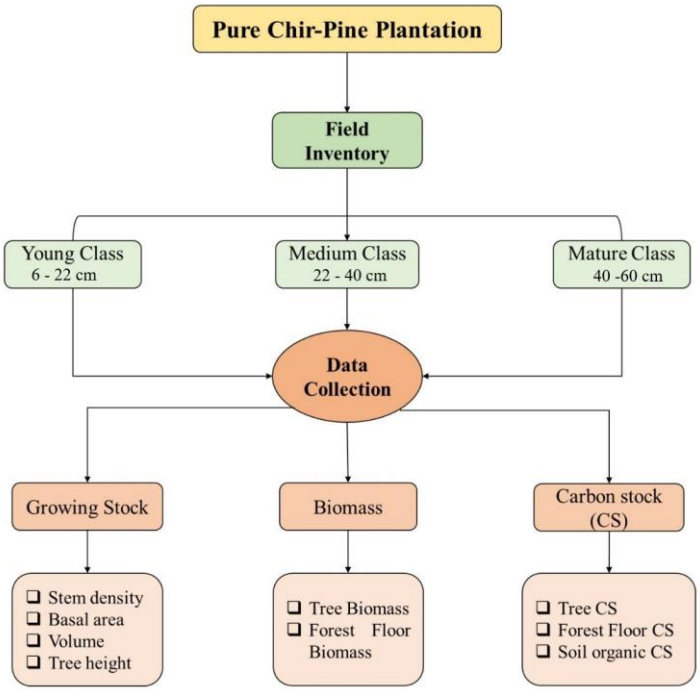


Figure 2. *The layout of the research design*

Growing stock and biomass calculation

The tree volume (m^3) was determined by using the following formula (Philips, 1994):

$$Tree\ volume(m^3) = \left[\left(\frac{\pi}{4}\right) \times d^2 \times h \times f\right] \quad \text{(Eq.1)}$$

The stem biomass of identified tree species in the area was calculated from the following formula:

$$Stem\ biomass = Volume(m^3) \times Basic\ wood\ density(kgm^{-3}) \quad \text{(Eq.2)}$$

Overall, tree biomass was determined using the following formulas:

$$AGB\ (t\ ha^{-1}) = Stem\ biomass(t\ ha^{-1}) \times BEF \quad \text{(Eq.3)}$$

http://www.aloki.hu ● ISSN 1589 1623 (Print) ● ISSN 1785 0037 (Online)
DOI: http://dx.doi.org/10.15666/aeer/1902_14571472
© 2021, ALÖKI Kft., Budapest, Hungary

$$BGB\ (t\ ha^{-1}) = AGB(t\ ha^{-1}) \times R \quad \text{(Eq.4)}$$

$$Total\ tree\ biomass(t\ ha^{-1}) = AGB + BGB \quad \text{(Eq.5)}$$

where: AGB = above ground biomass; BGB = below ground biomass; BEF = biomass expansion factor; R = root to shoot ratio.

The leaves, branches, twig role in overall above-ground biomass was assessed by biomass expansion factor (BEF) of the corresponding tree species. According to the literature, the BEF value for *P. roxburghii* used recently was 1.51 (Amir et al., 2019).

Carbon stocks calculation

The carbon stock conversion factor (0.5) (Amir et al., 2018) was used to convert total biomass to total carbon stock. This adaptation aspect has been used extensively around the Globe.

The total carbon stock was determined by using the following formula (Nizami, 2012; Ahmad et al., 2014a):

$$Total\ carbon\ stock(t\ C\ ha^{-1}) = Total\ Tree\ Biomass\ (t\ ha^{-1}) \times 0.5 \quad \text{(Eq.4)}$$

Quantities of understory vegetation biomass: The understory vegetation such as shrubs, herbs, and grasses were collected from each sample plot. Then the fresh weight of all samples (kg) was documented, and the average weight was taken and extrapolated to calculate the current weight of the whole plot. The collected samples were dried at 72 °C for 48 h (Roy et al., 2001).

Calculation of soil bulk density (SBD)

Soil bulk density in each age group was determined from the soil sample's weight and known soil core volume according to the given Equation.

$$Soil\ Bulk\ Density(g\ cm^{-3}) = \frac{weight\ of\ soil\ sample\ (g)}{volume\ soil\ core\ (cm^3)} \quad \text{(Eq.5)}$$

Calculation of soil carbon (t C/ha)

The bulk density (g cm-3) of soil samples was measured individually. The oxidizable organic carbon method (Walkley and Black, 1934) was used to find out soil carbon using the following formula (Pearson et al., 2007):

$$Soil\ carbon\ (t\ C\ ha^{-1}) = SBD(g\ cm^{-3}) \times SOC(\%) \times SHT(m) \times 100 \quad \text{(Eq.6)}$$

where: SBD = Soil Bulk Density (g/cm^3), STH = Soil horizon thickness (m).

For statistical analysis, we used Statistics (8.1 version), Origin (9.0 version), Excel pro professional (2016 version) software; for graphs and figures, Excel pro professional (2016 version) was used. Analysis of variance (ANOVA) was used to calculate the significant level at ($P < 0.05$, $P < 0.01$, $P < 0.001$) respectively, Tukey HSD post-hock test was used to indicate the significane for mean biomass and carbon stock values. A regression model (Linear, Polynomial) was used to illustrate the relationship between different factors for tree biomass and carbon stock.

http://www.aloki.hu ● ISSN 1589 1623 (Print) ● ISSN 1785 0037 (Online)
DOI: http://dx.doi.org/10.15666/aeer/1902_14571472
© 2021, ALÖKI Kft., Budapest, Hungary

Results

Growing stock characteristics

Stand density ranges from 20 to 260 (trees ha^{-1}) in three different diameter classes with the maximum mean value 166.11 ± 21.63 (t ha^{-1}) for diameter class (23-40 cm) and minimum value 33.89 ± 5.89 (tree ha^{-1}) for diameter class (41-60 cm) (*Table 1*). There was polynomial linear relationship between DBH (cm) and stand density (tree ha^{-1}) ($y = -0.2097x^2 + 13.002x - 69.713$; $R^2 = 0.54$) was observed (*Fig. 3*). With the increase in diameter (cm) the tree height (m ha^{-1}) increase positively ($y = 0.3763 + 1.9855$; $R^2 = 0.73$) and the maximum mean height was 33.89 ± 5.89 (m ha^{-1}) for DBH (41-60 cm). While mean basal area, stand volume and total tree biomass was also recorded maximum (14.19 ± 3.67 m^2 ha^{-1}, 16.69 ± 4.64 m^3 ha^{-1} and 16.71 ± 4.51 t ha^{-1}) for DBH (41-60 cm) (*Table 1*).

Table 1. *Distribution of stem density, volume, basal area, and mean height in different diameter classes*

DBH (cm)	Mean density (trees/ha)	Mean height (m/ha)	Mean basal area (m^2/ha)	Mean stand volume (m^3/ha)	Mean total tree biomass (t/ha)
6-22	38.89 ± 7.87	5.54 ± 1.04	1.49 ± 0.32	0.79 ± 0.18	0.83 ± 0.20
23-40	166.11 ± 21.63	13.49 ± 0.93	7.66 ± 1.59	6.70 ± 1.28	7.78 ± 0.64
41-60	33.89 ± 5.89	16.65 ± 1.56	14.19 ± 3.67	16.69 ± 4.64	12.76 ± 1.43

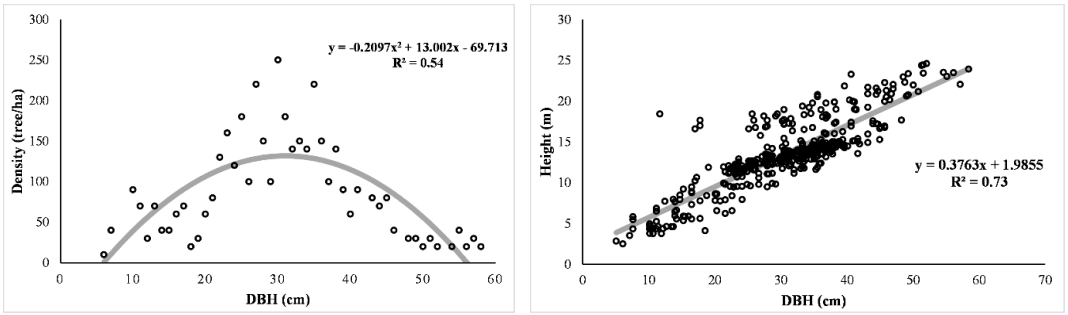


Figure 3. *The relation of diameter (cm) with wood density (trees ha^{-1}) and height (m)*

Relationship of different tree growth factors with basal area (m^2/ha)

The relation between stem volume, stem biomass, tree carbon stock with the basal area is illustrated in (*Fig. 4*) for three different diameter classes (6-22 cm, 23-40 cm, 41-60 cm).

The association of stem volume (m^3 ha^{-1}), stem biomass (t ha^{-1}) and total stem biomass (t ha^{-1}) with stem basal area (m^2 ha^{-1}) were significantly positive for all three diameter classes (6-22 cm, 23-40 cm, 41-60 cm). As the basal area (m^2 ha^{-1}) increases the stem volume (m^3 ha^{-1}), biomass (t ha^{-1}) and total stem biomass (t ha^{-1}) values also increase positively. The best result of linear regression for stem volume (m^3 ha^{-1}) against basal area (m^2 ha^{-1}) was obtained ($y = 1.8541x - 10.682$; $R^2 = 0.86$; $P = 0.04$) for DBH (41-60 cm), while the highest significant value was observed [$F(1, 26) = 8.22$, $P = 0.008$ ($P < 0.01$)] for DBH (6-22 cm). For stem biomass (t ha^{-1}) the maximum linear regression value against basal area (m^2 ha^{-1}) was ($y = 1.2404x - 7.8463$ $R^2 = 0.80$; $P = 0.0008$) and the highly significant value [$F(1,30) = 13.90$, $P = 0.0008$ ($P < 0.001$)]

http://www.aloki.hu ● ISSN 1589 1623 (Print) ● ISSN 1785 0037 (Online)
DOI: http://dx.doi.org/10.15666/aeer/1902_14571472
© 2021, ALÖKI Kft., Budapest, Hungary

were observed for DBH (41-60cm). In case of total tree biomass (t ha^{-1}) the best figures of linear regression against basal area (m^2 ha^{-1}) was (y = 1.4885x - 9.4155; R^2 = 0.80) for DBH (41-60 cm) respectively.

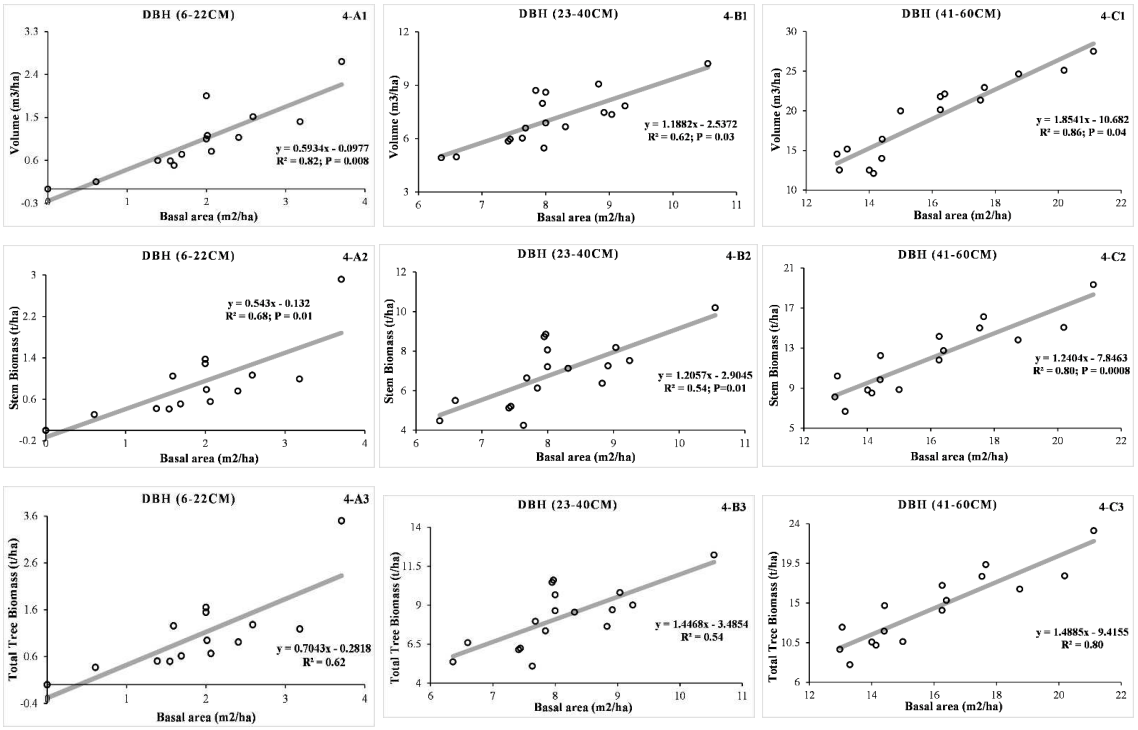


Figure 4. *Relationship between the factors, Volume (m^3/ha), Stem Biomass (t/ha), Total Tree Biomass (t/ha) with the Basal area (m^2/ha) for three different diameter classes (6-22 cm, 23-40 cm, 41-60 cm) at a significant level (P ≤ 0.05, ≤ 0.01, ≤ 0.001)*

Assessment of forest floor and soil carbon stock

One of this study's main objectives was to evaluate the forest floor carbon stock and soil carbon stock for three different dia classes.

We observed that stand of small-diameter trees (6-22 cm) has significantly more grasses cover, which ultimately results in sequestering more carbon (0.1 ± 0.04 t C ha^{-1}) compared to the other two diameter classes (*Table 2*). In the case of litter and dead-wood deposits, the quantity of both dead forest floor components was significantly increased with the increase in diameter; therefore, the significantly highest values of litter and dead-wood carbon stock [0.19 ± 0.06 t C ha^{-1} and 0.1 ± 0.03 t C ha^{-1}) were observed for diameter class (41-60 cm). So the three different diameter classes had significant effect on the amount of grasses carbon stock [F(1,4) = 13.67, P = 0.02 (P < 0.05)], litter carbon stock [F(1,4) = 13.62, P = 0.02 (P < 0.05)] and dead-wood carbon stock [F(1,4) = 13.68, P = 0.02 (p < 0.05)] respectively.

Association of soil bulk density (SBD) and soil organic carbon (SOC) with a diameter

Overall Soil Bulk density (SBD) in four different soil depths (0-20 cm, 21-40 cm, 41-60 cm, 61-80 cm) ranges (0.99 – 1.16 g/cm^3) for all three diameter classes (6-22 cm, 23-40 cm, 41-60 cm). There was significant difference observed [F = 53.47, df = 11,

http://www.aloki.hu ● ISSN 1589 1623 (Print) ● ISSN 1785 0037 (Online)
DOI: http://dx.doi.org/10.15666/aeer/1902_14571472
© 2021, ALÖKI Kft., Budapest, Hungary

P = 0.0001 (P < 0.001)] for SBD values at four different soil depths with regards to three different diameter classes (*Fig. 5*). The SBD in relation with four different soil depths for three diameter classes represented positive linear relationship ($y = 0.0011x + 1.0554$; $R^2 = 0.84$; $P = 0.0003$) with the highest value (1.16 ± 0.02 g/cm^3) [$F(1,6) = 14.33$, $P = 0.009$ ($P < 0.01$)] at soil depth (60-80 cm) for diameter class (41-60 cm). As the soil depth increases the SBD value also increased.

Table 2. *Carbon stock of forest floor (grasses, litter and dead wood) and soil (t ha^{-1}) in planted P. roxburghii forest at the level of significance (P < 0.05)*

DBH (cm)	MGCS (t C ha^{-1})	MLCS (t C ha^{-1})	MDwCS (t C ha^{-1})	SOC (t C ha^{-1})			
				Soil depth (cm)			
				0 - 20	21 - 40	41 - 60	61 - 80
6 - 22	0.1 ± 0.04**	0.14 ± 0.04**	0.04 ± 0.01**	2.30 ± 0.25**	2.10 ± 0.21**	1.93 ± 0.198**	1.14 ± 0.19**
23 - 40	0.09 ± 0.03**	0.16 ± 0.05**	0.07 ± 0.02**	2.81 ± 0.28**	2.53 ± 0.26**	2.12 ± 0.24**	1.53 ± 0.25**
41 - 60	0.06 ± 0.01**	0.19 ± 0.06**	0.1 ± 0.03**	3.33 ± 0.36**	2.78 ± 0.35**	2.28 ± 0.33**	1.65 ± 0.32**
Sum	0.25 ± 0.05	0.49 ± 0.06	0.21 ± 0.03	8.44 ± 0.41	7.41 ± 0.39	6.33 ± 0.37	4.32 ± 0.28

MGCS = Mean grasses carbon stock, MLCS = Mean litter carbon stock, MDwCS = Mean deadwood carbon stock, SOC = Soil organic carbon stock. ** indicates that according to Tukey (HSD) variables are significant different for different diameter classes

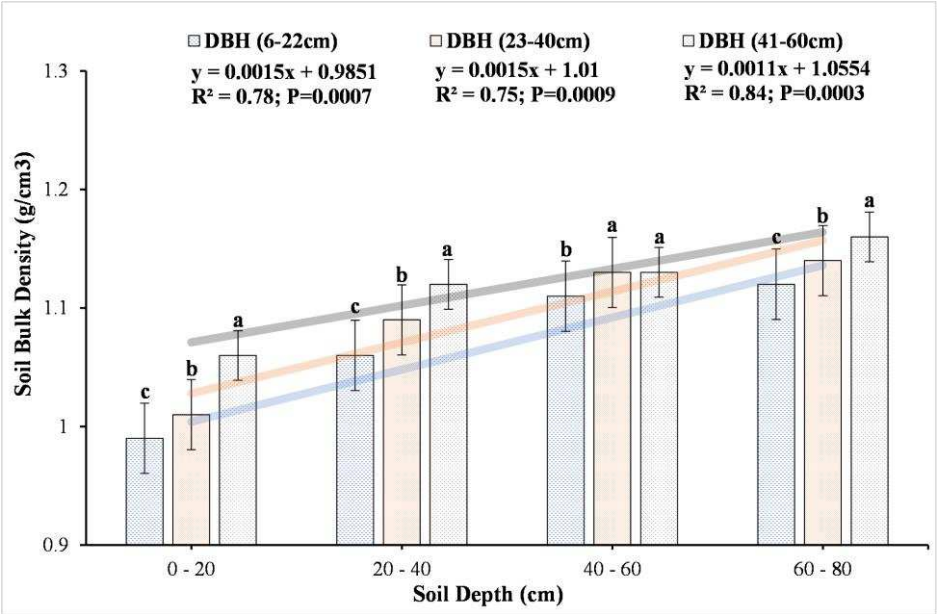


Figure 5. *Soil Bulk density in three different diameter classes (6-22, 23-40, 41-60 cm) of planted Pinus roxburghii stand at various depths. The relationship between soil bulk density and soil depth for different diameter classes are illustrated using linear regression. The different letters (a, b, c) on the bar show significant differences while the same letters on the bar show the non-significant difference between different diameter classes*

Soil organic carbon (SOC) in four different soil depths (0-20 cm, 21-40 cm, 41-60 cm, 61-80 cm) ranges (1.14 – 3.33 t C ha^{-1}) for all three diameter classes (6-22 cm, 23-40 cm, 41-60 cm). There was significant difference observed [$F = 45.37$, $df = 11$,

http://www.aloki.hu ● ISSN 1589 1623 (Print) ● ISSN 1785 0037 (Online)
DOI: http://dx.doi.org/10.15666/aeer/1902_14571472
© 2021, ALÖKI Kft., Budapest, Hungary

P = 0.0001 (P < 0.001)] for SOC values at four different soil depths with regards to three different diameter classes (*Table 2*; *Fig. 6*). The SOC in relation with four different soil depths for three diameter classes represented negative linear relationship [(y = -0.0277x + 3.8936, R^2 = 0.99; P = 0.01 (P < 0.05)] with the highest value (3.33 ± 0.36 t C ha^{-1}) [F(1,6) = 13.52, P = 0.01 (P < 0.05)] at soil depth (0-20 cm) for diameter class (41-60 cm). We observed that diameter class has significant association with soil carbon stock at various depth, as the soil depth increases the SOC value decreases.

Soil organic carbon analysis showed that the young diameter class (6-22 cm) stand holds minimum soil carbon, but as the diameter increase (41-60) with age, soil carbon holding capacity also increased. The results showed an increasing trend from young diameter class (6-22 cm) to older diameter class (41-60 cm) in soil carbon.

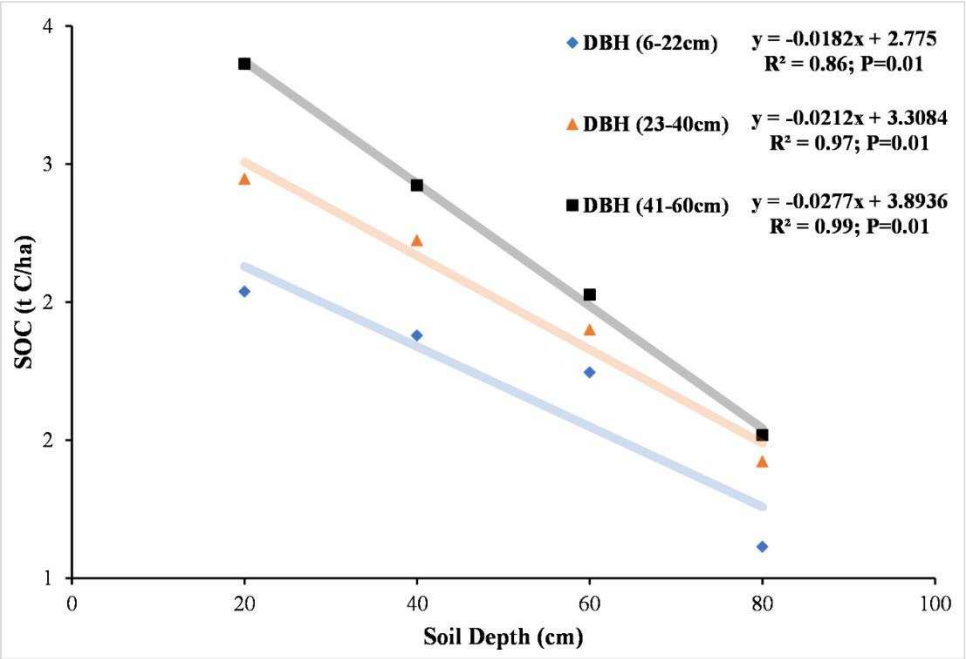


Figure 6. *Relationship of soil organic carbon (SOC) with a soil depth of three different diameter classes (6-22 cm, 23-40 cm, 41-60 cm) of planted Pinus roxburghii stand at a significant level (P = 0.01)*

The research data found that there was a clear association between the diameter and the age of the tree, with the diameter being directly proportional to the age of the stand. The lower diameter (8.47 ± 2.21 cm) has age (6.83 ± 1.79 years) and height (3.82 ± 0.97 m), while the high diameter (51.56 ± 2.21 cm) has age (41.62 ± 1.79 years) and height (22.35 ± 0.97 m) in the study area. The relationship between diameter and age was (y = 0.8071x + 3E-14; R^2 = 0.99) and between diameter and height was (y = 0.4165x + 0.4743; R^2 = 0.88) respectively (*Fig. 7*).

The total standing carbon stock of planted *P. roxburghii* forest was (59.86 ± 8.62 t C ha^{-1}) with the highest value for the diameter (41-60 cm) (*Fig. 8*). As the diameter class interval shifted from lower to the higher class, all carbon stock forms, including live tree, forest floor and soil, increased significantly with the highest total carbon stock value (29.89 ± 4.63 t C ha^{-1}) for diameter class (41-60 cm).

http://www.aloki.hu ● ISSN 1589 1623 (Print) ● ISSN 1785 0037 (Online)
DOI: http://dx.doi.org/10.15666/aeer/1902_14571472
© 2021, ALÖKI Kft., Budapest, Hungary

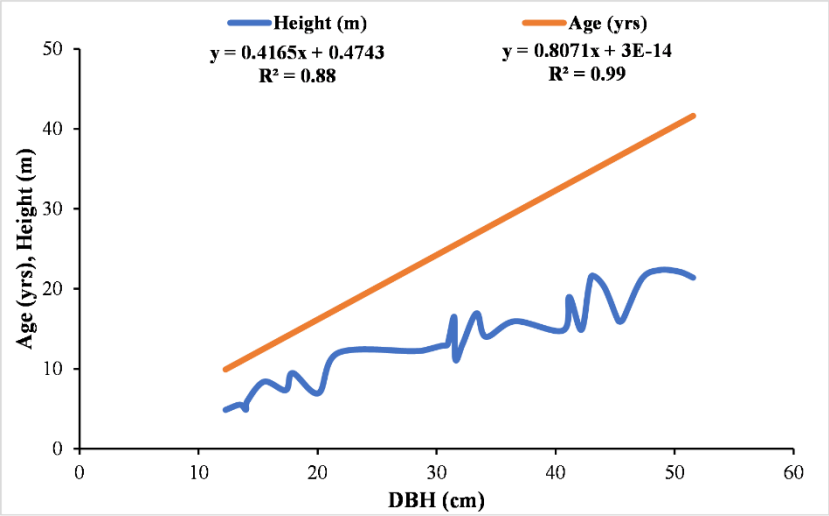


Figure 7. *The relation between diameter classes versus age (yrs) and height (m)*

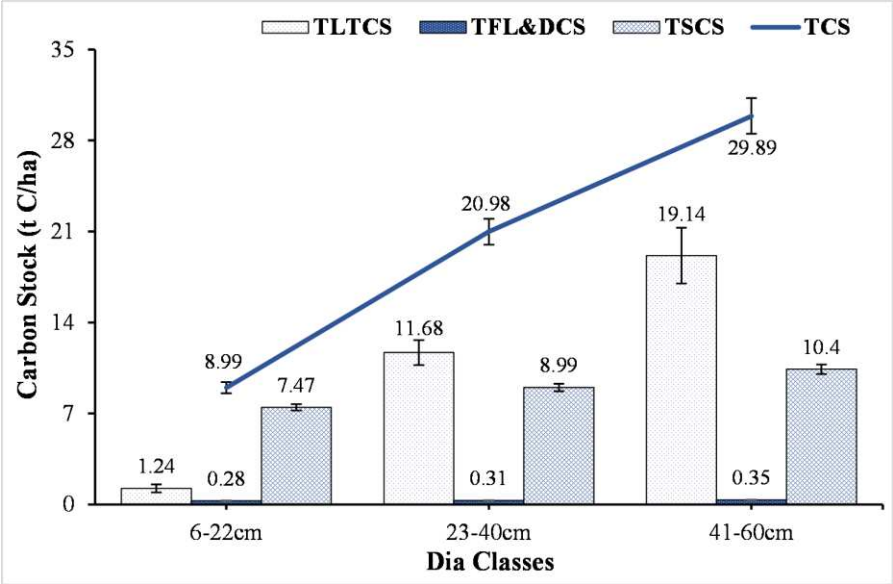


Figure 8. *Carbon stock distribution pattern for three diameter classes of planted P. roxburghii forest. TLTCS = total live tree carbon stock, TFL&DCS = total floor live and dead carbon stock, TSCS = total soil carbon stock, TCS = total carbon stock*

Discussion

In the present study, through investigating young planted *P. roxburghii* forest find out that stem density was maximum (166.11 ± 21.63 trees ha^{-1}) for the diameter class (23-40 cm) and was minimum (33.89 ± 5.89 trees ha^{-1}) for diameter class (41-60 cm) as the diameter increases the stem density per hectare decreases significantly (R2 = 0.54); which means that increased tree diameter results in the decrease of stem density (Nizami, 2012). The young planted stand volume has a positive association with the diameter with the highest volume (16.69 ± 4.64 m^3 ha^{-1}) for the diameter class (41-60 cm); as the diameter increase, the stand volume increased significantly (Amir et al., 2018).

http://www.aloki.hu ● ISSN 1589 1623 (Print) ● ISSN 1785 0037 (Online)
DOI: http://dx.doi.org/10.15666/aeer/1902_14571472
© 2021, ALÖKI Kft., Budapest, Hungary

Association between tree age and diameter was observed positive linear ($R^2 = 0.99$); our findings are in contrast with Siddiqui et al. (2013) that for conifer species age and diameter have significant association, and relationship between diameter and height was also observed positive linear ($R^2 = 0.88$) (*Fig. 7*), this finding is in line with the findings of Khan et al. (2016).

The current research found significant variation in the living tree biomass for three diameter classes of planted *P. roxburghii* forest. As the diameter increases with age, live tree biomass carbon of planted *P. roxburghii* also increases gradually. These findings are steady with Cao et al. (2012) and Li et al. (2013) that stand age/diameter effect the tree biomass carbon significantly.

With the increase in diameter, the overall tree growth variables effects significantly, i.e., in current studies, we found that out of three diameter classes, the highest diameter class (41-60 cm) has the highest values for basal area (14.19 ± 3.67 m^2 ha^{-1}), volume (16.69 ± 4.64 m^3 ha^{-1}), total tree biomass (12.76 ± 1.43 t ha^{-1}) and total live tree carbon stock (19.14 ± 2.15 t C ha^{-1}). Recent studies are also in contrast with our findings increasing carbon stock throughout the different growth periods of trees (Peichl and Arain, 2006; En et al., 2012).

Trees can impact the heterogeneity and distribution of understory vegetation (Svenning and Skov, 2002). Due to its impacts on micro-environment, humus layer decomposition, soil moisture and forest management practices, forest stand configuration such as tree age and tree density has a high impact on understory vegetation. In every forest biome, the carbon content varies with different variables, such as decomposition rate, maintenance practices, tree types, and litter fertility (Kang et al., 2006).

In the below-ground biomass, we found out that grasses cover decreases with the increase in diameter class/age while litter and dead wood deposits accumulation increased significantly with the increase of diameter class/age. It could be because an increase in diameter, causing the increase in tree height and canopy, ultimately enhances natural pruning and shredding of leaves, due to this forest floor covered with dead leaves and wood, stopping the growth of grasses. This finding is inconsistent with the finding of Ming et al. (2014) that an increase in diameter ultimately increasing litter productivity.

The observed carbon stocking pattern for three different diameter classes was as follows: live tree > Soil > forest cover (*Fig. 8*). Our result is in association with (Amir et al., 2018) that living trees absorb and distill more carbon than some other foliage forms.

Comparing SOC with forest biomass is very difficult (Laganiere et al., 2010) since SOC can be influenced by different variables, such as standing age, tree types, the form of forest, environment, and chemical and physical properties of the soil (Mora et al., 2014; Wang et al., 2014).

As compared to deeper soil, the soil carbon was recorded higher in the topsoil of each diameter class stand. It may be attributed to SOC's development by decomposing the root system and litter that first reached the topsoil near the ground, as other studies have shown (Zhang et al., 2012). There was a negative correlation of soil carbon with different diameter classes at various depths, as soil carbon values tend to decline in depth. Furthermore, with the increase in diameter, the soil carbon value significantly increased; our results are in line with the findings of (Amir et al., 2019) that with the relevant stand diameter and soil depth, the mean soil carbon showed a decrease.

http://www.aloki.hu ● ISSN 1589 1623 (Print) ● ISSN 1785 0037 (Online)
DOI: http://dx.doi.org/10.15666/aeer/1902_14571472
© 2021, ALÖKI Kft., Budapest, Hungary

Our study showed an increasing trend of soil carbon for different diameter classes as the highest value of SOC was obtained for the highest diameter class (41-60 cm). Besides this, litter and dead wood deposits were also recorded significantly high for the highest diameter class; Due to the deposition of organic matter in higher diameter stand, soil organic carbon typically increased with the stand age in conifer forest (Li et al., 2013). According to facts and figures, our hypothesis sustained that young afforested plantations are also vital sources to sequester the carbon.

Global warming is one of the main issues for the current century, mainly caused due to greenhouse gases; for the reduction of greenhouse gases, there is a need to increase and enhance the sinks in biomass (Zhao et al., 2014). Moreover, the simplest and the best way is to plant trees; so, the afforestation could be the critical step to control global warming (Sharma et al., 2011; Misir et al., 2013). To minimize atmospheric CO2 emissions by sequestering carbon in soils, afforestation, and reforestation have been seen as necessary (Smal and Olszewska, 2008). While on the other side, afforestation can also play a pivotal role in increasing the forest area and ultimately result in mitigating the global warming issue by sequestrating more carbon contents in the form of the living tree, forest floor cover and soil; this idea is agreed with the proposed suggestions of the (Watson, 2000). So, planting trees is much better than planting nothing; increasing forest area is an effective way to reduce elevated atmospheric carbon (Taylor et al., 2007); as the tree increases its diameter, absorption capacity increases (Huy and Tuan, 2008). The mountain ranges of the Karakorum-Hindukush region in northwest Pakistan has great potential to sequester and sink atmospheric carbon dioxide.

Limitations and uncertainties

This research was performed using a field inventory approach to investigate biomass and carbon distribution trends through the planted *P. roxburghii* forest in Pakistan. For the whole stem (above ground) biomass calculation, we used fixed BEF value 1.51 following (IPCC, 2006). We used a root to shoot ratio (*R*) of 0.19 (Amir et al., 2018). These values may vary with stand diameter/age; the present estimates of carbon allocation along the planted *P. roxburghii* may hold some qualms, which might tempt errors in carbon stock assessment along the diameter.

Conclusion

The present study showed a correlation between diameter and different tree growth factors and soil; as the diameter increases, all the mentioned factors increased significantly in a positive linear manner. There is a slight association of forest cover (grasses, litter and deadwood) with the diameter with the increase in diameter litter and deadwood accumulation increases while grasses cover decreases. Overall, the average carbon stocking values demonstrated the significant capacity for biomass and carbon sequestration during stand growth in the planted *P. roxburghii*. We further concluded that the proper management, increasing afforestation of bare land, and increasing vegetation cover in the region could increase carbon sequestration potential in the future. The conducted study may provide guidelines for managing pure planted *P. roxburghii* forest to enhance annual carbon potential based on growing and structure unique relationships. Current research has revealed that afforestation practice played an

http://www.aloki.hu ● ISSN 1589 1623 (Print) ● ISSN 1785 0037 (Online)
DOI: http://dx.doi.org/10.15666/aeer/1902_14571472
© 2021, ALÖKI Kft., Budapest, Hungary

essential role in carbon sequestration, the amount of sequestration could be increased furthermore by adopting mixed forest stand, and for this purpose, *Quercus* spp could be used. Therefore, we strongly recommended that forests consider rehabilitation and sustainable management for forest restoration and conservation.

Acknowledgements. We would like to thanks the forest department of district Swat for assistance, thanks to Soil testing and Conservation Lab, Rawalpindi, Pakistan, for soil samples analysis. It was a self-supported study.

REFERENCES

[1] Ahmad, A., Nizami, S. M. (2015): Carbon stocks of different land uses in the Kumrat valley, Hindu Kush Region of Pakistan. – Journal of Forestry Research 26(1): 57-64. https://doi.org/10.1007/s11676-014-0008-6.

[2] Ahmad, A., Mirza, N., Nizami, S. M. (2014a): Assessment of biomass and carbon stocks in coniferous forest of Dir Kohistan, KPK. – Pakistan Journal of Agricultural Sciences 51(2): 335-340. http://www.pakjas.com.pk/papers/2282.pdf.

[3] Ahmad, S., Ahmad, A., Moazzam, N. S. (2014b): Assessment of biomass expansion factor of Picea smithiana (Wall) Boiss. – Int. J. Sci. Eng. Res. 5(11): 1232–1239.

[4] Amir, M., Liu, X., Ahmad, A., Saeed, S., Mannan, A., Muneer, M. A. (2018): Patterns of biomass and carbon allocation across chronosequence of Chir pine (Pinus roxburghii) forest in Pakistan: inventory-based estimate. – Advances in Meteorology 8. https://doi.org/10.1155/2018/3095891.

[5] Amir, M., Saeed, S., Liu, X. D., Mannan, A., Khan, A., Li, Z. Z., Muneer, M. A. (2019): Soil organic content of stands of different ages in a subtropical chir pine (Pinus roxburghii) forest of Pakistan. – Applied Ecology and Environmental Research 17(5): 11475-11487. http://dx.doi.org/10.15666/aeer/1705_114751487.

[6] Arif, M., Shahzad, M. K., Elzaki, E. E. A., Hussain, A., Zhang, B., Yukun, C. (2017): Biomass and carbon stocks estimation in Chichawatni irrigated plantation in Pakistan. – Int J Agric Biol 19: 1339-1349. http://www.fspublishers.org/published_papers/12397_.pdf.

[7] Baishya, R., Barik, S. K., Upadhaya, K. (2009): Distribution pattern of aboveground biomass in natural and plantation forests of humid tropics in northeast India. – Tropical ecology 50(2): 295. http://tropecol.com/pdf/open/PDF_50_2/J-10.pdf.

[8] Bauhus, J., Pokorny, B., van der Meer, P. J., Kanowski, P. J., Kanninen, M. (2010): Ecosystem goods and services–the key for sustainable plantations. – CIFOR 2010: 205-227. https://www.cifor.org/publications/pdf_files/Books/BKanninen010208.pdf.

[9] Bonner, M. T. L., Schmidt., Shoo, L. P. (2013): A meta-analytical global comparison of aboveground biomass accumulation between tropical secondary forests and monoculture plantations. – Forest Ecology and Management 291: 73-86. https://doi.org/10.1016/j.foreco.2012.11.024.

[10] Canadell, J. G., Kirschbaum, M. U., Kurz, W. A., Sanz, M. J., Schlamadinger, B., Yamagata, Y. (2007): Factoring out natural and indirect human effects on terrestrial carbon sources and sinks. – Environmental Science & Policy 10(4): 370-384. https://doi.org/10.1016/j.envsci.2007.01.009.

[11] Cao, J., Wang, X., Tian, Y., Wen, Z., Zha, T. (2012): Pattern of carbon allocation across three different stages of stand development of a Chinese pine (Pinus tabulaeformis) forest. – Ecological Research 27(5): 883-892. https://doi.org/10.1007/s11284-012-0965-1.

http://www.aloki.hu ● ISSN 1589 1623 (Print) ● ISSN 1785 0037 (Online)
DOI: http://dx.doi.org/10.15666/aeer/1902_14571472
© 2021, ALÖKI Kft., Budapest, Hungary

[12] Chrsquo, H. Y., Ahmed, O. S., Majid, N. M. A. (2011): Assessment of soil carbon storage in a tropical rehabilitated forest. – International Journal of Physical Sciences 6(26): 6210-6219. https://doi.org/10.5897/IJPS11.076.
[13] Cossalter, C., Pye-Smith, C. (2003): Fast-Wood Forestry: Myths and Realities. Vol. 1. – CIFOR, Bogor.
[14] Delmotte, M. V., Zhai, P., Pörtner, H. O., Roberts, D., Skea, J., Shukla, P. R., Pirani, A., Okia, M. W., Péan, C., Pidcock, R., Connors, S. (2018): An IPCC Special Report on the Impacts of Global Warming of 1.5 C. – https://www.cooperacionsuiza.pe/wp-content/uploads/2018/03/3.reporte-especial-calentamiento-global-a-1.5c.pdf.
[15] En, L., Hui, W., Shi-rong, L. (2012): Characteristics of carbon storage and sequestration in different age beech (Castanopsis hystrix) plantations in south subtropical area of China. – Yingyong Shengtai Xuebao 23(2): 335-340.
[16] FAO (2006): Global Forest Resources Assessment 2005: Progress Towards Sustainable Forest Management.– FAO Forestry Paper 147. FAO, Rome.
[17] Gross, C. D., Harrison, R. B. (2018): Quantifying and comparing soil carbon stocks: underestimation with the core sampling method. – Soil Science Society of America Journal 82(4): 949-959. https://doi.org/10.2136/sssaj2018.01.0015.
[18] Holl, K. D., Zahawi, R. A. (2014): Factors explaining variability in woody aboveground biomass accumulation in restored tropical forest. – Forest Ecology and Management 319: 36-43. https://doi.org/10.1016/j.foreco.2014.01.024.
[19] Huy, B., Tuan, Ahn. P. (2008): Estimating CO2 sequestration in natural broad-leaved evergreen forests in Vietnam. – APA News (FAO) 32: 7-10.
[20] IPCC (2006): Intergovernmental Panel on Climate Change (IPCC) Guidelines for National Greenhouse Gas. – IPCC, Geneva.
[21] Kang, B., Liu, S., Zhang, G., Chang, J., Wen, Y., Ma, J., Hao, W. (2006): Carbon accumulation and distribution in Pinus massoniana and Cunninghamia lanceolata mixed forest ecosystem in Daqingshan, Guangxi, China. – Acta Ecologica Sinica 26(5): 1320-1327. https://doi.org/10.1016/S1872-2032(06)60024-3.
[22] Khan, M. S., Khan, S., Shah, W., Hussain, A., Masaud, S. (2016): Height growth, diameter increment and age relationship response to sustainable volume of subtropical Chir pine (Pinus roxburghii) forest of Karaker Barikot forest. – Pure and Applied Biology 5(4): 1. http://dx.doi.org/10.19045/bspab.2016.50095.
[23] Laganiere, J., Angers, D. A., Pare, D. (2010): Carbon accumulation in agricultural soils after afforestation: a meta-analysis. – Global Change Biology 16(1): 439-453. https://doi.org/10.1111/j.1365-2486.2009.01930.x.
[24] Laurance, W. F. (2007): A new initiative to use carbon trading for tropical forest conservation. – Biotropica 39(1): 20-24. https://doi.org/10.1111/j.1744-7429.2006.00229.x.
[25] Li, C., Zha, T., Liu, J., Jia, X. (2013): Carbon and nitrogen distribution across a chronosequence of secondary lacebark pine in China. – The Forestry Chronicle 89(2): 192-198. https://doi.org/10.5558/tfc2013-037.
[26] Ming, A., Jia, H., Zhao, J., Tao, Y., Li, Y. (2014): Above-and below-ground carbon stocks in an indigenous tree (Mytilaria laosensis) plantation chronosequence in subtropical China. – PLoS ONE 9(10): e109730. https://doi.org/10.1371/journal.pone.0109730.
[27] Misir, M., Misir, N., Bayburtlu, S., Bilgili, F. (2013): The yield of natural trembling aspen (Populus tremula L.) Stands (Northern and Eastern Anatolia). – Pakistan Journal of Agricultural Sciences 50(4): 537-547. http://pakjas.com.pk/papers/2190.pdf.
[28] Mora, J. L., Guerra, J. A., Armas-Herrera, C. M., Arbelo, C. D., Rodríguez-Rodríguez, A. (2014): Storage and depth distribution of organic carbon in volcanic soils as affected by environmental and pedological factors. – Catena 123: 163-175. https://doi.org/10.1016/j.catena.2014.08.004.

http://www.aloki.hu ● ISSN 1589 1623 (Print) ● ISSN 1785 0037 (Online)
DOI: http://dx.doi.org/10.15666/aeer/1902_14571472
© 2021, ALÖKI Kft., Budapest, Hungary

[29] Nizami, S. M. (2012): The inventory of the carbon stocks in subtropical forests of Pakistan for reporting under Kyoto Protocol. – Journal of Forestry Research 23(3): 377-384. https://doi.org/10.1007/s11676-012-0273-1.
[30] Nizami, S. M., Mirza, S. N., Livesley, S., Arndt, S., Fox, J. C., Khan, I. A., Mahmood, T. (2009): Estimating carbon stocks in sub-tropical pine (Pinus roxburghii) forests of Pakistan. – Pakistan Journal of Agricultural Sciences 46(4): 266-270. http://pakjas.com.pk/papers/78.pdf.
[31] Pan, Y., Luo, T., Birdsey, R., Hom, J., Melillo, J. (2004): New estimates of carbon storage and sequestration in China's forests: effects of age–class and method on inventory-based carbon estimation. – Climatic Change 67(2-3): 211-236. https://doi.org/10.1007/s10584-004-2799-5.
[32] Pearson, T. R. (2007): Measurement Guidelines for the Sequestration of Forest Carbon Vol. 18. – US Department of Agriculture, Forest Service, Northern Research Station, Washington, DC.
[33] Peichl, M., Arain, M. A. (2006): Above-and belowground ecosystem biomass and carbon pools in an age-sequence of temperate pine plantation forests. – Agricultural and Forest Meteorology 140(1-4): 51-63. https://doi.org/10.1016/j.agrformet.2006.08.004.
[34] Roy, J., Mooney, H. A., Saugier, B. (2001): Terrestrial Global Productivity. – Academic Press, San Diego.
[35] Saeed, S., Ashraf, M. I., Ahmad, A., Rahman, Z. (2016): The Bela forest ecosystem of district Jhelum, a potential carbon sink. – Pakistan Journal of Botany 48(1): 121-129.
[36] Sharma, C. M., Gairola, S., Baduni, N. P., Ghildiyal, S. K., Sarvesh, S. (2011): Variation in carbon stocks on different slope aspects in seven major types of temperate region of Garhwal Himalaya. – India. J. Biosci. 36(4): 701-708. https://doi.org/10.1007/s12038-011-9103-4.
[37] Siddiqui, M. F., Shaukat, S. S., Ahmed, M., Khan, N., Khan, I. A. (2013): Age and growth rates of dominant conifers from moist temperate areas of Himalayan and Hindukush region of Pakistan. – Pak. J. Bot. 45(4): 1135-1147.
[38] Smal, H., Olszewska, M. (2008): The effect of afforestation with Scots pine (Pinus silvestris L.) of sandy post-arable soils on their selected properties. II. Reaction, carbon, nitrogen and phosphorus. – Plant and Soil 305(1-2): 171-187. https://doi.org/10.1007/s11104-008-9538-z.
[39] Sullivan, M. J., Talbot, J., Lewis, S. L., Phillips, O. L., Qie, L., Begne, S. K., Chave, J., Cuni-Sanchez, A., Hubau, W., Lopez-Gonzalez, G., Miles, L. (2017): Diversity and carbon storage across the tropical forest biome. – Scientific Reports 7(1): 1-12. https://doi.org/10.1038/srep39102.
[40] Svenning, J. C., Skov, F. (2002): Mesoscale distribution of understorey plants in temperate forest (Kalø, Denmark): the importance of environment and dispersal. – Plant Ecology 160(2): 169-185. https://doi.org/10.1023/A:1015885321263.
[41] Taylor, A. R., Wang, J. R., Chen, H. Y. (2007): Carbon storage in a chronosequence of red spruce (Picea rubens) forests in central Nova Scotia, Canada. – Canadian Journal of Forest Research 37(11): 2260-2269. https://doi.org/10.1139/X07-080.
[42] Ullah, S., Muhammad, B., Amin, R., Abbas, H., Muneer, M. (2019): Sensitivity of arbuscular mycorrhizal fungi in old-growth forests: direct effect on growth and soil carbon storage. – Appl. Ecol. Environ. Res. 17: 13749-13758. http://dx.doi.org/10.15666/aeer/1706_1374913758.
[43] Walkley, A., Black, J. B. (1934): An examination of the Degtjareff method for determining soil organic matter and proposed modification of the chromic titration method. – Soil Science 37(1): pp29-38.
[44] Wang, D., Wang, B., Niu, X. (2014): Forest carbon sequestration in China and its benefits. – Scandinavian Journal of Forest Research 29(1): 51-59. https://doi.org/10.1080/02827581.2013.856936.

http://www.aloki.hu ● ISSN 1589 1623 (Print) ● ISSN 1785 0037 (Online)
DOI: http://dx.doi.org/10.15666/aeer/1902_14571472
© 2021, ALÖKI Kft., Budapest, Hungary

[45] Watson, R. T., Noble, I. R., Bolin, B., Ravindranath, N. H., Verardo, D. J., Dokken, D. J. (2000): Land Use, Land-Use Change and Forestry. A Special Report of the IPCC. – Cambridge University Press, Cambridge.
[46] Winjum, J. K., Schroeder, P. E. (1997): Forest plantations of the world: their extent, ecological attributes, and carbon storage. – Agricultural and Forest Meteorology 84(1-2): 153-167. https://doi.org/10.1016/S0168-1923(96)02383-0.
[47] Zhang, H., Guan, D., Song, M. (2012): Biomass and carbon storage of eucalyptus and acacia plantations in the Pearl River Delta, South China. – Forest Ecology and Management 277: 90-97. https://doi.org/10.1016/j.foreco.2012.04.016.
[48] Zhao, J., Kang, F., Wang, L., Yu, X., Zhao, W., Song, X. et al. (2014): Patterns of biomass and carbon distribution across a chronosequence of Chinese pine (Pinus tabulaeformis) forests. – PLoS ONE 9(4): e94966. https://doi.org/10.1371/journal.pone.0094966.

APPENDIX

Table A1. *Data of sampling plots (with reference to Figure 1)*

Plot no	Elevation (m)	Latitude	Longitude	Tree density	Slope	Aspect
1	1180	34.971	72.21	20	44%	Eastern
2	1222	34.947	72.206	43	58%	Northern
3	1232	34.912	72.174	11	60%	Southern
4	1229	34.883	72.274	13	60%	Southern
5	1193	34.855	72.179	33	52%	Northern
6	1148	34.882	72.204	24	34%	Northern
7	1231	34.923	72.279	36	54%	Northern
8	1274	34.928	72.236	15	78%	Eastern
9	1286	34.84	72.248	10	56%	Southern
10	1273	34.847	72.269	21	79%	Western
11	1191	34.799	72.236	18	37%	Eastern
12	1235	34.765	72.24	26	50%	Northern
13	1259	34.798	72.28	28	63%	Northern
14	1294	34.799	72.311	31	51%	Southern
15	1348	34.831	72.323	25	80%	Northern
16	1390	34.819	72.366	8	84%	Southern
17	1376	34.832	72.416	19	79%	Western
18	1301	34.872	72.357	24	80%	Eastern

http://www.aloki.hu ● ISSN 1589 1623 (Print) ● ISSN 1785 0037 (Online)
DOI: http://dx.doi.org/10.15666/aeer/1902_14571472
© 2021, ALÖKI Kft., Budapest, Hungary

FLORA DIVERSITY OF FIELD FOREST PATCHES IN LANDSCAPES WITH VARIED GEOMORPHOLOGICAL UNITS AND LAND USE IN POLAND

GAMRAT, R.[1*] – GAŁCZYŃSKA, M.[2]

[1]*Department of Environmental Management, West Pomeranian University of Technology, Słowackiego 17, PL-71-434 Szczecin, Poland*

[2]*Department of Bioengineering, West Pomeranian University of Technology, Słowackiego 17, PL-71-434 Szczecin, Poland*
(e-mail: Malgorzata.Galczynska@zut.edu.pl; phone: +48-91-449-6322)

[*]*Corresponding author*
e-mail: Renata.Gamrat@zut.edu.pl; phone: +48-91-449-6343

(Received 21st Nov 2020; accepted 8th Feb 2021)

Abstract. A diverse terrain is one of the essential natural features of a balanced landscape and the specific features of its geomorphological units (sandur, moraine) contribute to regional diversity. The present work describes research designed to verify the hypothesis that the diversity of flora in the ecotone zone of woodland in Poland relates to variability both in the terrain and in land use. By using phytoindication it was possible to assess differentiation in the surfaces under study. It was found that land use (agricultural and forest use) was responsible for the occurrence of a positive interrelationship between trophy and synanthropisation values, no matter what kind of geomorphological unit there was. On the basis of the species composition in the areas under research, within the ecotone zone of woodland, it was established that in the area within moraine which had previously been used agriculturally there was a cumulation of species due to habitat diversity in ecological niches resulting from the terrain, the amount of mineral nutrients in the soil and a large amount of, in particular, native and neutral species in the gene pool.
Keywords: *sandur, moraine, ecological indicators, agricultural land*

Abbreviations: s: Object is located on the sandur; m: Object is located on the moraine; fd: Object is located in the area previously used for agriculture; ft: Object is located in a previously forested area.

Introduction

Forest patches within the agricultural landscape are considered valuable due to their production or protective functions (lumber, regulation of water and temperature conditions on the fields) as well as ecological function (maintaining phytodiversity, including that of forest species in areas related to agrocenosis), aesthetic and landscape values (Jamoneau et al., 2012; Foli et al., 2015; Decocq et al., 2016; Hladnik et al., 2020). A particular role in maintaining phytodiversity is played by the most external part of forest patches, i.e. the ecotone zone (Chabrerie et al., 2013; Gamrat and Gałczyńska, 2014; Skrajna, 2020). The gene pool of seeds of the plant species found in that area depends on various factors, among others, the shape and size of the area, the length of borderline and the type of tree stand (Esseen et al., 2016).

The effect of tree stands on improving the natural features of sustainable landscape is especially valuable with respect to anthropogenic areas - a category encompassing arable fields (Forrest et al., 2015; Proesmans et al., 2019). Apart from the effect of anthropic pressure, the species composition of these ecosystems is determined by landscape features such as, for example, location within the specific geomorphological units such

http://www.aloki.hu ● ISSN 1589 1623 (Print) ● ISSN1785 0037 (Online)
DOI: http://dx.doi.org/10.15666/aeer/1902_14731489
© 2021, ALÖKI Kft., Budapest, Hungary

as sandur or moraine (Batary et al., 2011; Stepanovich, 2019; Majewski and Marszałek, 2020). Topography of the surface determines the available soil moisture regimes and nutrient gradients contributing to differentiation of habitat conditions, and thus plant composition (Jia et al., 2015).

The previous form of use of forest patches as an afforested production area or arable field may affect the species composition of the area through modifications of the vertical structure of flora or habitat mosaic due to specific characteristics of land use (Chabrerie et al., 2013; Lõhmus et al., 2014; Jia et al., 2019).

The present paper shows the effects of the two most essential factors consequential for the species composition of the ecotone zone of forest patches, i.e. topography (Jia et al., 2015) and the previous form of land use (Haddad et al., 2015). Research was conducted to verify the thesis stipulating that flora diversity in the ecotone zone of forest patches within sandur is lower than that within the moraine area. It was also stipulated that previous agricultural use of forest patches favours diversity of herbaceous synanthropic species. The said research fills the knowledge gap in terms of previous use of the analysed ecosystem in various geomorphological units. The increasing steppe formation on agricultural lands (Baude et al., 2019) may be a crucial factor in selecting the adequate management strategy of such landscapes to maintain biodiversity of fields affected by drought (Liu et al., 2020). The ecological factors affecting the fields with heavily dried surface layer of soil may be comparable to the factors determining biocenoses on sandur areas. The aim of the studies is to raise awareness of the impact of factors such as the type of geomorphological unit and prior use of land - covered at present with forest patches - on their phytodiversity.

Material and Methods

Study area

During 2011-2013, floristic and phytosociological research was carried out in forest patches in their outer ecotone zone within the range of ground moraine and sandur (the GPS coordinates of the central part of the studies areas of maps, respectively N 53°37'3.502", E 16°16'52.862" and N 53°31'36.046", E 16°18'14.964") in Drawsko Lakeland in West Pomeranian province in N-W Poland (*Fig. 1*). The detailed analysis concerned the outermost part of the ecotone zone in contact with the surroundings. The terrain floristic research included three growing seasons in the subsequent years of the study, i.e. from April to September in 2011, 2012 and 2013.

The most significant features determining a forest, as well as affecting the flora composition, are origin - presence on the previously afforested areas or those not classified as a forest (Haddad et al., 2015; Chazdon et al., 2016), and location of the analysed objects on different geomorphological units (Jia et al., 2015; Stepanovich, 2019).

The analysed forest patches were of different origin (the objects previously used as forest or arable lands) and geomorphological location. The objects within the moraine plain were labelled “m”, and those located within sandur as “s”. In the present paper, the following abbreviations are used: “field-forest” / (the present forest patches area was used as agriculture fields in 1948), “fd” (field) or “forest-forest” (the present forest patches area was used as a forest in 1948) and “ft” (forest). The previous use of the analysed objects as forest or field was confirmed with archive aerial photographs taken in 1947-48. The geomorphological location of the forest patches under analysis was confirmed with

http://www.aloki.hu ● ISSN 1589 1623 (Print) ● ISSN1785 0037 (Online)
DOI: http://dx.doi.org/10.15666/aeer/1902_14731489
© 2021, ALÖKI Kft., Budapest, Hungary

geomorphological maps. The soil granulometric composition on which the studied forest patches were located was read from the soil maps.

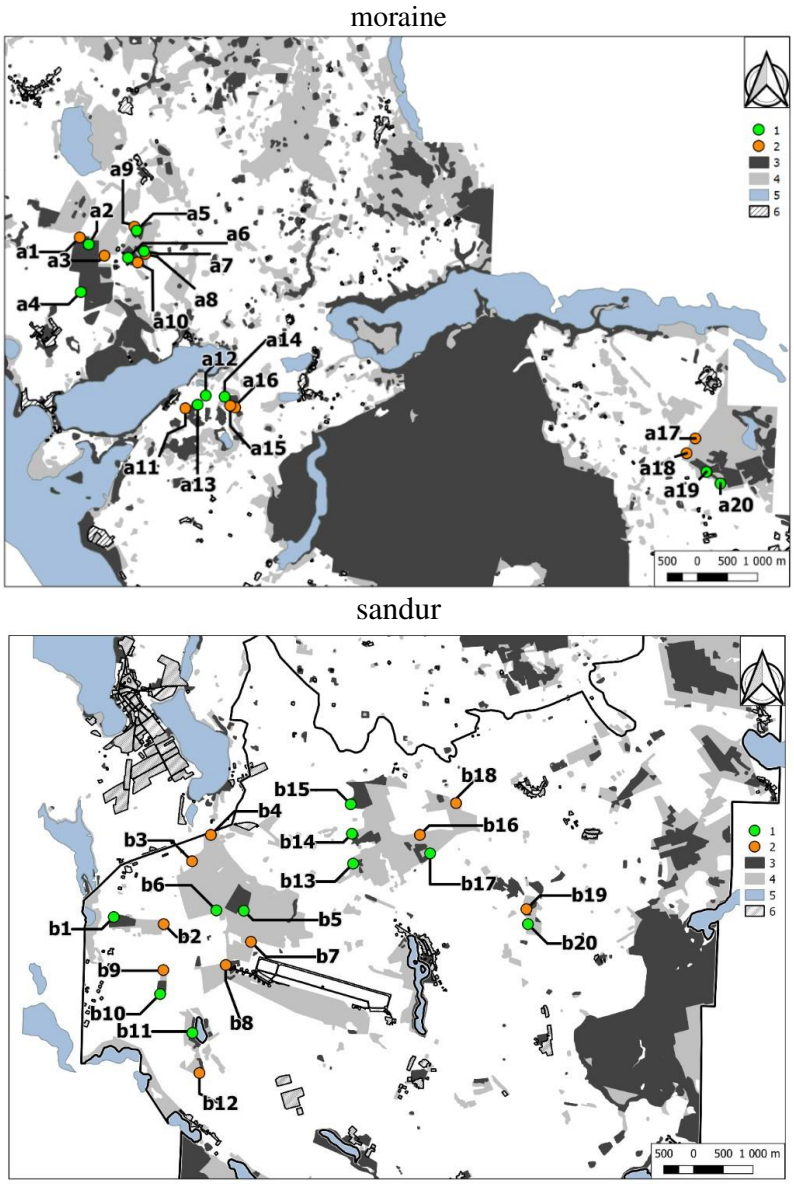


Figure 1. *Location of studied forest patches on moraine and sandur. 1: field-forest research stand (the present forest patches area was used as agriculture fields in 1948), 2: forest-forest research stand (the present forest patches area was used as a forest in 1948), 3: forest-forest areas (areas used as forest in 1948), 4: field-forest areas (areas used as agriculture fields in 1948), 5: water, 6: build area*

In the analysed forest patches, predominant was fresh mixed forest with a significant share of approx. 56-year-old pine trees *Pinus sylvestris* L. (mean value, *Table 1*). The height of the trees ranged from 8 to 12 m. The studies were conducted on 6 fragments of forest patches (both on the moraine and sandur areas) located within or only in some part in arable lands, specifically wheat farming. The elevations of the rolling moraine plains ranged from 150 m to 180 m asl, and on the sandur area about 140 m asl.

http://www.aloki.hu ● ISSN 1589 1623 (Print) ● ISSN1785 0037 (Online)
DOI: http://dx.doi.org/10.15666/aeer/1902_14731489
© 2021, ALÖKI Kft., Budapest, Hungary

Table 1. *Age of the stands at the examined points*

Geomorphological units	Land use	Number of object and age of the pine stand
moraine	field-forest	a1 - 55, a3 - 68, a7 - 55, a9 - 60, a10 - 66, a11 - 40, a15 - 55 (and *Betula pendula*), a16 - 25 (and *Fagus sylvatica*), a17 - 52, a18 - 52
	forest-forest	a2 - 90, a4 - 5, a5 - 110, a6 - 50, a12 - 50, a8 - 90, a13 - 70, a14 - 110 (and *Fagus sylvatica*), a19 - 85, a20 - 30
sandur	field-forest	b7 - 56, b8 - 52, b2 - 25, b3 - 55, b4 - 55, b9 - 60, b12 - 56, b16 - 46 (and *Picea abies*), b18 - 25 (and *Betula pendula*), b19 - 50
	forest-forest	b1, 20 - 66, 20 (and *Betula pendula*), b5 - 73, b6 - 73, b10 - 80, b11 - 111, b13 - 12, b14 - 25, b15 - 45, b17 - 46

a: objects located on the moraine, b: objects located on the sandur

Physical features of ecotone zones

Within the area of the selected forest patches, the ecotone zones of a width of 10 m and length of 20 m were analysed (Gamrat and Gałczyńska, 2014). Prior to the selection of the said areas and their size, terrain studies were conducted providing the analysis of plant structure, diameter at breast height of trees (comparable to the diameter results) and species diversity of trees (domination of *Pinus sylvestris* L.). Flora was categorised according to the vertical structure: the highest layer was constituted by the trees (a), the layer with lower location - shrubs and tree saplings (b), the layer with even lower location - herbaceous species (c), and the ground or arboreal level - mosses and lichens (d) (*Table A1*). Legally protected species were distinguished among the identified flora (JL, 2014).

On both geomorphological units, i.e. sandur and moraine, 40 phytosociological releve's were taken using the classic Braun-Blanquet method, allowing for the determination of the degree of surface coverage according to a 7-step scale following Dzwonko (2008) from 5 to r. The calculated constancy values and that of the coverage coefficient for 10 phytosociological releve's (S-D) are synthesized in *Table A1*, presenting data of the constancy and coefficient of the identified communities (Matuszkiewicz, 2017). The selected area of each releve's was 200 m^2.

Features of ecological indicators

For the purpose of the assessment of the degree of flora transformation, according to the identified geographical-historical groups, the synanthropization index (St) was calculated following Wysocki and Sikorski (2002), according to the formula:

$$St = \frac{Ap+A}{C} \cdot 100\ \% \qquad \text{(Eq.1)}$$

where St is the synanthropization index; Ap is the number of apophyte species (native plants that entered the habitats changed by man); A is the number of anthropophyte species (foreign plants); C is the total number of all plant species.

This index identifies total transformation in the vegetation cover due to human activity (anthropic pressure). This process is manifested by the displacement of native species which are replaced by foreign or cosmopolitan elements (Stepanovich, 2019) or their quantitative transformation within the sociological structure.

http://www.aloki.hu ● ISSN 1589 1623 (Print) ● ISSN1785 0037 (Online)
DOI: http://dx.doi.org/10.15666/aeer/1902_14731489
© 2021, ALÖKI Kft., Budapest, Hungary

Flora is an ecological indicator of numerous changes taking place in the environment. In Central Europe, the commonly accepted method of assessing the habitats with the use of habitat preference of flora is the Ellenberg scale (Ellenberg et al., 1991). For the purpose of verification of the habitat conditions, selected values of the percentage share of ecological groups were calculated for the found flora, i.e., acidity (pH) and nitrogen content (Trophy) in soil (*Table 2*).

Table 2. *Numerical indicators determining flora's preferences according to the pH and nitrogen content in soil*

No	Soil acidity (pH) value	Trophy value
1	strong indicator of acidity, never occur very weakly acidic to alkaline soils	habitats most poor in nitrogen
2	habitats intermediate between 1 and 3	habitats intermediate between 1 and 3
3	indicator of acidity on acid soils rarely neutral	habitat poor in nitrogen more than average fertile
4	habitats intermediate between 3 and 5	habitats intermediate between 3 and 5
5	habitats strongly acidified, at neutral and alkaline soils	an average of habitats rich in nitrogen
6	habitats intermediate between 5 and 7	habitats intermediate between 5 and 7
7	weaker indicator of acidity or alkalinity indicator of poor, never occurs on strongly acidic soils	often to be rich in nitrogen positions
8	habitats between 7 and 9	habitats rich in nitrogen
9	ratio of calcium to the soil very rich in calcium	habitats excessively rich in nitrogen

The possibility of spreading plant species was analyzed after Chmiel (1993), classifying the species into three synanthropodynamic groups. This classification included the following species: native (Native) - species that are very poorly spreading and endangered due to the destruction of their habitats, neutral (Neutral) - species poorly spreading and occurring only in habitats appropriate for them, invasive (Invasive) - rapidly spreading and colonizing species other than their own habitats.

The natural values of the flora were determined by average values of the natural valorization index (Valorisation) were calculated according to the modified Oświt method (Gamrat et al., 2019 after Oświt, 2000, *Table 3*).

Table 3. *Values of the natural classification of flora*

No	Values	Terms	No	Values	Terms
1	< 1.4	very low	6	3.1 - 3.4	measures high
2	1.5 - 1.8	medium low	7	3.5 - 3.8	high
3	1.9 - 2.2	low	8	3.9 - 4.2	very high
4	2.3 - 2.6	moderate	9	4.3-4.6	eminent
5	2.7 - 3.0	medium moderate	10	> 4.6	unique

Statistical analysis

The results of the research on the indices characterising the habitat properties of the vegetation and the number of synanthropodynamic groups were subjected to two-factor variance analysis (1st factor - the form of the terrain - 2 levels, 2nd factor - land use - 2 levels). Also analysed was the correlation between selected indices (trophy, soil pH and valorisation) and those of the remaining research parameters, which, as regards the factors

http://www.aloki.hu ● ISSN 1589 1623 (Print) ● ISSN1785 0037 (Online)
DOI: http://dx.doi.org/10.15666/aeer/1902_14731489
© 2021, ALÖKI Kft., Budapest, Hungary

tested, were significantly different (synanthropisation index, total number of species, including native, invasive and neutral). The significance of differences between the mean values was calculated based on of Tukey's t- test with significance level $\alpha = 0.05$. The calculations were performed by means of the Statistica 10 program.

Results

In the forest patches area, within the ground moraine and sandur, in the ecotone zone, 213 plant species were found, including 15 tree species, 12 species of shrubs, 7 lichens and 4 mosses (*Table A1*).

There were 5 partial protected species in the study area, including 3 mosses, 1 tree and 1 herbaceous plant. These species were found on prior forested forest patches on sandur. They were: *Leucobryum glaucum* Hedw., *Pleurozium schreberi* (Willd. ex Brid.) Mitt.), *Dicranum scoparium* Hedw. and *Taxus baccata* L. except for *Pyrola rotundifolia* L. - present in the area previously cultivated in agriculture.

On the moraine in the ecotone zone of forest patches significantly more plant species (177 species) were found as compared to sandur areas (95 plant species) (*Table A1*). Of all the plant species, forest and scrub flora (92 species) dominated and there were also meadow and grassland plants (77 species). The diversity of the number of species at 20 research sites was, in the case of forest grasslands, not large, contrary to meadow grassland flora. The plant species from the remaining sociological and ecological groups were less common (ruderal - 29; marsh - 15). Flora belonging to the remaining groups occurred mainly in the post-cultivated moraine areas (marsh species - 100%, ruderal - 86%, meadow - 65%).

The identified plant species belonged to 13 phytosociological classes (*Fig. 2*), with a predominance of forest habitats, i.e. *Vacccinio-Piceetea* - coniferous forests, *Querco-Fagetea* - eutrophic deciduous forests and *Epilobietea angustifolii* - semi-natural field communities (from 33 to 55 species) and meadow habitats - the *Molinio-Arrhenatheretea* class (from 26 to 50 species).

Table 4 and *Figure 3* show a statistical description of the results of the studies and variance analysis for synanthropisation and environmental indices (Trophy: soil nitrogen content indicator, pH: the value of the acidity index in the soil, Valorisation: the value of the natural valorisation index).

The synathropisation index took on larger values in an area previously used as an arable field in an afforested area, while the terrain had no influence on the value of the index calculated. The larger number of alien species such as *Lupinus polyphyllus* L., *Myosotis arvensis* (L.) Hill., *Sonchus asper* (L.) Hill. was responsible for the quantity of this parameter.

Error bars represente of the variability of data and used on graphs to indicate the error or uncertainty in a reported measurement. In our studies, the amount of variability in the data corresponds to field studies. The largest index values (4.3 and 3.4) characterising plant habitat properties (trophy, soil pH) occurred in an area used earlier as an arable field within moraine. The natural valorisation index for this research area was smaller than the previously wooded area and situated within sandur. In this area, there were numerous species with high valorisation values: *Hypogymnia psysodes* (L.) Nyl., *Hypocenomyce scalaris* (Ach. ex Lilj.) M. Choisy, *Taxus baccata* L. From the indices analysed (synanthropization W_s, naturalness W_n and flora anthropophytization W_a) only the synanthropization index turned out to be a parameter sensitive to land use, which indicates its usability at the assessment of transformations of the small areas of woodland studied.

http://www.aloki.hu ● ISSN 1589 1623 (Print) ● ISSN1785 0037 (Online)
DOI: http://dx.doi.org/10.15666/aeer/1902_14731489
© 2021, ALÖKI Kft., Budapest, Hungary

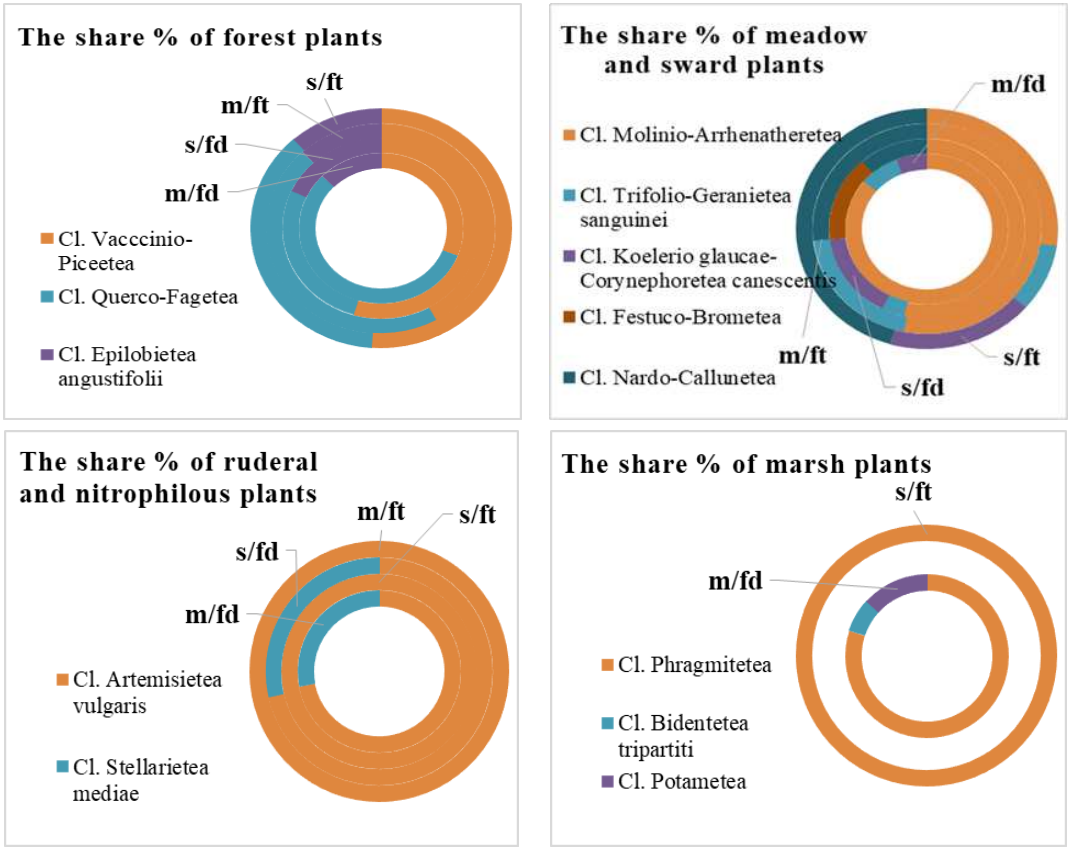


Figure 2. *The share of plant species belonging to phytosociological classes identified on the studied forest patches. s: object is located on the sandur, m: object is located on the moraine, fd: object is located in the area previously used for agriculture, ft: object is located in a previously forested area*

Table 4. *Synanthropization index values on the studied forest patches*

Geomorphological unit	Prior land use	Medium	Standard error	-95.00%	+95.00%
m	fd	230 [b]	± 48	129	331
m	ft	71 [a]	± 10	50	91
s	fd	178 [b]	± 23	129	227
s	ft	39 [a]	± 6	26	52

a, b: homogeneous groups, N: 20 research areas, s: object is located on the sandur, m: object is located on the moraine, fd: object is located in the area previously used for agriculture, ft: object is located in a previously forested area

The species occurring in the post-cultivated areas of moraine are characteristic of low-pH habitats, for example *Juncus effusus* L., *Maianthemum bifolium* (L.) F. W. Schmidt, *Oxalis acetosella* L. (acidification indicators). The species occurring in post-cultivated moraine terrain need habitats with a soil of larger trophic values, including: *Aegopodium podagraria* L., *Galium aparine* L., *Urtica dioica* L.

http://www.aloki.hu ● ISSN 1589 1623 (Print) ● ISSN1785 0037 (Online)
DOI: http://dx.doi.org/10.15666/aeer/1902_14731489
© 2021, ALÖKI Kft., Budapest, Hungary

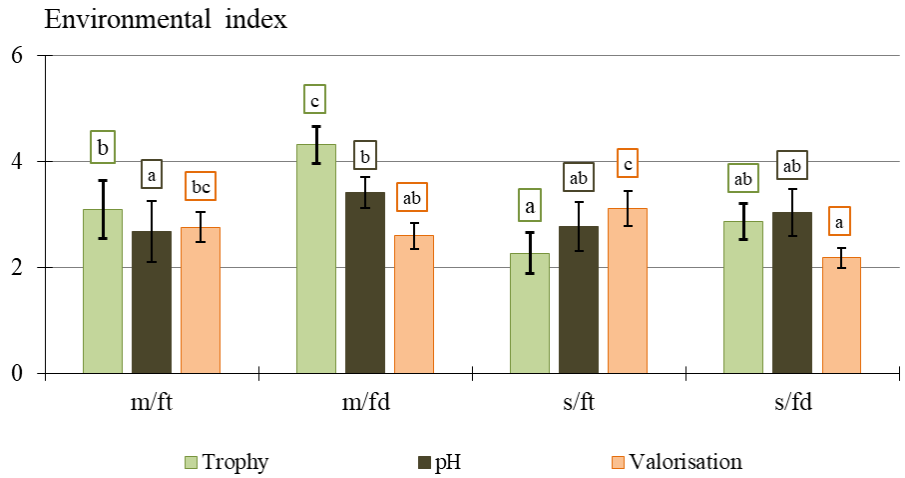


Figure 3. *Values of environmental indexes on studied areas (Mean ± standard error (SE)), Means with the same uppercase letter are not significantly different (p > 0.05), a, b, c: homogeneous groups, n: 20 research areas, s: object is located on the sandur, m: object is located on the moraine, fd: object is located in the area previously used for agriculture, ft: object is located in a previously forested area, Trophy: soil nitrogen content indicator, pH: the value of the acidity index in the soil, Valorisation: the value of the natural valorisation index*

The statistical analysis showed (*Fig. 4*), that the largest number of plant species occurred within moraine in an area previously used as an arable field which, at the same time, resulted in the largest number of species, including neutral species, i.e. poorly spreading and occurring only in habitats appropriate for them. These were, among others: *Carex elata* All., *Equisetum palustre* L., *Scirpus sylvaticus* L.

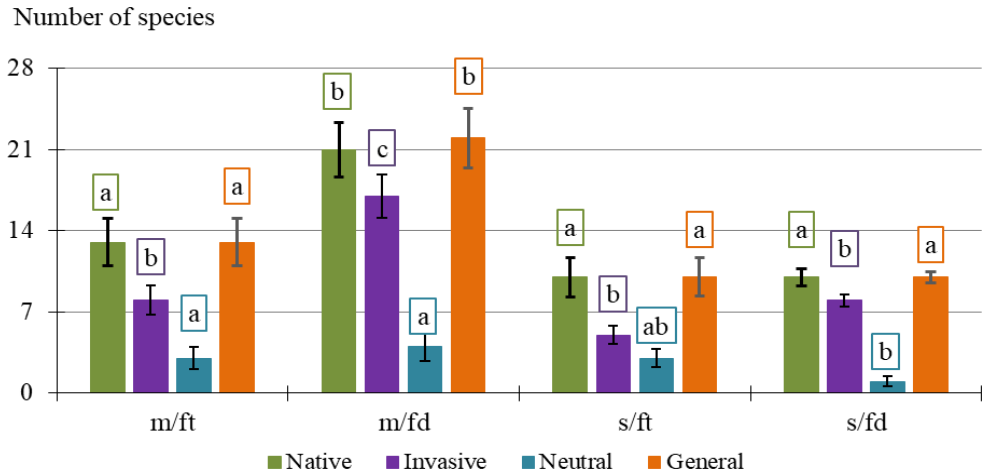


Figure 4. *The number of native, invasive and neutral species on the studied forest patches. (Mean ± standard error (SE)), Means with the same uppercase letter are not significantly different (p > 0.05), a, b, c: homogeneous groups, n: 20 research areas, s: object is located on the sandur, m: object is located on the moraine, fd: object is located in the area previously used for agriculture, ft: object is located in a previously forested area, Native: very poorly spreading species, Invasive: invasive rapidly spreading species, Neutral: neutral species, i.e. poorly spreading, General: the total number of species*

http://www.aloki.hu ● ISSN 1589 1623 (Print) ● ISSN1785 0037 (Online)
DOI: http://dx.doi.org/10.15666/aeer/1902_14731489
© 2021, ALÖKI Kft., Budapest, Hungary

Error bars represente of the variability of the number of species. In our studies, the amount of variability in this data corresponds to botanical studies. The fewest number of species was recorded in an area previously afforested within sandur. The species were under mutual influence, which mainly referred to the impingement of invasive species. In the assessment of transformations, the ecological indices including the trophy, soil pH and valorisation indices showed differentiation as regards to the varied terrain and land use.

It was established that there was a significance linear correlation between the plant habitat trophy and soil pH indices, and the total number of species, including native, invasive and neutral (*Table 5*). The value of the natural valorisation index was negatively correlated with the number of invasive species. The presented values indicate strong (r = 0.60), moderate (r = 0.42 or 0.56), and weak (r = -0.24 or 0.25 or 0.28 or 0.34) correlation between the evaluated parameters, but it is clear evidence that there is a correlation between the soil parameters first of all the soil pH and the species diversity because all species have an optimum range in terms of all environmental parameters. Additionally, it is a natural phenomenon that the occurrence of the invasive species is more frequent under non-optimum conditions such as too high or low pH.

Table 5. *The linear correlation coefficient between the analyzed indexes, and the number of species in the studied forest patches*

Parameter	Index				Number			
	St	**Trophy**	**pH**	**Valorisation**	**Native**	**Invasive**	**Neutral**	**Σ**
Index trophy	0.25*	1.00	0.42*	-	0.60*	0.56*	0.34*	0.60*
Index pH	-	0.42*	1.00	-	-	0.28*	-	-
Index valorisation	-	-	-	1.00	-	-0.24*	-	-

Level of significance, *<0.05. St: synanthropization index, Trophy: soil nitrogen content indicator, pH: the value of the acidity index in the soil, Valorisation: the value of the natural valorisation index, Native: very poorly spreading species, Invasive: invasive rapidly spreading species, Neutral: neutral species, i.e. poorly spreading

The species classified as invasive, i.e. characterized by rapid spreading and colonizing all available habitats, and also characterized by low valorisation number values are *Artemisia vulgaris* L., *Calamagrostis epigejos* (L.) Roth., *Elymus repens* (L.) Gould.

Discussion

Currently available knowledge on the ecosystem services of forest patches (Takkis et al., 2018), is still lacking in comparison with that on large forest areas (Gamfeldt et al., 2013; Biber et al., 2015). Therefore, it is vital to extend the knowledge on the role of forest patches in maintaining, among others, biological diversity in a landscape under heavy anthropogenic pressure, such as agricultural lands. As a result of economic and social transformations, the areas under study are characterised by the emergence of large areas of fallow lands, particularly on sandur areas (Majewski and Marszałek, 2020), and the only way in which these poor soils (complex 6 and 7 of agricultural use) could be developed and used was afforestation (Schmidt, 2015). In the analysed area, the predominant were slightly loamy sand (85% in sandur and 70% in moraine). In individual forest patches there were also sand and clay, respectively.

http://www.aloki.hu ● ISSN 1589 1623 (Print) ● ISSN1785 0037 (Online)
DOI: http://dx.doi.org/10.15666/aeer/1902_14731489
© 2021, ALÖKI Kft., Budapest, Hungary

The complexity of the landscape composition (e.g. kame, esker, valley, ravine) due to glacier retreat determines the occurrence of small elements of landscape (Pieńkowski et al., 2019), including forest patches. In the analysed moraine areas, which show greater diversity in terms of land relief and, consequently, are richer in other natural ecosystems, there were almost 2 times more plant species in comparison with the sandur areas. The diversity of herbaceous flora resulted from a low density of the shrub layer (from 0 to 40%). According to Hladnik et al. (2020), the limit values preventing the rejuvenation of tree stand and development of forest floor vegetation is 60% area covered with shrubs. In the analysed areas, the most diverse tree stand, and forest floor vegetation were found on the previously afforested moraine area. However, the richest layer of moss and forest floor vegetation was found on previously afforested sandur areas.

The previous use of forest patches as agricultural lands may have a negative effect on the quality of the tree stand as well as plants of the forest floor vegetation. The studies by Buffa et al. (2018) and Jelonek et al. (2019) showed a decrease in wood biomass production and flora diversity with the increasing age of forest patches. Similar results were obtained by Foli et al. (2015) and Van Dijk (2018), who reported changes in flora composition and deterioration of habitats due to the change of the form of land use. This is confirmed by own studies which indicate fewer plant species in the areas which previously had been used for agricultural purposes in comparison with previously afforested areas. The origin of forest patches determined the rate of flora succession. The flora changes in the areas previously used for agricultural purposes concerned 30% of species, whereas in the afforested areas the changes were non-substantial. Skrajna (2020) showed that with the high number of typically forest species in the extreme parts, the diversity of the whole ecotone zone increases. The share of coniferous and deciduous species (respectively, class *Vaccinio-Piceetea* and *Querco-Fagetea*) in the analysed areas was 25%.

The studies by Dzwonko (2015) showed that the previously afforested areas were characterised by a greater flora diversity of ecotone zones, particularly of forest species - a fact explained by Meszaros (2012) by their fast rate of vegetative propagation. The following forest species, among others, were observed in the analysed areas: *Asarum europaeum* L., *Convallaria majalis* L., *Oxalis acetosella* L., *Hedera helix* L., *Viola reichenbachiana* Jordan ex Bor., *Poa nemoralis* L., *Luzula pilosa* (L.) Willd. or *Vaccinium myrtillus* L. In the forest patches which were previously used for agricultural purposes, ruderal species were expansive, e.g. *Cirsium arvense* (L.) Scop.), *Rubus idaeus* L. and *Urtica dioica* L.

Additionally, floristic diversity depends on the tree stand. According to Gamfeldt et al. (2013) and Lõhmus et al. (2014), diversity is hindered by a high share of coniferous trees, particularly in the borderline zone - in the analysed area, *Pinus sylvestris* L. showed the highest share among other forest-forming species. With the presence of *Pinus sylvestris*, the forest floor vegetation was dominated by *Deschampsia flexuosa* L. (forest species forming aggregations). With the presence of deciduous species (e.g. *Betula pendula* Roth., *Fagus sylvatica* L., *Populus tremula* L., *Quercus robur* L.), ruderal species were numerous (e.g. *Aegopodium podagraria* L., *Rubus idaeus* L., *Geum urbanum* L.). The studies by Kryszak et al. (2014) showed high occurrence of *Deschampsia flexuosa* L. and *Poa nemoralis* L. on sandur areas. The preference of these grass species i.e., dry and slightly acidic habitats (Plue et al., 2020), made the analysed forest patches an unsuitable habitat for these plants.

http://www.aloki.hu ● ISSN 1589 1623 (Print) ● ISSN1785 0037 (Online)
DOI: http://dx.doi.org/10.15666/aeer/1902_14731489
© 2021, ALÖKI Kft., Budapest, Hungary

In Europe, the characteristics of a given environment, the so-called filtering, consists of the analysis of the preference of a given species in terms of a specified factor (Silvertown et al., 2006; Bartelheimer and Poschlod, 2015). The study on the transformation of the vascular flora of forest, after a period of 20 years, showed high values of the synantrophization index (>50%) and a low degree of flora naturalness (24.4%) (Ziaja and Wójcik, 2015). The values of the synantrophization index in pine stand ranged from 0.39 to 0.52 (Stepanovich, 2019). In the present study, the obtained values of syntantrophization index (*Eq. 1*) were 3.8 times higher in comparison to afforested areas, and 1.4 times higher within moraine areas.

The studies by Stepanovich (2019) on the occurrence of invasive species in pine forests showed 16 very invasive species - capable of inducing a radical transformation of native phytocenoses and the creation of own communities (e.g. *Robinia pseudoacacia* L.), 14 species resilient to unfavourable environmental conditions (e.g. *Impatiens parviflora* DC.), and 2 species quickly reacting to substrate disturbances (np. *Conyza canadensis* (L.) Cronquist). In the analysed area, the highest number of invasive species (according to synanthropodynamic classification) was found in forest patches previously used for agricultural purposes.

The studies conducted by Skrajna (2020) indicated greater differences in the values of Ellenberg ecological indices with respect to nitrogen content and acidity of the habitat between forest patches located in areas previously used for agricultural purposes and those located in previously afforested areas. The values of environmental valorisation index of forest ecotone zone ranged from moderately high to low (Gamrat et al., 2019). The said values determined for the analysed areas were even lower.

The effect of forest patches on the flow of ecosystemic services, including preservation of biodiversity (Takkes et al., 2018; Bergès and Dupouey, 2020), is critical for agricultural landscape. The objects with sustainable ecological continuity, such as forest patches located in areas which have been afforested for a long time, are considered particularly valuable for nature protection (Nordén et al., 2014).

Conclusions

The applied method of phytoindication with Ellenberg's and Oświt's indices made it possible to assess differences in the research areas. Land use (agricultural and forest use) was found to be responsible for a positive interrelationship between trophy and synanthropisation indices, no matter the type of geomorphological unit. On the basis of species composition in the ecotone zone of small areas of woodland in the research areas it was established that within the moraine area previously used agriculturally (the most species of trees, shrubs, green vegetation, mosses and lichens) there was a cumulation of species due to the habitat diversity of ecological niches resulting from the terrain, the amount of mineral nutrients in the soil and the large number of particularly native and neutral species in the gene pool. The ecotone zones in sandur areas of forest patches offer better conditions for the preservation of protected species owing to the smaller variability in habitat parameters. In view of the observed climate change, it is now important to properly manage the drought-affected fields. Monitoring of biodiversity in sandur areas can help in choosing the right direction in maintaining the phytodiversity of the agricultural landscape.

http://www.aloki.hu ● ISSN 1589 1623 (Print) ● ISSN1785 0037 (Online)
DOI: http://dx.doi.org/10.15666/aeer/1902_14731489
© 2021, ALÖKI Kft., Budapest, Hungary

REFERENCES

[1] Bartelheimer, M., Poschlod, P. (2015): Functional characterizations of Ellenberg indicator values - a review on ecophysiological determinants. – Functional Ecology 30(4): 506-516.
[2] Batary, P., Baldi, A., Kleijn, D., Tscharntke, T. (2011): Landscape moderated biodiversity effects of agri environmental management: a meta analysis. – Proceedings of the Royal Society B: Biological Sciences 278: 1894-1902.
[3] Baude, M., Meyer, B. C., Schindewolf, M. (2019): Land use change in an agricultural landscape causing degradation of soil based ecosystem services. – Science of the Total Environment 659: 1526-1536.
[4] Bergès, L., Dupouey, J.-L. (2020): Historical ecology and ancient forests: progress, conservation issues and scientific prospects, with some examples from the French case. – Journal of Vegetation Science 32(1): e12846.
[5] Biber, P., Borges, J. G., Moshammer, R., Barreiro, S., Botequim, B., Brodrechtová, Y., Brukas, V., Chirici, G., Cordero-Debets, R., Corrigan, E., Eriksson, L. O., Favero, M., Galev, E., Garcia-Gonzalo, J., Hengeveld, G., Kavaliauskas, M., Marchetti, M., Marques, S., Mozgeris, G., Navrátil, R., Nieuwenhuis, M., Orazio, C., Paligorov, I., Pettenella, D., Sedmák, R., Smreček, R., Stanislovaitis, A., Tomé, M., Trubins, R., Tuček, J., Vizzarri, M., Wallin, I., Pretzsch, H., Sallnäs, O. (2015): How sensitive are ecosystem services in European forest landscapes to silvicultural treatment? – Forests 6: 1666-1695.
[6] Buffa, G., Del Vecchio, S., Fantinato, E., Milano, V. (2018): Local versus landscape-scale effects of anthropogenic land-use on forest species richness. – Acta Oecologica 86: 49-56.
[7] Chabrerie, O., Jamoneau, A., Gallet-Moron, E., Decocq, G. (2013): Maturation of forest edges is constrained by neigh-bouring agricultural land management. – Journal of Vegetation Science 24: 58-69.
[8] Chazdon, R. L., Brancalion, P. H. S., Laestadius, L., Bennett-Curry, A., Buckingham, K., Kumar, C., Moll-Rocek, J., Guimara ˜es Vieira, I. C., Wilson, S. J. (2016): When is a forest a forest? Forest concepts and definitions in the era of forest and landscape restoration. – Ambio 45(5): 538-550.
[9] Chmiel, J. (1993): The flora of vascular plants in the eastern part of the Gniezno Lake District and its anthropogenic transformations in the 19th and 20th centuries. Part II. Plant distribution. – University of Adam Mickiewicz in Poznań, Poznań, 212p. (in Polish).
[10] Decocq, G., Andrieu, E., Brunet, J., Chabrerie, O., De Frenne, P., De Smedt, P., Deconchat, M., Diekmann, M., Ehrmann, S., Giffard, B., Gorriz, Mifsud, E., Hansen, K., Hermy, M., Kolb, A., Lenoir, J., Liira, J., Moldan, F., Prokofieva, I., Rosenqvist, L., Varela, E., Valdés, A., Verheyen, K., Wulf, M. (2016): Ecosystem services from small forest patches in agricultural landscapes. – Current Forestry Reports 2(1): 30-44.
[11] Dzwonko, J. (2008): Guide to phytosociological's research. – Publisher Sorus, Poznań - Kraków, 304p. (in Polish).
[12] Dzwonko, Z. (2015): Herb layer plants as indicators of woodland origin and changes. – Studia i Materiały CEPL w Rogowie 42(1): 27-38.
[13] Ellenberg, H., Weber, H. E., Düll, R., Wirth, V., Werner, W., Paulissen, D. (1991): Central European plant index values. – Scripta Geobotanica, Göttingen, 248p. (in German).
[14] Esseen, P., Hedström, A., Ringvall, A., Harper, K. A., Christensen, P., Svensson, J. (2016): Factors driving structure of natural and anthropogenic forest edges from temperate to boreal ecosystems. – Journal of Vegetation Science 27: 482-492.
[15] Foli, S., Reed, J., Clendenning, J., Petrokofsky, G., Padoch, C., Sunderland, T. C. (2015): To what extent does the presence of forests and trees contribute to food production in humid and dry forest landscapes? – Environmental Evidence 3(1): 1-8.
[16] Forrest, J. R., Thorp, R. W., Kremen, C., Williams, N. M. (2015): Contrasting patterns in species and functional-trait diversity of bees in an agricultural landscape. – Journal of Applied Ecology 52(3): 706-715.

http://www.aloki.hu ● ISSN 1589 1623 (Print) ● ISSN1785 0037 (Online)
DOI: http://dx.doi.org/10.15666/aeer/1902_14731489
© 2021, ALÖKI Kft., Budapest, Hungary

[17] Gamfeldt, L., Snäll, T., Bagchi, R., Jonsson, M., Gustafsson, L., Kjellander, P., Ruiz-Jaen, M. C., Fröberg, M., Stendahl, J., Philipson, C. D., Mikusiński, G., Andersson, E., Westerlund, B., Andrén, H., Moberg, F., Moen, J., Bengtsson, J. (2013): Higher levels of multiple ecosystem services are found in forests with more tree species. – Nature Communication 4: 1340.

[18] Gamrat, R., Gałczyńska, M. (2014): Influence of the forest ecotone structure on the phytodiversity. – Sylwan 158(1): 34-40. (in Polish).

[19] Gamrat, R., Gałczyńska, M., Sotek, Z., Stasińska, M. (2019): The impact of neighbouring ecosystems on species composition in the ecotone of small forest plots: case study in Choszczno Forest Inspectorate in NW Poland. – Russian Journal of Ecology 50: 465-473.

[20] Haddad, N. M., Brudvig, L. A., Clober, T. J., Davies, K. F., Gonzalez, A., Holt, R. D., Lovejoy, T. E., Sexton, J. O., Austin, M. P., Collins, C. D., Cook, W. M., Damschen, E. I., Ewers, R. M., Foster, B. L., Jenkins, C. N., King, A. J., Laurance, W. F., Levey, D. J., Margules, C. R., Melbourne, B. A., Nicholls, A. O., Orrock, J. L., Song, D.-X., Townshend, J. R. (2015): Habitat fragmentation and its lasting impact on Earth's ecosystems. – Science of Advanced Materials 1(2): e1500052.

[21] Hladnik, D., Kobler, A., Pirnat, J. (2020): Evaluation of forest edge structure and stability in peri-urban forests. – Forests 11(3): 338.

[22] Jamoneau, A., Chabrerie, O., Closset-Kopp, D., Decocq, G. (2012): Fragmentation alters beta-diversity patterns of habitat specialists within forest metacommunities. – Ecography 35: 124-33.

[23] Jelonek, T., Arasimowicz-Jelonek, M., Gzyl, J., Tomczak, A., Łakomy, P., Grzywiński, W., Remlein, A., Klimek, K., Kopaczyk, J., Jaszczak, R., Kuźmiński, R. (2019): Influence of former farmland on the characteristics and properties of scots pine (*Pinus sylvestris* L.) tree tissue. – Bioresources 14(2): 3247-3265.

[24] Jia, H. R., Chen, Y., Yuan, Z. L., Ye, Y. Z., Huang, Q. C. (2015): Effects of environmental and spatial het-erogeneity on tree community assembly in Baotianman National Nature Reserve, Henan, China. – Polish Journal of Ecology 63(2): 175-183.

[25] Jia, H. R., Chen, Y., Wang, X. Y., Li, P. K., Yuan, Z. L., Ye, Y. Z. (2019): The relationships among topographically-driven habitats, dominant species and vertical layers in temperate forest in China. – Russian Journal of Ecology 50(2): 172-186.

[26] JL (2014): Regulation of the Minister of the Environment on the Protection of Plant Species. – Journal of Laws 2014 no. 0, item 1409.

[27] Kryszak, A., Maćkowiak, K., Klarzyńska, A., Szczepańska, N., Kryszak, J. (2014): Fluctuation in grasses cover during the growing season in some types of forests. – Grassland Science in Poland 17: 61-71. (in Polish).

[28] Liu, Z., Jia, G., Yu, X. (2020): Variation of water uptake in degradation agroforestry shelterbelts on the North China Plain. – Agriculture, Ecosystems and Environment 287: 106697.

[29] Lõhmus, K., Paal, T., Liira, J. (2014): Long-term colonization ecology of forest-dwelling species in a fragmented rural landscape - dispersal versus establishment. – Ecology and Evolution 4: 3113-3126.

[30] Majewski, M., Marszałek, L. (2020): Forest cover changes over historical times in the area of Lake Jasień (northern Poland) recorded in slope sediments and archival maps - a case study. – Proceedings of the Estonian Academy of Sciences 69(1): 43-52.

[31] Matuszkiewicz, W. (2017): Guide to the identification of plant communities in Poland. – State Scientific Publishers, 3th edition, Warsaw, 540p. (in Polish).

[32] Meszaros, I. (2012): Community pattern in a small scale forest ecotone. – In: Teller, A., Mathy, P., Jeffers, J. N. R. (eds.) Responses of forest ecosystems to environmental changes. Springer, Dodrecht, pp. 906-909.

[33] Nordén, B., Dahlberg, A., Brandrud, T. E., Fritz, Ö., Ejrnaes, R., Ovaskainen, O. (2014): Effects of ecological continuity on species richness and composition in forests and woodlands: a review. – Écoscience 21(1): 34-45.

http://www.aloki.hu ● ISSN 1589 1623 (Print) ● ISSN1785 0037 (Online)
DOI: http://dx.doi.org/10.15666/aeer/1902_14731489
© 2021, ALÖKI Kft., Budapest, Hungary

[34] Oświt, J. (2000): The method of valuation of natural wetlands and the results of its application on selected objects. – IMUZ Press 35, Falenty: 36. (in Polish).
[35] Pieńkowski, P., Podlasiński, M., Szpigiel, M. (2019): Reasons for the occurence of small forest patches within post-glacial areas used for agriculture in northern Poland. – Applied Ecology and Environmental Research 17(5): 11995-12011.
[36] Plue, J., Cousins, S. A. O., De Pauw, K., Diekmann, M., Hagenblad, J., Helsen, K., Hermy M., Liira, J., Orczewska, A., Vanneste, T., Wulf, M., De Frenne, P. (2020): Biological flora of the British Isles: *Poa nemoralis*. – Journal of Ecology 108(4): 1750-1774.
[37] Proesmans, W., Bonte, D., Smagghe, G., Meeus, I., Decocq, G., Spicher, F., Kolb, A., Lemke, I., Diekmann, M., Bruun, H. H., Wulf, M., Van Den Berge, S., Verheyen, K. (2019): Small forest patches as pollinator habitat: oases in an agricultural desert? – Landscape Ecology 34: 487-501.
[38] Schmidt, C. (2015): The forests in Germany. – Federal Ministry of Food and Agriculture, 56p.
[39] Silvertown, J., Dodd, M., Gowing, D., Lawson, C., McConway, K. (2006): Phylogeny and the hierarchical organization of plant diversity. – Ecology 87: 39-49.
[40] Skrajna, T. (2020): Impact of agriculture intensification on the floristic diversity of the forest-field ecotone. – Polish Journal of Ecology 68(1): 47-66.
[41] Stepanovich, I. M. (2019): The invasive potential of synanthropic components of pine forests in Belarus. – Trudy 1(2): 90-98. (in Russian).
[42] Takkis, K., Kull, T., Hallikma, T., Jaksi, P., Kaljund, K., Kauer, K., Kull, T., Kurina, O., Külvik, M., Lanno, K., Liira, J., Melts, I., Pehlak, H., Raet, J., Sammet, K., Sepp, K., Väli, Ü., Laanisto, L. (2018): Drivers of species richness and community integrity of small forest patches in an agricultural landscape. – Journal of Vegetation Science 26(6): 978-988.
[43] Van Dijk, J. (2018): Biodiversity and nature. The Netherlands and the Dutch. – World Regional Geography Book Series, pp. 81-104.
[44] Wysocki, C., Sikorski, P. (2002): Phytosociology applied. – SGGW Press, Warsaw, 449p. (in Polish).
[45] Ziaja, M., Wójcik, T. (2015): Changes in vascular flora of the Rzeszow reservoir after 20 years (SE Poland). – Polish Journal of Environmental Studies 24(4): 1845-1854.

http://www.aloki.hu ● ISSN 1589 1623 (Print) ● ISSN1785 0037 (Online)
DOI: http://dx.doi.org/10.15666/aeer/1902_14731489
© 2021, ALÖKI Kft., Budapest, Hungary

APPENDIX

Table A1. *Phytosociological classification of the founded plant species*

No.	1	2	3	4
Geomorphological unit	**Moraine**	**Sandur**	**Moraine**	**Sandur**
Prior land use	**Field**	**Field**	**Forest**	**Forest**
Cover a [% min., max., av.]	**0, 100, 16**	**100**	**10, 100, 67**	**30, 100, 84**
Cover b [% min., max., av.]	**0, 20, 4**	**0, 40, 14**	**0, 40, 13**	**10, 30, 17**
Cover c [% min., max., av.]	**10, 100, 41**	**100**	**20, 100, 41**	**100**
Cover d [% min., max., av.]	**1, 1, 1**	**1, 1, 1**	**0, 10, 3**	**0, 10, 6**
Constancy S-Coefficient D for 10 phytosociological releve's	**S-D**	**S-D**	**S-D**	**S-D**
I. Cl. *Vaccinio-Piceetea*, O. *Cladonio-Vaccinietalia*				
Pinus sylvestris a	I-88	II-285	II-230	II-248
Vaccinium myrtillus c	.	I-38	II-270	II-53
Pleurozium schreberi d	I-<1	.	I-10	I-20
All. *Dicrano-Pinion*, Ass. *Leucobryo-Pinetum*				
Deschampsia flexuosa c	I-43	V-436	II-245	IV-615
Sorbus aucuparia b	I-<1	III-19	IV-71	V-12
Lepraria incana d	.	.	I-20	II-38
Leucobryum glaucum d	.	.	.	II-10
Rumex acetosella c	I-<1	III-1	.	I-1
O. *Vaccinio-Piceetalia*, All. *Piceion abietis*				
Agrostis capillaris c	.	III-278	I-18	III-11
Maianthemum bifolium c	I-0.1	.	I-90	.
Dryopteris filix-mas c	II-63	III-1	III-36	II-36
Betula pendula a	I-18	I-38	IV-133	III-88
Populus tremula a	I-80	I-18	I-75	.
Picea abies a	I-88	.	I-63	I-10
Betula pubescens b	.	.	.	I-75
Veronica officinalis c	I-<1	II-53	I-18	.
Pteridium aquilinum c	.	I-<1	I-<1	I-35
Holcus mollis c	I-<1	II-15	.	I-<1
II. Cl. *Querco-Fagetea*				
Quercus robur a	.	.	III-136	III-1
Alnus glutinosa a	.	I-1	I-150	I-35
Impatiens noli-tangere c	.	I-18	.	II-76
Oxalis acetosella c	I-75	.	II-93	.
Milium effusum c	I-<1	.	I-73	II-11
Fagus sylvatica a	I-18	.	II-73	.
Scirpus sylvaticus c	I-40	.	.	.
Hypogymnia physodes d	.	.	.	II-38
Quercus robur b	I-23	III-1	.	.
Carex sylvatica c	.	.	I-18	I-<1
Acer platanoides a	.	I-1	I-18	.
Rubus caesius b	.	.	II-18	I-18
Geum rivale c	I-18	.	I-<1	I-<1
Hedera helix c	.	.	I-18	.
III. Cl. *Epilobietea angustifolii*				
Rubus idaeus b	I-<1	IV-1	III-170	V-257
Fragaria vesca c	I-<1	I-<1	I-55	I-<1
Calamagrostis epigejos c	.	II-37	I-1	I-1
Sambucus nigra b	I-18	I-<1	I-<1	I-<1

http://www.aloki.hu ● ISSN 1589 1623 (Print) ● ISSN1785 0037 (Online)
DOI: http://dx.doi.org/10.15666/aeer/1902_14731489
© 2021, ALÖKI Kft., Budapest, Hungary

IV. Cl. *Molinio-Arrhenatheretea*				
Trifolium pratense c	II-98	.	.	.
Equisetum palustre c	I-88	.	.	.
Lotus corniculatus c	II-53	.	.	.
Juncus effusus c	II-38	.	I-1	.
Deschampsia caespitosa c	II-56	.	I-<1	.
Caltha palustris c	I-<1	.	I-35	.
Ranunculus acris c	III-1	.	I-<1	.
Cirsium oleraceum c	I-35	.	.	.
Agropyron repens c	I-23	I-<1	.	.
Daucus carota c	II-18	.	.	.
Heracleum sphondylium c	II-18	.	.	.
Trifolium dubium c	II-18	.	.	.
Stellaria graminea c	I-5	II-1	.	I-<1
Knautia arvensis c	I-<1	II-1	I-<1	.
Dactylis glomerata c	II-1	I-<1	I-<1	.
V. Cl. *Artemisietea vulgaris*				
Urtica dioica c	III-195	I-<1	I-63	.
Aegopodium podagraria c	I-63	.	II-88	.
Geum urbanum c	II-18	.	III-88	.
Galium aparine c	III-63	I-<1	I-18	.
Chelidonium majus c	.	.	I-38	.
Glechoma hederacea c	I-<1	.	I-38	.
Geranium robertianum c	I-<1	.	II-35	I-<1
Rumex obtusifolius c	I-35	.	.	.
Artemisia vulgaris c	II-23	.	.	.
Epilobium hirsutum c	II-5	.	I-<1	.
Melilotus officinalis c	I-18	.	.	.
VI. Cl. *Phragmitetea*				
Phragmites australis c	I-61	.	.	.
Carex elata c	I-31	.	.	I-<1
Typha latifolia c	I-43	.	.	.
Salix cinerea b	I-38	.	.	.
Carex disticha c	I-38	.	.	.
Others:				
Polygonum amphibium c	I-18	.	.	.
Vinca minor c	.	.	I-18	.
Solidago virgaurea c	.	.	I-16	I-<1
Hieracium pilosella c	.	II-5	I-<1	.
Anthoxanthum odoratum c	.	II-5	.	I-5

The species occurring in the I constancy class and the coverage factor below 10: I. *Calamagrostis arundinacea* c (1, 3, 4), *Convallaria majalis* c (1), *Dicranum scoparium* d (3, 4), *Epilobium montanum* (1-4), *Luzula pilosa* c (4), *L. sylvatica* c (4), *Melampyrum nemorosum* c (3), *Monotropa hypopitys* c (2), *Mycelis muralis* c (1, 2), *Pyrola rotundifolia* c (2), *Quercus petraea* a (1, 2); II. *Ajuga reptans* c (3), *Asarum europaeum* c (1), *Calamagrostis canescens* c (2), *Campanula persicifolia* c (2, 3), *Corydalis cava* c (1), *Corylus avellana* b (1), *Crataegus monogyna* b (1), *Equisetum sylvaticum* c (1), *Festuca gigantea* c (1), *Ficaria verna* c (1), *Fraxinus excelsior* b (1), *Hepatica nobilis* c (1, 3), *Humulus lupulus* c (1), *Hypericum perforatum* c (1, 3), *Hypnum cupressiforme* d (3), *Hypocenomyce scalaris* d (4), *Isopyrum thalictroides* c (1), *Larix decidua* a (4), *Luzula luzuloides* c (3, 4), *Lycopus europaeus* c (3), *Malus sylvestris* a (1), *Padus serotina* b (4), *Paris quadrifolia* c (1), *Petasites albus* c (1), *Poa nemoralis* c (1, 3), *Polygonatum odoratum* c (1), *Pulmonaria obscura* c (3), *Ranunculus lanuginosus* c (1-3), *R. repens* c (1), *Rubus plicatus* b (4), *Salix alba* a (1), *Scrophularia nodosa* c (3), *Solanum dulcamara* c (1-4), *Stachys sylvatica* c (1), *Stellaria nemorum* c (2, 4), *Symphoricarpos albus* b (1), *Taxus baccata* b (4),

http://www.aloki.hu ● ISSN 1589 1623 (Print) ● ISSN1785 0037 (Online)
DOI: http://dx.doi.org/10.15666/aeer/1902_14731489
© 2021, ALÖKI Kft., Budapest, Hungary

Tussilago farfara c (1), *Viola reichenbachiana* c (1, 3); III. *Centaurium umbellatum* c (1), *Epilobium angustifolium* c (1, 2, 4), *Omalotheca sylvatica* c (1-3), *Senecio sylvaticus* c (1, 3); IV. *Achillea millefolium* c (2), *Arrhenatherum elatius* c (2, 4), *Briza media* c (1), *Bromus hordeaceus* c (2), *Cirsium palustre* c (1), *Cynosurus cristatus* c (1), *Festuca arundinacea* c (1), *F. rubra* c (1-3), *Filipendula ulmaria* c (1), *Geranium palustre* c (1, 3), *Holcus lanatus* c (1, 2), *Lathyrus pratensis* c (1, 2), *Leontodon hispidus* c (2), *Lychnis flos-cuculi* c (1), *Lysimachia vulgaris* c (1), *Lythrum salicaria* c (1), *Mentha arvensis* c (1), *Myosotis palustris* c (1), *Parnassia palustris* c (1), *Phleum pratense* c (1), *Pimpinella major* c (1), *Plantago lanceolata* c (1), *Poa pratensis* c (2), *P. trivialis* c (1), *Potentilla anserina* c (1), *P. reptans* c (1), *Prunella vulgaris* c (1), *Rorippa sylvestris* c (1), *Rumex acetosa* c (2, 4), *Selinum carvifolia* c (2), *Stellaria palustris* c (1), *Taraxacum officinale* c (1), *Trifolium hybridum* c (1), *T. repens* c (1), *Vicia cracca* c (1); V. *Anthriscus sylvestris* c (1, 3, 4), *Arctium lappa* c (1), *Calystegia sepium* c (1, 2), *Cichorium intybus* c (1), *Cirsium vulgare* c (1, 3), *Erysimum cheiranthoides* c (1), *Eupatorium cannabinum* c (1), *Juglans regia* b (1), *Lamium album* c (1), *L. purpureum* c (4), *Lapsana communis* c (1), *Malva neglecta* c (1), *Melilotus alba* c (1), *Moehringia trinervia* c (4), *Picris hieracioides* c (1); VI. *Acorus calamus* c (1), *Carex acutiformis* c (1), *Galium palustre* c (1), *Glyceria fluitans* c (1), *Phalaris arundinacea* c (1), *Rumex hydrolapathum* c (1), *Scutellaria galericulata* c (1); Others (*Bidentetea tripartiti*, *Festuco-Brometea*, *Koelerio glaucae-Corynephoretea canescentis*, *Nardo-Callunetea*, *Potametea*, *Stellarietea mediae*, *Trifolio-Geranietea sanquinei*): *Astragalus glycyphyllos* c (4), *Bromus inermis* c (2), *Calluna vulgaris* c (4), *Centaurea scabiosa* c (2), *Cerastium arvense* c (2), *Cladonia coniocraea* d (4), *C. fimbriata* d (4), *C. macilenta* d (1), *C. subulata* d (1), *Dianthus carthusianorum* c (2), *Equisetum arvense* c (1), *Erodium cicutarium* c (1, 3), *Galium mollugo* c (1, 3), *Hieracium umbellatum* c (2, 3), *Hottonia palustris* c (1), *Jasione montana* c (2), *Lathyrus sylvestris* c (1), *Lupinus polyphyllus* c (1, 2), *Luzula campestris* c (3), *Myosotis arvensis* c (1, 2), *Nardus stricta* c (4), *Odontites serotina* c (1), *Origanum vulgare* c (1), *Polygonum hydropiper* c (1), *P. persicaria* c (1), *Potentilla argentea* c (1), *P. erecta* c (2), *Senecio vulgaris* c (1), *Silene vulgaris* c (2), *Sonchus asper* c (1, 2), *Thymus serpyllum* c (4), *Veronica chamaedrys* c (1, 2, 3), *Vicia hirsuta* c (1), *Viola canina* c (4).

Cl.: class, O.: order, All.: alliance, Ass.: association; constancy S: I: proportional participation of species < 20%, II: 40-20%, III: 60-40%, IV: 80-60 %, V: 100-80%; D: the coefficients of cover (from 1 to 8 750) were estimated for 10 phytosociological releve's, .: not present; a: trees, b: bushes, c: herbs, d: mosses and lichens; 1-4: information on which surface the species was recorded; min.: minimum values, max.: maximum values, av.: average values

http://www.aloki.hu ● ISSN 1589 1623 (Print) ● ISSN1785 0037 (Online)
DOI: http://dx.doi.org/10.15666/aeer/1902_14731489
© 2021, ALÖKI Kft., Budapest, Hungary

IMPROVEMENTS IN THE GROWTH, QUALITY, AND YIELD OF WUYI ROCK TEA (*CAMELLIA SINENSIS*) AFTER BREEDING EARTHWORMS IN SITU IN TEA GARDENS IN CHINA

HUO, D.[1] – YAN, K. Q.[1] – MENG, F. H.[1] – ZHANG, H. M.[1] – SONG, Y. Z.[1] – HONG, Y. C.[1] – LI, L.[1] – CAI, P. M.[1,2,3*]

[1]*Department of Horticulture, College of Tea and Food Science, Wuyi University, Wuyishan 354300, China*

[2]*Biological Control Research Institute, College of Plant Protection, Fujian Agriculture and Forestry University, Fuzhou 350002, China*

[3]*Key Laboratory of Biopesticide and Chemical Biology, Ministry of Education, Fuzhou 350002, China*

**Corresponding author*
e-mail: caipumo@qq.com; phone: +86-150-8045-6908

(Received 27th Nov 2020; accepted 27th Jan 2021)

Abstract. This study aimed to evaluate in situ the effects of earthworms on the growth, quality, and yield of the tea plant, *Camellia sinensis* (L.) O. Kuntze. Our results show that the incorporation of earthworms and organic waste in the soil significantly enhanced both the tea bud density and hundred-bud weight for both summer and autumn tea, but did not significantly influence the number of leaves per shoot or single leaf area. Furthermore, earthworms enhanced the quality of summer and autumn tea, in terms of significantly higher amino acid content, lower polyphenol and caffeine content, and maintenance of the total water extract content. Principal component analysis found that the four groups of samples were well separated at the first principal component and that free amino acids and polyphenols had the greatest effect between the treatment and the control group. Furthermore, these two parameters were also the primary reasons for differences between summer and autumn teas under the same treatment. Therefore, in situ earthworm breeding could be a promising alternative to chemical fertilizers and assist in the sustainable, pollution-free production of tea since it can improve both the quality and yield of tea and eliminate considerable amount of organic waste.
Keywords: *earthworm inoculation, organic fertilization, summer tea, autumn tea, quality and production*

Introduction

Tea, one of the world's most popular drinks, contains numerous bioactive ingredients which are responsible for its pleasurable taste and health-promoting benefits (Wei et al., 2018). The tea plant, *Camellia sinensis* (L.) O. Kuntze, originates from southwest China and its leaves have been used to make many kinds of tea for thousands of years. Today, it is cultivated all over the world (Kingdom-Ward, 1950; Taniguchi et al., 2014). Over the past decade, the worldwide production of tea has steadily increased, with the total cultivated area in 2020 being 66% greater than in 2010, and has achieved 5.3 million tons of tea from 3.5 million ha across more than 50 tea-cultivating countries (www.fao.org/faostat). This yield increase can be attributed to many factors, including the use of modern technical equipment, improvements in agronomic practices, adaptation of inorganic fertilizers and pesticides, huge capital investment, and the use of newly developed clones with higher production capabilities (Giri, 1995). However, intensive agriculture is often criticized for its detrimental influences on the environment and human health, particularly through its use of chemical fertilizers (Bertrand et al., 2015). These

http://www.aloki.hu ● ISSN 1589 1623 (Print) ● ISSN 1785 0037 (Online)
DOI: http://dx.doi.org/10.15666/aeer/1902_14911503
© 2021, ALÖKI Kft., Budapest, Hungary

fertilizers can damage the soil structure and reduce soil fertility by decreasing the nitrogen and carbon content (Ngo et al., 2012). Furthermore, chemical fertilizers have adverse effects on animal and human health due to their heavy metal content which can pass through the food chain (Vu et al., 2007). As a result, interest in organic fertilizers is growing, and proper organic amelioration involving composting, vermicomposting, and in situ earthworm breeding have become promising biological avenues for enhancing the growth, quality and production of tea.

Most tea growing regions are in hilly terrain. The soil in these regions this is often vulnerable to constant leaching from heavy rainfall, adversely affecting its biological and physicochemical parameters (Giri, 1995). Such effects can include reduced organic matter content, decreased water-holding capacity, acidification, lower cation exchange, soil surface compaction, soil erosion, nutrient leaching, and loss of important organisms from the soil (Giri, 1995). The incorporation of compost with the soil is considered a form of sustainable agriculture, contributing to improvements in soil fertility and plant nutrition (Caravaca et al., 2002). The presence of earthworms is of great interest since, as an important functional group in soil, they are marvelous in their ability to improve its structure, microbe diversity, and physicochemical properties and help plant development by their peculiar feeding, burrowing, and casting activities (Edwards and Bohlen, 1996). Earthworms have been present in soils for several hundred million years and constitute more than 80% of the soil invertebrate biomass in most terrestrial ecosystems (Lavelle and Spain, 2001); therefore, earthworms very likely co-evolved with plants (Bertrand et al., 2015). The positive impact of earthworms on plant growth and health has been known for over a century, with works dating as far back as the late 1800s (Darwin, 1881). Indeed, the effect that earthworms exert on primary yield has been fully explored both in the laboratory and the field, with some investigations taking place over several years (Giri, 1995; Blanchart et al., 1997). However, there are two previous studies which found that earthworms could have an unfavorable impact on plant growth (Brown et al., 1999, 2004). The authors found that in 4% of 246 assays (performed in tropical countries) there was a 20% decrease in crop production correlating with the occurrence of earthworms, and that several environmental determinants like soil type, soil texture and carbon content could account for variation in the productive response of the plants.

In China, the application and promotion of earthworms in tea plantations is low in comparison to the other major tea-growing country, India. Earthworms are only used over 0.4% China's tea-growing area (Kamel et al., 2002; Zhang et al., 2018), heavily concentrated in southern China such as Guangdong and Hainan Province (Tang et al., 2008, 2011, 2016; Zhuo et al., 2007, 2017). Until now, rare work has been undertaken in the other main tea-growing areas such as Fujian, Yunnan and Sichuan Provinces.

The present study focuses on Wuyi Mountain, situated in the north of Fujian Province. It is a UNESCO World Heritage site famous for oolong tea; the consumption of this tea has increased substantially worldwide in recent years due to its favorable taste and pleasant aroma (Chen et al., 2011). It is widely accepted that abundant earthworm populations are beneficial to agricultural production; however, these earthworm-mediated ecological services may not always enhance the performance of a particular cropping system because the effects are both species- and site-dependent (Bertrand et al., 2015). Therefore, the purpose of our research was to determine in situ the effects of earthworm breeding in a tea plantation on Wuyi Mountain, measured in terms of the growth, quality, and yield of oolong tea. We thus considered their use as a potential organic fertilizer as a substitute for chemical fertilizer to improve tea quality and yield.

http://www.aloki.hu ● ISSN 1589 1623 (Print) ● ISSN 1785 0037 (Online)
DOI: http://dx.doi.org/10.15666/aeer/1902_14911503
© 2021, ALÖKI Kft., Budapest, Hungary

Materials and methods

Test site description

The research was conducted from March to September 2019 at the Tea Science and Education Park of Wuyi University (27°43'38"N and 118°0'2"E) which covers an area of 0.4 ha (width 80 m × length 50 m, *Fig. 1*). The area is located at northern Fujian Province, China and characterized by a subtropical monsoon climate with an average annual precipitation of 1926.9 mm; most of the rainfall is concentrated in the wet season between March and June. The relative humidity (RH) of the experimental site is moderately high, ranging from 64 to 85%, and the mean temperature was 22.6 °C for whole year (Municipal Government of Wuyishan, 2019). Weeds were manually removed using a hand hoe wherever needed. The initial properties of the soil were investigated and are shown in *Table 1*.

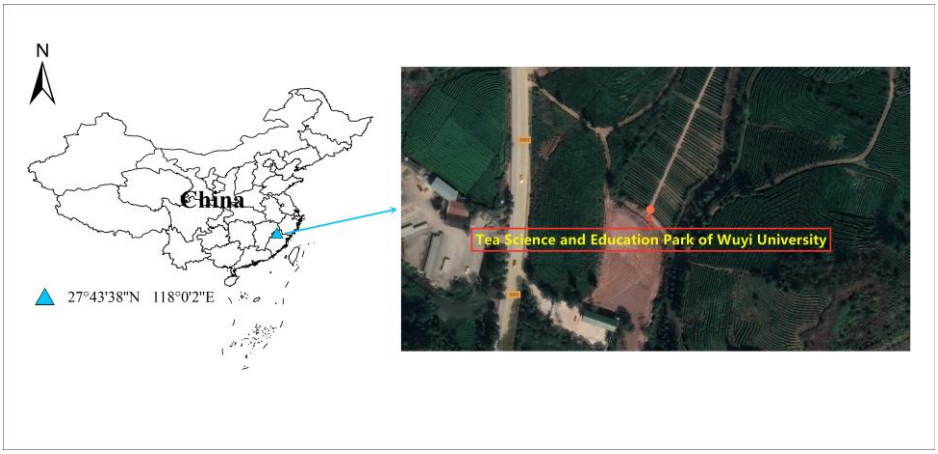


Figure 1. *Map of study area*

Table 1. *Initial chemical properties of the soil at the experimental site*

Index	Initial status of soil
pH value	4.05
Available N (mg kg^{-1} soil)	20.17
Available P (mg kg^{-1} soil)	10.85
Available K (mg kg^{-1} soil)	53.98
Organic carbon (%)	1.74

Earthworms and materials

In the present experiment, five-year-old *C. sinensis* cv. Shuixian tea plants were used. Based on our previous field, the predominant indigenous earthworm species for the local tea gardens is *Eisennia foetida* Savigny (unpublished data); this species was reared under laboratory conditions in accordance with the procedure by Dai (2014). The organic fertilizer used in the experiment was cow dung, which was naturally decomposed for one month prior to the experiment; the water and total nitrogen content was about 50% and 1%, respectively. Tea leaf litter was collected from tea garden ground and naturally dried in the field, with a total nitrogen content was about 2%.

http://www.aloki.hu ● ISSN 1589 1623 (Print) ● ISSN 1785 0037 (Online)
DOI: http://dx.doi.org/10.15666/aeer/1902_14911503
© 2021, ALÖKI Kft., Budapest, Hungary

Experimental design and treatments

The experimental area was divided into six plots, each covering an area of 5 × 5 m. To minimize the effects caused by other plots and surroundings, each plot was separated by concrete boards made from calcium silicate, and were 0.5 m apart. The boards were placed 0.6 m deep into the soil with 0.2 m of the board showing above the ground in order to prevent the escape of earthworms and fertilizer runoff. The treatment group plots contained organic fertilizer mixed with composting species of *E. foetida*, and the control group plots contained organic fertilizer alone without any earthworms. There were three replicates of each treatment and control plot, and these six plots were randomly arranged in the experimental area (*Fig. 2*). The field pattern of in situ earthworm breeding is shown in *Figure 3*. Finally, tea leaf litter and a sun shading net were placed upon the bed, and organic waste and water were provided regularly in order to create a better environment for the development and reproduction of the earthworms. The introduction of earthworms and fertilizers to the beds was performed in early March. Field management practices such as watering and artificial weeding were used for all plots in the tea garden to ensure the normal activity of earthworms. No chemical pesticide was applied during the experiment.

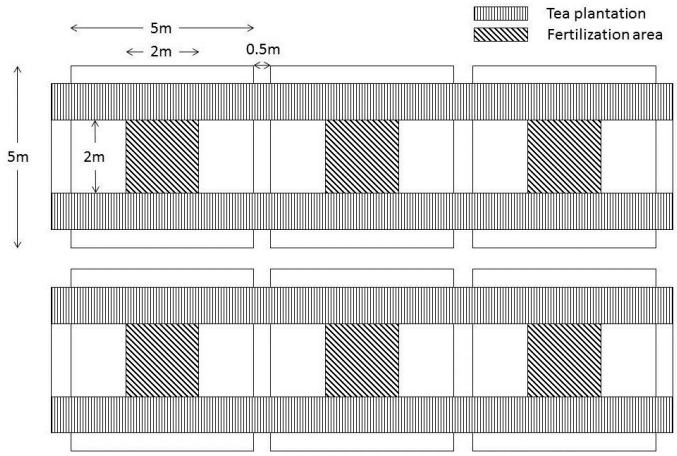


Figure 2. *Diagram of the experimental area. Treatment and control groups were randomly arranged into six plots*

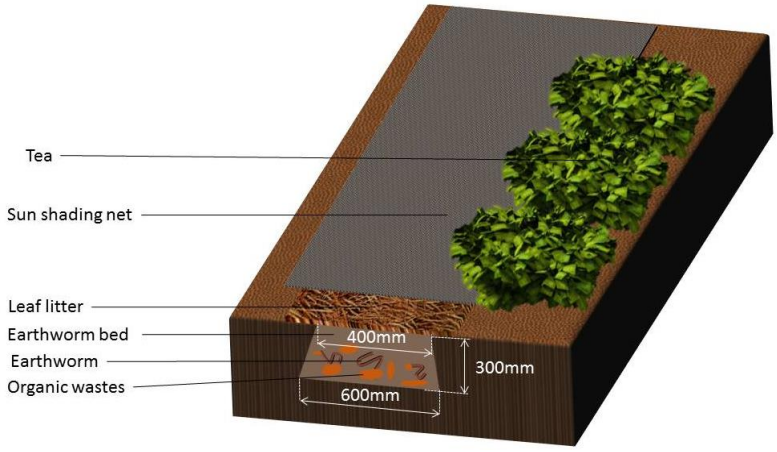


Figure 3. *The field pattern of in situ earthworm breeding in each plot*

http://www.aloki.hu ● ISSN 1589 1623 (Print) ● ISSN 1785 0037 (Online)
DOI: http://dx.doi.org/10.15666/aeer/1902_14911503
© 2021, ALÖKI Kft., Budapest, Hungary

Earthworm bed (length: 6 m, surface width: 0.4 m; bottom width: 0.6 m; height: 0.3 m) was prepared approximately 0.5 m away from the tea plantation for each plot. For each bed, 5 kg/m^3 of organic waste, derived from the process of manufacturing beer, was supplied to the bottom of the bed. In the treatment plots, 20 g of *E. foetida* were introduced into the central of bed.

Assessments

Determination of the growth indicators of tea

Several months after introducing the earthworms, tea leaves that collected in early June (from 1st to 5th June) were named summer tea, while tea leaves that collected in early September (from 1st to 5th September) were named autumn tea. The number of leaves on mature shoots, leaf area, one-hundred-bud weight, and bud density were evaluated during the summer (summer tea) and autumn (autumn tea) tea-picking season as mentioned below. All measurements were performed in triplicate for each plot.

Leaf number and area: Twenty mature shoots were randomly picked from each plot and the number of leaves on each shoot were calculated. The width and length of the leaves were gauged and the area of one leaf was calculated according to the following formula: length × width × 0.7 (Zhang and Wang, 2006).

Bud density: The number of buds in a 0.1 × 0.1 m area wooden-frame was counted.

One hundred bud weight: One hundred tea buds were randomly selected from each plot and then weighed in total.

After the above assessments, fresh leaves were collected fixed at a temperature of 105 °C for 1 h, followed by drying at 80 °C to a constant weight. They were then ground, screened using a 60-mesh sieve, and refrigerated at -20 °C prior to the tea quality assessments.

Determination of the quality of tea leaves

For both summer and autumn tea-picking season, the total mass of water extracts, polyphenols and free amino acid were assessed in accordance with the National Standards of People's Republic of China. All measurements were performed in triplicate for each plot.

Assessment of tea water extract

The tea leaves were first ground and approximately 2 g of leaf sample (measured with an analytical balance accurate to 0.0001 g) was placed in an aluminum box; the initial weight of each tea leaf sample was recorded as m_0. The samples were then placed in an electric drying oven (DH-9146A, Suzhou Weir Experimental Supplies Co., Ltd, PR China), held at 120 °C for 60 min, and then transferred to a drier (IPC250-1, Hebei Rixiang Experimental Supplies Co., Ltd, PR China) for cooling to room temperature. The weight of the dried tea sample was recorded as m_1. The dried tea sample was then soaked in 300 mL of boiling distilled water (100 °C) for 45 min using a water bath, and manually shaken every 10 min. The leach liquor was then immediately subjected to decompression filtration and the tea residue was washed multiple times using a small amount of 100 °C distilled water. The tea residue was transferred to a new aluminum box and placed in an oven for drying at 120 °C for 60 min, removed for 60 min cooling,

http://www.aloki.hu ● ISSN 1589 1623 (Print) ● ISSN 1785 0037 (Online)
DOI: http://dx.doi.org/10.15666/aeer/1902_14911503
© 2021, ALÖKI Kft., Budapest, Hungary

again placed in the oven at 120 °C for 60 min, and finally transferred to the drier for cooling to room temperature. The weight of this treated tea residue was recorded as m_2. The content of water extract was calculated using the following formula (GB/T 8305-2013, 2013):

$$(1-\frac{m_2}{m_0 \times m_1}) \times 100\%$$

Assessment of polyphenol content

Tea samples of 0.2 g were blended in 5 mL of 70% (v/v) methanol preheated to 70 °C. The polyphenol content was determined using Folin-Ciocalteu reagent and checked with a spectrophotometer (UV2900, Sunny Optical Technology Co., Ltd., China) at 765 nm. Gallic acid was used as the standard (GB/T 8313-2008, 2008).

Assessment of total free amino acid content

The free amino acid content was assessed by combining 1 mL of tea infusion, 0.5 mL of phosphate-buffered solution (pH 8.0) and 0.5 mL of 2% ninhydrin solution including 0.8 mg/mL of tin chloride in a 25-mL volumetric flask. The optical density of the solution was determined using the UV2900 spectrophotometer at 570 nm (GB/T 8314-2013, 2013).

Assessment of caffeine content

The process for extracting caffeine from tea samples was similar to that for free amino acids. The caffeine content was measured according to the method described by Wang et al. (2011) using a HPLC system (SPD-20A, Shimadzu, Japan) with a UV detector (LC-20AT, Shimadzu, Japan), RPC18 column (5 um, 250 mm × 4.6 mm i.d.) and analytical software.

Assessment of soluble sugar content

The soluble sugar content was determined based on the procedure proposed by Zhou et al. (2017). In order to extract the sugar content, tea leaf samples each weighing 0.3 g were soaked in 450 mL of boiling (100 °C) distilled water and kept at this temperature for 45 min in a water bath. The whole 450 mL of samples were then centrifuged for 4 min at 3500 × *g*. After collecting the tea infusion by vacuum suction filtration, water was added to make a final volume of 500 mL. The soluble sugar content was measured against a standard curve of glucose solution with concentrations ranging from 50 to 1000 ug/mL.

Statistical analysis

Statistical analysis was performed using SPSS Statistics 17.0 (SPSS, Inc., Chicago, Illinois, USA); significant differences between the means of replicates were evaluated by an independent sample t-test with a significance level of $P \leq 0.05$. Graphs were created using GraphPad Prism 7.0 (GraphPad Software, San Diego, CA, USA). SIMCA-P (Sartorius Stedim Data Analytics AB, Umeh, Sweden) was used for principal component analysis.

http://www.aloki.hu ● ISSN 1589 1623 (Print) ● ISSN 1785 0037 (Online)
DOI: http://dx.doi.org/10.15666/aeer/1902_14911503
© 2021, ALÖKI Kft., Budapest, Hungary

Results

Tea growth and yield

As shown in *Figure 4*, the addition of earthworms to the soil significantly enhanced the tea bud density and hundred-bud weight; these positive effects were observed both in summer and autumn tea (bud density: summer tea, F = 0.582, df = 4, t = 4.243, P = 0.013; autumn tea, F = 2.882, df = 4, t = 5.588, P = 0.005; hundred-bud weight: summer tea, F = 0.542, df = 4, t = 4.243, P = 0.023; autumn tea, F = 3.152, df = 4, t = 7.102, P = 0.002). However, for both summer and autumn tea, leaf number per shoot and single leaf area were not significantly different between the control and treatment groups (leaf number per shoot: summer tea, F = 0.571, df = 4, t = 1.044, P = 0.492; autumn tea, F = 1.96, df = 4, t = 0.64, P = 0.234; single leaf area: summer tea, F = 0, df = 4, t = 0.766, P = 0.487; autumn tea, F = 1.469, df = 4, t = 2.553, P = 0.292).

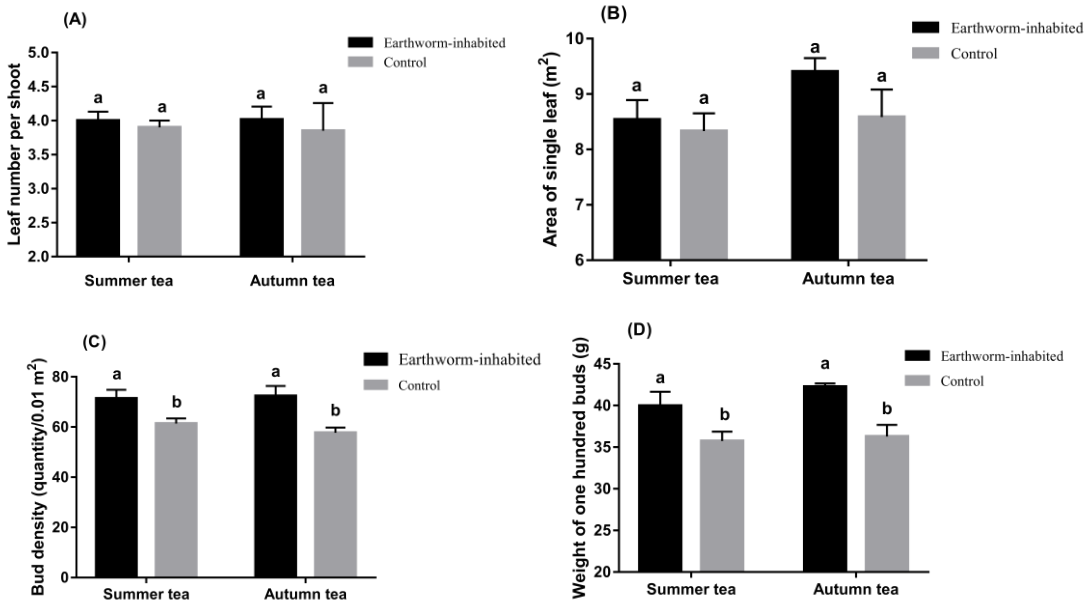


Figure 4. *Growth indicators of summer and autumn tea for the treatment and control groups. Data are shown as mean ± SD. Different letters above the bars indicate significant differences (independent sample t-test, P < 0.05)*

Tea quality

As shown in *Figure 5A* and *B*, there were no significant differences between the control and treatment group on water extract content or soluble sugar for summer and autumn tea (water extracts: summer tea, F = 9.119, df = 4, t = -2.789, P = 0.051; autumn tea, F = 5.841, df = 4, t = -0.74, P = 0.5; soluble sugar: summer tea, F = 0.87, df = 4, t = 3.611, P = 0.404; autumn tea, F = 0.447, df = 4, t = 0.683, P = 0.54). As shown in *Figure 5C*, in situ earthworm breeding significantly increased the total free amino acid content for both summer and autumn tea (summer tea, F = 0.086, df = 4, t = -5.124, P = 0.007; autumn tea, F = 0, df = 4, t = -2.99, P = 0.041). As shown in *Figure 5D, E* and *F*, the polyphenol to amino acid ratio and the content of caffeine and polyphenols for summer and autumn tea were significantly less in the experimental group (caffeine: summer tea, F = 9.799, df = 4, t = -3.771, P = 0.035; autumn tea, F = 9.728, df = 4, t = -

http://www.aloki.hu ● ISSN 1589 1623 (Print) ● ISSN 1785 0037 (Online)
DOI: http://dx.doi.org/10.15666/aeer/1902_14911503
© 2021, ALÖKI Kft., Budapest, Hungary

2.557, P = 0.036; polyphenols: summer tea, F = 0.015, df = 4, t = -4.792, P = 0.001; autumn tea, F = 2.761, df = 4, t = -4.57, P = 0.002; polyphenol to amino acid ratio: summer tea, F = 1.307, df = 4, t = -5.265, P = 0.006; autumn tea, F = 1.865, df = 4, t = -4.431, P = 0.011).

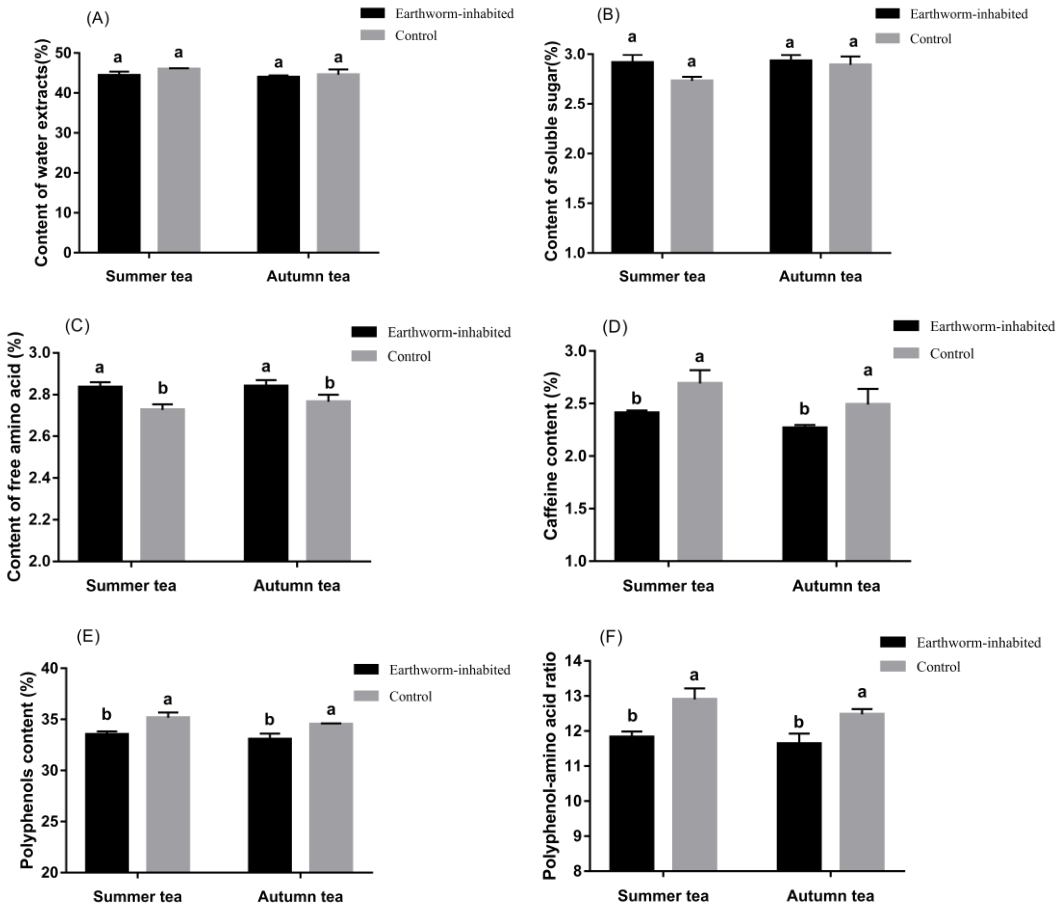


Figure 5. *Quality indicators of summer and autumn tea for the treatment and control groups. The quality parameters includes water extract content (A), soluble sugar content (B), free amino acid content (C), caffeine content (D), polyphenol content (E) and polyphenol to amino acid ratio (F). Bars show mean ± SD and the same letters above the bars indicate no significant differences (independent sample t-test, P < 0.05)*

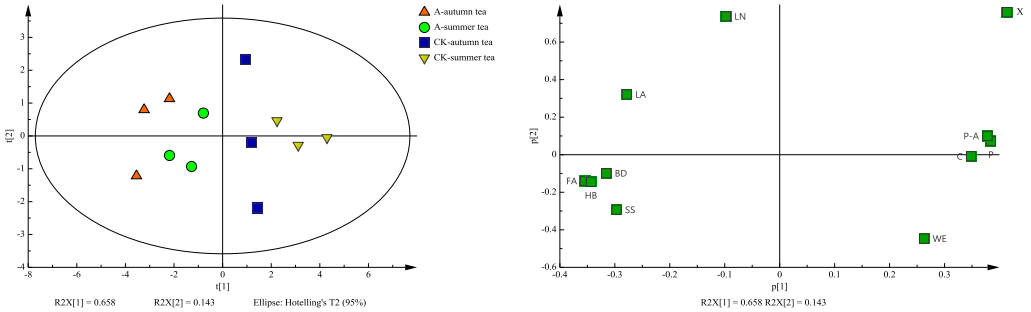
Principal component analysis

From the score graph (*Fig. 6A*), the four sample groups are well separated for the first principal component with a 65.8% model contribution rate. For the first principal component, treated autumn tea, treated summer tea, control autumn tea and control summer tea were in order from the negative to the positive direction. For the second principal component, the separation of the four sample groups was not clear, with a 14.3% model contribution rate.

From the perspective of load graph (*Fig. 6B*), the parameters that contributed more to the first principal component are FA (free amino acid), HB (hundred bud weight), BD (bud density), C (caffeine), P-A (polyphenol to amino acid ratio) and P (polyphenols).

http://www.aloki.hu ● ISSN 1589 1623 (Print) ● ISSN 1785 0037 (Online)
DOI: http://dx.doi.org/10.15666/aeer/1902_14911503
© 2021, ALÖKI Kft., Budapest, Hungary

The parameters that contributed more to the second principal component are LN (leaf number), WE (water extracts), LA (leaf area) and SS (soluble sugar). The differences between the control group and treatment group mainly came from FA, HB, C, P-A and P; of these FA and P had more significant roles between control and treatment group, meanwhile these two parameters made the great contribution to different season tea under the same treatment.



A **B**

Figure 6. *Principal component analysis for yield and quality components of tea treated with in situ earthworm breeding. LN, leaf number; LA, leaf area; BD, bud density; FA, free amino acid; HB, hundred-bud weight; SS, soluble sugar; P-A, polyphenols-amino acid; P, polyphenols; C, caffeine; WE, water extracts*

Discussion

Water extracts, free amino acid, polyphenols, caffeine and soluble sugar content are very important indices of tea quality. Indeed, the flavor of a particular tea comes from the balance of these components in the tea leaves (Chen et al., 2010). During the present field evaluation, it was found that in situ earthworm breeding significantly enhanced the tea quality because it significantly increased the content of free amino acids, reduced the content of caffeine and polyphenols, and maintained the total content of water-soluble substances. Lower caffeine and polyphenol contents in particular are good indicators for tea quality since high levels of these components tend to make tea infusions bitter and astringent (Zhang and Wei, 2012). Our results are consistent with other studies on the effect of earthworms on tea plants in other tea-producing regions of China (Tang et al., 2011; Zhou et al., 2017).

Amino acids are the products of nitrogen metabolism in tea plants, which are synthesized in the roots and transported to the young shoots. Tea plants growing in fertile soil and with well-developed roots can produce more amino acids which generally have a fresh and slightly sweet taste. Moreover, they are important ingredients that contribute to the pleasant aroma of tea. Thus, a greater free amino acid content in the plant indicates that the infusion will have a superior aroma and taste (Tang et al., 2011). In our study, the free amino acid content for both summer and autumn tea were increased in the presence of earthworms. Based on our unpublished data, the results demonstrated that inoculating the soil with earthworms significantly enhanced soil fertility, which contributed to the tea plant absorbing more nitrogen from the soil. The term “water extracts” refer to total amount of water-soluble ingredients in tea and contains the following nine groups: alkaloids, polyphenols, free amino acids and proteins, lipids, carbohydrates, vitamins, pigments, minerals, and aromatic compounds.

http://www.aloki.hu ● ISSN 1589 1623 (Print) ● ISSN 1785 0037 (Online)
DOI: http://dx.doi.org/10.15666/aeer/1902_14911503
© 2021, ALÖKI Kft., Budapest, Hungary

These are positively related to the quality of the tea infusion, considering factors such as color, aroma, persistence, and taste (Chen et al., 2010), where persistence is an explanation of the number of one tea can be brew. In this study, although some quality indices were lower in earthworm-treated groups, the content of water-soluble ingredients were not significantly different between the treatment and control groups. The positive correlation between earthworm and plant growth is not systematic, but the primary reason may be the occurrence of earthworm casts, which are also known as vermicompost. The positive effects of vermicompost application for increasing crop quality have been investigated in other horticultural settings (Xiang et al., 2016).

In our study, in situ earthworm breeding significantly promoted tea plant growth and yield; this treatment led to a higher bud density and heavier hundred bud weight, while buds were generally utilized to produce tea and their weight was considered as the one of important quality parameter of tea. Our findings are in-line with other research on the effect of earthworms on tea plants in other tea-producing regions of China (Tang et al., 2008; Zhuo et al., 2007) or in other above-ground plant communities such as *Carica papaya* L., *Plantago lanceolata* L. and *Trifolium repens* L. (Xiang et al., 2016). The following mechanisms may account for these results.

First, earthworm activities can improve the soil structure (e.g. increase porosity) and nutrient content, therefore supplying a better medium for root development; their actions change the soil's biological, chemical, and physical characteristics which helps the plant to develop (Lee, 1985). A previous study found that soil aggregation and water infiltration were significantly influenced by earthworm communities (Derouard et al., 1997). The function of earthworms in increasing plant yield and growth relies on the synchronization and synlocalization of their activities with the sphere and period of active root development and nutrient requirement. Most earthworm species release considerable quantities of assimilable nutrients in their fresh casts that can be utilized by plants (Lavelle et al., 1992). Moreover, earthworm activities intensely promote soil mineralization, releasing significant amounts of nitrogen (N), phosphorous (P), and potassium (K); an increase in these nutrients may stimulate plant growth and thus enhance the tea yield (Chaoui et al., 2003). In our previous study (unpublished data), we found that the nutrient content of the soil (measured as available N, P, and K) was greater in earthworm-inoculated plots was higher than in the control. This demonstrated that earthworm inoculation results in better conditions for tea plant growth.

Secondly, plant-growth hormones contained within the earthworm casts can regulate tea plant growth. Several studies have suggested that regulators such as auxins, gibberellins, and cytokinins (Krishnamoorthy and Vajrabhiah, 1986; Grappelli et al., 1987; Tomati et al., 1990) and plant-growth-regulating materials such as humic acids (Atiyeh et al., 2002) are present in the casts and can result in better plant growth for many crops (Atiyeh et al., 2002). Our research revealed that in situ earthworm breeding in a tea garden can contribute to enhanced plant growth. Other mechanisms by which earthworms can improve plant growth incorporate interactions with other organisms: (1) earthworms could be beneficial for pest biocontrol, and (2) earthworms could help to spread symbionts via their colonization (Bertrand et al., 2015).

The earthworms in our study were added to the sample plots only once and at a density of only 8 g/m^2. We therefore hypothesize that increasing the earthworm density could have a positive effect on tea leaf yield and quality; this should be examined in a further study. Furthermore, since the price of earthworms is low, agricultural management costs could be decreased by using this method rather than chemical

http://www.aloki.hu ● ISSN 1589 1623 (Print) ● ISSN 1785 0037 (Online)
DOI: http://dx.doi.org/10.15666/aeer/1902_14911503
© 2021, ALÖKI Kft., Budapest, Hungary

fertilizers. However, a drawback is that we found the preparation of earthworm beds in the field to be complicated. Finally, we did not investigate whether this technique is appropriate for other types of tea garden, if other earthworm species are also beneficial, or if this technique maintains the growth and yield performance long-term. These issues require further exploration.

Conclusion

Tea is one of the most well-known and popular drinks found all over the globe. However, the heavy use of chemical fertilizers to achieve higher yields is contributing to serious environmental problems. Whilst organic fertilizers can be used, their application is greatly limited in tea gardens due to problems with low efficiency and effective duration. The present study investigated the effects of in situ earthworm breeding on the growth, yield and quality of tea plants. We demonstrated that earthworm breeding in soil offers the best growth medium for the tea plant and conferred higher leaf quality and total bud yield. The incorporation of earthworm and organic waste in soil could be a potential organic substitute for chemical fertilizers since it not only improves the yield and quality but also decreases (through the action of the earthworms) the amount of organic waste. Therefore, it is advised that the ecological function of the earthworm should be taken into account and intensifies research of the earthworms in other tea produced regions so as to harness its potentials to improve plant performance in the studied regions especially now organic farming is the order of the day. Additionally, extra long-term field investigations will be essential to adequately understand the influences of earthworms on tea quality and yield.

Acknowledgements. The authors express their sincere thanks to Ms. Meimei Zhao, student of Horticulture Department, College of Tea and Food Science, Wuyi University, for rearing the earthworm species. This research was funded by Collaborative Innovation Center of Chinese Oolong Tea Industry—Collaborative Innovation Center (2011) of Fujian Province, Research Fund Project of Wuyi University (XL201702), Science & Technology Innovation Platform Construction Project of Fujian Province (2018N2004), Innovation and Entrepreneurship Training Program for College Students in Fujian Province (201710397001), Advanced Talents Introduction Project of Wuyi University (YJ201910), Education and Scientific Research Project for Young and Middle-aged Teachers in Fujian Province (JAT190801, JAT190805).

Author contributions. DH and PMC led the project and designed and conceived the study. PMC, YZS, FHM and YCH prepared the manuscript. DH, KQY and LL performed the data analysis. DH, FHM, PMC and HMZ performed sampling and experiments. All authors revised and approved the final manuscript.

Conflict of interests. The authors declare that they have no competing interests.

REFERENCES

[1] Atiyeh, R. M., Lee, S. S., Edwards, C. A., Arancon, N. Q., Metzger, J. (2002): The influence of humic acid derived from earthworm-processed organic waste on plant growth. – Bioresource Technology 84(1): 7-14.

[2] Bertrand, M., Barot, S., Blouin, M., Whalen, J., Oliveira, T., Roger-Estrade, J. (2015): Earthworm services for cropping systems. A review. – Agronomy for Sustainable Agriculture 35: 553-67.

http://www.aloki.hu ● ISSN 1589 1623 (Print) ● ISSN 1785 0037 (Online)
DOI: http://dx.doi.org/10.15666/aeer/1902_14911503
© 2021, ALÖKI Kft., Budapest, Hungary

[3] Blanchart, E., Lavelle, P., Braudeau, E., Bissonnais, Y. L., Valentin, C. (1997): Regulation of soil structure by geophagous earthworm activities in humid savannas of Côte d'Ivoire. – Soil Biology and Biochemistry 29(3-4): 431-39.
[4] Brown, G. G., Pashanasi, B., Villenave, C., Patron, J. C., Senapati, B. K., Giri, S., Barois, I., Lavelle, P., Blanchart, E., Blakemore, R. J., Spain, A. V., Boyer, J. (1999): Effects of Earthworms on Plant Production in the Tropics. – In: Lavelle, P., Brussaard, L., Hendrix, P. (eds.) The Management of Earthworms in Tropical Agroecosystems. CAB International, Wallingford, pp 87-148.
[5] Brown, G. G., Edwards, C. A., Brussaard, L. (2004): How Earthworms Affect Plant Growth: Burrowing into the Mechanisms. – In: Edwards, C. A. (ed.) Earthworm Ecology. CRC Press, Boca Raton, pp 13-49.
[6] Caravaca, F., Hernandez, T., Garcia, C., Roldan, A. (2002): Improvement of rhizosphere aggregate stability of afforested semiarid plant species subjected to mycorrhizal inoculation and compost addition. – Geoderma 108(1-2): 133-44.
[7] Chaoui, H. I., Zibilske, L. M., Ohno, T. (2003): Effects of earthworm casts and compost on soil microbial activity and plant nutrient availability. – Soil Biology and Biochemistry 35(2): 295-302.
[8] Chen, Y. S., Liu, B. L., Chang, Y. N. (2010): Bioactivities and sensory evaluation of pu-erh teas made from three tea leaves in an improved pile fermentation process. – Journal of Bioscience and Bioengineering 109(6): 557-63.
[9] Chen., Y. L., Duan, J., Jiang, Y. M., Shi, J., Peng, L., Xue, S., Kakuda, Y. (2011): Production, quality, and biological effects of oolong tea (*Camellia sinensis*). – Food Research International 27(1): 1-15.
[10] Dai, M. N. (2014): Biological Treatment of Live Stock and Poultry Excrement and the Study of Earthworm Breeding. – Hunan Agriculture University, Changsha Hunan.
[11] Darwin, C. (1881): The Formation of Vegetable Mould through the Action of Worms with Observations on their Habits. – John Murray, London.
[12] Derouard, L., Tondoh, J., Vilcosqui, L., Lavelle, P. (1997): Effects of earthworm introduction on soil processes and plant growth. – Soil Biology and Biochemistry 29(3-4): 541-45.
[13] Edwards, C. A., Bohlen, P. J. (1996): Biology and Ecology of Earthworms. 3rd Ed. – Chapman and Hall, London.
[14] GBT 8305-2013 (2013): State Standard of the People's Republic of China. Tea-Determination of Caffeine Content. Method Using High-Performance Liquid Chromatography.
[15] GBT 8313-2008 (2008): State Standard of the People's Republic of China. Determination of Total Polyphenols and Catechins Content in Tea.
[16] GBT 8314-2013 (2013): State Standard of the People's Republic of China. Tea-Determination of Free Amino Acids Content.
[17] Giri, S. (1995): Short Term Input Operational Experiment in Tea Garden with Application of Organic Matter and Earthworm. – Sambalpur University, Sambapur.
[18] Grappelli, D. H., Gallli, E., Tomati, U. (1987): Earthworm casting effect on *Agaricus bisporus* fructification. – Agrochimica 31(4-5): 457-62.
[19] Kamel, B. S., Martinez, O. B. (2002): Restoring soil fertility and enhancing productivity in Indian tea plantations with earthworms and organic fertilizers. – Annales de Chirurgie Thoracique et Cardio-Vasculaire 5: 738-41.
[20] Kingdom-Ward, F. (1950): Does wild tea exist? – Nature 165: 297-99.
[21] Krishnamoorthy, R. V., Vajrabhiah, S. N. (1986): Biological activity of earthworm casts: an assessment of plant growth promoter levels in the casts. – Proceedings of Indian Academy of Sciences (Animal Science) 95: 341-351.
[22] Lavelle, P., Spain, A. V. (2001): Soil Ecology. – Kluwer Scientific Publications, Amsterdam.

http://www.aloki.hu ● ISSN 1589 1623 (Print) ● ISSN 1785 0037 (Online)
DOI: http://dx.doi.org/10.15666/aeer/1902_14911503
© 2021, ALÖKI Kft., Budapest, Hungary

[23] Lavelle, P., Melendez, C. L., Pashanasi, B., Schaefer, R. (1992): Nitrogen mineralization and reorganization in casts of the geophagous tropical earthworm *Pontoscolex corethurus* (Glossoscolecidae). – Biology and Fertility of Soils 14: 49-53.
[24] Lee, K. E. (1985): Earthworms: Their Ecology and Relationships with Soils and Land Use. – Academic Press, Sydney.
[25] Municipal Government of Wuyishan (2019): http://www.wys.gov.cn/.
[26] Ngo, P. T., Rumpel, C., Doan, T. T., Jouquet, P. (2012): The effect of earthworms on carbon storage and soil organic matter composition in tropical soil amended with compost and vermicompost. – Soil Biology and Biochemistry 50: 214-220.
[27] Tang, J. C., Zhang, C., Zhao, C. Y., Tang, H., Li, J. L., Dai, J. (2008): Application of fertilization bio-organic system in tea plantation of south China. – Journal of Tea Sciences 28: 201-206.
[28] Tang, H., Tang, J. C., Li, J. L., Dai, J. (2011): Research on the influence of different soil fertilizing mode on tea quality. – Guangdong Agriculture Sciences 38(21): 71-73.
[29] Tang, J. C., Zhou, B., Li, J. L., Tang, H., Cao, J. X. (2016): Effects of earthworm bio-organic fertilization technology on soil microbial characteristics and enzyme activities of tea plants. – Journal of Tea Sciences 36: 45-51.
[30] Taniguchi, F., Kimura, K., Saba, T., Ogino, A., Yamaguchi, S., Tanaka, J. (2014): Worldwide core collections of tea (*Camellia sinensis*) based on SSR markers. – Tree Genetics and Genomes 10: 1555-1565.
[31] Tomati, U., Galli, E., Grappelli, A., Dihena, G. (1990): Effect of earthworm casts on protein synthesis in radish (*Raphanus sativum*) and lettuce (*Lactuca sativa*) seedlings. – Biology and Fertility of Soils 9: 288-289.
[32] Vu, T. K. V., Tran, M. T., Dang, T. T. S. (2007): A survey of manure management on pig farms in northern Vietnam. – Livestock Science 112: 288-297.
[33] Wang, Q., Peng, C., Gong, J. (2011): Effects of enzymatic action on the formation of theabrownin during solid state fermentation of pu-erh tea. – Journal of Science Food and Agriculture 91: 2412-2818.
[34] Wei, C., Yang, H., Wang, S., Zhao, J., Liu, C., Gao, L., Xia, E., Lu, Y., Tai, Y., She, G., et al. (2018): Draft genome sequence of *Camellia sinensis var. sinensis* provides insights into the evolution of the tea genome and tea quality. – Proceedings of the National Academy of Sciences of the United States of America 115(18): 201719622.
[35] Xiang, H., Zhang, J. E., Guo, L., Zhao, B. L. (2016): In situ earthworm breeding in orchards significantly improves the growth, quality and yield of papaya (*Carica papaya* L.). – PeerJ 4: e2752.
[36] Zhang, Z. C., Wang, X. P. (2006): The use of diversity of tea cultivars for bud blight control. – Chinese Journal of Tea Science 26: 253-58.
[37] Zhang, Q., Wei, C. X. (2012): Effects of different organic fertilizers on chief qualities of tea. – Guizhou Agriculture Sciences 40(8): 65-67.
[38] Zhang, C., Zhou, B., Wu, J. L., Lv, M. R., Chen, X. F., Yuan, Z. Y., Xiao, L., Dai, J. (2018): Application of earthworms on soil remediation in southern china. – Biodiversity Science 26: 1091-1102.
[39] Zhou, B., Li, J. L., Tang, H., Tang, J. C. (2017): Effects of earthworm bio-organic fertilization on quality components of jinxuan green tea. – Journal of Southern Agriculture 48: 1261-65.
[40] Zhuo, S. M., Wu, X. F., Wu, H. J. (2007): Effect of different of earthworm on tea output in tea plantations with different soil fertilities. – Chinese Journal of Tropical Agriculture 27: 1-3.

http://www.aloki.hu ● ISSN 1589 1623 (Print) ● ISSN 1785 0037 (Online)
DOI: http://dx.doi.org/10.15666/aeer/1902_14911503
© 2021, ALÖKI Kft., Budapest, Hungary

THE ALLOMETRY OF BIOMASS ALLOCATION TO VARIOUS ORGANS IN COTTON (*Gossypium hirsutum* L.) DEPENDING GROWTH PERIOD

GAO, X. – TANG, F.*

Key Laboratory of Crop Physiology, Ecology and Genetic Breeding, College of Agronomy, Ministry of Education, Jiangxi Agricultural University, Nanchang 330045, China

**Corresponding author*
e-mail: fytangcau@163.com

(Received 29th Nov 2020; accepted 27th Jan 2021)

Abstract. Biomass allocation to various components of the cotton plant is an important determinant of lint yield. Two Near-isogenic upland cotton lines 4003-6 and 4003-10 differing in growth period were employed to explore ontogenetic allometric relationships between various structures of field-grown cotton plants during reproduction using Standardized Major Axis. Compared to the later maturing line (4003-6), the earlier maturing line (4003-10) allocated i) proportionally more biomass to reproductive structures at a given vegetative biomass, and initiated reproduction at smaller plant sizes; ii) proportionally less biomass to roots at a given aerial biomass at early reproduction stage but this process was reversed at late reproduction stage; iii) proportionally less biomass to branches at a given stem biomass at late reproduction stage. It is concluded that the earlier maturing cotton line was characterized by deficient root growth at early reproduction stage and limited branch growth at late reproduction stage relative to later maturing line.
Keywords: *root-shoot relationship, reproductive biomass, vegetative biomass, Standardized Major Axis, early maturing*

Introduction

Upland cotton (*Gossypium hirsutum* L.) has an indeterminate growth habit, which leads to the simultaneous production of both vegetative and reproductive structures during considerable period of growing season. Moreover, cotton is exceedingly sensitive to environmental constrains to which it responds mainly by shedding reproductive structures (Oosterhuis and Stewart, 2004). The different organs of cotton take on distinct functions, such as leaves for photosynthesis, roots for uptake of water and nutrient. The growths of these organs depend heavily on the biomass partitioned to them, and in turn affect final lint yield. According to the optimal partitioning theory, environmental constraints usually result in greater biomass allocation to organs under growth limitations (Reynolds and Thornley, 1982; Ploschuk et al., 2005; Luo et al., 2006; Wang and Taub, 2010; Cheng et al., 2015; Luo et al., 2016).

Traditionally, allocation patterns have been defined and calculated as ratios (Weiner et al., 2009). However, allocation in the term of ratios is size-independent, whereas plant allocation is allometric and size-dependent as found in a wide range of plant species (McConnaughay and Coleman, 1999; Weiner, 2004; Otárola et al., 2016; Hill and Roberts, 2017; Chen et al., 2018). Allometric studies indicated that there were strong couplings between various plant components. i.e. between roots and shoots biomass (Niklas, 2005; Yang et al., 2010), between leaf mass and leaf area (Pan et al., 2013), between rate and duration of seed growth (Sadras and Egli, 2008), between leaf size and twig size (Westoby and Wright, 2003). Understanding of allometric

http://www.aloki.hu ● ISSN 1589 1623 (Print) ● ISSN1785 0037 (Online)
DOI: http://dx.doi.org/10.15666/aeer/1902_15051515
© 2021, ALÖKI Kft., Budapest, Hungary

relationships in crops is of agronomical significance both in developing crop simulation models and in estimating crop parameters which are difficult to measure. For example, the allometric function relating below-ground biomass (M_B) to above-ground biomass (M_A) can be employed to estimate M_B from the more easily measured M_A (Mokany et al., 2006; Yang et al., 2010; Yang and Luo, 2011). Up to date, allometric analysis primarily has concentrated on wild-born species spread within a certain terrestrial ecosystem. For field-grown crops exposed to man-created environment, the biomass allometry between various parts is poorly understood. Cotton is not the exception.

Earliness is an important consideration in the selection of cultivars for those cotton grown areas with low thermal availability or limited growing season. Short-season cotton cultivars had different reproductive allocation strategies from long-season ones (Bange and Milroy, 2000, 2004). Early cotton genotypes partitioned a greater proportion of biomass to reproductive forms than late genotypes (Pace et al., 1999; Bange and Milroy, 2000), but in another study by Bange and Milroy (2004) who argued that early genotypes did not show a preferential partitioning of dry matter to reproductive structures, and higher rate of partitioning did not necessarily cause early maturity. A majority of previous works dealt with relationships between dry matter production and allocation and cotton maturity in the partitioning-ratio context rather than the allometric view. Moreover, those works were not involved in the relationship between agronomically important traits, such as between M_B and M_A. M_A is commonly equated with plant size deemed as an important determinant to reproductive output (Weiner et al., 2009). Presently, it remains obscure how cotton allocates its resources to organs or functions during its ontogenetic development. The process involves investment trade-off because resources allocated to one organ are not available to other organs (Guo et al., 2012). In the present study, we have hypothesized that the allometric patterns between various components of cotton plants vary with the time to reproductive maturity. In an attempt to test the hypothesis, two Near-isogenic cotton lines 4003-6 and 4003-10 with the same genetic background but differing in growth period were employed to explore allometric relationships i) between reproductive and vegetative biomasses; ii) between above- and below ground biomasses; iii) between paired and physically linked organs (stem vs branch, branch vs leaf, carpel vs seedcotton). Knowledge of these allometric relationships would help establish optimal management practices to promote cotton growth and maximize lint yield.

Materials and Methods

Experimental Design

The experiment was conducted at the experimental station of Jiangxi Agricultural University (JXAU), Nanchang, China in 2017 and 2018. Two Near-isogenic upland cotton lines 4003-6 and 4003-10 were employed to examine biomass allocation among various plant structures and functions. 4003-10 was derived from a variant plantlet of 4003-6 and has been developed after successive generations of self-pollination in an attempt to reach homozygosity. They have the same genetic background and perform similarly in a wide range of attributes but differing in growth period with 4003-6 being a middle maturing line and 4003-10 being an early maturing line. The soil type was clay, mixed, thermic, Typic alfisols (udalfs; FAO luvisol) with a slightly acid pH of 5.6. The upper 20 cm soil layer contained 23.0 and 26.2 g kg^{-1} organic matter, 1.3 and 1.5 g kg^{-1} total N, 85.8 and 92.4 g kg^{-1} available N, 58.6 and 72.2 g kg^{-1} available P, and

http://www.aloki.hu ● ISSN 1589 1623 (Print) ● ISSN1785 0037 (Online)
DOI: http://dx.doi.org/10.15666/aeer/1902_15051515
© 2021, ALÖKI Kft., Budapest, Hungary

170.4 and 190.7g kg^{-1} available K in 2017 and 2018, respectively. Seeds were sowed in a nursery bed on 15 April 2017 and 26 April 2018, and seedlings were transplanted into the experimental field on 14 May 2017 and 17 May 2018, respectively. Plots were arranged in a randomized complete block design with three replications. Each plot contained six rows spaced 1 m apart and 9.3 m long with a 0.3 m of interplant distance. The four centered rows were used for plant sampling and the remaining outside rows were used to determine yield. A total of 240 kg N ha^{-1}, 108 kg P ha^{-1} and 225 kg K ha^{-1} was incorporated into fields. The P and K fertilizers were split applied in 1:1 ratio prior to planting and at first flowering, respectively. The N fertilizer was distributed in 1:2:1 ratio prior to planting, first flowering and peak flowering, respectively. Management practices including irrigation, insect and weed control were performed as needed during each of the growing seasons.

Sampling Procedure and Data Collection

Seven or eight samplings were taken at two-week intervals from 77 to 161 days after planting (DAP) in 2017, and 64 to 162 DAP in 2018. The sampling commenced at the squaring stage when 50% of plants produced flower buds (squares) for the middle maturing line (4003-6) and terminated until peak boll opening. Two lines were sampled on the same date, not by the exact growth stage. Within a plot, selected plants were located far apart from one another, to ensure that the growth of remaining plants was not affected by the earlier sampling of other plants. Three individual plants in each of plots were uprooted and washed free of soil, and then transferred in an icebox to the lab where they were separated into six parts: roots, main stems, branches, leaves, reproductive parts. Subsamples were oven-dried at 105 ℃ for 0.5 h and then at 60 ℃ to a constant weight. At the cotton maturation stage, a 50-bolls sample was collected from the unsampled rows of each plot for determining boll weight and lint percentage. All plots were hand-harvested three or four times before frost, and lint yields were determined by weighing seedcotton per plot and multiplying by lint percentage and expressed as kilogram per hectare (kg/ha). The growth period was termed as a period of planting date to cotton maturity (60% of bolls open) (Bange and Milroy, 2000).

Data Analysis

The data of cotton lint yield and yield components were subjected to Independent-Samples *t*-test. Means were separated at the probability level of 0.05. The other raw data were $\log_{10}$ transformed to fit the assumption of normality and homogeneity which were certified using Kolmogorov-Smirnov and Levene's tests, respectively. Standardized Major Axis regression and correlation analyses were applied to the $\log_{10}$ transformed data. Correlation analysis showed there were significant high log-log relationships between paired variables. The log-log linear function can be expressed as $\log_{10}Y = a\log_{10}X + b$, which is the $\log_{10}$ transformed version of the classical power function $Y = bX^a$, where a is the scaling exponent (slope) and b is the allometric constant (Y-intercept). A likelihood ratio method was employed to test for homogeneity of slopes and calculation of common slopes (Warton and Weber, 2002). Elevation (i.e. Y-intercept) differences between two linear regression models with the common slope were tested by Wald statistic. The slope and Y-intercept were determined using the software package "Standardized Major Axis Tests and Routines version 2.0" (Falster et al., 2006). All figures were produced by Origin 8.5.

http://www.aloki.hu ● ISSN 1589 1623 (Print) ● ISSN1785 0037 (Online)
DOI: http://dx.doi.org/10.15666/aeer/1902_15051515
© 2021, ALÖKI Kft., Budapest, Hungary

Results

Yield, Yield Components and Growth Period

4003-6 had a longer growth period than 4003-10 with the former being around two weeks longer than the latter (*Table 1*). 4003-10 initiated flowering about one week earlier than 4003-6. Higher seedcotton yield and lint yield were observed in 4003-6 than in 4003-10 in 2018, but not significant in 2017. 4003-6 exhibited a higher lint percentage than 4003-10, but no difference was found in bolls per plant across two years.

Table 1. *Cotton yield, yield components and growth period in lines 4003-10 and 4003-6 across 2017 to 2018*

Year	Genotype	Bolls (plant^{-1})	Boll size(g)	Lint percentage (%)	Seedcotton	Lint yield (kg)	Growth period (d)
2017	4003-10	38.1	4.4	37.2	2658.0	991.0	116
	4003-6	39.7	4.7	40.0**	2661.4	1063.6	130
	$P > F$†	0.536	0.211	0.002	0.996	0.790	
2018	4003-10	30.4	3.9	39.0	2345.9	913.7	113
	4003-6	28.5	4.6	41.2**	2737.0*	1126.9*	125
	$P > F$	0.187	0.100	0.007	0.048	0.014	

† t-test was conducted for means between two lines. *,** indicated significantly different at 0.05 and 0.01 level, respectively

Relationships between Reproductive Biomass and Vegetative Biomass

There was a significant positive relationship between log reproductive biomass (M_R) and log vegetative biomass (M_V) for each of the lines (*Fig. 1*). Two lines shared the commonly fitted slopes of log M_R to log M_V relationship at 2.39 in 2017 and at 2.27 in 2018, respectively. The scaling exponents of M_R to M_V were significantly greater than 1 (lower and upper 95% confidence intervals CIs equaled 2.24 and 2.54 in 2017, 2.11 and 2.45 in 2018, respectively), indicating larger individuals allocated proportionally more biomass to reproductive structures than to the other structures as reproduction progressed.

Allometric constants (*Y*-intercept) were negative irrespective of genotypes and years, suggesting there is a minimum size for cotton reproduction. This may be the case because cotton plant must have sufficient resources to build the reproductive support structures before the first boll can be produced. The *Y*-intercept was significantly different between two lines with 4003-10 being greater than 4003-6 ($P < 0.001$ for 2017, $P < 0.014$ for 2018). This result showed that the earlier maturing line tended to have more reproductive biomass at given vegetative biomass.

The *X*-intercept of linear regression on the M_R-M_V relationship is considered as the threshold size for reproduction (Bonser and Aarssen, 2009). 4003-10 exhibited a smaller threshold size for reproduction than 4003-6 (1.58 versus 1.73 in 2017, and 1.61 versus 1.67 in 2018), which means that earlier maturing line is capable of initiating reproduction at relatively smaller sizes.

http://www.aloki.hu ● ISSN 1589 1623 (Print) ● ISSN1785 0037 (Online)
DOI: http://dx.doi.org/10.15666/aeer/1902_15051515
© 2021, ALÖKI Kft., Budapest, Hungary

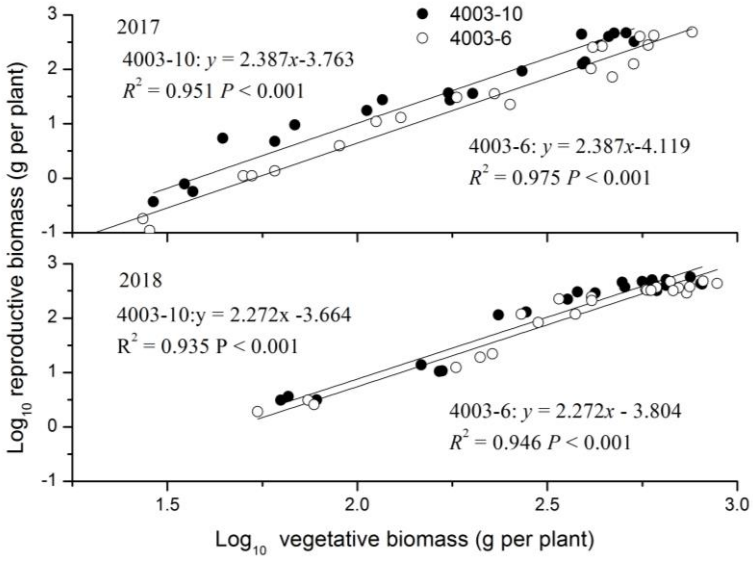


Figure 1. *Allometric relationships between reproductive mass and vegetative mass of cotton over two Near-isogenic lines 4003-6 and 4003-10*

Relationships between Below-ground Biomass and Above-ground Biomass

Log above-ground biomass (M_A) was significantly positively correlated with log below-ground biomass (M_B) for either of two lines (*Fig. 2*). The regression slope of log M_B on log M_A in 4003-10 was significantly > 1 with a 95% CI of 1.003 to 1.115 in 2017, but = 1 with a 95% CI of 0.963 to 1.165 in 2018, indicating that biomass allocated to roots disproportionately exceeded that to shoots or both increased in the same proportion. The slopes with 4003-6 were significantly < 1 with 95% CIs of 0.794 to 0.920 in 2017, and of 0.863 to 0.983 in 2018, indicating that a marginal increase in M_A caused a proportionally smaller increase in M_B. The result showed that the scaling relationship between M_A and M_B varied between cotton genotypes.

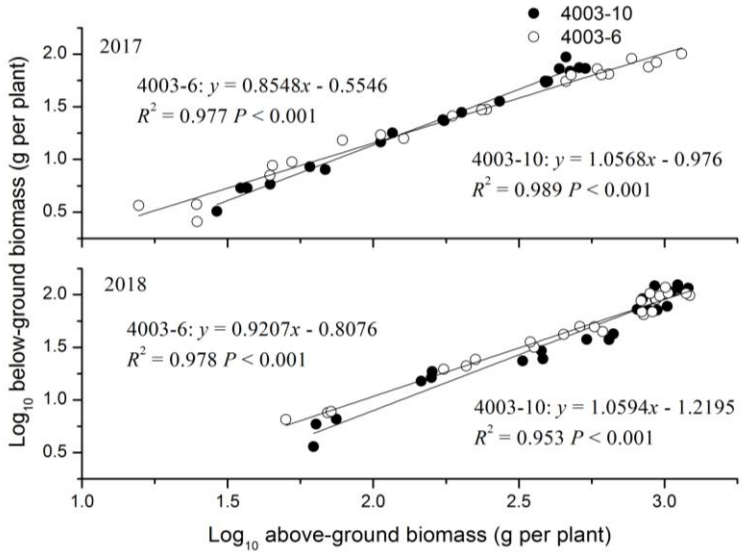


Figure 2. *Allometric relationships between below- and above-ground mass of cotton over two Near-isogenic lines 4003-6 and 4003-10*

http://www.aloki.hu ● ISSN 1589 1623 (Print) ● ISSN1785 0037 (Online)
DOI: http://dx.doi.org/10.15666/aeer/1902_15051515
© 2021, ALÖKI Kft., Budapest, Hungary

The *Y*-intercept of the regression of log M_B - log M_A was greater in 4003-6 than in 4003-10 over two years (*Fig. 2*). Moreover, allometric regression lines of both were crossed (*Fig. 2*), which means 4003-10 had a smaller M_B at a given M_A than 4003-6 prior to the cross point and the opposite was true of after the cross point. The combination of the higher slope and the lower *Y*-intercept for the earlier maturing line indicated that it allocates proportionately less biomass to roots at early reproductive growth stage and more at late reproductive growth stage compared with the later maturing line.

Relationships between Branch Biomass and Stem Biomass

Significant and positive correlations were observed between log stem biomass and log branch biomass (*Fig. 3*). The slopes of the log branch biomass to log stem biomass were all above 1 irrespective of genotypes and years, and differed between two lines, indicating cotton allocated proportionally more biomass to branches than to main stem after reproduction initiation (*Fig. 3*). 4003-6 had larger slopes and smaller *Y*-intercept compared to 4003-10 over two years, which means the former exhibited a smaller branch biomass at a given stem biomass at early reproductive stage, but the reversed appeared as reproduction progressed.

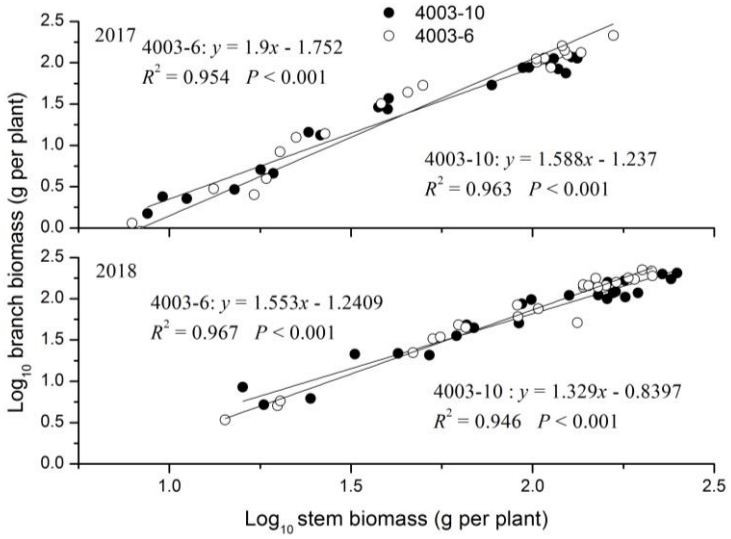


Figure 3. *Allometric relationships between branch mass and stem mass of cotton over two Near-isogenic lines 4003-6 and 4003-10*

Relations between Leaf Biomass and Branch Biomass

Log branch biomass correlated positively with log leaf biomass (*Fig. 4*). The slopes of the log leaf biomass to branch biomass were all below 1 regardless of genotypes and years, indicating cotton allocated proportionally less biomass to leaves than to branches during reproduction period. Greater slope and smaller elevation were recorded in 4003-10 relative to 4003-6 in 2017, but two lines shared a common slope at 0.5413 with no difference in *Y*-intercepts in 2018 (*Fig. 4*).

http://www.aloki.hu ● ISSN 1589 1623 (Print) ● ISSN1785 0037 (Online)
DOI: http://dx.doi.org/10.15666/aeer/1902_15051515
© 2021, ALÖKI Kft., Budapest, Hungary

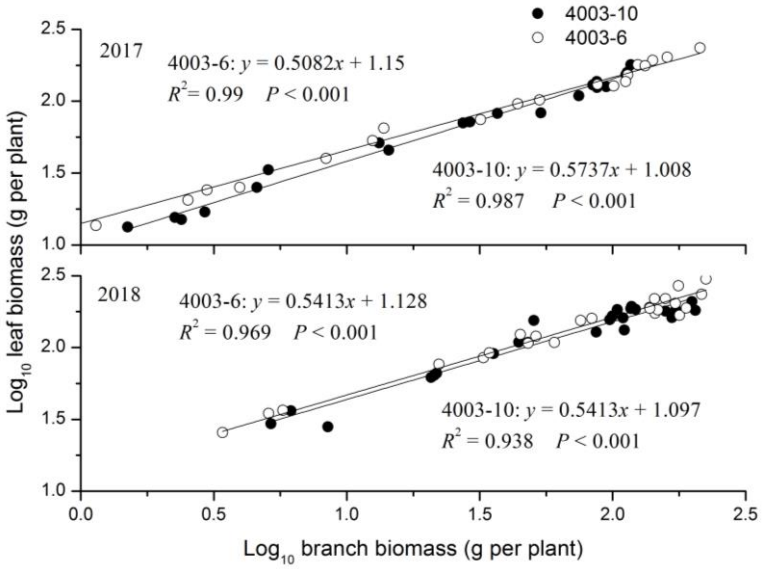


Figure 4. *Allometric relationships between leaf mass and branch mass of cotton over two Near-isogenic lines 4003-6 and 4003-10*

Relations between Boll (fibers plus seeds) Biomass and Carpel Biomass

There was a positive and significant correlation between log boll biomass and log carpel biomass (*Fig. 5*). The slope of log boll biomass to log carpel biomass was greater than 1 over two lines across two years, indicating cotton partitioned proportionally more biomass to fibers and seeds than to carpels with advancing boll development (*Fig. 5*). Two lines shared common slopes and no significant difference in elevation was observed.

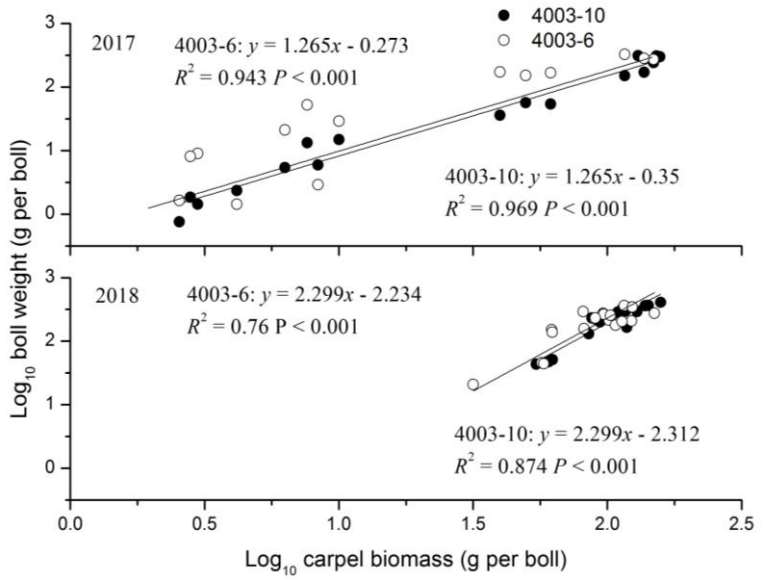


Figure 5. *Allometric relationships between boll mass and carpel mass of cotton over two Near-isogenic lines 4003-6 and 4003-10*

http://www.aloki.hu ● ISSN 1589 1623 (Print) ● ISSN1785 0037 (Online)
DOI: http://dx.doi.org/10.15666/aeer/1902_15051515
© 2021, ALÖKI Kft., Budapest, Hungary

Discussion

Allocation pattern with field-grown crops was largely investigated in the view of ratios. The method did not take into account plant size. With plant size being one of the most important factors affecting reproductive output, allocation patterns would be better understood by analyzing and interpreting the allometric relationship between reproductive and vegetative biomass within a population compared with traditional reproductive allocation approach based on ratios (Samson and Werk, 1986; Sugiyama and Bazzaz, 1998; Karlsson and Mendez, 2005).

4003-10 exhibited greater *Y*-intercepts of log M_R to log M_V relationship on the basis of the common slope over two years, indicating the former tended to have proportionally more reproductive biomass at given vegetative biomass. The result is somewhat similar to an early report by Bange and Milroy (2000) that the shorter-season cultivar partitioned significantly more of dry matter increment to reproductive structures than the long-season cultivar during the initial period of boll growth. The difference of *Y*-intercept may be the result of the difference in the growth period, because the shorter lifespan in the earlier maturing cultivar may prompt it to convert proportionally more biomass to reproductive biomass in an effort to complete its life cycle as soon as possible. 4003-10 exhibited a smaller threshold size for reproduction than 4003-6 over two years (*Fig. 1*), indicating the former can initiate reproduction at smaller sizes than the latter, as consistent with the report of Bange and Milroy (2004) that partitioning to the fruit began earlier in early genotypes. Similar to this, individuals living in adverse environments tend to allocate more of their biomass to reproduction (e.g., seeds) at small sizes compared with ones growing in more benign environments because of a high risk of early death before reproduction (Guo et al., 2012). Environmental adversity is apt to trigger reproduction at relatively small sizes (Bonser and Aarssen, 2009).

Two cotton lines exhibited different scaling relationship between M_A and M_B from one another across two years (*Fig. 2*). 4003-6 recorded a slope of log M_A to log M_B. regression below 1 over two years, but $\geqq 1$ for 4003-10. In a pot experiment with five alpine plant species where Luo et al. (2016) observed that the allometry between M_A and M_B was altered by the N:P supply ratio. By contrast, a substantial amount of studies with forest or grassland ecosystems reported that M_B scaled nearly isometrically with M_A and the scaling relationship changed little with various environmental conditions (Cheng et al., 2015; Niklas, 2005; Yang et al., 2010; Yang and Luo, 2011). The fluctuation in scaling relationships with changing environments was considered as increased individual fitness, which can be a disadvantage for plant production system where optimal population is preferred instead of individual performance (Weiner, 2004). 4003-10 had higher regression slopes but lower *Y*-intercepts than 4003-6 over two years (*Fig. 3*), which means proportionally less biomass partitioning to 4003-10 roots at early reproduction stage and the reversed at late reproduction stage. Root to shoot ratio is easily affected by environmental conditions (Weiner, 2004). Increased root to shoot ratio in cotton under soil moist deficit was largely due to a significant increase in root biomass with little change in shoot biomass (McMichael and Quisenberry, 1991). Early reproduction in cotton (i.e. squaring) is seen as the most critical phase for the development of roots system. A greater biomass partition to roots in 4003-6 at that stage should contribute to increasing its capacity of taking up water and nutrients at successive stages of development (i.e. flowering and fruiting), which may translate into a higher reproductive output. Contrarily, 4003-10 distributed less dry mass to roots at early reproduction, which may lead to deficient roots growth and

http://www.aloki.hu ● ISSN 1589 1623 (Print) ● ISSN1785 0037 (Online)
DOI: http://dx.doi.org/10.15666/aeer/1902_15051515
© 2021, ALÖKI Kft., Budapest, Hungary

limited nutrient uptake, and in turn fail to meet the resource requirement for growing boll loading, and thus produce a potential risk of premature. Those resources failing to trigger the initiation of new fruit sits are potentially transported into roots and stored there for the next growth cycle. This maybe the reason that a greater biomass partition to roots at late reproduction for 4003-10 relative to 4003-6. The improvement of root growth with early maturing genotype prior to reproduction initiation is supposed to be a promising strategy for further enhancing cotton yield.

The slopes of log branch biomass to either log stem biomass or log leaf biomass were above 1 irrespective of genotypes and years (*Fig. 3, Fig.4*), indicating cotton allocated proportionally more biomass to branches than either of stem and leaves after reproduction initiation. More branches potentially grow more fruiting forms which can help to achieve higher yield. It has been well known that sympodials per plant correlates positively with seedcotton yield per plant (Rao and Gopinath, 2013; Majeedano et al., 2014). 4003-6 presented greater slope and smaller *Y*-intercept with regard to the regression relationship of log branch biomass on log stem biomass, indicating it allocated proportionally more biomass to branches than to stem compared to 4003-10 as reproduction progressed. The result reflects that 4003-6 expressed more vigorous growth potential at late reproduction stage.

Allometric relationships have generally been deemed to be genetically determined, i.e. species- or genotype-specific (Weiner, 2004). On the other hand, allometric patterns varied with environmental and developmental constraints especially in short-lived (annual) ones (Reekie and Bazzaz, 1987; Weiner and Thomas, 1992). Presumably, Cotton is featured by comparatively high plasticity in growth allometry owing to its indeterminate growth habit. Allometric relationships from the present study may apply simply to the cotton population with enough growing season, low plant density and limited soil fertility availability which can create a symmetric competition among individuals (Bazzaz et al., 2005). The allometry of biomass allocation in cotton may be changed with varying plant density and soil fertility levels.

Based on the allocation patterns between M_R and M_V, and between M_A and M_B, it can be concluded that the early maturing genotype experiences greater developmental constraints, e.g. deficient root growth at early developmental stages, and reproduction initiation at smaller sizes, etc. Thus, cultivation practices should be applied to the early genotypes earlier than others aiming to establish well-developed roots and enlarge plant size before reproduction initiation. The alternative managements should prioritize intertillage weeding during seedling through squaring and increasing resources availability to them at early development.

Conclusions

During reproduction period, the earlier maturing line (4003-10) allocated i) proportionally more biomass to reproductive structures at a given vegetative biomass, and initiated reproduction at smaller plant sizes; ii) proportionally less biomass to roots at a given aerial biomass at early reproduction stage but the reversed at late reproduction stage; iii) proportionally less biomass to branches at a given stem biomass at late reproduction stage. It is suggested that earlier maturing cotton line was characterized by deficient root growth at early reproduction stage and limited branch growth at late reproduction stage relative to later maturing line. It is worth noting that those allometric relationships may apply simply to the cotton population with enough growing season,

http://www.aloki.hu ● ISSN 1589 1623 (Print) ● ISSN1785 0037 (Online)
DOI: http://dx.doi.org/10.15666/aeer/1902_15051515
© 2021, ALÖKI Kft., Budapest, Hungary

low plant density and limited soil fertility availability which can create a symmetric competition among individuals. The issue deserves further study how the allometry of biomass allocation in cotton responds to varying plant density and soil fertility levels.

Acknowledgments. This study was funded by the National Natural Science Foundation of China (Grand number: 31960385, 31560364).

REFERENCES

[1] Bange, M. P., Milroy, S. P. (2000): Timing of crop maturity in cotton: impact of dry matter production and partitioning. – Field Crops Research 68(2): 143-155.
[2] Bange, M. P., Milroy, S. P. (2004): Growth and dry matter partitioning of diverse cotton genotypes. – Field Crops Research 87(1): 73-87.
[3] Bazzaz, F. A., Ackerly, D. D., Reekie, E. G. (2005): Reproductive allocation in plants. – In: Fenner, M. (ed.) Seeds: The Ecology of Regeneration in Plant Communities. Wallingford, UK: CAB International 2000, pp. 1-29.
[4] Bonser, S. P., Aarssen, L. W. (2009): Interpreting reproductive allometry: individual strategies of allocation explain size-dependent reproduction in plant populations. – Perspectives in Plant Ecology Evolution and Systematics 11: 31-40.
[5] Chen, G., Hobbie, S. E., Reich, P. B., Yang, Y., Robinson, D. (2018): Allometry of fine roots in forest ecosystems. – Ecology Letter 22(2): 322-331.
[6] Cheng, D., Zhong, Q., Niklas, K. J., Ma, Y., Yang, Y., Zhang, J. (2015): Isometric scaling of above- and below-ground biomass at the individual and community levels in the understorey of a sub-tropical forest. – Annals of Botany http://dx.doi.org/10.1093/aob/mcu238.
[7] Falster, D. S., Warton, D. I., Wright, I. J. (2006): SMATR: Standardized major axis tests and routines, ver 2.0. – http://www.bio.mq.edu.au/ecology/SMATR/.
[8] Guo, H., Weiner, J., Mazer, S. J., Zhao, Z., Du, G., Li, B. (2012): Reproductive allometry in Pedicularis species changes with elevation. – Journal of Ecology 100: 452-458.
[9] Hill, T. D., Roberts, B. J. (2017): Effects of seasonality and environmental gradients on Spartina alterniflora allometry and primary production. – Ecology and Evolution 7: 9676-9688.
[10] Karlsson, P. S., Mendez, M. (2005): The resource economy of plant reproduction. – In: Reekie, E. G., Bazzaz, F. A. (ed.) Reproductive Allocation in Plants. Burlington, MA: Elsevier Academic Press, pp. 1-49.
[11] Luo, Y., Hui, D., Zhang, D. (2006): Elevated CO_2 stimulates net accumulations of carbon and nitrogen in land ecosystems: a meta-analysis. – Ecology 87: 53-63.
[12] Luo, X., Mazer, S. J., Guo, H., Zhang, N., Weiner, J., Hu, S. (2016): Nitrogen: phosphorous supply ratio and allometry in five alpine plant species. – Ecology and Evolution 6(24): 8881-8892.
[13] Majeedano, M. S., Ahsan, M. Z., Soomro, A. W., Panhwar, F. A., Channa, A. R. (2014): Heritability and corrrelations estimates for some yield traits of *Gossypium hirsutum* L. – American Research Thoughts 1(2): 781-790.
[14] McConnaughay, K. D. M., Coleman, J. S. (1999): Biomass allocation in plants: ontogeny or optimality? A test along three resource gradients. – Oecologia 113: 447-455.
[15] McMichael, B. L., Quisenberry, J. E. (1991): Genetic variation for root-shoot relationships among cotton germplasm. – Environmental and Experimental Botany 31(4): 461-470.
[16] Mokany, K., Raison, R. J., Prokushkin, A. S. (2006): Critical analysis of root: shoot ratios in terrestrial biomes. – Global Change Biology 12: 84-96.

http://www.aloki.hu ● ISSN 1589 1623 (Print) ● ISSN1785 0037 (Online)
DOI: http://dx.doi.org/10.15666/aeer/1902_15051515
© 2021, ALÖKI Kft., Budapest, Hungary

[17] Niklas, K. J. (2005): Modeling below- and above- ground biomass for non-woody and woody plants. – Annals of Botany 95: 315-321.
[18] Oosterhuis, D. M., Stewart, J. M. (2004): Physiological basis of yield and environmental adaptation in cotton. – In: Nguyen, H. T., Blum, A. (ed.) Physiology and Biotechnology Integration for Plant Breeding. – New York: Marcel Dekker Inc., pp. 363-401.
[19] Otárola, M. F., Sazima, M., Solferini, V. N. (2016): Stem and crown allometry in four congeneric species of dioecious tropical trees. – Trees 30(6): 2041-2049.
[20] Pace, P. F., Cralle, H. T., Cothren, J. T., Senseman, S. A. (1999): Photosynthate and dry matter partitioning in short- and long- season cotton cultivars. – Crop Science 39: 1065-1069.
[21] Pan, S., Liu, C., Zhang, W., Xu, S., Wang, N., Li, Y., Gao, J., Wang, Y., Wang, G. (2013): The scaling relationships between leaf mass and leaf area of vascular plant species change with altitude. – PLoS One 8(10): e76872. http://dx.doi.org/10.1371/journal.pone.0076872.
[22] Ploschuk, E. L., Slafer, G. A., Ravetta, D. A. (2005): Reproductive allocation of biomass and nitrogen in annual and perennial Lesquerella crops. – Annals of Botany 96: 127-135.
[23] Rao, P. J. M., Gopinath, M. (2013): Association analysis of yield and fibre quality characters in upland cotton (*Gossypium hirsutum* L.). – Australian Journal of Basic and Applied Science 7(8): 787-790.
[24] Reekie, E. G., Bazzaz, F. A. (1987): Reproductive effort in plants. I. Carbon allocation to reproduction. – American Naturalist 129: 876-896.
[25] Reynolds, J. F., Thornley, J. H. M. (1982): A shoot: root partitioning model. – Annals of Botany 49: 585-597.
[26] Sadras, V. O., Egli, D. B. (2008): Seed size variation in grain crops: allometric relationships between rate and duration of seed growth. – Crop Science 48: 408-416.
[27] Samson, D. A., Werk, K. S. (1986): Size-dependent effects in the analysis of reproductive effort in plants. – American Naturalist 127: 667-680.
[28] Sugiyama, S., Bazzaz, F. A. (1998): Size dependence of reproductive allocation: the influence of resource availability, competition and genetic identity. – Functional Ecology 12: 280-288.
[29] Wang, X., Taub, D. R. (2010): Interactive effects of elevated carbon dioxide and environmental stresses on root mass fraction in plants: a meta-analytical synthesis using pairwise techniques. – Oecologia 163: 1-11.
[30] Weiner, J., Thomas, S. C. (1992): Competition and allometry in three species of annual plants. – Ecology 73: 648-656.
[31] Weiner, J. (2004): Allocation, plasticity and allometry in plants. – Perspectives in Plant Ecology, Evolution and Systematics 6: 207-215.
[32] Weiner, J., Campbell, L. G., Pino, J., Echarte, L. (2009): The allometry of reproduction within plant populations. – Journal of Ecology 97: 1220-1233.
[33] Westoby, M., Wright, I. J. (2003): The leaf size – twig size spectrum and its relationship to other important spectra of variation among species. – Oecologia 135: 621-628.
[34] Yang, Y., Fang, J., Ma, W., Guo, D., Mohammat, A. (2010): Large-scale pattern of biomass partitioning across China's grasslands. – Global Ecology and Biogeography 19: 268-277.
[35] Yang, Y., Luo, Y. (2011): Isometric biomass partitioning pattern in forest ecosystems: evidence from temporal observations during stand development. – Journal of Ecology 99: 431-437.

http://www.aloki.hu ● ISSN 1589 1623 (Print) ● ISSN1785 0037 (Online)
DOI: http://dx.doi.org/10.15666/aeer/1902_15051515
© 2021, ALÖKI Kft., Budapest, Hungary

METHODOLOGY FOR ANALYSING PESTICIDE MULTI-RESIDUE IN WUYI ROCK TEA USING MODIFIED QUECHERS FOLLOWED BY GAS CHROMATOGRAPHY-TANDEM MASS SPECTROMETRY

XU, Z. Y.[1] – XIAO, X.[2] – JIANG, X. B.[1] – CAI, P. M.[1,3,4*]

[1]*College of Tea and Food Science, Wuyi University, Wuyishan 354300, China*

[2]*Wuyishan Food Hygiene Supervision and Inspection Center, Wuyishan 354300, China*

[3]*Biological Control Research Institute, College of Plant Protection, Fujian Agriculture and Forestry University Fuzhou 350002, China*

[4]*Key Laboratory of Biopesticide and Chemical Biology, Ministry of Education, Fuzhou 350002, China*

**Corresponding author*
e-mail: caipumo@qq.com; telephone number: +86-150-8045-6908

(Received 4th Dec 2020; accepted 8th Feb 2021)

Abstract. Tea is one of the most commonly consumed drinks worldwide, the production of which often uses a variety of multi-class pesticides. Development of a reliable method to determine the presence and quantity of any pesticide residue is therefore highly important. In the present study, we developed a validated method for the analysis of 33 pesticides in Wuyi Rock tea using the QuEChERS sample preparation method and capillary gas chromatography-tandem mass spectrometry (GC-MS/MS). After extracting the target components from the tea matrix using acetonitrile, a mixture of adsorbents [primary secondary amine (PSA; 400 mg), graphite carbon black (GCB; 400 mg), octadecylsilane (C18; 100 mg)] and salting-out solvents [anhydrous NaCl (1 g) and $MgSO_4$ (4 g)] were used for clean-up, and an analyte protectant solution [sorbitol (10 mg/mL) and L-gulonic acid-γ-lactone (20 mg/mL)] was added. For accurate quantification, a matrix-matched calibration method was applied. For all pesticides at concentration levels of 20–500 ng/ml, good linear calibrations with coefficients of (R^2) ≥ 0.994 were acquired. The recovery values of samples spiked with 20, 100, and 400 ng/kg doses of analytes ranged from 72.3 to 110.6%, and the relative standard deviations (RSD) ranged from 2.8 to 6.7%. The repeatability and recovery rates were in-line with criteria set by the GB 2763-2019 Guideline. Therefore, this validated method is suitable for the simultaneous determination of multi-class pesticide residues in Wuyi Rock tea.
Keywords: *GC-MS/MS, QuEChERs, Camellia sinensis, multi-pesticide residues, matrix interference*

Introduction

Tea, the agricultural product made from dried leaves of various cultivars of *Camellia sinensis* (L.) O. Kuntze, is the most popular non-alcoholic beverage throughout the world, particularly in Asian countries (Nie and Xie, 2011; Sharangi, 2009). Due to its beneficial effects on humans, tea is regarded as a healthy drink and should be free from contaminants. Throughout the growth of the plant, as well as in post-harvest treatments, pesticides are commonly used to protect the tea from weeds, pests, and diseases to guarantee high-quality products (Gurusubramanian et al., 2008). Even though some pesticide residues can be naturally degraded due to their instability, eliminating them completely is a difficult task. Considering that pesticide residues may present health risks to the consumer and potentially adverse influences on the environment, there are

http://www.aloki.hu ● ISSN 1589 1623 (Print) ● ISSN 1785 0037 (Online)
DOI: http://dx.doi.org/10.15666/aeer/1902_15171532
© 2021, ALÖKI Kft., Budapest, Hungary

strict regulations on maximum residues limits (MRLs). These exist for several hundred types of residues in many counties, including Australia, Japan, USA, and China, as well as several international organizations, including the European Union (EU) and the World Health Organization (WHO)/Food and Agriculture Organization (FAO). Based on the EU regulation, which includes a list of more than 480 pesticides, the default MRL of a pesticide residue is generally 0.01 mg/kg (European Union, 2016), which approaches the detection limit of most analytical methods. Therefore, in order to produce safer tea products, it is necessary to establish and modify a reliable, valid, sensitive, and high-throughput analytical method to simultaneously determine pesticide residues.

The analysis of trace substances in tea samples is challenging due to the significant amount of interference from highly complex compounds such as sugar, alkaloids, polyphenols, fatty acids, organic acids, caffeine, pigments, as well as other pesticides (Guillarme et al., 2010; Xu et al., 2011). Many approaches have been developed to detect the extremely small amounts of multi-class pesticide in tea samples; for example, solid-phase extraction (SPE) (Liu et al., 2019), dispersive solid-phase extraction (dSPE) (Dil et al., 2018), supercritical fluid extraction (SFE) (Huang et al., 2019b), matrix solid phase dispersion (MSPD) (Ramos, 2019), gel permeation chromatography (GPC) (Zhu et al., 2019), dispersive liquid-liquid microextraction (Dil et al., 2019), and magnetic dispersive micro-solid phase extraction (Mehrabi et al., 2017).

Among these methods, an extraction procedure based on the dSPE clean-up step named as QuEChERS (quick, easy, cheap, effective, rugged and safe) is a powerful method of sample preparation, first proposed by Anastassiades et al. (2003) and which has become very popular in the past few years. The technique has been successfully applied to detect one and more groups of pesticide residues in several agricultural products, including fruits and vegetables (Gómez-Ramos et al., 2013), animal-derived food (Surma et al., 2013), milk (Li et al., 2013), and cereals (Zheng et al., 2013). The technique utilizes a single-step or buffered acetonitrile extraction and a salting-out phase which separates the analyte from the water using anhydrous magnesium sulphate. Afterwards, a clean-up step is conducted to eliminate redundant water and interferences with a combination of sorbents containing $MgSO_4$ and sorbent primary secondary amine (PSA). Then, the final extracts undergo separation using either liquid chromatography (LC) or gas chromatography (GC) followed by detection through mass spectrometry (MS) (A.O.A.C., 2010). This method has many merits. First, the final extracts, which are dissolved in acetonitrile, can be utilized both for LC and GC. Secondly, various types of pesticides can be measured by this method in a single procedure. Thirdly, the QuEChERS method is definitely low-cost, simple, fast, solid, safe and effective, as per its name (Lehotay et al., 2005). Currently, the QuEChERS method has been successfully used to extract and purify pesticides from green, black, white, oolong and red tea (Shoeibi et al., 2013; Rajski et al., 2013; Guan et al., 2013; Chen et al., 2014a, b; Tran et al., 2015; Hou et al., 2016; Li et al., 2017; Wu, 2017; Huang et al., 2019a; Yu et al., 2020; Ly et al., 2020). However, several previous QuEChERS methodologies have concentrated on only a few types of pesticide; for example, only seven benzoylurea pesticides were determined in manufactured oolong tea (Chen et al., 2014b). Guan et al. (2013) presented a multi-residue method based on the utilization of a modified QuEChERS protocol combined with LC-MS/MS applied in tea, but only five organophosphorus and six carbamate pesticides were selected. Similarly, Yu et al. (2020) ameliorated the QuEChERS method that used only one absorbent and used LC-

http://www.aloki.hu ● ISSN 1589 1623 (Print) ● ISSN 1785 0037 (Online)
DOI: http://dx.doi.org/10.15666/aeer/1902_15171532
© 2021, ALÖKI Kft., Budapest, Hungary

MS/MS to simultaneously determine ten organophosphorus pesticide residues in tea. Since various classes of pesticides could reside in the tea, it is necessary to explore a novel method to analyze as many types as possible.

In a previous study by Li et al. (2017), the authors found that GC coupled with tandem mass spectrometry (GC-MS/MS) significantly enhanced the simultaneous determination of multi-pesticide residues due to its high selectivity and sensitivity compared to single quadrupole MS, with low limits of detection (LOD), low limits of quantification (LOQ) and excellent accuracy. The analytical method based on the QuEChERS method followed by GC-MS/MS has been standardized for the determination of 208 pesticides and their metabolite residues in foods of plant origin in China (GB 23200.113-2018), which was implemented on December 1, 2019. However, literature regarding the determination of multi-pesticide residues specifically in tea using GC-MS/MS and QuEChERS (or improved versions) are rare (Wu, 2017).

Teas from different regions have different tastes, flavors, colors, and appearances due to different cultivars, cultivation conditions, climate, and processing technology (Yener et al., 2016). One particular region of interest is Wuyi Mountain, located at the north part of Fujian Province, which is a UNESCO World Heritage site and considered the origin of oolong tea. In recent years, the yield and consumption of oolong tea has raised substantially worldwide thanks to its favorable taste and pleasant aroma (Chen et al., 2011). Moreover, Wuyi Rock tea is considered to be the most prestigious and premium subcategory of oolong tea in China, owing to its special and complicated processing procedures (Chen et al., 2018). The distinct processing steps of Wuyi Rock tea makes the interfering components of tea more abundant and complex, which result in stronger matrix interferences than other tea types. However, to the best of our knowledge, there is little information on pesticide residue analysis in Wuyi Rock tea based on QuEChERS sample pre-treatment combined with GC-MS/MS.

The present study focused on the removal of matrix effects by QuEChERS extraction using acetonitrile mixed with analyte protectants. This was combined with mixed-mode SPE clean-up using different adsorbents (C18, GCB and PSA), and salting-out using anhydrous NaCl and $MgSO_4$, as part of the sample preparation procedure. As such, a methodology was developed to simultaneously quantify multi-class pesticides in Wuyi Rock tea with low matrix interferences and high recovery rates by GC-MS/MS.

Materials and methods

Chemicals and reagents

A total of 33 pesticide reference standards with initial concentrations of 100 μg/mL and purities of 98.0–99.9% were supplied by the Agro-Environmental Protection Institute, Ministry of Agriculture and Rural Affairs, China (see *Table A1* in the *Appendix*). These pesticides were selected based upon their common application on tea plants and could be analyzed through GC-MS/MS. Primary secondary amine (PSA), graphitized carbon black (GCB), and C18 sorbents were purchased from Agela Technologies (Tianjin, China). HPLC grade acetonitrile and toluene were purchased from Sigma-Aldrich (Merck, Germany). Analytical grade sodium chloride (NaCl) and anhydrous magnesium sulfate ($MgSO_4$) were purchased from China National Medicines Corporation Ltd. (Shanghai, China). Heptachlor epoxide with a purity $\geq$ 98.0% was used as an internal standard (IS) for GC-MS/MS analysis. The stock IS solution was prepared in acetonitrile to a concentration of 4 μg/mL and preserved at -20 °C until

http://www.aloki.hu ● ISSN 1589 1623 (Print) ● ISSN 1785 0037 (Online)
DOI: http://dx.doi.org/10.15666/aeer/1902_15171532
© 2021, ALÖKI Kft., Budapest, Hungary

used. An analyte protectant (AP) solution was also prepared in acetonitrile, comprising 10 mg/mL of sorbitol and 20 mg/mL of L-gulonic acid-γ-lactone (both ≥ 98.0% purity; Macklin, Shanghai, China).

Instrumentation

Target analytes were determined using an Agilent 6890 Gas Chromatograph in combination with an Agilent 7000A triple quadrupole mass spectrometer in electron ionization mode (EI, 70 eV). A DB-5MS capillary column (30 m × 0.25 mm i.d. and 0.25-μm thick film) was used to separate the analytes. The oven temperature changes in the column were as follows: 40 °C for 1.5 min; increased by 25 °C/min to 90 °C, held for 1.5 min; increased by 25 °C/min to 180 °C, then by 5 °C/min to 280 °C, then by 10 °C/min to 300 °C, where it was held for 5 min. The injection volume was 1 μL in splitless mode at a constant flow rate of 1 mL/min; the injector temperature was held at 280 °C. The multiple reaction monitoring mode (MRM) with two transitions for each pesticide was applied to scan the ions, the higher intensities of the precursor-to-product ion transition were utilized for quantification, and the others were applied for confirmation. Retention time (RT), quantitative peak, confirmation peak and collision energy (CE) were set (see *Table A1*).

For the preparation of tea samples, a disintegrator (FW100, Tianjin Taisite Instrument Co., Ltd, Tianjin, China), nitrogen evaporator (QSC-12T, Quandao, Shanghai, China), high speed centrifuge (TG-16W, Biobase Scientifc Instrument Co., Ltd., Shandong, China) and horizontal oscillator (HT-100W, Zhongkai Scientifc Instrument Co., Ltd., Guangdong, China) were used.

Sample preparation procedure

The samples used in this study were dried Wuyi Rock tea, which is produced from *C. sinensis* leaves and buds, collected from the local market. Blank samples were selected from the samples in which no pesticides were detected. Five hundred grams of the collected samples were first ground, homogenized, and sieved through a 20-mesh sieve. Two grams of the tea powder was placed into a 50-mL centrifuge tube, to which 1 g of anhydrous NaCl and 4 g of anhydrous $MgSO_4$ were then added. The tube was sealed and hand-shaken for 1 min. Then, 15 mL of acetonitrile was added, the tube was again shaken vigorously for 1 min, then centrifuged at 4200 r/min for 10 min. For the clean-up step, 5 mL of the supernatant was transferred to a 15 mL centrifuge tube including 400 mg of PSA, 200 mg of GCB, and 100 mg of C18. The tube was shaken vigorously for 1 min and centrifuged at 4200 r/min for 3 min. One milliliter of the supernatant was pipetted and filtered through a 0.22-μm filter membrane (Minisart RC 15, Sartorius, Germany) to a GC-MS/MS autosampler vial. Prior to GC injection, the filtered supernatant was re-dissolved in 20 μL of the IS solution, and 20 μL of AP solution was added to ensure a good signal and peak shape (Wang et al., 2011).

Preparation of matrix-match standards solutions

Each stock solution of pesticide was prepared at a concentration of 1000 ng/mL in acetonitrile and stored at -20 °C until use. The composite working standard solutions were freshly prepared at concentrations of 0, 20, 50, 100, 200, and 500 ng/mL by diluting the stock solutions with acetonitrile. The working standard solutions were applied to prepare a standard curve (concentration range from 0 to 500 ng/mL) in a

http://www.aloki.hu ● ISSN 1589 1623 (Print) ● ISSN 1785 0037 (Online)
DOI: http://dx.doi.org/10.15666/aeer/1902_15171532
© 2021, ALÖKI Kft., Budapest, Hungary

blank tea sample for obtaining a matrix-match and spike sample for the validation measurement. The pesticide-free tea sample was extracted with acetonitrile using the same above-mentioned method.

Method validation

The method was validated to investigate linearity, repeatability, accuracy, precision, and limit of quantification (LOQ). Linearity was tested using matrix-matched calibration by analyzing pesticide-free tea samples spiked at six concentration levels, achieved by gradually diluting the mixed standard solution in acetonitrile. Calibration curves were established by plotting the peak areas of analytes/IS ratio against analyte concentration. Based on their concentrations, x axis, peak area, y axis, which were calculated by regression analysis of standard inspection lines:

$$y = a + bx$$

where a and b are constant.

Recovery and repeatability experiments were conducted to investigate the accuracy and precision of the method based on three concentration levels (20, 100, and 400 μg/kg) of each spiked sample with five replicates at every level. LOQs were evaluated at 10× S/N ratios for the target ion (the less intense transition).

Results and discussion

Optimization of extraction solvent

To enhance the extraction efficiency and lessen matrix effects, the extraction solvent should possess a similar polarity to that of the pesticides. Earlier research suggested that acetonitrile is an appropriate extraction solvent since it has a suitable polarity for most components and produces less matrix interference from co-extracts and greater recover rates and compatibility with LC and GC systems (da Costa-Morais et al., 2018; Lehotay et al., 2010). In order to obtain the optimal extraction efficiency for pesticides in a tea sample, a recovery experiment was conducted by comparing the addition of either 1% acetic acid or 10% ethyl acetate to acetonitrile, for a 100 mg/kg spiked standard solution of a composite pesticide. The extraction was performed as per the previously mentioned methodology, and each treatment was replicated five times.

Recovery rates of the 33 pesticides used in our study ranged from 65.7% (acephate) and 106.7% (bifenthrin) when only acetonitrile was used as the extraction agent (*Fig. 1*).

Acetic acid improved the recovery of only 3 pesticides (cyfluthrin, thiosulfan, and isocarbophos) whilst lowering the rates of more than 20, with an overall range from 52.4% (acephate) to 108.3% (cyfluthrin). A previous study found that 1% acetic acid added to acetonitrile improved the recovery of alkali-sensitive pesticides, such as pyrethroids in apples, to a satisfactory level (>80%) without obvious matrix effects (Liu et al., 2009). Similarly, Lehotay et al. (2010) found that an acid buffer extraction method had a higher efficiency and higher recovery rate in fruits and vegetables, which is inconsistent with our research. This may be attributed to the fact that tea extracts contain a large amount of tea polyphenol, a type of weak acid component. Therefore,

http://www.aloki.hu ● ISSN 1589 1623 (Print) ● ISSN 1785 0037 (Online)
DOI: http://dx.doi.org/10.15666/aeer/1902_15171532
© 2021, ALÖKI Kft., Budapest, Hungary

since the tea extract solution may naturally act as an acid buffer, the addition of an extra acid buffer was confirmed as an unnecessary step.

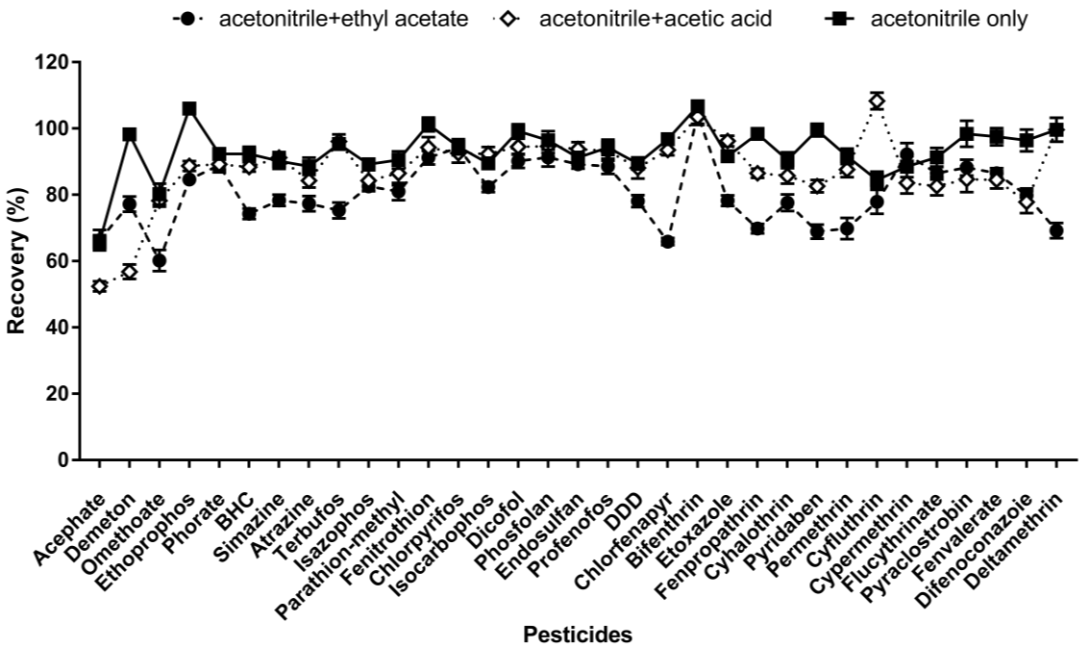


Figure 1. *Comparison of three QuEChERS extraction solution combinations for extracting pesticide residues in Wuyi Rock tea (spiked levels = 0.1 mg/kg, n = 5)*

When a mixture of acetonitrile and ethyl acetate (90% + 10%) was used as an extraction solvent, the recovery rates ranged from 66.3% (acephate) to 104.2% (cyfluthrin), and the mean recovery rate was lower than for acetonitrile only. Additionally, the colors of the extracts from this combination were too intense for further QuEChERS clean-up, in-line with a previous study on tea extracts (Chen et al., 2014b). This may be because ethyl acetate has a weak polarity, which could better dissolve the non-polar or weak polar pesticide components, but also dissolve the non-polar interference components, making purification more difficult.

Thus, from the above findings, acetonitrile alone was chosen for the preliminary extraction of tea samples.

Addition of analyte protectants (APs)

The application of APs to compensate for matrix effects in the GC system has recently gained attention (Li et al., 2012). In the present study, we compared the peak response of pesticides (spiked at a level of 50 μg/kg) in acetonitrile solutions containing APs (10 mg/mL of sorbitol and 20 mg/mL L-gulonic acid-γ-lactone) versus the peak response obtained in acetonitrile alone. All other steps were in accordance with the previously mentioned procedure.

As shown in *Figure 2*, the response values of targeted pesticides with APs were significantly higher than those of the control. Moreover, the presence of APs significantly improved the peak shape of polar pesticides, such as omethoate and methamidophos, which are easily adsorbed by the liner and injection port. Our results are similar to a previous study which indicated that a mixture of ethylglycerol,

http://www.aloki.hu ● ISSN 1589 1623 (Print) ● ISSN 1785 0037 (Online)
DOI: http://dx.doi.org/10.15666/aeer/1902_15171532
© 2021, ALÖKI Kft., Budapest, Hungary

sorbitol, and L-gulonic acid-γ-lactone was the most promising combination in reducing the matrix-induced response (Mastovská et al., 2005). Hence, the mixture of 20 mg/ml L-gulonic acid-γ-lactone and 10 mg/ml sorbitol was considered a suitable AP.

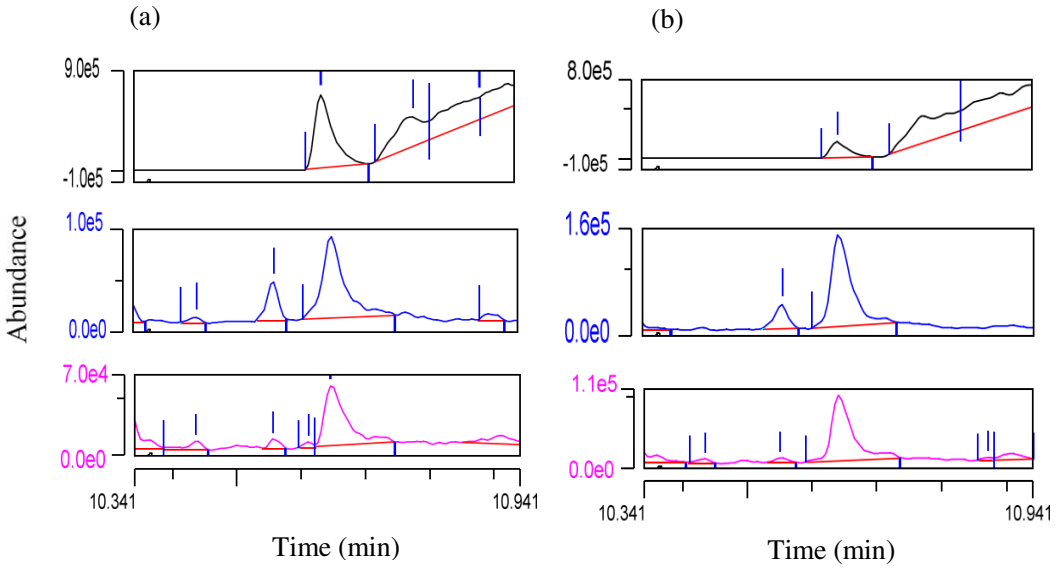


Figure 2. *GC-MS/MS chromatograms of omethoate pesticides with (a) and without (b) adding APs (spiked levels = 50 ug/mL)*

Optimization of clean-up conditions

Tea has a complicated matrix and includes a large amount of interferences, such as tea polyphenols, pigments, fatty acids, and caffeine, which can be co-extracted during sample preparation and influence the chromatographic separation (Pan et al., 2003). In order to solve this problem, we added sorbents (namely PSA, GCB, C18, and anhydrous $MgSO_4$) prior to injection as a purification step. PSA is a weak anion exchanger that be responsible for the elimination of sugars, fatty acids and other compounds that can form hydrogen-bonds, while C18 is used to eliminate lipids and non-polar components. GCB is responsible for removing pigments, such as chlorophyll. To remove water residue in the solvent, anhydrous $MgSO_4$ and NaCl was applied, resulting in a lower polarity of the final acetonitrile extracts and precipitation of certain polar matrix co-extracts (Cajka, et al., 2012). The salting-out conditions and QuEChERS adsorbents were optimized at spiked levels of 100 μg/kg for five replicates. Other than the different salting-out sorbents and QuEChERS adsorbents, all other steps were in performed as per the previously mentioned methodology.

Optimization of salting-out conditions

Different combinations of anhydrous NaCl and $MgSO_4$, namely 1 g NaCl + 4 g $MgSO_4$, 1 g NaCl + 2 g $MgSO_4$, and 4 g $MgSO_4$ without NaCl, were compared based on the recovery rate experiments. As shown in *Figure 3*, the different combinations of anhydrous NaCl and $MgSO_4$ have significant impacts on the recovery rate of pesticides. For 1 g NaCl + 4 g $MgSO_4$, the recovery value ranged from 77.3% to 106%, meaning

http://www.aloki.hu ● ISSN 1589 1623 (Print) ● ISSN 1785 0037 (Online)
DOI: http://dx.doi.org/10.15666/aeer/1902_15171532
© 2021, ALÖKI Kft., Budapest, Hungary

that it was more suitable for consistent multi-residue extraction than the other two groups. For 1 g NaCl + 2 g $MgSO_4$ and 4 g $MgSO_4$ without NaCl, the recovery rates were 53.2–103.5% and 65.4–107.8%, respectively. When acetonitrile was used as the extractant, the combination of anhydrous $MgSO_4$ and NaCl improved the recovery of polar pesticides, but too much NaCl was unfavorable for improving the recovery rate (Anastassiades et al., 2003; Andersson et al., 1991). Based on the current EU guidelines for quality control in pesticide residue determination (SANCO/10232/2006, 2006), the recovery values from routine analysis should be between 60% and 140%. Thus, 1 g NaCl + 4 g $MgSO_4$ was selected as the optimal combination.

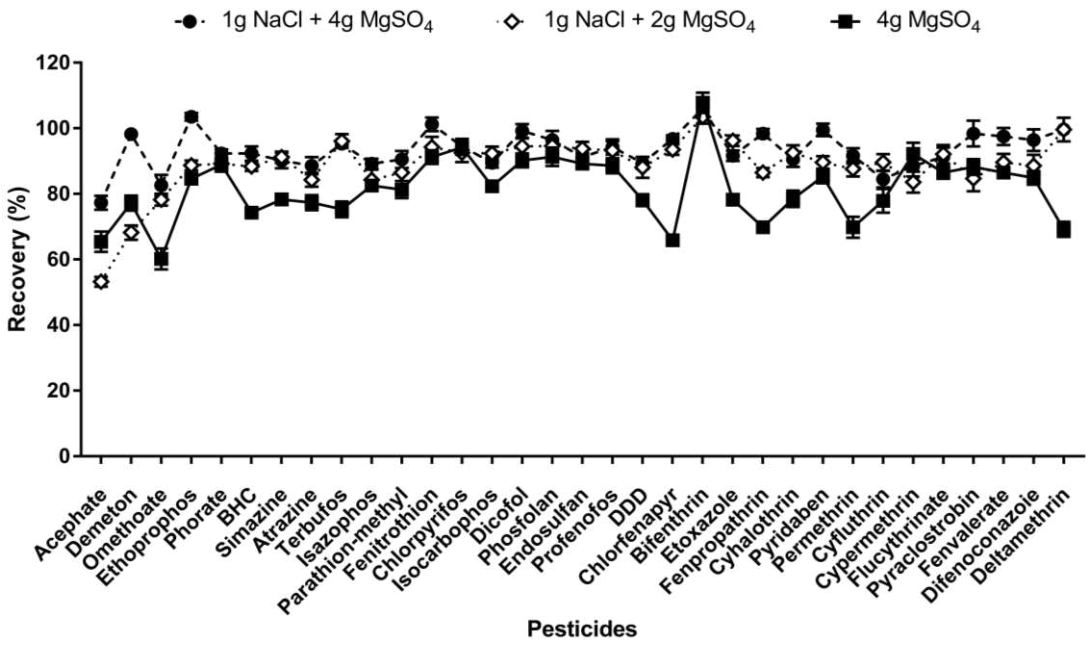


Figure 3. *Comparison of three QuEChERS salting-out solutions for purifying extracts in Wuyi Rock tea (spiked levels = 1 mg/kg, n = 5)*

Optimization of QuEChERS adsorbents

The main purpose of QuEChERS clean-up is to absorb as much interfering matrix as possible and maintain the targeted compounds in the solution without any negative effects. PSA has been suggested as a suitable adsorbent for eliminating interfering substances among the several carbon materials during the QuEChERS clean-up procedure for tea samples (Yu et al., 2020). To ensure optimal clean-up efficiency, recovery experiments were conducted by comparing different combinations of C18 and GCB with 400 mg of PSA. These were 400 mg PSA with 400 mg GCB + 50 mg C18 (combination adsorbent A), 400 mg PSA with 600 mg GCB + 50 mg C18 (combination adsorbent B), and 400 mg PSA with 400 mg GCB + 100 mg C18 (combination adsorbent C). According to the results shown in *Figure 4*, the recovery rates using combinations A, B, and C were 56.3–114.6%, 53.1–102.8%, and 78.4–108.6%, respectively. Only the rates resulting from C were within the range of the EC guidelines (SANCO/10232/2006, 2006). Moreover, the recovery rates of all 33 pesticides were more stable and greater than 78.4%, when combination adsorbent C was used. The use of combination adsorbent B resulted in very low recovery rates for chlorpyrifos,

http://www.aloki.hu ● ISSN 1589 1623 (Print) ● ISSN 1785 0037 (Online)
DOI: http://dx.doi.org/10.15666/aeer/1902_15171532
© 2021, ALÖKI Kft., Budapest, Hungary

fenvalerate, cyhalothrin, and DDT, although other pesticides were greater than 100%. Previous studies have indicated that increasing the volume of GCB led to reduced recovery rates of some pesticides due to the strong retention ability of GCB for these pesticides (Walorczyk and Gnusowski, 2009; Lu et al., 2012; Zheng et al., 2013). GCB possesses a planar structure, and therefore particularly adsorbs pesticides with planar structures, thus leading to low recovery rates for these pesticides (Tran et al., 2015). When combination adsorbent A was used, the test solution was light green, which indicated that the pigment was not cleaned completely. In summary, combination adsorbent C (400 mg PSA + 400 mg GCB + 100 mg C18) was found to the most suitable QuEChERS adsorbents for Wuyi Rock tea samples.

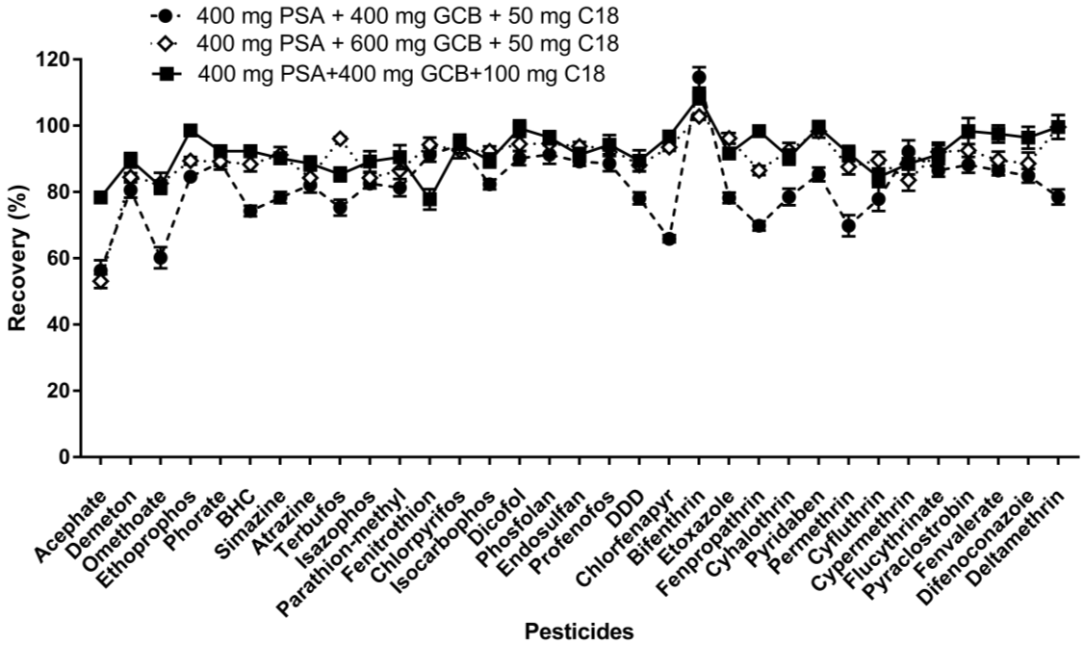


Figure 4. *Comparison of three QuEChERS adsorbent combinations for purifying extracts in Wuyi Rock tea (spiked levels = 1 mg/kg, n = 5)*

Method validation

The calibration curve was prepared using matrix-matched standards analyzed at five concentration levels (20, 50, 100, 200, and 500 ng/mL). The results, shown in *Table 1*, indicate that good linearity with correlation coefficients (R^2) greater than 0.994 was obtained for all pesticides at the concentration levels of 0.02, 0.2, 0.4 mg/kg after six parallel determinations. For all analyzed pesticides at three levels of concentration, the relative standard deviations (RSD%) ranged from 2.8% to 6.7%, with recovery rates between 72.3% and 110.6%. This suggests that this method has an accuracy appropriate for quantifying multi-class pesticide residues in Wuyi Rock tea. The limit of quantification (LOQ) for this determination method were estimated in spiked samples and calculated by considering a signal-to-noise ratio (S/N) of 10:1. All pesticides could be quantified at 0.02 mg/kg without any concentration steps; LOQ values ranged from 1.8 to 15.5 μg/kg and were acceptable compared to the maximum residue level from GB 2763-2019. Therefore, this method is suitable for the trace determination of pesticide multi-residue in Wuyi Rock tea.

http://www.aloki.hu ● ISSN 1589 1623 (Print) ● ISSN 1785 0037 (Online)
DOI: http://dx.doi.org/10.15666/aeer/1902_15171532
© 2021, ALÖKI Kft., Budapest, Hungary

Table 1. *Linearity, limits of quantification (LOQ) and recovery rates obtained with a modified QuEChERS method in Wuyi Rock tea, analyzed by GC-MS/MS (n = 6)*

Pesticide	R^2	LOQ (μg/kg)	Spiked level = 0.02 mg/kg		Spiked level = 0.2 mg/kg		Spiked level = 0.4 mg/kg	
			Recovery (%)	RSD (%)	Recovery (%)	RSD (%)	Recovery (%)	RSD (%)
Acephate	0.9948	15.3	72.3	4.3	78.1	3.9	81.6	2.9
Demeton	0.9994	13.2	102.1	5.2	95.3	2.2	92.3	2.6
Omethoate	0.9991	10.6	83.2	3.5	88.6	4.6	79.6	2.8
Ethoprophos	0.9999	6.8	106.3	2.6	102.3	2.1	88.6	3.1
Phorate	0.9991	8.6	94.2	3.7	95.3	1.6	94.5	2.1
α-BHC	0.9997	3.4	99.6	2.8	88.4	3.2	79.1	1.6
Simazine	0.9991	6.9	94.2	1.6	96.5	2.3	96.4	2.1
Atrazine	0.9957	12.6	96.8	3.6	94.3	2.8	89.3	1.8
β-BHC	0.9997	4.8	89.5	2.8	88.6	1.6	99.3	3.1
γ-BHC	0.9997	6.1	90.8	3.9	93.2	2.5	87.4	2.8
Terbufos	0.9991	5.9	84.9	5.1	90.5	3.1	95.2	1.2
Isazophos	0.9985	8.7	94.2	3.8	95.3	2.6	91.8	0.6
δ-BHC	0.9998	6.3	81.4	2.4	83.4	2.0	83.9	2.1
Parathion-methyl	0.9976	5.2	95.2	1.6	91.2	1.6	79.6	1.0
Fenitrothion	0.9998	8.7	102.5	3.1	94.6	2.5	95.6	1.3
Chlorpyrifos	0.9989	6.3	96.5	2.8	93.1	1.3	89.2	0.9
Isocarbophos	0.9992	4.9	94.1	4.6	97.6	0.5	94.6	2.1
Dicofol	0.9993	1.8	96.8	2.1	89.3	2.3	88.7	1.3
Quinalphos	0.9989	11.3	97.2	1.8	91.8	2.4	93.1	1.8
Phosfolan	0.9997	6.2	99.2	4.5	97.2	3.2	89.4	2.6
Endosulfan	0.9999	4.1	99.4	3.9	88.9	2.5	95.3	3.5
Profenofos	0.9992	13.5	95.6	3.1	95.6	1.4	87.4	1.4
p.p′－DDE	0.9995	6.4	86.5	5.8	89.2	1.1	86.3	0.5
Chlorfenapyr	0.9998	8.5	99.6	3.5	94.5	2.5	92.1	1.3
p.p′－DDD	0.9996	8.4	88.2	4.1	92.3	1.6	95.7	0.8
o.p′－DDT	0.9994	6.3	87.9	3.2	94.0	3.2	98.4	1.2
p.p′－DDT	0.9996	7.4	92.6	2.8	85.6	1.7	101.0	1.9
Bifenthrin	0.9948	5.2	110.6	2.6	101.2	2.8	98.6	1.3
Etoxazole	0.9967	7.6	98.4	3.1	95.3	3.5	84.3	2.5
Fenpropathrin	0.9999	5.2	99.8	4.8	93.1	1.9	96.5	1.6
Cyhalothrin	0.9999	15.5	86.5	5.0	82.3	2.0	86.7	2.8
Pyridaben	0.9998	8.9	97.5	3.5	94.6	3.3	95.2	1.3
Permethrin	0.9978	14.7	89.4	4.7	88.6	2.1	84.5	3.5
Cyfluthrin	0.9993	12.6	102.5	2.3	97.1	2.4	93.2	3.2
Cypermethrin	0.9998	10.4	99.5	4.1	89.5	3.1	88.6	1.2
Flucythrinate	0.9999	8.4	98.3	3.5	95.4	2.5	95.8	2.0
Pyraclostrobin	0.9996	6.6	94.6	2.9	91.5	1.8	79.6	1.6
Fenvalerate	0.9999	7.8	98.4	3.3	97.4	3.6	96.4	2.1
Difenoconazoie	0.9999	6.5	102.3	4.6	92.8	2.9	89.1	3.6
Deltamethrin	0.9996	11.6	98.9	3.8	97.1	1.4	92.4	2.1

Conclusion

QuEChERS is a tried and tested approach for determining pesticide residues in fruit and vegetables. However, in Wuyi Rock tea there are many complex chemical substances that cause matrix interferences and seriously influence the detection limits for pesticide analysis. Moreover, whilst most QuEChERS extraction methods are sufficient for LC/MS/MS analysis (Chen et al., 2014b; Guan et al., 2013; Rajski et al., 2013; Tran et al., 2015; Li et al., 2017; Huang et al., 2019a; Yu et al., 2020; Ly et al., 2020), few papers have focused on GC/MS/MS analysis to reduce matrix interference.

http://www.aloki.hu ● ISSN 1589 1623 (Print) ● ISSN 1785 0037 (Online)
DOI: http://dx.doi.org/10.15666/aeer/1902_15171532
© 2021, ALÖKI Kft., Budapest, Hungary

Thus, in the present study, a modified QuEChERS preparation method was developed to simultaneously quantify 33 pesticide residues in Wuyi Rock tea using GC-MS/MS. This involved applying a QuEChERS extraction and clean-up technique with three different adsorbents (PSA, GCB, and C18), salting-out sorbents (anhydrous $MgSO_4$ and NaCl), and analyte protectants (L-gulonic acid-γ-lactone and sorbitol) to minimize matrix interference, before analysis through a gas chromatography system coupled to tandem mass spectrometry. The results exhibited good analytical performance based on the repeatability and recovery obtained in the Wuyi Rock tea matrices, demonstrating that this quantitative method is suitable for the accurate analysis of pesticide multi-residue in tea samples.

Compared with the traditional method of pesticide analysis, the modified QuEChERS method has proven to be fast, easy to conduct, and uses only small quantities of reagents. It is therefore more environmentally friendly than conventional methods. To the best of our knowledge, this is the first time that the pesticide levels of Wuyi Rock tea in Fujian Province, China has been recorded; our data offers valuable information for the supervision department in China. In future research, the QuEChERS sample prepare method could also be optimized and validated for analysis through LC-MC/MC for polar, thermally unstable, and non-volatile pesticide residues in tea. Furthermore, we plan to use a similar methodology to optimize and evaluate pesticides in other tea commodities (e.g. black, white, and green tea) collected from different locations in China. Finally, the risk posed by pesticides in various tea infusions also warrants investigation.

Acknowledgements. This work was sponsored by the Education and Scientific Research Project for Young and Middle-aged Teachers in Fujian Province (JAT190793), the Advanced Talents Introduction Project of Wuyi University (YJ201910), and Science & Technology Innovation Platform Construction Project of Fujian Province (2018N2004).

Conflict of interests. The authors declare that they have no known competing financial interests or personal relationships that could have appeared to influence the work reported in this paper.

REFERENCES

[1] Anastassiades, M., Lehotay, S. J., Stajnbaher, D. Schenck, F. J. (2003): Fast and easy multiresidue method employing acetonitrile extraction/partitioning and dispersive solid-phase extraction for the determination of pesticide residues in produce. – Journal of AOAC International 86: 412-431.

[2] Andersson, A., Pålsheden, H. (1991): Comparison of the efficiency of different GLC multi-residue methods on crops containing pesticide residues. – Fresenius' Journal of Analytical Chemistry 339(6): 365-367.

[3] A.O.A.C. (2010): Official Methods of Analysis (18th rev. 3) – In: Horwitz, W., Latimer, G. W. (eds.) Official Method 2007.01 Pesticide Residues in Foods by Acetonitrile Extraction and Partitioning with Magnesium Sulfate. Association of Official Analytical Chemists, Inc., Guithersburg, MD, pp. 17-26.

[4] Cajka, T., Sandy, C., Bachanova, V., Drabova, L., Kalachova, K., Pulkrabova, J., Hajslova, J. (2012): Streamlining sample preparation and gas chromatography–tandem mass spectrometry analysis of multiple pesticide residues in tea. – Analytica Chimica Acta 743: 51-60.

http://www.aloki.hu ● ISSN 1589 1623 (Print) ● ISSN 1785 0037 (Online)
DOI: http://dx.doi.org/10.15666/aeer/1902_15171532
© 2021, ALÖKI Kft., Budapest, Hungary

[5] Chen., Y. L., Duan, J., Jiang, Y. M., Shi, J., Peng, L., Xue, S., Kakuda, Y. (2011): Production, quality, and biological effects of oolong tea (*Camellia sinensis*). – Food Research International 27: 1-15.
[6] Chen, H., Yin, P., Wang, Q., Jiang, Y., Xin, L. (2014a): A modified QuEChERS sample preparation method for the analysis of 70 pesticide residues in tea using gas chromatography-tandem mass spectrometry. – Food Analytical Methods 7(8): 1577-1587.
[7] Chen, L., Chen, J., Guo, Y., Li, J., Yang, Y., Xu, L., Fu, F. (2014b): Study on the simultaneous determination of seven benzoylurea pesticides in oolong tea and their leaching characteristics during infusing process by HPLC–MS/MS. – Food Chemistry 143: 405-410.
[8] Chen, S., Li, M., Zheng, G., Wang. T., Lin, J., Wang, S., Wang, X., Chao, Q., Cao, S., Yang, Z., Yu, X. (2018): Metabolite profiling of 14 Wuyi Rock Tea cultivars using UPLC-QTOF MS and UPLC-QqQ MS combined with chemometrics. – Molecules 81(2): 321.
[9] da Costa-Morais, E. H., Collins, C. H., Jardim, I. C. S. F. (2018): Pesticide determination in sweet peppers using QuEChERS and LC–MS/MS. – Food Chemistry (249): 77-83.
[10] Dil, E. A., Ghaedi, M., Asfaram, A., Mehrabi, F., Bazrafshan, A. A. (2018): Optimization of process parameters for determination of trace hazardous dyes from industrial wastewaters based on nanostructures materials under ultrasound energy. – Ultrasonics Sonochemistry 40: 238-248.
[11] Dil, E. A., Ghaedi, M., Asfaram, A., Tayebi, L., Mehrabi, F. (2019): A ferrofluidic hydrophobic deep eutectic solvent for the extraction of doxycycline from urine, blood plasma and milk samples prior to its determination by high-performance liquid chromatography-ultraviolet. – Journal of Chromatography A 1613: 460695.
[12] European Union. (2016): Pesticide residues and maximum residue levels. – http://ec.europa.eu/food/plant/pesticides/eu-pesticides-database/public/?event=download. MRL (accessed: July 2019).
[13] GB 23200.113-2018 National Standard for Food Safety: Determination of 208 pesticide residues and their metabolites in plant-derived foods by gas chromatography-mass spectrometry.
[14] GB 2763-2019 National Food Safety Standard Maximum Limit of Pesticide Residues in Food.
[15] Gómez-Ramos, M. M., Ferrer, C., Malato, O., Agüera, A., Fernández-Alba, A. R. (2013): Liquid chromatography-high-resolution mass spectrometry for pesticide residue analysis in fruit and vegetables: screening and quantitative studies. – Journal of Chromatography A 1287: 24-37.
[16] Guan, Y., Tang, H., Chen, D., Xu, T., Li, L. (2013): Modified QuEChERS method for the analysis of 11 pesticide residues in tea by liquid chromatography-tandem mass spectrometry. – Analytical Methods 5(12): 3056-3067.
[17] Guillarme, D., Casetta, C., Bicchi, C., Veuthey, J. L. (2010): High throughput qualitative analysis of polyphenols in tea samples by ultra-high pressure liquid chromatography coupled to UV and mass spectrometry detectors. – Journal of Chromatography A 1217: 6882-6890.
[18] Gurusubramanian, G., Rahman, A., Sarmah, M., Roy, S., Bora, S. (2008): Pesticide usage pattern in tea ecosystem, their retrospects and alternative measures. – Journal of Environmental Biology 29(6): 813-826.
[19] Hou, X., Lei, S., Guo, L., Qiu, S. (2016): Optimization of a multi-residue method for 101 pesticides in green tea leaves using gas chromatography-tandem mass spectrometry. – Brazilian Journal of Pharmacognosy 26(4): 401-407.

http://www.aloki.hu ● ISSN 1589 1623 (Print) ● ISSN 1785 0037 (Online)
DOI: http://dx.doi.org/10.15666/aeer/1902_15171532
© 2021, ALÖKI Kft., Budapest, Hungary

[20] Huang, Y. S., Shi, T., Luo, X., Xiong, H. L., Min, F. F. (2019a): Determination of multi-pesticide residues in green tea with a modified QuEChERS protocol coupled to HPLC-MS/MS. – Food Chemistry 275: 255-264.
[21] Huang, Y., Wang, T., Fillet, M., Crommen, J., Jiang, Z. (2019b): Simultaneous determination of amino acids in different teas using supercritical fluid chromatography coupled with single quadrupole mass spectrometry. – Journal of Pharmaceutical Analysis 9(4): 254-258.
[22] Lehotay, S. J., Kok, A., Hiemstra, M., Bodegraven, P. (2005): Validation of a fast and easy method for the determination of residues from 229 pesticides in fruits and vegetables using gas and liquid chromatography and mass spectrometric detection. – Journal of AOAC International 88: 595-614.
[23] Lehotay, S. J., Son, K. A., Kwon, H., Koesukwiwat, U., Fu, W., Mastovska, K., Hoh, E., Leepipatpiboon, N. (2010): Comparison of QuEChERS sample preparation methods for the analysis of pesticide residues in fruits and vegetables. – Journal of Chromatography 1217(16): 2548-2560.
[24] Li, Y., Chen, X., Fan, C., Pang, G. F. (2012): Compensation for matrix effects in the gas chromatography–mass spectrometry analysis of 186 pesticides in tea matrices using analyte protectants. – Journal of Chromatography 1266: 131-142.
[25] Li, N., Lei, L., Nian, L., Zhang, R., Wu, S. T., Ren, R. B., Wang, Y. Q., Zhang, H. Q., Yu, A. M. (2013): A modified QuEChERS method for the determination of some herbicides in yogurt and milk by high performance liquid chromatography. – Talanta 105: 219-228.
[26] Li, J. X., Sun, M. Y., Chang, Q. Y., Hu, X. Y., Kang, J., Fan, C. L. (2017): Determination of pesticide residues in teas via QuEChERS combined with dispersive liquid–liquid microextraction followed by gas chromatography-tandem mass spectrometry. – Chromatographia 80: 1447-1458.
[27] Liu, Y. B., Fan, M. T., Liang, J., Zhao, Z. Y., Yuan, H. (2009): Determination of 4 pyrethroids in apple by QuEChERS-GC-ECD. – Acta Agriculturae Boreali-Occidentalis Sinica 18(4): 61-65.
[28] Liu, C., Ji, Y., Jiang, X., Yuan, X., Zhang, X., Zhao, L. (2019): The determination of pesticides in tea samples followed by magnetic multiwalled carbon nanotube-based magnetic solid-phase extraction and ultra-high performance liquid chromatography tandem mass spectrometry. – New Journal of Chemistry 43(14): 5395-5403.
[29] Lu, D. S., Qiu, X. L., Feng, C., Jin, Y. E., Lin, Y. J., Xiong, L. B., Wen, Y. M., Wang, D. L., Wang, G. Q. (2012): Simultaneous determination of 45 pesticides in fruit and vegetable using an improved QuEChERS method and online gel permeation chromatography–gas chromatography/mass spectrometer. – Journal of Chromatography B 895-896: 17-24.
[30] Ly, T. K., Ho, T. D., Behra, P., Nhu-Trang, T. D. (2020): Determination of 400 pesticide residues in green tea leaves by UPLC-MS/MS and GC-MS/MS combined with QuEChERS extraction and mixed-mode SPE clean-up method. – Food Chemistry 326: 126928.
[31] Mastovská, K., Lehotay, S. J., Anastassiades, M. (2005): Combination of analyte protectants to overcome matrix effects in routine GC analysis of pesticide residues in food matrixes. – Analytical Chemistry 77: 8129.
[32] Mehrabi, F., Vafaei, A., Ghaedi, M., Ghaedi, M. A., Dil, E. A., Asfaram, A. (2017): Ultrasound assisted extraction of Maxilon Red GRL dye from water samples using cobalt ferrite nanoparticles loaded on activated carbon as sorbent: optimization and modeling. – Ultrasonics Sonochemistry 38: 672-680.
[33] Nie, S. P., Xie, M. Y. (2011): A review on the isolation and structure of tea polysaccharides and their bioactivities. – Food Hydrocolloid 25(2): 144-149.

http://www.aloki.hu ● ISSN 1589 1623 (Print) ● ISSN 1785 0037 (Online)
DOI: http://dx.doi.org/10.15666/aeer/1902_15171532
© 2021, ALÖKI Kft., Budapest, Hungary

[34] Pan, X., Niu, G., Liu, H. (2003): Microwave-assisted extraction of tea polyphenols and tea caffeine from green tea leaves. – Chemical Engineering and Processing: Process Intensification 42(2): 129-133.
[35] Rajski, L., Lozano, A., Belmonte-valles, N., Ucles, A., Ucles, S., Mezcua, M., Fernandez-alba, A. R. (2013): Comparison of three multiresidue methods to analyse pesticides in green tea with liquid and gas chromatography/tandem mass spectrometry. – Analyst 138: 921-931.
[36] Ramos, L. (2019): Use of new tailored and engineered materials for matrix solid-phase dispersion. – Trends in Analytical Chemistry 118: 751-758.
[37] SANCO/10232/2006. (2006): Quality control procedures for pesticide residue analysis. – http://www.crlpesticides.eu/library/docs/allcrl/AqcGuidance_Sanco_2006_10232.pdf (accessed 10.02.20).
[38] Sharangi, A. B. (2009): Medicinal and therapeutic potentialities of tea (*Camellia sinensis* L.) - a review. – Food Research International 42: 529-535.
[39] Shoeibi, S., Amirahmadi, M., Rastegar, H., Khosokhavar, R., Khanghah, A. M. (2013): An applicable strategy for improvement recovery in simultaneous analysis of 20 pesticides residue in tea. – Journal of Food Science 78: 792-796.
[40] Surma, M. K., Sadowska-Rociek, A. B., Cielik, E. J. (2014): Evaluation of the QuEChERS method with GC-MS detection for the determination of organochlorine pesticides in food of animal origin. – Food Analytical Methods 7(2): 366-376.
[41] Tran, S. C., Le, H. T., Thai-Nguyen, T. H. (2015): Determination of pesticide multi-residues in green tea using a modified QuEChERS extraction and liquid chromatography tandem mass spectrometry technique. – Acta Alimentaria 44(3): 412-422.
[42] Walorczyk, S., Gnusowski, B. (2009): Development and validation of a multi-residue method for the determination of pesticides in honeybees using acetonitrile-based extraction and gas chromatography - tandem quadrupole mass spectrometry. – Journal of Chromatography A 1216(37): 6522-6531.
[43] Wang, Y., Jin, H. Y., Ma, S. C., Lu, J., Lin, R. C. (2011): Determination of 195 pesticide residues in Chinese herbs by gas chromatography-mass spectrometry using analyte protectants. – Journal of Chromatography 1218(2): 334-342.
[44] Wu, C. C. (2017): Multiresidue method for the determination of pesticides in Oolong tea using QuEChERS by gas chromatography - triple quadrupole tandem mass spectrometry. – Food Chemistry 229: 580-587.
[45] Xu, X. M., Yu, C., Han, J. L., Li, J. P., El-Sepai, F., Zhu, Y., Huang, B. F., Cai, Z. X., Wu, H. W., Ren, Y. P. (2011): Multi-residue analysis of pesticides in tea by online SEC-GC/MS. – Journal of Separation Science 34(2): 210-216.
[46] Yener, S., Sánchez-López, J. A., Granitto, P. M., Cappellin, L., Märk, T. D., Zimmermann, R., Bonn, G. K., Yeretzian, C., Biasioli, F. (2016): Rapid and direct volatile compound profiling of black and green teas (*Camellia sinensis*) from different countries with PTR-ToF-MS. – Talanta 152: 45-53.
[47] Yu, C. C., Hao, D. Y., Chu, Q., Wang, T., Liu, S. N., Lan, T., Wang, F. H., Pan, C. P. (2020): A one adsorbent QuEChERS method coupled with LC-MS/MS for simultaneous determination of 10 organophosphorus pesticide residues in tea. – Food Chemistry 321: 126657.
[48] Zheng, H. B., Zhao, Q., Mo, J. Z., Huang, Y. Q., Luo, Y. B., Yu, Q. W., Feng, Y. Q. (2013): Quick, easy, cheap, effective, rugged and safe method with magnetic graphitized carbon black and primary secondary amine as adsorbent and its application in pesticide residue analysis. – Journal of Chromatography A 1300: 127-133.
[49] Zhu, B., Xu, X., Luo, J., Jin, S., Chen, W., Liu, Z., Tian, C. (2019): Simultaneous determination of 131 pesticides in tea by on-line GPC-GC–MS/MS using graphitized multi-walled carbon nanotubes as dispersive solid phase extraction sorbent. – Food Chemistry 276: 202-208.

http://www.aloki.hu ● ISSN 1589 1623 (Print) ● ISSN 1785 0037 (Online)
DOI: http://dx.doi.org/10.15666/aeer/1902_15171532
© 2021, ALÖKI Kft., Budapest, Hungary

APPENDIX

Table A1. *List of targeted pesticides with GC retention times and MS/MS condition*

Pesticide	Chemical formula	CAS No.	Class	Retention time/min	MRM transition/m/z (collision energy/eV)
Heptachlor epoxide	$C_{10}H_5Cl_7O$	1024-57-3	Organochlorine insecticides	16.094	354.8-264.9(10)[a] 352.8-262.9(10)[b]
Acephate	$C_4H_{10}NO_3PS$	30560-19-1	Organophosphorus insecticides	9.560	136.0-94.0(10)[a] 136.0-42.0(5)[b]
Demeton	$C_8H_{19}O_3PS_2$	8065-48-3	Organophosphorus insecticides	10.670	171.1-115(10)[a] 88.1-59.8(6)[b]
Omethoate	$C_5H_{12}NO_4PS$	1113-02-6	Organophosphorus insecticides	10.814	110.0-79.0(10)[a] 156.0-110.0(8)[b]
Ethoprophos	$C_8H_{19}O_2PS_2$	13194-48-4	Organophosphorus insecticides	10.952	157.9-96.9(16)[a] 157.9-113.9(6)[b]
Phorate	$C_7H_{17}O_2PS_3$	298-02-2	Organophosphorus insecticides	11.460	260.0-75.0(5)[a] 230.9-128.9(25)[b]
α-BHC	$C_6H_6Cl_6$	319-84-6	Organochlorine insecticides	11.616	218.8-146.6(20)[a] 218.8-183.0(8)[b]
Simazine	$C_7H_{12}ClN_5$	122-34-9	Triazine herbicides	12.033	201.1-731.1(5)[a] 201.1-186.2(5)[b]
Atrazine	$C_8H_{14}ClN_5$	1912-24-9	Triazine herbicides	12.034	214.9-58.1(10)[a] 214.9-200.2(5)[b]
β-BHC	$C_6H_6Cl_6$	319-85-7	Organochlorine insecticides	12.099	218.7-183.0(8)[a] 218.7-146.6(18)[b]
γ-BHC	$C_6H_6Cl_6$	58-89-9	Organochlorine insecticides	12.280	218.7-183.0(8)[a] 180.9-145.0(14)[b]
Terbufos	$C_9H_{21}O_2PS_3$	13071-79-9	Organophosphorus insecticides	12.300	230.9-175.0(10)[a] 230.9-129.0(20)[b]
Isazophos	$C_9H_{17}ClN_3O_3PS$	42509-80-8	Organophosphorus insecticides	12.677	161.0-119.0(5)[a] 161.0-146.0(5)[b]
δ-BHC	$C_6H_6Cl_6$	319-86-8	Organochlorine insecticides	12.863	218.8-146.5(20)[a] 218.8-182.9(8)[b]
Parathion-methyl	$C_8H_{10}NO_5PS$	298-00-0	Organophosphorus insecticides	13.791	262.9-109.0(10)[a] 232.9-109.0(10)[b]
Fenitrothion	$C_9H_{12}NO_6P$	2255-17-6	Organophosphorus insecticides	14.404	277.0-109.0(16)[a] 277.0-260.0(6)[b]
Chlorpyrifos	$C_9H_{11}Cl_3NO_3PS$	2921-88-2	Organophosphorus insecticides	14.795	196.9-169.0(15)[a] 198.9-171.0(15)[b]
Isocarbophos	$C_{11}H_{16}NO_4PS$	24353-61-5	Organophosphorus insecticides	15.142	135.9-108.0(15)[a] 135.9-69.0(30)[b]
Dicofol	$C_{14}H_9Cl_5O$	115-32-2	Organochlorine insecticides	15.227	250.9-139.0(12)[a] 139.0-111.0(12)[b]
Quinalphos	$C_{12}H_{15}N_2O_3PS$	13593-03-8	Organophosphorus insecticides	16.178	157.1-129.0(14)[a] 157.1-102.0(22)[b]
Phosfolan	$C_7H_{14}NO_3PS_2$	947-02-4	Organophosphorus insecticides	16.376	195.8-139.9(10)[a] 168.0-140.0(10)[b]
Endosulfan	$C_9H_6Cl_6O_3S$	115-29-7	Organochlorine insecticides	17.144	240.6-205.9(14)[a] 194.7-159.4(8)[b]
Profenofos	$C_{11}H_{15}BrClO_3PS$	41198-08-7	Organophosphorus insecticides	17.620	207.9-63.0(30)[a] 338.8-268.7(15)[b]

http://www.aloki.hu ● ISSN 1589 1623 (Print) ● ISSN 1785 0037 (Online)
DOI: http://dx.doi.org/10.15666/aeer/1902_15171532
© 2021, ALÖKI Kft., Budapest, Hungary

p.p′—DDE	$C_{14}H_8Cl_4$	72-55-9	Organochlorine insecticides	17.711	317.8-246.0(20)[a] 317.8-248.0(18)[b]
Chlorfenapyr	$C_{15}H_{11}BrClF_3N_2O$	122453-73-0	Pyrrole insecticides, acaricides	18.238	248.9-137.1(18)[a] 248.9-112.0(24)[b]
p.p′—DDD	$C_{14}H_{10}Cl_4$	72-54-8	Organochlorine insecticides	19.031	235.0-199.0(14)[a] 235.0-165.1(20)[b]
o.p′—DDT	$C_{14}H_{10}Cl_4$	53-19-0	Organochlorine insecticides	19.097	235.0-199.0(14)[a] 235.0-165.1(20)[b]
p.p′—DDT	$C_{14}H_{10}Cl_4$	72-54-8	Organochlorine insecticides	20.247	235.0-199.0(14)[a] 235.0-165.1(22)[b]
Bifenthrin	$C_{23}H_{22}ClF_3O_2$	82657-04-3	Pyrethroid insecticides	21.920	181.0-179.0(12)[a] 181.0-165.9(10)[b]
Etoxazole	$C_{21}H_{23}F_2NO_2$	153233-91-1	Acaricide	22.202	141.0-113.0(15)[a] 141.0-63.1(30)[b]
Fenpropathrin	$C_{22}H_{23}NO_3$	39515-41-8	Pyrethroid insecticides	22.239	207.9-181.0(5)[a] 264.9-210.0(10)[b]
Cyhalothrin	$C_{23}H_{19}ClF_3NO_3$	91465-08-6	Pyrethroid insecticides	23.775	197.1-141.1(10)[a] 197.1-161.1(5)[b]
Pyridaben	$C_{19}H_{25}ClN_2OS$	96489-71-3	Acaricide	25.472	147.1-132.1(12)[a] 147.1-119.1(8)[b]
Permethrin	$C_{21}H_{20}Cl_2O_3$	52645-53-1	Pyrethroid insecticides	25.475	183.0-168.1(10)[a] 183.0-153.1(10)[b]
Cyfluthrin	$C_{22}H_{18}Cl_2F_2NO_3$	68359-37-5	Pyrethroid insecticides	26.686	226.0-206.0(15)[a] 198.9-170.1(25)[b]
Cypermethrin	$C_{22}H_{19}Cl_2NO_3$	52315-07-8	Pyrethroid insecticides	27.287	163.0-127.0(6)[a] 163.0-91.0(10)[b]
Flucythrinate	$C_{26}H_{23}F_2NO_4$	70124-77-5	Pyrethroid insecticides	27.609	199.0-157.1(8)[a] 157.1-107.0(12)[b]
Pyraclostrobin	$C_{19}H_{18}ClN_3O_4$	175013-18-0	Bactericide	28.740	116.0-89.0(15)[a] 116.0-63.0(30)[b]
Fenvalerate	$C_{25}H_{22}ClNO_3$	51630-58-1	Pyrethroid insecticides	28.951	167.0-125.0(32)[a] 225.0-119.0(25)[b]
Difenoconazoie	$C_{19}H_{17}Cl_2N_3O_3$	119446-68-3	Bactericide	29.504	265.0-202.0(16)[a] 323.0-265.0(14)[b]
Deltamethrin	$C_{22}H_{19}Br_2NO_3$	52918-63-5	Pyrethroid insecticides	29.886	252.8-172.0(8)[a] 252.8-92.9(16)[b]

[a]Quantification ion
[b]Confirmation ion
α-BHC, β-BHC, γ-BHC and δ-BHC are isomers of the hexachlorocyclohexane; p.p'-DDE, p.p'-DDD, o.p'-DDT and p.p'-DDT are isomers of the clofenotane
Abbreviations: CAS, Chemical Abstracts Service; MRM, Multiple Reaction Monitoring; α-BHC, α-hexachlorocyclohexane; β-BHC, β-hexachlorocyclohexane; γ-BHC, γ-hexachlorocyclohexane; δ-BHC, δ-hexachlorocyclohexane; p.p'-DDE, 2-bis(4-chorophenyl)ethylene; p.p'-DDD, 1,1-Dichloro-2,2-bis(p-chlorophenyl)ethane; p.p'-DDT, 2, 2-bis(4-chlorophenyl)-1,1,1-trichloroethane; o.p'-DDT, 1,1,1-Trichloro-2-(2-chlorophenyl)-2-(4-chlorophenyl)ethane

http://www.aloki.hu ● ISSN 1589 1623 (Print) ● ISSN 1785 0037 (Online)
DOI: http://dx.doi.org/10.15666/aeer/1902_15171532
© 2021, ALÖKI Kft., Budapest, Hungary

COMPARISON OF INVADED AND NON-INVADED SITES: A CASE STUDY OF ROUGH COCKLEBUR (*XANTHIUM STRUMARIUM* L.) AN ALIEN INVASIVE SPECIES

ULLAH, R. – KHAN, N.* – RAHMAN, A.

Department of Botany, University of Malakand, Chakdara Dir Lower 18800, Khyber Pakhtunkhwa, Pakistan

**Corresponding author*
e-mail: nasrullah.uom@gmail.com

(Received 30th Nov 2020; accepted 27th Jan 2021)

Abstract. The present research focuses on the comparison of soil physiochemical properties, nutrients, and vegetation that are important factors influenced by the invasive species in the new environment. We compared the abiotic and biotic factors between *Xanthium strumarium* invaded sites and adjacent non-invaded *Vitex negundo* native populations. Sampling was conducted at 60 locations with extensively diverse soil and vegetation characteristics along road, rural and urban areas for comparison in Khyber Pakhtunkhwa, Pakistan. Our results revealed that *Xanthium* populations are growing in nutrient-deficient soils compared to *Vitex*. Invaded sites were of low nutrients level compared to non-invaded where phosphorus ($P<0.001$) and nitrogen ($P<0.05$) varied significantly. Soil textural properties were found to be highly fluctuating with the highest variation in clay particles ($P<0.001$). Electrical conductivity ($P<0.001$) was detected to be higher in non-invaded sites indicating that these sites are nutrient-rich compared to invaded ones. This fact is further evidenced by the species richness and diversity in invaded sites which were found to be floristically poor compared to the non-invaded sites. We concluded from this study that *X. strumarium* invasion can be successful in nutrient-deficient habitats and can invade the native plant communities with higher frequency because of the ample amount of nutrients available.
Keywords: *biotic and abiotic factors, low resources environment, poor floristic, native plant communities*

Introduction

Plant invasion has dramatic effects worldwide on biodiversity and materials cycling disturbing many ecosystem services throughout the globe (Rai and Singh, 2020). It is generally believed that invasive species have suitable traits with evolutionary adaptations that enable them to flourish well in a new environment (Rout and Callaway, 2009) thereby altering communities' composition and ecological association with ultimate effects on ecosystem conservation and services (Bartz and Kowarik, 2019). Besides, plant invasion provides key information about the usefulness of plant species in ecosystem development and their economic role (Díaz and Cabido, 2001). Most prominently, the non-native plants disturbed nutrients cycling and soil composition (Wang et al., 2015) by adapting and inheriting certain traits in the new prevailing environmental conditions and thus negatively affecting plant communities and endangering native useful plant species (Milanović et al., 2020).

Successful invasion depends on the environmental resources of a habitat where the plant species can grow and interact with native plants, ultimately leads to its disturbance and destruction (Thompson et al., 2001). It is generally believed that plants usually grow faster and densely populated in nutrient rich habitats with good yield and economic benefits (Gross et al., 2005). Conversely, invasive plants adjust in low resource conditions by the positive feedback mechanism and efficiently utilize the materials promoting disturbance thus making the conditions suitable for their growth temporally (Funk, 2013).

http://www.aloki.hu ● ISSN 1589 1623 (Print) ● ISSN1785 0037 (Online)
DOI: http://dx.doi.org/10.15666/aeer/1902_15331548
© 2021, ALÖKI Kft., Budapest, Hungary

Limited resources caused many adaptations in plants like the lower concentration of chemicals in tissues making the leaves thick, chemical compounds for defense, and resource use efficiency (Coley et al., 1985; Funk, 2013). Among these, resource use efficiency (RUE) is a key mechanism that enables the invasive plants to get success in a new environment with a high rate of propagation, growth, and development (Reed, 2005). In theoretical and community ecology the concept of limiting similarity theory (LST) has revealed that invasive species differ from native plants in many traits to enable themselves in invading the new harsh environment acquitting their requirements from low resources condition (MacArthur and Levins, 1967; Deng et al., 2004). In this context, several factors have been reported that affect successful invasion i.e., type and frequency of limited resources, the density of individuals, disturbance regime, and traits for resources conservation (Foxcroft et al., 2011). Plants invading environments with low resources completely use a different mechanism from those invading environments with high resources (Craine et al., 2005). Researchers have suggested that plant invading environment with high resources succeeded through resource acquisition while low resource species adapted to resource conservation (Craine, 2009).

Xanthium strumarium L. (hereafter *X. strumarium*) is one of the invading noxious weeds that significantly reduced the yield of different cereals and economically important crops like cotton, maize, soybeans, corns, and groundnuts (Hussain et al., 2014). In Pakistan, this plant has been reported as a predominant weed by Baloch et al. (1968) which was originated from northern Afghanistan through domesticated animals' and refugees' movement with rapid invasion in different parts of Khyber Pakhtunkhwa province during the late 1970s (Hashim and Marwat, 2002). Owing to the invasiveness and invasibility, we conducted this research to elucidate the complex relationships involved in the successful invasion of *X. strumarium* in the recipient ecosystem. Besides many other reasons, this research aimed to address whether this species can successfully invade and adopt in the condition of the low resources in different ecological habitats. We take into account the abiotic environment and vegetation in *X. strumarium* invaded and nearby non-invaded sites dominated by *Vitex negundo* (hereafter *V. negundo*) populations for the comparison of soil physiochemical properties and nutrients. This research will not only provide baseline information on how this species successfully invaded and occupied the areas with scarce resources in the native vegetation by modifying the soil's physical and chemical characteristics but will also be helpful in better understanding the invasion of other species in the region.

Materials and methods

Study area

This study was conducted in Khyber Pakhtunkhwa which is one of the five administrative provinces of Pakistan situated in the north-west region. The province is surrounded by Azad Jammu & Kashmir (AJK) in the north-east, Afghanistan and FATA in the west, Punjab in the east while Balochistan province lies southward (Khan, 2015). The province is covered with different mountainous ranges on the north-west and eastern part i.e., Himalayan, Hindukush and Karakorum ranges. The elevation of the province varies greatly from plains (327 m at Peshawar) towards mountains (7708 m at Tirch Mir) that lies in the Hindukush range (Rahman and Dawood, 2016). The sampling sites cover an elevation ranging from 360 m to 1200 m above sea level and are located between 34.59 to 34.85 N° latitudes and 71.44 to 72.82 E° longitudes (*Fig. 1*).

http://www.aloki.hu ● ISSN 1589 1623 (Print) ● ISSN1785 0037 (Online)
DOI: http://dx.doi.org/10.15666/aeer/1902_15331548
© 2021, ALÖKI Kft., Budapest, Hungary

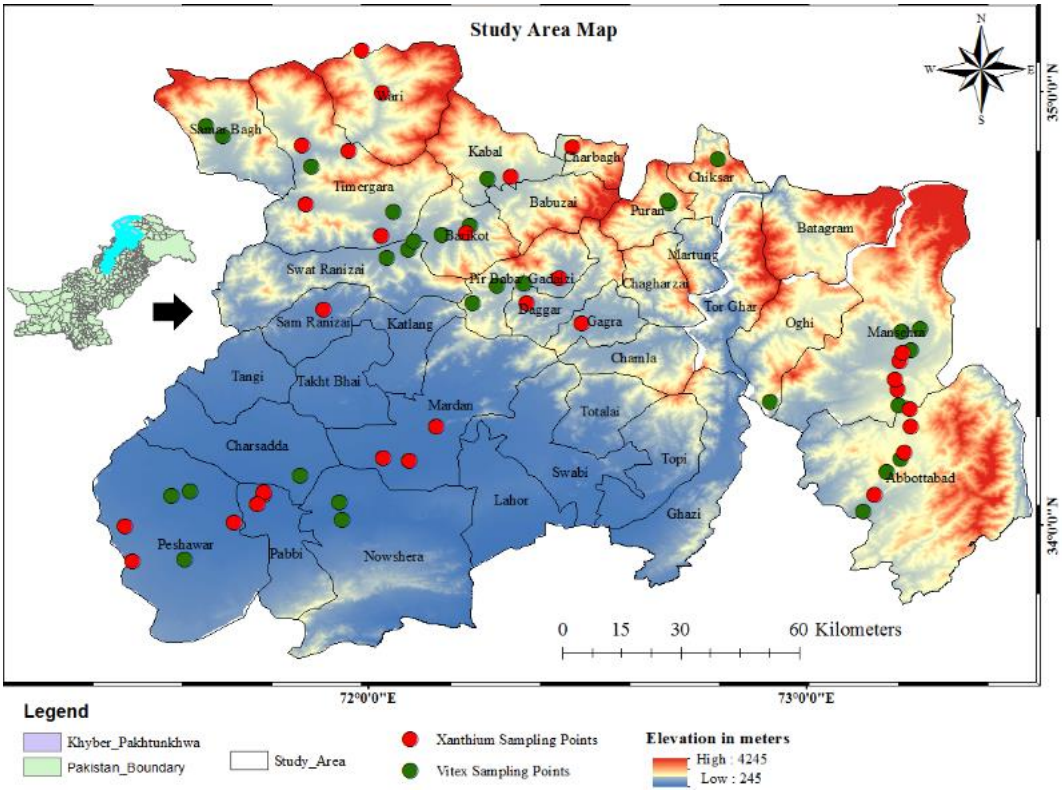


Figure 1. *Map of the study area with digital elevation model of Arc GIS while sampling sites of Xanthium are shown in red and that of Vitex in green legends*

The environmental protection agency (EPA) has divided the province into four agro-ecological zones (*Table 1*), based on the physiographic attributes and climate. The province has characterized by undulating valleys and plains surrounded by high mountains which significantly affect the climate along the elevation gradient from south to north and northwest in the region. Highlands are cold in winter and mild in summer with an obvious rise of temperature towards the South (Ali et al., 2018). June is the hottest month with a mean maximum and minimum temperature of 34.96±1.36 °C and 19.10±1.50 °C, respectively. January is the coldest month with a mean maximum and minimum temperature of 13.72±1.39 °C and 0.67±0.97 °C indicating that winters are more severe where the temperature generally falls below freezing point (Rahman and Khan, 2013). The average annual precipitation ranges from 384 mm to 639 mm whereas the relative humidity varies between 54.81±2.18% to 77.35±3.12% (Ali et al., 2018) as summarized in *Table 2*. The climate of the area plays a pivotal role in the economic, social, hydrological, and agricultural activities of the area and thus necessary in vegetation structure analysis (Deo and Sahin, 2015).

Table 1. *Showing the agro-ecological zones in Khyber Pakhtunkhwa, Pakistan*

Zone Name	A	B	C	D
Districts	Northern mountainous region (Swat, Dir Lower and Upper, Shangla, Bunir, Chitral)	Eastern mountainous region (Torghar, Kohistan, Haripur, Mansehra, Abbotabd, Battagram	Central plains (Mardan, Swabi, Kohat, Nowshera, Hangu, Karak, Peshwar, Charsadda)	Piedmont plains and Suleiman (Bannu, Lakki Marwat, Tank, Dera Ismail Khan)

http://www.aloki.hu ● ISSN 1589 1623 (Print) ● ISSN1785 0037 (Online)
DOI: http://dx.doi.org/10.15666/aeer/1902_15331548
© 2021, ALÖKI Kft., Budapest, Hungary

Table 2. *Geographic co-ordinates, elevation and climatic conditions of studied sites*

Latitude (°)		**Longitude (°)**		**Elevation (m)**		**Temperature (°C)**		**Relative Humidity**		**Precipitation (mm)**	
Min	Max	Min	Max	Min	Max	Min	Max	Min	Max	Min	Max
34.59	34.85	71.44	72.82	327	1200	7.19	37.03	54.81	77.35	384	639

Note: the coldest and warmest months' temperature were taken as mean as well as relative humidity

Studied species

We studied two different populations for comparison including an exotic invasive (*Fig. 2a*) and a native species (*Fig. 2b*) in this research. *X. strumarium* is a member of the family Asteraceae, which grow as an annual herb (about 150 cm in height) with a tap root system and usually propagate by seeds (Alex et al., 1980; Venodha, 2016). The morphometric characteristics of the plant show ovate, triangular alternate leaves, hairy stem and racemose inflorescence with pistillate heads below the staminate inflorescence (Love and Dansereau, 1959). Physiologically, it is a short-day plant that approximately requires 7.5 hours for flowering in northern while 10-hours photoperiods in southern areas (Abdulrahman and Winstead, 1977). The fruits (spiny bur) are up to 2 cm long with two stouts at the end and two achenes (Hicks, 1971) and often grow along shores and cultivated lands (Nadeau, 1961) as weed particularly in soybeans and cotton, thereby enormously reducing (up to 70%) yield of both crops (McWhorter and Anderson, 1976). Besides, it has also reduced wool production and caused many disorders in livestock due to harmful chemical constituents (Holm et al., 1977). This plant has been introduced from North America to many Asian countries including Pakistan especially in Khyber Pakhtunkhwa province where it spread from plains to higher zones and massively damaged District Nowshera and Abbottabad in the last two decades (Marwat, 2010). *X. strumarium* is more evident in open patches and along the road-sides and agriculture cropland due to its transport from Afghanistan through sheep's and goats during the Afghan nomad's movement (Hashim and Marwat, 2002) and now it acts as a strong ruderal component in the ecosystem. *V. negundo* commonly known as Marwadai that belongs to family Lamiaceae often grow as a shrub and rarely small deciduous tree with specific aroma (Ilyas, 2015). The plant reaches 3-9 ft in height and distributed in Indo-Malaysia, Asia, West Indies and America (Liu et al., 2005). The plant has a fairly thick brown root (about 8-10 cm dbh) (Vinuchakkaravarthy et al., 2011) and distinct by its palmately compound leaves with 3-5 leaflets. The flowers are usually axillary or terminal panicle and succulent black color ripped fruits are typical with four rounded seeds about 4 mm in diameter (Meena et al., 2011). Ecologically, this plant grows vigorously on loamy soils and usually preferred wet areas and forest lands (Khare, 2004). Medicinally, it is very important and often used as an analgesic, anti-inflammatory, anthelminthic, and anti-venom while its extracted oil is used as a diuretic and expectorant (Arora et al., 2011). It's has been used to strengthen immunity and frequently used in many Ayurvedic remedies for treating a wide range of diseases (Tiwle and Sanghi, 2015).

Soil sampling and floristic data collection

Collection of soil samples and vegetation data was carried from May to October 2018. The sampling sites were of two categories i.e., invaded and non-invaded which were further divided into three types i.e., road-sides, urban and rural to understand the intra and

http://www.aloki.hu ● ISSN 1589 1623 (Print) ● ISSN1785 0037 (Online)
DOI: http://dx.doi.org/10.15666/aeer/1902_15331548
© 2021, ALÖKI Kft., Budapest, Hungary

interspecific changes. The selection for sampling was based on the target species under investigation from sites with least to moderate (non-invaded) and more or entirely (invaded) anthropogenically disturbed often perceived as detrimental to plant biodiversity (Vanderhoeven et al., 2005). Finally, vegetation sampling was performed in 60 different stands (30 each) by using a plot size of 5 m^2 along 50 m transects at various physiographic situations and habitats. Five replicates of soil were collected from each plot at a depth of 10-30 cm in sites dominated by *X. strumarium* or *V. negundo* vegetation. The replicates were mixed to make a homogenized sample of 500 g following Elberling et al. (2004). Plant debris and small pebbles were removed from each sample by crushing peds with the grinding machine and were then allowed to air-dry. Each sample was passed through a sieve of 2-mm before physiochemical properties and nutrients analysis. Bouyoucos hydrometer method was used for determining soil texture properties (Day, 1965) and a soil suspension (1:5) was made for the determination of pH using a pH meter (Model CON.3173) immediately in the field. Soil organic matter was estimated by oxidation method following Walkley and Black (1934), whereas potassium was estimated in unbuffered NH4OAc of 1 molar (M) concentration (Thomas, 1982) using an Atomic absorption spectrophotometer (VARIAN model-AA2407, USA). Nitrogen was determined by digesting the samples in H_2SO_4–H_2O_2 and analyzed with an auto-analyzer whereas, phosphorus was estimated calorimetrically by using $NaHCO_3$ of 0.5M concentration (Murphy and Riley, 1962; Olsen and Sommers, 1982). Electrical conductivity was determined by using a conductometer (Model CON 5).



a) b)

Figure 2. a) *Xanthium strumarium L. with pistillate flowers surrounded by a spiny involucre and* ***b)*** *Vitex negundo L. with palmate compound leaves and inflorescence having bluish purple color flowers*

Statistical analysis

Phytosociological attributes for individual species were obtained and the importance values index (IVI) were calculated by transforming the relative values i.e., frequency, density, and the cover as IVI = 100 × (F_3 + D_3 + C_3/3) following Mueller-Dumbois and Ellenberg (1974) and Brower et al. (1998). We computed descriptive statistics (Mean±SE) for soil characteristics and the difference among the sites mean (i.e., urban, rural, and road-sides) were compared by using one-way analysis of variance (ANOVA) following a post hoc Tukey HSD test (Hughes and Uowolo, 2006). Additionally, a paired t-test was performed for the physiochemical and nutrient characteristics to seek any statistical differences between invaded and non-invaded sites. All the statistical analysis was carried out in Microsoft Excel and Graph Pad (ver.8.0).

http://www.aloki.hu ● ISSN 1589 1623 (Print) ● ISSN1785 0037 (Online)
DOI: http://dx.doi.org/10.15666/aeer/1902_15331548
© 2021, ALÖKI Kft., Budapest, Hungary

Results

Soil physiochemical properties and nutrients

Multiple resources in soil were found to be of low concentration in sites invaded by *X. strumarium* compared to *V. negundo*. The variations among soil textural properties and nutrients concentrations were found to be significant between the invaded and non-invaded sites. Site types i.e., roads, urban and rural was also found to play a significant role in the distribution and variation of nutrients in the study areas as shown in *Figure 3*, respectively. Concerning soil textural properties, clay particles exhibited a significantly strong variation (F =49.38, df =5, 54, p<0.01) among invaded and non-invaded sites. In soil physical characteristics, pH and electrical conductivity were found to be lower in invaded sites resulting in low resource condition that suggest comparatively higher availability of nutrients in non-invaded sites. The difference in pH (F-value= 11.409, df =5, 54, p<0.05) and electrical conductivity was statistically significant (F-value= 12.43, df =5, 54, p<0.05). Besides, significantly high differences in two important soil nutrients i.e., phosphorus (F=12.09, df=5, 54, p<0.05) and potassium (F=7.93, df=5, 54, p<0.05) were found between invaded and non-invaded sites indicating that invaded sites were of low nutrient concentration followed by organic matter, organic carbon, total carbon and nitrogen (p<0.05). This pattern was consistent among the road, urban, and rural sites respectively indicating that the nutrient level has a significantly lower value in invaded sites than the non-invaded sites. The results demonstrated that *X. strumarium* population has established faster with high efficiency than the *V. negundo* vegetation thereby utilizing and sustaining in the environment with low nutrients. The nutrient concentrations between invaded and non-invaded sites were also compared using a paired t-test which shows a considerably high variance of nutrients in non-invaded sites which generally elucidate an environment with low resources in invaded sites (*Fig. 3*).

Vegetation associations

We found 114 plant species belonging to 58 families in both the invaded and non-invaded sampling sites. Native vegetation was found to be species-rich with 92 different species compared to stands dominated by exotic invasive species. The most representative families were Asteraceae (26 spp), Amaranthaceae (10 spp), Moraceae, Lamiaceae (5 spp each), Poaceae, and Papilionaceae (3 spp each). The remaining 9 families were represented by 2 species each whereas 43 of the families were represented by single species. The invaded sites were usually dominated by *X. strumarium* with mean importance values ranging from 42.49 to 47.26% whereas, the non-invaded sites dominated by *V. negundo* with importance values ranging from 48% to 55% (*Table 3*). The IV values show that exotic species have densely invaded the urban sites where only 2 species were found as co-dominant with IV greater than 5%. *Table 3* shows that *Cannabis sativa* of the family Cannabaceae was a strong companion (IV= 10.81 to 11.98%) with the vegetation in road, rural and urban sampling sites, whereas, *Chenopodium album* (IV=8.23%) and *Datura innoxia* (IV=7.54%) were prominently associated species along road-sites. Conversely, the vegetation composition of non-invaded sites was different and predominated by *V. negundo* and *Justicia adhatoda* (9.33 to 23%) in the road and urban sites followed by *Cannabis sativa* (IV=13%) in rural sites vegetation (*Table 3*).

http://www.aloki.hu ● ISSN 1589 1623 (Print) ● ISSN1785 0037 (Online)
DOI: http://dx.doi.org/10.15666/aeer/1902_15331548
© 2021, ALÖKI Kft., Budapest, Hungary

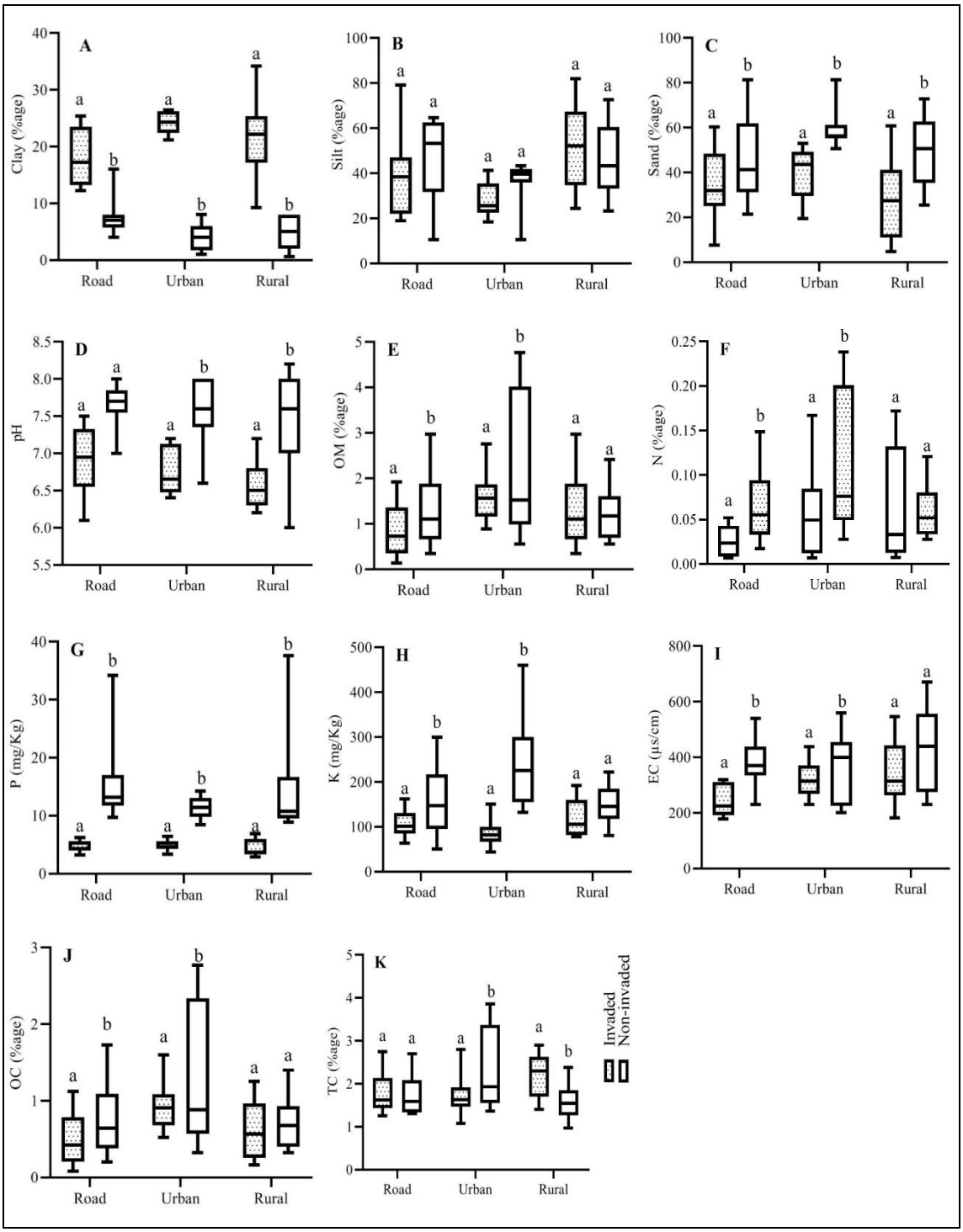


Figure 3. *Comparisons among different physiochemical properties of road, urban and rural sampling sites. * Same letters i.e. a:a indicating no significant difference between invaded and non-invaded sites while different letters i.e. a:b indicating significant difference between invaded and non-invaded. (Calculated through paired t-test at $p<0.05$). A. %age Clay: B. %age Silt: C. %age Sand: D. pH: E. %age Organic matter: F. Nitrogen %age: G. Phosphorus (mg/Kg): H. Potassium (mg/Kg): I. Electrical conductivity (µs/cm): J. %age Organic Carbon: K. %age Total Carbon*

http://www.aloki.hu ● ISSN 1589 1623 (Print) ● ISSN1785 0037 (Online)
DOI: http://dx.doi.org/10.15666/aeer/1902_15331548
© 2021, ALÖKI Kft., Budapest, Hungary

Table 3. *Top fifteen dominant plant species in different habitats (road, rural and urban) recorded in invaded and non-invaded sites. Importance Value Index was computed as Mean ± Standard Error*

Plant Name	Road		Rural		Urban	
	M±SE (In)	M±SE (N)	M±SE (In)	M±SE (N)	M±SE (In)	M±SE (N)
Xanthium strumarium L.	42.49±1.46	-	43.44±1.84	-	47.26±3.27	-
Vitex negundo L.	-	48±1.47	-	54.5±1.45	-	55±2.51
Cannabis satia L.	10.81±1.64	13±1.23	11.98±1.54	7.34±4.67	11.4±3.04	4.15±1.88
Adathoda viscosa L.	-	23±2.3	-	1.37±1.11	-	9.33±2.17
Eryngium caeruleum M.Bieb.	-	6.5±6.5	-	12±1.2	4.17±1.50	4±1.53
Datura inoxia L.	7.54±1.49	-	4.20±2.04	-	6.34±2.85	-
Chenopodium album L.	8.23±0.93	-	4.86±1.42	-	-	-
Ailanthus altissima (Mill.) Swingle	-	5±2.42	-	2.5±2.5	-	2.12±0.93
Verbascum thapsus L.	-	3.33±1.20	-	2.25±1.93	-	2.12±0.93
Amaranthus viridis L.	3.37±1.55	-	3.60±1.10	-	3.71±1.62	-
Cynodon dactylon (L.) Pers.	6.54±1.46	-	-	-	2.08±0.89	-
Carthamus oxycantha Bieb	-	-	3.64±1.39	-	-	-
Silybum marianum (L.) Geartn	-	-	5.87±1.95	-	-	-
Tagetes erectus L.	-	-	-	-	3.27±2.44	-
Daphne mucronata Royle	-	6.166±2.12	-	1.75±1.75	-	0.5±0.5

In: Invaded sites, N: Non-invaded sites: -: absence of species in given group: Details of all the plant species are available as supplementary materials in *Table A1*

Discussions

Humans are believed to play a key role in the dispersion of invasive plants especially in crossing aquatic barriers after which the exotic species establish, naturalized, and propagate efficiently (Seabloom, 2003). However, discovering the mechanism adopted by the invasive plants for finding ways in a new environment was a challenging task for ecologists for decades (Qureshi and Arshad, 2017). Researchers have reported that invasive species grow in environment with rich resources which brings variations in the invaded areas (Davis et al., 2000; Stohlgren et al., 2008). Our results did not support this concept rather the idea of limiting resources as formulated by Han et al. (2012). In the low resource system, invasive species conserved resources for better development and propagated even in harsh environments as reported by Funk and Vitousek (2007) which provide strength to our findings. The invasive plants have certain traits that enable them to maintain life even in low resources (Funk, 2008) efficiently with a complicated mechanism. *X. strumarium* an invasive species in northern Pakistan may have one of the possible adaptations reported by Grime (1977) and Funk (2008).

It was argued by Davis et al. (2000) that invasive plants used their traits efficiently according to the needs and requirements in the environment with fluctuating resources and has therefore gained the attention of researchers. It is believed that invasion in environment with low resources has resulted in disturbance and increased resource concentration with time (Antonio et al., 1999) despite the fact that native plants compete strongly with invasive species. Nevertheless, in certain conditions, the invasive plants get success in a new environment with a high growth rate and propagation pressure with a

http://www.aloki.hu ● ISSN 1589 1623 (Print) ● ISSN1785 0037 (Online)
DOI: http://dx.doi.org/10.15666/aeer/1902_15331548
© 2021, ALÖKI Kft., Budapest, Hungary

less known mechanism (Suding et al., 2004). This efficiency enables the invasive plants to establish well and compete the native plant species in low resource environments (Blumenthal, 2005). These statements proactively support the establishment of *X. strumarium* which propagates well in low resource conditions and will propagate rapidly if invaded the resource-rich environment compared to native plants like *V. negundo* (*Fig. 3*).

Identification of characters that enable the plants to occupy low resource conditions is difficult and complex to be realized since plants have a complex internal mechanism that needs to be evaluated (Tecco et al., 2010). However, invasive plants rather used completely different mechanisms from native plants to grow and establish in low resource environments thereby absorbing and conserving resources more efficiently (Wright et al., 2004; Funk and Vitousek, 2007). This behavior of invasive plants poses serious threats to native biodiversity as indicated by Holmes and Cowling (1997). Somewhat similar behavior was also shown by *X. strumarium* (*Table 3*), resulting in poor vegetation composition in the invaded sites compared to non-invaded. On the other hand, homogenization of biotic communities is a challenging task for ecologists throughout the globe because it rapidly and unnoticeably decreases the native flora by invasive alien species (Mckinney and Lockwood, 1999). The Present study reveals higher diversity in non-invaded sites compared to the invaded site as non-invaded sites were found to have ninety-two different species while invaded sites have forty-five species only. These findings are supported by studies like that of Qian and Guo (2010), who recorded invaded areas to be less diversified compared to native plant communities in North America. Several other factors that enable invasive species to be naturalized and dominate in an area varies considerably due to efficient dispersal of seeds and fruits, fecundity and fidelity, an adjustment in the prevailing environmental conditions, growth rate and biomass production, etc. (Devin and Beisel, 2007; Gosper and Vivian-Smith, 2009). These characteristics enable the invasive plants to occupy a variety of habitats with higher distribution in many regions and in some cases become cosmopolitan (Rejmánek and Richardson, 1996).

The key factor in promoting biotic homogenization is plant habits and their life-forms which contribute to promoting plant communities' disturbance. It was found that biennial and annual plants have more severely homogenized plant communities as compared to perennial plants (Qian and Guo, 2010). In the present study, *X. strumarium* was usually found to be the strong companion with annual and rarely with biennial plants advocating the findings of Qian and Guo (2010). Contrary to our results, researchers have also reported the homogenization of perennial plants (e.g., Milchunas et al., 1988; Tappeiner et al., 1991). Also, herbs were found with a more pronounced effect on homogenization of plant communities compared to shrubs and trees due to their efficient propagation potential and reproduction compared to other life-forms (Ricklefs et al., 2008). Although, *X. strumarium* is a shrub it produces a large number of seeds and fruits and is therefore spreading and propagating rapidly compared to *V. negundo* in the region.

Conclusions and limitations

Invasive plants have great potential to grow and propagate in diverse environmental conditions. *X. strumarium* an alien invasive species in Khyber Pakhtunkhwa has been established and adapted to a wide range of environmental conditions compared to native plant species. The eradication and control of invasive plants may better be understood

http://www.aloki.hu ● ISSN 1589 1623 (Print) ● ISSN1785 0037 (Online)
DOI: http://dx.doi.org/10.15666/aeer/1902_15331548
© 2021, ALÖKI Kft., Budapest, Hungary

by understanding the mechanism that favors invasive plant growth and reproduction. Our study focuses on the comparison of soil and vegetation between invaded and non-invaded sites in terms of soil physiochemical and nutrients concentration levels with phytosociological characters of associated plant species. Many other factors may enhance or decrease plant growth of invasive and native plants like climate, atmospheric moisture, light, and others, thus our study has the limitation in considering these factors in plants propagation and growth. This study is also restricted only to plant species with no animal invasion and its associated phenomenon. We further recommended that government departments like agriculture, livestock and forestry, and non-governmental organizations should immediately take steps for the eradication of this invasive plant species to protect the *V. negundo* communities in particular which is an important native medicinal plant and other native plant communities in general for the safety of the crops.

Acknowledgments. The authors sincerely acknowledge the local communities for providing hospitality and accommodation during the field survey. We also thank Dr. Kishwar Ali for their review and comments on the early version of this manuscript. The comments and suggestions of the anonymous reviewers also considerably improved the quality of this manuscript.

Competing Interests. The authors have declared that no competing interests exist.

Data Availability. The authors confirm that all data underlying the findings are fully available without restriction. All relevant data are within the paper along with supporting information files. Raw data can also be provided by the authors on request.

Funding. This study was self-supported by the authors and no funding agency was involved in the study design, data collection, and analysis, decision to publish, or preparation of the manuscript.

REFERENCES

[1] Abdulrahman, F. S., Winstead, J. E. (1977): Chlorophyll levels and leaf ultrastructure as ecotypic characters in *Xanthium strurmarium* L. – American Journal of Botany 64: 1177-1181.
[2] Alex, J. F., Cayouette, R., Mulltgan, G. A. (1980): Common and botanical names of weeds in Canada. – Research Branch, Agriculture Canada, 132p.
[3] Ali, A., Khan, T. A., Ahmad, A. (2018): Analysis of Climate Data of Khyber Pakhtunkhwa, Pakistan. – International Research Journal of Engineering and Technology 5(5): 4266-4283.
[4] Arora, V., Lohar, V., Singhal, S., Bhandari, A. (2011): *Vitex negundo* A Chinese Chaste Tree. – International Journal of Pharmaceutical Innovations 1(5): 9-20.
[5] Baloch, G. M., Mohyuddin, A. I., Ghani, M. A. (1968): *Xanthium strumarium* L.-insects and other organisms with it in West Pakistan. – Commonwealth Institute Biol. Control Tech. Bull 10: 103-111.
[6] Bartz, R., Kowarik, I. (2019): Assessing the environmental impacts of invasive alien plants: a review of assessment approaches. – NeoBiota 43: 69-99.
[7] Blumenthal, D. (2005): Interrelated causes of plant invasion. – Science 310(5746): 243-244.
[8] Brower, J. E., Zar, J. H., Von Ende, C. N. (1998): Field and laboratory methods for general ecology. – Wm. C. Brown company publisher.
[9] Coley, P. D., Bryant, J. P., Chapin, F. S. (1985): Resource availability and plant antiherbivore defense. – Science 230(4728): 895-899.

http://www.aloki.hu ● ISSN 1589 1623 (Print) ● ISSN1785 0037 (Online)
DOI: http://dx.doi.org/10.15666/aeer/1902_15331548
© 2021, ALÖKI Kft., Budapest, Hungary

[10] Craine, J. M., Fargione, J., Sugita, S. (2005): Supply pre-emption, not concentration reduction, is the mechanism of competition for nutrients. – New Phytologist 166: 933-940.
[11] Craine, J. M. (2009): Resource Strategies of Wild Plants. – Princeton University Press, Princeton.
[12] D'Antonio, C. M., Dudley, T. L., Mack, M. (1999): Disturbance and Biological Invasions: Direct Effects and Feedbacks. – In: Walker, L. R. (ed.) Ecosystems of Disturbed Ground. Elsevier, The Netherlands, pp. 413-452.
[13] Davis, M. A., Grime, J. P., Thompson, K. (2000): Fluctuating resources in plant communities: a general theory of invasibility. – Journal of ecology 88(3): 528-534.
[14] Day, P. R. (1965): Particle fractionation and particle-size analysis. – In: Page, A. L., Miller, R. H., Keeney, D. R. (eds.) Methods of soil analysis, Part 1. American Society of Agronomy, Soil Science Society of America.
[15] Deo, R. C., Şahin, M. (2015): Application of the Artificial Neural Network model for prediction of monthly Standardized Precipitation and Evapotranspiration Index using hydrometeorological parameters and climate indices in eastern Australia. – Atmospheric Research 161: 65-81.
[16] Devin, S., Beisel, J. N. (2007): Biological and ecological characteristics of invasive species: a gammarid study. – Biological Invasions 9: 13-24.
[17] Díaz, S., Cabido, M. (2001): Vive la différence: plant functional diversity matters to ecosystem processes. – Trends in ecology & evolution 16(11): 646-655.
[18] Elberling, B., Jakobsen, B. H., Berg, P., Søndergaard, J., Sigsgaard, C. (2004): Influence of vegetation, temperature, and water content on soil carbon distribution and mineralization in four High Arctic soils. – Arctic, Antarctic, and Alpine Research 36(4): 528-538.
[19] Foxcroft, L. C., Pickett, S. T. A., Cadenasso, M. L. (2011): Expanding the conceptual frameworks of plant invasion ecology. – Perspectives in Plant Ecology, Evolution and Systematics 13: 89-100.
[20] Funk, J. L., Vitousek, P. M. (2007): Resource-use efficiency and plant invasion in low-resource systems. – Nature 446(7139): 1079. https://doi.org/10.1038/nature 05719.
[21] Funk, J. L. (2008): Differences in plasticity between invasive and native plants from a low resource environment. – Journal of Ecology 96(6): 1162-1173.
[22] Funk, J. L. (2013): The physiology of invasive plants in low-resource environments. – Conservation physiology 1(1): 026.
[23] Gosper, C. R., Vivian-Smith, G. (2009): The role of fruit traits of bird-dispersed plants in invasiveness and weed risk assessment. – Diversity and Distributions 15: 1037-1046.
[24] Grime, J. P. (1977): Evidence for the existence of three primary strategies in plants and its relevance to ecological and evolutionary theory. – The American Naturalist 111(982): 1169-1194.
[25] Gross, K. L., Mittelbach, G. G., Reynolds, H. L. (2005): Grassland invasibility and diversity: responses to nutrients, seed input, and disturbance. – Ecology 86(2): 476-486.
[26] Han, Y., Buckley, Y. M., Firn, J. (2012): An invasive grass shows colonization advantages over native grasses under conditions of low resource availability. – Plant ecology 213(7): 1117-1130.
[27] Hashim, S., Marwat, K. B. (2002): Invasive weeds a threat to the biodiversity: a case study from Abbotabad District, N-W Pakistan. – Pakistan Journal of Weed Sciences and Research 8: 1-12.
[28] Hicks, A. J. (1971): Systematic studies of Xanthium (Compositae: Ambrosieae); the cockleburs of Tazewell County, Illinois. – Unpubl. Ph.D. thesis. University of Illinois. C' hampaign- Urbana, Ill. 60.
[29] Holm, L. G., Plunknett, D. L., Pancho, J. V., Herberger, J. P. (1977): The world worst weeds. – East-West Center Book Univ. Press of Hawaii, Honolulu, Hawaii. 609.

http://www.aloki.hu ● ISSN 1589 1623 (Print) ● ISSN1785 0037 (Online)
DOI: http://dx.doi.org/10.15666/aeer/1902_15331548
© 2021, ALÖKI Kft., Budapest, Hungary

[30] Holmes, P. M., Cowling, R. M. (1997): The effects of invasion by Acacia saligna on the guild structure and regeneration capabilities of South African fynbos shrub lands. – Journal of Applied Ecology 34(2): 317-332.
[31] Hughes, R. F., Uowolo, A. (2006): Impacts of *Falcataria moluccana* invasion on decomposition in Hawaiian lowland wet forests: The importance of stand- level controls. – Ecosystems 9: 977-991.
[32] Hussain, Z., Marwat, K. B., Cardina, J., Khan, I. A. (2014): *Xanthium strumarium* L. impact on corn yield and yield components. – Turkish journal of agriculture and forestry 38(1): 39-46.
[33] Ilyas, M. (2015): Phytosociological and ethnobotanical appraisal of Kabal valley swat with especial reference to plant biodiversity conservation. – PhD thesis Department of Botany Arid agriculture university Islamabad.
[34] Khan, F. K. (2015): Pakistan geography economy and people, 4th ed. – Oxford University Press, Pakistan.
[35] Khare, C. P. (2004): Encyclopedia of India Medicinal plants. – Spinger Verlange, Berline, Heidelberge, New York, pp. 474-476.
[36] Liu, C., Tseng, A., Yang, S. (2005): Chinese herbal medicine: modern applications of traditional formulas. – Florida, USA: CRC Press.
[37] Love, D., Dansereau, P. (l959): Biosystematic studies on Xanthium: Taxonomic appraisal and ecological status. – Canadian Journal of Botany 37: 193-208.
[38] MacArthur, R., Levins, R. (1967): The limiting similarity, convergence, and divergence of coexisting species. – The American Naturalist 101(921): 377-385.
[39] Marwat, K. B., Hashim, S., Ali, H. (2010): Weed Management: A case study from North-West Pakistan. – Pakistan Journal of Botany 42: 341-353.
[40] McKinney, M. L., Lockwood, J. L. (1999): Biotic homogenization: a few winners replacing many losers in the next mass extinction. – Trends in Ecology and Evolution 14: 450-453.
[41] McWhorter, C. G., Anderson, J. M. (1976): Effectiveness of metribuzin applied preemergence for economical control of common cocklebur in soybeans. – Weed Science 24(4): 385-390.
[42] Meena, A. K., Niranjan, U. S., Rao, M. M., Padhi, M. M., Ramesh, B. (2011): A review of the important chemical constituents and medicinal uses of Vitex genus. – Asian Journal of Traditional Medicines 6(2): 54-60.
[43] Milanović, M., Knapp, S., Pyšek, P., Kühn, I. (2020): Trait–environment relationships of plant species at different stages of the introduction process. – NeoBiota 58: 55-74.
[44] Milchunas, D. G., Salsa, O. E., Lauenroth, W. K. (1988): A generalized model of the effects of grazing by large herbivores on grassland community structure. – American Naturalist 132: 87-106.
[45] Mueller-Dombois, D., Ellenberg, H. (1974): Aims and Methods of Vegetation Ecology. – John Wiley and Sons, New York, 547.
[46] Murphy, J., Riley, J. P. (1962): A modified single solution method for the determination of phosphate in natural waters. – Analytica Chimica Acta 27: 31-36.
[47] Nadeau, L. H. (1961): Etude Biosystematique sur le genre *Xanthium*. – Doctoral dissertation, Université de Montréal.
[48] Olsen, S. R., Sommers, L. E. (1982): Phosphorus. – In: Page, A. L., Miller, R. H., Keeney, D. R. (eds.) Methods of soil analysis, Part 2. American Society of Agronomy, Madison, WI.
[49] Qian, H., Guo, Q. (2010): Linking biotic homogenization to habitat type, invasiveness and growth form of naturalized plants in North America. – Diversity and Distributions 16: 119-125.
[50] Qureshi, H., Arshad, M. (2017): Assumptions for successful plant invasion and Pakistan's stance regarding biological pollution. – Advances in Biology & Earth Sciences 2(2): 143-151.

http://www.aloki.hu ● ISSN 1589 1623 (Print) ● ISSN1785 0037 (Online)
DOI: http://dx.doi.org/10.15666/aeer/1902_15331548
© 2021, ALÖKI Kft., Budapest, Hungary

[51] Rahman, A., Khan, A. N. (2013): Analysis of 2010-flood causes, nature and magnitude in the Khyber Pakhtunkhwa, Pakistan. – Natural Hazards 66(2): 887-904.
[52] Rahman, A., Dawood, M. (2016): Spatio-statistical analysis of temperature fluctuation using Mann–Kendall and Sen's slope approach. – Climate dynamics 48(3): 783-797.
[53] Rai, P. K., Singh, J. S. (2020): Invasive alien plant species: Their impact on environment, ecosystem services and human health. – Ecological Indicators 111: 106020.
[54] Reed, H. E., Seasteadt, T. R., Blair, J. M. (2005): Ecological consequences of C4 grass invasion of a C4 grassland: a dilemma for management. – Ecological applications 15: 1560-1569.
[55] Rejmánek, M., Richardson, D. M. (1996): What attributes make some plant species more invasive? – Ecology 77: 1655-1661.
[56] Ricklefs, R. E., Guo, Q., Qian, H. (2008): Growth form and distribution of introduced plants in their native and nonnative ranges in Eastern Asia and North America. – Diversity and Distributions 14: 381-386.
[57] Rout, M. E., Callaway, R. M. (2009): An invasive plant paradox. – Science 324(5928): 734-735.
[58] Seabloom, E. W., Harpole, W. S., Reichman, O. J., Tilman, D. (2003): Invasion, competitive dominance, and resource use by exotic and native California grassland species. – Proceedings of the National Academy of Sciences 100(23): 13384-13389.
[59] Stohlgren, T. J., Barnett, D. T., Jarnevich, C. S., Flather, C., Kartesz, J. T. (2008): The myth of plant species saturation. – Ecol Lett 11: 313-326.
[60] Suding, K. N., LeJeune, K. D., Seastedt, T. R., (2004): Competitive impacts and responses of an invasive weed: dependencies on nitrogen and phosphorus availability. – Oecologia 141(3): 526-535.
[61] Tappeiner, J., Zasada, J., Ryan, P., Newton, M. (1991): Salmonberry clonal and population structure: the basis for a persistent cover. – Ecology 72: 609-618.
[62] Tecco, P. A., Díaz, S., Cabido, M., Urcelay, C. (2010): Functional traits of alien plants across contrasting climatic and land use regimes: do aliens join the locals or try harder than them? – Journal of Ecology 98(1): 17-27.
[63] Thomas, G. W. (1982): Exchangeable cations. – In: Page, A. L., Millar, R. H., Keeney, D. R. (eds.) Methods of soils analysis, Part 1. American Society of Agronomy, Madison, WI, pp. 159-166.
[64] Thompson, K., Hodgson, J. G., Grime, J. P., Burke, M. J. (2001): Plant traits and temporal scale: evidence from a 5-year invasion experiment using native species. – Journal of Ecology 89(6): 1054-1060.
[65] Tiwle, R., Sanghi, D. K. (2015): Comprehensive Study of Nirgundi Plant: A Survey Report. – JIPBS 2(2): 125-130.
[66] Vanderhoeven, S., Dassonville, N., Meerts, P. (2005): Increased topsoil mineral nutrient concentrations under exotic invasive plants in Belgium. – Plant Soil 275: 169-179.
[67] Venodha, P. M. (2016): Landscape Degradation and Restoration–A Planning Approach. – International Journal of Environmental Science and Development 7(3): 229-233.
[68] Vinuchakkaravarthy, T., Kumaravel, K. P., Ravichandran, S., Velmurugan, D. (2011): Active compound from the leaves of *Vitex negundo* L. shows anti-inflammatory activity with evidence of inhibition for secretory phospholipase A2 through molecular docking. – Bioinformation 7: 199-206.
[69] Walkley, A., Black, A. (1934): An examination of the Degtjareff method for determining soil organic matter and a proposed modification of the chromic acid titration method. – Soil Sciences 37: 29-38.
[70] Wang, C., Xiao, H., Liu, J., Wang, L., Du, D. (2015): Insights into ecological effects of invasive plants on soil nitrogen cycles. – American Journal of Plant Sciences 6(01): 34.
[71] Wright, I. J., Reich, P. B., Westoby, M., Ackerly, D. D., Baruch, Z., Bongers, F., Cavender-Bares, J., Chapin, T., Cornelissen, J. H., Diemer, M., Flexas, J. (2004): The worldwide leaf economics spectrum. – Nature 428(6985): 821.

http://www.aloki.hu ● ISSN 1589 1623 (Print) ● ISSN1785 0037 (Online)
DOI: http://dx.doi.org/10.15666/aeer/1902_15331548
© 2021, ALÖKI Kft., Budapest, Hungary

APPENDIX

Table A1. *Overall species reported in invaded and non-invaded sites during field sampling in X. strumarium and V. negundo communities of Khyber Pakhtunkhwa, Pakistan*

Plan Binomial	Road		Rural		Urban	
	In	N	In	N	In	N
***Xanthium strumarium* L.**	**42.49±1.46**	**-**	**43.44±1.84**	**-**	**47.26±3.27**	**-**
***Vitex negundo* L.**	**-**	**48±1.47**	**-**	**54.5±1.45**	**-**	**55±2.51**
***Cannabis sativa* L.**	**10.81±1.64**	**13±1.23**	**11.98±1.54**	**7.34±4.67**	**11.4±3.04**	**4.15±1.88**
Parthenium hysterosporus L.	0.98±0.05	-	0.89±0.18	-	0.61±0.88	-
***Datura inoxia* L.**	**7.54±1.49**	**-**	**4.20±2.04**	**-**	**6.34±2.85**	**-**
Sonchus asper (L.) Hill	0.24±0.17	-	0.83±0.28	-	0.42±0.42	-
***Verbascum thapsus* L.**	**-**	**3.33±1.20**	**-**	**2.25±1.93**	**-**	**2.12±0.93**
Erigeron canadensis (L.) Cronq.	0.55±0.55	0.45±0.32	0.65+0.15	-	.75±00.52	-
Capsella bursaa pestoris (L.)Medik	-	-	1.61±0.78	-	-	-
Trifolium repens L.	-	0.54±0.11	-	0.21±0.21	-	0.43±0.11
Calotropis procera (Aiton) W.T.Aiton	0.31±0.31		-	0.12±0.12	-	0.61±0.40
***Chenopodium album* L.**	**8.23±0.93**	**-**	**4.86±1.42**	**-**	**-**	**-**
***Amaranthus viridis* L.**	**3.37±1.55**	**-**	**3.60±1.10**	**-**	**3.71±1.62**	**-**
Lipidium sativa L.	0.73±0.25	-	0.42±0.42	-	0.99±0.38	-
Persicaria maculosa S.F.Gray	0.34±0.31	-	0.30±0.19		0.64±.49	-
***Adhatoda viscosa* L.**	**-**	**23±2.3**	**-**	**1.37±1.11**	**-**	**9.33±2.17**
Taraxicum officinale Weber	0.62±0.62	-	0.72±0.34	-	0.45±0.45	0.47±0.47
Brassica campestris L.	0.42±0.34	-	0.41±0.41	0.42±0.42	-	0.54±.32
Eclipta alba L.	0.69±0.42	0.47±0.43	-	0.68±0.68	0.41±0.41	-
Alternanthera pungens Kunth	0.34±0.34	0.80±0.32	-	0.72±0.62	-	0.87±0.80
***Eryngium coereculum* M-Bieb.**	**-**	**6.5±6.5**	**-**	**12±1.2**	**4.17±1.50**	**4±1.53**
Amarathus spinosus L.	0.67±0.67	-	-	-	0.71±0.44	-
Dysphania ambrosioides L.	-	-		-	0.88±0.09	-
Chrozophora tinctoria (L.) Raf.	0.71±0.71	-	-	-	0.43±0.43	-
Tribulus terrestris L.	0.46±0.42	-	0.49±0.49	0.64±0.33	-	0.87±0.54
Polygonum aviculare L.	-	-	0.58±0.15	-	-	-
Heliotropium curassavicum L.	0.26±0.23	-	-	-	-	-
Helianthus annus L.	0.15±0.15	-	1.10±0.54	-	0.19±0.19	-
Mirabilis jalapa L.	-	0.5±0.21	1.19±0.75	-	-	-
Centaurea cyanus L.	-	-	-	0.29±0.11	1.09±0.72	-
***Tagetes erectus* L.**	**-**	**-**	**-**	**-**	**3.27±2.44**	**-**
***Carthamus oxycantha* Bieb**	**-**	**-**	**3.64±1.39**	**-**	**-**	**-**
Cirsium arvense (L.) Scop.	-	-	0.92±0.73	-	-	0.94±0.74
Urtica dioica L.	0.85±0.43	-	0.92±0.72		0.09±0.07	1.09±0.72
Oxalis carniculata L.	0.21±0.21	0.23±0.23	-	0.76±0.76	0.92±0.72	-
Zea mays L.	-	0.43±0.43	-	0.29±0.29	-	-
***Silybum marianum* (L.) Geartn**	**-**	**-**	**5.87±1.95**	**-**	**-**	**-**
Cyprus rotundus L.	-	-	0.82±0.42	-	0.35±0.35	-
Eichornia cresipes (Mart.) Solma in DC	0.78±0.78	-	-	-	-	-

http://www.aloki.hu ● ISSN 1589 1623 (Print) ● ISSN1785 0037 (Online)
DOI: http://dx.doi.org/10.15666/aeer/1902_15331548
© 2021, ALÖKI Kft., Budapest, Hungary

Plan Binomial	Road		Rural		Urban	
	In	N	In	N	In	N
Brossentia papyrifera (L.) L'Herit. ex Vent	1.10±0.78	-	0.39±0.39	-	-	-
Cucurbita pepo L.	0.45±0.45	0.22±0.22	-	0.33±0.33	-	-
Solanum nigrum L	0.65±0.45	-	0.41±0.41	0.42±0.42	-	0.61±0.61
Trianthema portulacastrum L.	-	-	-	0.56±0.42	-	0.76±0.42
Prosopis julifolia (Sw.) DC.	-	0.34±0.34	-	-	0.43±0.43	-
Mentha longifolia L.	-	-	-	-	0.42±0.42	-
Acacia nilotica Willd.	-	-	0.57±0.57	-	0.29±0.29	-
Physalis minima L.	0.74±0.49	-	-	-	-	0.34±0.34
Cassia occidentalis L.	-	-	-	-	-	0.29±0.29
Achyranthus aspera L.	0.54±0.54	0.42±0.21	-	0.11±0.11	-	-
***Cynodon dactylon* (L.) Pers.**	**6.54±1.46**		**-**	**-**	**2.08±0.89**	**-**
Tagetes minuta L.	0.78±0.67	0.64±0.21	-	0.53±0.27	0.89±0.37	-
Centaurea ibrica L.	-	1.2±0.54	-	0.51±0.37	-	0.64±0.47
Cichorium intybus L.	-	0.5±0.5	-	0.56±0.56	-	0.74±0.74
Dicliptera bupleuroides (Nees) C. B. Clarke.	-	0.76±0.43	-	0.64±0.64	-	0.89±0.89
Melia azedarach L.		1±1	-	1±1	-	1±1
Olea ferruginea Royle	-	0.81±0.42	-	0.98±0.47	-	0.78±0.33
***Ailanthus altisima*(Mill.) Swingle**	**-**	**5±2.42**	**-**	**2.5±2.5**	**-**	**2.12±0.93**
Morus alba L.	-	0.5±0.5	-	0.5±0.5	-	0.5±0.5
*Pentanema visitum*L.	-	0.6±0.6	-	0.6±0.6	-	0.6±0.6
Dodonaea viscosa Jacq.	-	1±0.21	-	0.3±0.3	-	0.30±0.30
Celtis cuascaica L.	-	0.96±0.67	-	0.52±32	-	0.96±0.67
Pheonix dacatylifera L.	-	1±0.21	-	0.87±0.32	-	0.56±0.32
Plantago lanceolata L.	-	0.8±0.8	-	0.8±0.8	-	0.8±0.8
Thlaspi arvenses L.	-	0.33±0.33	-	0.33±0.33	-	0.33±0.33
Mytenious roylensis L.	-	1±1	-	0.53±0.53	-	0.31±0.31
Oryza sativa L.	-	1.5±1.5	-	-	-	-
***Daphne mucronata* Royle**	**-**	**6.166±2.12**	**-**	**1.75±1.75**	**-**	**0.5±0.5**
Asparagus gracilis L.	-	0.4±0.5	-	0.4±0.5	-	0.4±0.5
Zizypus mauritiana Lam.	-	0.25±0.25	-	0.25±0.25	-	0.25±0.25
Maytenus wallichiana (Spreng.) Raju & Babu in Bull.Bot. Surv.Ind.	-	-	-	0.33±0.33	-	-
Periploca aphylla Tourn. ex. L	-	0.16±0.16	-	0.16±0.16	-	0.16±0.16
Oenanthe janvanica (Blume) DC.	-	0.33±0.33	-	-	-	0.5±0.32
Artimisia scoparia Waldst. & Kit. 1802 not Maxim. 1859	-	0.5±0.32	-	0.65±0.43	-	-
Len culinaris Medikus	-	-	-	1±1	-	-
Pimpinella diversifolia L.	-	1±1	-	-	-	-
Oenthera rosea L'Hér. ex Aiton	-	0.16±0.16	-	-	-	0.16±0.16
Stachys parviflora (Benth.) Vved.	-	-	-	0.4±0.6	-	0.4±0.6
Micromeria biflora (Buch.-Ham. ex D. Don) Benth.	-	0.67±0.67	-	-	-	0.67±0.67
Otostegia lambata (Benth.) Boiss.	-	0.16±0.16	-	-	-	-
Zizypus sativa Mill.	-	-	-	0.16±0.16	-	0.16±0.16

http://www.aloki.hu ● ISSN 1589 1623 (Print) ● ISSN1785 0037 (Online)
DOI: http://dx.doi.org/10.15666/aeer/1902_15331548
© 2021, ALÖKI Kft., Budapest, Hungary

Plan Binomial	Road		Rural		Urban	
	In	N	In	N	In	N
Geramnium ocellatum Camb. in Jacq. Voy. Ind.	-	0.16±0.16	-	-	-	0.37±0.37
Robinia pseudoacacia L.	-	0.33±0.21	-	0.12±0.12	-	-
Euphorbia helioscopia L.	-	0.75±0.27	-	0.75±0.14	-	0.75±0.24
Acacia modesta (Wall.) P. J. H. Hurter	-	0.75±0.49	-	0.75±0.49	-	-
Tagetus minuta L.	-	0.37±0.26	-	-	-	-
Zanthoxylum armatum DC.	-	-	-	1.33±0.56	-	-
Morus nigra L.	-	0.33±0.33	-	0.33±0.33	-	-
Berberis vulgaris L.	-	-	-	0.83±0.83	-	-
Asphodelus tenuioflius Cav.	-	0.83±0.83	-	-	-	-
Rubus fruicosus L.	-	0.33±0.33	-	0.33±0.33	-	-
Ricinus communis L.	-	0.33±0.33	-	-	-	0.33±0.33
Boerhavia procumbent L.	-	0.6±0.6	-	0.6±0.6	-	-
Monotheca buxifolia (Falc.) A. DC.	-	-	-	1.25±1.25	-	-
Portulaca quadrifida L.	-	-	-	0.5±0.5	-	-
Morus lavegata L.	-	0.2±0.2	-	1.5±0.5	-	-
Verbina officinalis L.	-	0.25±0.25	-	-	-	0.61±0.61
Amaranthus caudatus L.	-	-	-	1.25±1.25	-	-
Marrubium vulgare L.	-	-	-	0.5±0.5	-	-
Galinosega perviflora Cav.	-	0.75±0.75	-	-	-	0.75±0.32
Limium album L.	-	-	-	0.25±0.25	-	0.25±0.25
Chenopodium ambrosoides (L.) Mosyakin & Clemants	-	0.5±0.5	-	-	-	0.5±0.5
Ajuga bracteosa Wall. ex. Benth.	-	0.5±0.5	-	0.6±0.6	-	-
Carthmus lanatus L.	-	0.33±0.33	-	-	-	0.34±0.12
Avena sativa L.	-	1±1	-	-	-	-
Ficus palmata Forsskål	-	1.4±0.34	-	-	-	-
Euclaptus lanceolata Andrews	-	1±0.45	-	-	-	0.8±0.52
Medicago sativa L.	-	0.8±0.48	-	-	-	0.65±0.23
Cassia fistula L.	-	-	-	0.4±0.4	-	-
Cactus dillenii (Haw.) Haw.	-	0.2±0.2	-	-	-	0.2±0.2
Euphorbia hirta L.	-	0.4±0.4	-	-	-	-
Poplus nigra L.	-	-	-	0.2±0.2	-	0.2±0.2
Rabdosia rugosa (Wall. ex Benth.) H.Hara	-	1.2±1.2	-	-	-	-
Zizyphus jujuba Mill.	-	0.2±0.2	-	-	-	0.2±0.2
Allium cepa L.	-	0.2±0.2	-	0.2±0.2	-	0.2±0.2

http://www.aloki.hu ● ISSN 1589 1623 (Print) ● ISSN1785 0037 (Online)
DOI: http://dx.doi.org/10.15666/aeer/1902_15331548
© 2021, ALÖKI Kft., Budapest, Hungary